ORGANOMETALLICS

Volume 14, Number 12, December 1995

Communications

An Unusual Hydrogen Migration from a Cyclopentadienyl to a μ-Carbyne Carbon in the Reaction of Grignard Reagents with $[Fe_2(CO)_2(cp)_2(\mu\text{-}CO)(\mu\text{-}CSMe)]SO_3CF_3$

Vincenzo G. Albano,[†] Silvia Bordoni,[‡] Luigi Busetto,[‡] Magda Monari,[†] and Valerio Zanotti*,[‡]

Dipartimento di Chimica Fisica ed Inorganica, Università di Bologna, Viale Risorgimento 4, I-40136 Bologna, Italy, and Dipartimento di Chimica "G. Ciamician", Università di Bologna, Via Selmi 2, I-40126 Bologna, Italy

Received August 9, 1995[⊗]

*Summary: Reaction of $[Fe_2(CO)_2(cp)_2(\mu\text{-}CO)(\mu\text{-}CSMe)]SO_3CF_3$ (**1**; cp = η-C_5H_5) with Grignard reagents RMgCl (R = benzyl, phenyl, isopropyl) forms the alkylidene compounds $[Fe_2(CO)_2(cp)(C_5H_4R)(\mu\text{-}CO)\{\mu\text{-}C(SMe)H\}]$ (**2**) and the corresponding cyclopentadiene complexes $[Fe_2(CO)_2(cp)(C_5H_5R)(\mu\text{-}CO)(\mu\text{-}CSMe)]$ (**3**). The latter complexes are the intermediates in the formation of **2** which are formed by hydrogen migration from the C_5H_5R ring to the μ-C carbyne carbon. The molecular structure of $[Fe_2(CO)_2(cp)(C_5H_4Bz)(\mu\text{-}CO)\{\mu\text{-}C(SMe)H\}]$ has been determined by X-ray crystallography. Spectroscopic properties of the complexes are also presented.*

Extensive investigations on the chemistry of the bridging thiocarbyne complex $[Fe_2(CO)_2(cp)_2(\mu\text{-}CO)(\mu\text{-}CSMe)]SO_3CF_3$ (**1**; cp = η-C_5H_5)[1] with nucleophiles have evidenced several reactivity patterns which include addition at the μ-C carbon,[2] NCO^- insertion into the μ-C–S bond,[3] carbonyl substitution,[1,4] and more recently, carbyne–carbonyl migratory coupling promoted by nucleophilic attack at the CO ligand.[5] While examining the reactions of dinuclear μ-alkylidyne complexes with carbon nucleophiles, we have found that the reaction of **1** with BzMgCl at 0 °C forms two compounds which have been separated by chromatography on an alumina column. The nature of the major red product $[Fe_2(CO)_2(cp)(C_5H_4Bz)(\mu\text{-}CO)\{\mu\text{-}C(SMe)H\}]$ (**2a**; 40%) has been ascertained by an X-ray structural study, which has shown that C–C bond formation has occurred at the cp ligand, accompanied by a hydrogen migration at the μ-C carbon.[6] The η^4-pentadienyl–alkylidyne nature of the second product, $[Fe_2(CO)_2(cp)(C_5H_5Bz)(\mu\text{-}CO)(\mu\text{-}CSMe)]$ (**3a**; 17%), spectroscopically ascertained, demonstrates well the nucleophilic addition at the cp ring, which is well-known in mononuclear complexes,[7] including iron compounds,[8] but, to our knowledge, has never been observed in polynuclear species.

It has been previously reported[2a] that the addition of BzMgCl to **1**, at room temperature, results in an exothermic reaction yielding, after silica gel column chromatography, the alkylidene complex $[Fe_2(CO)_2(cp)_2(\mu\text{-}CO)\{\mu\text{-}C(Me)Bz\}]$. At this point, it is not clear why

[†] Dipartimento di Chimica "G. Ciamician".
[‡] Dipartimento di Chimica Fisica ed Inorganica.
[⊗] Abstract published in *Advance ACS Abstracts,* November 1, 1995.

(1) Quick, M. H.; Angelici, R. J. *Inorg. Chem.* **1981**, *20*, 1123.
(2) (a) Schroeder, N. C.; Funchess, R.; Jacobson, R. A.; Angelici, R. J. *Organometallics* **1989**, *8*, 521. (b) Busetto, L.; Bordoni, S.; Zanotti, V.; Albano, V. G.; Braga, D. *Gazz. Chim. Ital.* **1988**, *118*, 667.
(3) Busetto, L.; Carlucci, L.; Zanotti, V.; Albano V. G.; Braga, D. *J. Chem. Soc., Dalton Trans.* **1990**, 243.
(4) Schroeder, N. C.; Angelici, R. J. *J. Am. Chem. Soc.* **1986**, *108*, 3688.
(5) Busetto, L.; Zanotti, V.; Norfo, L.; Palazzi, A.; Albano, V. G.; Braga, D. *Organometallics* **1993**, *12*, 190.

0276-7333/95/2314-5455$09.00/0

Scheme 1

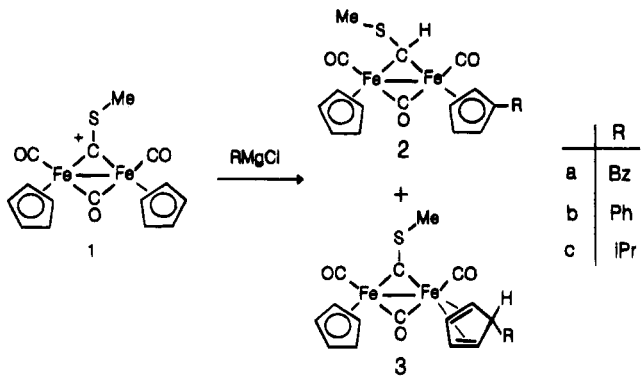

the different reaction conditions lead to such different products; however, it seems reasonable that the lower reaction temperature may result in a different reaction pathway, directing the nucleophilic addition at the Cp ring. Reactions of **1** with hydrides are known as well to give different products under different conditions: addition of $NaBH_4$ at room temperature occurred at the bridging carbon,[2a] whereas reaction with $LiHBEt_3$ at low temperature involved the carbonyl, affording the aldehyde complex $[FeFe(CO)(cp)_2(\mu\text{-}CO)\{\mu\text{-}C(SMe)(CHO)\}]$.[5] In order to prove that our findings are of general applicability, we have investigated the reaction with other Grignard reagents (RMgCl; R = Ph, *i*Pr): the results are consistent with those obtained in the case of R = Bz (Scheme 1).

Type **2** and **3** complexes have been characterized by spectroscopy (IR and NMR).[9,10] The IR spectra of type **3** complexes exhibit a ν(CO) band pattern (e.g. for **3a** in CH_2Cl_2 at 1980 s, 1945 w, and 1790 m cm^{-1}) that is consistent with the presence of two terminal and one bridging CO ligand. One single resonance, attributable to the cp group, is observed in both the ^1H and ^{13}C NMR spectra (e.g. for **3a** signals at δ 4.73 and 86.2). The C_5H_5R ring carbons, being diastereotopic, give rise tofive distinct signals in the ^{13}C NMR spectra (e.g. for **3a** δ 91.1, 87.5, 72.2, 69.2, and 59.0). The key feature in the ^{13}C NMR spectra of **3** is the low-field resonance (for **3a** at δ 398.0) in the region typical of bridging thioalkylidyne carbons.[1,2a,5]

A direct attack of R^- at the η^5-C_5H_5 ring normally occurs at the *exo* side of the ring, affording the L_nM-η^4-*exo*-RC_5H_5, unless nucleophilic addition takes place at the metal followed by a rearrangement to the cp ring to yield the *endo*-RC_5H_5 isomer. The IR criterion, based upon the characteristic absorption of the cyclopentadiene H_{exo} atom around 2750 cm^{-1}, provides a reliable method for distinguishing between the isomers.[11] In our case the absence of the IR C–H_{exo} band suggests that a direct nucleophilic attack at the cp ring has occurred.

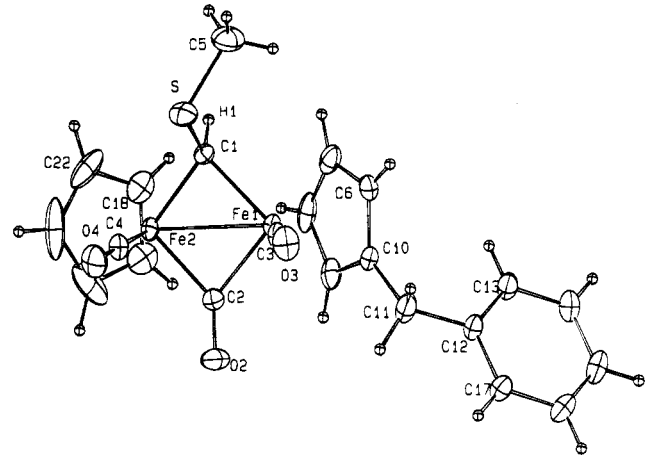

Figure 1. Ortep drawing of $[Fe_2(CO)_2(cp)(C_5H_4Bz)(\mu\text{-}CO)\{\mu\text{-}C(SMe)H\}]$ (**2a**). Selected bond distances (Å) and angles (deg) are as follows: Fe(1)–Fe(2), 2.519(1); Fe(1)–C(1), 1.982(3); Fe(2)–C(1), 1.957(3); Fe(1)–C(2), 1.903(4); Fe(2)–C(2), 1.915(3); C(1)–H(1), 0.96(4); C(2)–O(2), 1.171(4); C(3)–O(3), 1.141(4); C(4)–O(4), 1.143(5); C(1)–S, 1.774(3); C(5)–S, 1.761(6); C(1)–S–C(5), 102.4(2); S–C(1)–H(1), 107(2); S–C(1)–Fe(2), 117.8(2); S–C(1)–Fe(1), 123.9(2).

Complexes **2a–c** exhibit spectroscopic properties[9,10] similar to those of the previously reported bridgingmethylidene complexes of the type $[Fe_2(CO)_2(cp)_2(\mu\text{-}CO)\{\mu\text{-}C(R)H\}]$.[2a,12] In particular the methylidene proton gives rise to the expected low-field resonance at about δ 11 and the methylidene carbon resonance occurs at about δ 170. One single resonance is observed for the cp as well as for the SMe group (e.g. for **2a** at δ 4.90 and 2.87, respectively), indicating the existence, in solution, of a single isomer, presumably that bearing the SMe group on the less hindered CO side of the

(6) Crystal data for **2a**: $C_{22}H_{20}Fe_2O_3S$, fw 476.14; triclinic, space group $P\bar{1}$ (No. 2), a = 6.833(2) Å, b = 7.747(2) Å, c = 19.275(3) Å, α = 93.26(2)°, β = 93.62(2)°, γ = 100.21(2)°, V = 999.8(4) Å^3, Z = 2, d(calcd) = 1.582 Mg m^{-3}; ambient temperature; crystal dimensions 0.28 × 0.22 × 0.05 mm; graphite-monochromated Mo Kα radiation; μ(Mo Kα) = 1.575 mm^{-1}. Data were collected on an Enraf-Nonius CAD-4 diffractometer using the ω-scan mode; 4350 independent reflections ($\pm h, \pm k, +l$) were collected to $2\theta_{max}$ = 54° and corrected for absorption using the azimuthal scan method. Direct methods (SHELXS-86) identified the positions of the metal atoms and iterative cycles of least-squares refinement (on F^2), and difference Fourier syntheses located the remaining non-hydrogen atoms. The non-hydrogen atoms were refined anisotropically, and the carbene hydrogen was refined with fixed isotropic displacement parameters. The remaining hydrogen atoms were placed in calculated positions. Refinement on F^2 (SHELXL93) against 4344 data led to final convergence with R1 = 0.0437, wR2 = 0.1191, and S = 1.089 ($F_o > 4\sigma F_o$) for 232 refined parameters.

(7) (a) Davies, S. G.; Green, M. L. H.;. Mingos, D. M. P. *Tetrahedron* **1978**, *34*, 3047. (b) Maitlis, P. M. *Chem. Soc. Rev.* **1981**, *10*, 1.

(8) (a) Treichel, P. M.; Shubkin, R. L. *Inorg. Chem.* **1967**, *6*, 1328. (b) Green, M. L. H.; Whiteley, R. N. *J. Chem. Soc. A* **1971**, 1943. (c) Liu, L. K.; Luh, L. S. *Organometallics* **1994**, *13*, 2816. (d) Brown, D. A.; Fitzpatrick, N. J.; Groarke, P. J.; Koga, N.; Morokuma, K. *Organometallics* **1993**, *12*, 2521.

(9) Synthesis and characterization of **2a** and **3a**: freshly prepared BzMgBr (0.29 mmol) in thf solution was added to a stirred suspension of **1** (0.14 g, 0.26 mmol) in thf (15 mL) cooled to 0 °C with an external ice bath. The mixture was stirred for about 90 min, warmed to room temperature, and then filtered on an alumina pad. The solution was evaporated under reduced pressure, and the residue was chromatographed on an alumina column with a CH_2Cl_2–hexane mixture (1:4, v:v) as eluent. A first green fraction was collected, evaporated to dryness, and crystallized from CH_2Cl_2 layered with pentane at −20 °C, yielding $[Fe_2(CO)_2(cp)(C_5H_5Ph)(\mu\text{-}CO)(\mu\text{-}CSMe)]$ (**3a**; C_5H_5Bz = η^4-benzylcyclopentadiene; yield 50 mg, 40%). Anal. Calcd for $C_{22}H_{20}Fe_2O_3S$: C, 55.50; H, 4.23. Found: C, 55.44; H, 4.27. IR (CH_2Cl_2): ν(CO) 1980 s, 1945 w, 1790 m cm^{-1}. ^1H NMR (CD_2Cl_2): δ_H 7.28–7.04 (5 H, m, Ph), 4.73 (5 H, s, cp), 4.65, 4.16, 3.70 (5 H, m, C_5H_5Bz), 3.09 (3 H, s, Me), 2.08 (2 H, d, J = 2 Hz, CH_2Ph). ^{13}C NMR (CD_2Cl_2): δ_C 398.0 (br, μ-*C*SMe), 265.5 (μ-CO), 221.7, 212.7 (CO), 139.8, 129.2, 128.5, 125.9 (Ph), 86.2 (cp), 91.1, 87.5, 72.2, 69.2, 59.0 (C_5H_5Bz), 50.8 (CH_2Ph), 33.2 (SMe). Further elution with CH_2Cl_2–hexane (1:1, v:v) gave a red fraction which yielded, by crystallization, $[Fe_2(CO)_2(cp)(C_5H_4Bz)(\mu\text{-}CO)\{\mu\text{-}C(SMe)H\}]$ (**2a**; 21 mg, 17%; C_5H_4Bz = η^5-benzylcyclopentadienyl). Anal. Calcd for $C_{22}H_{20}Fe_2O_3S$: C, 55.50; H, 4.23. Found: C, 55.58; H, 4.32. IR (CH_2Cl_2): ν(CO) 1981 s, 1943 w, 1779 m cm^{-1}. ^1H NMR (CD_3CN): δ_H 11.55 (1 H, s, μ-CH), 7.35 (5 H, m, Ph), 4.90 (5 H, s, cp), 4.85, 4.78, 4.55 (4 H, m, C_5H_4Bz), 3.90 (1 H, d, J_{AB} = 15 Hz, CH_2Ph), 3.81 (1 H, d, J_{AB} = 15 Hz, CH_2Ph), 2.87 (3 H, s, Me). ^{13}C NMR (CD_3CN): δ_C 274.1 (μ-CO), 212.5, 212.4 (CO), 171.3 (μ-*C*HSMe), 140.8, 128.7, 128.6, 126.5 (Ph), 87.4 (cp), 105.9, 88.2, 86.9, 86.7, 67.2 (C_5H_4Bz), 33.5 (SMe), 25.1 (CH_2Ph).

molecule. This is the configuration found in the solid state for **2a** and $[Fe_2(CO)_2(cp)_2(\mu\text{-}CO)\{\mu\text{-}C(SMe)H\}]$[2a] (see Figure 1). The latter structure is strictly comparable with that of **2a**, the only difference being the benzyl appendage.

The migration of the R group from the metal to the the cyclopentadienyl ring has been observed in $[Fe(cp)(CO)_2R]$ (for R = $COCH_3$,[13] $SiMe_3$,[14] Bz[15]). In the complex $[Fe(\eta^4C_5H_5Bz)(CO)_3]$ the opposite transfer of Bz from the cyclopentadiene ring to the iron atom is also known[16] to occur in connection with light-induced loss of CO. Therefore, it is quite obvious to assume that complexes **3** are formed *via* hydrogen migration from the cyclopentadiene ligand to the μ-thioalkylidyne carbon. Conditions which favor this migration are currently under investigation: pure samples of **3** in CH_2Cl_2 solution do not exhibit appreciable conversion into **2** after 24 h. The relative amounts of the complexes **2**and **3** does not change appreciably upon chromatography on an alumina column; however, we have found that, upon treatment with silica gel, the conversion of **3** to **2** becomes significant.

Acknowledgment. Financial support from the MURST (Ministero dell'Università e della Ricerca Scientifica) and the CNR (Consiglio Nazionale delle Ricerche) is gratefully acknowledged.

Supporting Information Available: Listings of crystal data, positional and thermal parameters, and bond distances and angles for **2a** (8 pages). Ordering information is given on any current masthead page.

OM950630N

(10) **2b**: IR (CH_2Cl_2) ν(CO) 1981 s, 1944 w, 1780 m cm^{-1}; ^1H NMR: ($CDCl_3$) δ_H 10.93 (1 H, s, μ-CH), 7.41–7.19 (5 H, m, Ph), 4.53 (5 H, s, cp), 5.20, 4.95, 4.81, 4.67 (4 H, m, C_5H_4Ph), 2.50 (3 H, s, SMe). **3b**: IR (CH_2Cl_2) ν(CO) 1982 s, 1947 w, 1790 m cm^{-1}; ^1H NMR(CD_2Cl_2) δ_H 7.22–6.94 (5 H, m, Ph), 4.20 (5 H, s, cp), 4.87, 4.34, 3.94, 3.71 (5 H, m, C_5H_5Ph), 2.48 (3 H, s, Me). **2c**: IR (CH_2Cl_2) ν(CO) 1979 s, 1941 w, 1779 m cm^{-1}; ^1H NMR ($CDCl_3$) δ_H 11.39 (1 H, s, μ-CH), 4.74 (5 H, s, cp), 4.90, 4.79, 4.09 (4 H, m, C_5H_4Ph), 2.82 (3 H, s, SMe), 2.90 (1 H, m, $CHMe_2$), 1.30 (6 H, d, $CHMe_2$); ^{13}C NMR (CD_2Cl_2) δ_C 274.2 (μ-CO), 212.7, 212.2 (CO), 170.3 (μ-CHSMe), 87.6 (cp), 114.2, 88.5, 87.0, 85.3, 85.2 (C_5H_4iPr), 27.3 (SMe), 23.5, 23.1 (*i*Pr). **3c**: IR (CH_2Cl_2) ν(CO) 1979 s, 1943 w, 1786 m cm^{-1}; ^1H NMR ($CDCl_3$) δ_H 4.74 (5 H, s, cp), 4.63, 4.14, 3.79 (m, C_5H_5iPr), 3.13 (3 H, s, Me), 1.31 (1 H, m, $CHMe_2$), 0.72 (6 H, s, br, $CHMe_2$).

(11) (a) Davison, A.; Green, M. L. H.; Wilkinson, G. *J. Chem. Soc.* **1961**, 3172. (b) White, D. A. *Organomet. Chem. Rev. Sect. A* **1968**, *3*, 497. (c) Khand, I. U.; Pauson, P. L.; Watts, W. E. *J. Chem. Soc. C* **1969**, 2024. (d) Faller, J. W. *Inorg. Chem.* **1980**, *19*, 2857.

(12) Kao, S. C.; Lu, P. P. Y.; Pettit, R. *Organometallics* **1982**, *1*, 911. (b) Casey, C. P.; Fagan, P. J.; Miles, W. H. *J. Am. Chem. Soc.* **1982**, *104*, 1134. (c) Aime, S.; Cordero, L.; Gobetto, R.; Bordoni, S.; Busetto, L.; Zanotti, V.; Albano, V. G.; Braga, D.; Grepioni, F. *J. Chem. Soc., Dalton Trans.* **1992**, 2961.

(13) Liebeskind, L. S.; Welker, M. E. *Organometallics* **1983**, *2*, 194.

(14) (a) Berryhill, S. R.; Sharenow, B. *J. Organomet. Chem.* **1981**, *221*, 143. (b) Berryhill, S. R.; Clevenger, G. L.; Burdurlu, F. Y. *Organometallics* **1985**, *4*, 1509.

(15) Blaha, J. P.; Wrighton, M. S. *J. Am. Chem. Soc.* **1985**, *107*, 2694.

(16) Zou, C.; Wrighton, M. S.; Blaha, J. P. *Organometallics* **1987**, *6*, 1452.

Zwitterionic Metal Complexes of the New Triphosphine $NaO_3S(C_6H_4)CH_2C(CH_2PPh_2)_3$ in Liquid Biphasic Catalysis: An Alternative to Teflon "Ponytails" for Facile Catalyst Separation without Water

Claudio Bianchini,*[1a] Piero Frediani,[1b] and Volker Sernau[1a]

Istituto per lo Studio della Stereochimica ed Energetica dei Composti di Coordinazione del CNR, ISSECC, Via J. Nardi 39, 50132 Firenze, Italy, and Dipartimento di Chimica Organica, Università degli Studi di Firenze, Via G. Capponi 9, 50121 Firenze, Italy

Received August 8, 1995[⊗]

Summary: The new ligand $NaO_3S(C_6H_4)CH_2C(CH_2PPh_2)_3$ (sulphos) has been synthesized. The application of the zwitterionic Rh(I) complexes (sulphos)Rh(cod) and (sulphos)Rh(CO)$_2$ in liquid biphasic catalysis has been demonstrated for the hydrogenation of styrene and the hydroformylation of 1-hexene, respectively. The latter reaction gives C_7 alcohols in an alcohol/hydrocarbon system and C_7 aldehydes in an alcohol–water/hydrocarbon system. All rhodium is recovered in the polar phase at the end of the catalytic reactions.

In the field of liquid biphase catalysis, increasingly endeavors are being directed toward the elaboration of new techniques and new concepts in order to achieve selective chemical transformations and easy and efficient catalyst/product recovery.

An exciting approach to biphasic reactions has recently been developed by Horváth and Rabái.[2] The method is based on the limited miscibility of fluorinated solvents in hydrocarbons and the immobilization of the metal catalyst in the fluorocarbon phase by means of perfluoroalkylated phosphines (Teflon ponytails).

In this communication, we describe an alternative to fluorous biphasic systems for facile catalyst separation without water. Our strategy has involved the modification of a phosphine ligand, the tripodal triphosphine $MeC(CH_2PPh_2)_3$ (triphos) which has seen wide use in catalysis,[3] so as to make its metal complexes exclusively soluble in light alcohols (*e.g.* methanol) which have low miscibility in hydrocarbons at room temperature.

The new ligand $NaO_3S(C_6H_4)CH_2C(CH_2PPh_2)_3$ (sulphos) is basically a triphos ligand with a hydrophilic tail attached to the bridgehead carbon atom. The synthesis of sulphos is outlined in Scheme 1. The procedure involves the treatment of benzyltris(chloromethyl)methane[4] with concentrated H_2SO_4 (96%) at 100 °C, which results in the regioselective *para* sulfonation of the phenyl ring. Reaction of $NaO_3S(C_6H_4)CH_2C(CH_2Cl)_3$ with $KPPh_2$ in DMSO at 100 °C gives sulphos, which is recovered as colorless needles after recrystallization from hot ethanol (65% yield based on the trichloride).[5]

Scheme 1

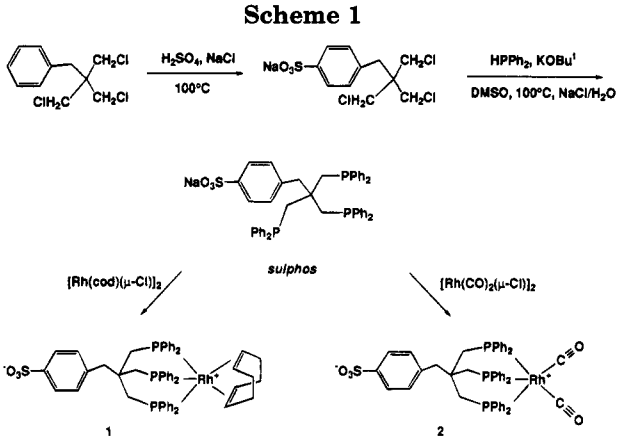

The complexes (sulphos)Rh(cod)[6] (**1**; cod = 1,5-cyclooctadiene) and (sulphos)Rh(CO)$_2$[7] (**2**) have been prepared by following the procedures used for the synthesis of the analogous triphos complexes (Scheme 1). Because of the distance of the negative charge from the phosphorus donors, the coordination properties of sulphos do not significantly differ from those of triphos. However, the complexes which are cationic with triphos[3a] are zwitterionic with sulphos, as this ligand can act as an internal counteranion itself. As a matter of fact, the main spectroscopic characteristics (NMR, IR) of the sulphos complexes are identical with those of the triphos

[⊗] Abstract published in *Advance ACS Abstracts,* October 15, 1995.

(1) (a) ISSECC-CNR. (b) Università degli Studi di Firenze.

(2) Horváth, I. T.; Rábai, J. *Science* **1994**, *266*, 72.

(3) (a) Bianchini, C.; Meli, A.; Peruzzini, M.; Vizza, F.; Frediani, P.; Ramirez, J. A. *Organometallics* **1990**, *9*, 226. (b) Bianchini, C.; Meli, A.; Peruzzini, M.; Vizza, F.; Zanobini, F. *Coord. Chem. Rev.* **1992**, *120*, 193. (c) Sernau, V.; Huttner, G.; Fritz, M.; Zsolnai, L.; Walter, O. *J. Organomet. Chem.* **1993**, *453*, C23. (d) Mayer, H. A.; Kaska, W. C. *Chem. Rev.* **1994**, *94*, 1239. (e) Barbaro, P.; Bianchini, C.; Frediani, P.; Meli, A.; Vizza, F. *Inorg. Chem.* **1992**, *31*, 1523. (f) Bianchini, C.; Farnetti, E.; Graziani, M.; Kaspar, J.; Vizza, F. *J. Am. Chem. Soc.* **1993**, *115*, 1753. (g) Bianchini, C.; Jimenez, M. V.; Meli, A.; Moneti, S.; Vizza, F.; Herrera, V.; Sánchez-Delgado, R. A. *Organometallics* **1995**, *14*, 2342.

(4) (a) Cooper, G. H.; Lawston, I. W.; Rickard, R. L.; Inch, T. D. *Eur. J. Med. Chem.* **1978**, *13*, 207. (b) Janssen, B.; Sernau, V.; Huttner, G.; Asam, A.; Walter, O.; Büchner, M.; Zsolnai, L. *Chem. Ber.* **1995**, *128*, 63.

(5) Anal. Calcd for $C_{47}H_{42}NaO_3P_3S$ (M_r = 802.82): C, 70.32; H, 5.27; P, 11.57. Found: C, 69.88; H, 5.10; P, 11.32. $^{31}P\{^1H\}$ NMR (24 °C, CD_3OD, 81.01 MHz): −29.5 ppm. ^1H NMR (20 °C, CD_3OD, 200.13 MHz): 2.21 ppm, s, br, 6H (CH_2P); 2.81 ppm, s, 2H ($PhCH_2C$); 7.11 ppm, d, 7 Hz, 2H (*o*-H of NaO_3SPh); 7.18 ppm, s, br, ~30H (PPh); 7.57 ppm, d, 7 Hz, 2H (*m*-H of NaO_3SPh).

(6) Anal. Calcd for $C_{55}H_{54}O_3P_3RhS$ (M_r = 990.21): C, 66.65; H, 5.50; P, 9.38. Found: C, 67.08; H, 5.40; P, 9.51. $^{31}P\{^1H\}$ NMR (20 °C, CD_2Cl_2, 81.01 MHz): 5.80 ppm, d, J_{RhP} = 104.5 Hz. ^1H NMR (20 °C, CD_2Cl_2, 200.13 MHz): 2.41 ppm, m, br, 4H (CH_2 of cod); 2.62 ppm, s, br, 6H (CH_2P); 2.78 ppm, m, br, 4H (CH_2 of cod); 3.12 ppm, s, br, 2H ($PhCH_2C$); 4.05 ppm, s, br, 4H (*CH* of cod); 6.92 ppm, br, 12H (*o*-H of PPh); 7.17 ppm, t, 5 Hz, 12H (*m*-H of PPh); 7.30 ppm, d, 8 Hz, 2H (*o*-H of ^-O_3SPh); 7.34 ppm, t, 5 Hz, 6H (*p*-H of PPh); 7.94 ppm, d, 8 Hz, 2H (*m*-H of ^-O_3SPh).

(7) Anal. Calcd for $C_{49}H_{42}O_5P_3RhS$ (M_r = 938.76): C, 62.69; H, 4.51; P, 9.90. Found: C, 62.50; H, 4.43; P, 9.70. $^{31}P\{^1H\}$ NMR (20 °C, CD_2Cl_2, 81.01 MHz): 6.60 ppm, d, J_{RhP} = 98 Hz. ^1H NMR (20 °C, CD_2Cl_2, 200.13 MHz): 2.65 ppm, d, 8 Hz, br, 6H (CH_2P); 3.27 ppm, s, br, 2H ($PhCH_2C$); 7.04 ppm, br, 12H (*o*-H of PPh); 7.15 ppm, t, 6 Hz, (*m*-H of PPh); 7.27 ppm, t, 6 Hz, 6H (*p*-H of PPh); 7.35 ppm, d, 8 Hz, 12H (*o*-H of ^-O_3SPh); 8.01 ppm, d, 8 Hz, 2H (*m*-H of ^-O_3SPh). IR: ν_{CO} 1971 (sst) cm^{-1}.

0276-7333/95/2314-5458$09.00/0

Table 1. Hydroformylation of 1-Hexene Catalyzed by 2[a]

		product composition[b]		
entry	solvent	hexane, %[c]	aldehyde (amt, %)	alcohol (amt, %)
1	methanol/isooctane (1:1, v:v)	24	heptanal (5) 2-methylhexanal (9) 2-ethylpentanal (3)	1-heptanol (43) 2-methylhexanol (14) 2-ethylpentanol (2)
2	H_2O–methanol/isooctane (1:1:1, v:v:v)	46	heptanal (37) 2-methylhexanal (17)	1-heptanol (traces)

[a] Conditions: 80 °C, 5 h, 15 bar of CO, 15 bar of H_2, [cat] = 2.5×10^{-4} mol^{-1}, 1:100 catalyst to substrate ratio. [b] Analyzed as a unique phase obtained by addition of THF. [c] Mixture of hexenes: entry 1, hexane (2%), 1-hexene (10%), *trans*-2-hexene (49%), *cis*-2-hexene (24%), *trans*-3-hexene (14%), *cis*-3-hexene (1%); entry 2, hexane (2%), 1-hexene (24%), *trans*-2-hexene (52%), *cis*-2-hexene (19%), *trans*-3-hexene (3%), *cis*-3-hexene (1%).

complexes apart from the differences intrinsically due to the $^-O_3S(C_6H_4)CH_2$ tail.[3a]

The sulphos Rh complexes are not soluble in water, hydrocarbons, or diethyl ether, whereas they dissolve in light alcohols (MeOH, EtOH) or in 1:1 (v:v) alcohol–water mixtures. Most importantly, *an alcohol phase containing either* ***1*** *or* ***2*** *(yellow color) is well-separated from a hydrocarbon phase (e.g. n-heptane) at room temperature, whereas a single homogeneous phase*[8] *is observed as the temperature of the biphasic system is increased above 60 °C. Cooling the homogeneous solution back to room temperature gives phase separation again.*[8] This characteristic of sulphos complexes allows the quantitative recovery of the metal in the polar phase after **1** and **2** have been used as catalyst precursors in liquid biphasic systems.

A preliminary investigation of the potential of **1** and **2** in liquid biphasic catalysis has been carried out. Styrene is hydrogenated to ethylbenzene in the presence of **1** in a 1:1 (v:v) mixture of methanol and *n*-heptane (30 atm of H_2, 65 °C, 1:500 catalyst to substrate ratio, 3 h, conversion >90%). Complete disappearance of styrene occurs after a further 2 h of reaction. After cooling to room temperature, the separation of the two phases does not give complete organic product separation, whereas all the rhodium in the form of a soluble species, as yet unidentified,[9] remains in the alcoholic phase.[10] However, the simple addition of water leads to the complete elimination of ethylbenzene (as well as residual styrene, if any) from the alcoholic phase. Interestingly, the same catalytic activity for the hydrogenation of styrene is shown by **1** in pure methanol, which confirms that truly a homogeneous phase forms at the reaction temperature.

Table 1 summarizes the results obtained for the hydroformylation of 1-hexene catalyzed by **2** in either methanol/isooctane or methanol–water/isooctane. In the absence of water, the reaction (15 atm of H_2, 15 atm of CO, 80 °C, 5 h) gives alcohols (1-heptanol, 2-methylhexanol, and 2-ethylpentanol) and aldehydes (heptanal, 2-methylhexanal, and 2-ethylpentanal) in an overall ratio of 78:22. For longer reaction times only alcohols are produced. The formation of alcohols is quite surprising, since rhodium catalysts typically only produce aldehydes (*e.g.* the triphos/Rh system).[3a] The typical chemoselectivity is found in the presence of water, as only aldehydes are formed (heptanal and 2-methylhexanal in a 69:31 ratio), although with a lower turnover frequency. Most importantly, in this latter case, it is not necessary to add water for product separation as only traces of aldehydes (as well as all the rhodium)[10] remain in the water/methanol phase after cooling to room temperature.

To the best of our knowledge, the overall characteristics of the present sulphos complexes have no precedent in the literature.

Current investigations center on the use of **1** and **2** in other liquid biphasic catalytic processes (*e.g.* the hydrogenation of carbonylic componds in light of the capability of **1** to catalyze the reduction of aldehydes) as well as the design of other tail-sulfonated polydentate ligands, possibly bearing stereocenters for use in asymmetric liquid biphase catalysis.

Acknowledgment. This work was partially supported by Progetto Strategico "Tecnologie Chimiche Innovative", CNR, Rome, Italy, and the EC (Contract No. CI1*-CT93-0329). A postdoctoral grant to V.S. from the EC (Contract No. CHBI CT94 1568) is also gratefully acknowledged.

Supporting Information Available: Text giving experimental details of the synthesis and characterization of the ligand $NaO_3S(C_6H_4)CH_2C(CH_2PPh_2)_3$ (sulphos) and of the new complexes described in this paper (4 pages). Ordering information is given on any current masthead page.

OM9506173

(8) In the absence of either **1** or **2**, the methanol/*n*-heptane mixture does not form a homogeneous phase at a temperature as high as 65 °C.

(9) Studies aimed at identifying the catalytically active species are currently in progress.

(10) After the hydrocarbon layer was separated, the solvent was removed in vacuo and the residue was analyzed by ^{31}P NMR spectroscopy and atomic absorption spectrometry. No appreciable amount of either phosphorus compounds or rhodium was detected.

New 58 VSE Clusters from the Oxidation of $Cp^{Et}_2Mo_2Co_2S_4(CO)_2$: Structural and Magnetic Effects and Catalytic Desulfurization Activity

M. Adnan Mansour, M. David Curtis,* and Jeff W. Kampf

The Willard H. Dow Laboratory, Department of Chemistry, The University of Michigan, Ann Arbor, Michigan 48109-1055

Received September 25, 1995[⊗]

Summary: The 60 VSE cubane cluster $Cp^{Et}_2Mo_2Co_2S_4(CO)_2$ *(1), where* $Cp^{Et} = C_5Me_4Et$*, reacts with* X_2 *to give the 58 VSE clusters* $Cp^{Et}_2Mo_2Co_2S_4(X)_2$ *(X = SPh (2), I (3), Cl (4), Br (5)). Structures and magnetic susceptibility data are reported for 2–4, and a catalytic desulfurization reaction of 1 with PhSH is described.*

Molybdenum sulfur compounds are important in the desulfurization of organic sulfur compounds,[1] including the commercially important hydrodesulfurization (HDS) catalytic reaction,[2] as well as in biological catalysis, e.g. nitrogenases[3] and hydrogenases.[4] We have been investigating the reactions of Mo/Co/S containing clusters, principally $Cp'_2Mo_2Co_2S_3(CO)_4$, as related to the commercially important "CoMoS" HDS catalyst.[5-7] This cluster reacts with a variety of organic sulfur compounds to give the cubane cluster $Cp'_2Mo_2Co_2S_4(CO)_2$ and the desulfurized organic radical. We have now observed that the cubane cluster is also an active agent for the desulfurization of certain sulfur donors, e.g. thiiranes and thietanes. The organometallic product of these desulfurization reactions is a black, insoluble powder whose elemental analysis agrees well with the formula $Cp'_2Mo_2Co_2S_5$, which we believe to consist of $Cp'_2Mo_2Co_2S_4$ cubes linked with sulfide bridges.[8] In this communication, we report a study of oxidative substitution reactions of the heterometallic cubane-type cluster $Cp^{Et}_2Mo_2Co_2S_4(CO)_2$ (**1**),[9] where $Cp^{Et} = C_5Me_4Et$, as models for the sulfur-bridged clusters obtained in the desulfurization reactions. These studies have also revealed the first *catalytic* desulfurization reaction with a Mo/Co/S cluster.[10]

Cluster **1** reacts with PhSSPh to give the new, paramagnetic, 58-electron cluster $Cp^{Et}_2Mo_2Co_2S_4(SPh)_2$ (**2**) (Scheme 1).[11] An alternate route to **2** is the reaction of **1** with PhSH in refluxing toluene. Cluster **2**, in turn, was found to react with CO to regenerate **1** along with PhSSPh, thus permitting a catalytic cycle for the conversion of PhSH to PhSSPh and H_2 (Scheme 2). When this catalytic cycle was attempted, **1** was allowed to react with an excess of PhSH under 1000 psi of CO.[12] The observed products were PhSSPh (171%) and PhS(CO)Ph (161%) and **2** (56% isolated yield, all yields based on **1**). The cluster **2** and PhSSPh were the expected products, but the phenyl thiobenzoate product must result from a *catalytic* desulfurization of the benzene thiol, followed by insertion of CO into an intermediate product. The noncatalytic formation of PhSC(O)Ph has been observed previously in a similar reaction.[6]

Cluster **2**, along with a series of halide clusters prepared from **1** and the corresponding halogen, have been structurally characterized as models for the insoluble, sulfide-bridged clusters formed from **1** and sulfur donors (Figure 1). Thus, cluster **1** reacted with an equivalent quantity of I_2 in toluene at room temperature to afford $Cp^{Et}_2Mo_2Co_2S_4(I)_2$ (**3**) as an analytically pure crystalline material.[13,14] Similarly, $Cp^{Et}_2Mo_2Co_2S_4(Cl)_2$ (**4**)[15] and $Cp^{Et}_2Mo_2Co_2S_4(Br)_2$ (**5**)[16] were prepared and characterized.

The most striking structural feature of these clusters is the variation in Co–Co distance upon going from the 60 VSE, electron-precise cubane, **1**, to the 58 VSE, electron-deficient cubanes, **2–5**. Cluster **1** has a Co–Co bond distance of 2.571(3) Å which corrresponds favorably to the Co–Co single bond distance of 2.665 Å

[⊗] Abstract published in *Advance ACS Abstracts,* November 1, 1995.

(1) (a) Dubois, M. R. *Chem. Rev.* **1989,** *89* (1), 1. (b) Lopez, L.; Godziela, G.; Dubois, M. R. *Organometallics* **1991,** *10,* 2660.

(2) Chianelli, R. R.; Daage, M.; Ledoux, M. J. *Adv. Catal.* **1994,** *40,* 177.

(3) (a) Holm, R. H.; Simhon, E. D. In *Molybdenum Enzymes*; Spiro, T. G., Ed.; Wiley-Interscience: New York, 1985; Chapter 1. (b) Burgess, B. K. *Chem. Rev.* **1990,** *90,* 1377. (c) Coucouvanis, D. *Acc. Chem. Res.* **1991,** *24,* 1. (d) Holm, R. H. *Adv. Inorg. Chem.* **1992,** *38,* 1.

(4) (a) Tan, G. O.; Ensign, S. A.; Cuirli, S.; Scott, M. J.; Hedman, B.; Holm, R. H.; Ludden, P. W.; Korszun, Z. R.; Stephens, P. J.; Hodgson, K. O. *Proc. Natl. Acad. Sci. U.S.A.* **1992,** *89,* 4427. (b) Bridya, N.; Olmstead, M. M.; Whitehead, J. P.; Bagyinka, C.; Maroney, M. J.; Mascharak, P. K. *Inorg. Chem.* **1992,** *31,* 3612. (c) Zhou, J.; Scott, M. J.; Hu, Z.; Peng, G.; Munck, E.; Holm, R. H. *J. Am. Chem. Soc.* **1992,** *114,* 10843. (d) Cuirli, S.; Ross, P. K.; Scott, M. J.; Yu, S.-B.; Holm, R. H. *J. Am. Chem. Soc.* **1992,** *114,* 5415.

(5) Curtis, M. D. *Appl. Organomet. Chem.* **1992,** *6,* 429.

(6) Riaz, U.; Curnow, O. J.; Curtis, M. D. *J. Am. Chem. Soc.* **1994,** *116,* 4357.

(7) Druker, S. H.; Curtis, M. D. *J. Am. Chem. Soc.* **1995,** *117,* 6366–6367.

(8) Druker, S. H.; Mansour, M. A.; Sielemann, D.; Curtis, M. D. To be published.

(9) This compound was prepared as described in: Brunner, H.; Wachter, J. *J. Organomet. Chem.* **1982,** *240,* C41.

(10) A solution of cluster **1** (0.059 g, 0.0744 mmol) and PhSSPh (0.018 g, 0.0824 mmol) in toluene (30 mL) was refluxed for 1 h and then filtered hot through Celite. Recrystallization from toluene/hexane at −18 °C gave 0.041 g (58%) of dark, needlelike crystals. No NMR was possible due to paramagnetism. Anal. Calcd for $C_{34}H_{44}Co_2Mo_2S_6$: C, 42.77; H, 4.64. Found: C, 42.49; H, 4.55. Mass spectral analysis was not possible due to loss of integrity of the cluster upon ionization.

(11) Bianchini et al. have recently observed the first homogeneously catalyzed HDS reaction with a (triphos)iridium complex: (a) Bianchini, C.; Meli, A.; Peruzzini, M.; Vizza, F.; Frediani, P.; Herrera, V.; Sanchez-Delgado, R. A. *J. Am. Chem. Soc.* **1993,** *115,* 2731. (b) Bianchini, C.; Jimenez, M. V.; Meli, A.; Moneti, S.; Vizza, F.; Herrera, V.; Sanchez-Delgado, R. A. *Organometallics* **1995,** *14,* 2342.

(12) A solution of **1** (0.095 g, 0.120 mmol) and PhSH (2.0 mL, 19.5 mmol) in toluene (50 mL) was prepared in a 300 mL Parr pressure reactor, which was subsequently charged with CO (1000 psi) and heated at 150 °C for 46 h. The vessel was depressurized, and the contents were transferred to a 100 mL Schlenk flask. The solvent and volatiles were distilled off, and a GC/MS analysis showed only excess PhSH present. PhSSPH and PhS(CO)Ph were sublimed from the reaction mixture after removal of solvent and volatiles and analyzed by GC/MS and NMR spectroscopy. Recrystallization of the reaction mixture from toluene/hexane gave **2**.

0276-7333/95/2314-5460$09.00/0

Scheme 1

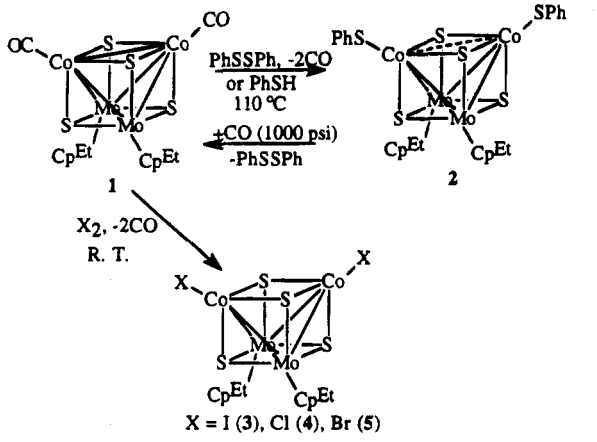

Scheme 2

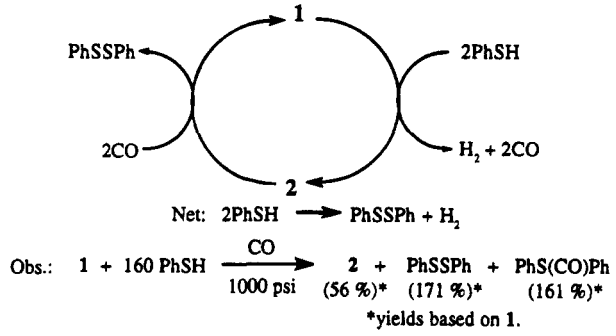

in $[Co(CO)_3Bu_3P]_2$.[17] The Co–Co bond distance increases to 2.934(3) Å in **3** and 2.953(3) Å in **4**. Harris has published a qualitative molecular orbital study of heterometallic cubane-type clusters with an $Mo_2M_2S_4$ core (M = Fe, Co, Ni), describing the HOMO as a tetrahedral, metal–metal bonding orbital and the LUMO as a metal–metal antibonding orbital.[18] The lengthening of the Co–Co distance observed upon oxidation of the $Mo_2Co_2S_4$ cubane is consistent with the removal of a pair of electrons from the HOMO of **1**, thus reducing the Co–Co bond order to zero. This behavior is quite different from that observed in the homometallic cluster $Cp_4Mo_4S_4$, which undergoes two, successive one-electron

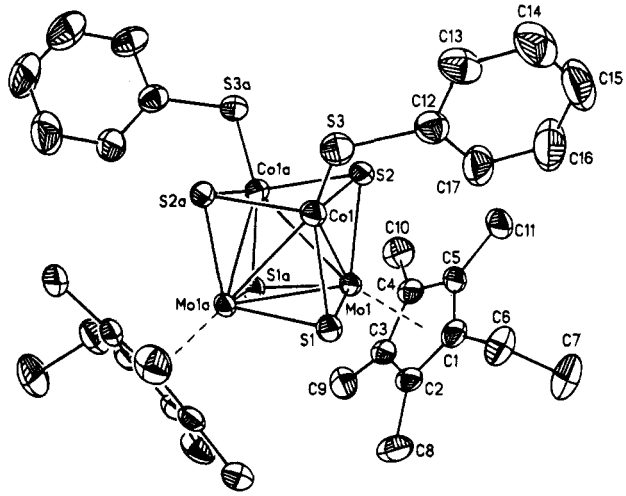

Figure 1. ORTEP plot of $C_{22}H_{34}Co_2Mo_2S_4(SPh)_2$ (**2**), showing 50% probability thermal ellipsoids.

oxidations with essentially no structural changes.[19] Similarly, $Cp_3Mo_3Fe(SH)S_4$, a 58 VSE cluster, has essentially the same bond lengths as found in the 60 VSE, all metal–metal-bonded cluster $Cp_3Mo_3Co(CO)S_4$.[20] Thus, it appears that in the Mo_2Co_2 clusters, the HOMO is more localized in the Co–Co bond, whereas, in the Mo_4 and Mo_3Fe clusters, the HOMO is at most weakly metal–metal bonding and more delocalized over the cluster.[19,21]

In contrast to the Co–Co distances in the two halide cluster, **3** and **4**, the Co–Co distance in the thiolato cluster **2** is 2.741(1) Å, a value nearly identical to that in the radical anion of **1** in which a Co–Co bond order of $^1/_2$ has been assigned.[22] The variation in the length of the Co–Co distance is also related to the magnetic behavior of these complexes (see below). The Mo–Mo and Mo–Co distances in the oxidized clusters change very little from the value in the electron-precise cluster, **1**. Thus, the Mo–Mo bond length is 2.831(1) Å in **1** and 2.8156(3), 2.803(1), and 2.804(1) Å in **2**–**4**, respectively. The Co–Mo distance varies from 2.712(1) Å in **1** to 2.733(3), 2.738(5), and 2.756(6) Å in **2**–**4**, respectively.

The solution ^{1}H-NMR behavior of these oxidized clusters is puzzling. At room temperature, the iodo cluster **3** showed a clean NMR pattern, corresponding to that expected for the Cp^{Et} ligand on a *diamagnetic* cluster. At lower temperatures (to −40 °C), there was no shift in the resonances, only slight broadening. Analogous behavior was seen for **4** and **5**, but the thiolato cluster **2** behaved as a paramagnetic system and no ^{1}H-NMR spectrum was observed.

The magnetic susceptibility of the clusters was measured on a SQUID magnetometer. As expected, cluster **2** exhibited paramagnetic behavior. A plot of $1/\chi$ *vs* T is a straight line, the slope of which gives an effective magnetic moment of 3.49 μ_B. This value is in the range

(13) $Cp^{Et}{}_2Mo_2Co_2S_4(I)_2$: Rectangular black crystals in 83% yield from dichloromethane–isobutanol. ^{1}H-NMR ($CDCl_3$): δ 3.07 (br s, 6H), 2.88 (br s, 6H), 2.01 (br t, 3H), 1.88 (br q, 2H), 5.30 (s, CH_2Cl_2). Anal. Calcd for $C_{22}H_{34}Co_2Mo_2S_4I_2 \cdot {}^1/_2CH_2Cl_2$: C, 26.17; H, 3.42. Found: C, 26.19; H, 3.21. HRMS (*m/z*): predicted, 981.6433; obsd, 981.6432.

(14) $C_{22}H_{34}Co_2Mo_2S_4I_2$: monoclinic, $C2/c$; $Z = 8$; $a = 39.540(7)$, $b = 10.737(2)$, $c = 16.485(2)$ Å; $\beta = 106.95(1)°$; $V = 6694(2)$ Å^3; $T = 295$ K; $R = 0.0329$; $R_w = 0.0388$ based on 3489 reflections for $(F_o) \geq n\sigma(F_o)$ ($n = 3$).

(15) Cluster **1** (0.146 g, 0.184 mmol) was dissolved in 100 mL of CH_2Cl_2, and Cl_2 (5 mL, 0.223 mmol) was added using a gastight syringe. The reaction mixture was stirred for 2 h at room temperature and then filtered through Celite. Recrystallization from CH_2Cl_2/hexane gave 0.071 g (48%) of black, rectangular crystals. ^{1}H-NMR ($CDCl_3$): δ 2.77 (br s, 6H), 2.56 (br s, 6H), 1.95 (mult, 5H), 5.30 (s, CH_2Cl_2). MS (EI) (*m/z*): 808 (P^+), 771 (P^+ − Cl), 734 (P^+ − 2Cl). Anal. Calcd for $C_{22}H_{34}Co_2Mo_2S_4Cl_2 \cdot {}^1/_2CH_2Cl_2$: C, 31.80; H, 4.15. Found: C, 31.80; H, 4.12.

(16) To a solution of cluster **1** (0.132 g, 0.167 mmol) in CH_2Cl_2 was added Br_2 (0.6 mL of a 0.291 M solution in CH_2Cl_2, 0.174 mmol) *via* syringe. The reaction mixture was stirred for 15 min at room temperature and then filtered through Celite. Recrystallization from CH_2Cl_2/hexane gave 0.101 g (68%) of black rectangular crystals. ^{1}H-NMR ($CDCl_3$): δ 2.90 (br s, 6H), 2.69 (br s, 6H), 1.98 (mult, 5H), 5.30 (s, CH_2Cl_2). MS (EI) (*m/z*): 896 (P^+), 815 (P^+ − Br), 735 (P^+ − 2Br). Anal. Calcd for $C_{22}H_{34}Co_2Mo_2S_4Br_2$: C, 29.48; H, 3.82. Found: C, 29.13; H, 3.70.

(17) Ibers, J. A. *J. Organomet. Chem.* **1968**, *14*, 423.

(18) Harris, S. *Polyhedron* **1989**, *8* (24), 2843.

(19) (a) Davies, C. E.; Green, J. C.; Kaltsoyannis, N.; MacDonald, M. A.; Qin, J.; Rauchfuss, T. B.; Redfern, C. M.; Stringer, G. H.; Woolhouse, M. G. *Inorg. Chem.* **1992**, *31*, 3779. (b) Bandy, J. A.; Davies, C. E.; Green, J. C.; Green, M. L. H.; Prout, K.; Rodgers, D. P. S. *J. Chem. Soc., Chem. Commun.* **1983**, 1395.

(20) Curtis, M. D.; Riaz, U.; Curnow, O. J.; Kampf, J. W.; Rheingold, A. L.; Haggerty, B. S. *Organometallics*, in press.

(21) Williams, P. D.; Curtis, M. D. *Inorg. Chem.* **1986**, *25*, 4562–4570.

(22) Druker, S. H. Ph.D. Thesis, The University of Michigan, 1995. The Co–Co distance in $Na[Cp^{Et}{}_2Mo_2Co_2S_4(CO)_2]$ is 2.735(1) Å.

observed for $S = 1$ spin systems.[23] The EPR silence of **2** is also consistent with an integer spin state. Contrary to the expectation based on the NMR spectrum, however, **3** also exhibited paramagnetic behavior. A plot of $1/\chi$ *vs* T (Figure 2) is not linear. At higher temperatures (125−300 K), the plot appears linear with $\mu_{eff} = 4.79\ \mu_B$, consistent with an $S = 2$ spin system. In the low-temperature regime (5−100 K), $\mu_{eff} = 3.07\ \mu_B$, a value consistent with an $S = 1$ spin system. These results suggested that the cluster behaves as a spin ladder, with increasing number of unpaired electrons with increasing temperature. Accordingly, the data were fit with the Van Vleck equation shown as follows:

$$\frac{1}{\chi_m(T)} = \frac{\sum_i (2S_i + 1) \exp\left(-\frac{\Delta E_i}{kT}\right)}{\sum_i (2S_i + 1)\chi_i \exp\left(-\frac{\Delta E_i}{kT}\right)} + C$$

$$\chi_i = \frac{N\mu_i^2\beta^2}{3kT}$$

This fit showed the population of S = 1, 2, and 3 levels near room temperature. The final best fit for $1/\chi_{corr}$ *vs* T was given by

$$\frac{1}{\chi_m(T)} = 6.61 + T\frac{3 + 5\exp\left(-\frac{a}{T}\right) + 7\exp\left(-\frac{b}{T}\right)}{3.34 + 14.34\exp\left(-\frac{a}{T}\right) + 42\left(-\frac{b}{T}\right)}$$

where $a = \Delta E_1/k = 292.3$ K and $b = \Delta E_2/k = 985.6$ K. Hence, $\Delta E_1 = 2.43$ kJ/mol or 203 cm^{-1} and $\Delta E_2 = 8.20$ kJ/mol or 686 cm^{-1}. Corresponding to these values, the ground state is a triplet, and the occupations of the excited $S = 2$ and $S = 3$ levels are 37.5% and 3.7% at room temperature. The corresponding values for **4** and **5** are $\Delta E_1 = 318$ cm^{-1} and 282 cm^{-1}, and $\Delta E_2 = 1655$ cm^{-1} and 1140 cm^{-1}, respectively. As the π-donor ability of X (Cl, Br, or I) increases, the energies of the higher spin states increase. Thus, the simple paramagnetism observed for **2** (X = SPh) may mean simply that the $S = 2$ state is not thermally populated at the temperatures studied.

The observation of paramagnetism for **3**−**5** seemed to be inconsistent with their diamagnetic-appearing NMR spectra and suggested different magnetic behavior in solution than in the solid state. The Evan's method for magnetic susceptibility[24] was used to extract solution magnetic data. The effective moments obtained for **2**−**5** at room temperature were $\mu_{eff} = 2.36$, 3.24, 1.84, and 2.52 μ_B, respectively. These values are all lower than their corresponding solid-state values. At this time, we have no good explanation for the anomalous NMR behavior of the halide clusters nor for the differences in the solid and solution states.

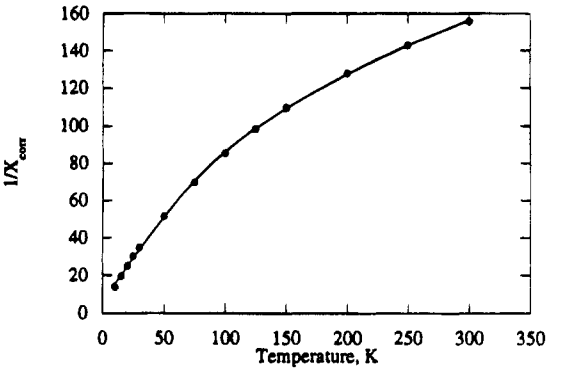

Figure 2. Plot of $1/\chi_{corr}$ *vs* temperature for $Cp^{Et}{}_2Co_2Mo_2S_4(I)_2$ (**3**). The points are experimental values; the solid line is calculated as described in the text.

The electron-deficient, oxidized cubane clusters described here appear to be good models for products formed during the desulfurization of thiiranes and thietanes by **1**. These results also suggest that oxidized cubanes may be desulfurization catalysts in their own right, and work is in progress to determine the structure and catalytic behavior of the sulfided cubane clusters.

Acknowledgment. The authors thank the National Science Foundation for support of this research (Grant CHE-9205018).

Supporting Information Available: Tables of X-ray structural data, atomic positional parameters, thermal parameters, bond distances, and bond angles and ORTEP diagrams for **2**, **3**, and **5**, $1/\chi$ *vs* T plots for **2**−**4**, and a ^{1}H-NMR spectrum of **3** (27 pages). This material is contained in many libraries on microfiche, immediately follows this article in the microfilm version of the journal, and can be ordered from the ACS; see any current masthead page for ordering information.

OM950759X

(23) Drago, R. S. *Physical Methods in Chemistry*; Saunders College Publishing: Chicago, 1977.

(24) (a) Evans, D. F. *J. Chem. Soc.* **1959**, 2005. (b) Loliger, J.; Scheffold, R. *J. Chem. Educ.* **1972**, *49* (9), 646. (c) Ostfeld, D.; Cohen, I. A. *J. Chem. Educ.* **1972**, *49* (12), 829. (d) For the correct Evans formula for superconducting NMR spectrometers, see: Schubert, E. M. *J. Chem. Educ.* **1992**, *69*, 62.

Fragmentation of 2-Pyridyl Esters Gives both η^2(C,O)- and η^2(C,C)-Bound Ketene Ligands on ClIr[P(*i*-Pr)$_3$]$_2$

D. B. Grotjahn* and H. C. Lo

Department of Chemistry and Biochemistry, Arizona State University, Tempe, Arizona 85287-1604

Received October 5, 1995[⊗]

Summary: 2-Pyridyl esters react with a source of ClIr[Pr(i-Pr)$_3$]$_2$ in a net elimination reaction to give η^2(C,O)-bound ketene complexes **4** *in the case of diaryl- or aryl(alkyl)-substituted ketenes and η^2(C,C)-bound isomers* **3** *in the case of monosubstituted ketenes, explainable by invoking an electronic preference for* **3** *which can be sterically overridden (***4***). The mechanism by which* **3** *or* **4** *is formed appears to involve the spectroscopically detectable acyl* **8**, *from oxidative addition of Ir(I) to the ester acyl–oxygen bond, followed by metal-induced β-hydride elimination.*

Metal–ketene complexes[1] have received attention because of their potential as models of reactions of CO and CO_2 activation or reduction (e.g. the Fischer–Tropsch process)[2] and because of the altered reactivity of the ketene ligand in a bound state.[3] Putative mononuclear ketene complexes of group 6 metals generated from carbene complexes by thermal[4] or photochemical[5] means have found increasing utility as intermediates in enantioselective organic synthesis, but their structures and the factors responsible for enantioselectivity are unknown. The factors governing binding to late transition metals are not completely understood.[1b] Isolable ketene complexes, however, are mainly made by direct reaction between a ketene ligand and a metal fragment,[1] a process essentially restricted to diaryl- or aryl(alkyl)ketenes because of slower dimerization or polymerization. Free ketenes have been reported as the organic product in the reaction of Ru(0)[6a] or Pt(0)[6b] complexes with acid chlorides. In contrast, here we report that Ir–ketene *complexes*, the first examples involving a group 9 metal, are formed from interaction of ClIr[P(*i*-Pr)$_3$]$_2$[7] with 2-pyridyl esters.[8] Depending on substitution, either η^2(C,O)- or η^2(C,C)-bound examples are isolated, pointing to the importance of steric factors in ketene binding.

Scheme 1[a]

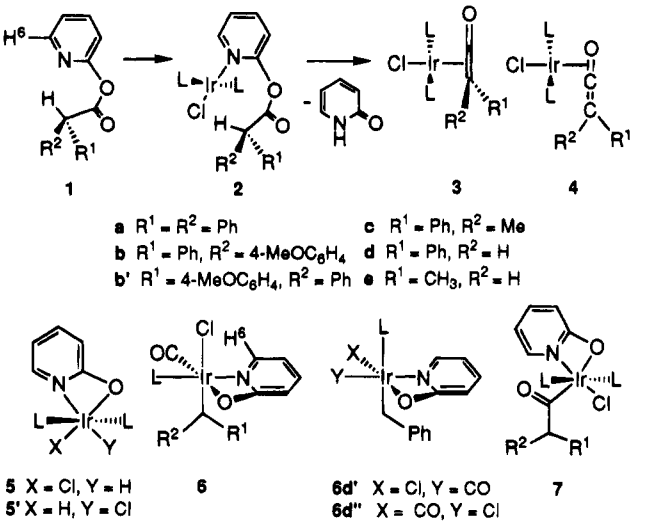

[a] L = P(*i*-Pr)$_3$.

Decarbonylation of 2-pyridyl formate by Rh(I) releases 2-pyridone and forms a CO ligand on Rh.[9] In analogy to this, reaction of 2-pyridyl esters **1** (Scheme 1) with 1 mol of ClIr[P(*i*-Pr)$_3$]$_2$ was anticipated to give 2-pyridone and the ketene ligand in **3** or **4** after N-complexation (**2**). The fragment ClIr[P(*i*-Pr)$_3$]$_2$ and its Rh analog are competent in C–H bond activation,[7d] giving products which predictably have the two bulky P(*i*-Pr)$_3$ ligands trans-disposed. In NMR tube experiments, P(*i*-Pr)$_3$ was added to a mixture of **1** and [Ir(μ-Cl)(cyclooctene)$_2$]$_2$ in C_6D_6 at room temperature.[10] The rapid formation of **2** was suggested by immediate broadening of the resonance for H6.[11] Over a period of time, resonances for the products[12] in Table 1 appeared. However, because of the irreversible formation of **5**[13] (Scheme 1), 2 mol of metal was required to consume **1**.

Ester **1a** afforded ketene complex **4a**, in which C,O binding was assigned on the basis of inequivalence of the two phenyl rings in ^{1}H and ^{13}C NMR spectra[1b,14] and ^{13}C resonances for the CCO unit. A summary of yield, IR, and ^{31}P and ^{13}C NMR data for ketene complexes appears in Table 1.[12] C,O binding is confirmed by the crystal structure of **4a** (Figure 1).[15] Of note is the slightly distorted square-planar geometry (if the η^2(C,O)-coordinated ketene is taken as occupying

[⊗] Abstract published in *Advance ACS Abstracts,* November 1, 1995.

(1) (a) Geoffroy, G. L.; Bassler, S. L. *Adv. Organomet. Chem.* **1988**, *28*, 1. (b) For an especially good leading reference, see: Hofmann, P.; Perez-Moya, L. A.; Steigelmann, O.; Riede, J. *Organometallics* **1992**, *11*, 1167 and references therein.

(2) (a) Keim, W. *Catalysis in C1 Chemistry;* D. Reidel: Dordrecht, The Netherlands, 1983. (b) Rofer-dePoorter, C. K. *Chem. Rev.* **1981**, *81*, 447. (c) Hermann, W. A. *Angew. Chem., Int. Ed. Engl.* **1982**, *21*, 117.

(3) (a) Galante, J. M.; Bruno, J. W.; Hazin, P. N.; Folting, K.; Huffman, J. C. *Organometallics* **1988**, *7*, 1066. (b) Tidwell, T. T. *Acc. Chem. Res.* **1990**, *23*, 273.

(4) (a) Dötz, K.-H. In *Organometallics in Organic Synthesis*; de Meijere, A., tom Dieck, H., Eds.; Springer: Berlin, 1988. (b) Wulff, W. D. In *Comprehensive Organic Synthesis*; Trost, B., Fleming, I., Eds.; Pergamon: Oxford, U.K., 1991; Vol. 5, p 1065. (c) Kim, O. K.; Wulff, W. D.; Jiang, W.; Ball, R. C. *J. Org. Chem.* **1993**, *58*, 5571. (d) Harvey, D. F.; Grenzer, E. M.; Gantzel, P. K. *J. Am. Chem. Soc.* **1994**, *116*, 6719.

(5) (a) Review: Schmalz, H.-G. *Nachr. Chem., Tech. Lab.* **1994**, *42*, 608. (b) Hegedus, L. S.; deWeck, G.; D'Andrea, S. *J. Am. Chem. Soc.* **1988**, *110*, 2122. (c) Merlic, C. A.; Xu, D.; Gladstone, B. G. *J. Org. Chem.* **1993**, *58*, 538.

(6) (a) Hommeltoft, S. I.; Baird, M. C. *J. Am. Chem. Soc.* **1985**, *107*, 2548. (b) Ishii, Y.; Kobayashi, Y.; Iwasaki, M.; Hidai, M. *J. Organomet. Chem.* **1991**, *405*, 133.

(7) (a) In our hands, NMR spectra of solutions of [Ir(μ-Cl)(cyclooctene)$_2$]$_2$ (0.5 mol) and P(*i*-Pr)$_3$ (2 mol) in C_6D_6 show several hydride resonances upfield of δ 0 ppm. In a footnote,[7b] evidence in a thesis is cited for formation of ClIr[P(*i*-Pr)$_3$]$_2$(cyclooctene) from these reagents, but for simplicity we use ClIr[P(*i*-Pr)$_3$]$_2$ to refer to the species derived from the above reagents. (b) Reference 12 in: Werner, H.; Höhn, A.; Schulz, M. *J. Chem. Soc., Dalton Trans.* **1991**, 777. (c) Binger, P.; Haas, J.; Glaser, G.; Goddard, R.; Krüger, C. *Chem. Ber.* **1994**, *127*, 1927. (d) Werner, H.; Höhn, A.; Dziallas, M. *Angew. Chem., Int. Ed. Engl.* **1986**, *25*, 1090.

(8) Dutta, A. S.; Morley, J. S. *J. Chem. Soc. C* **1971**, 2896.

(9) Suggs, J. W.; Pearson, G. D. N. *Tetrahedron Lett.* **1980**, *21*, 3853.

0276-7333/95/2314-5463$09.00/0

Table 1. Isolated Yields of Products from 1 and ClIr[P(*i*-Pr)$_3$]$_2$

			yields based on Ir[a] (%)		key spectral data for **3/4**		
entry no.	ester	time[b] (h)	**3/4**	**5**[c]	$^{31}P\{^1H\}$ (C_6D_6)[d]	IR (KBr; cm^{-1})	^{13}C (C_6D_6; *C*=C=O, C=*C*=O)[d]
1	**1a**	55	**4a**, 45 (46)	48 (48)	20.90 (s)	1636, 1589	74.26 (s), 143.39 (t, 3.2)
2	**1b**	55	**4b**	47 (47)	20.76 (s)	1632, 1589	73.38 (s), 143.19 (t, 4.0)
			4b′, 47 (47)[e]		20.03 (s)	1632, 1588	73.03 (s), 143.29 (t, 4.2)
3	**1c**	156[f]	**4c**, 30 (32)	34 (34)	22.31 (s)	1661, 1589	72.82 (s),[g] 157.42 (t, 3.6)
4	**1d**[h]	110	**3d**, 20 (20)	25 (25)	25.43 (d, 323.5) 23.30 (d, 323.5)	1763, 1460	−33.03 (dd),[g] 198.18 (t, 2.9)

[a] NMR yields, in parentheses, for those compounds whose signal(s) could be integrated reliably. Separation was performed with a Chromatotron over SiO_2 under N_2 or Ar. [b] Time required for disappearance of **1**/**2**[11] at 25 °C. [c] Combined yield for **5** and **5′**.[13] [d] In ppm (multiplicity, *J* in Hz). [e] Combined yield for **4b** and **4b′** (**4b**:**4b′** = 1:1). [f] Reaction was only ~80% complete at the time indicated. [g] In $CDCl_3$. For **3d**, the signal at −33.03 is not well-resolved, consisting of two slightly broad lines with equal intensities ca. 1.3 Hz apart. [h] Combined yield for **6d**, **6d′**, and **6d″** is 42% (**6d**:**6d′**:**6d″** ≈ 3:2:1) and for **7d** is 2%.[20]

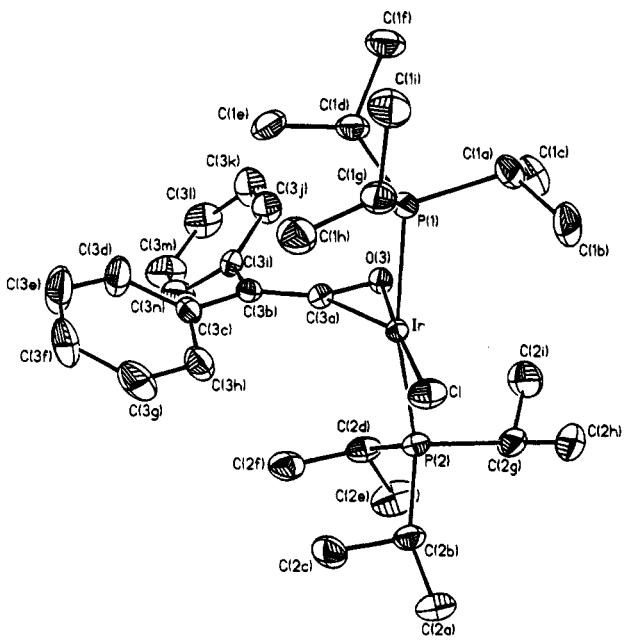

Figure 1. Molecular structure of **4a**, shown with 30% thermal ellipsoids. Key bond lengths (Å) and angles (deg): Ir−Cl, 2.285(2); Ir−O3, 2.092(4); Ir−C3a, 1.972(5); C3a−O3, 1.286(6); C3a−C3b, 1.348(6); C3b−C3a−O3, 136.6(6); P1−Ir−P2, 168.0(1).

one coordination site): the mutually trans phosphines are tilted away from the Ph ring nearer the ClIr[P(*i*-Pr)$_3$]$_2$ unit (P−Ir−P angle 168.0(1)°). The C−C−O angle of 136.6(6)° is consistent with a significant degree of back-bonding to the C=O bond.

From **1b**, equimolar amounts of separable diastereomers **4b** and **4b′** were formed, whereas from **1c**, only **4c** was isolated.[16] Consistent with C,O binding in these disubstituted examples for which $R^1 \neq R^2$, a singlet is seen in $^{31}P\{^1H\}$ NMR spectra.[17] Significantly, from monosubstituted ester **1d**, the ketene complex **3d**, bearing two inequivalent ^{13}P nuclei[17] with a large mutual coupling indicative of trans orientation, was obtained. These data and resonances for the −CH=C=O unit[18] are consistent with C,C binding in **3d**. The η^2-(C,C)-bound complex **3e**,[19] with key spectroscopic data similar to those of **3d**, was obtained from **1e** as well.

Some insight into the formation of **3/4** and **5** may be gleaned from other products and their behavior. Ester **1d** (entry 4, Table 1) not only gives **3d** but also is diverted to a mixture of four complexes (Scheme 1; **6**, **7**),[19] each bearing all of the atoms of the 2-pyridyl ester. The major components are the three isomeric monophosphine alkyl complexes **6d**, **6d′**, and **6d″**,[20] and the minor component is the bis(phosphine) acyl complex **7d**.[21] Particularly striking in the NMR spectra of **6d**, whose structure has been confirmed by X-ray diffraction,[12] is the coupling from P to H6 (indicative of a P(*i*-Pr)$_3$ ligand trans to N) and the coupling of P to only one of the methylene protons.[22] In the ^{13}C NMR spectra of **6d′** and **6d″**, large couplings between P and the

(10) In a typical reaction, a J. Young NMR tube was charged with [ClIr(cyclooctene)$_2$]$_2$ (50.1 mg, 55.9 × 10^{-3} mmol) and [(CH$_3$)$_3$Si]$_4$C (2.3 mg, 7.5 × 10^{-3} mmol, as internal standard) in a glovebox, and C_6D_6 (~0.6 mL) was added to give a suspension. To this was added **1a** (16.1 mg, 55.6 × 10^{-3} mmol), and additional C_6D_6 (~0.1 mL) was used to wash down any residue left on the top of the NMR tube. P(*i*-Pr)$_3$ (44 μL, 226 × 10^{-3} mmol) was then added into the mixture via syringe. Upon the addition of P(*i*-Pr)$_3$, a clear brownish yellow solution was formed. Additional C_6D_6 (~0.1 mL) was used to rinse the walls of the NMR tube. The tube was sealed and shaken to mix the contents well before removal from the glovebox. The tube contents were further degassed by two successive freeze−pump−thaw cycles, and the tube was kept at room temperature, protected from light with Al foil. The reaction was followed by ^1H or $^{31}P\{^1H\}$ NMR spectra and was considered to be complete when there was no detectable 2-pyridyl ester. TLC analysis of the final reaction mixture was conducted in a glovebox, and the reaction mixture was then subjected directly to radial chromatography (Chromatotron, 1 mm SiO_2 plate, gradient elution starting with 1:50 EtOAc−hexanes) to yield (in order of elution) complex **4a** as a red solid, complex **5** as a pale yellow solid, and **5′** as a pale yellow solid. If a residue was obtained after the removal of solvent on a high-vacuum line, it was recrystallized at −25 °C in a glovebox.

(11) The altered resonance for H6 in **2** was broad ($w_{1/2}$ = ca. 45 Hz) and shifted at least 1 ppm downfield from that of **1**; other resonances, all sharp, were shifted from those of **1** to a lesser extent.

(12) All new compounds were characterized by NMR, IR, and elemental analysis. See the Supporting Information for experimental procedures and data not provided in the footnotes, including the crystal structure of **6d**.

(13) (a) Only **5**[13b] is isolated from rapid reactions of **1**, but **5** isomerizes to **5′** at the rate of ca. 1% per day. (b) Grotjahn, D. B.; Lo, H.; Groy, T. L. *Acta Crystallogr., Sect. C*, in press.

(14) **4a**: ^1H NMR (C_6D_6) δ 8.63 (d, *J* = 7.2 Hz, 2H), 7.63 (d, *J* = 7.2, 2H), 7.33 (t, *J* = 7.6, 2H), 7.29 (t, *J* = 8.0, 2H), 7.09 (t, *J* = 7.2, 1H), 7.03 (t, *J* = 7.1, 1H), 2.45 (m, 6H), 1.19 (q, *J* = 7.1, 18H), 1.16 (q, *J* = 7.2, 18H).

(15) At 20 °C: triclinic, space group $P\bar{1}$ with *a* = 8.647(2) Å, *b* = 11.140(2) Å, *c* = 18.735 Å, α = 93.32(3)°, β = 102.96(3)°, γ = 107.82(3)°, V = 1658.7(6) Å^3, *Z* = 2, d_{calcd} = 1.486 g cm^{-3}, μ(Mo Kα) = 4.224 mm^{-1}, *R* = 2.96, and R_w = 3.95 for 3909 reflections with F > 4σ(*F*).

(16) Irradiation of the ketene methyl of **4c** (δ 2.62, s) led to 11.3% enhancement of the signals for *i*-Pr methyl.[12] The proximity of an aryl substituent to the metal appears to cause strong deshielding of the ortho protons: δ 8.63 (**4a**), 8.56 (**4b**), 8.65 (**4b′**). In contrast, the chemical shifts of the Ph protons of **4c** are unexceptional: δ 7.69 (d, 2H), 7.33 (t, 2H), 6.99 (t, 1H).

(17) For a ketene with $R^1 \neq R^2$, η^2(C,C) binding will lead to inequivalence of the two trans ^{31}P nuclei; see **3d** in Table 1.

(18) **3d**: ^1H NMR (C_6D_6) δ 7.76 (d, *J* = 6.5 Hz, 2H), 6.90−7.07 (m, 3H), 3.51 (dd, *J* = 6.5, 11.1, 1H, O=C$_1$=C$_2$(*H*)Ph), 2.54 and 2.26 (two octet of d, *J* = 7.2 ($^3J_{HH}$ = $^4J_{HP}$), 14.4 ($^2J_{HP}$), each 3H), 1.27−1.33 (m, 36H).

(19) (a) **3e**: ^1H NMR (C_6D_6) δ 2.19 (m, 1H), 1.05 (d, *J* = 7.8 Hz, 3H); $^{31}P\{^1H\}$ NMR δ 20.93, 20.50 (two d, *J* = 285.3). (b) Reaction of **1e** with ClIr[P(*i*-Pr)$_3$]$_2$ gave **3e**, **5**, **6e**, and **7e**, where **3e** and **6e** have not yet been isolated in a pure state. The slow conversion of **3e** (and **3d**) to phosphine cyclometalation products is under investigation.

(20) **6d′** isomerizes to **6d** over days at 25 °C in C_6D_6.

(21) The orientation of the four non-phosphine ligands in **7d** is assumed to be the same as that in crystallographically characterized **7e**: Grotjahn, D. B.; Lo, H. C.; Groy, T. L. *Acta Crystallogr., Sect. C*, in press.

Scheme 2[a]

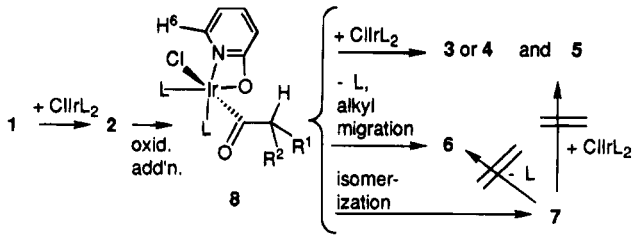

[a] L = P(*i*-Pr)$_3$.

benzylic CH_2 (and, remarkably, coupling to all carbons of the benzyl ligand) indicate the benzyl and P(*i*-Pr)$_3$ ligands are trans-disposed.[23]

In the reactions of **1** with less hindered R^1 and R^2 groups (e.g. **1d,e**), we see the buildup and decay of a chromatographically unstable intermediate, tentatively identified as **8** (Scheme 2). Spectral data for the intermediate from **1d**[24] include a ^{13}C resonance at δ 197.60 (t) with small splitting (6.2 Hz), consistent with an acyl cis to two phosphines, as in **7d** (acyl carbon δ 196.10 (t, J = 5.6)). However, two inequivalent ^{31}P nuclei with a small mutual coupling (10.7 Hz) are inconsistent with trans disposition, and coupling of one ^{31}P nucleus to H6[24] suggests that one P and N are trans as in **6d**. The disposition of N, acyl C, and both P atoms in **8** follows from these data, although the O and Cl atoms might be interchanged. Acyl **8** would be the product of oxidative addition of Ir(I) to the C–O bond of **1**, usually a difficult reaction for esters.[25]

The strain implied in structure **8** (cis-oriented phosphines) could be released by isomerization to **7**, or by phosphine loss, allowing alkyl migration to give **6**. In confirmation, the appearance of **6d,d′,d″** was suppressed by addition of excess P(*i*-Pr)$_3$ to a mixture of **1d** and ClIr[P(*i*-Pr)$_3$]$_2$, and **7d,e** showed no sign of forming **6** in pure C_6D_6 (25 °C, 2–3 days). Further observations clarify the relationship of isomeric acyls **7** and **8** to products **3–5**. Acyls **7d,e** are stable in the presence of ClIr[P(*i*-Pr)$_3$]$_2$ (25 °C, 3 days), showing that **7** is not a precursor to **3–5**. In contrast, in reactions of **1d,e** with ClIr[P(*i*-Pr)$_3$]$_2$, if less than 2 mol of Ir/mol of **1** is used, a significant amount of **8d** or **8e** persists until the proper amount of metal is added. Thus, **8** could bind to a second mole of ClIr[P(*i*-Pr)$_3$]$_2$, perhaps on the acyl oxygen, triggering formation of **3** or **4** and **5** by β-hydride elimination, a rare process for acyls.[26] That this β-hydride elimination does not depend strongly on phosphine loss from **8** is suggested by qualitative observation that, in the presence of added phosphine, the rate at which **3d** is formed from **1d** does not change, yet the formation of **6d,d′,d″** is suppressed. The relative rates of formation and fragmentation of **8** could be determined by the steric and electronic nature of R^1 and R^2, with fragmentation being faster in the case of at least one aryl group[27a] (**8a–c** were not detected). Evidence against formation of **3/4** by expulsion of free ketene[6a,28a] from **8** and subsequent trapping by ClIr[P(*i*-Pr)$_3$]$_2$[28b] comes from the unaltered ratio of **4a** to **5** in the reaction of **1a** with ClIr[P(*i*-Pr)$_3$]$_2$ in C_6D_6 saturated with H_2O (calculated to be 1 equiv). Considering the high reactivity of diphenylketene toward water,[3b] either free ketene is not formed to a significant extent or, if it is, ClIr[P(*i*-Pr)$_3$]$_2$ traps it faster than water.

The method described here affords the first isolable complexes of monosubstituted C,C-bound ketenes (**3d,e**), which are chiral species. Contradictory theoretical and experimental work summarized by Hofmann[1b] focused on electronic factors in determining ketene binding. From the examples of **3/4** isolated so far, disubstituted and monosubstituted ketenes give C,O- and C,C-complexes respectively, suggesting that steric factors are also important.[29] At present, we do not know which isomer is the kinetic product from reactions of **1** and ClIr[P(*i*-Pr)$_3$]$_2$.[30] Future topics under investigation in our laboratories will include the interconversion of **3** and **4**, the stereospecificity of transformation of **1** to **3**,[27] and the ability of the 16-electron complexes **3/4** to bind unsaturated molecules and facilitate bond-forming reactions. As it stands, the fragmentation reported here is the first method for generating ketene complexes under essentially neutral conditions from carboxylic acid esters.

Acknowledgment. We thank the donors of the Petroleum Research Fund, administered by the American Chemical Society, for partial support of this work and Johnson Matthey Aesar Alfa for a loan of iridium salts. Dr. Ron Nieman and Camil Joubran assisted with vital 2D NMR experiments. We warmly thank Prof. John Hubbard and Dr. Thomas Groy for acquisition and refinement of the crystal structures of **6d** and **4a**, respectively.

Supporting Information Available: Text giving spectral data and preparations of 15 compounds and tables and figures giving crystallographic data and refinement information for **4a** and **6d** (36 pages). This material is contained in many libraries on microfiche, immediately follows this article in the microfilm edition of this journal, can be ordered from the ACS, and can be downloaded from the Internet; see any current masthead page for ordering formation and Internet access instructions.

OM9507888

(22) (a) A version of the Karplus relationship may apply; see footnote 9 of: Nguyen, S. T.; Grubbs, R. H.; Ziller, J. W. *J. Am. Chem. Soc.* **1993**, *115*, 9858. (b) Methylene protons on **6d** (C_6D_6): δ 3.69 (dd, J = 4.6 ($^3J_{HP}$), 9.5 Hz ($^2J_{HH}$), 1H, C*H*HPh), 3.35 (d, J = 9.5 ($^2J_{HH}$), $^3J_{HP}$ = 0, 1H, CH*H*Ph).

(23) (a) ^{13}C NMR ($CDCl_3$) for CH_2Ph of **6d**, **6d′**, and **6d″**: δ 11.18 (d, J = 2.9 Hz), 25.26 (d, J = 75.7), 31.06 (d, J = 52.7). (b) $^{3-6}J_{PC}$ for C_6H_5 carbons of **6d′/6d″** (in Hz): ipso (5.2/5.6), ortho (2.0/3.4), meta (3.3/2.2), para (2.5/3.4). (c) $^nJ_{PC}$ has been reported in organic systems: Kalinowski, H.-O.; Berger, S.; Braun, S. *^{13}C-NMR-Spektroskopie*; Georg Thieme Verlag: Stuttgart, Germany, 1984; p 537.

(24) Other data for **8d**: $^{31}P\{^1H\}$ NMR δ −13.36, −18.53 (two d, J = 10.7 Hz); ^1H δ 7.98 (m, 1H, *H6*), 5.38 and 4.53 (two d, J = 17.1, each 1H, CH_2Ph). Irradiation of the ^{31}P resonance at δ −18.53 led to simplification of the ^1H signal for H6 to dd, J = 1.2, 5.2 Hz, confirming H6–P coupling as seen in spectra of **6d**. IR spectroscopy on the mixture was not informative.

(25) (a) Grotjahn, D. B.; Joubran, C. *Organometallics*, in press. (b) Review: Yamamoto, A. *Adv. Organomet. Chem.* **1992**, *34*, 111. (c) For the influence of steric effects, see: Ittel, S. D.; Tolman, C. A.; English, A. D.; Jesson, J. P. *J. Am. Chem. Soc.* **1978**, *100*, 7577.

(26) Only one acyl complex has been reported to undergo β-H transfer, giving a free ketene.[6a]

(27) (a) Reaction of the ester **1** derived from (*S*)-2-methylbutanoic acid seemed to stop at the stage of **2**. (b) The ester from (*S*)-2-methoxypropionic acid gave products other than **3** or **4**, whose structures are still under investigation.

(28) Khimtaveeporn, K.; Alper, H. *J. Am. Chem. Soc.* **1994**, *116*, 5662.

(29) It appears that $Ni(PPh_3)_2$ gives C,O- and C,C-bound ketene complexes with Ph(R)C=C=O and H_2C=C=O, respectively: Miyashita, A.; Sugai, R.; Yamamoto, J. *J. Organomet. Chem.* **1992**, *428*, 239 and references to earlier work.

(30) The fluxional behavior of ketenes on a single metal center has not been reported; for η^2(C,O)–Ni(0) complexes, a binuclear ketene exchange reaction with coordination mode switching has been proposed.[29] For allenes, see: Foxman, B.; Marten, D.; Rosan, A.; Raghu, S.; Rosenblum, M. *J. Am. Chem. Soc.* **1977**, *99*, 2160.

Synthesis and Structure of Bis(phenyltetramethylcyclopentadienyl)titanium(III) Hydride: First Monomeric Bis(cyclopentadienyl)titanium(III) Hydride

Jeannette M. de Wolf, Auke Meetsma, and Jan H. Teuben

Organometallics, **1995**, 14 (12), 5466-5468• DOI: 10.1021/om00012a005 • Publication Date (Web): 01 May 2002

Synthesis and Structure of Bis(phenyltetramethylcyclopentadienyl)titanium(III) Hydride: The First Monomeric Bis(cyclopentadienyl)titanium(III) Hydride

Jeannette M. de Wolf, Auke Meetsma, and Jan H. Teuben*

Groningen Center for Catalysis and Synthesis, Department of Chemistry, University of Groningen, Nijenborgh 4, 9747 AG Groningen, The Netherlands

Received October 2, 1995[⊗]

*Summary: The first structurally characterized monomeric bis(cyclopentadienyl)titanium(III) hydride, $(C_5PhMe_4)_2TiH$ (**4**), was synthesized by hydrogenolysis of $(C_5PhMe_4)_2TiMe$ (**5**). Hydride **4** was found to be a monomeric bent sandwich by X-ray diffraction methods, and the pentamethylcyclopentadienyl analogue $(C_5Me_5)_2TiH$ (**3**) is concluded to possess a similar molecular structure by comparison between the spectroscopic and reactivity data for **3** and **4**.*

Titanocene hydrides are intriguing compounds, often postulated as intermediates in catalytic reactions.[1,2] They also have relevance in olefin polymerization as the products of chain-terminating β-hydride transfer reactions.[3] Furthermore "titanocene" was proposed to be a dimeric fulvalene-bridged titanium complex with bridging hydrides $[\mu\text{-}\eta^5\text{:}\eta^5\text{-}C_{10}H_8][(\eta^5\text{-}C_5H_5)Ti(\mu\text{-}H)]_2$ (**1**),[4] which was recently confirmed by an X-ray structure determination.[5] Bercaw and Brintzinger were the first to isolate a titanocene(III) hydride, $[(C_5H_5)_2TiH]_2$ (**2**), despite its marginal stability.[6] This structure was, however, never confirmed by X-ray crystallography.

During an investigation of $(C_5Me_5)_2TiR$ (R = alkyl, aryl) compounds at our laboratory,[2,7] $(C_5Me_5)_2TiH$ (**3**) was synthesized by hydrogenolysis of $(C_5Me_5)_2TiR$,[8] extensively characterized, and, in contrast with **2**, formulated as a monomeric titanocene(III) hydride. X-ray crystal structure determinations were hampered by poor crystal quality. An ordinary bent-sandwich geometry, in analogy with $(C_5Me_5)_2TiR$, seems most likely for **3**, but a fulvene–dihydride structure $((C_5Me_5)(\eta^6\text{-}C_5Me_4CH_2)TiH_2)$ cannot be ruled out.[9] To lower the symmetry of the ligand environment, 1-phenyl-2,3,4,5-tetramethylcyclopentadienyl[10] was employed, resulting in the synthesis and X-ray structure determination of bis(1-phenyl-2,3,4,5-tetramethylcyclopentadienyl)titanium(III) hydride. $(C_5PhMe_4)_2TiH$ (**4**) is the first structurally characterized monomeric bis(cyclopentadienyl)titanium(III) hydride.

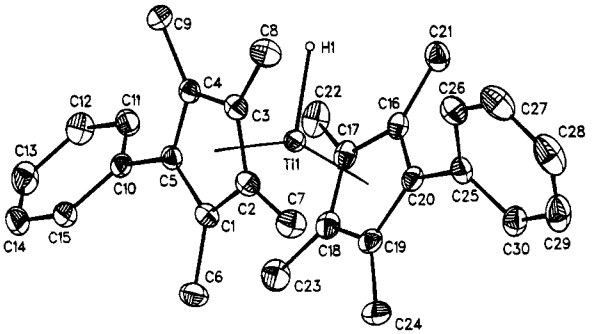

Figure 1. ORTEP drawing of $(C_5PhMe_4)_2TiH$ (**4**) with 50% probability ellipsoids. Hydrogens bonded to carbon are omitted for clarity.

A red-brown solution of **4** is formed quantitatively within minutes after exposing a green pentane solution of $(C_5PhMe_4)_2TiMe$ (**5**) to 1 atm of H_2 at room temperature.[11] Beautiful red-brown crystals of **4** separate after cooling to −20 °C. A single-crystal X-ray diffraction

[⊗] Abstract published in *Advance ACS Abstracts,* November 1, 1995.

(1) Reviews of titanocene chemistry: (a) Bottrill, M.; Gavens, P. D.; McMeeking, J. In *Comprehensive Organometallic Chemistry*; Wilkinson, G., Stone, F., Abel, E. W., Eds.; Pergamon Press: New York, 1982; Chapter 22. (b) Pez, G. P.; Armor, J. N. *Adv. Organomet. Chem.* **1981**, *19*, 1–50.

(2) (a) Akita, M.; Yasuda, H.; Nagasuna, K.; Nakamura, A. *Bull. Chem. Soc. Jpn.* **1983**, *56*, 554–558. (b) Akita, M.; Yasuda, H.; Nakamura, A. *Bull. Chem. Soc. Jpn.* **1984**, *57*, 480–487. (c) Broene, R. D.; Buchwald, S. L. *J. Am. Chem. Soc.* **1993**, *115*, 12569–12570. (d) Lee, N. E.; Buchwald, S. L. *J. Am. Chem. Soc.* **1994**, *116*, 5985–5986. (e) Willoughby, C. A.; Buchwald, S. L. *J. Am. Chem. Soc.* **1992**, *114*, 7562–7564. (f) Willoughby, C. A.; Buchwald, S. L. *J. Org. Chem.* **1993**, *58*, 7627–7629. (g) Willoughby, C. A.; Buchwald, S. L. *J. Am. Chem. Soc.* **1994**, *116*, 11703–17714. (h) Carter, M. B.; Schiøtt, B.; Gutiérrez, A.; Buchwald, S. L. *J. Am. Chem. Soc.* **1994**, *116*, 11667–11670. (i) Cesarotti, E.; Ugo, R.; Kagan, H. B. *Angew. Chem., Int. Ed. Engl.* **1979**, *18*, 779–780. (j) Halterman, R. L.; Vollhardt, K. P. C. *Organometallics* **1988**, *7*, 883–892. (k) Halterman, R. L.; Vollhardt, K. P. C.; Welker, M. E.; Bläser, D.; Boese, R. *J. Am. Chem. Soc.* **1987**, *109*, 8105–8107. (l) Luinstra, G. A.; Teuben, J. H. *J. Am. Chem. Soc.* **1992**, *114*, 3361–3367.

(3) Burger, B. J.; Thompson, M. E.; Cotter, W. D.; Bercaw, J. E. *J. Am. Chem. Soc.* **1990**, *112*, 1566–1577 and references therein.

(4) (a) Brintzinger, H. H.; Bercaw, J. E. *J. Am. Chem. Soc.* **1970**, *92*, 6182–6185. (b) Davison, A.; Wreford, S. S. *J. Am. Chem. Soc.* **1974**, *96*, 3017–3018.

(5) Troyanov, S. I.; Antropiusová, H.; Mach, K. *J. Organomet. Chem.* **1992**, *427*, 49–55.

(6) Bercaw, J. E.; Brintzinger, H. H. *J. Am. Chem. Soc.* **1969**, *91*, 7301–7306.

(7) (a) Pattiasina, J. W.; Heeres, H. J.; Van Bolhuis, F.; Meetsma, A.; Teuben, J. H.; Spek, A. L. *Organometallics* **1987**, *6*, 1004–1010. (b) Luinstra, G. A.; Ten Cate, L. C.; Heeres, H. J.; Pattiasina, J. W.; Meetsma, A.; Teuben, J. H. *Organometallics* **1991**, *10*, 3227–3237 and references therein.

(8) (a) Teuben, J. H. In *Fundamental and Technological Aspects of Organo-f-Element Chemistry*; Marks, T. J., Fragala, I. L., Eds.; Reidel: Dordrecht, The Netherlands, **1985**; pp 195–227. (b) Bercaw, J. E.; Marvich, R. H.; Bell, L. G.; Brintzinger, H. H. *J. Am. Chem. Soc.* **1972**, *94*, 1219–1238. (c) Bercaw, J. E. *J. Am. Chem. Soc.* **1974**, *96*, 5087–5094.

(9) When **3** is reacted with 1 atm of D_2 at room temperature, not only the deuteride $(C_5Me_5)_2TiD$ is formed but H/D scrambling into the methyl groups of the Cp* rings also occurs.[8a] This facile deuteration of the Cp* rings distinguishes **3** from analogous $(C_5Me_5)_2MH$ compounds (M = Sc, Y, Lu), where the metal deuteride can be prepared without simultaneous H/D scrambling of the Cp* protons. (a) Thompson, M. E.; Bercaw, J. E. *Pure Appl. Chem.* **1984**, *56*, 1–11. (b) Den Haan, K. H.; Wielstra, Y.; Teuben, J. H. *Organometallics* **1987**, *6*, 2053–2060. (c) Booy, M.; Deelman, B.-J.; Duchateau, R.; Postma, D. S.; Meetsma, A.; Teuben, J. H. *Organometallics* **1993**, *12*, 3531–3540. (d) Watson, P. L. *J. Chem. Soc., Chem. Commun.* **1983**, *276*–277.

(10) (a) Fischer, B.; Wijkens, P.; Boersma, J.; van Koten, G.; Smeets, W. J. J.; Spek, A. L.; Budzelaar, P. H. M. *J. Organomet. Chem.* **1989**, *376*, 223–233. (b) Threlkel, R. S.; Bercaw, J. E. *J. Organomet. Chem.* **1977**, *136*, 1–5.

0276-7333/95/2314-5466$09.00/0

analysis determined the molecular structure shown in Figure 1.[12a]

4 is a monomeric bent sandwich, in which the C_5PhMe_4 ligands behave as regular cyclopentadienyl ligands.[12b] The phenyl rings are pointing away from each other, and their planes are at angles of 49.61(9) and 53.66(9)° with the respective Cp planes. The $Cp_{centroid}-Ti-Cp_{centroid}$ angle is very large (150.84°), which apparently is allowed by the fact that the hydride is very small. The Ti–H distance (1.768(15) Å) is comparable to other monomeric ($(C_5Me_5)(C_5Me_4CH_2(C_5H_3MeN))TiH$[13] (Ti–H = 1.70(4) Å), $CpTi(CO)_2(dmpe)H$[14] (1.75(7) Å), $CpTi(dmpe)_2H$[15] (1.96(6) Å)) and dimeric titanium hydrides (**1**[5] ($Ti-H_{av}$ = 1.73 Å), $[\mu-C_5H(CH_3)_2(CH_2)_2][(C_5HMe_4)Ti(\mu-H)]_2$[16] (1.81 Å), *rac*-$[(C_2H_4(\eta^5\text{-tetrahydroindenyl})_2)Ti(\mu-H)]_2$[17] (1.90 Å)).

The position of the hydride ligand with respect to the plane defined by Ti and both centers of gravity of the cyclopentadienyl rings deserves special attention. On the basis of extended Hückel calculations, Lauher and Hoffmann predicted that the Ti–H axis will be about 35° outside this plane in a d^1 Cp_2TiH complex.[18] In a recent paper however, Bercaw and Goddard performed ab initio calculations on Cl_2TiH and concluded that the hydride will reside in the plane through Ti and both ring centroids.[19] In **4** the hydride is found only 2.8(5)° outside the plane, supporting the theoretical considerations of Bercaw and Goddard.

We assume that the pentamethyl analogue **3** has a molecular structure identical to **4**, because of the close resemblance in spectroscopic and experimental data.[8a] Both **3** and **4** are d^1 15 electron paramagnetic complexes. The ^{1}H-NMR spectrum of **4** only shows resonances of the C_5PhMe_4 ligands, which are considerably narrower than for the corresponding methyl compound **5**. No hydride resonance could be detected for either **3** or **4**.[20] In the IR spectrum a band at 1505 cm^{-1} is assigned to ν(Ti–H), which shifts to 1092 cm^{-1} after deuteration of **4** via reaction with 1 atm D_2. Simultaneously, H/D scrambling of the methyl and the *o*-phenyl protons of the C_5PhMe_4 ligands is observed. The UV/vis spectrum of **4** shows an absorption at 480 nm, comparable to an absorption at 483 nm for **3**, resulting in a red-brown color for both compounds.[21] The ESR spectrum of a pentane solution of **4** shows a singlet (g = 1.976) with hyperfine coupling to Ti isotopes (a(Ti) = 8.9 G) at both room temperature and −100 °C.[22] No coupling with the hydride nuclear spin is observed. In contrast with **4**, the ESR spectrum of a pentane solution of **3** only shows a poorly resolved doublet (g = 1.973, a(H) = 10 G) at room temperature. Below −100 °C a singlet (g = 1.976) is observed. Thermolysis of **3** yields the fulvene complex $(C_5Me_5)Ti(\eta^6\text{-}C_5Me_4CH_2)$.[2l,7b] On thermolysis of **4**, only the methyl protons of the C_5PhMe_4 ligand are activated, producing a mixture of two isomers ($(C_5PhMe_4)Ti(C_5\text{-}1\text{-}CH_2\text{-}2\text{-}Ph\text{-}3,4,5\text{-}Me_3)$ and $(C_5PhMe_4)Ti(C_5\text{-}1\text{-}CH_2\text{-}3\text{-}Ph\text{-}2,4,5\text{-}Me_3)$). No products due to activation of the phenyl protons of the C_5PhMe_4 ligand were observed. A convenient way to characterize paramagnetic Ti(III) complexes consists of oxidation with $PbCl_2$ to the corresponding diamagnetic Ti(IV) chloride compounds.[23] As expected, oxidation of **4** with $PbCl_2$ yields $(C_5PhMe_4)_2Ti(H)Cl$, while **3** gives $(C_5Me_5)_2Ti(H)Cl$. Both **3** and **4** catalyze the hydrogenation of 1-hexene to hexane and the dimerization of phenylacetylene.

It was reported that **3** is not capable of ethene polymerization.[7b] Instead, only one insertion of ethene

(11) Experimental details are as follows: **General comments.** All manipulations of air-sensitive compounds were carried out under N_2, using standard Schlenk-line and glovebox techniques. 1-Phenyl-2,3,4,5-tetramethylcyclopentadiene was prepared according to published procedures.[10a] A small portion of all new paramagnetic Ti(III) compounds was oxidized with $PbCl_2$[23] to the corresponding diamagnetic Ti(IV) compounds for facile characterization by ^{1}H NMR. **Synthesis of $(C_5PhMe_4)_2TiCl$.** A 3.59 g amount of $TiCl_3$·3THF (9.70 mmol) was added to a suspension of 4.06 g of LiC_5PhMe_4 (20.0 mmol) in 150 mL of THF and stirred at RT (room temperature) for 10 min. The dark green solution was heated under reflux for 48 h, yielding a blue-green solution. The solvent was evaporated, and the residue was extracted with toluene. After concentration and cooling to −80 °C, a dark blue crystalline solid was obtained. Yield: 3.29 g (71%). ^{1}H NMR (C_6D_6): δ −4.6 (s, 12H, $C_5PhMe_2Me_2$, WHM = 1320 Hz), 2.0 (m, 2H, *p*-Ph), 5.21 (s, 4H, *o*-Ph, 100 Hz), 7.89 (s, 4H, *m*-Ph, 115 Hz), 12.0 (s, 12H, $C_5PhMe_2Me_2$, 4430 Hz). Oxidation with $PbCl_2$ yielded purple-red $(C_5PhMe_4)_2TiCl_2$.[10b] ^{1}H NMR ($CDCl_3$): δ 1.89, 2.05 (s, 12H, $C_5PhMe_2Me_2$), 7.4 (m, 10H, C_5PhMe_4). **Synthesis of $(C_5PhMe_4)_2TiMe$ (5).** A 4.5 mL amount of 1.33 M MeLi in ether (5.99 mmol) was added to a solution of 2.70 g of $(C_5PhMe_4)_2TiCl$ (5.66 mmol) in 75 mL of THF at −30 °C. The reaction mixture was allowed to warm to RT under stirring, yielding a green solution. The solvent was evaporated, and the residue was extracted with toluene. After evaporation of toluene the green product was dissolved in pentane and cooled to −80 °C. Dark green crystals (1.80 g (70%)) were isolated. ^{1}H NMR (C_6D_6): δ −20.5 (s, 3H, Ti–*Me*, WHM = 3390 Hz), 1.0 (m, 4H, *o*-Ph), 1.9 (s, 12H, $C_5PhMe_2Me_2$, 500 Hz), 6.16 (s, 2H, *p*-Ph, 64 Hz), 8.11 (s, 4H, *m*-Ph, 100 Hz), 20.0 (s, 12H, $C_5PhMe_2Me_2$, 4525 Hz). Oxidation with $PbCl_2$ yielded brown-orange $(C_5PhMe_4)_2Ti(Me)Cl$. ^{1}H NMR (C_6D_6): δ 0.60 (s, 3H, Ti–*Me*), 1.66, 1.83, 1.87, 1.93 (s, 6H, $C_5PhMeMe_3$), 7.0 (m, 10H, C_5PhMe_4). **Synthesis of $(C_5PhMe_4)_2TiH$ (4).** A dark green solution of 1.83 g of **5** (4.01 mmol) in 175 mL of pentane was exposed to 1 atm of H_2, and within 2 min the solution turned brown-red. After cooling of the solution to −80 °C, brown-red crystals were isolated. Yield: 1.47 g (83%). ^{1}H NMR (C_6D_6): δ 2.0 (s, 4H, *o*-Ph, WHM = 300 Hz), 4.87 (s, 2H, *p*-Ph, 26 Hz), 6.33 (s, 12H, $C_5PhMe_2Me_2$, 190 Hz), 7.80 (s, 4H, *m*-Ph, 34 Hz), 25.2 (s, 12H, $C_5PhMe_2Me_2$, 465 Hz). IR (cm^{-1}): 2955 (s), 2857 (s), 2726 (w), 1599 (m), 1505 (s), 1466 (s), 1377 (s), 1179 (w), 1074 (m), 1026 (m), 916 (m), 760 (s), 704 (s), 588 (m), 455 (m). UV/vis (THF): λ_{max} = 480 nm (ϵ = 78 $L\cdot mol^{-1}\cdot cm^{-1}$), 575 (sh). ESR (pentane) (RT and −100 °C): singlet (g = 1.976, a(Ti) = 8.9 G, peak to peak width 3.5 G). Magnetic susceptibility (corrected for diamagnetism): μ_{eff} = 1.79 μ_B. Anal. Calcd for $C_{30}H_{35}Ti$: C, 81.25; H, 7.96; Ti, 10.80. Found: C, 81.11; H, 7.99; Ti, 10.72. Oxidation with $PbCl_2$ yielded orange-brown $(C_5PhMe_4)_2Ti(H)Cl$: ^{1}H NMR (C_6D_6) δ 1.87, 1.89, 1.95, 1.98 (s, 6H, $C_5PhMeMe_3$), 5.16 (s, 1H, Ti–H), 7.1 (m, 10H, *Ph*).

(12) (a) Crystal data for **4**: $C_{30}H_{35}Ti$, triclinic, space group $P\bar{1}$ with a = 9.097(1) Å, b = 12.102(1) Å, c = 12.317(1) Å, α = 76.646(4)°, β = 72.618(4)°, γ = 69.643(4)°, V = 1201.0(2) Å^3, d_{calcd} = 1.226 g cm^{-3}, and Z = 2. Data were collected on an Enraf-Nonius CAD-4F diffractometer at 130 K with Mo K$\bar{\alpha}$ (λ = 0.710 73 Å). The structure was solved by Patterson methods. Difference Fourier synthesis resulted in the location of all hydrogen atoms, which positions were included in the refinement. R_F = 0.033 with wR = 0.041 for 4633 unique reflections with $I \geq 2.5\sigma(I)$ and 422 parameters. (b) Ti–Cen(1), 2.0298(8) Å, C–C_{av}(1), 1.4244 Å; ring slippage(1), 0.035 Å. Ti–Cen(2), 2.0305(8) Å; C–C_{av}(2), 1.4230 Å; ring slippage(2), 0.070 Å.

(13) Pattiasina, J. W.; Van Bolhuis, F.; Teuben, J. H. *Angew. Chem., Int. Ed. Engl.* **1987**, *26*, 330–331.

(14) Frerichs, S. R.; Stein, B. K.; Ellis, J. E. *J. Am. Chem. Soc.* **1987**, *109*, 5558–5560.

(15) You, Y.; Wilson, S. R.; Girolami, G. S. *Organometallics* **1994**, *13*, 4655–4657.

(16) Troyanov, S. I.; Mach, K.; Varga, V. *Organometallics* **1993**, *12*, 3387–3389.

(17) Xin, S.; Harrod, J. F.; Samuel, E. *J. Am. Chem. Soc.* **1994**, *116*, 11562–11563.

(18) Lauher, J. W.; Hoffmann, R. *J. Am. Chem. Soc.* **1976**, *98*, 1729–1742.

(19) Bierwagen, E. P.; Bercaw, J. E.; Goddard, W. A. *J. Am. Chem. Soc.* **1994**, *116*, 1481–1489.

(20) This may be explained by either a very broad hydride resonance or by a fast H/D exchange with the solvent.

(21) Upon oxidation with air to Ti(IV) species, these absorption bands disappear.

(22) Any trace of N_2 needs to be rigorously removed, otherwise on cooling to −100 °C a doublet (g = 1.992, a(H) = 11.9 G) appears in the ESR spectrum of **4** at the expense of the intensity of the singlet at g = 1.976, due to formation of a dinitrogen adduct, $(C_5PhMe_4)_2Ti(H)N_2$. Because of the lower symmetry of this adduct, mixing occurs between the orbital in which the unpaired electron resides and the Ti–H bonding orbital, resulting in the observation of a doublet.

(23) Luinstra, G. A.; Teuben, J. H. *J. Chem. Soc., Chem. Commun.* **1990**, 1470–1471.

occurred, producing $(C_5Me_5)_2TiEt$ for which compound a β-H agostic interaction was anticipated on the basis of IR spectroscopy. Similarly, **4** reacts with only 1 equiv of ethene, but the IR spectrum of the paramagnetic d^1 product does not show any β-H agostic interaction. The structure and reactivity of this complex is being studied at the moment.

The phenyltetramethylcyclopentadienyl ligand proves to be a very useful ligand for the investigation of titanocene chemistry, resulting in formation of well-crystallizable products. The molecular structure of the first monomeric bis(cyclopentadienyl)titanium(III) hydride, $(C_5PhMe_4)_2TiH$, was determined to be a bent-sandwich. Since the spectroscopic and experimental data of $(C_5PhMe_4)_2TiH$ and Cp^*_2TiH are very similar, Cp^*_2TiH is assumed to have a bent-sandwich geometry as well. We are currently exploring the chemistry of (phenyltetramethylcyclopentadienyl)titanium compounds further.

Supporting Information Available: Text giving details of the structure determination of **4** and tables of crystal data, thermal displacement parameters, atomic coordinates, bond lengths, and bond angles (17 pages). This material is contained in many libraries on microfiche, immediately follows this article in the microfilm version of the journal, can be ordered from the ACS, and can be downloaded from the Internet; see any current masthead page for ordering information and Internet access instructions.

OM9507787

Novel Example of Thermally Induced Metal–Metal Bond Homolysis in a Bimetallic Fulvalene Complex, the New Dichromium Compound $(\eta^5{:}\eta^5\text{-}C_{10}H_8)Cr_2(CO)_4(PMe_2Ph)_2$

István Kovács† and Michael C. Baird*

Department of Chemistry, Queen's University, Kingston, Ontario, Canada K7L 3N6

Received September 8, 1995®

Summary: Treatment of the fulvalene compound $FvCr_2(CO)_4(PMe_2Ph)_2H_2$ *with 2 molar equiv of trityl radicals* ($Ph_3C^\bullet$) *results in hydride hydrogen atom abstraction and formation of triphenylmethane and the new chromium–chromium-bonded dimer trans-*$FvCr_2(CO)_4(PMe_2Ph)_2$ *(4). Chemical reactivity patterns and variable-temperature IR and* ^1H, $^{13}C\{^1H\}$, *and* $^{31}P\{^1H\}$ *NMR investigations of 4 suggest that this 18-electron compound exists in thermal equilibrium with its 17-electron, biradical isomer* $PMe_2Ph(CO)_2Cr(\mu\text{-}Fv)Cr(CO)_2PMe_2Ph$, *at room temperature.*

The chemistry of 17-electron organotransition-metal radicals continues to attract interest,[1] with particular attention being paid in recent years to the cyclopentadienylchromium carbonyl system, in which the 18-electron chromium–chromium-bonded dimer exists in facile thermal equilibrium with the corresponding 17-electron monomer (eq 1).[1a,b,2]

$$[CpCr(CO)_3]_2 \rightleftharpoons 2CpCr(CO)_3^\bullet \qquad (1)$$

It has also been found that bulky substituents, either on the Cp ligand (Me, Ph) or in place of a CO ligand (phosphines, phosphites) greatly enhance the extent of homolysis of the chromium–chromium bond.[1b,2d–h,3]

Surprisingly, however, while the metal–metal bonds in the very similar fulvalene complexes $FvM_2(CO)_6$ (M = Cr, Mo, W)[4] are all longer than that of $[CpCr(CO)_3]_2$,[2a] there has been reported no direct evidence for homolysis of the metal–metal bonds in these fulvalene complexes (eq 2), either thermally or photochemically.[4d,f]

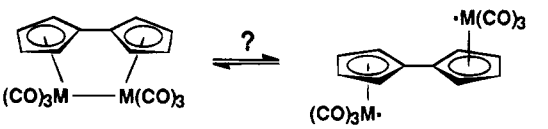

(2)

We therefore decided to investigate the possible effects of CO substitution by bulky phosphines in these compounds and have recently reported the preparation and properties of several (fulvalene)dimolybdenum carbonyl dimers, $FvMo_2(CO)_4L_2$ (L = PPh_3, PCy_3 (Cy = cyclohexyl), PXy_3 (Xy = 3,5-dimethylphenyl)).[5] In no cases do these compounds undergo thermal molybdenum–molybdenum bond homolysis. We now report preliminary results on the preparation and chemistry of a chromium analogue, $FvCr_2(CO)_4(PMe_2Ph)_2$, which would be expected to have a weaker metal–metal bond than the molybdenum analogues[1o] and which indeed does undergo spontaneous thermal homolysis.

The new hydride $FvCr_2(CO)_4(PMe_2Ph)_2H_2$ was synthesized essentially as reported previously for the molybdenum analogues $FvMo_2(CO)_4L_2H_2$ (L = PMe_3, PPh_3).[5] The carbonylate salt $(Et_4N)_2[FvCr_2(CO)_6]$ (**1**)[6,7] was protonated with glacial acetic acid in hexane–toluene (1:3) solution, forming the unstable dihydride $FvCr_2(CO)_6H_2$ (**2**).[6,7] Subsequent *in situ* reaction of **2** with PMe_2Ph at room temperature resulted in the formation of yellow, crystalline $FvCr_2(CO)_4(PMe_2Ph)_2H_2$

† NATO Science Fellow; Research Group for Petrochemistry of the Hungarian Academy of Sciences, Veszprém, Hungary.

® Abstract published in *Advance ACS Abstracts,* November 1, 1995.

(1) Some most recent advances: (a) Huber, T. A.; Macartney, D. H.; Baird, M. C. *Organometallics* **1995**, *14*, 592. (b) Richards, T. C.; Geiger, W. E.; Baird, M. C. *Organometallics* **1994**, *13*, 4494. (c) Kuksis, I.; Baird, M. C. *Organometallics* **1994**, *13*, 1551. (d) Koeslag, M. D.; Baird, M. C. *Organometallics* **1994**, *13*, 11. (e) Creutz, C.; Song, J.-S.; Bullock, R. M. *Pure Appl. Chem.* **1995**, *67*, 47. (f) Kiss, G.; Nolan, S. P.; Hoff, C. D. *Inorg. Chim. Acta* **1994**, *227*, 285. (g) Balla, J.; Bakac, A.; Espenson, J. H. *Organometallics* **1994**, *13*, 1073. (h) Zhu, Z.; Espenson, J. H. *Organometallics* **1994**, *13*, 1893. (i) Atwood, C. G.; Geiger, W. E. *J. Am. Chem. Soc.* **1994**, *116*, 10849. (j) Milukov, V. A.; Sinyashin, O. G.; Ginzburg, A. G.; Kondratenko, M. A.; Loim, N. M.; Gubskaya, V. P.; Musin, R. Z.; Morozov, V. I.; Batyeva, E. S.; Sokolov, V. I. *J. Organomet. Chem.* **1995**, *493*, 221. (k) Huang, Y.; Carpenter, G. B.; Sweigart, D. A.; Chung, Y. K.; Lee, B. Y. *Organometallics* **1995**, *14*, 1423. (l) Avey, A.; Nieckarz, G. F.; Keana, K.; Tyler, D. R. *Organometallics* **1995**, *14*, 2790. (m) Lang, R. F.; Ju, T. D.; Kiss, G.; Hoff, C. D.; Bryan, J. C.; Kubas, G. J. *J. Am. Chem. Soc.* **1994**, *116*, 7917. (n) Tilset, M. *Inorg. Chem.* **1994**, *33*, 3121. For reviews of earlier results, see: (o) Baird, M. C. *Chem. Rev.* **1988**, *88*, 1217. (p) Trogler, W. C., Ed. *Organometallic Radical Processes*; J. Organomet. Chem. Library 22; Elsevier: Amsterdam, 1990; p 49.

(2) (a) Adams, R. D.; Collins, D. E.; Cotton, F. A. *J. Am. Chem. Soc.* **1974**, *96*, 749. (b) Madach, T.; Vahrenkamp, H. *Z. Naturforsch.* **1979**, *34B*, 573. (c) McLain, S. J. *J. Am. Chem. Soc.* **1988**, *110*, 643. (d) Goh, L. Y.; Lim, Y. Y. *J. Organomet. Chem.* **1991**, *402*, 209. (e) Fortier, S.; Baird, M. C.; Preston, K. F.; Morton, J. R.; Ziegler, T.; Jaeger, T. J.; Watkins, W. C.; MacNeil, J. H.; Watson, K. A.; Hensel, K.; LePage, Y.; Charland, J.-P.; Williams, A. J. *J. Am. Chem. Soc.* **1991**, *113*, 542. (f) Watkins, W. C.; Jaeger, T.; Kidd, C. E.; Fortier, S.; Baird, M. C.; Kiss, G.; Roper, G. C.; Hoff, C. D. *J. Am. Chem. Soc.* **1992**, *114*, 907. (g) O'Callaghan, K. A. E.; Brown, S. J.; Page, J. A.; Baird, M. C.; Richards, T. C.; Geiger, W. E. *Organometallics* **1991**, *10*, 3119. (h) Yao, Q.; Bakac, A.; Espenson, J. H. *Organometallics* **1993**, *12*, 2010. (i) McConnachie, C. A.; Nelson, J. M.; Baird, M. C. *Organometallics* **1992**, *11*, 2521.

(3) (a) Goh, L.-Y.; D'Aniello, M. J., Jr.; Slater, S.; Muetterties, E. L.; Tavanaiepour, I.; Chang, M. I.; Fredrich, M. F.; Day, V. W. *Inorg. Chem.* **1979**, *18*, 192. (b) Cooley, N. A.; MacConnachie, P. T. F.; Baird, M. C. *Polyhedron* **1988**, *7*, 1965. (c) Watkins, W. C.; Hensel, K.; Fortier, S.; Macartney, D. H.; Baird, M. C.; McLain, S. J. *Organometallics* **1992**, *11*, 2418. (d) Hoobler, R. J.; Hutton, M. A.; Dillard, M. M.; Castellani, M. P.; Rheingold, A. L.; Rieger, A. L.; Rieger, P. H.; Richards, T. C.; Geiger, W. E. *Organometallics* **1993**, *12*, 116.

(4) (a) Abrahamson, H. B.; Heeg, M. J. *Inorg. Chem.* **1984**, *23*, 2281. (b) Drage, J. S.; Vollhardt, K. P. C. *Organometallics* **1986**, *5*, 280. (c) Moulton, R.; Weidman, T. W.; Vollhardt, K. P. C.; Bard, A. J. *Inorg. Chem.* **1986**, *25*, 1846. (d) McGovern, P. A.; Vollhardt, K. P. C. *Synlett* **1990**, 493. (e) Tilset, M.; Vollhardt, K. P. C.; Boese, R. *Organometallics* **1994**, *13*, 3146. (f) The compound $[CpCr(CO)_3]_2$ catalyzes the 1,4-dihydrogenation of conjugated dienes[4g] via $CpCr(CO)_3$ and the hydride $CpCr(CO)_3H$,[1o,4g] and thus indirect evidence for the diradical isomer of $FvCr_2(CO)_6$ is found in observations that this compound and the corresponding dihydride effect similar chemistry: Vollhardt, K. P. C., private communication. (g) Miyake, A.; Kondo, H. *Angew. Chem., Int. Ed. Engl.* **1968**, *7*, 631.

(5) (a) Kovács, I.; Baird, M. C. *Organometallics* **1995**, *14*, 4074. (b) Kovács, I.; Baird, M. C. *Organometallics* **1995**, *14*, 4084.

(6) The compounds $(Et_4N)_2[FvCr_2(CO)_6]$ and $FvCr_2(CO)_6H_2$ have also been prepared elsewhere: McGovern, P. A.; Vollhardt, K. P. C., private communication.

0276-7333/95/2314-5469$09.00/0

(**3**) in good yield. Attempted substitutions of **2** failed with the bulkier PPh_2Me and PPh_3 but proceeded smoothly with the smaller PMe_3.[8] Room-temperature IR and NMR spectra[7] of **3** were fully consistent with its formulation, which was confirmed by elemental and mass spectroscopic analyses.[9]

Treatment of **3** with trityl radical ($Ph_3C^{\bullet}$, 1:2 molar ratio) in toluene at room temperature resulted in a rapid color change from yellow to yellow-brown. The complete consumption of **3** and the concomitant formation of a single heat- and light-sensitive organometallic product were established by spectroscopic methods. The IR spectrum of the reaction mixture exhibited absorbances at 1926 (s) and 1850 (vs) cm^{-1}, at positions very similar to those of **3** but with different relative intensities.[7] The ^1H NMR spectrum of a reaction mixture in toluene-d_8 exhibited broad resonances attributable to PMe (δ 1.68), fulvalene (δ 3.69 and 3.92), and phenyl protons, all significantly different from those of **3**,[7] and a singlet at δ 5.37 attributable to Ph_3CH. In addition, the UV–vis spectrum exhibited a strong $d\sigma \rightarrow d\sigma^*$ transition at 460 nm, indicative of a metal–metal bond in the product which, on the basis of comparisons with data for the (fulvalene)molybdenum dimers *trans*-$FvMo_2(CO)_4L_2$ (L = PPh_3, PCy_3, PXy_3),[5] is tentatively identified as the chromium–chromium-bonded dimer *trans*-$FvCr_2(CO)_4(PMe_2Ph)_2$ (**4**). Thus, as anticipated,[5] the reaction between trityl radicals and **3** took place according to eq 3.

$$FvCr_2(CO)_4(PMe_2Ph)_2H_2 + 2Ph_3C^{\bullet} \rightarrow FvCr_2(CO)_4(PMe_2Ph)_2 + 2Ph_3CH \quad (3)$$

Since **4** was found to be too unstable to be isolated analytically pure, it was also obtained in an alternative way, by the treatment of **3** with 1,3,5-hexatriene. It has been demonstrated that hydrogenation of a number of conjugated dienes by $CpM(CO)_3H$ (M = Cr, Mo, W) can be utilized to prepare the corresponding dimers, $[CpM(CO)_3]_2$, in excellent yields.[3b,4g,10]

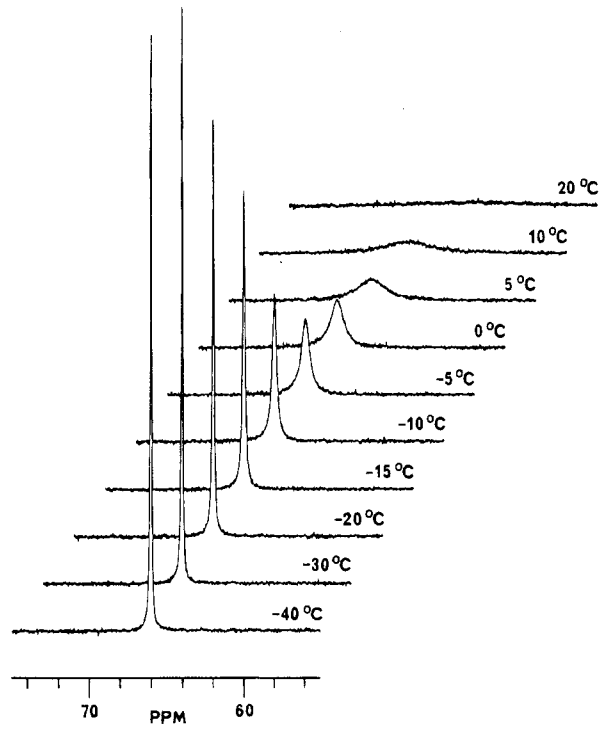

Figure 1. Stacked variable-temperature $^{31}P\{^1H\}$ NMR spectra (toluene-d_8) of compound **4**.

Interestingly, the ^1H, $^{13}C\{^1H\}$, and $^{31}P\{^1H\}$ NMR spectra of **4** are all strongly temperature-dependent. A variable-temperature ^1H NMR experiment revealed that both the fulvalene and the PMe resonances shifted downfield and broadened significantly as the temperature was raised from −80 to +80 °C. Although decomposition became evident above 50 °C, the line broadening and the chemical shift changes were both clearly reversible. Similar effects, resulting from dissociation to paramagnetic monomer, are observed in the ^1H NMR spectrum of $[CpCr(CO)_3]_2$.[2d,i]

The room-temperature $^{13}C\{^1H\}$ NMR spectrum of **4** in acetone-d_6 exhibited only tertiary carbon resonances in both the fulvalene (δ 82.3, 87.5) and the phenyl regions. The quaternary carbon (C-1 Fv, *ipso*-Ph, CO) and PMe resonances were not observed at room temperature but were at −50 °C.[7] Furthermore, the $^{31}P\{^1H\}$ NMR spectrum of **4** exhibited no phosphorus resonance at room temperature, but a very broad resonance appeared at δ 66.0 at 10 °C and gradually sharpened upon further cooling to appear as a normal $^{31}P\{^1H\}$ NMR spectrum at −40 °C (Figure 1).

A complementary variable-temperature IR experiment was also carried out in the temperature range 25–80 °C. As the temperature was raised, the absorbances of **4** at 1926 (s) and 1850 (vs) cm^{-1} weakened and two new ν_{CO} bands emerged at 1949 (s) and 1800 (s, br) cm^{-1}, very similar to those of $CpCr(CO)_2(PMe_2Ph)$ (1925 (s) and 1807 (m, br) cm^{-1}).[3b] Only the new absorbances were present at 80 °C.

The most plausible rationale for the temperature dependence of the IR and NMR spectra is that the chromium–chromium-bonded form of **4** exists in a facile

(7) Spectroscopic data are as follows. **1**: IR (THF) ν_{CO} 1889 (vs), 1800 (vs, br), 1717 (vs, br) cm^{-1}; ^1H NMR (200 MHz, acetone-d_6) δ 1.36 (tt, J_1 = 7 Hz, J_2 = 2 Hz, 24H, CH_3), 3.42 (q, J = 7 Hz, 16H, CH_2N), 4.13 ("t", 4H, Fv), 4.61 ("t", 4H, Fv); $^{13}C\{^1H\}$ NMR (100.6 MHz, acetone-d_6) δ 7.7 (s, CH_3), 52.8 (s, CH_2N), 80.0 (s, Fv), 81.7 (s, Fv), 100.9 (s, C-1 Fv), 247.4 (s, CO). **2**: IR (hexane) ν_{CO} 2014.5 (s), 1948 (s, sh), 1940 (vs) cm^{-1}; ^1H NMR (200 MHz, toluene-d_8) δ −5.46 (s, 2H, CrH), 4.08 ("t", 4H, Fv), 4.34 ("t", 4H, Fv); $^{13}C\{^1H\}$ NMR (100.6 MHz, toluene-d_8) δ 83.7 (s, Fv), 85.9 (s, Fv), 99.8 (s, C-1 Fv), 234.7 (br s, CO). **3**: IR (toluene) ν_{CO} 1924.5 (vs), 1856 (vs), 1846 (sh) cm^{-1}; ^1H NMR (200 MHz, toluene-d_8) δ −6.07 (d, J_{PH} = 73 Hz, 2H, CrH), 1.26 (d, J_{PH} = 8.5 Hz, 12H, PCH_3), 4.04 ("q", 4H, Fv), 4.35 ("q", 4H, Fv), ~7.06 (m, 6H, *m,p*-Ph), 7.30 ("t", 4H, *o*-Ph); $^{13}C\{^1H\}$ NMR (100.6 MHz, toluene-d_8) δ 83.7 (s, Fv), 84.8 (s, Fv), 99.9 (s, C-1 Fv), 128.5 (d, J_{PC} = 8.5 Hz, *m*-Ph), 129.2 (s, *p*-Ph), 129.6 (d, J_{PC} = 8.8 Hz, *o*-Ph), 143.0 (d, J_{PC} = 36 Hz, *ipso*-Ph) (no PMe and CO resonances were observed); $^{31}P\{^1H\}$ NMR (162 MHz, toluene-d_8) δ 59.9. **4**: IR (toluene) ν_{CO} 1926 (s), 1850 (vs) cm^{-1}; UV–vis (THF) $\lambda_{max}(d\sigma \rightarrow d\sigma^*)$ 460 (vs) nm; ^1H NMR (200 MHz, toluene-d_8) δ 1.68 (br s, 12H, PCH_3), 3.69 (br m, 4H, Fv), 3.92 (br m, 4H, Fv), ~7.05 (br m, 4H, Ph), 7.41 (br m, 6H, Ph); $^{13}C\{^1H\}$ NMR (100.6 MHz, acetone-d_6, 25 °C) δ 88.4 (s, Fv), 82.6 (s, Fv), 129.3, 130.0, 130.6 (s, all Ph) (no quaternary or PMe resonances were observed); $^{13}C\{^1H\}$ NMR (100.6 MHz, acetone-d_6, −50 °C) δ 18.7 (d, J_{PC} = 32 Hz, PMe), 82.5 (s, Fv), 87.3 (s, C-1 Fv), 88.1 (s, Fv), 129.0, 129.7, 129.8 (s, all Ph), 143.8 (d, J_{PC} = 33.5 Hz, *ipso*-Ph), 254.8 (d, J_{PC} = 35 Hz, CO); $^{31}P\{^1H\}$ NMR (162 MHz, toluene-d_8, −40 °C) δ 66.0.

(8) Kovács, I.; Baird, M. C., unpublished results.

(9) Anal. Calcd for $C_{30}H_{32}Cr_2O_4P_2$: C, 57.88; H, 5.18. Found: C, 57.30, H, 5.33. EI-MS (*m/z* (%)): no $[M]^+$ appeared; $[M - 2H - CO]^+$, 592 (0.2); $[M - 2H - 2CO]^+$, 564 (0.8); $[M - 2H - 3CO]^+$, 538 (2.2); $[M - 2H - 4CO]^+$, 508 (0.5); $[M - 2H - PMe_2Ph]^+$, 482 (0.4); $[M - 2H - PMe_2Ph - CO]^+$, 454 (0.2); $[M - 2H - PMe_2Ph - 2CO]^+$, 426 (0.2); $[M - 2H - PMe_2Ph - 3CO]^+$, 398 (0.2); $[M - 2H - PMe_2Ph - 4CO]^+$, 370 (3.3); $[FvCrH]^+$, 181 (11); $[O{=}PMe_2Ph]^+$, 154 (69); $[PMe_2PhH]^+$, 139 (100); $[PMe_2Ph]^+$, 138 (58); $[Fv]^+$, 128 (33).

(10) Miyake, A.; Kondo, H. *Angew. Chem., Int. Ed. Engl.* **1968**, *7*, 880.

equilibrium with its biradical isomer, as shown in eq 4.

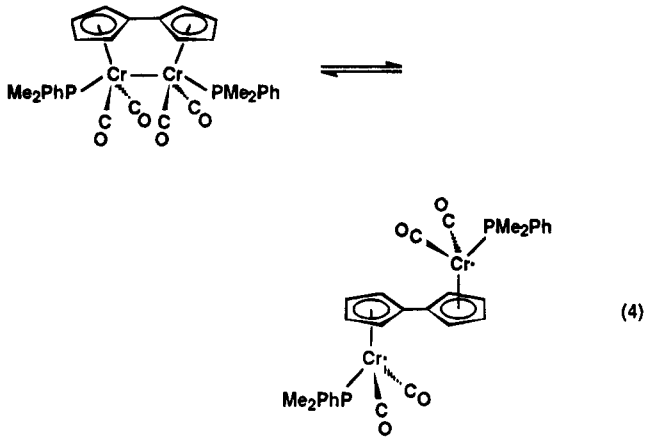

(4)

While the NMR studies established that rapid exchange between the 18-electron dimer and 17-electron biradical occurs above −40 °C, at least, as in eq 4, the ^{1}H NMR and IR studies demonstrate that the equilibrium is shifted considerably to the right above room temperature such that the predominant species in solution at higher temperatures is the biradical isomer. Thus, **4** behaves much like $[CpCr(CO)_3]_2$,[2d,i] although the changes in the ^{1}H NMR spectrum (downfield shifts of ~1 ppm) are much smaller.

The radical-like properties of **4** were further supported by studies on its reactions with activated alkyl halides. It has been shown that the solution chemistry of $[CpCr(CO)_3]_2$ is dominated by the reactivity of the small amount of monomer present in solution and that $[CpCr(CO)_3]_2$ takes part in halogen atom abstraction reactions with a wide variety of alkyl bromides and iodides. The primary products are $CpCr(CO)_3X$ (X = Br, I) and $CpCr(CO)_3R$ (R = alkyl) if the starting halide contains no β-hydrogen atom(s);[1a,2i,11] the halochromium product arises from initial halogen abstraction by one chromium-centered radical and the alkylchromium product from coupling of the resulting alkyl radical with a second chromium-centered radical. We have found that **4** reacts instantaneously at room temperature in the dark with ICH_2CO_2Et, allyl iodide, $CHBr_3$, $BrCH_2CN$, and CCl_4, but only slowly (several hours) with $PhCH_2Br$ and $BrCH_2CO_2Me$. Reactions with unactivated alkyl iodides occur very slowly (1 day), in the order EtI < *i*-PrI < *t*-BuI. IR and ^{1}H and $^{31}P\{^1H\}$ NMR spectroscopic studies showed that the major or sole products in the fast reactions were the dihalides $FvCr_2(CO)_4(PMe_2Ph)_2X_2$ (X = Cl, Br, I), identified spectroscopically.[5]

There remains the question of why fulvalene compounds, with very long metal−metal bonds, do not undergo spontaneous thermal homolysis as do analogous cyclopentadienyl compounds with much shorter metal−metal bonds. The factors inducing compounds with metal−metal bonds to undergo spontaneous thermal homolysis are not well understood, as there are as yet few examples of homologous series from which to draw conclusions.[2f] Mention has already been made of the effects of steric factors, metal−metal bonds often being destabilized with respect to homolytic dissociation on substitution of small ligands by more sterically demanding ligands, *e.g.* CO by tertiary phosphines and η^5-C_5H_5 by η^5-C_5Me_5 and η^5-C_5Ph_5. While it seems implicit in this apparent correlation that the principal factor at play here is weakening of metal bonds through steric strain, in fact such does not appear to be the case with $[CpCr(CO)_3]_2$ and $[Cp^*Cr(CO)_3]_2$.[2f] Although the latter has a much longer Cr−Cr bond and dissociates much more extensively in solution, the enthalpies of dissociation of the two dimers in toluene are identical within experimental error and the differing degrees of dissociation are related primarily to entropic factors. Thus, dissociation of $[Cp^*Cr(CO)_3]_2$ apparently gives rise to a much greater release of steric strain than is the case with $[CpCr(CO)_3]_2$, making possible degrees of ligand rotational motion in monomeric $Cp^*Cr(CO)_3$ not possible in $[Cp^*Cr(CO)_3]_2$.[2f] This type of increase in entropy would be much less of a factor in the fulvalene complexes under consideration here. While increased rotation of the ML_3 fragments relative to the cyclopentadienyl rings would occur, as with $[CpCr(CO)_3]_2$, the increase in rotational motion around the fulvalene central C−C bond would not be equivalent to the effect of dissociation of $[CpCr(CO)_3]_2$, nor would there be entropic factors equivalent to the probable increase in methyl rotational effects in $[Cp^*Cr(CO)_3]_2$.

Acknowledgment. We thank NATO for a Science Fellowship to I.K. (administered by the Natural Sciences and Engineering Research Council), the NSERC for a Research Grant to M.C.B., and the Hungarian Science Fund for support provided by Grant No. OTKA F7419.

OM950719T

(11) (a) Cooley, N. A.; Watson, K. A.; Fortier, S.; Baird, M. C. *Organometallics* **1986**, *5*, 2563. (b) Goulin, C. A.; Huber, T. A.; Nelson, J. M.; Macartney, D. H.; Baird, M. C. *J. Chem. Soc., Chem. Commun.* **1991**, 798. (c) Huber, T. A.; Macartney, D. H.; Baird, M. C. *Organometallics* **1993**, *12*, 4715.

Polysilyl Group Isomerization via Migrations in Rhodium and Iridium Derivatives $(Me_3P)_3MSi(SiMe_3)_3$

Gregory P. Mitchell and T. Don Tilley*

Department of Chemistry, University of California at Berkeley, Berkeley, California 94720-1460

Glenn P. A. Yap and Arnold L. Rheingold*

Department of Chemistry and Biochemistry, University of Delaware, Newark, Delaware 19716-2522

Received August 15, 1995[⊗]

*Summary: Reaction of $(Me_3P)_3RhCl$ with $(THF)_3LiSi(SiMe_3)_3$ generates the thermally unstable complex $(Me_3P)_3RhSiMe_2SiMe(SiMe_3)_2$ (**1**), probably via a series of 1,2- and 1,3-migrations. The analogous iridium reaction results in a similar rearrangement to give the iridacycle $(Me_3P)_3(H)IrSiMe_2SiMe(SiMe_3)SiMe_2CH_2$ as a mixture of diastereomers (**2a,b**), which is catalytically converted to an equilibrium mixture by hydrogen.*

Intramolecular 1,2- and 1,3-migrations appear to pervade transition metal–silicon chemistry and are thought to mediate many important pathways for silicon–element bond reactivity.[1] For example, such processes have been invoked in proposed mechanisms for metal-mediated redistributions at silicon[2] and silane dehydrocoupling.[3] Although neither type of migration has been directly observed, convincing evidence for such steps has been amassed by Pannell, Ogino, and Turner for reactions involving the Cp(CO)Fe fragment.[4] These photochemically-driven processes result in rearrangement of silyl ligands, possibly by series of migration steps as generalized in eq 1. An interesting example of

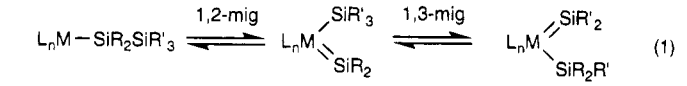

(1)

this chemistry is the photochemical conversion of $Cp(CO)_2Fe(SiMe_2)_3SiMe_3$ to $Cp(CO)_2FeSi(SiMe_3)_3$, for which 1,2- and 1,3-migrations are inferred.[4c] In recent work of Berry, the 1,3-migration of methyl groups in $Cp_2W(SiMe_3)(SiR'_2OTf)$ complexes has been probed.[5]

In attempts to study this important and fundamental rearrangement chemistry, we have sought to observe isolated migrations that might be amenable to further scrutiny. One approach involves the generation of coordinatively unsaturated silyl derivatives which could rearrange to more stable 18-electron, silyl–silylene complexes via a 1,2-migration. We have previously employed a related strategy in the synthesis of η^2-silene complexes.[6] Here we report an attempt to observe such transformations in rhodium and iridium systems of the type L_3M-SiR_3, which has led to observation of rather dramatic migratory rearrangements.

Reaction of $(THF)_3LiSi(SiMe_3)_3$[7] with $(Me_3P)_3RhCl$[8] in pentane resulted in a deep red solution, from which dark red crystals were obtained in 53% yield. Complete characterization of this compound was complicated by its thermal instability ($t_{1/2} \approx 6$ h in benzene-d_6), but the NMR data strongly support formulation of the compound as $(Me_3P)_3RhSiMe_2SiMe(SiMe_3)_2$ (**1**, eq 2).[9] A

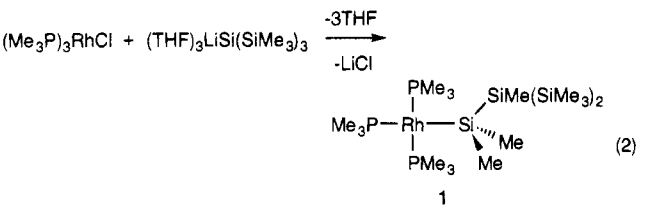

(2)

1

single resonance at 1.16 ppm is assigned to the fluxional PMe_3 ligands.[10] The SiMe groups give rise to resonances at 0.73, 0.44, and 0.36 ppm, in a relative intensity ratio of 2:6:1. The $^{29}Si\{^1H\}$NMR spectrum contains resonances at δ −80.7, −11.9, and −4.9, which may be attributed to the β, γ, and α silicon atoms, respectively, on the basis of relative intensities and published chemical shift data.[1,11] Compound **1** decomposes to several uncharacterized products (by NMR spectroscopy), but the appearance of a resonance in the hydride region (δ −9.63) suggests that a major decomposition pathway involves metalation of the silyl ligand.

The analogous reaction of "$(Me_3P)_3IrCl$", generated in THF by addition of PMe_3 to $[(COE)_2IrCl]_2$ (COE =

[⊗] Abstract published in *Advance ACS Abstracts,* November 1, 1995.

(1) (a) Tilley, T. D. In *The Chemistry of Organic Silicon Compounds*; Patai, S., Rappoport, Z., Eds.; Wiley: New York, 1989; Chapter 24, p 1415. (b) Tilley, T. D. In *The Silicon-Heteroatom Bond*; Patai, S., Rappoport, Z., Eds.; Wiley: New York, 1991; Chapters 9 and 10, pp 245 and 309. (c) Pannell, K. H.; Sharma, H. K. *Chem. Rev.* **1995**, *95*, 1351.

(2) (a) Curtis, M. D.; Epstein, P. S. *Adv. Organomet. Chem.* **1981**, *19*, 213. (b) Kobayashi, T.; Hayahi, T.; Yamashita, H.; Tanaka, M. *Chem. Lett.* **1988**, 1411. (c) Okinoshima, H.; Yamamota, K.; Kumada, M. *J. Organomet. Chem.* **1971**, *27*, C31.

(3) Tilley, T. D. *Comments Inorg. Chem.* **1990**, *10*, 37.

(4) (a) Pannell, K. H.; Cervantes, J.; Hernandez, C.; Cassias, J.; Vincenti, S. *Organometallics* **1986**, *5*, 1056. (b) Pannell, K. H.; Rozell, J. M., Jr.; Hernandez, C. *J. Am. Chem. Soc.* **1989**, *111*, 4482. (c) Pannell, K. H.; Wang, L.-J.; Rozell, J. M. *Organometallics* **1989**, *8*, 550. (d) Jones, K. L.; Pannell, K. H. *J. Am. Chem. Soc.* **1993**, *115*, 11336. (e) Hernandez, C.; Sharma, H. K.; Pannell, K. H. *J. Organomet. Chem.* **1993**, *462*, 259. (f) Pannell, K. H.; Brun, M.-C.; Sharma, H.; Jones, K.; Sharma, S. *Organometallics* **1994**, *13*, 1075. (g) Tobita, H.; Ueno, K.; Ogino, H. *Bull. Chem. Soc. Jpn.* **1988**, *61*, 2797. (h) Ueno, K.; Tobita, H.; Ogino, H. *Chem. Lett.* **1990**, 369. (i) Haynes, A.; George, M. W.; Haward, M. T.; Poliakoff, M.; Turner, J. J.; Boag, N. M.; Green, M. *J. Am. Chem. Soc.* **1991**, *113*, 2011. (j) Pannell, K. H.; Sharma, H. *Organometallics* **1991**, *10*, 954. (k) Ueno, K.; Hamashima, N.; Shimoi, M.; Ogino, H. *Organometallics* **1991**, *10*, 959.

(5) Pestana, D. C.; Koloski, T. S.; Berry, D. H. *Organometallics* **1994**, *13*, 4173.

(6) Campion, B. K.; Heyn, R. H.; Tilley, T. D. *J. Am. Chem. Soc.* **1988**, *110*, 7558.

(7) Gutekunst, G.; Brook, A. G. *J. Organomet. Chem.* **1982**, *225*, 1.

(8) Jones, R. A.; Real, F. R.; Wilkinson, G.; Galas, A. M. R.; Hursthouse, M. B.; Malik, K. M. A. *J. Chem. Soc., Dalton Trans.* **1980**, 511.

0276-7333/95/2314-5472$09.00/0

Scheme 1

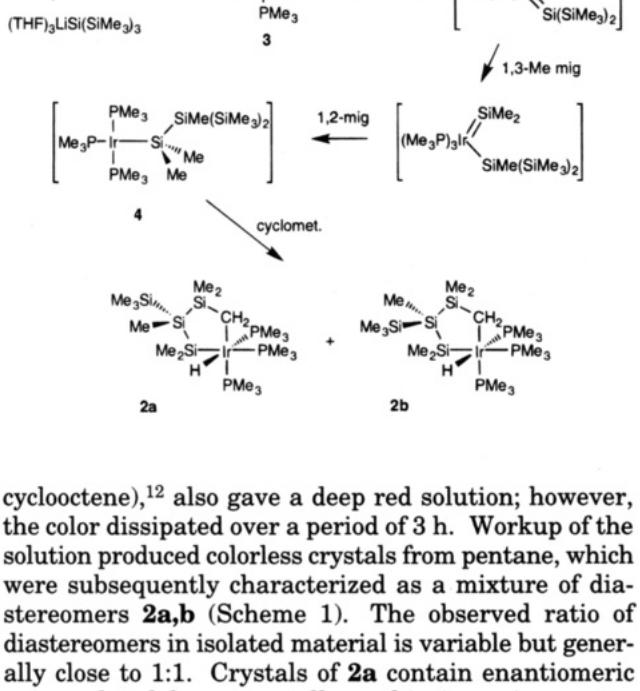

cyclooctene),[12] also gave a deep red solution; however, the color dissipated over a period of 3 h. Workup of the solution produced colorless crystals from pentane, which were subsequently characterized as a mixture of diastereomers **2a,b** (Scheme 1). The observed ratio of diastereomers in isolated material is variable but generally close to 1:1. Crystals of **2a** contain enantiomeric pairs related by a crystallographic inversion center (Figure 1). The substitution pattern about Ir is the same as that observed previously for $(Me_3P)_3\overline{Ir(C_6H_4)}SiPh_2(H)$, which forms via orthometalation of $(Me_3P)_3IrSiPh_3$.[13] The hydride ligand was located and refined at a distance of 1.74(3) Å from Ir, and the Ir–Si bond length of 2.441(3) Å is quite normal.[1] This silairidacycle is strongly folded, such that the angle between the C(81)–Ir–Si(1) and the C(81)–Si(3)–Si(2)–Si(1) planes is 124.7°.

A likely mechanism for the formation of **2**, shown in Scheme 1, involves rearrangement of an initially formed silyl complex $(Me_3P)_3IrSi(SiMe_3)_3$ (**3**) to $(Me_3P)_3IrSiMe_2SiMe(SiMe_3)_2$ (**4**) via 1,2- and 1,3-migration steps and silyl (silylene) intermediates. Intramolecular metalation then produces the observed products **2a,b**. Attempts to trap a silylene intermediate with PhC≡CPh[1] or $[Bu_4N]Cl$ failed to change the course of the reaction. Monitoring the reaction at −80 °C by ^{31}P NMR spectroscopy revealed the formation of an intermediate which exhibited two resonances (δ −20.5 (d) and −14.5 (t), J = 32 Hz, 2:1 ratio) consistent with square-planar substitution about Ir. We tentatively assign this spectrum to the Ir(I) silyl complex **3**.

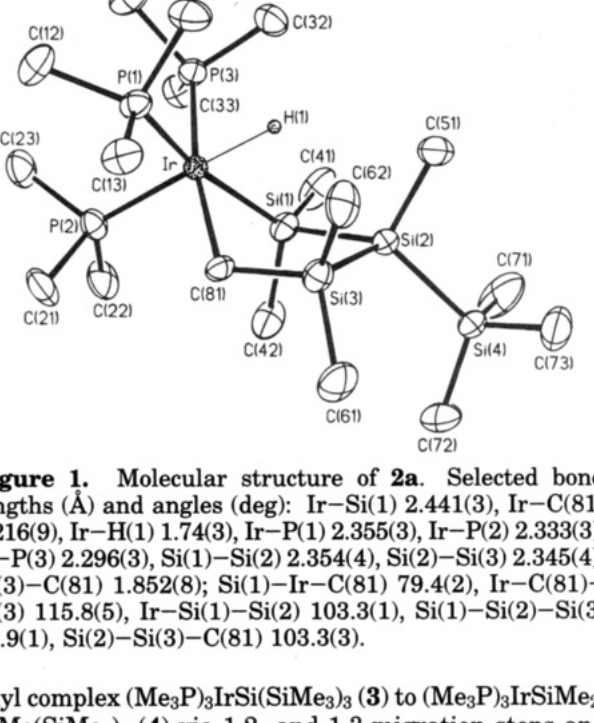

Figure 1. Molecular structure of **2a**. Selected bond lengths (Å) and angles (deg): Ir–Si(1) 2.441(3), Ir–C(81) 2.216(9), Ir–H(1) 1.74(3), Ir–P(1) 2.355(3), Ir–P(2) 2.333(3), Ir–P(3) 2.296(3), Si(1)–Si(2) 2.354(4), Si(2)–Si(3) 2.345(4), Si(3)–C(81) 1.852(8); Si(1)–Ir–C(81) 79.4(2), Ir–C(81)–Si(3) 115.8(5), Ir–Si(1)–Si(2) 103.3(1), Si(1)–Si(2)–Si(3) 93.9(1), Si(2)–Si(3)–C(81) 103.3(3).

Variations in the observed ratio of diastereomers **2a,b** (depending on reaction conditions) indicate that the distribution of products obtained is kinetically determined. Attempts to equilibrate the mixtures with heating (80 °C in benzene-d_6) resulted only in decomposition. Interestingly, isomerization of the diastereomeric mixtures is catalyzed by hydrogen at room temperature. Under 1 atm of hydrogen, a 1.3:1 ratio of diastereomers (in benzene-d_6 solution) is converted to a ratio of 1:9 within 12 h. Longer reaction times under hydrogen or nitrogen do not change this ratio, indicating that it represents the thermodynamic equilibrium. We are not sure which isomer is more stable, but we assume that it is **2a**, which has the $-SiMe_3$ group furthest removed from the $Ir(H)(PMe_3)_3$ fragment (see Figure 1). A proposed mechanism for isomerization (illustrated for the conversion of **2b** to **2a**) is shown in Scheme 2. Presumably, **2b** is in equilibrium with the Ir(I) silyl complex **4**, and thermal isomerization (slow at room temperature) would be accomplished via rotation about the Si_α–Si_β bond of **4**. Given the relatively rapid effect of hydrogen, we conclude that an open coordination site is made readily available by C–H reductive elimination to form **4**. The slow rate of thermal isomerization thus implies that $k_{rot} < k_{-1}$. Apparently, rotation about this Si–Si bond is facilitated by formation of an intermediate H_2 adduct (which was not observed by NMR spectroscopy), for which Si_α–Si_β bond rotation is competitive with H_2 reductive elimination (Scheme 2).

(9) Selected data are as follows. **1**: ^1H NMR (benzene-d_6, 400 MHz) δ 0.36 (s, 3H), 0.44 (s, 18 H), 0.73 (s, 6 H), 1.16 (s, 27 H); $^{13}C\{^1H\}$ NMR (benzene-d_6, 100.6 MHz) δ −6.20 (s, β-SiMe), 1.86 (s, γ-SiMe), 9.92 (s, α-SiMe), 22.88 (m, PMe_3); $^{31}P\{^1H\}$ NMR (benzene-d_6, 162.0 MHz) δ 20.00 (d, $^1J_{PRh}$ = 145 Hz); $^{29}Si\{^1H\}$ NMR (benzene-d_6, 59.63 MHz) δ −80.7 (s, β-Si), −11.9 (s, γ-Si), −4.9 (s, α-Si). **2** (more stable diastereomer): ^1H NMR (benzene-d_6, 300 MHz) δ −12.46 (dt, $^2J_{HP}$ = 136 Hz, 17.6 Hz, 1 H), −0.25 (m, 1 H), −0.01 (m, 1 H), 0.42 (s, 3 H), 0.49 (s, 3 H) 0.51 (s, 9 H) 0.70 (s, 3 H), 0.77 (d, $^4J_{HP}$ = 3 Hz), 0.86 (d, $^4J_{HP}$ = 3 Hz), 1.06 (d, $^2J_{HP}$ = 7.2 Hz), 1.09 (d, $^2J_{HP}$ = 7.2 Hz), 1.25 (d, $^2J_{HP}$ = 7.8 Hz); $^3P\{^1H\}$ NMR (benzene-d_6, 121.5 MHz) δ −64.22 (dd, $^2J_{PP}$ = 19.0 Hz, 15.7 Hz), −59.58 (dd, $^2J_{PP}$ = 14.9 Hz), −57.19 (t). **2** (less stable diastereomer): ^1H NMR (benzene-d_6, 300 MHz) δ −13.41 (ddd, $^2J_{HP}$ = 140 Hz, 18.2 Hz, 17.0 Hz, 1 H), −0.24 (m, 1 H), −0.04 (m, 1 H), 0.45 (s, 3 H), 0.46 (s, 9 H) 0.58 (s, 3 H) 0.63 (s, 3 H), 0.66 (d, $^4J_{HP}$ = 3 Hz), 0.69 (d, $^4J_{HP}$ = 3 Hz), 1.16 (d, $^2J_{HP}$ = 7.4 Hz), 1.20 (d, $^2J_{HP}$ = 7.4 Hz), 1.31 (d, $^2J_{HP}$ = 8.0 Hz); $^{31}P\{^1H\}$ NMR (benzene-d_6, 121.5 MHz) δ −69.30 (dd, $^2J_{PP}$ = 24.0 Hz, 18.2 Hz), −66.29 (dd, $^2J_{PP}$ = 16.2 Hz), −65.75 (dd). Anal. (C, H). **3**: $^{31}P\{^1H\}$ NMR (toluene-d_8, 162.0 MHz, −83 °C) δ −20.50 (d, $^2J_{PP}$ = 30 Hz), −14.5 (t). ^1H NMR resonances for **3** were largely obscured by those for the product.

(10) A similar observation was made for $(Me_3P)_3RhSiPh_3$: Thorn, D. L.; Harlow, R. L. *Inorg. Chem.* **1990**, *29*, 2017.

(11) Williams, E. A. *Annu. Rep. NMR Spectrosc.* **1983**, *15*, 235.

(12) (a) Bleeke, J. R.; Haile, T.; Chiang, M. Y. *Organometallics* **1991**, *10*, 19. (b) Herskovitz, T.; Guggenberger, L. J. *J. Am. Chem. Soc.* **1976**, *98*, 1615.

(13) Aizenberg, M.; Milstein, D. *Angew. Chem., Int. Ed. Engl.* **1994**, *33*, 317.

(14) Crystal data for **2a**: $C_{18}H_{54}IrP_3Si_4$, fw = 668.1, colorless, triclinic, $P\bar{1}$, a = 10.585(3) Å, b = 10.822(3) Å, c = 14.692(5) Å, α = 83.82(3)°, β = 84.99(3)°, γ = 77.16(2)°, V = 1627.9(9) Å^3, Z = 2, μ(Mo Kα) = 44.0 cm^{-1}, T = 298 K. Of 4553 empirically absorption corrected data ($2\theta_{max}$ = 45°), 3380 were independent and observed. The H atom bonded to Ir was located and refined. $R(F)$ = 3.76%; $R(wF)$ = 4.01%.

Scheme 2

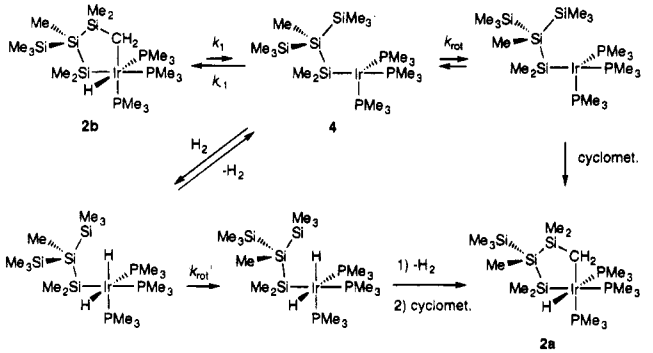

The silyl group rearrangement reported here (Scheme 1), like the ones observed by Pannell for $Cp(CO)_2Fe$ complexes, undoubtedly occurs via intramolecular processes. Because conclusive mechanistic data is still lacking in both systems, alternative mechanisms cannot be definitively ruled out. However other pathways, for example ones involving disilene intermediates or Si–Si/Si–C oxidative additions of $Si(SiMe_3)_n$ derivatives, seem less likely to us.[1] Interestingly, the rearrangement of $(Me_3P)_3IrSi(SiMe_3)_3$ to $(Me_3P)_3IrSiMe_2SiMe(SiMe)_3$ represents the *elongation* of a polysilyl chain, in contrast to what has typically been observed by Pannell.[4] In one case, however, Pannell's group has observed the $Cp(Ph_3P)_2RuMe$-catalyzed isomerization of $Me_3Si(SiMe_2)_3H$ to a mixture of $(Me_3Si)_3SiH$ and $(Me_3Si)_2SiMeSiMe_2H$, which probably also occurs via a $M-SiMe_2SiMe(SiMe_3)_2$ intermediate.[4f] Formation of a metalated, trivalent iridium center may provide some driving force for stabilizing the Ir product, but this is apparently not required for the analogous Rh rearrangement (to **1**). Thus, while it is yet to be determined whether this difference has electronic and/or steric origins, the implications is that migrations of this kind might be used to produce linear polysilanes.

Acknowledgment is made to the National Science Foundation for support of this work.

Supporting Information Available: Text giving experimental procedures and characterization data for compounds and tables of crystal, data collection, and refinement parameters, atom positional and U parameters, bond distances and angles, and anisotropic displacement parameters (11 pages). Ordering information is given on any current masthead page.

OM9506431

Synthesis and Solid-State Structure of $[Cu_5(Bu^tC{\equiv}C)_2(bpy)_4][CF_3SO_3]_3{\cdot}CH_2Cl_2$: An Unusual Cationic Organocopper(I) Complex Held Together by Two Bridging Alkynyl Ligands

Daniel L. Reger,* James E. Collins, and Mark F. Huff

Department of Chemistry and Biochemistry, University of South Carolina, Columbia, South Carolina 29208

Arnold L. Rheingold and Glenn P. A. Yap

Department of Chemistry and Biochemistry, University of Delaware, Newark, Delaware 19716

Received August 7, 1995[⊗]

Summary: The reaction of $Cu(NCMe)_4(O_3SCF_3)$ with $LiC{\equiv}CBu^t$ and 2,2′-bipyridine in an approximate 5/2/4 molar ratio leads to the formation of $[Cu_5(Bu^tC{\equiv}C)_2(bpy)_4][CF_3SO_3]_3$. The solid-state structure shows that the cation contains a nearly planar array of five copper atoms held together solely by two bridging alkynyl ligands.

As part of a long-term investigation of transition-metal complexes of alkynes,[1] we have discovered an unusual class of multimetal, cationic alkynylcopper(I) derivatives stabilized by bipyridine (bpy) ligands. Reported here are the syntheses of compounds containing the unusual cationic organocopper group $[Cu_5(alkynyl)_2(bpy)_4]^{3+}$, which contain a nearly planar Cu_5 central core held together by two bridging alkynyl ligands. The compound $[Cu_5(Bu^tC{\equiv}C)_2(bpy)_4][CF_3SO_3]_3{\cdot}CH_2Cl_2$ has been characterized in the solid state by X-ray crystallography. A second class of complexes containing a cation with the empirical formula $[Cu_3(alkynyl)(bpy)_3]^{2+}$ has also been prepared.

Treatment of a THF solution of $Cu(NCMe)_4(O_3SCF_3)$ with $LiC{\equiv}CBu^t$ and 2,2′-bipyridine in an approximate 5/2/4 molar ratio leads to the precipitation of $[Cu_5(Bu^tC{\equiv}C)_2(bpy)_4][CF_3SO_3]_3$.[2] The solid-state structure of the CH_2Cl_2 solvate has been determined crystallographically.[3] A PLUTO diagram of the cationic part of the compound, showing the two coordinated CF_3SO_3 groups, is shown in Figure 1. The five copper(I) atoms are arranged in a nearly planar array. The Cu1 and Cu3 atoms are 0.14 Å on one side of the least-squares plane and the Cu2 and Cu4 atoms 0.15 Å on the other side, with Cu5 only 0.010 Å out of the plane. The Cu1···Cu5···Cu3 angle is 172.4(1)°, and the Cu2···Cu5···Cu4 angle is 173.3°. The Cu1···Cu5 and Cu3···Cu5 separations are similar at 2.482(2) and 2.458(2) Å and shorter than the Cu2···Cu5 and Cu4···Cu5 separations of 2.810(2) and 2.707(2) Å.

Four of the copper atoms, Cu1–4, are bonded to bipyridine ligands that are arranged in parallel pairs on each side of the cation. Cu1 and Cu3 are also weakly coordinated to one oxygen atom from the CF_3SO_3 anions. The cation is held together by the two bridging $Bu^tC{\equiv}C$ ligands. The terminal carbon atoms of the two alkynyl ligands symmetrically bridge the shorter Cu···Cu distances. The Cu1–C43 and Cu3–C49 distances of 1.966(8) and 1.976(8) Å are just slightly longer than the Cu5–C43 and Cu5–C49 distances of 1.924(9) and 1.942(10) Å. Cu5 is two-coordinate, bonded only to C43 and C49 with a nearly linear C43–Cu5–C49 bond angle of 178.2(4)°. The Cu2 and Cu4 atoms are held in the cation solely by symmetrical π-bonding interactions to the carbon–carbon triple bonds, with typical Cu–C distances averaging 2.02 Å.[4] The C–C alkyne distances are 1.245(11) and 1.211(12) Å, just slightly longer than the normal distances of 1.21 Å in free alkynes and typical of alkynes bonded to transition metals that do not strongly back-bond.[1b] The C43–C44–C45 and C49–C50–C51 bond angles are 156.4(8) and 159.3(8)°, again typical of Cu(I)–η^2-alkyne structures.[4] The draw-

[⊗] Abstract published in *Advance ACS Abstracts,* November 15, 1995.

(1) (a) Reger, D. L. *Acc. Chem. Res.* **1988**, *21*, 229. (b) Reger, D. L.; Klaeren, S. A.; Lebioda, L. *Organometallics* **1988**, *7*, 189. (c) Reger, D. L.; Huff, M. F. *Organometallics* **1990**, *9*, 2807. (d) Reger, D. L.; Huff, M. F. *Organometallics* **1992**, *11*, 69.

(2) $Cu(NCMe)_4(O_3SCF_3)$ (0.50 g, 1.3 mmol) was dissolved in THF (8 mL). This solution was treated dropwise by cannula transfer with a THF (5 mL) solution of $LiC{\equiv}CBu^t$ (0.047 g, 0.53 mmol) and 2,2′-bipyridine (0.17 g, 1.1 mmol). A yellow solid precipitated while the mixture was stirred overnight. This solid was collected and washed with hexanes (3 × 5 mL; 0.21 g, 0.14 mmol, 51%). Slow diffusion of hexanes into a saturated CH_2Cl_2 solution provided crystals which were collected and dried (crystals turn into a powder) to yield $[Cu_5(bpy)_4(C{\equiv}CBu^t)_2][O_3SCF_3]_3{\cdot}0.5CH_2Cl_2$ (0.18 g, 0.11 mmol, 43%); mp 158–165 °C. Half an equivalent of CH_2Cl_2 is retained by the compound, as determined by ^1H NMR and elemental analysis. ^1H NMR (acetone-d_6): δ 8.97, 8.51, 8.22, 7.71 (br, d, J = 8.0 Hz, m, m; 8, 8, 8, 8; bpy); 5.63 (s; 1; CH_2Cl_2); 1.56 (s; 18; $C(CH_3)_3$). ^{13}C NMR (acetone-d_6): δ 152.3, 150.3, 140.9, 127.4, 122.8 (bpy); 122.3 (q; O_3SCF_3); 98.6 ($C{\equiv}CBu^t$); 88.8 (br; $C{\equiv}CBu^t$); 32.9 ($C(CH_3)_3$); 32.1 ($C(CH_3)_3$). Anal. Calcd for $C_{55}H_{50}Cu_5F_9N_8O_9S_3{\cdot}0.5CH_2Cl_2$: C, 41.81; H, 3.22; N, 7.03. Found: C, 41.15; H, 3.23; N, 6.75.

(3) A single crystal, grown from CH_2Cl_2/hexane, of $[Cu_5(bpy)_4(C{\equiv}CBu^t)_2][O_3SCF_3]_3{\cdot}CH_2Cl_2$ was mounted, immediately upon removal from the mother liquor (crystals degrade rapidly when dry, even under N_2), with epoxy cement at the end of a glass fiber. All specimens studied diffracted weakly, in keeping with the ionic composition of the compound. Photographic characterization revealed no symmetry greater than triclinic. Data collection was performed at 298 K on a Siemens P4 diffractometer with Mo Kα graphite-monochromated radiation (λ = 0.7107 Å). A total of 7430 reflections ($4 \le 2\theta \le 48°$) were collected, with 4685 being observed having $I > 4\sigma$. Corrections for absorption were applied using a semiempirical procedure (transmission ratio 1.24). Direct methods were used to locate the metal atoms. Due to the large number of parameters refined (549), blocked methods were used. Only atoms with atomic numbers of 7 or greater were refined with anisotropic thermal parameters, and hydrogen atoms were idealized ($R(F) = 5.14$; $R_w(F) = 6.23$). All computations used the SHELXTL 4.2 library of programs (G. Sheldrick, Siemens XRD, Madison, WI). Crystal data for $C_{56}H_{52}Cl_2Cu_5F_9N_8O_9S_3$: fw = 1648.0, triclinic, space group $P\bar{1}$, a = 11.570(3) Å, b = 15.650(4) Å, c = 19.072(6) Å, α = 86.76(2)°, β = 73.42(2)°, γ = 79.18(2)°, V = 3250(1) Å^3, Z = 2, D_{calc} = 1.672 g cm^{-3}, μ = 18.7 cm^{-1}.

(4) (a) Reger, D. L.; Huff, M. F.; Wolfe, T. A.; Adams, R. D. *Organometallics* **1989**, *8*, 848. (b) Pasquali, M.; Leoni, P.; Floriani, C.; Gaetani-Manfredotti, A. *Inorg. Chem.* **1982**, *21*, 4324.

0276-7333/95/2314-5475$09.00/0

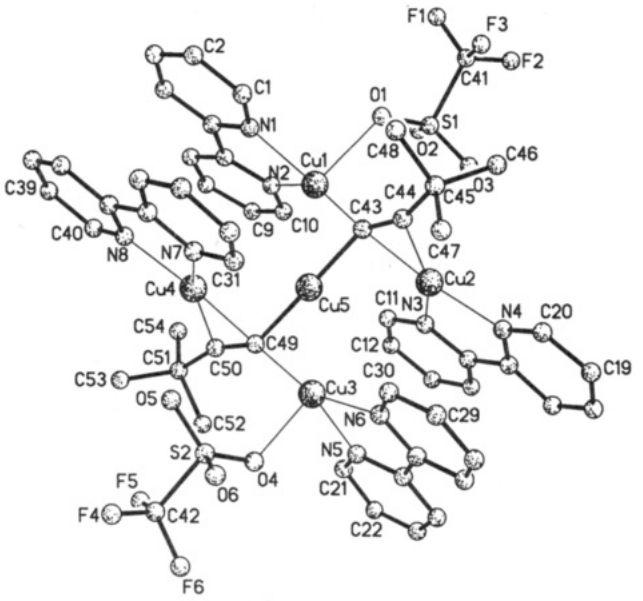

Figure 1. Pluto drawing of $[Cu_5(bpy)_4(C{\equiv}CBu^t)_2(O_3SCF_3)_2]^+$ showing the atomic labeling scheme. Selected distances (Å): Cu1···Cu5 = 2.482(2), Cu2···Cu5 = 2.810(2), Cu3···Cu5 = 2.458(2), Cu4···Cu5 = 2.707(2), Cu1···C43 = 1.966(8), Cu2−C43 = 2.018(8), Cu2−C44 = 2.010(8), Cu3−C49 = 1.976(8), Cu4−C49 = 2.038(8), Cu4−C50 = 2.016(8), Cu5−C43 = 1.924(9), Cu5−C49 = 1.942(10), C43−C44 = 1.245(11), C49−C50 = 1.211(12), Cu1−O1 = 2.327(8), Cu3−O4 = 2.267(11). Selected angles (deg): Cu1···Cu5···Cu2 = 85.6(1), Cu1···Cu5···Cu3 = 172.4(4), Cu1···Cu5···Cu4 = 94.4(1), Cu2···Cu5···Cu3 = 90.3(1), Cu2···Cu5···Cu4 = 173.3(1), Cu3···Cu5···Cu4 = 90.5(1), C43−Cu5−C49 = 178.2(4), C43−C44−C45 = 156.4(8), C49−C50−C51 = 159.3(8).

Chart 1

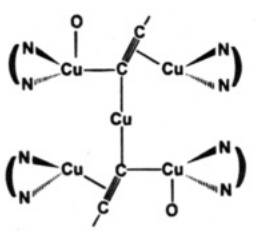

Chart 2

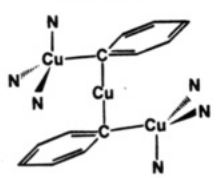

ing in Chart 1 depicts the bonding of the central Cu_5 core and the donor atoms bonded to it.

This structure represents the second example of a cationic organocopper(I) complex. The first is the trimetallic cation $[Cu_3Ph_2(PMDTA)_2]^+$ (PMDTA = *N*,*N*,*N*′,*N*″,*N*″-pentamethyldiethylenetriamine).[5] A drawing of the $Cu_3C_2N_6$ core of this cation is shown in Chart 2. The structure is remarkably similar to the linear $Cu_3(\mu\text{-}C)_2$ part of the Cu_5 cation that runs from the top left to the bottom right of Chart 1. Even the terminal copper atoms are bonded to three other donor atoms. In the cation $[Cu_3Ph_2(PMDTA)_2]^+$, the Cu···Cu distances are 2.444 Å, less than 0.03 Å shorter than the average of the Cu1···Cu5 and Cu3···Cu5 separations. The Cu−C distances of 2.006(7), 1.989(5), 1.980(7), and 2.064(5) Å are slightly longer, with the shorter distances to the central copper atom as observed in the Cu_5 cation. These slightly longer Cu−C bonds are explained by the fact that the bridging carbon atoms in this structure are sp^2-hybridized, whereas in the structure of $[Cu_5(Bu^tC{\equiv}C)_2(bpy)_4]^{3+}$ the bridging carbon atoms are sp-hybridized. The main difference in the two structures is that the presence of the two C−C triple bonds in $[Cu_5(Bu^tC{\equiv}C)_2(bpy)_4]^{3+}$ allows the coordination of two additional (bipyridine)copper(I) groups.

Two other compounds containing the $[Cu_5(RC{\equiv}C)_2(bpy)_4]^{3+}$ cation have been prepared.[6] A reaction similar to that described above using $Cu(NCMe)_4(PF_6)$ with $LiC{\equiv}CBu^t$ and 4,4′-dimethylbipyridine yields, after crystallization from CH_2Cl_2/hexane, $[Cu_5(Me_2bpy)_4(C{\equiv}CBu^t)_2][PF_6]_3{\cdot}0.5CH_2Cl_2$. Reaction of $Cu(NCMe)_4(SbF_6)$ with $LiC{\equiv}CPh$ and 4,4′-dimethylbipyridine yields $[Cu_5(Me_2bpy)_4(C{\equiv}CPh)_2][SbF_6]_3$. Both of these compounds have been characterized in the solid state by X-ray crystallography, but the structures suffered disorder problems. In both cases the structures of the cations were clearly identified and are essentially the same as that observed for $[Cu_5(Bu^tC{\equiv}C)_2(bpy)_4][CF_3SO_3]_3{\cdot}CH_2Cl_2$.

Surprisingly, a similar reaction using $Cu(NCMe)_4(PF_6)$ with $LiC{\equiv}CBu^t$ and 2,2′-bipyridine yields a compound with an entirely different empirical formula, $[Cu_3(bpy)_3(C{\equiv}CBu^t)][PF_6]_2{\cdot}0.5CH_2Cl_2$.[7] Repeated attempts to grow single crystals of this compound that are suitable for a crystallographic study have not proven successful. A reasonable structure would have the three copper atoms, two bpy ligands, and the bridging alkynyl ligands arranged as in the top of Chart 1. The $Cu_2(alkynyl)(bpy)_2$ group would be removed from the bottom of the drawing and replaced with a bpy ligand bonded to the central copper atom. This synthesis indicates that additional cationic alkynylcopper(I) compounds stabilized by chelating nitrogen donor ligands are possible.

(5) He, X.; Ruhlandt-Senge, K.; Power, P. P.; Bertz, S. H. *J. Am. Chem. Soc.* **1994**, *116*, 6963.

(6) $[Cu_5(Me_2bpy)_4(C{\equiv}CBu^t)_2][PF_6]_3$ was prepared as described in ref 2 (0.34 g, 0.21 mmol; 77%) using $Cu(NCMe)_4PF_6$ (0.50 g, 1.3 mmol), $LiC{\equiv}CBu^t$ (0.047 g, 0.53 mmol), and 4,4′-Me_2bpy (0.20 g, 1.1 mmol). Crystallization from CH_2Cl_2/hexanes provided analytically pure $[Cu_5(Me_2bpy)_4(C{\equiv}CBu^t)_2][PF_6]_3{\cdot}0.5CH_2Cl_2$. ^{1}H NMR (acetone-$d_6$): 8.77, 8.35, 7.54 (s, s, s; 8, 8, 8; bpy); 5.63 (s; 1; CH_2Cl_2); 2.52 (s; 24; $(H_3C)_2$-bpy); 1.57 (s; 18; $C(CH_3)_3$). Anal. Calcd for $C_{60}H_{66}Cu_5F_{18}N_8P_3{\cdot}0.5CH_2Cl_2$: C, 42.89; H, 3.99; N, 6.61. Found: C, 42.88; H, 4.03; N, 6.69. $[Cu_5(Me_2bpy)_4(C{\equiv}CPh)_2][SbF_6]_3$ was prepared as described in ref 2 from $Cu(NCMe)_4SbF_6$ (0.500 g, 1.08 mmol), 4,4′-Me_2bpy (0.16 g, 0.86 mmol), and $LiC{\equiv}CPh$ (0.047 g, 0.43 mmol) in THF (30 mL). The yellow powder that formed over ca. 2.5 h was filtered and dried overnight in vacuo (0.221 g, 0.113 mmol, 52%). ^{1}H NMR (acetone-d_6): δ 8.59, 8.31, 7.43 (s, s, s; 8, 8, 8; bpy); 7.90, 7.58 (d; m; J = 8 Hz; 4, 6; C_6H_5); 2.49 (s; 24; $(H_3C)_2$bpy).

(7) $[Cu_3(bpy)_3(C{\equiv}CBu^t)][PF_6]_2$ (0.37 g, 0.36 mmol, 80%) was prepared by treating a THF (10 mL) solution of $Cu(NCMe)_4PF_6$ (0.50 g, 1.3 mmol) and 2,2′-bipyridine (0.21 g, 1.3 mmol) with a THF (5 mL) solution of $LiC{\equiv}CBu^t$ (0.039 g, 0.45 mmol) by slow cannula transfer. After the mixture was stirred overnight, the product was isolated as described above for $[Cu_5(bpy)_4(C{\equiv}CBu^t)_2][O_3SCF_3]_3$; mp 210−215 °C. Crystallization from CH_2Cl_2/hexanes provided analytically pure $[Cu_3(bpy)_3(C{\equiv}CBu^t)][PF_6]_2{\cdot}0.5CH_2Cl_2$. ^{1}H NMR (acetone-$d_6$): δ 8.98, 8.59, 8.27, 7.73 (br d, J = 7.1, m, m; 6, 6, 6, 6; bpy); 5.63 (s; 1; CH_2Cl_2); 1.66 (s; 9; $C(CH_3)_3$). ^{13}C NMR (acetone-d_6): δ 152.5, 150.3, 140.8, 127.5, 122.9 (bpy); 88.7 ($C{\equiv}CBu^t$); 34.2 ($C(CH_3)_3$); 32.9 ($C(CH_3)_3$). Anal. Calcd for $C_{36}H_{33}Cu_3F_{12}N_6P_2{\cdot}0.5CH_2Cl_2$: C, 40.87; H, 3.19; N, 7.83. Found: C, 40.45; H, 3.21; N, 7.46.

Acknowledgment is made to Professor Lucas Lebioda for solving the crystal structure of $[Cu_5(Me_2bpy)_4(C{\equiv}CPh)_2][SbF_6]_3$. The NSF (Grants CHE-8411172 and CHE-8904942) and NIH (Grant RR-02425) have supplied funds to support NMR equipment at the University of South Carolina.

Supporting Information Available: Tables of complete data collection information, bond distances, angles, anisotropic thermal parameters, and positional parameters and a stereoview of the unit cell (13 pages). Ordering information is given on any current masthead page.

OM950614Q

Sterically Demanding Diamide Ligands: Synthesis and Structure of d0 Zirconium Alkyl Derivatives

John D. Scollard, David H. McConville, and Jagadese J. Vittal

Organometallics, **1995**, 14 (12), 5478-5480• DOI: 10.1021/om00012a009 • Publication Date (Web): 01 May 2002

Sterically Demanding Diamide Ligands: Synthesis and Structure of d^0 Zirconium Alkyl Derivatives

John D. Scollard, David H. McConville,* and Jagadese J. Vittal

Department of Chemistry, University of Western Ontario, London, Ontario, Canada N6A 5B7

Received July 11, 1995[⊗]

*Summary: The chelating diamide complexes (BDAP)Zr(NMe$_2$)$_2$ (**2**), (BDAP)ZrCl$_2$(py)$_2$ (**4**), (BDAP)ZrR$_2$ (**5a**, R = CH$_2$Ph; **5b**, R = Me), (BDAP)Zr(η^5-Cp)Cl (**5c**), and (BDAP)Zr(η^2(N,C)-NC$_5$H$_4$)(CH$_2$CMe$_2$Ph) (**5d**) (BDAP = ArNCH$_2$CH$_2$CH$_2$NAr; Ar = 2,6-^{i}Pr$_2$-C$_6$H$_3$) have been prepared. An X-ray study of (BDAP)Zr(η^2(N,C)-NC$_5$H$_4$)(CH$_2$CMe$_2$Ph) (**5d**) revealed an η^2-pyridyl moiety bound to zirconium. Proton and carbon NMR data suggest that the pyridyl moiety in **5d** is rotating rapidly about the Zr–C bond on the NMR time scale.*

Homogeneous "single site" olefin polymerization catalysts have developed rapidly in the last 15 years. Initial studies[1] on the polymerization activity of Cp_2ZrMe_2 (methylaluminoxane (MAO) cocatalyst) gave way to the ingeniously designed bridged-metallocene catalysts (e.g., [*rac*-ethylenebis(η^5-tetrahydroindenyl)]$ZrCl_2$[2] and [isopropyl(η^5-cyclopentadienyl)(η^5-1-fluorenyl)]$ZrCl_2$[3]). Recent interest in constrained-geometry catalysts (e.g., [(η^5-C$_5$Me$_4$)SiMe$_2$(NCMe$_3$)]ML$_n$; M = Ti, Zr, Hf, Sc; L = halide, alkyl)[4–6] that contain a linked cyclopentadienylamide ligand[7–9] prompted us to investigate the chemistry of group 4 chelating diamide complexes. In fact, the bis(amide) complex [(Me$_3$Si)$_2$N]$_2$$ZrCl_2$[10] is reported to polymerize propylene to 90% isotactic poly(propylene) when activated with MAO.[11] A number of chelating diamide complexes of group 4 have been prepared;[12–16] however, most contain silyl substituents at nitrogen. We are particularly interested in the steric and electronic effects of diamide ancillaries that incorporate the voluminous 2,6-diisopropylphenyl moiety.[17] We report here the synthesis of d^0 alkyl complexes of zirconium stabilized by a new bulky chelating diamide ligand.

The reaction of 2 equiv of LiNHAr (Ar = 2,6-^{i}Pr$_2$-C$_6$H$_3$) with 1,3-dibromopropane yields the diamine ligand (BDAP)H$_2$ (**1**),[18] as a viscous oil (eq 1). The

$$2\mathrm{LiNHAr} + \mathrm{Br(CH_2)_3Br} \xrightarrow[-2\mathrm{LiBr}]{\mathrm{THF/tmeda/0-25\ ^\circ C}} \underset{\mathbf{1}}{\mathrm{ArHN(CH_2)_3NHAr}} \quad (1)$$

$$\mathrm{tmeda} = \mathrm{Me_2NCH_2CH_2NMe_2}$$

aminolysis reaction between (BDAP)H$_2$ and Zr(NMe$_2$)$_4$[19] provides 2 equiv of HNMe$_2$ and the mixed-amide complex (BDAP)Zr(NMe$_2$)$_2$ (**2**), in high yield (eq 2).

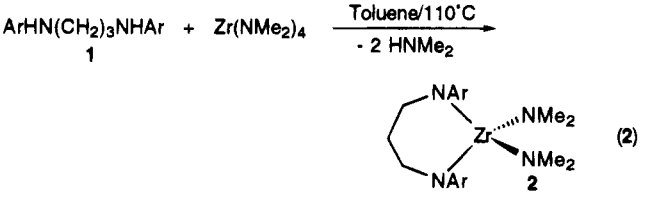

Characteristic second-order patterns are observed for the methylene protons (NCH_2 and NCH$_2$CH_2) of the coordinated BDAP ligand in the proton NMR spectrum of complex **2**.[20] Additionally, the isopropyl methyl groups of the arene are diastereotopic, which we interpret as a consequence of restricted rotation about the N-C$_{ipso}$ bond.[17,21]

Chloride derivatives were desired as precursors to alkyl derivatives. Compound **2** reacts with 2 equiv of [Me$_2$NH$_2$]Cl to afford the octahedral dimethylamine adduct (BDAP)ZrCl$_2$(NHMe$_2$)$_2$ (**3**).[18] We do not observe protonolysis of the BDAP ligand, although other amide donors are prone to this reaction.[9] Compound **3** is unstable toward loss of dimethylamine, possibly due to steric congestion about the zirconium center. The bis(pyridine) adduct proved to be more stable. Reaction of complex **2** with 2 equiv of [Me$_2$NH$_2$]Cl in the presence of excess pyridine affords a single bis(pyridine) geometrical isomer, (BDAP)ZrCl$_2$py$_2$ (**4**), in good yield.

[⊗] Abstract published in *Advance ACS Abstracts,* November 15, 1995.

(1) Sinn, H.; Kaminsky, W.; Vollmer, H. J.; Woldt, R. *Angew. Chem., Int. Ed. Engl.* **1980**, *19*, 390.
(2) Kaminsky, W.; Kulper, K.; Brintzinger, H. H.; Wild, F. R. W. P. *Angew. Chem., Int. Ed. Engl.* **1985**, *24*, 507.
(3) Ewan, J. A.; Jones, R. L.; Razavi, J. A. *J. Am. Chem. Soc.* **1988**, *110*, 6255.
(4) Shapiro, P. J.; Bunel, E.; Schaefer, W. P.; Bercaw, J. E. *Organometallics* **1990**, *9*, 867.
(5) Stevens, J. C.; Timmers, F. J.; Wilson, D. R.; Schmidt, G. F.; Nickias, P. N.; Rosen, R. K.; Knight, G. W.; Lai, S. Y. (Dow) European Patent Application EP-416-815-A2, March 13, 1991.
(6) Canich, J. A. (Exxon) European Patent Application EP-420-436-A1, April 4, 1991.
(7) Okuda, J. *Chem. Ber.* **1990**, *123*, 1649.
(8) Hughes, A. K.; Meetsma, A.; Teuben, J. A. *Organometallics* **1993**, *12*, 1936.
(9) Mu, Y.; Piers, W. E.; MacGillivray, L. R.; Zaworotko, M. J. *Polyhedron* **1995**, *14*, 1.
(10) Anderson, R. A. *Inorg. Chem.* **1979**, *18*, 2928.
(11) Canich, J. A.; Turner, H. W. (Exxon) PCT Int. Appl. WO 92/12162, July 23, 1992.
(12) Bürger, H.; Wiegel, K.; Thewalt, U.; Schomburg, D. *J. Organomet. Chem.* **1975**, *87*, 301.
(13) Brauer, D. J.; Bürger, H.; Wiegel, K. *J. Organomet. Chem.* **1978**, *150*, 215.
(14) Bürger, H.; Beiersdorf, D. *Z. Anorg. Allg. Chem.* **1979**, *459*, 111.
(15) Bürger, H.; Geschwandtner, W.; Liewald, G. R. *J. Organomet. Chem.* **1983**, *259*, 145.
(16) Herrmann, W. A.; Denk, M.; Albach, R. W.; Behm, J.; Herdtweck, E. *Chem. Ber.* **1991**, *124*, 683.
(17) Guérin, F.; McConville, D. H.; Vittal, J. J. *Organometallics* **1995**, *14*, 3154.
(18) See the Supporting Information for experimental and spectroscopic details.
(19) Bradley, D. C.; Thomas, I. M. *Proc. Chem. Soc., London* **1959**, 225.
(20) (BDAP)Zr(NMe$_2$)$_2$ (**2**): ^{1}H NMR δ 7.20 (m, 6H, Ar), 3.78 (sept, 4H, C*H*Me$_2$), 3.55 (m, 4H, NCH_2), 2.64 (s, 12H, N*Me*$_2$), 2.44 (m, 2H, NCH$_2$CH_2), 1.34 (d, 12H, CH*Me*$_2$), 1.32 (d, 12H, CH*Me*$_2$); ^{13}C{^{1}H} NMR δ 146.4, 145.8, 125.2, 124.1, 59.1, 41.8, 32.3, 28.3, 26.2, 25.0. Anal. Calcd for C$_{31}$H$_{52}$N$_4$Zr: C, 65.09; H, 9.16; N, 9.79. Found: C, 64.75; H, 9.19; N, 9.65.
(21) With the exception of **5b**, the proton NMR spectra of compounds **2–5** display temperature-independent signals for diastereotopic isopropyl methyl groups.

0276-7333/95/2314-5478$09.00/0

Scheme 1. Alkylation of Compound 4[a]

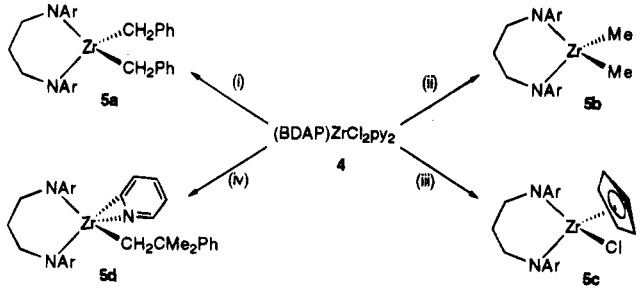

[a] Reagents and conditions: (i) 2 equiv of $PhCH_2MgCl$, Et_2O, −20 °C to room temperature, 18 h; (ii) 2 equiv of MeMgCl, Et_2O, −20 °C to room temperature, 18 h; (iii) 1 equiv of NaCp(DME), toluene, room temperature, 18 h; (iv) 2 equiv of $PhMe_2CCH_2MgCl$, THF, −20 °C to room temperature 18 h.

$$\underset{\mathbf{2}}{(BDAP)Zr(NMe_2)_2} + 2[Me_2NH_2]Cl \xrightarrow[-4HNMe_2]{py/CH_2Cl_2/-78\text{ to }+25\text{ °C}} \underset{\mathbf{4}}{(BDAP)ZrCl_2(py)_2} \quad (3)$$

The ^1H NMR spectrum of compound **4** displays a downfield shift for the ortho protons and an upfield shift for the meta and para protons of the coordinated pyridine.[18] The C_{2v} symmetry of compound **4** necessitates a *cis,trans* arrangement (as opposed to *cis,cis*) of the chlorides and pyridines about zirconium; however, the specific arrangement is not possible to deduce from the available spectroscopic data.

With the aim of preparing zirconium alkyl derivatives, the reaction of compound **4** with various alkylating reagents has been investigated (Scheme 1). The addition of 2 equiv of $PhCH_2MgCl$ to an ether suspension of compound **4** yields the formally 12-electron dibenzyl complex $(BDAP)Zr(CH_2Ph)_2$ (**5a**). The proton NMR spectrum[22] of complex **5a** displays a resonance at 1.95 ppm for the benzylic protons; however, more interestingly the ortho protons of the C_6H_5 ring appear as a high-field doublet at 6.65 ppm. In the carbon NMR spectrum, the $Zr-CH_2Ph$ resonance is observed at 64.2 ppm with $^1J_{C-H}$ = 124 Hz. Although the coupling constant for the CH_2Ph group is low, these data are consistent[23] with some η^2-benzyl character in the bonding with zirconium.[8,24-28] Perhaps the steric bulk of the BDAP ligand prevents the close approach of the ipso carbon to zirconium, thus lowering the observed C−H coupling constant.

The white crystalline dimethyl derivative $(BDAP)ZrMe_2$ (**5b**) was isolated from the reaction of compound **4** with 2 equiv of MeMgBr. The ^1H and $^{13}C\{^1H\}$ NMR spectra[29] of complex **5b** display a $Zr-CH_3$ resonance at 0.42 ppm and a $Zr-CH_3$ signal at 39.9 ppm. These data are comparable to those for the closely related complex $[(Me_3Si)_2N]_2ZrMe_2$ ($Zr-CH_3$, δ 0.94 ppm; $Zr-CH_3$, δ 48.8 ppm)[10] and others.[30-32] Additionally, the proton NMR spectrum of the dimethyl derivative **5b** is temperature-dependent. Above 35 °C the resonances attributed to the diastereotopic isopropyl methyl groups of the BDAP ligand sharpen to a single resonance, which we interpret as rapid rotation about the $N-C_{ipso}$ bond.

Compound **4** reacts with 1 equiv of NaCp(DME)[33] to yield the 16-valence-electron cyclopentadienyl complex $(BDAP)Zr(\eta^5\text{-Cp})Cl$ (**5c**). The proton and carbon NMR spectra[18] of compound **5c** are consistent with a pseudotetrahedral geometry and local C_s symmetry about zirconium. The remaining chloride in complex **5c** can be metathesized with alkylating reagents such as MeMgBr, $PhCH_2MgCl$, and $LiCH_2SiMe_3$ to afford the alkyl derivatives $(BDAP)Zr(\eta^5\text{-Cp})R$ (R = Me, CH_2Ph, CH_2SiMe_3).[34] The local C_s symmetry is retained in these compounds.

The reaction of the dichloride complex **4** with 2 equiv of $PhMe_2CCH_2MgCl$ in THF did not give the anticipated dineophyl complex but rather the η^2-pyridyl compound $(BDAP)Zr(\eta^2(N,C)\text{-}NC_5H_4)(CH_2CMe_2Ph)$ (**5d**). Spectroscopic data[35] suggest that compound **5d** has C_s symmetry, as evidenced by the AB pattern observed for the BDAP methylene protons (NCH_2 and NCH_2CH_2). The ^1H NMR resonances for the η^2-pyridyl moiety are comparable to those for other known complexes.[36-38] We have observed nearly identical η^2-pyridyl resonances (by ^1H NMR) in the reaction of compound **4** with 2 equiv of $LiCH_2SiMe_3$ but were unable to isolate pure product. We are exploring the use of other bases to stabilize the "$(BDAP)ZrCl_2$" fragment.

Colorless single crystals of **5d** suitable for an X-ray analysis were grown from a saturated pentane solution at −30 °C.[39] The molecular structure of complex **5d** and selected bond distances and angles are shown in Figure 1. Overall the structure is best described as a capped tetrahedron with the pyridyl nitrogen occupying the

(22) $(BDAP)Zr(CH_2Ph)_2$ (**5a**): ^1H NMR δ 7.19 (m, 6H, Ar), 7.01 (tt, 4H, Ph), 6.82 (tt, 4H, Ph), 6.65 (dd, 2H, Ph), 3.78 (sept, 4H, $CHMe_2$), 3.49 (m, 2H, NCH_2), 2.31 (m, 2H, NCH_2CH_2), 1.95 (s, 2H, CH_2Ph), 1.32 (d, 12H, $CHMe_2$), 1.27 (d, 12H, $CHMe_2$); $^{13}C\{^1H\}$ NMR δ 145.9, 145.1, 145.0, 130.1, 126.6, 126.5, 124.7, 122.7, 64.2 (CH_2Ph, $^1J_{CH}$ = 124 Hz), 58.8, 29.1, 28.4, 26.6, 25.1. Anal. Calcd for $C_{41}H_{54}N_2Zr$: C, 73.93; H, 8.17; N, 4.21. Found: C, 73.54; H, 8.33; N, 4.27.

(23) Latesky, S. L.; McMullen, A. K.; Niccolai, G. P.; Rothwell, I. P.; Huffman, J. C. *Organometallics* **1985**, *4*, 902.

(24) Wolczanski, P. T.; Bercaw, J. E. *Organometallics* **1982**, *1*, 793.

(25) Lubben, T. V.; Wolczanski, P. T.; Van Duyne, G. D. *Organometallics* **1984**, *3*, 977.

(26) Jordan, R. F.; Lapointe, R. E.; Baenziger, N.; Hinch, G. D. *Organometallics* **1990**, *9*, 1539.

(27) Crowther, D. J.; Jordan, R. F.; Baenziger, N.; Verma, A. *Organometallics* **1990**, *9*, 2574.

(28) Fryzuk, M. D.; Mao, S. S. H.; Duval, P. B.; Rettig, S. J. *Polyhedron* **1995**, *14*, 11.

(29) $(BDAP)ZrMe_2$ (**5b**): ^1H NMR (20 °C) δ 7.17 (m, 6H, Ar), 3.75 (sept, 4H, $CHMe_2$), 3.47 (m, 2H, NCH_2), 2.25 (m, 2H, NCH_2CH_2), 1.36 (m, 12H, $CHMe_2$), 1.34 (m, 12H, $CHMe_2$), 0.42 (s, 6H, $ZrMe_2$), $^{13}C\{^1H\}$ NMR (20 °C) δ 145.6, 143.2, 126.8, 124.5, 59.4, 39.9 ($ZrMe_2$), 29.9, 28.6, 25.8. Anal. Calcd for $C_{29}H_{46}N_2Zr$: C, 67.78; H, 9.02; N, 5.45. Found: C, 68.04; H, 9.27; N, 5.40.

(30) Anderson, R. A. *Inorg. Chem.* **1979**, *18*, 1724.

(31) Jordan, R. F.; Dasher, W. E.; Echols, S. F. *J. Am. Chem. Soc.* **1986**, *108*, 1718.

(32) Cummins, C. C.; Baxter, S. M.; Wolczanski, P. T. *J. Am. Chem. Soc.* **1988**, *110*, 8731.

(33) Smart, J. C.; Curtis, C. J. *Inorg. Chem.* **1977**, *16*, 1788.

(34) Scollard, J. D.; McConville, D. H. To be published.

(35) $(BDAP)Zr(\eta^2(N,C)\text{-}NC_5H_4)(CH_2CMe_2Ph)$ (**5d**): ^1H NMR δ 7.33–7.10 (m, 10H, Ar, Ph, py), 6.88 (m, 1H, Ph), 6.78 (tt, 1H, py), 6.72 (m, 2H, Ph), 6.35 (ddd, 1H, py), 4.26 (sept, 2H, $CHMe_2$), 3.82 (m, 2H, NCH_2), 3.58 (m, 2H, NCH_2), 3.26 (sept, 2H, $CHMe_2$), 2.76 (m, 1H, NCH_2CH_2), 2.64 (m, 1H, NCH_2CH_2), 1.70 (s, 2H, CH_2CMe_2Ph), 1.59 (d, 6H, $CHMe_2$), 1.47 (d, 6H, $CHMe_2$), 1.18 (d, 6H, $CHMe_2$), 1.17 (s, 6H, CMe_2Ph), 0.64 (d, 6H, $CHMe_2$); $^{13}C\{^1H\}$ NMR δ 153.9, 149.7, 145.5, 144.6, 144.5, 134.8, 129.3, 128.1, 125.3, 125.1, 125.1, 124.7, 124.0, 123.8, 68.0, 59.6, 41.0, 35.5, 31.7, 28.3, 28.1, 27.0, 26.6, 25.2, 24.1. Anal. Calcd for $C_{42}H_{57}N_3Zr$: C, 72.57; H, 8.26; N, 6.04. Found: C, 72.85; H, 8.61; N, 5.95.

(36) Thompson, M. E.; Baxter, S. M.; Bulls, A. R.; Burger, B. J.; Nolan, M. C.; Santarsiero, B. D.; Schaefer, W. P.; Bercaw, J. E. *J. Am. Chem. Soc.* **1987**, *109*, 203.

(37) den Haan, K. H.; Wielstra, Y.; Teuben, J. H. *Organometallics* **1987**, *6*, 2053.

(38) Jordan, R. F.; Taylor, D. F.; Baenziger, N. C. *Organometallics* **1990**, *9*, 1546.

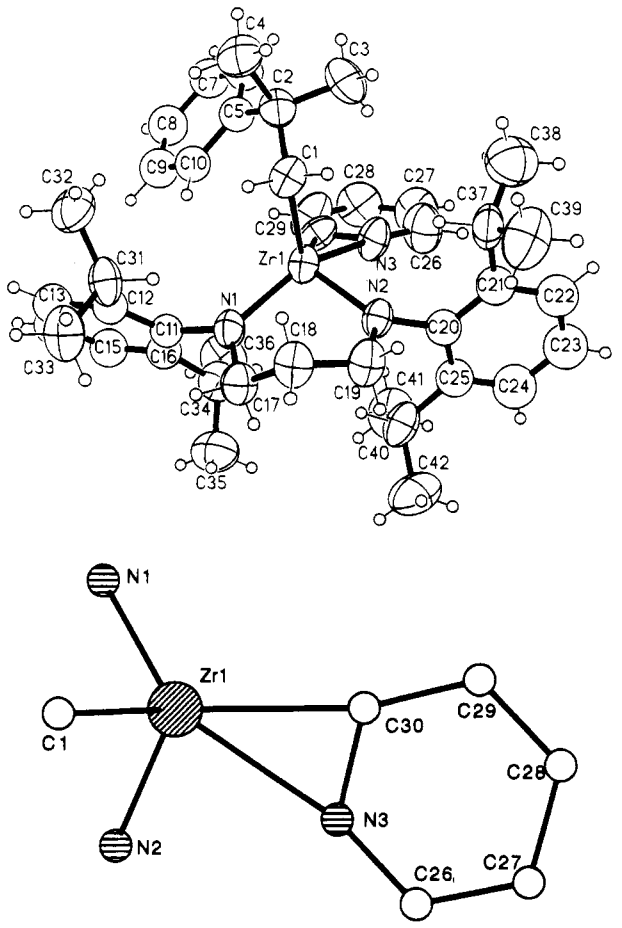

Figure 1. (top) ORTEP drawing of **5d**. (bottom) Chem 3D Plus representation of the core of **5d**. Selected bond distances (Å) and angles (deg): Zr1–N1 = 2.050(9), Zr1–N2 = 2.031(9), Zr–C1 = 2.268(12), Zr1–C30 = 2.219(12), Zr1–N3 = 2.260(10); N1–Zr1–N2 = 95.4(4), C30–Zr1–C1 = 113.2(4), N1–Zr1–C1 = 103.9(4), N1–Zr1–C30 = 120.8(4).

capping position. The Zr1–N3–C30 ring is structurally similar to the Zr–N–C ring in the cationic complex [Cp_2-$Zr(\eta^2$-picolyl)(PMe_3)][BPh_4].[38] Each amide donor in **5d** is sp^2-hybridized, as evidenced by the sum of the angles about each nitrogen (N1, 360.0°; N2, 359.8°). The solid-state C_1 symmetry of compound **5d** coupled with the spectroscopically observed C_s symmetry in solution suggests that rapid rotation about the Zr1–C30 bond is occurring on the NMR time scale.

It is interesting that the pyridyl complex **5d** is formed only with a large alkylating reagent. A preliminary investigation into the mechanism of formation of compound **5d** is presented.[40] Two possible pathways for this reaction are depicted in Scheme 2. Substituting (BDAP)-$ZrCl_2(d_5$-py$)_2$ for (BDAP)$ZrCl_2$(py)$_2$ readily discriminates between these two mechanisms. Path A outlines the formation of the pyridyl complex via an intermediate zirconium alkylidene[41] complex. Transferring a deuterium from coordinated d_5-pyridine to the alkylidene yields a d_1-neophyl group. Alternatively (path B), the pyridyl complex could result from neophyl abstraction of deuterium from coordinated d_5-pyridine.[38] In this case the retained neophyl group would show no deuterium incorporation. The reaction of (BDAP)$ZrCl_2(d_5$-py$)_2$ with 2 equiv of $PhMe_2CCH_2MgCl$ yields a single pyridyl species, (BDAP)$Zr(\eta^2(N,C)$-$NC_5D_4)(CH_2CMe_2Ph)$ (***d*₄-5d**) (as confirmed by NMR spectroscopy), suggesting that the mechanism in path B is operative.

Scheme 2. Possible Mechanisms for the Formation of Compound 5d

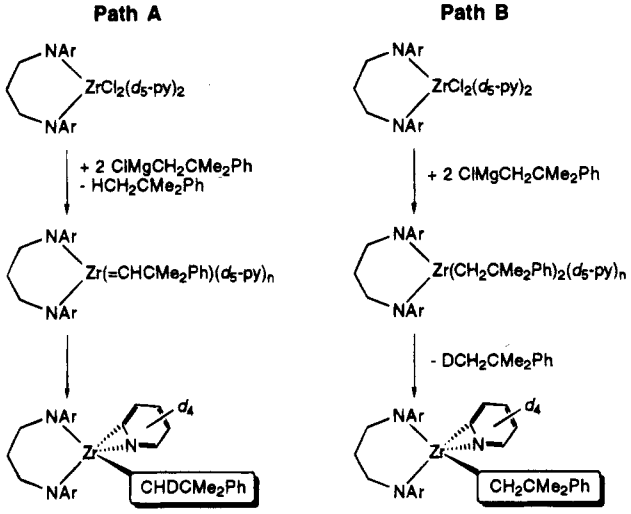

The new chelating diamide ligand BDAP has been shown to stabilize d^0 dialkyl derivatives of zirconium. The rigid coordination of the ligand and enforced location of the aryl isopropyl groups creates a "pocket" opposite the ligand and necessarily protects the metal above and below the zirconium–diamide plane. We are currently exploring the catalytic olefin polymerization chemistry of putative cationic derivatives of compounds **5a,b** (e.g., [(BDAP)ZrR]$^+$). In addition, we are preparing other chelating diamide complexes of groups 4 and 5 with different substitution on the arene ring.

Acknowledgment. This research was supported by the NSERC (Canada) and a University of Western Ontario Internal Research Grant (to D.H.M.).

Supporting Information Available: Text giving experimental details for compounds **1–5** and tables of crystal data, data collection details, final positional parameters, final thermal parameters, and all bond distances and angles (14 pages). Ordering information is given on any current masthead page.

OM950534M

(39) X-ray data for **5d**. Data were collected at 25 °C on a Siemens P4 diffractometer using graphite-monochromated Mo Kα radiation. A total of 6209 reflections were collected in the θ range 2.0–23°, of which 5405 were independent (R_{int} = 0.0558). The structure was solved by a combination of Patterson and difference Fourier techniques. Non-hydrogen atoms were refined anisotropically except for two phenyl ring carbon atoms. In the final least-squares refinement cycle on F^2, the model converged at R = 0.0951, R_w = 0.2287, and GOF = 1.014 for 2999 reflections with $F_o \geq 4\sigma(F_o)$ and 289 parameters. Crystal data are a = 10.146(2) Å, b = 12.336(2) Å, c = 16.723(2) Å, α = 81.00(6)°, β = 74.99(10)°, γ = 76.24(9)°, V = 1953.6(6) Å^3, space group $P\bar{1}$, Z = 2, mol wt 695.13, and ρ(calcd) = 1.182 g/cm^3.

(40) We are pursuing routes to base-stabilized alkylidenes of the form (BDAP)Zr(=CHR)(L), (L = PR_3). We thank a reviewer for suggesting the deuterium labeling experiment.

(41) Fryzuk, M. D.; Mao, S. S. H.; Zaworotko, M. J.; MacGillivray, L. R. *J. Am. Chem. Soc.* **1993**, *115*, 5336.

A Puckered Titanacyclobutane Fragment as the Result of a C–C Coupling between a Fulvene and a 2-Methylallyl Ligand: Structure of $(\eta^5\text{-}C_5Me_5)[\eta^5{:}\eta^2\text{-}C_5Me_4CH_2CMe(CH_2)_2]Ti$

Peter H. P. Brinkmann, Marc-H. Prosenc, and Gerrit A. Luinstra*

Department of Chemistry, University of Konstanz, Postfach 5560 M738, D-78343 Konstanz, Germany

Received August 1, 1995[⊗]

*Summary: Reaction of $(C_5Me_5)(C_5Me_4CH_2)TiCl$ and (2-methylallyl)MgBr leads to $(\eta^5\text{-}C_5Me_5)[\eta^5{:}\eta^2\text{-}C_5Me_4CH_2CMe(CH_2)_2]Ti$ (**2**), a bent metallocene complex wherein a four-membered metallacycle is tethered to a tetramethyl Cp ligand by a methylene bridge. Thermolysis of **2** gives a new fulvene compound: $(C_5Me_4CH_2)(\eta^5{:}\eta^1\text{-}C_5Me_4CH_2CMe_2CH_2)Ti$ (**4**).*

Fulvene complexes of the early transition metals are easily accessible through thermolysis of alkyl or hydride complexes.[1] These very reactive organometallics undergo coupling reactions with oxygen- or nitrogen-containing unsaturated substrates (ketones or nitriles) to yield functionalized Cp ligands, which are tethered to the metal by an alkoxide or amide bridge.[2] Asymmetric ketones are inserted with high regioselectivity resulting in one pair of diastereomers only.[2ab,3] It would be desirable to extend this high-yield C–C coupling to a wider range of unsaturated reactants. Unfortunately, coupling of the fulvene exo methylene group with olefins or alkynes to give either alkyl or alkenyl bridges has not been observed, except for the insertion of butadiene in the Zr–C of the cationic fulvene complex $(C_5Me_5)[C_5Me_4CH_2]Zr$.[4] We have been studying allyl(fulvene)-titanium complexes of generic type $Cp^*FvTi(\eta^3\text{-}CH_2CR{=}CH_2)$[5] ($Cp^*$, $\eta^5\text{-}C_5Me_5$; Fv, $C_5Me_4CH_2$) with a view toward the possibility that allyl ligands—with orbitals of comparable symmetry and energy as fulvene fragments—might engage in a reaction with the fulvene exocyclic methylene group.[6]

The orange $Cp^*FvTi(\eta^3\text{-}CH_2CH{=}CH_2)$ (**1**), which contains an η^3-coordinated allyl fragment, is not stable at room temperature: it slowly isomerizes to $Cp^*FvTi(\eta^1\text{-}CH{=}CHMe)$, apparently by a C–H activation of the central carbon atom.[5] To explore this type of C–H activation further, we tried to prepare the corresponding 2-methylallyl derivative, $Cp^*FvTi(\eta^3\text{-}CH_2CMe{=}CH_2)$, by reaction of $Cp^*FvTiCl$ and $CH_2{=}CMeCH_2MgBr$. A red compound (**2**) was obtained, which showed all the anticipated NMR signals for $Cp^*FvTi(\eta^3\text{-}CH_2CMe{=}CH_2)$.[7] The fulvene exocyclic methylene carbon has, surprisingly, a $^1J(C-H)$ of 132 Hz, characteristic for an sp^3-hybridized center, rather than an sp^2 carbon as in **1**, where a coupling constant of 153 Hz was found. A determination of the molecular structure by X-ray crystallography (Figure 1[8]) revealed that a C–C coupling had taken place between the fulvene exocyclic methylene carbon and the central carbon of the methylallyl fragment (Scheme 1), resulting in a tethered metallacyclobutane ligand, $\eta^5{:}\eta^2\text{-}C_5Me_4CH_2CMe(CH_2)_2$. The binding of the new ligand yields a highly symmetric molecule: a nearly perfect plane is formed by C(1), C(11), C(24), C(22), and Ti (deviation < 0.0026 Å). The distances of C(23) and C(21) to that plane are about equal (1.17 and 1.18 Å). The Ti–C distances of about 2.19 Å are in the usual range.[9] The Cp* ligand is planar (deviation from least square plane < 0.0013 Å) with the ring methyl groups pushed slightly out of the plane of the ring (deviation < 0.33 Å for C(16)–C(20)).[10] The same is observed for the tetramethylneopentadiyl-substituted Cp ring (deviation of the ring carbon atoms from the least square plane < 0.011 Å); the ring methyl groups are pushed away from the metal (deviation < 0.28 Å), except for C(11) which points toward the metal (by 0.33 Å). In this way C(23) and C(21) can bind in

[⊗] Abstract published in *Advance ACS Abstracts,* November 1, 1995.

(1) (a) Bercaw, J. E.; Marvich, R. H.; Bell, L. G.; Brintzinger, H.-H. *J. Am. Chem. Soc.* **1972**, *94*, 1219. (b) Schock, L. E.; Brock, C. P.; Marks, T. J. *Organometallics* **1987**, *6*, 232. (c) Den Haan, K.; Teuben, J. H. *J. Chem. Soc., Chem. Commun.* **1986**, 682. (d) Luinstra, G. A.; Teuben, J. H. *J. Am. Chem. Soc.* **1992**, *114*, 3361. (e) Booij, M.; Meetsma, A.; Teuben, J. H. *Organometallics* **1991**, *10*, 3246.

(2) (a) Pattiasina, J. W.; Hissink, C. E.; De Boer, J. L.; Meetsma, A.; Teuben, J. H.; Spek, A. *J. Am. Chem. Soc.* **1985**, *107*, 7758. (b) Erker, G.; Korek, U. Z. *Naturforsch.* **1989**, *44B*, 1593. (c) Fandos, R.; Meetsma, A.; Teuben, J. H. *Organometallics* **1991**, *10*, 2665. (d) Fandos, R.; Meetsma, A.; Teuben, J. H. *Organometallics* **1991**, *10*, 1637. (e) Pattiasina, J. W. Thesis, University of Groningen, 1989.

(3) Luinstra, G. A.; Dros, A. C.; Eshuis, J. W.; Meetsma, A.; Teuben, J. H. Manuscript in preparation.

(4) Horton, A. D. *Organometallics* **1992**, *11*, 3271.

(5) Brinkmann, P. H. P.; Luinstra, G. A. Manuscript in preparation.

(6) The bonding of the fulvene ligand can be described in either of two ways: as a 6π, neutral ligand (η^6-FvM) or as a dianionic, σ,π ligand (η^5,η^1-FvM^{2+}). The formal oxidation state of the metal thus differs by two. Accordingly, the reaction between the exocyclic CH_2 group and an unsaturated substrate is an oxidative coupling or an insertion, respectively.

(7) ^1H NMR (250 MHz, benzene-d_6): δ = 1.17 (d, $^2J(H-H)$ = 7.8 Hz, 2H; CH_2), 1.308 (s, 3H; Me), 1.31 (d, $^2J(H-H)$ = 7.8 Hz, 2H; CH_2), 1.6 (s, 6H; 2Me), 1.68 (s, 15H; Cp*), 1.87 (s, 6H; 2 Me), 2.6 (s, 2H; CH_2). Yield: 490 mg (1.31 mmol, 83%). ^{13}C NMR (62.9 MHz, benzene-d_6): δ = 11.3 and 15.1 (q, $^1J(C-H)$ = 126 Hz; Me), 12.2 (q, $^1J(C-H)$ = 126 Hz; Cp*), 26.1 (s; C metallacycle), 29.1 (q, $^1J(C-H)$ = 125 Hz; Me), 37.4 (t, $^1J(C-H)$ = 128 Hz; CH_2–Ti), 75.4 (t, $^1J(C-H)$ = 132 Hz; CH_2), 118.2 (s; Cp*), 115 and 117.6 and 119.3 (s; C ring).

(8) Crystal data and structure refinement for **2**: $C_{24}H_{36}Ti$, 0.3 × 0.2 × 0.15 mm, monoclinic, $P2_1/c$, a = 12.476(6) Å, b = 8.657(4) Å, c = 19.608(9) Å, β = 90.61(4)°, V = 2118(2) Å^3, Z = 4, 1.63 < θ < 26.52°, Mo Kα λ = 0.710 73 Å, Wyckoff type scan, T = 293 K, 4393 reflections collected, 4214 independent with $F > 2\sigma$, 4209 reflections refined, data collection with Siemens Nicolet P3R3, solution by direct methods using SHELXL-93 software, 226 parameters, all non-hydrogens refined anisotropically, hydrogens refined by a riding model, R = 0.0766, wR^2 = 0.1894, full-matrix least-squares treatment on F^2, residual electron density of 1.123 e Å^{-3}.

(9) (a) Atwood, J. L.; Hunter, W. E.; Alt, H.; Rausch, M. D. *J. Am. Chem. Soc.* **1976**, *98*, 2454. (b) Atwood, J. L.; Hunter, W.; Hrncir, D. C.; Samuel, E.; Alt, H.; Rausch, M. D. *Inorg. Chem.* **1975**, *14*, 1757. (c) Green, M. L.; Hazel, N. J.; Grebenik, P. D.; Mtetwa, V. S. B.; Prout, K. *J. Chem. Soc., Chem. Commun.* **1983**, 356. (d) Gómez-Sal, M. P.; Mena, M.; Royo, P.; Serrano, R. *J. Organomet. Chem.* **1988**, *358*, 147.

(10) This has been noticed before: Pattiasina, J. W.; Heeres, H. J.; van Bolhuis, F.; Meetsma, A.; Teuben, J. H.; Spek, A. L. *Organometallics* **1987**, *6*, 1004 and references therein.

0276-7333/95/2314-5481$09.00/0

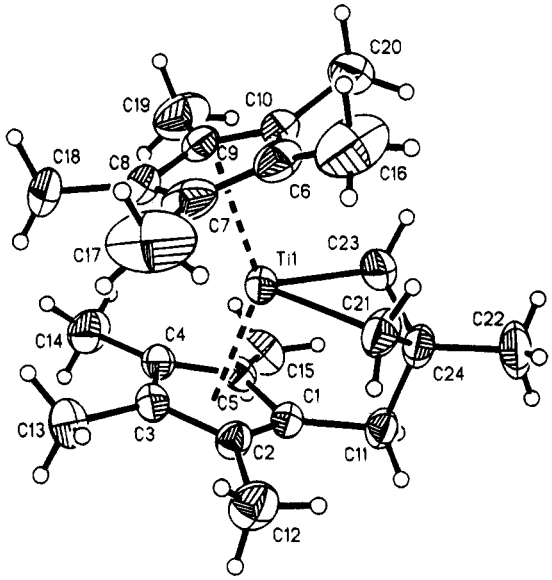

Figure 1. ORTEP drawing of **2**, showing thermal ellipsoids (50% probability level). Selected bond lengths (Å): Ti–CE1 2.102, Ti–CE2 2.096, Ti–C(21) 2.190(5), Ti–C(23) 2.187(4), C(23)–C(24) 1.538, C(24)–C(21) 1.547(7), C(11)–C(24) 1.549(6), C(1)–C(11), 1.497(5). Selected bond angles (deg): C(23)–Ti–C(21) 65.3(2), Ti–C(21)–C(24) 88.4(3), C(21)–C(24)–C(23) 99.9(3), CE1–Ti–CE2 141.6 (CE1: centroid C(1) → C(5), CE2: C(6) → C(10)).

Scheme 1

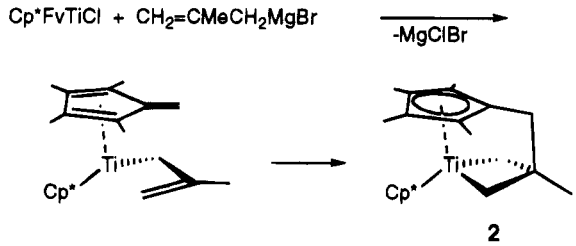

2

the equatorial plane (torsion angle CE2–Ti–C(21)–C(23) is 90.2°). In contrast to other structurally characterized titanacyclobutanes, which are planar,[11] a strongly puckered ring is found in **2** (the dihedral angle between Ti, C(21), C(23), C(24) is 44.4°).

Titanacyclobutanes may ring-open to give an olefin and a titanium carbene.[12] However no evidence for opening of the puckered metallacycle was found. Compound **2** does not react with but-2-yne, and no formation of an analog of Tebbe's reagent was observed when **2** was treated with dimethylaluminum chloride or with trimethylaluminum.[13]

When **2** is treated with 1 equiv of HCl in toluene, one Ti–C bond is cleaved selectively to yield Cp*[$C_5Me_4CH_2C(Me)_2CH_2$]TiCl (**3**). In the reaction of **2** with 2 equiv of HCl (−30 °C) the second Ti–C bond is cleaved as well to give Cp*($C_5Me_4CH_2CMe_3$)$_2$TiCl$_2$ (Scheme 2). This provides an attractive, high-yield route to mixed bent sandwich complexes of titanium.

Scheme 2

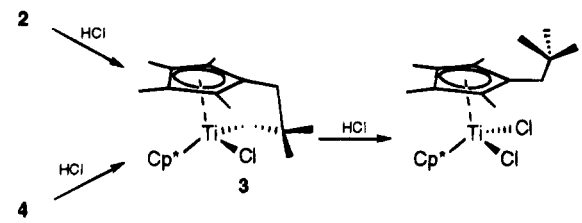

Scheme 3

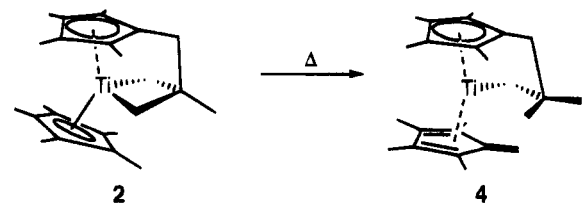

Thermolysis of **2** in toluene at 70 °C results in the formation of ($C_5Me_4CH_2$)Ti(η^5:η^1-$C_5Me_4CH_2CMe_2CH_2$) (**4**) (Scheme 3). Compound **4** was identified by its NMR spectra. In the ^{1}H NMR, 8 singlets are observed for the ring-bound methyl groups, one singlet of double intensity for the $CH_2C\mathit{Me}_2CH_2$ group, and three CH_2 groups with diastereotopic protons (each as doublet with ^2J(H–H) = 4, 11.6, and 13 Hz, for the fulvene methylene group, Ti–CH_2, and $C_5Me_4C\mathit{H}_2CMe_2$, respectively). After this thermal rearrangement, the molecule again has two reactive centers. Complex **4**, like **2**, reacts with HCl at low temperature to form **3** (Scheme 2).

It is unclear how the thermolysis of **2** proceeds. Cp*$_2$TiR$_2$ complexes (R = alkyl, aryl) usually decompose in a concerted $2_s + 2_s$ process, with the intermediate formation of a reactive species like a benzyne, or a carbene, which is formed by a ligand C–H abstraction reaction from either a Ti–Ph or Ti–alkyl entity in the equatorial plane.[1,14] In this case, such a pathway seems unlikely since no easily accessible C–H bonds are present in the equatorial plane. The detailed decomposition pathway is still under investigation.

Acknowledgment. Dr. A. Geyer and Ms. M. Cavegen are thanked for measurements of 2-D spectra. We thank Prof. H.-H. Brintzinger for useful discussions.

Supporting Information Available: Full details of the X-ray structure, including tables of atomic coordinates and *U* values, bond lengths, bond angles, and anisotropic displacement coefficients, and text giving details of the synthesis and characterization of complexes **3**, **4**, and Cp*($C_5MeCH_2CMe_3$)$_2$TiCl$_2$ (10 pages). Ordering information is given on any current masthead page.

OM950598X

(11) Lee, J. B.; Gajda, G. J.; Schaefer, W. P.; Howard, T. R.; Ikarariya, T.; Straus, D. A.; Grubbs, R. H. *J. Am. Chem. Soc.* **1981**, *103*, 7358. Beckhaus, R.; Flatau, S.; Trojanov, S.; Hofmann, P. *Chem. Ber.* **1992**, *125*, 291.

(12) (a) Straus, D. A.; Grubbs, R. H. *Organometallics* **1982**, *1*, 1658. (b) Anslyn, E. V.; Grubbs, R. H. *J. Am. Chem. Soc.* **1987**, *109*, 4880. (c) Katz, T. J. *Adv. Organomet. Chem.* **1977**, *16*, 283.

(13) Tebbe, F. N.; Parshall, G. W.; Reddy, G. S. *J. Am. Chem. Soc.* **1978**, *100*, 3611. Compound **2** does not react with Me_3Al. Reaction of **2** with 2 equiv of Me_2AlCl gave a complex NMR spectrum with no evidence for the formation of a vinylic entity. See: Ott, K. C.; Lee, J. B.; Grubbs, R. H. *J. Am. Chem. Soc.* **1982**, *104*, 2942.

(14) (a) McDade, C.; Green, J. C.; Bercaw, J. E. *Organometallics* **1982**, *1*, 1629. (b) Luinstra, G. A.; Teuben, J. H. *Organometallics* **1992**, *11*, 1793. (c) Luinstra, G. A. Thesis, University of Groningen, 1991.

Reversible C–C Bond Scission and C–H Bond Activation in the Butterfly Acetylide Clusters $Cp^*WOs_3(CO)_{11}(CCR)$ (R = Ph, Bu, CH_2OMe)

Yun Chi,*,† Pei-Chiun Su,† Shie-Ming Peng,*,‡ and Gene-Hsiang Lee‡

Departments of Chemistry, National Tsing Hua University, Hsinchu 30043, Taiwan, Republic of China, and National Taiwan University, Taipei 10764, Taiwan, Republic of China

Received September 18, 1995®

Summary: The tetranuclear acetylide compounds $Cp^*WOs_3(CO)_{11}(CCR)$ (R = Ph, Bu, CH_2OMe), depending on the substituents of the acetylide ligand, undergo reversible C–C bond scission and C–H activation to afford the carbido–alkylidyne cluster $Cp^*WOs_3(CO)_{10}(\mu_4\text{-}C)(\mu\text{-}CPh)$ and the carbido–vinylidene clusters $Cp^*WOs_3(CO)_9(\mu_4\text{-}C)(\mu\text{-}H)(\mu\text{-}CCHR')$ (R' = Pr, OMe), respectively.

The chemistry of metal acetylide complexes has been the subject of intense study in recent years.[1] Condensation with terminal alkynes,[2] phosphinoacetylenes,[3] and mononuclear acetylide complexes[4] has provided versatile synthetic entries for a variety of such complexes. Their successful synthesis has not only led to the observation of fascinating structural chemistry but also formed a basis for understanding the reactivity of chemisorbed acetylides on metal surfaces.[5] Attention is now focused on their novel chemical transformation, which requires multisite interaction of the polynuclear frameworks.[6] Of particular interest in this regard is the conversion between acetylides and alkylidyne carbides.[7] This transformation represents a possible pathway for the conversion of interstitial carbides to hydrocarbon fragments of higher carbon content, a process which has been recognized to play an important role in the CO reduction and activation of hydrocarbons on catalytic surfaces.[8] Here we report the results of our investigation on the reactivity of unique WOs_3 acetylide clusters which offers an informative comparison.

Scheme 1

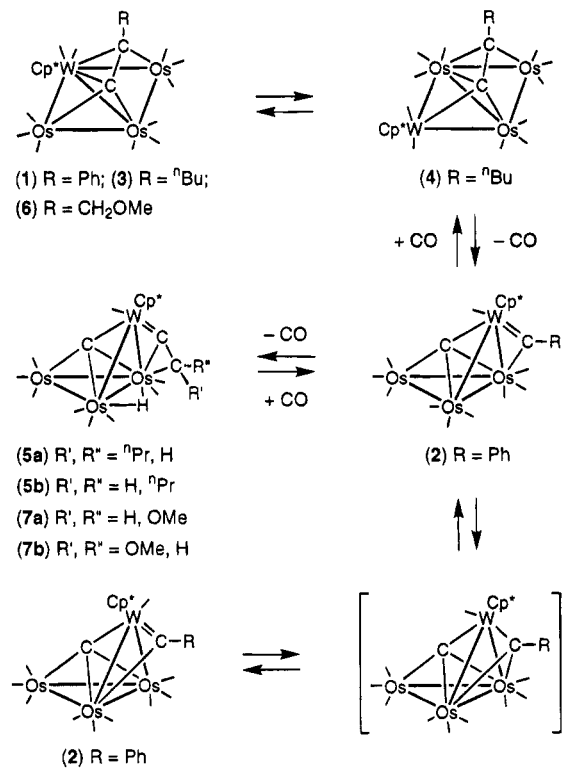

The butterfly cluster $Cp^*WOs_3(CO)_{11}(CCPh)$ (**1**), which contains a hinge W atom and a multisite-bound acetylide ligand (Scheme 1), was obtained directly from combination of the triosmium cluster $Os_3(CO)_{10}(NCMe)_2$ and the mononuclear acetylide complex $Cp^*W(CO)_3(CCR)$ according to the published method.[9] When a solution of **1** was allowed to react with 1.1 equiv of anhydrous Me_3NO in dichloromethane/acetonitrile solution at room temperature (30 min), followed by heating in refluxing toluene (10 min), a stable orange product (**2**) was formed in 80% yield, which was purified by chromatography followed by recrystallization from a

† National Tsing Hua University.
‡ National Taiwan University.
® Abstract published in *Advance ACS Abstracts,* November 15, 1995.

(1) (a) Nast, R. *Coord. Chem. Rev.* **1982,** *47,* 89. (b) Bruce, M. I.; Swincer, A. G. *Adv. Organomet. Chem.* **1983,** *22,* 59. (c) Bruce, M. I. *Chem. Rev.* **1991,** *91,* 197. (d) Akita, M.; Moro-oka, Y. *Bull. Chem. Soc. Jpn.* **1995,** *68,* 420.

(2) (a) Sappa, E.; Tiripicchio, A.; Braunstein, P. *Chem. Rev.* **1983,** *83,* 203. (b) Raithby, P. R.; Rosales, M. J. *Adv. Inorg. Chem. Radiochem.* **1985,** *29,* 169. (c) Rosenberg, E. *Polyhedron* **1989,** *8,* 383.

(3) (a) Doherty, S.; Corrigan, J. F.; Carty, A. J.; Sappa, E. *Adv. Organomet. Chem.* **1995,** *37,* 39. (b) Corrigan, J. F.; Taylor, N. J.; Carty, A. J. *J. Chem. Soc., Chem. Commun.* **1994,** 1769. (c) Sun, Y.; Taylor, N. J.; Carty, A. J. *Organometallics* **1992,** *11,* 4293. (d) Adams, C. J.; Bruce, M. I.; Skelton, B. W.; White, A. H. *Aust. J. Chem.* **1993,** *46,* 1811. (e) Adams, C. J.; Bruce, M. I.; Skelton, B. W.; White, A. H. *Inorg. Chem.* **1992,** *31,* 3336.

(4) (a) Yasufuku, K.; Aoki, K; Yamazaki, H. *Bull. Chem. Soc. Jpn.* **1975,** *48,* 1616. (b) Boyar, E.; Deeming, A. J.; Felix, M. S. B.; Kabir, S. E.; Adatia, T.; Bhusate, R.; McPartlin, M.; Powell, H. R. *J. Chem. Soc., Dalton Trans.* **1989,** 5. (c) Albiez, T.; Powell, A. K.; Vahrenkamp, H. *Chem. Ber.* **1990,** *123,* 667. (d) Bernhardt, W.; Vahrenkamp, H. *J. Organomet. Chem.* **1988,** *355,* 427. (e) Roland, E.; Bernhardt, W.; Vahrenkamp, H. *Chem. Ber.* **1986,** *119,* 2566. (f) Chi, Y. *J. Chin. Chem. Soc.* **1992,** *39,* 591.

(5) (a) Muetterties, E. L.; Rhodin, T. N.; Band, E.; Brucker, C. F.; Pretzer, W. R. *Chem. Rev.* **1979,** *79,* 91. (b) Albert, M. R.; Yates, J. T., Jr. *The Surface Scientist's Guide to Organometallic Chemistry*; American Chemical Society: Washington, DC, 1987.

(6) Sappa, E.; Tiripicchio, A.; Carty, A. J.; Toogood, G. E. *Prog. Inorg. Chem.* **1987,** *35,* 437.

(7) (a) Carty, A. J. *Pure Appl. Chem.* **1982,** *54,* 113. (b) Carty, A. J.; Taylor, N. J.; Sappa, E.; Tiripicchio, A.; Camellini, M. T. *Organometallics* **1991,** *10,* 1907. (c) Chiang, S.-J.; Chi, Y.; Su, P.-C.; Peng, S.-M.; Lee, G.-H. *J. Am. Chem. Soc.* **1994,** *116,* 11181. (d) Blenkiron, P.; Taylor, N. J.; Carty, A. J. *J. Chem. Soc., Chem. Commun.* **1995,** 327.

(8) (a) Tachikawa, M.; Muetterties, E. L. *J. Am. Chem. Soc.* **1980,** *102,* 4541. (b) Hriljac, J. A.; Swepston, P. N.; Shriver, D. F. *Organometallics* **1985,** *4,* 158.

(9) (a) Chi, Y.; Lee, G.-H.; Peng, S.-M.; Wu, C.-H. *Organometallics* **1989,** *8,* 1574. (b) Chi, Y.; Wu, C.-H.; Peng, S.-M.; Lee, G.-H. *Organometallics* **1990,** *9,* 2305.

0276-7333/95/2314-5483$09.00/0

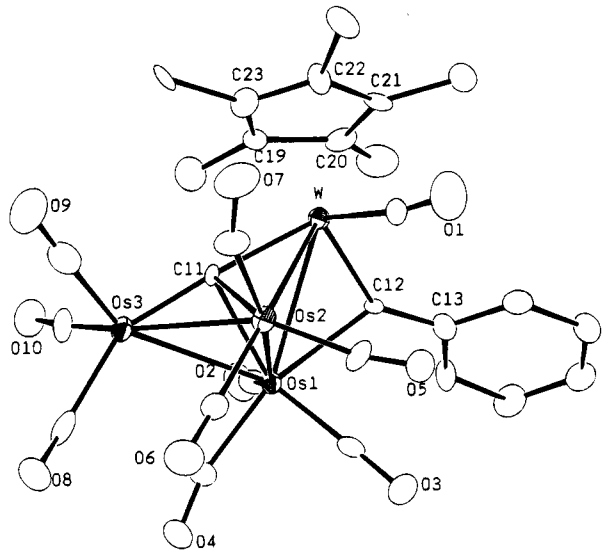

Figure 1. Molecular structure of **2** and the atomic numbering scheme. Selected bond lengths (Å): W–Os(1) = 2.896(3), W–Os(2) = 2.974(3), Os(1)–Os(2) = 2.751(2), Os(1)–Os(3) = 2.899(2), Os(2)–Os(3) = 2.850(3), W–C(11) = 2.10(4), Os(1)–C(11) = 2.22(4), Os(2)–C(11) = 2.12(4), Os(3)–C(11) = 1.81(4), W–C(12) = 1.89(3), Os(1)–C(12) = 2.22(4). Selected bond angles (deg): W–C(11)–Os(3) = 175(3), Os(1)–C(11)–Os(2) = 79(1), W–C(12)–C(13) = 142(3).

mixture of chloroform and methanol.[10] The stoichiometry was initially confirmed by FAB mass analysis, which gave a parent ion at *m/z* 1276, showing that this complex contains one CO less than its precursor. The loss of CO ligand strongly suggested the formation of carbide and alkylidyne species via fission of the acetylide C–C bond. Thus, an X-ray diffraction study was carried out to reveal the identity of this compound.

Crystals of **2** contain two crystallographically distinct, but structurally similar, molecules in the asymmetric unit.[11] A perspective view of one of these molecules is depicted in Figure 1. The overall structure consists of a butterfly WOs_3 arrangement with an acute dihedral angle (99.5(1)°). The W atom is located at a wingtip position. A similar skeletal arrangement has been observed in the carbide clusters $CpWRu_3(CO)_{11}(\mu_4\text{-}C)(\mu\text{-}H)$[12] and $CpWOs_3(CO)_{11}(\mu_4\text{-}C)(\mu\text{-}SMe)$[13] and in the carbonyl clusters $Cp^*MRu_3(CO)_{11}(\mu_4\text{-}CO)(\mu\text{-}H)$ (M = Mo, W), with a quadruply bridging CO ligand.[14] The carbido atom C(11), liberated from the acetylide fragment, is bound to the cluster with short M(wingtip)–C distances (average 1.96(4) Å) and long M(hinge)–C distances (average 2.17(4) Å), typical for such carbides in a butterfly environment.[15] The alkylidyne ligand bridges the W–Os(1) edge with angles W–C(12)–C(13) = 142(3)°, Os(1)–C(12)–C(13) = 127(3)°, and W–C(12)–Os(1) = 89(1)°. Since these structural features invoke a trigonal-planar carbon atom, a substantial degree of W–C double-bond interaction is indicated (W–C(12) = 1.89(3) Å).

In accordance with the solid-state structure, the ^{13}C NMR spectrum showed two signals at δ 357.0 (J_{W-C} = 104 Hz) and 293.9 (J_{W-C} = 150 Hz), which were assigned to the carbido and alkylidyne carbon atoms, respectively. Moreover, the ^{13}C NMR spectrum recorded at 253 K showed one W–CO signal at δ 226.7 and eight Os–CO resonances in the region δ 187.2–164.9 with one signal at δ 182.1 possessing intensity equivalent to two CO ligands. When the temperature was raised to 338 K, the signal at δ 164.9 broadened substantially and the seven Os–CO signals in the range δ 187.2–173.3 coalesced to one broad signal centered at δ 181.3. Although this exchange pattern supports the onset of alkylidyne migration from one W–Os edge to the second via the formation of a μ_3-alkylidyne intermediate on the WOs_2 plane (Scheme 1), it is possible that this migration requires a higher reaction temperature.

The related *n*-butyl-substituted acetylide complex **3** and its isomer **4**, in which the W atom resides at the wingtip position, were prepared and subjected to the same decarbonylation reaction in attempts to extend the scope of the reaction. Unexpectedly, both complexes **3** and **4** slowly eliminated two CO ligands in refluxing toluene solution (30 min) to afford the vinylidene complexes $Cp^*WOs_3(CO)_9(\mu_4\text{-}C)(\mu\text{-}H)(\mu\text{-}CCH^nPr)$ as a mixture of two isomers (**5a**:**5b** = 4:3) in 75% yield.[16] Their identities were revealed on the basis of the NMR data, and they are obviously caused by the asymmetric nature of the vinylidene fragment. In the ^1H NMR spectrum, two sets of signals are observed at δ 4.08 and −24.23 and at δ 4.15 and −24.29, indicating the presence of a C=CH^{n}Pr vinylidene ligand and a bridging hydride ligand (Scheme 1). The ^{13}C NMR spectrum was

(10) Spectral data for **2**: MS (FAB, ^{184}W, ^{192}Os) *m/z* 1276 (M^+); IR (C_6H_{12}) ν(CO) 2076 (s), 2040 (vs), 2021 (s), 2003 (s), 1981 (m, br), 1976 (vw), 1958 (w), 1950 (vw), 1922 (vw, br) cm^{-1}; ^1H NMR ($CDCl_3$, 294 K) δ 2.51–2.47 (m, 3H), 7.37 (t, 2H, J_{H-H} = 7.3 Hz), 1.99 (s, 15H, C_5Me_5); ^{13}C NMR ($CDCl_3$, 258 K) δ 357.0 (μ_4-*C*, J_{W-C} = 104 Hz), 293.9 (μ-*C*Ph, J_{W-C} = 150 Hz), 226.7 (CO, J_{W-C} = 178 Hz), 187.2 (CO, br), 182.1 (2CO), 181.3 (CO), 179.4 (CO), 178.8 (CO, br), 175.1 (CO, br), 173.3 (CO), 164.9 (CO), 155.8 (*i*-C_6H_5), 130.1 (*o*,*m*-C_6H_5), 129.8 (*m*,*o*-C_6H_5), 128.6 (*p*-C_6H_5), 107.1 (C_5Me_5), 11.0 (C_5Me_5). Anal. Calcd for $C_{28}H_{20}O_{10}Os_3W$: C, 26.46; H, 1.59. Found: C, 26.52; H, 1.63.

(11) Crystal data for **2**: $C_{28}H_{20}O_{10}Os_3W$, M_r = 1270.90, orthorhombic, space group *Pca*21, a = 30.773(5) Å, b = 9.678(2) Å, c = 20.561(3) Å, V = 6124(2) Å^3, Z = 8, ρ_{calcd} = 2.757 g cm^{-3}, $F(000)$ = 4518, λ(Mo Kα) = 0.7107 Å, T = 298 K, μ = 163.0 cm^{-1}. The intensities were measured on a Nonius CAD4 diffractometer on a crystal with dimensions 0.20 × 0.20 × 0.25 mm. Of the 5546 unique reflections collected, 3139 reflections with $I > 2\sigma(I)$ were used for the refinement. The structure was solved by using the NRCC-SDP-VAX package and refined to R_F = 0.053, R_w = 0.047, and GOF = 1.21 for 757 parameters, weighting scheme $w^{-1} = \sigma^2(F_o) + 0.00002F_o^2$, and highest Δ/σ ratio 0.07. A difference map following convergence showed residual electron density within the range −1.49 to +2.24 e/Å^3 (min–max). In addition, this crystal belongs to the noncentric space group $Pca2_1$. The presence of two crystallographically distinct molecules in the asymmetric unit doubles the number of variables used in the refinement, which gives a relatively poor data-to-parameter ratio (4.2:1) and undesired large standard deviations for the bond distances and angles.

(12) Chi, Y.; Chuang, S.-H.; Chen, B.-F.; Peng, S.-M.; Lee, G.-H. *J. Chem. Soc., Dalton Trans.* **1990**, 3033.

(13) Gong, J.-H.; Tsay, C.-W.; Tu, W.-C.; Chi, Y.; Peng, S.-M.; Lee, G.-H. *J. Cluster Sci.* **1995**, *6*, 289.

(14) (a) Chi, Y.; Wu, F.-J.; Liu, B.-J.; Wang, C.-C.; Wang, S.-L. *J. Chem. Soc., Chem. Commun.* **1989**, 873. (b) Chi, Y.; Su, C.-J.; Farrugia, L. J.; Peng, S.-M.; Lee, G.-H. *Organometallics* **1994**, *13*, 4167.

(15) (a) Bradley, J. S. *Adv. Organomet. Chem.* **1982**, *22*, 1. (b) Harris, S.; Bradley, J. S. *Organometallics* **1984**, *3*, 1086. (c) Hriljac, J. A.; Harris, S.; Shriver, D. F. *Inorg. Chem.* **1988**, *27*, 816.

(16) Spectral data for **5**: MS (FAB, ^{184}W, ^{192}Os) *m/z* 1228 (M^+); IR (C_6H_{12}) ν(CO) 2075 (m), 2044 (vs), 2008 (s), 2002 (m), 1995 (s), 1976 (w), 1959 (m), 1946 (vw), 1931 (vw, br) cm^{-1}; ^1H NMR ($CDCl_3$, 294 K) isomer **a** δ 4.08 (t, C*H*, J_{H-H} = 7.4 Hz), 2.10 (s, 15H, C_5Me_5), 1.69 (m, 1H), 1.56 (m, 1H), 1.00 (t, C*H*$_3$, J_{H-H} = 7.4 Hz), and −24.23 (s, 1H) isomer **b** δ 4.15 (t, C*H*, J_{H-H} = 7.4 Hz), 2.15 (s, 15H, C_5Me_5), 1.68 (m, 1H), 1.48 (m, 1H), 1.02 (t, C*H*$_3$, J_{H-H} = 7.4 Hz), and −24.29 (s, 1H); ^{13}C NMR ($CDCl_3$, 294 K) isomer **a** δ 343.1 (μ_4-*C*, J_{W-C} = 100 Hz), 273.1 (*C*CH^{i}Pr, J_{W-C} = 100 Hz), 222.6 (CO, J_{W-C} = 169 Hz), 186.7 (CO), 180.2 (CO), 175.6 (CO), 172.5 (CO), 166.0 (CO), 106.4 (C_5Me_5), 65.1 (CCH^{i}Pr), 36.2 (CH_2), 26.9 (CH_2), 13.3 (CH_3), and 11.0 (C_5Me_5) isomer **b** δ 345.7 (μ_4-*C*, J_{W-C} = 100 Hz), 269.5 (*C*CH^{n}Pr, J_{W-C} = 100 Hz), 221.2 (CO, J_{W-C} = 169 Hz), 187.3 (CO), 179.5 (CO), 175.3 (CO), 173.3 (CO), 166.1 (CO), 106.5 (C_5Me_5), 65.0 (*C*CH^{i}Pr), 34.2 (CH_2), 27.4 (CH_2), 13.5 (CH_3), 11.2 (C_5Me_5). Anal. Calcd for $C_{25}H_{24}O_9Os_3W$: C, 24.55; H, 1.98. Found: C, 24.53; H, 2.02.

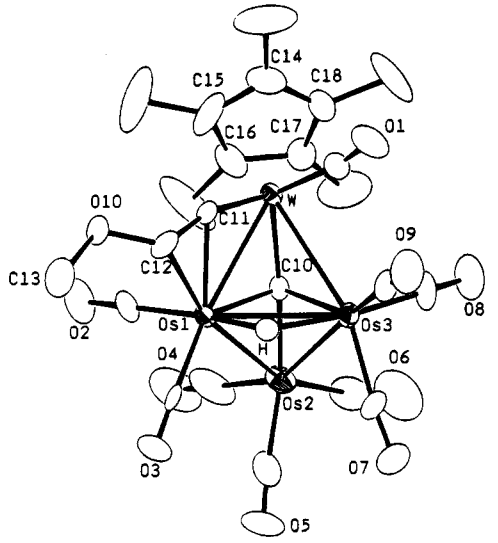

Figure 2. Molecular structure of **7a** and the atomic numbering scheme. Selected bond lengths (Å): W–Os(1) = 2.840(2), W–Os(3) = 2.985(1), Os(1)–Os(2) = 2.815(1), Os(1)–Os(3) = 2.883(1), Os(2)–Os(3) = 2.857(1), W–C(10) = 2.02(2), Os(1)–C(10) = 2.13(1), Os(2)–C(10) = 1.91(2), Os(3)–C(10) = 2.18(1), W–C(11) = 1.93(2), Os(1)–C(11) = 2.18(2), Os(1)–C(12) = 2.27(2), C(11)–C(12) = 1.36(2). Selected bond angles (deg): W–C(10)–Os(2) = 174.4(8), Os(1)–C(10)–Os(3) = 84.0(5), W–C(11)–C(12) = 163(1).

interpreted accordingly. In addition to the carbide and the W–CO resonances, the ^{13}C resonances arising from the α- and β-carbons of the vinylidene group in **5a** appeared at δ 273.1 (J_{W-C} = 100 Hz) and 65.1, while those of **5b** occurred at δ 269.5 (J_{W-C} = 100 Hz) and 65.0. We propose that the dominant isomer **5a** contains the *exo* hydrogen, while the less abundant **5b** has an *endo* hydrogen atom, as a positive NOE enhancement (≥3.6%) was observed for the hydride signal of **5b** upon irradiating the respective vinylidene hydrogen signal.

The identification of the previously mentioned vinylidene complexes was further confirmed by the characterization of the two methoxy derivatives $Cp^*WOs_3(CO)_9(\mu_4\text{-}C)(\mu\text{-}H)(\mu\text{-}CCHOMe)$ (**7a,b**), which were obtained from the thermolysis of the acetylide derivative $Cp^*WOs_3(CO)_{11}(CCCH_2OMe)$ (**6**).[17] The methoxy derivatives **7a,b** were isolated in pure form by TLC separation and recrystallization. An X-ray diffraction study on **7a** confirmed that the molecule possesses the WOs_3 butterfly arrangement with dihedral angle 104.24(3)° (Figure 2),[18] which is essentially identical with that of **2**. The hydride, which is located on the difference Fourier map, spans the slightly elongated hinge Os–Os bond. The vinylidene ligand, containing a linear W–C–C skeleton and an *endo* hydrogen atom, is best visualized as possessing a W=C double bond and as π-bonding to the adjacent Os atom. These parameters are in agreement with those observed for the "side-on" coordinated vinylidene ligands of dinuclear and polynuclear systems.[19]

The pathways leading to the formation of vinylidene from acetylide ligands were easily established (Scheme 1), which consist of (i) cluster skeletal rearrangement, (ii) C–C bond cleavage, and (iii) C–H bond activation. Our previous experiments suggested that the W atom in this butterfly system can undergo migration between the wingtip and the hinge sites through a process involving reversible cleavage of the M–M bond.[17] After the occurrence of cluster skeletal rearrangement, the acetylide complexes then liberate one CO ligand to induce the scission of the C–C bond and to afford the carbide and alkylidyne fragments. If the acetylide ligands contained a methylene group adjacent to the C_2 fragment, the reaction proceeded further to the production of vinylidene via hydrogen activation, a process which is akin to that observed in the metal clusters and crystal surfaces.[20] In the present system, two configurations are anticipated due to the poor selectivity in abstracting the diastereotopic methylene hydrogen atoms.

Finally, in view of these pronounced changes starting from the coordinated acetylide, it is even more remarkable that the carbide in both **2** and **5** can be transformed back to the acetylide upon addition of CO. Thus, exposure of **2** to CO (110 °C, 5 min) resulted in the formation of **1** in 85% yield, whereas the reaction of **5** proceeded much more slowly (40 min, 65% completion) to afford **3** and **4** in 61% combined yield and a trace amount of the trinuclear acetylide cluster $Cp^*WOs_2(CO)_8(CCBu)$ due to fragmentation.[9] This rarely reported pattern of reactivity highlights the exciting chemistry of carbide in reacting with small organic hydrocarbon fragments.[21] An extensive investigation regarding C–C bond formation with these carbido cluster compounds will be described in the future.

Acknowledgment. We are grateful to the National Science Council of the Republic of China for financial support (Grant No. NSC 85-2113-M007-008).

Supporting Information Available: Text describing the experimental details and the spectroscopic data for **1**, **3**, **4**, and **7** and full details of crystal structure analyses, including tables of bond distances, atomic coordinates, and anisotropic thermal parameters, for **2** and **7a** (14 pages). Ordering information is given on any current masthead page.

OM950742E

(17) Su, P.-C.; Chiang, S.-J.; Chang, L.-L.; Chi, Y.; Peng, S.-M.; Lee, G.-H. *Organometallics* **1995**, *14*, 4844.

(18) Crystal data for **7a**: $C_{23}H_{20}O_{10}Os_3W$, M_r = 1210.84, monoclinic, space group $P2_1/n$, a = 10.666(5) Å, b = 14.779(3) Å, c = 18.540(5) Å, β = 103.62(3)°, V = 2841(2) Å^3, Z = 4, ρ_{calcd} = 2.831 g cm^{-3}, $F(000)$ = 2139, λ(Mo Kα) = 0.7107 Å, T = 298 K, μ = 175.7 cm^{-1}. The intensities were measured on a crystal with dimensions 0.25 × 0.30 × 0.50 mm. Of the 4998 unique reflections collected, 3635 reflections with $I > 2\sigma(I)$ were used for the refinement. The structure was refined to R_F = 0.037, R_w = 0.037, and GOF = 1.83 for 339 parameters, weighting scheme $w^{-1} = \sigma^2(F_o) + 0.00005F_o^2$, and highest Δ/σ ratio 0.008. A difference map following convergence showed residual electron density within the range −1.38 to +2.49 e/Å^3 (min–max).

(19) (a) Hwang, D.-K.; Lin, P.-J.; Chi, Y.; Peng, S.-M.; Lee, G.-H. *J. Chem. Soc., Dalton Trans.* **1991**, 2161. (b) Doherty, N. M.; Elschenbroich, C.; Kneuper, H.-J.; Knox, S. A. R. *J. Chem. Soc., Chem. Commun.* **1985**, 170.

(20) (a) Shapley, J. R.; Park, J. T.; Churchill, M. R.; Ziller, J. W.; Beannan, L. R. *J. Am. Chem. Soc.* **1984**, *106*, 1144. (b) Park, J. T.; Chi, Y.; Shapley, J. R.; Churchill, M. R.; Ziller, J. W. *Organometallics* **1994**, *13*, 813. (c) Dutta, T. K.; Vites, J. C.; Fehlner, T. P. *Organometallics* **1986**, *5*, 385. (d) Hills, M. M.; Parmeter, J. E.; Weinberg, W. H. *J. Am. Chem. Soc.* **1987**, *109*, 597.

(21) (a) Holt, E. M.; Whitmire, K. H.; Shriver, D. F. *J. Organomet. Chem.* **1981**, *213*, 125. (b) Bradley, J. S.; Hill, E. W.; Ansell, G. B.; Modrick, M. A. *Organometallics* **1982**, *1*, 1634. (c) Wijeyesekera, S. D.; Hoffmann, R.; Wilker, C. N. *Organometallics* **1984**, *3*, 962. (d) Bogdan, P. L.; Woodcock, C.; Shriver, D. F. *Organometallics* **1987**, *6*, 1377. (e) Dutton, T.; Johnson, B. F. G.; Lewis, J.; Owen, S. M.; Raithby, P. R. *J. Chem. Soc., Chem. Commun.* **1988**, 1423.

Chiral Oxazolinylferrocene–Phosphine Hybrid Ligand for the Asymmetric Hydrosilylation of Ketones

Yoshiaki Nishibayashi, Kyohei Segawa, Kouichi Ohe, and Sakae Uemura*

Division of Energy and Hydrocarbon Chemistry, Graduate School of Engineering, Kyoto University, Sakyo-ku, Kyoto 606-01, Japan

Received September 1, 1995[⊗]

Summary: A new type of chiral oxazolinylferrocene–phosphine hybrid is a very effective ligand for Rh(I)-catalyzed asymmetric hydrosilylation of simple ketones to give the corresponding sec-alcohols (91% ee) after acid hydrolysis. Similar reactions also proceed highly selectively (96% ee) by use of Ir(I) catalyst, but the configuration of the products is completely reverse.

Molecular design of a chiral ligand is essential for obtaining highly enantiomerically pure compounds in transition-metal-catalyzed asymmetric reactions, and there has been much effort devoted to prepare efficient ligands.[1] The enantioselective reduction of prochiral ketones is an important reaction, because the optically active alcohol products are useful intermediates in synthetic organic chemistry.[2] We now envisage the preparation of newly designed chiral ligands and their use in the rhodium(I)- and iridium(I)-catalyzed asymmetric hydrosilylation of ketones. Preliminary results are reported here.

A new type of chiral ligand, an oxazolinylferrocene–phosphine hybrid ligand, was designed because the ligand could be easily prepared from reactions of either ferrocenecarboxylic acid or ferrocenecarbonitrile with chiral amino alcohols and also ferrocenes with planar chirality were known to be useful ligands for asymmetric reactions.[3] At first, the four ligands **1**,[4a,b] **2**,[4a] **3**, and **4**[4a] were prepared and applied to the hydrosilylation of acetophenone with diphenylsilane in the presence of a catalytic amount of $[Rh(COD)Cl]_2$ in Et_2O at 25 °C. The enantiomeric excesses of 1-phenylethanol obtained by acid hydrolysis of the hydrosilylation product were 60% ee (*R*), 48% ee (*R*), 37% ee (*R*), and 13% ee (*R*), respectively. Generally, in hydrosilylation, oxidative addition of hydrosilane to the rhodium(I) complex takes place first and coordination of the carbonyl group of the ketone to vacant sites of the complex follows. Therefore,

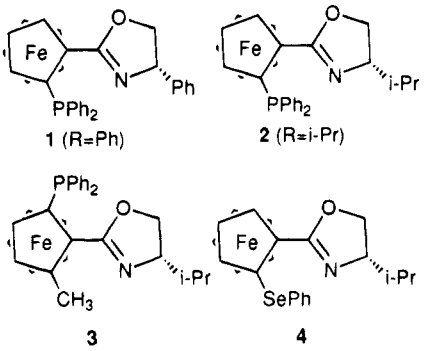

the bulkiness and the position of substituents on an oxazoline ring might affect the stereoselectivity.

With the intention of obtaining a much higher selectivity, we then designed and prepared the ligand **5**, (*S,S,S*)-[2-(4,5-*dip*henyl*o*xazolin-2-yl)*f*errocenyl]diphenylphosphine. It was abbreviated as (*S,S,S*)-DIPOF and separated from its diastereoisomer (*S,S,R*)-DIPOF (**6**) (Scheme 1). Hydrosilylation of several ketones with diphenylsilane was then investigated in the presence of a catalytic amount of $[Rh(COD)Cl]_2$ and **5** (Scheme 2).[5] As shown in Table 1, the reaction proceeded highly stereoselectively. The reactions with aryl methyl ketones gave a high enantioselectivity (runs 1–3), but those with propiophenone and α-chloroacetophenone were slow and the enantioselectivity was quite low (runs 5 and 6), in contrast to hydrosilylation using nitrogen-containing chiral ligands such as Pybox, Pythia, etc.[6] Interestingly, the ligand **5** acted effectively not only for aryl methyl ketones but also for alkyl methyl ketones (runs 7 and 8; 87–89% ee), the ee values being the highest among those obtained so far in the hydrosilylation of these alkyl methyl ketones.[7,8] Even the simple dialkyl ketone, 2-octanone, afforded moderate enantioselectivity (run 9; 60% ee).

[⊗] Abstract published in *Advance ACS Abstracts,* November 15, 1995.

(1) For reviews, see: (a) Ojima, I., Ed. *Catalytic Asymmetric Synthesis;* VCH: New York, 1993. (b) Noyori, R. *Asymmetric Catalysis in Organic Synthesis;* Wiley: New York, 1994.

(2) For examples: (a) Ohkuma, T.; Ooka, H.; Hashiguchi, S.; Ikariya, T.; Noyori, R. *J. Am. Chem. Soc.* **1995**, *117*, 2675. (b) Noyori, R.; Ohkuma, T.; Kitamura, M.; Takaya, H.; Sayo, N.; Kumobayashi, H.; Akutagawa, S. *J. Am. Chem. Soc.* **1987**, *109*, 5856. (c) Kitamura, M.; Ohkuma, T.; Inoue, S.; Sayo, N.; Kumobayashi, H.; Akutagawa, S.; Ohta, T.; Takaya, H.; Noyori, R. *J. Am. Chem. Soc.* **1988**, *110*, 629. (d) Corey, E. J.; Bakshi, R. K.; Shibata, S.; Chen, C. P.; Singh, V. K. *J. Am. Chem. Soc.* **1987**, *109*, 7925. (e) Noyori, R.; Tomino, I.; Tanimoto, Y. *J. Am. Chem. Soc.* **1979**, *101*, 3129. (f) Dumont, W.; Poulin, J. C.; Dang, T.-P.; Kagan, H. B. *J. Am. Chem. Soc.* **1973**, *95*, 8295.

(3) For example: Sawamura, M.; Ito, Y. *Chem. Rev.* **1992**, *92*, 867.

(4) (a) Nishibayashi, Y.; Uemura, S. *Synlett* **1995**, 79. (b) Richards, C. J.; Damalidis, T.; Hibbs, D. E.; Hursthouse, M. B. *Synlett* **1995**, 74. (c) Sammakia et al. have also reported the highly diastereoselective ortho-lithiation of chiral oxazolinylferrocenes: Sammakia, T.; Latham, H. A.; Schaad, D. R. *J. Org. Chem.* **1995**, *60*, 10.

(5) After $[Rh(COD)Cl]_2$ (0.0025 mmol) and the ligand **5** (0.005 mmol) were stirred in Et_2O (3 mL) at 25 °C, acetophenone (1 mmol) and then diphenylsilane (1.3 mmol) were slowly added to the mixture, the temperature being kept at 25 °C. After the mixture was stirred for suitable time at 25 °C, the addition of 1 N aqueous HCl (5 mL) and the general workup procedure afforded 1-phenylethanol quantitatively with 91% ee. The optical purity was determined by GLC or HPLC with a chiral phase. The absolute configuration was determined by an optical rotation. The ee value obtained by similar treatment with the ligand **6** was moderate.

(6) For example: (a) Brunner, H.; Becker, R.; Roepl, G. *Organometallics* **1984**, *3*, 1354. (b) Nishiyama, H.; Kondo, M.; Nakamura, T.; Itoh, K. *Organometallics* **1991**, *10*, 500. (c) Nishiyama, H.; Yamaguchi, S.; Kondo, M.; Itoh, K. *J. Org. Chem.* **1992**, *57*, 4306.

(7) With the chiral aminophosphine ligand AMPHOS, 72% ee was obtained in the hydrosilylation of *tert*-butyl methyl ketone: Payne, N. C.; Stephan, D. W. *Inorg. Chem.* **1982**, *21*, 182.

(8) With the trans-chelating diphosphine *n*-BuTRAP, 80% ee was obtained in the hydrosilylation of cyclohexyl methyl ketone: Sawamura, M.; Kuwano, R.; Ito, Y. *Angew. Chem., Int. Ed. Engl.* **1994**, *33*, 111.

0276-7333/95/2314-5486$09.00/0

Scheme 1[a]

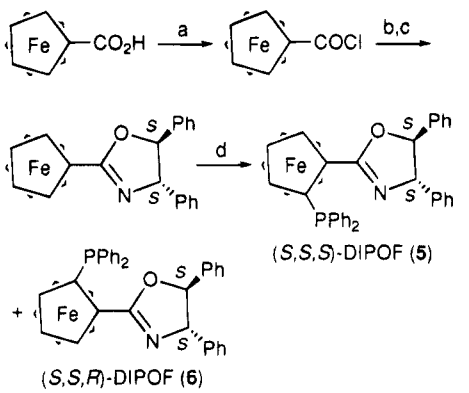

[a] Conditions: (a) $SOCl_2$, 50 °C, 54%; (b) (1*R*,2*S*)-(−)-2-amino-1,2-diphenylethanol, Et_3N, room temperature, 40%; (c) $SOCl_2$, −78 to 0 °C then 20% K_2CO_3(aq), 0 °C, 51%; (d) *s*-BuLi, −78 °C, PPh_2Cl, reflux, 68% (**5**/**6** = 35/65), **5** isolated (24%) with column chromatography (SiO_2).

Scheme 2

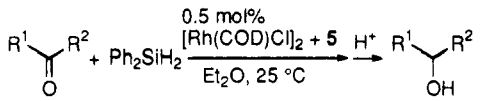

Scheme 3

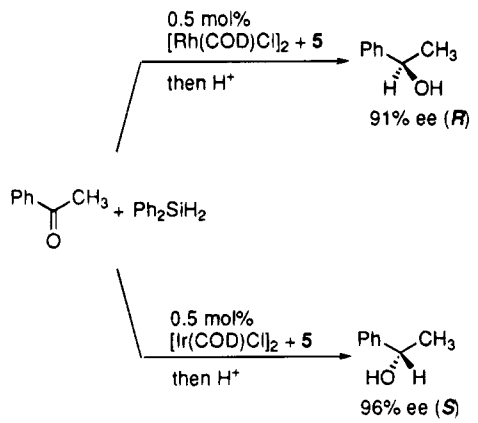

Surprisingly, in the presence of $[Ir(COD)Cl]_2$ as a catalyst in place of $[Rh(COD)Cl]_2$, hydrosilylation of acetophenone with the ligand **5** at 0 °C for 20 h afforded 1-phenylethanol of the opposite configuration (*S*) with high enantioselectivity (96% ee) almost quantitatively (Scheme 3). Although similar phenomena have been observed in a few cases, only low enantioselectivity has been obtained to the best of our knowledge.[9] This is also the first example of highly enantioselective Ir-catalyzed asymmetric hydrosilylation of ketones. We are making efforts to apply this DIPOF/Ir(I) system to other ketones, the results of which will be reported in due course.[10]

In conclusion, we designed and prepared a new type of chiral oxazolinylferrocene−phosphine hybrid ligand, (*S,S,S*)-DIPOF (**5**), for the Rh(I)-catalyzed asymmetric hydrosilylation of simple ketones lacking a secondary coordinating functional group. This ligand was found to be a very effective ligand for the reduction of aryl and alkyl methyl ketones to the corresponding *sec*-alcohols with *R* configuration after acid hydrolysis. On the other hand, enantioselective hydrosilylation of acetophenone with the (*S,S,S*)-DIPOF/Ir(I) system occurred highly selectively (96% ee) to give the alcohol with an *S* configuration.

Table 1. Asymmetric Hydrosilylation of Various Ketones Catalyzed by Rh(I)−(*S,S,S*)-DIPOF (5)[a]

run	ketones	alcohols yield(%)[b]	ee(%)[c]	config.
1	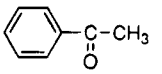	100	91	*R*
2	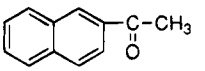	99	88	*R*
3	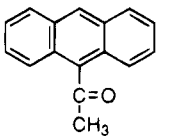	100	90	*R*
4	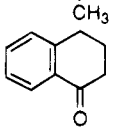	95	57	*R*
5	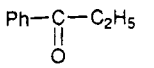	12	23	*S*
6	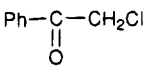	19	8	*S*
7	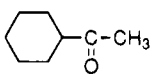	45	89	*R*
8	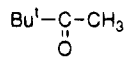	100	87	*R*
9	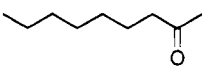	92	60	*R*

[a] All the reactions were carried out in the presence of $[Rh(COD)Cl]_2$ (0.25 mol %) and (*S,S,S*)-DIPOF (**5**) (0.5 mol %) with diphenylsilane (1.5 mmol) and ketones (1.0 mmol) in Et_2O at 25 °C for 15−25 h. [b] Isolated yield. [c] The ee was determined by HPLC and GLC.

Acknowledgment. The present work was supported in part by a Grant-in-Aid for Scientific Research from the Ministry of Education, Science and Culture of Japan and by a Fellowship (to Y.N.) of the Japan Society for the Promotion of Science for Japanese Junior Scientists.

Supporting Information Available: Text giving the preparative methods and spectral details for the ligands **1**−**5** (8 pages). This material is contained in many libraries on microfiche, immediately follows this article in the microfilm version of the journal, and can be ordered from the ACS; see any current masthead page for ordering information.

OM950694Y

(9) The enantioselectivity of the Ir(I)-catalyzed hydrosilylation of acetophenone was up to 32% ee: (a) Faller, J. W.; Chase, K. J. *Organometallics* **1994**, *13*, 989. (b) Kinting, A.; Kreuzfeld, H.-J.; Abicht, H.-P. *J. Organomet. Chem.* **1989**, *370*, 343.

(10) The preliminary results for several ketones are as follows: propiophenone (100%, 92% ee), phenyl *n*-propyl ketone (100%, 91% ee), and *p*-chloroacetophenone (97%, 88% ee).

Synthesis and Structural Characterization of $\{LiN(SiMe_3)_2MMe_3\}_\infty$ (M = Al, Ga): Amido Ligands Isoelectronic to the Alkyl Group $-C(SiMe_3)_3$

Mark Niemeyer and Philip P. Power*

Department of Chemistry, University of California, Davis, California 95616

Received September 29, 1995[⊗]

*Summary: The synthesis and structural characterization of the lithium salts $\{LiN(SiMe_3)_2MMe_3\}_\infty$ (M = Al (**1**), Ga (**2**)) are described. The compounds are essentially isostructural and are associated into infinite chains that involve bridging by the lithium ion to an aluminum or gallium methyl group of a neighboring molecule.*

The ligands $-C(SiMe_3)_3$ and $-N(SiMe_3)_2AlMe_3$ are isoelectronic. Yet, there are very few examples of structurally characterized compounds in which the properties of these two ligands can be directly compared (vide infra).[1,2] The alkyl group $-C(SiMe_3)_3$ has been employed throughout the periodic table and has been shown to be effective in stabilizing low coordination numbers and unusual oxidation states in a variety of elements.[2-4] Its lithium salt $LiC(SiMe_3)_3$ is of key importance in the synthesis of most of these derivatives. When crystallized in the presence of THF, it exists as the "ate" complex $[Li(THF)_4][Li\{C(SiMe_3)_3\}_2]$,[4] but as a solvent-free species it exists as the dimer $\{LiC(SiMe_3)_3\}_2$.[5] The structure of the related amide $LiN(SiMe_3)_2$ (either unsolvated[6] or solvated by various donors[7]) has been well studied, and it exists as the trimer $\{LiN(SiMe_3)_2\}_3$ when uncomplexed.[6] The simple addition of trimethylaluminum to $LiN(SiMe_3)_2$ affords a species $LiN(SiMe_3)_2AlMe_3$ which is isoelectronic to $LiC(SiMe_3)_3$. It is therefore of some interest to examine the relationship between their structures. In this paper the synthesis and structure of $LiN(SiMe_3)_2AlMe_3$ and its gallium analogue are now reported.

The compounds $\{LiN(SiMe_3)_2MMe_3\}_\infty$ (M = Al (**1**), Ga (**2**)) were isolated[8] in high yield as colorless, isomorphous crystals by the addition of trimethylaluminum or -gallium to $LiN(SiMe_3)_2$ in toluene solution. X-ray crystallographic data[9] for **1** and **2** show that the structures are composed of infinite chains in which monomeric units of $LiN(SiMe_3)_2MMe_3$ (M = Al, Ga) are linked by an interaction between the lithium ion and a methyl group (i.e. C(1a)) from the MMe_3 moiety in the neighboring molecule. The structure of **1** is illustrated in Figure 1, and further structural details are provided in Table 1. From these data it can be seen that the two structures are almost identical. Each Li^+ ion interacts most strongly with the amido nitrogen and with C(3) and C(1a) methyl groups such that the nitrogen and two carbons define an approximately trigonal planar coordination sphere for the metal. The strong[10] interaction between Li^+ and the C(3) methyl group is consistent with M–C(3) bonds that are longer (by *ca.* 0.06 Å) than

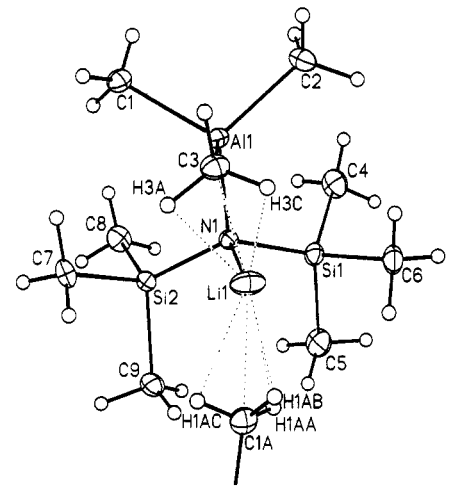

Figure 1. Thermal ellipsoidal plot (30%) of **1** illustrating the coordination of the Li^+ ion.

[⊗] Abstract published in *Advance ACS Abstracts,* November 15, 1995.

(1) Boncella, J. M.; Andersen, R. A. *Organometallics* **1985**, *4*, 205.
(2) Eaborn, C.; Hitchcock, P. B.; Izod, K.; Smith, J. D. *J. Am. Chem. Soc.* **1994**, *116*, 12071.
(3) (a) Al-Juaid, S. S.; Eaborn, C.; Hitchcock, P. B.; McGeary, C. A.; Smith, J. D. *J. Chem. Soc., Chem. Commun.* **1989**, 273. (b) Buttrus, N. H.; Eaborn, C.; Hitchcock, P. B.; Smith, J. D.; Sullivan, A. C. *J. Chem. Soc., Chem. Commun.* **1985**, 1380.
(4) Eaborn, C.; Hitchcock, P. B.; Smith, J. D.; Sullivan, A. C. *J. Chem. Soc., Chem. Commun.* **1983**, 827.
(5) Hiller, W.; Layh, M.; Uhl, W. *Angew. Chem., Int. Ed. Engl.* **1991**, *30*, 324.
(6) Mootz, D.; Zinnius, A.; Böttcher, B. *Angew. Chem., Int. Ed. Engl.* **1969**, *8*, 378.
(7) (a) Lappert, M. F.; Slade, M. J.; Singh, A.; Atwood, J. L.; Rogers, R. D.; Shakir, R. *J. Am. Chem. Soc.* **1983**, *105*, 302. (b) Engelhardt, L. M.; May, A. S.; Raston, C. L.; White, A. H. *J. Chem. Soc., Dalton Trans.* **1983**, 1671. (c) Power, P. P.; Xu, X. *J. Chem. Soc., Chem. Commun.* **1984**, 358. (d) Engelhardt, L. M.; Jolly, B. S.; Punk, P. C.; Raston, C. L.; White, A. H. *Austr. J. Chem.* **1986**, *39*, 1337.

(8) All manipulations were carried out under anaerobic and anhydrous conditions. Al_2Me_6 in PhMe (2 M), $GaMe_3$, and $HN(SiMe_3)_2$ were obtained from commercial suppliers and used as received. $LiN(SiMe_3)_2$ was generated in solution by the addition of 1 equiv of 1.6 M *n*-BuLi in hexane and was purified by sublimation. With stirring at room temperature a 2 M solution of $AlMe_3$ (5.25 mL, 10.5 mmol) in PhMe was added dropwise via a syringe to $LiN(SiMe_3)_2$ (1.75 g, 10.5 mmol) in toluene (30 mL). Within 5 min colorless crystals began to precipitate. These were partly redissolved by warming with a heat gun. Stirring was then discontinued, and the solution was cooled to room temperature over several hours to give large crystals of the product **1** that were suitable for X-ray crystallographic studies. A further crop of crystals was obtained by cooling in a −30 °C freezer overnight. The synthesis of **2** as colorless crystals was accomplished in a similar manner with use of $GaMe_3$ (0.78 g, 6.8 mmol) and $LiN(SiMe_3)_2$ (1.12 g, 6.8 mmol) and *ca.* 20 mL total volume of PhMe. Data for **1**, with those for **2** in braces, are as follows: Yield 2.11 g (84%) {1.50 g (79%)}, mp 175–177 °C {129–130 °C}; ^1H NMR (C_6D_6) δ 0.21 {0.19} ($SiMe_3$, 18H), −0.55 {−0.33} (MMe_3, 9H); ^{13}C NMR (C_6D_6) δ 6.1 {6.0} ($SiMe_3$), 2.6 {−0.9} (MMe_3); ^7Li NMR (C_6D_6) δ −2.3 {−2.2}; IR (Nujol, cm^{-1}) 2175 w, 1923 w, 1862 w, 1616 w, 1402 m, 1294 sh, 1264 sh, 1252 vs, 1208 s, 1189 s, 1108 s, 930–580 vs br, 521 s, 465 s, 403 m, 371 m, 340 m-s; {2210 w, 1920 w, 1858 w, 1625 w, 1397 m, 1290 sh, 1262 sh, 1250 vs, 1204 m-s, 1193 s, 1124 s, 947 vs br, 876–727 vs br, 677 vs, 634 m-s, 609 vs, 527 vs, 482 vs, 402 m, 350 sh, 330 m-s}.

(9) Crystal data at 130 K with Cu Kα (λ = 1.541 84 Å) radiation: **1**, $C_9H_{27}AlNSi_2$, a = 12.334(3) Å, b = 15.563(3) Å, c = 16.449(3) Å, orthorhombic, space group *Pbca*, Z = 8, R = 0.048 for 1622 ($I > 2\sigma(I)$) data; $C_9H_{27}GaNSi_2$, **2**, a = 12.336(3) Å, b = 15.563(3) Å, c = 16.434(3) Å, orthorhombic, space group *Pbca*, Z = 8, R = 0.062 for 1745 ($I > 2\sigma(I)$) data.

0276-7333/95/2314-5488$09.00/0

Table 1. Selected Distances (Å) and Angles (deg) in 1 and 2

	compd	
	1 (M = Al)	**2** (M = Ga)
Li(1)–N(1)	2.027(7)	2.014(12)
Li(1)- - -C(1)	2.252(8)	2.233(13)
Li(1)- - -C(3)	2.157(8)	2.205(13)
M(1)–N(1)	1.944(3)	2.038(4)
N(1)–Si(1)	1.741(3)	1.742(4)
N(1)–Si(2)	1.749(3)	1.727(4)
M(1)–C(1)	2.005(4)	2.022(6)
M(1)–C(2)	1.974(4)	1.987(7)
M(1)–C(3)	2.032(4)	2.044(6)
Li(1)–N(1)–M(1)	82.4(2)	81.7(3)
Li(1)–N(1)–Si(1)	102.5(3)	101.4(4)
Li(1)–N(1)–Si(2)	106.5(2)	107.9(4)
N(1)–M(1)–C(1)	114.6(2)	112.4(2)
N(1)–M(1)–C(2)	117.3(2)	117.1(2)
N(1)–M(1)–C(3)	103.0(2)	101.9(2)
N(1)–Li(1)–C(1a)	129.9(4)	129.2(6)
N(1)–Li(1)–C(3)	96.0(3)	97.4(5)
C(1a)–Li(1)–C(3)	128.5(4)	126.6(5)

the M–C(2) bonds which involve terminal methyl groups bound solely to Al or Ga. In addition, the longer M–C(1) distances are in agreement with the role of this methyl group in bridging the $LiN(SiMe_3)_2MMe_3$ moieties. The interaction between the Li^+ ion and the methyl groups can also be expressed in the form of Li- - -H distances. For this purpose the hydrogens in **1** were located on a difference map and refined isotropically. The Li–H(1AA, AB, and AC) distances are 2.05(4), 2.25(4), and 2.10(4) Å, whereas the corresponding distances for Li- - -H(3A and C) are 2.15(4) and 2.11(4) Å. The Li–N bond lengths are slightly longer than that observed (Li–N = 2.00 Å) in the unsolvated trimer $\{LiN(SiMe_3)_2\}_3$.[6] The only significant differences between the structures of **1** and **2** involve the M–N and Li- - -C(3) distances which are respectively *ca.* 0.09 and 0.05 Å longer in the case of the gallium derivative. This difference is probably due to the weaker Lewis base character of $GaMe_3$[11] and the lowered ionic effects in the Ga–N and Ga–C bonding owing to the higher electronegativity of gallium in comparison to aluminum.[12]

Why are structures of $\{LiN(SiMe_3)_2AlMe_3\}_\infty$ (**1**) and $\{LiC(SiMe_3)_3\}_2$ (**3**) different? The answer may lie in the difference in the strengths of the interaction between the Li^+ ion and the methyl groups in the two molecules. These are very much stronger in the nitrogen derivative, *ca.* 2.16 and 2.25 Å in **1** (marginally weaker in **2**) versus *ca.* 2.47 and 2.54 Å in **3**.[5] Significantly, both Li- - -CH_3 interactions in **1** involve aluminum methyl rather than silyl methyl groups. Apparently the more electropositive aluminum center[12] induces a greater $\delta-$ charge on its methyl substituents which causes the stronger Li- - -CH_3 interaction. In addition, the fact that the Al–N and Ga–N bonds are dative ones and are probably weaker than the corresponding C–Si bond in **3** may permit greater flexibility in the orientation of MMe_3 moieties. As a result of this, the N(1)–Al(Ga)–C(3) angles are at least 10° narrower than the corresponding angles involving C(1) and C(2). By the same token the Li^+ ion is displaced toward the C(3) carbons so that the Li–N–M angles are only *ca.* 82° in each compound. Nonetheless, interaction of Li^+ with just one of the methyl groups is insufficient to saturate the Li^+ coordination sphere and a second strong Li- - -CH_3 interaction is not possible within a dimeric structure due to the fact that the $AlMe_3$ groups would adopt a trans-orientation with respect to the Li_2N_2 ring plane. In other words, the polymeric structure in **1** occurs in order to preserve two strong Li- - -CH_3 interactions involving the aluminum methyl groups. Increased crowding is also probably involved in determining the structure. This is due to the fact that the Li–N and N–Si bonds are shorter than corresponding Li–C and C–Si bonds so that a dimeric arrangement which had a structure similar to **3** would be more sterically encumbered. The polymeric structure seen in **1** and **2** has not been previously observed for amides; however, polymeric structures with a different Li- - -N- - -Li- - -N backbone are known for $\{LiN(i\text{-}Pr)_2\}_\infty$[13] and $\{(TMEDA)LiN(i\text{-}Pr)_2\}_2$.[14] The species $\{LiCH(SiMe_3)_2\}_\infty$[15] also has a polymeric backbone, and in this case it is composed of a Li- - -C- - -Li- - -C array.

It remains to be seen if the differences in structure between **1** or **2** and **3** will be observed in other metal derivatives. Only one other pair of compounds is currently available for comparison—the species $Yb\{N(SiMe_3)_2AlMe_3\}_2$[1] and $Yb\{C(SiMe_3)_3\}_2$.[2] The structures of these two compounds bear a very close similarity and have comparable Yb- - -Me interactions in each compound. It is possible in this case that the large size of the Yb^{2+} ion ensures a sterically more relaxed species in which almost equal Yb- - -Me contacts can occur in each compound. Investigations of other metal $-N(SiMe_3)_2AlMe_3$ derivatives are in hand.

Acknowledgment. We are grateful to the National Science Foundation for financial support.

Supporting Information Available: Tables of data collection parameters, complete atom coordinates and *U* values, distances and angles, and anisotropic thermal parameters (18 pages). Ordering information is given on any current masthead page.

OM950771P

(10) The Li- - -C distances in **1** and **2** are similar to those observed in many typical organolithium structures in which there is a direct interaction between the Li^+ and a carbanionic center: Setzer, W. N.; Schleyer, P. v. R. *Adv. Organomet. Chem.* **1985**, *24*, 353.

(11) This compound is a monomeric liquid at room temperature whereas trimethylaluminum is associated as dimers.

(12) The Allred–Rochow electronegativity values for aluminum and gallium are 1.47 and 1.82, respectively.

(13) Barnett, N. D. R.; Mulvey, R. E.; Clegg, W.; O'Neil, P. A. *J. Am. Chem. Soc.* **1991**, *113*, 8187.

(14) Bernstein, M. P.; Romesberg, F. E.; Fuller, D. J.; Harrison, A. T.; Collum, D. B.; Liu, Q.-Y; Williard, P. G. *J. Am. Chem. Soc.* **1992**, *114*, 5100.

(15) Atwood, J. L.; Fjeldberg, T.; Lappert, M. F.; Luong-Thi, T.; Shakir, R.; Thorne, A. J. *J. Chem. Soc., Chem. Commun.* **1984**, 1163.

Synthesis of the Cationic Silyleneiron Complex [(.eta.-C5H5)Fe(CO)2:SiMe{2-(Me2NCH2)C6H4}]PF6 by Hydride Abstraction from a (Hydrosilyl)iron Complex with Ph3CPF6

Hideki Kobayashi, Keiji Ueno, and Hiroshi Ogino

Organometallics, **1995**, 14 (12), 5490-5492• DOI: 10.1021/om00012a014 • Publication Date (Web): 01 May 2002

Synthesis of the Cationic Silyleneiron Complex $[(\eta\text{-}C_5H_5)Fe(CO)_2{=}SiMe\{2\text{-}(Me_2NCH_2)C_6H_4\}]PF_6$ by Hydride Abstraction from a (Hydrosilyl)iron Complex with Ph_3CPF_6

Hideki Kobayashi, Keiji Ueno,* and Hiroshi Ogino*

Department of Chemistry, Graduate School of Science, Tohoku University, Sendai 980-77, Japan

Received August 14, 1995[⊗]

Summary: A cationic intramolecular base-stabilized silyleneiron complex, $[(\eta\text{-}C_5H_5)Fe(CO)_2{=}SiMe\{2\text{-}(Me_2NCH_2)C_6H_4\}]PF_6$, was synthesized by hydride abstraction from the (hydrosilyl)iron complex $(\eta\text{-}C_5H_5)Fe(CO)_2SiHMe\{2\text{-}(Me_2NCH_2)C_6H_4\}$ with Ph_3CPF_6. Reaction of the silylene complex with MeOH afforded the methoxysilyl complex $[(\eta\text{-}C_5H_5)Fe(CO)_2SiMeOMe\{2\text{-}(Me_2N(H)CH_2)C_6H_4\}]PF_6$ in good yield. The molecular structures of the silylene and methoxysilyl complexes were determined by X-ray crystal structure analysis.

One of the useful synthetic routes for carbene complexes is abstraction of a leaving group from the carbon atom of an alkylmetal complex with an electrophile.[1] A similar strategy, i.e., abstraction of a leaving group from the silicon atom of a silylmetal complex, seems applicable for the synthesis of silylene complexes. However, such attempts to prepare silylene complexes have failed, principally due to the occurrence of secondary reactions.[2] For example, reaction of $FpSiCl_3$ (Fp = $CpFe(CO)_2$; Cp = η-C_5H_5) with 3 equiv of $AgBF_4$ caused fluorination of the silyl group and $FpSiF_3$ was isolated (eq 1).[2a] In 1987, Tilley and his colleagues succeeded

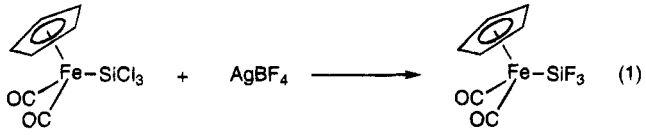

(1)

in obtaining the cationic silylene complex $[Cp^*(Me_3P)_2Ru{=}SiPh_2{\cdot}NCMe]BPh_4$ (Cp^* = η-C_5Me_5) by the abstraction method.[3] They selected $Cp^*Ru(PMe_3)_2SiPh_2OTf$ as a precursor complex, which contains the good leaving group OTf and the electron-rich ruthenium fragment $Cp^*Ru(PMe_3)_2$ to stabilize the generated silylene ligand. In addition, they used a mild electrophile which does not contain a fluorine source, $NaBPh_4$, to prevent undesirable secondary reactions. Their result clearly shows that selection of the leaving group and the electrophile, especially the counteranion in the electrophile, is important for the preparation of the silylene complex by the abstraction method.

Many hydrosilyl complexes have been prepared so far.[4] Thus, it would be worthwhile to find a new synthetic route to silylene complexes using hydrosilyl complexes as precursors. This prompted us to investigate hydride abstraction from the hydrosilyl complex by electrophiles. Our efforts, at first, were focused on finding substituents for the silicon atom which sufficiently stabilize the cationic silylene complex generated by hydride abstraction. We employed an Ar^N group (Ar^N = $2\text{-}(Me_2NCH_2)C_6H_4$) for the substituent on the silyl ligand, since the generated silylene ligand may be effectively stabilized by the intramolecular base.[5,6] We then attempted to abstract the hydride from $FpSiMeHAr^N$ (**1**)[7] with several electrophiles and finally found that the reaction of the (hydrosilyl)iron complex **1** with Ph_3CPF_6 resulted in the formation of the cationic silylene complex $[Fp{=}SiMeAr^N]PF_6$ (**2**). This is a surprising result, since the cationic silylene complex is stable enough even in the presence of PF_6^- ions. Here we report the details of the synthesis of the cationic silyleneiron complex by hydride abstraction and the reactivity of the silylene complex.

An initial attempt to carry out the hydride abstraction from the silyl group of $FpSiHMeAr^N$ (**1**) with Ph_3CBF_4 was unsuccessful. For example, reaction of $FpSiHMeAr^N$ (**1**) with 1 equiv of Ph_3CBF_4 in dichloromethane at room temperature afforded a complex reaction mix-

[⊗] Abstract published in *Advance ACS Abstracts,* November 15, 1995.

(1) (a) Hayes, J. C.; Cooper, N. J. *J. Am. Chem. Soc.* **1982,** *104,* 5570. (b) Kegley, S. E.; Brookhart, M.; Husk, G. R. *Organometallics* **1982,** *1,* 760. (c) Tam, W.; Lin, G.-Y.; Wong, W.-K.; Kiel, W. A.; Wong, V. K.; Gladysz, J. A. *J. Am. Chem. Soc.* **1982,** *104,* 141. (d) Yu, Y. S.; Angelici, R. J. *Organometallics* **1983,** *2,* 1018. (e) Guerchais, B.; Astruc, D. *J. Chem. Soc., Chem. Commun.* **1985,** 835. (f) Bly, R. S.; Silverman, G. S. *Organometallics* **1984,** *3,* 1765. (g) Richmond, T. G.; Crespi, A. M.; Shriver, D. F. *Organometallics* **1984,** *3,* 314. (h) Cutler, A. R. *J. Am. Chem. Soc.* **1979,** *101,* 604. (i) Casey, C. P.; Miles, W. H.; Tukada, H. *J. Am. Chem. Soc.* **1985,** *107,* 2924. (j) Barefield, E. K.; McCarten, P.; Hillhouse, M. C. *Organometallics* **1985,** *4,* 1682. (k) Jolly, P. W.; Pettit, R. *J. Am. Chem. Soc.* **1966,** *88,* 5044. (l) Hoskins, S. V.; Richard, C. E. F.; Roper, W. R. *J. Chem. Soc., Chem. Commun.* **1984,** 1000. (m) Calabrese, J. C.; Roe, D. C.; Thorn, D. L.; Tulip, T. H. *Organometallics* **1984,** *3,* 1223.

(2) (a) Marks, T. J.; Seyam, A. M. *Inorg. Chem.* **1974,** *13,* 1624. (b) Schmid, G.; Balk, H.-J. *J. Organomet. Chem.* **1974,** *80,* 257. (c) Thum, G.; Malisch, W. *J. Organomet. Chem.* **1984,** *264,* C5. (d) Malisch, W. *Chem. Ber.* **1974,** *107,* 3835.

(3) Straus, D. A.; Tilley, T. D.; Rheingold, A. L.; Geib, S. J. *J. Am. Chem. Soc.* **1987,** *109,* 5872.

(4) (a) Aylett, B. J. *Adv. Inorg. Chem. Radiochem.* **1982,** *25,* 1. (b) Tilley, T. D. In *The Chemistry of Organic Silicon Compounds*; Patai, S., Rappoport, Z., Eds.; Wiley: New York, 1989; Vol. 2, Chapter 24.

(5) (a) Handwerker, H.; Leis, C.; Probst, R.; Bissinger, P.; Grohmann, A.; Kiprof, P.; Herdtwech, E.; Blümel, J.; Auner, N.; Zybill, C. *Organometallics* **1993,** *12,* 2162. (b) Probst, R.; Leis, C.; Gamper, S.; Herdtweck, E.; Zybill, C.; Auner, N. *Angew. Chem., Int. Ed. Engl.* **1991,** *30,* 1132.

(6) (a) Chauhan, B. P. S.; Corriu, R. J. P.; Lanneau, G. F.; Priou, C. *Organometallics* **1995,** *14,* 1657. (b) Corriu, R. J. P.; Chauhan, B. P. S.; Lanneau, G. F. *Organometallics* **1995,** *14,* 1646. (c) Corriu, R. J. P.; Chauhan, B. P. S.; Lanneau, G. F. *Organometallics* **1995,** *14,* 4014.

(7) ^1H NMR (300 MHz, CD_2Cl_2): δ 0.62 (d, $^3J_{HH}$ = 3.8 Hz, 3H, SiMe), 2.23 (s, 6H, NMe_2), 3.42 (d, $^2J_{HH}$ = 12.8 Hz, 1H, CH_2), 3.62 (d, $^2J_{HH}$ = 12.8 Hz, 1H, CH_2), 4.72 (s, 5H, Cp), 5.04 (q, $^3J_{HH}$ = 3.8 Hz, 1H, SiH), 7.21–7.34 (m, 3H, Ar), 7.61–7.64 (m, 1H, Ar). ^{29}Si NMR (59.6 MHz, CD_2Cl_2): δ 13.4. ^{13}C NMR (75.5 MHz, CD_2Cl_2): δ 2.9 (SiMe), 45.0 (NMe_2), 64.1 (CH_2), 84.5 (Cp), 126.3, 128.0, 129.3, 135.1, 143.7, 144.5 (Ar), 215.4, 215.8 (CO). IR (KBr): $\tilde{\nu}$ (cm^{-1}) 2107 (ν_{SiH}), 1994, 1911 (ν_{CO}). MS (EI, 70 eV): m/z 354 (2.9, $M^+ - H$), 179 (100), 135 (100), 121 (100). Anal. Calcd for $C_{17}H_{21}FeNO_2Si$: C, 57.47; H, 5.96; N, 3.94. Found: C, 57.42; H, 5.89; N, 3.92.

0276-7333/95/2314-5490$09.00/0

ture. NMR investigation revealed that the mixture contained Ph_3CH, BF_3, and compounds with Si–F bonding. This result suggests that hydride abstraction occurred during the reaction but was followed by secondary reactions. Our attention then turned to Ph_3CPF_6, since fluoride ion affinity toward PF_5 is considerably greater than that toward BF_3.[8]

The reaction of $FpSiHMeAr^N$ (**1**) with Ph_3CPF_6 in dichloromethane afforded complex **2** and Ph_3CH.[9] Complex **2** crystallized out as an air-sensitive yellow solid when the reaction mixture was cooled to −30 °C. The ^{29}Si NMR spectrum of **2** in acetonitrile-d_3 showed a singlet peak at δ 118.3 ppm, which appears at much lower field than that of the precursor complex **1** (δ 13.4 ppm) and at comparable field to those of the known silylene complexes stabilized by the Ar^N group (δ 110–145 ppm).[5,6] The fact that the ^{29}Si NMR gave a singlet peak and the SiMe signal in the ^1H NMR spectrum was observed as a singlet peak at δ 0.92 ppm shows that fluorination of the silicon did not take place during the reaction. From the spectroscopic and mass spectral data as well as the elemental analysis, complex **2** was identified as a cationic silylene complex with PF_6^-, $[Fp{=}SiMeAr^N]PF_6$ (**2**; eq 2). The existence of PF_6^- ions was also confirmed by ^{19}F NMR and IR spectroscopy. The structure of the complex **2** was unequivocally confirmed by X-ray crystal structure analysis.

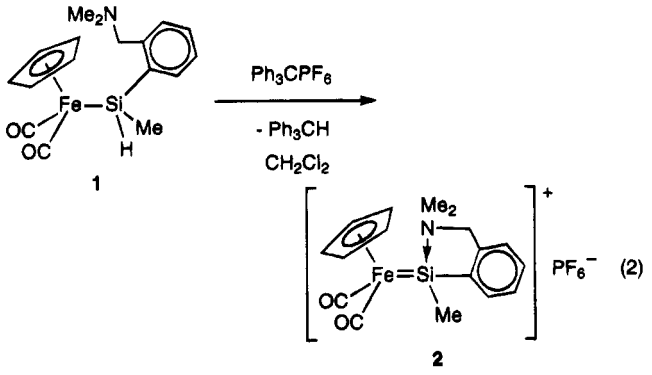

Figure 1 shows an ORTEP drawing of the cationic silyleneiron moiety $[Fp{=}SiMeAr^N]^+$ in complex **2**.[10] The short Fe–Si bond distance (2.2659(11) Å) of **2** suggests the unsaturated character of the Fe–Si bond, which is shorter than those of the usual silyliron complexes (2.32–2.37 Å)[4] and comparable to those of the known base-stabilized silyleneiron complexes (2.21–2.29 Å).[6a,13,14]

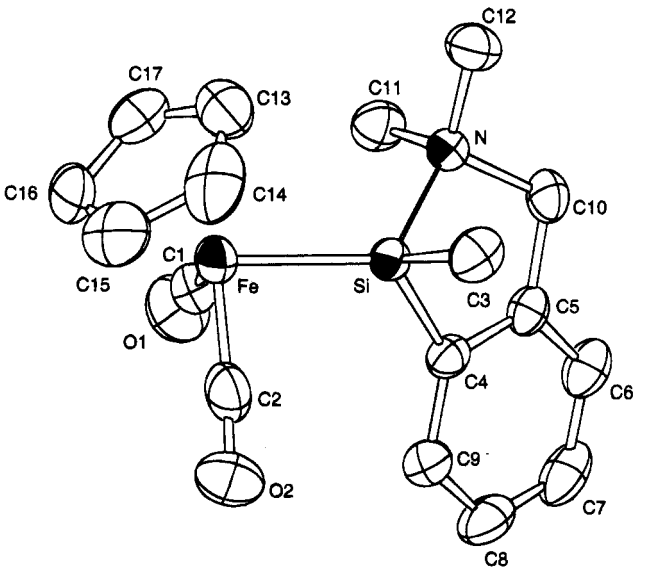

Figure 1. ORTEP drawing for the cationic silyleneiron moiety $[Fp{=}SiMeAr^N]^+$ in **2**. Atoms are represented by thermal ellipsoids at the 50% probability level. Selected bond lengths (Å) and angles (deg): Fe–Si, 2.2659(11); Fe–C(1), 1.748(5); Fe–C(2), 1.748(5); Fe–C(Cp), 2.097 (av); Si–C(3), 1.867(4); Si–C(4), 1.871(4); Si–N, 1.949(3); O(1)–C(1), 1.148(5); O(2)–C(2), 1.149(5); C(1)–Fe–Si, 89.85(14); C(2)–Fe–Si, 87.92(14); C(1)–Fe–C(2), 93.4(2); N–Si–Fe, 118.53(10); C(3)–Si–Fe, 116.6(2); C(4)–Si–Fe, 120.02(12); C(3)–Si–C(4), 107.0(2).

The Si–N bond distance (1.949(3) Å) is longer than the normal values of Si–N σ-bonds (1.70–1.76 Å) and much shorter than the sum of the van der Waals radii (3.2 Å).[6,15] Interestingly, the Si–N distance is shorter than that of the dative bonding in $H_2Si{\leftarrow}NH_3$ (2.06 Å) obtained by ab initio calculations[16] and those of other silylene complexes stabilized by the Ar^N group (1.962–2.046 Å).[5,6a] The sum of bond angles of the three covalently bonded substituents at silicon (343.6°) is also slightly smaller than those of other silylene complexes stabilized by the Ar^N group (346.7–351.3°).[5,6a] These results suggest that the Si←N dative interaction in **2** is relatively strong, which is expected due to the high electrophilicity of the silylene ligand imparted by the presence of a monopositive charge on complex **2**. The strong coordination of NMe_2 to the silylene ligand is also revealed by a VT ^1H NMR experiment. The silyleneiron complex **2** shows a rigid coordination of the dimethylamino group to silicon even at 80 °C in CD_3CN solution (300 MHz); i.e., no broadening of the diastereotopic Me_2N signals and the AB pattern signals of the CH_2 group was observed. This is in contrast to Zybill's silylene complex $(OC)_5Cr{=}SiPhAr^N$, which shows si-

(8) Haartz, J. C.; McDaniel, D. H. *J. Am. Chem. Soc.* **1973**, *95*, 8562.

(9) ^1H NMR (300 MHz, CD_3CN): δ 0.92 (s, 3H, SiMe), 2.84 (s, 3H, NMe), 3.00 (s, 3H, NMe), 4.39 (d, $^2J_{HH}$ = 15.1 Hz, 1H, CH_2), 4.64 (d, $^2J_{HH}$ = 15.1 Hz, 1H, CH_2), 5.28 (s, 5H, Cp), 7.37–7.67 (m, 4H, Ar). ^{29}Si NMR (59.6 MHz, CD_3CN): δ 118.3 (s). ^{13}C NMR (75.5 MHz, CD_3CN): δ 7.8 (SiMe), 48.0, 49.9 (NMe_2), 68.7 (CH_2), 68.4 (Cp), 125.7, 129.8, 132.1, 133.1, 139.8, 139.8 (Ar), 212.9, 213.3 (CO). ^{19}F NMR (282 MHz, CD_3CN): δ −71.0 (d, $^1J_{PF}$ = 714 Hz, PF_6^-). IR (CH_2Cl_2): $\bar{\nu}$ (cm^{-1}) 2025 (s), 1975 (s) (ν_{CO}), 849 (s) (PF_6^-, ν_{PF}), 557 (m) (PF_6^-, δ_{FPF}). MS (EI, 70 eV): *m/z* 354 (7, $M^+ - PF_6$), 326 (6), 121 (77). Anal. Calcd for $C_{17}H_{20}F_6FeNO_2PSi$: C, 40.90; H, 4.04; N, 2.81. Found: C, 40.62; H, 3.99; N, 2.80.

(10) Crystal data for **2**: $C_{17}H_{20}F_6FeNO_2PSi$, M_r = 499.25, triclinic, space group $P\bar{1}$, a = 9.4771(14) Å, b = 13.267(2) Å, c = 8.8592(14) Å, α = 104.94(2)°, β = 102.778(14)°, γ = 79.516(13)°, V = 1040.3(2) Å^3, Z = 2, D_{calcd} = 1.594 g/cm^3, μ = 0.925 mm^{-1}, $F(000)$ = 508. Data in the range 1.60 ≤ θ ≤ 32.49° were collected with graphite-monochromated Mo Kα radiation at 293 K (7524 reflections). The structure was solved by heavy-atom methods (SHELXS-86)[11] and refined by full-matrix least-squares techniques on all measured F^2 data (SHELXL-93);[12] GOF = 1.008. R1 = 0.0637 and wR2 = 0.1399 for 3647 reflections with $I > 2\sigma(I)$.

(11) Sheldrick, G. M. SHELXS-86, Program for Crystal Structure Determination; University of Göttingen, Göttingen, Germany, 1986.

(12) Sheldrick, G. M. SHELXL-93, Program for Crystal Structure Determination; University of Göttingen, Göttingen, Germany, 1993.

(13) (a) Ueno, K.; Tobita, H.; Shimoi, M.; Ogino, H. *J. Am. Chem. Soc.* **1988**, *100*, 4092. (b) Tobita, H.; Ueno, K.; Shimoi, M.; Ogino, H. *J. Am. Chem. Soc.* **1990**, *112*, 3415. (c) Ueno, K.; Ito, S.; Endo, K.; Tobita, H.; Inomata, S.; Ogino, H. *Organometallics* **1994**, *13*, 3309.

(14) (a) Leis, C.; Wilkinson, D. L.; Handwerker, H.; Zybill, C. *Organometallics* **1992**, *11*, 514. (b) Zybill, C.; Wilkinson, D. L.; Leis, C.; Müller, G. *Angew. Chem., Int. Ed. Engl.* **1989**, *28*, 203. (c) Leis, C.; Zybill, C.; Lachmann, J.; Müller, G. *Polyhedron* **1991**, *10*, 1163. (d) Zybill, C.; Müller, G. *Organometallics* **1988**, *7*, 1368. (e) Zybill, C.; Müller, G. *Angew. Chem., Int. Ed. Engl.* **1987**, *26*, 669.

(15) Sheldrick, W. S. In *The Chemistry of Organic Silicon Compounds*; Patai, S., Rappoport, Z., Eds.; Wiley: New York, 1989; Vol. 2, Chapter 3, p 227.

(16) (a) Conlin, R. T.; Laakso, D.; Marshall, P. *Organometallics* **1994**, *13*, 838. (b) Raghavachari, K.; Chandrasekhar, J.; Gordon, M. S.; Dykema, K. J. *J. Am. Chem. Soc.* **1984**, *106*, 5853.

multaneous coalescence of both Me_2N and CH_2 signals at 95 °C.[5] It is noteworthy that the cationic silyleneiron complex coexists with the fluorine-containing anion, PF_6^-. The surprising inertness of the cationic complex **2** toward the PF_6^- ion even at elevated temperature could be attained by the strong intramolecular coordination of the dimethylamino group in Ar^N to the highly electrophilic silylene ligand.

Some reactivity studies of complex **2** were carried out. Heating a CD_3CN solution of complex **2** in a sealed tube at 95 °C for 3 days afforded Ar^NSiMeF_2, Fp^-, and Fp_2, which would be generated by a reaction including fluorination of the silylene ligand by PF_6^- and successive cleavage of the silicon–iron linkage by PF_5.[2a] Thus, the stabilization of the silylene ligand by the Ar^N group is critical for the reactivity toward PF_6^-.

The silylene complex shows particular susceptibility to nucleophiles. Reaction of **2** with 1 equiv of MeOH led to the formation of the cationic methoxysilyl complex $[FpSiMeOMeAr^{NH}]PF_6$ (**3**, Ar^{NH} = 2-{$Me_2N(H)CH_2$}-C_6H_4; eq 3).[17] The ^{29}Si NMR signal of **3** appeared at

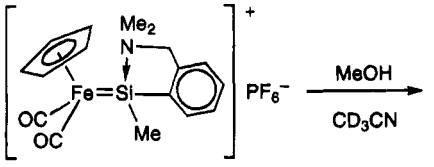

2

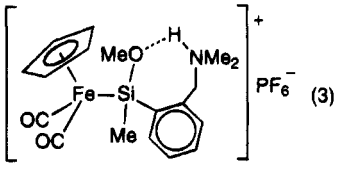

(3)

3

much higher field (δ 7.40 ppm) than that of the silylene complex **2**, indicating the loss of unsaturated character of the Fe–Si bond. The complex **3** showed a broad ^1H NMR signal at 8.8 ppm, which is assignable to the proton in the dimethylammonium group. The signals of the diastereotopic Me_2N and the CH_2 groups appeared as two doublets and an ABX pattern, respectively, due to the spin–spin coupling with the proton on the nitrogen atom.

Figure 2 shows an ORTEP drawing of the cationic (methoxysilyl)iron moiety $[FpSi(OMe)MeAr^{NH}]^+$ of complex **3**.[18] The Fe–Si bond distance of **3** (2.305(2) Å) is longer by 0.04 Å than that of the silylene complex **2** but is still shorter than those of the known (alkylsilyl)iron complexes (2.32–2.37 Å).[4] The relatively short Fe–Si distance of **3** may be attributed to the presence of the electron-withdrawing methoxy substituent on the silicon

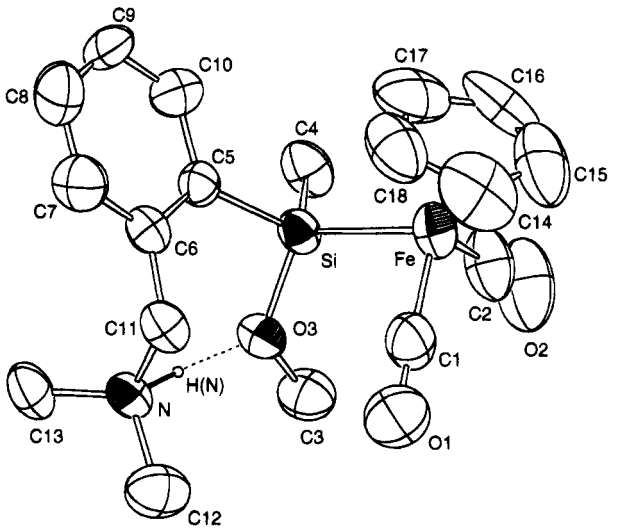

Figure 2. ORTEP drawing for the cationic (methoxysilyl)-iron moiety $[FpSi(OMe)MeAr^N]^+$ in **3**. Atoms are represented by thermal ellipsoids at the 50% probability level. Selected bond lengths (Å) and angles (deg): Fe–Si, 2.305(2); N···O3, 2.721(8); Fe–C(1), 1.723(10); Fe–C(2), 1.761(11); O(1)–C(1), 1.156(10); O(2)–C(2), 1.121(10); Si–O(3), 1.670(5); Si–C(4), 1.878(8); Si–C(5), 1.889(8); Fe–C(Cp), 2.071 (av); C(4)–Si–C(5), 108.3(4); O(3)–Si–Fe, 114.3(2); C(4)–Si–Fe, 112.3(3); C(5)–Si–Fe, 114.8(2); C(1)–Fe–C(2), 94.5(5); C(1)–Fe–Si, 87.5(3); C(2)–Fe–Si, 88.3(3); O(3)–Si–C(4), 104.7(3); C(3)–O(3)–Si, 123.3(5); O(1)–C(1)–Fe, 177.6(10); O(2)–C(2)–Fe, 179.2(10).

atom.[4] The Si–O(3) bond distance lies within the range for a covalent bond (1.670(5) Å).[15] The sum of the C–Si–C and two C–Si–Fe bond angles in **3** (335.4°) is smaller than that of **2** (343.6°), indicating the sp^3 character of the silicon atom in **3**. The N–H(N) bond in the dimethylammonium unit is directed toward oxygen O(3) (N···O(3) = 2.74(1) Å) by hydrogen bonding (N–H(N)···O(3)).

The cationic silyleneiron complex **2** reacts with some nucleophiles, such as HMPA, HCl, H_2O, and PMe_3. Further studies on the reactivity of the silylene complex **2** and related complexes are in progress.

Acknowledgment. This work was supported by Grants-in-Aid for Scientific Research (Nos. 05236104 and 07740516) from the Ministry of Education, Science and Culture of Japan. We are grateful to Shin-Etsu Chemical Co., Ltd., for a gift of silicon compounds.

Supporting Information Available: Text giving experimental details for the syntheses of **1**–**3** and the crystal structure analyses of **2** and **3** and tables of crystal data and structural refinement, positional and thermal parameters, and bond lengths and angles for **2** and **3** (18 pages). Ordering information is given on any current masthead page.

OM950640O

(17) ^1H NMR (300 MHz, CD_2Cl_2): δ 0.89 (s, 3H, SiMe), 2.78 (d, $^3J_{HH}$ = 5.3 Hz, 3H, NMe), 3.02 (d, $^3J_{HH}$ = 5.1 Hz, 3H, NMe), 3.65 (s, 3H, OMe), 4.17 (dd, $^2J_{HH}$ = 12.7 Hz, $^3J_{HH}$ = 7.4 Hz, 1H, CH_2), 4.55 (dd, $^2J_{HH}$ = 12.7 Hz, $^3J_{HH}$ = 4.3 Hz, 1H, CH_2), 4.97 (s, 5H, Cp), 7.38–7.68 (m, 4H, Ar), 8.78 (br, 1H, NH). ^{29}Si NMR (59.6 MHz, CD_2Cl_2): δ 74.0 (s). ^{13}C NMR (75.5 MHz, CD_2Cl_2): δ 7.4 (SiMe), 41.9, 43.8 (NMe_2), 52.0 (OMe), 63.9 (CH_2), 85.1 (Cp), 130.2, 130.3, 133.3, 133.7, 135.0, 146.1 (Ar), 214.9, 215.7 (CO). ^{19}F NMR (282 MHz, CD_2Cl_2): δ −72.0 (d, $^1J_{PF}$ = 701 Hz, PF_6^-). IR (CH_2Cl_2): $\tilde{\nu}$ (cm^{-1}) 2002 (s), 1946 (s) (ν_{CO}), 849 (s) (PF_6^-, ν_{PF}), 557 (m) (PF_6^-, δ_{FPF}). MS (FAB, Xe, NBA): *m/z* 917 (10, $2M^+ - PF_6$), 386 (100, $M^+ - PF_6$), 208 (16). Anal. Calcd for $C_{18}H_{24}F_6FeNO_3PSi \cdot 0.8CH_2Cl_2$: C, 37.68; H, 4.31; N, 2.34. Found: C, 37.67; H, 4.28; N, 2.55.

(18) Crystal data for **3**: $C_{19}H_{26}Cl_2F_6FeNO_3PSi$, M_r = 616.22, monoclinic, space group $P2_1/n$, a = 14.157(2) Å, b = 16.027(3) Å, c = 11.843(2) Å, β = 92.83(2)°, V = 2683.8(8) Å^3, Z = 4, D_{calcd} = 1.525 g/cm^3, μ = 0.928 mm^{-1}, $F(000)$ = 1256. Data in the range 1.92 ≤ θ ≤ 27.51° were collected with graphite-monochromated Mo Kα radiation at 293 K (6474 reflections). The structure was solved by heavy-atom methods (SHELXS-86)[11] and refined by full-matrix least-squares techniques on all collected F^2 data (SHELXL-93);[12] GOF = 0.990. R1 = 0.0729 and wR2 = 0.1622 for 1864 reflections with $I > 2\sigma(I)$.

Organometallic Complexes for Nonlinear Optics. 4.[1] Cubic Hyperpolarizabilities of (Cyclopentadienyl)bis(phosphine)ruthenium σ-Arylacetylides

Ian R. Whittall and Mark G. Humphrey*

Department of Chemistry, Australian National University, Canberra, ACT 0200, Australia

Marek Samoc, Jacek Swiatkiewicz,† and Barry Luther-Davies

Laser Physics Centre, Research School of Physical Sciences and Engineering, Australian National University, Canberra, ACT 0200, Australia

Received June 26, 1995[⊗]

Summary: Third-order molecular optical nonlinearities of a systematically varied series of (cyclopentadienyl)-bis(phosphine)ruthenium arylacetylide complexes have been determined by Z-scan and degenerate four-wave mixing techniques: the influence on the nonlinear response of replacing the acetylide by a chloro ligand, varying the phosphine, extending the acetylide chain length, or modifying the substituent at the 4-position of the arylacetylide has been studied.

New materials exhibiting large nonlinear optical (NLO) responses are required for applications in photonics. Organometallic compounds have been attracting attention recently, but the vast majority of such studies have been concerned with quadratic optical nonlinearities—third-order responses have been little investigated.[2] In particular, very little is known of the effect of systematic structural variation on cubic hyperpolarizability. We have recently commenced a detailed investigation of the NLO behavior of organometallic compounds[3] and report herein the results of studies on the third-order hyperpolarizabilities of systematically varied (cyclopentadienyl)ruthenium complexes.

The complexes studied are of general formula $RuX(L)_2(\eta\text{-}C_5H_5)$ (L = PPh_3, PMe_3; X = Cl, C≡CR (R = C_6H_5, 4-C_6H_4Br, 4-$C_6H_4NO_2$, (*E*)-4,4′-$C_6H_4CH{=}CHC_6H_4NO_2$, 4,4′-$C_6H_4C{\equiv}CC_6H_4NO_2$)) and were synthesized by either literature procedures[4] or extensions thereof (full details of the synthesis, spectroscopic properties, and X-ray structural characterization of complexes **4a**,**b**, **5**, and **6** will be reported elsewhere);[1,3b] the numbering scheme used in the subsequent discussion is shown in Table 1. The third-order nonlinearities were evaluated by the Z-scan technique[5] with some additional experiments performed using degenerate four-wave mixing (DFWM). Z-scan does not provide information on the temporal behavior of the NLO response. It does, however, have a significant advantage over DFWM: the signs of the NLO susceptibility components (both real and imaginary) are accessible without the need to carry out measurements on many solutions with a wide range of concentrations. A combination of both techniques is therefore an advantage. Measurements were performed at 800 nm using a system consisting of a Coherent Mira Ar-pumped Ti–sapphire laser generating a mode-locked train of approximately 100 fs pulses and a home-built Ti–sapphire regenerative amplifier pumped with a frequency-doubled Q-switched pulsed YAG laser (Spectra Physics GCR) at 30 Hz and employing chirped pulse amplification.

Results of the measurements are given in Table 1. A number of conclusions from comparisons across these data can be made. The observed responses are not simply the sums of components of the complexes; γ for **4b** is much larger than that for **1b** and 4-nitrophenylethyne (20×10^{-36} esu), indicating that electronic communication between the ligated metal and acetylide fragments is important. The cubic nonlinearities of the chloro complexes are quite low, and the stated values incorporate a substantial error margin; for comparison, γ values for titanocene and zirconocene halides are also very low ($\leq 5 \times 10^{-36}$ esu) by third-harmonic generation.[6] Phosphine ligand replacement causes little difference in γ, as shown by **4a**,**b**, where there is a substantial variation in donor power of the phosphine; the possibility of varying the ligand environment to tune nonlinear optical response is a potential benefit of organometallic materials, but the result here does not support that idea. Not surprisingly, extension from a one-ring chromophore (**4a**) to an extended-chain two-ring chromophore (**5**) leads to a large increase in γ, which parallels results from the "all-organic" system. Minor variation in the acetylide ligand (replacement of 4-H by 4-Br in proceeding from **2** to **3**) has no discernible effect on γ. However, replacement of H by the strongly withdrawing NO_2 (**2** to **4a**) makes a significant difference in the cubic nonlinearity; a similar increase was observed in proceeding from styrene to its 4-nitro derivative.[6] The real component of γ is the same for

* To whom correspondence should be addressed.
† On leave from the Photonics Research Laboratory, State University of New York, Buffalo, NY.
⊗ Abstract published in *Advance ACS Abstracts,* November 15, 1995.
(1) Part 3: Whittall, I. R.; Humphrey, M. G.; Hockless, D. C. R. To be submitted for publication.
(2) (a) Nalwa, H. S. *Appl. Organomet. Chem.* **1991**, *5*, 349. (b) Long, N. J. *Angew. Chem., Int. Ed. Engl.* **1995**, *34*, 21.
(3) (a) Whittall, I. R.; Cifuentes, M. P.; Costigan, M. J.; Humphrey, M. G.; Goh, S. C.; Skelton, B. W.; White, A. H. *J. Organomet. Chem.* **1994**, *471*, 193. (b) Whittall, I. R.; Humphrey, M. G.; Hockless, D. C. R.; Skelton, B. W.; White, A. H. *Organometallics* **1995**, *14*, 3970.
(4) (a) Bruce, M. I.; Wallis, R. C. *Aust. J. Chem.* **1979**, *32*, 1471. (b) Bruce, M. I.; Hameister, C.; Swincer, A. G.; Wallis, R. C. *Inorg. Synth.* **1982**, *21*, 78. (c) Bruce, M. I.; Koutsantonis, G. A.; Liddell, M. J.; Nicholson, B. K. *J. Organomet. Chem.* **1987**, *320*, 217.
(5) Sheikh-bahae, M.; Said, A. A.; Wei, T.; Hagan, D. J.; van Stryland, E. W. *IEEE J. Quantum Electron.* **1990**, *26*, 760.
(6) Myers, L. K.; Langhoff, C.; Thompson, M. E. *J. Am. Chem. Soc.* **1992**, *114*, 7560.

0276-7333/95/2314-5493$09.00/0

Table 1. Cubic Hyperpolarizabilities of $Ru(R)(PR'_3)_2(\eta\text{-}C_5H_5)$ Complexes[a] from Z-Scan and DFWM Measurements

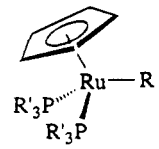

			γ (10^{-36} esu)[b]			
			DFWM	Z-scan		
complex	R	R'	real part	real part	imag part	λ_{max}[c]
1a	Cl	Ph	50 ± 20	150 ± 100		348
1b	Cl	Me	80 ± 30	≤80		346
2	C≡CPh	Ph		≤150		311
3	$C{\equiv}CC_6H_4Br$-4	Ph		≤150		325
4a	$C{\equiv}CC_6H_4NO_2$-4	Ph	−260 ± 60	−210 ± 50	≤10	461
4b	$C{\equiv}CC_6H_4NO_2$-4	Me		−230 ± 70	74 ± 30	480
5	(*E*)-4,4′-$C{\equiv}CC_6H_4CH{=}CHC_6H_4NO_2$	Ph		−450 ± 100	210 ± 100	476, 346
6	4,4′-$C{\equiv}CC_6H_4C{\equiv}CC_6H_4NO_2$	Ph		−450 ± 100	≤20	447, 346

[a] Measurements at 800 nm (all complexes are optically transparent at this wavelength) for tetrahydrofuran (THF) solutions. [b] All results are referenced to the hyperpolarizability of THF, $\gamma = 1.6 \times 10^{-36}$ esu. [c] All as THF solutions.

the ene-linked complex **5** and the yne-linked complex **6**, but the former has a substantial imaginary component which results in a larger vectorial sum; for these complexes, the cubic hyperpolarizability increases faster with chain length for the ene-linked organometallic chromophore compared to the yne-linked analogue, paralleling our observations on computationally derived quadratic optical nonlinearities in this system.[1]

Complexes **1a,b**, **2**, and **3** have positive γ values, whereas the nitro complexes **4a,b**, **5**, and **6**, presumably incorporating a strong donor−acceptor interaction, have negative γ values. It was of interest to ascertain the origin of the negative responses, the first reports of negative γ values for organometallic complexes. Investigations on **4a** and **4b** by femtosecond time-resolved DFWM confirm that the negative γ values are not due to thermal lensing; the observed response of solutions shows a concentration dependence characteristic for a negative real part of γ of the solute, while the DFWM signal retains its femtosecond response. The observation of a negative real component of γ together with a complex component (as evident for complexes **4b** and **5**) is suggestive of electronic resonance enhancement, with the imaginary part relating to nonlinear absorption. It is perhaps significant that negative γ is observed for complexes with λ_{max} longer than 400 nm and positive γ for complexes with λ_{max} shorter than 400 nm, consistent with the dispersion effect of two photon states contributing to the observed responses, and we favor this explanation at present, although the possibility of negative static hyperpolarizabilities (for the acetylide complexes bearing nitro substituents) cannot be dismissed.

Off-resonant negative γ is rather unusual; however, results thus far do not permit us to eliminate this possibility (measurements at other wavelengths may resolve this issue). Off-resonant electronic third-order optical susceptibility has been discussed for organic systems.[7-9] A simplified three-level model has been applied with success to a variety of molecular types, including conjugated donor−acceptor dipolar molecules with a large second-order susceptibility β, organic compounds similar to the organometallic complexes considered here; off-resonance susceptibilities are predicted to be positive-definite for such molecules, but it has not been shown that a simplified three-level model is justifiable for an organometallic complex. According to this model, negative susceptibilities are only observable in simple organic systems such as charged polymethine dyes with an odd number of atoms in the conjugative unit,[8] or in molecules with little or no bond-length alternation in conjugated bridges. For the latter, Marder *et al.* have demonstrated the solvent dependence of γ for polyene structures capped by donor and acceptor groups;[10] changes in molecular geometry from a highly bond-length-alternated form in nonpolar solvents to one with little bond-length alternation in polar solvents resulted in a change from positive γ to negative γ. Similarly, polarization by external point charges resulted in decreased bond-length alternation and negative γ.[11] In the organometallic complexes considered here, there is no evidence for variation in bond-length alternation (from an arylacetylide structure to one with quinoidal vinylidene character) on modifying solvent polarity. In **4b**, for example, λ_{max} shifts dramatically (440 nm (cyclohexane), 480 nm (tetrahydrofuran), 505 nm (dimethylformamide)) on increasing the solvent polarity, but solvatochromism is normally considered to reflect electron polarization without atomic displacement.[12] Infrared data from key structural elements in the organometallic chromophore provide a better indication of changes in molecular geometry; $\nu(C{\equiv}C)$ does not decrease significantly (2060 cm^{-1} (cyclohexane), 2047 cm^{-1} (tetrahydrofuran), 2041 cm^{-1} (dimethylformamide)) on varying solvent polarity, indicating that the arylacetylide structure is maintained, and indeed minimal bond-length variation for arene-containing chromophores would be predicted due to the potential loss

(7) Kuzyk, M. G.; Dirk, C. W. *Phys. Rev. A* **1990**, *41*, 5098.
(8) Dirk, C. W.; Cheng, L.-T.; Kuzyk, M. G. *Int. J. Quantum Chem.* **1992**, *43*, 27.
(9) Dirk, C. W.; Caballerro, N.; Kuzyk, M. G. *Chem. Mater.* **1993**, *5*, 733.
(10) Marder, S. R.; Perry, J. W.; Bourhill, G.; Gorman, C. B.; Tiemann, B. G.; Mansour, K. *Science* **1993**, *261*, 186.
(11) Gorman, C. B.; Marder, S. R. *Proc. Natl. Acad. Sci. U.S.A.* **1993**, *90*, 11297.
(12) Paley, M. S.; Harris, J. M.; Looser, H.; Baumert, J. C.; Bjorklund, G. C.; Jundt, D.; Twieg, R. J. *J. Org. Chem.* **1989**, *54*, 3774.

of aromatic stabilization energy. We do not believe that bond-length-alternation effects are operative in giving rise to negative γ values for these donor–acceptor organometallic acetylides.

Few comparisons of cubic molecular nonlinearities with other organometallic complexes are possible, given the paucity of extant data; it should also be stressed that comparisons between systems examined by different techniques are very difficult. Ferrocene (16×10^{-36} esu) and some cyclopentadienyl-ring-substituted derivatives ($(85-305) \times 10^{-36}$ esu) were investigated by DFWM;[13] interestingly, dimeric and oligomeric derivatives gave larger responses ($(504-1550) \times 10^{-36}$ esu), but overall the ferrocenyl group itself made little contribution to nonlinearity. 1,8-Bis(ferrocenyl)octatetrayne has a reported γ value of 110×10^{-36} esu (by dc electric field induced second-harmonic generation).[14] A series of titanium and zirconium acetylide complexes are reported to have γ values of $(50-100) \times 10^{-36}$ esu (by third-harmonic generation, THG) with the larger values being bis(acetylide) complexes; these studies showed that the response can be tuned by metal replacement.[6] Oligomeric group 10 metal acetylides have also been investigated ($\gamma = (56-856) \times 10^{-36}$ esu by THG and DFWM); the type of metal, arene spacer, and conjugation length were all important.[2b] The present investigation is important in that, by employing a systematically varied series of complexes, it establishes the significance of (i) phosphine ligand substitution and (ii) variation in acetylide substituent, (iii) it suggests that chain lengthening by ene linkage is the most effective method for maximizing γ in acetylide complexes, and (iv) it reports the first negative γ value for organometallic complexes; thermal lensing and bond-length-alternation effects have been rejected as the cause of negative γ, and two-photon dispersion seems likely, but a negative static hyperpolarizability is also possible. Further studies with systematically varied molecules are currently underway.

Acknowledgment. We thank the Australian Research Council and the Harry Triguboff AM Syndicate for support of this work and Johnson-Matthey Technology Centre for the loan of ruthenium salts. I.R.W. is the recipient of an Australian Postgraduate Research Award (Industry), and M.G.H. holds an ARC Australian Research Fellowship.

OM950497Z

(13) Ghosal, S.; Samoc, M.; Prasad, P. N.; Tufariello, J. T. *J. Phys. Chem.* **1990**, *94*, 2847.
(14) Yuan, Z.; Taylor, N. J.; Sun, Y.; Marder, T. B. *J. Organomet. Chem.* **1993**, *449*, 27.

Articles

Synthesis, Characterization, and Homopolymerization and Copolymerization Behavior of the Silicon-Bridged [1]Chromarenophane $Cr(\eta\text{-}C_6H_5)_2SiMe_2$

Kai C. Hultzsch, James M. Nelson, Alan J. Lough, and Ian Manners*

Department of Chemistry, University of Toronto, 80 St. George Street, Toronto M5S 1A1, Ontario, Canada

Received June 21, 1995[⊗]

The silicon-bridged [1]chromarenophane $Cr(\eta\text{-}C_6H_5)_2SiMe_2$ (**7**) was synthesized by the reaction of $[Cr(\eta\text{-}C_6H_5Li)_2]\cdot$TMEDA (TMEDA, *N,N,N,N*-tetramethyl-1,2-ethylenediamine) with Me_2SiCl_2 in hexanes. The molecular structure of **7** was determined by single-crystal X-ray diffraction and was shown to be strained, with an angle between the planes of the arene rings of 16.6(3)°. In addition, significant distortion from planarity was detected in **7** for the arene carbon atom bonded to the bridging silane moiety, with angles between the planes of the arene ligands and the C(arene)–Si bonds of 37.9(4)° and 38.2(4)°. Compound **7** does not undergo thermal ring-opening polymerization at temperatures approaching 180 °C, but instead decomposes to yield chromium metal and Ph_2SiMe_2. This behavior contrasts with that of silicon-bridged [1]ferrocenophanes such as $Fe(\eta\text{-}C_5H_4)_2SiMe_2$ (**1**), which readily thermally polymerize to yield poly(ferrocenylsilanes) at 130 °C and above. However, thermal treatment of equimolar mixtures of **7** and **1** at 140 °C for 72 h resulted in the formation of the air-sensitive, heterobimetallic copolymer $[Cr(\eta\text{-}C_6H_5)_2SiMe_2]_x[Fe(\eta\text{-}C_5H_4)_2SiMe_2]_y$ (**9a**), which was identified by ^1H, ^{13}C, and ^{29}Si NMR. Treatment of equimolar mixtures of **7** and **1** in THF with anionic initiators such as BuLi/hexanes resulted in the formation of an analogous copolymer **9b**. ^1H NMR integration and, after selective cleavage of the silicon–arene bonds in the copolymers by treatment with methanol, analysis of the residual ferrocenylsilane segments by GPC allowed an estimate of the molecular weights of **9a** and **9b**. These results indicated that the minimum value of M_w for **9a** was *ca.* 2.4×10^3 and that for **9b** was *ca.* 1.2×10^4.

Introduction

Well-defined, high molecular weight, transition-metal-containing polymers currently are a topic of considerable interest due to their interesting properties and potential applications.[1,2] In 1992, we reported[3] that strained, ring-tilted, silicon-bridged [1]ferrocenophanes (*e.g.*, **1**) undergo ring-opening polymerization (ROP) to yield high molecular weight poly(ferrocenylsilanes) **2**.[4–6] These silicon-bridged [1]ferrocenophanes have also been shown to undergo anionic ring-opening oligomerization and polymerization in solution in the presence of anionic initiators to produce, in some cases, living systems.[5c,7] In addition, transition-metal-catalyzed ROP of species such as **1** has recently been reported.[8] We have also described the successful extension of this ROP methodology to related species, such as other [1]ferrocenophanes and hydrocarbon-bridged [2]metallocenophanes **3**.[9,10] In all cases in which ROP has been shown

[⊗] Abstract published in *Advance ACS Abstracts,* October 15, 1995.

(1) (a) Pittman, C. U., Jr.; Carraher, C. E., Jr.; Reynolds, J. R. In *Encyclopedia of Polymer Science and Engineering*; Mark, H. F., Bikales, N. M., Overberger, C. G., Menges, G., Eds.; Wiley: New York, 1989; Vol. 10, p 541. (b) Mark, J. E.; Allcock, H. R.; West, R. *Inorganic Polymers*; Prentice Hall: Englewood Cliffs, NJ, 1992. (c) Allcock, H. R. *Adv. Mater.* **1994**, *6*, 106. (d) Manners, I. *Adv. Mater.* **1994**, *6*, 68.

(2) For recent examples of transition-metal-based polymeric materials, see the following: (a) Fyfe, H. B., Mlekuz, M.; Zargarian, D.; Taylor, N. J.; Marder, T. B. *J. Chem. Soc., Chem. Commun.* **1991**, 188. (b) Tenhaeff, S. C.; Tyler, D. R. *Organometallics* **1992**, *11*, 1466. (c) Davies, S. J.; Johnson, B. F. G.; Khan, M. S.; Lewis, J. *J. Chem. Soc., Chem. Commun.* **1991**, 187. (d) Lewis, J.; Khan, M. S.; Kakkar, A. K.; Johnson, B. F. G.; Marder, T. B.; Fyfe, H. B.; Whittmann, F.; Friend, R. H.; Dray, A. E. *J. Organomet. Chem.* **1992**, *425*, 165. (e) Nugent, H. M.; Rosenblum, M.; Klemarczyk, P. *J. Am. Chem. Soc.* **1993**, *115*, 3848. (f) Dembek, A. A.; Fagan, P. J.; Marsi, M. *Macromolecules* **1993**, *26*, 2992. (g) Brandt, P. F.; Rauchfuss, T. B. *J. Am. Chem. Soc.* **1992**, *114*, 1926. (h) Roesky, H. W.; Lücke, M. *Angew. Chem., Int. Ed. Engl.* **1989**, *28*, 493. (i) Bayer, R.; Pöhlmann, T.; Nuyken, O. *Makromol. Chem., Rapid Commun.* **1993**, *114*, 6246.

(3) Foucher, D. A.; Tang, B. Z.; Manners, I. *J. Am. Chem. Soc.* **1992**, *114*, 6246.

(4) Manners, I. *Adv. Organomet. Chem.* **1995**, *37*, 131.

(5) (a) Foucher, D. A.; Ziembinski, R.; Tang, B.-Z.; Macdonald, P. M.; Massey, J.; Jaeger, C. R.; Vancso, G. J.; Manners, I. *Macromolecules* **1993**, *26*, 2878. (b) Foucher, D.; Ziembinski, R.; Petersen, R.; Pudelski J.; Edwards, M.; Ni, Y.; Massey, J.; Jaeger, C. R.; Vancso, G. J.; Manners, I. *Macromolecules* **1994**, *27*, 3992. (c) Rulkens, R.; Ni, Y.; Manners, I. *J. Am. Chem. Soc.* **1994**, *116*, 12121. (d) Foucher, D. A.; Honeyman, C. H.; Nelson, J. M.; Tang, B. Z.; Manners, I. *Angew. Chem., Int. Ed. Engl.* **1993**, *32*, 1709.

(6) For the work of other groups on poly(ferrocenylsilanes) and related materials, see the following: (a) Rosenberg, H. U.S. Patent 3,-426,053, 1969. (b) Tanaka, M.; Hayashi, T. *Bull. Chem. Soc. Jpn.* **1993**, *66*, 334. (c) Nguyen, M. T.; Diaz, A. F.; Dement'ev, V. V.; Pannell, K. H. *Chem. Mater.* **1993**, *5*, 1389.

(7) Rulkens, R.; Lough, A. J.; Manners, I. *J. Am. Chem. Soc.* **1994**, *116*, 797.

(8) Ni, Y.; Rulkens, R.; Pudelski, J. K.; Manners, I. *Makromol. Chem., Rapid Commun.* **1995**, *16*, 637.

0276-7333/95/2314-5496$09.00/0

to take place, the monomers have been found to possess strained structures in which the cyclopentadienyl ligands are tilted substantially by *ca.* 18–31°.[4,11,12]

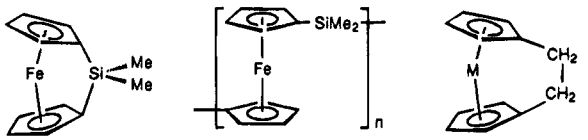

1 2 3 M = Fe, Ru

The first silicon-bridged [1]chromarenophane, $Cr(\eta\text{-}C_6H_5)_2SiPh_2$ (**4**), was synthesized in 1990 by Elschenbroich and co-workers.[13] An X-ray diffraction study of this species indicated that this compound possesses a strained structure with a tilt angle between the planes of the arene ligands of *ca.* 14°. Related compounds such as **5** and **6** have also been characterized, and these also have strained, ring-tilted structures. These results suggest that [*n*]metalloarenophanes may also function as precursors to novel transition-metal-based polymers via ROP. In this paper, we report on the synthesis, molecular structure, and polymerization behavior of $Cr(\eta\text{-}C_6H_5)_2SiMe_2$ (**7**), the chromarenophane analog of **1**.[14]

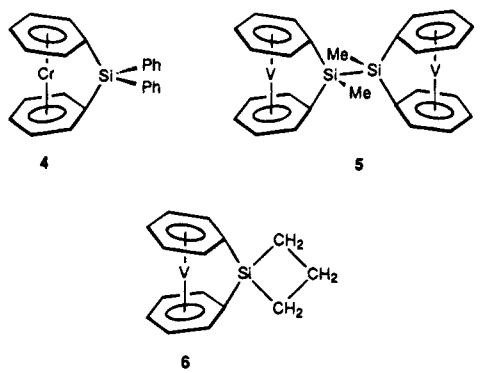

4 5 6

Results and Discussion

Various silicon-bridged [1]metalloarenophanes have previously been synthesized and structurally characterized. For example, the previously mentioned species **4** was found to possess a substantially ring-tilted structure with a tilt angle of 14.4°.[13] In addition, the silicon-bridged [1]vanadarenophanes **5** and **6** were found to possess tilt angles of 20.8° [15] and 19.9°,[16] respectively. The structures of these species are strikingly similar to those of silicon-bridged [1]ferrocenophanes, and this suggests that similar ROP behavior might be anticipated. To study the ROP behavior of these silicon-bridged chromarenophanes, we targeted the chromarenophane analog of the ferrocenophane **1** rather than phenylated **4**, as the ferrocenophane analog of the latter yields a poly(ferrocenylsilane) that is insoluble and difficult to characterize.[3,5a]

Synthesis and Characterization of the Silicon-Bridged [1]Chromarenophane $Cr(\eta\text{-}C_6H_5)_2SiMe_2$ (7). The [1]chromarenophane **7** was prepared as a maroon crystalline material in 56% yield via the reaction of $[Cr(\eta\text{-}C_6H_5Li)_2]\cdot$TMEDA with Me_2SiCl_2 in hexanes, a route analogous to that previously reported by Elschenbroich and co-workers for the synthesis of **4**.[13] The synthesis $[Cr(\eta\text{-}C_6H_5Li)_2]\cdot$TMEDA was carried out by reaction of bis(benzene)chromium with BuLi/TMEDA in refluxing cyclohexane.

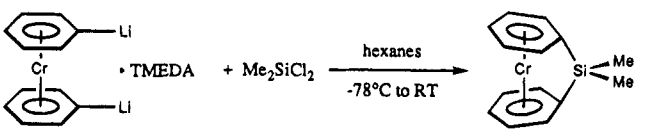

7

The identity of **7** was confirmed by ^1H, ^{13}C, and ^{29}Si NMR and mass spectrometry, which gave data consistent with the assigned structure. Significantly, the ^{13}C NMR spectroscopic data for **7** indicated that this species is significantly strained. Thus, an upfield ^{13}C NMR chemical shift for the *ipso*-arene carbons bonded to silicon was found (39.5 ppm) compared to bis(benzene)-chromium (73.2 ppm).[17] By comparison, a similar trend has been found for strained, ring-tilted [1]ferrocenophanes (*e.g.*, **1**), where the *ipso*-cyclopentadienyl carbon atom bonded to silicon is shifted 35–60 ppm upfield compared to analogous unstrained species.[18] To allow a comparison of the molecular structure of compound **7** with those of related species, a single-crystal X-ray diffraction study was carried out.

Discussion of the X-ray Structure of 7. Maroon-colored single crystals of **7** suitable for an X-ray diffraction study were obtained from a solution of the compound in hexanes at −30 °C. Two alternative views of the molecular structures of **7** are shown in Figure 1a,b. A summary of cell constants and data collection parameters is included in Table 1, the fractional coordinates are listed in Table 2, and important bond lengths and angles are listed in Table 4 of the supporting information for **7**. The angles α, β, θ, and δ used in discussing the structures are defined in Figure 2.[18]

The most interesting structural feature of **7** is the tilt of the virtually planar arene ligands with respect to one another (Figure 1). The tilt angle of 16.6(3)° in **7** is slightly larger than that in the previously characterized phenylated analog **4** (α = 14.4°). The degree of tilting in **7** can also be appreciated by considering the arene-

(9) (a) Nelson, J. M.; Rengel, H.; Manners, I. *J. Am. Chem. Soc.* **1993**, *115*, 7035. (b) Nelson, J. M.; Lough, A. J.; Manners, I. *Angew. Chem., Int. Ed. Engl.* **1994**, *33*, 989.

(10) Foucher, D. A.; Edwards, M.; Burrow, R. A.; Lough, A. J.; Manners, I. *Organometallics* **1994**, *13*, 4959.

(11) (a) Stoeckli-Evans, H.; Osborne, A. G.; Whiteley, R. H. *Helv. Chim. Acta* **1976**, *59*, 2402. (b) Stoeckli-Evans, H.; Osborne, A. G.; Whiteley, R. H. *J. Organomet. Chem.* **1980**, *194*, 91. (c) Seyferth, D.; Withers, H. P. *Organometallics*, **1982**, *1*, 1275. (d) Butler, I. R.; Cullen, W. R.; Einstein, F. W. B.; Rettig, S. J.; Willis, A. J. *Organometallics* **1983**, *2*, 128. (e) Fischer, A. B.; Bruce, J. A.; McKay, D. R.; Maciel, G. E.; Wrighton, M. S. *Inorg. Chem.* **1982**, *21*, 1766. (f) Osborne, A. G.; Whiteley, R. H.; Meads, R. E. *J. Organomet. Chem.* **1980**, *193*, 345.

(12) Pudelski, J. K.; Gates, D. P.; Rulkens, R.; Lough, A. J.; Manners, I. *Angew. Chem., Int. Ed. Engl.* **1995**, *34*, 1506.

(13) Elschenbroich, C.; Hurley, J.; Metz, B.; Massa, W.; Baum, G. *Organometallics* **1990**, *9*, 889.

(14) Elschenbroich and co-workers have mentioned in a footnote in a paper published in 1990 that they have prepared compound **7**, but no characterization data were reported (see ref 13, footnote 16). After this manuscript was submitted, we were informed by Professor Elschenbroich that the characterization data are described in a Ph.D. Thesis (Hurley, J. Doktorarbeit, Philipps-Universität Marburg, 1989).

(15) Elschenbroich, C.; Bretschneider-Hurley, A.; Hurley, J.; Massa, W.; Wocadio, S.; Pebler, J.; Reijerse, E. *Inorg. Chem.* **1993**, *32*, 5421.

(16) Elschenbroich, C.; Bretschneider-Hurley, A.; Hurley, J.; Behrendt, A.; Massa, W.; Wocadlo, S.; Reijerse, E. *Inorg. Chem.* **1995**, *34*, 743.

(17) Elschenbroich, C.; Koch, J. *J. Organomet. Chem.* **1982**, *229*, 139.

(18) Osborne, A. G.; Whiteley, R. H.; Meads, R. E. *J. Organomet. Chem.* **1980**, *193*, 345.

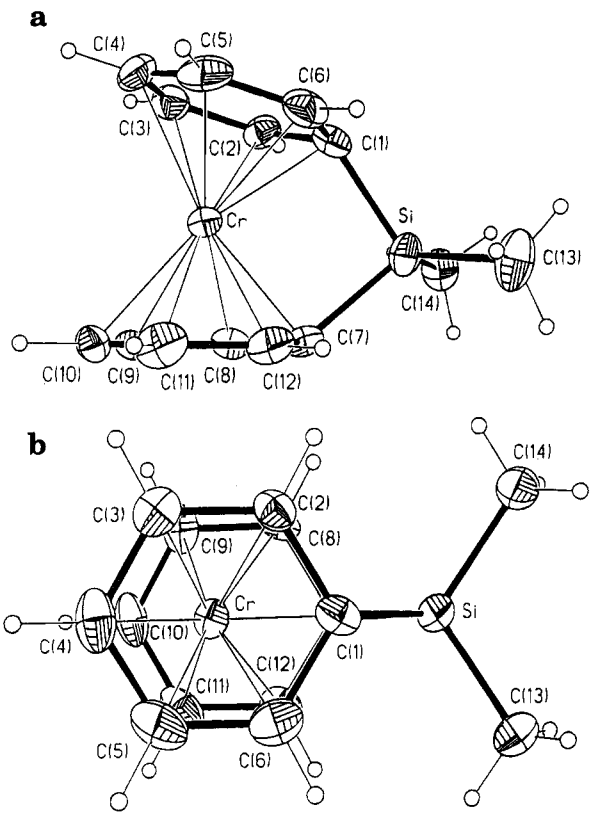

Figure 1. (a) Molecular structure of **7** and (b) alternative view of the molecular structure of **7** (vibrational ellipsoids at the 50% probability level; hydrogen atoms are shown as small spheres for clarity).

(centroid)–Cr–arene(centroid) angle (δ), which is 167.6(3)° compared to 180° in bis(benzene)chromium.[19] The tilting of the arene rings results in a displacement (away from silicon) of the chromium atom from the line joining the two centroids of the arene ligands of 0.173(8) Å. Additionally, the tilting of the arene ligands in **7** results in a significant distortion from planarity at the arene carbon bonded to silicon, with angles between the planes of the arene ligands and the C(arene)–Si bonds (β) in **7** of 37.9(4)° and 38.2(4)°, which are slightly smaller than that for **4** (40.8°). This substantial deviation from planarity also helps to explain the large upfield ^{13}C NMR shift associated with the arene carbon atom bonded to silicon. The C(arene)–Si–C(arene) angle θ in **7** [92.9(3)°] is smaller than that of **4** [96.0(2)°] and in both cases is substantially less than the ideal angle for a sp^3-hybridized silicon atom. The smaller θ angle results in a slight scissoring effect at silicon, with a widening of the C(R)–Si–C(R) [**7**, C(R) = Me; **4**, C(R) = Ph] angle to values of 111.0(4)° in **7** and 110.9(2)° in **4**. The Si–C(arene) bond lengths in **7** [1.868(8) and 1.881(8) Å] are essentially identical to those in **4** [1.882(4) Å]. The Cr–Si distance in **7** of 2.906(1) Å is longer than both the sum of the covalent radii (2.42 Å)[20] and the corresponding value in **4** [2.842(2) Å]. These distances indicate that any interaction between the Cr center and silicon is weak at best. The arene ligands in **7** are essentially eclipsed with a staggering angle of 0.1(8)°. There is an appreciable variance in the C–C bond lengths associated with the arene ligands. The bond lengths for the carbon atoms directly bonded to the *ipso*-carbons [C(1)–C(6) = 1.441(10) Å, C(1)–C(2) = 1.431(10) Å] are significantly longer than the other C–C bond lengths [*e.g.*, C(2)–C(3) = 1.403(10) Å]. This lengthening is consistent with the substantial deviation from sp^2 hybridization for the arene carbon atom bonded to silicon.

(19) Keulen, E.; Jellinek, F. *J. Organomet. Chem.* **1965**, *5*, 490.
(20) Stark, J. G.; Wallace, H. G. *Chemistry Data Book*; John Murray: London, 1975.

Table 1. Summary of Crystal Data and Intensity Collection Parameters[a]

	7
empirical formula	$C_{14}H_{16}CrSi$
M_r	264.36
crystal class	orthorhombic
space group	*Pbca*
a (Å)	13.773(2)
b (Å)	10.829(3)
c (Å)	16.180(3)
V (Å^3)	2413.2(9)
Z	8
D_{calcd} (g cm^{-3})	1.455
μ(Mo K) (cm^{-1})	0.10
F(000)	1104
ω scan width (deg)	0.57
range θ collected (deg)	3.47–25.0
total no. rflns	1981
no. of unique flns	1981
refinement coefficient	F^2
no. of data used	1981
no. of obsd data [$I > 2\sigma(I)$]	1066
weighting a, b	0.0282, 0.00
R_1 [$I > 2\sigma(I)$]	0.067
R_{w2} (all data)	0.144
GOF	1.03
$(\Delta/\sigma)_{max}$ in last cycle	0.00
no. of params refined	150
$\Delta\rho$ (max) in final ΔF map (e Å^{-3})	0.43

[a] Definition of R indices: $R_1 = \sum w(F_o - F_c)/\sum(F_o)$; $R_{w2} = \{\sum[w(F_o^2 - F_c^2)]^2/\sum[w(F_o^2)^2]\}^{1/2}$.

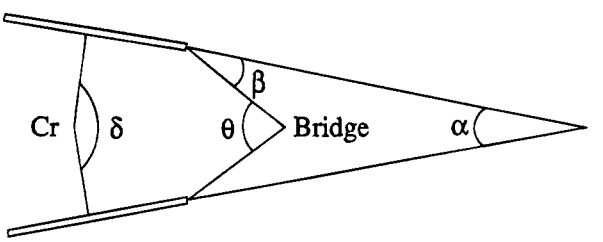

Figure 2. Distortions in arenophanes defining angles α, β, δ, and θ.

Table 2. Final Fractional Coordinates (×10^4) and Equivalent Isotropic Displacement Coefficients (Å^2 × 10^3) for the Non-Hydrogen Atoms of 7

	x	y	z	U(eq)
Cr	1120(1)	732(1)	6462(1)	22(1)
Si	1286(2)	1245(2)	8219(1)	28(1)
C(1)	457(5)	1824(7)	7381(5)	25(2)
C(2)	898(5)	2611(7)	6778(5)	25(2)
C(3)	722(5)	2476(8)	5929(5)	31(2)
C(4)	57(6)	1575(7)	5641(5)	35(2)
C(5)	−422(5)	833(8)	6228(5)	36(2)
C(6)	−235(5)	941(8)	7071(5)	33(2)
C(7)	1964(5)	214(7)	7497(4)	23(2)
C(8)	2565(5)	835(7)	6899(4)	23(2)
C(9)	2598(5)	458(8)	6057(5)	29(2)
C(10)	2041(5)	−535(8)	5777(5)	34(2)
C(11)	1466(5)	−1195(7)	6348(5)	36(2)
C(12)	1440(5)	−839(7)	7190(5)	30(2)
C(13)	622(6)	371(8)	9026(5)	45(2)
C(14)	2048(5)	2478(7)	8688(5)	35(2)

Thermal and Anionic Homopolymerization Behavior of 7. Attempts to thermally polymerize **7** involved heating this species in the melt in a manner analogous to that used to successfully polymerize **1**. However, when **7** was heated in an evacuated tube at a temperature of 180 °C for 1 h, a substantial amount of lustrous metallic chromium coated the sides of the tube and no increase in viscosity was detected. Analysis of the tube contents by ^1H and ^{29}Si NMR, as well as by mass spectrometry, showed only the presence of Ph_2SiMe_2.

Anionic ROP has previously been reported for cyclic tetrasilanes[21] and also for the ROP of the [1]ferrocenophane **1**.[5c,7] Similar anionic ROP methods were investigated in an attempt to induce **7** to polymerize under more mild conditions.

Initial experiments focused on stoichiometric ring-opening reactions of **7**. When a solution of **7** in THF was treated with 1 molar equiv of MeLi in diethyl ether followed by quenching of the reaction with Me_3SiCl, examination of the reaction products by NMR spectroscopy provided evidence for the formation of the bis[(trimethylsilyl)benzene]chromium species **8**. A ^1H NMR spectrum (in C_6D_6) of the products revealed that, in fact, no monomer remained and displayed only broad resonances at 4.33–4.25 (br s, arene) and 0.25 (s, $SiMe_3$) ppm. Further evidence for the formation of **8** was provided by a ^{29}Si NMR (in C_6D_6) spectrum, which displayed a sharp resonance at 1.9 ppm that was identical to that of an authentic sample of **8** prepared via reaction of $[Cr(\eta\text{-}C_6H_5Li)\cdot TMEDA$ with Me_3SiCl in hexanes. The formation of **8** demonstrated that **7** can indeed be ring-opened stoichiometrically by anionic reagents. To explore whether oligomerization or polymerization could be induced, the reaction of **7** with low concentrations (10%) of alkyllithium reagents was investigated. However, only uncharacterized mixtures of products were formed in these reactions according to ^{29}Si NMR analysis. GPC analysis was unsuccessful, presumably as a consequence of the acute air and moisture sensitivity of the material. Mass spectral analysis also provided no useful information in the form of peaks assignable to monomeric or oligomeric fragments. In an attempt to yield products that were amenable to characterization, the thermal and anionic copolymerization reactions of **7** with the silicon-bridged [1]ferrocenophane **1** were explored.

Thermal and Anionic Copolymerization of 7 with 1. A sealed tube containing an equimolar ratio of **7** and **1** was heated for 3 h at 140 °C. No significant increase in viscosity was detected. Analysis of the tube contents by ^1H NMR and GPC showed a significant amount of the two starting monomers and small quantities (yield = 10%) of the poly(ferrocenylsilane) **2**. Under identical conditions, as a control, a pure sample of **1** underwent ROP to yield poly(ferrocenylsilane) **2** in greater than 80–90% yield.[22] Extended heating (72 h) of a 1:1 molar mixture of **1** and **7** at 140 °C in a sealed Pyrex tube produced an immobile black solid, which showed partial solubility in hexanes and good solubility in C_6D_6. Analysis of this material by multinuclear (^1H, ^{29}Si, ^{13}C) NMR afforded data consistent with the formation of a cooligomer or copolymer **9a**, presumably mixed with poly(ferrocenylsilane) **2** on the basis of the results of the 3 h experiment.[23] Treatment of an equimolar amount of **7** and **1** in THF with 10 mol % *n*-BuLi in THF yielded an analogous copolymer **9b**. The ^1H NMR spectra of the poly(ferrocenylsilane)–poly(chromarenosilane) copolymers displayed broad resonances at 4.2–4.3 ppm assigned to both arene and Cp protons, 4.1–4.2 ppm assigned to Cp protons, and 0.5–0.6 ppm assigned to $SiMe_2$ protons (see Figure 3 for **9b**). The integration ratio for the arene and cyclopentadienyl regions of the ^1H NMR spectrum showed that the ratios of Cr:Fe in the copolymers were *ca.* 1:4.6 in **9a** and 1:1.6 in **9b**. Further structural characterization of **9a** and **9b** was provided by ^{29}Si and ^{13}C NMR spectroscopy. Analysis of the copolymers by ^{29}Si NMR (in C_6D_6) showed resonances for the ferrocenyldimethylsilane units at −6.4 ppm[3] and a broad resonance for chromarenodimethylsilane segments at +3.7 ppm and also revealed a small peak for a $SiMe_2$ crossover group between the ferrocenyldimethylsilane and chromarenodimethylsilane segments at −1.3 ppm (see Figure 4 for **9b**).

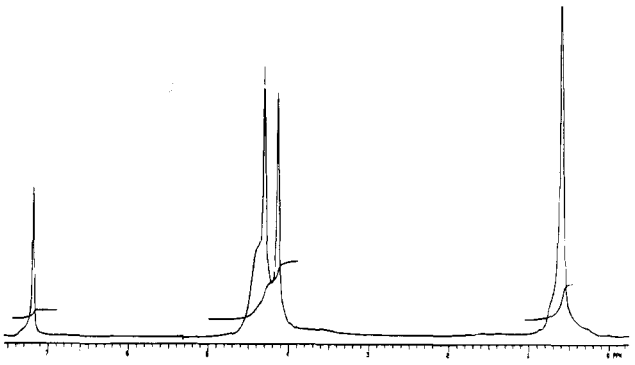

Figure 3. ^1H NMR spectrum of copolymer **9b** in C_6D_6.

Very little information has been published concerning the ^{29}Si NMR shifts of ring substituted bis(benzene)-chromium compounds, and to provide additional support for our assignments, we synthesized the bis(dimethylphenylsilane)-substituted species **10** by reaction of $[Cr(\eta\text{-}C_6H_5Li)_2]\cdot TMEDA$ with $Me_2PhSiCl$ in hexanes. Compound **10** was found to display a ^{29}Si NMR resonance at +0.7 ppm. As uncomplexed Ph_2SiMe_2 displays a ^{29}Si NMR resonance at −7.9 ppm, a comparison suggests that complexation of both phenyl groups in Ph_2SiMe_2 chromium would result in a significant downfield chemical shift from +0.7 ppm, which is reasonably consistent with our value for a ring-opened chromarenosilane segment in **9a** and **9b** at +3.4 ppm.

The ^{13}C NMR spectra of **9a** and **9b** were also consistent with the assigned copolymer structure. Further evidence for the copolymeric nature of these materials was provided by mass spectrometric analysis of samples, which were heated under vacuum at 100 °C in the mass spectrometer probe, and the thermal decomposition

(21) Cypryk, M.; Gupta, Y.; Matyjaszewski, K. *J. Am. Chem. Soc.* **1991**, *113*, 1046.

(22) Interestingly, in other experiments it was found that the addition of 10–25% of **7** to **1** led to an effective inhibition of the thermally induced ROP process, with dramatic reductions in both yield and molecular weight. In contrast, polymerizations of **1** carried out in 1:1 molar ratios with bis(benzene)chromium showed no signs of significant inhibition. See the Experimental Section for details.

(23) Elemental analysis data for **9a** and **9b** were repeatedly low for C (*e.g.*, for **9b** Anal. calcd C, 61.10; H, 5.89. Found: C, 53.70; H, 5.64). Similar problems have been noted for Cr–arene compounds (see footnote 13 in ref 15).

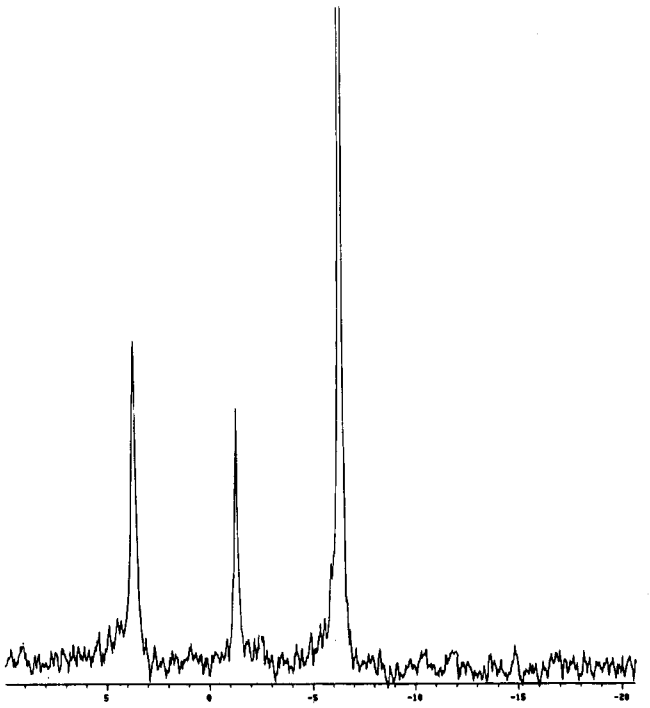

Figure 4. ^{29}Si NMR spectrum of copolymer **9b** in C_6D_6.

products were found to contain the oligomer species $C_6H_5SiMe_2((\eta\text{-}C_5H_4)Fe(\eta\text{-}C_5H_4)SiMe_2)_xC_6H_5$ (x = 1–4).

GPC analysis of the molecular weights of the copolymers **9a** and **9b** was not possible due to the acute air sensitivity of the materials. An alternative method to measure the molecular weights of the copolymers **9a** and **9b** involved treatment with methanol, which is known to cleave arene–silicon bonds in these bis(benzene)chromium-based systems to afford C_6H_6 and SiOH groups.[13,24] This resulted in partial, but controlled decomposition of the copolymer to leave the ferrocenyldimethylsilane segments intact. Similar partial decomposition techniques using UV light were previously used to confirm the nature of poly(ferrocenylsilane)–poly(silane) copolymers.[25] GPC analysis of **9a** after methanolysis provided a minimum molecular weight estimate (assuming a block copolymer) and gave an approximate weight-average molecular weight (M_w) of 2.0 × 10^3 and a number-average molecular weight (M_n) of 0.9 × 10^3. This suggests that the M_w for the copolymer **9a** is at least 2.4 × 10^3 on the basis of the Cr:Fe ratio from ^{1}H NMR integration. The polymeric nature of this methanolysis product was confirmed by ^{1}H NMR spectroscopy, which showed characteristic resonances associated with the poly(ferrocenyldimethylsilane) (**2**).[3] An analogous procedure for **9b** showed that the value of M_w is at least 1.2 × 10^4. The lower molecular weight for the thermally derived copolymer **9a** is also consistent with the partial solubility of this material in hexanes, which is a nonsolvent for **9b** and **2**.

(24) In an attempt to estimate of the molecular weights of **9a** and **9b**, these materials were first oxidized with $[Fe(\eta\text{-}C_5H_5)_2][PF_6]$ in THF. However, analysis of the oxidized materials by GPC showed only peaks with M_w < *ca.* 2000, which trailed into that of the solvent. Presumably due to the ionomeric nature of oxidized **9a** and **9b**, the use of GPC analysis with polystyrene standards provides a poor estimate of the molecular weight.

(25) Fossum, E.; Matyjaszewski, K.; Rulkens, R.; Manners, I. *Macromolecules* **1995**, *28*, 401.

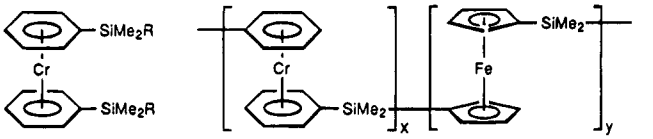

8 R = Me
10 R = Ph

9a-b

Summary and Conclusions

The silicon-bridged [1]chromarenophane **7** has been synthesized and structurally characterized. Unlike the silicon-bridged [1]ferrocenophane **1**, this compound is resistant to thermal and anionic homopolymerization via ROP; however, through thermal and anionic copolymerization with polymerizable **1**, the bimetallic air-sensitive oligomeric/polymeric materials **9a** and **9b** have been prepared.

Recent work has shown that the thermal ROP of silicon-bridged [1]ferrocenophane occurs by cleavage of the cyclopentadienyl carbon-bridging atom (*i.e.*, silicon) bond via a process that is probably heterolytic in nature.[26] The difference in polymerization behavior observed for the [1]chromarenophane **7** compared to the analogous [1]ferrocenophane **1** can be attributed to the lower Cr–arene bond energy, which is *ca.* 170 kJ mol^{-1} compared to *ca.* 220 kJ mol^{-1} for a Fe–Cp bond.[27] Thus, at elevated temperatures (*e.g.*, 180 °C) exclusive extrusion of Cr is detected. At lower temperatures (*ca.* 140 °C), this extrusion process is much slower and it is possible to induce copolymerization with **1**. Analogous air- and moisture-sensitive copolymers were also formed by anionic copolymerization of **7** with **1**.

We are now investigating the synthesis and polymerization behavior of other strained, transition-metal-containing rings, and our results will be the subject of future publications.

Experimental Section

Materials. Dimethyldichlorosilane (Me_2SiCl_2), dimethylphenylchlorosilane ($Me_2PhSiCl$), trimethylchlorosilane (Me_3SiCl), 1.6 M butyllithium in hexanes, 1.4 M methyllithium in diethyl ether, tetramethylethylenediamine (TMEDA), ferrocenium hexafluorophosphate, and chromium(III) chloride were purchased from Aldrich. Bis(benzene)chromium, dilithio[bis(benzene)chromium]·TMEDA, and dilithioferrocene·TMEDA were synthesized by literature procedures.[5a,13]

Equipment. All reactions and manipulations were carried out under an atmosphere of prepurified nitrogen using either Schlenk techniques or an inert-atmosphere glove box (Vacuum Atmospheres). Solvents were dried by standard methods, distilled, and stored under nitrogen over activated molecular sieves. ^{1}H NMR spectra (200 MHz) and ^{13}C NMR spectra (50.3 MHz) were recorded on either a Varian Gemini 200 or a Varian XL 400 spectrometer, respectively. The 79.4 MHz ^{29}Si NMR spectra were referenced externally to $SiMe_4$ (TMS) and were recorded on a Varian XL 400 spectrometer utilizing either a normal (proton-coupled) or a DEPT pulse sequence (proton-decoupled) with a $^2J_{Si-H}$ coupling of 6.7 Hz. All NMR spectra were performed in benzene-d_6, which was dried over sodium and stored under nitrogen over activated molecular sieves, and were referenced internally to TMS. Mass spectra were obtained with the use of a VG 70-250S mass spectrometer

(26) Pudelski, J. K.; Manners, I. *J. Am. Chem. Soc.* **1995**, *117*, 7265.

(27) (a) The Cr–(η-C_6H_6) bond energy of $Cr(\eta\text{-}C_6H_6)_2$ is *ca.* 170 kJ/mol, and the Fe–(η-C_5H_5) bond energy of $Fe(\eta\text{-}C_5H_5)_2$ is *ca.* 220–270 kJ/mol [see Elschenbroich, C.; Salzer, A. *Organometallics*; VCH: Weinheim, Germany, 1992].

operating in an electron impact (EI) mode. Molecular weights were estimated by gel permeation chromatography (GPC) by using a Waters Associates liquid chromatograph equipped with a 510 HPLC pump, U6K injector, and ultrastyragel columns packed with high-performance, fully porous, highly cross-linked styrene–divinylbenzene copolymer particles, with a pore size between 10^3 and 10^5 Å, and a Waters 410 differential refractometer. A flow rate of 1.0 mL/min was used, and the eluent was a solution of 0.1% tetra-*n*-butylammonium bromide in THF. Polystyrene standards were used for calibration purposes.

Synthesis of the Silicon-Bridged [1]Chromarenophane 7. To a suspension of $[Cr(\eta\text{-}C_6H_5Li)_2\cdot$TMEDA (2.42 g, 7.2 mmol) in hexane (40 mL) was added Me_2SiCl_2 (0.93 g, 7.4 mmol) at −78 °C. The reaction mixture was stirred at this temperature for 3 h and was then allowed to warm to room temperature over a 12 h period. Removal of solvent under vacuum left **7** as a black powder that was isolated and purified by recrystallization from hexanes at −20 °C (yield, 1.04 g (56%)). ^{1}H NMR (200 MHz) ($CDCl_3$): δ 4.7 (t, $^3J_{HH}$ = 5.3 Hz, 2H, *p*-C_6H_5), 4.5 (t, $^3J_{HH}$ = 5.4 Hz, 4H, *m*-C_6H_5), 3.9 (d, $^3J_{HH}$ = 5.1 Hz, 4H, *o*-C_6H_5), 0.3 (s, 6H, SiMe). ^{13}C NMR ($CDCl_3$): δ 82.7 (*p*-C_6H_5), 79.1 (*o*-C_6H_5), 75.4 (*m*-C_6H_5), 39.5 (ipso, CpSi), −4.9 (SiMe). ^{29}Si NMR (79.5 MHz) (C_6D_6): δ 21.0. MS (EI, 70 eV): *m/z* 264 (M^+, 100), 249 ($M^+ - CH_3$, 39), in good agreement with isotopic abundance calculations. HRMS calculated for $C_{14}H_{16}{}^{52}Cr^{28}Si$ 264.0426, found 264.0427.

Synthesis of Bis[(trimethylsilyl)benzene]chromium (8). To a suspension of $[Cr(\eta\text{-}C_6H_5Li)_2]\cdot$TMEDA (0.20 g, 0.6 mmol) in cyclohexane (40 mL) was added Me_3SiCl (0.40 g, 3.2 mmol) at −20 °C. The reaction mixture was stirred at this temperature for 3 h and was then allowed to warm to room temperature over a 12 h period. Removal of solvent under vacuum left **8** as a black powder that was isolated and purified by sublimation at high vacuum (70 °C/0.005 mmHg) to give very air-sensitive dark brown crystals (yield, 0.15 g (72%)). ^{1}H NMR (200 MHz) (C_6D_6): δ 4.33–4.25 (br s, 10H, C_6H_5), 0.25 (br s, 18H, $SiMe_3$). ^{29}Si NMR (79.5 MHz) (C_6D_6): δ 1.9 (s, $SiMe_3$). MS (EI, 70 eV): *m/z* 352 (M^+, 35), 280 ($M^+ - SiMe_3$, 12), 135 ($SiPhMe_2$, 100), in good agreement with isotopic abundance calculations.

Synthesis of Bis[(dimethylphenylsilyl)benzene]-chromium (10). To a suspension of $[Cr(\eta\text{-}C_6H_5Li)_2]\cdot$TMEDA (0.22 g, 0.7 mmol) in cyclohexane (40 mL) was added $PhMe_2SiCl$ (0.34 g, 3.2 mmol) at −20 °C. The reaction mixture was stirred at this temperature for 3 h and was then allowed to warm to room temperature over a 12 h period. Removal of solvent under vacuum left **9** as a black powder that was isolated and purified by sublimation at high vacuum (70 °C/0.005 mmHg) to give very air-sensitive dark brown crystals (yield, 0.21 g (72%)). ^{1}H NMR (200 MHz) (C_6D_6): δ 7.77 (m, 2H, SiPh), 7.16–7.19 (m, 3H, SiPh), 4.38 (br s, 3H, C_6H_5), 4.28 (br s, 2H, C_6H_5), 0.25 (br s, 6H, $SiMe_2$). ^{29}Si NMR (79.5 MHz) (C_6D_6): δ 0.7 (s, $SiPhMe_2$). MS (EI, 70 eV): *m/z* 476 (M^+, 38), 341 ($M^+ - SiPhMe_2$, 9), 135 ($SiPhMe_2$, 100), in good agreement with isotopic abundance calculations. HRMS calculated for $C_{28}H_{32}{}^{52}Cr^{28}Si_2$ 476.1448, found 476.1450.

Attempted Thermal ROP of 7. Samples of **7** (*ca.* 120 mg, 0.43 mmol) were heated in evacuated, sealed Pyrex glass tubes at temperatures of 180 °C for 1 h, resulting in the production of chromium metal and Ph_2SiMe_2, as confirmed by ^{1}H and ^{29}Si NMR and mass spectrometry. ^{1}H NMR (200 MHz) (C_6D_6): δ 7.45 (m, 4H, SiPh), 7.15–7.19 (m, 6H, SiPh), 0.41 (br s, 6H, $SiMe_2$). ^{29}Si NMR (79.5 MHz) (C_6D_6): δ −7.9 (s, Me_2SiPh_2). MS (EI, 70 eV): *m/z* 212 (M^+, 26), 197 (M^+ − Me, 9), 135 ($SiPhMe_2$, 12). No increase in melt viscosity was noted, and analysis of the tube contents by mass spectrometry and GPC in THF showed that no high molecular weight (M_w > 1000), GPC-active material was present.

(28) Sheldrick, G. M. *SHELXA-90, Program for Absorption Correction*; University of Göttingen: Göttingen, Germany, 1994.

Anionic Ring-Opening Reactions of 7. (a) To a solution of **7** (30 mg, 0.11 mmol) in 2 mL of THF was added 0.08 mL (0.11 mmol) of a 1.4 M solution of MeLi in diethyl ether The reaction mixture was stirred for 1.5 h and quenched with an excess of Me_3SiCl. Analysis of the reaction mixture by ^{1}H and ^{29}Si NMR showed resonances consistent with the formation of bis[(trimethylsilyl)benzene]chromium (**8**). ^{1}H NMR (200 MHz) (C_6D_6): δ 4.33–4.25 (br s, 10H, C_6H_5), 0.25 (br s, 18H, $SiMe_3$). ^{29}Si NMR (79.5 MHz) (C_6D_6): δ 1.9 (s, $SiMe_3$).

(b) To a solution of **7** (100 mg, 0.38 mmol) in 3 mL of THF was added 0.027 mL (0.038 mmol) of a 1.4 M solution of MeLi in diethyl ether. The reaction mixture was stirred for 1.5 h and quenched with 0.04 mL of Me_3SiCl (0.38 mmol). ^{1}H NMR (200 MHz) (C_6D_6): δ 4.40–4.10 (br s, arene), 0.54 (br s). ^{29}Si NMR (79.5 MHz) (C_6D_6): δ 30.6, 7.6, and 4.8. Analysis of this solid by GPC was not possible due to the acute air sensitivity of the material.

(c) To a solution **7** (100 mg, 0.38 mmol) in 3 mL of THF was added 0.023 mL (0.037 mmol) of a 1.6 M solution of BuLi/hexanes. The reaction mixture was stirred for 1.5 h and quenched with 0.04 mL of Me_3SiCl (0.38 mmol). ^{1}H NMR (200 MHz) (C_6D_6): δ 4.40–4.10 (br s, arene), 0.54 (br s). ^{29}Si NMR (79.5 MHz) (C_6D_6): δ 27.5, 7.6, and 4.6. Analysis of this solid by GPC was not possible due to the acute air sensitivity of the material.

Attempted Thermal Copolymerization of 7 with the [1]Ferrocenophane 1. (a) A mixture consisting of a 1:1 molar ratio of **7** (100 mg, 0.38 mmol) and **1** (90 mg, 0.37 mmol) was heated at 140 °C for (i) 1, (ii) 3, (iii) 47, and (iv) 72 h. In the cases of i–iii, no significant increase in melt viscosity was noted, and analysis of the tube contents by ^{1}H and ^{29}Si NMR revealed that a varying amount of the poly(ferrocenylsilane) **2** was either (i) not detectable, (ii) *ca.* 10% and (iii) 50% based on ^{1}H NMR integration together with the two starting monomers. In the case of iv, heat treatment resulted in the formation of an immobile black solid, which was analyzed by multinuclear (^{1}H, ^{29}Si, ^{13}C) NMR and found to possess resonances consistent with the formation of a poly(ferrocenylsilane)–poly(chromarenosilane) copolymer **9a**. For **9a**: ^{1}H NMR (200 MHz) (C_6D_6) δ 4.28 (br s), 4.11 (br s), 0.55 (br s); ^{13}C NMR (50.3 MHz) (C_6D_6) δ 79.1 (s, arene), 76.5 (s, arene), 74.8 (s, arene), 74.1 (s, *ipso*-arene), 73.7 (s, Cp), 71.9 (s, *ipso*-Cp), 71.4 (s, Cp), −0.5 (s, $CpSiMe_2Cp$), −1.0 (s, $CpSiMe_2$-arene), −1.6 (s, arene-$SiMe_2$-arene); ^{29}Si NMR (79.5 MHz) (C_6D_6) δ 3.4 (br s, arene-Si-arene), −1.3 (br s, CpSi-arene), −6.4 (br s, CpSiCp). This material was treated with methanol (20 mL) and filtered, and the solvent was removed in vacuo, leaving a brown residue. Analysis of this material by ^{1}H NMR in C_6D_6 showed resonances at 4.28 (br s, 4H, η-C_5H_4), 4.11 (br s, 4H, η-C_5H_4), and 0.56 (br s, 6H, SiMe) ppm, consistent with the formation of poly(ferrocenylsilane) **2**. Analysis of this solid by GPC revealed that this material possesses a weight-average molecular weight (M_w) of *ca.* 2.0 × 10^3 and a number-average molecular weight (M_n) of *ca.* 0.9 × 10^3. On the basis of ^{1}H NMR integration, this suggests that a minimum estimate of molecular weight for this material is *ca.* 2.4 × 10^3.

(b) A mixture consisting of a 1:4 molar ratio of **7** (20 mg, 0.076 mmol) of **1** (70 mg, 0.29 mmol) was heated for (i) 3 and (ii) 47 h at 140 °C. In each case, no increase in melt viscosity was noted, and analysis of the tube contents by ^{1}H and ^{29}Si NMR and GPC revealed that a small to moderate amount of the poly(ferrocenylsilane) **2** was present: (i) *ca.* 10%, M_w = 6.6 × 10^3, M_n = 4.7 × 10^3, polydispersity (M_w/M_n) = 1.4; (ii) 55%, M_w = 5.5 × 10^3, M_n = 4.3 × 10^3, polydispersity (M_w/M_n) = 1.4. The two starting monomers were also identified by ^{1}H NMR.

Influence of Bis(benzene)chromium on the Thermal ROP of the [1]Ferrocenophane 1. A mixture consisting of a 1:1 molar ratio of bis(benzene)chromium (50 mg, 0.24 mmol) and **1** (58 mg, 0.24 mmol) was heated for 10 min at 150 °C, at which point a considerable increase in viscosity was noted and the tube contents became immobile. Analysis of the tube

contents by ^{1}H NMR revealed that the poly(ferrocenylsilane) **2** (approximately 10% based on NMR integrations) was present along with the two starting monomers. For polymer **2**: M_w = 3.6 × 10^5, M_n = 2.3 × 10^5, polydispersity (M_w/M_n) = 1.6.

Anionic Copolymerization of 7 with the [1]Ferrocenophane 1. To a 1:1 molar mixture of **7** (50 mg, 0.19 mmol) and **1** (45 mg, 0.19 mmol) in 10 mL of THF was added 0.01 mL (0.016 mmol) of a 1.6 M solution of BuLi in hexanes. The reaction mixture was stirred for 1.5 h and quenched with 0.02 mL of Me_3SiCl (0.16 mmol). Analysis of the black reaction product **9b** by ^{1}H and ^{29}Si NMR showed resonances consistent with the formation of a poly(ferrocenylsilane)−poly(chromarenosilane) copolymer. ^{1}H NMR (200 MHz) (C_6D_6): δ 4.37 (br s, arene), 4.26 (br s, Cp), 4.10 (br s, Cp), 0.54 (br s, $SiMe_2$). ^{13}C NMR (50.3 MHz) (C_6D_6): δ 79.1 (s, arene), 76.5 (s, arene), 74.8 (s, arene), 74.1 (s, *ipso*-arene), 73.7 (s, Cp), 71.9 (s, *ipso*-Cp), 71.4 (s, Cp), −0.5 (s, $CpSiMe_2Cp$), −1.0 (s, $CpSiMe_2$-arene), −1.6 (s, arene-$SiMe_2$-arene). ^{29}Si NMR (79.5 MHz) (C_6D_6): δ 3.4 (br s, arene-Si-arene), −1.3 (br s, CpSi-arene), −6.4 (br s, CpSiCp). MS (EI, 70 eV): *m/z* 1180 (((Fe(η-C_5H_4)$_2$-$SiMe_2$)$_4$(C_6H_5)$_2$$SiMe_2$, 8), 938 ((Fe($\eta$-$C_5H_4$)$_2$$SiMe_2$)$_3$($C_6H_5$)$_2$-$SiMe_2$), 4), 726 (((Fe($\eta$-$C_5H_4$)$_2$$SiMe_2$)$_3$, 30), 696 ((Fe($\eta$-$C_5H_4$)$_2$-$SiMe_2$)$_2$($C_6H_5$)$_2$$SiMe_2$), 5), 528 (($C_6H_5$)$_2$$CrSiMe_2$)$_2$), 36), 502 ((Fe($\eta$-$C_5H_5$)($\eta$-$C_5H_4$)($SiMe_2OSiMe_2$)(Fe($\eta$-$C_5H_4$)($\eta$-$C_5H_5$)), 75), 484 ((Fe($\eta$-$C_5H_4$)$_2$$SiMe_2$)$_2$, 36), 454 ((Fe($\eta$-$C_5H_4$)$_2$$SiMe_2$)(($C_6H_5$)$_2$-$SiMe_2$), 100), 428 ((Fe($\eta$-$C_5H_4$)$_2$$SiMe_2$(Fe($\eta$-$C_5H_4$)$_2$, 6), 363 ((Fe($\eta$-$C_5H_4$)$_2$$SiMe_2$($\eta$-$C_5H_4$)Fe, 14), 243 ((Fe($\eta$-$C_5H_4$)$_2$$SiMe_2$ + H, 33), 197 (Ph_2SiMe, 18), 186 ((Fe(η-C_5H_5)$_2$, 12), 135 ($PhSiMe_2$, 49). This material was treated with methanol (20 mL) and filtered, and solvent was removed in vacuo, leaving a brown residue. Analysis of this material by ^{1}H NMR in C_6D_6 showed resonances at 4.28 (br s, 4H, η-C_5H_4), 4.11 (br s, 4H, η-C_5H_4), and 0.56 (br s, 6H, SiMe) ppm, consistent with the formation of poly(ferrocenylsilane) **2**. Analysis of this solid by GPC revealed that this material possesses a weight-average molecular weight (M_w) of *ca.* 7.5 × 10^3 and a number-average molecular weight (M_n) of *ca.* 6.7 × 10^3. On the basis of ^{1}H NMR integration, which showed a 1:1.6, Cr:Fe ratio, this suggests that a minimum estimate of molecular weight for this material is *ca.* 1.2 × 10^4.

X-ray Structural Determination Technique. Intensity data were collected on an Enraf-Nonius CAD4 (Siemens P4) diffractometer at 173 K, using graphite monochrominated Mo Kα radiation (λ = 0.710 73 Å). The ω scan technique was applied with variable scan speeds (4 to 45 deg/min in ω). The intensities of three standard reflections measured every 97 reflections showed no decay. The data were corrected for Lorentz and polarization effects. A semiempirical absorption correction was carried out using SHELXA-90[28] (in SHELXL-93). The program used for absorption correction was SHELXA-90,[28] which uses ΔF refinement for corrections. The structure was solved by direct methods. Non-hydrogen atoms were refined with anisotropic thermal parameters by full-matrix least squares to minimize $\sum\omega(F_o - F_c)^2$, where $W^{-1} = \sigma^2(F_o) + (aP)^2 + bP$, where $P = (F_o^2 + 2F_c^2)/3$. Hydrogen atoms were included in calculated positions (C−H distance of 0.96 Å) with U_{iso} of 0.030(6) Å^2 for ring hydrogens and 0.01(2) Å^2 for methyl hydrogens. Crystal data, data collection, and least-squares parameters are listed in Table 1. All calculations were performed and structural diagrams were created by using SHELXTL PC[29] on a 486-66 personal computer. Atomic coordinates are listed in Table 2; other data concerning the crystal structure are given in the supporting information.

Acknowledgment. This work was supported by the Petroleum Research Fund (PRF), administered by the American Chemical Society, and the Natural Science and Engineering Research Council of Canada (NSERC). We also thank the University of Toronto for an Open Research Fellowship for J.M.N., the Deutscher Akademischer Austauchdienst (DAAD) for an overseas exchange award for K.C.H., and Mr. Nick Plavac for obtaining the ^{29}Si NMR spectra. In addition, I.M. is grateful to the Alfred P. Sloan Foundation for a Fellowship (1994−1996).

Supporting Information Available: Tables of atomic coordinates, complete bond lengths and angles, anisotropic thermal parameters, hydrogen atom coordinates, torsion angles, and least squares plane data and a figure showing the structure of **7** (9 pages). Ordering information is given on any current masthead page.

OM950477X

(29) Sheldrick, G. M. *SHELXTL-93, Program for Crystal Structure Refinement*; Göttingen, Germany, 1994.

Thermal Ring-Opening Polymerization (ROP) of Strained, Ring-Tilted, Phosphorus-Bridged [1]Ferrocenophanes: Synthesis of Poly(ferrocenylphosphines) and Poly(ferrocenylphosphine sulfides)

Charles H. Honeyman, Daniel A. Foucher, Francisco Y. Dahmen, Rudy Rulkens, Alan J. Lough, and Ian Manners*

Department of Chemistry, University of Toronto, 80 St. George Street, Toronto, Ontario M5S-1A1, Canada

Received May 22, 1995[⊗]

A series of phosphorus(III)-bridged [1]ferrocenophanes Fe[(η-C_5H_3R)(η-C_5H_3R')]PX (X = Ph, R = R′ = H (**3**); X = Cl, R = R′ = H (**4**); X = Ph, R = H, R′ = ^{n}Bu (**5**); X = Ph, R = R′ = $SiMe_3$ (**6**)) have been synthesized via the reaction of Fe[(η-C_5H_3RLi)(η-$C_5H_3R'Li$)]·*n*TMEDA with $PXCl_2$ (X = Cl, Ph). The reaction of **6** with an excess of elemental sulfur resulted in the quantitative formation of the phosphorus(V)-bridged species Fe[η-$C_5H_3SiMe_3$]$_2$P(S)Ph (**7**). The new compounds **4**–**7** were characterized by multinuclear NMR, by mass spectrometry and, in the cases of **4**, **6**, and **7**, by single-crystal X-ray diffraction and elemental analysis. Ring-tilt angles (α) for **4** and **6** were found to be typical of phosphorus(III)-bridged [1]ferrocenophanes (**4**, 27.0(6)°; **6**, 27.5(6)°) whereas in the case of the phosphorus(V)-bridged species **7** the tilt angle was slightly less (α = 25.3(3)°). The thermal ring-opening polymerization of **3**, **5**, and **6** at 120–250 °C yielded the poly(ferrocenylphosphines) **8**–**10**, respectively. These materials were characterized by multinuclear NMR and by elemental analysis. The molecular weight of the trimethylsilyl-substituted polymer **10** was determined by GPC in THF versus polystyrene standards to be M_w = 66 000, PDI = 1.98, whereas **8** and **9** failed to elute from the GPC column. The phosphorus(V)-bridged species **7** also underwent thermal ring-opening polymerization to yield the poly(ferrocenylphosphine sulfide) **13** which was analyzed by GPC (M_w = 22 000, PDI = 1.24); thermally-induced elimination of $S(SiMe_3)_2$ from the ring-opened polymer was identified as a side reaction. The macromolecular reactions of **8**–**10** with elemental sulfur yielded the poly(ferrocenylphosphine sulfides) **11**–**13**. These were structurally characterized by multinuclear NMR and elemental analysis and their molecular distributions were analyzed by GPC (M_w = 18 000–65 000, PDI = 1.5–2.3).

Introduction

Polymers with transition elements in the main chain structure are of current interest as a result of their novel physical and catalytic properties.[1–5] However, the synthesis of well-defined, high molecular weight, and soluble examples of these materials has posed a considerable synthetic challenge. With this in mind, we recently reported the discovery that strained ring-tilted [1]ferrocenophanes (e.g. **1**) undergo thermal ring-opening polymerization (ROP) to yield high molecular weight poly(ferrocenylsilanes) (e.g. **2**).[6] Subsequent studies have focused on the interesting properties of these materials.[2,5,7–10] We have also recently described that, in the presence of anionic initiators in solution, silicon-bridged [1]ferrocenophanes yield linear oligo(ferrocenylsilanes). Moreover, in the presence of small quantities

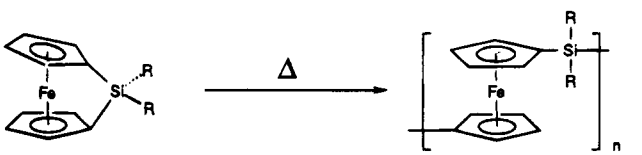

1 **2**

of an initiator such as ^{n}BuLi, living anionic ROP is possible.[11] This allows for the preparation of poly(ferrocenylsilanes) with controlled molecular weights and end group structures and also permits access to novel block copolymers.[11] Recently, transition metal-catalyzed ROP of silicon-bridged [1]ferrocenophanes in solution at ambient temperatures has also been achieved.[12]

[⊗] Abstract published in *Advance ACS Abstracts,* November 1, 1995.

(1) Hagihara, N.; Sonogashira, K.; Takahashi, S. *Adv. Polym. Sci.* **1981**, *41*, 149.
(2) Foucher, D. A.; Honeyman, C. H.; Nelson, J. M.; Tang, B.-Z.; Manners, I. *Angew. Chem., Int. Ed. Engl.* **1993**, *32*, 1709.
(3) Manners, I. *Adv. Mater.* **1994**, *6*, 68.
(4) Brandt, P. F.; Rauchfuss, T. B. *J. Am. Chem. Soc.* **1992**, *114*, 1926.
(5) Manners, I. *Adv. Organomet. Chem.* **1995**, *37*, 131.
(6) Foucher, D. A.; Tang, B.-Z.; Manners, I. *J. Am. Chem. Soc.* **1992**, *114*, 6246.
(7) Foucher, D.; Ziembinski, R.; Petersen, R.; Pudelski, J.; Edwards, M.; Ni, Y.; Massey, J.; Jaeger, C. R.; Vancso, G. J.; Manners, I. *Macromolecules* **1994**, *27*, 3992.
(8) Zechel, D.; Foucher, D. F.; Pudelski, J. K.; Yap, G. P. A.; Rheingold, A. L.; Manners, I. *J. Chem. Soc., Dalton Trans.* **1995**, 1893.
(9) Tang, B.; Petersen, R.; Foucher, D.; Lough, A.; Coombs, N.; Sodhi, R.; Manners, I. *J. Chem. Soc., Chem. Commun.* **1993**, 523.
(10) For the work of other groups on poly(ferrocenylsilanes) and related materials, see: (a) Tanaka, M.; Hayashi, T. *Bull. Chem. Soc. Jpn.* **1993**, *66*, 334. (b) Nguyen, M. T.; Diaz, A. F.; Dement'ev, V. V.; Pannell, K. H. *Chem. Mater.* **1993**, *5*, 1389. (c) Hmyene, M.; Yasser, A.; Escorne, M.; Percheron-Guegan, A.; Garnier, F. *Adv. Mater.* **1994**, *6*, 564.

0276-7333/95/2314-5503$09.00/0

We have also described the extension of the ROP approach to germanium-bridged [1]ferrocenophanes.[13,14] ROP of these species yields poly(ferrocenylgermanes) which have been shown to possess similar electrochemical and thermal transition behavior to their silicon analogues.[2,15] Strained, ring-tilted hydrocarbon-bridged [2]metallocenophanes also undergo thermally-induced ROP to yield new classes of organometallic polymers, poly(metallocenylethylenes).[16]

As part of our efforts to further extend this ROP methodology, we have studied the polymerization behavior of phosphorus-bridged [1]ferrocenophanes.[17] Polymers derived from these species are of interest as they possess phosphorus(III) centers which could function as coordination sites for the complexation of transition metals and as crosslinking sites through derivatization.[18,19] In this paper we report our studies of the thermal ring-opening polymerization behavior of [1]ferrocenophanes which possess either a phosphorus(III) or phosphorus(V) unit in the bridge.

Experimental Section

Equipment. Reactions and manipulations were carried out strictly under an atmosphere of prepurified nitrogen (Canox) using either Schlenk techniques or an inert-atmosphere glovebox (VAC Atmospheres) where required. Solvents were all dried and distilled using standard methods, and all reactions were carried out with solvents that had been stored under an inert (N_2) atmosphere. ^1H and ^{13}C NMR spectra were obtained using either a Varian XL 400 (400 and 100.5 MHz, respectively) or a Varian Gemini 200 spectrometer (200 and 50.3 MHz, respectively) and were referenced to $SiMe_4$ (TMS). ^{31}P NMR spectra were obtained using a Gemini 300 spectrometer (121.5 MHz) and were referenced externally to 85% H_3PO_4 in D_2O. ^{29}Si NMR spectra were obtained on a Varian XL 400 spectrometer (79.4 MHz) using either a normal or a DEPT pulse sequence and were referenced externally to TMS. Mass spectra were obtained with the use of a VG 70-250S mass spectrometer using an 70 eV electron impact ionization source. Molecular weights were determined by GPC (Waters 410 refractometer, Waters 510 HPLC pump, Waters 710 data module) on the basis of a comparison to polystyrene standards using a two column system in THF with 0.1% $[^nBu_4N]Br$ (w/w) with Waters Ultrastyragel columns (1×10^5, 1×10^3).

Materials. All reagents purchased from Aldrich were used as received (ferrocene, butylferrocene, 1.6 M butyllithium in hexanes, dichloro(phenyl)phosphine, TMEDA, $S(SiMe_3)_2$, and Grignard reagents). Inert-atmosphere nitrogen was supplied by Canox as prepurified N_2. Trichlorophosphine was supplied by BDH Inc. and was used without further purification. Elemental sulfur was supplied by BDH and was sublimed before use. 1,1'-Bis(trimethylsilyl)ferrocene was synthesized using a literature procedure.[20]

Synthesis of Fe(η-C_5H_4)$_2$PPh (3). This procedure was adapted from that previously described by Seyferth and Withers.[19]

Fe[(η-C_5H_4)Li]$_2$·nTMEDA (2.33 g, 7.34 mmol) was slurried in 150 mL of hexanes with stirring and was cooled to −78 °C. To this mixture was added a 40 mL solution of $PhPCl_2$ (1.0 mL, 7.36 mmol) in hexanes dropwise by cannula. Stirring was continued as the reaction solution was slowly warmed to ca. 15 °C over which period (2.5 h) the color had become dark red. The resulting reaction solution was then filtered, the solvent was removed from the filtrate in vacuo, and the residue was dried overnight under high vacuum. The resulting solid was extracted with hexanes until the extracts were colorless. The washings were combined and concentrated by the removal of solvent under vacuum. The solution was cooled to −50 °C which resulted in the formation of red crystals. Yield of **3**: 1.0 g (48%). These dark red crystals were identified as **3** by ^1H, ^{13}C, and ^{31}P NMR spectroscopy and by MS which afforded data in excellent agreement with those found in the literature.[19]

Data for **3**: ^{31}P NMR (CH_2Cl_2) δ = 13.1 ppm; ^1H NMR (C_6D_6) δ = 7.7−7.5 (m, *o*-Ph, 2H), 7.3−7.0 (m, *p,m*-Ph, 3H), 4.6−4.5 (m, Cp, 2H), 4.4−4.3 (m, Cp, 2H), 4.3−4.1 (m, Cp, 4H); ^{13}C NMR (C_6D_6) δ = 18.6 (d, ipso Cp, J_{PC} = 54.5 Hz), 78.2 (s, Cp), 77.3 (d, Cp, J_{PC} = 33.6 Hz), 77.6 (d, Cp, J_{PC} = 7.6 Hz), 77.2 (d, J_{PC} = 8.0 Hz), 137.9 (d, ipso Ph, J_{PC} = 10.9 Hz), 130.7 (d, *o*-Ph, $^2J_{PC}$ = 13.9 Hz), 128.8 (d, *m*-Ph, $^3J_{PC}$ = 3.4 Hz), 127.7 (s, *p*-Ph) ppm.

Synthesis of Fe(η-C_5H_4)$_2$PCl (4). Fe[η-$C_5H_4Li]_2$·nTMEDA (11.34 g, 36.1 mmol) was slurried in 700 mL of freshly distilled hexanes with stirring, and the suspension was cooled to −78 °C. To this mixture was added a solution of PCl_3 (4.5 mL, 40 mmol) in 100 mL of hexanes dropwise by cannula. The resulting mixture was allowed to slowly warm (to ca. 15 °C) at which point it was filtered. The dark red filtrate was immediately cooled to −78 °C and stored at this temperature overnight. This resulted in the formation of a fine red powder which was decanted and dried under vacuum and found to be highly reactive to both air and moisture. This red powder which was found to decompose rapidly in solution (ca. 30 min) at room temperature was subsequently identified as **4** by ^1H, ^{13}C, and ^{31}P NMR and MS. Yield: 4.67 g (52%). Brick-red colored crystals of **4** suitable for a single-crystal X-ray diffraction study were grown from hexanes at −78 °C over several days.

Data for **4**: ^{31}P NMR (C_6D_6) δ = 86.9 ppm; ^{13}C NMR (C_6D_6) δ = 19.2 ppm (d, ipso, $^1J_{PC}$ = 77.9 Hz), 72.2 (d, Cp, 37.3 Hz), 75.7 (d, Cp, 3.7 Hz), 77.8 ppm (d, Cp, 7.4 Hz), 79.4 ppm (s, Cp); ^1H NMR (C_6D_6) δ = 4.0 (m, Cp, 4H), 4.2 (m, Cp, 2H), 4.6 (m, Cp, 2H) ppm; MS (EI, 70 eV) *m/z* (%) = 250 (M^+, 100%), 214 (M^+ − HCl, 90%).

Synthesis of Fe[(η-$C_5H_3{}^nBu$)(η-C_5H_4)]PPh (5). This species was prepared in a similar manner to **3** using Fe[(η-$C_5H_3{}^n$BuLi)(η-C_5H_4Li)]·nTMEDA. However, since the product, which consisted of a mixture of isomers, proved to be a liquid even at low temperature (ca. −70 °C), **5** was isolated in vacuo as a red liquid, yield 6.0 g (71%). Purification beyond ca. 95% from n-butylferrocene impurity was not possible.

Data for **5**: ^{31}P NMR (CH_2Cl_2) δ = 15.6, 14.0, 12.0, 10.2 ppm; ^1H NMR ($CDCl_3$) δ = 7.8−7.2 (br, Ph, 5H), 4.7−3.7 (br, Cp, 7H), 1.8−1.1 (br, CH_2 (butyl), 6H), 1.1−0.7 (br, CH_3, 3H) ppm; MS (EI, 70 eV) *m/z* (%) 348 (M^+, 100), 333 ($M^+ - CH_3$, 8), 319 ($M^+ - C_2H_5$, 25), 305 ($M^+ - C_3H_7$, 27), 291 ($M^+ - C_4H_9$, 13), 271 (M^+ − Ph, 10), 240 (M^+ − PPh, 18); HRMS (*m/z*) $C_{20}H_{21}{}^{56}$FeP calcd 348.0730, found 348.0745.

Synthesis of Fe[η-$C_5H_3SiMe_3$]$_2$PPh (6). This species was prepared in a similar manner to **3** using Fe[η-$C_5H_3SiMe_3$-Li]$_2$·nTMEDA[20] except that the reaction solution was filtered

(11) Rulkens, R.; Ni, Y.; Manners, I. *J. Am. Chem. Soc.* **1994**, *116*, 12121.
(12) Ni, Y.; Rulkens, R.; Pudelski, J. K.; Manners, I. *Makromol. Chem. Rapid Commun.* **1995**, *16*, 637.
(13) Foucher, D. A.; Manners, I. *Makromol. Chem., Rapid Commun.* **1993**, *14*, 63.
(14) Foucher, D. A.; Edwards, M.; Burrow, R. A.; Lough, A. J.; Manners, I. *Organometallics* **1994**, *13*, 4959.
(15) Foucher, D. A.; Ziembinski, R.; Rulkens, R.; Nelson, J.; Manners, I. *Inorganic and Organometallic Polymers II*; Wisian-Neilson, P., Allcock, H. R., Wynne, K. J., Eds.; American Chemical Society: Washington, DC, 1994; p 449.
(16) (a) Nelson, J. M.; Rengel, H.; Manners, I. *J. Am. Chem. Soc.* **1993**, *115*, 7035. (b) Nelson, J. M.; Lough, A. J.; Manners, I. *Angew. Chem., Int. Ed. Engl.* **1994**, *33*, 989.
(17) Honeyman, C. H.; Foucher, D. A.; Mourad, O.; Rulkens, R.; Manners, I. *Polymer Prepr., Am. Chem. Soc. Div. Polym. Chem.* **1993**, *34* (1), 330.
(18) Neuse, E. W.; Chris, G. J. *J. Macromol. Sci., Chem.* **1967**, *3*, 371.
(19) Withers, H. P.; Seyferth, D.; Fellmann, J. D.; Garrou, P. E.; Martin, S. *Organometallics* **1982**, *1*, 1283.
(20) Brown, R. A.; Houlton, A.; Roberts, R. M. G.; Silver, J.; Frampton, C. S. *Polyhedron* **1992**, *11*, 2611.

and the solvent was then removed using high vacuum. The residue was placed under high vacuum for 3–4 h at 80 °C ensuring that all TMEDA and $Fe(\eta\text{-}C_5H_4SiMe_3)_2$ had been removed. The resulting dark-red oil was redissolved in a minimum of hexanes and cooled to −70 °C for 3 d. This resulted in the formation of a fine red powder. The product was filtered off at −70 °C resulting in the isolation of 2.0 g (yield 16%) of a fine rose-colored powder. Dissolution of this powder in hexanes and cooling to −70 °C for 3 d resulted in the formation of dark red-purple crystals suitable for a single-crystal X-ray diffraction study.

Data for **6**: ^{31}P NMR (CD_2Cl_2) δ = 10.0 ppm; ^{29}Si NMR ($CDCl_3$) δ = −4.4(s), −4.2 (s) ppm; ^{13}C NMR ($CDCl_3$) δ = 137.0 (d, ipso Ph, J_{PC} = 50.5 Hz), 130.3 (d, *o*-Ph, $^2J_{PC}$ = 13.9 Hz), 128.5 (d, *m*-Ph, $^3J_{PC}$ = 3.6 Hz), 127.5 (s, *p*-Ph), 83.9 (s, ipso C−Si), 82.0 (s, ipso C−Si), 82.9 (s, Cp), 82.8 (d, Cp, J_{PC} = 6.6 Hz), 81.7 (s, Cp), 81.6 (d, Cp, J_{PC} = 8.1 Hz), 79.2 (d, Cp, J_{PC} = 2.9 Hz), 79.0 (d, Cp, J_{PC} = 2.9 Hz), 21.8 (d, ipso Cp−P, J_{PC} = 50.5 Hz), 21.3 (d, ipso Cp−P, J_{PC} = 49.8 Hz), −0.03 (s, $SiMe_3$), −0.04 (s, $SiMe_3$) ppm; ^1H NMR (C_6D_6) δ = 7.7 (tt, *o*-Ph, $^3J_{PH}$ = 13.3 Hz, $^3J_{HH}$ = 6.7 Hz, $^4J_{HH}$ = 1.5 Hz, 2H), 7.3–7.0 (m, *m*- and *p*-Ph, 3H), 4.7 (m, Cp, 1H), 4.6 (m, Cp, 1H), 4.56 (m, Cp, 1H), 4.5 (m, Cp, 1H), 4.3 (m, Cp, 1H), 4.2 (m, Cp, 1H), 0.2 (s, $SiMe_3$, 9H), 0.1 (s, $SiMe_3$, 9H) ppm; MS (EI, 70 eV) *m/z* (%) = 436 (100, M^+), 421 (38, $M^+ - CH_3$); HRMS (*m/z*) $C_{22}H_{29}{}^{56}FeP^{28}Si_2$ calcd 436.0895, found 436.0905. Anal. Calcd: C, 60.54; H, 6.70. Found: C, 60.12; H, 6.60.

Synthesis of $Fe[\eta\text{-}C_5H_3SiMe_3]_2P(S)Ph$ (7). **6** (3.06 g, 6.9 mmol) was dissolved in 100 mL of THF, and an excess of elemental sulfur, 0.5 g (15.6 mmol), was added. After being stirred under nitrogen for 24 h, the solution was filtered. A ^{31}P NMR spectrum of this reaction solution showed the sulfurization to be quantitative. The solvent was then removed by vacuum, and the product was recrystallized from hexanes twice. This resulted in the isolation of a fine red powder, yield 2.2 g (68%). Bright red crystals suitable for single-crystal X-ray diffraction study were obtained by sublimation at 90 °C (0.02 mmHg) following recrystallization from a toluene/hexanes (1:2) mixture at −15 °C.

Data for **7**: ^{31}P NMR (CD_2Cl_2) δ = 46.1 ppm; ^{29}Si NMR (C_6D_6) δ = −4.2 (s, $SiMe_3$), −4.4 (s, $SiMe_3$) ppm; ^{13}C NMR (C_6D_6) δ = 134.8 (d, ipso Ph, J_{PC} = 87.9 Hz), 132.1 (d, *p*-Ph, $^4J_{PC}$ = 3.0 Hz), 129.7 (d, *m*-Ph, $^3J_{PC}$ = 12.5 Hz), 129.3 (d, *o*-Ph, $^2J_{PC}$ = 14.0 Hz), 86.6 (d, Cp ipso Si, $^3J_{PC}$ = 7.3 Hz), 85.3 (d, Cp ipso Si, $^3J_{PC}$ = 5.8 Hz), 84.9 (d, Cp, J_{PC} = 11.7 Hz), 83.7 (d, Cp, J_{PC} = 9.5 Hz), 81.7 (d, Cp, J_{PC} = 15.4 Hz), 79.0 (d, Cp, J_{PC} = 2.9 Hz), 78.9 (d, Cp, J_{PC} = 2.9 Hz), 76.6 (d, Cp, J_{PC} = 11.0 Hz), 34.9 (d, P ipso Cp, J_{PC} = 34.4 Hz), 34.2 (d, P ipso Cp, J_{PC} = 35.1 Hz), −0.1 (s, $SiMe_3$), −0.2 (s, $SiMe_3$) ppm; ^1H NMR (C_6D_6) δ = 7.9 (m, *o*-Ph, 2H), 7.3–7.0 (m, *m*- and *p*-Ph, 3H), 5.2 (m, Cp, 1H), 5.13 (d, Cp, J = 1.5 Hz, 1H), 4.4 (m, Cp, 1H), 4.3 (m, Cp, 1H), 4.0 (m, Cp, 1H), 3.9 (m, Cp, 1H), 0.2 (s, $SiMe_3$, 9H), 0.1 (s, $SiMe_3$, 9H), ppm; MS (EI, 70 eV) *m/z* (%) = 468 (100, M^+), 453 (21, $M^+ - CH_3$), 436 (11, $M^+ - S$); HRMS (*m/z*) $C_{22}H_{29}{}^{56}FeP^{32}S^{28}Si_2$ calcd 468.0616, found 468.0606. Anal. Calcd: C, 56.40; H, 6.24. Found: C, 56.22; H, 6.17.

Reaction of 4 with PhMgBr. Alternative Synthesis of 3. A cold (−78 °C) solution of **4** (3.7 g, 15.0 mmol) in 50 mL of ether was made as described above and used *in situ*. Once this solution had warmed to 15 °C, PhMgBr in ether (9.0 mL, 2.0 M, 18.0 mmol) was added quickly by syringe. A ^{31}P NMR spectrum of the reaction solution at this point revealed 2 singlet resonances at δ = 86.9 and 13.0 ppm assigned to **4** and **3**, respectively. After 20 min reaction time $SiMe_3Cl$ (0.2 mL, 1.6 mmol) was added to destroy any remaining lithiated ferrocene products and/or excess Grignard reagent. The resulting solution was then filtered, and the solvent was removed in vacuo. The residue was extracted with dry hexanes until the washings were colorless. These washings were then combined and solvent was removed in vacuo to give 3.3 g (75%) of **3** which was identified by ^{31}P NMR spectroscopy and mass spectrometry.

Thermal Ring-Opening Polymerization of 3 and 5–7. A general procedure was used for the thermal ROP of **3** and **5–7**. The procedure for the synthesis of polymer **9** serves as a representative example.

A Pyrex tube was charged with **5** (1.50 g, 4.3 mmol) and was sealed under vacuum (0.01 mmHg). This was then heated in an oven to 175 °C for 2 h. The initially molten sample became immobile after 10 min. The tube was allowed to cool and was then opened, and the contents were dissolved in 50 mL of THF. The resulting solution was filtered, and the volume of THF was reduced to 5–6 mL using a water aspirator. The concentrated polymer solution was then slowly added to stirred hexanes (500 mL) which resulted in the formation of a fine tan powder precipitate (1.24 g, 83%). The precipitate was identified as **9** by ^{31}P and ^1H NMR spectroscopy.

Data for polymer **8**: Thermal ROP conditions for **3** with 1 h at 120 °C, 15 min at 130 °C, precipitation into hexanes; ^{31}P NMR identical to literature.[19] ^1H NMR (CD_2Cl_2) δ = 7.9–6.8 (br, Ph, 5H), 4.7–3.6 (br, Cp, 8H) ppm. Polymer **8** was found not to elute from the GPC column. However GPC was performed on the sulfurized derivative **11**, which confirmed **8** was polymeric indirectly. Yield: 60%.

Data for polymer **9**: Thermal ROP conditions for **5** with 2 h at 175 °C, precipitation into hexanes; ^{31}P NMR (CH_2Cl_2) δ = −30.0 to −33.0 ppm; ^1H NMR (C_6D_6) δ = 8.2–6.8 (br, Ph, 5 H), 4.8–3.1 (br, Cp, 7 H), 2.5–0.5 (br, ^nBu, 9 H) ppm. Anal. Calcd: C, 68.99; H, 6.08. Found: C, 67.78; H, 6.13. Polymer **9** was found not to elute from the GPC column. However GPC was performed on the sulfurized derivative **12**, which confirmed **9** was polymeric indirectly. Yield: 83%.

Data for polymer **10**: Thermal ROP conditions for **6** with 1 h at 250 °C, precipitation into MeOH; ^{31}P NMR (CD_2Cl_2) δ = −27.0 to −31.0 ppm; ^1H NMR (CD_2Cl_2) δ = 8.3–6.6 (br m, Ph, 5 H), 5.2–3.5 (br m, Cp, 6 H), 0.9 to −0.3 (br, $SiMe_3$, 18 H) ppm; ^{13}C NMR ($CDCl_3$) δ = 140.0 (br, ipso Ph), 137.0–134.0 (br, *p*-Ph), 130.0–129.0 (*o*-, *m*-Ph), 87.3–73.0 (br, Cp), 0.9 (br, $SiMe_3$) ppm; ^{29}Si NMR ($CDCl_3$) δ = −2.2 to −3.3 (br, $SiMe_3$) ppm; GPC M_w = 66 000, PDI = 1.98. Anal. Calcd: C, 60.54; H, 6.70. Found: C, 59.82; H, 6.44. Yield: 66%.

Data for polymer **13**: Thermal ROP conditions for **7** with 15 min at 250 °C, precipitation into MeOH; ^{31}P NMR (CD_2Cl_2) δ = 38 (br) ppm; GPC M_w = 22 000, PDI = 1.24. For full characterization, see polymer prepared by sulfurization of **10**.

Note: *The thermal ROP of **4** was attempted at 250 °C and resulted in the detonation of the sample. Extreme care should be exercised if this experiment is to be repeated!*

Reaction of the Poly(ferrocenylphosphines) 8–10 with Elemental Sulfur: Synthesis of the Poly(ferrocenylphosphine sulfide)s 11–13. All reactions were carried out in a similar fashion, and that for **10** serves as a representative example.

Polymer **10** (250 mg, 0.6 mmol, M_w = 66 000, PDI = 1.98) was dissolved in 2–3 mL of dry dichloromethane with stirring. To this solution was added an excess of elemental sulfur (100 mg, 0.4 mmol of S_8). This reaction solution was allowed to stir overnight. There was no noticeable color change of the reaction solution over this time. The reaction mixture was then filtered, and solvent was removed. The resultant product was then redissolved in a minimum of CH_2Cl_2 and filtered again. A ^{31}P NMR spectrum of this product revealed a broad resonance centered at δ ca. 38 ppm characteristic of **13** (similar to the polymer produced via thermal ROP of **7**). The molecular weight of **13** produced in this manner was M_w = 65 000, PDI = 1.90. The yield was quantitative (ca. 100%) as was indicated by ^{31}P NMR spectroscopy. The isolated yield was 95%.

Data for polymer **11**: ^{31}P NMR (CD_2Cl_2) δ = 37.5 ppm; ^1H NMR (CD_2Cl_2) δ = 9.1–7.5 (br, Ph, 5 H), 5.6–3.0 (br, Cp, 8 H) ppm; M_w = 18 000, PDI = 1.52. Anal. Found: C, 58.77; H, 4.04. Calcd: C, 59.28; H, 4.05. Yield: 95%

Data for polymer **12**: ^{31}P NMR (CD_2Cl_2) δ = 38.1 ppm; ^{13}C NMR (CD_2Cl_2) δ = 135.5–133.0 (br, *ipso*-Ph), 132.6–130.5 (br, Ph), 129.0–128.5 (br, Ph), 94.7 (br, Cp ipso J_{PC} = 100 Hz), 82–69 (br, Cp), 35.0–33.3 (br, CpCH_2), 29.5–27.8 (br, CH_2), 23.5–22.0 (br, MeCH_2), 14.6–13.2 (br, CH_3) ppm; ^1H NMR

(CD_2Cl_2) δ = 8.1–6.9 (br, Ph, 5 H), 4.5–3.5 (br, Cp, 7 H), 2.6–2.0 (br, P–CH_2, 2 H), 1.8–1.0 (br, CH_2, 4H), 1.0–0.8 (d, CH_3, 3H) ppm; M_w = 19 000, PDI = 2.26. Anal. Calcd: C, 63.17; H, 5.57. Found: C, 62.50; H, 5.57. Yield: 90%.

Data for polymer **13**: ^{31}P NMR (CH_2Cl_2) δ = 36–39 (br) ppm; ^1H NMR (CD_2Cl_2) δ = 8.2–7.1 (br, Ph, 5 H), 5.1–4.5 (br, Cp, 6 H), 1.0 to −0.4 (br, $SiMe_3$, 18 H) ppm; ^{13}C NMR (CD_2Cl_2) δ = 134–130 (br, Ph), 130.0–127.0 (br, Ph), 84.0–70.0 (br, Cp), 3.5 to −2.0 (br, $SiMe_3$) ppm; M_w = 65 000, PDI = 1.90. Anal. Calcd: C, 56.40; H, 6.24. Found: C, 55.51; H, 6.06. Yield: 95%.

Elimination of $S(SiMe_3)_2$ from (A) the Thermal ROP of 7 and (B) the Thermal Decomposition of Polymer 13. (A) From Thermal ROP of 7. A Pyrex tube was charged with **7** (0.5 g, 1.1 mmol) and was sealed under vacuum (0.01 mmHg). This was heated to 250 °C for 1 h. The tube was then opened under a nitrogen atmosphere, and the clear liquid contents were collected (ca. 10 μL). Subsequent characterization of this liquid by ^{29}Si and ^1H NMR spectroscopy and mass spectrometry confirmed it was $S(SiMe_3)_2$.[27]

(B) From Thermal Decomposition of Polymer 13. A small glass capillary was loaded with ca. 5 mg of polymer **13**. This was then placed into the mass spectrometer sample head and heated under vacuum to approximately 150 °C. Ions ascribable to $S(SiMe_3)_2$ appeared as well as other peaks identifiable as polymer decomposition products. The residual sample was insoluble in THF. MS (EI, 70 eV) [*m/z* (%)]: $S(SiMe_3)_2$, 178 (10, M^+), 163 (33, M^+ − Me), 105 (10, M^+ − $SiMe_3$); other polymer decomposition products, 256 (100, Fe[(η-$C_5H_3SiMe_3$)(η-C_5H_3)]), 192 (55, Fe[(η-$C_5H_3SiMe_3$)]).

Single-Crystal X-ray Diffraction Technique. Intensity data for **4** and **6** were collected on an Enraf-Nonius CAD-4 diffractometer whereas **7** was collected on a Siemens P4 diffractometer using graphite-monochromated Mo Kα radiation (λ = 0.710 73 Å) with ω scans. In each case the intensities of 3 standard reflections measured periodically showed no decay. Data were corrected for Lorentz and polarization effects and for absorption. The absorption corrections for all compounds were carried out using the SHELXA-90 routine in SHELXL. The structures were solved by direct methods. All structures were refined anisotropically by full-matrix least squares. For all structures the hydrogen atoms were visible in difference Fourier maps and were included in idealized positions. Crystal data and data collection parameters are listed in Table 2. All calculations were performed and all diagrams were created using SHELXTL-PC[28] and SHELXL-93[29] on a 486-66 personal computer.

Results and Discussion

Phosphorus-bridged [1]ferrocenophanes were first reported in 1980 by Osborne et al.[21] and by Seyferth and co-workers.[22] Important studies in this area have also been reported by Cullen.[23] These species were prepared via the reaction of dilithioferrocene·*n*TMEDA[24] with dichloroorganophosphines PR'''Cl_2 (R''' = Me, Ph) in nonpolar solvents such as hexanes (Scheme 1). Single-crystal X-ray diffraction studies have shown that phosphorus-bridged [1]ferrocenophanes such as **3** possess highly strained structures with tilt angles between the planes of the cyclopentadienyl rings of ca. 26–27°.[23,25] These compounds have been shown to undergo facile stoichiometric ring-opening reactions with aryllithium reagents.[22] Moreover, Seyferth et al. have reported that in the presence of small amounts of anionic initiator oligo(ferrocenylphosphines) with 2–5

Scheme 1

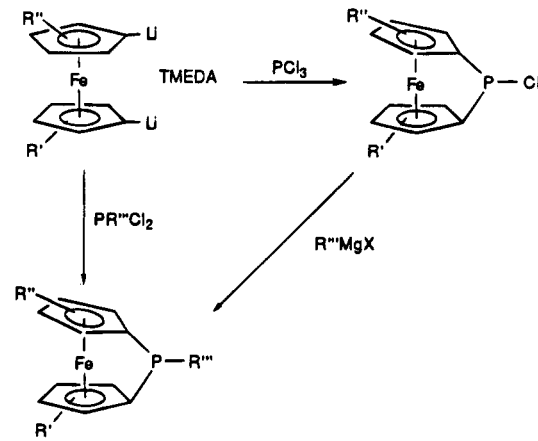

repeat units are formed. However, attempts to generate high molecular weight poly(ferrocenylphosphines) via anionic ROP by using small quantities of initiator were reported to be unsuccessful and led only to the same oligomeric products. Low molecular weight poly(ferrocenylphosphines) were also formed (instead of the [1]ferrocenophane **3**) by condensation polymerization reactions when the reaction of dilithioferrocene·*n*TMEDA with $PPhCl_2$ was carried out in ether solvents rather than in hexanes.[19] In addition, under certain conditions, these polycondensation reactions were reported to yield surprisingly[26] high molecular weight materials.

As part of our program to develop ROP as a route to transition metal-based macromolecules we initially focused on the [1]ferrocenophane **3** for our thermal polymerization studies.

Synthesis and Thermal ROP of Fe(η-C_5H_4)$_2$PPh (3). The synthesis of **3** was accomplished by the reaction of $PPhCl_2$ with 1,1′-dilithioferrocene·*n*TMEDA in hexanes.[19] This yielded red crystalline **3** in 48% yield, and the product gave ^{31}P and ^1H NMR and mass spectra in excellent agreement with those in the literature.[22] A Pyrex tube was charged with **3** and then sealed under vacuum. The tube was then heated to 120 °C for 1 h and then to 130 °C for 15 min. During this time the tube contents melted and then became viscous and subsequently immobile. The tube contents were then dissolved in CH_2Cl_2 over 24 h. A ^{31}P NMR spectrum of the solution exhibited two broad resonances, one of high intensity at δ = −30.5 to −31.2 ppm, which was assigned to the internal phosphorus atoms of **8**, and one

(21) Osborne, A. G.; Whiteley, R. H.; Meads, R. E. *J. Organomet. Chem.* **1980**, *193*, 345.
(22) Withers, H. P.; Seyferth, D. *Organometallics* **1982**, *1*, 1275.
(23) Butler, I. R.; Cullen, W. R.; Einstein, F. W. B.; Rettig, S. J.; Willis, A. J. *Organometallics* **1983**, *2*, 128.
(24) Reaction of 2 equiv of BuLi and ferrocene in the presence of 2 equiv of TMEDA produces dilithioferrocene·*n*TMEDA. A crystal structure has been reported for the species n = 1.5. However, the value of n in the isolated bulk product is not necessarily the same as in the crystal structure. See: Butler, I. R.; Cullen, W. R.; Ni, J.; Rettig, S. J. *Organometallics* **1985**, *4*, 2196 and references therein. For the purposes of this paper we have assumed that n = 1.
(25) Stoeckli-Evans, H.; Osborne, A. G.; Whiteley, R. H. *J. Organomet Chem.* **1980**, *194*, 91.
(26) The formation of high molecular weight products via polycondensation reactions using dilithioferrocene·*n*TMEDA as a difunctional monomer would be highly unexpected as this reagent, which is generated via the reaction of ferrocene with n-butyllithium·TMEDA, is generally only 90–95% pure. A major impurity is monolithioferrocene which serves as a polymer chain capping agent and therefore favors the formation of only low molecular weight products. On the basis of the hindsight provided by the recent discovery of the anionic ROP of silicon-bridged [1]ferrocenophanes, it appears far more likely to us that the high molecular weight poly(ferrocenylphosphines) are not formed by polycondensation but instead arise via a chain growth reaction, namely the anionically (i.e. lithiated ferrocene) induced ROP of the phosphorus-bridged [1]ferrocenophane **3** which is generated *in situ*. See: Manners, I. *Adv. Organomet. Chem.* **1995**, *37*, 131–136 and 153–154.

Scheme 2

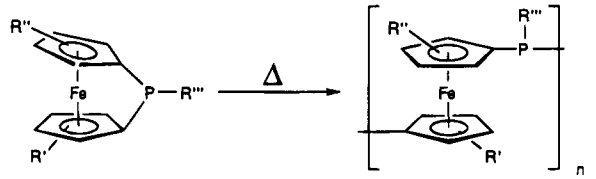

3 R' = R'' = H, R''' = Ph
4 R' = R'' = H, R''' = Cl
5 R' = H, R'' = nBu, R''' = Ph
6 R' = R'' = $SiMe_3$, R''' = Ph
7 R' = R'' = $SiMe_3$, R''' = Ph; P(S)

8 R' = R'' = H, R''' = Ph
9 R' = H, R'' = nBu, R''' = Ph
10 R' = R'' = $SiMe_3$, R''' = Ph

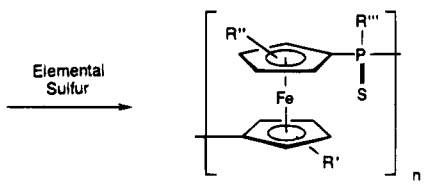

11 R' = R'' = H, R''' = Ph
12 R' = H, R'' = nBu, R''' = Ph
13 R' = R'' = $SiMe_3$, R''' = Ph

of low intensity at $\delta = -26.3$ ppm, which was assigned to the phosphorus atoms at the chain terminii. These assignments agree with those for the oligomers and polymers **8** generated by condensation routes.[19] Precipitation into hexanes yielded **8** as a fluffy, tan-colored solid in 60% yield. A ^{1}H NMR spectrum of **8** (in CD_2Cl_2) showed broad resonances in the correct integration ratio for the Ph and Cp protons. However, an estimation of the molecular weight of **8** could not be obtained by gel permeation chromatography (GPC) as found previously by Seyferth and co-workers.[19] After injection onto the GPC column, no polymer was detected in the eluted solvent at any time. This result suggests that significant polymer–column interactions may be interfering with normal elution based on size exclusion. We were subsequently able to obtain molecular weight information for the sulfurized derivative of **8** (Scheme 2) which was found to be GPC-analyzable (see below).

Synthesis and Characterization of Fe(η-C_5H_4)$_2$PCl (4). The synthesis of phosphorus-bridged [1]ferrocenophanes from dilithioferrocene·*n*TMEDA involves reaction with dichlorophosphines PR'''Cl_2. Of these, only $PPhCl_2$ is readily available at reasonable cost, and this species, together with the other more expensive examples (especially alkyl derivatives), is extremely malodorous and toxic. We were therefore interested in investigating whether an alternative and potentially general approach to the synthesis of phosphorus-bridged [1]ferrocenophanes might be possible. An attractive approach would be to use readily available PCl_3 to react with dilithioferrocene·*n*TMEDA to form the chloroderivative **4** and to subsequently react this with organometallic nucleophiles to form P-substituted derivatives (Scheme 1).

The synthesis of **4** involved the addition of PCl_3 in hexanes to a slurry of dilithioferrocene·*n*TMEDA in hexanes at −78 °C. However, once formed in solution this [1]ferrocenophane was found to quickly decompose at temperatures above −20 °C. Nevertheless, under certain conditions and appreciable care **4** can be isolated in moderate yield (ca. 50%). The structure of **4** was assigned on the basis of ^{31}P and ^{1}H NMR spectroscopy as well as mass spectrometry. Once isolated, it was found that large brick red crystals of **4** could be grown by first dissolving the species in hexanes at −20 °C and then cooling further to −78 °C. This permitted further characterization of **4** via a single-crystal X-ray diffraction study (see below).

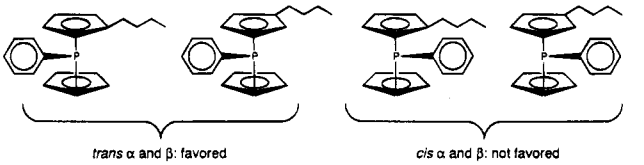

Figure 1.

Reaction of 4 with PhMgBr. Alternative Synthesis of 3. In order to investigate whether nucleophilic substitution of the chlorine substituent in **4** could be achieved, this species was reacted with PhMgBr in ether. The reaction was monitored in solution by ^{31}P NMR spectroscopy which showed that **3** ($\delta = 13.0$ ppm) was formed from **4** ($\delta = 86.9$ ppm) quantitatively. Furthermore, the isolated yield of **3** (75%) indicated that this type of reaction sequence might, in principle, be used in the future to generate a wide range of substituted phosphorus-bridged [1]ferrocenophanes.

Synthesis and ROP of Fe[(η-C_5H_3^{n}Bu)(η-C_5H_4)]PPh (5). One possible explanation for the GPC-inactivity of **8** is the fairly poor solubility of this polymer in THF which might lead to adsorption to the GPC column. We therefore aimed to prepare a more soluble derivative via the attachment of alkyl chains to the cyclopentadienyl ligands. The synthesis of the monomer Fe[(η-C_5H_3^{n}Bu)(η-C_5H_4)]PPh (**5**) was therefore investigated.

The synthesis of **5** involved the dilithiation of n-butylferrocene and the subsequent reaction of the product with $PPhCl_2$. This led to an overall crude yield of 71% of **5** which was isolated as a red liquid. A ^{31}P NMR spectrum of **5** (in CH_2Cl_2) revealed four unique resonances at $\delta = 15.6$, 14.0, 12.0, and 10.2 with the two lower field peaks of greater intensity than the others. This result was consistent with the formation of four different structural isomers. The formation of these isomers can be explained by the lithiation of the n-butylferrocene at both the α and β positions in combination with the possible *cis* or *trans* relation of the Ph group to that of the n-butyl group in **5**. The formation of isomers with the Ph and ^{n}Bu groups *trans* to one another is likely to be favored (Figure 1). Further characterization of **5** was achieved by high-resolution mass spectrometry, which showed the expected molecular ion, and ^{1}H NMR, which clearly showed broad resonances in the correct intensity ratios which were assigned to the Ph, Cp, and to the n-butyl group, respectively.

When **5** was heated in an evacuated Pyrex tube to 175 °C for 2 h, the sample immediately became free flowing and then increasingly viscous and finally immobile. The tube was then opened under nitrogen, and the entire contents were dissolved in THF. Purification yielded **9**, which presumably contains a mixture of monomer units derived from the various isomers of **5**, as a light brown powder in 83% yield. The poly(ferrocenylphosphine) **9** was characterized by ^{31}P and ^{1}H NMR spectroscopy. The ^{31}P NMR spectrum of **9** (in CH_2Cl_2) consisted of a single, broad resonance at $\delta = -30$ to −33 ppm which was similar to that for polymer **8**. The ^{1}H NMR spectrum of **9** (in C_6D_6) consisted of broad resonances in the correct integration ratio for the

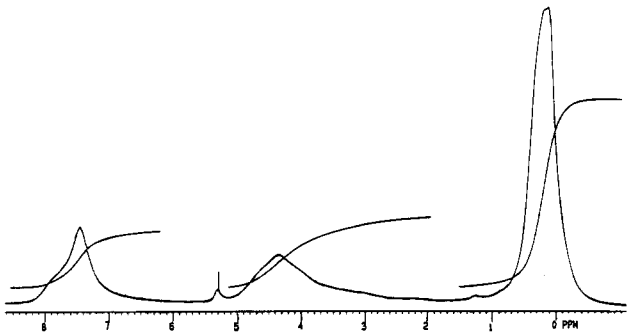

Figure 2. ^{1}H NMR spectrum of **10** in CD_2Cl_2.

phenyl, Cp, and alkyl regions. Polymer **9**, which showed good solubility in polar solvents, formed well-defined but brittle films when cast from a solution in CH_2Cl_2. However, attempts to estimate the molecular weight of **9** by GPC were unsuccessful as in the case of **8**. Again, sulfurization provided a GPC-analyzable derivative (see below) which confirmed that **9** was indeed polymeric.

Synthesis and ROP of Fe[η-$C_5H_3SiMe_3$]$_2$PPh (6). An alternative precursor to more soluble poly(ferrocenylphosphines), the bis(trimethylsilyl)-substituted species Fe[η-$C_5H_3SiMe_3$]$_2$PPh, **6**, was also synthesized. This was accomplished by the dilithiation of 1,1′-bis(trimethylsilyl)ferrocene with 2 equiv of BuLi·TMEDA in hexanes and the subsequent reaction of the product with 1 equiv of $PPhCl_2$. The [1]ferrocenophane **6** was isolated as a rose-colored solid which was characterized by ^{31}P, ^{29}Si, ^{13}C, and ^{1}H NMR and high-resolution mass spectrometry. The spectroscopic data were all consistent with the assigned structure for **6**. However, in contrast to the situation for **5**, the NMR data indicated the presence of a single structural isomer. For example, a single ^{31}P NMR resonance at 10.0 ppm (in CD_2Cl_2) was detected for both the bulk product and for that of the single crystals of **6**. The formation of a single structural isomer is consistent with the previously noted regiospecifically β- and stereospecifically *anti*-dilithiation of 1,1′-bis(trimethylsilyl)ferrocene which has been attributed to the bulky nature of the $SiMe_3$ groups.[20] Additional characterization of **6** was obtained by X-ray diffraction (see below).

The thermal ROP of **6** was carried out at 250 °C over 1 h. A ^{31}P NMR spectrum of the products showed a small singlet resonance at δ = 10 ppm assigned to unreacted **6** and a very broad resonance from δ = −27 to −31 ppm which was assigned to the polymer **10**. Precipitation into methanol resulted in the isolation of a tan solid in a 66% yield. A ^{1}H NMR spectrum of this polymer revealed broad resonances for the Ph, Cp, and $SiMe_3$ groups in the correct intensity ratios (Figure 2). As noted above and by others previously,[19] molecular weight analysis of poly(ferrocenylphosphines) by GPC techniques has until now been complicated by the fact the polymers do not elute from the column properly.[19] However, we found that the introduction of the trimethylsilyl groups allowed us to overcome this difficulty and a GPC investigation of **10** in THF revealed that the material possessed a M_w of 66 000 and a polydispersity (PDI) of 1.98 versus polystyrene standards.

Synthesis and Polymerization Behavior of Fe[η-$C_5H_3SiMe_3$]$_2$P(S)Ph (7). In order to investigate whether phosphorus (V)-bridged [1]ferrocenophanes would also undergo thermally-induced ROP, we synthesized the phosphine sulfide **7** via the reaction of **6** with an excess of S_8 in THF. The reaction was monitored by ^{31}P NMR which after 24 h showed a single, new singlet resonance at δ = 44 ppm. Species **7** was isolated as a red powder and was characterized by multinuclear NMR and high-resolution mass spectrometry. As in the case of **6**, each hydrogen atom bound to the cyclopentadienyl (Cp) ligands was found to be unique. Thus 6 signals were observed in the Cp region of the ^{1}H NMR spectrum, and a set of 10 resonances were assigned to the Cp carbons in the ^{13}C NMR spectrum. As with other strained, ring-tilted [1]ferrocenophanes, the Cp−P ipso carbon ^{13}C NMR resonances are considerably upfield at δ = 34.9 (d, J_{PC} = 34.4 Hz) and 34.2 ppm (d, J_{PC} = 35.1 Hz) whereas the other 8 Cp resonances appear in the typical region between 76 and 87 ppm. Further characterization of **7** was achieved by single-crystal X-ray diffraction (see below).

In a manner similar to that for the other [1]ferrocenophanes, **7** was sealed in an evacuated Pyrex tube and was then heated (to 250 °C). The sample became molten, viscous, and then immobile after 15 min. However, only a small fraction of the tube contents were found to be soluble in THF. Furthermore, a clear colorless liquid was observed within the Pyrex tube before the products were analyzed. Isolation and characterization of this liquid showed it to be the sulfide, $S(SiMe_3)_2$. This was confirmed by mass spectrometry and a comparison of the ^{29}Si and ^{1}H NMR spectra of this species to those of an authentic sample.[27] The soluble polymer fraction exhibited a broad ^{31}P NMR resonance centered at δ = 38 ppm. The insoluble material was presumably crosslinked polymer having further P−Cp bonds. However, this has not been established and the insoluble products may be poorly defined decomposition products. Studies of polymer **13** synthesized by an alternative route (i.e. the sulfurization of **10**) have shown that the elimination of $S(SiMe_3)_2$ occurs at temperatures below that needed to generate polymer by thermal ROP (see below).

Sulfurization of the Poly(ferrocenylphosphines) 8−10 with Elemental Sulfur. Synthesis of the Poly(ferrocenylphosphine sulfides) 11−13. In order to investigate the ability of **8** to undergo macromolecular reactions and in order to attempt to obtain a derivative that could be analyzed by GPC, we reacted **8** with an excess of elemental sulfur in THF. The reaction was monitored by ^{31}P NMR which showed a singlet resonance at δ = ca. 37 ppm which was dramatically downfield shifted from that of **8** (δ = ca. −30 ppm). The polymer product was identified as **11** by ^{31}P and ^{1}H NMR and elemental analysis. Furthermore, analysis by GPC showed that this species successfully eluted from the column and that it possessed M_w = 18 000 and PDI = 1.52.

The poly(ferrocenylphosphines) **9** and **10** were similarly reacted with sulfur to yield **12** and **13**, respectively. Similar ca. 60 ppm downfield shifts in the ^{31}P NMR spectra of the sulfurized polymers were noted. ^{1}H and ^{13}C NMR spectroscopy and elemental analysis provided additional characterization for **12** and **13**. Both poly-

(27) The elimination product exhibited chemical shifts as follows: ^{1}H NMR (C_6D_6) δ = 0.28 ppm (0.28); ^{29}Si NMR (C_6D_6) δ = 14.3 ppm (14.3). Those of the authentic sample are in parentheses.

(28) Sheldrick, G. M. SHELXTL-PC, Siemens Analytical X-ray Instruments Inc., Madison, WI, 1990.

(29) Sheldrick, G. M. SHELXL-93. Program for the Refinement of Crystal Structures. University of Göttingen, Germany, 1994.

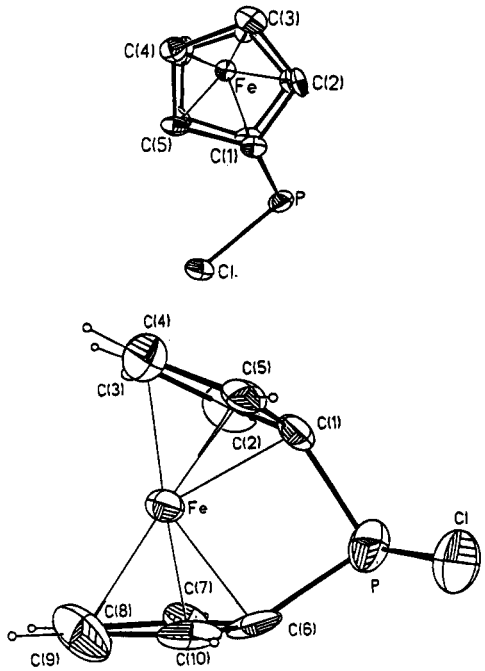

Figure 3. Alternative views of the molecular structure of **4** with thermal ellipsoids at the 50% probability level.

Table 1. Selected Structural Data for Phosphorus-Bridged [1]Ferrocenophanes, with Esd's in Parentheses (Where Available)

	compd			
	3	**4**	**6**	**7**
Fe–P dist (Å)	2.774(3)	2.715(6)	2.784(2)	2.688(2)
Fe displacement (Å)		0.277(8)	0.291(7)	0.259(2)
ring tilt α (deg)	26.7	27.0(6)	27.5(6)	25.3(3)
β(av) (deg)	32.5	31.9(7)	32.0(3)	35.0(4)
θ (deg)	90.6(3)	90.1(7)	95.7(4)	95.0(2)
δ (deg)	159.8	160.4(6)	159.5(3)	161.8(2)
C_{ipso}–C'_{ipso} (Å)	2.619(12)	2.606(17)	2.638(9)	2.673(7)

Table 2. Summary of Crystal Data and Intensity Collection Parameters for 4, 6, and 7

	4	**6**	**7**
formula	$C_{10}H_8ClFeP$	$C_{22}H_{29}FePSi_2$	$C_{22}H_{29}FePSi_2S$
M_r	250.4	436.5	468.5
cryst class	monoclinic	triclinic	monoclinic
space group	$P2_1/c$	$P\bar{1}$	$P2_1/c$
temp, K	292	223	173
a, Å	7.306(1)	8.0748(8)	11.580(2)
b, Å	19.442(8)	11.4391(14)	13.472(2)
c, Å	7.421(1)	12.7716(17)	15.314(3)
α, deg	90	103.46(1)	90
β, deg	118.870(12)	93.87(1)	90.89(1)
γ, deg	90	97.51(1)	90
V, Å^3	923.1(4)	1131.54(24)	2388.8(7)
Z	4	2	4
D_{calcd}, g cm^{-3}	1.802	1.281	1.303
μ(Mo Kα), mm^{-1}	2.036	0.846	0.891
λ(Mo Kα), Å	0.709 30	0.710 73	0.710 73
R_{int}, %	3.43	0.00	5.23
R,[a] %	5.08	5.90	4.98
R_w*,[a] %	4.23	7.55	8.74
abs cor	1.175/0.843	1.1640/0.8120	0.9353/0.6018

[a] Definition of R factors: $R = \Sigma\Delta/\Sigma(F(\text{obs}))$. $R_w = [\Sigma(\text{weight} \times \Delta)^2/\Sigma(\text{weight} \times F(\text{obs})^2)]^{1/2}$, where $\Delta = [F(\text{obs}) - F(\text{calc})]$.

(ferrocenylphosphine sulfides) were also found to elute from the GPC column (**12**, M_w = 19 000, PDI = 2.26; **13**, M_w = 65 000, PDI = 1.90). In the case of **11** and **12** the GPC activity allowed an estimation of the molecular weights of their poly(ferrocenylphosphine) precursors **8** and **9**. Comparison of the value for **13** (M_w = 65 000, PDI = 1.90) with that for the sole example of a GPC-analyzable poly(ferrocenylphosphine) precursor **10** (M_w = 66 000, PDI = 1.98) is significant. This suggests sulfurization occurs without significant molecular weight decline assuming that the hydrodynamic volumes of each species are similar. This suggests that GPC analysis of the sulfurized derivatives provided a good method for evaluating the molecular weights of poly(ferrocenylphosphines) which adsorb to the GPC column and removes the necessity of resorting to the use of light scattering (or other) techniques which are considerably more time consuming.

The facile formation of soluble **13** via the sulfurization of **10** compares favorably with the small amount of soluble material formed in the thermal ROP of the phosphine sulfide **7** discussed previously. In the latter reaction the other products were $S(SiMe_3)_2$ and insoluble material. The possibility that $S(SiMe_3)_2$ was formed by the thermal decomposition of the ring-opened polymer **13** was investigated by heating a well-characterized sample of **13**, prepared by the sulfurization of **10**, from 25 to 150 °C under vacuum. The formation of the sulfide $S(SiMe_3)_2$ was detected by simultaneous mass spectrometry. Furthermore, the resulting polymeric product was rendered insoluble. Thus, the thermal treatment of the soluble polymer **13** might allow the introduction of controlled degrees of crosslinking.

Table 3. Atomic Coordinates (×10^4) and Equivalent Isotropic Displacement Coefficients (Å^2 × 10^3) for the Non-Hydrogen Atoms of 4 with Esd's in Parentheses

atom	x	y	z	U(eq)[a]
Fe	7382(3)	8960(1)	1938(3)	28(1)
Cl	12953(6)	8414(2)	6333(5)	53(2)
P	10731(7)	8069(2)	3492(7)	46(2)
C(1)	10070(21)	8870(8)	1988(20)	30(7)
C(2)	8454(24)	8857(8)	−98(22)	41(8)
C(3)	7310(23)	9465(7)	−547(22)	40(8)
C(4)	8265(21)	9875(8)	1214(22)	39(9)
C(5)	9949(20)	9536(7)	2750(21)	32(7)
C(6)	8362(23)	8157(7)	3760(22)	38(9)
C(7)	6389(23)	7981(7)	1932(22)	36(9)
C(8)	4884(23)	8449(8)	1890(22)	39(9)
C(9)	5779(27)	8874(8)	3556(26)	53(10)
C(10)	7889(24)	8706(7)	4743(20)	26(7)

[a] Equivalent isotropic U defined as one-third of the trace of the orthogonalized U_{ij} tensor.

Table 4. Bond Lengths (Å) for 4 with Esd's in Parentheses

Fe–P	2.755(5)	Fe–C(1)	1.954(17)
Fe–C(2)	2.019(20)	Fe–C(3)	2.068(18)
Fe–C(4)	2.052(16)	Fe–C(5)	2.011(14)
Fe–C(6)	1.960(14)	Fe–C(7)	2.036(15)
Fe–C(8)	2.063(18)	Fe–C(9)	2.050(24)
Fe–C(10)	1.992(16)	Cl–P	2.055(5)
P–C(1)	1.840(15)	P–C(6)	1.843(20)
C(1)–C(2)	1.423(17)	C(1)–C(5)	1.431(21)
C(2)–C(3)	1.393(21)	C(3)–C(4)	1.397(20)
C(4)–C(5)	1.376(17)	C(6)–C(7)	1.465(17)
C(6)–C(10)	1.427(23)	C(7)–C(8)	1.415(24)
C(8)–C(9)	1.364(22)	C(9)–C(10)	1.396(22)

Discussion and Comparison of the X-ray Structures of 4, 6, and 7. Crystals of **4** suitable for a single-crystal X-ray diffraction study were obtained from hexanes at −78 °C. Two views of the molecular structure of **4** are shown in Figure 3. Table 1 gives selected structural data for important features for this and related [1]ferrocenophanes. The angles α, β, and θ are defined in Figure 6.

The summary of the crystal data and collection parameters is found in Table 2. Tables of the fractional

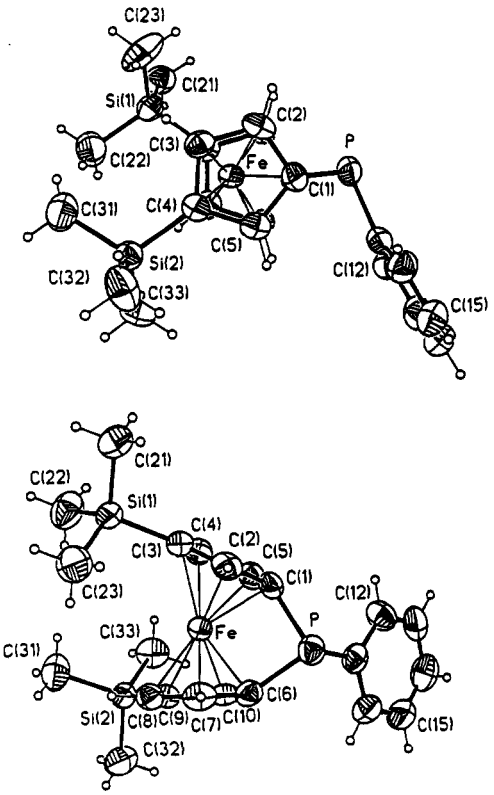

Figure 4. Alternative views of the molecular structure of **6** with thermal ellipsoids at the 50% probability level.

Table 5. Selected Bond Angles (deg) for 4 with Esd's in Parentheses

Cl–P–C(1)	101.1(4)	P–C(6)–C(7)	115.7(13)
Cl–P–C(6)	100.2(5)	P–C(6)–C(10)	126.6(11)
C(1)–P–C(6)	90.1(7)	C(2)–C(1)–C(5)	105.6(12)
P–C(1)–C(2)	118.8(11)	C(7)–C(6)–C(10)	106.0(13)
P–C(1)–C(5)	125.0(12)		

coordinates, bond lengths, and selected angles for **4** are found in Tables 3–5, respectively. X-ray diffraction quality crystals of **6** were grown from hexanes at −70 °C over several days. Views of the molecular structure of **6** are shown in Figure 4. Fractional coordinates, bond lengths, and selected angles can be found in Tables 6–8, respectively. Suitable crystals of **7** were grown by vacuum sublimation. Views of the molecular structure are shown in Figure 5, and fractional coordinates, bond lengths, and selected bond angles can be found in Tables 9–11, respectively.

The single-crystal X-ray diffraction studies confirmed the structures of **4**, **6**, and **7** as phosphorus-bridged [1]ferrocenophanes. Although both **6** and **7** consisted of a single structural isomer, both are chiral. Two enantiomers were found for each species in the crystals as indicated by the symmetries of the unit cells (**6**, $P\bar{1}$, $Z = 2$; **7**, $P2_1/c$, $Z = 4$). The most notable features of the phosphorus(III)-bridged [1]ferrocenophanes **4** and **6** are the large ring tilt angles (α) of ca. 27° compared to their silicon-bridged analogs (α = ca. 21°). This phenomenon has been previously noted and analyzed by Cullen[23] and by Osborne.[30] A significant difference between the structures of the molecules is the larger θ angle for the trimethylsilyl-substituted species **6** and **7** compared to **4**. Average θ angles for phosphorus(III)-bridged [1]ferrocenophanes are normally within the range 90.5–91.5° (e.g. for **3**, θ = 90.7(2)°). However, none exceed 94° and values of this magnitude are more

Table 6. Atomic Coordinates (×10⁴) and Equivalent Isotropic Displacement Coefficients (Å² × 10³) for the Non-Hydrogen Atoms of 6 with Esd's in Parentheses

atom	*x*	*y*	*z*	*U*(eq)[a]
Fe	2190(1)	8521(1)	1744(1)	34(1)
P	−296(3)	10003(2)	2026(2)	47(1)
Si(1)	3465(3)	7034(2)	−768(2)	47(1)
Si(2)	4708(3)	7617(2)	3716(2)	43(1)
C(1)	413(9)	8883(7)	2717(6)	41(3)
C(2)	56(9)	7628(8)	2125(6)	47(3)
C(3)	1410(9)	7047(7)	2362(6)	43(3)
C(4)	2659(9)	7893(7)	3127(6)	39(3)
C(5)	2026(9)	9006(7)	3342(6)	39(3)
C(6)	1473(10)	9858(7)	1162(6)	42(3)
C(7)	1312(10)	8784(7)	309(6)	45(3)
C(8)	2939(10)	8394(7)	166(6)	44(3)
C(9)	4087(10)	9292(7)	976(7)	48(3)
C(10)	3193(10)	10172(7)	1587(6)	45(3)
C(11)	443(9)	11443(8)	3025(7)	48(3)
C(12)	1174(11)	12440(8)	2711(8)	58(4)
C(13)	1561(12)	13567(9)	3459(9)	68(4)
C(14)	1145(12)	13692(10)	4514(9)	71(4)
C(15)	407(12)	12720(9)	4827(8)	64(4)
C(16)	38(10)	11603(9)	4082(7)	58(4)
C(21)	1909(14)	5692(8)	−728(9)	93(5)
C(22)	5653(12)	6847(10)	−365(8)	81(5)
C(23)	3333(11)	7183(8)	−2187(7)	62(4)
C(31)	5378(12)	6247(9)	2825(8)	77(5)
C(32)	6284(10)	8962(8)	3794(7)	62(4)
C(33)	4476(11)	7399(10)	5097(7)	75(5)

[a] Equivalent isotropic *U* defined as one-third of the trace of the orthogonalized $\mathbf{U}_{ij}$ tensor.

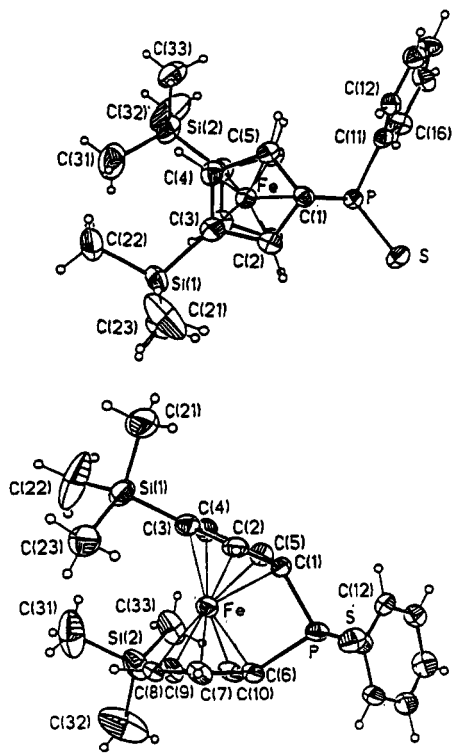

Figure 5. Alternative views of the molecular structure of **7** with thermal ellipsoids at the 50% probability level.

common in silicon-bridged ferrocenophanes. Both **6** and **7** have θ values greater than 94° (**6**, 95.7(4)°; **7**, 95.0(2)°).

The tilt angle (α) of **6** was found to be 27.5(6)° whereas the α angle of **7** was significantly smaller (25.3(3)°). Interestingly, this difference was not accompanied by a significant change in the θ angle in the two complexes.

(30) Stoeckli-Evans, H.; Osborne, A. G.; Whiteley, R. H. *J. Organomet. Chem.* **1980**, *194*, 91.

Table 7. Bond Lengths (Å) for 6 with Esd's in Parentheses

Fe–P	2.784(2)	Si(2)–C(31)	1.868(9)
Fe–C(1)	1.987(7)	Si(2)–C(32)	1.859(9)
Fe–C(2)	2.033(7)	Si(2)–C(33)	1.859(9)
Fe–C(3)	2.067(8)	C(1)–C(2)	1.447(10)
Fe–C(4)	2.086(7)	C(1)–C(5)	1.455(9)
Fe–C(5)	2.004(6)	C(2)–C(3)	1.406(11)
Fe–C(6)	1.980(8)	C(3)–C(4)	1.436(8)
Fe–C(7)	2.024(7)	C(4)–C(5)	1.420(10)
Fe–C(8)	2.123(7)	C(6)–C(7)	1.425(9)
Fe–C(9)	2.084(8)	C(6)–C(10)	1.425(9)
Fe–C(10)	2.009(7)	C(7)–C(8)	1.443(10)
P–C(1)	1.846(8)	C(8)–C(9)	1.447(9)
P–C(6)	1.869(7)	C(9)–C(10)	1.423(10)
P–C(11)	1.831(7)	C(11)–C(12)	1.379(12)
Si(1)–C(4)	1.864(7)	C(11)–C(16)	1.379(11)
Si(1)–C(21)	1.860(9)	C(12)–C(13)	1.389(11)
Si(1)–C(22)	1.845(8)	C(13)–C(14)	1.378(14)
Si(1)–C(23)	1.851(9)	C(14)–C(15)	1.360(14)
Si(2)–C(8)	1.842(7)	C(15)–C(16)	1.379(11)

Table 8. Selected Bond Angles (deg) for 6 with Esd's in Parentheses

C(1)–P–C(6)	90.5(3)	C(21)–Si(1)–C(22)	108.5(4)
C(1)–P–C(11)	102.8(3)	C(31)–Si(2)–C(33)	109.6(4)
C(3)–Si(1)–C(22)	108.2(3)	P–C(1)–C(2)	116.9(5)
C(3)–Si(1)–C(21)	111.0(4)	P–C(1)–C(5)	123.4(5)
C(6)–P–(C)11	102.0(3)	P–C(6)–C(7)	116.5(5)
C(9)–Si(2)–C(31)	109.2(3)	P–C(6)–C(10)	125.8(5)
C(9)–Si(2)–C(33)	108.6(4)		

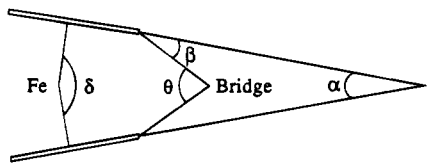

Figure 6. Definition of structural parameters for [1]metallocenophanes.

However, a significant increase in the β angle was observed. This angle, which represents a distortion from planarity for the ipso carbon atoms of the cyclopentadienyl rings bonded to phosphorus, increased from 32.0(3)° in **6** to 35.0(4)° in **7**. The difference in the β angle may be a consequence of the change in the length of the ipso carbon–phosphorus bonds which shorten from an average value of 1.857(8) Å in **6** to a value of 1.799(5) Å in **7**.

Previous structural studies on [1]ferrocenophanes have provided evidence for a possible dative interaction between the iron center and the bridging element. Further evidence for this Fe···E interaction has also been provided by physical methods such as Mössbauer spectroscopy.[31,32] A comparison of the structures of **6** and **7** offers some additional insight. The sulfurization of **6** to yield **7** formally alters the oxidation state of the phosphorus center. Thus an increase in the magnitude in the dative interaction between the iron atom and the phosphorus center might be expected. Indeed, the Fe···P distance in **7** (2.688(2) Å) is shorter than in **6** (2.784(2) Å). By comparison, in the previously studied phosphorus(III)-bridged [1]ferrocenophanes the Fe···P distances range from 2.715(6) to 2.784(2) Å. This shortening of the Fe···P distances in **7** relative to **6** was also accompanied by a decrease in the displacement of the Fe (in an opposite direction to the phosphorus atom) from the line joining the Cp centroids. Thus, in **7** this displacement is 0.259(2) Å, significantly less than in **6** (0.291(7) Å). This also provides evidence that the phosphorus(V) center in **7** may be acting as a better acceptor of electron density than the phosphorus(III) center in **6**. However, it should be noted that the decreased length of the ipso carbon–phosphorus bonds in **7** relative to **6** mentioned above would also be expected to decrease the Fe···P distance. Thus, as noted

(31) Clemance, M.; Roberts, R. M. G.; Silver, J. *J. Organomet. Chem.* **1983**, *243*, 461.
(32) Silver, J. *J. Chem. Soc., Dalton Trans.* **1990**, 3513.
(33) Pudelski, J. K.; Foucher, D. A.; Honeyman, C. H.; Lough, A. J.; Manners, I.; Barlow, S.; O'Hare, D. *Organometallics* **1995**, *14*, 2470.

Table 9. Atomic Coordinates (×10⁴) and Equivalent Isotropic Displacment Coefficients (Å² × 10³) for the Non-Hydrogen Atoms of 7 with Esd's in Parentheses

atom	x	y	z	U(eq)[a]
Fe	2470(1)	446(1)	2348(1)	27(1)
Si(1)	2393(2)	1337(1)	131(1)	42(1)
Si(2)	−292(2)	798(1)	3217(1)	55(1)
P	4350(1)	−337(1)	3135(1)	25(1)
S	5922(1)	155(1)	3125(1)	35(1)
C(1)	3686(4)	−534(4)	2069(3)	25(1)
C(2)	3735(4)	295(4)	1461(3)	30(1)
C(3)	2672(4)	385(4)	992(3)	32(1)
C(4)	1970(4)	−414(4)	1285(3)	32(1)
C(5)	2578(4)	−972(4)	1937(3)	31(1)
C(6)	3264(4)	529(4)	3502(3)	27(1)
C(7)	3190(5)	1501(4)	3112(3)	31(1)
C(8)	2010(5)	1744(4)	2987(3)	32(1)
C(9)	1301(5)	933(4)	3286(4)	38(2)
C(10)	2089(4)	207(4)	3603(3)	32(1)
C(11)	4099(4)	−1436(4)	3756(3)	26(1)
C(12)	3974(4)	−2367(4)	3380(4)	30(1)
C(13)	3762(4)	−3188(4)	3881(4)	35(1)
C(14)	3701(4)	−3096(4)	4764(4)	38(2)
C(15)	3869(5)	−2200(4)	5158(4)	41(2)
C(16)	4049(5)	−1363(4)	4661(3)	32(1)
C(21)	3312(7)	1014(5)	−821(4)	92(3)
C(22)	873(6)	1281(6)	−198(5)	114(4)
C(23)	2783(5)	2571(4)	538(4)	50(2)
C(31)	−847(6)	1574(5)	2323(5)	102(3)
C(32)	−938(6)	1188(7)	4245(5)	112(3)
C(33)	−653(5)	−507(5)	2997(5)	67(2)

[a] Equivalent isotropic U defined as one-third of the trace of the orthogonalized $\mathbf{U}_{ij}$ tensor.

Table 10. Bond Lengths (Å) for 7 with Esd's in Parentheses

Fe–C(1)	1.981(5)	Fe–C(6)	1.984(5)
Fe–C(10)	2.005(5)	Fe–C(7)	2.013(5)
Fe–C(5)	2.015(5)	Fe–C(2)	2.024(5)
Fe–C(4)	2.072(5)	Fe–C(8)	2.078(5)
Fe–C(3)	2.094(5)	Fe–C(9)	2.095(5)
Fe···P	2.688(2)	Si(1)–C(22)	1.824(6)
Si(1)–C(23)	1.829(6)	Si(1)–C(3)	1.864(6)
Si(1)–C(21)	1.869(7)	Si(2)–C(32)	1.831(7)
Si(2)–C(31)	1.831(7)	Si(2)–C(33)	1.838(7)
Si(2)–C(9)	1.855(6)	P–C(11)	1.785(5)
P–C(6)	1.811(5)	P–C(1)	1.814(5)
P–S	1.938(2)	C(1)–C(5)	1.424(6)
C(1)–C(2)	1.455(7)	C(2)–C(3)	1.421(6)
C(3)–C(4)	1.426(7)	C(4)–C(5)	1.426(7)
C(6)–C(10)	1.439(7)	C(6)–C(7)	1.443(7)
C(7)–C(8)	1.415(7)	C(8)–C(9)	1.444(7)
C(9)–C(10)	1.417(7)	C(11)–C(12)	1.387(7)
C(11)–C(16)	1.392(6)	C(12)–C(13)	1.370(7)
C(13)–C(14)	1.360(7)	C(14)–C(15)	1.361(7)
C(15)–C(16)	1.378(7)		

Table 11. Selected Bond Angles (deg) for 7 with Esd's in Parentheses

C(1)–P–C(6)	95.0(2)	C(21)–Si(1)–C(22)	109.5(4)
C(1)–P–C(11)	106.8(2)	C(31)–Si(2)–C(33)	109.4(3)
C(3)–Si(1)–C(22)	108.8(3)	P–C(1)–C(2)	116.3(4)
C(3)–Si(1)–C(21)	107.3(3)	P–C(1)–C(5)	123.8(4)
C(6)–P–C(11)	104.4(2)	P–C(6)–C(7)	119.6(4)
C(9)–Si(2)–C(31)	108.9(3)	P–C(6)–C(10)	120.1(4)
C(9)–Si(2)–C(33)	109.1(3)	C(1)–P–S	115.3(2)

elsewhere,[33] the different structural parameters in [1]ferrocenophanes are interrelated and it is difficult to distinguish definitively between which structural change is a "cause" which is an "effect".

Cullen has suggested that the ring strain in phosphorus-bridged [1]ferrocenophanes is manifest in different structural distortions compared to their silicon or germanium analogues.[23] Thus, on the basis of an analysis of the structures available at that time, it was noted that phosphorus-bridged [1]ferrocenophanes exhibit higher tilt angles (α) whereas the silicon and germanium complexes have higher θ and β angles. It is therefore interesting to note that, while the characteristics of **4** agree with this assessment, the θ and β angles for **6** and in particular **7** are between those typically found in silicon-bridged and phosphorus-bridged [1]ferrocenophanes. Thus, the θ and β angles in **7** (θ = 95.0(2)°, β = 35.0(4)°) are intermediate between those found in **3** (θ = 90.6(3)°, β = 32.5°) and $Fe(\eta\text{-}C_5H_4)_2SiPh_2$ (θ = 99.2(5)°, β = 40.0(9)°).

Summary

A series of strained, ring-tilted phosphorus(III)-bridged [1]ferrocenophanes have been shown to undergo thermal ROP to yield poly(ferrocenylphosphines). Sulfurization of these materials yielded poly(ferrocenylphosphine sulfides) which were GPC-analyzable and which were completely characterized. The phosphorus(V)-bridged [1]ferrocenophane **7** also underwent thermally-induced ROP, but the resulting polymer partially decomposed under the thermolysis conditions.

Future work will be focused on detailed studies of the properties of the polymers, and we recently reported electrochemical studies of **9** which showed that the iron centers interact with one another in a similar manner to those in poly(ferrocenylsilanes) and poly(ferrocenylgermanes).[2] We are also investigating alternative methods for the initiation of the ROP of phosphorus-bridged [1]ferrocenophanes, and our results of this study will be reported in the near future.

Acknowledgment. This work was supported by the donors of the Petroleum Research Fund (PRF), administered by the American Chemical Society (ACS), and the Natural Science and Engineering Research Council of Canada (NSERC). In addition, I.M. is grateful to the Alfred P. Sloan Foundation for a Research Fellowship (1994–1996).

Supporting Information Available: Tables of crystallographic details, bond angles, anisotropic thermal parameters, and hydrogen coordinates and thermal parameters (17 pages). Ordering information is given on any current masthead page.

OM950376Z

Reactions of $[Et_3NH][(\mu\text{-RE})(\mu\text{-CO})Fe_2(CO)_6]$ (E = S, Se) Salts with Sulfur(I) Chloride and with Carbon Disulfide. Crystal Structure of the $(\mu\text{-PhSe})(\mu\text{-PhCH}_2\text{SC=S})Fe_2(CO)_6$ Complex

Li-Cheng Song,* Chao-Guo Yan, and Qing-Mei Hu

Department of Chemistry, Nankai University, Tianjin 300071, China

Ru-Ji Wang

Department of Chemistry, Tsinghua University, Beijing 100084, China

Thomas C. W. Mak

Department of Chemistry, The Chinese University of Hong Kong, Shatin, New Territories, Hong Kong

Received June 8, 1995[⊗]

The salts of $[Et_3NH][(\mu\text{-RE})(\mu\text{-CO})Fe_2(CO)_6]$ (**1**) react with S_2Cl_2 to give double-cluster complexes $[(\mu\text{-RE})Fe_2(CO)_6]_2(\mu\text{-S–S-}\mu)$ (**2a–f**) (**2a**, RE = EtS; **2b**, PhS; **2c**, *n*-BuS; **2d**, *t*-BuS; **2e**, PhSe; **2f**, *p*-$CH_3C_6H_4Se$), whereas the salt of $[Et_3NH][(\mu\text{-PhSe})(\mu\text{-CO})Fe_2(CO)_6]$ reacts with CS_2 followed by treatment with diverse organic halides to afford single-cluster complexes $(\mu\text{-PhSe})(\mu\text{-ZSC=S})Fe_2(CO)_6$ (**3a–c**) (**3a**, Z = $PhCH_2$; **3b**, $PhCOCH_2$; **3c**, EtO_2CCH_2), double-cluster complexes $[(\mu\text{-PhSe})Fe_2(CO)_6]_2(1,3\text{-}(\mu\text{-S=C–SCH}_2)_2C_6H_4]$ (**3d**) and $[(\mu\text{-PhSe})Fe_2(CO)_6]_2$-$[1,4\text{-}(\mu\text{-S=C–SCH}_2)_2C_6H_4]$ (**3e**), and triple-cluster complex $[(\mu\text{-PhSe})Fe_2(CO)_6]_3[1,3,5\text{-}(\mu\text{-S=C–SCH}_2)_3C_6H_3]$ (**3f**). The crystal structure of **3a** was determined by X-ray diffraction techniques.

Introduction

Over the past decade, the chemical reactivities of triethylammonium salts of the $(\mu\text{-RS})(\mu\text{-CO})Fe_2(CO)_6$ anions have been studied extensively[1–14] relative to those of their Li^+,[2] Na^+,[5] and Mg^+X[15] salts, as well as Et_3N^+H salts of the $(\mu\text{-RSe})(\mu\text{-CO})Fe_2(CO)_6$ anions.[6] Reactions of such salts with most electrophiles can be rationalized in terms of their action as iron-centered nucleophiles and may fall into two categories according to the nature of the electrophiles. In one category, reactions with the electrophiles having a leaving group gave neutral products in which the organic group replaced the μ-CO ligand, such as is shown in ref 5, or the μ-CO ligand remains untouched, which was found only in ref 14. In the other category, however, reactions with the electrophiles that have no leaving group initially gave the corresponding salts of other anions and finally gave the neutral products by protonation of the anions from their counterion Et_3N^+H[2] or by interaction of the anions with extra electrophiles further added.[2] In order to develop the chemistry of such salts, particularly the Se analogs, we initiated the study on the reactions of the Et_3N^+H salts of $(\mu\text{-RE})(\mu\text{-CO})Fe_2(CO)_6$ (E = S, Se) with S_2Cl_2 and with CS_2. Herein we report the interesting results.

Results and Discussion

Reactions of salts $[Et_3NH][(\mu\text{-RE})(\mu\text{-CO})Fe_2(CO)_6]$ (E = S, Se) (**1**) prepared from $Fe_3(CO)_{12}$, Et_3N, and RSH or RSeH with S_2Cl_2 in an approximate molar ratio 2:1 resulted in the formation of the S–S-bonded, double-cluster complexes **2**. The products **2** could be produced *via* an intermediate **M1** formed by nucleophilic attack of the negatively charged iron in **1** at sulfur atoms in S_2Cl_2, followed by the intramolecular displacement of two μ-CO groups by the S–S moiety in **M1**, as shown in Scheme 1. **2a** and **2b** were previously prepared by another route and identified by comparison of their IR and ^1H NMR spectra to those of authentic samples.[16,17]

[⊗] Abstract published in *Advance ACS Abstracts,* October 15, 1995.

(1) Seyferth, D.; Womack, G. B.; Dewan, J. C. *Organometallics* **1985**, *4*, 398.
(2) Seyferth, D.; Hoke, J. B.; Dewan, J. C. *Organometallics* **1987**, *6*, 895.
(3) Seyferth, D.; Anderson, L. L.; Davis, W. M. *J. Organomet. Chem.* **1993**, *459*, 271.
(4) Seyferth, D.; Ruschke, D. P.; Davis, W. M.; Cowie, M.; Hunter, A. D. *Organometallics* **1994**, *13*, 3834.
(5) Seyferth, D.; Womack, G. B.; Archer, C. M.; Dewan, J. C. *Organometallics* **1989**, *8*, 430.
(6) Song, L.-C.; Yan, C.-G.; Hu, Q.-M. *Acta Chim. Sin.* **1995**, *53*, 402.
(7) Song, L.-C.; Liu, J.-T.; Wang, J.-T. *Chem. J. Chin. Univ.* **1989**, *10*, 905.
(8) Song, L.-C.; Wang, R.-J.; Liu, J.-T.; Wang, H.-G.; Wang, J.-T. *Acta Chim. Sin.* **1990**, *48*, 1141.
(9) Song, L.-C.; Liu, J.-T.; Wang, J.-T. *Acta Chim. Sin.* **1990**, *48*, 110.
(10) Song, L.-C.; Li, Y.; Hu, Q.-M.; Liu, R.-G.; Wang, J.-T. *Acta Chim. Sin.* **1990**, *48*, 1180.
(11) Song, L.-C.; Wang, R.-J.; Li, Y.; Wang, H.-G.; Wang, J.-T. *Acta Chim. Sin.* **1990**, *48*, 867.
(12) Song, L.-C.; Hu, Q.-M. *J. Organomet. Chem.* **1991**, *414*, 219.
(13) Song, L.-C.; Hu, Q.-M.; He, J.-L.; Wang, R.-J.; Wang, H.-G. *Heteroatom. Chem.* **1992**, *3*, 465.
(14) Delgado, E.; Hernández, E.; Rossell, O.; Seco, M.; Puebla, E. G.; Ruiz, C. *J. Organomet. Chem.* **1993**, *455*, 177.
(15) Song, L.-C.; Hu, Q.-M.; Cao, X.-C. *Chem. J. Chin. Univ.* **1994**, *15*, 1331.
(16) Seyferth, D.; Kiwan, A. M.; Sinn, E. *J. Organomet. Chem.* **1985**, *281*, 111.
(17) Song, L.-C.; Kadiata, M.; Wang, J.-T. *Youji Huaxue* **1990**, *10*, 270.

0276-7333/95/2314-5513$09.00/0

Scheme 1

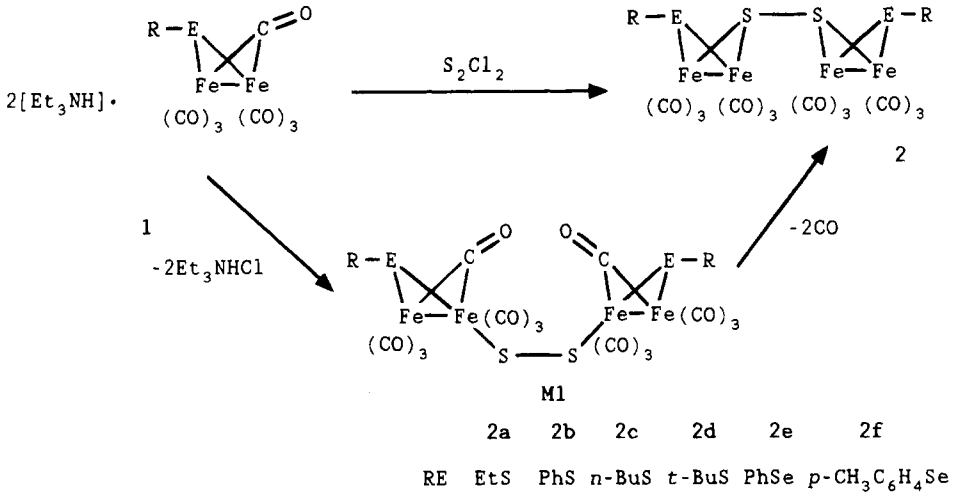

2c–f are new and their constitutions were proven by combustion analysis, IR, ^{1}H NMR spectroscopy, and EI mass spectrometry. The latter showed the molecular ion M^+ for **2f**, M^+-*n*CO for **2c** and **2d**, and the largest fragment $(CO)_4Fe_2SSePh$ for **2e**. According to the orientations of the S–S and C–E bonds to the subcluster core, Fe_2SE (E = S or Se), there are essentially 10 different conformation isomers in all for double-cluster repulsion interactions between R and subcluster (μ-RE)(μ-S)$Fe_2(CO)_6$.[18,19] It is interesting to note that ^{1}H NMR spectroscopy can provide information about the presence of those isomers, which was developed on the basis of the study on the relationship between the structure of (μ-$C_2H_5S)_2Fe_2(CO)_6$[20] and King's ^{1}H NMR data.[21] The ^{1}H NMR spectrum of **2a** showed one axial ethyl group signal at δ_{CH_2} 1.92 ppm[22] and one equatorial ethyl group signal at δ_{CH_2} 2.44 ppm,[22] with an integration ratio of 3:1; therefore, **2a** could not exist as one isomer **ii** (aeee) or **iv** (eaea), but should be a mixture of two or more isomers, such as **i** (aeea) and **iii** (eeee) or **i** and **vi** (eaae) in a ratio of 3:1 (Chart 1). Similarly, since the ^{1}H NMR spectrum of **2d** showed one axial *t*-Bu signal at $\delta_{t\text{-Bu}}$ 1.17 ppm[22] and one equatorial signal at $\delta_{t\text{-Bu}}$ 1.42 ppm,[22] and due to the unequal integrations of two *t*-Bu signals (4:1), **2d** also exists as a mixture, such as **i** and **iii** or **i** and **vi** with a ratio of 4:1. The ^{1}H NMR spectrum of **2f** only showed one signal for *p*-CH_3 at δ 2.34, which means that the two *p*-$CH_3C_6H_4$ are bonded to E atoms *via* one type of bond. Thus, **2f** may exist as one either **i**, **iii**, or **vi**. Unfortunately, the ^{1}H NMR spectra of **2b**, **2c**, and **2e** showed complicated multiplets for their phenyl groups and *n*-Bu groups attached to E atoms, which did not provide any useful information for the identification of their isomers. Although the double clusters of type **2** with E = S were prepared previously by oxidative coupling of the monoanion [(μ-RS)(μ-S)$Fe_2(CO)_6$]$^-$ with SO_2Cl_2,[16,17] the double clusters of type **2** with E = Se were first prepared by this new method from the corresponding salts of complexes **1**. However, the yields of such double clusters prepared by this method are usually low, which is possibly due to the formation of the corresponding byproduct (μ-RE)$_2Fe_2(CO)_6$.

It is known that salts of type **1** with E = S react with CS_2 and diverse halides to form dithioformate cluster complexes.[2] To compare the reactivity of the salts of type **1** (E = Se) toward CS_2 with that of E = S analogs, and to prepare the novel cluster complexes containing both bridged alkylselenido and dithioformate ligands, we carried out the reaction of [Et_3NH][(μ-PhSe)(μ-CO)$Fe_2(CO)_6$] with CS_2, followed by *in situ* reaction with various organic halides. It was observed that the solution turned cherry red with brisk gas evolution when CS_2 was added to the red-brown solution of [Et_3NH][(μ-PhSe)(μ-CO)$Fe_2(CO)_6$] prepared from $Fe_3(CO)_{12}$, PhSeH, and Et_3N. This means that the μ-CO group was replaced by CS_2, and the selenium salt intermediate **M2** was formed in which dithioformato acted as a bridging group. Treatment of the intermediate **M2** solution with organic mono-, di-, or trihalides followed by further workup gave the corresponding single-cluster complexes **3a–c**, double-cluster complexes **3d–e**, and triple-cluster complex **3f**, as shown in Scheme 2.

The cluster complexes **3a–f** are all new and were characterized by combustion analysis and IR, ^{1}H NMR, and mass spectroscopies. Their IR spectra all exhibited two groups of bands: one group consisted of four or five strong peaks in the region of 1960–2100 cm^{-1} and the other had one medium peak around 1000 cm^{-1}. The former was attributed to terminal carbonyls and the latter to the bridged thiocarbonyl C=S group. The C=S vibrational band in free CS_2 is situated at 1533 cm^{-1}, but in CS_2 complexes it is usually shifted to the region of 860–1120 cm^{-1}.[23] As seen from the IR spectra of **3a–f**, the nature of the organic moiety attached to the *exo* sulfur atom may affect the C=S vibrational band. The C=S band in **3a** and **3d–f** is at 999 and 1007 cm^{-1}, respectively, while that in **3b** and **3c** is at 1015 cm^{-1}. This is possible due to the stronger electron-withdrawing effects of the benzoyl and ethoxycarbonyl groups in **3b** and **3c** than those of the corresponding organic groups in **3a** and **3d–f**. The ^{1}H NMR spectra of **3a–f** indicated the proton signals for their respective organic

(18) Shaver, A.; Fitzpatrick, P.; Steliou, K.; Butler, I. S. *J. Am. Chem. Soc.* **1979**, *101*, 1313.
(19) Seyferth, D.; Henderson, R. S.; Song, L.-C. *Organometallics* **1982**, *1*, 125.
(20) Dahl, L. F.; Wei, C.-H. *Inorg. Chem.* **1963**, *2*, 328.
(21) King, R. B. *J. Am. Chem. Soc.* **1962**, *84*, 2460.
(22) De Beer, J. A.; Haines, R. J. *J. Organomet. Chem.* **1970**, *24*, 757.
(23) Patin, H.; Mignani, G.; Mahe, C.; Le Marouille, J.-Y.; Southern, T. G.; Benoit, A.; Grandjean, D. *J. Organomet. Chem.* **1980**, *197*, 315.

Chart 1

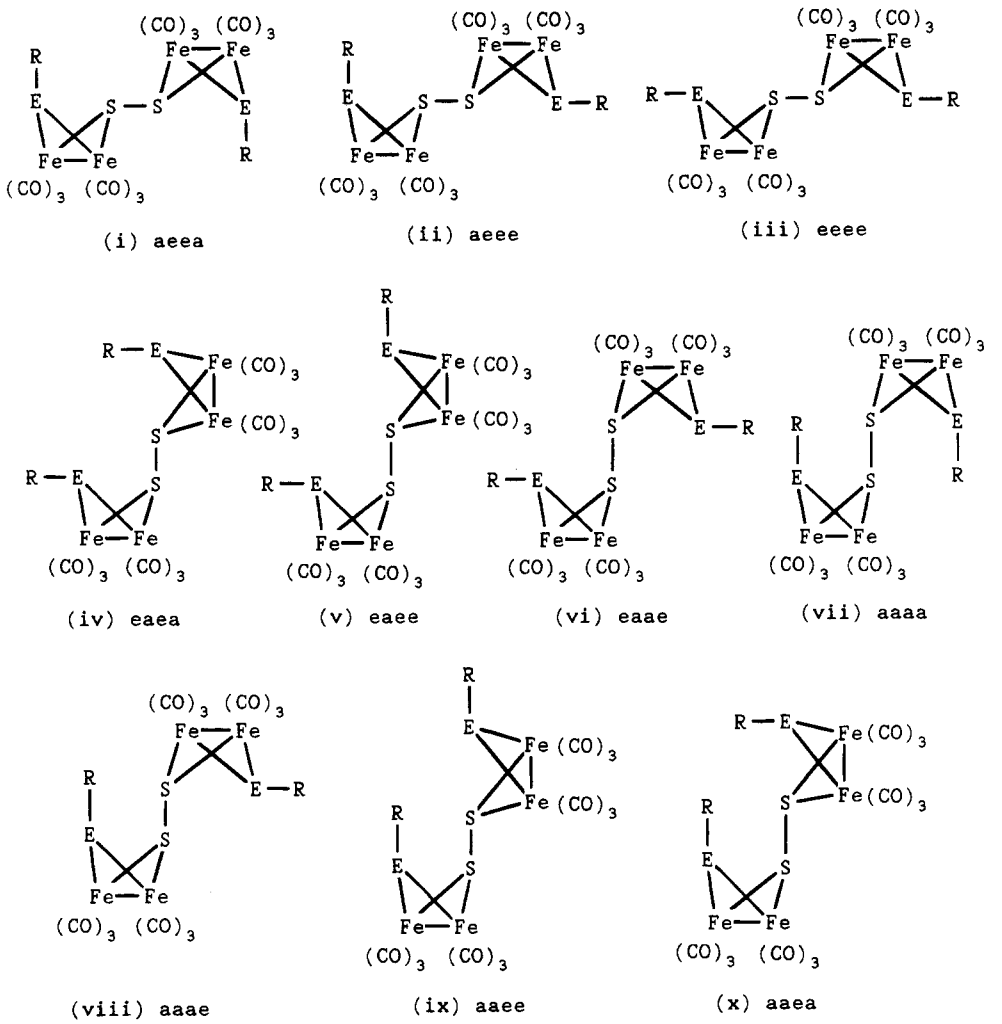

groups, and the mass spectra showed the fragment ions, such as $M^+ - nCO$ for **3a**–**c** and smaller fragment ions for **3d**–**f**.

With the phenyl groups attached to Se atoms as axial or equatorial groups, there are two possible conformation isomers for **3a**–**c**, three for **3d**,**e**, and four for **3f**. Since ^{1}H NMR data for the phenyl groups could not provide information for the identification of isomers (due to their complicated multiplets), an X-ray crystal diffraction analysis for **3a** was undertaken.

The data collection and processing parameters, atomic coordinates, equivalent isotropic thermal parameters, and selected bond lengths and angles are listed in Tables 1–3. Figure 1 shows the ORTEP representation of the molecule. As seen from Figure 1, the structure of **3a** is very similar to that of μ-(thioferrocenylmethyl-methane thiomethylene-C^1-S^2)-1,1,1,2,2,2-hexacarbonyl-μ-methylthiodiiron (abbreviated as Tf hereafter),[23] where both contain a butterfly core with Fe_2E and Fe_2SC as two wings, with E = Se for **3a** and E = S for Tf. The dihedral angle between the two wing planes in **3a** is 89.3°, which is smaller than the corresponding one in Tf (91°).[23] The six-coordinate atoms or groups around each iron atom display as a distorted octahedron. The Fe–Fe distance in **3a** is 2.648(3) Å, which is slightly longer than that of Tf (2.62 Å),[23] but much longer than those in complexes containing two thioalkyl or thioaryl bridges.[24,25]

The angle of S(1)···Se(1)–C(7) = 160.2° reveals that the phenyl group attached to the selenium atom is at an equatorial position, namely, **3a** is an e-type isomer, which can be seen from Figure 1 intuitively. The two Fe–Se distances are almost the same [Fe(1)–Se(1) = 2.380(2) Å, Fe(2)–Se(1) = 2.368(3) Å]. Similar to Tf, the thiocarbonyl C(13)=S(1) in the S(2)–C(13)=S(1) moiety is bridged to Fe(1) *via* a σ bond [Fe(1)–C(13) = 1.98(1) Å] with a carbene character[23] and to Fe(2) *via* the donation of an unshared electron pair from S(1) [Fe(2)–S(1) = 2.307(5) Å]. In comparison with a typical C=S double bond in CS_2 (1.554 Å),[26] the bond length of the double bond C(13)=S(1) extends to 1.63(1) Å [corresponding C–S length is 1.658(4) Å in Tf],[23] but is still much shorter than that of the single bond S(2)–C(13) [1.72(1) Å; the corresponding length in Tf is 1.698(4) Å].[23]

Experimental Section

1. General Comments. All reactions were carried out under an atmosphere of prepurified tank nitrogen. Tetrahy-

(24) Le Borgne, G.; Grandjean, D.; Mathieu, R.; Poilblance, R. *J. Organomet. Chem.* **1977**, *131*, 429.
(25) Henslee, W.; Davis, R. E. *Crystallogr. Struct. Commun.* **1972**, *1*, 403.
(26) Butler, I. S.; Fenster, A. E. *J. Organomet. Chem.* **1974**, *66*, 161.

Scheme 2

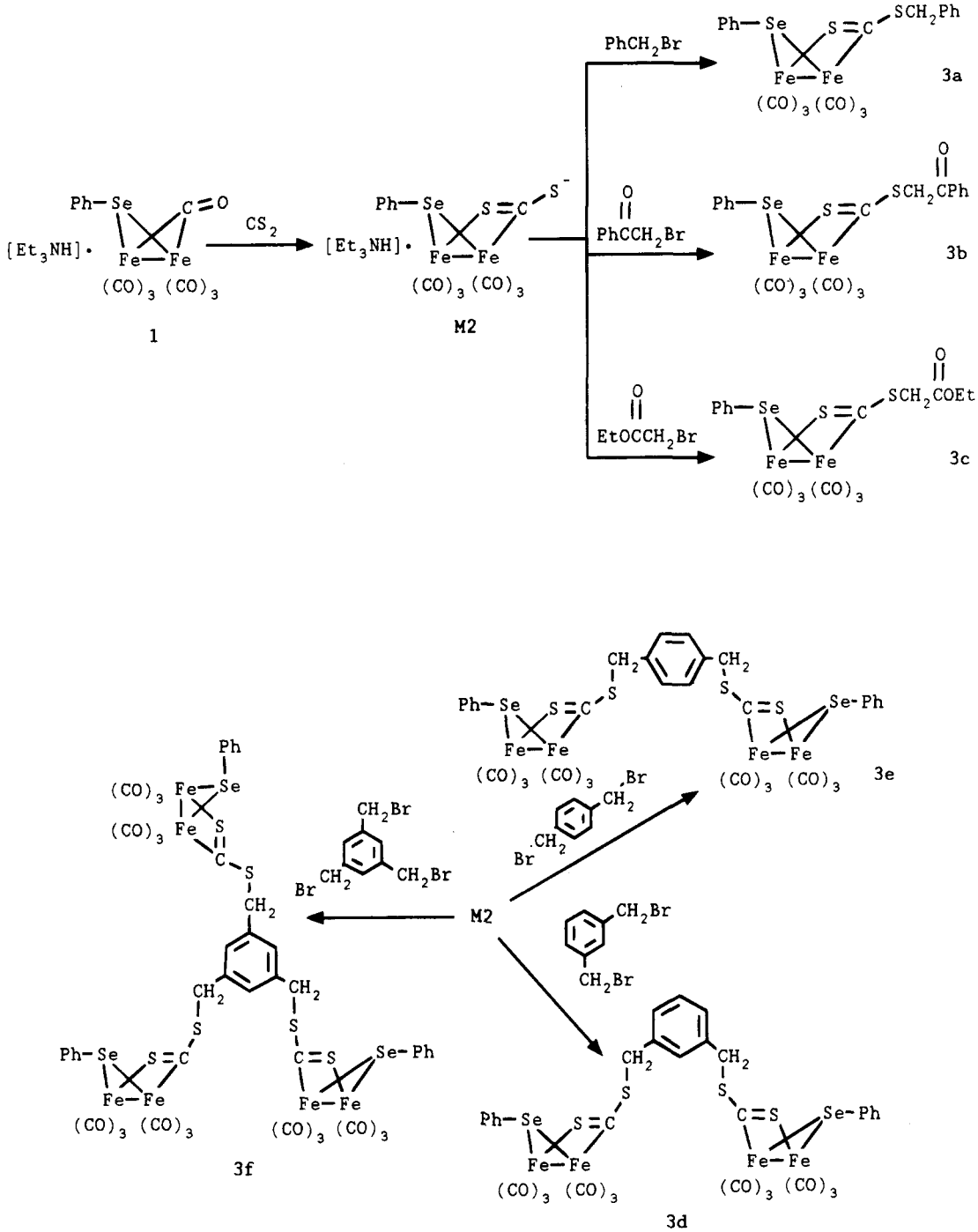

drofuran (THF) was distilled under nitrogen from sodium/benzophenone ketyl, triethylamine from potassium hydroxide, sulfur(I) chloride from elemental sulfur, and carbon disulfide from phosphorus pentoxide. Ethyl, *n*-propyl, *n*-butyl, and *tert*-butyl mercaptans, thiophenol, benzyl bromide, ethyl bromoacetate, and bromoacetophenone were of commercial origin and used without further purification. 1,3-Bis(bromomethyl)-benzene, 1,4-bis(bromomethyl)benzene, 1,3,5-tris(bromomethyl)benzene,[27] triiron dodecacarbonyl,[28] and benzeneselenol[29] were prepared by literature procedures.

The progress of all reactions was monitored by thin-layer chromatography (TLC). Products were purified by column chromatography (30 × 2.4 cm, 200–300 mesh silica gel) and by TLC (20 × 25 × 0.025 cm, silica gel G). Chromatography was completed without the exclusion of atmospheric oxygen or moisture. The eluents were light petroleum ether (60–90 °C) and methylene chloride, which were chemical reagents and used without further purification. Solid products were recrystallized from deoxygenated, mixed solvents of CH_2Cl_2/petroleum ether.

Melting points were determined on a Yanaco MP-500 melting point apparatus and were uncorrected. Combustion analysis was performed on a 240C Model analyzer. Proton NMR spectra were recorded on a JEOL FX-90Q spectrometer with a $CDCl_3$ solvent and a TMS internal standard. Infrared spectra were obtained on a NICOLET FT-IR 5DX spectrophotometer with a KBr disk. Mass spectra were obtained with a HP 5988A spectrometer.

2. Reaction of [Et$_3$NH][(μ-RE)(μ-CO)Fe$_2$(CO)$_6$] (1) with

(27) Werner, W. *J. Org. Chem.* **1952**, *17*, 523.
(28) King, R. B. *Organometallic Syntheses*; Academic Press: New York, 1965; Vol. 1, Transition-Metal Compounds, p 95.
(29) Foster, D. G. *Organic Syntheses*; Wiley: New York, 1955; Collect. Vol. III, p 771.

Table 1. Data Collection and Processing Parameters for 3a

molecular formula	$C_{20}H_{12}Fe_2O_6S_2Se$
molecular weight	603.08
color and habit	red plate
crystal size (mm^3)	0.05 × 0.10 × 0.10
crystal system	monoclinic
space group	$P2_1/n$ (No. 14)
unit cell parameters	a = 9.584(2) Å
	b = 21.871(4) Å
	c = 11.061(2) Å
	β = 98.92(3)°
	Z = 4
	V = 2291(1) Å^3
	$F(000)$ = 1192
density (calcd, g cm^{-3})	1.749
Rigaku R-AXIS II	imaging plate size, 200 × 200 mm
camera length (mm)	69.95 (start angle −20.0°)
frame number	24 (oscillation angle 6°)
exposure time (min)	16
radiation	graphite-monochromatized Mo Kα, λ = 0.710 73 Å
absorption coefficient (mm^{-1})	3.071
collection range	$0 \le h \le 12$, $0 \le k \le 25$, $-13 \le l \le 13$; $2\theta = 55°$
unique data measured	4101
R_{int} (from merging of equiv reflections)	0.074
obs data with $\|F_o\| \ge 10\sigma(\|F_o\|)$, n	1746
no. of variables, p	256
weighting scheme	$w = 1/\sigma^2(F)$
$R_F = \sum\|\|F_o\| - \|F_c\|\|/\sum\|F_o\|$	0.066
$R_w = [\sum w(\|F_o\| - \|F_c\|)^2/\sum w\|F_o\|^2]^{1/2}$	0.066
$S = [\sum w(\|F_o\| - \|F_c\|)^2/(n-p)]^{1/2}$	2.91
largest and mean Δ/σ	0.24 and 0.04
residual extrema in final difference map (eÅ^{-3})	+0.92 to −0.44

Table 2. Atomic Coordinates (×10^4) and Equivalent Isotropic Temperature Factors[a] (×10^4 Å^2 for Se and Fe; ×10^3 Å^2 for Others) for 3a

atom	x	y	z	U_{eq}
Se(1)	2957(2)	339(1)	3626(2)	549(5)
Fe(1)	1354(2)	−412(1)	2675(2)	543(7)
Fe(2)	3884(2)	−205(1)	2078(2)	571(8)
S(1)	4292(4)	−922(2)	3623(4)	61(1)
S(2)	1956(4)	−1463(2)	4721(4)	63(1)
O(1)	764(12)	−1453(4)	993(10)	81(2)
O(2)	−1016(11)	−514(5)	4069(11)	93(2)
O(3)	−294(11)	483(5)	1071(10)	81(2)
O(4)	4056(12)	−1173(5)	289(12)	100(2)
O(5)	6756(11)	32(5)	2381(12)	102(2)
O(6)	2746(12)	597(5)	67(11)	91(2)
C(1)	987(14)	−1028(7)	1653(13)	61(2)
C(2)	−85(15)	−466(6)	3582(15)	70(2)
C(3)	362(13)	128(7)	1679(13)	58(2)
C(4)	3998(15)	−800(7)	1021(15)	69(2)
C(5)	5669(15)	98(7)	2290(16)	79(2)
C(6)	3183(14)	299(6)	889(13)	59(2)
C(7)	2407(14)	1141(6)	3131(13)	58(2)
C(8)	3323(15)	1529(6)	2572(15)	72(2)
C(9)	3013(16)	2133(7)	2389(16)	83(2)
C(10)	1814(17)	2387(7)	2703(16)	90(2)
C(11)	917(17)	2029(6)	3229(14)	77(2)
C(12)	1225(16)	1418(6)	3416(15)	76(2)
C(13)	2621(13)	−969(5)	3744(12)	51(2)
C(14)	3464(14)	−1882(7)	5517(13)	67(2)
C(15)	3030(13)	−2269(6)	6483(13)	55(2)
C(16)	2761(15)	−2877(7)	6346(15)	75(2)
C(17)	2334(17)	−3250(7)	7246(15)	84(2)
C(18)	2326(15)	−2981(7)	8356(16)	77(3)
C(19)	2599(16)	−2380(7)	8574(16)	84(3)
C(20)	2981(16)	−2025(8)	7628(16)	86(3)

[a] U_{eq} is defined as one-third of the trace of the orthogonalized **U** tensor.

Table 3. Selected Bond Lengths (Å) and Bond Angles (deg) for 3a

atom	distance	atom	distance
Fe(1)−Fe(2)	2.648(3)	Fe(1)−Se(1)	2.380(2)
Fe(1)−C(1)	1.76(2)	Fe(1)−C(2)	1.83(2)
Fe(1)−C(3)	1.79(1)	Fe(1)−C(13)	1.98(1)
Fe(2)−Se(1)	2.368(3)	Fe(2)−S(1)	2.307(5)
O(1)−C(1)	1.18(2)	O(3)−C(3)	1.15(2)
O(5)−C(5)	1.12(2)	Se(1)−C(7)	1.89(1)
S(1)−C(13)	1.63(1)	S(2)−C(13)	1.72(1)
S(2)−C(14)	1.82(1)	C(14)−C(15)	1.47(2)

atom	angle	atom	angle
Se(1)−Fe(1)−Fe(2)	55.9(1)	Se(1)−Fe(1)−C(1)	149.8(5)
Fe(2)−Fe(1)−C(1)	94.0(5)	Se(1)−Fe(1)−C(2)	107.0(5)
Fe(2)−Fe(1)−C(2)	160.8(5)	C(1)−Fe(1)−C(2)	102.1(7)
Se(1)−Fe(1)−C(3)	93.5(4)	Fe(2)−Fe(1)−C(3)	98.8(5)
Se(1)−Fe(1)−C(13)	82.3(4)	Fe(2)−Fe(1)−C(13)	75.7(4)
Se(1)−Fe(2)−Fe(1)	56.3(1)	Se(1)−Fe(2)−S(1)	81.1(1)
Fe(1)−Fe(2)−S(1)	75.9(1)	Se(1)−Fe(2)−C(4)	156.7(5)
Fe(1)−Fe(2)−C(4)	101.1(5)	S(1)−Fe(2)−C(4)	88.2(5)
Se(1)−Fe(2)−C(5)	100.1(5)	Fe(1)−Fe(2)−C(5)	155.6(6)
Se(1)−Fe(2)−C(6)	94.7(5)	Fe(1)−Fe(2)−C(6)	92.0(5)
S(1)−Fe(2)−C(6)	167.5(5)	Fe(1)−C(1)−O(1)	178(1)
Fe(2)−C(4)−O(4)	177(1)	Fe(1)−Se(1)−Fe(2)	67.8(1)
Fe(1)−Se(1)−C(7)	112.4(4)	Fe(2)−Se(1)−C(7)	112.1(5)
Se(1)−C(7)−C(8)	121(1)	Fe(2)−S(1)−C(13)	92.7(5)
C(13)−S(2)−C(14)	106.1(7)	Fe(1)−C(13)−S(1)	115.6(7)
Fe(1)−C(13)−S(2)	120.7(7)	S(1)−C(13)−S(2)	123.8(8)
S(2)−C(14)−C(15)	110(1)		

Sulfur(I) Chloride. A 100 mL three-necked round-bottomed flask equipped with a stir-bar, a N_2 inlet tube, and serum caps was charged with 1.50 g (2.98 mmol) of $Fe_3(CO)_{12}$ and 40 mL of THF. To the resulting green solution were added 0.50 mL (3.58 mmol) of triethylamine and about 3 mmol of the corresponding mercaptan, thiophenol, or areneselenol. The solution immediately turned red-brown and was stirred for 10 min in the case of areneselenol and for 30 min in the case of mercaptan and thiophenol. The resulting [Et$_3$NH][(μ-RE)(μ-CO)Fe$_2$(CO)$_6$] reagent (**1**) then was utilized *in situ* without further purification.

2.1. Preparation of 2a. The THF solution of **1** (RE = EtS) prepared by using EtSH as above was cooled to −78 °C with a dry ice/acetone bath, to which was added 0.13 mL (1.6 mmol) of sulfur(I) chloride. The reaction mixture was maintained for 10 min at −78 °C and then allowed to warm to room temperature and stirred for an additional 2 h. TLC analysis of the reaction mixture indicated the formation of two major orange-red products. The solvent was removed *in vacuo* to give a dark red residue, which was purified by column

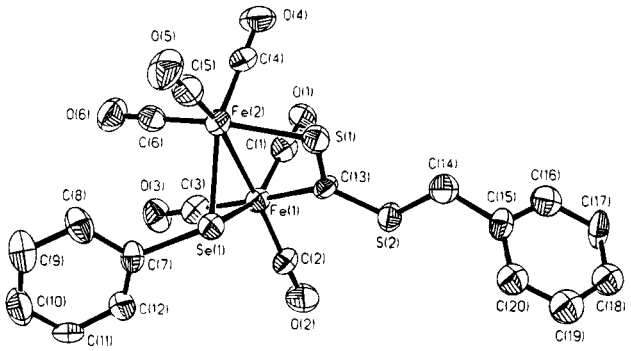

Figure 1. ORTEP view of **3a** as drawn with 35% probability ellipsoids.

chromatography. Elution with 1:9 (v/v) CH_2Cl_2/petroleum ether gave a red oil, which was further purified by TLC. Elution with 1:18 (v/v) CH_2Cl_2/petroleum ether gave two red bands. The first red band gave 0.076 g (4%) of $(\mu\text{-EtS})_2Fe_2(CO)_6$, which was identified by comparison of its melting point and ^1H NMR spectrum with those given in the literature.[7] The second major red band gave 0.331 g (30%) of $[(\mu\text{-EtS})Fe_2(CO)_6]_2(\mu\text{-S-S-}\mu)$ (**2a**) as a slightly air-sensitive red crystal, which was also identified by comparison of its melting point and ^1H NMR spectrum with those of an authentic sample.[17]

2.2. Preparation of 2b. The same procedure as in section 2.1 was followed, but **1** where RE = EtS was replaced by **1** where RE = PhS and gave two major products. The first orange band gave 0.349 g (24%) of $(\mu\text{-PhS})_2Fe_2(CO)_6$, which was identified by comparison of its melting point and ^1H NMR spectrum with those given in the literature.[30] The second red band gave 0.080 g (6%) of $[(\mu\text{-PhS})Fe_2(CO)_6]_2(\mu\text{-S-S-}\mu)$ (**2b**) as a slightly air-sensitive red solid, which was also identified by comparison of its melting point and ^1H NMR spectrum with those of an authentic sample.[16]

2.3. Preparation of 2c. The same procedure as in section 2.1 was followed, but **1** where RE = EtS was replaced by **1** where RE = *n*-BuS and gave two major products. The first red band gave 0.054 g (4%) of $(\mu\text{-}n\text{-BuS})_2Fe_2(CO)_6$, which was identified by comparison of its ^1H NMR spectrum with that given in the literature.[22] The second major red band gave 0.294 g (30%) of $[(\mu\text{-}n\text{-BuS})Fe_2(CO)_6]_2(\mu\text{-S-S-}\mu)$ (**2c**) as a slightly air-sensitive red solid (mp 85–86 °C). Anal. Calcd for $C_{20}H_{18}Fe_4O_{12}S_4$: C, 29.95; H, 2.26. Found: C, 29.90; H, 1.98. IR (KBr disk): terminal C≡O 2065(vs), 2049(vs), 1991(vs) cm^{-1}. ^1H NMR ($CDCl_3$): δ 0.60–2.70 (m, 18H, $2CH_2CH_2CH_2CH_3$). MS (EI) *m/z* (relative intensity): 718 [$(M - 3CO)^+$, 0.6], 662 [$(M - 5CO)^+$, 0.4], 578 [$(M - 8CO)^+$, 0.6], 550 [$(M - 9CO)^+$, 0.5], 522 [$(M - 10CO)^+$, 3.0], 494 [$(M - 11CO)^+$, 8.2], 466 [$(M - 12CO)^+$, 1.8], 402 [$(CO)_6Fe_2SH{\cdot}SBu\text{-}n^+$, 2.6], 374 [$(CO)_5Fe_2SH{\cdot}SBu\text{-}n^+$, 5.2], 346 [$(CO)_4Fe_2SH{\cdot}SBu\text{-}n^+$, 8.1], 318 [$(CO)_3Fe_2SH{\cdot}SBu\text{-}n^+$, 19.7], 233 [$Fe_2S{\cdot}SBu\text{-}n^+$, 8.0), 201 [$Fe_2SBu\text{-}n^+$, 4.0), 176 [$Fe_2S_2^+$, 24.3), 144 [$Fe_2S^+$, 11.4), 112 [$Fe_2^+$, 4.8), 90 [*n*-$BuSH^+$, 6.1), 57 [*n*-$Bu^+$, 21.6), 56 [$Fe^+$, 100), 41 [$CH_2{=}CHCH_2^+$, 85.6).

2.4. Preparation of 2d. The same procedure as in section 2.1 was followed, but **1** where RE = EtS was replaced by **1** where RE = *t*-BuS and gave two major products. The first red band gave 0.058 g (4%) of $(\mu\text{-}t\text{-BuS})_2Fe_2(CO)_6$, which was identified by comparison of its melting point and ^1H NMR spectrum with those given in the literature.[22] The second major red band gave 0.616 g (52%) of $[(\mu\text{-}t\text{-BuS})Fe_2(CO)_6]_2(\mu\text{-S-S-}\mu)$ (**2d**) as a slightly air-sensitive red crystal (mp 140 °C (dec)). Anal. Calcd for $C_{20}H_{18}Fe_4O_{12}S_4$: C, 29.95; H, 2.26. Found: C, 29.77; H, 2.23. IR (KBr, disk): terminal C≡O 2065(s), 2032(vs), 2008(s), 1983(vs) cm^{-1}. ^1H NMR ($CDCl_3$): δ 1.17 [s, a-$C(CH_3)_3$], 1.42 [s, e-$C(CH_3)_3$], a/e = 4:1. MS (EI) *m/z* (relative intensity): 522 [$(M - 10CO)^+$, 0.7], 494 [$(M - 11CO)^+$, 1.8], 466 [$(M - 12CO)^+$, 0.5], 409 ($Fe_4S_4Bu\text{-}t^+$, 0.7), 352 ($Fe_4S_4^+$, 2.0), 233 ($Fe_2S{\cdot}SBu\text{-}t^+$, 2.6), 177 ($Fe_2S{\cdot}SH^+$, 7.1), 176 ($Fe_2S_2^+$, 1.1), 144 ($Fe_2S^+$, 0.6), 112 ($Fe_2^+$, 1.2), 90 (*t*-$BuSH^+$, 16.8), 89 (*t*-$BuS^+$, 0.6), 57 (*t*-$Bu^+$, 37.3), 56 ($Fe^+$, 33.7), 41 ($CH_2{=}CHCH_2^+$, 100).

2.5. Preparation of 2e. The same procedure as in section 2.1 was followed, but **1** where RE = EtS was replaced by **1** where RE = PhSe and gave two major products. The first red band gave 0.337 g (19%) of $(\mu\text{-PhSe})_2Fe_2(CO)_6$, which was identified by comparison of its melting point and ^1H NMR spectrum with those of an authentic sample.[6] The second red band gave 0.122 g (9%) of $[(\mu\text{-PhSe})Fe_2(CO)_6]_2(\mu\text{-S-S-}\mu)$ (**2e**) as a slightly air-sensitive red solid (mp 190 °C (dec)). Anal. Calcd for $C_{24}H_{10}Fe_4O_{12}S_2Se_2$: C, 30.80; H, 1.08. Found: C, 30.75; H, 0.98. IR (KBr, disk): terminal C≡O 2082(s), 2057(vs), 2032(vs), 1991(vs), 1975(vs) cm^{-1}. ^1H NMR ($CDCl_3$): δ 7.16–6.80 (m, 10H, $2C_6H_5$). MS (EI, ^{80}Se) *m/z* (relative intensity): 413 [$(CO)_4Fe_2S{\cdot}SePh^+$, 98.6], 357 [$(CO)_2Fe_2S{\cdot}SePh^+$, 12.4], 301 ($Fe_2S{\cdot}SePh^+$, 5.6), 269 (Fe_2SePh^+, 3.7), 224 ($Fe_2S{\cdot}Se^+$, 8.6), 196 (Fe_2Se^+, 4.7), 144 (Fe_2S^+, 4.8), 112 (Fe_2^+, 8.2), 77 ($C_6H_5^+$, 8.6), 56 (Fe^+, 26.8).

2.6. Preparation of 2f. The same procedure as in section 2.1 was followed, but **1** where RE = EtS was replaced by **1** where RE = 4-$CH_3C_6H_4Se$ and gave two major products. The first red band gave 0.439 g (24%) of $(\mu\text{-4-}CH_3C_6H_4Se)_2Fe_2(CO)_6$ as an air-stable red solid. It is a new compound (mp 96–98 °C). Anal. Calcd for $C_{20}H_{14}Fe_2O_6Se_2$: C, 38.75; H, 2.28. Found: C, 38.83; H, 2.22. IR (KBr disk): terminal C≡O 2032(s), 2000(vs), 1967(vs) cm^{-1}. ^1H NMR ($CDCl_3$): δ 2.20 (s, 6H, $2CH_3$), 6.88, 6.96, 7.08, 7.18 (AA'BB' quartet, 8H, $2C_6H_4$). MS (EI, ^{80}Se) *m/z* (relative intensity): 622 (M^+, 0.9), 566 [$(M - 2CO)^+$, 1.2], 538 [$(M - 3CO)^+$, 0.6], 510 [$(M - 4CO)^+$, 0.4], 482 [$(M - 5CO)^+$, 1.4], 454 [$(M - 6CO)^+$, 8.2], 363 ($Fe_2SeSeC_6H_4CH_3\text{-}4^+$, 1.2), 272 ($Fe_2Se_2^+$, 21.7), 283 ($Fe_2SeC_6H_4CH_3\text{-}4^+$, 1.5), 269 ($Fe_2SeC_6H_5^+$, 7.1), 192 ($Fe_2Se^+$, 9.4), 182 ($CH_3C_6H_4C_6H_4CH_3^+$, 26.7), 167 ($C_6H_5Se^+$, 18.4), 112 ($Fe_2^+$, 3.8), 91 ($C_6H_4CH_3^+$, 100), 56 ($Fe^+$, 16.5). The second red band gave 0.095 g (7%) of $[(\mu\text{-4-}CH_3C_6H_4Se)Fe_2(CO)_6]_2(\mu\text{-S-S-}\mu)$ (**2f**) as a slightly air-sensitive red solid (mp 105 °C (dec)). Anal. Calcd for $C_{26}H_{14}Fe_4O_{12}S_2Se_2$: C, 32.40; H, 1.46. Found: C, 32.19; H, 1.43. IR (KBr disk): terminal C≡O 2082(s), 2057(vs), 2032(vs), 1991(vs) cm^{-1}. ^1H NMR ($CDCl_3$): δ 2.34 (s, 6H, $2CH_3$), 7.09, 7.18, 7.33, 7.44 (AA'BB' quartet, 8H, $2C_6H_4$). MS (EI, ^{80}Se) *m/z* (relative intensity): 315 ($Fe_2S{\cdot}SeC_6H_4CH_3\text{-}4^+$, 1.3), 282 ($Fe_2SeC_6H_4CH_3\text{-}4^+$, 1.4), 224 ($Fe_2S{\cdot}Se^+$, 3.5), 192 ($Fe_2Se^+$, 2.1), 171 (4-$CH_3C_6H_4Se^+$, 23.2), 144 ($Fe_2S^+$, 3.2), 112 ($Fe_2^+$, 1.9), 91 ($C_6H_5CH_2^+$, 100), 56 ($Fe^+$, 11.7).

3. Reactions of $[Et_3NH][(\mu\text{-PhSe})(\mu\text{-CO})Fe_2(CO)_6]$ with Carbon Disulfide. Standard in Situ Preparation of $[Et_3NH][(\mu\text{-PhSe})(\mu\text{-SC=S})Fe_2(CO)_6]$ (M2). A 100 mL three-necked flask equipped with a magnetic stir-bar, a N_2 inlet, and serum caps was charged with 1.50 g (2.98 mmol) of $Fe_3(CO)_{12}$ and 40 mL of THF. To the resulting green solution were added 0.50 mL (3.58 mmol) of triethylamine and 0.32 mL (3.03 mmol) of benzeneselenol, which was stirred for 10 min. When 0.60 mL (10.0 mmol) of CS_2 was added to this THF solution of $[Et_3NH](\mu\text{-PhSe})(\mu\text{-CO})Fe_2(CO)_6]$, gas evolution was observed and the color of solution changed from red-brown to cherry red in 30 min. The $[Et_3NH][\mu\text{-PhSe})(\mu\text{-S=C-S}^-)Fe_2(CO)_6]$ (**M2**) solution was thus prepared and utilized *in situ* without further purification.

3.1. Preparation of 3a. To the solution prepared as above was added 0.72 mL (6.0 mmol) of benzyl bromide. The reaction mixture was stirred for 2 h at room temperature. TLC analysis indicated that two main red products were formed. The solvent was removed *in vacuo* to give a red residue, which was subjected to column chromatography. Elution with 1:9 (v/v) CH_2Cl_2/petroleum ether followed by evaporation of the solvent gave 0.322 g (18%) of $(\mu\text{-PhSe})_2Fe_2(CO)_6$, which was identified by comparison of its melting point and ^1H NMR spectrum with those of an authentic sample,[6] and 1.016 g (57%) of $(\mu\text{-PhSe})(\mu\text{-PhCH}_2SCS)Fe_2(CO)_6$ (**3a**) as a red air-

(30) Nametkin, N. S.; Tyurin, V. D.; Kukina, M. A. *J. Organomet. Chem.* **1978**, *149*, 355.

stable solid (mp 116–117 °C). Anal. Calcd for $C_{20}H_{12}Fe_2O_6S_2Se$: C, 39.83; H, 2.01. Found: C, 39.79; H, 2.03. IR (KBr disk): terminal C≡O 2065(s), 2016(vs), 1983(s), 1867(s) cm^{-1}, C=S 999(m) cm^{-1}. ^{1}H NMR ($CDCl_3$): δ 4.35 (s, 2H, CH_2), 7.08–7.64 (m, 10H, $2C_6H_5$). MS (EI, ^{80}Se) *m/z* (relative intensity): 520 [(M − 3CO)$^+$, 1.0], 492 [(M − 4CO)$^+$, 0.7], 436 [(M − 6CO)$^+$, 3.3], 345 ($Fe_2SePhCS_2^+$, 1.9), 301 ($Fe_2S{\cdot}SePh^+$, 4.0), 269 (Fe_2SePh^+, 6.1), 224 ($Fe_2S{\cdot}Se^+$, 6.0), 192 (Fe_2Se^+, 3.7), 157 ($PhSe^+$, 11.7), 144 (Fe_2S^+, 2.3), 91 ($C_6H_5CH_2^+$, 100), 77 ($C_6H_5^+$, 15.6), 56 (Fe^+, 2.9).

3.2. Preparation of 3b. A procedure similar to that in section 3.1 was followed, but 0.995 g (5.0 mmol) of bromoacetophenone was used instead of benzyl bromide. Elution with 1:18 (v/v) CH_2Cl_2/petroleum ether yielded 0.310 g (18%) of (μ-PhSe)$_2$Fe$_2$(CO)$_6$. Further elution with 3:7 (v/v) CH_2Cl_2/petroleum ether afforded 0.906 g (48%) of (μ-PhSe)(μ-$PhCOCH_2$SCS)$Fe_2(CO)_6$ (**3b**) as a red air-sensitive solid (mp 38–40 °C). Anal. Calcd for $C_{21}H_{12}Fe_2O_7S_2Se$: C, 39.97; H, 1.92. Found: C, 40.36; H, 1.78. IR (KBr disk): terminal C≡O 2065(s), 2024(vs), 2000(s), 1983(s) cm^{-1}, C=O 1680(m) cm^{-1}, C=S 1015(m) cm^{-1}. ^{1}H NMR ($CDCl_3$): δ 4.74 (s, 2H, CH_2), 7.34–8.20 (m, 10H, $2C_6H_5$). MS (EI, ^{80}Se) *m/z* (relative intensity): 548 [(M − 3CO)$^+$, 0.4], 520 [(M − 4CO)$^+$, 0.4], 464 [(M − 6CO)$^+$, 2.1], 301 ($Fe_2S{\cdot}SePh^+$, 1.7), 269 (Fe_2SePh^+, 4.2), 224 (Fe_2SSe^+, 4.1), 192 (Fe_2Se^+, 5.2), 157 ($PhSe^+$, 24.7), 144 (Fe_2S^+, 3.5), 119 ($PhCOCH_2^+$, 1.9), 105 ($PhCO^+$, 69.9), 91 ($C_6H_5CH_2^+$, 22.8), 77 ($C_6H_5^+$, 100), 56 (Fe^+, 9.5).

3.3. Preparation of 3c. A procedure similar to that in section 3.1 was followed, but 0.56 mL (5.0 mmol) of ethyl bromoacetate was used instead of benzyl bromide. Elution with 1:18 (v/v) CH_2Cl_2/petroleum ether yielded 0.392 g (22%) of (μ-PhSe)$_2$Fe$_2$(CO)$_6$. Further elution with 1:4 (v/v) CH_2Cl_2/petroleum ether afforded 0.836 g (47%) of (μ-PhSe)(μ-EtO_2CCH_2SCS)$Fe_2(CO)_6$ (**3c**) as a red air-stable solid (mp 74–75 °C). Anal. Calcd for $C_{17}H_{12}Fe_2O_8S_2Se$: C, 34.09; H, 2.02. Found: C, 34.19; H, 2.13. IR (KBr disk): terminal C≡O 2065(s), 2032(vs), 2008(s), 1983(s), 1951(s) cm^{-1}, C=O 1721 cm^{-1}, C=S 1015(m) cm^{-1}. ^{1}H NMR ($CDCl_3$): δ 1.20 (t, J = 7.2 Hz, 3H, CH_3), 3.91 (s, 2H, CH_2CO), 4.16 (q, J = 7.2 Hz, 2H, CH_2), 7.04–7.80 (m, 5H, C_6H_5). MS (EI, ^{80}Se) *m/z* (relative intensity): 544 [(M − 2CO)$^+$, 2.0], 516 [(M − 3CO)$^+$, 21.7], 488 [(M − 4CO)$^+$, 14.4], 460 [(M − 5CO)$^+$, 0.9], 432 [(M − 6CO)$^+$, 58.3], 387 ($Fe_2SePh{\cdot}SCSCH_2CO^+$, 5.3), 359 ($Fe_2SePh{\cdot}SCSCH_2^+$, 2.8), 346 ($Fe_2SePh{\cdot}SCSH^+$, 100), 345 ($Fe_2SePh{\cdot}SCS^+$, 13.9), 301 ($Fe_2SePh{\cdot}S^+$, 18.5), 269 ($Fe_2SePh^+$, 33), 192 ($Fe_2Se^+$, 61.7), 157 ($PhSe^+$, 52.7), 144 ($Fe_2S^+$, 28.2), 112 ($Fe_2^+$, 14.7), 77 ($C_6H_5^+$, 62.1), 56 ($Fe^+$, 42.1).

3.4. Preparation of 3d. A procedure similar to that in section 3.1 was followed, but 0.370 g (1.4 mmol) of 1,3-bis(bromomethyl)benzene was used instead of benzyl bromide. Elution with 1:18 (v/v) CH_2Cl_2/petroleum ether yielded 0.403 g (23%) of (μ-PhSe)$_2$Fe$_2$(CO)$_6$. Further elution with 1:4 (v/v) CH_2Cl_2/petroleum ether afforded 0.501 g (30%) of [(μ-PhSe)$Fe_2(CO)_6$]$_2$[1,3-(μ-$SCSCH_2$)$_2C_6H_4$] (**3d**) as a red air-stable solid (mp 44–46 °C). Anal. Calcd for $C_{34}H_{18}Fe_4O_{12}S_4Se_2$: C, 36.20; H, 1.61. Found: C, 36.58; H, 2.01. IR (KBr disk): terminal C≡O 2065(s), 2024(s), 2000(s), 1983(s) cm^{-1}, C=S 1007(m) cm^{-1}. ^{1}H NMR ($CDCl_3$): δ 3.96–4.20, 4.24–4.48 (m, m, 4H, $2CH_2$), 7.12–7.72 (m, 14H, $2C_6H_5$, C_6H_4). MS (EI, ^{80}Se) *m/z* (relative intensity): 157 ($PhSe^+$, 94.8), 105 ($CH_3C_6H_4CH_2^+$, 16.7), 104 ($CH_2C_6H_4CH_2^+$, 97.5), 91 ($C_6H_5CH_2^+$, 29.3), 78 ($C_6H_6^+$, 84.6), 77 ($C_6H_5^+$, 100).

3.5. Preparation of 3e. A procedure similar to that in section 3.1 was followed, but 0.370 g (1.4 mmol) of 1,4-bis(bromomethyl)benzene was used instead of benzyl bromide. Elution with 1:9 (v/v) CH_2Cl_2/petroleum ether yielded 0.303 g (17%) of (μ-PhSe)$_2$Fe$_2$(CO)$_6$ and then gave 0.503 g (30%) of [(μ-PhSe)$Fe_2(CO)_6$]$_2$[1,4-(μ-$SCSCH_2$)$_2C_6H_4$] (**3e**) as a red air-stable solid (mp 52–54 °C). Anal. Calcd for $C_{34}H_{18}Fe_4O_{12}S_4Se_2$: C, 36.20; H, 1.61. Found: C, 36.26; H, 1.54. IR (KBr disk): terminal C≡O 2065(s), 2024(vs), 2000(s), 1983(s) cm^{-1}, C=S 1007(m) cm^{-1}. ^{1}H NMR ($CDCl_3$): δ 4.16, 4.41 (s, s, 4H, $2CH_2$), 7.12–7.60 (m, 14H, $2C_6H_5$, C_6H_4). MS (EI, ^{80}Se) *m/z* (relative intensity): 269 (Fe_2SePh^+, 0.3), 192 (Fe_2Se^+, 0.2), 157 ($PhSe^+$, 35.9), 105 ($CH_3C_6H_4CH_2^+$, 21.8), 104 ($CH_2C_6H_4CH_2^+$, 100), 78 ($C_6H_6^+$, 26.3), 77 ($C_6H_5^+$, 36.8).

3.6. Preparation of 3f. A procedure similar to that in section 3.1 was followed, but 0.358 g (1.0 mmol) of 1,3,5-tris(bromomethyl)benzene was used instead of benzyl bromide. Elution with 1:18 (v/v) CH_2Cl_2/petroleum ether gave 0.334 g (19%) of (μ-PhSe)$_2$Fe$_2$(CO)$_6$. Further elution with 1:5 (v/v) CH_2Cl_2/petroleum ether yielded 0.259 g (16%) of [(μ-PhSe)$Fe_2(CO)_6$]$_3$[1,3,5-(μ-$SCSCH_2$)$_3C_6H_3$] (**3f**) as a red air-stable solid (mp 78–80 °C). Anal. Calcd for $C_{48}H_{24}Fe_6O_{18}S_6Se_3$: C, 34.88; H, 1.46. Found: C, 34.76; H, 1.39. IR (KBr disk): terminal C≡O 2065(s), 2032(vs), 2000(s), 1983(s) cm^{-1}, C=S 1007(m) cm^{-1}. ^{1}H NMR ($CDCl_3$): δ 3.94–4.12, 4.16–4.48 (m, m, 6H, $3CH_2$), 7.04–7.60 (m, 18H, C_6H_3, $3C_6H_5$). MS (EI, ^{80}Se) *m/z* (relative intensity): 346 ($Fe_2SePh{\cdot}SCSH^+$, 0.3), 314 ($Fe_2SePh{\cdot}SCH^+$, 37.5), 301 (Fe_2SePhS^+, 0.4), 269 (Fe_2SePh^+, 0.7), 224 ($Fe_2Se{\cdot}S^+$, 1.3), 192 (Fe_2Se^+, 0.8), 157 ($PhSe^+$, 91.4), 144 (Fe_2S^+, 0.9), 117 [$C_6H_3(CH_2)_3^+$, 15.7], 104 ($CH_2C_6H_4CH_2^+$, 1.8), 91 ($C_6H_5CH_2^+$, 19.4), 78 ($C_6H_6^+$, 16.4), 77 ($C_6H_5^+$, 100), 56 (Fe^+, 2.3).

4. Crystal Structure Determination of 3a. Details of crystal parameters, data collection, and structure refinement are given in Table 1. Raw intensities were collected on a Rigaku R-AXIS II camera with a rotating anode source (50 kV, 150 mA) at room temperature (294 K). Patterson superposition yielded the positions of all non-hydrogen atoms, which were subjected to anisotropic refinement. All hydrogens were generated geometrically (C–H bonds fixed at 0.96 Å) and allowed to ride on their respective parent C atoms; they were assigned the same isotropic temperature factors (U = 0.08 Å^2) and included in the structure factor calculations. Computations were performed using the SHELXTL PC program package on a PC 486 computer. Analytical expressions of atomic scattering factors were employed, and anomalous dispersion corrections were incorporated.[31]

Acknowledgment. We are grateful to the National Natural Science Foundation of China and the State Key Laboratory of Elemento-Organic Chemistry for financial support of this work.

Supporting Information Available: Tables of crystallographic data, positional and thermal parameters including hydrogen atoms, and anisotropic parameters (6 pages). Ordering information is given on any current masthead page.

OM950432W

(31) *International Tables for X-ray Crystallography*; Kynoch Press: Birmingham, 1974 (now distributed by Kluwer: Dordrecht, The Netherlands); Vol. 4, pp 55, 99, 149.

Preparation and Diels–Alder Reactions of (1,3-Dienyl)- and (1,2-Dienyl)cobaloxime Complexes

Heather L. Stokes, B. Matthew Richardson, Marcus W. Wright, Stacia M. Vaughn, and Mark E. Welker*,†

Department of Chemistry, Wake Forest University, P.O. Box 7486, Winston-Salem, North Carolina 27109

Louise Liable-Sands and Arnold L. Rheingold

Department of Chemistry, University of Delaware, Newark, Delaware 19716

Received June 27, 1995®

The synthesis and characterization (including crystallographic data) of several cobaloxime-substituted 1,3- and 1,2-dienes are reported here. Diels–Alder reactions of some of the 1,3-dienyl complexes are then reported along with reactions which demonstrate that the cobalt–carbon bonds in the Diels–Alder cycloadducts can be cleaved so that cobalt complexes as well as functionalized organic cycloadducts are recovered.

Introduction

We recently reported that pyr(glyoxime)$_2$Co anions (**1**) react via a S_N2' pathway with simple, unsubstituted allenic electrophiles (**2**: R = H, X = OTs, Cl) and a monosubstituted allenic electrophile (**2**: R = Me, X = OAc) to produce cobalt-substituted 1,3-dienes.[1] Tada

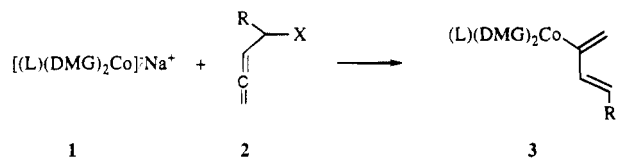

1 2 3

and Shimizu have also reported an alternative preparation of a cobalt-substituted 1,3-butadiene complex[2a] as well as a 3-furylmethyl)cobaloxime.[2b] This transition-metal substitution enhanced the reactivity and controlled the diastereoselectivity of 1,3-dienes in cycloaddition reactions. In the present paper, we first report reactions of a variety of substituted allenic electrophiles (**4**) with cobaloxime anions (**1**). Depending upon allene

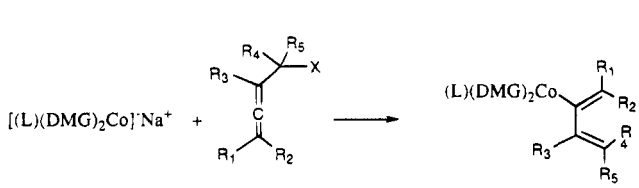

1 4 5

substitution and reaction conditions, we isolate either 1,3- (**5**) or 1,2-dienes in all cases. Diels–Alder reactions of the 1,3-dienes (**5**) are then reported, followed by a discussion of how to cleave the cobalt–carbon bonds in the cycloadducts so that cobalt complexes as well as functionalized organic cycloadducts are recovered.

Experimental Section

General Considerations. All nuclear magnetic resonance (NMR) spectra were obtained using a Varian VXR-200 FT NMR. All absorptions are expressed in parts per million relative to tetramethylsilane. Infrared (IR) spectra were obtained using a Perkin-Elmer 1620 FTIR. All elemental analyses were performed by Atlantic Microlab, Inc., of Norcross, GA. High-resolution mass spectral analyses were performed by the Midwest Center for Mass Spectrometry, University of Nebraska–Lincoln. Low-resolution EI mass spectra were obtained on a Hewlett-Packard 5989 GC/MS system. Melting points were determined on a Mel-Temp apparatus and are reported uncorrected.

Alumina (80–200 mesh) for column chromatography was purchased from Fisher Scientific and deactivated with an acetone/water mixture (90/10 immediately prior to use. Flash silica gel (40 μm) was purchased from Universal Scientific Inc. Cobalt chloride hexahydrate was purchased from Strem Chemicals and used as received. 4-Chloro-2-butyn-1-ol,[3] 5-(*p*-tolylsulfonyl)-2,3-pentadiene (**16c**),[1b] 2-acetoxy-3,4-pentadiene (**16a**),[1b] 2-(trimethylacetoxy)-3,4-pentadiene (**16b**),[1b] 2-acetoxy-5-methyl-3,4-hexadiene (**16f**),[1b] 2-methyl-3,4-pentadien-2-ol (**15d**),[4] (dmg)$_2$CoCl$_2$,[5] (3*E*)-(1,3-pentadien-2-yl)(pyridine)bis(dimethylgloxyimato)cobalt(III) (**17a**),[1b] and 1-ethynyl-7-oxabicyclo[4.1.0]heptane (**12**)[6] were prepared according to previously described methods.

2-[(1,2,3,4-Tetrahydropyranyl)oxy]-3-butyne (7). This compound was prepared in 90% yield on a 50 g scale according to the method of Landor et al.[7] ^{1}H NMR data ($CDCl_3$) were not previously reported: major diastereomer 4.87–4.94 (m, 1H), minor 4.71–4.76 (m, 1H), 4.56–4.35 (m, 1H), 4.05–3.75 (m, 2H), 3.43–3.56 (m, 2H), minor 2.38 (d, J = 2Hz, 1H), major 2.35 (d, J = 2Hz, 1H), 1.90–1.50 (m, 4H), minor 1.46 (s, 3H), major 1.43 (s, 3H).

† Henry Dreyfus Teacher-Scholar Awardee (1994–1999). E-mail: welker@wfu.edu.

® Abstract published in *Advance ACS Abstracts,* November 1, 1995.

(1) (a) Smalley, T. L.; Wright, M. W.; Garmon, S. A.; Welker, M. E.; Rheingold, A. L. *Organometallics* **1993**, *12*, 998. (b) Wright, M. W.; Smalley, T. L.; Welker, M. E.; Rheingold, A. L. *J. Am. Chem. Soc.* **1994**, *116*, 6777.

(2) (a) Tada, M.; Shimizu, T. *Bull. Chem. Soc. Jpn.* **1992**, *65*, 1252. (b) Tada, M.; Mutoh, N.; Shimizu, T. *J. Org. Chem.* **1995**, *60*, 550.

(3) Brandsma, L.; Verkruijsse, H. D. *Synthesis of Acetylenes, Allenes, and Cumulenes*; Elsevier: New York, 1981; p 65.

(4) Gelin, R.; Gelin, S.; Albrand, M. *Bull. Chim. Soc. Fr.* **1972**, 720.

(5) Burkhardt, E. W.; Burmeister, L. *Inorg. Chim. Acta* **1978**, *27*, 115.

(6) Alexakis, A.; Marek, I.; Mangeney, P.; Normant, J. F. *Tetrahedron* **1991**, *47*, 1677.

(7) Landor, P. D.; Landor, S. R.; Pepper, E. S. *J. Chem. Soc. C* **1967**, 185.

0276-7333/95/2314-5520$09.00/0

4-[(1,2,3,4-Tetrahydropyranyl)oxy]-2-pentyn1-ol (8). By a modified literature procedure,[7] **7** (22.92 g, 0.149 mol) was added to anhydrous Et_2O (200 mL) and cooled (−78 °C). *n*-Butyllithium (65.0 mL of 2.5 M BuLi in hexanes, 0.163 mol) was added dropwise, and the mixture was stirred (0.75 h). Paraformaldehyde (7.0 g, 0.078 mol) was added quickly, and the mixture was stirred (0.5 h) and then warmed slowly to 25 °C to afford a golden colored solution which was refluxed (2.5 h). The mixture was cooled (25 °C), and ice water (45 mL) was added; it then was extracted with Et_2O (2 × 25 mL). The extracts were dried ($MgSO_4$), and the solvent was removed by rotary evaporation. The resulting oil was vacuum-distilled to afford a clear, viscous liquid (**8**: bp 110−120 °C, 1 mmHg; yield 22.92 g, 0.125 mol (84%)). ^1H NMR data ($CDCl_3$) were not previously reported: 4.86−4.95 (major) (m, 1H), 4.76−4.70 (minor) (m, 1H), 4.60−4.36 (m, 1H), 4.23 (s, 2H), 4.00−3.68 (minor) (m, 2H), 3.55−3.40 (major) (m, 2H), 2.60−2.90 (broad s, 1H), 1.78−1.45 (m, 6H), 1.37 (major) (d, J = 6 Hz, 3H).

2,3-Pentadien-1-ol (9). Compound **8** (22.60 g, 0.123 mol; dissolved in anhydrous Et_2O (40 mL)) was added dropwise over 1.5 h to a slurry of $LiAlH_4$ (5.68 g, 0.150 mol) in anhydrous Et_2O (300 mL) at 0 °C. The mixture was stirred (0.5 h) and then warmed to 25 °C over 0.75 h. The mixture was refluxed (2 h) and then cooled to 0 °C, and ice−water (28 mL) was added dropwise to quench the remaining hydride. Et_2O was removed by decantation, and the resulting off-white salts were washed with Et_2O (3 × 25 mL). The Et_2O extracts were combined and dried ($MgSO_4$). Solvent was distilled at 760 mmHg, and the remaining solution was vacuum-distilled to afford a clear, viscous liquid (bp 50−53 °C at 20 mmHg;[7] yield 6.74 g, 0.080 mol (65.3%)). ^1H NMR data ($CDCl_3$) were not previously reported: 5.28−5.08 (m, 2H), 4.05 (dd, J = 6, 2 Hz, 2H), 2.10 (broad s, 1H), 1.66 (dd, J = 6, 2 Hz, 3H).

1-Acetoxy-4-chloro-2-butyne (10). This compound was prepared according to the method of Colonge and Poilane.[8] ^1H NMR data ($CDCl_3$) were not reported previously: 4.69 (t, J = 1.98 Hz, 2H), 4.14 (t, J = 1.98 Hz, 2H), 2.07 (s, 3H).

1-Acetoxy-2-methyl-2,3-butadiene (11). Methyllithium (85.0 mL of a 1.4 M solution, 0.119 mol) was added dropwise to a suspension of CuI (11.456 g, 0.06 mol) in anhydrous Et_2O (300 mL) at −20 °C. After the mixture was stirred at −20 °C for 30 min, **10** (8.0 g, 0.054 mol) in Et_2O (56 mL) was added dropwise. The reaction mixture was warmed to just below 25 °C, and ice−water (150 mL) followed by saturated aqueous NH_4Cl (100 mL) was added slowly. The solution was extracted with Et_2O (3 × 100 mL), and the extracts were dried ($MgSO_4$). The solvent was removed via rotary evaporation at 25 °C, and the residue was vacuum-distilled to afford **11** (bp 30−40 °C at 12 mmHg; yield 4.9 g, 0.0389 mol (72.0%)). ^1H NMR ($CDCl_3$): 4.73 (apparent q, J = 2.4 Hz, 2H), 4.52 (t, J = 2.4 Hz), 2.08 (s, 3H), 1.72 (t, J = 2.41 Hz, 3H). IR ($CDCl_3$) 3154.6, 2987.9, 2947.2, 2864.5, 1962.1, 1735.1, 1440.8, 1381.5, 1244.1 cm^{-1}. HRMS: *m/z* calcd for $C_7H_{10}O_2$ 126.0681, found 126.0681. This compound was mentioned by Huche,[9] but no experimental procedure or data were reported.

Preparation of 2-Ethenylidene-1-cyclohexanol (13). The acetylenic epoxide **12**[6] (5.75 g, 0.047 mol) was dissolved in anhydrous Et_2O (200 mL) and cooled to 0 °C. DIBAL-H (56.6 mL of a 1.0 M solution in cyclohexane; 0.0566 mol) was added dropwise, and the solution was warmed to 25 °C and stirred (1 h). Water (100 mL) was added slowly, the ether was removed by decantation, and the remaining white gelatinous material was extracted with Et_2O (5 × 25 mL). The ether extracts were dried ($MgSO_4$) and the ether removed by rotary evaporation at 0 °C. The remaining liquid was distilled to afford the alcohol **13** (bp 45−50 °C at 12 mmHg; yield 3.641 g, 0.029 mol (62%)), identical by spectroscopic and bp comparison with literature data.[7]

Preparation of 1-Acetoxy-2-ethenylidenecyclohexane (14). The acetylenic epoxide **12** (8.598 g, 0.070 mol) was reduced with DIBAL-H as described above, and the crude product after solvent removal via rotary evaporation was added slowly to acetic anhydride (19 mL) containing sodium acetate (0.065 g). The solution was refluxed 6 h after addition, and the acetate **14** was removed by distillation (bp 84−86 °C at 20 mmHg, 5.253 g, 0.032 mol (46%) for two steps). ^1H NMR ($CDCl_3$): 5.25 (m, 1H), 4.82 (m, 1H), 4.78 (m, 2H), 2.38 (m, 1H), 2.18 (m, 1H), 2.10 (s, 3H), 1.95−1.49 (m, 6H). ^{13}C NMR ($CDCl_3$): 202.6, 170.0, 101.3, 76.1, 71.0, 32.0, 28.8, 26.0, 22.7, 21.1. IR ($CDCl_3$): 2944, 2862, 1728, 1646, 1559, 1468, 1381, 1248, 1168, 1097 cm^{-1}. Anal. Calcd for $C_{10}H_{14}O_2$: C, 72.26; H, 8.49. Found: C, 72.47; H, 8.57.

1-(*p*-Tolylsulfonyl)-2,3-pentadiene (16c). This compound was prepared in a manner analogous to that which we have reported previously for an allenic tosylate[1b] from 2,3-pentadien-1-ol (**9**; 1.74 g, 0.021 mol) and *p*-toluenesulfonyl chloride (3.82 g, 0.020 mol) to afford a white, waxy solid (3.78 g, 0.018 mol (89.0%)). Mp: <25 °C. ^1H NMR ($CDCl_3$): 7.79 (d, J = 8.3 Hz, 2H), 7.34 (d, J = 8.3 Hz, 2H), 5.16 (m, 2H), 4.52 (dd, J = 5.0, 2.1 Hz, 2H), 2.44 (s, 3H), 1.62 (dd, J = 7.0, 3.4 Hz, 3H). ^{13}C NMR ($CDCl_3$): 207.0, 144.7, 133.4, 129.8, 127.8, 88.1, 85.0, 69.1, 21.6, 13.5. IR ($CDCl_3$): 3154, 2956, 1540, 1308, 1212 cm^{-1}. This tosylate decomposed rapidly at 25 °C, and multiple attempts to obtain a satisfactory elemental analysis were unsuccessful. HRMS showed only $M^+ - C_5H_6$ at *m/z* 172.0195.

1-Diethyl 2,3-Pentadienyl Phosphate (16d). This compound has been prepared previously from 2,3-pentadien-1-ol (**9**) using pyridine and diethyl chlorophosphate in CH_2Cl_2.[10] 2,3-Pentadien-1-ol (**9**; 1.01 g, 12.0 mmol) was placed in dry THF (25 mL) and the solution cooled to −15 °C. Methyllithium (9.0 mL of a 1.4 M solution in Et_2O, 12.6 mmol) was added over 20 min, and the resultant mixture was stirred for 2 h. Diethyl chlorophosphate (2.29 g, 13.3 mmol) was added quickly, and the resultant solution was stirred for 2 h after warming slowly to 25 °C. Saturated aqueous $NaHCO_3$ (75 mL) was added to the solution, and this mixture was extracted with CH_2Cl_2 (2 × 25 mL). The extracts were dried ($MgSO_4$) and excess solvent removed under reduced pressure to yield an orange liquid (2.21 g, 10.0 mmol (84.0%)) spectroscopically analogous to that prepared by the alternative method mentioned above.[10]

(3*E*)-(1,3-Pentadien-2-yl)(4-cyanopyridine)bis(dimethylglyoximato)cobalt(III) (17d). 4-Cyanopyridine (0.150 g, 1.4 mmol) and diene **17a** (0.140 g, 0.32 mmol) were combined in $CHCl_3$ (2 mL) and refluxed (4 h). The solvent was removed under vacuum, and the residue was chromatographed on silica (EtOAc). The orange band was collected (0.059 g, 0.13 mmol (39.8%)), Mp: 181−183 °C dec. ^1H NMR ($CDCl_3$): 8.86 (d, J = 6.7 Hz, 2H), 7.53 (d, J = 6.7 Hz, 2H), 6.07 (dq, J = 14.9, 1.7 Hz, 1H), 5.25 (dq, J = 14.9, 6.6 Hz, 1H), 4.41 (s, 1H), 4.24 (s, 1H), 2.07 (s, 12H), 1.48 (dd, J = 6.6, 1.7, 3H). IR ($CDCl_3$): 3152.0, 3055.6, 2960.2, 2930.0, 2850.2, 1811.7, 1792.2, 1610.1, 1561.1, 1503.8, 1482.0, 1465.6, 1447.8, 1431.0, 1392.2, 1383.5, 1375.7, 1090.4 cm^{-1}. Anal. Calcd for $C_{19}H_{25}O_4N_5Co$: C, 49.57; H, 5.47. Found: C, 49.65; H, 5.49.

(3*E*)-(1,3-Pentadien-2-yl)(diphenylmethylphosphine)bis(dimethylglyoximato)cobalt(III) (17e). At 25 °C, diphenylmethylphosphine (0.24 mL, 1.3 mmol) was added dropwise to diene **17a** (0.303 g, 0.7 mmol) in $CHCl_3$ (12 mL) and the solution was stirred overnight. The solvent was removed under vacuum and the pyridine and excess phosphine were removed with repeated washings of 50/50 ether/hexane to yield an orange-yellow solid (0.351 g, 0.631 mmol (90.6%)). Mp: 157−158 °C. ^1H NMR ($CDCl_3$): 7.55−7.25 (m, 10H), 6.12 (d, J = 14.3 Hz, 1H), 5.15 (dq, J = 14.3, 7.1 Hz, 1H), 4.50 (d,

(8) (a) Colonge, J.; Poilane, G. *Bull. Chim. Soc. Fr.* **1955**, 502. (b) For an alternate preparation of this compound see: Voronkov, M. G.; Shirchin, B.; Golovanova, N. I.; Albanov, A. I. *Russ. Bull. Div. Chem. Sci. (Engl. Transl.)* **1984**, 838−841.

(9) Huche, M. *Bull. Soc. Chim. Fr.* **1975**, 2369.

(10) Djahanbini, D.; Cazes, B.; Gore, J. *Tetrahedron* **1984**, *40*, 3645.

$J(^{31}P-^{1}H)$ = 17.8 Hz, 1H), 4.55 (d, $J^{31}P-^{1}H$) = 7.1 Hz, 1H), 1.85 (d, J = 8.9 Hz, 3H), 1.75 (s, 12H), 1.45 (d, J = 7.1 Hz, 3H). IR ($CDCl_3$): 3607.6, 3397.1, 3155.3, 3062.1, 2987.5, 2922.6, 1794.3, 1557.8, 1475.9, 1439.9, 1380.4, 1235.6 cm^{-1}. Anal. Calcd for $C_{26}H_{34}O_4N_4PCo$: C, 56.12; H, 6.16. Found: C, 55.96; H, 6.21.

(3*E*)-(1,3-Pentadien-2-yl)(tributylphosphine)bis(dimethylglyoximato)cobalt(III) (17f). At 25 °C, tributylphosphine (0.6 mL, 2.4 mmol) was added to diene **17a** (0.500 g, 1.2 mmol) in toluene (15 mL), and the solution was refluxed (8 h). Solvent was removed under vacuum, and the residue was chromatographed on silica (Et_2O) to yield the product as a yellow oil (0.158 g, 0.28 mmol (23.7%)). ^1H NMR ($CDCl_3$): 6.12 (d, J = 13.8 Hz, 1H), 5.10 (m, 1H), 4.54 (d, $J(^{31}P-^{1}H)$ = 15.4 Hz, 1H), 4.43 (d, $J(^{31}P-^{1}H)$ = 6.2 Hz, 1H), 2.08 (s, 6H), 2.10 (s, 6H), 1.47 (d, J = 7.7 Hz, 3H), 1.25 (m, 18H), 0.85 (t, J = 7.1 Hz, 9H). IR ($CDCl_3$): 3689.2, 2963.1, 1604.9, 1556.3, 1482.5, 1459.9, 1235.0 cm^{-1}. Anal. Calcd for $C_{25}H_{48}O_4N_4PCo$: C, 53.76; H, 8.66. Found: C, 53.50; H, 8.57.

(4-Cyanopyridine)bis(dimethylglyoximato)cobalt(III) Chloride (18a). $CoCl_2(dmg)_2$[5] (1.065 g, 3.01 mmol) was suspended in 95% ethanol (10 mL) at 25 °C; then NaOH (0.312 g, 3.9 mmol) as a 50% aqueous solution was added dropwise. The solution was stirred for 10 min; then 4-cyanopyridine (0.305 g, 2.93 mmol) was added. The brown product was collected by vacuum filtration 30 min later and dried to yield **18a** (1.101 g, 2.4 mmol (79.5%)). Mp: >200 °C. ^1H NMR ($CDCl_3$): 8.52 (d, J = 6.1 Hz, 2H), 7.48 (d, J = 6.1 Hz, 2H), 2.39 (s, 12H). IR ($CDCl_3$): 3689.7, 3607.4, 3154.3, 3106.6, 3061.8, 2981.3, 2901.7, 1793.7, 1616.3, 1562.4, 1503.6, 1466.1, 1243.2 cm^{-1}. Anal. Calcd for $C_{14}H_{18}O_4N_6ClCo$: C, 39.22; H, 4.23. Found: C, 38.35; H, 4.30.

(4-Ethyl-2,6,7-trioxa-1-phosphatricyclo[2.2.2]octane)bis(dimethylglyoximato)cobalt(III) Chloride (18b). This complex was prepared in a manner analogous to that reported for **18a** above using $CoCl_2(dmg)_2$[5] (1.506 g, 4.3 mmol) and 4-ethyl-2,6,7-trioxa-1-phosphatricyclo[2.2.2]octane (Strem; 1.137 g, 7.0 mmol) to yield a yellow product (1.504 g, 3.13 mmol (72.9%)). Mp: >200 °C. ^1H NMR ($CDCl_3$): 4.17 (d, J = 4.9 Hz, 6H), 2.26 (s, 12H), 1.16 (q, J = 7.6 Hz, 2H), 0.691 (t, J = 7.6 Hz, 3H). ^{13}C NMR: 151.74, 36.86, 36.21, 22.38 ($J(^{31}P)$ = 2.4 Hz), 12.94, 7.13. IR ($CDCl_3$): 3152.3, 2977.6, 2948.0, 2926.8, 2901.2, 2867.1, 1563.3, 1463.3, 1382.9, 1375.5, 1348.9, 1248.4, 1184.8, 1152.4, 1100.6 cm^{-1}. Anal. Calcd for $C_{14}H_{25}O_7N_4PClCo$: C, 34.55; H, 5.18. Found: C, 34.39; H, 5.25.

(3*E*)-(1,3-Pentadien-2-yl)(4-cyanopyridine)bis(dimethylglyoximato)cobalt(III) (17d). At −20 °C, $NaBH_4$ (0.087 g, 2.3 mmol) in water (0.3 mL) was added to a suspension of cobalt chloride **18a** (1.0 g, 2.2 mmol) in degassed THF (20 mL). Acetate **16a** (0.230 g, 2.09 mmol) was added dropwise, and the solution was warmed to 25 °C overnight. The THF was removed under reduced pressure; then the product was redissolved in EtOAc and washed with water. The EtOAc extracts were dried with $MgSO_4$, and solvent was removed under vacuum. The resulting solid was redissolved in a minimum amount of CH_2Cl_2 and cooled to −78 °C and precipitation induced with pentane. The orange product was collected by vacuum filtration (0.512 g, 1.1 mmol, 51.2%) and was identical by spectroscopic comparison with **17d** prepared by the alternate method described above.

(3*E*)-(1,3-Pentadien-2-yl)(4-ethyl-2,6,7-trioxa-1-phosphatricyclo[2.2.2]octane)bis(dimethylglyoximato)cobalt(III) (17g). This complex was prepared from **18b** in a manner analogous to that described for **17d** just above to yield diene **17g** (0.226 g, 0.436 mmol, 20.7%). ^1H NMR ($CDCl_3$): 6.12 (bd, J = 15.3 Hz, 1H), 5.21 (dq, J = 15.3, 6.8 Hz, 1H), 4.90 (d, J = 17.0 Hz, 1H), 4.68 (d, J = 10.2 Hz, 1H), 4.10 (d, J = 5.1 Hz, 6H), 2.12 (s, 6H), 2.14 (s, 6H), 1.51 (apparent dt, J = 6.8, 3.0 Hz, 3H), 1.19 (q, J = 7.5 Hz, 2H), 0.78 (t, J = 7.5 Hz, 3H). IR ($CDCl_3$): 3689.0, 3606.5, 3154.7, 2975.9, 2945.9, 2897.9, 1605.7, 1560.3, 1238.4, 1092.0, 1035.2 cm^{-1}. Repeated purification attempts involving chromatography or recrystallization failed to yield analytically pure material.

Isomerization of (3*E*)-(1,3-Pentadien-2-yl)(pyridine)bis(dimethylglyoximato)cobalt(III) (17a). Pure diene **17a** (0.250 g, 0.574 mmol) was added to MeOH (13 mL) and the solution degassed with N_2. $NaBH_4$ (0.087 g, 2.296 mmol) was added and the solution refluxed (1.5 h). There was a color change from orange to green that faded back to orange after 10 min, and the solution became homogeneous while green. The reaction mixture was cooled and stirred for 8 h at 25 °C. The volume was reduced to about 8 mL via rotary evaporation, and the remaining liquid was poured into water (25 mL) containing pyridine (3−4 drops). The orange precipitate was collected and washed with water (3 × 20 mL) and Et_2O (2 × 15 mL). After vacuum drying, a 1:1 mixture of dienes **17a** and **20** (0.177 g, 0.407 mmol (71%)) was obtained. Diene **20**'s structure was proposed on the basis of ^1H NMR data ($CDCl_3$): 8.64 (d, J = 6.2 Hz, 2H), 7.72 (app t, J = 6.2 Hz, 1H), 7.33 (d, J = 6.2 Hz, 2H), 6.62 (ddd, J = 16.7, 11.0, 8.8 Hz, 1H), 5.87 (broad d, J = 11.0 Hz, 1H), 4.87 (dd, J = 16.7, 2.7 Hz, 1H), 4.63 (dd, J = 8.8, 2.7 Hz, 1H), 2.04 (s, 12H), 1.65 (d, J = 2.7 Hz, 3H). NOE data are discussed in the text.

(3-Methyl-1,3-butadien-2-yl)(pyridine)bis(dimethylglyoximato)cobalt(III) (21). At 0 °C, $CoCl_2 \cdot 6H_2O$ (0.662 g, 2.78 mmol) and dmg (0.648 g, 5.6 mmol) were added to degassed DMF (13 mL). NaOH (0.5 g, 6.25 mmol) was added as a 50% aqueous solution (0.5 g, 6.25 mmol) followed by pyridine (0.23 mL, 2.84 mmol). After 1 h, NaOH (0.260 g, 3.25 mmol) was added as a 50% aqueous solution followed by $NaBH_4$ (0.036 g, 0.95 mmol) in H_2O (0.25 mL) at −20 °C. After 0.75 h, acetate **11** (0.356 g, 2.82 mmol) was added dropwise to the brick red solution, which was warmed to 25 °C overnight. Water (100 mL) was added, and an orange solid precipitated. The precipitate was removed by filtration and subsequently washed with water and then pentane. The filtrate was extracted with CH_2Cl_2 until the extracts were colorless. The CH_2Cl_2 extracts were washed with water (5 × 200 mL) to remove the DMF. The CH_2Cl_2 extracts were dried ($MgSO_4$) and then concentrated under reduced pressure. Both solid from the filtrate and residue from the filtration were combined and washed with ether to yield an orange solid (0.589 g (49%)). Mp: 172−173 °C dec. ^1H NMR ($CDCl_3$): 8.58 (d, J = 5.2 Hz, 2H), 7.32 (t, J = 5.2 Hz, 1H), 7.29 (t, J = 5.2 Hz, 2H), 4.70−4.63 (m, 1H), 4.44 (s, 1H), 4.18 (d, J = 2.9 Hz, 1H), 4.12 (s, 1H), 2.12 (s, 12H), 1.71 (s, 3H). ^{13}C NMR ($CDCl_3$): 154.05, 150.01, 149.84, 137.52, 125.08, 114.79, 108.12, 24.26, 12.38. IR ($CDCl_3$): 3155.9, 2982.8, 2921.2, 2337.5, 1817.5, 1793.9, 1605.7, 1562.3, 1471.7, 1450.2, 1382.0, 1235.6, 1166.3 cm^{-1}. Anal. Calcd for $C_{18}H_{26}O_4N_5Co$: C, 49.66; H, 6.02. Found: C, 49.76; H, 6.02.

(3-Methyl-1,3-butadien-2-yl)[4-(dimethylamino)pyridine]bis(dimethylglyoximato)cobalt(III) (22a). Diene **21** (0.400 g, 0.91 mmol) and DMAP (0.112 g, 0.91 mmol) were refluxed in degassed MeOH (10 mL) for 1.5 h. Solvent was removed under vacuum, and the product was triturated with Et_2O (10 mL) to yield **22a** (0.425 g, 0.88 mmol, 97%). Mp: 185−187 °C dec. ^1H NMR ($CDCl_3$): 8.03 (d, J = 6.7 Hz, 2H), 6.37 (d, J = 6.7 Hz, 2H), 4.65−4.60 (m, 1H), 4.40 (s, 1H), 4.17 (s, 1H), 4.12 (d, J = 3.5 Hz, 1H), 2.95 (s, 6H), 2.11 (s, 12H), 1.69 (br s, 3H). ^{13}C NMR ($CDCl_3$): 154.49, 154.08, 149.34, 148.62, 114.31, 107.37, 107.26, 39.02, 24.71, 12.33. IR ($CDCl_3$): 3155.9, 3072.0, 2921.6, 2358.0, 2336.8, 1819.9, 1793.9, 1622.0, 1562.7, 1562.7, 1537.8, 1475.8, 1469.2, 1447.2, 1387.2, 1376.4 cm^{-1}. Anal. Calcd for $C_{20}H_{31}O_4N_6Co$: C, 50.21; H, 6.53. Found: C, 50.35; H, 6.48.

(3-Methyl-1,3-butadien-2-yl)(methyldiphenylphosphine)bis(dimethylglyoximato)cobalt(III) (22b). Diene **21** (0.293 g, 0.67 mmol) was dissolved in degassed MeOH (7 mL). Diphenylmethylphosphine (0.15 mL, 0.80 mmol) was added and the solution stirred overnight at 25 °C. The resulting yellow-orange precipitate was collected by vacuum filtration. Excess diphenylmethylphosphine was removed with

repeated pentane washes to yield **22b** (0.328 g, 0.59 mmol (87.6%)). Mp: 137–140 °C dec. ^{1}H NMR ($CDCl_3$): 7.40 (m, 10H), 4.60–4.54 (m, 1H), 4.41 (d, $J(^{31}P-^1H)$ = 8.7 Hz, 1H), 4.34 (d, $J(^{31}P-^1H)$ = 1.5, 1H), 4.01 (s, 1H), 1.88 (d, $J(^{31}P-^1H)$ = 8.5 Hz, 3H), 1.79 (s, 6H), 1.77 (s, 6H), 1.65 (s, 3H). IR ($CDCl_3$): 3153.5, 3065.6, 2981.5, 2923.9, 1817.3, 1792.6, 1601.7, 1558.0, 1485.0, 1474.2, 1465.6, 1436.3, 1385.5, 1378.4, 1339.3, 1293.9, 1235.9, 1170.3, 1093.5 cm^{-1}. Anal. Calcd for $C_{26}H_{34}O_4N_4PCo$: C, 56.12; H, 6.16. Found: C, 56.13; H, 6.27.

Preparation of (1-Vinylcyclohexen-2-yl)(pyridine)bis(dimethylglyoximato)cobalt(III) (23a). This complex was prepared in MeOH in a manner analogous to that reported above for **21**, using acetate **14** (1.00 g, 6.02 mmol), $CoCl_2 \cdot 6H_2O$ (1.43 g, 6.02 mmol), dmg (1.40 g, 12.05 mmol), NaOH (0.904 g, 0.026 mol), and $NaBH_4$ (0.096 g, 2.54 mmol) to produce **23a** as a yellow-orange solid (1.571 g, 3.30 mmol, 55%). Mp: 118–121 °C dec. ^{1}H NMR ($CDCl_3$): 8.58 (br d, J = 6.5 Hz, 2H), 7.70 (t, J = 6.5 Hz, 1H), 7.30 (t, J = 6.5 Hz, 2H), 4.94 (br m, 1H), 4.40 (s, 1H), 4.07 (s, 1H), 2.11 (s, 12H), 1.91 (m, 2H), 1.73 (m, 2H), 1.50 (m, 4H). ^{13}C NMR (C_6D_6): 150.3, 149.6, 146.8, 137.2, 124.8, 120.0, 115.5, 31.1, 26.7, 24.0, 22.8, 11.9. IR ($CDCl_3$): 2982, 2932, 2857, 1731, 1605, 1561, 1469, 1385, 1236 cm^{-1}. Anal. Calcd for $C_{21}H_{28}N_5O_4Co$: C, 53.05; H, 6.36. Found: C, 52.77; H, 6.46.

Preparation of (1-Vinylcyclohexen-2-yl)[4-(dimethylamino)pyridine]bis(diphenylglyoximato)cobalt(III) (23b). This complex was prepared in DMF in a manner analogous to that described for **21** using $CoCl_2 \cdot 6H_2O$ (1.36 g, 5.27 mmol), acetate **14** (0.950 g, 5.27 mmol), diphenylglyoxime (2.75 g, 11.0 mmol), DMAP (0.70 g, 5.72 mmol), NaOH (0.860 g, 21.5 mmol), and $NaBH_4$ (0.109 g, 2.86 mmol). The crude yellow-orange product obtained after CH_2Cl_2 removal was suspended in Et_2O (100 mL) and cooled to 0 °C. Pentane (100 mL) was then added, and the yellow-orange precipitate was isolated by vacuum filtration (3.00 g, 3.92 mmol, 74%). Mp: 189–191 °C dec. ^{1}H NMR ($CDCl_3$): 8.38 (d, J = 7.5 Hz, 2H), 7.38–7.05 (m, 20H), 6.52 (d, J = 7.5 Hz, 2H), 5.38 (m, 1H), 4.92 (s, 1H), 4.42 (s, 1H), 3.03 (s, 6H), 2.27 (m, 2H), 1.85 (m, 2H), 1.56 (m, 4H). ^{13}C NMR ($CDCl_3$): 154.2, 150.7, 148.5, 146.5, 130.3, 129.5, 128.6, 127.6, 119.8, 115.0, 107.6, 39.0, 31.0, 25.9, 23.5, 22.2. IR ($CDCl_3$): 3063, 2929, 1671, 1623, 1537, 1479, 1445, 1386, 1286, 1135, 1012 cm^{-1}. HRMS FAB: *m/z* calcd for $C_{43}H_{43}N_6O_4Co$ 766.2677, found 766.2647.

Preparation of (1-Vinylcyclohexen-2-yl)[4-(dimethylamino)pyridine]bis(dimethylglyoximato)cobalt(III) (23c). This complex was prepared via ligand exchange in MeOH as described above previously using complex **23a** (0.375 g, 0.782 mmol) and DMAP (0.105 g, 0.859 mmol) to produce **23c** as a yellow-orange solid (0.231 g, 0.446 mmol (57%)). Mp: 198–200 °C dec. ^{1}H NMR ($CDCl_3$): 8.06 (d, J = 7.5 Hz, 2H), 6.39 (d, J = 7.5 Hz, 2H), 4.90 (m, 1H), 4.38 (m, 1H), 4.12 (m, 1H), 2.98 (s, 6H), 2.12 (s, 12H), 1.90 (m, 2H), 1.75 (m, 2H), 1.62 (m, 2H), 1.50 (m, 2H). IR ($CDCl_3$): 2987, 2928, 1622, 1539, 1471, 1382, 1234, 1167, 1094 cm^{-1}. Anal. Calcd for $C_{23}H_{35}N_6O_4Co$: C, 53.18; H, 6.98. Found: C, 53.35; H, 6.79.

Preparation of (1-Vinylcyclohexen-2-yl)[4-(dimethylamino)pyridine]bis(diphenylglyoximato)cobalt(III) (23b) via Ligand Exchange. This complex was prepared from the dpg pyr diene complex (170 mg, 0.0235 mmol) and DMAP (32 mg, 0.0262 mmol), which were refluxed in MeOH (5 mL) under N_2 for 3 h. The solution was then cooled to 0 °C, and the orange precipitate was isolated by vacuum filtration (0.059 g, 0.0077 mmol, 33%). This material was identical by spectroscopic comparison with the material (**23b**) reported above.

Preparation of (3*E*)-(1,3-Pentadien-3-yl)(pyridine)bis(dimethylglyoximato)cobalt(III) (24a). $CoCl_2 \cdot 6H_2O$ (1.35 g, 5.68 mmol) and dmg (1.32 g, 11.34 mmol) were dissolved in degassed MeOH (40 mL). The rapidly stirred mixture was degassed throughout the addition of subsequent reagents. NaOH (0.45 g, 11.25 mmol) dissolved in water (1 mL) was added dropwise. Pyridine (0.47 g, 5.9 mmol) was then added slowly. The mixture was stirred at 25 °C for 10 min and then cooled to −15 °C. NaOH (0.23 g, 5.7 mmol) dissolved in water (1 mL) was added very slowly. $NaBH_4$ (0.054 g, 5.70 mmol) dissolved in water (1 mL) was added very slowly over 5 min to avoid heating the solution. 1-(*p*-Tolylsulfonyl)-2,3-pentadiene (**16c**; 1.5 g, 7.07 mmol) was added quickly and the mixture warmed to 25 °C overnight. The reaction volume was reduced by 25% by rotary evaporation, and the mixture was poured into water (200 mL, 0 °C) which contained pyridine (about 2 mL). The precipitate was collected by vacuum filtration and vacuum-dried to yield an orange solid (**24a**; 1.49 g, 3.4 mmol (43.0%)). When amounts used above were held constant but the solvent was changed to DMF, the yield increased to 56.3%. Mp: 183 °C dec. ^{1}H NMR ($CDCl_3$): 8.60 (d, J = 6.2 Hz, 2H), 7.67 (t, J = 6.2 Hz, 1H), 7.28 (t, J = 6.2 Hz, 2H), 6.04 (dd, J = 15.2, 11.4 Hz, 1H), 4.93 (dd, J = 11.4, 2.3 Hz, 1H), 4.87 (q, J = 6.2 Hz, 1H), 4.55 (dd, J = 15.2, 2.3 Hz, 1H), 2.10 (s, 12H), 1.72 (d, J = 6.2 Hz, 3H). ^{13}C NMR ($CDCl_3$): 149.9, 149.6, 149.5, 141.1, 137.4, 125.0, 122.2, 110.9, 16.7, 12.3. IR ($CDCl_3$): 3155, 2902, 2854, 1994, 1604, 1297, 1038, 922 cm^{-1}. Anal. Calcd for $C_{18}H_{26}N_5O_4Co$: C, 49.66; H, 6.02. Found: C, 49.38; H, 5.94.

Complex **24a** was also synthesized using 1-diethylphosphonate-2,3-pentadiene (**16d**) (1.5 g, 7.07 mmol) keeping all other reagents constant. The reaction was run in DMF rather than MeOH so a work-up analogous to that reported for **21** above was used to yield **24a** (0.750 g, 1.73 mmol, 30%). This material proved identical by spectroscopic comparison to the material (**24a**) isolated above.

Preparation of (3*E*)-(1,3-Pentadien-3-yl)[4-(dimethylamino)pyridine]bis(dimethylglyoximato)cobalt(III) (24b). This complex was prepared on the same scale as **24a** in DMF above except that (dimethylamino)pyridine (DMAP; 1.10 g, 9 mmol) was used instead of pyridine to yield a light orange solid after purification by silica chromatography (EtOAc) (2.09 g, 6.1 mmol (63%)). Mp: 192 °C dec. ^{1}H NMR ($CDCl_3$): 8.03 (d, J = 6.1 Hz, 2H), 6.35 (d, J = 6.1 Hz, 2H), 6.03 (dd, J = 17.2, 10.5 Hz, 1H), 4.87–4.77 (m, 2H), 4.48 (dd, J = 17.2, 3.2 Hz, 2H), 2.93 (s, 6H), 2.07 (s, 12H), 1.67 (d, J = 6.7 Hz, 3H). ^{13}C NMR ($CDCl_3$): 154.1, 149.1, 148.9, 141.6, 121.9, 110.4, 107.4, 39.0, 16.8, 12.2. IR ($CDCl_3$): 3155, 2985, 2902, 1794, 1624, 1472, 1385, 1094 cm^{-1}. Anal. Calcd for $C_{20}H_{31}O_4N_6Co$: C, 50.21; H, 6.53. Found: C, 49.95; H, 6.49.

Preparation of (3*E*)-(1,3-Pentadien-3-yl)[4-(dimethylamino)pyridine]bis(diphenylglyoximato)cobalt(III) (24c). This compound was prepared on the same scale as for **24b** above, except diphenylglyoxime (1.65 g, 14.2 mmol) was used instead of dmg to yield an orange-red solid after purification by chromatography on silica (1/1 ethyl acetate/pentane) (2.35 g, 3.31 mmol (70%)). Mp: 130–132 °C dec. ^{1}H NMR ($CDCl_3$): 8.39 (d, J = 7.2 Hz, 2H), 7.29–7.06 (m, 20H), 6.51 (d, J = 7.2 Hz, 2H), 6.41 (m, partially obscured by neighboring aromatic H, 1 J of 10.7 Hz observable, 1H), 5.27 (quartet, J = 6.6 Hz, 1H), 5.12 (dd, J = 10.7, 3.3 Hz, 1H), 4.89 (dd, J = 17.3, 3.3 Hz, 1H), 3.03 (s, 6H), 1.88 (d, J = 6.6 Hz, 3H). ^{13}C NMR ($CDCl_3$): 154.4, 150.8, 149.0, 141.0, 130.4, 129.9, 129.7, 128.7, 122.7, 114, 111.4, 107.8, 39.1, 17.2. IR ($CDCl_3$): 3155, 2985, 2902, 1794, 1623, 1472, 1385, 1094 cm^{-1}. LRMS (*m/z*) found for $C_{33}H_{29}O_4N_4Co$: M + 1 − DMAP 605.2(33), 538(100), 299-(20), 179(63). Anal. Calcd for $C_{40}H_{39}O_4N_6Co$: C, 66.11; H, 5.41. Found: C, 64.46; H, 5.62.

Preparation of (3*E*)-(1,3-Pentadien-3-yl)[4-(dimethylamino)pyridine]bis(dimethylglyoximato)cobalt(III) via Ligand Exchange (24b). Complex **24a** (0.25 g, 0.58 mmol) was added to degassed MeOH (20 mL) with DMAP (80 mg, 0.66 mmol). The mixture was stirred (2 h) and then cooled to 0 °C. The resulting precipitate was vacuum-filtered and washed with cold Et_2O. The yellow-orange solid was vacuum-dried (0.22 g, 0.449 mmol, 78.1%)) and proved identical by spectroscopic comparison with **24b** reported above.

Preparation of (3*E*)-(1,3-Pentadien-3-yl)(methyldiphenylphosphine)bis(dimethylglyoximato)cobalt(III) (24d). Complex **24a** (0.13 g, 0.29 mmol) was added to degassed MeOH

(20 mL). Methyldiphenylphosphine (75 mg, 0.38 mmol) was added to the solution and stirred (2 h). The mixture was cooled to 0 °C and vacuum-filtered to obtain a dark orange solid, which was vacuum-dried (0.150 g, 0.27 mmol (94%)). Mp: 162–163 °C. ^{1}H NMR ($CDCl_3$): 7.44–7.26 (m, 10 H), 6.05 (dd, J = 17.2, 10.8 Hz, 1H), 4.89–4.78 (m, 2H), 4.42 (apparent dt, J = 17.2, 3.2 Hz, 1H), 1.84 (d, $J(^{31}P-^1H)$ = 9.2 Hz, 3H), 1.75 (s, 6H), 1.74 (s, 6H), 1.66 (d, J = 6.6 Hz, 3H). ^{13}C NMR ($CDCl_3$; all J couplings reported to ^{31}P): 148.1 (d, J = 2.8 Hz), 140.4, 131.3 (d, J = 8.9 Hz), 129.9 (d, J = 2.4 Hz), 129.4 (d, J = 30.4 Hz), 128.1 (d, J = 9.0 Hz), 120.1, 111.0 (d, J = 5.3 Hz), 17.1 (d, J = 7.8 Hz), 11.8 (d, J = 1.7 Hz), 6.6 (d, J = 21.0 Hz). IR ($CDCl_3$): 3745, 3155, 2986, 1797, 1470, 1383, 1095, 947 cm^{-1}. Anal. Calcd for $C_{21}H_{32}N_4O_4PCo$: C, 55.91; H, 6.50. Found, C, 56.16; H, 6.40.

Preparation of (3*E*)-(1,3-Pentadien-3-yl)(dimethylphenylphosphine)bis(dimethylglyoximato)cobalt(III) (24e). Complex **24e** was prepared using the same method described for **24d** above, except that dimethylphenylphosphine (52 mg, 0.38 mmol) was used to yield a bright yellow solid (0.120 g, 0.25 mmol (85%)). Mp: 170–172 °C. ^{1}H NMR ($CDCl_3$): 7.36–7.26 (m, 3H), 7.14–7.04 (m, 2H), 6.05 (dd, J = 17.4, 10.7 Hz, 1H), 4.88 (dq, $J(^{31}P)$ = 8.7 Hz, J = 6.6 Hz, 1H), 4.79 (dd, J = 10.7, 3.2 Hz, 1H), 4.38 (apparent ddd, J = 17.4, 3.2, $J(^{31}P)$ = 1.2 Hz, 1H), 1.88 (s, 6H), 1.86 (s, 6H), 1.65 (d, J = 6.6 Hz, 3H), 1.37 (d, $J(^{31}P)$ = 9.3 Hz, 6H). ^{13}C NMR ($CDCl_3$; all J couplings reported as coupled to ^{31}P): 147.4 (d, J = 2.3 Hz), 140.6, 131.3, 130.6, 129.6 (d, J = 7.8 Hz), 128.0 (d, J = 9.0 Hz), 119.9, 110.5 (d, J = 5.1 Hz), 17.1 (d, J = 7.8 Hz), 11.9, 8.0 (d, J = 20.3 Hz). IR ($CDCl_3$): 3856, 3690, 2986, 2904, 1797, 1469, 1383 cm^{-1}. Anal. Calcd for $C_{21}H_{32}N_4O_4PCo$: C, 51.02; H, 6.52. Found: C, 51.24; H, 6.53.

Preparation of (3*E*)-(1,3-Pentadien-3-yl)(4-*tert*-butylpyridine)bis(dimethylglyoximato)cobalt(III) (24f). Complex **24a** (0.130 g, 0.29 mmol) was added to degassed MeOH (20 mL) along with 4-*tert*-butylpyridine (75 mg, 0.38 mmol) and the mixture was stirred overnight at 25 °C. The solvent was removed by rotary evaporation and the remaining solid triturated with cold Et_2O (20 mL) and then vacuum-dried to yield a dark orange solid (**24f**; 0.34 g, 0.27 mmol (89%)). Mp: 178–181 °C dec. ^{1}H NMR ($CDCl_3$): 8.41 (d, J = 6.7 Hz, 2 H), 7.22 (d, J = 6.7 Hz, 2H), 6.05 (dd, J = 17.5, 10.5 Hz, 1H), 4.90 (dd, J = 10.5, 3.5 Hz, 1H), 4.85 (q, J = 6.3 Hz, 1H), 4.54 (dd, J = 17.5, 3.5, 1H), 2.10 (s, 12H), 1.70 (d, J = 6.3 Hz, 3H), 1.26 (s, 9H). ^{13}C NMR ($CDCl_3$): 161.7, 149.6, 149.4, 141.3, 122.3, 110.9, 34.8, 30.2, 16.8, 12.4. IR ($CDCl_3$): 3154, 2971, 1794, 1560, 1471, 1384, 1234, 1094 cm^{-1}. HRMS FAB for $C_{22}H_{34}N_5O_4Co$: *m/z* calcd 491.1942, found 491.1926.

Crystallography Experimental Details for Complex 24f. Crystal data collection and refinement parameters are given in Table 5. The unit-cell parameters were obtained by the least-squares refinement of the angular settings of 24 reflections (19° < 2θ < 24°).

Axial photographs and unit-cell parameters indicate that this crystal system is monoclinic. Occurrence of equivalent reflections and systematic absences are consistent with the space groups *C*2/*c* and *Cc*. E statistics suggest a centrosymmetric space group, and solution of the structure in *C*2/*c* gave chemically reasonable results.

The structure was solved using direct methods and refined by full-matrix least-squares procedures. The asymmetric unit consists of two independent molecules, one in a general position and one on a crystallographic 2-fold axis containing Co(1), N(8), C(23), C(28), and C(29). C(14) and C(18) are disordered over two positions with an occupancy of 60/40. All atoms with the exception of C(14), C(18), and C(23)–C(32) were refined with anisotropic displacement coefficients. Hydrogen atoms were treated as idealized contributions. Corrections for absorption were not required.

All software and sources of scattering factors are contained in either SHELXTL (5.1) or the SHELXTL PLUS (4.2) program libraries (G. Sheldrick, Siemans XRD, Madison, WI).

1-[(Pyridine)bis(dimethylglyoximato)cobaltio(III)]-4-methyl-2,3-pentadiene (26). Polar Aprotic Solvent Conditions. Pyr(dmg)$_2$CoCl[11] (0.200 g, 0.506 mmol) was added to Na(Hg) (0.58 g, 2.53 mmol of Na) and THF (100 mL) with rapid stirring at −30 °C. The solution was heterogeneous for about 5 min and then turned dark purple, indicating anion formation. After the solution was stirred for 2 h, 5-(*p*-toluenesulfonyl)-2-methyl-2,3-pentadiene (**16e**; 0.130 g, 0.515 mmol) was added and the reaction mixture warmed to 25 °C and stirred for 8 h. The solution was decanted from the spent amalgam, which was washed with THF (3 × 10 mL). Water (10 mL) was added to the combined THF extracts and the THF removed by rotary evaporation. The dark brown aqueous solution was extracted with CH_2Cl_2 (3 × 20 mL). The combined organic layers were washed with water (50 mL). After drying with $MgSO_4$, the solvent was removed to yield **26** (0.100 g, 0.223 mmol (44%)), identical by spectroscopic comparison with previously reported material.[1b]

(3*Z*)-(1,3-Pentadien-2-yl)(pyridine)bis(dimethylglyoximato)cobalt(III) (32). At −20 °C, $NaBH_4$ (0.138 g, 3.64 mmol) in H_2O (0.1 mL) was added to cobalt chloride **18** (L = pyr; 1.500 g, 3.71 mmol) in ethanol (20 mL). Enyne **31** (Wiley) was added at −20 °C after 45 min and the solution warmed to 25 °C and stirred for 2 h. The solution was poured into ice–water (100 mL). The resulting orange precipitate was collected by filtration and vacuum-dried (1.271 g, 70%, >20:1 *Z*:*E* by ^{1}H NMR analysis). The filtrate was extracted with CH_2Cl_2 to yield a mixture of **32Z** and **32E** (1.66:1; 0.126 g (8%)). Mp for **32Z**: 195–196 °C. ^{1}H NMR ($CDCl_3$): 8.62 (d, J = 5.7 Hz, 2H), 7.69 (t, J = 7.6 Hz, 1H), 7.28 (t, J = 7.6 Hz, 2H), 6.00 (dq, J = 11.3 Hz, 1.7 Hz, 1H), 5.3 (m, 1H), 4.77 (s, 1H), 4.13 (s, 1H), 2.07 (s, 12 H), 1.30 (dd, J = 6.7, 1.7 Hz, 3H). ^{13}C NMR: 149.953, 149.666, 138.302, 137.488, 125.108, 119.332, 116.579, 13.800, 11.993. IR ($CDCl_3$): 3688.3, 3582.7, 3078.4, 3006.8, 2929.1, 1828.1, 1562.1, 1490.6, 1452.4, 1377.4, 1235.3 cm^{-1}. Anal. Calcd for $C_{18}H_{26}CoN_5O_4$: C, 49.66; H, 6.02. Found: C, 49.55; H, 6.04.

Preparation of [*cis*- and *trans*-1-(1-Oxoethyl)-2-methyl-3-cyclohexen-4-yl](4-cyanopyridine)bis(dimethylglyoximato)cobalt(III) (36d, 37d). At 25 °C, diene **17d** (0.045 g, 0.097 mmol) was dissolved in THF (8 mL). Methyl vinyl ketone (0.10 mL, 1.20 mmol) was added dropwise, and the solution was refluxed for 8 h. Additional methyl vinyl ketone (0.10 mL, 1.20 mmol) was added, and the solution was refluxed for 16 h before the solvent was removed under reduced pressure. The residue was dissolved in $CHCl_3$ and cooled to −78 °C and precipitation induced with pentane. The product was a yellow solid (0.039 g, 0.073 mmol (76%)). ^{1}H NMR ($CDCl_3$): 8.89 (d, J = 6.9 Hz, 2H), 7.55 (d, J = 6.9 Hz, 2H), 5.10–5.0 (m, 1H) major, 4.95–4.85 (m, 1H) minor, 2.75–2.15 (m, 3H), 2.11 (s, 6H), 2.10 (s, 6H), 2.02 (s, 3H, overlapping acetyl methyls), 2.0–1.5 (m, 3H), 0.79 (d, J = 6.9 Hz, 3H) minor, 0.63 (d, J = 6.9 Hz, 3H) major. IR (benzene): 4066.5, 4051.8, 2325.7, 1961.0, 1826.7, 1808.2, 1708.9, 1558.1, 1528.1, 1236.7 cm^{-1}. FAB HRMS: *m/z* for $C_{23}H_{31}CoN_6O_5$ ((M + H)$^+$) 531.1766, found 531.1780.

Preparation of [*cis*- and *trans*-1-(1-Oxoethyl)-2-methyl-3-cyclohexen-4-yl](tributylphosphine)bis(dimethylglyoximato)cobalt(III) (36f, 37f). At 25 °C, methyl vinyl ketone (0.10 mL, 0.86 mmol) was added to diene **17f** (0.162 g, 0.29 mmol) in degassed THF (10 mL). The solution was refluxed (8 h) and then the solvent was removed via rotary evaporation. The residue was chromatographed on silica (ether) to yield the adduct (0.103 g, 1.6 mmol, 54.2%) as a yellow oil. ^{1}H NMR ($CDCl_3$): 5.12 (m, 1H), major, 4.95 (m, 1H) minor, 2.70–2.15 (m, 3H), 2.11 (s, 6H), 2.09 (s, 6H), 2.06 (s, 3H) minor, 2.05 (s, 3H) major, 2.0–1.65 (m, 3H), 1.40–1.05 (m, 18H0, 1.85 (t, J = 7.92 Hz, 9H), 0.745 (d, J = 7.45 Hz, 3H) minor, 0.57 (d, J = 7.45 Hz, 3H) major. IR ($CDCl_3$): 3686.0,

(11) Schrauzer, G. N. In *Inorganic Syntheses*; Jolly, W. L., Ed.; McGraw-Hill: New York, 1968; Vol. XI, pp 61–70.

3600.8, 2960.9, 2871.0, 1703.7, 1605.6, 1553.6, 1457.0, 1373.3, 1234.2 cm^{-1}. FAB HRMS: *m/z* for $C_{29}H_{54}CoN_4O_5P$ ($(M + H)^+$) 629.3242, found 629.3253.

Preparation of [*cis*- and *trans*-1-(1-Oxoethyl)-2-methyl-3-cyclohexen-4-yl](diphenylmethylphosphine)bis(dimethylglyoximato)cobalt(III) (36e, 37e). Cobalt diene **17e** (0.097 g, 0.17 mmol) and methyl vinyl ketone (0.05 mL, 0.60 mmol) were combined in degassed THF (10 mL). The solution was refluxed (15.5 h), and the solvent was removed under vacuum. The crude product was chromatographed on silica (EtOAc) to yield a yellow solid (0.059 g, 0.09 mmol (54.1%)). ^1H NMR ($CDCl_3$): 7.50–7.24 (m, 10H), 5.15 (m, 1H) major, 4.95 (d, J = 7.8 Hz, 1H) minor, 2.71–2.06 (m, 3H), 2.05 (s, 3H) minor, 2.00 (s, 3H) major, 1.85 (d, J = 7.8 Hz, 3H), 1.75 (apparent t, J = 3.9 Hz, 12H), 1.65–1.45 (m, 3H), 0.75 (d, J = 7.84 Hz, 3H) minor, 0.57 (d, J = 7.84, 3H) major. IR ($CDCl_3$): 3689.6, 3155.4, 3062.9, 2959.1, 2925.4, 2337.2, 1699.7, 1557.7, 1484.4, 1468.0, 1436.1, 1382.8, 1375.2, 1234.0 cm^{-1}. Anal. Calcd for $C_{30}H_{40}O_4N_4Co$: C, 57.51; H, 6.43. Found: C, 57.23; H, 6.51.

Synthesis of (*syn*- and *anti*-4,4,7,7,8,9-hexahydro-4-methyl-1,3-dioxoisobenzofuran-5-yl)(methyldiphenylphosphine)bis(dimethylglyoximato)cobalt(III) (38a, 39a). Diene **24d** (175 mg, 0.32 mmol) and maleic anhydride (124 mg, 1.26 mmol) were added to degassed THF (4 mL) in a sealed tube which has heated to 100 °C for 2 h. The mixture was cooled to 25 °C, and the solvent was removed by rotary evaporation. The remaining black oil was purified by silica chromatography (1:1 ethyl acetate/pentane) to yield a dark yellow waxy solid (**38a**, **39a**; 28 mg, 0.04 mmol (14%)). Mp: 132–134 °C. ^1H NMR ($CDCl_3$): 7.46–7.30 (m, 10 H), 5.70–5.58 (m, 1H) minor, 5.40–5.38 (m, 1H) major, 3.22 (m, 1H), 3.04 (m, 1H), 2.62 (dd, J = 10.4, 5.6 Hz, 1H), 2.56–2.45 (m, 2H), 1.84 (d, J = 8.4 Hz, 3H), 1.73 (d, J = 3.5 Hz, 6H), 1.71 (d, J = 3.5 Hz, 6H), 0.83 *minor* (d, J = 6.9 Hz, 3H), 0.57 *major* (d, J = 6.9 Hz, 3H). IR ($CDCl_3$): 3688, 3156, 2984, 1783, 1469, 1382, 1231, 1095 cm^{-1}. FAB MS: *m/z* calcd for M + 1 − H_2 ($C_{30}H_{37}O_7N_4PCo$) 655.1, found 655.1.

Synthesis of (*syn*- and *anti*-4,4,7,7,8,9-hexahydro-4-methyl-1,3-dioxoisobenzofuran-5-yl)(dimethylphenylphosphine)bis(dimethylglyoximato)cobalt(III) (38b, 39b). Diene **24e** (160 mg, 0.32 mmol) and maleic anhydride (63.5 mg, 0.65 mmol) were added to degassed THF (3 mL) in a sealed tube which was heated to 100 °C for 2 h. The mixture was cooled to 25 °C and solvent removed by rotary evaporation. The remaining black oil was purified by silica chromatography (1:1 EtOAc/pentane) to yield a yellow waxy solid (**38b**, **39b**; 65 mg, 0.011 mmol (34%)). Mp: 96–100 °C. ^1H NMR ($CDCl_3$): 7.42–7.26 (m, 3H), 7.22–7.05 (m, 2H), 5.71–5.55 (m, 1H) *minor*, 5.46–5.32 (m, 1H) *major*, 3.19 (m, 1H), 3.04 (m, 1H), 2.60 (dd, 1H, J = 10.6, 5.6 Hz), 2.54–2.42 (m, 2H), 1.97 (d, 6*H*, J = 9.4 Hz), 1.89 (s, 6H), 1.87 (s, 6H), 0.84 (d, 3H, J = 7.0 Hz) *minor*, 0.55 (d, 3H, J = 7.0 Hz) *major*. IR ($CDCl_3$): 3156, 2985, 2905, 1794, 1558, 1471, 1383, 1096 cm^{-1}. FAB HRMS: *m/z* calcd for M + 1 ($CoC_{25}H_{34}O_7N_4P$) 593.1575, M + 1 found 593.1550.

Synthesis of (*syn*- and *anti*-4,4,7,7,8,9-hexahydro-4-methyl-1,3-dioxoisobenzofuran-5-yl)[4-(dimethylamino)-pyridine]bis(dimethylglyoximato)cobalt(III) (38c, 39c). Complex **24b** (200 mg, 0.42 mmol) and maleic anhydride (82 mg, 0.84 mmol) were added to degassed toluene (3 mL) in a sealed tube which was heated to 50 °C for 5 h. The mixture was cooled to 25 °C, and pentane (15 mL) was added. The product was collected by vacuum filtration and vacuum-dried to give a yellow powder (**38c**, **39c**; 230 mg, 0.41 mmol (98%)). Mp: decomposes at 110–112 °C. ^1H NMR ($CDCl_3$): 8.01 (d, J = 7.1 Hz, 2H), 6.37 (d, J = 7.1 Hz, 2H), 5.37 (apparent t, J = 5.8 Hz, 1H), 3.08 (dd, J = 9.9, 5.6 Hz, 1H), 2.96 (s, 6H), 2.69 (dd, J = 9.9, 5.6 Hz, 1H), 2.54–2.47 (m, 2H), 2.10 (s, 6H), 2.08 (s, 6H), 0.88 (d, J = 8.0 Hz, 3H) minor, 0.62 (d, J = 8.0 Hz, 3H) major. ^{13}C NMR ($CDCl_3$): 175.6, 172.6, 154.2, 149.8, 149.79, 149.71 (2 dmg C=N), 148.6, 123.3, 107.5, 47.5, 39.0, 38.9, 35.9, 23.3, 13.7, 12.10, 12.05 (2 dmg Me). IR ($CDCl_3$): 3691, 3156, 1785, 1624, 1469, 1384, 1095, 936 cm^{-1}. Analysis calculated for $C_{24}H_{33}O_7N_6Co$: C, 48.94; H, 5.89. Found: C, 49.13; H, 5.87.

Lewis Acid Mediated Cleavage of the Cobalt–Carbon Bond in 38c and 39c To Yield *syn*- and *anti*-4-4,7,7,8,9-hexahydro-4-methyl-1,3-dioxoisobenzofuran. Complexes **38c** and **39c** (150 mg, 0.266 mmol) were dissolved in dry THF (10 mL), and the solution was cooled to 0 °C. $AlMe_3$ in hexanes (0.27 mL of a 2 M solution, 0.532 mmol) was added. After 0.5 h, the ice bath was removed and the mixture was warmed to 25 °C and stirred for 12 h. Ice–water (10 mL) was added and the mixture extracted with CH_2Cl_2 (4 × 25 mL). The CH_2Cl_2 extracts were combined and dried over $MgSO_4$. The solvent was removed under vacuum and the resultant orange oil vacuum-dried. The crude product was microdistilled under vacuum (Kugelrohr) to give the white solid **40** (20 mg, 0.12 mmol, 45.1%), identical by spectroscopic comparison with an authentic sample prepared from (*E*)-piperylene and maleic anhydride.[12] The remaining orange solid in the distillation flask was found to be methyl [4-(dimethylamino)pyridine]bis(dimethylglyoximato)cobalt(III) (**41**; 78 mg, 0.18 mmol (68.8%)), which was proven to be identical with an authentic sample prepared by the method of Schrauzer et al.[11] Mp: 177–180 °C dec. ^1H NMR ($CDCl_3$): 8.06 (d, J = 7.1 Hz, 2H), 6.39 (d, J = 7.1 Hz, 2H), 2.95 (s, 6H), 2.10 (s, 12H), 0.68 (s, 3H). ^{13}C NMR ($CDCl_3$): 154.2, 148.8, 148.4, 107.4, 39.0, 11.9. IR ($CDCl_3$): 3155, 2986, 2902, 1793, 1472, 1384, 1094 cm^{-1}. Anal. Calcd for $CoC_{16}H_{27}O_4N_6$: C, 45.07; H, 6.38. Found: C, 45.06; H, 6.36.

Cycloaddition between the 3-Cobaltio-(3*E*)-1,3-pentadiene Complex 24b and Methyl Vinyl Ketone. Complex **24b** (510 mg, 1.07 mmol) was dissolved in methyl vinyl ketone (6 mL) and heated to 75 °C in a sealed tube (90 h). The mixture was cooled to 25 °C, and excess dienophile was removed by rotary evaporation. The resultant dark red-brown oil was purified by silica chromatography (ethyl acetate/diethyl ether (1:1)) to give an orange-red waxy solid (**42a,b** and **43a,b**; 550 mg, 1.03 mmol (96.2%)) as a mixture of regioisomers and diastereomers: 1:3.4:1.2:3.3 ortho-trans (**43b**), meta-trans (**42a**), meta-cis (**42b**), and ortho-cis (**43a**) (meta products 2.95:1 (trans:cis), ortho products 3.4:1 (cis:trans)). ^1H NMR ($CDCl_3$; cyclohexenyl ring methyls only are reported): 0.90 (J = 6.7 Hz, ortho-trans), 0.79 (J = 6.6 Hz, meta-trans), 0.66 (J = 7.0 Hz, meta-cis), 0.52 (J = 6.7 Hz, ortho-cis).[13b] IR ($CDCl_3$): 3156, 2925, 1622, 1540, 1383, 1236, 1093 cm^{-1}.

Lewis Acid Mediated Cleavage of the Cobalt–Carbon Bond in 42a,b and 43a,b To Yield *trans*- and *cis*-1-(1-Oxoethyl)-5-methyl-3-cyclohexen-1-yl (44a,b) and *cis*- and *trans*-1-(1-Oxoethyl)-2-methyl-3-cyclohexen-1-yl (45a,b). The mixture of **42a,b** and **43a,b** (550 mg, 1.03 mmol) from the cycloaddition described above was dissolved in dry THF (20 mL) and the solution cooled to 0 °C. $AlMe_3$ (0.75 mL, 2 M in hexanes, 1.5 mmol) was added and the solution stirred (1 h). The dark orange mixture was then warmed to 25 °C slowly and stirred for 15 h. Ice–water (10 mL) was added and the mixture extracted with CH_2Cl_2 (5 × 25 mL). The CH_2Cl_2 extracts were combined and dried over $MgSO_4$, and the solvent was removed by rotary evaporation to yield an orange waxy solid. The solid was chromatographed on silica (1:1 Et_2O/pentane), and the solvent was removed by rotary evaporation (15 °C bath) to afford a pale yellow oil (**44** and **45**; 112 mg, 0.811 mmol (78.7%)). ^1H NMR ($CDCl_3$; cyclohexenyl ring methyls only are reported): 0.955 (J = 7.2 Hz, meta-cis (minor, **44b**)), 0.943 (J = 7.0 Hz, meta-trans (major, **44a**)), 0.867 (J = 7.0 Hz, ortho-trans (minor, **45b**)), 0.771 (J = 7.0 Hz, ortho-cis

(12) (a) Brocksom, T. J.; Constantino, M. G. *J. Org. Chem.* **1982**, *47*, 3450. (b) Brocksom, T. J.; Constantino, M. G. *An. Acad. Bras. Cienc.* **1982**, *54*, 655.

(major, **45a**)).[13] ^{13}C NMR ($CDCl_3$; diagnostic peaks only (alkene peaks and C(2) or C(5) (carbon with Me subst.) reported): meta-cis (**44b**), 133.2, 124.3, 47.87; meta-trans (**44a**), 132.4, 124.2, 43.7; ortho-trans (**45b**), 132.3, 125.2, 55.4; ortho-cis (**45a**), 131.7, 126.2, 51.2. The organometallic complex was removed from the silica using EtOAc. The solvent was removed by rotary evaporation and high vacuum to afford an orange solid, **41** (274 mg, 0.64 mmol, (62.4%)), which was identical by spectroscopic comparison with the sample characterized above.

Preparation of *trans*- and *cis*-1-(1-Oxoethyl)-5-methyl-3-cyclohexen-1-yl (44a,b) and *cis*- and *trans*-1-(1-Oxoethyl)-2-methyl-3-cyclohexen-1-yl (45a,b) via Thermal Reaction of (*E*)-Piperylene and MVK. *trans*-Piperylene (380 mg, 5.59 mmol) and methyl vinyl ketone (1.00 g, 14 mmol) were placed in a sealed tube and heated (150 °C) for 15 h.[13c] The mixture was cooled, and a yellow gel formed. The gel was chromatographed on silica (1:1 Et_2O/pentane). The solvent was removed by rotary evaporation (15 °C bath) to yield a pale yellow liquid (**44** and **45**; 439 mg, 3.18 mmol (56.9%)) as a mixture of regioisomers and diastereomers. The products were spectroscopically identical with reported ^1H NMR data for cis and trans 1,2- and 1,3-compounds.[13b] The products have an overall ratio of 1:4 meta:ortho (**44**:**45**) products. The ratio of total products was meta-trans:meta-cis:ortho-trans:ortho-cis = 1.0:1.6:3.1:4.5.

Results and Discussion

The preparation of the allenic electrophiles required to test the scope and limitations of the S_N2' reaction presented in the Introduction was straightforward. Most of the simple allenic alcohol precursors to the allenic electrophiles were known.[7-9] All reported yields are of isolated, purified materials which have been prepared on a multigram scale. All allenic electrophiles, except the tosylates, appear to be stable for at least 1 month at −20 °C. Terminally unsubstituted allenic electrophiles are prepared from propargyl chloride, whereas terminally substituted allenes are prepared from substituted propargyl alcohols (**6**). Preparation of 2,3-pentadien-1-ol (**9**) is presented as a representative example:

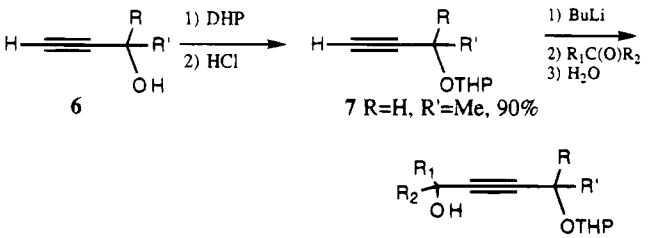

6 **7** R=H, R'=Me, 90%

8 R'=Me, R=R_1=R_2=H, 79%

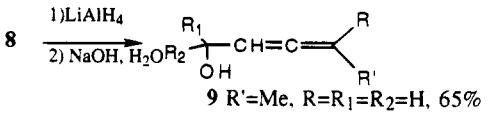

9 R'=Me, R=R_1=R_2=H, 65%

1-Acetoxy-2-methyl-2,3-butadiene (**11**) was prepared (72%) by addition of a methyl cuprate reagent to 1-acetoxy-4-chloro-2-butyne (**10**). 2-Ethenylidene-1-cyclohexanol (**13**) was prepared via S_N2' hydride opening of the alkynyl epoxide **12**, and then the alcohol **13** was acetylated. The chloride or acetate of 2-methyl-3,4-pentadien-2-ol (**15d**, $R_1 = R_2 = H$, $R_3 = R_4 = Me$)[4] could not be prepared cleanly, presumably due to the acid and/or aqueous sensitivity of these tertiary alcohols and electrophiles. Table 1 summarizes the conditions used to prepare all acyclic allenic tosylates, acetates, pivalates, and phosphates (except as described above or described previously: **16a**, R_{1-3} = H, R_4 = Me, X = OAc;[1] **16b**, R_{1-3} = H, R_4 = Me, X = OPiv;[1] **16e**, $R_{1,2}$ = Me, $R_{3,4}$ = H, X = OTs;[1] **16f**, R_{1-3} = Me, R_4 = H, X = OAc[1]) used in the preparation of dienyl complexes.

Table 1. Preparation of Allenic Electrophiles (16) from Allenic Alcohols (15)

allenic alcohol			allenic electrophile		
R_1,R_2,R_3,R_4	compd no.	conditions	X	yield (%)	compd no.
Me,H,H,H	**9**	tosylCl/KOH/Et_2O	OTs	89	**16c**
Me,H,H,H	**9**	$ClP(O)(OEt)_2$/MeLi	$OP(O)(OEt)_2$	84	**16d**
H,H,Me,Me	**15d**[a]				

[a] Neither the chloride nor the tosylate could be prepared cleanly.

Table 2. (3*E*)-1,3-Pentadiene Complexes from in Situ Generated Anionic Cobalt Complexes

entry no.	L	glyoxime	solvent	allenic electrophile	yield (%)	product
1	pyr	dmg	MeOH	**16a**	59	**17a**
2	pyr	dmg	MeOH	**16b**	56	**17a**
3	DMAP	dmg	MeOH	**16a**	45	**17b**
4	pyr	dpg	MeOH	**16a**	35	**17c**
5	pyr	dpg	MeOH	**16b**	40	**17c**
6	pyr	dpg	DMF	**16a**	73	**17c**
7	pyr	dpg	DMF	**16b**	66	**17c**

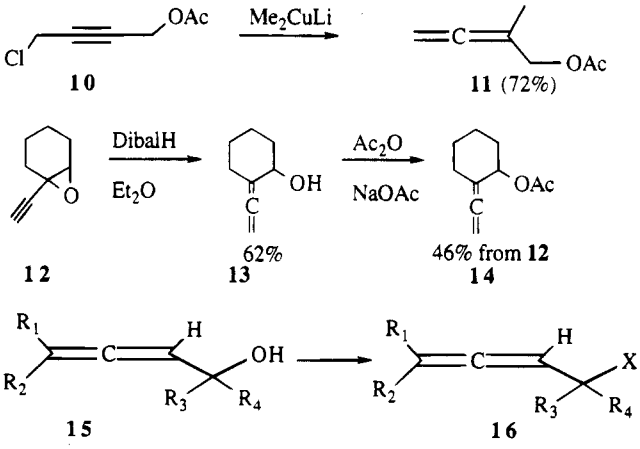

10 **11** (72%)

12 **13** **14**

15 **16**

Preparation of 2-Cobalt-Substituted (3*E*)-1,3-Pentadienes (17a−g). We prepared these dienyl complexes (**17**) with axial ligands other than pyridine by one of three routes;[14] (1) via reactions of anionic cobalt complexes generated in situ with allenic electrophiles, (2) via axial ligand exchange from 2-(pyr-$(dmg)_2$Co)-(3*E*)-1,3-pentadiene (**17a**), or (3) via reduction of a cobalt chloride (**18**) to the anion, which is then treated with allenic electrophiles. For complexes prepared by route 1, we found acetates and pivalates to be virtually interchangeable as electrophiles (Table 2, entries 1 and 2, 4 and 5, 6 and 7). Increasing the size of the equatorial ligands from dimethylglyoxime (dmg)

(13) (a) Guner, O. F.; Ottenbrite, R. M.; Shillady, D. D.; Alston, P. V. *J. Org. Chem.* **1988**, *53*, 5348. (b) Bonnesen, P. V.; Puckett, C. L.; Honeychuck, R. V.; Hersh, W. H. *J. Am. Chem. Soc.* **1989**, *111*, 6070. (c) Smith, D. A.; Sakan, K.; Houk, K. N. *Tetrahedron Lett.* **1986**, *27*, 4877.

(14) For previously reported examples of these types of reactions see refs 1b and 11 in addition to: (a) Bulkowski, J.; Cutler, A.; Dolphin, D.; Silverman, R. B. *Inorganic Syntheses*; **1980**, *20*, 127. (b) Bigotto, A.; Costa, C.; Mestroni, G.; Pellizer, G.; Puxeddu, A.; Reisenhofer, E.; Stefani, L.; Tauzher, G. *Inorg. Chim. Acta Rev.* **1970**, *4*, 41.

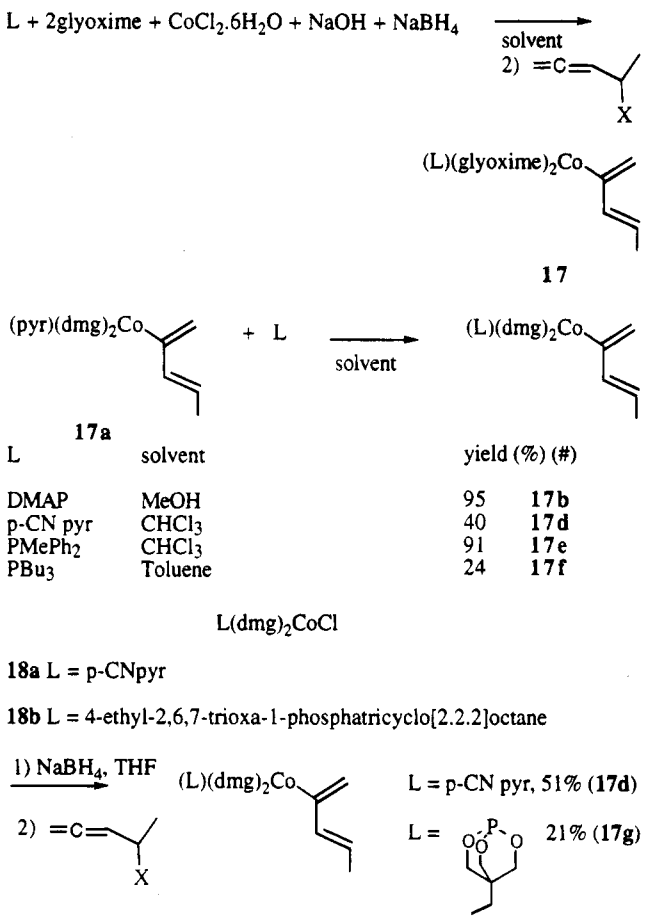

to diphenylglyoxime (dpg) significantly lowered the yields of diene complexes obtained in polar protic solvents (Table 2, entries 4 and 5). It is less convenient to perform these reactions in DMF, since an extraction is required, but with the bulkier dpg, the polar aprotic solvent is necessary in order to obtain yields of diene complexes >50%.[14a]

Complexes with axial ligands other than pyridine (**17b,e**) are conveniently prepared via ligand exchange (route 2) for strongly electron donating ligands such as DMAP or $PMePh_2$.[15] When an axial ligand which is less electron donating than pyridine, such as 4-cyanopyridine, is desired, then the complex is best prepared via reduction of the preformed chloride **18** (route 3). The *E* double-bond stereochemistry is determined by $J(H_3-H_4)$, which is >14 Hz in all complexes. The C_1 H's show coupling to ^{31}P in the phosphine complexes (**17e,f,g**).

In order to obtain *E* double-bond isomers (**17**) cleanly, one must carefully follow our protocols with respect to concentration, hydride reducing equivalents present, and temperature. In our previously reported protocol,[1] the anionic cobalt complex **1** was generated (0.262 M) in methanol at −10 °C using 1.1 equiv (based on Co) of $NaBH_4$ and then the allenic acetate (**16a**) was added and the solution was warmed to 25 °C overnight. The crude product contained traces of *Z* isomer (**19**) and 2-substituted diene (**20**), which were removed by one recrystallization from MeOH (entry 1, Table 3). Increasing the amount of $NaBH_4$ to 2.0 equiv caused essentially no change. However, maintaining the temperature at −10 °C after allenic electrophile addition

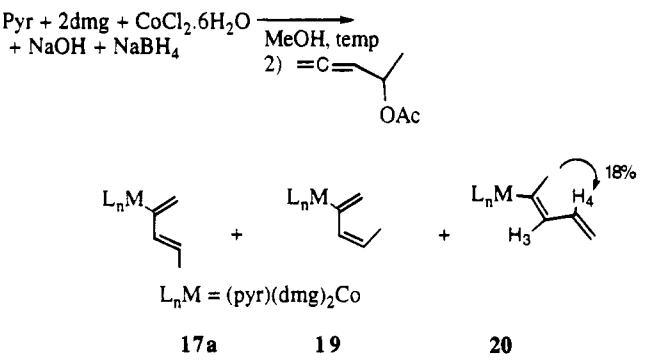

followed by addition of water containing a few drops of pyridine provided **17a** as the clean *E* isomer without recrystallization (entry 3). When the concentration is reduced by a factor of 4, the percentage of **20** present increases significantly and is independent of hydride over the range 1.1−4 equiv (entries 4 and 5). Further dilution by a factor of 2 and refluxing the MeOH solution prior to aqueous workup have little additional effect (entry 6). Heating pure **17a** in methanol (1.5 h) produced a 77:23 mixture of **17a** and **19** but no **20**. Treatment of pure **17a** with a large excess of $NaBH_4$ (16 equiv) and refluxing in MeOH (1.5 h) produced a 1:1 mixture of **17a** and **20**. DMAP diene **17b** showed no evidence of double-bond isomerization over a period of 5 days at 25 °C in $CDCl_3$ or 1 day in THF. Pyridine diene **17a** does isomerize slowly under these conditions with an *E*:*Z* ratio of 28:1 being observed by ^1H NMR after 3.5 days in $CDCl_3$ at 25 °C. Heating in THF, as for MeOH, accelerated isomerization rapidly. DMAP diene **17b** is a 3.2:1 mixture of *E*:*Z* isomers after 4 h, and this ratio is 2.5:1 after 8 and 24 h at reflux. Likewise, complex **17a** is a 2.6:1 mixture of *E*:*Z* isomers after 24 h reflux in THF. Isolated yields for all these reactions are in the 55−75% range (except for entry 3, 30−40%).

A detailed investigation of this isomerization will be reported in a forthcoming manuscript, but several comments relevant to the preparation of *E* diene complexes discussed in this paper are in order. The *E* diene complex **17a** appears to be the kinetic product of this reaction (entry 3). The cobalt and hydrogen 1,3-transpositions are hydride rather than polar protic solvent or NaOMe mediated, since heating **17a** alone in methanol (1.5 h) produces a 77:23 mixture of **17a** to **19** but no **20** and heating **17a** with 16 equiv of NaOMe in MeOH (1.5 h) produced a 84:16 mixture of **17a** to **19** with no **20** observed. Only one double-bond isomer of **20** is produced, and the *E* geometry is postulated on the basis of the observation that the methyl to H_4 NOE is much larger than the methyl to H_3 NOE.

Preparation of 2-Cobalt-Substituted 3-Methyl-1,3-Butadienes and 2-Cobalt-Substituted 1-Vinylcyclohexenyl Complexes. The (pyr)(dmg)$_2$Co anion generated in situ in DMF reacted with 1-acetoxy-2-methyl-2,3-butadiene (**11**) to produce the 2-cobalt-substituted 1,3-butadiene **21**. None of this diene complex (**21**) could be isolated when this same reaction was performed in MeOH. The DMAP (**22a**) and Me(Ph)$_2$P (**22b**) complexes of this same diene were prepared via ligand exchange in MeOH from the pyr complex **21**, as mentioned above for the (3*E*)-pentadiene complex **17a**. Likewise, the exocyclic allenic acetate **14** reacted cleanly with the pyr(dmg)$_2$Co anion and the DMAP(dpg)$_2$ cobalt

(15) (a) Trogler, W. C.; Marzilli, L. G. *Inorg. Chem.* **1975**, *14*, 2942. (b) Dodd, D.; Johnson, M. D. *Organomet. Chem. Rev.* **1973**, *52*, 1.

Table 3. Effect of Concentration, Reducing Agent, and Temperature on the Ratio 17a:19:20

entry no.	molarity ($CoCl_2$)	amt of $NaBH_4$ (equiv)	temp (°C)	amt of product (%) 17a	19	20
1	0.262	1.1	25	90	5	5
2	0.262	2.0	25	90	5	5
3	0.262	2.0	−10	100	<1	<1
4	0.075	1.1	25	75	10	15
5	0.075	4.0	25	85	<1	15
6	0.035	2.0	Δ 1.5 h	80	6	14

anion to produce complexes **23a,b**. DMAP complexes **23b,c** were also available via ligand exchange from the pyridine complexes.

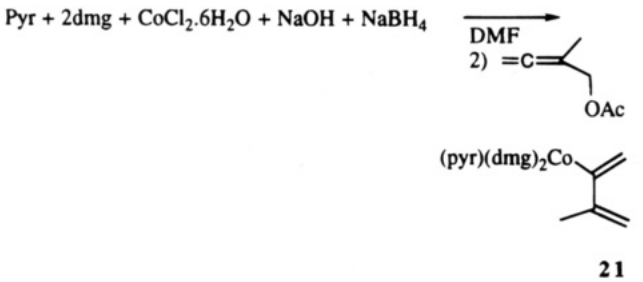

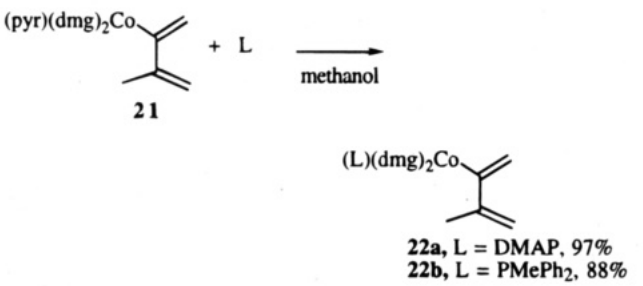

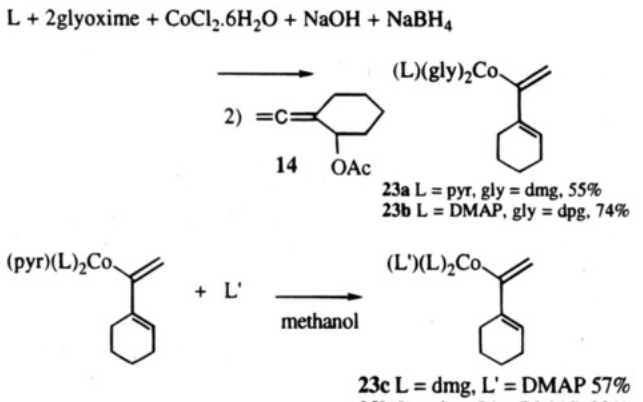

Preparation of 3-Cobalt-Substituted (3*E*)-1,3-Pentadienes. The $(pyr)(dmg)_2Co$ anion was generated in situ in both MeOH and DMF and treated with tosylate (**16c**) to produce the 3-cobalt-substituted 1,3-pentadiene **24a** as the only isolated complex in 43% and 56% yields, respectively (Table 4). In both cases, only the *E* geometry in the alkene was observed. Refluxing these dienes (**24**) in THF, $CHCl_3$, or methanol for extended periods led to some (30−50%) diene decomposition, but no other alkene isomers were observed. The $DMAP(dmg)_2Co$ anion and the $DMAP(dpg)_2Co$ anion react similarly in DMF to produce the corresponding diene complexes **24b,c** in 63 and 71% yields. A phosphate (**16d**) could be used in place of the tosylate; however, the yield of dienyl complex **24a** was significantly lower and there was no effect on alkene geometry.[10] The DMAP, $Me(Ph)_2P$, $(Me)_2PhP$, and 4-*tert*-butylpyridine complexes (**24b,d−f**) of this same diene could all also be prepared via ligand exchange in MeOH from the pyr complex **24a**.

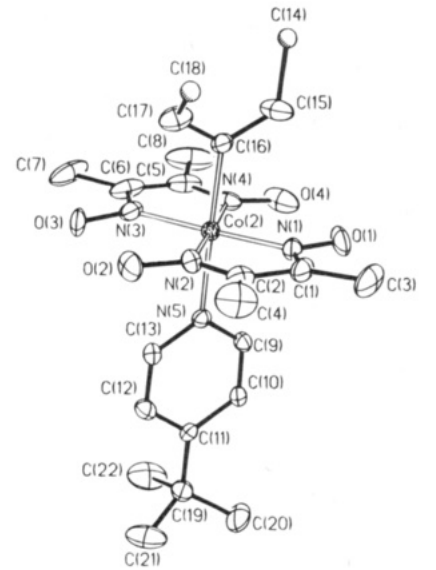

Figure 1. Molecular structure of complex **24f**.

Table 4. 3-Cobaltio-(3*E*)-1,3-pentadiene Complexes from in Situ Generated Anionic Cobalt Complexes

entry no.	L	glyoxime	solvent	electrophile	yield (%)	product
1	pyr	dmg	MeOH	**16c**	43	**24a**
2	pyr	dmg	DMF	**16c**	56	**24a**
3	pyr	dmg	DMF	**16d**	30	**24a**
4	DMAP	dmg	DMF	**16c**	63	**24b**
5	DMAP	dpg	MeOH	**16c**	70	**24c**

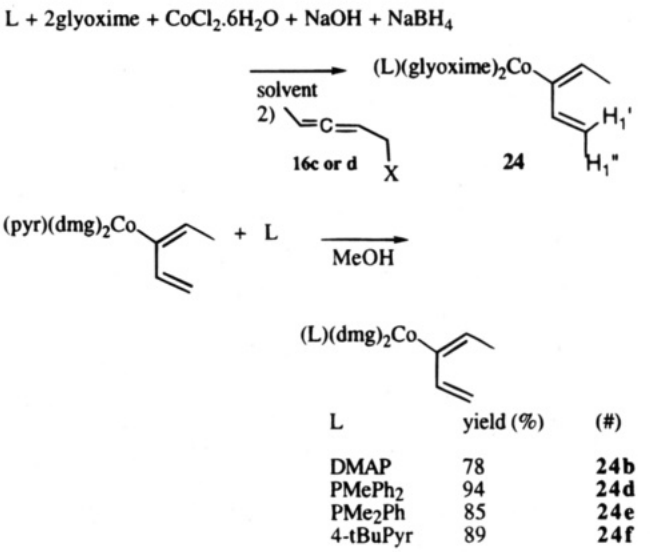

We postulated an *E* double-bond stereochemistry and more *s-cis*- than *s-trans*-like diene conformation initially on the basis of NOE data, in which irradiation of H_1' produced a 2.2% enhancement of the pentadiene methyl and no enhancement of the dmg methyls. This postulate about diene geometry was subsequently proven by an X-ray crystallographic analysis of the *tert*-butylpyridine complex **24f**. The ORTEP drawing of this complex is provided in Figure 1, and data collection and

Table 5. Crystallographic Data for $C_{22}H_{34}CoN_5O_4$

(a) Crystal Parameters

formula	$C_{22}H_{34}CoN_5O_4$	V, Å^3	7383(4)
fw	491.5	Z	12
cryst syst	monoclinic	cryst dimens, mm	0.21 × 0.26 × 0.34
space group	$C2/c$	cryst color	orange-red
a, Å	29.313(9)	D(calc), g cm^{-3}	1.326
b, Å	15.033(3)	μ(Mo Kα), cm^{-1}	7.33
c, Å	17.856(7)	temp, K	240
β, deg	110.24(2)		

(b) Data Collection

diffractometer	Siemens P4
monochromator	graphite
radiation	Mo Kα (λ = 0.710 73 Å)
2θ scan range, deg	4–52
data collected (h,k,l)	±33, +18, +22
no. of rflns collected	7493
no. of indpt rflns	7243
no. od indpt obsd rflns, $F_o \geq 4\sigma(F_o)$	4974
std/rfln	3 std/197 rflns

(c) Refinement[a]

$R(F)$, %	7.70	$\Delta(\rho)$, e Å^{-3}	0.69
$R(wF)$, %	11.28	N_o/N_v	12.3
Δ/σ (max)	0.273	GOF	1.76

[a] Quantity minimized: $\Sigma w\Delta^2$; $R = \Sigma\Delta/\Sigma(F_o)$; $R(w) = \Sigma\Delta w^{1/2}/\Sigma(F_o w^{1/2})$, $\Delta = |(F_c - F_c)|$.

Table 6. Selected Bond Lengths and Bond Angles for Co(dmg)$_2$(4-*t*-Bu(py))(σ-C_5H_7) (24f)

Bond Lengths (Å)

Co(2)–N(1)	1.876(6)	Co(2)–N(2)	1.889(6)	Co(2)–N(3)	1.877(6)
Co(2)–N(4)	1.877(6)	Co(2)–N(5)	2.064(4)	Co(2)–C(16)	2.019(6)
N(1)–O(1)	1.350(9)	N(1)–C(1)	1.308(10)	N(2)–O(2)	1.324(9)
N(2)–C(2)	1.294(9)	N(3)–O(3)	1.361(9)	N(3)–C(6)	1.288(9)
N(4)–O(4)	1.326(9)	N(4)–C(5)	1.286(10)	C(14)–C(15)	1.539(23)
C(15)–C(16)	1.428(12)	C(16)–C(17)	1.375(12)	C(17)–C(18)	1.513(34)

Bond Angles (deg)

N(1)–Co(2)–N(2)	81.3(3)	N(1)–Co(2)–N(3)	178.1(2)
N(2)–Co(2)–N(3)	98.2(3)	N(1)–Co(2)–N(4)	99.1(3)
N(2)–Co(2)–N(4)	177.9(2)	N(3)–Co(2)–N(4)	81.4(3)
N(1)–Co(2)–N(5)	90.9(2)	N(2)–Co(2)–N(5)	91.3(2)
N(3)–Co(2)–N(5)	90.9(2)	N(4)–Co(2)–N(5)	90.8(2)
N(1)–Co(2)–C(16)	87.5(2)	N(2)–Co(2)–C(16)	87.9(2)
N(3)–Co(2)–C(16)	90.6(2)	N(4)–Co(2)–C(16)	90.0(2)
N(5)–Co(2)–C(16)	178.3(2)	C(14)–C(15)–C(16)	118.7(13)
Co(2)–C(16)–C(15)	116.7(5)	Co(2)–C(16)–C(17)	117.8(6)
C(15)–C(16)–C(17)	125.5(6)	C(16)–C(17)–C(18)	123.1(17)

refinement parameters as well as selected bond lengths and angles are provided in Tables 5 and 6. The cobalt to dmg nitrogen (N(1)–N(4)) and cobalt to N(5) bond lengths are all very similar to those we have observed previously in related dienyl complexes.[1] The cobalt–C(16) bond length (2.019(6) Å) is the longest cobalt to sp^2 carbon bond length we have seen in a dienyl complex to date.[1] C(14) and C(18) of the diene portion of this molecule are disordered over two positions with occupancies of 60/40; therefore, comparisons of C–C bond lengths within this diene to those in our other crystallographically characterized dienyl complexes are not meaningful. The C(18)–C(17)–C(16)–C(15) torsion angle (diene torsion angle) is 56°, within the range of torsion angles we have previously observed.[1]

Preparation of 1-Cobalt-Substituted 4-Methyl-2,3-pentadiene and 3-Cobalt-Substituted 2-Methyl-2,4-hexadienes. The terminally disubstituted allenic tosylate **16e** proved to be the only instance where we observed an S_N2 rather than S_N2' product from the reaction of a cobalt nucleophile with an allenic electrophile. This reaction was initially performed in MeOH,[1b] where hydrogen bonding increases the effective size of the cobalt nucleophile such that S_N2 dominated over S_N2'. However, performing the same reaction in THF[14b] still produced only the S_N2 product **26** (44%). With a terminally disubstituted secondary rather than primary allenic electrophile (**16f**), reaction with the cobalt anion **25** once again produced the S_N2' product **27**. Surprisingly, this reaction failed in all attempts in polar aprotic solvents and failed using the pivalate **16g** rather than the acetate **16f**, possibly due to the fact that E2 or E2′ is the dominant reaction in those solvents with these hindered electrophiles (**16f,g**).

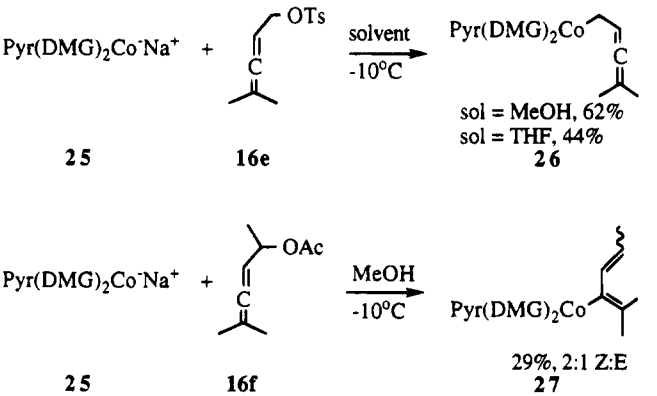

4 + 2 Cycloaddition Reactions of Cobalt-Substituted 1,3-Diene Complexes. We had previously shown that complexes **17a–c** reacted with a variety of disubstituted dienophiles in *exo* selective Diels–Alder reactions performed at 25 °C, where no double-bond isomerization is taking place.[1b] However, we also noted that these same complexes (**17a–c**) reacted with methyl vinyl ketone (MVK) with poor *endo*:*exo* selectivity ranging from 5.0:1 for **17a** to 2.1:1 for **17f**. Unlike the cycloadditions with dienophiles containing two electron-withdrawing groups, these reactions had to be performed in refluxing solvents where double-bond isomerization is occurring simultaneously with cycloaddition. What effect does this double-bond isomerization have on the *endo*:*exo* selectivity of the cycloadditions? Clean **17aE** reacted with maleic anhydride (**28**) in THF at 25 °C to provide a 2.3:1 mixture of *anti*:*syn* cycloadducts (**29**:**30**). A 2.4:1 mixture of *E*:*Z* isomers of **17a** also reacted with maleic anhydride (**28**) in THF at 25 °C to provide a 2.3:1 mixture of *anti*:*syn* cycloadducts (**20**:**30**). The same two reactions performed in $CDCl_3$ produced identical results. Qualitatively, by ^{1}H NMR spectroscopy in $CDCl_3$, we can say that the rate constant for the *E* isomer cycloaddition is faster than *Z* to *E* isomerization, since the relative *E*:*Z* amount of **17a** dropped from 2.4:1 to 1:1 after 5 min. We conclude that the rate of *Z* isomer cycloaddition must be much slower than *E* cycloaddition and *Z*:*E* isomerization. To prove this, we independently prepared the *Z* isomer **32** from the enyne **31**,[16] and we found that it (**32**) isomerized slowly at 25 °C and faster in refluxing THF (16 h, 2.4:1 *E*:*Z*). Treatment of initially pure *Z* isomer **32** with maleic anhydride (**28**) (5 h reflux in THF) produced the same ratio of cycloadducts (**29**:**30**) as the *E* isomer of **17a**. To check for the unlikely possibility that the *Z* isomer was reacting through an *endo* transition state

(16) Pasto, D. J.; Timmers, D. A. *Inorg. Chem.* **1984**, *23*, 4117.

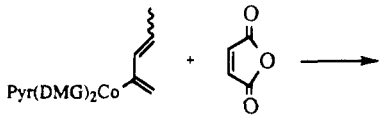

17a **28**

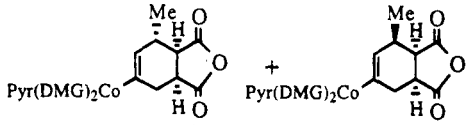

anti syn

29 **30**

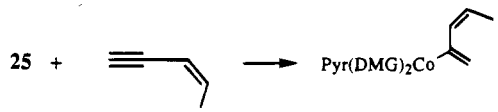

31 **32** (70%)

with the same selectivity that the *E* isomer had for an *exo* transition state, we treated **32** with MA under conditions where the *Z* isomer **32** did not isomerize (0 °C, $CDCl_3$). The reaction required 10 days to go to completion and produced a 1:1 mixture of *anti* and *syn* cycloadducts (**29**:**30**). We therefore conclude (since the *E* isomer is so much more reactive in cycloaddition) that even if we perform cycloadditions under conditions where the *E* double bond isomerizes, the cycloaddition product ratios that we observe have not been affected by this concurrent isomerization.

As shown in Table 7, we next surveyed a variety of solvents and temperatures for the reaction of the pyr-$(dmg)_2Co$ diene **17a** with MVK. Performing the cycloaddition under conditions where the diene isomerized (THF reflux) or not ($CHCl_3$, 25 °C, −22 °C) has little effect on *syn*:*anti* (*endo*:*exo*) selectivity (consistent with the results reported for MA). Selectivity also changes little in going from nonpolar to polar aprotic to polar protic solvents.

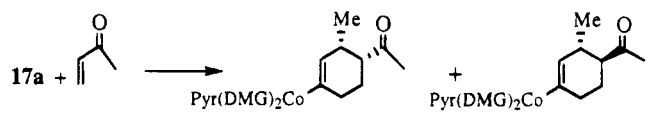

syn (endo) anti (exo)

33 **34** **35**

The effect of changes in axial ligand on syn:anti selectivity were investigated on the basis of literature precedent that electron-withdrawing axial ligands lead to shorter cobalt−carbon bonds[17] (better exo selectivity?) and electron-donating ligands lead to longer cobalt−carbon bonds[17] (better endo selectivity?). Phosphines as axial ligands were known to distort the equatorial glyoximes up toward the cobalt−carbon bond in related alkyl cobaloxime chemistry,[17] and this could be expected to influence the stereochemical outcome of subsequent 4 + 2 cycloadditions. The results of these cycloadditions

(17) For reviews of structural aspects of cobaloxime and related complexes see: (a) Randaccio, L.; Bresciani Pahor, N.; Zangrando, E.; Marzilli, L. G. *Chem. Soc. Rev.* **1989**, *18*, 225. (b) Bresciani-Pahor, N.; Forcolin, M.; Marzilli, L. G.; Randaccio, L.; Summers, M. F.; Toscano, P. J. *Coord. Chem. Rev.* **1985**, *63*, 1. (c) Toscano, P. J.; Marzilli, L. G. *Prog. Inorg. Chem.* **1984**, *31*, 105.

Table 7. Reactions of 17a with MVK

entry no.	conditions	**34:35**	yield (%)
1	THF/reflux	5.0:1	95
2	$CHCl_3$, 25 °C	2.7:1	98
3	$CHCl_3$, −22 °C	3.8:1	99
4	95% EtOH, 25 °C	4.2:1	87
5	acetone/reflux	2.2:1	94
6	toluene/reflux	4.8:1	47

Table 8. Axial Ligand Variation on *syn*:*anti* (36:37) Ratios

L	ratio (**37**:**37**)	yield (%)
pyr (**17a**)	5.0:1	95
DMAP (**17b**)	3.0:1	85
4-CN-pyr (**17d**)	4.2:1	76
PBu_3 (**17f**)	2.1:1	54
PPh_2Me (**17e**)	2.8:1	54

are presented in Table 8. None of these axial ligand changes had a tremendous impact on *syn*:*anti* selectivity. *Syn* (*endo*) selectivity decreased with phosphine substitution, probably due to phosphine-induced out-of-plane distortion of the dmgs up toward the diene. Assignment of *syn* and *anti* stereochemistry was done by ^1H NMR spectral analogy to cycloadducts whose stereochemistry had previously been rigorously proven.[1b] The ^1H NMR signal for the methyl on the cyclohexene ring in the *syn* isomer is always further upfield than that for the *anti* isomer.

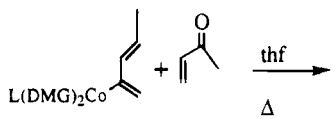

17 **33**

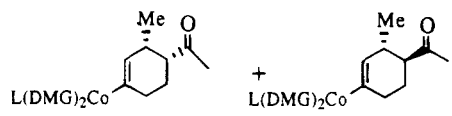

syn (endo) anti (exo)

36 **37**

Dienyl complexes containing cobalt and carbon substituents on internal diene carbons (**21**−**23**) unfortunately proved unreactive in Diels−Alder reactions under a variety of conditions with several different dienophiles. Pyridine complex **21** proved to be unreactive toward MA in refluxing THF or in a sealed tube (85 °C, 13 h). Unreacted **21** was recovered nearly quantitatively. At temperatures above 100 °C there is significant decomposition of **21**. Complexes **21** and **22a** proved unreactive toward MVK in neat refluxing MVK, and **21** did not react with dimethyl fumarate which had been precomplexed with $AlCl_3$ at −20 °C. The DMAP dienyl complex **22a** proved less thermally stable than **21**, and when heated with maleic anhydride in THF, we noted significant diene decomposition with the remaining material (29%) being unreacted **22a**. Diphenylmethylphosphine complex **22b** proved to be the most thermally sensitive. This complex was unreactive toward MA, *N*-phenylmaleimide and MVK at 25 °C in THF and rapidly decomposed when refluxed in neat MVK.

The vinylcyclohexenyl complexes **23** proved to be more thermally robust than the methyl-substituted dienes **21** and **22**, but they were equally unreactive in Diels−Alder

reactions. The pyridine and DMAP dmg complexes **23a,c** proved to be unreactive toward benzoquinone and diethyl acetylenedicarboxylate when heated in a sealed tube at 120 °C in THF, toluene, or 1,2-dichloroethane. The DMAP dpg complex **23b** was slightly more thermally sensitive than **23a** or **23c** and proved to be unreactive toward benzoquinone or MA when heated at 80 °C for 24 h in THF (sealed tube). Likewise a Lewis acid catalyzed reaction of **23b** with MVK ($AlMe_3$, CH_2Cl_2, −45 °C, 24 h, $iPrOH/H_2O$ −45 °C quench) also yielded only recovered **23b**. Lewis acid catalyzed attempts must be done at low temperature only, since at −10 °C and above Lewis acids cleave the cobalt−carbon bond in these complexes.[1]

The 3-cobalt-substituted (3*E*)-1,3-pentadiene complexes (**24**) proved less reactive in Diels−Alder reactions than the 2-cobalt-substituted dienes **17**. The position of the methyl in the 3-cobalt-substituted dienes **24** should hinder attaining an *s-cis* diene conformation. Initially, we tried benzoquinone with pyridine complex **24a**. No cycloadduct was seen, and significant diene decomposition was noted (35−55%) in refluxing THF or $CHCl_3$ (6−12 h). DMAP dmg diene **24b** proved equally unreactive toward benzoquinone but more thermally robust. We recovered 95% of unreacted **24b** after heating 24 h with benzoquinone in a sealed tube in toluene at 50 °C. The DMAP diene complex **24b** did react with MA, as did the methyldiphenyl- and phenyldimethylphosphine complexes **24d,e**. The DMAP diene **24b** reacted with excellent syn (*exo*) selectivity (**38c**:**39c** = 17.5:1). These reaction conditions are much milder than those typically used for (*Z*)-piperylene,[12] and again with transition-metal-substituted dienes and a disubstituted dienophile we see predominantly products which arise via reaction through *exo* transition states.[18,19] Since the mass balance of the phosphine diene cycloadditions **24d,e** was low, we hesitate to compare diastereoselectivities with **24b**. However, the anti (*exo*) selectivity noted here for DMAP complex **24b** (17.5:1) is significantly better than the selectivity we observed with 2-cobalt-substituted (3*E*)-pentadienes **17**. Presumably in the case of complex **24b**, the methyl substituent on the diene and the metal's equatorial ligands provide steric hindrance to an *endo* transition state.

The relative stereochemistry in **38c** was proven by cleavage to anhydride **40**, which had a ^1H NMR spectrum identical with that of an authentic sample.[12] The cobalt with ligand set intact (**41**) is also recovered (69%) in a form which can be recycled into preparation of the dienyl complex. Complex **24b** proved unreactive toward citraconic anhydride or cyclohexenone under similar

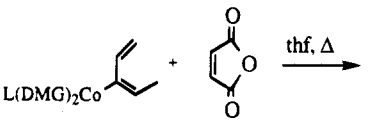

24b L = DMAP
24d L = PPh_2Me
24e L = $PPhMe_2$

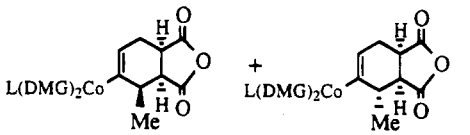

syn (exo) **38** anti (endo) **39**

a) L = PPh_2Me	3.7	:	1	14%
b) L = $PPhMe_2$	2.2	:	1	34%
c) L = DMAP	17.5	:	1	98%

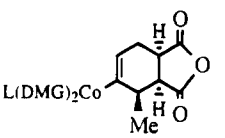

38c

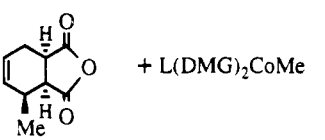

40 (45%) **41** (69%)

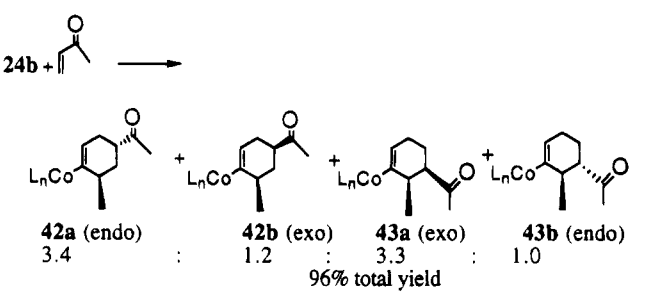

42a (endo)		**42b** (exo)	**43a** (exo)		**43b** (endo)
3.4	:	1.2	: 3.3	:	1.0

96% total yield

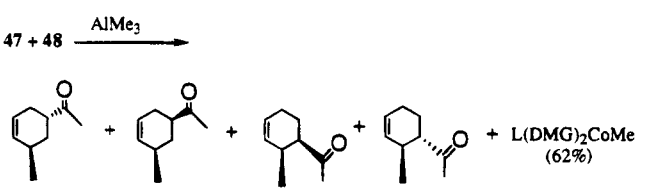

44a	**44b**	**45a**	**45b**
4.8	1.4	3.2	1.0

79% total yield (meta:ortho products 1.1:1.0)

E-piperylene/MVK	1.0	1.6	4.5	3.1
150°C	56% total yield (ortho:meta products 4.0:1.0)			

conditions but did react with MVK (neat, 75 °C, 72 h) to produce a mixture of regio- and stereoisomers (**42a,b** and **43a,b**) in 96% yield. The regio- and stereoisomeric mixture (**44a,b** and **45a,b**) obtained was also proven after cobalt−carbon bond cleavage via ^1H NMR spectral comparison with authentic samples.[13] Cobalt complex **41** was also recovered from this cleavage reaction. The regio- and stereochemical outcome of the thermal Diels−Alder reaction of this cobalt-substituted diene (**24b**) with MVK is very different from the outcome of the reaction of (*E*)-piperylene with MVK. 1,2-Disubstituted cyclohexenes **45** are the major products of the (*E*)-piperylene

(18) For some other recent examples of stoichiometric reactions of transition-metal complexes in Diels−Alder reactions see: (a) Sabat, M.; Reynolds, K. A.; Finn, M. G. *Organometallics* **1994**, *13*, 2084. (b) Gilbertson, S. R.; Zhao, X.; Dawson, D. P.; Marshall, K. L. *J. Am. Chem. Soc.* **1993**, *115*, 8517. (c) Laschat, S.; Noe, R.; Riedel, M.; Kruger, C. *Organometallics* **1993**, *12*, 3738. (d) Wulff, W. D.; Powers, T. S. *J. Org. Chem.* **1993**, *58*, 2381. (e) Rahm, A.; Wulff, W. D.; Rheingold, A. L. *Organometallics* **1993**, *12*, 597. (f) Uemura, M.; Hayashi, Y.; Hayashi, Y. *Tetrahedron: Asymmetry* **1993**, *4*, 2291. (g) Anderson, B. A.; Wulff, W. D.; Powers, T. S.; Tribbitt, S.; Rheingold, A. L. *J. Am. Chem. Soc.* **1992**, *114*, 10784. (h) Bhaduri, D.; Nelson, J. H.; Day, C. L.; Jacobson, R. A.; Solujic, L.; Milosavljevic, E. B. *Organometallics* **1992**, *11*, 4069. (i) Park, J.; Kang, S.; Whang, D.; Kim, K. *Organometallics* **1992**, *11*, 1738. (j) Muller, G.; Jas, G. *Tetrahedron Lett.* **1992**, *33*, 4417−4420.

(19) For a recent report of an alternative approach to achieving *exo* selective Diels−Alder reactions, see: Maruoka, K.; Imoto, H.; Yamamoto, H. *J. Am. Chem. Soc.* **1994**, *116*, 12115.

reaction, and there is a preference for the 1,2-product **45a** resulting from an *endo* transition state. In contrast, cobalt-substituted diene **24b** yielded 1,3-disubstituted cyclohexenes (**44**) as the major products. Presumably, this gives an indication of the electron-donating effect of the transition-metal complex in comparison to the electron-donating effect of an alkyl substituent on the diene. The major 1,3-product **42a** results from reaction through an *endo* transition state. With monosubstituted dienophiles, we had previously observed this *endo* preference for other related cobalt dienes (i.e. the bulk of the complex is not sufficient to override the *endo* Diels–Alder preference for small dienophiles).[1] However, the major 1,2-product (**43a**) was the result of reaction through an *exo* transition state. Presumably, the bulk of the cobalt's equatorial ligands in conjunction with the methyl on the diene have caused this *exo* preference for the 1,2-product. While we have reported many cases of *exo*-selective Diels–Alder reactions of cobalt dienes with disubstituted dienophiles, this is the first *exo*-selective result for a monosubstituted dienophile.

Conclusions

A variety of cobaloxime-substituted 1,3-dienes can be conveniently prepared via reactions of cobaloxime anions with allenic electrophiles. Ligands axial to the diene are easily exchanged. When cobalt is in the 2-position of a 1,3-diene, substituents can be stereospecifically placed in the 1- or 4-position of the diene (complexes **24** and **17**) and these dienes will participate in 4 + 2 cycloadditions under conditions which are much milder than their organic counterparts ((*E*)- and (*Z* piperylenes). When dienophiles contain two electron-withdrawing substituents, preference for Diels–Alder reactions through *exo* transition states can be quite high. Unfortunately, *syn*:*anti* Diels–Alder selectivity for monosubstituted dienophiles is low regardless of which commercially available glyoxime (dmg or dpg) or axial ligand is used, and this problem will probably be solved via modified glyoxime synthesis in conjunction with Lewis acid catalysis. The regiochemical outcome of the Diels–Alder reaction between **24b** and MVK hints that, with the right ligand set and conditions, we might gain clean access to 1,3-disubstituted (meta) cyclohexenes which are not accessible via standard Diels–Alder chemistry. 1,3-Dienes substituted by cobalt and carbon in the 2- and 3-positions (**21**–**23**) proved unreactive in Diels–Alder reactions. The solution to this problem will probably require synthesis of analogous dienes with cobalt substituents in the 1-position.

Acknowledgment. We thank the National Science Foundation (Grant No. CHE-9321454), the Wake Forest University Research and Creative Activities Fund, the donors of the Petroleum Research Fund, administered by the American Chemical Society, the Exxon Education Foundation, and the Camille and Henry Dreyfus Foundation (Henry Dreyfus Teacher-Scholar Award to M.E.W, 1994–1999) for their support. Low-resolution mass spectra were obtained on an instrument purchased with the partial support of the NSF (Grant No. CHE-9007366). The Midwest Center for Mass Spectrometry (Grant No. NSF DIR9017262) performed high-resolution mass spectral analyses. M.W.W. and H.L.S. acknowledge Sigma Xi for student grants-in-aid of research.

Supporting Information Available: Tables of atomic coordinates, thermal parameters, bond distances, and bond angles for **24f** (7 pages). This material is contained in many libraries on microfiche, immediately follows this article in the microfilm version of the journal, can be ordered from the ACS, and can be downloaded from the Internet; see any current masthead page for ordering information and Internet access instructions.

OM950499J

Synthesis of a Novel Cyclic Germanium Enamine from Germylene and 2-Vinylpyridine and Its Stereoselective Aldol Type Reaction with Aldehydes

Satoru Iwata, Shin-ichiro Shoda, and Shiro Kobayashi*

Department of Molecular Chemistry and Engineering, Faculty of Engineering, Tohoku University, Aoba, Sendai 980, Japan

Received July 21, 1995[⊗]

A novel cyclic germanium(IV) enamine **3** has been prepared by the reaction of a germylene, bis[bis(trimethylsilyl)aminato]germanium(II) (**1**), and 2-vinylpyridine (**2**). The aldol type reaction of the resulting enamine with various aldehydes **4** gave condensation products of 4,5-disubstituted 1-oxa-2-germacyclopentane derivatives **5**. The reaction proceeds in a stereoselective manner to give *trans* products when aliphatic aldehydes were used as electrophiles. In the case of using aromatic aldehydes, *cis* isomers predominate. The preferential formation of a *cis* or *trans* isomer was explained by assuming an acyclic transition state for the aldol type reaction.

Introduction

Enamines have greatly contributed to the progress of synthetic organic chemistry because of their high reactivity toward various electrophiles.[1] Especially, lithoenamines have most frequently been utilized as nucleophiles in cross aldol reactions, alkylations, and asymmetric syntheses.[2] In recent years, the development of a C–C bond-forming reaction which proceeds via a novel organometallic intermediate having a central metal of higher atomic number is of growing interest in organic synthesis. Much attention has been paid to the structure and reactivity of organogermanium species as reactive intermediates. Although there are several reports on germanium enolate formation and their reactivities,[3–5] little is known about the synthesis and reactivity of germanium enamines. Normally, a germanium enamine is obtained only as the tautomer of an *N*-germylimine prepared by the reaction of tetravalent halogermanes and iminolithium derivatives;[6] there has been no report of the preparation of a germanium enamine starting from a divalent germanium compound (germylene).

Recently, in the course of our investigations on the development of new polymerizations using germylene species,[7] we found that a stable germylene, bis[bis(trimethylsilyl)aminato]germanium(II),[8] undergoes a rapid addition reaction to various α,β-unsaturated carbonyl compounds with *s-cis* conformation to give the corresponding cyclic germanium enolate.[4] We have also demonstrated the synthesis of a poly(germanium enolate) by using a cyclic α,β-unsaturated ketone with *s-trans* conformation.[5] Here, we report synthesis of a novel bicyclic germanium(IV) enamine **3** by the reaction of the germylene **1** and 2-vinylpyridine (**2**). The aldol type reaction of the resulting enamine with various aldehydes **4** gives rise to 4,5-disubstituted 1-oxa-germacyclopentane derivatives **5**.[9]

Results and Discussion

Synthesis of Germanium Enamine 3. The addition reaction of the germylene **1** to 2-vinylpyridine (**2**) occurred instantaneously at room temperature to afford the corresponding germanium(IV) enamine **3** in 95% yield (Scheme 1). The resulting enamine has a novel bicyclic structure fused by a 1-aza-2-cyclogermapent-4-ene ring (five-membered) and a 1-azacyclohexa-3,5-diene ring (six-membered).

The reaction was carried out in benzene-d_6 in an NMR sample tube, and the formation of the enamine was directly confirmed by ^{1}H NMR spectroscopy. The ^{1}H NMR spectrum of the resulting enamine showed a signal at δ 4.33 ppm ascribable to the olefinic proton in the 1-aza-2-cyclogermapent-4-ene (five-membered) moiety. The peak at δ 1.84 ppm can be assigned to the methylene protons adjacent to the germanium atom. The signals at δ 0.36 and 4.3–7.1 are due to the protons

[⊗] Abstract published in *Advance ACS Abstracts,* November 1, 1995.

(1) (a) Dyke, S. F. *The Chemistry of Enamine*; Cambridge University Press: Cambridge, U.K., 1973. (b) Reiff, H. *Newer Methods of Preparative Organic Chemistry*; Foerst, W., Ed.; Academic Press: New York, 1971; Vol. 6, p 48. (c) Wittig, G.; Hesse, A. *Org. Synth.* **1970**, *50*, 66.

(2) (a) Stork, G.; Terrell, R.; Szmuszkovisz, J. *J. Am. Chem. Soc.* **1954**, *76*, 2029. (b) Meyers, A. I.; Williams, D. R.; Druelinger, M. *J. Am. Chem. Soc.* **1976**, *98*, 3072. (c) Meyers, A. I. *Acc. Chem. Res.* **1978**, *11*, 375.

(3) (a) Lutsenko, I. F.; Baukov, Y. I.; Belavin, I. Y.; Tvorogov, A. N. *J. Organomet. Chem.* **1968**, *14*, 229. (b) Michel, E.; Neumann, W. P. *Tetrahedron Lett.* **1986**, *27*, 2455. (c) Inoue, S.; Sato, Y. *Organometallics* **1987**, *6*, 2568. (d) Yamamoto, Y.; Hatsuya, S.; Yamada, J. *J. Chem. Soc., Chem. Commun.* **1988**, 1639.

(4) Kobayashi, S.; Iwata, S.; Shoda, S. *Chem. Express* **1989**, *4*, 41.

(5) (a) Kobayashi, S.; Iwata, S.; Yajima, K.; Shoda, S. *J. Am. Chem. Soc.* **1992**, *114*, 4929. (b) Kobayashi, S.; Shoda, S. *Adv. Mater.* **1993**, *5*, 57.

(6) (a) Chan, L. H.; Rochow, E. G. *J. Organomet. Chem.* **1967**, *9*, 231. (b) Lappert, M. F.; Palmer, D. E. *J. Chem. Soc., Dalton Trans.* **1973**, 157. (c) Keable, J.; Othen, D. G.; Wade, K. *J. Chem. Soc., Dalton Trans.* **1976**, 1.

(7) (a) Kobayashi, S.; Iwata, S.; Abe, M.; Shoda, S. *J. Am. Chem. Soc.* **1990**, *112*, 1625. (b) Kobayashi, S.; Cao, S. *Chem. Lett.* **1993**, 25. (c) Kobayashi, S.; Cao, S. *Chem. Lett.* **1993**, 1385. (d) Kobayashi, S.; Iwata, S.; Hiraishi, M. *J. Am. Chem. Soc.* **1994**, *116*, 6047. (e) Kobayashi, S.; Iwata, S.; Abe, M.; Shoda, S. *J. Am. Chem. Soc.* **1995**, *117*, 2187.

(8) (a) Harris, D. H.; Lappert, M. F. *J. Chem. Soc., Chem. Commun.* **1974**, 895. (b) Gynane, M. J. S.; Harris, D. H.; Lappert, M. F.; Power, P. P.; Rivière, P.; Rivière-Baudet, M. *J. Chem. Soc., Dalton Trans.* **1977**, 2004.

(9) The present study was previously presented in part: Kobayashi, S.; Shoda, S.; Iwata, S. *Annu. Meet. Chem. Soc. Jpn. Prepr.* **1991**, *61*, 1818.

0276-7333/95/2314-5533$09.00/0

Scheme 1

Scheme 2

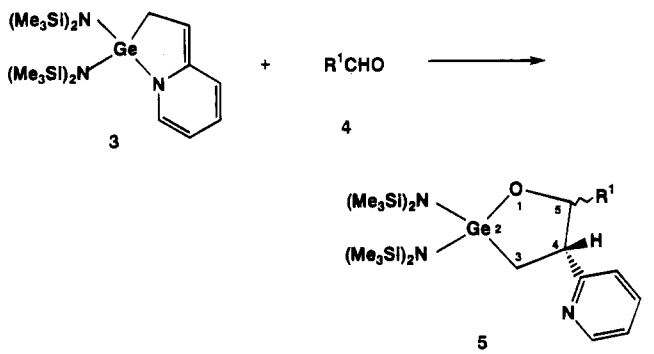

Table 1. Aldol Reaction of Cyclic Germanium Enamine 3 with Various Aldehydes[a]

entry	aldehyde	aldol product	yield (%)[b]	diasteromer ratio[c] *cis:trans*
1	CCl_3CHO	**5a**	87	4:96
2	MeCHO	**5b**	82	26:74
3	EtCHO	**5c**	79	35:65
4	$PhCH_2CHO$	**5d**	78	28:72
5	PhCHO	**5e**	90	75:25
6	*m*-ClPhCHO	**5f**	90	75:25
7	*m*-ClPhCHO	**5f**	87	76:24
8	*m*-ClPhCHO	**5f**	89	71:29

[a] Reaction was carried out in toluene at room temperature under argon. [b] Isolated yield. [c] Determined by ^1H NMR.

of the trimethylsilyl groups and the olefins in the 1-azacyclohexa-3,5-diene (six-membered ring) moiety, respectively. The ^{13}C NMR spectrum also supported the bicyclic germanium enamine structure **3**. These results clearly show that germylene **1**, having a bulky electron-donating group on the germanium atom, has a strong nucleophilicity toward the carbon–carbon double bond conjugated with the pyridine ring. It is to be noted that the pyridine structure is destroyed and transformed to the bicyclic enamine structure as a result of the germanium–carbon bond formation at the terminal vinyl carbon of 2-vinylpyridine and the germanium–nitrogen bond formation.

Aldol Type Reaction of 3 with Aldehydes. The germanium enamine **3** showed nucleophilic reactivity, which is characteristic of a metal–enamine compound. When the enamine **3** was treated with an aldehyde **4** which acts as an electrophile in toluene at room temperature, an aldol type reaction took place smoothly to afford a 1-oxa-2-germacyclopentane derivative **5** having a pyridyl group and an alkyl group at the 4 and 5 positions, respectively (Scheme 2).

The yield of the aldol reaction and the diastereomer ratio (*cis:trans*) of the condensation product **5** are summarized in Table 1. All the reactions proceeded smoothly at room temperature to give **5** in good yield (78–90%). The nucleophilic attack at the aldehyde takes place regioselectively at the carbon–carbon double bond in the five-membered ring of **3**. At the same time, cleavage of the germanium–nitrogen bond occurs, regenerating the pyridine ring. It is assumed that the stabilization due to the aromaticity of the pyridine is an important driving force to promote the aldol reaction.

Table 2. NMR Parameters and NOE for the *Cis* or *Trans* Isomer of Aldol Product 5

aldol product	irradiated H	NOE (%) at H^1	NOE (%) at H^3	NOE (%) at H^4	$J(H^3-H^4)$	^{13}C NMR chem shift of $GeCH_2$(ppm)
5a						
cis	H^3	5.0		8.2	6.9	23.3
	H^4		6.2			
trans	H^3	2.6		1.0	8.6	33.7
5b						
cis	H^3	7.5		5.7	6.4	21.0
	H^4		4.9			
trans	H^3	5.3			10.1	29.9
5c						
cis	H^3	6.1		*a*	6.3	22.2
	H^4		0.7			
trans	H^3	3.1			10.1	30.0
5d						
cis	H^3	4.3		7.5	6.3	23.2
	H^4		9.2			
trans	H^3	2.4		1.6	10.2	30.6
	H^4		1.7			
5e						
cis	H^3	6.0		9.9	6.2	23.1
	H^4		11.0			
trans	H^3	2.9		1.8	9.9	30.1
	H^4		1.8			
5f						
cis	H^3	5.3		10.3	6.6	22.7
	H^4		10.6			
trans	H^3	1.1		1.1	9.9	30.2
	H^4		2.5			

[a] NOE was not detected because of the short distance between H^3 and H^4.

The aldol reaction was found to proceed in a stereoselective manner. When aliphatic aldehydes were used as electrophiles, *trans* isomers were obtained preferentially (entries 1–4). Especially, a product of higher diastereoselectivity (*cis:trans* = 4:96) was obtained with chloral (trichloroacetaldehyde) as the electrophile (entry 1). Treatment of **3** with aromatic aldehydes (benzaldehyde and *m*-chlorobenzaldehyde) also gave the corresponding condensation products in good yield. In this case, the *cis* isomers were obtained predominantly (entries 5–8). The diastereomeric ratio of the aldol product was determined by comparing the integral values of the peaks due to the methyne proton (4 positions) of **5** in the ^1H NMR spectrum of the mixture of *cis* and *trans* isomers (*cis* isomer, δ 3.59–3.93; *trans* isomer, δ 2.93–3.52). The resulting 1-oxa-2-germacyclopentane derivative **5** was found to be stable at room temperature, and each diastereomer can be separated by silica gel column chromatography without decomposition.

Structure Determination of Aldol Product 5. The relative configuration (*cis:trans*) between the pyridyl group at the 4 position and the alkyl group at the 5 position of the product **5** was determined by a nuclear Overhauser effect (NOE) measurement on the ^1H NMR spectra (Table 2). For example, when the signal derived from the proton on carbon 4 (denoted by H^3 in Figure 1) of product **5e** was irradiated, the spectrum of the main isomer showed a larger NOE between H^3 and H^4 (9.9%). Irradiation of the proton on carbon 5 (denoted by H^4 in Figure 1) also caused a large NOE (11.0%) observation between H^3 and H^4. These results clearly indicate that proton H^3 and proton H^4 are located close each other, suggesting that these substituents on the 4 and 5 positions of the main isomer have a *cis* relationship. On the other hand, the minor isomer showed a smaller NOE (1.8%) between H^3 and H^4, indicating that

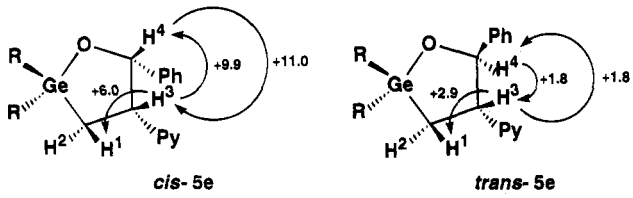

cis-5e *trans*-5e

Figure 1. NOE of aldol products *cis*-**5e** and *trans*-**5e**.

Scheme 3

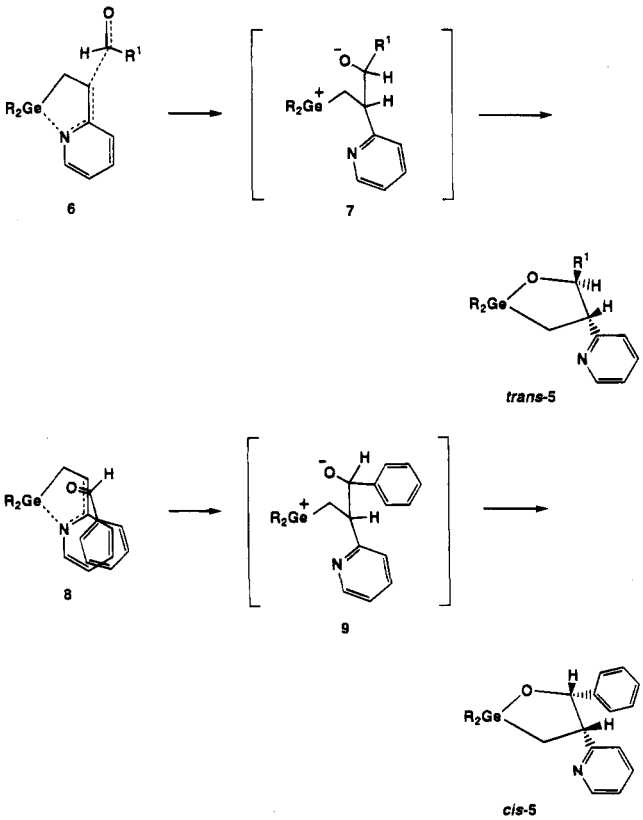

the relative configuration of these substituents is *trans*. The structure determinations of other products (**5a–d** and **5f**) were carried out in a similar manner.

In addition to the NOE measurements, the coupling constant between H^3 and H^4 ($J(H^3-H^4)$) as well as the ^{13}C chemical shift of the methylene carbon adjacent to the germanium atom ($GeCH_2$) also give useful information about the structure of *cis* and *trans* isomers (Table 2). The coupling constants ($J(H^3-H^4)$) of the *trans* isomer are 8.6–10.2 Hz, whereas those of *cis* isomer show smaller values of 6.2–6.9 Hz. The chemical shifts for the carbon atoms adjacent to the germanium atom in the two isomers show a remarkable difference; the chemical shift values for the *cis* isomer are 21.0–23.3 ppm whereas those of *trans* isomer are 29.9–33.7 ppm. These NMR parameters are especially useful to confirm the relative configuration of the product **5c** whose NOE can only be partly detected.

Reaction Mechanism. At present, the formation of the 1-oxa-2-germacyclopentane skeleton **5** may be explained as follows (Scheme 3). The nucleophilic attack of germanium enamine **3** on the aldehyde takes place regioselectively at the carbon atom on the five-membered ring to give a corresponding zwitterionic intermediate **7** (or **9**) having an alkoxide ion and a germanium cation. Then, this intermediate undergoes a nucleophilic intramolecular attack of the alkoxide ion at the germanium cation giving rise to the cyclic aldol product **5**.

Concerning the stereoselectivity of the present reaction, the preferential formation of the *trans* isomer can be explained by assuming an acyclic transition state **6**,[10] where a chelate formation between Ge and oxygen does not occur because of the lower Lewis acidity of the germanium atom having bulky electron-donating groups. As mentioned above, the use of benzaldehyde or *m*-chlorobenzaldehyde as the electrophile affords the *cis* isomer preferentially. These results suggest that the reaction proceeds via a different transition state in the case of an aromatic aldehyde. The transition state **8** may be preferable due to the $\pi-\pi$ interaction between the 1-azacyclohexa-3,5-diene part of the enamine and benzene ring of the aldehyde, leading to the preferential formation of the *cis* isomer via the intermediate **9**.

Conclusion

The oxidative addition of 2-vinylpyridine to the germylene bis[bis(trimethylsilyl)aminato]germanium(II) gave a novel bicyclic germanium enamine having a 1-azacyclohexa-3,5-diene structure. The resulting enamine was successfully condensed with various aldehydes via an aldol type reaction giving rise to the corresponding 4,5-disubstituted 1-oxa-2-germacyclopentane derivatives in good yield. To our best knowledge, the present reaction is the first example of a carbon–carbon bond-forming reaction using a cyclic germanium enamine species which can be constructed by a redox process starting from a divalent germanium compound, a germylene. It is also to be noted that the aldol product is a new 1-oxa-2-germacyclopentane derivative having a pyridyl group and an alkyl group at the 4 and 5 positions, respectively, where the stereochemistry of these groups can be fairly well controlled. The skeleton of the resulting 4,5-disubstituted 1-oxa-2-germacyclopentane is very difficult to construct by the conventional methodology of using a germanium(IV) compound as starting material.

Experimental Section

General Procedure. The germylene bis[bis(trimethylsilyl)aminato]germanium(II) (**1**) was prepared according to the literature.[8] 2-Vinylpyridine and aldehydes were distilled over calcium hydride. Toluene was purified by distillation from benzophenone ketyl before use. All reactions were carried out under an argon atmosphere. Column chromatography was performed with silica gel 60 (70–230 mesh) (Merck). NMR spectra (^1H and ^{13}C) were recorded on a Brucker AM-250T spectrometer.

Preparation of Germanium Enamine 3. A solution of bis[bis(trimethylsilyl)aminato]germanium(II) (**1**) (65 mg, 0.17 mmol) in C_6D_6 (0.2 mL) was added to a solution of 2-vinylpyridine (**2**) (17 mg, 0.16 mmol) in C_6D_6 (0.3 mL) at room temperature under argon. The reaction mixture was transferred to a NMR sample tube, and the formation of the germanium enamine **3** was directly confirmed by NMR spectroscopy (95% yield determined by ^1H NMR): ^1H NMR (C_6D_6) δ 0.36 (s, $SiMe_3$, 36H), 1.84 (d, J = 3.6 Hz, CH_2, 2H), 4.33 (t, J = 3.6 Hz, $-CH_2CH{=}C$, 1H), 4.3–7.1 (m, olefin, 4H); ^{13}C NMR (C_6D_6) δ 5.9 ($SiMe_3$), 25.4 (CH_2), 84.6 ($-CH_2CH{=}C$), 101.0, 121.4, 128.0, 137.8, 148.6.

Aldol Type Reaction of 3 with Aldehydes. To a toluene solution (1.6 mL) of the germylene **1** (0.631 g, 1.60 mmol) was added a toluene solution (1.6 mL) of 2-vinylpyridine (**2**) (0.173 g, 1.64 mmol) at 0 °C, and the reaction mixture was stirred

(10) Noyori, R.; Nishida, I.; Sakata, J. *J. Am. Chem. Soc.* **1983**, *105*, 1598.

for 15 min. To this mixture was added a toluene solution (1.6 mL) of chloral (0.240 g, 1.63 mmol) in toluene (1.6 mL) at 0 °C. After being stirred for 15 min, the reaction mixture was concentrated to dryness. The residue was dissolved in $CDCl_3$, and an ^1H NMR spectrum of the condensation products was taken in order to determine the diastereomer ratio (*cis:trans*). After recovery of the products, each diastereomer was separated by silica gel column chromatography (eluent:*n*-hexane/diethyl ether = 5/1) to give 0.041 g of the *cis* isomer and 0.882 g of the *trans* isomer.

Aldol Product 5a. *Cis* isomer: ^1H NMR ($CDCl_3$) δ 0.30 (s, $SiMe_3$, 18H), 0.33 (s, $SiMe_3$, 18H), 1.41 (dd, J_{AB} = 13.1 Hz, J_{BX} = 6.8 Hz, $-CH_AH_B$, 1H), 2.44 (dd, J_{AB} = 13.1 Hz, J_{AX} = 13.7 Hz, CH_AH_B, 1H), 3.91 (ddd, J_{AX} = 13.7 Hz, J_{BX} = 6.8 Hz, J_{XY} = 6.9 Hz, $-CH_2CH_X-$, 1H), 4.83 (d, J_{XY} = 6.9 Hz, CH_Y-O, 1H), 7.1−8.7 (m, pyridyl, 4H); ^{13}C NMR ($CDCl_3$) δ 5.5 ($SiMe_3$), 23.3 (CH_2), 50.2 (CH_2CH), 86.5 (OCH), 102.6 (CCl_3), 122.2, 123.1 (Py, C3, C5), 135.9 (py, C4), 149.0 (py, C6), 159.0 (py, C2).

Trans isomer: ^1H NMR ($CDCl_3$) δ 0.31 (s, $SiMe_3$, 18H), 0.32 (s, $SiMe_3$, 18H), 1.57 (dd, J_{AB} = 13.6 Hz, J_{BX} = 13.2 Hz, CH_AH_B, 1H), 2.16 (dd, J_{AB} = 13.6 Hz, J_{AX} = 7.2 Hz, CH_AH_B, 1H), 3.52 (ddd, J_{AX} = 7.2 Hz, J_{BX} = 13.2 Hz, J_{XY} = 8.6 Hz, CH_2CH_X, 1H), 5.02 (d, J_{XY} = 8.6 Hz, OCH, 1H), 7.1−8.6 (m, pyridyl, 4H); ^{13}C NMR ($CDCl_3$) δ 5.30, 5.66 ($SiMe_3$), 33.7 (CH_2), 49.7 (CH_2CH), 88.3 (OCH), 103.6 (CCl_3), 121.3, 123.2 (py, C3, C5). Anal. Calcd for $C_{21}H_{44}Cl_3GeN_3OSi_4$: C, 39.05; H, 6.87; N, 6.51; Cl, 16.47. Found: C, 39.00; H, 6.96; N, 5.92; Cl, 16.61.

Aldol type reaction using other aldehydes were carried out in a similar manner to afford the corresponding condensation products.

Aldol Product 5b. *Cis* Isomer: ^1H NMR ($CDCl_3$) δ 0.30 (s, $SiMe_3$, 18H), 0.31 (s, $SiMe_3$, 18H), 0.72 (d, J = 6.4 Hz, CH_3, 3H), 1.34 (dd, J_{AB} = 12.9 Hz, J_{BX} = 6.3 Hz, CH_AH_B, 1H), 1.93 (dd, J_{AB} = 12.9 Hz, J_{AX} = 13.0 Hz, CH_AH_B, 1H), 3.59 (ddd, J_{AX} = 13.0 Hz, J_{BX} = 6.3 Hz, J_{XY} = 6.4 Hz, CH_2CH_X, 1H), 4.58 (dq, J_{XY} = 6.4 Hz, J_{Me-HY} = 6.4 Hz, OCH_Y, 1H), 7.1−8.6 (m, pyridyl, 4H); ^{13}C NMR ($CDCl_3$) δ 5.53, 5.66 ($SiMe_3$), 18.7 (Me), 21.0 (CH_2), 49.8 (CH_2CH), 73.4 (OCH), 121.3, 122.1 (py, C3, C5), 136.0 (py, C4), 149.2 (py, C6), 161.5 (py, C2). Anal. Calcd for $C_{21}H_{47}GeN_3OSi_4$: C, 46.49; H, 8.73; N, 7.74. Found: C, 46.06; H, 8.84; N, 7.63.

Trans isomer: ^1H NMR ($CDCl_3$) δ 0.29 (s, $SiMe_3$, 36H), 1.13 (d, J = 5.9 Hz, CH_3, 3H), 1.68 (dd, J_{AB} = 13.5 Hz, J_{BX} = 12.8 Hz, CH_AH_B, 1H), 1.77 (dd, J_{AB} = 13.5 Hz, J_{AX} = 7.2 Hz, CH_AH_B, 1H), 2.93 (ddd, J_{AX} = 7.2 Hz, J_{BX} = 12.8 Hz, J_{XY} = 10.1 Hz, CH_2CH_X, 1H), 4.00 (dq, J_{XY} = 10.1 Hz, J_{Me-HY} = 5.9 Hz, OCH_Y, 1H), 7.1−8.5 (m, pyridyl, 4H); ^{13}C NMR ($CDCl_3$) δ 5.4, 5.7 ($SiMe_3$), 21.4 (CH_3), 29.9 (CH_2), 55.1 (CH_2CH), 75.0 (OCH), 121.3, 122.4 (py, C3, C5), 136.1 (py, C4), 149.5 (py, C6), 163.1 (py, C2). Anal. Calcd for $C_{21}H_{47}GeN_3OSi_4$: C, 46.49; H, 8.73; N, 7.74. Found: C, 46.49; H, 8.56; N, 7.65.

Aldol Product 5c. *Cis* isomer: ^1H NMR ($CDCl_3$) δ 0.27 (s, $SiMe_3$, 18H), 0.29 (s, $SiMe_3$, 18H), 0.77, 0.79 (CH_3, 3H), 0.9−1.1 (m, $MeCH_2$, 2H), 1.35 (dd, J_{AB} = 12.9 Hz, J_{BX} = 6.8 Hz, $GeCH_AH_B$, 1H), 1.89 (dd, J_{AB} = 12.9 Hz, J_{AX} = 12.7 Hz, $GeCH_AH_B$, 1H), 3.64 (ddd, J_{AX} = 12.7 Hz, J_{BX} = 6.8 Hz, J_{XY} = 6.3 Hz, CH_2CH_X, 1H), 4.19 (m, OCH_Y, 1H), 7.1−8.6 (m, pyridyl, 4H); ^{13}C NMR ($CDCl_3$) δ 5.48, 5.69 ($SiMe_3$), 10.8 (CH_3), 22.2 ($GeCH_2$), 25.6 ($MeCH_2$), 49.6 (CH_2CH_X), 78.6 (OCH), 121.3, 122.3 (py, C3, C5), 135.9 (py, C4), 149.2 (py, C6), 161.6 (py, C2). Anal. Calcd for $C_{22}H_{49}GeN_3OSi_4$: C, 47.48; H, 8.87; N, 7.55. Found: C, 47.08; H, 8.87; N, 7.35.

Trans isomer: ^1H NMR ($CDCl_3$) δ 0.29 (s, $SiMe_3$, 36H), 0.93 (t, CH_3, 3H), 1.2−1.4 (m, $MeCH_2$, 2H), 1.62 (dd, J_{AB} = 13.3 Hz, J_{BX} = 13.0 Hz, $GeCH_AH_B$, 1H), 1.81 (dd, J_{AB} = 13.3 Hz, J_{AX} = 6.8 Hz, $GeCH_AH_B$, 1H), 2.97 (ddd, J_{AX} = 6.8 Hz, J_{BX} = 13.0 Hz, J_{XY} = 10.1 Hz, CH_2CH_X, 1H), 3.77 (m, J_{XY} = 10.1 Hz, OCH_Y, 1H), 7.1−8.5 (m, pyridyl, 4H); ^{13}C NMR ($CDCl_3$) 5.4, 5.7 ($SiMe_3$), 11.0 (CH_3), 28.6, 30.0 (CH_2), 53.5 (CH_2CH_X), 80.1 (OCH), 121.3, 122.4 (py, C3, C5), 136.0 (py, C4), 150.0 (py, C6), 163.2 (py, C2). Anal. Calcd for $C_{22}H_{49}GeN_3OSi_4$: C, 47.48; H, 8.87; N, 7.55. Found: C, 47.29; H, 9.02; N, 7.38.

Aldol Product 5d. *Cis* isomer: ^1H NMR ($CDCl_3$) δ 0.24 (s, $SiMe_3$, 18H), 0.29 (s, $SiMe_3$, 18H), 1.48 (dd, J_{AB} = 13.2 Hz, J_{BX} = 6.7 Hz, CH_AH_B, 1H), 1.99 (dd, J_{AB} = 13.2 Hz, J_{AX} = 11.2 Hz, CH_AH_B, 1H), 2.24 (dd, J_{AB} = 14.2 Hz, J_{BX} = 3.5 Hz, CH_AH_B-Ph, 1H), 2.46 (dd, J_{AB} = 14.2 Hz, J_{AX} = 9.2 Hz, CH_AH_BPh, 1H), 3.72 (ddd, J_{AX} = 9.2 Hz, J_{BX} = 3.5 Hz, J_{XY} = 6.3 Hz, OCH_Y, 1H), 7.1−8.6 (m, pyridyl, phenyl, 9H); ^{13}C NMR ($CDCl_3$) δ 5.5, 5.6 ($SiMe_3$), 23.2 ($GeCH_2$), 39.2 (CH_2Ph), 49.6 (CH_2CH_X), 77.9 (OCH_Y), 121.4, 122.6 (py C3, 5), 125.3, 127.6, 129.1 (Ph, C2-6), 135.9 (py, C4), 140.0 (Ph, C1), 149.2 (py, C6), 161.3 (py, C2).

Trans isomer: ^1H NMR ($CDCl_3$) δ 0.09 (s, $SiMe_3$, 18H), 0.29 (s, $SiMe_3$, 18H), 1.60 (dd, J_{AB} = 13.4 Hz, J_{BX} = 13.2 Hz, CH_AH_B, 1H), 1.85 (dd, J_{AB} = 13.4 Hz, J_{AX} = 6.9 Hz, CH_AH_B, 1H), 2.65 (dd, J_{AB} = 13.7 Hz, J_{BX} = 8.5 Hz, CH_AH_BPh, 1H), 2.72 (dd, J_{AB} = 13.7 Hz, J_{AX} = 2.5 Hz, CH_AH_BPh, 1H), 3.09 (ddd, J_{AX} = 6.9 Hz, J_{BX} = 13.2 Hz, J_{XY} = 10.2 Hz, CH_2CH_X, 1H), 4.14 (ddd, J_{AX} = 2.5 Hz, J_{BX} = 8.5 Hz, J_{XY} = 10.2 Hz, OCH_Y, 1H), 7.1−8.6 (m, pyridyl, phenyl, 9H); ^{13}C NMR ($CDCl_3$) δ 5.3, 5.7 ($SiMe_3$), 30.0 ($GeCH_2$), 41.6 (CH_2Ph), 53.1 (CH_2CH_X), 79.6 (OCH_Y), 121.4, 122.5 (py, C3, 5), 125.5, 127.6, 129.6 (Ph, C2-6), 136.2 (py, C4), 140.0 (Ph, C1), 149.6 (py, C6), 163.0 (py, C2).

Aldol Product 5e. *Cis* isomer: δ 0.33 (s, $SiMe_3$, 18H), 0.34 (s, $SiMe_3$, 18H), 1.35 (dd, J_{AB} = 12.7 Hz, J_{BX} = 5.8 Hz, CH_AH_B, 1H), 1.76 (dd, J_{AB} = 12.7 Hz, J_{AX} = 12.4 Hz, CH_AH_B, 1H), 3.93 (ddd, J_{AX} = 12.4 Hz, J_{BX} = 5.8 Hz, J_{XY} = 6.2 Hz), 5.47 (d, J_{XY} = 6.2 Hz, OCH_Y, 1H), 6.6−8.6 (m, pyridyl, phenyl, 9H); ^{13}C NMR ($CDCl_3$) δ 5.4, 5.5 ($SiMe_3$), 23.1 (CH_2), 51.3 (CH_2CH_X), 79.4 (OCH_Y), 121.3, 122.0 (py, C3, C5), 126.3, 126.8, 126.9 (Ph, C2-6), 135.5 (py, C4), 141.2 (Ph, C1), 148.8 (py, C6), 160.1 (py, C2); IR 1582, 1461, 1426, 1399, 1249, 1021, 895, 869, 769, 734, 702, 672, 647 cm^{-1}. Anal. Calcd for $C_{26}H_{49}GeN_3OSi_4$: C, 51.65; H, 8.17; N, 6.95. Found: C, 51.32; N, 8.27; N, 6.67.

Trans isomer: ^1H NMR ($CDCl_3$) 0.32 (s, $SiMe_3$, 18H), 0.35 (s, $SiMe_3$, 18H), 1.88 (dd, J_{AB} = 13.3 Hz, J_{BX} = 12.9 Hz, CH_AH_B, 1H), 2.00 (dd, J_{AB} = 13.3 Hz, J_{AX} = 6.9 Hz, CH_AH_B, 1H), 3.13 (ddd, J_{AX} = 6.9, J_{BX} = 12.9, J_{XY} = 9.9 Hz, CH_2CH_X, 1H), 4.96 (d, J_{XY} = 9.9 Hz, OCH_Y, 1H), 6.6−8.6 (m, pyridyl, phenyl, 9H); ^{13}C NMR ($CDCl_3$) δ 5.43, 5.73 ($SiMe_3$), 30.1 (CH_2), 56.0 (CH_2CH_X), 81.2 (OCH_Y), 121.3, 123.6 (py, C3, C5), 126.3, 126.7, 127.5 (Ph, C2-6), 135.7 (py, C4), 143.8 (Ph, C1), 149.4 (py, C6), 161.8 (py, C2); IR 1581, 1428, 1250, 1010, 876, 854, 761, 701, 672 cm^{-1}. Anal. Calcd for $C_{26}H_{49}GeN_3OSi_4$: C, 51.65; H, 8.17; N, 6.95. Found: C, 51.59; H, 8.14; N, 6.94.

Aldol Product 5f. *Cis* isomer: ^1H NMR ($CDCl_3$) δ 0.33 (s, $SiMe_3$, 18H), 0.36 (s, $SiMe_3$, 18H), 1.35 (dd, J_{AB} = 12.7 Hz, J_{BX} = 5.7 Hz, CH_AH_B, 1H), 1.73 (dd, J_{AB} = 12.7 Hz, J_{AX} = 12.8 Hz, CH_AH_B, 1H), 3.92 (ddd, J_{AX} = 12.8 Hz, J_{BX} = 5.7 Hz, J_{XY} = 6.6 Hz, CH_2CH_X 1H), 5.44 (d, J_{XY} = 6.6 Hz, OCH_Y, 1H), 6.7−8.5 (m, pyridyl, phenyl, 9H); ^{13}C NMR ($CDCl_3$) δ 5.4, 5.5 ($SiMe_3$), 22.7 (CH_2), 51.2 (CH_2CH), 79.0 (OCH), 121.5, 121.9 (py, C3, C5), 125.0, 126.5, 126.7, 128.1 (Ph, C2, 4, 5, 6), 133.3 (Ph, C1), 135.7 (py, C4), 143.7 (Ph, C3), 148.9 (py, C6), 160.5 (py, C2). Anal. Calcd for $C_{26}H_{48}ClGeN_3OSi_4$: C, 48.87; H, 7.57; N, 6.58; Cl, 5.55. Found: C, 48.44; H, 7.86; N, 6.44; Cl, 5.62.

Trans isomer: ^1H NMR ($CDCl_3$) δ 0.32 (s, $SiMe_3$, 18H), 0.35 (s, $SiMe_3$, 18H), 1.85 (dd, J_{AB} = 13.5 Hz, J_{BX} = 13.3 Hz, CH_AH_B, 1H), 2.00 (dd, J_{AB} = 13.5 Hz, J_{AX} = 6.7 Hz, CH_AH_B, 1H), 3.07 (ddd, J_{AX} = 6.7 Hz, J_{BX} = 13.3 Hz, J_{XY} = 9.9 Hz, CH_2CH_X, 1H), 4.98 (d, J_{XY} = 9.9 Hz, OCH_Y, 1H), 6.7−8.6 (m, pyridyl, phenyl, 9H); ^{13}C NMR ($CDCl_3$) δ 5.4, 5.7 ($SiMe_3$), 30.2 (CH_2), 56.0 (CH_2CH), 80.5 (OCH), 121.6, 123.6 (py, C3, C5), 124.3, 126.4, 126.8, 128.7, (Ph, C2, 4, 5, 6), 133.6 (Ph, Cl), 135.8 (py, C4), 146.3 (Ph, C3), 149.6 (py, C6), 161.4 (py, C2). Anal. Calcd for $C_{26}H_{48}ClGeN_3OSi_4$: C, 48.87; H, 7.57; N, 6.58; Cl, 5.55. Found: C, 48.36; H, 7.77; N, 6.49; Cl, 5.85.

Acknowledgment. This work was partially supported by a Grant-in Aid for Scientific Research on Priority Area (07216209) and a Grant-in Aid for Scientific Research (06453145). We thank Asai Germanium Research Institute for providing us with germanium tetrachloride.

OM950559L

Synthesis and Reactivity of Trinuclear Gold(III) Dithiolate Complexes. X-ray Structure of $[Au(C_6F_5)(S_2C_6H_4)]_3$ and $[Au(C_6F_5)(S_2C_6H_4)(SC_6H_4SPPh_3)]$

Elena Cerrada,[†] Eduardo J. Fernández,[‡] Peter G. Jones,[§] Antonio Laguna,[†] Mariano Laguna,*[,†] and Raquel Terroba[‡]

Departamento de Química Inorgánica, Instituto de Ciencia de Materiales de Aragón, Universidad de Zaragoza-CSIC, 50009 Zaragoza, Spain, Departamento de Química, Universidad de la Rioja, 26001 Logroño, Spain, and Institut für Anorganische und Analytische Chemie der Technischen Universität, Postfach 3329, 38023 Braunschweig, Germany

Received June 9, 1995[⊗]

$Q_2[Zn(S\text{-}S)_2]$ or $[SnMe_2(S\text{-}S)]$ (Q = NBu_4 or PPN, S-S = $S_2C_6H_4$, $S_2C_6H_3CH_3$, or C_3S_5 (dmit)) reacts with *trans*-$[Au(C_6F_5)Cl_2(tht)]$ affording trinuclear species $[Au(C_6F_5)(S\text{-}S)]_3$ (**1**–**3**). When $[AuX_3(tht)]$ (X = Cl or Br) are used instead, $[AuBr(S\text{-}S)]_n$ (**4**–**6**) and $[AuCl(dmit)]_n$ (**7**) are obtained. Complex **1** further reacts with PPh_3 to give $[Au(C_6F_5)(S_2C_6H_4)(SC_6H_4SPPh_3)]$. Complexes **1**–**3** react with neutral (pyridine) or anionic (Cl, Br, or SCN) ligands affording $[Au(C_6F_5)(S\text{-}S)(py)]$ (**9a**–**c**) or $Q[Au(C_6F_5)(S\text{-}S)X]$ (**10a**–**c**–**12a**–**c**) complexes. The structures of **1** and **8** have been established by X-ray crystallography. Complex **1** shows a six-membered Au_3S_3 ring which adopts a chair configuration and shows a gold–gold distance of 3.515 Å. Complex **8** is a mononuclear square-planar gold(III) complex with a new $SC_6H_4SPPh_3$ thiolate ligand, the P–S bond length being 2.058(5) Å.

Introduction

The synthesis of gold complexes containing Au–S bonds has attracted considerable attention in recent years because of their potential applications in various areas such as medicine,[1] mainly as antiarthritic drugs, deposition of gold films in electronic devices, and the glass industry[2] or as gold thiol interfaces.[3] Recent discoveries showing that aurothiolates have some inhibitory effects on HIV-1 (the etiologic agent of AIDS),[4] cytotoxicity, and anticancer activity[5] have encouraged the research activity in these areas.

Au–S complexes are known in oxidation states I, II, or III and in complexes formally containing gold(IV),[6] which probably contain gold(III) with partially oxidized ligands. Most are mononuclear, but there are noteworthy exceptions such as the dinuclear gold(II) complexes,[7] the recently reported $[S(AuPR_3)_3]$ (PR_3 = PPh_3, PPh_2Me, PMe_3),[8] $[S(AuPR_3)_4]$ (PR_3 = PPh_3),[9] $[Au_4(S\text{-}S)_2(PEt_3)_2]$ (S-S = 1,2-$S_2C_6H_4$ or 3,4-$S_2C_6H_3CH_3$),[10,11] $[Au_3(S\text{-}S)(PR_3)_3]^+$,[12] $[Au_4(\mu\text{-}(C_3S_5)_2(\mu\text{-dppm})_2]$,[13] or the benzenehexathiol derivative "golden wheel" $[\{CSAu(PPh_3)\}_6]$.[14] Only a few examples of dinuclear gold(III) complexes have been reported such as $[Au_2(CH_2PPh_2CH_2)_2(S_2C_6H_4)_2]$[15] and $[Au_2Me_2(SR)_2]$ (R = Ph,[16a] $COCH_3$,[16b] Et[16c]).

In this paper we report the synthesis of the trinuclear gold(III) derivatives $[AuX(S\text{-}S)]_3$ (S-S = 1,2-benzenedithiolate ($S_2C_6H_4$), 3,4-toluenedithiolate ($S_2C_6H_3CH_3$), and 2-thioxo-1,3-dithiole-4,5-dithiolate (C_3S_5, dmit); X = Br, Cl, or C_6F_5) by dithiolate ligand transfer from $Q_2[Zn(S\text{-}S)_2]$ and $[SnMe_2(S\text{-}S)]$. The reaction of the trinuclear derivatives with various neutral or organic ligands breaks the thiolate bridge, affording $[Au(C_6F_5)(S\text{-}S)L]$ (L = PPh_3 or py) or $Q[Au(C_6F_5)(S\text{-}S)X]$ (X = Cl, Br, SCN; Q = NBu_4 or PPN). The reaction of PPh_3 with $[Au(C_6F_5)(S_2C_6H_4)]_3$ leads to the expected addition product, but a side reaction involves an unprecedented thiolate–phosphine coupling, affording $[Au(C_6F_5)(S_2C_6H_4)(SC_6H_4SPPh_3)]$ as a byproduct. The molecular structures of $[Au(C_6F_5)(S_2C_6H_4)]_3$ and $[Au(C_6F_5)(S_2C_6H_4)(SC_6H_4SPPh_3)]$ have been established by single-

[†] Universidad de Zaragoza-CSIC.
[‡] Universidad de la Rioja.
[§] Technische Universität Braunschweig.
[⊗] Abstract published in *Advance ACS Abstracts,* November 1, 1995.

(1) (a) Shaw, C. F., III; Isab, A. A.; Hoeschele, J. D.; Starich, M.; Jocke, J.; Schulteis, P.; Xiao, J. *J. Am. Chem. Soc.* **1994**, *116*, 2254. (b) Graham, G. C.; Champion, G. D.; Ziegher, J. B. *Inflammopharmacology* **1991**, *1*, 99.
(2) (a) Rapson, W. S.; Groenewald, T. In *Gold Usage*; Academic Press: London, 1978. (b) Papazian, A. N. *Gold Bull.* **1982**, *15*, 81.
(3) Fenter, P.; Eberhardt, A.; Eisenberger, P. *Science* **1994**, *226*, 1216.
(4) (a) Okada, T.; Patterdon, B. K.; Ye, O. S.; Gurney, M. E. *Virology* **1993**, *192*, 631. (b) Blough, H. A.; Richetti, M.; Montagnier, B. H. *Chem. Abstr.* **1991**, *115*, 174630p.
(5) Sadler, P. J. In *Metal Complexes in Cancer Chemotherapy*; Keppler, K. B., Ed.; VCH: Weinheim, Germany. 1993.
(6) Rinford, G.; Thorup, N.; Bjornholm, T.; Bechgaard, K. *Acta Crystallogr.* **1990**, *C46*, 1437.
(7) Bardají, M.; Jones, P. G.; Laguna, A.; Laguna, M. *Organometallics* **1995**, *14*, 1310 and references therein.
(8) a) Jones, P. G.; Thöne, C. *Acta Crystallogr.* **1980**, *1336*, 2777. (b) Angermaier, K.; Schmidbaur, H. *Chem Ber.* **1994**, *127*, 2387.
(9) Canales, F.; Gimeno, M. C.; Jones, P. G.; Laguna, A. *Angew. Chem., Int. Ed. Engl.* **1994**, *33*, 769.
(10) Davila, R. M.; Elduque, A.; Grant, T.; Staples, R. J.; Fackler, J. P., Jr. *Inorg. Chem.* **1993**, *32*, 1749.
(11) Nakamoto, M.; Schier, A.; Schmidbaur, H. *J. Chem. Soc., Dalton Trans.* **1993**, 1347.
(12) Gimeno, M. C.; Jones, P. G.; Laguna, A.; Laguna, M.; Terroba, R. *Inorg. Chem.* **1994**, *33*, 3932.
(13) Cerrada, E.; Jones, P. G.; Laguna, A.; Laguna, M. *J. Chem. Soc., Dalton Trans.* **1994**, 1315.
(14) Yip, H. K.; Schier, A.; Riede, J.; Schmidbaur, H. *J. Chem. Soc., Dalton Trans.* **1994**, 2333.
(15) Heinrich, D. H.; Fackler, J. P., Jr. *Inorg. Chem.* **1990**, *29*, 4402.
(16) (a) Johnson, A.; Puddephatt, R. J. *J. Chem. Soc. Dalton Trans.* **1975**, 115. (b) Bergfeld, M.; Schmidbaur, H. *Chem. Ber.* **1969**, *102*, 2408. (c) Paparizos, Ch. Dissertation, Case Western Reserve University, 1977, pp 1–186; *Diss. Abstr. Int.* **1978**, *B38*, 4227.
(17) Cerrada, E.; Fernandez, E. J.; Gimeno, M. C.; Laguna, A.; Laguna, M.; Terroba, R.; Villacampa, M. D. *J. Organomet. Chem.* **1995**, *492*, 105.

0276-7333/95/2314-5537$09.00/0

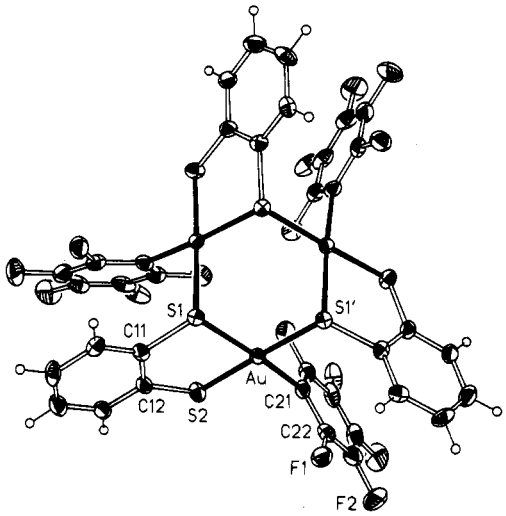

Figure 1. Molecule of compound **1** in the crystal with view direction (approximately) along the crystallographic 3-fold axis. Ellipsoids correspond to 50% probability levels. Hydrogen radii are arbitrary. The asymmetric unit and the equivalent atom S1′ are labeled.

crystal analysis, showing a six-membered Au_3S_3 ring in the former and the above-mentioned combination of dithiolate and triphenylphosphine in the latter.

Results and Discussion

Recently[17] we have shown that dithiolate complexes [$SnMe_2$(S-S)] or Q_2[Zn(S-S)$_2$] [S-S = 1,2-benzenedithiolate ($S_2C_6H_4$), 3,4-toluenedithiolate ($S_2C_6H_3CH_3$), and 2-thioxo-1,3-dithiole-4,5-dithiolate (dmit); Q = NEt_4 or PPh_3=N=PPh_3 (PPN)] transfer dithiolate groups to gold centers, on reaction with gold(III) complexes *cis*-[Au(C_6F_5)Cl_2L] (L = phosphine or arsine ligand) (eq 1).

$$\begin{matrix}[SnMe_2(S\text{-}S)] \\ {}^1/_2Q_2[Zn(S\text{-}S)_2]\end{matrix} + [Au(C_6F_5)Cl_2L] \rightarrow [Au(C_6F_5)(S\text{-}S)L] \begin{matrix}+ SnMe_2Cl_2 \\ + {}^1/_2Q_2[ZnCl_4]\end{matrix} \quad (1)$$

The analogous reaction starting from *cis*- or *trans*-[Au(C_6F_5)Cl_2(tht)] (tht = tetrahydrothiophene), in acetone or dichloromethane, and S-S = 1,2-$S_2C_6H_4$ affords a brown complex **1**, and from the mother liquors $SnMe_2Cl_2$ or $(PPN)_2[ZnCl_4]$ can be recovered. The reaction thus proceeds in a similar way to the previous one[17] (eq 1), but the spectroscopic properties of complex **1** indicate that there are important differences (eq 2). Thus ^{1}H NMR shows only signals assignable to the dithiolate ligand and no tetrahydrothiophene resonances, in accordance with the stoichiometry [Au(C_6F_5)($S_2C_6H_4$)] deduced by elemental analysis. ^{19}F NMR of complex **1** shows five signals of equal intensity, which can be assigned to one type of C_6F_5 with hindered rotation around the *ipso*-carbon atom.

A polymeric formulation for complex **1** is further evidenced by mass spectrometry (FAB+); it shows peaks at *m/z* 1512 (80%), which can be assigned to [Au(C_6F_5)-($S_2C_6H_4$)]$_3^+$, and species lacking 1, 2, or 3 C_6F_5 groups of the parent ion (75%, 40%, 35%, respectively).

Final proof of the structure of complex **1** was furnished by X-ray diffraction (Figures 1 and 2). Atomic coordinates are given in Table 2 and selected bond lengths and angles in Table 3.

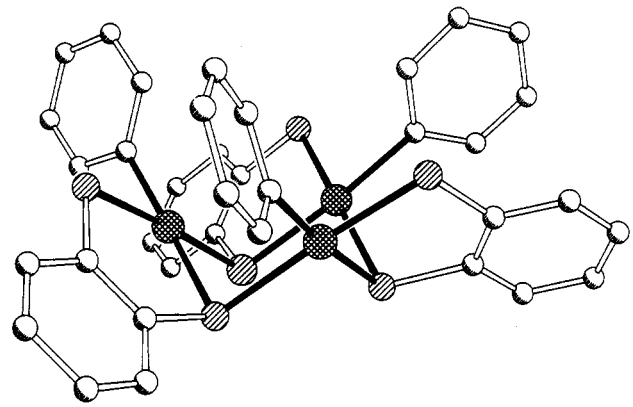

Figure 2. Molecule of compound **1** in the crystal (side view, arbitrary radii, H and F atoms omitted for clarity).

Table 1. Details of X-ray Structure Analyses for Compounds 1 and 8

	compd	
	1	**8**·2CH_2Cl_2
formula	$C_{36}H_{12}Au_3F_{15}S_6$	$C_{38}H_{27}AuCl_4F_5PS_4$
M_r	1512.72	1076.57
cryst habit	dark red tablet	pink platelet
cryst size (mm)	0.60 × 0.27 × 0.12	0.25 × 0.15 × 0.02
space group	$P\bar{3}$	$P\bar{1}$
temp (°C)	−130	−100
cell constants		
a (Å)	16.005(2)	12.677(3)
b (Å)	16.005(2)	13.288(3)
c (Å)	9.384(2)	13.534(3)
α (deg)	90	72.02(2)
β (deg)	90	82.19(2)
γ (deg)	120	67.72(2)
V (Å^3)	2081.8(6)	2006.1(8)
Z	2	2
D_x (Mg m^{-3})	2.413	1.782
F(000)	1392	1052
μ (mm^{-1})	10.9	4.23
transm factors	0.44−0.98	0.38−0.73
$2\theta_{max}$ (deg)	55	50
no. of reflcns		
measd	5848	7087
indpdt	3190	6727
R_{int}	0.052	0.117
w$R(F_2$, all reflcns)	0.098	0.114
$R(F, F > 4\sigma(F))$	0.039	0.066
no. of params	181	228
no. of restraints	160	107
S	1.05	0.76
max Δ/σ	0.001	<0.001
max $\Delta\rho$ (e Å^{-3})	1.9	1.4

The molecule displays crystallographic 3-fold symmetry. The immediate environment of each gold atom consists of one carbon atom and three sulfur atoms in a slightly distorted square-planar arrangement (root-mean-square deviation of five atoms 0.04 Å). One sulfur atom (S(1)) of each benzenedithiolate ligand bridges a pair of gold atoms and is thus three-coordinate, whereas the other (S(2)) only coordinates to one gold. The central six-membered Au_3S_3 ring adopts a chair configuration (Figure 2) analogous to that reported in [Au(CH_3)$_2$-NH_2]$_3$;[18] all three C_6F_5 groups lie on one side of the ring and all three dithiolate rings on the other side. The gold−gold distance is 3.515 Å, very similar to the 3.563 and 3.545 Å in [Au(CH_3)$_2NH_2$]$_3$[18] and longer than in dinuclear gold(III) derivative [Au_2(μ-CH_2)(μ-CH_2PPh_2-

(18) Grässle, U.; Strähle, J. *Z. Anorg. Allg. Chem.* **1985**, *531*, 26.
(19) Bardají, M.; Gimeno, M. C.; Jimenez, J.; Laguna, A.; Laguna, M. *J. Organomet. Chem.* **1992**, *441*, 339.

Table 2. Atomic Coordinates ($\times 10^4$) and Equivalent Isotropic Displacement Parameters ($Å^2 \times 10^3$) for Compound 1

	x	y	z	U(eq)[a]
Au	4720.7(2)	6955.6(2)	2811.9(3)	17.5(1)
S(1)	3629.3(11)	5634.5(12)	4202(2)	18.7(3)
S(2)	5113.8(13)	5961.1(13)	1587(2)	25.1(4)
C(11)	3973(5)	4764(5)	3783(7)	20.1(13)
C(12)	4627(5)	4929(5)	2659(8)	23.0(14)
C(13)	4870(5)	4225(5)	2384(8)	25.4(14)
C(14)	4494(6)	3406(5)	3208(8)	33(2)
C(15)	3854(6)	3250(5)	4315(8)	31(2)
C(16)	3600(5)	3936(5)	4605(7)	23.8(14)
C(21)	5671(5)	8007(5)	1483(7)	24.7(14)
C(22)	6604(5)	8655(5)	1890(8)	26.6(15)
C(23)	7275(5)	9326(6)	989(9)	34(2)
C(24)	7024(6)	9357(6)	−416(8)	38(2)
C(25)	6105(6)	8719(5)	−857(8)	32(2)
C(26)	5442(5)	8065(5)	89(8)	27.3(15)
F(1)	6903(3)	8604(3)	3228(5)	34.2(10)
F(2)	8179(3)	9937(4)	1420(6)	52.1(14)
F(3)	7670(4)	9976(4)	−1334(6)	57(2)
F(4)	5846(4)	8732(3)	−2213(5)	44.0(13)
F(5)	4543(3)	7448(3)	−398(5)	34.1(10)

[a] U(eq) is defined as one-third of the trace of the orthogonalized U_{ij} tensor.

Table 3. Selected Bond Lengths (Å) and Angles (deg) for Compound 1[a]

Au−C(21)	2.035(7)	Au−S(2)	2.292(2)
Au−S(1)	2.352(2)	Au−S(1′)	2.395(2)
S(1)−C(11)	1.779(7)	S(2)−C(12)	1.750(7)
C(21)−Au−S(2)	85.2(2)	C(21)−Au−S(1)	174.6(2)
S(2)−Au−S(1)	89.55(6)	C(21)−Au−S(1′)	95.7(2)
S(2)−Au−S(1′)	176.73(6)	S(1)−Au−S(1′)	89.70(8)
C(11)−S(1)−Au	101.5(2)	C(11)−S(1)−Au″	108.1(2)
Au−S(1)−Au″	95.53(6)	C(12)−S(2)−Au	102.7(2)

[a] Symmetry transformations used to generate equivalent atoms: (′) $-y+1, x-y+1, z$; (″) $-x+y, -x+1, z$.

$CH_2)_2(C_6F_5)_2]$[19] at 3.113 Å. Although metal−metal interactions with gold(III)−gold(I) distances of 3.470 Å[20] (av) have been postulated, we believe that in our complex the mentioned Au···Au distance is imposed by the six-membered ring.

The three Au−S bond lengths differ significantly. As expected, those to the bridging S (Au−S(1) and Au−S(1′)) are longer (2.352(2) and 2.395(2) Å) than Au−S(2) (2.292(2) Å). It is surprising that Au−S(1′) (*trans* to S) is longer than Au−S(1) (*trans* to C) in view of the appreciable expected *trans* influence of carbon ligands at gold; however, a comparison of Au−S bond lengths in $[Au(dmit)_2]^-$ [21,22] and $[Au(dmit)(C_6F_5)_2]^-$ [23] shows no significant differences. The shorter distance Au−S(2) is very similar to those observed in other dithiolate gold(III) complexes with two-coordinate sulfur, such as $[Au(C_6F_5)(1,2\text{-}S_2C_6H_4)(PPh_3)]$[17] (2.314(1) and 2.299(1) Å) and $[Au(1,2\text{-}S_2C_6H_4)_2]$ (2.305 Å),[6] and shorter than in related gold(I) derivatives, e.g. $[Au_2(1,2\text{-}S_2C_6H_4)(PPh_3)_2]$ (2.325(3) and 2.316(3) Å).[10,11] The Au−C bond of 2.035 Å is similar to those in $[Au(1,2\text{-}S_2C_6H_4)(C_6F_5)(PPh_3)]$[17] (2.061(4) Å) or $[Au(C_6F_5)_2\{S_2CN(CH_2Ph)_2\}]$[24] (2.047(6) and 2.049(6) Å].

The formation of **1** can be represented as shown in process 2.

$$3[SnMe_2(S_2C_6H_4)] + 3trans\text{-}[Au(C_6F_5)Cl_2(tht)] \xrightarrow{-tht} \underset{\mathbf{1}}{[Au(C_6F_5)(S\text{-}S)]_3} + 3SnMe_2Cl_2 \quad (2a)$$

$$^3/_2Q_2[Zn(S_2C_6H_4)_2] + 3trans\text{-}[Au(C_6F_5)Cl_2(tht)] \xrightarrow{-tht} \underset{\mathbf{1}}{[Au(C_6F_5)(S\text{-}S)]_3} + {}^3/_2Q_2[ZnCl_4] \quad (2b)$$

When reaction 2 is carried out with the toluene analog $3,4\text{-}S_2C_6H_3CH_3$, a brown complex **2** is formed, for which analysis and mass spectra indicate the same type of trinuclear derivative $[Au(C_6F_5)(S_2C_6H_3CH_3)]_3$; however ^1H NMR (two singlets for the Me groups) and ^{19}F NMR (two types of nonrotating C_6F_5 groups) show that probably it is a mixture of isomers, because the dithiolate ligand is not symmetrical. The mass spectrum shows the trinuclear parent peak at *m/z* 1554 (55%) and the loss of 1, 2, or 3 C_6F_5 groups at *m/z* 1387 (55%), 1220 (20%), and 1066 (20%), respectively.

Reaction 2 proceeds in a similar way with 2-thioxo-1,3-dithiole-4,5-dithiolate (dmit) as ligand, affording a dark purple product $[Au(C_6F_5)(dmit)]_n$ (**3**) that has an uninformative mass spectrum, with no peaks assignable to $[Au(C_6F_5)(dmit)]_n^+$. Its ^{19}F NMR shows one type of C_6F_5 group, for which only three signals are present because both *ortho*-F and *meta*-F are equivalent. Although the reactivity of complex **3** (see below) is very similar to that shown by complexes **1** and **2**, we do not have conclusive data to propose a trinuclear structure for complex **3**.

Process 2 can be extended to the synthesis of halo−gold derivatives starting from $[AuX_3(tht)]$ (X = Cl, Br), but in these cases the reaction is not a general procedure; only with the dmit ligand does the reaction work as intended with the tin and zinc derivatives and X = Cl or Br. In contrast, when $1,2\text{-}S_2C_6H_4$ or $3,4\text{-}S_2C_6H_3CH_3$ are used, only the bromide derivatives can be isolated by the reaction of the tin complex (eqs 3 and 4)

$$[SnMe_2(S\text{-}S)] + [AuBr_3(tht)] \rightarrow \underset{\substack{S\text{-}S = 1,2\text{-}S_2C_6H_4\ (\mathbf{4}),\\ 3,4\text{-}S_2C_6H_3CH_3\ (\mathbf{5})}}{[AuBr(S\text{-}S)]_3} + SnMe_2Br_2 \quad (3)$$

$$\underset{(NEt_4)_2[Zn(dmit)_2]}{[SnMe_2(dmit)]} + [AuX_3(tht)] \xrightarrow{-tht} \underset{X = Br(\mathbf{6});\ Cl\ (\mathbf{7})}{(1/n)[AuX(dmit)]_n} + SnMe_2X_2 + (NEt_4)_2[ZnX_4] \quad (4)$$

^1H NMR of complexes **4** and **5** shows only dithiolate resonances, in accordance with their formulation. We have only analytical data for complexes **6** and **7**, because their insolubility precludes spectroscopic techniques. Only the mass spectrum of **4** shows the trinuclear parent peak (*m/z* 1512, 15%); complexes **5**−**7** give a very poor ionization pattern with the lack of signals of the trinuclear species. We presume that complexes **4** and

(20) Bovio, B.; Calagero, S.; Wagner, F. E.; Burini, A.; Pietroni, B. R. *J. Organomet. Chem.* **1994**, *470*, 275.
(21) Matsubayashi, G.; Yokozawa, A. *J. Chem. Soc., Dalton Trans.* **1990**, 3535.
(22) Cerrada, E.; Gimeno, M. C.; Jones, P. G.; Laguna, M. *Z. Kristallogr.* **1994**, *209*, 827.
(23) Cerrada, E.; Jones, P. G.; Laguna, A.; Laguna, M. Unpublished results.
(24) Usón, R.; Laguna, A.; Laguna, M.; Castrilla, M. L.; Jones, P. G.; Meyer-Bäse, K. *J. Organomet. Chem.* **1987**, *336*, 453.

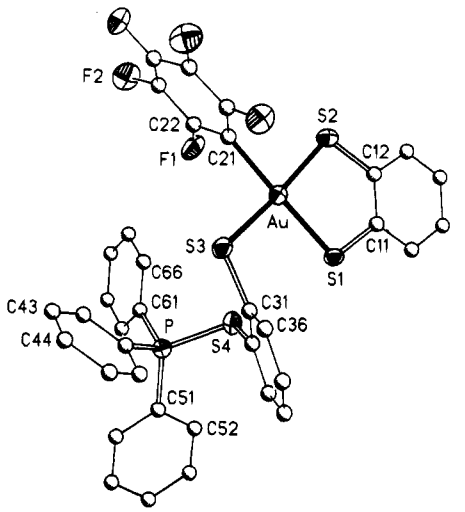

Figure 3. Molecule of compound **8** in the crystal. Ellipsoids correspond to 50% probability levels. Hydrogen and carbon radii are arbitrary.

(probably) **5** present trinuclear structures similar to **1**, but in the case of the dmit derivatives, **6** and **7**, only polynuclear structures can be proposed.

Complexes **1**–**3** react under very mild conditions (diethyl ether, room temperature, reaction times of the order of minutes) with neutral ligands such as PPh_3 (gold/ligand ratio 1:1) to give the previously known complexes $[Au(C_6F_5)(S\text{-}S)(PPh_3)]$.[17] When complex **2** is involved, the resulting product shows one ^{31}P NMR signal, one ^1H NMR resonance for the methyl group, and three resonances in the ^{19}F NMR spectra, as reported for $[Au(C_6F_5)(S_2C_6H_3CH_3)(PPh_3)]$[17] in accordance with a formulation of **2** as a mixture of isomers. When S-S = $S_2C_6H_4$ is used, a small quantity of a pink complex **8** precipitates and can be easily recovered. Analytical data and the mass spectrum are in accordance with the composition "$[Au(C_6F_5)(S_2C_6H_4)_2(PPh_3)]$" ($m/z$ = 906 [M^+], 32%). The apparent presence of two dithiolate ligands and a pentafluorophenyl group would indicate five negative charges; however, the base peak ($SC_6H_4SPPh_3$) (m/z = 403) in the spectrum suggested that this modified ligand might be present in the complex.

The molecular structure of complex **8** was resolved by an X-ray study of its bis(dichloromethane) solvate (Figure 3), confirming its formulation as $[Au(C_6F_5)(S_2C_6H_4)(SC_6H_4SPPh_3)]$. Atomic coordinates are given in Table 4 and selected bond lengths and angles in Table 5. The complex is mononuclear and exhibits square-planar geometry (mean deviation of five atoms 0.04 Å); one benzenedithiolate acts as a chelating anion, and a new thiolate ligand is observed, formed by an unprecedented coupling of triphenylphosphine and one S terminus of dithiolate. It is noteworthy that the $[Au(C_6F_5)(S_2C_6H_4)]$ fragment in this complex is very similar to the recently reported $[Au(C_6F_5)(S_2C_6H_4)(PPh_3)]$.[17] The Au–S(dithiolate) bond lengths are Au–S(1) = 2.314(4) and Au–S(2) = 2.299(4) Å, the longer being *trans* to the C_6F_5, but Au–S(3), the bond to the new ligand, is longer again at 2.338(4) Å. The P–S(4) bond length of 2.058(5) Å is consistent with its formulation as a formally single bond (cf. standard P=S bond length of ca. 1.95 Å), although there are few examples of P–S single bonds at four-coordinate phosphorus (2.0737(9) Å in a recently measured NC_2PS system[25]).

The yield of complex **8** can be increased using a higher gold/PPh_3 ratio; the best result (11%) is obtained with the ratio 1:1.5. Neither other phosphines as PPh_2Me or $PPhMe_2$ nor $AsPh_3$ give coupling thiolate-ligand complexes; only the known[17] $[Au(C_6F_5)(S_2C_6H_4)L]$ (L = PPh_2Me, $PPhMe_2$, $AsPh_3$) are obtained. Complex **8** is only formed when the reaction takes place in diethyl ether, probably because of its insolubility in this solvent. When the reaction is done in dichloromethane, the ^{31}P NMR shows that $[Au(C_6F_5)(S_2C_6H_4)(PPh_3)]$ is the only gold product containing PPh_3. Complex **8** is not an

Table 4. Atomic Coordinates ($\times 10^4$) and Equivalent Isotropic Displacement Parameters (Å^2 $\times 10^3$) for Compound 8

	x	y	z	U(eq)[a]
Au	8874.2(6)	3305.6(7)	2629.0(6)	24.8(2)
P	4399(3)	5919(3)	2934(3)	25.6(10)
S(1)	8901(3)	4310(3)	3745(3)	26.9(10)
S(2)	10257(3)	1723(4)	3573(3)	34.8(12)
S(3)	7554(4)	4829(4)	1495(3)	33.7(12)
S(4)	5989(3)	5377(3)	3539(3)	30.4(10)
C(11)	9863(7)	3244(7)	4710(6)	27(4)
C(12)	10458(8)	2162(8)	4605(6)	32(4)
C(13)	11210(7)	1355(6)	5367(7)	37(4)
C(14)	11366(7)	1629(7)	6234(6)	41(4)
C(15)	10771(7)	2711(8)	6339(5)	35(4)
C(16)	10019(7)	3519(6)	5577(7)	23(4)
C(21)	8869(11)	2350(12)	1679(10)	37(5)
C(22)	8200(10)	1704(10)	1900(10)	28(4)
C(23)	8167(11)	1052(11)	1275(10)	34(4)
C(24)	8745(11)	1126(13)	350(11)	41(4)
C(25)	9464(12)	1724(12)	119(12)	45(5)
C(26)	9500(11)	2308(12)	811(10)	32(4)
F(1)	7551(7)	1627(7)	2782(6)	45(2)
F(2)	7470(7)	452(7)	1515(6)	50(3)
F(3)	8708(7)	550(7)	−268(6)	55(3)
F(4)	10061(7)	1780(7)	−779(6)	55(3)
F(5)	10157(7)	2989(7)	468(6)	47(3)
C(31)	7258(7)	6093(5)	1859(7)	15(3)
C(32)	6567(7)	6352(6)	2702(6)	23(4)
C(33)	6291(6)	7407(7)	2865(5)	31(4)
C(34)	6707(7)	8202(6)	2183(7)	25(4)
C(35)	7398(7)	7943(6)	1340(6)	33(4)
C(36)	7673(6)	6888(7)	1177(5)	34(4)
C(41)	4357(7)	6404(7)	1540(5)	24(4)
C(42)	4050(7)	5838(6)	984(7)	30(4)
C(43)	4026(7)	6218(7)	−95(7)	47(5)
C(44)	4309(8)	7164(8)	−617(5)	41(4)
C(45)	4616(7)	7729(6)	−61(7)	40(4)
C(46)	4640(7)	7349(7)	1017(7)	26(4)
C(51)	3352(7)	7030(7)	3396(7)	30(4)
C(52)	3480(6)	7169(7)	4344(7)	28(4)
C(53)	2622(8)	7984(8)	4731(6)	40(4)
C(54)	1636(7)	8660(7)	4169(7)	47(5)
C(55)	1508(6)	8522(7)	3221(7)	42(5)
C(56)	2366(8)	7707(8)	2834(6)	34(4)
C(61)	4058(8)	4661(6)	3454(6)	24(4)
C(62)	3074(7)	4658(6)	4048(7)	30(4)
C(63)	2857(6)	3658(8)	4456(6)	32(4)
C(64)	3623(8)	2659(6)	4268(7)	34(4)
C(65)	4607(7)	2662(6)	3673(7)	38(4)
C(66)	4824(6)	3662(8)	3266(6)	40(5)
C(98)	3242(22)	508(22)	2804(20)	146(11)
Cl(1)	3594(6)	296(6)	1561(7)	154(3)
Cl(2)	4322(6)	−1(6)	3592(7)	156(3)
C(99)	8697(15)	5485(15)	8550(14)	77(6)
Cl(3)	7296(4)	6491(4)	8549(4)	75(2)
Cl(4)	8817(4)	4426(4)	8086(4)	72(2)

[a] U(eq) is defined as one-third of the trace of the orthogonalized U_{ij} tensor.

(25) Pinchuk, V. A.; Müller, C.; Fischer, A.; Thönnessen, H.; Jones, P. G.; Schmutzler, R.; Markowsky, L. N.; Shermolovich, Y. G.; Pinchuk, A. M. *Phosphorus, Sulfur Silicon*, submitted for publication.

intermediate in the formation of $[Au(C_6F_5)(S_2C_6H_4)(PPh_3)]$ because when a solution is stirred in diethyl ether or dichloromethane, the starting complex is recovered without change. We do not have the evidence of the formation mechanism of complex **8**, but a way could be the attack of PPh_3 on one nonbridging S atom and the reduction of one gold center giving rise with one extra triphenylphosphine to $[Au(C_6F_5)(PPh_3)]$, which can be detected by ^{31}P and ^{19}F NMR in the reaction solvent, and complex **8**. The third Au appears as $[Au(C_6F_5)(S_2C_6H_4)(PPh_3)]$. A possible reaction is presented in eq 5.

$$[Au(S_2C_6H_4)(C_6F_5)]_3 + 3PPh_3 \rightarrow [Au(C_6F_5)(PPh_3)] + [Au(C_6F_5)(S_2C_6H_4)(PPh_3)] + [Au(C_6F_5)(S_2C_6H_4)(SC_6H_4SPPh_3)] \quad (5)$$
8

The reaction of polynuclear complexes **1**–**3** with pyridine, a ligand with limited affinity for gold(III), breaks the dithiolate bridge, affording mononuclear complexes **9a-c** (eq 6).

$$[Au(C_6F_5)(S\text{-}S)]_3 + py \rightarrow 3[Au(C_6F_5)(S\text{-}S)(py)] \quad (6)$$
S-S = 1,2-$S_2C_6H_4$ (**9a**), 3,4-$S_2C_6H_3CH_3$ (**9b**), dmit (**9c**)

The analytical data and spectroscopic properties of complexes **9a**–**c** are in accordance with their formulation. ^1H NMR shows pyridine protons in a 1:1 ratio, and ^{19}F NMR show in all cases three signals indicating one type of C_6F_5 group with free rotation around the C-*ipso* atom. The mass spectra show the parent peak as follows: **9a** (*m/z* 583, 50%) and **9b** (*m/z* 597, 45%).

The reaction with pyridine to give complexes **9a**–**c** demonstrates the ease of breaking the sulfur bridges. This makes the complexes **1**–**3** an excellent starting point to extend gold(III) dithiolate chemistry. As an example we have carried out reactions with various halides and pseudohalogenides affording anionic complexes **10**–**12** (eq 7).

$$[Au(C_6F_5)(S\text{-}S)]_3 + 3XQ \rightarrow Q[Au(C_6F_5)(S\text{-}S)X] \quad (7)$$
X = Br, Q = NBu_4 (**10a**–**c**)
X = Cl, Q = PPN (**11a**–**c**)
X = SCN, Q = PPN (**12a**–**c**)

Complexes **10a,b**, **11a,b**, and **12a,b** are violet, and **10c**, **11c**, and **12c** are yellow-green solids. They show conductivities of 95–110 Ω^{-1} cm^2 mol^{-1} characteristic of 1:1 electrolytes, in agreement with their formulation. The ^1H NMR spectra show the ligand and cation resonances in the expected ratio. ^{19}F NMR again shows three resonances assignable to one C_6F_5 group, as expected for the monuclear complexes. The toluenedithiolate complexes **10b**, **11b**, and **12b** only show one absorption assignable to the Me group, as is usual in mononuclear complexes, although the two isomers should be present. Their mass spectra (FAB−) show peaks assignable to the parent anions as follows (*m/z*): **10a** (583, 100%), **10b** (598, 50%), **10c** (640, 15%), **11a** (539, 55%), **11b** (533, 5%), **12a** (562, 55%), **12b** (576, 100%), **12c** (618, 15%). **11c** does not show the parent anion, but $[M - Cl]^-$ is present at *m/z* = 560 (10%).

Table 5. Selected Bond Lengths (Å) and Angles (deg) for Compound 8

Au–C(21)	2.07(2)	Au–S(2)	2.299(4)
Au–S(1)	2.314(4)	Au–S(3)	2.338(4)
P–C(51)	1.786(7)	P–C(61)	1.793(7)
P–C(41)	1.797(7)	P–S(4)	2.058(5)
S(1)–C(11)	1.784(7)	S(2)–C(12)	1.753(7)
S(3)–C(31)	1.784(7)	S(4)–C(32)	1.757(7)
C(21)–Au–S(2)	87.5(4)	C(21)–Au–S(1)	177.8(4)
S(2)–Au–S(1)	90.5(2)	C(21)–Au–S(3)	86.4(4)
S(2)–Au–S(3)	173.0(2)	S(1)–Au–S(3)	95.6(2)
C(51)–P–C(61)	108.6(5)	C(51)–P–C(41)	106.5(5)
C(61)–P–C(41)	112.5(5)	C(51)–P–S(4)	113.7(4)
C(61)–P–S(4)	100.7(4)	C(41)–P–S(4)	114.8(3)
C(11)–S(1)–Au	102.0(3)	C(12)–S(2)–Au	102.7(4)
C(31)–S(3)–Au	109.6(3)	C(32)–S(4)–P	102.1(3)

Experimental Section

The starting materials $[Sn(CH_3)_2(S\text{-}S)]$,[17] $(PPN)_2[Zn(S\text{-}S)_2]$.[17] $(NEt_4)_2[Zn(dmit)_2]$,[26] $[Au(C_6F_5)Cl_2(tht)]$,[27] and $[AuX_3(tht)]$[28] were prepared as described previously. All other reagents were commercially available.

The C, H, N, and S analyses were carried out on a Perkin-Elmer 2400 microanalyzer. Conductivities were measured in approximately 5 × 10^{-4} mol dm^{-3} acetone solutions, with a Jenway 4010 conductimeter. The infrared spectra were recorded (4000–200 cm^{-1}) on a Perkin-Elmer 599 spectrophotometer, using Nujol mulls between polyethylene sheets. The NMR spectra were recorded on Varian UNITY 300 and Bruker ARX 300 spectrometers, in $CDCl_3$, except for complexes **11** and **12** in HDA. Chemical shifts are cited relative to $SiMe_4$ (^1H), 85% H_3PO_4 (external ^{31}P), and $CFCl_3$ (^{19}F). Mass spectra were recorded on a VG Autospec, with the FAB technique using 3-nitrobenzyl alcohol as the matrix.

Syntheses. $[Au(C_6F_5)(S\text{-}S)]_3$ [S-S = 1,2-$S_2C_6H_4$ (1), 3,4-$S_2C_6H_3CH_3$ (2)]. Method a. To a dichloromethane (30 cm^3) solution of $[Sn(CH_3)_2(1,2\text{-}S_2C_6H_4)]$ (0.029 g, 0.1 mmol) or $[Sn(CH_3)_2(3,4\text{-}S_2C_6H_3CH_3)]$ (0.030 g, 0.1 mmol) was added $[Au(C_6F_5)Cl_2(tht)]$ (0.052 g, 0.1 mmol), and the resulting solution was stirred for 1 h. Evaporation of the solvent to 5 cm^3 and addition of hexane (20 cm^3) resulted in the precipitation of brown complexes. Yield (%): 84 (**1**), 86 (**2**). **Method b.** To a dichloromethane (30 cm^3) solution of $(PPN)_2[Zn(1,2\text{-}S_2C_6H_4)_2]$ (0.076 g, 0.05 mmol) or $(PPN)_2[Zn(3,4\text{-}S_2C_6H_3CH_3)_2]$ (0.077 g, 0.05 mmol) was added $[Au(C_6F_5)Cl_2(tht)]$ (0.052 g, 0.1 mmol). After being stirred for 3 h, the solution was concentrated to 5 cm^3. Addition of diethyl ether (15 cm^3) gave a white precipitate $(PPN)_2[ZnCl_4]$. The solution was filtered through 1 cm of diatomaceous earth and the solvent removed to 5 cm^3. Addition of hexane (20 cm^3) led to the precipitation of brown solids. Yield (%): 84 (**1**), 86 (**2**). Data for **1** are as follows. Anal. Calcd for $C_{36}H_{12}Au_3F_{15}S_6$: C, 28.6; H, 0.8; S, 12.7. Found: C, 28.4; H, 0.85; S, 12.3. Λ_M: 5 Ω^{-1} cm^2 mol^{-1}. ^1H NMR: δ = 7.42 and 7.04 (m, 4H, $S_2C_6H_4$). ^{19}F NMR: δ = −111.4 (m, 1F, F_o), −120.65 (m, 1F, F_o), −155.5 (t, $^3J_{F_pF_m}$ = 23.6 Hz, 1F, F_p), −158.15 (m, 1F, F_m), −158.7 (m, 1F, F_m). Data for **2** are as follows. Anal. Calcd for $C_{39}H_{18}Au_3F_{15}S_6$: C, 30.15; H, 1.2; S, 12.35. Found: C, 30.35; H, 1.25; S, 12.3. Λ_M: 22 Ω^{-1} cm^2 mol^{-1}. ^1H NMR: δ = 7.20 and 6.82 (m, 3H, $S_2C_6H_3CH_3$), 2.28 (s, 3H, $S_2C_6H_3CH_3$). ^{19}F NMR: δ = −111.7 (m, 1F, F_o), −120.5 (m, 1F, F_o), −122.1 (m, F_o), −156.2 (t, $^3J_{F_pF_m}$ = 20.0 Hz, F_p), −157.1 (t, $^3J_{F_pF_m}$ = 19.3 Hz, 1F, F_p), −159.15 (m, 1F, F_m), −159.5 (m, 1F, F_m), −159.7 (m, F_m).

(26) a) Steimecke, G.; Kirmse. R.; Hoyer, E. *Z. Chem.* **1975**, *15*, 28. (b) Valade, L.; Legros, J. P.; Bosseau, M.; Cassoux, P.; Barbauskas, M.; Interrante, L. V. *J. Chem. Soc., Dalton Trans.* **1985**, 783.
(27) Usón, R.; Laguna, A.; Bergareche, B. *J. Organomet. Chem.* **1980**, *184*, 411.
(28) Allen, E. A.; Wilkinson, W. *Spectrochim. Acta* **1972**, *28A*, 2257.

$[Au(C_6F_5)(dmit)]_n$ (3). Method a. To an acetone (30 cm^3) solution of $[Sn(dmit)(CH_3)_2]$ (0.034 g, 0.1 mmol) was added $[Au(C_6F_5)Cl_2(tht)]$ (0.052 g, 0.1 mmol), and the resulting solution was stirred for 4 h. Evaporation of the solvent to 5 cm^3 and addition of hexane (20 cm^3) resulted in the precipitation of the dark purple complex **3**. Yield: 65%. **Method b.** To an acetone (30 cm^3) solution of $(NEt_4)_2[Zn(dmit)_2]$ (0.071 g, 0.1 mmol) under dinitrogen was added $[Au(C_6F_5)Cl_2(tht)]$ (0.104 g, 0.2 mmol). After being stirred for 3 h, the solution was concentrated to 1 cm^3. Addition of diethyl ether (15 cm^3) left a white solid $(PPN)_2[ZnCl_4]$; the solution was filtered through 1 cm of diatomaceous earth and solvent removed to 5 cm^3. Addition of hexane (20 cm^3) led to the precipitation of dark purple solid **3**, which was washed with water and dried *in vacuo*. Yield: 65%. Anal. Calcd for $C_9AuF_5S_5$: C, 19.3; S, 29.3. Found: C, 19.45 ; S, 28.6. ^{19}F NMR: $\delta = -121.0$ (m, 2F, F_o), -154.1 (t, $^3J_{F_pF_m} = 19.8$Hz, 1F, F_p), -159.7 (m, 2F, F_m).

$[AuBr(S\text{-}S)]_3$ [S-S = 1,2-$S_2C_6H_4$ (4), 3,4-$S_2C_6H_3CH_3$ (5)]. Method a. To a dichloromethane (30 cm^3) solution of $[Sn(CH_3)_2(1,2\text{-}S_2C_6H_4)]$ (0.029 g, 0.1 mmol) or $[Sn(CH_3)_2(3,4\text{-}S_2C_6H_3CH_3)]$ (0.030 g, 0.1 mmol) was added $[AuBr_3(tht)]$ (0.052 g, 0.1 mmol), and the resulting solution was stirred for 1 h. Evaporation of the solvent to 5 cm^3 and addition of diethyl ether (20 cm^3) resulted in the precipitation of dark brown complexes. Yield (%): 55 (**4**), 48 (**5**). Data for **4** are as follows. Anal. Calcd for $C_{18}H_{12}Au_3Br_3S_6$: C, 17.3; H, 0.95; S, 15.35. Found: C, 17.5; H, 1.0; S, 16.0. ^1H NMR: $\delta = 7.70-7.04$ (m, 4H, $S_2C_6H_4$). Data for **5** are as follows. Anal. Calcd for $C_{21}H_{18}Au_3Br_3S_6$: C, 19.5; H, 1.4; S, 14.9. Found: C, 19.8; H, 1.6; S, 15.5. ^1H NMR: $\delta = 7.62$, 7.34 and 6.82 (m, 3H, $S_2C_6H_3CH_3$), 2.21(s, 3H, $S_2C_6H_3CH_3$).

$[Au(X)(dmit)]_n$ [X = Br (6), Cl (7)]. Method a. To an acetone (30 cm^3) solution of $[Sn(dmit)(CH_3)_2]$ (0.034 g, 0.1 mmol) was added $[AuCl_3(tht)]$ (0.039 g, 0.1 mmol) or $[AuBr_3(tht)]$ (0.052 g, 0.1 mmol). Immediately black solids **6** and **7** precipitated, which were filtered off and dried *in vacuo*. Yield (%): 90 (**6**), 74 (**7**). **Method b.** To an acetone solution under dinitrogen of $(NEt_4)_2[Zn(dmit)_2]$ (0.071 g, 0.1 mmol) was added $[AuCl_3(tht)]$ (0.078 g, 0.2 mmol) or $[AuBr_3(tht)]$ (0.104 g, 0.2 mmol). Black solids **6** and **7** appeared immediately, which were filtered off, washed with water, and dried *in vacuo*. Yield (%): 97 (**6**), 90 (**7**). Anal. Calcd for C_3AuBrS_5: C, 7.6; S, 33.8. Found: C, 7.7; S, 31.55.Anal. Calcd for C_3AuClS_5: C, 8.4; S, 37.3. Found: C, 9.0; S, 36.45.

$[Au(C_6F_5)(S_2C_6H_4)(SC_6H_4SPPh_3)]$ (8). To a diethyl ether (30 cm^3) solution of **1** (0.015 g, 0.05 mmol) was added PPh_3 (0.059 g, 0.225 mmol), and the resulting solution was stirred for 1 h. A pink solid appeared, which was filtered off and washed with diethyl ether (2 × 5 cm^3). Yield: 11%. Anal. Calcd for $C_{36}H_{23}AuF_5PS_4$: C, 47.7; H, 2.55; S, 14.1. Found: C, 47.9; H, 2.6; S, 14.6. Λ_M: 7 Ω^{-1} cm^2 mol^{-1}. ^{31}P NMR: $\delta = 44.1$ (s). ^{19}F NMR: $\delta = -120.8$ (m, 2F, Fo), -159.1 (t, $^3J_{F_pF_m} = 19.5$ Hz, 1F, F_p), -162.7 (m, 2F, F_m).

$[Au(C_6F_5)(S\text{-}S)py]$ [S-S = 1,2-$S_2C_6H_4$ (9a), 3,4-$S_2C_6H_3CH_3$ (9b), dmit (9c)]. To a diethyl ether (30 cm^3) solution of **1** (0.151 g, 0.04 mmol) or **2** (0.155 g, 0.04 mmol) or to an acetone (30 cm^3) of **3** (0.168g, 0.1 mmol) was added excess pyridine. After being stirred for 2 h, the solutions were concentrated to 5 cm^3. Addition of hexane (20 cm^3) led to the precipitation of pink (**9a**, 33%; **9b**, 60%) or dark brown (**9c**, 65%) solids. Data for **9a** are as follows. Anal. Calcd for $C_{17}H_9AuF_5NS_2$: C, 35.0; H, 1.55; N, 2.4; S, 11.0. Found: C, 35.4; H, 1.3; N, 1.9; S, 11.7. Λ_M: 5 Ω^{-1} cm^2 mol^{-1}. ^1H NMR: $\delta = 8.97$ (m, 1H, py), 8.70 (m, 1H, py), 7.96 (m, 1H, py), 7.65 (m, 3H, py and $S_2C_6H_4$), 7.22 (m, 2H, $S_2C_6H_4$), 6.98 (m, 1H, $S_2C_6H_4$). ^{19}F NMR: $\delta = -122.3$ (m, 2F, F_o), -157.2 (t, $^3J_{F_pF_m} = 19.4$ Hz, 1F, F_p), -161.7 (m, 2F, F_m). Data for **9b** are as follows. Anal. Calcd for $C_{18}H_{11}AuF_5NS_2$: C, 36.2; H, 1.85; N, 2.35; S, 10.75. Found: C, 36.4; H, 1.25; N, 2.35; S, 10.55. Λ_M: 3 Ω^{-1} cm^2 mol^{-1}. ^1H NMR: $\delta = 8.95$ (m, 1H, py), 8.60 (m, 1H, py), 7.94 (m, 1H, py), 7.50 (m, 2H, py), 7.05 (m, 2H, $S_2C_6H_3CH_3$), 6.80 (m, 1H, $S_2C_6H_3CH_3$), 2.25 (s, 3H, CH_3). ^{19}F NMR: $\delta = -122.3$ (m, 2F, F_o), -157.3 (t, $^3J_{F_pF_m} = 19.5$ Hz, 1F, F_p), -161.7 (m, 2F, F_m). Data for **9c** are as follows. Anal. Calcd for $C_{14}H_5AuF_5NS_5$: C, 26.3; H, 0.8; N, 2.2; S, 25.1. Found: C, 26.15; H, 0.8; N, 2.6; S, 23.85. ^1H NMR: $\delta = 7.35$ (m, 2H), 7.75 (t, 2H), 8.7 (m, 1H). ^{19}F NMR: $\delta = -121.0$ (m, 2F, F_o), -154.1 (t, $^3J_{F_pF_m} =$ 19Hz, 1F, F_p), -159.7 (m, 2F, F_m).

$Q[Au(C_6F_5)X(S\text{-}S)]$ [Q = NBu_4, X = Br, S-S = 1,2-$S_2C_6H_4$ (10a), 3,4-$S_2C_6H_3CH_3$ (10b), dmit (10c); Q = PPN, X = Cl, S-S = 1,2-$S_2C_6H_4$ (11a), 3,4-$S_2C_6H_3CH_3$ (11b), dmit (11c); Q = PPN, X = SCN, S-S = 1,2-$S_2C_6H_4$ (12a), 3,4-$S_2C_6H_3CH_3$ (12b), dmit (12c)]. To an acetone (30 cm^3) solution of **1** (0.151 g, 0.1 mmol), **2** (0.155 g, 0.1 mmol), or **3** (0.168 g, 0.1 mmol) was added NBu_4Br (0.096 g, 0.3 mmol), PPN(Cl) (0.172 g, 0.3 mmol) or PPN(SCN) (0.178 g, 0.3 mmol). After being stirred for 4 h, the solutions were concentrated to 5 cm^3. Addition of hexane (20 cm^3) led to the precipitation of violet (**10**−**12a,b**) or yellow-green (**10**−**12c**) solids. Data for **10a** are as follows. Yield: 41%. Anal. Calcd for $C_{28}H_{40}AuBrF_5NS_2$: C, 40.7; H, 4.9; N, 1.7; S, 7.75. Found: C, 40.9; H, 4.9; N, 1.9; S, 6.85. Λ_M: 111 Ω^{-1} cm^2 mol^{-1}. ^1H NMR: $\delta = 7.06$ and 6.76 (m, 4H, $S_2C_6H_4$), 3.07, 1.50, 1.36 and 0.94 (m, 9H, NBu_4). ^{19}F NMR: $\delta = -120.7$ (m, 2F, F_o), -158.8 (t, $^3J_{F_pF_m} = 19.9$ Hz, 1F, F_p), -162.35 (m, 2F, F_m). Data for **10b** are as follows. Yield: 68%. Anal. Calcd for $C_{29}H_{42}AuBrF_5NS_2$: C, 41.45; H, 5.05; N, 1.65; S, 7.85. Found: C, 41.6; H, 5.25; N, 1.65; S, 7.0. Λ_M: 113 Ω^{-1} cm^2 mol^{-1}. ^1H NMR: $\delta = 6.94$ and 6.65 (m, 3H, $S_2C_6H_3CH_3$), 3.02, 1.45, 1.31 and 0.91 (m, 9H, NBu_4), 2.19 (s, 3H, $S_2C_6H_3CH_3$). ^{19}F NMR: $\delta = -120.7$ (m, 2F, F_o), -158.85 (t, $^3J_{F_pF_m} = 19.9$ Hz 1F, F_p), -162.35 (m, 2F, F_m), 2.19 (s, 3H, $S_2C_6H_3CH_3$). Data for **10c** are as follows. Yield: 85%. Anal. Calcd for $C_{25}H_{36}AuBrF_5NS_5$: C, 34.0; H, 4.1; N, 1.6; S, 18.2. Found: C, 34.6; H, 4.4; N, 1.7; S, 16.8. Λ_M: 123 Ω^{-1} cm^2 mol^{-1}. ^{19}F NMR: $\delta = -121.4$ (m, 2F, F_o), -157.6 (t, $^3J_{F_pF_m} = 19.9$ Hz, 1F, F_p), -162.0 (m, 2F, F_m). Data for **11a** are as follows. Yield: 60%. Anal. Calcd for $C_{48}H_{34}AuClF_5NP_2S_2$: C, 53.45; H, 3.2; N, 1.3; S, 5.95. Found: C, 53.65; H, 3.2; N, 1.2; S, 5.55. Λ_M: 94 Ω^{-1} cm^2 mol^{-1}. ^1H NMR: $\delta = 7.63-7.41$ (m, 30H, PPN), 7.06 and 6.76 (m, 4H, $S_2C_6H_4$). ^{19}F NMR: $\delta = -120.3$ (m, 2F, F_o), -160.1 (t, $^3J_{F_pF_m} = 20.05$ Hz, 1F, F_p), -168.0 (m, 2F, F_m). Data for **11b** are as follows. Yield: 64%. Anal. Calcd for $C_{49}H_{36}AuClF_5NP_2S_2$: C, 53.9; H, 3.3; N, 1.3; S, 5.85. Found: C, 53.15; H, 3.45; N, 0.95; S, 5.65. Λ_M: 99 Ω^{-1} cm^2 mol^{-1}. ^1H NMR: $\delta = 7.62-7.41$ (m, 30H, PPN), 7.10 and 6.50 (m, 3H, $S_2C_6H_3CH_3$), 2.15 (s, 3H, $S_2C_6H_3CH_3$). ^{19}F NMR: $\delta = -120.2$ (m, 2F, F_o), -160.2 (t, $^3J_{F_pF_m} = 20.1$ Hz, 1F, F_p), -163.0 (m, 2F, F_m). Data for **11c** are as follows. Yield: 70%. Anal. Calcd for $C_{45}H_{30}AuClF_5NP_2S_5$: C, 47,6; H, 2.7; N, 1.2; S, 14.1. Found: C, 47.6; H, 3.2; N, 1.5; S, 12.3. Λ_M: 120 Ω^{-1} cm^2 mol^{-1}. ^{19}F NMR: $\delta = -120.1$ (m, 2F, F_o), -158.1 (t, $3J_{F_pF_m} = 20$Hz, 1F, F_p), -162.05 (m, 2F, F_m). Data for **12a** are as follows. Yield: 89%. Anal. Calcd for $C_{49}H_{34}AuF_5N_2P_2S_3$: C, 53.45; H, 3.1; N, 2.25; S, 8.75. Found: C, 53.4; H, 3.45; N, 2.1; S, 8.2. Λ_M: 115 Ω^{-1} cm^2 mol^{-1}. ^1H NMR: $\delta = 7.72-7.30$ (m, 30H, PPN) 7.10 and 6.80 (m, 4H, $S_2C_6H_4$). ^{19}F NMR: $\delta = -119.7$ (m, 2F, F_o), -158.5 (t, $^3J_{F_pF_m} = 20.5$ Hz, 1F, F_p), -162.3 (m, 2F, F_m). Data for **12b** are as follows. Yield: 44%. Anal. Calcd for $C_{50}H_{36}AuF_5N_2P_2S_3$: C, 53.85; H, 3.25; N, 2.5; S, 8.65. Found: C, 53.4; H, 3.4; N, 2.2; S, 8.3. Λ_M: 107 Ω^{-1} cm^2 mol^{-1}. ^1H NMR: $\delta = 7.65-7.33$ (m, 30H, PPN), 6.94 and 6.63 (m, 3H, $S_2C_6H_3CH_3$). Data for **12c** are as follows. Yield: 83%. Anal. Calcd for $C_{46}H_{30}AuF_5N_2P_2S_6$: C, 47.75; H, 2.6; N, 2.4; S, 16.6. Found: C, 48.2; H, 2.4; N, 2.35; S, 14.4. Λ_M: 113 Ω^{-1} cm^2 mol^{-1}. ^{19}F NMR: $\delta = -120.7$ (m, 2F, F_o), -157.0 (t, $^3J_{F_pF_m} = 20$ Hz, 1F, F_p), -161.7 (m, 2F, F_m).

X-Ray Structure Determinations. Compound 1. *Data collection:* Data were measured with Mo Kα radiation on a Stoe STADI-4 diffractometer fitted with a Siemens LT-2 low-temperature device. Cell constants were refined from $\pm\omega$ values of ca. 50 reflections in the 2θ range 20−23°. Absorption corrections were based on ψ-scans. *Structure solution:* heavy-atom method. *Structure refinement:* anisotropic on F^2 (program SHELXL-93, G. M. Sheldrick, Univ. of Göttingen) using

all reflections; H atoms using riding model. Other details are given in Tables 1–3.

Compound 8. The structure was determined as for compound **1** except for the following. *Data collection:* Siemens P4 diffractometer, cell constants refined from setting angles, absorption correction using SHELXA (G. M. Sheldrick, unpublished). *Structure refinement:* C atoms isotropic, phenyl rings idealized. Other details are in Tables 1, 4, and 5.

Acknowledgment. We thank the Direction General de Investigación Científica y Técnica (Grant PB92-1078) for financial support. We also thank the Fonds der Chemischen Industrie and Ministerio de Educación y Ciencia for a grant (to R.T.).

Supporting Information Available: Descriptions of the crystal structure determinations, including tables of crystal data, data collection, and solution and refinement parameters, hydrogen coordinates, bond distances and angles, and thermal parameters (8 pages). Ordering information is given on any current masthead page.

OM9504415

Preparation of Five-Membered Nickelacycles of N-Donor Ligands by Activation of C–X Bonds (X = F, Cl, or Br). X-ray Crystal Structure of [NiBr{2-(CH=NCH$_2$Ph)C$_6$H$_4$}(2,4,6-Me$_3$C$_5$H$_2$N)]

Rosa M. Ceder, Jaume Granell,* and Guillermo Muller*

Department de Química Inorgànica, Universitat de Barcelona, Diagonal, 647, 08028 Barcelona, Spain

Mercè Font-Bardía and Xavier Solans

Departament de Cristallografia, Mineralogia i Dipòsits Minerals, Universitat de Barcelona, Martí i Franquès, s/n, 08028 Barcelona, Spain

Received May 12, 1995[⊗]

The five-membered metallacycles [Ni(C–N)XL] (L = 2-picoline, 2,4-lutidine, or 2,4,6-collidine, X = Cl or Br) have been prepared by reaction of [Ni(cod)$_2$] with *ortho* halo-substituted imines or *N,N*-dimethylbenzylamines in toluene or tetrahydrofuran, in the presence of an aromatic amine as stabilizing ligand. The molecular structure of [NiBr{2-(CH=NCH$_2$Ph)C$_6$H$_4$}{2,4,6-Me$_3$(C$_5$H$_2$N)}] has been determined by a single-crystal X-ray crystallographic study. The reaction of [Ni(cod)$_2$] with *ortho* halo-substituted imines or with C$_6$Cl$_5$CH$_2$NMe$_2$, in toluene or THF, in the presence of dimethylphenylphosphine, gave the metalated compounds [NiX(C–N)(PMe$_2$Ph)$_2$], **8** or **9**, through oxidative addition of one of the *ortho* C–X bonds (X = Br or Cl) of the N-donor ligand. All the spectroscopic evidence indicates a square-planar geometry for these compounds, with the phosphine molecules in a *trans* arrangement and the iminic nitrogen atom in an axial position around the metal, giving a pseudopentacoordinated compound. Surprisingly, when the oxidative addition reaction was performed in a 1/1 molar ratio of nickel/phosphine, the formation of the metallacycles [NiX(C–N)(PMe$_2$Ph)] was not observed, but **8** or **9**, containing two phosphine molecules by the metal atom, were formed. The oxidative addition of one of the *ortho* C–F bonds of the imine C$_6$F$_5$CH=NCH$_2$Ph to [Ni(cod)$_2$] was also observed under very mild conditions, and compound [NiBr(C$_6$F$_4$CH=NCH$_2$Ph)(PMe$_2$Ph)$_2$] was obtained when the reaction was performed in the presence of LiBr and PMe$_2$Ph.

Introduction

The preparation of metal complexes containing polydentate ligands has become a field of increasing interest. The selection of the number and type of coordinating atoms, the size of the metallacycle, and the neutral or ionic nature of the ligand allows extensive modulation of the chemical properties of compounds of this type. The study of nickel complexes with such ligands is especially interesting because of their reactivity and their catalytic activity. Nickel compounds with anionic P–O ligands have been widely studied and are highly active and selective catalysts in the oligomerization of ethylene to linear α-olefins.[1] Van Koten *et al.* have reported the synthesis and reactivity of many complexes which contain monoanionic ligands, potentially terdentate (N–C–N),[2] and one of them is an effective catalyst in the Karasch addition.[3] In contrast, few nickelacycles containing bidentate anionic N–C ligands have been described, and there is no systematic process to obtain them. Pfeffer *et al.* have described the preparation of cyclonickelated compounds by reaction between *ortho-N,N*-(dimethylamino)benzyllithium and [NiCl$_2$(PR$_3$)$_2$].[4] Longoni *et al.* have reported the synthesis of compounds of nickel(II), palladium(II), and platinum(II) of type [M(C–N)$_2$], HC–N = *N,N*-dimethylbenzylamine, by reaction between 2-[(dimethylamino)methyl]phenyllithium and [MCl$_2$(PEt$_3$)$_2$].[5] Azobenzene derivatives have been obtained from NiCp$_2$ and *ortho*-halogenated azobenzene;[6] isocyanide insertion into Ni–C(benzylic) bonds[7] and also reactions with organomercury compounds have been used to obtain N–C nickelocycles.[8]

[⊗] Abstract published in *Advance ACS Abstracts,* September 1, 1995.

(1) (a) Peuckert, M.; Keim, W. *Organometallics* **1983**, *2*, 594. (b) Keim, W.; Behr, A.; Gruber, B.; Hoffmann, B.; Kowaldt, F. H.; Kürschner, U.; Limbäcker, B.; Sistig, F. P. *Organometallics* **1986**, *5*, 2356. (c) Keim, W. *Angew. Chem., Int. Ed. Engl.* **1990**, *29*, 235. (d) Klabunde, U.; Ittel, S. D. *J. Mol. Cat.* **1987**, *41*, 123. (e) Keim, W.; Schulz, R. P. *J. Mol. Cat.* **1994**, *92*, 21. (f) Braunstein, P.; Chauvin, I.; Mercier, S.; Saussine, L.; De Cian, A.; Fischer, J. *J. Chem. Soc., Chem. Commun.* **1994**, 2203. (g) Bonnet, M. C.; Dahan, F.; Ecke, A.; Keim, W.; Schulz, R. P.; Tkatchenko, I. *J. Chem. Soc., Chem. Commun.* **1994**, 615.

(2) (a) van de Kuil, L. A.; Luitjes, H.; Grove, D. M.; Zwikker, J. W.; van der Linden, J. G. M.; Roelofsen, A. M.; Jenneskens, L. W.; Drenth, W.; van Koten, G. *Organometallics* **1994**, *13*, 468. (b) van Beek, J. A. M.; van Koten, G.; Ramp, M. J.; Coenjarts, N. C.; Grove, D. M.; Goubitz, K.; Zoutberg, M. C.; Stam, C. H.; Smeets, W. J. J.; Spek, A. L. *Inorg. Chem.* **1991**, *30*, 3059. (c) Grove, D. M.; van Koten, G.; Ubbels, H. J. C.; Zoet, R. *Organometallics* **1984**, *3*, 1003.

(3) Grove, D. M.; van Koten, G.; Verschuuren, A. H. M. *J. Mol. Cat.* **1988**, *45*, 169.

(4) Arlen, C.; Pfeffer, M.; Fischer, J.; Mitschler, A. *J. Chem. Soc., Chem. Commun.* **1983**, 928.

(5) Longoni, G.; Fantucci, P.; Canzani, F. *J. Organomet. Chem.* **1972**, *39*, 413.

0276-7333/95/2314-5544$09.00/0

We have described the synthesis and reactivity of five- and four-membered nickelacycles containing the anionic P–C chelate,[9] and now we extend our studies to N–C anionic ligands. In this paper we report the reactions of $[Ni(cod)_2]$ and *ortho* halo-substituted amines or imines in the presence of heterocyclic amines or $PPhMe_2$ as stabilizing ligands. This reaction appears to be quite general and permits the synthesis of the corresponding metallacycles in good yields.

Fluorocarbons are reluctant to coordinate to metal centers and resistant to chemical attack as a consequence of the strength of the C–F bond, but it has been shown recently that several low-valent transition metal compounds can insert into an aromatic carbon–fluorine bond of N-donor ligands.[10] There are very few reports of activation of C–F bonds by nickel compounds. Fahey reported the intermolecular oxidative addition of C_6F_6 to $[Ni(PEt_3)_2(cod)]$ at 30–35° over a period of days in a 7% yield.[11] Richmond *et al.* have shown that the reaction between $[Ni(cod)_2]$ and the terdentate ligand $2\text{-}NMe_2C_6H_4N{=}CHC_6F_5$ results in intramolecular C–F activation at room temperature.[10b] We report here that the reaction between $[Ni(cod)_2]$ and the imine $C_6F_5\text{-}CH{=}NCH_2Ph$, in the presence of PMe_2Ph and LiBr, affords a metalated complex by activation of one of the *ortho* C–F bonds of the imine in very mild conditions.

Results and Discussion

Synthesis of [NiX(C–N)L], L = Aromatic Amine. The reaction of $[Ni(cod)_2]$ with *ortho* halo-substituted imines or *N,N*-dimethylbenzylamines in toluene or THF, in the presence of an aromatic amine (2-picoline, 2,4-lutidine, or 2,4,6-collidine), gave five-membered metallacycles through oxidative addition of one of the *ortho* C–X bonds (X = Br or Cl) of the N-donor ligand (Scheme 1). The new compounds obtained are stable either as dry solids or in benzene, toluene, or tetrahydrofuran solutions under nitrogen, and they were characterized by elemental analyses, infrared spectra, ^1H NMR in C_6D_6 solution under nitrogen, and crystal structure determination of **7c** (see below). Mass spectra of selected compounds were also recorded. The proton NMR spectra of imine derivatives (Table 1 and Figure 1) and the spectrum of the amine metallacycle **3a** are well-defined. The aromatic protons of both the heterocyclic amine and the metalated ring are high-field shifted, suggesting a *cis* arrangement between both moieties (the crystal structure determination of **7c** confirms this). The *ortho* methyl groups of the aromatic amines appear to be low-field shifted. This shift can be explained by the paramagnetic anisotropy of the

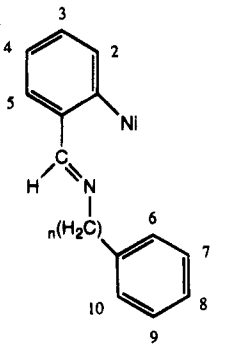

Figure 1.

Scheme 1

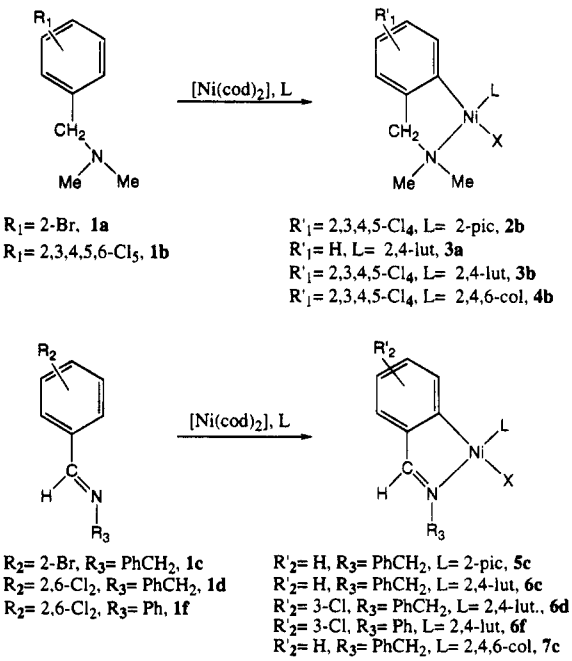

metal and shows that these methyl groups occupy the axial position of the metal atom, due to the hindered rotation around the Ni–N bond.[12] In the ^1H NMR spectrum of **3a**, the CH_2 protons appear as a well-defined AB quartet and the NMe_2 protons appear as two singlets. These facts show the coordination of the nitrogen atom of the NMe_2 group to the nickel and that the coordination plane is not a symmetry plane (only one of the axial positions of the metal is occupied by a methyl group of the lutidine). In contrast, the ^1H NMR spectra of pentachloroamine derivatives **2b–4b** in C_6D_6 or toluene-d_8 at room temperature give broad signals, and compound **4b** shows a magnetic moment of 1.78 μ_B (298 K). Similar anomalous magnetic moments have been measured for some nickel derivatives, and an isomeric equilibrium in solution between the tetrahedral and the square-planar form or the formation of a mixture of the two isomers in solid has been proposed to explain this.[13] The release of steric interaction between the chlorine in *ortho* position relative to the Ni–C bond and the ligands of the nickel atom when the tetrahedral isomer is formed could be the driving force of this process, and this may explain the fact that only

(6) (a) Kleimann, J. P.; Dubeck, M. *J. Am. Chem. Soc.* **1963**, *85*, 1544. (b) Ustynyuk, Y. A.; Barinov, I. V. *J. Organomet. Chem.* **1970**, *23*, 551. (c) Barinov, I. V.; Voyevodskaya, T. Y.; Ustynyuk, Y. A. *J. Organomet. Chem.* **1971**, *30*, C28.

(7) Cámpora, J.; Gutiérrez, E.; Monge, A.; Poveda, M. L.; Ruiz, C.; Carmona, E. *Organometallics* **1993**, *12*, 4025.

(8) (a) Isaeva, L. S.; Morozova, L. N.; Bashilov, V. V.; Petrovskii, P. V.; Sokolov, V. I.; Reutov, O. A. *J. Organomet. Chem.* **1983**, *243*, 253. (b) Cross, R. J.; Tennent, N. H. *J. Organomet. Chem.* **1974**, *72*, 21.

(9) (a) Muller, G.; Panyella, D.; Rocamora, M.; Sales, J.; Font-Bardia, M.; Solans, X. *J. Chem. Soc., Dalton Trans.* **1993**, 2959. (b) Font-Bardia, M.; González-Platas, J.; Muller, G.; Panyella, D.; Rocamora, M.; Solans, X. *J. Chem. Soc., Dalton, Trans.* **1994**, 3075.

(10) (a) Richmond, T. G. *Coord. Chem. Rev.* **1990**, *105*, 221. (b) Kiplinger, J. L.; Richmond, T. G.; Osterberg, C. E. *Chem. Rev.* **1994**, *94*, 373.

(11) Fahey, D. R.; Mahan, J. E. *J. Am. Chem. Soc.* **1977**, *99*, 2501.

(12) Miller, R. G.; Stauffer, R. D.; Fahey, D. R.; Parnell, D. R. *J. Am. Chem. Soc.* **1970**, *92*, 1511.

(13) Frömmel, T.; Peters, W.; Wunderlich, H.; Kuchen, W. *Angew. Chem., Int. Ed. Engl.* **1992**, *5*, 612.

Table 1. Proton[a] NMR Data

compd	aromatic	others
2b	8.83 (br s, 1H, pic) 6.55 (br m, 1H, pic) 6.18 (br m, 1H, pic)	3.47 (s, 2H, CH_2N) 3.43 (s, 3H, pic) 1.95 [s, 6H, $N(CH_3)_2$]
3a	8.99 [d, ^3J(HH) = 5.6, 1H, lut] 6.70 [br m, 2H, H^3, H^5] 6.97 [t, ^3J(HH) = 7.8, 1H, H^4] 6.20 (s, 1H, lut) 6.08 [d, ^3J(HH) = 5.6, 1H, lut] 5.36 [d, ^3J(HH) = 7.3, 1H, H^2]	3.52 (s, 3H, lut) 3.18 [q(AB), 2H, NCH_2] 2.55 [s, 3H, $N(CH_3)$] 2.51 [s, 3H, $N(CH_3)$] 1.55 (s, 3H, lut)
3b	8.82 [d, ^3J(HH) = 5.9, 1H, lut] 6.08 (s, 1H, lut) 6.02 [d, ^3J(HH) = 5.9, 1H, lut]	3.43 (s, 3H, lut) 1.50 (s, 3H, lut) 1.97 [s, 6H, $N(CH_3)_2$] 3.50 (s, 2H, CH_2N)
4b[b,c]	6.15 (s, 2H, col)	3.93 (s, 6H, col) 3.45 (s, 2H, CH_2N) 2.06 [s, 6H, $N(CH_3)_2$] 1.79 (s, 3H, col)
5c	8.84 (br s, 1H, pic) 7.41 (br s, 2H, H^6, H^{10}) 7.03–6.70 (br m, 7H imine) 6.51 (br m, 1H, pic) 6.24 (br m, 2H, pic) (H^2)[e]	HC=N[d] 5.05 [q(AB), 2H, NCH_2] 3.30 (s, 3H, Me)
6c	8.72 [d, ^3J(HH) = 6.0, 1H, lut] 7.45 [d, ^3J(HH) = 7.0, 2H, H^6, H^{10}] 7.18–6.72 (br m, 7H, imine) 6.15 (s, 1H, lut) 6.05 [d, ^3J(HH) = 6.0, 1H, lut] 5.35 [d, ^3J(HH) = 7.5, 1H, H^2]	HC=N[d] 5.05 q(AB), 2H, NCH_2] 3.30 (s, 3H, lut) 1.50 (s, 3H, lut)
6d	8.61 [d, ^3J(HH) = 5.9, 1H, lut] 7.45 [d, ^3J(HH) = 7.0, 2H, H^6, H^{10}] 7.15 (br m, 3H, H^7, H^8, H^9) 6.74 [d, ^3J(HH) = 7.8, 1H, H^4] 6.41 [t, ^3J(HH) = 7.8, 1H, H^3] 6.11 (s, 1H, lut) 6.05 [d, ^3J(HH) = 5.9, 1H, lut] 5.23 [d, ^3J(HH) = 7.2, 1H, H^2]	7.95 (s, 1H, HC=N) 4.85 [q(AB), 2H, NCH_2] 3.26 (s, 3H, lut) 1.52 (s, 3H, lut)
6f[c]	8.90 [d, ^3J(HH) = 4.8, 1H, lut] 7.47 [d, ^3J(HH) = 7.2, 2H, H^6, H^{10}] 7.35–7.20 [br m, 3H, H^7, H^8, H^9] 6.96 [d, ^3J(HH) = 8.1, 1H, H^4] 6.63 [t, ^3J(HH) = 8.1, 1H, H^3] 6.49 (s, 1H, lut) 6.33 [d, ^3J(HH) = 4.8, 1H, lut] 5.47 [d, ^3J(HH) = 7.8, 1H, H^2]	8.25 (s, 1H, CH=N) 3.54 (s, 3H, lut) 1.76 (s, 3H, lut)
7c	7.55 [d, ^3J(HH) = 7.0, 2H, H^6, H^{10}] 7.18–6.70 (br m, 7H, imine) 6.21 (s, 2H, col) 5.25 [d ^3J(HH) = 7.0, 1H, H^2]	HC=N[d] 5.19 (s, 2H, NCH_2) 3.66 (s, 6H, col) 1.71 (s, 3H, col)
8b	7.41 (br s, 4H, P–Ph) 7.15–7.00 (br m, 6H, P–Ph)	2.17 [s, 6H, $N(CH_3)_2$] 3.93 (s, 2H, NCH_2) 1.22 (br s, 12H, P–Me)
9c	7.65 [d, ^3J(HH) = 7.5, 2H, H^6, H^{10}] 7.54 (br s, 4H, P–Ph) 7.21–7.00 (br m, 9H, P–Ph, H^7, H^8, H^9) 6.85 [d, ^3J(HH) = 7.5, 1H, H^2] 6.72–6.50 (m, 3H, H^3, H^4, H^5)	8,11 (s, 1H, HC=N) 5.19 (s, 2H, CH_2N) 0.95 (br s, 12H, P–Me)
9d	7.64 [d, ^3J(HH) = 7.6, 2H, H^6, H^{10}] 7.39 (br s, 4H, P–Ph) 7.15–7.00 (br m, 9H, P–Ph, H^7, H^8, H^9) 6.85 [d, ^3J(HH) = 7.8 H^2] 6.33 [d, ^3J(HH) = 7.8, H^4] 6.20 [t, ^3J(HH) = 7.8, H^3]	8.97 (s, 1H, HC=N) 5.16 (s, 2H, CH_2N) 0.92 (br s, 12H, P–Me)
9e	7.90 [d, ^3J(HH) = 7.8, 2H, H^6, H^{10}] 7.73 (br s, 4H, P–Ph) 7.46 [t, ^3J(HH) = 7.8, 2H, H^7, H^9] 7.18 (br m, 9H, P–Ph, H^2, H^5, H^8) 6.85 (t, ^3J(HH) = 7.7, H^4) 6.72 (t, ^3J(HH) = 7.7, H^3)	8.47 (s, 1H, HC=N) 1.50 (br s, 6H, P–Me) 0.70 (br s, 6H, P–Me)
9f	7.93 [d, ^3J(HH) = 7.6, 2H, H^6, H^{10}] 7.48 (br s, 4H, P–Ph) 7.30 [t, ^3J(HH) = 7.6, 2H, H^7, H^9]	9.23 (s, 1H, HC=N) 1.39 (br s, 6H, P–Me) 0.58 (br s, 6H, P–Me)

Table 1 (Continued)

compd	aromatic	others
9f	7.15–7.00 (br m, 7H, P–Ph, H^8) 6.85 [d, ^3J(HH) = 7.5, H^2] 6.72 [d, ^3J(HH) = 7.5, H^4] 6.30 [t, ^3J(HH) = 7.5, H^3]	
9g	7.50 [d, ^3J(HH) = 7.0, 2H, H^6, H^{10}] 6.90–7.15 (br m, 13H, P–Ph, H^7, H^8, H^9)	8.41 [d, 1H, ^4J(HF) = 2.3, CH=N] 4.91 (s, 2H, CH_2N) 1.41 (br s, 6H, P–Me) 1.03 (br s, 6H, P–Me)

[a] In C_6D_6, at room temperature; chemical shifts in ppm with respect to internal $SiMe_4$; coupling constants in Hz; numbering as in Figure 1. [b] In toluene–d_8 at 220 K. [c] Spectrum recorded in toluene–d_8 at 300 MHz. [d] Overlapped by aromatic protons. [e] Partially overlapped with AB quartet.

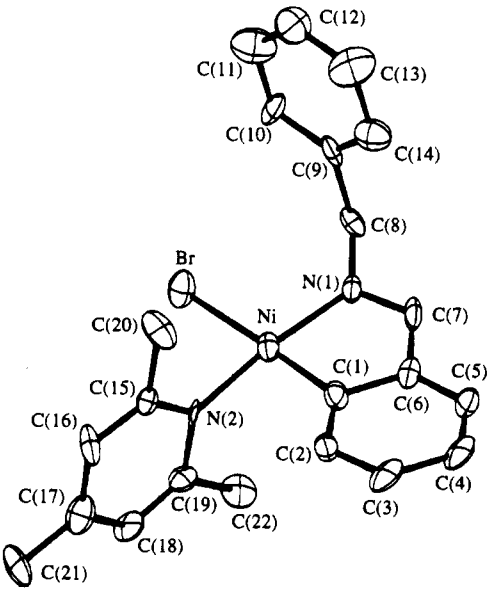

Figure 2. Molecular structure of **7c**.

the pentachloroamine derivatives present broad bands in the NMR spectra. As concerns to the spectra of the imine metallacycles **5**–**7**, the CH_2 protons appear as a singlet in the 2,4,6-collidine derivative **7c**, but in the 2-picoline or 2,4-lutidine derivatives these protons appear as an AB quartet because the coordination plane is not a symmetry plane in these complexes, and, as a consequence, the methylene protons are diastereotopic.

When the oxidative addition reaction was performed either using pyridine or 4-picoline as neutral ligands or in the absence of aromatic amines, no organometallic compound was obtained. These results show that an aromatic amine containing at least one methyl group in *ortho* position is needed to obtain such metalated species. The low stability of dinuclear halo-bridged organonickel compounds and the necessity of some steric protection to stabilize the organometallic nickel complex could explain this.

Molecular Structure of 7c. The crystal structure of **7c** has been determined (Figure 2). Crystallographic data, atomic coordinates for non-hydrogen atoms, and selected bond lengths and angles are listed in Tables 2–4 respectively.

The crystal structure consists of discrete molecules separated by van der Waals distances. The nickel atom is in a slightly distorted square-planar environment, coordinated to carbon, bromine, and the two nitrogen atoms, with deviations from the mean plane as follows: Ni, −0.0451 Å, Br, −0.0096 Å, N(1), 0.0345 Å; N(2) 0.0353 Å; C(1), −0.0151 Å. The nitrogen atoms adopt a *trans* arrangement. The angles between adjacent atoms in the coordination sphere lie in the range 97.2(2)°, (N1–Ni–Br) to 83.6(4)° (C1–Ni–N1). The distance between nickel and the coordinated atoms are similar to those reported for other analogous compounds.[2b]

Table 2. Crystal Data and Structure Refinement for 7c

empirical formula	$C_{22}H_{23}BrN_2Ni$
fw	478.06
temp	293(2) K
wavelength	0.710 69 Å
cryst syst	monoclinic
space group	$P2_1/a$
unit cell dimens	a = 12.564(2) Å, α = 90° b = 14.704(3) Å, β = 104.98(2)° c = 11.615(2) Å, γ = 90°
volume	2072.8(6) Å^3
Z	4
density (calcd)	1.532 g/cm^3
abs coeff	2.875 mm^{-1}
F(000)	976
cryst size	0.1 × 0.1 × 0.2 mm^3
θ range for data collcn	2.18–25.05°
index ranges	$-14 \le h \le 14$, $0 \le k \le 17$, $0 \le l \le 13$
no. of reflns collcd	3648
no. of indpt reflns	3648 [R(int) = 0.0000]
ref method	full-matrix least-squares on F^2
data/restraints/params	2830/0/237
goodness-of-fit on F^2	0.938
final R indices [$I > 2\sigma(I)$]	R1 = 0.0650, wR2 = 0.1585
R indices (all data)	R1 = 0.1633, wR2 = 0.2927
extinct coeff	0.0000(8)
largest diff peak and hole	1.150 and −0.999 e Å^{-3}

The coordination plane and the collidine molecule are almost perpendicular (88.51°), and the *ortho* methyl groups of the aromatic amine occupy the apical sites in the coordination sphere, the Ni···C22 and Ni···C20 distances being 3.002(11) and 3.033(11) Å, respectively.

The metalated phenyl ring and the methinic moiety are nearly planar, and the angle between normals to both planes is 9.5°. The metalated phenyl and the benzylamine groups are in *trans* position relative to the C=N bond, showing that the imine is in the *E*-conformation; the angle between normals to both planes is 93.3°.

Synthesis of [NiX(C–N)(PMe_2Ph)$_2$]. The reaction of [Ni(cod)$_2$] with *ortho* halo-substituted imines or with $C_6Cl_5CH_2NMe_2$, in toluene or THF, in the presence of dimethylphenylphosphine gave the metalated compounds [NiX(C–N)(PMe_2Ph)$_2$], **8b** and **9c**–**f**, through oxidative addition of one of the *ortho* C–X bonds (X = Br or Cl) of the N-donor ligand (Scheme 2). Although no organometallic compound was isolated as a pure solid when the reaction was performed with *N*,*N*-dimethyl-2-bromobenzylamine, their formation was detected by

Table 3. Atomic Coordinates ($\times 10^4$) and Equivalent Isotropic Displacement Parameters ($A^2 \times 10^3$) for 7c

atom	x	y	z	U(eq)[a]
Br	1760(1)	989(1)	914(1)	61(1)
Ni	3253(1)	−91(1)	1456(1)	40(1)
N(1)	2469(6)	−1121(5)	646(7)	36(2)
N(2)	4080(7)	825(4)	2403(6)	34(2)
C(1)	4432(10)	−940(7)	1940(9)	48(3)
C(2)	5525(9)	−824(7)	2527(9)	47(3)
C(3)	6262(11)	−1571(8)	2784(9)	65(4)
C(4)	5844(11)	−2478(8)	2505(10)	62(3)
C(5)	4809(10)	−2563(7)	1932(9)	50(3)
C(6)	4084(9)	−1842(6)	1636(9)	41(3)
C(7)	2985(9)	−1880(6)	914(9)	47(3)
C(8)	1357(9)	−1125(7)	−211(9)	53(3)
C(9)	1361(8)	−856(6)	−1495(9)	44(3)
C(10)	733(10)	−126(7)	−2041(10)	61(3)
C(11)	717(13)	123(11)	−3172(12)	98(5)
C(12)	1381(12)	−358(9)	−3770(12)	77(4)
C(13)	2035(12)	−1093(11)	−3239(12)	94(5)
C(14)	2072(9)	−1361(9)	−2027(10)	67(3)
C(15)	4743(8)	1404(6)	1990(8)	35(2)
C(16)	5282(9)	2109(6)	2622(11)	59(3)
C(17)	5331(10)	2212(8)	3863(11)	62(3)
C(18)	4669(9)	1614(8)	4278(10)	58(3)
C(19)	4112(9)	949(7)	3581(9)	48(3)
C(20)	4759(10)	1263(8)	692(10)	67(4)
C(21)	5942(12)	2981(8)	4607(12)	103(5)
C(22)	3365(10)	256(8)	4031(9)	63(3)

[a] U(eq) is defined as one-third of the trace of the orthogonalized U_{ij} tensor.

Table 4. Selected Bond Distances (Å) and Angles (deg) for 7c

Br−Ni	2.413(2)	C(1)−C(2)	1.376(14)
Ni−N(2)	1.875(7)	C(1)−C(6)	1.413(13)
Ni−C(1)	1.908(11)	C(2)−C(3)	1.418(14)
Ni−N(1)	1.915(7)	C(3)−C(4)	1.44(2)
N(1)−C(7)	1.288(11)	C(4)−C(5)	1.305(14)
N(1)−C(8)	1.491(12)	C(5)−C(6)	1.382(14)
N(2)−C(15)	1.362(11)	C(6)−C(7)	1.419(14)
N(2)−C(19)	1.370(11)	C(8)−C(9)	1.545(14)
N(2)−Ni−C(1)	91.5(4)	C(1)−C(2)−C(3)	121.5(10)
N(2)−Ni−N(1)	173.2(3)	C(1)−C(2)−H(2)	119.2(6)
C(1)−Ni−N(1)	83.6(4)	C(3)−C(2)−H(2)	119.3(7)
N(2)−Ni−Br	87.4(2)	C(2)−C(3)−C(4)	119.3(11)
C(1)−Ni−Br	178.0(3)	C(5)−C(4)−C(3)	117.5(11)
N(1)−Ni−Br	97.2(2)	C(4)−C(5)−C(6)	124.0(11)
C(7)−N(1)−C(8)	119.0(8)	C(5)−C(6)−C(7)	126.6(9)
C(7)−N(1)−Ni	113.8(7)	C(5)−C(6)−C(1)	121.1(10)
C(8)−N(1)−Ni	127.2(6)	C(7)−C(6)−C(1)	112.1(9)
C(15)−N(2)−C(19)	114.0(8)	N(1)−C(7)−C(6)	117.5(9)
C(15)−N(2)−Ni	122.6(6)	N(1)−C(8)−C(9)	114.0(8)
C(19)−N(2)−Ni	123.4(7)	C(10)−C(9)−C(14)	123.7(11)
C(2)−C(1)−C(6)	116.4(10)	C(10)−C(9)−C(8)	119.8(10)
C(2)−C(1)−Ni	131.6(8)	C(14)−C(9)−C(8)	116.5(10)
C(6)−C(1)−Ni	112.0(8)		

^{31}P NMR spectroscopy (singlet at δ −10.3 ppm). These results show that the metalated amine complexes are less stable than the metalated imines derivatives, but the presence of electron-withdrawing substituents in the aromatic ring stabilizes the Ni−C bond and allows the formation of the amine nickelacycles. No metalated compound was obtained when the reaction was performed in the presence of PEt_3, PPh_3, or $P(CH_2Ph)_3$, in contrast with the results described for related five-membered phosphanickelacycles.[9a] The new compounds prepared are stable under nitrogen as dry solids or as benzene, toluene, or THF solutions, and they were characterized by elemental analyses, infrared spectra, and multinuclear NMR in C_6D_6 solution, under nitrogen. Mass spectra of selected compounds were also

Scheme 2

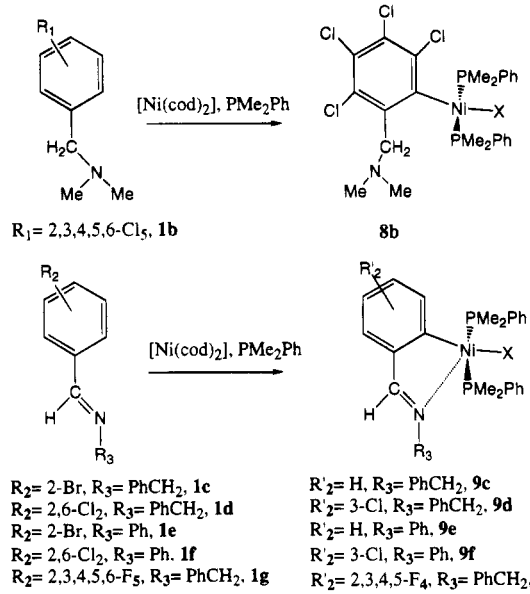

recorded. The IR spectra show the typical bands of coordinated dimethylphenylphosphine, imines, or amines. The wavenumbers corresponding to ν(C=N) appear to be shifted to low values (20−30 cm^{-1}) in the imine derivatives. These values have been taken as an indication of some interaction between the iminic nitrogen and the metal atom in analogous palladium complexes.[14] The $^{31}P\{^1H\}$ spectra display a singlet from δ −12 to −19 ppm, showing a *trans* arrangement of phosphorus atoms. The $^{13}C\{^1H\}$ spectrum of **9e** confirms the *trans* arrangement between these atoms because the signals of the P−Me carbons appear as two triplets, $J(^{13}C-^{31}P)$ = 15.5 Hz, due to "virtual coupling".[15] The proton NMR spectra are very well defined and permit the assignment of nearly all the signals (Table 1). The aromatic protons of the metalated ring appear to be high-field shifted, showing a *cis* arrangement between the phosphines and the metalated ring. The P−Me signals appear as a triplet (220 K), which is characteristic of a *trans* arrangement of the two phosphines. All this spectroscopic evidence points to a square-planar geometry for these compounds, with the phosphine molecules in a *trans* arrangement and the iminic nitrogen atom in an axial position around the metal (see Scheme 1), giving a pseudopentacoordinated compound. Analogous palladium complexes with imine ligands have been shown by X-ray studies to adopt this geometry.[14] Variable temperature ^1H NMR spectra also confirm that the iminic nitrogen occupies an axial position in the nickel coordination sphere (see below).

Surprisingly, when the oxidative addition reaction was performed in a 1/1 molar ratio of nickel/phosphine, the formation of the metallacycles [NiX(C−N)(PMe_2Ph)] was not observed, but **8** or **9**, containing two phosphine molecules per metal atom, was formed. These nickel compounds were also obtained by substitution reactions when the complexes [NiX(C−N)L], L = aromatic amine, were treated with PMe_2Ph, even if a 1/1 molar ratio of nickel/phosphine was used. The great reactivity of the

(14) Granell, J.; Sainz, D.; Sales, J.; Solans, X.; Font-Altaba, M. *J. Chem. Soc., Dalton Trans.* **1986**, 1785.
(15) Akitt, J. W. In *NMR and Chemistry*; Chapman and Hall: London, 1983; p 56.

metallacycle in the presence of PMe_2Ph is remarkable, because the five-membered phosphanickelacycles [NiCl(P−C)(PMe_2Ph)] and the cyclopalladated complexes [Pd(C−N)X(PR_3)] are easily obtained.[9a,16] This behavior is similar to that of the four-membered phosphanickelacycles, in which the metallacycle opens up easily giving pseudopentacoordinated complexes by reaction with aliphatic phosphines.[9b] The results described here show that it is not easy to obtain organometallic nickel derivatives containing monodentate P- and N-donor ligands simultaneously, and the small number of X-ray structures determined of nickel complexes of this type confirms this.[7,17] Contrary to what may be expected ("hard" *vs.* "soft" donors), the weakness of the nitrogen−nickel bonds in the new metallacycles obtained, in comparison with the palladium−nitrogen or nickel−phosphorous bonds of related metallacycles, is surprising. Pfeffer *et al.* have obtained cyclonickelated compounds by reaction between *ortho-N,N*-(dimethylamino)benzyllithium and [$NiCl_2(PR_3)_2$], and the spectroscopic data and the reactivity of the metallacycle suggest a weak interaction between nitrogen and nickel atoms.[4] The fact that few cyclonickelated compounds of N-donor ligands have been prepared, in sharp contrast with the large number of cyclopalladated or cycloplatinated derivatives described, can also be explained by the weakness of the Ni−N interaction, because it is widely accepted that the coordination of nitrogen to the metal is the initial step in the cyclometalation of N-donor ligands.[18] Crabtree *et al.* have recently studied the geometrical and electronic factors that favor the binding of soft ligands like CO to Ni(II), and they suggest that the binding properties of this metal can be significantly modified by changing the ligands and the coordination geometry.[19]

Synthesis of [NiBr($C_6F_4CH{=}NCH_2Ph$)(PMe_2Ph)$_2$]. The reaction of [Ni(cod)$_2$] with $C_6F_5CH{=}NCH_2Ph$ in THF in the presence of dimethylphenylphosphine and LiBr gave the metalated compound [NiBr($C_6F_4CH{=}NCH_2Ph$)(PMe_2Ph)$_2$], **9g**, through oxidative addition of one of the *ortho* C−F bonds of the N-donor ligand (Scheme 2). It should be noted that this reaction permits the activation of the strongest single bond to carbon in mild conditions (1 h at room temperature). The oxidative addition of C−F bonds of very similar imines to platinum(II) complexes, even in the presence of weaker carbon−chlorine or −bromine bonds, has been previously described.[20] The IR, ^{1}H, and ^{31}P NMR spectroscopic data are similar to those of compounds **9c−f**, showing that **9g** adopts a pseudopentacoordinated geometry. The ^{19}F NMR spectrum (see Experimental Section) is consistent with the proposed structure. Variable temperature ^{1}H NMR spectra also confirm that the imine nitrogen occupies an axial position in the nickel coordination sphere (see below). Correct carbon, hydrogen, and nitrogen analyses were not obtained if the reaction was performed in the absence of LiBr. The easy hydrolysis of the Ni−F bond could explain this.[10b]

Table 5. Fluxional Processes in Compounds 9c−g

compd	T_c (K)	$\Delta G^{\ddagger}$ (kJ mol^{-1})[a]
9c	285	57 ± 4
9d	278	56 ± 4
9e	325	65 ± 4
9f	317	64 ± 4
9g	308	64 ± 4

[a] Data calculated from ^{1}H NMR spectra (toluene-d_8, 80.13 MHZ) using the chemical shift differences in the slow exchange limit.

Variable Temperature ^{1}H NMR. The Me−P protons appear as one or two signals in the ^{1}H NMR spectra of compounds **9**, depending on the temperature, the magnetic field, and the N-donor ligand. It has been previously shown that Me−P protons appear as two triplets in arylnickel complexes containing dimethylphenylphosphine, if there is no plane of symmetry through the P−Ni bond.[21] Moreover, the observation of two triplets in such nickel complexes has been taken as an indication that one asymmetric ligand is fixed perpendicularly to the coordination plane, occupying one of the axial positions in the metal coordination sphere.[22] Two triplets assigned to the Me−P protons were observed in the spectra of all the imine derivatives at 220 K in toluene-d_8 solutions. This confirms that the iminic nitrogen occupies one of the axial positions in the coordination sphere of the metal. The coalescence of the signals is observed when the temperature is increased because of the rotation around the C−Ni bond. Table 5 shows T_c and $\Delta G^{\ddagger}$ for this process.[23] The coalescence of the Me−P signals in organometallic nickel compounds containing dimethylphenylphosphine has been explained by free rotation around Ni−N[22a] or Ni−C bonds.[17c,22c] The $\Delta G^{\ddagger}$ value depends on the imine ligand and is *ca.* 10 kJ mol^{-1} higher in the aniline derivatives (compounds **9e,f**). This difference can be explained by the great flexibility of the benzylic group that facilitates the rotation around the Ni−C bond. The $\Delta G^{\ddagger}$ value for compound **9g** is higher than that for the other benzylimine derivatives, probably due to the presence of a bulkier F *ortho*-atom or to the great electronegativity of the pentafluorophenyl group.

The P−Me protons appear as one triplet at all the temperatures studied (220−330 K) in the amine complex **8b**, suggesting that the nitrogen is further away from the metal atom. The chemical shift of the Me−N and CH_2N protons in the ^{1}H NMR spectrum of **8b** are similar to those of the free ligand, confirming the lack of interaction between the nitrogen and the nickel. van Koten *et al.* have shown by crystallographic methods that the Ni···N distance in the amine derivative [NiBr-

(16) Albert, J.; Ceder, R. M.; Gómez, M.; Granell, J.; Sales, J. *Organometallics* **1992**, *11*, 1536 and references therein.

(17) (a) Klein, H. F.; Wiemer, T.; Menu, M. J.; Dartiguenave, M.; Dartiguenave, Y. *Inorg. Chim. Acta.* **1988**, *154*, 21. (b) Carmona, E.; Paneque, M.; Poveda, M. L.; Gutiérrez-Puebla, E.; Monge, A. *Polyhedron* **1989**, *8*, 1069. (c) Campora, J.; Carmona, E.; Gutiérrez, E.; Palma, P.; Poveda, M. L.; Ruiz, C. *Organometallics* **1992**, *11*, 11. (d) Gutiérrez, E.; Hudson, S. A.; Monge, A.; Nicasio, M. C.; Paneque, M.; Carmona, E. *J. Chem. Soc.*, Dalton *Trans.* **1992**, 2651.

(18) (a) Bruce, M. I. *Angew. Chem., Int. Ed. Engl.* **1977**, *16*, 73; (b) Newkome, G. R.; Puckett, W. E.; Gupta, W. K.; Kiefer, G. E. *Chem. Rev.* **1986**, *86*, 451; (c) Omae, I. *Coord. Chem. Rev.* **1988**, *83*, 137; (d) Dunina, V. V.; Zalevskaya, O. A.; Potatov, V. M. *Russ. Chem. Rev.* **1988**, *57*, 250.

(19) Macgregor, S. A.; Lu, Z.; Eisenstein, O.; Crabtree, R. *Inorg. Chem.* **1994**, *33*, 3616.

(20) (a) Crespo, M.; Martínez, M.; Sales, J. *J. Chem. Soc., Chem. Commun.* **1992**, 822. (b) Anderson, C. M.; Crespo, M.; Ferguson, G.; Lough, A. J.; Puddephatt, R. J. *Organometallics* **1992**, *11*, 1177.

(21) Moss, J. R.; Shaw, B. L. *J. Chem. Soc. A* **1966**, 1793.

(22) (a) Wada, M.; Shimohigashi, T. *Inorg. Chem.* **1976**, *15*, 954. (b) Wada, M.; Oguro, K.; Kawasaki, Y. *J. Organomet. Chem.* **1979**, *178*, 261. (c) Wada, M.; Koyama, Y. *J. Organomet. Chem.* **1980**, *201*, 477.

(23) The equation used was: $\Delta G^{\ddagger} = 2.303RT_c(10.319 - \log k' + \log T_c)$, where T_c is the coalescence temperature, $k' = \pi(\Delta\nu)/2^{1/2}$, and $\Delta\nu$ is the frequency separation of the coalescence peaks, although the equation is strictly valid only for coalescence of two singlets (Calder, I. C.; Garrat, P. J. *J. Chem. Soc. B* **1967**, 660).

(2,6-{$CH_2N(Ph)Me$}$_2C_6H_3$)(PEt_3)$_2$] is greater than 4 Å.[2b] The different conformation adopted by the amine and the imine in these nickel complexes can be explained because in the amine derivatives the pendant arms, where the nitrogen atoms are located, are very flexible owing to the sp^3 hybridization of the carbon atoms. As a consequence, the nitrogen atoms are far away from the metal atom. In contrast, the planarity of the imine moiety in compounds **9** forces the methinic nitrogen to occupy an axial position in the coordination sphere of the metal.

Experimental Section

^1H, $^{31}P\{^1H\}$, ^{19}F, and $^{13}C\{^1H\}$ NMR spectra were obtained by using Varian XL-200 (200 MHz), Bruker WP 80SY (32.4 MHz), Varian XL300 FT (282.2 MHz), and Varian XL-200 (50.3 MHz) spectrometers, respectively. Solvents used were C_6D_6 or [$^2H_8$] toluene. Infrared spectra were recorded as KBr disks on a Nicolet 520 FT-IR spectrometer. Microanalyses were performed by the Institut de Química Bio-Orgànica de Barcelona (CSIC) and by the Serveis Científico-Tècnics de la Universitat de Barcelona. Mass spectra were recorded on a Fisons VG-Quattro spectrometer. The samples were introduced in a matrix of 2-nitrobenzyl alcohol for FAB analysis and then subjected to bombardment with cesium atoms.

Materials and Synthesis. All manipulations of the organonickel compounds were carried out using Schlenk techniques under a nitrogen atmosphere. All solvents were dried and degassed by standard methods. Tetrahydrofuran and toluene were distilled over sodium–benzophenone under nitrogen before use. Amine **1a**, pyridines, and dimethylphenylphosphine were obtained commercially. Amine **1b**,[24] imines,[25] and [$Ni(cod)_2$][26] were prepared according to procedures described elsewhere.

[NiCl{2-(CH_2NMe_2)-3,4,5,6-Cl_4C_6}L] [L = 2-Me(C_5H_4N), 2b; L = 2,4-Me_2(C_5H_3N), 3b; L = 2,4,6-Me_3(C_5H_2N), 4b] and [NiBr{2-(CH_2NMe_2)C_6H_4}-2,4-Me_2(C_5H_3N)], 3a. To a suspension of [$Ni(cod)_2$] (0.65 g, 2.40 mmol) in THF (30 cm^3) at −78 °C were added the corresponding amine (2.40 mmol) and the substituted pyridine (2.40 mmol). The reaction mixture was warmed to room temperature and maintained for 1 h under these conditions. The solvent was partially removed under vacuum, and ether was added. Compounds **2**–**4** were precipitated and recrystallized in toluene–ether. Data for **2b**: 0.35 g, 32%. Anal. Found: C, 38.9; H, 3.5; N, 5.9. Calcd for $C_{15}H_{15}Cl_5N_2Ni$: C, 39.23; H, 3.29; N, 6.10. For **3a**: 0.45 g, 49%. Anal. Found: C, 50.0; H, 5.7; N, 7.3. Calcd for $C_{16}H_{21}BrN_2Ni$: C, 50.58; H, 5.57; N, 7.37. For **3b**: 0.45 g, 40%. Anal. Found: C, 39.5; H, 3.8; N, 5.24. Calcd for $C_{16}H_{17}Cl_5N_2Ni$: C, 40.61; H, 3.62; N, 5.92. For **4b**: 0.50 g, 43%. Anal. Found: C, 41.0; H, 4.2; N, 5.4. Calcd for $C_{17}H_{19}Cl_5N_2Ni$ (M_r 487): C, 41.90 H, 3.93; N, 5.75. MS: *m/z* 487 (M).

[NiX{2-(CH=NCH_2Ph)-6-YC_6H_3}L] [X = Br, Y = H, L = 2-Me(C_5H_4N), 5c; X = Br, Y = H, L = 2,4-Me_2(C_5H_3N), 6c; X = Y = Cl, L = 2,4-Me_2(C_5H_3N), 6d; X = Br, Y = H, L = 2,4,6-Me_3(C_5H_2N), 7c] and [NiCl{2-(CH=NPh)-6-ClC_6H_3}2,4-Me_2(C_5H_3N)], 6f. To a suspension of [$Ni(cod)_2$] (0.65 g, 2.40 mmol) in toluene or THF (25 cm^3) at −78 °C were added the corresponding imine (2.40 mmol) and the substituted pyridine (2.40 mmol). The reaction mixture was warmed to room temperature and maintained for 30 min under these conditions. The solvent was partially removed under vacuum, and, on cooling the solution at −40 °C for several hours, compounds **5**–**7** were precipitated. Data for **5c**: 0.6 g, 60%. Anal. Found: C, 56.1; H, 4.3; N, 6.4. Calcd for $C_{20}H_{19}BrN_2Ni$ (M_r 426): C, 56,38; H, 4.50; N, 6.57. MS: *m/z* 346 (M − Br). For **6c**: 0.74 g, 70%. Anal. Found: C, 57.0; H, 4.6; N, 6.3. Calcd for $C_{21}H_{21}BrN_2Ni$ (M_r 440): C, 57.32; H, 4.82; N, 6.36. MS: *m/z* 360 (M − Br). For **6d**: 0.72 g, 70%. Anal. Found: C, 58.5; H, 4.9; N, 6.3. Calcd for $C_{21}H_{20}Cl_2N_2Ni$ (M_r 430): C, 58.65; H, 4.70; N, 6.54. MS: *m/z* 395 (M − Cl). For **7c**: 0.65 g, 60%. Anal. Found: C, 58.0; H, 5.1; N, 5.9. Calcd for $C_{22}H_{23}BrN_2Ni$ (M_r 454): C, 58.20; H, 5.10; N, 6.15. MS: *m/z* 454 (M), *m/z* 374 (M − Br). For **6f**: 0.40 g, 40%. Anal. Found: C, 57.0; H, 4.7; N, 6.6. Calcd for $C_{20}H_{18}Cl_2N_2Ni$: C, 57.75; H, 4.36; N, 6.73.

[NiCl{2-(CH_2NMe_2)-3,4,5,6-Cl_4C_6}(PMe_2Ph)$_2$], 8b. To a suspension of [$Ni(cod)_2$] (0.65 g, 2.40 mmol) in THF (30 cm^3) at −78 °C were added the corresponding amine (2.40 mmol) and dimethylphenylphosphine (7.20 mmol). The reaction mixture was warmed to room temperature and then maintained for 2 h under these conditions. The solvent was partially removed under vacuum, and on adding methanol compound **8b** was obtained (0.95 g, 65%). Anal. Found: C, 45.8; H, 4.8; N, 2.0. Calcd for $C_{25}H_{30}Cl_5NNiP_2$ (M_r 642): C, 46.74; H, 4.71; N, 2.18. ^{31}P NMR: δ_P (toluene) −12.9. MS: *m/z* 642 (M).

[NiX{2-(CH=NCH_2Ph)-6-YC_6H_4}(PMe_2Ph)$_2$] [X = Br, Y = H, 9c; X = Y = Cl, 9d] and [NiX{2-(CH=NPh)-6-YC_6H_4}(PMe_2Ph)$_2$] [X = Br, Y = H, 9e; X = Y = Cl, 9f]. To a suspension of [$Ni(cod)_2$] (0.65 g, 2.40 mmol) in toluene or THF (40 cm^3) at −78 °C were added the corresponding imine (2.40 mmol) and dimethylphenylphosphine (4.80 mmol). The reaction mixture was warmed to room temperature and maintained for 1 h under these conditions. The solvent was removed under vacuum. Compounds **8** and **9** were precipitated on adding absolute ethanol. Data for **9c**: 0.95 g, 65%. Anal. Found: C, 59.0; H, 5.4; N, 2.4. Calcd for $C_{30}H_{34}BrNNiP_2$: C, 59.14; H, 5.64; N, 2.23. IR: ν/cm^{-1} 1604 s. ^{31}P NMR: δ_P (toluene) −18.9. For **9d**: 0.85 g, 60%. Anal. Found: C, 59.9; H, 5.6; N, 2.3. Calcd for $C_{30}H_{33}Cl_2NNiP_2$ (M_r 599): C, 60.13; H, 5.56; N, 2.33. IR: ν/cm^{-1} 1602 s. ^{31}P NMR: δ_P (toluene) −18.6. ^{13}C NMR δ_C (C_6D_6) 163.4 [1C, *HC*=N], 62.3 (1C, *CH*$_2$N], 13.1 [4C, P(*CH*$_3$)$_2$Ph]. MS: *m/z* 564 (*M* − Cl). For **9e**: 0.85 g, 60%. Anal. Found: C, 58.5; H, 5.5: N, 2.2. Calcd for $C_{29}H_{32}BrNNiP_2$ (M_r 595): C, 58.52; H, 5.40; N, 2.30. IR: ν/cm^{-1} 1602 s. ^{31}P NMR δ_P (toluene) −11.9. ^{13}C NMR: δ_C (C_6D_6) 163.8 [1C, *HC*=N], 16.3 [2C, t, *J*(PC) = 15.5 Hz, P(*CH*$_3$)$_2$Ph], 11.9 [2C, t, *J*(PC) = 15.5 Hz, P(*CH*$_3$)$_2$-Ph]. MS: *m/z* 515 (M − Br). For **9f**: 0.75 g, 55%. Anal. Found: C, 59.5; H, 5.7; N, 2.3. Calcd for $C_{29}H_{31}Cl_2NNiP_2$ (M_r = 585): C, 59.51; H, 5.35; N, 2.30. IR: ν/cm^{-1} 1610 m. ^{31}P NMR: δ_P (toluene) −12.6. ^{13}C NMR: δ_C (C_6D_6) 160.5 [1C, *HC*=N], 13.9 [2C, P(*CH*$_3$)$_2$Ph], 11.1 [2C, P(*CH*$_3$)$_2$Ph]. MS: *m/z* = 550 (M − Cl).

[NiBr{2-(CH=NCH_2Ph)-3,4,5,6-F_4C_6}(PMe_2Ph)$_2$], 9g. To a suspension of [$Ni(cod)_2$] (0.65 g, 2.40 mmol) in THF (30 cm^3) at −78 °C were added the corresponding imine (2.40 mmol), LiBr (0.21 g, 2.40 mmol), and dimethylphenylphosphine (4.80 mmol). The reaction mixture was warmed to room temperature and maintained for 1 h under these conditions. The solvent was removed under vacuum, and after addition of methanol a maroon solid was collected. Recrystallization from toluene–methanol gave **9g** in good yield (1.12 g, 68%). Anal. Found: C, 52.2; H, 4.4; N, 1.9. Calcd for $C_{30}H_{30}BrF_4NNiP_2$ (M_r 681): C, 52.90; H, 4.44; N, 2.06. ^{31}P NMR: δ_P (toluene) −16.2 ^{19}F NMR: δ_F (C_6D_6, reference $CFCl_3$) −121.7 [m, F_2], −152.0 [t, $J(F-F)_{ortho}$ = 20.0 Hz, F_3], −159.5 [dd, $J(F-F)_{para}$ = 30.0 Hz, $J(F-F)_{ortho}$ = 20.0 Hz, F_5], −171.2 [t, $J(F-F)_{ortho}$ = 20.0 Hz, F_4]. MS: *m/z* 681 (M).

Data Collection. A prismatic crystal (0.1 × 0.1 × 0.2 mm^3) was selected and mounted on a Philips PW-1100 four-circle diffractometer. Unit cell parameters were determined from automatic centering of 25 reflections ($8 \le \theta \le 12°$) and refined by the least-squares method. Intensities were collected with graphite-monochromatized Mo Kα radiation, using the $\omega/2\theta$ scan technique; 3648 reflections were measured in the range

(24) Foulger, N. J.; Wakefield, B. J. *J. Organomet. Chem.* **1974**, *69*, 321.
(25) Tennant, G. In *Comprehensive Organic Chemistry*; Barton, D., Ollis, W. D., Eds.; Pergamon: Oxford, U.K., 1979; Vol. 2, Part 8.
(26) Guerrieri, F.; Salerno, G. *J. Organomet. Chem.* **1976**, *114*, 339.

$2.18 \leq \theta \leq 25.05°$, and 1563 reflections were assumed as observed applying the condition $I \geq 2\sigma(I)$. Three reflections were measured every 2 h as orientation and intensity controls, and significant intensity decay was not observed. Lorentz–polarization and absorption corrections were made.

Structure Solution and Refinement. The structure was solved by Patterson synthesis using the SHELXS computer program[27] for crystal structure determination and refined by the full-matrix least-squares method with the SHELX93 computer program.[28] The function minimized was $\sum w[|F_o|^2 - k|F_c|^2]^2$, where $w = [\sigma^2(I) + (0.1049P)^2]^{-1}$ and $P = [|F_o|^2 + 2|F_c|^2)/3$; f, f', and f'' were taken from ref 29. The extinction coefficient was 0.0000(8); 23 hydrogen atoms were computed and refined with an overall isotropic temperature factor using a riding model. The final R (on F) factor was 0.065, wR (on $|F|^2$) = 0.054, and the goodness of fit was 1.049 for all observed reflections. The number of refined parameters was 237. Max shift/esd = 0.4, mean shift/esd = 0.03, and max and min peaks in the final difference synthesis were 1.150 and −0.999 e Å^{-3}, respectively.

(27) Sheldrick, G. M. *Acta Crystallogr.* **1990**, *A46*, 467.
(28) Sheldrick, G. M. In preparation.
(29) *International Tables for X-ray Crystallography*; Kynoch Press: Birmingham, U.K., 1974; Vol. IV, pp 99–100, 149.

Acknowledgment. We thank the DGICYT (Grant No. PB90-0058) for financial suport and the Serveis Científico-Técnics de la Universitat de Barcelona for many facilities in recording NMR spectra.

Supporting Information Available: Tables of all bond distances and angles, final hydrogen coordinates, and anisotropic displacement parameters for **7c** (4 pages). Ordering information is given on any current masthead page.

OM9503454

Mechanism of the Insertion Reactions of Alkynes with Phosphanickelacycles

Manuel Martinez,* Guillermo Muller,* David Panyella, and Mercè Rocamora

Departament de Química Inorgànica, Universitat de Barcelona, Diagonal 647, E-08028 Barcelona, Spain

Xavier Solans and Mercè Font-Bardía

Departament de Cristal.lografia, Mineralogia i Dipòsits Minerals, Universitat de Barcelona, Marti i Franqués s/n, E-08028 Barcelona, Spain

Received June 22, 1995[⊗]

The mechanism of the insertion reaction of substituted alkynes (PhCCPh (X), PhCCCOOEt (Y), MeOOCCCCOOMe (Z)) into the Ni–C bond of *trans*-[{Ni(2-$C_6H_4CH_2PPh_2$)(μ-Cl)}$_2$] and *trans*-[NiCl(C-P)P′] (C-P = 2-$C_6H_4CH_2PPh_2$, P′ = PBz_3 (**1a**), PMe_2Ph (**1b**); C-P = 2-C_6H_4-CH_2PEt_2, P′ = PBz_3 (**1′a**)) complexes has been investigated by means of ^{31}P NMR and UV–vis spectroscopy; in all cases insertion of only one molecule of alkyne has been found. The regioselectivity of the reaction is very well defined; only the regioisomer arising from a 1,2-*cis* addition on the Ni–C bond is obtained. The kinetics of the reactions have been studied *via* UV–vis spectroscopy. Results agree with the formation of a highly ordered transition state still containing the monodentate phosphine P′ in its coordination sphere, the effect of the metalated phosphine being less important (for example $\Delta H^{\ddagger}$ = 43, 60, 40 kJ mol^{-1} and $\Delta S^{\ddagger}$ = −118, −67, −125 J K^{-1} mol^{-1} for the **1a** + Y, **1b** + Y, and **1′a** + Y systems, respectively). A mechanism proceeding *via* the formation of a pentacoordinate intermediate aggregate, not detectable by NMR or visible spectroscopy, under the conditions of the study, is proposed. Only for the weaker π-acceptor alkyne PhCCPh is the observed rate constant found to be dependent on the alkyne concentration, indicating that for the other two alkynes studied the formation of the above-mentioned aggregate is complete under the kinetic conditions used (>10-fold excess of alkyne).

Introduction

The insertion of carbon–carbon multiple bonds into metal–carbon or metal–hydrogen bonds has been assumed to be a key step in many reactions in homogeneous catalysis.[1]

Reactions of acetylenes with *trans*-[PtClH(PEt_3)$_2$], in polar solvents such as methanol, proceed *via* a previous substitution of the chloride ligand followed by a migratory insertion of acetylene into the Pt–H bond, leading to the *cis* product. A reaction mechanism involving a four-center transition state seems to be operating for that reaction system. Nevertheless, when the same reaction is carried out in a nonpolar solvent, benzene, a mixture of *cis*- and *trans*-alkenyl compounds is produced. In this case a radical chain mechanism is interpreted to be responsible for the behavior observed.[2]

Electron-transfer processes are also involved in the formation of alkenyl compounds, as found in acetylene insertion reactions with platinum dihydrides.[3] The insertion of alkynes into Pt–C[4] and Pd–C[4,5] bonds has also been observed, usually leading to products that contain two molecules of alkyne; in particular, the reaction with cyclopalladated organometallic compounds has been studied thoroughly.[6] The insertion reaction of alkynes into [Ni(acac)(CH_3)(PPh_3)] has also been studied,[7] and the results observed have been interpreted as a 1,2-*cis* addition of the methyl–nickel bond to the alkyne plus a concurrent isomerization to produce *cis*- and *trans*-alkenyl derivatives. The same pattern has also been observed in other studies of reactions of PhCCPh or PhCCH with compounds containing Ni–alkyl or Ni–acyl bonds.[8,9]

Theoretical analysis of the reactions of ethylene and alkynes with *trans*-[PtClH(PH_3)$_2$][10] or [NiCl(CH_3)(C_2H_4)-(PH_3)][11] led to the common conclusion that the insertion reaction is likely to proceed *via* a tetracoordinate intermediate, having the unsaturated molecule in a position *cis* to the M–H or M–C bond. Nevertheless, insertion of tetrafluoroethylene in a Pt–O bond *via* a pentacoordinate intermediate has also been proposed.[12]

[⊗] Abstract published in *Advance ACS Abstracts,* October 15, 1995.

(1) Collman, J. P.; Hegedus, L. S.; Norton, J. R.; Finke, R. G. *Principles and Applications of Organotransition Metal Chemistry*; University Science Books: Mill Valley, CA, 1987.
(2) Clark, H. C.; Wong, C. S. *J. Am. Chem. Soc.* **1977**, *99*, 7073.
(3) Clark, H. C.; Ferguson, G.; Goel, A. B.; Janzen, E. G.; Ruegger, J. H.; Siew, P. Y.; Wong, C. S. *J. Am. Chem. Soc.* **1986**, *108*, 6961.
(4) Clark, H. C.; Milne, C. R. C.; Wong, C. S. *J. Organomet. Chem.* **1977**, *136*, 265.
(5) Albert, J.; Granell, J.; Sales, J.; Solans, X. *J. Organomet. Chem.* **1989**, *379*, 177.
(6) (a) Pfeffer, M. *Pure Appl. Chem.* **1992**, *64*, 335. (b) Pfeffer, M. *Recl. Trav. Chim. Pays-Bas* **1990**, *109*, 567. (c) Ryabov, A. D.; van Eldik, R.; Le Borgne, G.; Pfeffer, M. *Organometallics* **1993**, *12*, 1386.
(7) (a) Huggins, J. M.; Bergman, R. G. *J. Am. Chem. Soc.* **1981**, *103*, 3002. (b) Yang, K., Bott, S. G.; Richmond, M. G. *Organometallics* **1994**, *13*, 3767.
(8) Carmona, E.; Gutierrez-Puebla, E.; Marin, J. M.; Monge, A.; Paneque, M.; Poveda, M. L.; Ruiz, C. *J. Am. Chem. Soc.* **1989**, *111*, 2883.
(9) Carmona, E.; Gutierrez-Puebla, E.; Monge, A.; Marin, J. M.; Paneque, M.; Poveda, M. L. *Organometallics* **1989**, *8*, 967.
(10) Thorn, D. I.; Hoffmann, R. *J. Am. Chem. Soc.* **1978**, *100*, 2079.
(11) Trzcinska, B. M.; Fackler, J. P.; Anderson, A. B. *Organometallics* **1984**, *3*, 319.
(12) Bryndza, H. E. *Organometallics* **1985**, *4*, 406.

0276-7333/95/2314-5552$09.00/0

Scheme 1

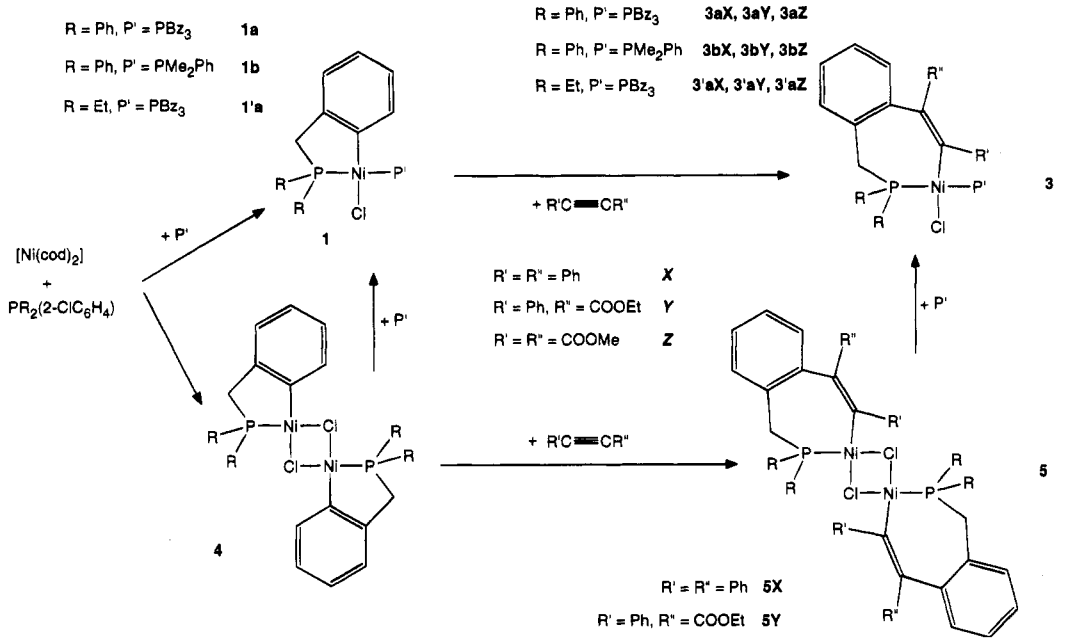

The insertion into the Ni–C bond has some characteristic features: (i) only one alkyne molecule is usually inserted; (ii) in spite of some differences,[7,13,14] the reaction is interpreted as a concerted 1,2-addition with a dissociation of neutral ligand prior to the insertion reaction; (iii) the regioselectivity is such that unsymmetrical alkynes produce the regioisomer that has the bulkier substituent attached to the nickel-bound carbon, but when PMe_3 is used as the stabilizing monodentate ligand, the reaction is less regioselective.[13,15]

In spite of the wide documentation available for the insertion reactions of alkynes, careful kinetic studies dealing with the proposed mechanisms are scarce. Only a few studies on insertions of alkynes into different Pd–C and Pt–C bonds are available.[16,17] Kinetic studies with organonickel compounds are severely limited by the instability of the organometallic compounds in the presence of a large excess of other ligands.

In this paper we present the study of the kinetics and mechanisms of a series of insertion reactions of metallacyclic organonickel compounds in nonpolar solvents as depicted in Scheme 1. The metallacyclic compounds **1a**, **1b**, **3aX**, **3aY**, and **3bX** have already been reported,[18a] and compounds **1'a**, **3aZ**, **3bY**, **3bZ**, **3'aX**, and **3'aY** have been prepared and fully characterized in this work. The stability of these metallacycles in the presence of a moderate excess of alkynes allows this type of work. Another fact that led us to consider this study is that the proposed mechanism for the isomerization of the alkenyl compounds[7] is disfavored in this case. It would include rotation about the vinyl C_α–C_β bond and, thus, the twist of the whole chelate ring on type **3** compounds.

Results

Compounds. The phosphanickelacycles **1a** and **1b** have been prepared as reported by reaction of $[Ni(cod)_2]$ with $(2\text{-}ClC_6H_4CH_2)PPh_2$ in the presence of the different free phosphine ligands.[18a] Compound **1'a** has been prepared by the same procedure using $(2\text{-}ClC_6H_4CH_2)PEt_2$ as chelating phosphine. When the synthesis of compounds **1** is carried out in the absence of free phosphine, the dinuclear complex *trans*-$[\{Ni(2\text{-}C_6H_4CH_2PPh_2)(\mu\text{-}Cl)\}_2]$ (**4**) is obtained.[18a] Addition of phosphine to solutions of compound **4** led to the cleavage of the chlorine bridge, giving type **1a** or **1b** compounds (see Scheme 1). Reactions of compounds **1** and **1'** with a slight excess of the corresponding PhCCPh (X) and PhCCCOOEt (Y) alkynes produce the corresponding compounds of types **3** and **3'** (see Scheme 1). The same reaction with MeOOCCCCOOMe (Z) produces dark red (with **1a**) or purple-violet solutions (with **1b** and **1'a**). ^{31}P NMR of these solutions shows that the inserted **3aZ**, **3bZ**, and **3'aZ** complexes and some other material are present in the solution. From these mixtures only a low yield of compounds **3aZ** and **3bZ** could be isolated and fully characterized. In order to increase yields, reaction of **1a** with MeOOCCCCOOMe (Z) was carried out in the presence of free PBz_3; under these conditions a better yield of a yellow compound, characterized as **3aZ** by elemental analyses and ^{31}P and ^1H NMR, is achieved. The same procedure is not useful to obtain compound **3bZ** since the formation of the previously described purple pentacoordinated species $[NiCl(2\text{-}C_6H_4CH_2PPh_2)(PMe_2Ph)_2]$[18a] is dominant. For compound **3a'Z** the secondary material becomes the predominant species after the insertion reaction, and isolation of a pure sample has not been possible with any of the above-mentioned procedures.

The nature of the other species present in the **1** + Z → **3** reaction medium could be associated with the formation of a pentacoordinated or a zwitterionic species

(13) Bochmann, M.; Hawkins, I.; Sloan, M. P. *J. Organomet. Chem.* **1987**, *332*, 371.
(14) Hernandez, J.; Muller, G.; Rocamora, M.; Solans, X.; Aguílo, M. *J. Organomet. Chem.* **1988**, *345*, 383.
(15) Cámpora, J.; Llebaría, A.; Moreto, J. M.; Poveda, M. L.; Carmona, E. *Organometallics* **1993**, *12*, 4032.
(16) Samsel, E. G.; Norton, J. R. *J. Am. Chem. Soc.* **1984**, *106*, 5505.
(17) Romeo, R.; Alibrandi, G.; Scolaro, L. M. *Inorg. Chem.* **1993**, *32*, 4668.
(18) (a) Muller, G.; Panyella, D.; Rocamora, M.; Sales, J.; Font-Bardia, M.; Solans, X. *J. Chem. Soc., Dalton Trans.* **1993**, 2959. (b) Font-Bardía, M.; González-Platas, J.; Muller, G.; Panyella, D.; Rocamora, M.; Solans, X. *J. Chem. Soc., Dalton Trans.* **1994**, 3075.

Table 1. ^{1}H NMR Data[a] for the Nonaromatic Protons of the Compounds Studied in Toluene Solution

compd	R_2PCH_2Ph bridge	R' and R'' alkyne substituents	P′ monodentate phosphine
1a[b]	3.58 (d, J_{PH} = 9.0)		PCH_2Ph, 3.17 (d, J_{PH} = 8.2)
1b[b]	3.6		PCH_3, 1.46
3aX[b]	3.88 (t, $J_{PH} = J_{HH'} \simeq 10$), 2.91 (t, $J_{PH} = J_{HH'} \simeq 10$)		PCH_2Ph, 3.51 (dd, J_{PH} = 7.6, $J_{HH'}$ = 14.2), 3.26 (dd, J_{PH} = 7.3, $J_{HH'}$ = 14.2)
3aY[b]	4.07 (dd, $J_{HH'}$ = 12, J_{PH} = 8), 2.86 (t, $J_{PH'} = J_{HH'} \simeq 12$)	$CO_2CH_2CH_3$, 3.84 (q, J_{HH} = 7); $CO_2CH_2CH_3$, 0.66 (t, J_{HH} = 7)	PCH_2Ph, 3.34 (dt, $J_{PH+P'H} \simeq 14$, $J_{HH'} \simeq 8$), 3.21 (dt, $J_{PH+P'H} \simeq 14$, $J_{HH'} \simeq 8$)
3aZ	3.7 (t, $J_{PH} = J_{HH'} \simeq 10$), 2.7 (t, $J_{PH'} = J_{HH'} \simeq 10$)	NiC−CO_2CH_3, 3.27; NiC=CCO_2CH_3, 3.33	PCH_2Ph, 3.7 (t, $J_{PH} = J_{HH'} \simeq 10$), 2.7 (t, $J_{PH} = J_{HH'} \simeq 10$)
3bX[b]	3.71 (t, $J_{PH} = J_{HH'} \simeq 8$), 2.91 (t, $J_{PH'} = J_{HH'} \simeq 8$)		PCH_3, 1.61 (d, J_{PH} = 8.8), 1.43 (d, J_{PH} = 8.32)
3bY	3.67 (dd, $J_{PH} \simeq 8$, $J_{HH'} \simeq 12$), 2.91 (t, $J_{PH'} = J_{HH'} \simeq 12$)	$CO_2CH_2CH_3$, 3.82 (q, J_{HH} = 7.2); $CO_2CH_2CH_3$, 0.78 (t, J_{HH} = 7.2)	PCH_3, 1.57 (d, J_{PH} = 8), 1.62 (d, J_{PH} = 9)
3bZ	4.3 (d, $J_{HH'} \simeq 13.2$), 2.64 (t, $J_{PH'} = J_{HH'} \simeq 13.5$)	NiC−CO_2CH_3, 3.30; NiC=CCO_2CH_3, 3.36	PCH_3, 1.71 (d, J_{PH} = 10.6), 1.51 (d, J_{PH} = 10)
3′aX	2.5 (t, $J_{PH} = J_{HH'} \simeq 10.7$), 2.85 (t, $J_{PH'} = J_{HH'} \simeq 10.7$) ($PCH_2CH_3$, 1.3 (m); PCH_2CH_3, 0.95 (m))		PCH_2Ph, 3.0 (m), 3.55 (m)
3′aY	2.65 (t, $J_{HH'} = J_{PH} \simeq 11$), 3.19 (dd, $J_{HH'} \simeq 9.5$, $J_{PH} \simeq 12.5$) (PCH_2CH_3, 1.55 (m), 2.22 (m); PCH_2CH_3, 1.2(m))	$CO_2CH_2CH_3$, 4.05, 4.15 (dq, J_{HH} = 7, $J_{HH'}$ = 11); $CO_2CH_2CH_3$, 0.91 (t, J_{HH} = 7)	PCH_2Ph, 3.30 (dd, $J_{PH} \simeq 13.8$, $J_{HH} \simeq 7$), 3.60 (dd, $J_{PH} \simeq 14.3$, $J_{HH} \simeq 7$)

[a] δ in ppm relative to TMS (J in Hz), in C_6D_6 or toluene-d_8. [b] Reference 23.

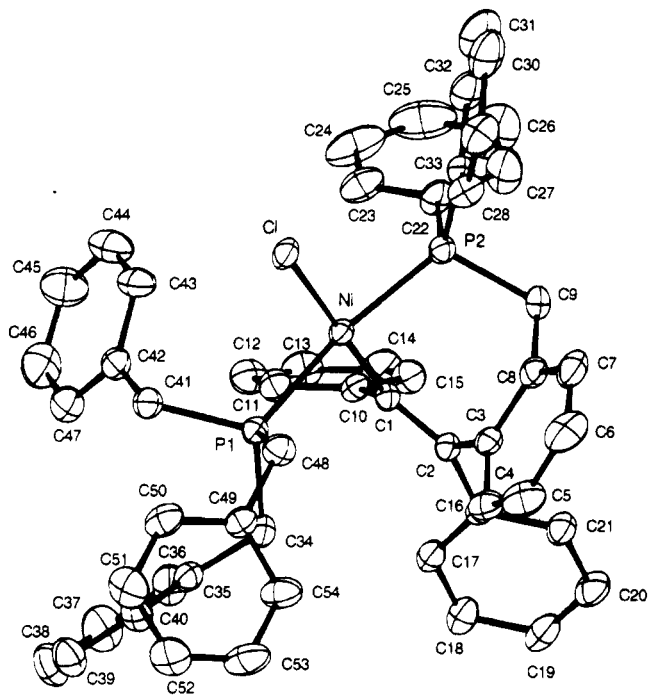

Figure 1. Ortep view of the structure of complex **3aX**, *trans*-[NiCl{PhC=CPh(2-$C_6H_4CH_2PPh_2$)}PBz_3], showing the atom-labeling scheme. Hydrogen atoms have been omitted for clarity.

and its subsequent decomposition.[7,9] When the stoichiometric reaction of **1′a** with MeOOCCCCOOMe (Z) is carried out in THF solution, two groups of signals, one corresponding to the **3′aZ** inserted compound and two doublets at 14.7 and 21.5 ppm ($J_{PP'}$ = 10.3 Hz) are observed by ^{31}P NMR immediately after mixing. This signal pattern collapses in a few minutes, producing a single signal at 18 ppm which is that observed under any other conditions. The same reaction and signal patterns are observed for the reactions of **1a** and **1b** with Z, but in these cases the formation of the inserted complexes is favored.

The insertion reactions of alkynes PhCCPh (X) and PhCCCOOEt (Y) have been studied also with compound **4**, only compound **5X** has been fully characterized in the solid state and the reaction of the inserted compounds with P′ (Scheme 1) allowed us to confirm its nature. Reactions run with a [Ni]/[alkyne] ratio of 1/2 at 273 K were complete in few minutes, and no intermediates were detected, as observed by ^{31}P NMR monitoring. Although compounds **1** are stable in solution under a dinitrogen atmosphere, compound **4** is much less stable and, even under these conditions, decompose rather quickly with the appearance of a yellow precipitate. The stabilities of all the **1** and **4** compounds studied are enhanced by the formation of the corresponding insertion products.

^{31}P and ^{1}H (Table 1) NMR spectra of compounds of types **1** and **3** have been recorded. The ^{31}P NMR spectra clearly indicate their *trans* geometry;[18a] however, dinuclear complexes **4** and **5** may be a mixture of the *sym* and *anti* isomers, since the phosphorus NMR signal is broad and complex. Small quantities of *cis*-**1a** were found in solutions of its *trans* isomer complex. The relative amount of *cis*/*trans* isomerization was found to be dependent on the size of the different ligands, compound **1b** not showing any percentage of *cis* isomer.[18a] This behavior was related to the production of a more labile species *via* the equilibrium process

$$[NiCl(2\text{-}C_6H_4CH_2PPh_2)P'] + S \rightleftharpoons [NiCl(2\text{-}C_6H_4CH_2PPh_2)S] + P' \quad (1)$$

S = solvent

This process is strongly displaced to the left-hand side, since no signals of free phosphine can be detected by ^{31}P NMR. An equimolar mixture of **1′a** and **1b** compounds in toluene solution at room temperature equilibrates on standing, producing an almost equimolar amount of the four organometallics **1′a**, **1b**, **1a**, and **1′b** (δ_P −8.1 ppm, $\delta_{P'}$ −57.3 ppm, $J_{PP'}$ = 340 Hz at 220 K), as can be monitored by ^{31}P NMR at 220 K. This fact agrees with the presence of catalytic amounts of free

Table 2. Selected Bond Distances and Angles (Esd's in Parentheses) for *trans*-[NiCl{PhC=CPh(2-$C_6H_4CH_2PPh_2$)}PBz_3]

Bond Lengths (Å)			
Cl–Ni	2.244(1)	C(2)–C(3)	1.548(4)
P(1)–Ni	2.256(1)	C(3)–C(8)	1.427(4)
P(2)–Ni	2.212(1)	C(8)–C(9)	1.500(4)
C(1)–Ni	1.929(3)	C(9)–P(2)	1.857(3)
C(1)–C(2)	1.362(4)		
Bond Angles (deg)			
P(1)–Ni–Cl	88.6(1)	Ni–P(2)–C(9)	112.1(1)
P(2)–Ni–Cl	93.8(1)	C(8)–C(9)–P(2)	109.9(2)
P(1)–Ni–P(2)	169.3(1)	C(9)–C(8)–C(3)	118.6(3)
C(1)–Ni–Cl	177.5(1)	C(8)–C(3)–C(2)	121.6(2)
C(1)–Ni–P(1)	92.2(1)	C(1)–C(2)–C(3)	119.9(2)
C(1)–Ni–P(2)	85.8(1)	Ni–C(1)–C(2)	119.3(2)

phosphine in solution. Nevertheless, when large amounts of free PBz_3 were added to toluene solutions of *trans*-[NiCl(2-$C_6H_4CH_2PPh_2$)PBz_3] (**1a**), no line broadening was observed. ^1H NMR signals, collected in Table 1, indicate that the two methylene protons of the ring give different signals according to the rigidity of the ring and the lack of a symmetry plane in the complex. ^1H NMR spectra (500 MHz) recorded for the **3a'Y** compound showed that all the methylene protons are diasterotopic.

Molecular Structure of *trans*-[NiCl{PhC=CPh-(2-$C_6H_4CH_2PPh_2$)}PBz_3] (3aX). The molecular and crystal structure of compound **3aX** was determined by X-ray diffraction. The crystal structure consists of discrete molecules (Figure 1) separated by van der Waals distances. Selected bond lengths and angles and atomic coordinates are listed in Tables 2 and 3, respectively. The bond distances are in the range expected; the complex exhibits a distorted-square-planar geometry. The observed displacements (Å) from the least-squares plane of the coordination sphere (plane A) are as follows: Ni, −0.0640; P1, 0.1372; Cl, −0.0962; P2, 0.1412; Cl, −0.1183. Despite the fact that a greater steric hindrance for the Ni–C(Ph)=C(Ph)– than for the Ni–C(Ph)=C(COOEt)– fragments of the rings can be assumed, these displacements are lower than those observed for the previously described **3aY** complex (−0.0402, −0.2908, 0.2843 −0.2897, 0.3365 Å).[18a] Nevertheless, the steric hindrance is present. On one hand, the alkenyl plane defined by C1C2C3C10C16 (plane B) in **3aX** shows a displacement from the least-squares plane of −0.1043, −0.0280, 0.0641, 0.0817, and −0.0135 Å, respectively, and the nickel atom directly bonded to C1 is displaced −0.4435 Å (compared with 0.3761 Å for the **3aY** compound). On the other hand, the bite angle for **3aX** (85.8(1)°) is very strained when compared with that for the **3aY** complex (90.1(2)°).

The benzyl group of the phosphine included in the seven-membered ring C2–C9 also forms a well-defined plane (C); the angles formed between normals to the planes AB, AC, and BC are respectively 94.89, 68.32, and 62.51°, showing a nearly perpendicular arrangement of the alkenyl group with respect to the square-planar coordination sphere.

Mechanistic Studies. The reaction of *trans*-[NiCl(C-P)P'] (**1**) and [NiCl(C-P)]$_2$ (**4**) compounds with several alkynes, (PhCCPh (X), PhCCCOOEt (Y), and MeOOCCCCOOMe (Z)) was studied kinetically in toluene solutions by means of UV–vis spectroscopy. The *in situ* monitoring of these processes *via* ^{31}P NMR (see above) proved that the reactions followed were effectively the

Table 3. Final Atomic Coordinates (×10^4; ×10^5 for Ni, Cl, P(1), and P(2)) for *trans*-[NiCl{PhC=CPh(2-$C_6H_4CH_2PPh_2$)}PBz_3]

	x/a	*y/b*	*z/c*	B_{eq} (Å^2)[a]
Ni	17667(3)	17162(1)	24306(2)	2.87(2)
P(1)	462(6)	13395(3)	17496(4)	3.10(3)
P(2)	32028(6)	21864(3)	31771(4)	3.29(3)
Cl	21464(6)	20341(3)	11813(4)	3.83(3)
C(1)	1502(2)	1424(1)	3503(2)	3.07(11)
C(2)	756(2)	1665(1)	4003(2)	3.09(11)
C(3)	344(3)	2213(1)	3799(2)	3.26(11)
C(4)	−923(3)	2334(1)	3593(2)	4.30(14)
C(5)	−1293(4)	2840(2)	3403(2)	5.66(19)
C(6)	−437(5)	3227(1)	3448(2)	6.06(21)
C(7)	816(4)	3121(1)	3687(2)	5.14(17)
C(8)	1227(3)	2615(1)	3860(2)	3.82(13)
C(9)	2591(3)	2496(1)	4086(2)	4.30(14)
C(10)	2156(2)	930(1)	3755(2)	3.37(12)
C(11)	2205(3)	508(1)	3209(2)	3.99(13)
C(12)	2822(3)	56(1)	3478(2)	5.02(16)
C(13)	3416(3)	10(1)	4293(3)	5.50(18)
C(14)	3420(3)	428(2)	4836(2)	5.64(18)
C(15)	2814(3)	881(1)	4571(2)	4.36(14)
C(16)	286(2)	1442(1)	4771(2)	3.27(11)
C(17)	−47(3)	921(1)	4827(2)	3.89(13)
C(18)	−520(3)	730(1)	5535(2)	4.72(15)
C(19)	−680(3)	1056(2)	6196(2)	5.12(16)
C(20)	−353(3)	1573(2)	6156(2)	5.17(17)
C(21)	126(3)	1765(1)	5456(2)	4.15(13)
C(22)	4576(3)	1823(1)	3610(2)	4.48(14)
C(23)	4876(3)	1381(2)	3190(3)	5.84(19)
C(24)	5907(4)	1089(2)	3501(4)	8.96(30)
C(25)	6639(5)	1238(3)	4243(6)	11.41(43)
C(26)	6362(5)	1662(3)	4639(4)	10.26(39)
C(27)	5327(4)	1965(2)	4354(3)	7.01(21)
C(28)	3814(3)	2743(1)	2642(2)	3.60(12)
C(29)	2982(3)	3096(1)	2215(2)	4.66(15)
C(30)	3394(4)	3519(2)	1806(2)	5.67(18)
C(31)	4661(5)	3591(2)	1789(3)	7.24(24)
C(32)	5487(4)	3240(2)	2191(3)	8.16(26)
C(33)	5079(3)	2823(2)	2622(2)	5.75(18)
C(34)	−1012(3)	975(1)	2380(2)	3.99(13)
C(35)	−1563(3)	461(1)	2066(2)	3.77(12)
C(36)	−1151(3)	0(1)	2459(2)	5.30(16)
C(37)	−1675(4)	−473(1)	2194(3)	6.62(22)
C(38)	−2619(4)	−497(1)	1533(3)	6.27(21)
C(39)	−3048(3)	−44(1)	1136(2)	5.47(17)
C(40)	−2523(3)	429(1)	1397(2)	4.40(14)
C(41)	261(3)	950(1)	805(2)	3.94(13)
C(42)	1286(3)	542(1)	941(2)	4.08(13)
C(43)	2541(3)	695(2)	1005(2)	5.23(17)
C(44)	3489(4)	335(2)	1159(3)	6.54(22)
C(45)	3234(5)	−178(2)	1241(3)	7.04(24)
C(46)	2011(5)	−337(2)	1159(3)	6.69(23)
C(47)	1029(4)	21(1)	1006(2)	5.34(17)
C(48)	−930(3)	1890(1)	1307(2)	4.15(13)
C(49)	−2255(3)	1786(1)	925(2)	3.66(11)
C(50)	−2542(3)	1604(1)	107(2)	4.72(15)
C(51)	−3766(4)	1497(2)	−234(2)	5.72(18)
C(52)	−4719(3)	1579(2)	237(3)	5.72(18)
C(53)	−4465(3)	1765(2)	1039(3)	6.38(20)
C(54)	−3241(3)	1866(2)	1378(2)	5.46(17)

[a] $B_{eq} = {}^8/_3\pi^2\sum U_{ij}A_i^*A_j^*\mathbf{A}_i\cdot\mathbf{A}_j$.

alkyne insertion into the Ni–C bond present in compounds **1** and **4** to produce compounds **3** and **5** (see Scheme 1).

Table 4 shows the spectral electronic data for the reactions studied. In all cases a good retention of isosbestic points was observed (Figure 2), indicating that only the insertion reaction was being monitored. For systems where a subsequent reaction was detected, only the first fast spectral changes were monitored as the insertion reaction.

The observed rate constants obtained for all these systems, collected in Table S1 (Supporting Information),

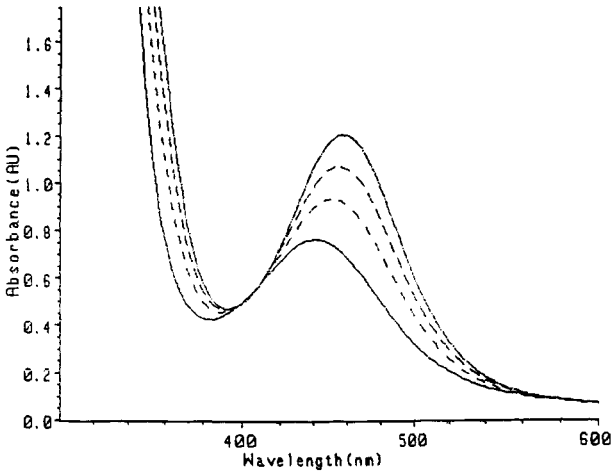

Figure 2. UV–vis consecutive spectra showing the advance of the insertion reaction of compound **1b** with the alkyne PhCCPh (X) (T = 15 °C, [**1b**] = 1 × 10^{-3} M, [X] = 0.0250 M, t = 0–600 s, toluene solution).

Table 4. UV–Vis Spectral Data for the Compounds Studied (T = 15 °C; Toluene Solution)

compd	λ/nm	ε/M^{-1} cm^{-1}	extra alkyne added (*ca.* 0.4 M)	λ/nm[a]
trans-[$NiCl_2(PBz_3)_2$]	488, 374	680, 17 500		
1a	448	1700	Z	570[b]
1b	442	850	Z	570[b]
1'a	428	1000	Z	575[b]
4	450			
3aX	456	1600	X	dec
			Y	450
			Z	475
3aY	448	1600	X	dec
			Y	446
			Z	472
3aZ	431	650		
3'aX	447	1300		
3'aY	436	1400		
3bX	462	1300		
3bY	456	2400		
3bZ	438	700		
5X	486[a]			

[a] No ε values are given due to subsequent decomposition reactions and/or concentration uncertainties. [b] Final purple solution, isosbestics points observed in all cases.

were found to have a linear correlation with the alkyne concentration only for the reaction of compounds of type **1** with the PhCCPh (X) alkyne to produce **3aX**, **3bX**, and **3'aX** inserted products. For all other systems the observed rate constants were found to be independent of the alkyne concentration used for the runs. Figure 3 represents an example of such behavior. Some runs were carried out in THF solution, and the observed rate constants were found to be independent of the solvent used.

The results obtained agree with any of the reaction mechanisms depicted in Schemes 2 and 3, which produces the rate law[19]

$$k_{obs} = \frac{kK[\text{alkyne}]}{1 + K[\text{alkyne}]} \qquad (2)$$

where

$$K = \frac{[\mathbf{2}]}{[\mathbf{1}][\text{alkyne}]} \qquad (3)$$

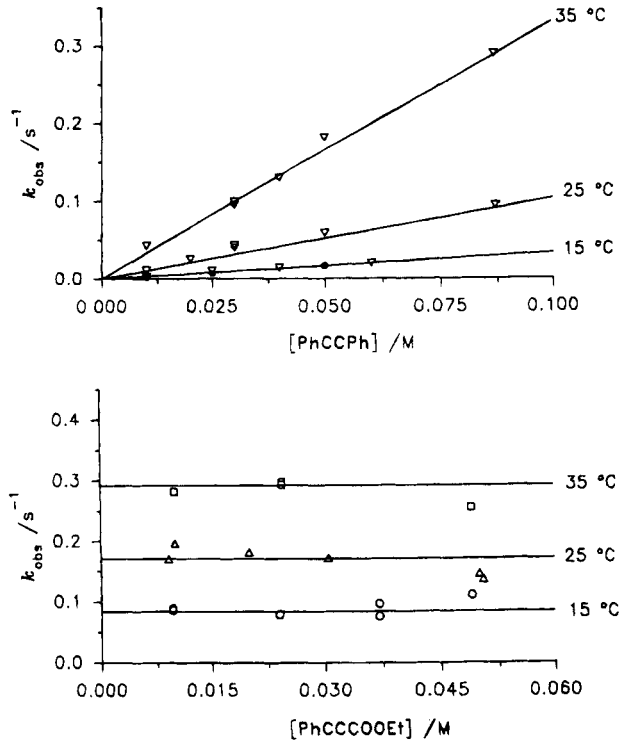

Figure 3. Alkyne concentration and temperature dependence on the observed rate constants for the insertion reaction of compound **1'a** with alkynes PhCCPh (X) (above) and PhCCCOOEt (Y) (below) alkynes. Open points correspond to toluene solution and solid points to THF solution.

For PhCCCOOEt (Y) and MeOOCCCCOOMe (Z) alkynes the K[alkyne] term becomes much larger than 1, and rate law 2 becomes $k_{obs} = k$, while for alkyne PhCCPh (X) the K[alkyne] term becomes very small and rate law 2 becomes $k_{obs} = kK$[alkyne].

Table 5 collects all the first- and second-order rate constants derived from these systems, as well as the thermal activation parameters derived from its temperature dependence and standard Eyring plots.

In view of these data a clear distinction must be made between the insertion reactions leading to **3aX**, **3bX**, and **3'aX** and the rest. These three reactions produce second-order rate constants that cannot be separated in equilibrium and kinetic constants; consequently, any comparison of these values with those for the reaction systems with the PhCCCOOEt (Y) and MeOOCCCCOOMe (Z) alkynes is meaningless.

In order to clarify the role of the two monodentate phosphine ligands of compounds **1** in the nature of the insertion reaction, compound **4** was reacted with alkynes PhCCPh (X) and PhCCCOOEt (Y) to produce compounds **5** shown in Scheme 1. Given the lesser stability of compound **4** when compared with **1a** or **1'a**, only runs at 15 °C at varying alkyne concentration were carried out, thermal activation parameters not being determined. The results obtained showed, again, different [alkyne]-dependence behavior, and the rate constants obtained are much larger than those corresponding to the mononuclear equivalent **1a** and **1b** species, as shown in Table 5.

(19) (a) Wilkins, R. G. *Kinetics and Mechanisms of Reactions of Transition Metal Complexes*; VCH: Weinheim, Germany, 1991. (b) Crespo, M.; Martinez, M.; Sales, J. *Organometallics* **1992**, *11*, 1288.

Scheme 2

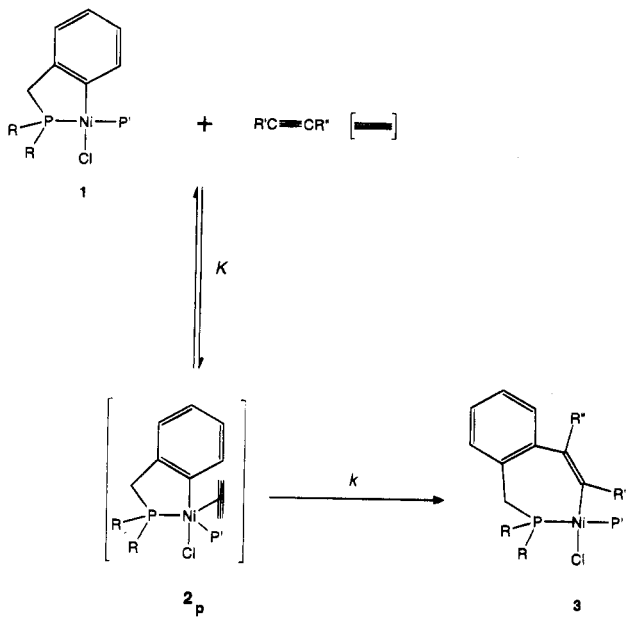

Table 5. Insertion Reaction Rate Constants and Thermal Activation Parameters for the Systems Studied ([Starting Nickel Compound] = 1×10^{-3} M, Toluene Solution)

compd	alkyne	T/°C	k	$\Delta H^{\ddagger}$/ kJ mol^{-1}	$\Delta S^{\ddagger}$/ J K mol^{-1}
1a	X	15	0.31 M^{-1} s^{-1}	57 ± 5	−57 ± 17
		25	0.61 M^{-1} s^{-1}		
		35	1.5 M^{-1} s^{-1}		
	Y	15	0.084 s^{-1}	43 ± 4	−118 ± 14
		25	0.17 s^{-1}		
		35	0.29 s^{-1}		
	Z	15	0.28 s^{-1}	41 ± 5	−114 ± 18
		25	0.57 s^{-1}		
		35	0.92 s^{-1}		
1'a	X	15	0.037 M^{-1} s^{-1}	81 ± 12	5 ± 1
		25	0.11 M^{-1} s^{-1}		
		35	0.29 M^{-1} s^{-1}		
	Y	15	0.10 s^{-1}	40 ± 3	−125 ± 10
		25	0.20 s^{-1}		
		35	0.32 s^{-1}		
	Z	15	0.14 s^{-1}	41 ± 1	−118 ± 3
		25	0.28 s^{-1}		
		35	0.51 s^{-1}		
1b	X	15	0.35 M^{-1} s^{-1}	84 ± 6	35 ± 12
		25	1.2 M^{-1} s^{-1}		
		35	3.4 M^{-1} s^{-1}		
	Y	15	0.031 s^{-1}	60 ± 1	−67 ± 3
		25	0.074 s^{-1}		
		35	0.17 s^{-1}		
	Z	15	0.049 s^{-1}	53 ± 3	−85 ± 8
		25	0.12 s^{-1}		
		35	0.22 s^{-1}		
4	X	15	4.18 M^{-1} s^{-1}		
	Y	15	1.25 s^{-1}		
1a	X	15	0.23 M^{-1} s^{-1} [a]		
			0.22 M^{-1} s^{-1} [b]		
			0.06 M^{-1} s^{-1} [c]		
1a	Z	15	0.23 s^{-1} [b]		

[a] [PBz_3]/[**1a**] = 0.01. [b] [PBz_3]/[**1a**] = 0.1. [c] [PBz_3]/[**1a**] = 1.

Some runs were also carried out in order to check possible concentration effects of the nickel starting organometallic, type **1** compounds, on the insertion rate constants. The results obtained for most of the systems indicate that a very important increase in the reaction rate constant is observed on decreasing the nickel starting material concentration. Decomposition reactions, occurring much more readily at lower concentrations, could be responsible for the dilution effects observed. For concentrations higher than 5×10^{-4} M no dilution effects were observed; consequently [**1**] was set to 1×10^{-3} M.

Experiments at varying added phosphine concentrations were carried out also for the reaction of **1a** with alkynes PhCCPh (X) and MeOOCCCCOOMe (Z) in order to check possible mass-retardation effects.[7] Even though the degree of advance of the reaction decreases on increasing the phosphine concentration, producing less reliable observed rate constants, the results clearly show (Table 5) that the rate constants for the insertion reaction do not vary significantly at reasonable concentration values of added PBz_3.

Discussion

Reactions of type **1** and **4** compounds in toluene solution with alkynes such as diphenylacetylene (X) ethyl phenylpropiolate (Y), and dimethyl acetylenedicarboxylate (Z) take place readily at room temperature. For example, 1 h is enough to complete the reaction when a [Ni]/[X] ratio of 1/2 is used. The insertion of only one molecule of alkyne into the Ni−C bond was observed for these compounds, further reaction with a second alkyne molecule being blocked by the bulky substituents of the alkenyl derivative. For the less sterically hindered alkyne MeOOCCCCOOMe, other definite changes that could be attributed to the formation of compounds where an attack at the double C=C bond by the neighboring P′ phosphine has occurred[9] or to the formation of a pentacoordinated species were observed in both the ^{31}P NMR and UV−vis spectra (Table 5). In this respect, changes in the UV−vis spectra of solutions of the inserted compounds with an excess of different alkynes (Table 4) seem to agree with the pentacoordinate assumption.

Only one of the two possible cyclic alkenyl isomers was obtained in each reaction (see Scheme 1). The stereochemistry of the addition was established unambiguously from the molecular structure determination for two of the alkenyl products, **3aX** and **3aY**.[18a] Both structures showed that the alkyne substituents remain in a *cis* distribution in the alkenyl addition products. For the ethyl phenylpropiolate inserted compound **3aY**, the largest substituent lies on the carbon directly bonded to the nickel center, indicating that possible interactions of the $-CO_2R$ groups with the nickel center should not be very important.

The stereochemistry of the reaction can be considered as a *cis* 1,2-addition of the nickel−carbon bond to the alkyne, which is in good agreement with proposals found in the literature.[7] Although results from other groups suggest that a *trans*-insertion alkenyl compound is the kinetic product of the reaction,[13] the fact that no isomerization processes are readily accessible in our case indicates that the *cis* addition must be the kinetic product of the reaction.

As a previous step to the insertion reaction, the existence of reaction equilibrium 1 suggests that the presence of large amounts of alkyne could favor the displacement of the phosphine in the starting type **1** nickel compounds. Although a ^{31}P signal of free phosphine is observed when a large excess of alkyne is present in the reaction medium, NMR measurements cannot rule out the decomposition of the organometallic

Scheme 3

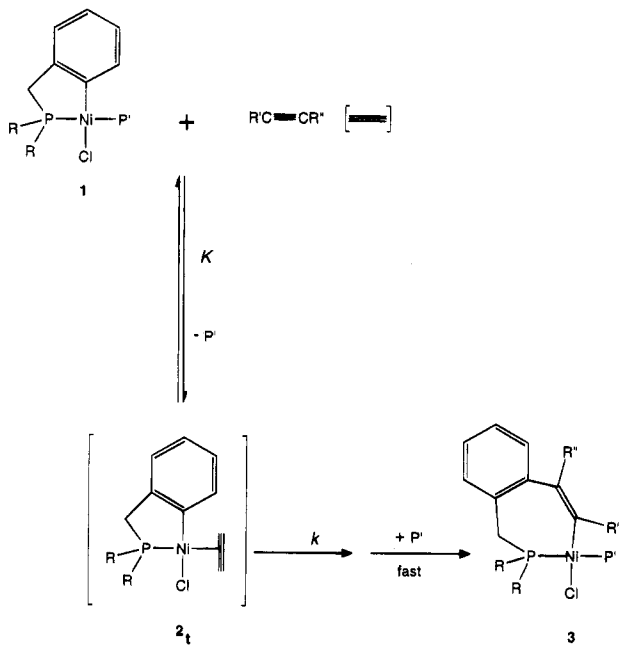

compound as the source of it. In this respect, compounds **5X** and **5Y** (the latter not characterized in the solid state) are stable in the presence of a large excess of the corresponding alkynes, indicating that such poor ligands cannot even displace the bridging chloride in the dinuclear compounds. Allowing for these facts, the alternate reaction mechanism depicted in Scheme 3 does not fit to the experimental observations.

Although the presence of free phosphine in the insertion reactions *via* intermediates of type $\mathbf{2_p}$ (Scheme 2) and $\mathbf{2_t}$ (Scheme 3) should not produce any difference in the first-order rate constants for alkynes PhCCCOOEt (Y) and MeOOCCCCCOOMe (Z) ($k_{obs} = k$ in both cases, given the large value of K), a $[P]_{added}$ mass-retardation effect should be observed in the second-order rate constants[7,10] obtained for the systems with alkyne PhCCPh (X), where the rate law derived is[20]

$$k_{obs} = kK\frac{[\text{alkyne}]}{[P']} \qquad (4)$$

The $[P]_{added}$ independence of the second-order rate constants of the reaction of compound **1a** with alkyne PhCCPh (X) (Table 5) indicates that a rate law such as that indicated in eq **4** does not apply. Consequently, an intermediate species of type $\mathbf{2_p}$ (Scheme 2) seems to fit much better to the experimental kinetic data. Formation of a tetracoordinate intermediate *via* displacement of the chloride ligands in type **1** compounds by alkynes is also unexpected. Kinetic runs carried out in THF solution showed that the observed rate constants were independent of the solvent used, as expected for the absence of ionic species during the insertion process.

The presence of an aggregate, similar to that depicted as $\mathbf{2_p}$ in Scheme 3, having two monodentate PBz_3 ligands and the chelating phosphine phosphorus interacting with the nickel center, could account for the lesser degree of advance in the insertion reaction when free PBz_3 is present in the solution. As already pointed out in the literature for Pt(II) systems,[21] it is very difficult to distinguish between a pentacoordinated compound and a tight outer-sphere complex; therefore, the nature of the possible intermediate aggregate is by no means clear. Furthermore, ^{31}P NMR at these concentrations, or UV–vis spectroscopy when other highly absorbing species exist in the reaction medium, makes it very difficult to assert its nature. Even so, the steric congestion around the Ni center has to be very important and the decomposition of type **1a** compounds in the presence of excess free PBz_3 to produce a nonreacting mixture of *trans*-$[NiCl_2(PBz_3)_2]$ and phosphonium salts seems to be another plausible explanation of the lesser extent of the insertion reaction observed under these conditions.

Examination of data in Table 5 clearly indicates that the insertion process goes through a highly ordered transition state, as seen by the very negative values of $\Delta S^{\ddagger}$ for the systems where these values have been derived from the first-order rate constants (alkynes PhCCCOOEt (Y) and MeOOCCCCCOOMe (Z)). The more negative $\Delta S^{\ddagger}$ values found for the systems having PBz_3 as the monodentate phosphine ligand have to be interpreted in view of the more important space rearrangement necessary for these systems for the insertion reaction to take place. For the **1a** and **1'a** systems $\Delta H^{\ddagger}$ values are smaller than those for the **1b** systems, indicating that the higher ν electronic parameter of the PBz_3 phosphine in these systems makes the insertion reaction more favorable.[22] An important fact that should also be considered is that $\Delta S^{\ddagger}$ and $\Delta H^{\ddagger}$ values derived from first-order rate constants, while independent of the metalated phosphine, vary significantly with the monodentate P' phosphine ligand. Given the fact that the alkyne has to be close to the P' ligand for the insertion reaction to take place, the above-mentioned difference seems to indicate that a reaction intermediate aggregate of type $\mathbf{2_p}$ (Scheme 2), where the chelating phosphine has very little influence on the transition state, is a very plausible explanation of the observed facts.

Furthermore, if this is true, a simultaneous interaction of the much bulkier PhCCPh (X) alkyne with type **1** compounds is very unfavorable with respect to that of the smaller PhCCCOOEt (Y) and MeOOCCCCCOOMe (Z) alkynes. The results for the systems studied agree with this assumption; the differences in the magnitude of K in rate law 2 are important enough as to make K unobservable for the two systems with less bulky and more electronically activated alkynes by its π-acceptor character.[7] A possible interaction of the $-CO_2R$ groups of alkynes PhCCCOOEt (Y) and MeOOCCCCCOOMe (Z) with the nickel center could also be related to the large magnitude of K. Nevertheless, the determined crystal structure of compound **3aY**[18a] does not show this interaction in the inserted species, and steric effects seem to dominate.

The insertion reactions studied with the dinuclear compounds type **4** agree, again, with the existence of this aggregate intermediate species. If the reaction takes place *via* a species where the chlorine bridge has been cleaved to introduce an alkyne in the coordination

(20) Crespo, M.; Martinez, M.; Sales, J. *Organometallics* **1993**, *12*, 4297.

(21) Alibrandi, G.; Romeo, R.; Scolaro, L. M.; Tobe, M. L. *Inorg. Chem.* **1992**, *31*, 5061.

(22) (a) Tolman, C. A. *Chem. Rev.* **1977**, *77*, 313. (b) Tolman, C. A. *J. Am. Chem. Soc.* **1970**, *92*, 2953.

sphere (to produce a species similar to $\mathbf{2_t}$), no important differences should be detected in the first-order rate constants when compared with those for the insertion of **1a** or **1'a**. Data in Table 5 show the contrary, indicating that in this case the intermediate species of the insertion reaction of compound **4** with alkyne PhCCCOOEt (Y) should be rather different from a compound of type $\mathbf{2_t}$. A dinuclear species having a pentacoordinate structure fits perfectly the experimental data. Furthermore, the final reaction mixture, as monitored by ^{31}P NMR, showed only the presence of the dinuclear inserted species, even in the presence of large amounts of free alkyne, somehow indicating that the dinuclear structure is maintained during the insertion process. Nevertheless, the fact that no activation parameters have been determined for these reactions (due to the inherent starting material instability) does not allow us to rule out that some other reaction mechanism, such as that observed for dimeric palladacycles,[6c] could be operating for the processes.

Experimental Section

Compounds. All manipulations of the organonickel compounds were carried out using Schlenk techniques under a dinitrogen atmosphere. All solvents were dried and degassed by standard methods. Tetrahydrofuran and toluene were distilled over sodium–benzophenone under a dinitrogen atmosphere before use. Phosphines were obtained commercially or prepared according to established procedures.[23] $[Ni(cod)_2]$ was prepared, with small modifications, by the method reported.[24]

^1H NMR spectra were recorded on Varian XL 200 or Bruker WP80SY instruments. ^{31}P NMR spectra at variable temperatures were obtained on a Bruker WP80SY instrument (32.38 MHz). The reference used was 85% H_3PO_4 for ^{31}P spectra; all chemical shifts are reported as downfield from standards. NMR solvents used were toluene and THF, with a 5 mm coaxial insert tube containing $[^2H_6]$acetone–$P(OMe)_3$. Infrared spectra were recorded on a Nicolet 520 FT-IR instrument. Elemental analyses were carried out at the Servei d'Anàlisis Elementals de la Universitat de Barcelona on an Eager 1108 microanalyzer.

***trans*-[NiCl(2-$C_6H_4CH_2PEt_2$)PBz_3] (1'a).** PBz_3 (4.80 × 10^{-3} mol) and (2-$ClC_6H_4CH_2$)PEt_2 (4.80 × 10^{-3} mol) were added to a suspension of $[Ni(cod)_2]$ (4.80 × 10^{-3} mol) in toluene (40 cm^3) at −78 °C. The reaction mixture was warmed to room temperature and maintained for 30 min under these conditions. After the solvent was partially removed under vacuum, the yellow complex was precipitated on adding absolute ethanol (yield 1.94 g, 70%; dec temp 155 °C). Anal. Found: C, 66.1; H, 6.30. Calcd for $C_{32}H_{37}ClNiP_2$: C, 66.57; H, 6.45. $^{31}P\{^1H\}$ NMR (in toluene solution, δ in ppm referenced to H_3PO_4, J in Hz): 55.9, 10.8, ^2J = 335.

***trans*-[NiCl{MeOOCC=CCOOMe(2-$C_6H_4CH_2PPh_2$)}PBz_3] (3aZ).** MeOOCC≡CCOOMe (0.1 g, 0.7 × 10^{-3} mol) dissolved in 20 cm^3 of THF was added at room temperature under nitrogen to a solution of **1a** (0.35 g, 0.5 × 10^{-3} mol) and PBz_3 (0.15 g, 0.5 × 10^{-3} mol) in THF (20 cm^3). After 45 min of stirring the brownish solution became red. The solvent was removed under vacuum, and after addition of methanol a yellow solid was collected. Recrystallization from methanol afforded the insertion product (yield 0.1 g, 25%). Anal. Found: C, 68.5; H, 5.4. Calcd for $C_{46}H_{43}ClNiO_4P_2$: C, 67.71; H, 5.32. $^{31}P\{^1H\}$ NMR (in toluene solution, δ in ppm referenced to H_3PO_4, J in Hz): 34.0, 4.6, ^2J = 318.

***trans*-[NiCl{PhC=CCOOEt(2-$C_6H_4CH_2PPh_2$)}PMe_2Ph] (3bY).** PhC≡CCOOEt (0.2 g, 1.12 × 10^{-3} mol) was added at −78 °C under nitrogen to a solution of **1b** (0.58 g, 1.12 × 10^{-3} mol) in toluene (20 cm^3). After 20 min of stirring at −78 °C the solution was warmed to room temperature. The solvent was removed under vacuum, and after addition of absolute ethanol a red solid was obtained (yield 0.5 g, 75%). Anal. Found: C, 67.2; H, 5.6; Cl, 5.0. Calcd for $C_{38}H_{37}ClNiO_2P_2$: C, 66.94; H, 5.47; Cl, 5.20. $^{31}P\{^1H\}$ NMR (in toluene solution, δ in ppm referenced to H_3PO_4, J in Hz): 29.5, −10.5, ^2J = 294.

***trans*-[NiCl{MeOOCC=CCOOMe(2-$C_6H_4CH_2PPh_2$)}PMe_2Ph] (3bZ).** MeOOCC≡CCOOMe (0.13 g, 0.9 × 10^{-3} mol) was added at 0 °C under nitrogen to a solution of **1b** (0.47 g, 0.9 × 10^{-3} mol) in THF (20 cm^3). The solution became violet, and after 30 min of stirring the solvent was removed under vacuum. After addition of hexane a dark red solid was collected (yield 0.1 g, 17%). Anal. Found: C, 59.3; H, 5.3. Calcd for $C_{33}H_{33}ClNiO_4P_2$: C, 61.00; H, 5.12. $^{31}P\{^1H\}$ NMR (in toluene solution, δ in ppm referenced to H_3PO_4, J in Hz): 33.48, −6.49, ^2J = 338.

***trans*-[NiCl{PhC=CPh(2-$C_6H_4CH_2PEt_2$)}PBz_3] (3'aX).** PhC≡CPh (0.2 g, 1.2 × 10^{-3} mol) was added at room temperature under nitrogen to a solution of **1'a** (0.58 g, 1 × 10^{-3} mol) in toluene (20 cm^3). After 60 min of stirring the solvent was removed under vacuum. The solid was extracted with 2 × 10 cm^3 of hexane. The hexane was removed under vacuum and the residue dissolved in 10 cm^3 of methanol. After the solution was cooled to −20 °C for several days, a yellow solid was collected (yield 0.27 g, 35%). Anal. Found: C, 72.5; H, 6.2. Calcd for $C_{46}H_{47}ClNiP_2$: C, 73.08; H, 6.26. $^{31}P\{^1H\}$ NMR (in toluene solution, δ in ppm referenced to H_3PO_4, J in Hz): 32.8, 5.7, ^2J = 310.

***trans*-[NiCl{PhC=CPCOOEt(2-$C_6H_4CH_2PEt_2$)}PBz_3] (3'aY).** PhC≡CCOOEt (0.2 g, 1.2 × 10^{-3} mol) was added at 0 °C under nitrogen to a solution of **1'a** (0.58 g, 1 × 10^{-3} mol) in toluene (20 cm^3). The solution was warmed to room temperature, and after 2 h of stirring the solution was filtered over Celite and the solvent removed under vacuum. The solid was extracted with 2 × 10 cm^3 of ether. The addition of hexane produced an orange solid that was collected and dried (yield 0.34 g, 45%). Anal. Found: C, 68.6; H, 6.5. Calcd for $C_{43}H_{47}ClNiO_2P_2$: C, 68.68; H, 6.30. $^{31}P\{^1H\}$ NMR (in toluene solution, δ in ppm referenced to H_3PO_4, J in Hz): 32.0, 4.85, ^2J = 301.

***trans*-[NiCl{CPh=CPh(2-$C_6H_4CH_2PPh_2$)}]$_2$ (5X).** PhC-CPh (2 × 10^{-3} mol) was added at room temperature and under a dinitrogen atmosphere to 25 cm^3 of a toluene solution of *trans*-[NiCl(2-$C_6H_4CH_2PPh_2$)]$_2$ (1 × 10^{-3} mol). After several minutes of stirring the orange solution became red. After the solvent was partially removed under vacuum, hexane was added and the red solid obtained was filtered (yield 0.60 g, 55%; dec temp 130 °C). Anal. Found: C, 72.0; H, 5.14. Calcd for $C_{52}H_{42}Cl_2Ni_2P_2$: C, 72.45; H, 4.80. $^{31}P\{^1H\}$ NMR (in toluene solution, δ in ppm referenced to H_3PO_4): 30.7.

Kinetics. All UV–vis spectra were recorded on a HP8452A instrument. Solutions for the kinetic measurements were made up in degassed toluene, and careful gastight syringe and dinitrogen handling techniques were necessary in order to avoid extensive decomposition of the nickel compounds at those concentrations.

Runs with $t_{1/2}$ > 170 s were recorded on a HP8452A instrument equipped with a thermostated multicell transport, and runs with 7 < $t_{1/2}$ < 170 s were recorded on a HP8452A instrument equipped with a High-Tech SFA-11 rapid kinetics accessory; for $t_{1/2}$ < 7 s runs were recorded on a Durrum D-110 stopped-flow instrument. All kinetic runs were initially followed at the full 700–325 nm range in toluene solutions. The observed rate constants, k_{obs}, were derived at the wavelength where the difference in absorbance between the initial and final species was large enough. Pseudo-first-order conditions were used for all runs with a nickel starting compound (**1**) concentration of 1 × 10^{-3} M. Absorbance *versus* time traces

(23) Kosolapoff, G. M.; Maier, L. *Organic Phosphorus Compounds*; Wiley: New York, 1972; Vol. 1.
(24) Guerrieri, F.; Salerno, G. *J. Organomet. Chem.* **1976**, *114*, 339.

Table 6. Crystallographic Data Collection for the *trans*-[NiCl{PhC=CPh(2-$C_6H_4CH_2PPh_2$)}PBz_3] Compound

formula	$C_{54}H_{47}P_2ClNi$
mol wt	852.08
cryst dimens (mm)	0.1 × 0.1 × 0.2
cryst syst	monoclinic
space group	$P2_1/c$
a (Å)	10.755(2)
b (Å)	26.657(4)
c (Å)	15.897(3)
β (deg)	97.39(2)
Z	4
$F(000)$	1784.0
V (Å^3)	4520(2)
T (K)	298
ρ (g cm^{-3})	1.252
μ (cm^{-1})	5.95 (Mo Kα)
radiation (Å)	0.710 69 (Mo Kα)
no. of data collected	13424
collecn range (deg)	$2 \leq \theta \leq 30$
scan method	$\omega/2\theta$
no. of independent data obsd	6980
R (obsd reflection)	0.042
R'	0.045

were fitted to exponential form by the Marquardt algorithm. All the k_{obs} errors were in the range of 5−15% of the actual value obtained, indicating a very good fit up to 3−4 half-lives. The k_{obs} *versus* [alkyne] plots were fitted by unweighted least squares. Thermal activation parameters were derived from standard Eyring plots by the same method.

Crystallographic Studies. Crystals of complex **3aX** were grown from a dichloromethane−ethanol mixture by cooling to −20 °C. A prismatic crystal (0.1 × 0.1 × 0.2 mm) was selected and mounted on an Enraf-Nonius CAD4 diffractometer. Unit-cell parameters were determined from automatic centering of 25 reflections ($12 \leq \theta \leq 22°$) and refined by the least-squares method.

Intensities were collected with graphite-monochromatized Mo Kα radiation, by the $\omega/2\theta$-scan technique. A total of 13 424 reflections were measured ($\pm h,k,l$) in the range $2 \leq \theta \leq 30°$, 6980 of which were assumed as observed by applying the condition $I \geq 2.5\sigma(I)$. R_{int} (on F) was 0.012. Three reflections were measured every 2 h as orientation and intensity control; significant intensity decay was not observed. Lorentz−polarization, but not absorption, corrections were made.

The structure was solved by Patterson synthesis, using the SHELXS computer program, and refined by full-matrix least squares with the SHELX76 computer program.[25] The function minimized was $\sum w[|F_o| - |F_c|]^2$, where $w = [\sigma^2(F_o) + 0.0008(F_o)^2]^{-1}$; f, f', and f'' were taken from ref 26.

The positions of all H atoms were computed from a difference synthesis and refined with an overall isotropic thermal parameter. The final R factor was 0.042 ($R' = 0.045$) for all observed reflections. The number of refined parameters was 664, the maximum shift/esd was 0.06, and maximum and minimum peaks in the final difference synthesis were 0.3 and −0.3 Å^{-3}, respectively. Crystal parameters, data collection details, and results of the refinements are summarized in Table 6.

Acknowledgment. We acknowledge financial support from the DGICYT (Ministerio de Educación y Ciencia), Project No. PB90-0058.

Supporting Information Available: Tables of observed reaction rate constants for **1a**, **1b**, **1'a**, and **4** and of bond lengths and angles, anisotropic thermal parameters, and H atom coordinates for **3aX** (10 pages). Ordering information is given on any current masthead page.

OM950480G

(25) (a) Sheldrick, G. M. *Acta Crystallogr., Sect. A* **1990**, *46*, 467. (b) SHELX, a Computer Program for Crystal Structure Determination; University of Cambridge, Cambridge, U.K., 1976.

(26) *International Tables of X-ray Crystallography*; Kynoch Press: Birmingham, U.K., 1974; Vol. 4, pp 99, 100, 149.

Optically Active Transition-Metal Complexes. 4.[1] Rhenium Complexes with the Enantiopure Cyclopentadienyl Ligand PCp: X-ray Structure of the *exo* Isomer of S_{Re}-(PCp)Re(NO)(PPh_3)(CH_3)

Bernhard Pfister, Ulli Englert, and Albrecht Salzer*

Institut für Anorganische Chemie der RWTH Aachen, D-52056 Aachen, Germany

Received June 27, 1995[⊗]

Treatment of a 1:1 mixture of the diastereomers S_{Re}- and R_{Re}-*exo*-[(η^5-PCp)Re(NO)(PPh_3)(CO)]$^+BF_4^-$ (**1a,b**) (PCp = "pinene-fused cyclopentadienyl") with sodium methoxide in methanol affords the derivative "esters" S_{Re}- and R_{Re}-*exo*-(η^5-PCp)Re(NO)(PPh_3)(COOMe) (**2a,b**) (S_{Re}:R_{Re} = 1:1). Reaction of **2a,b** with (+)-(*R*)-(1-naphthylethyl)amine gives the "amides" S_{Re}- and R_{Re}-*exo*-(η^5-PCp)Re(NO)(PPh_3)[$CONHCH(CH_3)C_{10}H_7$] (**3a,b**) (S_{Re}:R_{Re}= 1:1). **3a,b** are separated by recrystallization. **3a** is treated with CF_3CO_2H and $NaBF_4$ to give S_{Re}-(**1a**). **1a** is then converted to S_{Re}-*exo*-(η^5-PCp)Re(NO)(PPh_3)(CH_3) (**4a**). Protonolysis of **4a** with HBF_4/Et_2O in CD_2Cl_2 at −78 °C results in solvent-stabilized S_{Re}-*exo*-[(η^5-PCp)Re(NO)(PPh_3)($ClCD_2Cl$)]$^+BF_4^-$ (**5a**); the thermal and configurational stability of **5a** is investigated at various temperatures. An X-ray crystal structure of **4a** establishes the absolute configurations of **1a**, **3a**, and **4a**.

Introduction

We recently described the synthesis of the diastereomeric methylrhenium complexes S_{Re},R_{Re}-*exo*-(η^5-PCp)-Re(NO)(PPh_3)(CH_3) (**4a,b**) (Figure 1)[2] with the optically active pinane-related cyclopentadienyl ligand (1*R*,8*R*)-(−)-9,9-dimethyltricyclo[6.1.1.$0^{2,6}$]deca-2,5-dienyl (PCp^-; Figure 2).[3–5]

Starting from diastereomerically pure *exo*-(η^5-PCp)-$Re(CO)_3$, we obtained, after a sequence of ligand substitutions, the "chiral-at-rhenium" derivatives S_{Re},R_{Re}-*exo*-[(η^5-PCpRe(NO)(PPh_3)(CO)]$^+BF_4^-$ (**1a,b**) and S_{Re},R_{Re}-*exo*-(η^5-PCp)Re(NO)(PPh_3)(CH_3) (**4a,b**) in good overall yields as 1:1 inseparable mixtures of diastereomers. Crystallization of **4a,b**, for example, afforded the rare case that both diastereomers cocrystallized in a ratio of 1:1 in the unit cell.[2]

Gladysz and co-workers have demonstrated in a host of experiments with the Cp analogs of **4a,b** that methylrhenium complexes such as (η^5-Cp)Re(NO)(PPh_3)(CH_3) can readily be converted to chiral, pyramidal, substitution-labile dichloromethane complexes, [(η^5-PCp)Re-(NO)(PPh_3)($ClCH_2Cl$)]$^+BF_4^-$, which appear to be of stable configuration in dichloromethane at low temperatures. Generated by protonolysis of (η^5-Cp)Re(NO)-(PPh_3)(CH_3) with HBF_4·Et_2O in CH_2Cl_2 at −78 °C, [(η^5-Cp)Re(NO)(PPh_3)($ClCH_2Cl$)]$^+BF_4^-$ exhibits overall retention at rhenium after reaction with various neutral donor ligands.[6–17]

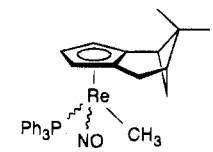

Figure 1. S_{Re},R_{Re}-*exo*-(η^5-PCp)Re(NO)(PPh_3)(CH_3) (**4a,b**).

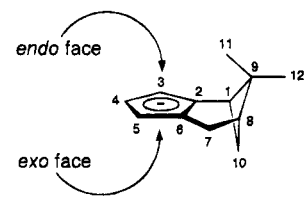

Figure 2. The PCp^- anion and its numbering scheme.

In our last paper we described the conversion of **4a** + **4b** with HBF_4·Et_2O to S_{Re},R_{Re}-*exo*-[(η^5-PCp)Re-(NO)(PPh_3)($ClCD_2Cl$)]$^+BF_4^-$ (**5a,b**) in CD_2Cl_2 at −78 °C. The experiment was performed in an NMR tube and immediately analyzed by ^{31}P-NMR at −80 °C. We observed two resonance peaks (δ 13.4 and 11.9 ppm) due to two diastereomers (ratio of integration: S_{Re}:R_{Re} = 1:1). By stepwise warming of the sample to −20 °C,

(1) Part 3: Käser, M.; Salzer, A. *J. Organomet. Chem.*, submitted for publication.

[⊗] Abstract published in *Advance ACS Abstracts,* November 1, 1995.

(2) Salzer, A.; Bosch, W. H.; Englert, U.; Pfister, B.; Stauber, R. *J. Organomet. Chem.*, in press.
(3) Paquette, L. A.; McLaughlin, M. L. *Org. Synth.* **1992**, *69*, 220.
(4) Salzer, A.; Schmalle, H.; Stauber, R.; Streiff, S. *J. Organomet. Chem.* **1991**, *408*, 403.
(5) Nelson, J. H.; Bhaduri, D.; Jacobson, R. A.; Wang, T. *Organometallics* **1994**, *13*, 2291.
(6) Gladysz, J. A.; Tam, W.; Lin, G. Y.; Wong, W. K.; Kiel, W. A.; Wong, V. K. *J. Am. Chem. Soc.* **1982**, *104*, 141.
(7) Gladysz, J. A.; Strouse, C. E.; Merrifield, J. M. *Organometallics* **1982**, *1*, 1204.
(8) Gladysz, J. A.; Fernandez, J. M.; Buhro, W. E.; Merrifield, J. M. *Inorg. Chem.* **1984**, *23*, 4022.
(9) Gladysz, J. A.; Fernandez, J. M. *Inorg. Chem.* **1986**, *25*, 2672.
(10) Gladysz, J. A.; Fernandez, J. M. *Organometallics* **1989**, *8*, 207.
(11) Gladysz, J. A.; Peng, T. S. *J. Am. Chem. Soc.* **1992**, *114*, 4174.
(12) Gladysz, J. A.; Agbossou, F.; O'Connor, E. J.; Garner, C. M.; Mendez, N. Q.; Fernandez, J. M.; Patton, A. T.; Ramsden, J. A. *Inorg. Synth.* **1992**, *29*, 211.
(13) Gladysz, J. A.; Mendez, N. Q.; Seyler, J. W.; Arif, A. M. *J. Am. Chem. Soc.* **1993**, *115*, 2323.
(14) Gladysz, J. A.; Arif, A. M.; Peng, T. S. *Helv. Chim. Acta* **1992**, *75*, 442.
(15) Gladysz, J. A.; Wang, Y.; Agbossou, F.; Dalton, D. M.; Liu, Y.; Arif, A. M. *Organometallics* **1993**, *12*, 2699.
(16) Gladysz, J. A.; Knight, D. A.; Dewey, M. A.; Stark, G. A.; Bennett, B. K.; Arif, A. M. *Organometallics* **1993**, *12*, 4523.
(17) Gladysz, J. A.; Peng, T. S.; Pu, J. *Organometallics* **1994**, *13*, 929.

0276-7333/95/2314-5561$09.00/0

Scheme 1

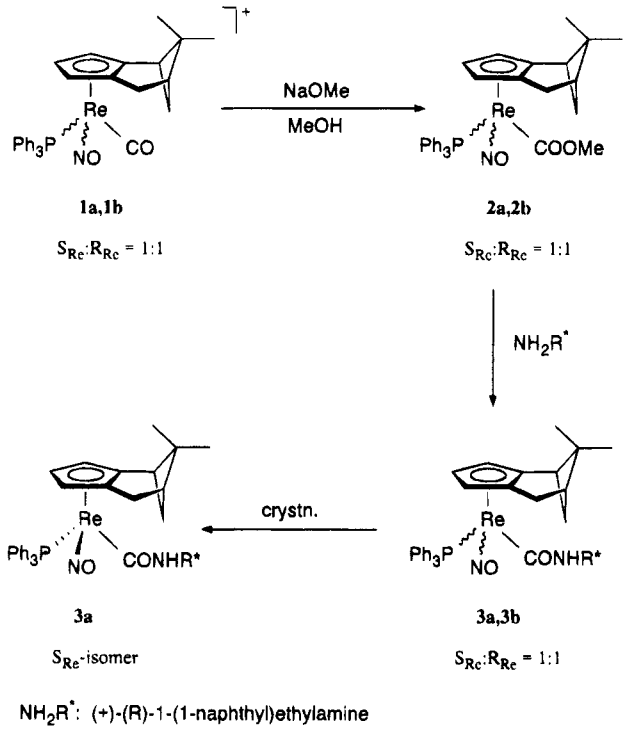

^{31}P-NMR spectra showed only two resonances, which shifted slightly to higher field, over the entire temperature range. Above −20 °C, decomposition of **5a,b** occurred.[2]

From these experiments, it was impossible to decide whether inversion of **5a,b** occurred on a time scale slower than that of the NMR experiment. To answer this question and unequivocally establish that **5a** and **5b** are configurationally stable at temperatures up to −20 °C, it was necessary to also investigate the stability of a single diastereomer, either **5a** or **5b**.

Our aim was therefore to find a synthetic route to diastereomerically pure S_{Re}- or R_{Re}-*exo*-(η^5-PCp)Re(NO)(PPh$_3$)(CH$_3$) in good overall yield.

Results and Discussion

1. Synthesis and Resolution of Optically Active S_{Re}-*exo*-(η^5-PCp)Re(NO)(PPh$_3$)[CONHCH(CH$_3$)-C$_{10}$H$_7$] (3a). To obtain diastereomerically pure *exo*-(η^5-PCp)Re(NO)(PPh$_3$)(CH$_3$), we used a reaction pathway quite similar to that found by Gladysz and co-workers.[7,12] S_{Re},R_{Re}-*exo*-[(η^5-PCp)Re(NO)(PPh$_3$)(CO)]$^+$BF$_4^-$ (**1a,b**) (ratio of **1a**:**1b** = 1:1) were prepared as described.[2,6,12] **1a** + **1b** were then treated with sodium methoxide in methanol and stirred for 10 h at ambient temperature. After work-up S_{Re},R_{Re}-*exo*-(η^5-PCp)Re(NO)(PPh$_3$)(COOMe) (**2a,b**) could be obtained in excellent yield as a light yellow solid with the ratio of diastereomers 1:1 (Scheme 1).

The ratio of diastereomers was determined by integration of both the ^{1}H-NMR peaks assigned to the methoxy groups (δ 3.12 and 3.08 ppm) and the ^{31}P-NMR peaks (δ 19.5 and 19.3 ppm) of **2a,b**. As **2a,b** exhibit the same IR absorptions in the nitrosyl and carbonyl region, they cannot be distinguished by IR spectroscopy. ^{13}C-NMR spectra of **2a,b** show only one doublet resonance for the CO ligands with identical chemical shifts for **2a,b**.

Scheme 2

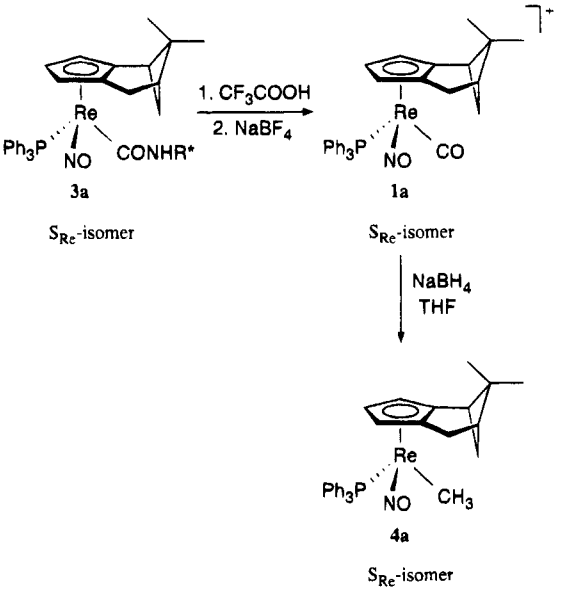

Conversion of **2a** + **2b** to their derivative "amides" could be performed in good yield in CH_2Cl_2 by addition of commercial (+)-(*R*)-(1-(1-naphthyl)ethyl)amine at room temperature. The course of the reaction can easily be monitored by IR. After removal of solvent, crude S_{Re},R_{Re}-*exo*-(η^5-PCp)Re(NO)(PPh$_3$)[CONHCH(CH$_3$)-C$_{10}$H$_7$] (**3a,b**) with the ratio of diastereomers 1:1 was obtained. However, the diastereomeric amides (**3a,b**) were readily separable by fractional crystallization in benzene/*n*-hexane. The yellow crystals of the less soluble diastereomer were collected, washed with *n*-hexane, and dried to give S_{Re}-*exo*-(η^5-PCp)Re(NO)-(PPh$_3$)[CONHCH(CH$_3$)C$_{10}$H$_7$] (**3a**) of ≥98% diastereomeric purity.[7]

For **3a,b**, ratios of diastereomers S_{Re}:R_{Re} were determined by ^{31}P-NMR spectra. The assignment of the absolute configuration at rhenium of **3a** and the subsequent derived rhenium complexes is based on an X-ray structure analysis of S_{Re}-*exo*-(η^5-PCp)Re(NO)-(PPh$_3$)(CH$_3$) (**4a**) (vide infra). As all these complexes undergo bond cleavages and metatheses which do not affect any rhenium−carbon bond; retention of the absolute configuration at rhenium has previously been established.

2. Preparation of S_{Re}-*exo*-(η^5-PCp)Re(NO)(PPh$_3$)-CH$_3$) (4a). The amide linkage of **3a** was cleaved with CF_3CO_2H in CH_2Cl_2 at 0 °C, and the optically active S_{Re}-*exo*-[(η^5-PCp)Re(NO)(PPh$_3$)(CO)]$^+$CF$_3$CO$_2^-$ thus formed was metathesized to the BF$_4^-$ salt, **1a**, which has a higher tendency to precipitate (Scheme 2).[12] Reduction of **1a** by treatment with $NaBH_4$ in THF at ambient temperature resulted in diastereomerically pure S_{Re}-*exo*-(η^5-PCp)Re(NO)(PPh$_3$)(CH$_3$) (**4a**) (Scheme 2). Evaporation of solvent, purification by chromatography, and subsequent crystallization from a saturated toluene solution, layered with 6 equiv of *n*-hexane, afforded red single crystals of **4a** after 2 d. A crystal structure analysis of **4a** established the absolute configuration at rhenium of **3a**, **1a**, and **4a**.

3. X-ray Structure of 4a. The solid-state structure analysis of complex **4a** shows the expected orientation of the bulky PPh$_3$ group positioned as far as possible away from the sterically demanding pinene part of the

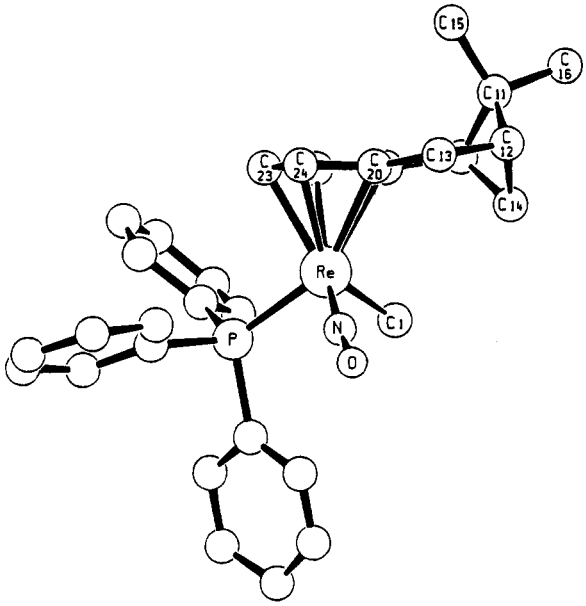

Figure 3. Molecular structure and crystallographic numbering scheme of S_{Re}-*exo*-(η^5-PCp)Re(NO)(PPh$_3$)(CH$_3$) (**4a**).

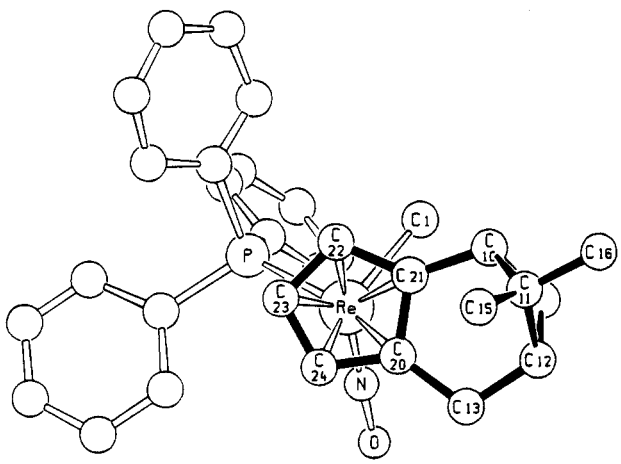

Figure 4. Top view of **4a**.

PCp ligand (Figures 3 and 4). The small NO and methyl ligand are well shielded below the π-plane. The bond angles at the metal center deviate distinctly from an octahedral coordination of 90°, and the Re–C distances to the cyclopentadienyl ring range from 2.20 to 2.30 Å. A summary of crystal data, data collection parameters, and convergence results for **4a** is given in Table 3. Fractional atomic coordinates and equivalent isotropic displacement parameters are listed in Table 1, and selected bond lengths and angles in Table 2.

4. Formation and Stability of S_{Re}-*exo*-[(η^5-PCp)Re(NO)(PPh$_3$)(ClCD$_2$Cl]$^+$BF$_4^-$ (5a). Similar to the NMR experiment which we had already conducted with the 1:1 mixture of diastereomers **4a**,**b**,[2,9] we treated optically active S_{Re}-*exo*-(η^5-PCp)Re(NO)(PPh$_3$)(CH$_3$) (**4a**) with a stoichiometric amount of HBF$_4$·Et$_2$O in CD$_2$Cl$_2$ at −78 °C. The conversion to the corresponding (dichloromethane)rhenium complex (**5a**) was performed in an NMR tube and immediately analyzed at −80 °C by ^{31}P-NMR (Scheme 3).

Only *one* resonance peak (δ 13.5 ppm) due to *one* diastereomer could be observed. When the probe was warmed stepwise to −20 °C, the ^{31}P-NMR spectra showed only *one* resonance over the entire temperature range (Figure 5). Above −20 °C, decomposition occurred with formation of new complexes (presumably chloro complexes), but even then no resonance due to **5b** could be observed.

Table 1. Fractional Atomic Coordinates and Equivalent Isotropic Displacement Parameters (Å^2) of S_{Re}-*exo*-(PCp)Re(NO)(PPh$_3$)(CH$_3$) (4a) with Estimated Standard Deviations in Parentheses

	x	y	z	U(eq)[a]
Re	0.34557(4)	0.99547(5)	0.83871(3)	0.02999(9)
P	0.5363(3)	1.0020(4)	0.8308(2)	0.0302(7)
O	0.3283(9)	0.999(1)	1.0216(5)	0.072(3)
N	0.3416(9)	1.001(1)	0.9465(6)	0.045(3)
C1	0.346(2)	1.153(1)	0.805(1)	0.059(5)
C10	0.118(1)	1.062(1)	0.7221(9)	0.040(4)
C11	0.004(1)	1.012(1)	0.7168(7)	0.050(4)
C12	−0.000(1)	1.016(1)	0.8144(7)	0.046(4)
C13	0.067(1)	0.934(1)	0.8550(8)	0.047(5)
C14	0.075(1)	1.108(1)	0.806(1)	0.053(5)
C15	−0.011(1)	0.909(1)	0.6793(9)	0.064(6)
C16	−0.084(1)	1.078(1)	0.674(1)	0.079(6)
C20	0.176(1)	0.922(1)	0.8121(9)	0.046(4)
C21	0.202(1)	0.987(1)	0.7449(7)	0.033(3)
C22	0.300(1)	0.949(1)	0.7091(8)	0.039(4)
C23	0.334(1)	0.866(1)	0.7512(9)	0.047(4)
C24	0.257(1)	0.849(1)	0.813(1)	0.041(4)
C31	0.611(1)	0.8977(9)	0.8733(7)	0.029(4)
C32	0.553(2)	0.833(1)	0.927(1)	0.062(6)
C33	0.614(2)	0.755(1)	0.965(1)	0.074(6)
C34	0.723(1)	0.739(1)	0.9411(9)	0.047(5)
C35	0.727(1)	0.880(1)	0.856(1)	0.063(6)
C36	0.777(1)	0.796(1)	0.8847(9)	0.045(5)
C41	0.606(1)	1.107(1)	0.8854(8)	0.032(4)
C42	0.562(1)	1.157(1)	0.9454(8)	0.038(4)
C43	0.612(1)	1.233(1)	0.982(1)	0.061(6)
C44	0.711(1)	1.266(1)	0.9642(8)	0.043(4)
C45	0.761(1)	1.212(1)	0.9021(9)	0.047(5)
C46	0.709(1)	1.135(1)	0.8595(7)	0.029(4)
C51	0.585(1)	1.006(1)	0.7232(6)	0.031(3)
C52	0.581(1)	1.0922(9)	0.6789(8)	0.028(3)
C53	0.619(1)	1.093(1)	0.5960(9)	0.050(5)
C54	0.645(1)	1.007(1)	0.5557(7)	0.066(4)
C55	0.639(2)	0.921(1)	0.598(1)	0.081(7)
C56	0.617(1)	0.916(1)	0.6810(8)	0.037(4)

[a] U values for anisotropically refined atoms are given in the form of the isotropic equivalent displacement parameter defined as one-third of the trace of the orthogonalized **U** tensor.

Table 2. Selected Bond Lengths (Å) and Angles (deg) of S_{Re}-*exo*-(PCp)Re(NO)(PPh$_3$)(CH$_3$) (4a) with Estimated Standard Deviations in Parentheses

Bond Lengths			
Re–P	2.324(3)	C11–C12	1.57(2)
Re–N	1.73(1)	C11–C15	1.53(3)
Re–C1	2.20(1)	C11–C16	1.55(2)
Re–C20	2.33(2)	C12–C13	1.52(2)
Re–C21	2.31(1)	C12–C14	1.55(2)
Re–C22	2.24(1)	C13–C20	1.51(2)
Re–C23	2.25(2)	C20–C21	1.42(2)
Re–C24	2.30(1)	C20–C24	1.39(2)
O–N	1.22(1)	C21–C22	1.42(2)
C10–C11	1.54(2)	C22–C23	1.38(2)
C10–C14	1.57(2)	C23–C24	1.38(2)
C10–C21	1.49(2)		

Bond Angles			
P–Re–N	94.6(4)	C11–C10–C21	109(1)
P–Re–C1	86.9(6)	C11–C12–C13	113(1)
N–Re–C1	101.6(7)	C11–C12–C14	86(1)
Re–N–O	173(1)	C12–C11–C15	115(2)
C21–C20–C24	107(1)	C12–C11–C16	114(1)
C10–C11–C12	88(1)	C12–C13–C20	111(1)
C10–C11–C15	122(2)	C13–C12–C14	108(1)
C10–C11–C16	113(2)	C13–C20–C21	118(1)
C10–C14–C12	87(1)	C13–C20–C24	134(2)
C10–C21–C20	117(1)	C14–C10–C21	107(1)
C10–C21–C22	136(1)	C15–C11–C16	106(1)
C11–C10–C14	86(1)		

Scheme 3

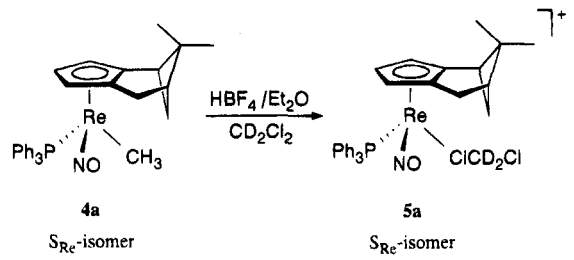

One might argue that **5a,b** are diastereomers of different thermodynamic stability so that an interconversion of **5a** to **5b** was not possible for thermodynamic reasons. However, as a 1:1 mixture of **5a,b** also did not change in ratio up to −20 °C, we conclude that the inversion barrier of **5a** is high enough so that decomposition occurs faster than inversion. These NMR measurements make it possible for the first time to estimate a lower value for the inversion barrier of these chiral, pyramidal dichloromethane complexes ($\Delta G^{\ddagger} \geq 47.9 \pm 0.8$ kJ mol^{-1}). These experiments also clearly establish the usefulness of optically active cyclopentadienyl ligands as spectroscopic probes in mechanistic studies where chirality is involved. Up to now, it had only been possible to determine the stability of functional equivalents of the chiral, 16-valence-electron Lewis acids S_{Re},R_{Re}-[(η^5-Cp)Re(NO)(PPh$_3$)]$^+$ by indirect methods[7,9,10] and not by a simple NMR experiment.

We are currently studying other organometallic systems, where the formation of metal-centered chirality can be monitored (and not induced) by chirality in the cyclopentadienyl ring.

Experimental Section

General Data. All reactions and manipulations were performed under nitrogen by use of standard vacuum line and Schlenk tube techniques. All solvents were degassed before use. Diethyl ether and THF were distilled from sodium benzophenone ketyl. Methanol was distilled from magnesium filings. Dichloromethane, benzene, toluene, and *n*-hexane were dried over molecular sieves. Unless otherwise indicated, all commercially available reagents were used as received. Column chromatography was performed on grade II (activated) silica gel (Merck Kieselgel 60). For organometallic complexes, all chromatography was carried out under nitrogen. (+)-(*R*)-(1-(1-naphthyl)ethyl)amine (Aldrich), HBF$_4$ (54% in Et$_2$O), CF$_3$CO$_2$H (Merck), NaBF$_4$, and NaBH$_4$ (Fluka) were used as supplied. S_{Re},R_{Re}-*exo*-[(η^5-PCp)Re(NO)(CO)(PPh$_3$)]$^+$BF$_4^-$ (**1a,b**) were prepared as described in the literature.[2,12] Infrared spectra were recorded on a Perkin-Elmer 1750 Fourier transform spectrophotometer as solutions in *n*-hexane or dichloromethane using NaCl cells. NMR spectra were recorded on either a Varian VXR 300 or a Varian Unity 500 spectrometer in CDCl$_3$ or CD$_2$Cl$_2$ solutions unless otherwise stated. ^{1}H- and ^{13}C-NMR spectra were referenced to tetramethylsilane (TMS) using internal solvent peaks; ^{31}P-NMR spectra were referenced to H$_3$PO$_4$ (external). In the Experimental Section, ^{13}C- and ^{31}P-NMR data are given in terms of the proton-decoupled (broad band) spectra.

S_{Re},R_{Re}-*exo*-(η^5-PCp)Re(NO)(PPh$_3$)(CO$_2$CH$_3$) (2a,b). A solution of 4.12 g (5.48 mmol) of **1a** + **1b** (ratio of **1a**:**1b** = 1:1) in 60 mL of methanol was treated with 4.37 M sodium methoxide in methanol (8.64 mL, 37.74 mmol). The suspension was stirred at room temperature for 10 h. The solvent was then removed and the brown residue extracted with hot *n*-hexane and filtered. The orange filtrate was concentrated and recrystallized at −30 °C to afford a light yellow precipitate of S_{Re},R_{Re}-*exo*-(η^5-PCp)Re(NO)(PPh$_3$)(CO$_2$CH$_3$) (**2a,b**), which was collected by filtration and dried under oil pump vacuum; yield of **2a** + **2b**, 3.63 g (5.21 mmol, 95%), with the ratio of diastereomers S_{Re}:R_{Re} = 1:1.

2a + 2b: IR 1681, 1596 cm^{-1} (*n*-hexane); IR 1655, 1585 cm^{-1} (CH$_2$Cl$_2$); ^{1}H-NMR (500 MHz, CDCl$_3$) δ 7.69−7.35 (m, 30H, 6 × Ph), 5.18 (br, 1H), 5.04 (br, 1H), 4.46 (br, 1H), 4.42 (dd, J = 2.8, 1.5 Hz, 1H), 4.34 (dd, J = 4.9, 2.5 Hz, 1H), 4.23 (dd, J = 4.9, 2.5 Hz, 1H), 3.12 (s, 3H, OCH$_3$), 3.08 (s, 3H, OCH$_3$), 2.88−2.59 (m, 8H), 2.24 (m, 2H), 1.70 (d, J = 10.1 Hz, 1H), 1.69 (d, J = 10.1 Hz, 1H), 1.42 (s, 3H, CH$_3$), 1.40 (s, 3H, CH$_3$), 0.77 (s, 3H, CH$_3$), 0.74 (s, 3H, CH$_3$) ppm; ^{13}C-NMR (125 MHz, CDCl$_3$) δ 198.5 (d, J_{CP} = 4.1 Hz), 135.7 (d, J_{CP} = 54.0 Hz), 133.7 (d, J_{CP} = 10.9 Hz), 130.1, 128.2 (d, J_{CP} = 10.9 Hz), 126.3, 121.0, 107.6, 104.7, 90.8, 90.0, 89.3, 88.7, 87.6, 85.9, 49.6, 49.2, 42.1, 41.8, 41.6, 41.5, 41.3, 41.1, 37.2, 35.9, 31.6, 27.1, 26.8, 26.6, 22.7, 22.0 ppm; ^{31}P-NMR (202 MHz, CDCl$_3$) δ 19.5, 19.3 ppm. Anal. Found: C, 55.15; H, 4.89; N, 1.90. Calc for C$_{32}$H$_{33}$NO$_3$PRe: C, 55.16; H, 4.77; N, 2.01.

S_{Re}-*exo*-(η^5-PCp)Re(NO)(PPh$_3$)[CONHCH(CH$_3$)C$_{10}$H$_7$] (3a). A 2.14 g amount (3.07 mmol) of **2a** + **2b** was dissolved in 10 mL of dichloromethane. A 0.99 mL amount (6.14 mmol) of commercial (+)-(*R*)-(1-(1-naphthyl)ethyl)amine was added by syringe, and the yellow solution was stirred for 8 h at ambient temperature. The progress of the reaction was monitored by IR. Evaporation of the solvent afforded a yellow-brown oil of crude S_{Re},R_{Re}-*exo*-(η^5-PCp)Re(NO)(PPh$_3$)[CONHCH(CH$_3$)C$_{10}$H$_7$] (**3a** + **3b**) and residual amine. This oil was dissolved in 10 mL of benzene, upon which 35 mL of *n*-hexane was layered. The layers were allowed to diffuse for 6 d, and the resulting yellow crystals were collected and washed with *n*-hexane to give S_{Re}-*exo*-(η^5-PCp)Re(NO)(PPh$_3$)[CONHCH(CH$_3$)C$_{10}$H$_7$] (**3a**) of ≥98% diastereomeric purity; yield of **3a**, 0.96 g (1.15 mmol, 75%).

3a: IR 1631, 1535 cm^{-1} (CH$_2$Cl$_2$); ^{1}H-NMR (500 MHz, CD$_2$Cl$_2$) δ 8.14 (d, J = 8.2 Hz, 1H, naphthyl), 7.83 (dd, J = 7.9, 1.2 Hz, 1H, naphthyl), 7.70 (d, J = 7.9 Hz, 1H, naphthyl), 7.57−7.41 (m, 19H, naphthyl and phenyl), 5.54 (m, 2H, NCH and NH), 5.24 (br, 1H), 4.63 (dd, J = 2.8, 1.5 Hz, 1H), 3.91 (dd, J = 2.8, 2.1 Hz, 1H), 2.73 (m, 2H), 2.51 (m, 1H), 2.34 (m, 1H), 2.09 (m, 1H), 1.34 (d, J = 10.1 Hz, 1H), 1.31 (s, 3H, CH$_3$), 0.99 (d, J = 6.7 Hz, 3H, CH$_3$), 0.71 (s, 3H, CH$_3$) ppm; ^{13}C-NMR (125 MHz, CD$_2$Cl$_2$) δ 191.5 (d, J_{CP} = 10.9 Hz), 142.6, 136.9 (d, J_{CP} = 53.4 Hz), 134.2 (d, J_{CP} = 10.9 Hz), 131.5, 130.5, 128.8, 128.6 (d, J_{CP} = 10.4 Hz), 127.2, 126.0, 125.7, 124.6, 122.6, 121.3, 105.0, 93.5, 91.4, 87.5, 44.5, 42.0, 41.64, 41.60, 37.7, 27.4, 26.8, 22.0, 21.5 ppm; ^{31}P-NMR (202 MHz, CD$_2$Cl$_2$) δ 18.6 ppm. Anal. Found: C, 61.89; H, 5.13; N, 3.32. Calc for C$_{43}$H$_{42}$N$_2$O$_2$PRe: C, 61.78; H, 5.06; N, 3.35.

S_{Re}-*exo*-(η^5-PCp)Re(NO)(PPh$_3$)(CH$_3$) (4a). **3a** (0.32 g, 0.38 mmol) was dissolved in 1.5 mL of dichloromethane, and the solution was kept at 0 °C with an ice bath. While the solution was stirring, 73 μL (0.96 mmol) of CF$_3$CO$_2$H was added by syringe. The solution was stirred for 10 min at 0 °C. The solvent was then removed under reduced pressure to give a yellow foam. The residue was taken up in 1.5 mL methanol, and a solution of NaBF$_4$ (0.08 g, 0.76 mmol) in water (0.75 mL) was added with vigorous stirring. A yellow solid precipitated. Additional water (2.5 mL) was added, and the mixture was stirred for 15 min. The yellow precipitate was collected by filtration, washed with water (4 × 2.5 mL), washed with *n*-hexane, and dried under oil pump vacuum to afford S_{Re}-*exo*-[(η^5-PCp)Re(NO)(CO)(PPh$_3$)]$^+$BF$_4^-$ (**1a**); yield of **1a**, 0.27 g (0.36 mmol, 95%).

A 0.27 g (0.36 mmol) amount of **1a** was dissolved in 25 mL of THF. While the mixture was stirred, 0.043 g (1.15 mmol) of NaBH$_4$ was added. The solution was stirred for 3 h at room temperature. The solvent was then removed under reduced pressure, and the residue was extracted with toluene and filtered. Chromatography over silica gel (1.5 × 20 cm) in toluene and evaporation of the solvent gave an orange solid. This was dissolved in 1 mL of toluene, upon which 6 mL of

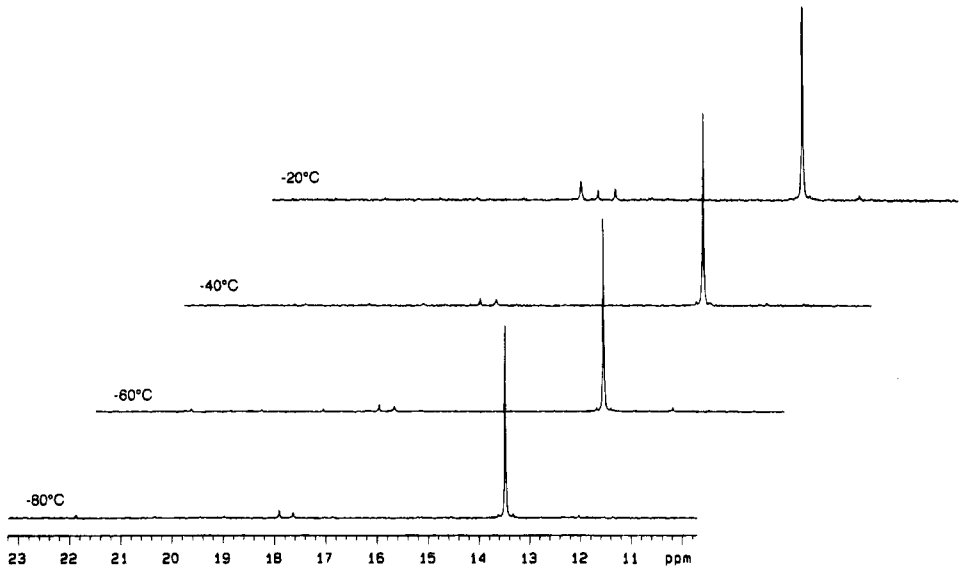

Figure 5. ^{31}P-NMR spectra of S_{Re}-*exo*-[(η^5-PCp)Re(NO)(PPh$_3$)(ClCD$_2$Cl)]$^+$BF$_4^-$ (**5a**) in CD_2Cl_2 at various temperatures. Note that the spectra at −60, −40, and −20 °C have been displaced to the right for clarity.

n-hexane was layered. The layers were allowed to diffuse for 2 d to afford red single crystals of S_{Re}-*exo*-(η^5-PCp)Re(NO)(PPh$_3$)(CH$_3$) (**4a**), which were filtered off and dried: yield of **4a**, 0.19 g (0.29 mmol, 80%); mp 150 °C.

1a: IR 2015, 1754 cm^{-1} (CH_2Cl_2); ^{1}H-NMR (500 MHz, acetone-d_6) δ 7.67 (m, 9H, Ph), 7.50 (m, 6H, Ph), 6.19 (br, 1H), 5.68 (br, 1H), 5.42 (dd, J = 6.1, 2.8 Hz, 1H), 3.27−2.83 (m, 4H), 2.40 (m, 1H), 1.46 (s, 3H, CH$_3$), 1.35 (d, J = 10.4 Hz, 1H), 0.80 (s, 3H, CH$_3$) ppm; ^{13}C-NMR (125 MHz, acetone-d_6) δ 197.9, 134.0 (d, J_{CP} = 9.9 Hz), 133.1, 131.8 (d, J_{CP} = 60.3 Hz), 130.5 (d, J_{CP} = 11.5 Hz), 129.2, 113.5, 96.3, 93.9, 87.4,42.1, 41.9, 41.8, 37.0, 27.2, 26.5, 22,1 ppm; ^{31}P-NMR (202 MHz, acetone-d_6) δ 11.3 ppm.

4a: IR 1631 cm^{-1} (THF); IR 1613 cm^{-1} (CH_2Cl_2); ^{1}H-NMR (500 MHz, CD_2Cl_2) δ 7.39 (m, 15H, 3 × Ph), 5.20 (br, 1H), 4.02 (dd, J = 2.8, 1.5 Hz, 1H), 3.62 (m, 1H), 2.83 (m, 3H), 2.56 (m, 1H), 2.21 (m, 1H), 1.54 (d, J = 9.8 Hz, 1H), 1.42 (s, 3H, CH$_3$), 0.93 (d, J = 6.1 Hz, 3H, CH$_3$), 0.78 (s, 3H, CH$_3$) ppm; ^{13}C-NMR (125 MHz, CD_2Cl_2) δ 137.2 (d, J_{CP} = 50.3 Hz), 134.0 (d, J_{CP} = 10.6 Hz), 130.2, 128.5 (d, J_{CP} = 10.1 Hz), 118.8, 101.6, 91.4, 88.5, 83.5, 41.7, 41.5,41.4, 37.2, 30.1, 27.3, 27.0, 22.0, −35.7 (d, J_{CP} = 6.6 Hz) ppm; ^{31}P-NMR(202 MHz, CD_2Cl_2) δ 26.9 ppm. Anal. Found: C, 56.85; H, 5.16; N, 2.21. Calc for $C_{31}H_{33}NOPRe$: C, 57.04; H, 5.10; N, 2.15.

Crystal Structure Determination of 4a. A saturated solution of **4a** in toluene, layered with 6 equiv of *n*-hexane, afforded red single crystals after 2 d of layer diffusion. The crystals of **4a** were filtered off and dried under oil pump vacuum. Data collection was performed with an Enraf-Nonius CAD4 diffractometer equipped with a graphite monochromator. Crystal data, data collection parameters, and convergence results are given in Table 3. Before averaging over symmetry-related reflections, a numerical absorption correction (crystal faces: 10$\bar{1}$, $\bar{1}$01, 101, $\bar{1}$0$\bar{1}$, $\bar{1}\bar{1}$1, 1$\bar{1}\bar{1}$, 010) was applied. The structure was solved by direct methods[18] and refined on F with the SDP program system.[19] In the final refinement cycles, hydrogen atoms were included as riding on the corresponding carbon atoms (C−H = 0.98 Å). Fractional coordinates of the non-hydrogen atoms are compiled in Table 1.

S_{Re}-*exo*-[(η^5-PCpRe(NO)(PPh$_3$)(ClCD$_2$Cl)]$^+$BF$_4^-$ (5a) (NMR Experiment). A 5-mm NMR tube was charged with 0.040 g (0.061 mmol) of **4a** and 0.50 mL of CD_2Cl_2. The tube was cooled to −78 °C, and HBF$_4$·Et$_2$O (8.4 μL, 0.061 mmol) was added by syringe. The tube was shaken and placed in a −80 °C NMR probe. ^{31}P-NMR spectra at various temperatures were recorded.

5a: ^{31}P-NMR (202 MHz, CD_2Cl_2) δ 13.5 ppm (at −80 °C).

Table 3. Summary of Crystal Data and Details of the Intensity Collection and Refinement for S_{Re}-*exo*-(PCp)Re(NO)(PPh$_3$)(CH$_3$) (4a)

formula	$C_{31}H_{33}NOPRe$
fw	652.79
color, habit	red rod
cryst size, mm^3	0.17 × 0.17 × 0.45
cryst system	orthorhombic
space group	$P2_12_12_1$ (No. 19)
a, Å	12.156(3)
b, Å	13.531(4)
c, Å	16.066(4)
V, Å^3	2643(1)
Z	4
d(calc), g cm^{-3}	1.640
F(000)	1296
abs coeff (μ, cm^{-1})	47.41
abs corr	numerical
max/min transm	0.53/0.26
radiation (λ, Å)	Mo Kα (0.710 73)
temp, K	263
scan mode (θ range, deg)	ω (3−25)
no. of unique rflns	3237
N_o, no. of obsd rflns	2407 ($I > 1.0\sigma(I)$)
N_p, no. of params refined	316
weighting scheme	$w^{-1} = \sigma^2(F_o)$
R	0.048
R_w	0.046
GOF	1.156
resid fluctuation in final DF map, e/Å^3	1.7, 0.8 Å from Re

Acknowledgment. The authors are grateful for financial support from the Deutsche Forschungsgemeinschaft (Grant SFB 380) and from the "Fonds der chemischen Industrie".

Supporting Information Available: Tables giving a structure report on the X-ray data collection and refinement, positional and thermal parameters for all atoms, anisotropic displacement parameters (U), and bond lengths and bond angles and an ORTEP drawing for **4a** (12 pages). Ordering information is given on any current masthead page.

OM950498R

(18) Sheldrick, G. M. SHELXS-86; Program for Crystal Structure Solution; University of Göttingen, Göttingen, Germany, 1986.
(19) Frenz, B. A. Enraf-Nonius Structure Determination Package, Version 5.0, Delft, The Netherlands, 1989.

Stable and Crystalline Allylium and Allenylium Salts with Ferrocenyl Substituents

Josef Lukasser,[†] Herbert Angleitner,[†] Herwig Schottenberger,*[,†,‡] Holger Kopacka,[†] Manuela Schweiger,[†] Benno Bildstein,*[,†,§] Karl-Hans Ongania,[||] and Klaus Wurst[†]

Institut für Allgemeine, Anorganische, und Theoretische Chemie and Institut für Organische Chemie, Universität Innsbruck, Innrain 52a, A-6020 Innsbruck, Austria

Received July 25, 1995[⊗]

Allylic and allenylic carbenium ions, which have been reported in the literature to be labile or not isolable at all, have no inherent instability. Progressive substitution with ferrocenyl groups affords allylic cations, whose stability toward photochemical decay and nucleophilic collapse increases with increasing number of ferrocenyl substituents, if the allylic moiety is at least 2-fold-substituted with ferrocenes in the 1,3-positions. The unmatched cation-stabilizing capacity of metallocenes is illustrated in cyclopentadienyl(1,3-diferrocenyl-1-yliumpentalenyl)iron tetrafluoroborate, a compound which survives exposure to sunlight in aqueous solution for days. In addition to full characterization for these allylium salts by the usual analytical and spectroscopic methods, X-ray analysis of cyclopentadienyl(1,3-diferrocenyl-1-yliumpentalenyl)iron tetrafluoroborate showed (a) deviations of the regular conformation of the ferrocenyl substituents in the 1,3-positions that are similar to those observed in other simple metallocenyl-stabilized carbenium ions, indicative of electronic stabilization by intramolecular charge delocalization, (b) these two ferrocenyl substituents are structurally distorted in an unequal manner and seem to contribute unequally in this charge delocalization, but the observed dissymmetric structure is most likely the result of crystal forces, and (c) the annelated ferrocene of this formal pentalene system is undistorted, ruling out (together with results from solution NMR measurements) any significant conjugation; therefore, this cation should be envisaged as an allylium system and not as an antiaromatic cyclopentadienyl cation. In the case of allenylium ↔ propargylium ions, attachment of two ferrocenes results in labile or intermediate propargylium ions, which can be trapped with triethylamine to afford ammonium allenes, formally Lewis base complexed allenylium salts, with an interesting bent allene unit as is evidenced by single-crystal structure analysis. Introduction of a third ferrocene into the allenylium ↔ propargylium system affords 1,3,3-triferrocenylallen-1-ylium tetrafluoroborate, the first stable and fully characterized allenylium compound, with only minor resonance contributions from the propargylium structure, proven most clearly by the observation of an extremely intense and acceptor-shifted cumulenic stretching vibration of 2151 cm^{-1} in the IR spectrum.

Introduction

Stabilization of an α-carbenium moiety by π-ligand complexes of transition metals[1] has been achieved with a wide range of organometallic fragments, including (arene)tricarbonyl chromium,[2] (cyclopentadiene)tricarbonylmanganese,[3] (cyclopentadiene)dicarbonylnitrosylchromium,[4] (cyclobutadiene)tricarbonyliron,[5] nonacarbonyltricobalt alkylidyne,[6] hexacarbonyldicobalt alkyne,[7] bis(methylcyclopentadienyl)tetracarbonyldimolybdenum,[8] and metallocenes.[1,9] Of these carbenium-stabilizing groups, metallocenes are probably the most efficient donors for satisfying the electron-deficiency of the carbenium moiety, which was recognized soon after the discovery of ferrocene.[10] This chemistry has been developed over the last decades with numerous studies concerning structural and spectroscopic properties and applications in organic synthesis.[1,9,11] Within this area

[†] Institut für Allgemeine, Anorganische, und Theoretische Chemie.
[‡] Correspondence regarding allylium salts to this author.
[§] Correspondence regarding allenylium salts to this author.
[||] Institut für Organische Chemie.
[⊗] Abstract published in *Advance ACS Abstracts,* November 1, 1995.

(1) Watts, W. E. In *Comprehensive Organometallic Chemistry*; Wilkinson, G., Stone, F. G. A., Abel, E. W., Eds.; Pergamon: Oxford, 1982; Vol. 8, Chapter 59, p 1051.

(2) (a) Seyferth, D.; Eschbach, C. S. *J. Organomet. Chem.* **1975,** *94,* C5. (b) Seyferth, D.; Merola, J. S.; Eschbach, C. S. *J. Am. Chem. Soc.* **1978,** *100,* 4124. (c) Jaouen, G. *Pure Appl. Chem.* **1986,** *58,* 597. (d) Edelmann, F.; Behrens, P.; Behrens, S.; Behrens U. *J. Organomet. Chem.* **1986,** *310,* 333.

(3) (a) Ginzburg, A. G.; Setkina, V. N.; Kursanov, D. N. *J. Organomet. Chem.* **1974,** *77,* C27. (b) Loim, N. M.; Malutschenko, L. A.; Parnes, Z. N.; Kursanov, D. N. *J. Organomet. Chem.* **1976,** *108,* 363. (c) Loim, N. M.; Petrovskii, P. V.; Robas, V. I.; Parnes, Z. N.; Kursanov, D. N. *J. Organomet. Chem.* **1976,** *117,* 265. (d) Ginzburg, A. G.; Setkina, V. N.; Petrovskii, P. V.; Kasumov, Sh. G.; Panosyan, G.A.; Kursanov, D. N. *J. Organomet. Chem.* **1976,** *121,* 381. (e) Ginzburg, A. G.; Panosyan, G. A.; Setkina, V. N.; Kasumov, Sh. G.; Petrovskii, P. V.; Kursanov, D.N. *J. Organomet. Chem.* **1979,** *164,* 59. (f) Seyferth, D.; Merola, J. S. *J. Organomet. Chem.* **1978,** *160,* 275.

(4) (a) Rausch, M. D.; Kowalski, D. J.; Mintz, E. A. *J. Organomet. Chem.* **1988,** *342,* 201. (b) Rausch, M. D.; Wang, Y.-P. *Organometallics* **1991,** *10,* 1438.

(5) (a) Fitzpatrick, J. D.; Watts, L.; Pettit, R. *Tetrahedron Lett.* **1966,** 1299. (b) Davis, R. E.; Simpson, H. D.; Conte, N.; Pettit, R. *J. Am. Chem. Soc.* **1971,** *93,* 6688. (c) Eschbach, C. S.; Seyferth, D.; Reeves, P. C. *J. Organomet. Chem.* **1976,** *104,* 363.

(6) (a) Seyferth, D. *Adv. Organomet. Chem.* **1976,** *14,* 97. (b) Seyferth, D.; Eschbach, C. S.; Nestle, M. O. *J. Organomet. Chem.* **1975,** *97,* C11. (c) Nicholas, K. M.; Nestle, M. O.; Seyferth, D. In *Transition Metal Organometallics in Organic Synthesis*; Alper, H., Ed.; Academic Press: New York, 1978; Vol. 2, Chapter 1, p 1.

0276-7333/95/2314-5566$09.00/0

of research, ferrocenyl-stabilized carbenium ions are the most frequently studied systems, but the even higher donor-capacity of ruthenocene, osmocene, and permethylated metallocenes[12] is illustrated by the recent isolation of metallocene-stabilized dications.[13] In addition, contrary to the above mentioned carbonyl-containing donors, metallocenes allow the synthesis of the carbenium-isoelectronic heterocations phosphenium[14] and silicenium.[15] For carbocations, mainly simple carbenium ions have been studied and no stable allyl or allenyl cations have been isolated so far. Here we describe the synthesis, properties, and structure of such cations, which are substituted and hence stabilized by two or three ferrocene moieties. These cations are of interest as electron and energy transfer model systems for molecular electronics.

Experimental Section

General Comments. All of the reactions were carried out in the absence of air using standard Schlenk techniques and vacuum-line manipulations. Solvents were deoxygenated, purified, and dried prior to use. Instrumentation: Bruker AC 200 (^{1}H and ^{13}C NMR); Nicolet 510 FT-IR (IR); Bruins Instruments Omega 20 (UV–vis); Varian CH-7, Finnigan MAT 95 (MS); Siemens P4 (X-ray). Melting points were determined on a Kofler hot-plate apparatus. Microanalyses were obtained from the Department for Microanalysis, University of Vienna, Austria; and from the Analytical Department of Lenzing AG, Lenzing, Austria.

Monolithioferrocene,[16] ferrocenylcopper–dimethylsulfide complex,[17] *trans*-1,3-diferrocenylpropenone,[18] diferrocenyl ketone,[19] ethinylferrocene,[20] (trimethylsilyl)ethinylferrocene,[17,21] and cyclopentadienyl(3-ferrocenyl-1-oxy-pentalenyl)iron[22] were prepared according to published procedures.

***rac*-1,3-Diferrocenylprop-2-en-1-ol (CAS Registry No. 72971-83-6).** Since no analytical and spectral data were given in ref 18b, the experimental procedure is reported in detail: 0.487 g (1.15 mmol) of 1,3-diferrocenylprop-2-en-1-one was dissolved in 40 mL of THF in a Schlenk vessel under an atmosphere of argon and cooled to −60 °C. A 1.27 mL amount of a 1.0 M solution of lithium triethylborohydride (1.27 mmol) was syringed slowly to the stirred solution. The reaction mixture was warmed to room temperature, reduced in volume to approximately 10 mL, hydrolyzed by addition of 30 mL of H_2O, and extracted with three portions of Et_2O. The combined organic layers were dried with Na_2SO_4, the solvents were removed in vacuo, and the residue was purified by chromatography on neutral Al_2O_3 with Et_2O (a few drops of *tert*-butylamine were added to ensure basic conditions) as eluent: 0.350 g (0.82 mmol, 71.4%) of *rac*-1,3-diferrocenylprop-2-en-1-ol, orange crystals, mp not observable because of ready reoxidation by air of the solid alcohol to an oily mixture of alcohol and ketone. For the same reason, no elemental analysis was attempted. MS (EI, 70 eV): m/z 426 (M^+). Selected IR data (KBr): 3436 (ν_{OH}), 1656 ($\nu_{C=C}$) cm^{-1}. ^{1}H NMR (DMSO-d_6; *cp* refers to cyclopentadienyl): δ 4.43 (1H, s, −O−*H*), 3.46 (10H, s, *unsubst. cp*), 4.14 (4H, m, *subst. cp*), 4.21 (4H, m, *subst. cp*), 4.92 (1H, m, C*H*−OH), 6.00−6.36 (2H, m, −C*H*=C*H*−). ^{13}C NMR (DMSO-d_6): δ 66.2, 66.5, 66.7, 67.2, 67.3, 67.4, 68.5, 67.0, 69.3 (*ferrocenyl*), 91.8 (*C*−OH), 125.8 [−*C*H=CH−CH(OH)], 130.3 [−CH=*C*H−CH(OH)].

1,3-Diferrocenylallylium Triiodide (1a), 1,3-Diferrocenylallylium Hexafluorophosphate (1b), and 1,3-Diferrocenylallylium Tetrafluoroborate (1c) (CAS Registry No. 68093-14-1). A 0.220 g (0.516 mmol) amount of *rac*-diferrocenylprop-2-en-1-ol was dissolved in 50 mL of Et_2O. After addition of 60 mL of 2 N H_2SO_4, the mixture was shaken in a separatory funnel, the resulting green aqueous layer was quickly added to a solution of 0.830 g (5.00 mmol) of KI and 1.27 g (5.00 mmol) of I_2 in 50 mL of H_2O, and the precipitated green solid was filtered off, washed with three portions of H_2O, and dried in vacuo, yielding 0.190 g (0.24 mmol, 46.6%) of 1,3-diferrocenylallylium triiodide (**1a**). Analogously, combining the 1,3-diferrocenylallylium hydrogensulfate solution with an aqueous solution of $NaPF_6$ yielded 0.420 g (0.758 mmol, 71.4%) of 1,3-diferrocenylallylium hexafluorophosphate (**1b**). Addition of 1.5 mol equiv (based on starting alcohol) of a 54% solution of fluoroboric acid in ether to the solution of *rac*-diferrocenylprop-2-en-1-ol in Et_2O yielded 0.179 g (0.361 mmol, 72.8%) of 1,3-diferrocenylallylium tetrafluoroborate (**1c**). Compounds **1a,c** are stable for a limited time only, after storage under argon at −30 °C for half a year, decomposition of the triiodide **1a** and the tetrafluoroborate **1c** were complete. The hexafluorophosphate **1b** showed NMR spectral parameters corresponding to less than 5% decomposition after storage at ambient temperature for 18 months.

Data for **1a**: Green microcrystalline solid. Mp not observable due to continuous decomposition on heating. Anal. Calcd

(7) (a) Nicholas, K. M.; Pettit, R. *J. Organomet. Chem.* **1972**, *44*, C21. (b) Connor, R. E.; Nicholas, K. M. *J. Organomet. Chem.* **1977**, *125*, C45. (c) Nicholas, K. M. *Acc. Chem. Res.* **1987**, *20*, 207. (d) Varghese, V.; Saha, M.; Nicholas, K. M. *Org. Synth.* **1989**, *67*, 141. (e) Takano, S.; Sugihara, T.; Ogasawara, K. *Synlett* **1992**, 70. (f) Grove, D. D.; Miskevich, F.; Smith, Ch. C.; Corte, J. R. *Tetrahedron Lett.* **1990**, *44*, 6277. (g) Buchmeiser, M.; Schottenberger, H. *Organometallics* **1993**, *12*, 2472.

(8) (a) Meyer, A.; McCabe, D. J.; Curtis, M. D. *Organometallics* **1987**, *6*, 1491. (b) Gruselle, M.; Cordier, C.; Salmain, M.; El Amouri, H.; Guérin, C.; Vaissermann, J.; Jaouen, G. *Organometallics* **1990**, *9*, 2993. (c) Barinov, I. V.; Reutov, O. A.; Polyakov, A. V.; Yanovsky, A. I.; Struchkov, Yu.T.; Sokolov, V. I. *J. Organomet. Chem.* **1991**, *418*, C24. (d) Le Berre-Cosquer, N.; Kergoat, R. *Organometallics* **1992**, *11*, 721. (e) Cordier, C.; Gruselle, M.; Vaissermann, J.; Troitskaya, L. L.; Bakhmutov, V. I.; Sokolov, V. I.; Jaouen, G. *Organometallics* **1992**, *11*, 3825. (f) Gruselle, M.; El Hafa, H.; Nikolski, M.; Jaouen, G.; Vaissermann, J.; Li, L.; McGlinchey, M. J. *Organometallics* **1993**, *12*, 4917. (g) El Amouri, H.; Besace, Y.; Vaissermann, J.; Jaouen, G.; McGlinchey, M. J. *Organometallics* **1994**, *13*, 4426. (h) El Hafa, H.; Cordier, C.; Gruselle, M.; Besace, Y.; Jaouen, G.; McGlinchey, M. J. *Organometallics* **1994**, *13*, 5149.

(9) Watts, W. E. *J. Organomet. Chem. Libr.* **1979**, *7*, 399.

(10) (a) Hill, E. A.; Richards, S. H. *J. Am. Chem. Soc.* **1959**, *81*, 3483. (b) Cais, M. *Organomet. Chem. Rev.* **1966**, *1*, 435.

(11) (a) Wagner, G.; Herrmann, R. In *Ferrocenes*; Togni, A., Hayashi, T., Eds.; VCH Verlagsgesellschaft mbH: Weinheim, Germany; 1995, Chapter 4, p 173. (b) Sokolov, V. I. *Chirality and Optical Activity in Organometallic Compounds*; Gordon & Breach: London, 1992. (c) Mayr, H.; Rau, D. *Chem. Ber.* **1994**, *127*, 2493. (d) Bildstein, B.; Denifl, P.; Wurst, K. *J. Organomet. Chem.* **1995**, *496*, 175; and references cited therin.

(12) (a) Rybinskaya, M. I.; Kreindlin, A. Z.; Fadeeva, S. S. *J. Organomet. Chem.* **1988**, *358*, 363. (b) Yanovsky, A. I.; Struchow, Yu.T.; Kreindlin, A. Z.; Rybinskaya, M.I. *J. Organomet. Chem.* **1989**, *369*, 125.

(13) (a) Kreindlin, A. Z.; Fedin, E. I.; Petrovskii, P. V.; Rybinskaya, M. I. *Organometallics* **1991**, *10*, 1206. (b) Rybinskaya, M. I.; Kreindlin, A. Z.; Petrovskii, P. V.; Minyaev, R. M.; Hoffmann, R. *Organometallics* **1994**, *13*, 3903.

(14) (a) Baxter, S. G.; Collins, R. L.; Cowley, A. H.; Sena, S. F. *J. Am. Chem. Soc.* **1981**, *103*, 714. (b) Baxter, S. G.; Collins, R. L.; Cowley, A. H.; Sena, S. F. *Inorg. Chem.* **1983**, *22*, 3475.

(15) (a) Corey, J. Y.; Gust, D.; Mislow, K. *J. Organomet. Chem.* **1975**, *101*, C7. (b) Lambert, J. B.; Zhang, S.; Ciro, S. M. *Organometallics* **1994**, *13*, 2430. (c) Ruffolo, R.; Decken, A.; Girard, L.; Gupta, H. K.; Brook, M. A.; McGlinchey, M.J. *Organometallics* **1994**, *13*, 4328.

(16) (a) Guillaneux, D.; Kagan, H. B. *J. Org. Chem.* **1995**, *60*, 2502. (b) Rebiere, F.; Samuel, O.; Kagan, H. B. *Tetrahedron Lett.* **1990**, *31*, 3121.

(17) Buchmeiser, M.; Schottenberger, H. *J. Organomet. Chem.* **1992**, *436*, 223.

(18) (a) Schlögl, K.; Egger, H. *Monatsh. Chem.* **1963**, *94*, 376. (b) Bunton, C. A.; Carrasco, N.; Watts, W. E. *J. Chem. Soc., Perkin Trans. 2* **1979**, *9*, 1267. (c) Kasahara, A.; Izumi, T.; Shimizu, I. *Bull. Chem. Soc. Jpn.* **1982**, *55*, 1901. (d) Schottenberger, H.; Buchmeiser, M.; Polin, J.; Schwarzhans, K.-E. *Z. Naturforsch.* **1993**, *48B*, 1524.

(19) O'Connor Salazar, D. C.; Cowan, D. O. *J. Organomet. Chem.* **1991**, *408*, 219 and references cited therein.

(20) Wurst, K.; Elsner, O.; Schottenberger, H. *Synlett* **1995**, *8*, 833 and references cited therein.

(21) Gvertsiteli, I. M.; Astiani, L. P.; Zurabinshvili, D. S. *Zh. Obshch. Khim.* **1975**, *45*, 577.

(22) (a) Abram, T. S.; Watts, W. E. *J. Chem. Soc., Perkin Trans. 1* **1977**, 1527. (b) Egger, H.; Schlögl, K. *Monatsh. Chem.* **1964**, *95*, 1750.

for $C_{23}H_{21}Fe_2I_3$: C, 34.98; H, 2.68. Found: C, 35.12; H, 2.52. MS (FAB): m/z 409.03375 (M^+ of cation; exact mass calcd for $C_{23}H_{21}Fe_2$, 409.03420). UV−vis data: unstable in solution, not determined. IR data (KBr): 3081 w, 1696 m, 1652 m, 1561 vs, 1451 vs, 1412 s, 1380 s, 1287 s, 1231 vs, 1167 m, 1108 s, 1054 s, 1036 s, 1003 s, 976 s, 922 s, 893 m, 847 vs, 826 vs, 641 s, 502 vs, 473 s, 459 vs, 419 s cm^{-1}. ^1H and ^{13}C NMR: unstable in solution due to Watts-type[40] oligomerization, not determined.

Data for **1b**: Green microcrystalline solid. Mp not observable due to continuous decomposition on heating. Anal. Calcd for $C_{23}H_{21}Fe_2PF_6$: C, 49.86; H, 3.82. Found: C, 49.20; H, 4.14. MS (FAB): m/z 409.03305 (M^+ of cation; exact mass calcd for $C_{23}H_{21}Fe_2$, 409.03420). UV−vis data (acetonitrile; λ_{max}/log ϵ): 419/4.2, 767/3.9 nm/log ϵ. IR data (KBr): 3108 w, 1706 w, 1642 w, 1569 vs, 1451 s, 1412 m, 1380 m, 1287 s, 1235 vs, 1167 m, 1108 m, 1052 m, 1042 s, 978 m, 924 s, 849 vs, 644 s, 558 vs, 509 s, 498 s, 475 s, 461 vs, 423 s cm^{-1}. ^1H NMR (CD_2Cl_2): δ 4.43 (10H, s, *unsubst. cp*), 4.97 (4H, br s, *subst. cp*), 5.54 (4H, br s, *subst. cp*), 6.48 [1H, br s, *allyl H(2)*], 8.30 [2H, br s, *allyl H(1) and H(3)*]. ^{13}C NMR (CD_2Cl_2): δ 74.6, 76.6, 83.5, 87.4 (*ferrocenyl*), 126.0 (*allyl*), 157.7 (*allyl*).

Data for **1c**: Green microcrystalline solid. Mp not observable due to continuous decomposition on heating. Anal. Calcd for $C_{23}H_{21}Fe_2BF_4$: C, 55.71; H, 4.27. Found: C, 55.47; H, 4.19. MS (FAB): m/z 409.03445 (M^+ of cation; exact mass calcd for $C_{23}H_{21}Fe_2$, 409.03420). UV−vis data (acetonitrile; λ_{max}/log ϵ): 420/4.1, 751/3.8 nm/log ϵ. ^1H NMR (CD_2Cl_2): δ 4.45 (10H, s, *unsubst. cp*), 5.00 (4H, br s, *subst. cp*), 5.52 (4H, br s, *subst. cp*), 6.50 [1H, br s, *allyl H(2)*], 8.35 [2H, br s, *allyl H(1) and H(3)*]. ^{13}C NMR (CD_2Cl_2): δ 74.3, 76.4, 83.2, 87.4 (*ferrocenyl*), 125.7 (*allyl*), 157.7 (*allyl*).

1,1,3-Triferrocenylprop-2-en-1-ol (2). A Schlenk vessel was charged with 1.30 g (6.77 mmol) of monolithioferrocene and 100 mL of THF at −80 °C. To the resulting suspension was added 2.73 g (6.45 mmol) of 1,3-diferrocenylprop-2-en-1-one, and the mixture was stirred magnetically at −80 °C for 5 min. The cooling bath was removed, and the stirred mixture was warmed to room temperature. The solvent THF was removed in vacuo, the resulting crude alcoholate was hydrolyzed with ice/water, the product mixture (containing alcohol **2** and traces of unreacted propenone and ferrocene) was extracted with three portions of ether, and all volatile materials were removed in vacuo, yielding 3.66 g (6.00 mmol, 93%) of crude **2**. For analytical purposes a small portion was purified by chromatography on neutral Al_2O_3 with petroleum ether/diethyl ether: orange crystals, mp 165−168 °C (decomp). Anal. Calcd for $C_{33}H_{30}Fe_3O$: C, 64.96; H, 4.96; O, 2.62. Found: C, 65.13; H, 4.82; O, 2.70. MS (EI, 70 eV): m/z 610 (M^+). Selected IR data (KBr): 3527 (ν_{OH}), 1652 ($\nu_{C=C}$) cm^{-1}. ^1H NMR (C_6D_6): δ 2.57 (1H, s, −O−*H*), 3.96 (4H, m, *subst. cp*), 4.07−4.14 (19H, m, *unsubst. and subst cp*), 4.23 (2H, m, *subst. cp*), 4.32 (2H, m, *subst. cp*), 6.49−6.60 (2H, dd, J = 15.4 Hz, −C*H*=C*H*−). ^{13}C NMR ($CDCl_3$): δ 66.7, 66.9, 67.4, 67.9, 68.6, 68.9, 69.6, 89.6, 91.7 (*ferrocenyl*), 96.8 (*C*−OH), 124.0 (−*C*H=CH−), 132.6 (−CH=*C*H−).

1,1,3-Triferrocenylallylium Tetrafluoroborate (3a) and 1,1,3-Triferrocenylallylium Tetraphenylborate (3b). The crude 1,1,3-triferrocenylprop-2-en-1-ol (**2**) was dissolved in dry ether, and 1.5 mol equiv of a 54% solution of fluoroboric acid in ether was added dropwise to the stirred solution. The precipitated dark green cation tetrafluoroborate was filtered off, washed with 5 portions of ether, and dried in vacuo, yielding 2.63 g (3.87 mmol, 64.5%) of 1,1,3-triferrocenylallylium tetrafluoroborate (**3a**).

Conversion of 3a into the Corresponding Tetraphenylborate 3b. Combining a solution of 900 mg (1.32 mmol) of **3a** in 200 mL of dry methanol with a solution of 500 mg (1.46 mmol) of sodium tetraphenylborate in 3 mL of methanol produces a dark green precipitate, which was filtered off, washed with three portions of H_2O and three portions of Et_2O, and dried in vacuo, yielding 600 mg (0.66 mmol, 50%) of 1,1,3-triferrocenylallylium tetraphenylborate (**3b**). These allylium salts are air-stable in the solid state but have to be protected from light to avoid photochemical decomposition.

Data for **3a**: Mp not observed, >300 °C. Anal. Calcd for $C_{33}H_{29}BF_4Fe_3$: C, 58.29; H, 4.30. Found: C, 58.51; H, 4.33. MS (FAB): m/z 593.03149 (M^+ of cation; exact mass calcd for $C_{33}H_{29}Fe_3$, 593.03174). UV−vis data (acetonitrile; λ_{max}/log ϵ): 388/4.0, 451/4.2, 840/4.0 nm/log ϵ. IR data (KBr): 471 m, 807 m, 822 m, 1036 vs, 1090 vs, 1108 vs, 1264 s, 1281 s, 1436 s, 1457 s, 1557 vs cm^{-1}. ^1H NMR (CD_3CN): δ 4.39 (10H, s, *unsubst. cp*), 4.46 (5H, s, *unsubst. cp*), 5.10 (2H, m, *subst. cp*), 5.27 (4H, m, *subst. cp*), 5.31 (2H, m, *subst. cp*), 5.45 (4H, m, *subst. cp*), 6.67 [1H, d, J = 14.6 Hz, *allyl H(3)*], 8.66 [1H, d, J = 14.6 Hz, *allyl H(2)*]. ^{13}C NMR ($CDCl_3$): δ 72.2, 73.6, 74.4, 74.8, 75.0, 79.2, 79.4, 84.8, 86.2 (*ferrocenyl*); 128.5, 154.1, 180.5 (*allyl*).

Data for **3b**: Mp not observed, >300 °C. Anal. Calcd for $C_{57}H_{49}BFe_3$: C, 75.04; H, 5.41. Found: C, 75.11; H, 5.18. MS (EI, 70 eV): m/z 593.03295 (M^+ of cation; exact mass calcd for $C_{33}H_{29}Fe_3$, 593.03174). UV−vis data (acetonitrile; λ_{max}/log ϵ): 389/4.0, 451/4.2, 841/4.0 nm/log ϵ. IR data (KBr): 3096 w, 3055 m, 2984 w, 1553 vs, 1456 s, 1435 s, 1271 s, 1107 m, 829 m, 733 m, 704 s, 470 m cm^{-1}. ^1H NMR (CD_3CN): δ 4.37 (10H, s, *unsubst. cp*), 4.44 (5H, s, *unsubst. cp*), 5.07 (2H, m, *subst. cp*), 5.25 (4H, m, *subst. cp*), 5.29 (2H, m, *subst. cp*), 5.42 (4H, m, *subst. cp*), 6.65 [1H, d, J = 14.6 Hz, *allyl H(3)*], 6.86−6.79 (8H, m, *phenyl*), 6.98 (12H, m, *phenyl*), 8.64 [1H, d, J = 14.6 Hz, *allyl H(2)*]. ^{13}C NMR ($CDCl_3$): δ 68.8, 69.2, 69.9, 72.1, 73.4, 74.5, 75.1, 79.3, 79.9, 84.2, 85.8 (*ferrocenyl*); 121.7, 125.5, 136.3 (*phenyl*); 164.2 [q, $J(^{13}C-^{11}B)$ = 195 Hz, *C(1) of phenyl*)]; 127.9, 154.1, 180.6 (*allyl*).

Cyclopentadienyl(3-ferrocenyl-1-hydroxypentalenyl)iron (4) and Cyclopentadienyl(3-ferrocenyl-1-yliumpentalenyl)iron Tetrafluoroborate (5). In an analogous manner as described for *rac*-1,3-diferrocenylprop-2-en-ol (see above), reduction of cyclopentadienyl-(3-ferrocenyl-1-oxypentalenyl)iron with lithium triethylborohydride yielded cyclopentadienyl(3-ferrocenyl-1-hydroxypentalenyl)iron (**4**) as a red solid of limited stability; therefore only NMR spectroscopy was used for the characterization of this intermediate. ^1H NMR (C_6D_6): δ 2.02 (1H, d, J = 9.5 Hz, −O−*H*), 3.90−4.48 (17H, m and two s, *subst. and unsubst. cp*), 4.94−5.00 (1H, dd, J = 9.5 Hz, J = 2 Hz, −C*H*−OH), 6.05 (1H, d, J = 2 Hz, −C*H*=). ^{13}C NMR (C_6D_6): δ 61.9, 63.3, 66.4, 69.1, 69.2, 69.8, 70.0, 70.2, 72.2, 80.2, 94.0 (*ferrocenyl*), 96.5 (*C*−OH), 122.8 (*C*−OH), 132.3 (−*C*H=C), 142.6 (−CH=*C*). Addition of 1.5 mol equiv (based on starting alcohol) of a 54% solution of fluoroboric acid in ether to the solution of **4** in Et_2O yielded 0.147 g (0.30 mmol, 60%) of cyclopentadienyl(3-ferrocenyl-1-yliumpentalenyl)iron tetrafluoroborate (**5**) as a green, microcrystalline solid. Mp: not observable due to continuous decomposition on heating. MS (FAB): m/z 407.02230 (M^+ of cation; exact mass calcd for $C_{23}H_{19}Fe_2$, 407.01855). UV−vis data (acetonitrile; λ_{max}): unstable in solution; 356, 476, 637 nm were observed for freshly prepared solutions, and during measurement of the spectrum these absorptions shifted to lower values with decreasing ϵ, indicative of destruction of the chromophore. IR data (KBr): 3100 m, 1669 m, 1530 s, 1410 s, 1387 s, 1339 m, 1300 m, 1233 w, 1107 s, 1084 s, 834 m, 469 m, 436 m cm^{-1}. ^1H and ^{13}C NMR: unstable in solution; attempted NMR analysis yielded too many signals with broad appearance, indicating decomposition during FID accumulation.

Cyclopentadienyl(1,3-diferrocenyl-1-hydroxypentalenyl)iron (6) and Cyclopentadienyl(1,3-diferrocenyl-1-yliumpentalenyl)iron Tetrafluoroborate (7). A Schlenk vessel was charged with 1.21 g (6.3 mmol) of monolithioferrocene and 100 mL of THF at −80 °C. To the resulting suspension was added 2.52 g (6.0 mmol) of cyclopentadienyl-(3-ferrocenyl-1-oxypentalenyl)iron, and the mixture was stirred magnetically at −80 °C for 5 min. The cooling bath was removed, and the stirred mixture was warmed to room

Table 1. Crystal Data and Structure Refinement for 7, 10a,b, and 11

	7	10a	10b	11
mol formula	$C_{33}H_{27}BF_4Fe_3$	$C_{30}H_{34}F_3Fe_2NO_3S$	$C_{53}H_{54}BFe_2N$	$C_{33}H_{28}Fe_3O$
fw	677.9	657.34	827.48	608.10
cryst syst	triclinic	monoclinic	monoclinic	orthorhombic
space group	*P*1 (No. 2)	$P2_1/c$ (No. 14)	$P2_1/c$ (No. 14)	$Pca2_1$ (No. 29)
a (pm)	1311.1(4)	2011.4(3)	1548.6(4)	3983.0(5)
b (pm)	1320.2(4)	729.8(1)	1561.6(3)	584.1(2)
c (pm)	1621.0(6)	2055.5(7)	1833.7(5)	1064.6(4)
α (deg)	91.61(2)	90	90	90
β (deg)	95.40(2)	102.81(2)	108.71(2)	90
γ (deg)	100.30(2)	90	90	90
vol (nm^3)	2.746(2)	2.9422(12)	4.200(2)	2.4768(13)
Z	4	4	4	4
temp (K)	223(2)	213(2)	213(2)	193(2)
density (calcd) (Mg/m^3)	1.640	1.484	1.309	1.631
abs coeff (mm^{-1})	1.614	1.108	0.729	1.760
F(000)	1376	1360	1744	1248
color, habit	black block	orange platelet	red prism	orange block
cryst size (mm^3)	0.3 × 0.2 × 0.15	0.34 × 0.19 × 0.09	0.60 × 0.25 × 0.20	0.35 × 0.2 × 0.15
θ range for data collecn (deg)	2.02–19.99	2.56–18.00	3.01–21.00	3.07–22.49
index ranges	$-1 \le h \le 11$; $-13 \le k \le 12$; $-15 \le l \le 15$	$-13 \le h \le 20$; $-5 \le k \le 7$; $-19 \le l \le 20$	$-6 \le h \le 16$; $-11 \le k \le 17$; $-20 \le l \le 15$	$-36 \le h \le 42$; $-6 \le k \le 6$; $-8 \le l \le 11$
no. of rflns collecd	5302	2774	5594	2442
no. of indep rflns	4981 (R_{int} = 0.0580)	2008 (R_{int} = 0.0369)	4500 (R_{int} = 0.0350)	1882 (R_{int} = 0.0410)
no. of rflns with $I > 2\sigma(I)$	2977	1511	2960	1534
abs corr	DIFABS	ψ-scan	none	ψ-scan
max and min transm		0.926 and 0.838		0.953 and 0.765
refinement method	full-matrix least-squares on F^2	full-matrix least-squares on F^2	full-matrix least-squares on F^2	full-matrix least-squares on F^2
data/restraints/parameters	4798/0/734	1872/0/285	4384/0/514	1810/0/333
goodness-of-fit on F^2	1.030	1.087	1.013	1.095
final *R* indices [$I > 2\sigma(I)$]	R1 = 0.0578; wR2 = 0.1042	R1 = 0.0792; wR2 = 0.1687	R1 = 0.0386; wR2 = 0.0701	R1 = 0.0578; wR2 = 0.1042
R indices (all data)	R1 = 0.1260; wR2 = 0.1394	R1 = 0.1118; wR2 = 0.2369	R1 = 0.0977; wR2 = 0.1153	R1 = 0.0685; wR2 = 0.1098
largest diff peak and hole (e nm^{-3})	383 and −393	510 and −354	377 and −386	430 and −391

temperature. The solvent THF was removed in vacuo, the resulting crude alcoholate was hydrolyzed with ice/water, the product mixture [containing alcohol **6** and traces of unreacted cyclopentadienyl(3-ferrocenyl-1-oxypentalenyl)iron and ferrocene] was extracted with three portions of ether, and all volatile materials were removed in vacuo, yielding crude **6**, which was used without further purification because of ready reoxidation and immobilization on basic alumina as the solid phase on attempted chromatography. Compound **6** was dissolved in dry ether, and 1.5 mol equiv of a 54% solution of fluoroboric acid in ether was added dropwise to the stirred solution. The precipitated dark blue cation tetrafluoroborate was filtered off, washed with five portions of ether, and dried in vacuo, yielding 2.09 g (3.1 mmol, 51.4%) of cyclopentadienyl-(1,3-diferrocenyl-1-yliumpentalenyl)iron tetrafluoroborate (**7**), which is air-stable in the solid state; for prolonged storage it should be protected from light to avoid photochemical decomposition. Mp not observed, >300 °C. Anal. Calcd for $C_{33}H_{27}Fe_3BF_4$: C, 58.47; H, 4.01. Found: C, 58.41; H, 4.28. MS (FAB): *m/z* 591.01611 (M^+ of cation; exact mass calcd for $C_{33}H_{27}Fe_3$, 591.01609). UV−vis data (acetonitrile; $\lambda_{max}/\log \epsilon$): 391/4.2, 558/3.5, 873/4.1 nm/log ϵ. IR data (KBr): 1040 s, 1063 s, 1084 s, 1106 s, 1127 s, 1412 s, 1445 s, 1509 vs, 1540 s cm^{-1}. ^1H NMR (CD_2Cl_2): δ 4.25 (10H, s, *unsubst. cp*), 4.39 (5H, s, *unsubst. cp*), 4.61 (2H, m, *subst. cp*), 4.74 (2H, m, *subst. cp*), 5.61−5.23 (5H, m, *subst. cp*), 5.58 (2H, d, J = 2.7 Hz, *subst. cp*), 6.19 (1H, t, J = 2.7 Hz, *allyl-H*). ^{13}C NMR (CD_2Cl_2): δ 70.2, 73.0, 75.0, 76.4, 79.4, 79.9, 82.2, 84.5, 88.8 (*ferrocenyl*); 127.7 (*allyl*), 162.6 (*allyl*).

X-ray Structure Determination of 7. (Figures 2−4) Single crystals, suitable for X-ray analysis, were obtained by recrystallization from dichloromethane. A Siemens P4 diffractometer with graphite-monochromatized Mo Kα radiation (λ = 71.073 pm) was used for data collection. Crystal data, data collection, and refinement parameters of **7** are summarized in Table 1. The unit cell was determined by the automatic indexing of 25 centered reflections and confirmed by examination of the axial photographs. Data were measured via ψ-scan and corrected for Lorentz and polarization effects. Scattering factors for neutral atoms and anomalous dispersion corrections were taken from the *International Tables for X-ray Crystallography*,[23] and an empirical absorption correction[24] was made. The structure was solved by direct methods, SHELXS-86,[25] and refined by a full-matrix least-squares procedure using SHELXL-93.[26] All non-hydrogen atoms were refined with anisotropic displacement parameters. Hydrogen atoms were placed in calculated positions. For complete crystallographic data, tables of bond lengths, bond angles, anisotropic thermal parameters, calculated hydrogen atomic coordinates, and final atomic coordinates, see supporting information.

1,1-Diferrocenyl-3-(trimethylsilyl)prop-2-yn-1-ol (8). A 0.80 mL (5.6 mmol) amount of ethynyl trimethylsilane [(trimethylsilyl)acetylene] was dissolved in 125 mL of THF and cooled to −60 °C in a Schlenk vessel under an atmosphere of argon. Addition of 3.6 mL (5.7 mmol) of a 1.6 M *n*-butyllithium solution in *n*-hexane and allowing the stirred mixture to warm to ambient temperature resulted in formation of lithium (trimethylsilyl)acetylide.[27] To this colorless solution was added 1.60 g (4.0 mmol) of diferrocenyl ketone in one portion, and the resulting red solution was stirred at room temperature for

(23) *International Tables for X-ray Crystallography*; Kynoch Press: Birmingham, U.K., 1974; Vol. 4, pp 72−98.

(24) (a) North, A. C. T.; Phillips, D.; Mathews, F. S. *Acta Crystallogr.* **1968**, *A24*, 351. (b) Walker, N.; Stuart, D. *Acta Crystallogr.* **1983**, *A39*, 158.

(25) Sheldrick, G. M. *SHELXS-86: Program for Crystal Structure Solutions*; University of Göttingen: Göttingen, Germany, 1986.

(26) Sheldrick, G. M. *SHELXL-93: Program for the Refinement of Crystal Structures*; University of Göttingen: Göttingen, Germany, 1993.

(27) Brandsma, L. *Preparative Acetylenic Chemistry*, 2nd ed.; Elsevier: Amsterdam 1988.

20 h during which time the color of the solution gradually changed from red to orange. The mixture was hydrolyzed with 1 mL of water, all volatile materials were removed in vacuo, and the resulting brown residue was dissolved in dichloromethane, washed with two portions of a 5% $NaHCO_3$ solution, dried with Na_2SO_4, and evaporated to dryness. The crude product was purified by chromatography on neutral Al_2O_3 with *n*-hexane/ether (3/1) as eluent, yielding 1.53 g (76% based on starting diferrocenyl ketone) of yellow, crystalline **8**. Mp: 149–151 °C (decomp). Anal. Calcd for $C_{26}H_{28}Fe_2OSi$: C, 62.92; H, 5.69; O, 3.22. Found: C, 63.34; H, 5.74; O, 3.20. MS (EI, 70 eV): *m/z* 496 (M^+). Selected IR data (KBr): 3568 (ν_{OH}), 2182 ($\nu_{C\equiv C}$), 1250 (ν_{Si-C}) cm^{-1}. ^1H NMR (C_6D_6): δ 0.32 (9H, s, Si–C*H*$_3$), 2.92 (1H, s, –O–*H*), 3.97 (4H, m, *subst. cp*), 4.25 (10H, s, *unsubst. cp*), 4.49–4.40 (4H, m, *subst. cp*). ^{13}C NMR (C_6D_6): δ 0.2 (Si–*C*H$_3$); 66.0, 68.0, 69.5 (*ferrocenyl*); 86.9, 95.7, 109.8 (*propargyl*).

1,1-Diferrocenylprop-2-yn-1-ol (9). A 250 mL round bottom flask was charged with 1.68 g (30 mmol) of powdered KOH, 100 mL of methanol, and 1.49 g (3.0 mmol) of 1,1-diferrocenyl-3-(trimethylsilyl)prop-2-yn-1-ol (**8**). This orange solution was refluxed for 18 h to remove the trimethylsilyl protecting group,[28] during which time a yellow precipitate of potassium 1,1-diferrocenylprop-2-yn-1-oxide was formed. Methanol and all volatiles were removed in vacuo, the residue was hydrolyzed with 50 mL of H_2O, the product was extracted with three portions of Et_2O, washed with H_2O, dried with Na_2SO_4, and evaporated to dryness, yielding 1.25 g (98%) of yellow, crystalline 1,1-diferrocenylprop-2-yn-1-ol (**9**). Mp: 158 °C (decomp). Anal. Calcd for $C_{23}H_{20}Fe_2O$: C, 65.14; H, 4.75; O, 3.77. Found: C, 64.94; H, 4.70; O, 4.34. MS (EI, 70 eV): *m/z* 424 (M^+). Selected IR data (KBr): 3583 (ν_{OH}), 3271 ($\nu_{C\equiv C-H}$), 2109 ($\nu_{C\equiv C}$) cm^{-1}. ^1H NMR ($CDCl_3$): δ 2.77 (1H, s, C≡C–*H*), 3.09 (1H, s, –O–*H*), 4.12 (4H, m, *subst. cp*), 4.22 (10H, s, *unsubst. cp*), 4.27–4.32 (4H, m, *subst. cp*). ^{13}C NMR ($CDCl_3$): δ 65.5, 67.6, 67.8, 68.0, 69.0 (*ferrocenyl*); 71.5, 86.4, 94.8 (*propargyl*).

(3,3-Diferrocenylallenyl)triethylammonium Trifluoromethanesulfonate (10a) and (3,3-Diferrocenylallenyl)-triethylammonium Tetraphenylborate (10b). To a solution of 424 mg (1.0 mmol) of 1,1-diferrocenylprop-2-yn-1-ol (**9**), dissolved in 30 mL of dry, deoxygenated dichloromethane in a small Schlenk tube was added 0.15 mL (1.1 mmol) of freshly distilled dry triethylamine. The brown solution was cooled in an ice/water bath, and after addition of 0.20 mL (1.1 mol) of trimethylsilyl trifluoromethanesulfonate[29] the mixture was stirred at 0 °C for 90 min and after warming to room temperature for additional 90 min at ambient temperature. The mixture was filtered through a bed of neutral Al_2O_3, prepared by pouring a slurry of Al_2O_3 in Et_2O into a small filter funnel, to absorb the polar product and to remove unreacted material and less polar side-products by washing with three portions of Et_2O. The product was eluted with ethanol, and after evaporation to dryness 354 mg (54%) of orange, crystalline (3,3-diferrocenylallenyl)triethylammonium trifluoromethanesulfonate (**10a**) was obtained. Performing the same reaction at –70 °C with inversed addition mode (first trimethylsilyl trifluoromethanesulfonate and second triethylamine) yields the product **10a** in 74% yield.

Conversion of 10a into the Corresponding Tetraphenylborate 10b. Combining a solution of 200 mg (0.304 mmol) of **10a** in 2 mL of dry methanol with a solution of 217 mg (0.634 mmol) of sodium tetraphenylborate in 0.5 mL of methanol produces a dark yellow precipitate, which was filtered off, washed with three portions of methanol and three portions of Et_2O, and dried in vacuo, yielding 174 mg (0.21 mmol, 69%) of (3,3-diferrocenylallenyl)triethylammonium tetraphenylborate (**10b**).

Data for **10a**: Mp 114 °C (decomp). Anal. Calcd for $C_{29}H_{34}BF_4Fe_2N$: C, 58.53; H, 5.76; N, 2.35. Found: C, 58.27; H, 5.62; N, 2.31. MS (FAB): *m/z* 508.13726 (M^+ of cation; exact mass calcd for $C_{29}H_{34}Fe_2N$, 508.13900); 407.01519 (M^+ of cation minus triethylamine; exact mass calcd for $C_{23}H_{19}Fe_2$, 407.01855). UV–vis data (acetonitrile; λ_{max}/log ϵ): 363/3.3, 455/3.0 nm/log ϵ. IR data (KBr): 3097 w, 2987 w, 2950 w, 1937 m ($\nu_{C=C=C}$), 1636 w, 1478 m, 1447 m, 1389 m, 1277 vs, 1264 vs, 1223 m, 1156 s, 1108 m, 1030 s, 830 s, 639 s, 519 m, 477 s cm^{-1}. ^1H NMR (CD_3CN): δ 1.31 (9H, t, J = 7.0 Hz, CH_2–C*H*$_3$), 3.38 (6H, q, J = 7.0 Hz, CH_2–CH_3), 4.22 (10H, s, *unsubst. cp*), 4.47 (4H, m, *subst. cp*), 4.69 (4H, m, *subst. cp*), 6.12 (1H, s, *allenyl-H*). ^{13}C NMR ($CDCl_3$): δ 8.5 (*C*H$_3$), 54.2 (*C*H$_2$); 68.5, 69.9, 77.6 (*ferrocenyl*); 106.6, 123.5, 195.2 (*allenyl*); (the ^{13}C signal of trifluoromethanesulfonate was not observed, probably due to unfavorable relaxation).

Data for **10b**: Mp 225 °C (decomp). Anal. Calcd for $C_{53}H_{54}BFe_2N$: C, 76.93; H, 6.58; N, 1.69. Found: C, 76.79; H, 6.47; N, 1.56. MS (FAB): *m/z* 508.13690 (M^+ of cation; exact mass calcd for $C_{29}H_{34}Fe_2N$, 508.13900); 407.01556 (M^+ of cation minus triethylamine; exact mass calcd for $C_{23}H_{19}Fe_2$, 407.01855). UV–vis data (acetonitrile; λ_{max}/log ϵ): 363/3.3, 455/3.0 nm/log ϵ. IR data (KBr): 3095 w, 3053 m, 3029 m, 2997 m, 2985 m, 1939 m ($\nu_{C=C=C}$), 1646 w, 1580 m, 1478 m, 1457 m, 1428 m, 1412 m, 1397 m, 1287 m, 1256 m, 1185 w, 1146 m, 1107 m, 1063 m, 1049 m, 1031 m, 1001 m, 823 s, 791 s, 742 s, 735 s, 708 s, 614 s, 512 m, 479 s cm^{-1}. ^1H NMR (CD_2Cl_2): δ 1.21 (9H, t, J = 7.0 Hz, CH_2–C*H*$_3$), 2.71 (6H, q, J = 7.0 Hz, CH_2–CH_3), 4.43 (10H, s, *unsubst. cp*), 4.71 (4H, m, *subst. cp*), 4.77 (2H, m, *subst. cp*), 4.80 (2H, m, *subst. cp*), 5.52 (1H, s, *allenyl-H*), 7.10–7.64 (20H, m, *phenyl*). ^{13}C NMR (CD_2Cl_2): δ 8.5 (*C*H$_3$), 54.5 (*C*H$_2$); 69.1, 69.2, 70.4, 70.6, 70.8, 77.8 (*ferrocenyl*); 105.5, 195.5 (*allenyl*, the third signal cannot be assigned unambiguously due to signal-overlap with the phenyl signals but is probably located at 122.4 according to the line shape of this signal); 122.4, 126.3, 136.4, (*phenyl*); 164.5 (q, J (^{13}C–^{11}B) = 195 Hz, *C1 of phenyl*).

X-ray Structure Determination of 10a. (Figures 5 and 6). Single crystals, suitable for X-ray analysis, were obtained by recrystallization from ethanol. Crystal data, data collection, and refinement parameters of **10a** are summarized in Table 1, and the general procedure was as described for **7**, except for isotropic refinement of the cyclopentadienyl carbons. The anion trifluoromethanesulfonate is disordered and was refined with two fixed positions for the sulfur atom (see Figure 6). For complete crystallographic data, tables of bond lengths, bond angles, anisotropic and isotropic thermal parameters, calculated hydrogen atomic coordinates, final atomic coordinates, see supporting information.

X-ray Structure Determination of 10b. (Figure 7.) Single crystals, suitable for X-ray analysis, were obtained by slow diffusion of methanol into a dichloromethane solution of **10b**. Crystal data, data collection, and refinement parameters of **10b** are summarized in Table 1, and the general procedure was as described for **7**. For complete crystallographic data, tables of bond lengths, bond angles, anisotropic thermal parameters, calculated hydrogen atomic coordinates, final atomic coordinates, see supporting information.

1,1,3-Triferrocenylprop-2-yn-1-ol (11). A 1.00 g (4.76 mmol) amount of ethinylferrocene (ferrocenylacetylene) was dissolved in 80 mL THF and cooled to –60 °C in a Schlenk vessel under an atmosphere of argon. Addition of 3.0 mL (4.8 mmol) of a 1.6 M *n*-butyllithium solution in *n*-hexane and allowing the stirred mixture to warm to ambient temperature resulted in formation of lithium ferrocenylacetylide. To this orange solution was added 1.33 g (3.34 mmol) of diferrocenyl ketone in one portion, and the resulting red solution was stirred at room temperature for 12 h, during which time the color of the solution gradually changed from red to brown with precipitation of yellow lithium 1,1,3-triferrocenylprop-2-yn-1-

(28) Eaborn, C.; Thompson, A. R.; Welton, D. R. M. *J. Chem. Soc. C* **1967**, 1364.

(29) Emde, H.; Domsch, D.; Feger, H.; Frick, U.; Götz, A.; Hergott, H. H.; Hofmann, K.; Kober, W.; Krägeloh, K.; Oesterle, T.; Steppan, W.; West, W.; Simchen, G. *Synthesis* **1982**, 1.

oxide. The mixture was hydrolyzed with 1 mL of dilute acetic acid, all volatile materials were removed in vacuo, and the resulting brown residue was dissolved in dichloromethane, washed with two portions of a 5% $NaHCO_3$ solution and with one portion of H_2O, dried with Na_2SO_4, and evaporated to dryness. The crude product was purified by chromatography on neutral Al_2O_3 with *n*-hexane/ether (1/1) as eluent, yielding 1.45 g (71% based on starting diferrocenyl ketone) of yellow, crystalline **11**. Mp: 155–156 °C (decomp). Anal. Calcd for $C_{33}H_{28}Fe_3O$: C, 65.18; H, 4.64; O, 2.63. Found: C, 64.80; H, 4.45; O, 2.84. MS (EI, 70 eV): *m/z* 608 (M^+). Selected IR data (KBr): 3551 (ν_{OH}), 2228 ($\nu_{C\equiv C}$) cm^{-1}. ^1H NMR ($CDCl_3$): δ 3.04 (1H, s, −O−*H*), 4.13 (4H, m, *subst. cp*), 4.22 (2H, m, *subst. cp*), 4.27 (10H, s, *unsubst. cp*), 4.32 (5H, s, *unsubst. cp*), 4.37 (4H, m, *subst. cp*), 4.54 (2H, m, *subst. cp*). ^{13}C NMR ($CDCl_3$): δ 67.7, 67.8, 68.6, 68.9, 69.7, 71.3 (*ferrocenyl*); 81.7, 88.5, 95.4 (*propargyl*).

X-ray Structure Determination of 11. (Figure 8.) Single crystals, suitable for X-ray analysis, were obtained by recrystallization from dichloromethane/*n*-hexane. Crystal data, data collection, and refinement parameters of **11** are summarized in Table 1, and the general procedure was as described for **7**. For complete crystallographic data, tables of bond lengths, bond angles, anisotropic thermal parameters, calculated hydrogen atomic coordinates, final atomic coordinates, see supporting information.

Triferrocenylallenylium tetrafluoroborate (12). A round bottom flask was charged with 350 mg (0.576 mmol) of 1,1,3-triferrocenylprop-2-yn-1-ol (**11**) dissolved in 700 of mL dry Et_2O. Addition of 0.090 mL (0.66 mmol) of a 54% solution of fluoroboric acid in Et_2O precipitated the dark green product, which was filtered off, washed with two portions of Et_2O, and dried in vacuo, yielding 307 mg (0.453 mmol, 79%) of triferrocenylallenylium tetrafluoroborate (**12**). Similarly, using trifluoromethanesulfonic acid or a mixture of a solution of sodium tetraphenylborate, dissolved in glacial acid and trifluoromethanesulfonic acid, yielded triferrocenylallenylium trifluoromethanesulfonate and triferrocenylallenylium tetraphenylborate, respectively. Of these three products, only the tetrafluoroborate (**12**) is air-stable in the solid state and sufficiently stable in solution for a full characterization. Mp not observed, >300 °C. Anal. Calcd for $C_{33}H_{27}BF_4Fe_3$: C, 58.47; H, 4.01. Found: C, 57.00; H, 4.03. MS (FAB): *m/z* 591.01733 (M^+ of cation; exact mass calcd for $C_{33}H_{27}Fe_3$, 591.01609). UV–vis data (methanol; λ_{max}/log ϵ): 376/3.9, 445/4.1, 760/3.9 nm. IR data (KBr): 3104 w, 2151 s ($\nu_{C=C=C}$), 1630 w, 1468 s, 1438 m, 1412 m, 1385 m, 1250 w, 1084 vs, 1036 m, 834 m, 706 m, 477 m cm^{-1}. ^1H NMR ($CDCl_3$): δ 4.35 (5H, s, *unsubst. cp*), 4.46 (10H, s, *unsubst. cp*), 4.76 (2H, m, *subst. cp*), 4.84 (2H, m, *subst. cp*), 5.28 (4H, m, *subst. cp*), 5.77 (4H, m, *subst. cp*). ^{13}C NMR ($CDCl_3$): δ 62.9, 72.4, 74.1, 74.3, 75.2, 77.5, 84.5, 90.2, (*ferrocenyl*); 96.0, 118.2, 155.6 (*allenyl*).

Results and Discussion

Stabilization of Carbenium Ions by Ferrocenyl Substituents. The phenomenon of the extraordinary stabilization of the carbenium ion center in α-metallocenyl cations has been adressed with a wide range of physical methods, mainly in solution by NMR spectroscopy[1,9,30] and for a limited number of cases in the crystalline state by X-ray spectroscopy.[8e,12a,b,30b,f,31] Together with the results obtained from ^{57}Fe Mössbauer studies[9,32] and ^{57}Fe NMR spectroscopy[33] the minimum-energy structure of Hückel calculations[34] with a bent exocyclic fulvenoid structure has been confirmed, although the amount of bending toward the metal (the dihedral angle of the exocyclic fulvene double bond) is dependent on sterical and electronic factors of the other substituents (Scheme 1). Therefore, it is generally agreed that these cations have important resonance contributions from the η^6-fulvene-η^5-cyclopentadienyl iron(II) form, similar to the well-known benzylic resonance in organic arene chemistry but with additional π-bonding of the metal with the exocyclic (formal) double bond. The direct participation of the iron atom in charge delocalization causes the two cyclopentadienyl rings to deviate from being parallel (tilt angle 4–5°) and forces the exocyclic substituent, bearing the positive charge, out of the plane of the cyclopentadienyl ring in a bent position in the direction of the iron atom (dihedral angle 10–20°). The partial double-bond character of the bond between the exocyclic cationic center and the ring carbon leads to hindered rotation around this bond with the consequence of optical activity for unsymmetrically substituted cations.[11a–c]

Scheme 1. Mesomeric Forms of Ferrocenylcarbenium Ions

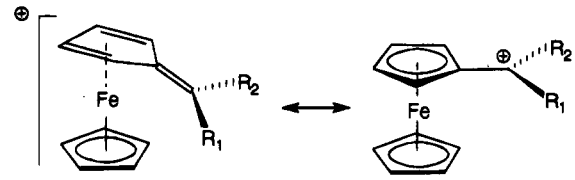

Synthesis. In general, the synthesis of α-metallocenyl carbocations starts from the corresponding carbinols (other but less useful methods have been reported).[1,9] Treatment of the α-metallocenyl alcohol with a strong acid affords the oxonium ion, which forms the carbenium ion by exoelimination of H_2O under anchimeric assistence by the metal. All the allylium and allenylium salts in this work were prepared according to this general synthetic route, starting from the respective alcohols as precursors, which were prepared as outlined in Schemes 2 and 3.

The synthesis of allylium salts (Scheme 2) is readily accomplished by nucleophilic addition of either hydride (in the form of triethylborohydride) or monolithioferrocene with ferrocenylated enone systems, best available by the chalcone reaction[18b] or, for polynuclear derivatives, by the Benary reaction.[18d] Reaction with *trans*-1,3-diferrocenylpropenone or cyclopentadienyl(3-ferrocenyl-1-oxy-pentalenyl)iron, respectively, yields the corresponding allylic alcohols (some of these are rather unstable toward oxidation by air; see Experimental Section); subsequent protonation affords the target allylium salts **1**, **3**, **5**, and **7**.

(30) (a) Braun, S.; Abram, T. S.; Watts, W. E. *J. Organomet. Chem.* **1975**, *97*, 429. (b) Lupan, S.; Kapon, M.; Cais, M.; Herbstein, F. H. *Angew. Chem.* **1972**, *84*, 1104; *Angew. Chem., Int. Ed. Engl.* **1972**, 1025. (c) Abram, T. S.; Watts, W. E. *J. Chem. Soc., Perkin Trans. 1* **1977**, 1522. (d) Abram, T. S.; Watts, W. E. *J. Chem. Soc., Perkin Trans. 1* **1977**, 1532. (e) Surya Prakash, G. K.; Buchholz, H.; Prakash Reddy, V.; de Meijere, A.; Olah, G. A. *J. Am. Chem. Soc.* **1992**, *114*, 1097. (f) Turpeinen, U.; Kreindlin, A. Z.; Petrovskii, P. V.; Rubinskaya, M. I. *J. Organomet. Chem.* **1992**, *441*, 109.

(31) (a) Sime, R. L.; Sime, R. J. *J. Am. Chem. Soc.* **1974**, *96*, 892. (b) Behrens, U. *J. Organomet. Chem.* **1979**, *182*, 89.

(32) (a) Neshvad, G.; Roberts, R. M. G.; Silver, J. *J. Organomet. Chem.* **1982**, *236*, 237. (b) Watanabe, M.; Iwamoto, T.; Nakashima, S.; Sakai, H.; Motoyama, I.; Sano, H. *J. Organomet. Chem.* **1993**, *448*, 167.

(33) Koridze, A. A.; Astakhova, N. M.; Petrovskii, P. V. *J. Organomet. Chem.* **1983**, *254*, 345.

(34) (a) Hoffmann, R.; Hofmann, P. *J. Am. Chem. Soc.* **1976**, *98*, 598. (b) Gleiter, R.; Seeger, R. *Helv. Chim. Acta* **1971**, *54*, 1217.

Scheme 2. Preparation of Compounds 1–7

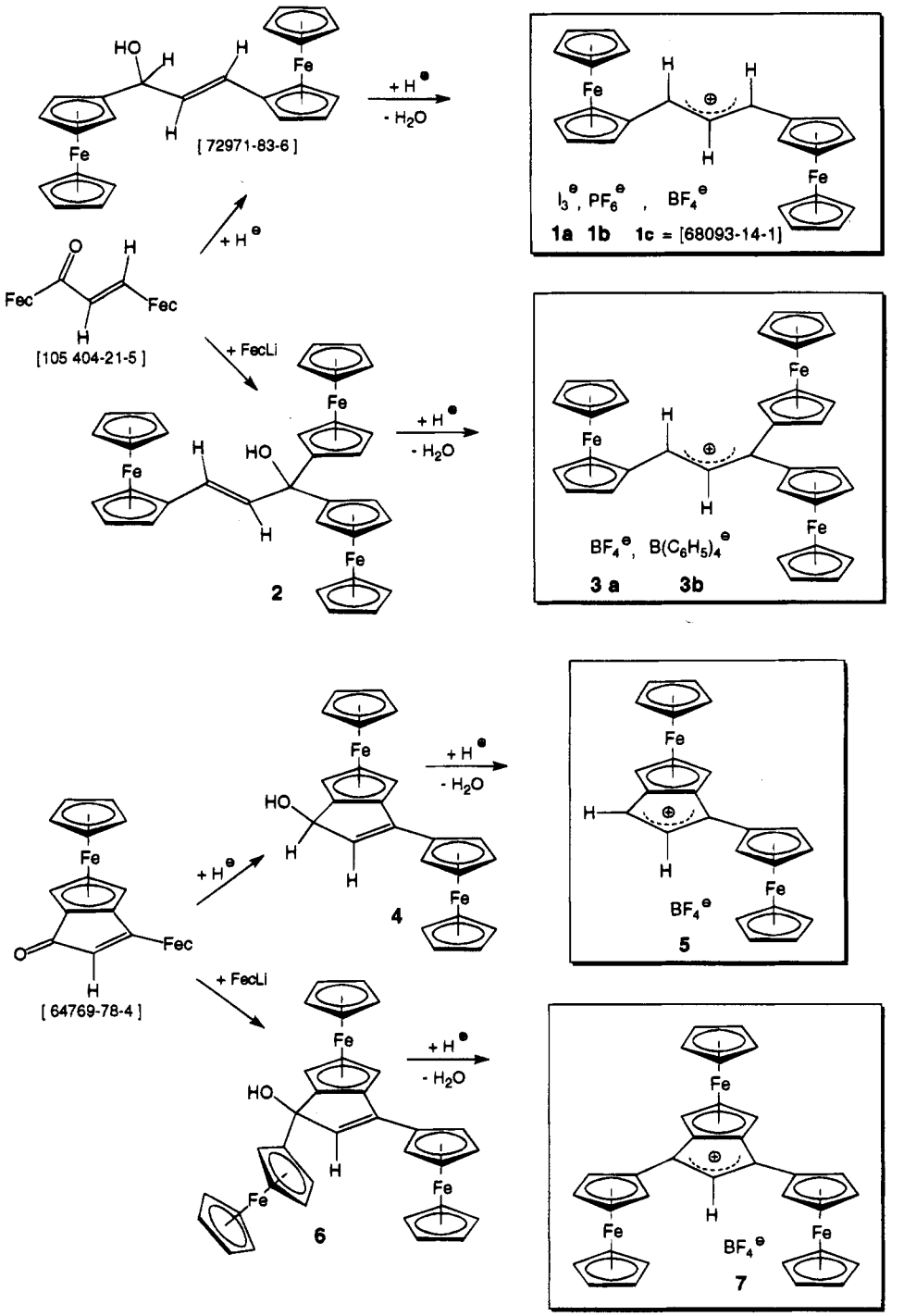

For allenylium salts, the necessary progenitors are the corresponding propargyl alcohols, which are generally prepared by nucleophilic addition of metalated acetylenes to the carbonyl functionality of an aldehyde or a ketone.[27] First we attempted the preparation of a 1,1-diferrocenylallenylium salt, although in light of the limited stability of **5** (see below) it is unlikely that such an allenylium ion, with only hydrogen as a substituent on one end of the allene moiety, is stable and can be isolated in pure form. To synthesize the precursor alcohol **9**, it proved necessary to react diferrocenyl ketone with a trimethylsilyl-protected acetylene, because simply using lithium acetylide or the corresponding TMEDA complex met with failure, obviously because (trimethylsilyl)acetylide is the better nucleophile due to the donor effect of the trimethylsilyl group. Protonation of **9** with fluoroboric acid produces a blue precipitate, probably ethinyldiferrocenylmethylium tetrafluoroborate, which decomposed rapidly, therefore no further characterization was possible. This is in accord with the reported solvolytic collapse of analogous ferrocenyl propargylic compounds.[30d,35] Unexpectedly, this propargyl cation is also formed by combining (**9**) with trimethylsilyl trifluoromethanesulfonate with subsequent spontaneous elimination of (trimethylsilyl)oxide, a reaction we attempted to protect the hydroxy group of **9**. The intermediate ethinyldiferrocenylmethylium reacts with triethylamine to give **10a** and, after anion-

(35) Abram, T. S.; Watts, W. E. *J. Organomet. Chem.* **1975**, *87*, C39.

Scheme 3. Preparation of Compounds 8–12

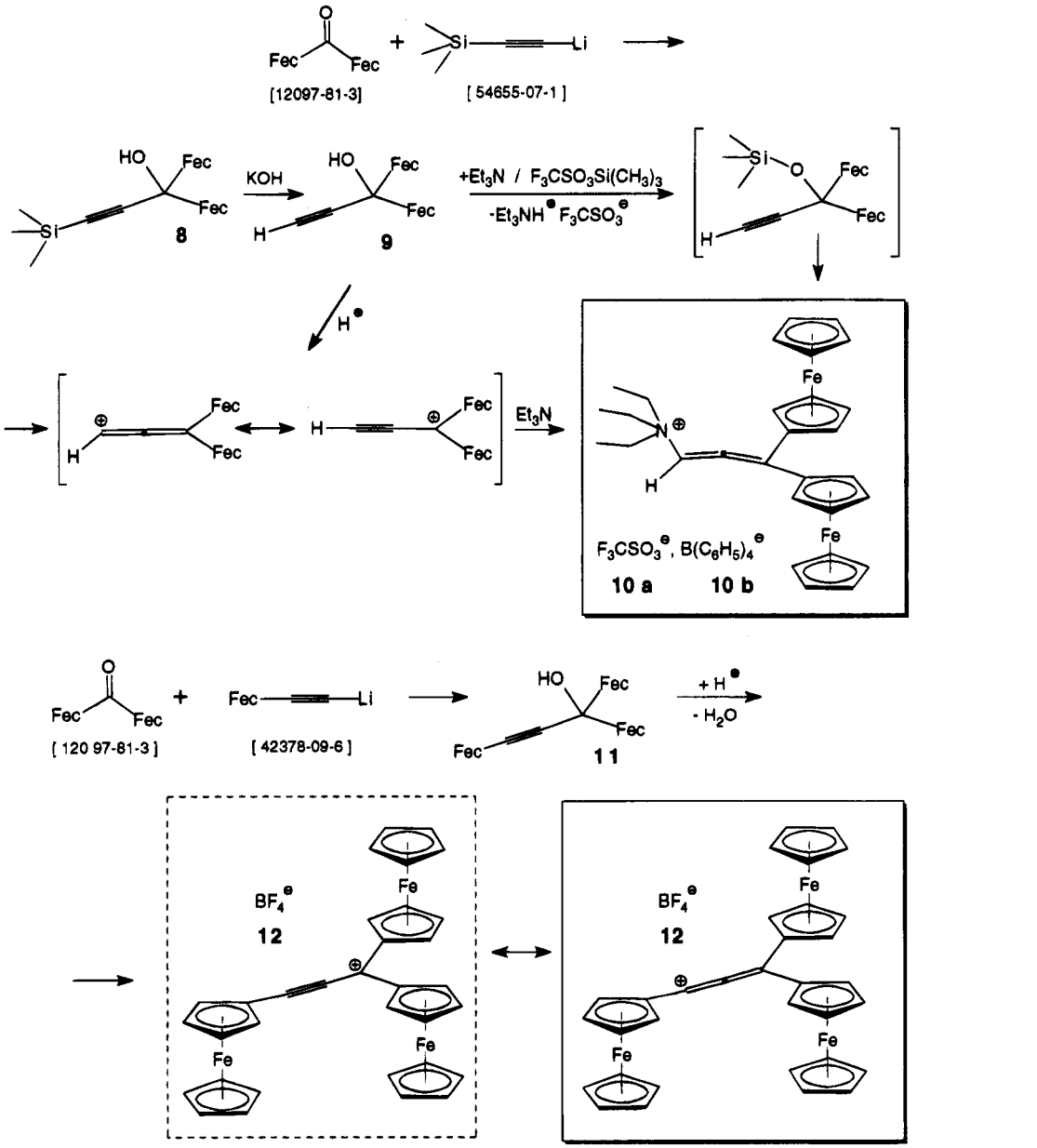

exchange with sodium tetraphenylborate, **10b**, formally Lewis base stabilized allenylium salts with unusual bent allene moietes in the solid state.

Introduction of three ferrocenyl substituents by the reaction sequence shown in Scheme 3 affords the maximally substituted compounds **11** and **12**; in this case, the combined stabilization by three ferrocenyl units allows the isolation of **12** as a true allenylium salt with only a minor resonance contribution from the ethinylmethylium form.

Stability. As expected, increasing the number of ferrocenyl substituents increases the stability of the allylium salts as is evidenced by comparing the physical properties of **1a–c** versus **3a,b** and **5** versus **7**. A prerequisite to stable allylium systems is further the 1,3-disubstitution of the allylium moiety with two ferrocenes, thereby affording charge delocalization by the metallocenes in α-position to the formally two possible locations of the positive charge. Cation **5**, which does not fulfill this criterion, although it incorporates an annelated ferrocene, is therefore the least stable allylium salt and decomposes gradually in solution within minutes, preventing complete spectral characterization. On the other hand, the comparison of **3a,b** with the more stable **7** (both of these cations have three ferrocenes) indicates that the annelated central ferrocene participates in cation stabilization of the 1- and 3-positions, whereas in **3a,b** one of these two positions can interact with only one ferrocene. Interestingly, the cyclic allylium compounds **5** and **7** can formally be envisaged as the first stable cyclopentadienyl cations, but the known instability and antiaromaticiy of the parent cyclopentadienyl cation[36] makes this formulation extremely unlikely.

Allenylium salts with fewer than three ferrocenes are unstable or have only fleeting existence as the mesomeric propargylic cations, which either decompose by solvolytic collapse[30d,35] or can be trapped with triethylamine under formation of ammonium allenes **10a,b**.

The effect of the counteranions on the stability of the

(36) (a) Breslow, R.; Hoffmann, J. M. *J. Am. Chem. Soc.* **1972**, *94*, 2110. (b) Breslow, R.; Mazur, S. *J. Am. Chem. Soc.* **1973**, *95*, 584. (c) Lossing, F. P.; Traeger, J. C. *J. Am. Chem. Soc.* **1975**, *97*, 1579. (d) Breslow, R.; Canary, J. W. *J. Am. Chem. Soc.* **1991**, *113*, 3950.

allylium and allenylium salts is less clear, the existence and relative stability of these salts depends obviously on specific cation–anion interactions which are, in relation to the counter-anion, different for each type of cation. For example, hexafluorophosphate **1b** has a shelf-life of at least 1 year at ambient temperature and does not decompose in solution (allowing, for example, UV–vis measurements), whereas the tetrafluoroborate **1c** survives only for a few hours in solution. In contrast, for allenylium salt **12** only the tetrafluoroborate is sufficiently stable (see Experimental Section).

The nature of the decomposition pathways of α-metallocenyl carbenium ions is still under investigation.[12a] Spin-trapping experiments[37] and the isolation of radical coupling decomposition products has been taken as evidence for the existence of a singlet–triplet equilibrium by an intramolecular redox tautomerism. Direct observation of the paramagnetic triplet species by NMR[38] or by Mössbauer[12a] spectroscopy showed for ferrocenyl carbenium ions a population of the triplet state of less than 1%, which allows characterization of these essentially diamagnetic ions by standard NMR spectroscopy.

The relative reactivity of ferrocenyl stabilized carbeniumions, including **(1c)**, with H_2O and other nucleophiles ("solvolytic collapse" and/or nucleophilic addition) has been studied in detail,[11c,18b,35,39,40] but, contrary to the findings of Watts and co-workers,[39] we observe a much slower decomposition in this regard in solution. One reason for this discrepancy could be the reported light sensitivity[41] of metallocenyl cations; the photometric concentration determinations in these kinetic experiments could be responsible for an accelerated decomposition by photochemical activation. The primary degradation pathways for the less congested allylium salts are dimerizations and electrophilic cyclizations;[9,22a,40,42] these processes are extremely accelerated by irradiation. In this respect, allylium salt **(7)** is of extraordinary stability; it survives for days in aqueous solution at pH 7 under irradiation by sunlight.

Spectroscopy and Structure of Allylium Salts. The high stability of these allylium and allenylium salts permits accurate mass detection of the cations by high-resolution positive FAB-MS (see Experimental Section) for all synthesized ionic compounds, including **1a** and **5**, which decompose in solution, thereby preventing further characterization by NMR or UV–vis spectroscopy. The increase in stability of allylium compounds **1–7** with progressive incorporation of ferrocenyl substituents is paralleled by a bathochromic shift of the λ_{max} absorption (Figure 1) in the UV–vis spectra, reflecting

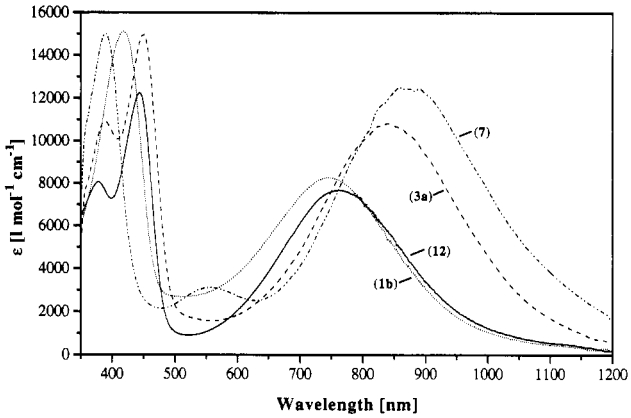

Figure 1. UV–vis–near-infrared spectra of allylium salts **1b**, **3a**, and **7** and of allenylium salt **12**.

Table 2. Allylium[a] ^1H and ^{13}C NMR Shifts (ppm)

	H_α	H_β	H_γ	C_α	C_β	C_γ
1b	8.30	6.48	8.30	157.7	126.0	157.7
1c	8.35	6.50	8.35	157.7	125.7	157.7
3a	8.66	6.67		154.1	128.5	180.5
3b	8.64	6.65		154.1	127.9	180.6
7		6.19		162.6	127.7	162.6

[a] Due to decomposition in solution no values for allylium salts **1a** and **5** were obtained. The labels α, β, and γ refer to the 1-, 2-, and 3-positions of the allylium moiety, respectively.

the increasing conjugation with increasing number of ferrocenyl substituents. Table 2 summarizes pertinent ^1H and ^{13}C NMR data for the allylium salts. The chemical shifts of the central allylic hydrogen (H_β) and carbon (C_β) are very similar and show almost no influence by the substitution pattern. The relative distribution of positive charge to the 1- and 3-positions in **3a,b** as an unsymmetrically substituted allylium system is reflected by two different ^{13}C chemical shifts of the C_α and C_γ carbons; the more deshielded signal (δ 180 ppm) is assigned to the carbon atom adjacent to two ferrocenyl groups, which direct the positive charge to their α-position. The least stable allylium salts **1b,c** in this series (with the exception of **5**, see above), with only one ferrocene on each terminal carbon, show chemical shifts for these carbons (δ 157.7 ppm) differing by only 5 ppm in comparison to the most stable ferrocene-annelated allylium salt **7** (δ 162.6 ppm). The observed higher stability of **7** versus **1a–c** might therefore be attributed to mainly sterical protection of the allylium moiety by the annelated ferrocene, ruling out any significant electronic contribution in terms of an antiaromatic cyclopentadienyl cationic sytem.[36]

Single-crystal X-ray analysis was performed in order to obtain further information on the structure and factors governing the stability of **7**. The structure of allylium salt **7** consists of two crystallographically independent molecules, **A** and **B**, with tetrafluoroborate as counteranions (Figure 2). These two molecules differ slightly in their conformation; selected bond lengths and angles are given in Table 3. The occurrence of these two conformationally similar but distinctly different molecules indicates that the structure is governed not only by intramolecular (electronic) factors, which are of prime interest for a deeper understanding of the mechanism of carbenium-ion stabilization by ferrocenes, but also and of equal rank by crystal forces. Both molecules have a planar pentalenyl subunit (Figure 3); the two

(37) Cais, M.; Ashkenazi, P.; Dani, S.; Gottlieb, J. *J. Organomet. Chem.* **1977**, *124*, 49.
(38) Edin, E. I.; Blumenfeld, A. L.; Petrovskii, P. V.; Kreindlin, A. Z.; Fadeev, S. S.; Rybinskaya, M. I. *J. Organomet. Chem.* **1985**, *292*, 257.
(39) Bunton, C. A.; Carrasco, N.; Davoudzadeh, F.; Watts, W. E. *J. Chem. Soc., Perkin Trans. 2* **1980**, 1520.
(40) (a) Perevalova, E. G.; Pushin, A. N.; Klimova, E. I.; Slovokhotov, Yu. L.; Struchkov, Yu. T. *Metalloorg. Khim.* **1989**, *2*, 1405. (b) Nesmeyanov, A. N.; Postnov, V. N.; Sazonova, V. A.; Galakhova, T. N.; Kuznetsov, A. A. *Izv. Akad. Nauk SSSR, Ser. Khim.* **1978**, *9*, 2172. (c) Boev, V. I.; Dombrovskii, A. V. *Zh. Obshch. Khim.* **1987**, *57*, 938.
(41) (a) Kerber, R. C.; Ehntholdt, D. J. *Synthesis* **1970**, 449 and references cited therein. (b) Miyazaki, H. *Chem. Abstr.* **1987**, *106*, JP Patent 61151544 A2, 41609f; July 10, 1986.
(42) Postnov, V. N.; Klimova, E. I.; Garzia, M. M.; Meleshonkova, N. N.; Rybakov, V. V.; Aslanov, L. A. *J. Organomet. Chem.* **1994**, *476*, 189.

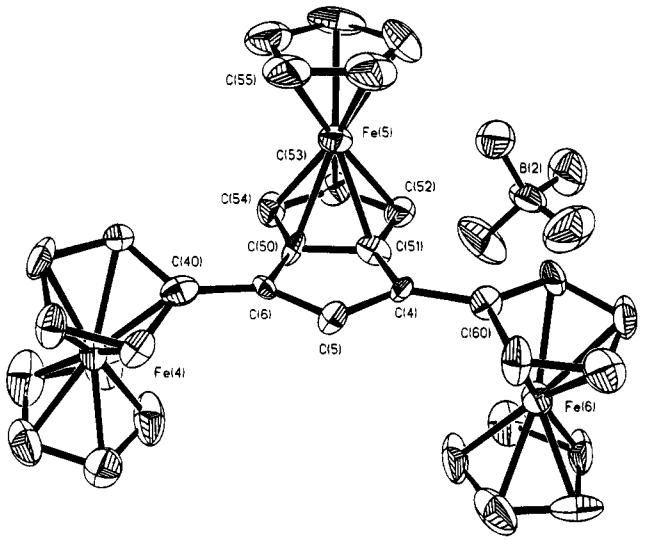

Figure 2. Molecular structure of **7**, molecule **B**, showing the atom-numbering scheme. Hydrogen atoms are omitted for clarity.

Table 3. Selected Bond Lengths (pm) and Angles (deg) for 7

	molecule **A**	molecule **B**
Bond Lengths		
C(1)–C(2)/C(4)–C(5)	138.9(13)	140.7(13)
C(2)–C(3)/C(5)–C(6)	142.8(13)	140.4(13)
C(1)–C(10)/C(4)–C(60)	141.2(13)	145.7(14)
C(3)–C(30)/C(6)–C(40)	145.6(14)	145.6(14)
C(1)–C(20)/C(4)–C(51)	146.4(13)	144.9(14)
C(3)–C(21)/C(6)–C(50)	145.8(13)	145.3(14)
C(20)–C(21)/C(50)–C(51)	144.1(13)	138.9(14)
Fe(1)–C(1)/Fe(6)–C(4)	303.8(10)	295.3(10)
Fe(3)–C(3)/Fe(4)–C(6)	283.1(11)	311.4(10)
Bond Angles		
C(1)–C(2)–C(3)/C(4)–C(5)–C(6)	110.1(0.9)	108.5(0.9)
C(10)–C(1)–C(2)/C(60)–C(4)–C(5)	127.3(0.10)	125.0(0.11)
C(30)–C(3)–C(2)/C(40)–C(6)–C(5)	124.9(0.10)	126.1(0.10)
twist angle C(1)–C(10)/C(4)–C(60)[a]	13.43(0.53)	9.68(0.58)
twist angle C(3)–C(30)/C(6)–C(40)[a]	18.19(0.51)	21.89(0.51)
dihedral angle C(1)–C(10)/ C(4)–C(60)[b]	4.8(0.8)	9.8(0.8)
dihedral angle C(3)–C(30)/ C(6)–C(40)[b]	15.7(0.9)	0.08(0.7)
tilt angle ferrocene[Fe(1)]/ ferrocene[Fe(6)][c]	3.9	2.85
tilt angle ferrocene[Fe(3)]/ ferrocene[Fe(4)][c]	4.88	3.45

[a] Twist angle, the angle between cyclopentadienyl and pentalenyl planes. [b] Dihedral angle, the bending of the exocyclic ferrocenyl toward allylium. [c] Tilt angle, the deviation of cyclopentadienyl planes from parallelism [angle (centroid of $Cp_{subst.}$) – (Fe)–(centroid of $Cp_{unsubst.}$)].

ferrocenyl substituents in 1- and 3-positions of the allylium moiety are twisted with values ranging from 9.7 to 21.9° (Table 3). The cyclopentadienyl rings of these ferrocenes are planar (max deviation 2.27 ± 1.23°), but not parallel, the corresponding ferrocene tilt angles (2.8–4.9°) are similar to reported values for other α-carbenium ferrocenes.[8c,30b,31] The bending of the ferrocenyl substituents toward the cationic allyl system, indicating a (weak) interaction of the iron atom with the α-C^+ is seen in the distances (Fe)–(α-C^+) and in the dihedral angles of the (α-C^+)–(ferrocene) bonds (Table 3; Figures 3 and 4). For symmetrically substituted allylic cations, the two terminal allylic positions are

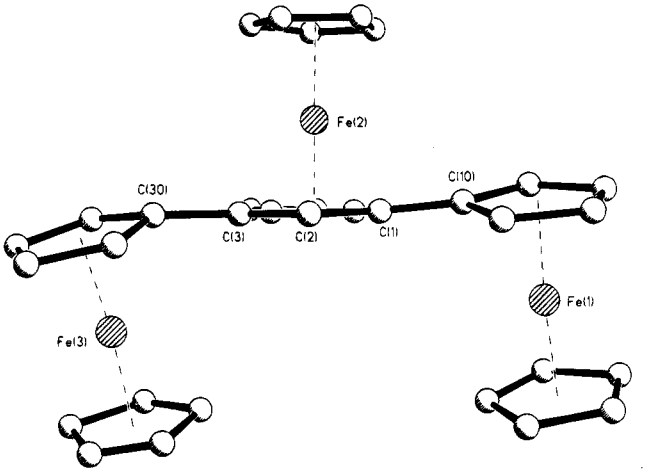

Figure 3. Molecular structure of **7**, molecule **A**, projecting into the pentalene plane.

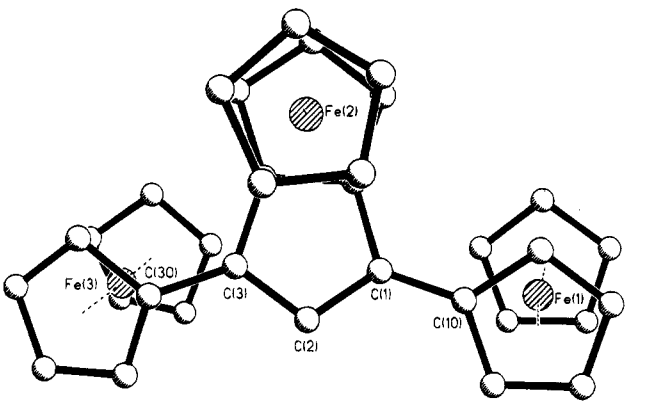

Figure 4. Molecular structure of **7**, molecule **A**, projecting perpendicular to the pentalene plane.

equal in terms of charge density and carry statistically only 50% of one positive charge, therefore one might expect an equal, but in comparison to simple carbenium ions (for example: diphenylferrocenylmethylium tetrafluoroborate[31b]), reduced bending of the two ferrocenyl substituents. In contrast to this expectation the two ferrocenyl substituents in both molecules **A** and **B** show unequal bending with values ranging from 0.08 to 15.7° and with corresponding (Fe)–(α-C^+) distances from 283.1 to 311.4 pm. Similar unequal bending has been observed in the crystal structure of diferrocenylmethylium tetrafluoroborate.[30b] The annelated ferrocene of the pentalene subunit is for both molecules a "normal" ferrocene, no significant deviations are observed, which is in accord with only steric, but not electronic, stabilization of the allylium moiety by this ferrocene. In summary, the expected distortions from the idealized ferrocene conformation are in both molecules observed for the ferrocenyl substituents in 1- and 3-positions of the allylic cation, albeit in varying degree, which is an indication of substantial contributions to the conformation by solid state packing effects.

Spectroscopy and Structure of Allenylium Salts. As described above, 1,1-diferrocenylallen-3-ylium tetrafluoroborate or the mesomeric ethinyldiferrocenylmethylium tetrafluoroborate (1,1-diferrocenylpropargylium tetrafluoroborate) is unstable or cannot be isolated in pure form, respectively (Scheme 3). However, the

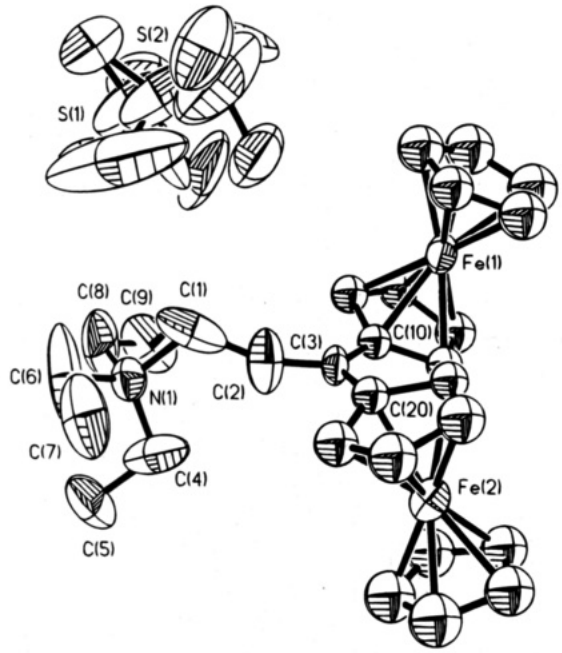

Figure 5. Molecular structure of **10a**, showing the atom-numbering scheme. Hydrogen atoms are omitted for clarity. The atom-numbering of the disordered trifluoromethanesulfonate is shown in Figure 6. Cyclopentadienyl carbons of ferrocene 1 are C(10)−C(19) and for ferrocene 2 C(20)−C(29), respectively.

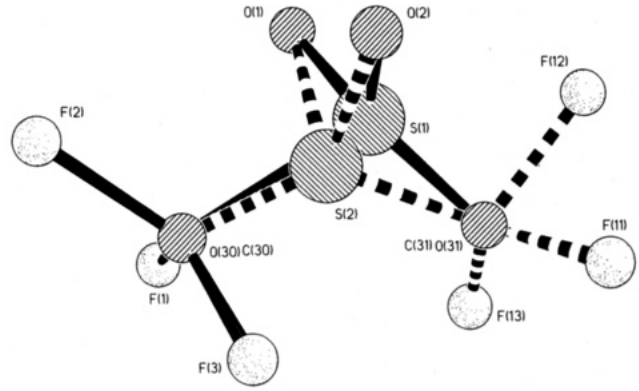

Figure 6. Atom-labeling for the disordered trifluoromethanesulfonate of **10a**.

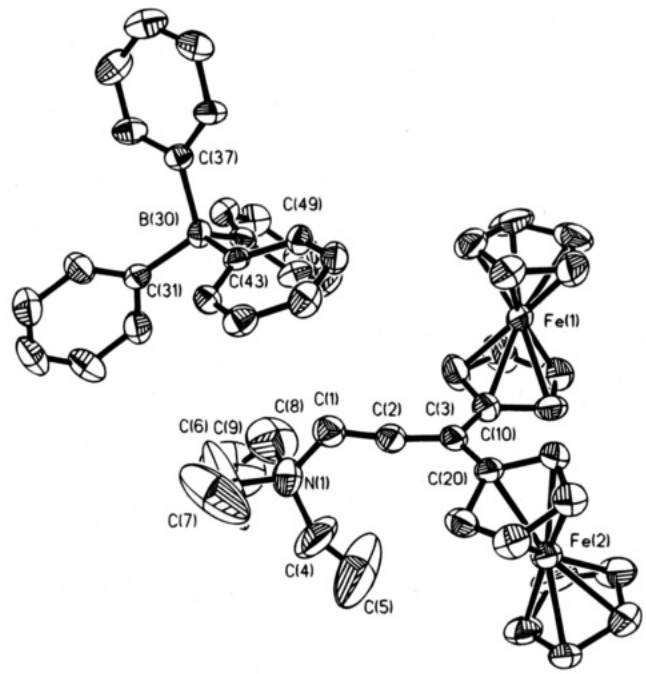

Figure 7. Molecular structure of **10b**, showing the atom-numbering scheme. Hydrogen atoms are omitted for clarity. Cyclopentadienyl carbons of ferrocene 1 are C(10)−C(19), and for ferrocene 2 C(20)−C(29), respectively. Phenyl carbons of tetraphenylborate are C(31)−C(36), C(37)−C(42), C(43)−C(48), and C(49)−C(54), respectively.

Lewis acid−base complexes **10a,b** with triethylamine as the Lewis base can be envisaged as donor-stabilized allenylium salts. The high-resolution positive FAB mass spectra show the molecular ion of the triethylammonium allene cation in low intensity (approximately 5%) and, in accord with the formulation of **10a,b** as adducts of triethylamine with 1,1-diferrocenylallen-3-ylium, the corresponding peak of 1,1-diferrocenylallen-3-ylium as the most intense signals. The UV−vis spectra of the orange-colored **10a,b**, on the other hand, are typical for regular allenic chromophores (see Experimental Section), and are therefore not included in Figure 1. Also, the value and intensity of the $\nu_{C=C=C}$ vibrations (1937 cm^{-1} for **10a** and 1939 cm^{-1} for **10b** with medium intensity; expected range for $\nu_{C=C=C}$: 1950−1930 cm^{-1}) are indicative of a normal allene functionality. The ^{13}C NMR data (δ_{allene} 106.6, 123.5, 195.2 ppm for **10a** and 105.5, 122.4, 195.5 ppm for **10b**) are also in agreement with the formulation of these compounds as unexceptional allenes, whereas the ^1H NMR chemical shifts of the allenic hydrogen ($\delta_{C=C=C-H}$ 6.12 ppm for **10a** and 5.52 ppm for **10b**) are quite different for these two analogous salts with supposedly identical cations.

To clarify this discrepancy, single-crystal analyses were performed for **10a** and **10b** (Table 1). Figure 5 shows the molecular structure of **10a**, and Figure 6 shows the positional disorder of the trifluoromethanesulfonate. Although the residuals for this structure analysis are relatively high due to a non-optimal data to parameter ratio, the structure of the cationic part, which is of main interest in this context, is sufficiently defined because the inaccurancy is chiefly restricted to the trifluoromethanesulfonate, as can be seen by the large thermal ellipsoids of the anion in Figure 5. The bond lengths of the allene moiety [C(1)−C(2) = 143(3) pm, C(2)−C(3) = 127(2) pm] show a deceptively large value for the C(1)−C(2) bond (expected value for C=C=C: 131 pm), which might indicate a (not resolved) disorder of the C(1) atom, in agreement with the relatively high value of 150(2) pm (expected value for $C(sp^2-Nsp^3)$: 142 pm) for the C(1)−N(1) bond. Despite these limitations, the most interesting structural feature is the unexpected angle C(1)−C(2)−C(3) of 161(2)° for the allenic unit. Even taking into consideration the aforementioned likely positional disorder of the C(1) atom, this surprising result is significant in terms of a qualitatively real nonlinearity. An analogous structure is shown by compound **10b** (Figure 7). In this case, no disordering was observed and the low residuals and the good data set (Table 1) allow a much more accurate description of the structure of the cationic part. In comparison to **10a**, the ethyl groups of the ammonium subunit are arranged in a less folded fashion, which is

simply a consequence of the different space-filling requirements due to the larger anion with corresponding increased anion–cation distances in **10b**. The relevant bond lengths [C(1)–C(2) = 130.4(8) pm, C(2)–C(3) = 131.9(8) pm] and C(1)–N(1) = 149.6(7) are in good agreement with the expected values for allenic bonds, and the C(1)–N(1) bond length is very similar to the corresponding value in the structure of trifluoromethanesulfonate **10a**. The C(1)–C(2)–C(3) angle of the allenic linkage is 173.1(6)°, which confirms the nonlinear allenic unit, albeit to a lesser degree in comparison to **10a** (the possible reason for the value being too high in the structure of **10a** has been discussed above). In summary, these two structures show an unexpected bent allene moiety in the solid state for both ammonium allene compounds which is probably not attributable to packing effects. In solution, the difference of the ^{1}H NMR chemical shift of the allenic hydrogen with a deshielded signal in **10a** in comparison to **10b** arises most likely by an increase in the Coulomb attraction between anion and cation in **10a** due to the smaller anion–cation distance. The only electronic explanation for the bending of the allene unit we can offer at this point is a nonclassical distortion of the cumulenic system by (formal) interaction of a singlet 1,1-diferrocenylcarbene (the singlet carbene should be stabilized by the combined donor ability of the two ferrocenes) with a triethylammonium vinylidene; experimental and theoretical results for related systems have been published.[43]

So far all published attempts to isolate an allenylium compound met with failure,[44] but strong evidence for relatively important contributions of the allenylic resonance form to the total ion structure (compare the two mesomeric forms of **12** in Scheme 3) has been obtained from ^{13}C NMR measurements of triply substituted propargylic alcohols in acidic solution at low temperatures[44a–f] and from theoretical calculations.[44h] The reported instability of 1,3-diferrocenylallenylium trifluoroacetate,[30d] a cation with two ferrocenyl substituents at the terminal allenic carbons, shows for allenylium salts the need for additional stabilizing metallocenyl substituents (contrary to the allylic systems, where this 2-fold substitution effects sufficient stabilization). Consequently, the triply substituted propargylic alcohol (**11**) was prepared. In addition to the usual characterization by spectroscopic methods a single-crystal structure analysis was performed (Table 1; Figure 8). The bond lengths and angles of the propargylic unit [C(31)–C(32) = 146.9(13) pm, C(32)–C(33) = 118.0(13) pm; C(31)–C(32)–C(33) = 174.8(10)°, C(32)–C(33)–C(21) = 178.2(10)°] show the expected linear conformation with small deviations from linearity due to packing effects. From this progenitor, the green stable salt **12** precipitates upon treatment with HBF_4. The high-resolution positive FAB mass spectrum gives

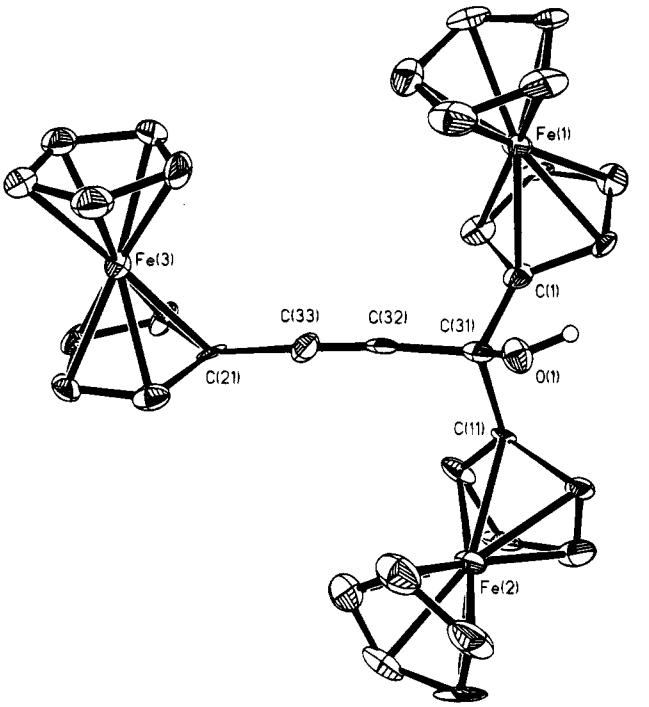

Figure 8. Molecular structure of **11**, showing the atom-numbering scheme. Hydrogen atoms are omitted for clarity, except for the hydroxyl hydrogen. Cyclopentadienyl carbons of ferrocene 1 are C(1)–C(10), for ferrocene 2 C(11)–C(20), and for ferrocene 3 C(21)–C(30), respectively.

the molecular ion of the cation (m/z 591.01733), in excellent agreement with the calculated exact mass (calcd for $C_{33}H_{27}Fe_3$: 591.01609). The UV–vis spectrum of **12** (Figure 1) is very similar to the spectrum of **1b**, indicating charge delocalization not only by the ferrocene chromophors but also, and more importantly by conjugation of the ethinyl group with the electron deficient carbocation. IR spectroscopy shows a very intense cumulenic absorption (Figure 9) at 2151 cm^{-1}, and the high intensity points to an acceptor-substituted unsymmetric allene, which strongly supports the allenium form as the predominant resonance structure (Scheme 3). This is further corroborated by the marked ^{13}C NMR deshieldings of the terminal carbons of the allenium ↔ propargylium moiety in **12** [$\delta(C_\alpha)$ 155.6 ppm, $\delta(C_\beta)$ 96,0 ppm, $\delta(C_\gamma)$ 118.2 ppm] in comparison to the corresponding signals of the precursor alcohol **11** [$\delta(C_\alpha)$ 81.7 ppm, $\delta(C_\beta)$ 95.4 ppm, $\delta(C_\gamma)$ 88.5 ppm]; similar arguments have been reported for the analogous triphenylallenium ion, obtained from the corresponding alcohol upon dissolution in superacidic medium at −60 °C.[44c] Although so far no suitable single crystals for X-ray structure analysis could be obtained, from the combined spectroscopic results we conclude that **12** comes as close as possible to a true allenylium salt with unprecedented stability.

Summary. The stability of allylium and allenylium cations can be increased by multiple incorporation of ferrocenyl substituents, allowing for the first time the isolation in pure form solid and air-stable representatives of these elusive species. Their structures in solution and in the solid state, investigated by NMR, IR, UV–vis, and single-crystal X-ray analysis, indicate ferrocene to be one of the most efficient stabilizing donors for electron deficient conjugated carbocations.

(43) Trinquier, G.; Malrieu, J.-P. *J. Am. Chem. Soc.* **1987**, *109*, 5303.
(44) (a) Richey, H. G., Jr.; Philips, J. C.; Rennick, L. E. *J. Am. Chem. Soc.* **1965**, *87*, 1381. (b) Pittmann, C. U., Jr.; Olah, G. A. *J. Am. Chem. Soc.* **1965**, *87*, 5632. (c) Olah, G. A.; Spear, R. J.; Westermann, P. W.; Denis, J.-M. *J. Am. Chem. Soc.* **1974**, *96*, 5855. (d) Olah, G. A.; Berrier, A. L.; Field, L. D.; Surya Prakash, G. K. *J. Am. Chem. Soc.* **1982**, *104*, 1349. (e) Olah, G. A.; Krishnamurti, R.; Surya Prakash, G. K. *J. Org. Chem.* **1990**, *55*, 6061. (f) Olah, G. A.; Prakash Reddy, V.; Surya Prakash, G. K. *Chem. Rev.* **1992**, *92*, 69. (g) Maas, G.; Rahm, R.; Mayer, D.; Baumann, W. *Organometallics* **1995**, *14*, 1061. (h) Hopkinson, A. C.; Lien, M. H. *J. Am. Chem. Soc.* **1986**, *108*, 2843.

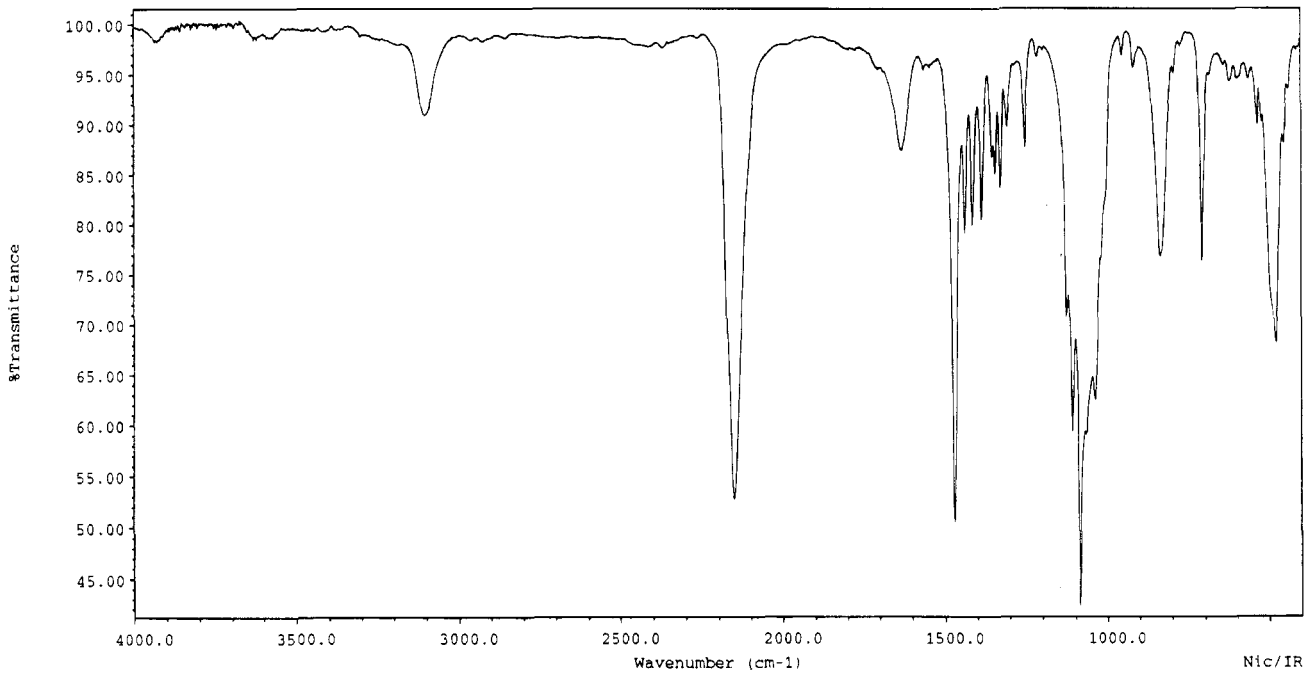

Figure 9. IR spectrum of allenylium tetrafluoroborate **12**.

Future work will focus on the electrochemistry and intervalence transfer of these model compounds for molecular electronics and on preparative chemistry, including the synthetic use of these electrophilic synthons and the chemical generation of neutral allylic radical or carbenoid species from the corresponding allylium salts. Results from Mössbauer measurements, which should give further insight into the role of the metallocenyl substituents as cation-stabilizing moieties and into the intramolecular electronic interaction among the conjugatively bridged ferrocenyl groups, will be reported in due course.

Acknowledgment. This work was supported by the European HCM project "Electron and Energy Transfer in Model Systems and their Implications for Molecular Electronics" (Grant No. CHRX-CT94-0538).

Supporting Information Available: Tables of crystal data and structure refinement details, anisotropic thermal parameters, fractional atomic coordinates and isotropic thermal parameters for the non-hydrogen atoms, all bond lengths and angles, and fractional atomic coordinates for the hydrogen atoms for **7**, **10a**,**b** and **11** (39 pages). Ordering information is given on any current masthead page. The authors have deposited atomic coordinates for structures **7**, **10a**,**b**, and **11** with the Cambridge Crystallographic Data Centre. The coordinates can be obtained, on request, from the Director, Cambridge Crystallographic Data Centre, Lensfield Road, Cambridge, CB2 1EW, U.K.

OM950579N

Water-Induced Isomerization of CpW(NO)(*o*-tolyl)$_2$ to CpW(O)(N-*o*-tolyl)(*o*-tolyl) and Related Chemistry†

Peter Legzdins,* Steven J. Rettig,‡ and Kevin J. Ross

Department of Chemistry, The University of British Columbia, Vancouver, British Columbia, Canada V6T 1Z1

Raymond J. Batchelor and Frederick W. B. Einstein§

Department of Chemistry, Simon Fraser University, Burnaby, British Columbia, Canada V5A 1S6

Received August 7, 1995⊗

Treatment of a THF solution of CpW(NO)(*o*-tolyl)$_2$ (**1**) with H_2O affords a structural isomer of **1**, namely CpW(O)(N-*o*-tolyl)(*o*-tolyl) (**2**), in 30% isolated yield as well as the expected product, CpW(O)$_2$(*o*-tolyl) (**3**), in low isolated yield (10%). Complexes **2** and **3** are formed in a ratio of approximately 1:1 upon treatment of a C_6D_6 solution of **1** with D_2O. Similar treatment of **1** with $^{18}OH_2$ results in the production of unlabeled complex **2**, thereby establishing the intramolecular nature of the water-catalyzed isomerization of **1** to **2**. The characteristic reactivity of CpW(NO)(*o*-tolyl)$_2$ toward various classes of reagents has been investigated to determine if the conversion of **1** to **2** can be effected with reagents other than water. In general, this reactivity has been found to be similar to that exhibited by other Cp′W(NO)R$_2$ (Cp′ = Cp or Cp*; R = alkyl or aryl) complexes, and treatment of **1** with reagents other than water does not result in isomerization of the organometallic reactant. The isomerization is also dependent upon the nature of the Cp ligand, the metal, and the aryl groups as evidenced by the fact that treatment of the related diaryl complexes, CpW(NO)(*p*-tolyl)$_2$, CpW(NO)Ph$_2$, CpMo(NO)(*o*-tolyl)$_2$, and Cp*W(NO)(*o*-tolyl)$_2$, with water does not result in the production of their arylimido oxo structural isomers. Consequently, the water-induced isomerization of **1** to **2** remains a unique chemical process. Crystals of CpW(NO)(*o*-tolyl)$_2$ (**1**) and CpW(O)(N-*o*-tolyl)(*o*-tolyl) (**2**) have been subjected to X-ray crystallographic analyses.

Introduction

Cleavage of the N–O bond in metal-bound nitric oxide is both of fundamental significance in inorganic chemistry and of relevance to biological and environmental chemistry.[1] We have recently encountered such nitrosyl N–O bond cleavage under a variety of mild conditions while investigating the characteristic chemistry of 16-valence-electron complexes which contain Cp′M(NO) (Cp′ = η^5-C_5H_5 (Cp) or η^5-C_5Me_5 (Cp*); M = Mo or W) fragments.[2] The first, and still the most intriguing, example of nitrosyl N–O bond cleavage observed in our laboratories involves the novel isomerization that occurs as part of the overall conversion depicted in eq 1.[3] This isomerization of the 16-valence-electron diaryl nitrosyl compound (**1**) to a thermodynamically more stable 18-valence-electron arylimido oxo complex (**2**) is intriguing since it could conceivably proceed via intramolecular nitrosyl-ligand N–O bond cleavage. Consequently, we decided to investigate transformation 1 and related

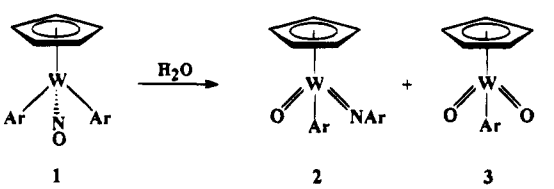

1 **2** **3** (1)

Ar = *o*-tolyl

chemistry in some detail. Presented in this paper are the results of our attempts to delineate the scope of this conversion as well as our investigations into the nature of the chemical entities capable of inducing this isomerization. Finally, we also compare the reactivity of CpW(NO)(*o*-tolyl)$_2$ with various classes of reagents to the reaction chemistry exhibited by related diaryl and dialkyl complexes.

Experimental Section

General Procedures Routinely Employed in the Legzdins Laboratories. All reactions and subsequent manipulations were performed under anaerobic and anhydrous conditions under an atmosphere of prepurified dinitrogen or argon unless otherwise specified. Purification of inert gases was achieved by passing them first through a column containing MnO and then a column of activated 4 Å molecular sieves. Conventional glovebox and vacuum line Schlenk techniques were utilized throughout.[4] The gloveboxes used during this work were two Vacuum Atmospheres Models HE-43-2 and HE-

†Dedicated to Prof. Dr. Max Herberhold on the occasion of his 60th birthday.

‡ Author to whom correspondence regarding the crystallography for complex **2** should be addressed.

§ Author to whom correspondence regarding the crystallography for complex **1** should be addressed.

⊗ Abstract published in *Advance ACS Abstracts,* November 1, 1995.

(1) (a) Sadler, P. J. *Adv. Inorg. Chem.* **1991**, *36*, 1. (b) Kummer, J. T. *J. Phys. Chem.* **1986**, *90*, 4747.

(2) Legzdins, P.; Young, M. A. *Comments Inorg. Chem.* **1995**, *17*, 239 and references cited therein.

(3) Legzdins, P.; Rettig, S. J.; Ross, K. J.; Veltheer, J. E. *J. Am. Chem. Soc.* **1991**, *113*, 4361.

0276-7333/95/2314-5579$09.00/0

493 and an Innovative Technologies Labmaster 130 two-station glovebox equipped with a cold well, freezer, and rotary evaporator. Some reactions were performed in a bomb, here defined as a thick-walled glass vessel with a Kontes greaseless Teflon stopcock and a side-arm for vacuum-line attachment. Filtrations were performed through columns supported on a medium-porosity glass frit. The column supports, which had been oven-dried and cooled in vacuo, included Celite 545 diatomaceous earth (Fisher), Florisil (Fisher, 60–100 mesh), or alumina (Fisher, neutral, activity I).

Solvents were either distilled from appropriate drying agents and purged with dinitrogen or argon for 15 min prior to use or were directly vacuum transferred from the drying agent.[5] CH_2Cl_2 was doubly distilled from P_2O_5. Et_2O was distilled from CaH_2 and sodium/benzophenone. Hexanes were distilled from CaH_2 and sodium/benzophenone/tetraglyme. Pentane was distilled from sodium/benzophenone/tetraglyme. THF was vacuum transferred from sodium/benzophenone. CH_3CN was vacuum transferred from CaH_2. $CDCl_3$ was dried over P_2O_5 and filtered through a short column of alumina (Woelm neutral, activity 1). Other deuterated solvents were dried over activated 4 Å molecular sieves, thrice freeze–pump–thaw degassed, and filtered through Celite.

All IR samples were run as solutions in NaCl cells or as Nujol mulls between NaCl plates. IR spectra were recorded on an ATI Mattson Genesis Series FTIR spectrometer, interfaced to a 486DX-33 PC using WinFIRST software. NMR spectra were obtained on either a Bruker AC-200 or Varian Associates XL-300 spectrometer. ^1H and $^{13}C\{^1H\}$ NMR spectra are referenced to the residual proton or natural abundance carbon signal(s) of the solvent employed. $^{31}P\{^1H\}$ NMR spectra are referenced to external $P(OMe)_3$ set as 141 ppm downfield from 85% aqueous H_3PO_4. Mrs. M. T. Austria, Ms. L. K. Darge, and Dr. S. O. Chan assisted in obtaining the NMR data. Low-resolution mass spectra (EI, 70 eV) were recorded on a Kratos MS50 spectrometer using the direct-insertion method. Fast-atom bombardment (6 kV ion source, 7–8 kV xenon FAB gun) mass spectra were recorded on an AEI MS9 spectrometer using 3-nitrobenzyl alcohol as matrix. All mass spectra were recorded by Dr. G. K. Eigendorf and the staff of the mass spectroscopy laboratory. Elemental analyses were performed by Mr. P. Borda of the UBC Department of Chemistry.

Procedures Specific to This Work. The organometallic reagents, $Cp'M(NO)Cl_2$ (M = Mo or W), were prepared by established procedures.[6] $Cp'Mo(NO)Cl_2$ complexes were further purified by Soxhlet extraction with CH_2Cl_2, and the $Cp'W(NO)Cl_2$ complexes were stored at −30 °C and used within a few months of preparation. *tert*-Butylamine (Aldrich) and isopropyl alcohol (BDH) were subjected to two freeze–pump–thaw cycles and dried over CaH_2. *p*-Tolyl isocyanate was vacuum transferred from P_2O_5. All $(aryl)_2Mg{\cdot}x(dioxane)$ complexes were prepared by a modification[7] of the standard methodology,[8] and the complexes $Cp^*W(NO)Ph_2$ and $Cp^*W(NO)(p\text{-tolyl})_2$ were prepared by established procedures.[7] D_2O (MSD, 99.8% D), $^{18}OH_2$ (Aldrich, 97% ^{18}O), elemental sulfur (Fisher), and CO (Matheson CP grade) were used as received.

Preparation of CpW(NO)(*o*-tolyl)$_2$ (1). THF (10 mL) was vacuum transferred onto a mixture of $CpW(NO)Cl_2$ (350 mg, 1.00 mmol) and $(o\text{-tolyl})_2Mg{\cdot}x(dioxane)$ (2.00 mmol of *o*-tolyl) at −196 °C. The reaction mixture was stirred while being slowly warmed to 0 °C until there was no noticeable starting material remaining in the flask (approximately 10 min). The final purple solution was taken to dryness in vacuo, and Et_2O (100 mL) was vacuum transferred onto the remaining purple residue. This purple solution was filtered quickly through Florisil (3 × 3 cm). The volume of the purple filtrate was reduced in vacuo, and the resulting solution was placed in a freezer (−30 °C) overnight. Purple needles of the desired complex (150 mg, 33% yield) were isolated by cannulating away the mother liquor.

Anal. Calcd for $C_{19}H_{19}NOW$: C, 49.48; H, 4.15; N, 3.04. Found: C, 49.19; H, 4.21; N, 3.05. IR (Nujol mull): ν_{NO} 1599 cm^{-1}. ^1H NMR (C_6D_6): δ 7.56–7.02 (m, 8H, Ar *H*), 6.11 (s, 5H, C_5H_5), 2.67 (s, 6H, 2 × *Me*). Low-resolution mass spectrum (probe temperature 120 °C): *m/z* 461 [P^+].

Isolation of CpW(O)(N-*o*-tolyl)(*o*-tolyl) (2). A solution of $CpW(NO)(o\text{-tolyl})_2$ (generated from 1.00 mmol $CpW(NO)Cl_2$) in THF was prepared as above. This solution was treated with excess H_2O (0.1 mL) at −70 °C. As the stirred reaction mixture was warmed to room temperature, its color changed from purple to brown. This mixture was taken to dryness in vacuo, and the residue was extracted with Et_2O (2 × 25 mL). The extracts were filtered through Florisil (3 × 5 cm). The resulting yellow filtrate was taken to dryness under reduced pressure, and the remaining residue was triturated with hexanes to obtain a yellow powder which was dissolved in Et_2O. Concentration and cooling of this solution to −30 °C led to the deposition of 138 mg (30% yield) of analytically pure **2**.

Anal. Calcd for $C_{19}H_{19}NOW$: C, 49.48; H, 4.15; N, 3.04. Found: C, 49.59; H, 4.30; N, 2.91. IR (Nujol mull): $\nu_{W=O}$ 897 (vs), also 1476 (s), 1379 (m), 1117 (m), 1022 (m), 1007 (m), 841 (m), 824 (s), 766 (s), and 750 (m) cm^{-1}. ^1H NMR (C_6D_6): δ 7.90 (dd, 1H, o-Ar *H*), 7.24–6.77 (m, 7H, Ar *H*), 5.72 (s, 5H, C_5H_5), 2.48 (s, 3H, *Me*), 2.32 (s, 3H, *Me*). Low-resolution mass spectrum (probe temperature 120 °C): *m/z* 461 [P^+].

Isolation of CpW(O)$_2$(*o*-tolyl) (3). Product **3** was obtained by elution with acetone of the Florisil column used during the isolation of **2** (vide supra). Solvent was evaporated from the acetone eluate to obtain a microcrystalline off-white solid which was crystallized from CH_2Cl_2/hexanes. Complex **3** was typically isolated in low yields (5–10% based on $CpW(NO)Cl_2$).

Anal. Calcd for $C_{12}H_{12}O_2W$: C, 38.73; H, 3.25. Found: C, 38.82; H, 3.30. IR (Nujol mull): 947 (m), 901 (m), 845 (w), 818 (w) cm^{-1}. ^1H NMR (CD_2Cl_2): δ 7.58 (dd (J_{HH} = 3.2 and 12.4 Hz), 1H, *o*-Ar *H*), 7.32 (m, 2H, Ar *H*), 7.19 (m, 1H, Ar *H*), 7.06 (m, 1H, Ar *H*), 6.52 (s, 5H, C_5H_5), 2.29 (s, 3H, *Me*). Low-resolution mass spectrum (probe temperature 120 °C): *m/z* 372 [P^+].

Reaction of CpW(NO)(*o*-tolyl)$_2$ with $^{18}OH_2$ or D_2O. Solutions of $CpW(NO)(o\text{-tolyl})_2$ (46 mg, 0.10 mmol) in C_6D_6 (0.7 mL) were treated with excess $^{18}OH_2$ or D_2O (0.05 mL). The solutions changed in color from purple to brown in a few seconds. The reaction mixtures were worked-up as described in the preceding paragraphs, and the resulting solids were characterized by mass spectrometry and ^1H NMR spectroscopy. In both cases, ^1H NMR spectroscopy indicated that two products had been formed in the approximate ratio of 1:1. These two products were identified as complexes **2** and **3** by comparisons to authentic samples. The mass spectrum of the solid isolated from the reaction with $^{18}OH_2$ exhibited a parent envelope at *m/z* 461 (probe temperature 120 °C).

Preparation of CpW(NO)(η^2-C{O}-*o*-tolyl)(*o*-tolyl) (4). A solution of $CpW(NO)(o\text{-tolyl})_2$ (generated from 1.00 mmol $CpW(NO)Cl_2$) in THF was prepared as described above. The stirred reaction mixture was treated with excess CO at room temperature, whereupon the solution changed from purple to yellow in a matter of seconds. This yellow solution was taken to dryness in vacuo, and the resulting yellow residue was triturated in CH_2Cl_2 (40 mL). The resulting mixture was filtered through Florisil (3 × 5 cm). Hexanes (30 mL) were added to the filtrate, the volume of the solution was reduced in vacuo, and the final solution was placed in a freezer (−30

(4) Shriver, D. F.; Drezdon, M. A. *The Manipulation of Air-Sensitive Compounds*, 2nd ed.; Wiley-Interscience: New York, 1986.
(5) Perrin, D. D.; Armarego, W. L. F.; Perrin, D. R. *Purification of Laboratory Chemicals*, 3rd ed.; Wiley-Interscience: New York, 1986.
(6) Dryden, N. H.; Legzdins, P.; Batchelor, R. J.; Einstein, F. W. B. *Organometallics* **1991**, *10*, 2077.
(7) Dryden, N. H.; Legzdins, P.; Rettig, S. J.; Veltheer, J. E. *Organometallics* **1992**, *11*, 2583.
(8) (a) Anderson, R. A.; Wilkinson, G. *J. Chem. Soc., Dalton Trans.* **1977**, 809. (b) Anderson, R. A.; Wilkinson, G. *Inorg. Synth.* **1979**, *19*, 262.

°C) overnight. Yellow-orange crystals of the desired complex (250 mg, 51% yield) were then isolated by removing the supernatant solution by cannulation and drying the crystals in vacuo.

Anal. Calcd for $C_{20}H_{19}NO_2W$: C, 49.10; H, 3.91; N, 2.86. Found: C, 49.18; H, 3.89; N, 2.80. IR (Nujol mull): 1584 (s), 1532 (s), 1219 (m), 925 (m), 819 (m) cm^{-1}. ^{1}H NMR (CD_2Cl_2): δ 8.26 (dd, 1H, *o*-Ar *H*), 7.74 (m, 2H, Ar *H*), 7.60 (m, 1H, Ar *H*), 7.48 (m, 1H, Ar *H*), 7.22 (m, 1H, Ar *H*), 7.11 (m, 2H, Ar *H*), 5.91 (s, 5H, C_5H_5), 2.83 (s, 3H, *Me*), 2.44 (s, 3H, *Me*). ^{13}C (CD_2Cl_2): δ 273.36 (*C*O), 161.39, 149.17 (2 × C_{ipso}), 142.03, 140.59, 140.52, 138.36, 136.77, 132.16, 129.51, 127.42, 125.79, 124.66 (10 × C_{aryl}), 100.61 (C_5H_5), 26.15, 21.14 (2 × *Me*). Low-resolution mass spectrum (probe temperature 120 °C): *m/z* 489 [P$^+$], 461 [P$^+$ − CO].

Preparation of CpW(NO)(*o*-tolyl)$_2$(PMe$_3$) (5). A solution of CpW(NO)(*o*-tolyl)$_2$ (generated from 1.00 mmol of CpW(NO)Cl_2) in THF was prepared as described above. The stirred reaction mixture was treated with approximately 1 atm of PMe_3 at room temperature, whereupon the solution changed from purple to yellow/brown in approximately 5 s. The reaction mixture was taken to dryness in vacuo, and the remaining brown residue was triturated in CH_2Cl_2 (10 mL). The resulting yellow powder was dissolved in CH_2Cl_2 (10 mL), and this solution was filtered through alumina I (3 × 3 cm). Hexanes (5 mL) were added to the filtrate, the volume of the solution was reduced in vacuo, and the final solution was placed in a freezer (−30 °C) overnight. The desired complex deposited as a yellow powder (360 mg, 67% yield) and was isolated by removing the supernatant solution by cannulation.

Anal. Calcd for $C_{22}H_{28}NOPW$: C, 49.18; H, 5.25; N, 2.61. Found: C, 48.96; H, 5.25; N, 2.57. IR (Nujol mull): 1587 (s), 1303 (m), 1281 (m), 954 (m), 826 (w) cm^{-1}. ^{1}H NMR ($CDCl_3$) (60:40 mixture of cis and trans isomers): δ 7.8 (m, *o*-Ar *H*), 7.2−6.8 (m, Ar *H*), 5.59 (s, C_5H_5), 5.56 (s, C_5H_5), 2.47 (s, *Me*), 2.33 (s, 3H, *Me*), 0.89, 0.79 (d ($^2J_{HP}$ = 9.3 Hz), 2 × P*Me*$_3$). Low-resolution mass spectrum (probe temperature 170 °C): *m/z* 461 [P$^+$ − PMe_3].

Generation of CpW(NO)(*o*-tolyl)(NHCMe$_3$) (6). Complex **1** (70 mg, 0.15 mmol) in CH_2Cl_2 (2 mL) was treated with excess Me_3CNH_2. There was no immediate color change, and there was no change evident in the ν_{NO} band in the solution IR spectrum. However, stirring of this solution at room temperature for 2 d resulted in a change in color from purple to orange. Cooling of the final solution to −30 °C afforded a dark orange powder which was identified by its physical properties as complex **6**. In solution this complex exists as a mixture of two isomers in the ratio 5:1. Only data for the major isomer are presented below.

^{1}H NMR ($CDCl_3$): δ 9.4 (s, 1H, N*H*), 7.7 (m, 1H, Ar *H*), 7.2 (m, 1H, Ar *H*), 7.0 (m, 2H, Ar *H*), 5.95 (s, 5H, C_5H_5), 2.24 (s, 3H, *Me*), 1.33 (s, 9H, C*Me*$_3$). ^{13}C ($CDCl_3$): δ 144.18, 141.40, 128.88, 126.28, 124.32 (5 × C_{aryl}), 102.60 (Cp), 64.99 (*C*Me$_3$), 33.02 (C*Me*$_3$), 28.69 (Ar *Me*). Low-resolution mass spectrum (probe temperature 120 °C): *m/z* 442 [P$^+$].

Generation of CpW(NO)(*o*-tolyl)(OCHMe$_2$) (7). A solution of CpW(NO)(*o*-tolyl)$_2$ (30 mg, 0.065 mmol) in $CDCl_3$ (0.7 mL) in an NMR tube was treated with an excess of Me_2CHOH (5 mg, 0.08 mmol). The solution changed color from purple to deep red in a matter of seconds. The reaction produced one major Cp-containing product (>95 %) as judged by ^{1}H NMR spectroscopy. The contents of the NMR tube were poured into a Schlenk tube and were taken to dryness. The resulting red solid was extremely air- and moisture-sensitive, and satisfactory mass spectral and elemental analysis data could not be obtained.

IR (Nujol mull): 1602 (br) cm^{-1}. ^{1}H NMR ($CDCl_3$): δ 7.6 (m, 1H, Ar *H*), 7.2 (m, 1H, Ar *H*), 7.1 (m, 2H, Ar *H*), 6.1 (s, 5H, C_5H_5), 5.4 (m, 1H, −C*H*−), 2.31 (s, 3H, *Me*), 1.30 (m, 6H, 2 × *Me*). ^{13}C ($CDCl_3$): δ 144.53, 137.40, 129.69, 127.49, 124.58 (5 × C_{aryl}), 104.55 (Cp), 85.34 (O*C*HMe$_2$), 27.02 (OCH*Me*$_2$), 26.61 (Ar *Me*), 26.08 (OCH*Me*$_2$).

Preparation of CpW(NO)(SAr)$_2$ (Ar = *o*-Tolyl (8), *p*-Tolyl (9)). A solution of CpW(NO)(*o*-tolyl)$_2$ (generated from 1.00 mmol of CpW(NO)Cl_2) in THF was prepared as described above. The stirred reaction mixture was treated with excess S_8 (80 mg, 2.5 equiv of S) at room temperature, whereupon the solution changed from purple to red in about 10 s. This red solution was taken to dryness in vacuo, and the resulting dark red residue was triturated in Et_2O (30 mL). This mixture was filtered through Florisil (3 × 5 cm). The volume of the filtrate was reduced in vacuo, and the resulting solution was placed in a freezer (−30 °C) overnight. Dark red crystals of the desired complex (270 mg, 51% yield) were isolated by removing the supernatant solution by cannulation.

Anal. Calcd for $C_{19}H_{19}NOS_2W$: C, 43.44; H, 3.64; N, 2.67. Found: C, 43.52; H, 3.65; N, 2.61. IR (Nujol mull): 1616 (s), 825 (m), 744 (m) cm^{-1}. ^{1}H NMR (C_6D_6): δ 7.62 (d, 2H, *o*-Ar *H*), 7.10 (m, 6H, Ar *H*), 5.06 (s, 5H, C_5H_5), 2.51 (s, 6H, 2 × *Me*). ^{13}C (CD_2Cl_2): δ 161.39, 149.17 (2 × C_{ipso}), 142.03, 140.59, 140.52, 138.36, 136.77, 132.16, 129.51, 127.42, 125.79, 124.66 (10 × C_{aryl}), 100.61 (C_5H_5), 21.14 (*Me*). Low-resolution mass spectrum (probe temperature 120 °C): *m/z* 525 [P$^+$].

CpW(NO)(S-*p*-tolyl)$_2$ (9) was prepared by using the same methodology as described above for complex **8**. Thus, treatment of CpW(NO)(*p*-tolyl)$_2$ generated in situ with excess S_8 afforded a dark red solution. Dark red crystals of complex **9** (230 mg, 45% yield) were isolated in a similar manner.

Anal. Calcd for $C_{19}H_{19}NOS_2W$: C, 43.44; H, 3.64; N, 2.67. Found; C, 43.59; H, 3.63; N, 2.74. IR (Nujol mull): 1614 cm^{-1}. ^{1}H NMR (C_6D_6): δ 7.6 (s (br), 4H, *o*-Ar *H*), 6.92 (d ($^3J_{HH}$ = 7.8 Hz), 4H, *p*-Ar *H*), 5.02 (s, 5H, C_5H_5), 2.05 (s, 6H, 2 × *Me*). Low-resolution mass spectrum (probe temperature 120 °C): *m/z* 525 [P$^+$].

Preparation of CpW(NO)(η^2-N(*p*-tolyl)C{O}-*o*-tolyl)(*o*-tolyl) (10). A sample of CpW(NO)(*o*-tolyl)$_2$ (46 mg, 0.10 mmol) in toluene (5 mL) was treated with an excess of *p*-tolyl isocyanate (25 mg, 0.18 mmol). The color of the solution changed from purple to yellow in a matter of seconds. Hexanes (5 mL) were added to the final reaction mixture, and the sample was placed in a freezer (−35 °C) overnight. A yellow microcrystalline powder of the desired complex (37 mg, 63% yield) was then isolated by decanting the supernatant solution and drying the powder in vacuo.

Anal. Calcd for $C_{27}H_{26}N_2O_2W$: C, 54.56; H, 4.41; N, 4.71. Found: C, 54.52; H, 4.54; N, 4.60. IR (Nujol mull): 1586 (s), 1573 (s), 1558 (m), 1394 (m) cm^{-1}. ^{1}H NMR ($CDCl_3$): δ 8.04 (m, 1H, Ar *H*), 7.3−6.9 (m, 11H, Ar *H*), 5.81 (s, 5H, C_5H_5), 2.58 (s, 3H, *Me*), 2.34 (s, 3H, *Me*) 2.31 (s, 3H, *Me*). Low-resolution mass spectrum (probe temperature 120 °C): *m/z* 594 [P$^+$].

Reaction of Cp*W(NO)(*o*-tolyl)$_2$ with D$_2$O. A solution of Cp*W(NO)(*o*-tolyl)$_2$ (53 mg, 0.10 mmol) in C_6D_6 (0.7 mL) was treated with excess D_2O (0.05 mL). The solution changed color from purple to brown in a few minutes. One major Cp*-containing product was produced in 95% yield (based on integration) as judged by ^{1}H NMR spectroscopy. This product was identified as Cp*W(O)$_2$(*o*-tolyl) on the basis of its characteristic ^{1}H NMR, IR, and mass spectral data.[9]

In Situ Treatment of CpW(NO)(*p*-tolyl)$_2$ with H$_2$O. A solution of CpW(NO)(*p*-tolyl)$_2$ was generated in THF from CpW(NO)Cl_2 (1.0 mmol) and (*p*-tolyl)$_2$Mg·*x*(dioxane) and was treated with excess H_2O (0.1 mL). The solution changed in color from dark blue to brown in a few seconds. The final reaction mixture was taken to dryness in vacuo, and the residue remaining was triturated in Et_2O (30 mL). The resulting yellow mixture was filtered through alumina I (3 × 3 cm). The filtrate was taken to dryness under reduced pressure to obtain a light yellow powder which was identified as 4,4′-dimethylbiphenyl (30 mg, 16% yield) by its ^{1}H NMR and mass spectra: ^{1}H NMR (C_6D_6): δ 7.44 (d, 2H, Ar *H*), 7.03 (d, 2H, Ar *H*), 2.14 (s, 3H, *Me*); low-resolution mass spectrum

(9) Legzdins, P.; Lundmark, P. J.; Phillips, E. C.; Rettig, S. J.; Veltheer, J. E. *Organometallics* **1992**, *11*, 2991.

(probe temperature 120 °C): *m/z* 182 [P$^+$]. No organometallic product was isolated.

In Situ Treatment of CpW(NO)Ph$_2$ with H$_2$O. CpW(NO)Ph$_2$ was generated in THF from CpW(NO)Cl$_2$ (1.0 mmol) and Ph$_2$Mg·*x*(dioxane) and was treated with excess H$_2$O (0.1 mL). The solution changed from dark blue to green to brown in a matter of seconds. The final reaction mixture was taken to dryness in vacuo, and the residue remaining was triturated in Et$_2$O (30 mL). The resulting yellow mixture was filtered through alumina I (3 × 3 cm). The filtrate was taken to dryness under reduced pressure to obtain a light yellow powder. Its IR and mass spectra indicated the material to be CpW(O)$_2$Ph. IR (Nujol mull): 950, 904 cm^{-1}. Low-resolution mass spectrum (probe temperature 180 °C): *m/z* 358 [P$^+$].

In Situ Treatment of CpMo(NO)(*o*-tolyl)$_2$ with H$_2$O. A THF solution of CpMo(NO)(*o*-tolyl)$_2$ was generated in a manner similar to its tungsten analogue (vide supra). This solution was treated at −20 °C with excess H$_2$O (0.1 mL). The purple color characteristic of the diaryl complex quickly changed to dark red. This solution was taken to dryness in vacuo, and the residue remaining was triturated with Et$_2$O (20 mL). The resulting red mixture was filtered through Florisil (3 × 3 cm). The filtrate was taken to dryness under reduced pressure, and the residue was triturated in hexanes to obtain a dark red powder. On the basis of its IR and mass spectra, the product was identified as [CpMo(NO)(*o*-tolyl)]$_2$(μ-O). IR (Nujol mull): ν_{NO} 1622 cm^{-1} and also 813 cm^{-1}. Low-resolution mass spectrum (probe temperature 120 °C): *m/z* 580 [P$^+$]. Attempts to obtain this complex analytically pure have to date been unsuccessful.

X-ray Crystallographic Analysis of CpW(O)(N-*o*-tolyl)-(*o*-tolyl) (2). A prismatic yellow crystal of **2** was mounted in a thin-walled glass capillary and was transferred to a Rigaku AFC6S diffractometer equipped with graphite-monochromated Mo Kα radiation ($\lambda_{K\alpha}$ = 0.710 69 Å). Final unit-cell parameters for the complex were obtained by least-squares analysis of setting angles for 25 reflections, 25.1 ≤ 2θ ≤ 29.7°. The intensities of three standard reflections were measured every 200 reflections during the data collection. These intensities remained constant throughout, thereby indicating crystal and electronic stability; no decay correction was therefore applied. The data were corrected for Lorentz and polarization effects and for absorption using the azimuthal scan method.[10] Pertinent crystallographic and experimental parameters for the complex are summarized in Table 1.

Interpretation of the Patterson function yielded the coordinates of the heaviest atoms in the structure, and the full structure of the compound was then derived by conventional electron-density methods and was refined by full-matrix least-squares methods on *F*, minimizing the function $\Sigma w(|F_o| - |F_c|)^2$, where $w = 4F_o^2/\sigma^2(F_o)^2$. Hydrogen atoms were fixed in calculated positions with C−H = 0.98 Å and $U_H = 1.2U_{\text{bonded atom}}$. Non-hydrogen atoms were refined with anisotropic thermal parameters. A correction for secondary extinction was applied, the final value of the extinction coefficient being 1.48(6) × 10^{-7}. Complex neutral-atom scattering factors (for all atoms) and anomalous scattering corrections for the non-hydrogen atoms were taken from ref 11. Final positional and equivalent isotropic thermal parameters for the complex are given in Table 2, and selected bond lengths (Å) and bond angles (deg) are listed in Table 3. A view of the solid-state molecular structure of complex **2** is displayed in Figure 2.

X-ray Crystallographic Analysis of CpW(NO)(*o*-tolyl)$_2$ (1). Under a dry N$_2$ atmosphere, a dark-purple-colored octagonal plate of complex **1** was cleaved, and a fragment was wedged into a glass capillary tube with a trace of fluorocarbon

Table 1. Crystallographic Data for Complexes 1 and 2[a]

compd	**2**[b]	**1**[c]
formula	$C_{19}H_{19}NOW$	$C_{19}H_{19}NOW$
fw	461.22	461.22
temp, K	294	205
color, habit	yellow, prism	purple, octagonal
cryst size, mm	0.06 × 0.15 × 0.32	0.09 × 0.21 × 0.23
cryst system	monoclinic	monoclinic
space group	$P2_1/n$	$P2_1/c$
a, Å	13.509(3)	9.636(2)
b, Å	7.003(3)	14.634(2)
c, Å	18.436(3)	12.347(3)
β, deg	107.24(1)	107.72(2)
V, Å^3	1666(1)	1658.5
Z	4	4
ρ_{calc}, g/cm^3	1.839	1.847
F(000)	883.81	883.81
μ(Mo K_α), cm^{-1}	70.82	71.10
transm factors (relative)	0.65−1.00	0.233−0.549
scan type	$\omega-2\theta$	$\omega-2\theta$
scan range, deg in ω	1.31 + 0.35 tan θ	0.9 + 0.35 tan θ
scan rate, deg/min	32	0.82−3.3
data collcd	$+h,+k,\pm l$	$\pm h,+k,+l$
$2\theta_{max}$, deg	60	48
cryst decay, %	0	negligible
tot. reflcns	5238	2575
obsd reflcns	2539	2075
R	0.030	0.022
R_w	0.029	0.026
gof	1.21	1.188
max Δ/σ (final cycle)	0.03	0.02
resid density, e/Å^3	−0.84 to 0.65 (near W)	−0.62(11) to 0.76(11)[d]

[a] Function minimized $\Sigma w(|F_o| - |F_c|)^2$, where $w = 4F_o^2/\sigma^2(F_o^2)$; $R = \Sigma||F_o| - |F_c||/\Sigma|F_o|$, $R_w = (\Sigma w(|F_o| - |F_c|)^2/\Sigma w|F_o|^2)^{1/2}$, and gof = $[\Sigma w(|F_o| - |F_c|)^2/(m-n)]^{1/2}$. Values given for *R*, R_w, and gof are based on those reflections with $I \geq 3\sigma(I)$ for complex **2** and $I \geq 2.5\sigma(I)$ for complex **1**. For complex **1**, $w = [\sigma(F_o)^2 + 0.0002F_o^2]^{-1}$. [b] Rigaku AFC6S diffractometer, Mo Kα radiation (λ = 0.710 69 Å), graphite monochromator, takeoff angle 6.0°, aperture 6.0 × 6.0 mm at a distance of 285 mm from the crystal, stationary background counts at each end of the scan (scan/background time ratio 2:1, up to 8 rescans), $\sigma^2(F^2) = [S^2(C + 4B)]/Lp^2$ (*S* = scan rate, *C* = scan count, *B* = normalized background count). [c] Enraf Nonius CAD4F diffractometer. [d] 0.93 Å from W.

Table 2. Final Positional and Equivalent Isotropic Thermal Parameters (Å^2) for CpW(O)(N-*o*-tolyl)(*o*-tolyl) (2)

atom	*x*	*y*	*z*	B_{eq}[a]
W(1)	0.49362(2)	0.51470(3)	0.13169(1)	2.867(9)
O(1)	0.4942(4)	0.7486(6)	0.1018(3)	4.4(2)
N(1)	0.3814(4)	0.4067(8)	0.0713(3)	3.4(2)
C(1)	0.6789(5)	0.497(1)	0.1490(4)	5.0(3)
C(2)	0.6262(5)	0.348(1)	0.1017(4)	4.5(3)
C(3)	0.5903(5)	0.218(1)	0.1477(4)	4.2(3)
C(4)	0.6145(5)	0.295(1)	0.2206(4)	4.0(3)
C(5)	0.6705(5)	0.465(1)	0.220(4)	4.3(3)
C(6)	0.4339(5)	0.5353(8)	0.2276(3)	3.4(2)
C(7)	0.4537(6)	0.684(1)	0.2806(4)	5.0(3)
C(8)	0.4073(7)	0.683(1)	0.3404(4)	5.3(4)
C(9)	0.3472(7)	0.533(1)	0.3488(4)	5.9(4)
C(10)	0.3261(6)	0.387(1)	0.2976(5)	5.7(4)
C(11)	0.3703(6)	0.385(1)	0.2391(4)	4.5(3)
C(12)	0.2954(5)	0.318(1)	0.0232(3)	3.5(3)
C(13)	0.2015(6)	0.407(1)	0.0050(4)	4.3(3)
C(14)	0.1157(6)	0.316(1)	−0.0441(4)	5.5(4)
C(15)	0.1263(7)	0.141(2)	−0.0745(5)	6.1(4)
C(16)	0.2222(8)	0.054(1)	−0.0571(5)	6.4(4)
C(17)	0.3068(6)	0.137(1)	−0.075(4)	5.1(4)
C(18)	0.5182(8)	0.852(1)	0.2750(5)	7.3(5)
C(19)	0.1898(6)	0.594(1)	0.0367(5)	6.2(4)

[a] $B_{eq} = (8/3)\pi^2\Sigma\Sigma U_{ij}a_i^*a_j^*(a_i a_j)$.

(10) TEXSAN/TEXRAY structure analysis package which includes versions of the following: MITHRIL, integrated direct methods, by C. J. Gilmore; DIRDIF, direct methods for difference structures, by P. T. Beurskens; ORFLS, full-matrix least-squares, and ORFFE, functions and errors, by W. R. Busing, K. O. Martin, and H. A. Levy; ORTEP II, illustrations, C. K. Johnson.

(11) *International Tables for X-ray Crystallography*; Kynoch Press: Birmingham, England, 1974; Vol. IV, Tables 2.2B and 2.3.1.

Table 3. Selected Metrical Parameters for CpW(O)(N-*o*-tolyl)(*o*-tolyl) (2)

atoms	bond length (Å)	atoms	bond angle (deg)
W(1)−O(1)	1.729(4)	O(1)-W(1)-N(1)	106.8(2)
W(1)−N(1)	1.764(5)	O(1)-W(1)-C(6)	103.6(2)
W(1)−C(6)	2.155(6)	N(1)-W(1)-C(6)	95.0(2)
N(1)−C(12)	1.382(8)	W(1)-N(1)-C(12)	178.2(5)
W(1)−CP[a]	2.119(3)		

[a] CP refers to the unweighted centroid of the cyclopentadienyl ring.

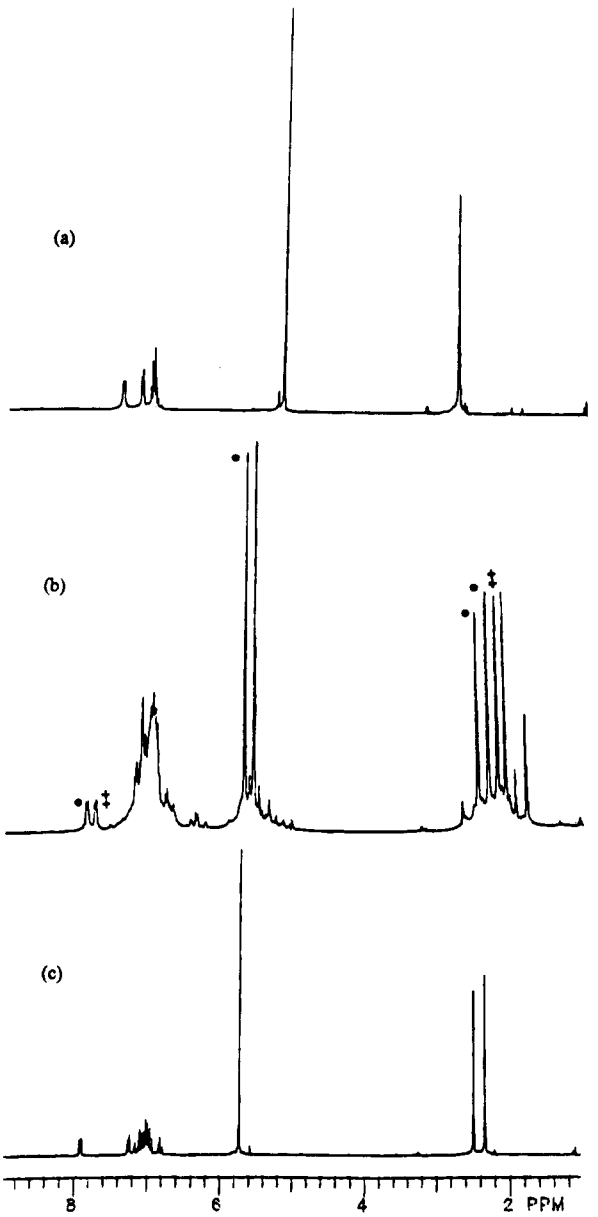

Figure 1. (a) 300 MHz ^{1}H NMR spectrum of CpW(NO)(*o*-tolyl)$_2$ (**1**) (C_6D_6). (b) 300 MHz ^{1}H NMR spectrum of the reaction mixture of D_2O and CpW(NO)(*o*-tolyl)$_2$ (**1**), where ● denotes CpW(O)(N-*o*-tolyl)(*o*-tolyl) (**2**) and ‡ denotes CpW(O)$_2$(*o*-tolyl) (**3**) (C_6D_6). (c) 300 MHz ^{1}H NMR spectrum of CpW(O)(N-*o*-tolyl)(*o*-tolyl) (**2**) (C_6D_6).

grease as adhesive. The tube was sealed with a hot wire inside the glovebox. Data were recorded at 205 K with an Enraf Nonius CAD4F diffractometer equipped with an in-house modified low-temperature attachment and using graphite-monochromatized Mo Kα radiation. Two intensity standards were measured every 1 h of exposure time and showed intensity fluctuations of ±2% during the course of the measurements. The data were corrected for absorption by the

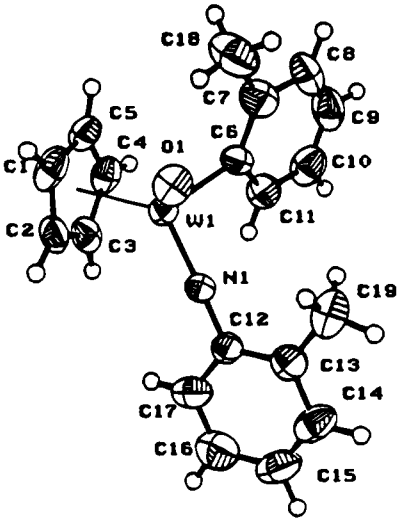

Figure 2. View of the solid-state molecular structure of complex **2**. Probability ellipsoids at the 33% level are shown.

Gaussian integration method, and corrections were carefully checked against ψ-scan measurements. Data reduction included corrections for intensity scale variation and for Lorentz and polarization effects.

Coordinates and anisotropic thermal parameters for all non-hydrogen atoms were refined. Hydrogen atoms were placed in calculated positions 0.95 Å from their respective carbon atoms and with isotropic temperature factors initially proportionate to the carbon-atom equivalent isotropic temperature factors. In subsequent cycles of refinement the coordinate shifts for the hydrogen atoms of the aryl and cyclopentadienyl rings were linked with those for their respectively bound carbon atoms. Each methyl group was refined as a rigid CH_3 group subject to restraints which maintained near axial symmetry for the respective CCH_3 fragment. Mean isotropic temperature factors were refined for each of five groups of hydrogen atoms, and the shifts were applied to the individual atomic values. An extinction parameter[12] was refined. A weighting scheme based on counting statistics was applied such that $\langle w(|F_o| - |F_c|)^2 \rangle$ was nearly constant as a function of both $|F_o|$ and $(\sin\theta)/\lambda$. Final full-matrix least-squares refinement of 211 parameters for 2075 data ($I \geq 2.5\sigma(I)$) and 6 restraints converged at $R_F = 0.022$. The final maximum shift/error was 0.02. Crystallographic details are summarized in Table 1. The programs used for absorption corrections, data reduction, structure solution, refinement, and plot generation were from the NRCVAX Crystal Structure System.[13] Final refinement was made using CRYSTALS.[14] Complex scattering factors for neutral atoms[11] were used in the calculation of structure factors. Computations were carried out on MicroVAX-II and 80486 computers.

Rigid-body analysis[15] of the anisotropic thermal parameters of the molecule yielded $R_w = 0.079$ for the agreement between observed and calculated U_{ij} values with an rms discrepancy of 0.0012 Å. While there remained some significant residual observed thermal motion for a few of the cyclopentadienyl-carbon atoms and the outer carbon atoms of one of the *o*-tolyl groups C(21−27), further modeling of the internal motion was deemed to be unwarranted. Pertinent crystallographic and

(12) Larson, A. C. In *Crystallographic Computing*; Munksgaard: Copenhagen, 1970; p 293.
(13) Gabe, E. J.; LePage, Y.; Charland, J.-P.; Lee, F. J.; White P. S. NRCVAX- An Interactive Program System for Structrue Analysis. *J. Appl. Crystallogr.* **1989**, *22*, 384.
(14) Watkin, D. J.; Carruthers, J. R.; Betteridge, P. W. CRYSTALS. Chemical Crystallography Laboratory, University of Oxford, Oxford, England, 1984.
(15) Schomaker, V.; Trueblood, K. N. *Acta Crystallogr.* **1968**, *B24*, 63.

Table 4. Final Positional and Equivalent Isotropic Thermal Parameters (Å²) for CpW(NO)(*o*-tolyl)₂ (1) at 205 K

atom	*x*	*y*	*z*	B_{eq}[a]
W	0.316284(21)	0.185482(12)	0.026673(16)	0.0252
O	0.3351(4)	0.0619(3)	−0.1604(3)	0.0431
N	0.3288(5)	0.1179(3)	−0.0878(3)	0.0288
C(1)	0.2876(9)	0.2080(5)	0.2129(6)	0.0534
C(2)	0.1763(9)	0.1503(5)	0.1493(6)	0.0532
C(3)	0.2410(7)	0.0710(4)	0.1277(5)	0.0487
C(4)	0.3924(8)	0.0791(4)	0.1690(5)	0.0463
C(5)	0.4208(9)	0.1636(5)	0.2250(5)	0.0524
C(11)	0.1194(6)	0.2540(4)	−0.0710(4)	0.0315
C(12)	0.0028(6)	0.2169(3)	−0.1569(5)	0.0362
C(13)	−0.1053(6)	0.2748(4)	−0.2231(5)	0.0397
C(14)	−0.1002(6)	0.3681(4)	−0.2051(5)	0.0443
C(15)	0.0106(6)	0.4047(4)	−0.1189(6)	0.0450
C(16)	0.1158(6)	0.3471(4)	−0.0522(5)	0.0389
C(17)	−0.0093(7)	0.1157(3)	−0.1824(6)	0.0510
C(21)	0.5091(6)	0.2624(3)	0.0477(4)	0.0306
C(22)	0.6245(6)	0.2477(3)	0.0031(4)	0.0345
C(23)	0.7177(7)	0.3201(4)	−0.0011(5)	0.0453
C(24)	0.6989(8)	0.4046(5)	0.0378(6)	0.0512
C(25)	0.5936(8)	0.4197(4)	0.0892(6)	0.0497
C(26)	0.5020(6)	0.3487(4)	0.0968(5)	0.0372
C(27)	0.6547(7)	0.1556(4)	−0.0402(5)	0.0477

[a] B_{eq} is the cube root of the product of the principle axes of the thermal ellipsoid.

Table 5. Selected Metrical Parameters for CpW(NO)(*o*-tolyl)₂ (1) at 205 K

atoms	bond length (Å)	atoms	bond angle (deg)
W−N	1.759(4)	N−W−CP[a]	124.1
W−C(11)	2.160(5)	W−N−O	172.5(4)
W−C(21)	2.120(5)	N−W−C(11)	94.35(19)
W−CP[a]	2.030	N−W−C(21)	97.20(21)
N−O	1.229(6)	C(11)−W−C(21)	114.20(20)

[a] CP refers to the unweighted centroid of the cyclopentadienyl ring.

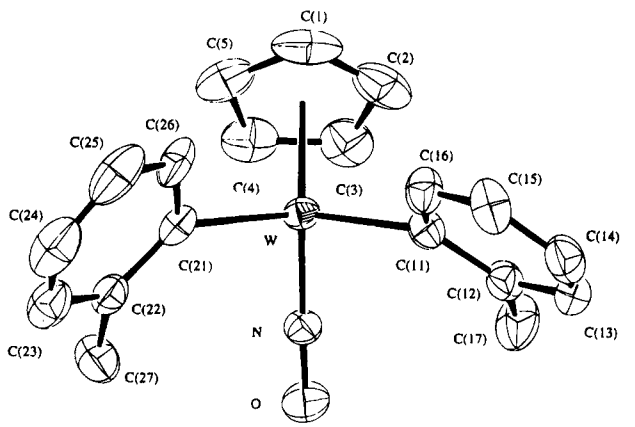

Figure 3. View of the solid-state molecular structure of complex **1**. Probability ellipsoids at the 50% level are shown.

experimental parameters for the complex are summarized in Table 1. Final positional and equivalent isotropic thermal parameters for the complex are given in Table 4, and selected bond lengths (Å) and bond angles (deg) are listed in Table 5. A view of the solid-state molecular structure of complex **1** is displayed in Figure 3.

Results and Discussion

Nitrosyl N−O Bond Cleavage. The cleavage of nitric oxide may be effected in the condensed phase, and this process has been viewed as a model for the catalytic degradation of nitrogen oxides.[16] The cleavage of bound nitric oxide (i.e. a nitrosyl ligand) can be viewed as a crude modeling of the crucial step in this process and is a fundamental transformation of interest in its own right since it permits the utilization of NO as a source of nitrogen and oxygen atoms in transition-metal chemistry. There have been several examples of nitrosyl-ligand N−O bond cleavage reported which involve the photolysis[17] or thermolysis[18] of mixtures of organometallic complexes to obtain mixed-metal nitrido cluster complexes. In addition, NO cleavage reactions involving metal cluster compounds are well-known.[19] Furthermore, there have been reports of the Lewis acid-induced conversion of a terminal nitrosyl ligand into terminal oxo and nitrido linkages, a process which has been termed intramolecular redox isomerization.[20] It has also been reported that nitric oxide can be used as a source of oxo ligands in an *intermolecular* fashion.[21] Very recently, Cummins and co-workers effected the synthesis of terminal chromium(VI) nitrido complexes, $(RR'N)_3Cr{\equiv}N$, via deoxygenation of the precursor nitrosyl complex, $(RR'N)_3Cr(NO)$, using $(THF)V(Mes)_3$ as the oxygen-atom acceptor.[22] Finally, tandem mass spectrometry has demonstrated that $Cp_2Fe_2(NO)^+$ undergoes N−O bond cleavage, the resulting fragments being pyridine and $CpFe_2O^+$.[23]

In contrast to the examples of nitrosyl N−O cleavage mentioned in the preceding paragraph, the transformation depicted in eq 1 in the Introduction is quite intriguing since it involves the inducement of such cleavage by water. Of particular interest is the specific nature of conversion 1, namely, the following: (a) Is the isomerization of **1** to **2** an intermolecular or an intramolecular process? (b) What role does the H_2O play in this isomerization and what other agents induce this reactivity? (c) What other complexes containing an NO ligand may be induced to undergo this isomerization? We have endeavored to answer these questions by studying the characteristic chemistry of CpW(NO)(*o*-tolyl)₂ and some of its analogues with a variety of reagents. The closest analogues to **1** are those containing a different Cp′ ligand, a different metal center, or different aryl groups. The reactions of some of these analogues of **1** with H_2O have been investigated to determine the generality of conversion 1. Furthermore, the characteristic chemistry of **1** has been investigated to elucidate whether its reactivity with other reagents does or does not parallel that of other related diaryl and dialkyl systems. It should be emphasized here that complex **1** (the only member of the class of molecules CpM(NO)(aryl)₂ (M = Mo or W) that has been isolated to date) is quite difficult to handle due to its hydrolytic and thermal instability in solution and that the isolation

(16) See, for example: (a) Gland, J. L.; Sexton, B. A. *Surf. Sci.* **1980**, *94*, 355. (b) Villarubia, J. S.; Ho, W. *J. Chem. Phys.* **1987**, *87*, 750.
(17) (a) Gibson, C. P.; Dahl, L. F. *Organometallics* **1988**, *7*, 543. (b) Gibson, C. P.; Bern, D. S.; Falloon, S. B.; Hitchens, T. K.; Cortopassi, J. E. *Organometallics* **1992**, *11*, 1742.
(18) Feasey, N. D.; Knox, S. A. R. *J. Chem. Soc., Chem. Commun.* **1982**, 1063.
(19) Gladfelter, W. L. *Adv. Organomet. Chem.* **1985**, *24*, 41.
(20) Seyferth, K.; Taube, R. *J. Mol. Catal.* **1985**, *28*, 53.
(21) The mechanism of this conversion is unclear and the fate of nitrogen of the nitric oxide has not been determined; see: Alt, H. G.; Hayen, H. I. *Angew. Chem., Int. Ed. Engl.* **1985**, *24*, 497.
(22) Odom, A. L.; Cummins, C. C.; Protasiewicz, J. D. *J. Am. Chem. Soc.* **1995**, *117*, 6613.
(23) Schröder, D.; Müller, J.; Schwarz, H. *Organometallics* **1993**, *12*, 1972.

of some derivatives of **1** has been precluded by their extreme sensitivity.

Intramolecular Water-Induced N–O Bond Cleavage. The first question that is raised by the isomerization of **1** to **2** is whether the oxo ligand of **2** is the result of intramolecular cleavage of the nitrosyl ligand of **1** or intermolecular transfer from the water reactant. This point can be addressed by treating complex **1** with $^{18}OH_2$. The final reaction mixture is worked up in a manner similar to that outlined in the Experimental Section for complex **2**. The mass spectrometric characterization of this product reveals an isotopic envelope centered at m/z 461 which is identical to that obtained from treatment of **1** with nonlabeled water. The observed result thus indicates that the imido *and* oxo ligands of complex **2** have their origins in the initial nitrosyl ligand and that the isomerization of **1** to **2** probably occurs intramolecularly (eq 2).

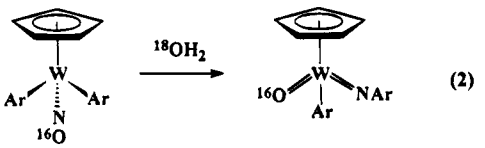

(2)

Ar = *o*-tolyl

Treatment of complex **1** with D_2O affords results similar to those obtained with H_2O and $^{18}OH_2$. Monitoring of the reaction of complex **1** in C_6D_6 with approximately 1 equiv of D_2O by ^1H NMR spectroscopy (Figure 1) reveals that **1** is converted to complexes **2** and **3** in the approximate ratio of 1:1. Similar product ratios are obtained from similar treatment of **1** in C_6D_6 with H_2O and $^{18}OH_2$.[24] The results of the ^1H NMR spectroscopic and mass spectrometric investigations therefore indicate that the formation of **2** and **3** takes place via independent pathways.

Characteristic Chemistry of Complex 1. Complex **1** exhibits reactivity toward several classes of reagents among which are included Lewis acids and bases, Brønsted acids, and electrophiles (Scheme 1). The chemistry involved generally resembles that observed for other Cp′W(NO)R_2 systems such as CpW(NO)$(CH_2SiMe_3)_2$.[25]

(A) Reactivity toward Lewis Bases. One possible function of the water in inducing transformation 1 may involve initial coordination as a Lewis base to the metal center. If so, other Lewis bases may also serve to induce this isomerization. However, the reaction of **1** with CO, a typical Lewis base, produces a monoinserted 18-valence-electron acyl–aryl complex, **4**. This complex is similar to the products obtained from the insertion of CO into related dialkyl[26] and diaryl[5] complexes. This insertion of CO into an M–C_{aryl} bond of complex **1** is more facile than for some analogous dialkyl complexes as evidenced by the much shorter reaction times for the aryl system. This difference in reactivity indicates that the metal center of **1** is more accessible and/or the metal

Scheme 1

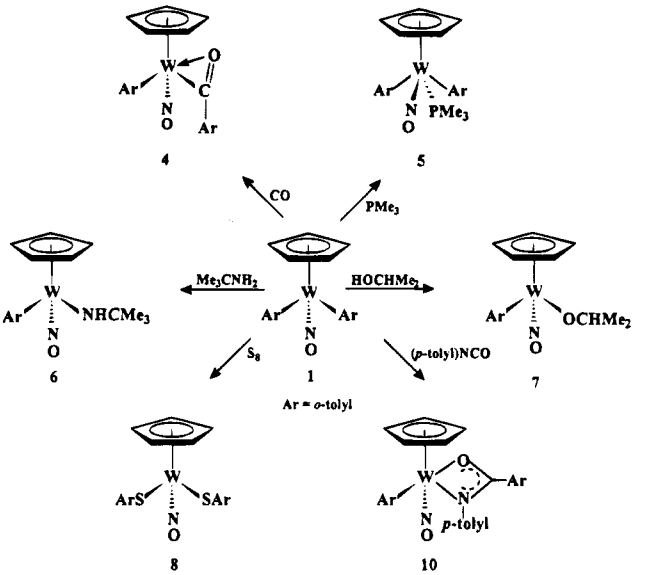

center of **1** is a more potent Lewis acid than that in the related dialkyl complexes.[27] Complex **1** also reacts with PMe_3, another typical Lewis base, at room temperature to afford the 1:1 PMe_3 adduct, **5**. Similar adducts of PMe_3 with Cp*-containing diaryls have been previously reported.[5] Complex **5** is formulated as the four-legged piano-stool adduct containing a terminal nitrosyl ligand on the basis of its ^1H NMR and IR spectra (e.g. ν_{NO} (Nujol mull): 1587 cm^{-1}). Its ^1H NMR spectrum (see Experimental Section) also indicates that this adduct exists as a 60:40 mixture of isomers in solution. Like other adducts of this type,[26] **5** is probably the trans isomer with the Lewis base trans to the nitrosyl ligand in the metal's coordination sphere, and the isomers in solution are the rotamers resulting from hindered rotation about the two W–*o*-tolyl bonds. Attempts to induce the thermal isomerization of **5** to its imido oxo isomer by warming benzene solutions of **5** simply result in its thermal decomposition to an intractable mixture. Furthermore, when solutions of complex **1** in a variety of solvents (e.g. C_6D_6, $CDCl_3$, and THF-d_8) are allowed to decompose thermally at room temperatures in the absence of a trapping agent, the ^1H NMR spectra of the final solutions exhibit a large number of peaks attributable to Cp resonances, thereby indicating that many products are formed.

(B) Reactivity toward RNH_2 and R′OH. It is possible that the reactivity of a Brønsted acid such as *tert*-butylamine with complex **1** may parallel that exhibited by water. At room temperature there is no initial adduct formation between the amine and the complex as determined by IR spectroscopy. Consistently, the color of the reaction mixture does not change from the initial purple color upon addition of the amine. However, the reaction mixture does change to yellow when cooled to approximately −50 °C, a feature consistent with adduct formation occurring only at low temperatures. Stirring of the reaction solution at room temperature for 2 days and then cooling to −30 °C results in the deposition of CpW(NO)(*o*-tolyl)$(NHCMe_3)$ (**6**) as an orange solid. The ^1H NMR spectrum of **6**

(24) The fact that the ^{18}O label ends up in **3** after this reaction is not conclusive by itself since we have established previously that such Cp′$M(O)_2R$ (M = Mo, W) complexes are prone to undergo oxygen-atom exchange processes; see, Legzdins, P.; Phillips, E. C.; Sánchez, L. Organometallics **1989**, *8*, 940.

(25) Legzdins, P.; Rettig, S. J.; Sánchez, L. *Organometallics* **1988**, *7*, 2394.

(26) Dryden, N. H.; Legzdins, P.; Lundmark, P. J.; Riesen, A.; Einstein, F. W. B. *Organometallics* **1993**, *12*, 2085.

(27) A discussion of the steric and electronic factors operative in complexes of this type has appeared; see: Legzdins, P.; Veltheer, J. E. *Acc. Chem. Res.* **1993**, *26*, 41.

indicates that it exists as two isomers in solution which are most likely rotational isomers resulting from restricted rotation about the W−N multiple bond, a phenomenon previously noted for similar complexes.[28] Complex **6** may result from protonolysis of a W−aryl bond in **1** by the amine.

Complex **1** also reacts with 2-propanol, a protic acid having a pK_a similar to H_2O.[29] Again, however, this reagent does not induce the isomerization conversion 1 but rather forms the alkoxo aryl complex, CpW(NO)(*o*-tolyl)(OCHMe$_2$) (**7**). This conversion again most likely involves protonolysis of the aryl ligand; similar reactions with analogous Cp* complexes proceed more slowly and also result in the formation of alkoxo complexes.[30] In summary, the reactions of **1** with reagents that have Lewis basic and weakly Brønsted acidic properties do not result in the isomerization of **1** to **2**.

(C) Other Reactivity of Complex 1. Complex **1** also exhibits reactivity toward elemental sulfur and *p*-tolyl isocyanate. These reactions (Scheme 1) provide the products expected on the basis of comparisons with related dialkyl or diaryl systems. Treatment of **1** with elemental sulfur provides the dithiolate complex, CpW(NO)(S-*o*-tolyl)$_2$ (**8**). Once again, this reaction is much more facile than that for the dialkyl systems. For example, when CpW(NO)(CH$_2$SiMe$_3$)$_2$ is treated with elemental sulfur, it proceeds through several isolable intermediates, namely CpW(NO)(SCH$_2$SiMe$_3$)(CH$_2$SiMe$_3$) and CpW(NO)(η^2-S$_2$CH$_2$SiMe$_3$)(CH$_2$SiMe$_3$).[31] However, complex **1** reacts with sulfur in less than 1 min at ambient temperatures to produce the dithiolate complex. This facile insertion of elemental sulfur appears to be a simple alkyl vs aryl dependence as evidenced by the fact that CpW(NO)(*p*-tolyl)$_2$ also reacts rapidly with elemental sulfur to form CpW(NO)(S-*p*-tolyl)$_2$ (**9**).

Complex **1** also reacts with *p*-tolyl isocyanate to give CpW(NO)(η^2-N(*p*-tolyl)C{O}-*o*-tolyl)(*o*-tolyl) (**10**). Again, this is the product expected on the basis of the reactivity found for the analogous Cp* systems.[32] Reactions of complex **1** with other heterocumulenes such as CO_2 and CS_2 do not result in any isolable products. These reactions (especially the CO_2 reaction) are slower than that of the isocyanate reaction, and thus the thermal decomposition of **1** and not the insertion of the heterocumulene into a W−C bond is the dominant process.

In summary, the characteristic chemistry of **1** parallels that established for the well-studied dialkyl systems with the exception that the diaryl systems undergo qualitatively more facile reactions. If, however, a reaction does not proceed rapidly (i.e. in a matter of minutes), then the thermal decomposition of complex **1** becomes the dominant process.

Reactivity of Analogues of CpW(NO)(*o*-tolyl)$_2$ with H_2O/D_2O. Since no other species besides water could be found to promote the isomerization outlined in eq 1, it became of interest to us to determine the generality of the water-induced isomerization in terms of the organometallic reactant. The closest analogues to **1** are found by (1) changing the nature of the cyclopentadienyl ligand, (2) changing the metal to another group 6 metal, and (3) changing the nature of the aryl ligands.

To investigate the dependence of this conversion on the Cp′ group, the reactivity of Cp*W(NO)(*o*-tolyl)$_2$ with D_2O was examined. Monitoring of this reaction by ^{1}H NMR spectroscopy reveals one major Cp*-containing product in approximately 90% yield (based on integration). This peak, along with other resonances further downfield, is attributable to the dioxo complex, Cp*W(O)$_2$(*o*-tolyl) (eq 3). Consistently, the EI mass spectrum

$$\text{Cp*W(NO)(}o\text{-tolyl)}_2 \xrightarrow{\text{xs } D_2O} \text{Cp*W(O)}_2\text{(}o\text{-tolyl)} \quad (3)$$

of the powder resulting from this reaction reveals a parent envelope centered at m/z 442 assignable to Cp*W(O)$_2$(*o*-tolyl). It thus appears that isomerization 1 is dependent on the nature of the cyclopentadienyl ligand such that upon changing this ligand from Cp to Cp* the isomerization does not take place.

A solution of the molybdenum analogue of **1,** CpMo(NO)(*o*-tolyl)$_2$, can be generated in THF at low temperatures. This complex has eluded isolation, but solutions of CpMo(NO)(*o*-tolyl)$_2$ can be generated that exhibit IR properties (ν_{NO} 1624 cm^{-1}) and color (purple) that are consistent with this formulation. Attempts to isolate this complex by cooling solutions containing it result in the deposition of a brown, intractable solid. When the solutions of CpMo(NO)(*o*-tolyl)$_2$ generated in situ are treated with H_2O, workup provides a dark red powder which is identified as [CpMo(NO)(*o*-tolyl)]$_2$-μ-O (eq 4). This finding is not surprising considering that similar molybdenum dialkyl and diaryl complexes generally react with water to form similar bridging oxo complexes.[9]

$$\text{CpMo(NO)(o-tolyl)}_2 \xrightarrow{\text{xs } H_2O} \text{\{CpMo(NO)(o-tolyl)\}}_2\text{-}\mu\text{-O} \quad (4)$$

The dependence of the isomerization of **1** to **2** on the nature of the aryl ligands can be investigated by preparing solutions of CpW(NO)Ph$_2$ (ν_{NO} 1601 cm^{-1}) and CpW(NO)(*p*-tolyl)$_2$ (ν_{NO} 1599 cm^{-1}) and treating them with H_2O. When CpW(NO)(*p*-tolyl)$_2$ is treated with H_2O, an immediate reaction takes place, but the only product isolable is 4,4′-dimethylbiphenyl. This organic product is most likely the result of reductive elimination of the aryl groups from the metal center. This type of reactivity has been observed during the thermolysis of a related arylnitrosylruthenium compound, Cp*Ru(NO)Ph$_2$.[33] The reaction of CpW(NO)Ph$_2$ with H_2O provides the corresponding dioxo complex CpW(O)$_2$Ph. Again, in these cases there is no evidence for the isomerization of these diaryl complexes upon changing the aryl ligands to groups other than *o*-tolyl ligands.

X-ray Crystallographic Analysis of Complex 2. The solid-state molecular structure of **2** has been established by a single-crystal X-ray crystallographic analysis, and an ORTEP plot of the structure is shown in Figure 2. The intramolecular metrical parameters of **2** (Table 3) indicate that the aryl and oxo ligands

(28) (a) Legzdins, P.; Young, M. A.; Veltheer, J. E.; Batchelor, R. J.; Einstein, F. W. B. *Organometallics* **1995**, *14*, 407. (b) Legzdins, P.; Rettig, S. J.; Ross, K. J. *Organometallics* **1993**, *12*, 2103.

(29) The pK_a values of water and 2-propanol are both approximately 16. See, for example: Streitweiser, A., Jr.; Heathcock, C. H. *Introduction to Organic Chemistry*; Macmillan: New York, 1985; Chapter 10.

(30) Lundmark, P. J. Ph.D. Dissertation, University of British Columbia, 1993.

(31) See ref 25 and: Legzdins, P.; Sánchez, L. *J. Am. Chem. Soc.* **1985**, *107*, 5525.

(32) Brouwer, E. B.; Legzdins, P.; Rettig, S. J.; Ross, K. J. *Organometallics* **1993**, *12*, 4234.

(33) Chang, J.; Bergman, R. G. *J. Am. Chem. Soc.* **1987**, *109*, 4298.

function as one- and two-electron donors, respectively, to the tungsten center. Also, according to the criteria developed by Parkin and Bercaw,[34] the $\nu_{W=O}$ of 897 cm^{-1} displayed by **2** in its Nujol mull IR spectrum indicates that the tungsten–oxygen linkage is principally a double bond. The relatively short W–N bond length (1.764(5) Å) and the essentially linear W–N–C grouping (the angle at N being 178.2(5)°) is consistent with the view that this ligand formally provides four electrons to the W≡N bond.[35]

The transformation in eq 1 thus results in the conversion of the 16-valence-electron reactant to its thermodynamically more stable 18-valence-electron structural isomer. For the simplified conversion shown in eq 5, a crude thermodynamic analysis can be instructive.

$$O{=}N{-}[W]{-}R \longrightarrow O{=}[W]{=}N{-}R \quad (5)$$

(R = *o*-tolyl; [W] = CpW(*o*-tolyl))

In complex **1**, both the M–C(aryl) and W–N bond strengths can be approximated at 210 kJ/mol,[36] while the minimum N=O bond strength can be estimated as 420 kJ/mol.[37] Little is known with regard to the strengths of transition-metal multiple bonds. However, Mayer and co-workers have estimated that the W=O and W=NR bonds are ≥577 and ≥420 kJ/mol, respectively, in complexes of the type $L_3Cl_2W{=}X$ (L = phosphine; X = O, NR).[38] Assuming these values for the W=O and W=NR bond strengths of complex **2** as well as a value of 290 kJ/mol for the N–R linkage,[29] an approximate value for ΔH of −400 kJ/mol is calculated for the conversion shown in eq 5. It thus appears that this reaction is thermodynamically driven by the propensity of the tungsten center to form strong multiple bonds with oxygen and nitrogen.

X-ray Crystallographic Analysis of Complex 1. It was also of interest to determine if the solid-state molecular structure of complex **1** could provide any insight into conversion 1. It was thought possible that some type of interaction of the *o*-methyl groups with the metal center which allows this conversion might be observed in the solid-state structure of **1**. After considerable effort, crystals of complex **1** suitable for an X-ray analysis were obtained, and the subsequently determined solid-state structure of **1** is shown in Figure 2. This structure can be compared to that of the Cp* analogue, Cp*W(NO)(*o*-tolyl)$_2$, which has been previously characterized crystallographically.[7] Somewhat disappointingly, the Cp complex, **1**, is essentially isostructural with the Cp* complex. The only major difference between the two structures is the fact that the Cp ligand is slightly further away from the metal center than is the Cp* ligand. The only feature of note in the Cp complex is that one of the W–C bonds (W–C(11) 2.160(5) Å) is slightly longer than the other (W–C(21) 2.120(5) Å). Thus, the comparison of these structures does not provide an explanation for the anomalous behavior of complex **1** with water.

Epilogue

To summarize, no complex other than CpW(NO)(*o*-tolyl)$_2$ (**1**) has been found to undergo isomerization to its arylimido oxo analogue upon treatment with water. Also, no other tested reagent induces the conversion of **1** to **2**. However, since our original communication in 1991 of this first example of N–O bond cleavage, we have discovered other systems that exhibit N–O bond cleavage.[2] These examples of nitrosyl N–O bond cleavage are quite varied both in the nature of the conditions used to promote this process and in the nature of the resulting organometallic complexes. However, attempts are being made to understand the factors involved in promoting and controlling N–O bond cleavage in these and other reactions. Many of these N–O bond cleavage reactions may be explained by the initial formation of an η^2-NO linkage which can eventually form oxo and imido/nitrido functionalities. For instance, we recently discovered a cationic nitrosyl complex that adds water to generate an η^2-hydroxylamido ligand.[39] Further studies to test the metal–η^2-NO linkage hypothesis are currently in progress.

Acknowledgment. We are grateful to the Natural Sciences and Engineering Research Council of Canada for support of this work in the form of grants to P.L. and F.W.B.E. and a postgraduate scholarship to K.J.R.

Supporting Information Available: Tables of hydrogen atom parameters, anisotropic thermal parameters, complete bond lengths and bond angles, torsion angles, intermolecular contacts, and least-squares planes for complexes **1** and **2** (17 pages). Ordering information is given on any current masthead page.

OM950606+

(34) Parkin, G.; Bercaw, J. E. *J. Am. Chem. Soc.* **1989**, *111*, 391.
(35) Nugent, W. A.; Mayer, J. M. *Metal-Ligand Multiple Bonds*; Wiley-Interscience: Toronto, 1988; Chapter 5.
(36) Collman, J. P.; Hegedus, L. S.; Norton, J. R.; Finke, R. G. *Principles and Applications of Organotransition Metal Chemistry*; University Science Books: Mill Valley, CA, 1987; Chapter 2.
(37) It is expected that this bond strength would be lower than the bond strength of 630 kJ/mol for NO(g); see: *Handbook of Chemistry and Physics*; Weast, R. C., Ed.; CRC Press: Boca Raton, FL, 1984; p F-180.
(38) Hall, K. A.; Mayer, J. M. *J. Am. Chem. Soc.* **1992**, *114*, 10402 and references cited therein.
(39) Legzdins, P.; Rettig, S. J.; Sayers, S. F. *J. Am. Chem. Soc.* **1994**, *116*, 12105.

Mechanistic Aspects of Carbon–Nitrogen Bond Cleavage in an $\eta^2(N,C)$-Pyridine Complex: Intimate Details of Metal to Ligand Aryl Migrations and Their Relevance to Hydrodenitrogenation Catalysis

Keith J. Weller, Steven D. Gray, Paula M. Briggs, and David E. Wigley*

Carl S. Marvel Laboratories of Chemistry, Department of Chemistry, University of Arizona, Tucson, Arizona 85721

Received September 5, 1995[⊗]

The reaction of the $\eta^2(N,C)$-pyridine complex $[\eta^2(N,C)$-2,4,6-$NC_5{}^tBu_3H_2]Ta(OAr)_2Cl$ (**1**, Ar = 2,6-$C_6H_3{}^iPr_2$) with PhLi affords the phenyl complex $[\eta^2(N,C)$-2,4,6-$NC_5{}^tBu_3H_2]Ta(OAr)_2$-Ph (**2**) in moderate yield. The *para*-substituted phenyl derivatives $[\eta^2(N,C)$-2,4,6-$NC_5{}^tBu_3H_2]$-$Ta(OAr)_2(4\text{-}C_6H_4X)$, where X = OMe (**3**), Me (**4**), Cl (**5**), and CF_3 (**6**), are prepared similarly from **1** and the appropriate aryl Grignard or lithium reagent. Complexes **2**–**6** represent the kinetic products of this reaction since, upon their thermolysis, aryl migration from metal to ligand occurs and the ring-opened compounds $Ta[{=}NC{}^tBu{=}CHC{}^tBu{=}CHC{}^tBu(4\text{-}C_6H_4X)]$-$(OAr)_2$, where X = H (**7**), OMe (**8**), Me (**9**), Cl (**10**), and CF_3 (**11**), are formed by C–N bond scission. Kinetic and mechanistic studies of the $[\eta^2(N,C)$-2,4,6-$NC_5{}^tBu_3H_2]Ta(OAr)_2(4\text{-}C_6H_4X)$ $\rightarrow Ta[{=}NC{}^tBu{=}CHC{}^tBu{=}CHC{}^tBu(4\text{-}C_6H_4X)](OAr)_2$ rearrangement reveal that aryl migration follows clean first-order kinetics, implying an intramolecular, *endo* attack of the migrating aryl group on the $\eta^2(N,C)$-pyridine ligand. An Eyring plot provides activation parameters for the $[\eta^2(N,C)$-2,4,6-$NC_5{}^tBu_3H_2]Ta(OAr)_2(4\text{-}C_6H_4OMe)$ (**3**) $\rightarrow Ta[{=}NC{}^tBu{=}CHC{}^tBu{=}CHC{}^tBu(4\text{-}C_6H_4OMe)](OAr)_2$ (**8**) rearrangement of $\Delta H^{\ddagger} = +19.2 \pm 1.3$ kcal mol^{-1} and $\Delta S^{\ddagger} = -27 \pm 4$ cal K^{-1} mol^{-1}, for a $\Delta G^{\ddagger} = +27.3 \pm 1.3$ kcal mol^{-1} at 25 °C, suggesting a highly ordered transition state leading to aryl transfer. Hammett considerations for the transformation of complexes **2**–**6** into **7**–**11** provide $\rho = -0.58 \pm 0.10$ for the aryl migration reaction. While the sign of ρ is in agreement with an electrophilic aromatic substitution at the migrating phenyl ligand, the small value of ρ argues against this pathway and against the involvement of the aryl π framework during migration. These data support the direct attack of the formal $[C_6H_4X]^-$ σ bond on C_α of the $\eta^2(N,C)$-pyridine ligand and C–N bond scission resulting from migration of the aryl group as a σ-nucleophile. Unlike their alkyl congeners, these ring-opened aryl derivatives $Ta[{=}NC{}^tBu{=}CHC{}^tBu{=}CHC{}^tBu(4\text{-}C_6H_4X)]$-$(OAr)_2$ (**7**–**11**) are stable to subsequent rearrangement. The structure of $Ta[{=}NC{}^tBu{=}CHC{}^tBu{=}CHC{}^tBuPh](OAr)_2$ (**7**) indicates a highly localized metallacycle with an imido nitrogen linkage characterized by a Ta–N–C angle of 145.3(3)° and Ta–N bond distance of 1.771(3) Å. Although an *endo* attack of the phenyl group is evident from mechanistic studies, the solid-state structure intimates an *exo* addition, and a simple pathway that interconverts *endo* and *exo* isomers is described to account for this observation. The reactions and structures of this model system are discussed in terms of a fundamental mechanistic knowledge of C–N bond scission that is relevant to hydrodenitrogenation catalysis.

Introduction

Of all the nitrogen compounds subject to hydrodenitrogenation (HDN) catalysis[1–3] during petroleum refining,[4,5] the basic heterocyclic compounds that contain pyridine rings are among the most difficult to process.[6–9] While the hydrogenation of pyridine heterocycles is facile under typical HDN conditions (300–450 °C, ≥2000 psi H_2),[9–11] C–N bond hydrogenolysis reactions are considerably slower.[8,12,13] Since C–N bond cleavage

[⊗] Abstract published in *Advance ACS Abstracts,* November 1, 1995.

(1) Angelici, R. J. In *Encyclopedia of Inorganic Chemistry*; King, R. B., Ed.; John Wiley and Sons: New York, 1994; Vol. 3; pp 1433–1443.
(2) Ho, T. C. *Catal. Rev.—Sci. Eng.* **1988**, *30*, 117.
(3) Ledoux, M. J. In *Catalysis*; The Chemical Society, London, 1988; Vol. 7, pp 125–148.
(4) Gary, J. H.; Handwerk, G. E. *Petroleum Refining: Technology and Economics*; 3rd ed., Marcel Dekker, Inc.: New York, 1993.
(5) Satterfield, C. N. *Heterogeneous Catalysis in Industrial Practice*; 2nd ed.; McGraw-Hill, Inc.: New York, 1991.
(6) Katzer, J. R.; Sivasubramanian, R. *Catal. Rev.—Sci. Eng.* **1979**, *20*, 155.
(7) Laine, R. M. *Catal. Rev.—Sci. Eng.* **1983**, *25*, 459.
(8) Laine, R. M. *Ann. NY Acad. Sci.* **1983**, *415*, 271.
(9) Fish, R. H. *Ann. NY Acad. Sci.* **1983**, *415*, 292.
(10) Fish and co-workers have developed a highly loaded nickel oxide catalyst system that promotes C–N bond cleavage prior to hydrogenation of the arene ring in quinoline; see: Fish, R. H.; Michaels, J. N.; Moore, R. S.; Heinemann, H. *J. Catal.* **1990**, *123*, 74.
(11) Fish, R. H.; Thormodsen, A. D.; Moore, A. D.; Perry, D. L.; Heinemann, H. *J. Catal.* **1986**, *102*, 270.

0276-7333/95/2314-5588$09.00/0

is typically rate-limiting,[14-22] the mechanistic details surrounding this reaction are of singular importance to understanding and improving HDN, especially since the metal's role in promoting this reaction remains unresolved.[1,2,23] Studies of thiophene hydrodesulfurization (HDS) have afforded several well-characterized C–S bond scission reactions,[24-32] but analogous model reactions of *N*-heterocycles are rare. Prior to our initial report,[33] the few examples of metal-mediated C–N bond scissions were limited to aliphatic amine substrates in systems not easily amenable to study;[34,35] several subsequent examples of C–N scissions have been reported.[36-40]

Recently, we described the reaction of $LiBEt_3H$ with the $\eta^2(N,C)$-pyridine complex $[\eta^2(N,C)$-2,4,6-$NC_5{}^tBu_3H_2]Ta(OAr)_2Cl$ (**1**, Ar = 2,6-$C_6H_3{}^iPr_2$) that resulted in C–N bond scission and formation of the ring-opened, metallacyclic complex $Ta[{=}NC^tBu{=}CHC^tBu{=}CHCH{-}{}^tBu](OAr)_2$.[33,41] Subsequent work demonstrated that nucleophiles attack the metal center in $[\eta^2(N,C)$-2,4,6-$NC_5{}^tBu_3H_2]Ta(OAr)_2Cl$ *first*, followed by their *intra*molecular migration to C_α of the η^2-pyridine to induce ring opening.[42] This migration reaction affords a unique opportunity to examine the mechanistic aspects of an elusive C–N bond cleavage and perhaps elucidate the metal's role in this process more clearly. In this paper,

Scheme 1

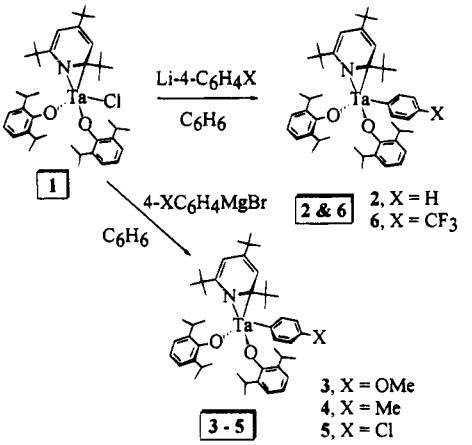

we report the preparations and properties of the aryl complexes $[\eta^2(N,C)$-2,4,6-$NC_5{}^tBu_3H_2]Ta(OAr)_2(4\text{-}C_6H_4X)$ and our use of these species to examine the mechanistic details of C–N bond cleavage.

Results

Reactions of an $\eta^2(N,C)$-Pyridine Complex with Aryl Nucleophiles. Upon reaction of $[\eta^2(N,C)$-2,4,6-$NC_5{}^tBu_3H_2]Ta(OAr)_2Cl$ (**1**, Ar = 2,6-$C_6H_3{}^iPr_2$) with 1 equiv of PhLi, a maroon oil is obtained from which dark red crystals of complex **2** can be isolated in moderate yield, Scheme 1. On the basis of the spectroscopic and analytical properties of this species, complex **2** is formulated as the phenyl derivative $[\eta^2(N,C)$-2,4,6-$NC_5{}^tBu_3H_2]Ta(OAr)_2Ph$. The room-temperature ^1H NMR spectrum of **2** reveals inequivalent ring protons of the $NC_5{}^tBu_3H_2$ ligand, supporting the preservation of its $\eta^2(N,C)$ bonding mode upon phenyl substitution. Upon heating solutions of **2** to ca. 100 °C (toluene-d_8), the $NC_5{}^tBu_3H_2$ ring protons become equivalent by a process that does not involve $NC_5{}^tBu_3H_2$ dissociation from the metal center, since this ligand does not exchange with pyridine, indicating that the $\eta^2(N,C)$ bonding mode is not static at this temperature. We propose that at higher temperatures a "ring rocking" process ensues by which pyridine *ortho* carbons sequentially coordinate and then dissociate from the metal, as suggested in eq 1. The related alkyl complexes $[\eta^2(N,C)$-2,4,6-$NC_5{}^tBu_3H_2]Ta(OAr)_2R$ (R = Et, ^{n}Pr, ^{n}Bu, CH_2SiMe_3) show similar spectroscopic properties, although the pyridine ligand of $[\eta^2(N,C)$-2,4,6-$NC_5{}^tBu_3H_2]Ta(OAr)_2Me$ ring rocks at room temperature.[42] Likely intermediates or transition states in this process have been discussed.[42]

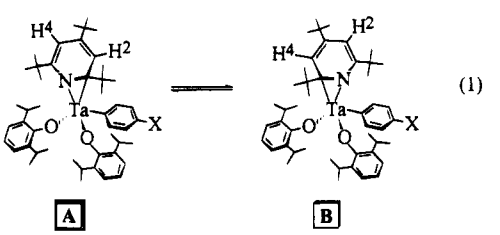

(1)

The *para*-substituted phenyl derivatives $[\eta^2(N,C)$-2,4,6-$NC_5{}^tBu_3H_2]Ta(OAr)_2(4\text{-}C_6H_4X)$, where X = OMe (**3**), Me (**4**), Cl (**5**), and CF_3 (**6**), are all prepared similarly from **1** and the appropriate aryl Grignard or lithium reagent, Scheme 1. Attempts to prepare the 4-C_6H_4-

(12) Satterfield, C. N.; Modell, M.; Wilkers, J. A. *Ind. Eng. Chem. Process Des. Dev.* **1980**, *19*, 154.
(13) Satterfield, C. N.; Yang, S. H. *Ind. Eng. Chem. Process Des. Dev.* **1984**, *23*, 11.
(14) Laine, R. M. *New J. Chem.* **1987**, *11*, 543.
(15) Satterfield, C. N.; Cocchetto, J. F. *Ind. Eng. Chem. Process Des. Dev.* **1981**, *20*, 53.
(16) Olalde, A.; Perot, G. *Appl. Catal.* **1985**, *13*, 373.
(17) Satterfield, C. N.; Modell, M.; Hites, R. A.; Declerck, C. J. *Ind. Eng. Chem. Process Des. Dev.* **1978**, *17*, 141.
(18) Yang, S. H.; Satterfield, C. N. *J. Catal.* **1983**, *81*, 168.
(19) Yang, S. H.; Satterfield, C. N. *Ind. Eng. Chem. Process Des. Dev.* **1984**, *23*, 20.
(20) Satterfield, C. N.; Smith, C. M.; Ingalls, M. *Ind. Eng. Chem. Process Des. Dev.* **1985**, *24*, 1000.
(21) Satterfield, C. N.; Gültekin, S. *Ind. Eng. Chem. Process Des. Dev.* **1981**, *20*, 62.
(22) Vivier, L.; Dominguez, V.; Perot, G.; Kasztelan, S. *J. Mol. Catal.* **1991**, *67*, 267.
(23) Allen, K. D.; Bruck, M. A.; Gray, S. D.; Kingsborough, R. P.; Smith, D. P.; Weller, K. J.; Wigley, D. E. *Polyhedron* **1995**, *14*, 3315.
(24) Spies, G. H.; Angelici, R. J. *Organometallics* **1987**, *6*, 1897.
(25) Ogilvy, A. E.; Skaugset, A. E.; Rauchfuss, T. B. *Organometallics* **1988**, *7*, 1171.
(26) Chen, J.; Daniels, L. M.; Angelici, R. J. *J. Am. Chem. Soc.* **1990**, *112*, 199.
(27) Chen, J.; Daniels, L. M.; Angelici, R. J. *Polyhedron* **1990**, *9*, 1883.
(28) Chen, J.; Daniels, L. M.; Angelici, R. J. *J. Am. Chem. Soc.* **1991**, *113*, 2544.
(29) Jones, W. D.; Dong, L. *J. Am. Chem. Soc.* **1991**, *113*, 559.
(30) Dong, L.; Duckett, S. B.; Ohman, K. F.; Jones, W. D. *J. Am. Chem. Soc.* **1992**, *114*, 151.
(31) Jones, W. D.; Chin, R. M. *Organometallics* **1992**, *11*, 2698.
(32) Bianchini, C.; Meli, A.; Peruzzini, M.; Vizza, F.; Frediani, P.; Herrera, V.; Sanchez-Delgado, R. A. *J. Am. Chem. Soc.* **1993**, *115*, 2731.
(33) Gray, S. D.; Smith, D. P.; Bruck, M. A.; Wigley, D. E. *J. Am. Chem. Soc.* **1992**, *114*, 5462.
(34) Kabir, S. E.; Day, M.; Irving, M.; McPhillips, T.; Minassian, H.; Rosenberg, E.; Hardcastle, K. I. *Organometallics* **1991**, *10*, 3997.
(35) Laine, R. M.; Thomas, D. W.; Cary, L. W. *J. Am. Chem. Soc.* **1982**, *104*, 1763.
(36) Adams, R. D.; Chen, G. *Organometallics* **1992**, *11*, 3510.
(37) Adams, R. D.; Chen, G. *Organometallics* **1993**, *12*, 2070.
(38) Adams, R. D.; Chen, L.; Wu, W. *Organometallics* **1993**, *12*, 4962.
(39) Hiraki, K.; Matsunaga, T.; Kawano, H. *Organometallics* **1994**, *13*, 1878.
(40) Hagadorn, J. R.; Arnold, J. *Organometallics* **1994**, *13*, 4670.
(41) Gray, S. D.; Fox, P. A.; Kingsborough, R. P.; Bruck, M. A.; Wigley, D. E. *ACS Prepr. Div. Petrol. Chem.* **1993**, *39*, 706.
(42) Gray, S. D.; Weller, K. J.; Bruck, M. A.; Briggs, P. M.; Wigley, D. E. *J. Am. Chem. Soc.*, in press.

NO_2 complex from **1** and Li-4-$C_6H_4NO_2$ resulted in the decomposition of **1** and rapid darkening of the solution, a feature that is probably related to the nitro group since **1** also decomposes in the presence of 4-$ClC_6H_4NO_2$. Compounds **3**–**6** are typically isolated as dark red solids in moderate yield, and like complex **2**, the pyridine ring protons of **3**–**6** can also be equilibrated at elevated temperatures.

Compounds **2**–**6** are proposed to have structures similar to structurally characterized [$\eta^2(N,C)$-2,4,6-NC_5-^{t}Bu$_3$H$_2$]Ta(OAr)$_2$Et[42] in which the short Ta–N and Ta–C_α distances and the long N–C_α bond support a formal Ta(V) "metallaaziridine" description of these species, as depicted in Scheme 1.[43–46] A 1,3-diene type π electron localization in the η^2 pyridine ligand of **2**–**6** is also presumed, as the interruption in pyridine aromaticity of this same type is evident in all $\eta^2(N,C)$-pyridine complexes that have been structurally characterized, viz. [$\eta^2(N,C)$-NC_5H_5]Ta(OSi^{t}Bu$_3$)$_3$,[47,48] [$\eta^2(N,C)$-2,4,6-NC_5^{t}Bu$_3$H$_2$]Ta(OAr)$_2$Cl,[49] [$\eta^2(N,C)$-2,4,6-NC_5^{t}Bu$_3$H$_2$]Ta(OAr)$_2$(S^{t}Bu),[50] and the 6-methylquinoline derivatives [$\eta^2(N,C)$-$NC_{10}H_9$]Ta(OAr)$_3$(PMe$_3$)[23,33] and [$\eta^2(N,C)$-$NC_{10}H_9$]Ta(OAr)$_2$Cl(OEt$_2$).[23] A molecular orbital description of $\eta^2(N,C)$ bonding in hypothetical [$\eta^2(N,C)$-NC_5H_5]Ta(OH)$_3$ has been presented that is consistent with the Ta(V) metallaaziridine description.[48]

Thermolysis of the Aryl Derivatives [$\eta^2(N,C)$-2,4,6-NC_5^{t}Bu$_3$H$_2$]Ta(OAr)$_2$(4-C_6H_4X): Transition Metal-Mediated C–N Bond Cleavage. While aryl nucleophiles attack the metal center in [$\eta^2(N,C)$-2,4,6-NC_5^{t}Bu$_3$H$_2$]Ta(OAr)$_2$Cl (**1**) to afford compounds **2**–**6**, these species constitute the *kinetic* products of this system. Upon thermolysis of benzene solutions of **2** (80 °C, C_6D_6), the solution darkens, and after 2 d (approximately 1 half-life), the concentration of **2** has significantly diminished and a single, new complex **7** is observed. The ^{1}H NMR signals for the NC_5^{t}Bu$_3$H$_2$ ring protons that were equivalent at high temperatures in complex **2** are replaced by two, new singlets at δ 6.35 and 5.78 (C_6D_6) in **7** that cannot be rendered equivalent even at elevated temperatures (100 °C, toluene-d_8). On the basis of these NMR data and the precedent observed in the alkyl compounds, this new product is formulated as the C–N bond cleavage isomer, Ta[=NC^{t}Bu=CHC^{t}Bu=CHC^{t}BuPh](OAr)$_2$ (**7**), Scheme 2. Kinetic studies reveal that the **2** → **7** conversion is cleanly first order (*vide infra*), thereby advancing an *intra*molecular transfer of the phenyl group from metal to ligand. This observation implies a formal *endo* attack of the migrating alkyl on the underside of the $\eta^2(N,C)$-pyridine ligand. Similarly, kinetic studies and crossover experiments revealed a strictly intramolecular transfer of the methyl ligand from metal to ligand in the conversion of [$\eta^2(N,C)$-2,4,6-NC_5^{t}Bu$_3$H$_2$]Ta(OAr)$_2$Me to Ta[=NC^{t}Bu=CHC^{t}Bu=CHC^{t}BuMe](OAr)$_2$.[42] We note that ring rocking is rapid at temperatures where aryl transfer ensues.

Scheme 2

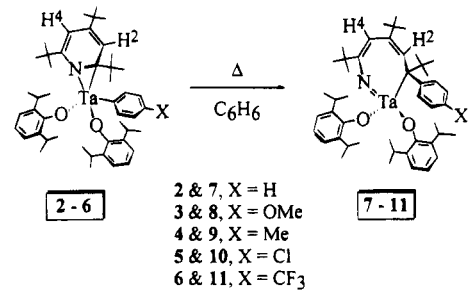

The other aryl derivatives [$\eta^2(N,C)$-2,4,6-NC_5^{t}Bu$_3$H$_2$]-Ta(OAr)$_2$(4-C_6H_4X) (**3**–**6**) all constitute kinetic products since, upon their thermolysis, aryl migration from metal to ligand occurs and the C–N bond-cleaved compounds Ta[=NC^{t}Bu=CHC^{t}Bu=CHC^{t}Bu(4-C_6H_4X)](OAr)$_2$ [X = OMe (**8**), Me (**9**), Cl (**10**), and CF_3 (**11**)] are formed.

Structural Study of Ta[=NC^{t}Bu=CHC^{t}Bu=CHC^{t}BuPh](OAr)$_2$ (7). Red-orange, single crystals of **7** suitable for an X-ray structural determination were grown from Et_2O/NCMe solutions at −35 °C. Tables 1 and 2 present details of the structural study and selected structural data, and Figures 1 and 2 present molecular and core structures of Ta[=NC^{t}Bu=CHC^{t}Bu=CHC^{t}BuPh](OAr)$_2$. These data clearly demonstrate that the carbon–nitrogen bond of the $\eta^2(N,C)$-pyridine ligand in **2** has been cleaved upon rearrangement by phenyl migration to form **7**. Considering the Ta(V), metallaaziridine[43–46] description of pyridine bonding in [$\eta^2(N,C)$-2,4,6-NC_5^{t}Bu$_3$H$_2$]Ta(OAr)$_2$Ph (**2**), a formal *amido* nitrogen[47,48] has been converted into a formal *imido* linkage upon aryl migration. The formation of the strong metal–nitrogen multiple bond in **7** certainly contributes a major driving force for this reaction, as does the reduction in the C–N bond order that arises from $\eta^2(N,C)$ coordination of the pyridine.

The local coordination about tantalum is a distorted tetrahedron with L–Ta–L angles ranging from 90.4(2)° for N–Ta–C(1) to 117.1(1)° for C(1)–Ta–O(10); thus the small metallacycle bite angle allows all other L–Ta–L angles to increase above that expected for a tetrahedron. The imido Ta–N–C(5) bond angle of 145.3(3)° represents a strongly bent terminal imido ligand,[51] though this angle is not unusual for a chelating imide.[42,52,53] It seems reasonable to propose the Ta–N–C bend arises from the constraints of the metallacycle, yet despite this distortion the Ta–N bond length of 1.771(3) Å compares well with that of other d^0 Ta=NR functional groups.[51] The metallacycle is clearly π-localized as represented in Scheme 2, as revealed by the

(43) Durfee, L. D.; Fanwick, P. E.; Rothwell, I. P.; Folting, K.; Huffman, J. C. *J. Am. Chem. Soc.* **1987**, *109*, 4720.
(44) Mayer, J. M.; Curtis, C. J.; Bercaw, J. E. *J. Am. Chem. Soc.* **1983**, *105*, 2651.
(45) Durfee, L. D.; Hill, J. E.; Kerschner, J. L.; Fanwick, P. E.; Rothwell, I. P. *Inorg. Chem.* **1989**, *28*, 3095.
(46) Chiu, K. W.; Jones, R. A.; Wilkinson, G.; Gales, A. M. R.; Hursthouse, M. B. *J. Chem. Soc., Dalton Trans.* **1981**, 2088.
(47) Neithamer, D. R.; Párkányi, L.; Mitchell, J. F.; Wolczanski, P. T. *J. Am. Chem. Soc.* **1988**, *110*, 4421.
(48) Covert, K. J.; Neithamer, D. R.; Zonnevylle, M. C.; LaPointe, R. E.; Schaller, C. P.; Wolczanski, P. T. *Inorg. Chem.* **1991**, *30*, 2494.
(49) Smith, D. P.; Strickler, J. R.; Gray, S. D.; Bruck, M. A.; Holmes, R. S.; Wigley, D. E. *Organometallics* **1992**, *11*, 1275.
(50) Fox, P. A.; Bruck, M. A.; Wigley, D. E. Unpublished results.
(51) Wigley, D. E. *Prog. Inorg. Chem.* **1994**, *42*, 239.
(52) Minelli, M.; Kuhlman, R. L.; Shaffer, S. J.; Chiang, M. Y. *Inorg. Chem.* **1992**, *31*, 3891.
(53) Minelli, M.; Carson, M. R.; Whisenhunt, D. W., Jr.; Imhof, W.; Huttner, G. *Inorg. Chem.* **1990**, *29*, 4801.

Table 1. Details of the X-ray Diffraction Studies for Ta[=NC^{t}Bu=CHC^{t}Bu=CHC^{t}BuPh](OAr)$_2$ (7)

Crystal Parameters	
molecular formula	$C_{47}H_{68}NO_2Ta$
M_n	860.02
$F(000)$	892
cryst color	red orange
space group	triclinic $P\bar{1}$ (No. 2)
unit cell vol, Å^3	2222.6(2)
a, Å	10.713(7)
b, Å	10.812(6)
c, Å	19.545(7)
α, deg	82.54(4)
β, deg	83.06(4)
γ, deg	85.08(5)
Z	2
D(calc), g cm^{-3}	1.29
cryst dimens, mm	0.25 × 0.25 × 0.08
ω width, deg	0.30
abs coeff, cm^{-1}	24.8
data collcn temp, °C	23 ± 1
Data Collection	
diffractometer	Enraf-Nonius CAD4
monochromator	graphite crystal, incident beam
attenuator	Zr foil, factor 13.6
Mo Kα radiation, λ, Å	0.710 73
2θ range, deg	0−50
octants collcd	$+h,\pm k,\pm l$
scan type	$\omega-2\theta$
scan speed, deg min^{-1}	1−7
scan width, deg	0.8 + 0.340 tan θ
tot. no. of reflns measd	8266 (7807 unique)
corrs	Lorentz−polarization refln averaging (agreement on I = 2.0%) empirical abs (from 0.58 to 1.00 on I)
Solution and Refinement	
solution	Patterson method
refinement	full-matrix least-squares
reflns used in refinement; $I > 3\sigma(I)$	6657
params refined	460
R	0.025
R_w	0.033
esd of obs of unit weight	1.27
convergence, largest shift	0.01σ
Δ/σ(max), e/Å^3	0.85(6)
Δ/σ(min), e/Å^3	−0.12(6)
computer hardware	VAX
computer software	MolEN (Enraf-Nonius)

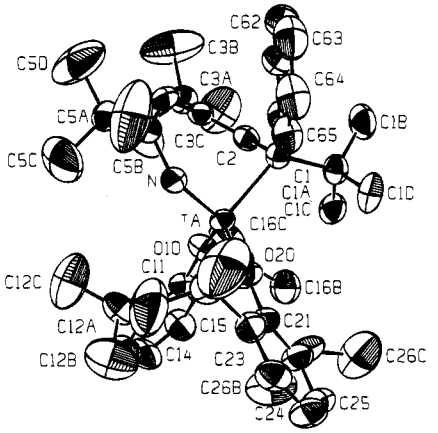

Figure 1. Molecular structure of Ta[=NC^{t}Bu=CHC^{t}Bu=CHC^{t}BuPh](OAr)$_2$ (**7**) with atoms represented as 50% ellipsoids.

alternating long and short bonds and the torsional angles about the metallacycle, Table 2. Thus, torsional

Table 2. Selected Bond Distances (Å), Bond Angles (deg), and Torsional Angles (deg) in Ta[=NC^{t}Bu=CHC^{t}Bu=CHC^{t}BuPh](OAr)$_2$ (7)[a]

Bond Distances			
Ta−N	1.771(3)	C(3)−C(4)	1.476(6)
Ta−C(1)	2.185(4)	C(4)−C(5)	1.334(6)
Ta−O(10)	1.914(3)	C(5)−N	1.388(6)
Ta−O(20)	1.875(3)	O(20)−C(21)	1.373(5)
C(1)−C(2)	1.494(6)	O(10)−C(11)	1.365(5)
C(2)−C(3)	1.370(6)		
Bond Angles			
Ta−N−C(5)	145.3(3)	N−Ta−O(10)	116.2(2)
Ta−C(1)−C(2)	85.3(3)	N−Ta−O(20)	110.7(2)
Ta−C(1)−C(1A)	116.2(3)	C(1)−Ta−O(10)	117.1(1)
Ta−C(1)−C(60)	116.1(3)	C(1)−Ta−O(20)	110.0(2)
C(2)−C(1)−C(1A)	111.1(3)	O(10)−Ta−O(20)	110.9(1)
C(2)−C(1)−C(60)	115.3(4)	C(1)−C(2)−C(3)	132.6(4)
C(1A)−C(1)−C(60)	110.8(4)	C(2)−C(3)−C(4)	125.5(4)
Ta−O(10)−C(11)	149.0(3)	C(3)−C(4)−C(5)	125.2(4)
Ta−O(20)−C(21)	175.2(3)	N−C(5)−C(4)	117.0(4)
N−Ta−C(1)	90.4(2)		
Torsional Angles			
Ta−C(1)−C(2)−C(3)		77.81(47)	
C(1)−C(2)−C(3)−C(4)		3.84(72)	
C(1)−C(2)−C(3)−C(3A)		175.51(41)	
C(2)−C(3)−C(4)−C(5)		46.46(66)	
C(3)−C(4)−C(5)−N		5.42(65)	
C(3)−C(4)−C(5)−C(5A)		175.72(42)	
C(4)−C(5)−N−Ta		2.56(74)	
C(5)−N−Ta−C(1)		45.72(52)	
N−Ta−C(1)−C(2)		78.51(24)	

[a] Numbers in parentheses are estimated standard deviations in the least significant digits.

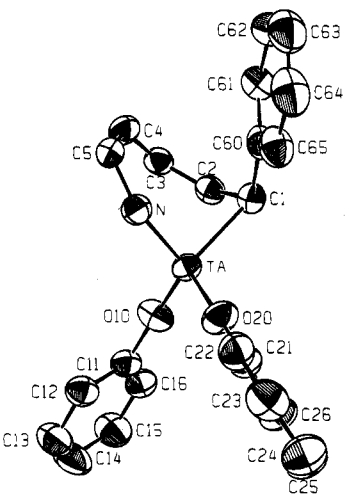

Figure 2. Core molecular structure of Ta[=NC^{t}Bu=CHC^{t}Bu=CHC^{t}BuPh](OAr)$_2$ (**7**) with atoms represented as 50% ellipsoids.

angles about the C(2)−C(3) and C(4)−C(5) bonds are close to 0 and 180° as expected for C=C double bonds.

Mechanistic Considerations of C−N Bond Cleavage: *Endo- vs Exo*-Attack of the $\eta^2(N,C)$-Pyridine Ligand. The simplest scenario for C−N bond cleavage in the **2** → **7** reaction involves an *endo* transfer of the aryl ligand from the metal to the η^2-pyridine. However, an examination of the molecular structure of **7** reveals that the phenyl group has apparently added to the face of the pyridine ligand directed *away* from the metal center, Figures 1 and 2. Thus it *appears* as if an *exo* addition to the pyridine has occurred with one molecule of **2** serving as a delivery agent to add a phenyl ligand

Scheme 3

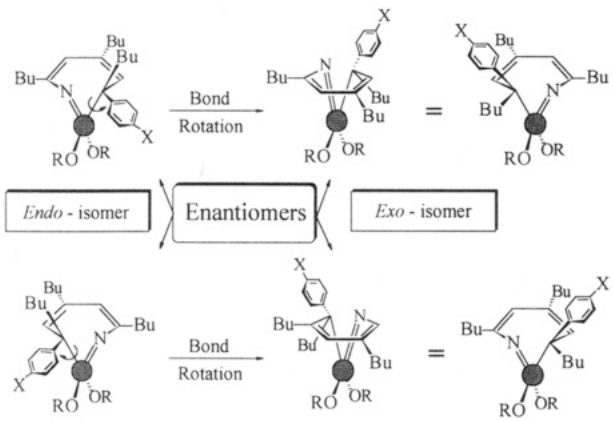

Table 3. Rate Data and Activation Parameters for the Thermal Decomposition of $[\eta^2(N,C)$-2,4,6-$NC_5{}^tBu_3H_2]Ta(OAr)_2(4\text{-}C_6H_4OMe)$ (3) to $Ta[=NC^tBu{=}CHC^tBu{=}CHC^tBu(4\text{-}C_6H_4OMe)](OAr)_2$ (8) in C_6D_5Br

Rate Data	
T, °C	10^4k, s^{-1}
140	6.4 ± 0.2
130	3.6 ± 0.1
118	2.0 ± 0.1
100	0.46 ± 0.01

Activation Parameters at 25 °C	
param	value
$\Delta H^‡$	+19.2 ± 1.3 kcal mol^{-1}
$\Delta S^‡$	−27 ± 4 cal K^{-1} mol^{-1}
$\Delta G^‡$	+27.3 ± 1.3 kcal mol^{-1}

to the top (*exo*) face of an η^2-pyridine ligand of a neighboring molecule.

However, kinetic studies of the **2** → **7** rearrangement reveal *intramolecular*, *endo* attack of the migrating phenyl group on the $\eta^2(N,C)$-pyridine (*vide infra*). This apparent discrepancy is readily understood by noting that *endo* attack is not ruled out from the molecular structure of **7**: simple rotation about the Ta−C(1) bond and the Ta−N−C(5) linkage of the metallacycle of the *endo* addition product, brought about by an "envelope ring flip", results in a nominal *exo* addition structure. This process is represented for both enantiomers of **7** in Scheme 3 and clearly indicates how an apparent *exo* addition product can arise from an *endo* transfer of the pyridine ligand. We conclude therefore that the most stable solid-state structure of $Ta[=NC^tBu{=}CHC^tBu{=}CHC^tBuPh](OAr)_2$ is generated by rearranging the kinetic *endo* addition isomer.

Mechanistic Studies of the Metal-to-Ligand Aryl Migration in the Conversion of $[\eta^2(N,C)$-2,4,6-$NC_5{}^tBu_3H_2]Ta(OAr)_2(4\text{-}C_6H_4X)$ to $Ta[=NC^tBu{=}CHC^tBu{=}CHC^tBu(4\text{-}C_6H_4X)](OAr)_2$. Thermolysis of the *para*-substituted phenyl derivatives $[\eta^2(N,C)$-2,4,6-$NC_5{}^tBu_3H_2]Ta(OAr)_2(4\text{-}C_6H_4X)$ (**2**−**6**) were examined in kinetic studies under conditions outlined in the Experimental Section. Table 3 summarizes first-order rate constants for the disappearance of $[\eta^2(N,C)$-2,4,6-$NC_5{}^tBu_3H_2]Ta(OAr)_2(4\text{-}C_6H_4OMe)$ (**3**) over several temperatures (in C_6D_5Br) along with calculated activation parameters for aryl migration in this complex. Table 4 presents rate data for the disappearence of the series of *para*-substituted phenyl derivatives $[\eta^2(N,C)$-2,4,6-$NC_5{}^tBu_3H_2]Ta(OAr)_2(4\text{-}C_6H_4X)$, along with the Hammett σ_p parameter for each substituent.

Table 4. Hammett σ_p Constants and Rate Data for the Thermal Decomposition of the Substituted Phenyl Derivatives $[\eta^2(N,C)$-2,4,6-$NC_5{}^tBu_3H_2]Ta(OAr)_2(4\text{-}C_6H_4X)$ (2−6) at 80 °C in C_6D_6

Rate Data			
X	σ_p[a]	10^6k, s^{-1}	R^2
OMe	−0.27	7.40 ± 0.17	0.992
Me	−0.17	6.98 ± 0.16	0.990
H	0	4.26 ± 0.07	0.994
Cl	+0.23	4.35 ± 0.09	0.991
CF_3	+0.54	2.40 ± 0.06	0.989

Hammett Parameter	
ρ	−0.58 ± 0.10

[a] From ref 54.

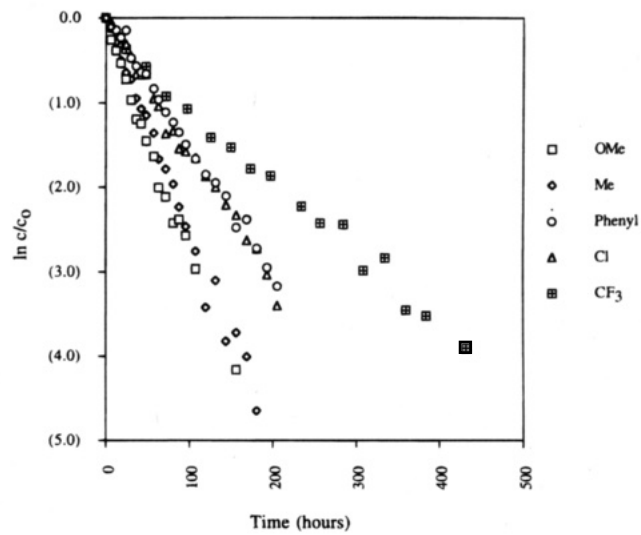

Figure 3. First-order kinetic plots for aryl migration in $[\eta^2(N,C)$-2,4,6-$NC_5{}^tBu_3H_2]Ta(OAr)_2(4\text{-}C_6H_4X)$ to form $Ta[=NC^tBu{=}CHC^tBu{=}CHC^tBu(4\text{-}C_6H_4X)](OAr)_2$ (for X = OMe, Me, H, Cl, and CF_3).

The disappearance of complexes **2**−**6** follows first-order kinetics as indicated in the plot of $\ln[c/c_{t=0}]$ vs time in Figure 3. Rate constants for these reactions exhibit only a moderate increase in the rate of aryl migration as the *para*-substituent in $4\text{-}C_6H_4X$ becomes more electron-donating, Table 4. The fastest aryl migration occurs in $[\eta^2(N,C)$-2,4,6-$NC_5{}^tBu_3H_2]Ta(OAr)_2(4\text{-}C_6H_4OMe)$ (**3**); therefore, the **3** → **8** reaction was examined over a range of temperatures. An Eyring plot for the disappearance of **3** provides activation parameters of $\Delta H^‡ = +19.2 \pm 1.3$ kcal mol^{-1} and $\Delta S^‡ = -27 \pm 4$ cal K^{-1} mol^{-1}, for a $\Delta G^‡ = +27.3 \pm 1.3$ kcal mol^{-1} at 25 °C. The large, negative entropy of activation supports a highly ordered transition state leading to aryl migration, consistent with an intramolecular ligand transfer that requires a confined ligand arrangement in the activation step. The large *entropic* barrier to initiate C−N bond cleavage presumably arises since bond scission occurs from only one of the two $\eta^2(N,C)$ isomers that equilibrate *via* ring rocking, viz. structure **A** (eq 1) with proximate C_α and aryl groups.

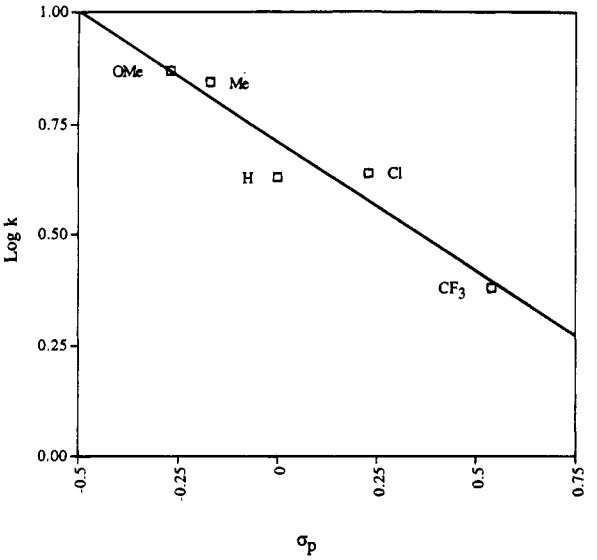

Figure 4. Hammett plot for aryl migration in $[\eta^2(N,C)$-2,4,6-$NC_5{}^tBu_3H_2]Ta(OAr)_2(4\text{-}C_6H_4X)$ to form $Ta[{=}NC{}^tBu{=}CHC{}^tBu{=}CHC{}^tBu(4\text{-}C_6H_4X)](OAr)_2$ (for X = OMe, Me, H, Cl, and CF_3) at 80 °C in C_6D_6.

Scheme 4

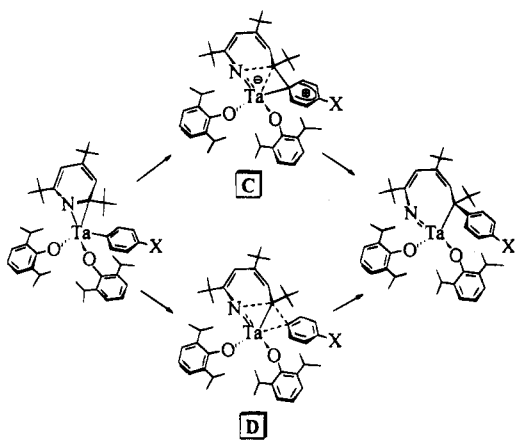

A plot of log k vs the Hammett constants σ_p for aryl migration in the $[\eta^2(N,C)$-2,4,6-$NC_5{}^tBu_3H_2]Ta(OAr)_2(4\text{-}C_6H_4X)$ series **2**–**6** gives a reasonably linear fit with $\rho = -0.58 \pm 0.10$ as presented in Figure 4. While the *sign* of ρ is in agreement with an electrophilic aromatic substitution at the migrating aryl ligand, the small value of ρ argues against this pathway and against the involvement of the aryl π framework during migration. Most electrophilic aromatic substitutions that involve Wheland intermediates such as **C** in Scheme 4 are typically characterized by values of ρ from ca. -2 to -12.[54,55] This observation, along with the fact that the *alkyl* complexes $[\eta^2(N,C)$-2,4,6-$NC_5{}^tBu_3H_2]Ta(OAr)_2R$ (R = Me, Et, ^{n}Pr, ^{n}Bu) undergo a similar ligand migration, also argues against a classic, electrophilic aromatic substitution at the migrating aryl ligand as depicted by **C**.[55] While ligand migration is relatively insensitive to the nature of the *para*-substituent, C–N bond scission by migration of the aryl group as a nucleophile, in particular as a *σ-nucleophile* as suggested by transition state **D**, is nevertheless indicated, Scheme 4.[56]

Scheme 5

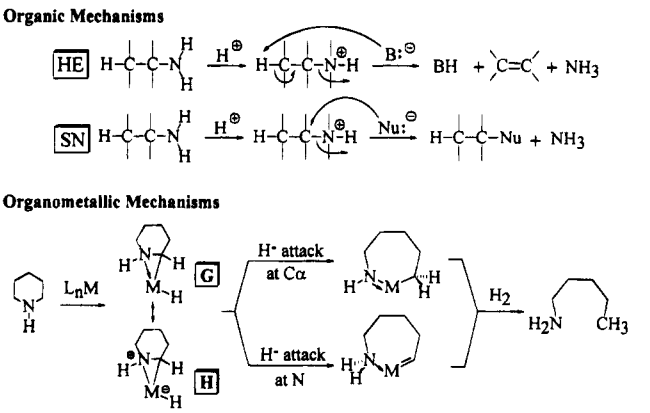

Discussion

Despite its importance in producing high-quality, low-cost fuels and in upgrading petroleum feedstocks, HDN catalysis is significantly less well-studied than HDS.[1,4,5] As a result, the mechanism of the C–N bond scission step in HDN and the metal's role in promoting this step remain unsettled.[2,57] Therefore, an examination of our HDN model in view of proposed mechanisms of C–N cleavage is instructive and allows us to draw some conclusions regarding the relevance of our system to HDN catalysis.

Quinoline is a prototypical HDN substrate that has proved particularly valuable in HDN model studies. It has been shown—primarily on the basis of product analyses—that over a range of conditions it is necessary to hydrogenate both the heterocyclic and carbocyclic rings in order to cleave both C–N bonds of quinoline.[2,3,15–17,22,58] Satterfield and co-workers have established that H_2S (formed in HDS reactions) *enhances* the rate of quinoline HDN, leading to the proposal of either a Hofmann elimination (HE), with SH^- serving as base, or a nucleophilic substitution (SN), with SH^- acting as nucleophile, as the principal mechanisms of C–N bond scission, Scheme 5.[2,3,7,8,17–22] Laine has discussed a similar finding.[59]

(54) Lowry, T. H.; Richardson, K. S. *Mechanism and Theory in Organic Chemistry*, 3rd ed.; Harper & Row: New York, 1987.

(55) Resonance structure **C** is proposed as the best representation of a possible Wheland intermediate in which the C_α–N bond is being broken while the Ta=N multiple bond is being formed. Therefore, **C** is perhaps best considered a resonance structure arising from contributions of both **E** and **F** shown as follows:

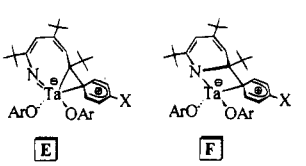

In Wheland intermediate **E**, the C_α–N bond has been cleaved, whereas in intermediate **F** the C_α–Ta bond is broken.

(56) Our terminology σ nucleophile (vs π nucleophile) is used to distinguish between transition states **C** vs **D** in Scheme 4 and should not be confused with the "σ complex" vs "π complex" terminology to describe intermediates in a generalized mechanisms of electrophilic, aromatic substitution. Thus, both structures **C** and **D** represent "σ complexes" in the classic sense; however, **C** arises from the reactivity of the aryl ligand as a π nucleophile, while **D** arises from its reactivity as a σ nucleophile, without involvement of the aryl π system.

(57) Prins, R.; de Beer, V. H. J.; Somorjai, G. A. *Catal. Rev.—Sci. Eng.* **1989**, *31*, 1.

(58) Shih, S. S.; Katzer, J. R.; Kwart, H.; Stiles, A. B. *Am. Chem. Soc., Div. Pet. Chem. Prepr.* **1977**, *22*, 919.

Scheme 6

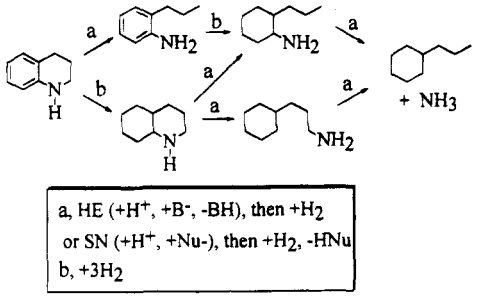

Unfortunately, few deliberations in the catalysis literature consider the participation of a metal center in discussing C−N bond scission mechanisms, though several metal-mediated C−N scission have recently been described.[36-40] Laine,[35] Adams,[36-38] and Rosenberg[34] have all uncovered C−N scission products at transition metal clusters from reactions that are not readily amenable to study. In particular, Laine and co-workers have shown that no C−N bond cleavage in tertiary amines occurs without the presence of a ruthenium catalyst,[35] a fact that led to the proposal that nucleophilic attack on a *coordinated* heterocycle is necessary to effect C−N bond scission.[7,8,14,60] Scheme 5 also outlines Laine's proposal for C−N bond cleavage in piperidine.[7] An important feature of Laine's proposal is the participation of an $\eta^2(N,C)$ piperidyl *amine* complex (**G** of Scheme 5) that is formed at the catalytic site. If the subsequent C−N bond cleavage results from hydride transfer to C_α, then formation of a ring-opened *amido* complex occurs. In our study, ligand migration and C−N scission in **1**−**6** transforms a formal *amido* nitrogen (in the metallaaziridine description) to a formal *imido* nitrogen in the ring-opened structure, which is simply a reflection of the saturation state of the pyridine ring. Whether the nature of the migrating hydrogen ligand in Laine's proposal is more hydridic $H^{\delta-}$ or acidic $H^{\delta+}$ throughout migration could not be specifically addressed in Laine's proposal. Our study provides a clear example of ring opening by migration of a σ nucleophile and therefore a model for hydride attack. Further similarities between the C−N bond cleavage we have observed with carbon nucleophiles and Laine's proposal for C−N scission have been detailed.[42]

In a recent mechanistic investigation particularly relevant to this study, Perot and co-workers obtained strong evidence that the SN mechanism is the major C−N cleavage pathway in tetrahydro*isoquinoline* (THIQ) HDN.[22,61] As suggested by Perot, an examination of HE vs SN pathways (Scheme 5) reveals that saturation and sp^3 hybridization at the carbon α to nitrogen is required for C−N scission by a nucleophilic substitution mechanism, while saturation at *both* C_α and C_β is required to effect C−N scission by a Hofmann elimination. Thus, hydrogenation of the carbocyclic ring of 1,2,3,4-tetrahydroquinoline (THQ) is required to cleave both C−N bonds of this compound by *either* mechanism, a feature consistent with propylcyclohexane as the principle product of quinoline HDN under a variety of conditions, Scheme 6.[61] However, Perot used this saturation difference between HE and SN reactions to distinguish between these pathways in the C−N cleavage reactions of 1,2,3,4-tetrahydro*iso*quinoline, Scheme 7.[22] Thus, the formation of any 2-ethyltoluene in tetrahydro*iso*quinoline HDN must arise from an SN mechanism of C−N bond cleavage from the sp^3 hybridization requirements described above, whereas 1-ethyl-2-methylcyclohexane will arise from HE chemistry, Scheme 7. The Perot experiment revealed that, under the same conditions that quinoline reacts to give primarily THQ, tetrahydroisoquinoline undergoes HDN to afford primarily 2-ethyltoluene, consistent with an SN mechanism of C−N bond cleavage in this compound. Perot notes that substitutions at the carbon α to nitrogen result in changes in the HDN product distribution, perhaps signaling a change in mechanism for the C−N scission step.[22]

Scheme 7

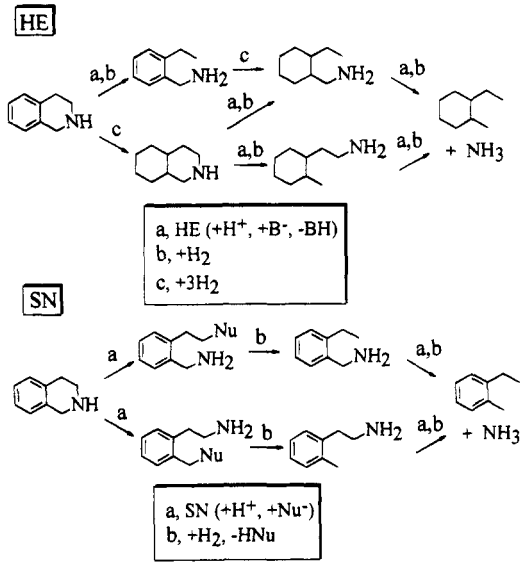

The overall reaction we have observed between the pyridine complex $[\eta^2(N,C)$-2,4,6-$NC_5{}^tBu_3H_2]Ta(OAr)_2Cl$ and an attacking carbon nucleophile (Schemes 1 and 2) can be partitioned into two stages: (1) nucleophilic attack at the metal center, followed by (2) nucleophilic migration to the η^2 ligand. In our model system, this migration is the rate-limiting step. The role of the metal center therefore is to mediate this process: it selectively activates the heterocyclic C−N bond and renders the pyridine C_α susceptible to nucleophilic attack. This nucleophilic designation is based upon a very slight rate enhancement in aryl migration using electron-donating substituents in the *para* position of the aryl ring. Nevertheless, our data are consistent with both nucleophilic attack of the migrating ligand on the pyridine C_α and with Perot's evidence for SN mechanisms in tetrahydroisoquinoline HDN.

Finally, we view our observations as a framework on which to unify the Laine and Perot theories of C−N scission in the following ways. As Laine suggests, substrate coordination is required, and we have found that $\eta^2(N,C)$ is the most relevant bonding mode since C−N bond cleavage has been observed only in $\eta^2(N,C)$-pyridine complexes. Furthermore, an *intra*molecular migration of the attacking nucleophile achieves C−N scission. Bonding the pyridine $\eta^2(N,C)$ allows the pyridine C_α (a formal sp^2 carbon) to attain sp^3 hybridiza-

(59) Hirschon, A. S.; Laine, R. M. *Fuel* **1985**, *64*, 868.
(60) Shvo, Y.; Laine, R. M. *J. Chem. Soc., Chem. Commun.* **1980**, 753.
(61) Perot, G. *Catal. Today* **1991**, *10*, 447.

tion and thereby renders this carbon subject to nucleophilic attack. If one considers the $\eta^2(N,C)$ piperidyl amine complex **G** ↔ **H** that is proposed by Laine, it is clear that the Lewis acidic, electrophilic metal center can take the place of H^+ in the classic nucleophilic substitution mechanism of Scheme 5, as indicated by structure **H**.[8] In this way, nucleophilic displacement of the C−N bonding electrons cleaves this bond while the N−metal bond is maintained; protonation of the substrate nitrogen is not necessary in this case since $\eta^2(N,C)$ binding serves the same purpose.

Conclusions

The results described in this report allow us to draw certain conclusions regarding one mechanism by which C−N bonds can be cleaved.

(1) The overall reaction between an $\eta^2(N,C)$-pyridine complex and an attacking nucleophile can be partitioned into two stages: nucleophilic attack at the metal center followed by ligand migration to the η^2 ligand. In our model system, this migration is rate-limiting.

(2) All available evidence indicates that the $\eta^2(N,C)$ bonding mode induces a *selective* activation of the heterocyclic C−N bond toward attack by the migrating ligand and that C−N bond scission invariably results from migration to the pyridine *carbon*, rather than nitrogen.

(3) The C−N bond scission reaction appears to be driven by, in large part, the formation of a strong metal−nitrogen multiple bond and the reduction in the pyridine C−N bond order that arises from its $\eta^2(N,C)$ coordination.

(4) Finally, C−N bond scission occurs unambiguously *via* an *intra*molecular, *endo* attack of the attacking aryl ligand that migrates to the HDN substrate as a σ *nucleophile*.

Experimental Section

General Details. All experiments were performed under a nitrogen atmosphere either by standard Schlenk techniques[62] or in a Vacuum Atmospheres HE-493 drybox at room temperature (unless otherwise indicated). Solvents were distilled under N_2 from an appropriate drying agent[63] and were transferred to the drybox without exposure to air. NMR solvents were passed down a short (6−8 cm) column of activated alumina prior to use. The "cold" solvents used to workup isolated products were typically cooled to −35 °C before use. Thermolyses were either conducted in sealed NMR tubes in an oil bath maintained at the specified temperature, in the NMR probe maintained at the specified temperature that had been calibrated using a thermocouple placed inside a 5 mm NMR tube, or in a refluxing still that was modified with a submerged, oil-containing side arm. Abbreviations: Ar = 2,6-$C_6H_3{}^iPr_2$.

Physical Measurements. ^1H (250 MHz) and ^{13}C (62.9 MHz) NMR spectra were recorded at probe temperature (unless otherwise specified) on a Bruker AM-250 or Varian Unity 300 spectrometer in C_6D_6 solvent; C_6D_5Br was used as NMR solvent in the variable-temperature experiments. Chemical shifts are referenced to protio impurities (δ 7.15 in C_6D_6) or solvent ^{13}C resonances (δ 128.0 in C_6D_6) and are reported downfield of Me_4Si. Carbon assignments were assisted by APT, DEPT, or gated $^{13}C\{^1H\}$-decoupled spectra. For ^1H and ^{13}C NMR assignments, numbering of the ring positions follows that shown in the X-ray structure of **2**, i.e. Ta[=N^5C^tBu=$^4CH^3C$-^tBu=$^2CH^1C^tBu$(4-C_6H_4X)] for the metallacycles and Ta[$\eta^2(N,C)$-N^5C^tBu=$^4CH^3C^tBu$=$^2CH^1C^tBu$] for the η^2-tri-*tert*-butylpyridine ligand. In most of the aryl complexes [$\eta^2(N,C)$-2,4,6-$NC_5{}^tBu_3H_2$]Ta$(OAr)_2$(4-C_6H_4X) (**2**−**6**), only two CMe_3 resonances were observed in the ^{13}C NMR spectrum; the higher field resonance most likely consists of two coincident signals. Microanalytical samples were handled under nitrogen and were combusted with WO_3 (Desert Analytics, Tucson, AZ).

Starting Materials. [$\eta^2(N,C)$-2,4,6-$NC_5{}^tBu_3H_2$]Ta$(OAr)_2$Cl (**1**) was prepared as previously described.[49] Solutions of PhLi (1.8 M in cyclohexane/Et_2O), 4-ClC_6H_4MgBr (1 M in Et_2O), 4-MeC_6H_4MgBr (1 M in Et_2O), and *n*-BuLi (1.6 M in hexanes) were obtained from Aldrich and used as received. 4-$MeOC_6H_4Br$ and 4-$BrC_6H_4CF_3$ were also obtained from Aldrich and used as received.

4-$MeOC_6H_4MgBr$. Solutions of 4-$MeOC_6H_4MgBr$ (1 M in THF) were prepared by reacting 4-$MeOC_6H_4Br$ with excess Mg in the appropriate volume of THF. The 4-$MeOC_6H_4MgBr$ solution was decanted from the excess Mg and used without further purification or standardization.

Li-4-$C_6H_4CF_3$. *Caution!! Solid samples of Li-4-$C_6H_4CF_3$ are shock sensitive and will explode violently upon gentle agitation! It is strongly recommended that Li-4-$C_6H_4CF_3$ be generated, used, and disposed of only in solution and that solid Li-4-$C_6H_4CF_3$* ***not*** *be isolated under any circumstances!*[64] Solutions of Li-4-$C_6H_4CF_3$ were prepared by a modification of the literature procedure.[64] A solution of *n*-BuLi (5.56 mL, 1.6 M in hexanes, 8.896 mmol) was slowly added to a stirred solution of 4-$BrC_6H_4CF_3$ (2.00 g, 8.89 mmol) in 35 mL of Et_2O, whereupon the solution turned from clear to yellow. This approximately 0.22 M Li-4-$C_6H_4CF_3$ solution was used without further purification or standardization. Fresh solutions of Li-4-$C_6H_4CF_3$ consistently gave the best results. Solutions of Li-4-$C_6H_4CF_3$ prepared in this manner turn progressively darker over a period of days, even when stored at −35 °C. *The authors of the literature procedure advise that Li-4-$C_6H_4CF_3$ "can only be handled safely when in solution or under hexane".*[64]

Preparations. [$\eta^2(N,C)$-2,4,6-$NC_5{}^tBu_3H_2$]Ta$(OAr)_2$Ph (2). A solution of PhLi (1.8 M in cyclohexane/Et_2O, 0.339 mL, 0.611 mmol) was slowly added to a rapidly stirred, room-temperature solution of [$\eta^2(N,C)$-2,4,6-$NC_5{}^tBu_3H_2$]Ta$(OAr)_2$Cl (**1**, 0.500 g, 0.610 mmol) in 10 mL of benzene. This mixture was stirred for 20 h after which time the reaction volatiles were removed under reduced pressure to yield a dark red oil. The oil was dissolved in cold pentane (ca. 20 mL) and filtered through Celite to remove the white solid that precipitated upon pentane addition. The resulting clear red filtrate was stripped of solvent to provide a maroon oil. This oil was dissolved in a minimal volume of diethyl ether (ca. 2 mL), ca. 20 mL of acetonitrile was added, and the solution was cooled to −35 °C. After 20 h the dark red crystals that had formed were collected on a frit and dried *in vacuo* to yield 0.256 g (0.298 mmol, 49%) of **2** as an analytically pure, red crystalline product. ^1H NMR (C_6D_6): δ 7.67 (d, 6.2 Hz, 2 H, H_o, C_6H_5), 7.19−6.92 (overlapping m, 9 H total, H_{aryl}, OAr; H_m and H_p, C_6H_5), 6.09 (br s, 1 H, C(2)H), 5.92 (br s, 1 H, C(4)H), 3.76, 3.48 (br spt, 2 H each, C*H*Me_2), 1.25−0.96 (br overlapping s and d, 51 H total, CHMe_2 and CMe_3). ^{13}C NMR (C_6D_6): δ 194.34 (C_{ipso}, C_6H_5), 169.21 (C(5), $NC_5{}^tBu_3H_2$), 157.41, 156.91 (C_{ipso}, OAr), 148.83 (C(3), $NC_5{}^tBu_3H_2$), 138.72, 138.12 (C_o, OAr), 136.13 (C_o, C_6H_5), 127.84 (C_m, C_6H_5), 127.62 (C_p, C_6H_5), 123.98, 123.71, 123.56, 123.48 (C_m and C_p, OAr), 109.18 (C(2), $NC_5{}^tBu_3H_2$), 106.39 (C(1), $NC_5{}^tBu_3H_2$), 103.37 (C(4), $NC_5{}^tBu_3H_2$), 41.70, 37.67, 34.64 (*C*Me_3), 30.44, 24.17, 24.11 (C*Me*$_3$), 27.25, 26.56 (*CH*Me_2), 29.55, 29.08 (CH*Me*$_2$). Anal. Calcd for $C_{47}H_{68}NO_2Ta$: C, 65.64; H, 7.97; N, 1.63. Found: C, 65.66; H, 7.93; N, 1.50.

(62) Shriver, D. F.; Drezdzon, M. A. *The Manipulation of Air-Sensitive Compounds*, 2nd ed.; John Wiley and Sons: New York, 1986.
(63) Perrin, D. D.; Armarego, W. L. F. *Purification of Laboratory Chemicals*, 3rd ed.; Pergamon Press: Oxford, U.K., 1988.
(64) Ladd, J. A.; Parker, J. *J. Chem. Soc., Dalton Trans.* **1972**, 930.

[η^2(*N,C*)-2,4,6-NC$_5$^{t}Bu$_3$H$_2$]Ta(OAr)$_2$(4-C$_6$H$_4$OMe) (3). The reaction of 4-MeOC$_6$H$_4$MgBr (1 M in THF, 0.670 mL, 0.670 mmol) with a benzene solution of [η^2(*N,C*)-2,4,6-NC$_5$^{t}Bu$_3$H$_2$]Ta(OAr)$_2$Cl (0.500 g, 0.611 mmol) for 40 h, according to the reaction and workup procedure outlined above for [η^2(*N,C*)-2,4,6-NC$_5$^{t}Bu$_3$H$_2$]Ta(OAr)$_2$Ph, afforded [η^2(*N,C*)-2,4,6-NC$_5$^{t}Bu$_3$H$_2$]Ta(OAr)$_2$(4-C$_6$H$_4$OMe) as a red oil. All attempts to crystallize this compound resulted in slight decomposition of the complex. However, analytically pure samples were obtained by triturating the oil several times with pentane to afford the product as a red powder that was collected by filtration and dried in vacuo; yield 0.314 g (0.354 mmol, 58%). ^{1}H NMR (C$_6$D$_6$): δ 7.75 (d, 7.8 Hz, 2 H, H$_o$, C$_6$H$_5$), 7.21−6.77 (overlapping m, 8 H total, H$_{aryl}$, OAr and H$_m$, C$_6$H$_5$), 6.06 (s, 1 H, C(2)H), 5.91 (s, 1 H, C(4)H), 3.51, 3.49 (br spt, 2 H each, C*H*Me$_2$), 3.23 (s, 3 H, OMe), 1.47−0.97 (br overlapping s and d, 51 H total, CH*Me*$_2$ and C*Me*$_3$). ^{13}C NMR (C$_6$D$_6$): δ 187.13 (C$_{ipso}$, 4-C$_6$H$_4$OMe), 169.05 (C(5), NC$_5$^{t}Bu$_3$H$_2$), 161.02 (C$_p$, 4-C$_6$H$_4$OMe), 157.56, 157.14 (C$_{ipso}$, OAr), 148.67 (C(3), NC$_5$^{t}Bu$_3$H$_2$), 138.76, 138.29 (C$_o$, OAr), 137.61 (C$_o$, 4-C$_6$H$_4$OMe), 123.96, 123.82, 123.71, 123.43 (C$_m$ and C$_p$, OAr), 113.27 (C$_m$, 4-C$_6$H$_4$OMe), 109.44 (C(2), NC$_5$^{t}Bu$_3$H$_2$), 106.52 (C(1), NC$_5$^{t}Bu$_3$H$_2$), 103.08 (C(4), NC$_5$^{t}Bu$_3$H$_2$), 54.47 (4-C$_6$H$_4$O*Me*), 41.60, 37.76, 34.65 (*C*Me$_3$), 30.42, 24.19 (C*Me*$_3$), 29.54, 29.07 (CH*Me*$_2$), 27.24, 26.61 (*C*HMe$_2$). Anal. Calcd for C$_{48}$H$_{70}$NO$_3$Ta: C, 64.78; H, 7.93; N, 1.57. Found: C, 64.94; H, 7.97; N, 1.87.

[η^2(*N,C*)-2,4,6-NC$_5$^{t}Bu$_3$H$_2$]Ta(OAr)$_2$(4-C$_6$H$_4$Me) (4). The reaction of MeC$_6$H$_4$MgBr (1 M in Et$_2$O, 0.805 mL, 0.805 mmol) with a benzene solution of [η^2(*N,C*)-2,4,6-NC$_5$^{t}Bu$_3$H$_2$]Ta(OAr)$_2$Cl (**1**, 0.600 g, 0.733 mmol), according to the reaction and workup procedure outlined above for [η^2(*N,C*)-2,4,6-NC$_5$^{t}Bu$_3$H$_2$]Ta(OAr)$_2$Ph, afforded [η^2(*N,C*)-2,4,6-NC$_5$^{t}Bu$_3$H$_2$]Ta(OAr)$_2$(4-C$_6$H$_4$Me) as a red oil that resisted repeated attempts at crystallization. However, solid product could be obtained by dissolving this oil in pentane and removing the solvent *in vacuo* (several times, if necessary) which afforded 0.270 g (0.309 mmol, 42%) of [η^2-(*N,C*)-2,4,6-NC$_5$^{t}Bu$_3$H$_2$]Ta(OAr)$_2$(4-C$_6$H$_4$Me) as an analytically pure solid. ^{1}H NMR (C$_6$D$_6$): δ 7.65 (d, 7.4 Hz, 2 H, H$_o$, 4-C$_6$H$_4$Me), 7.21−6.90 (overlapping m, 8 H total, H$_{aryl}$, OAr; H$_m$, 4-C$_6$H$_4$Me), 6.07 (s, 1 H, C(2)H), 5.92 (s, 1 H, C(4)H), 3.78, 3.48 (br spt, 2 H each, C*H*Me$_2$), 2.05 (s, 3 H, C$_6$H$_4$*Me*), 1.47−0.97 (br overlapping s and d, 51 H total, CH*Me*$_2$ and C*Me*$_3$). ^{13}C NMR (C$_6$D$_6$): δ 191.76 (C$_{ipso}$, 4-C$_6$H$_4$Me), 169.18 (C(5), NC$_5$^{t}Bu$_3$H$_2$), 157.58, 157.04 (C$_{ipso}$, OAr), 148.77 (C(3), NC$_5$^{t}Bu$_3$H$_2$), 138.73, 138.19 (C$_o$, OAr and coincident C$_p$, 4-C$_6$H$_4$Me), 136.12 (C$_o$, 4-C$_6$H$_4$Me), 128.50 (C$_m$, 4-C$_6$H$_4$Me), 123.96, 123.71, 123.56, 123.46 (C$_m$ and C$_p$, OAr), 109.18 (C(2), NC$_5$^{t}Bu$_3$H$_2$), 106.50 (C(1), NC$_5$^{t}Bu$_3$H$_2$), 103.19 (C(4), NC$_5$^{t}Bu$_3$H$_2$), 41.66, 37.69, 34.65 (*C*Me$_3$), 30.42, 24.14 (C*Me*$_3$), 29.57, 29.06 (CH*Me*$_2$), 27.24, 26.54 (*C*HMe$_2$), 21.63 (4-C$_6$H$_4$*Me*). Anal. Calcd for C$_{48}$H$_{70}$NO$_2$Ta: C, 65.96; H, 8.07; N, 1.60. Found: C, 65.63; H, 8.02; N, 1.71.

[η^2(*N,C*)-2,4,6-NC$_5$^{t}Bu$_3$H$_2$]Ta(OAr)$_2$(4-C$_6$H$_4$Cl) (5). The reaction of 4-ClC$_6$H$_4$MgBr (1 M in Et$_2$O, 0.850 mL, 0.850 mmol) with a benzene solution of [η^2(*N,C*)-2,4,6-NC$_5$^{t}Bu$_3$H$_2$]Ta(OAr)$_2$Cl (**1**, 0.600 g, 0.733 mmol), according to the reaction and workup procedure outlined above for [η^2(*N,C*)-2,4,6-NC$_5$^{t}Bu$_3$H$_2$]Ta(OAr)$_2$Ph, afforded [η^2(*N,C*)-2,4,6-NC$_5$^{t}Bu$_3$H$_2$]Ta(OAr)$_2$(4-C$_6$H$_4$Cl) as an analytically pure, red crystalline solid (yield 0.400 g, 0.447 mmol, 61%). ^{1}H NMR (C$_6$D$_6$): δ 7.49 (d, 7.9 Hz, 2 H, H$_o$, 4-C$_6$H$_4$Cl), 7.20 (d, 7.9 Hz, 2 H, H$_m$, 4-C$_6$H$_4$Cl), 7.08−6.83 (overlapping m, 6 H total, H$_{aryl}$, OAr), 6.05 (s, 1 H, C(2)H), 5.88 (s, 1 H, C(4)H), 3.68, 3.38 (br spt, 2 H each, C*H*Me$_2$), 1.47−0.92 (overlapping s and d, 51 H total, CH*Me*$_2$ and C*Me*$_3$). ^{13}C NMR (C$_6$D$_6$): δ 191.19 (C$_{ipso}$, 4-C$_6$H$_4$Cl), 169.13 (C(5), NC$_5$^{t}Bu$_3$H$_2$), 157.32, 156.78 (C$_{ipso}$, OAr), 148.94 (C(3), NC$_5$^{t}Bu$_3$H$_2$), 138.69, 137.74 (C$_o$, OAr, and coincident C$_o$, 4-C$_6$H$_4$Cl), 135.05 (C$_p$, 4-C$_6$H$_4$Cl), 127.87 (C$_m$, 4-C$_6$H$_4$Cl), 124.24, 124.04, 123.75 (C$_m$ and C$_p$, OAr; one resonance coincident), 109.27 (C(2), NC$_5$^{t}Bu$_3$H$_2$), 106.47 (C(1), NC$_5$^{t}Bu$_3$H$_2$), 103.49 (C(4), NC$_5$^{t}Bu$_3$H$_2$), 41.64, 37.60, 34.60 (*C*Me$_3$), 30.37, 24.07 (C*Me*$_3$), 29.48, 29.04 (CH*Me*$_2$), 27.24, 26.50 (*C*HMe$_2$). Anal. Calcd for C$_{47}$H$_{67}$ClNO$_2$Ta: C, 63.11; H, 7.55; N, 1.57. Found: C, 62.71; H, 7.59; N, 1.52.

[η^2(*N,C*)-2,4,6-NC$_5$^{t}Bu$_3$H$_2$]Ta(OAr)$_2$(4-C$_6$H$_4$CF$_3$) (6). The reaction of Li-4-C$_6$H$_4$CF$_3$ (*Caution!! See warning above!)* (0.22 M in Et$_2$O, 3.5 mL, 0.770 mmol) with a benzene solution of [η^2(*N,C*)-2,4,6-NC$_5$^{t}Bu$_3$H$_2$]Ta(OAr)$_2$Cl (0.569 g, 0.695 mmol), according to the reaction and workup procedure outlined above for [η^2(*N,C*)-2,4,6-NC$_5$^{t}Bu$_3$H$_2$]Ta(OAr)$_2$Ph, afforded [η^2(*N,C*)-2,4,6-NC$_5$^{t}Bu$_3$H$_2$]Ta(OAr)$_2$(4-C$_6$H$_4$CF$_3$) as a red oil. All attempts to crystallize this product provided an oil, accompanied by slight decomposition of the product. Therefore, pure samples were obtained by triturating the oil several times with pentane to afford [η^2(*N,C*)-2,4,6-NC$_5$^{t}Bu$_3$H$_2$]Ta(OAr)$_2$(4-C$_6$H$_4$-CF$_3$) as an analytically pure, red powder that was filtered off and dried in vacuo; yield 0.320 g (0.345 mmol, 50%). ^{1}H NMR (C$_6$D$_6$): δ 7.59 (d, J = 7.7 Hz, 2 H, H$_o$, 4-C$_6$H$_4$CF$_3$), 7.47 (d, J = 7.7 Hz, 2 H, H$_m$, 4-C$_6$H$_4$CF$_3$), 7.21−6.88 (overlapping m, 6 H total, H$_{aryl}$, OAr), 6.09 (s, 1 H, C(2)H), 5.89 (s, 1 H, C(4)H), 3.66, 3.31 (spt, 2 H each, C*H*Me$_2$), 1.48−0.88 (overlapping s and d, 51 H total, CH*Me*$_2$, OAr and C*Me*$_3$). ^{13}C NMR (C$_6$D$_6$): 197.16 (C$_{ipso}$, 4-C$_6$H$_4$CF$_3$), 169.25 (C(5), NC$_5$^{t}Bu$_3$H$_2$), 157.21, 156.80 (C$_{ipso}$, OAr), 148.98 (C(3), NC$_5$^{t}Bu$_3$H$_2$), 138.69, 137.74 (C$_o$, OAr), 136.79 (C$_o$, 4-C$_6$H$_4$CF$_3$), 124.46, 124.10, 123.77 (C$_m$ and C$_p$, OAr; one resonance coincident), 109.40 (C(2), NC$_5$^{t}Bu$_3$H$_2$), 106.65 (C(1), NC$_5$^{t}Bu$_3$H$_2$), 103.74 (C(4), NC$_5$^{t}Bu$_3$H$_2$), 41.66, 37.51, 34.58 (*C*Me$_3$), 30.37, 24.01 (C*Me*$_3$), 29.46, 29.04 (CH*Me*$_2$), 27.29, 26.48 (*C*HMe$_2$). Resonances assignable to C$_m$ (4-C$_6$H$_4$CF$_3$), C$_p$ (4-C$_6$H$_4$CF$_3$), or *C*F$_3$ were not located. Anal. Calcd for C$_{48}$H$_{67}$F$_3$NO$_2$Ta: C, 62.13; H, 7.28; N, 1.51. Found: C, 62.31; H, 7.32; N, 1.64.

Ta[=NC^{t}Bu=CHC^{t}Bu=CHC^{t}BuPh](OAr)$_2$ (7). An ampule (Teflon stopcock) was charged with 0.500 g (0.581 mmol) of [η^2(*N,C*)-2,4,6-NC$_5$^{t}Bu$_3$H$_2$]Ta(OAr)$_2$Ph (**2**) dissolved in 50 mL of toluene. The ampule was sealed, and the mixture was heated to 100 °C for 48 h during which time the solution became maroon in color. The reaction was cooled, and the volatiles were removed under reduced pressure to provide a dark maroon oil. This oil was dissolved in Et$_2$O (only ca. 2 mL) and acetonitrile (ca. 20 mL) and cooled to −35 °C. After 24 h the dark purple crystals that had formed were collected by filtration and dried *in vacuo* to afford 0.373 g (0.434 mmol, 75%) of Ta[=NC^{t}Bu=CHC^{t}Bu=CHC^{t}BuPh](OAr)$_2$ as a dark purple, analytically pure crystalline solid. This complex is also generated *in situ* upon thermolyzing [η^2(*N,C*)-2,4,6-NC$_5$^{t}Bu$_3$H$_2$]Ta(OAr)$_2$Ph as described in the text. ^{1}H NMR (C$_6$D$_6$): δ 8.10 (d, 2 H, H$_o$, C$_6$H$_5$), 7.40 (t, 1 H, H$_p$, C$_6$H$_5$), 7.17−6.80 (overlapping m, 8 H total, H$_{aryl}$, OAr; H$_m$, C$_6$H$_5$), 6.35 (s, 1 H, C(2)H), 5.78 (s, 1 H, C(4)H), 4.24, 3.77 (spt, 2 H each, C*H*Me$_2$), 1.35, 1.34, 1.25, 1.22 (overlapping d, 6 H each, CH*Me*$_2$), 1.10, 1.06, 0.83 (s, 9 H each, C*Me*$_3$). ^{13}C NMR (C$_6$D$_6$): δ 174.4, (C$_{ipso}$, C$_6$H$_5$), 165.2, 158.7, 155.8, 142.2, 139.4, 136.5, 136.3, 133.2, 126.2, 125.4, 124.8, 123.9, 123.6, 122.0, 121.4, 115.2, 109.8 (C$_{aryl}$, OAr and C$_6$H$_5$; C(1−5), metallacycle), 40.3, 36.9, 36.4 (*C*Me$_3$), 31.1, 30.3, 28.8, 26.9, 26.3, 24.6, 24.0, 23.5 (C*Me*$_3$, *C*HMe$_2$, and CH*Me*$_2$). Anal. Calcd for C$_{47}$H$_{68}$NO$_2$Ta: C, 65.64; H, 7.97; N, 1.63. Found: C, 65.92; H, 8.14; N, 1.72.

Ta[=NC^{t}Bu=CHC^{t}Bu=CHC^{t}Bu(4-C$_6$H$_4$OMe)](OAr)$_2$ (8). This complex is formed upon thermolyzing [η^2(*N,C*)-2,4,6-NC$_5$^{t}Bu$_3$H$_2$]Ta(OAr)$_2$(4-C$_6$H$_4$OMe) *in situ* as described in the text and was not isolated. ^{1}H NMR (C$_6$D$_6$): δ 8.04 (d, 2 H, H$_o$, 4-C$_6$H$_4$OMe), 7.17−6.78 (overlapping m, 8 H total, H$_{aryl}$, OAr; H$_m$, 4-C$_6$H$_4$OMe), 6.35 (s, 1 H, C(2)H), 5.79 (s, 1 H, C(4)H), 4.24, 3.78 (spt, 2 H each, C*H*Me$_2$), 3.44 (s, 3 H, 4-C$_6$H$_4$O*Me*), 1.34, 1.33, (overlapping d, 12 H total, CH*Me*$_2$), 1.25, 1.22 (overlapping d, 12 H total, CH*Me*$_2$), 1.14, 1.12, 0.87 (s, 9 H each, C*Me*$_3$). ^{13}C NMR (C$_6$D$_6$): δ 174.37 (C$_{ipso}$, 4-C$_6$H$_4$OMe), 165.31, 158.78, 158.06, 155.88, 139.40, 137.02, 136.32, 134.54, 134.00, 123.93, 123.58, 122.01, 121.33, 115.78, 111.95, 110.09, 109.73 (C$_{aryl}$, OAr and 4-C$_6$H$_4$OMe; C(1−5), metallacycle), 54.88

(4-C_6H_4OMe), 40.28, 37.10, 36.44 (CMe_3), 31.03, 30.57, 30.28, 28.82, 26.94, 26.34, 24.52, 23.99, 23.47 (CMe_3, $CHMe_2$, and $CHMe_2$).

Ta[=NC^{t}Bu=CHC^{t}Bu=CHC^{t}Bu(4-C_6H_4Me)](OAr)$_2$ (9). This complex is formed upon thermolyzing [$\eta^2(N,C)$-2,4,6-$NC_5{}^tBu_3H_2$]Ta(OAr)$_2$(4-C_6H_4Me) *in situ* as outlined in the text and was not isolated. ^{1}H NMR (C_6D_6): δ 8.03 (d, 2 H, H_o, 4-C_6H_4-Me), 7.24 (d, 2 H, H_m, 4-C_6H_4Me), 7.17–6.78 (overlapping m, 6 H total, H_{aryl}, OAr), 6.07 (s, 1 H, C(2)H), 5.92 (s, 1 H, C(4)H), 4.25, 3.77 (spt, 2 H each, $CHMe_2$), 2.28 (s, 3 H, 4-C_6H_4Me), 1.35 (d, 12 H each, $CHMe_2$), 1.25, 1.21 (d, 6 H each, $CHMe_2$), 1.13, 1.08, 0.85 (s, 9 H each, CMe_3).

Ta[=NC^{t}Bu=CHC^{t}Bu=CHC^{t}Bu(4-C_6H_4Cl)](OAr)$_2$ (10). This complex is formed upon thermolyzing [$\eta^2(N,C)$-2,4,6-$NC_5{}^tBu_3H_2$]Ta(OAr)$_2$(4-C_6H_4Cl) *in situ* as described in the text and was not isolated. ^{1}H NMR (C_6D_6): δ 8.00 (d, $J \sim 7$ Hz, 2 H, H_o, 4-C_6H_4Cl), 7.43 (d, $J \sim 7$ Hz, 2 H, H_m, 4-C_6H_4Cl), 7.17–6.62 (overlapping m, 6 H total, H_{aryl}, OAr), 6.27 (s, 1 H, C(2)H), 5.76 (s, 1 H, C(4)H), 4.16, 3.69 (spt, 2 H each, $CHMe_2$), 1.32–1.17 (overlapping d, 24 H total, $CHMe_2$), 1.04, 1.02, 0.81 (s, 9 H each, CMe_3).

Ta[=NC^{t}Bu=CHC^{t}Bu=CHC^{t}Bu(4-$C_6H_4CF_3$)](OAr)$_2$ (11). This complex is formed upon thermolyzing [$\eta^2(N,C)$-2,4,6-$NC_5{}^tBu_3H_2$]Ta(OAr)$_2$(4-$C_6H_4CF_3$) *in situ* as outlined in the text and was not isolated. ^{1}H NMR (C_6D_6): δ 8.12 (d, 2 H, H_o, 4-C_6H_4-CF_3), 7.70 (d, 2 H, H_m, 4-$C_6H_4CF_3$), ca. 7.38–6.73 (overlapping m, 6 H total, H_{aryl}, OAr), 6.26 (s, 1 H, C(2)H), 5.76 (s, 1 H, C(4)H), 4.14, 3.67 (spt, 2 H each, $CHMe_2$), ca. 1.33–0.95 (overlapping d, 24 H total, $CHMe_2$), ca. 1.18, 1.03, 0.76 (s, 9 H each, CMe_3).

Kinetic Experiments. Kinetics measurements of the cleavage reaction were obtained by monitoring the disappearance of the ^{1}H NMR resonances of the C(4)*H* or C(2)*H* protons of the $\eta^2(N,C)$ pyridine complexes **2** and **4–6** and were quantified by integration relative to $(Me_3Si)_2O$ as an internal standard. The kinetic data for the disappearance of **3** were obtained by monitoring the ^{1}H resonance of the 4-C_6H_4OMe protons. Although the disappearance of other resonances in the ^{1}H NMR spectra of complexes **2–6** and the appearance of various resonances in the ^{1}H NMR spectra of **7–11** were also examined, the disappearance data for C(4)*H* or C(2)*H* were found to be the most reproducible. The data recorded in Tables 3 and 4 report uncertainties as standard deviations of the slope of the $\ln[c/c_{t=0}]$ vs time plot from regression analysis. ^{1}H NMR spectra were recorded at timed intervals at 250 MHz using a Bruker AM250 spectrometer. NMR tubes were sealed under vacuum after three freeze/pump/thaw cycles to degas each sample. Reaction temperatures were maintained by placing NMR tubes in an oil-containing side arm that was immersed in refluxing benzene in a round bottom flask specially modified to incorporate the side arm. The samples were removed periodically, quenched by cooling, and examined by NMR. A typical experiment involved 45 mg of tantalum aryl compound in 0.5 mL of C_6D_6 solution containing 0.5% (by volume) of $(Me_3Si)_2O$ as an internal standard.

X-ray Structural Study of Ta[=NC^{t}Bu=CHC^{t}Bu=CHC^{t}BuPh](OAr)$_2$. A red-orange parallelpiped block crystal of Ta[=NC^{t}Bu=CHC^{t}Bu=CHC^{t}BuPh](OAr)$_2$ was crystallized from Et_2O/NCMe solution at −35 °C and was mounted in a glass capillary in a random orientation. Table 1 summarizes the crystal data and collection, solution, and refinement parameters for this sample. The space group was determined from the systematic absences and the subsequent least-squares refinement, and the structure was solved by the Patterson method. All non-hydrogen atoms were refined anisotropically. Hydrogen atoms were found in the difference maps but placed in ideal positions. Exceptions to this include H(2) and H(4); these atoms were taken directly from the difference map due to the unusual bond angles of the metallacycle.

Acknowledgment is made to the Division of Chemical Sciences, Office of Basic Energy Sciences, Office of Energy Research, U.S. Department of Energy (Grant DE-FG03-93ER14349) for support of this research.

Supporting Information Available: Text giving details of the structure solution and refinement, tables of crystal data and data collection parameters, atomic positional and thermal parameters, bond distances, bond angles, and least-squares planes, and ORTEP figures for Ta[=NC^{t}Bu=CHC^{t}Bu=CHC^{t}BuPh](OAr)$_2$ (22 pages). Ordering information is given on any current masthead page.

OM9506983

A Photochemical Route to Heterometallic Complexes. Synthesis and Structural Characterization of Di- and Trinuclear Complexes Having a Molybdenocene or Tungstenocene Unit

Takayuki Nakajima,[†] Takaya Mise,[‡] Isao Shimizu,[†] and Yasuo Wakatsuki*,[‡]

The Institute of Physical and Chemical Research (RIKEN), Wako-shi, Saitama 351-01, Japan, and Department of Applied Chemistry, School of Science and Engineering, Waseda University, 3-4-1 Ookubo, Shinjuku-ku, Tokyo 169, Japan

Received July 6, 1995[⊗]

Irradiation of a mixture of tungstenocene or molybdenocene dihydride and a metal–metal-bonded dimeric complex has been found to be a convenient route to homo- and heterometallic complexes. The photoreactions of $(\eta^5\text{-}C_5H_5)_2M^1H_2$ with $[(\eta^5\text{-}C_5H_5)M^2(CO)_3]_2$ (M^1, M^2 = W, Mo) in DME afford in good yields the bimetallic complexes $(\eta^5\text{-}C_5H_5)(CO)M^1(\mu,\sigma\text{-}\eta^5\text{-}C_5H_4)\text{-}M^2(CO)_2(\eta^5\text{-}C_5H_5)$ with a $M^1\text{–}M^2$ bond. (**1a**, M^1 = W, M^2 = Mo; **1b**, M^1 = Mo, M^2 = W; **1c**, $M^1 = M^2$ = W; **1d**, $M^1 = M^2$ = Mo). By use of $[(\eta^5\text{-}C_5R_5)Ni(CO)]_2$ as the dimer part, the heterobimetallic hydrides $(\eta^5\text{-}C_5H_5)_2M(\mu\text{-}H)(\mu\text{-}CO)Ni(C_5R_5)$ (**2a**, M = W, R = H; **2b**, M = W, R = Me; **2c**, M = Mo, R = H, **2d**, M = Mo, R = Me) were obtained, where the two metallocene cyclopentadienyl rings remain intact and the metal–metal bond is bridged by CO and hydride. Similar photolysis of a mixture of $(\eta^5\text{-}C_5H_5)_2MH_2$ and $[(\eta^5\text{-}C_5H_5)Ru(CO)_2]_2$ has afforded two trimetallic complexes: $(\eta^5\text{-}C_5H_5)(\mu,\sigma\text{-}\eta^5\text{-}C_5H_4)M(\mu\text{-}CO)_2Ru(\eta^5\text{-}C_5H_5)Ru(\eta^5\text{-}C_5H_5)\text{-}(CO)H$ (**3a**, M = W; **3b**, M = Mo), where the Ru–Ru bond still exists with a new M–Ru bond and one bridging $(\mu,\sigma\text{-}\eta^5\text{-}C_5H_4)$ ring between M and the other Ru, and $(\mu,\sigma\text{-}\eta^5\text{-}C_5H_4)_2\text{-}MH_2[(\eta^5\text{-}C_5H_5)Ru(CO)]_2$ (**4a**, M = W; **4b**, M = Mo), in which both of the cyclopentadienyl rings of the metallocene are metalated with Ru. The crystal and molecular structures of **1a**, **2d**, **3a**, and **4a** have been determined by single-crystal X-ray diffraction analysis.

In recent years heterometallic complexes have attracted considerable interest as the potential sites for cooperative reactions effected by different sorts of neighboring metals. A large number of heteronuclear metal–metal-bonded complexes have been known, and many synthetic approaches for them have been summarized and classified in the reviews by Roberts and Geoffroy[1] and Stephan.[2] Though synthetic methods for heterobimetallic complexes and triangular heterotrimetallic complexes are most extensively studied, that for open-chain framed hetero*tri*metallic complexes are much fewer with major rational synthetic methodologies being (1) substitution of the halide anions (X^-) in ML_nX_2 by an anionic metal complex or (2) ligand bridge-assisted substitution reactions.[1]

Photoactivation of Cp_2WH_2 (Cp = η^5-C_5H_5) has been reported to generate active tungstenocene [Cp_2W] species which can oxidatively add the C–H bond of solvent molecules (RH) to form $Cp_2W(R)(H)$.[3] If a similar oxidative addition of the metal–metal bond of an appropriatee $L_nM'\text{–}M'L_n$ complex can take place across the tungstenocene or molybdenocene, heterotrimetallic complexes of the form $(L_nM')\text{–}(Cp_2M)\text{–}(M'L_n)$ (M = W, Mo) may be expected. Alternatively, photolysis of the $L_nM'\text{–}M'L_n$ molecule might cleave the metal–metal bond to form a metal radical species[4] which could attack the metallocene dihydride to give a heterometallic complex. In any event, irradiation of a mixture of $Cp_2\text{-}MH_2$ (M = W, Mo) and a $L_nM'\text{–}M'L_n$ type complex seemed to be a reasonable system to produce new heterometallic compounds.

To examine this hypothesis we carried out several photoreactions of molybdenocene and tungstenocene dihydrides with dimeric metal complexes. Although some of the reactions ended up with the formation of bimetallic complexes, the present reaction system has been found to be useful in introducing a molybdenocene or tungstenocene unit into di- and trimetallic compounds. To the best of our knowledge, complexes possessing heteronuclear bonds between the molybdenocene or tungstenocene unit and other transition metals have only one precedent.[5]

Results and Discussion

W–Mo, W–W, and Mo–Mo Complexes. An equimolar amount of Cp_2WH_2 and $[CpMo(CO)_3]_2$ in 1,2-dimethoxyethane (DME) was irradiated with a high-pressure mercury lamp at room temperature until most

[†] Waseda University.
[‡] RIKEN.
[⊗] Abstract published in *Advance ACS Abstracts,* November 1, 1995.

(1) Roberts, D. A.; Geoffroy, G. L. In *Comprehensive Organometallic Chemistry*; Wilkinson, G., Stone, G., Abel, E. W., Eds.; Pergamon: New York, 1982; Vol. 6.
(2) Stephan, D. W. *Coord. Chem. Rev.* **1989**, *95*, 41.
(3) (a) Green, M. L. H. *Pure Appl. Chem.*, **1978**, *50*, 27. (b) Giannotti, C.; Green, M. L. H. *J. Chem. Soc., Chem. Commun.* **1972**, 1114. (c) Berry, M.; Elmitt, K.; Green, M. L. H. *J. Chem. Soc., Dalton Trans.* **1979**, 1950.
(4) (a) Wrighton, M. S.; Ginley, D. S. *J. Am. Chem. Soc.* **1975**, *97*, 2065. (b) Wrighton, M. S.; Ginley, D. S. *J. Am. Chem. Soc.* **1975**, *97*, 4246.
(5) Hoxmeier, R.; Deubzer, B.; Kaesz, H. D. *J. Am. Chem. Soc.* **1971**, *93*, 536.

0276-7333/95/2314-5598$09.00/0

of the tungstenocene dihydride was consumed (ca. 35 h), which was easily monitored by ^{1}H NMR spectra. Chromatography on an alumina column of the crude mixture gave dark red crystals which were not the expected trimetallic complex but turned out to be a heterobimetallic complex of the formula $Cp(C_5H_4)W-Mo(CO)_2Cp$ (**1a**) in 43% yield. The other half of the dimolybdenum unit obviously took up hydrogen since $CpMo(CO)_3H$ was detected in a reasonable amount when the reaction mixture was dried up and subjected to NMR measurement. Complex **1a** is air-stable in the crystalline form but begins to decompose gradually when kept in solution for a few days under argon. The ^{1}H NMR spectrum of **1a** shows two singlets with an integrated ratio equal to 10 protons, indicating the presence of two different Cp rings. The third cyclopentadienyl unit exhibits four protons which appear as four different multiplets. Subsequent characterization of this complex by a single-crystal X-ray diffraction analysis revealed the solid state structure shown in Figure 1. Crystal and data collection parameters are provided in Table 1, and selected bond distances and angles are tabulated in Table 2. One of the metallocene Cp rings has been metalated by molybdenum, and the two metals are directly bonded. To attain an 18-electron configuration, this metal–metal bond may be regarded as a dative bond from metallocene (W) to Mo. The W–Mo bond length of 3.069(2) Å is a little, but significantly, shorter than the Mo–Mo bond (3.089(1) Å) in the known analog (**1d**).[6] A similar trend has been observed in the metal–metal bond lengths in $[CpM(CO)_3]_2$: 3.222(1) Å for M = W and 3.235(1) Å for M = Mo.[7]

In the converse way, photolysis of a mixture of Cp_2MoH_2 and $[CpW(CO)_3]_2$ for 12 h gave the corresponding heterobimetallic complex $Cp(C_5H_4)Mo-W(CO)_2Cp$ (**1b**) in 42% yield. The reaction could also be applied to the syntheses of homobimetallic complexes of W and Mo: similar photoreactions of Cp_2MH_2 and $[CpM(CO)_3]_2$ in DME afforded $Cp(C_5H_4)M-M(CO)_2Cp$ (**1c**, M = W, 43%; **1d**, M = Mo, 56% yield). In all of these reactions, concomitant formation of the metal hydride $CpM(CO)_3H$ was confirmed by NMR spectra. The overall reaction may then be expressed as shown in eq 1.

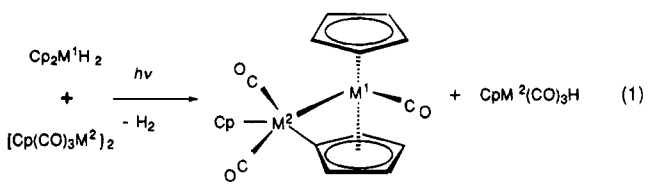

The homometallic complex **1d** has been prepared previously by two quite different methods, i.e. from $Mo_2(O_2CMe)_4$ and $Na(C_5H_5)/CO$,[6] and also by the reaction of $C_5H_4N_2$ with $Cp(CO)_2Mo{\equiv}Mo(CO)_2Cp$.[8] The very low terminal-carbonyl absorption of **1d** at 1765 cm^{-1} (mulls) has been assigned by Green et al.[6] to one of the

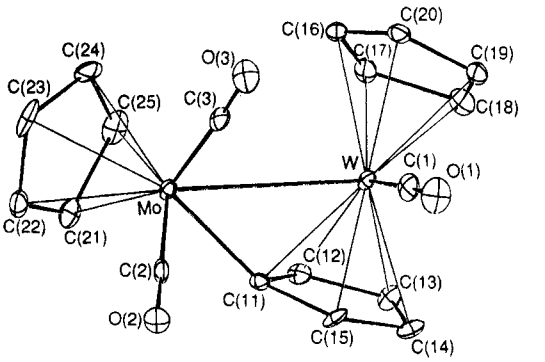

Figure 1. View of $Cp(C_5H_4)(CO)W-Mo(CO)_2Cp$ (**1a**) showing the atom-labeling scheme.

CO groups on M^2 and has been attributed to the strong dative bond from the molybdenocene unit (M^1), which causes accumulation of negative charge on M^2. In THF solutions, the present complexes exhibit three carbonyl stretching bands (**1a**, 1961, 1882, 1799; **1b**, 1971, 1880, 1790; **1c**, 1962, 1876, 1788; **1d**, 1970, 1887, 1803 cm^{-1}). Following the argument of Green et al., the two low-frequency bands may be assigned symmetric and asymmetric coupling of the two CO vibrations at M^2. Comparing the bands of **1a** with **1d**, and also **1b** with **1c**, we see the donation from tungstenocene unit is slightly stronger than that from molybdenocene.

W–Ni and Mo–Ni Complexes. The nickel dimer $[(\eta^5\text{-}C_5R_5)Ni(CO)]_2$ (R = H, Me) reacted successfully under the photolysis conditions with the metallocene dihydrides. Workup on an alumina column gave dark-red crystals of heterobimetallic complexes of the formula $Cp_2MH-Ni(CO)(\eta^5\text{-}C_5R_5)$ (**2a**, M = W, R = H, 56%; **2b**, M = W, R = Me, 23%; **2c**, M = Mo, R = H, 35%; **2d**, M = Mo, R = Me, 25% yield). Proton NMR spectra of these complexes indicated that the two metallocene Cp rings remain intact and magnetically equivalent. A peak with an intensity equivalent to one hydrogen was observed at δ −5.83 (**2a**), −6.47 (**2b**), −6.43 (**2c**), and −5.57 (**2d**) ppm. These complexes have a single carbonyl stretching absorption at the bridging carbonyl region, 1718–1755 cm^{-1}.

The crystal of **2d** has been characterized by X-ray analysis. The molecular structure with atom-labeling scheme is shown in Figure 2, and selected bond lengths and angles are listed in Table 3. The Mo–Ni distance is 2.657(1) Å indicating the presence of the metal–metal bond. For comparison, the Ni–Ni and Mo–Mo distances in $[CpNi(CO)]_2$[9] and $[CpMo(CO)_3]_2$[7] are 2.3627(9) and 3.235(1) Å, respectively. The hydride in complex **2d** could not be located from Fourier maps but must be present at the vacant site bridging the two metals. The Cp ring on Ni (C(21)–C(25)) is not perpendicular to the Mo–Ni vector but tilted, the angle between the Mo–Ni axis and the Cp(Ni) plane being 75°, and opens toward the bridging CO. Still there is enough space available for the hydride bridge opposite to the bridging CO. The metallocene wedge opens right to the direction of Ni. Reflecting the larger size of the molybdenum atom, the Mo–C(O) distance (2.226(4) Å) is much longer than the corresponding Ni–C(O) distance of 1.759(5) Å. The C–O vector is almost perpendicular to the Mo–Ni axis. In accord with this structure, the hydride ^{1}H NMR resonances of **2a**,**b** exhibit satellites due to ^{183}W ($|J_{W-H}|$

(6) Bashkin, J.; Green, M. L. H.; Poveda, M. L.; Prout, K. *J. Chem. Soc., Dalton Trans.* **1982**, 2485.
(7) Adams, R. D.; Collins, D. M.; Cotton, F. A. *Inorg. Chem.* **1974**, *13*, 1086.
(8) Herrmann, W. A.; Kriechbaum, G.; Bauer, C.; Guggolz, E.; Ziegler, M. L. *Angew. Chem., Int. Ed. Engl.* **1981**, 815.
(9) Byers, L. R.; Dahl, L. F. *Inorg. Chem.* **1980**, *19*, 680.

Table 1. Crystallographic Data for Complexes 1a, 2d, 3a, and 4a

	1a ($C_{18}H_{14}O_3MoW$)	**2d** ($C_{21}H_{26}OMoNi$)	**3a** ($C_{23}H_{20}O_3Ru_2W$)	**4a** ($C_{22}H_{20}O_2Ru_2W\cdot0.5C_7H_8$)
fw	558.1	449.1	730.5	748.5
cryst system	monoclinic	monoclinic	monoclinic	monoclinic
space group	$P2_1/n$	$P2_1/n$	$P2_1/c$	$P2_1/c$
a, Å	12.223(2)	15.026(2)	15.126(3)	9.848(3)
b, Å	15.229(2)	14.097(4)	11.956(2)	10.993(3)
c, Å	8.613(3)	9.085(2)	12.202(6)	21.658(6)
β, deg	92.27(2)	101.96(1)	112.78(2)	98.06(3)
V, Å^3	1605	1880	2039	2321
Z	4	4	4	4
cryst size, mm	0.54 × 0.23 × 0.11	0.58 × 0.29 × 0.07	0.29 × 0.14 × 0.07	0.43 × 0.22 × 0.07
d_{calc}, g·cm^{-3}	2.309	1.586	2.379	2.142
radiation	Cu Kα (λ = 1.541 84 Å)	MoKα (λ = 0.710 73 Å)	MoKα (λ = 0.710 73 Å)	MoKα (λ = 0.710 73 Å)
μ, cm^{-1}	198.5	16.6	72.1	63.3
2θ scan range, deg	4.0–136.0	4.0–55.0	4.0–55.0	4.0–55.0
data collcd (h,k,l)	±14,+18,+10	±19,+18,+11	±19,+15,+25	±12,+14,+28
no. of unique rflns ($F_o \geq 4\sigma(F_o)$)	2638	3210	3831	3878
R, %	7.91	3.58	3.85	5.12
R_w, %	8.41	3.60	4.27	5.79

Table 2. Selected Bond Distances (Å) and Angles (deg) for 1a

Bond Distances			
W–Mo	3.069(2)	W–C(1)	2.008(25)
W–C(11)	2.222(17)	W–C(16)	2.331(20)
W–C(12)	2.263(21)	W–C(17)	2.310(22)
W–C(13)	2.313(22)	W–C(18)	2.357(24)
W–C(14)	2.352(21)	W–C(19)	2.317(21)
W–C(15)	2.240(18)	W–C(20)	2.306(20)
C(11)–C(12)	1.481(27)	C(12)–C(13)	1.400(29)
C(13)–C(14)	1.373(31)	C(14)–C(15)	1.433(28)
C(15)–C(11)	1.472(28)		
Mo–C(2)	1.918(21)	Mo–C(3)	1.934(25)
Mo–C(11)	2.106(18)	Mo–C(21)	2.406(22)
Mo–C(22)	2.338(26)	Mo–C(23)	2.347(24)
Mo–C(24)	2.371(24)	Mo–C(25)	2.363(27)
C(1)–O(1)	1.150(3)		
C(2)–O(2)	1.180(26)	C(3)–O(3)	1.177(30)

Bond Angles			
Mo–W–C(11)	43.3(5)	W–C(11)–Mo	90.3(5)
C(11)–Mo–W	46.4(5)	Mo–W–C(1)	94.9(6)
W–Mo–C(2)	104.9(6)	W–Mo–C(3)	75.7(6)
C(11)–C(12)–C(13)	111.4(18)	C(12)–C(13)–C(14)	108.2(19)
C(13)–C(14)–C(15)	109.1(19)	C(14)–C(15)–C(11)	109.8(17)
C(15)–C(11)–C(12)	101.2(15)	Cp–W–Cp[a]	148.1(10)

[a] Angle between the two perpendicular lines from W to the Cp rings.

= 73.7 (**2a**), 76.8 (**2b**) Hz). If the 18-electron rule is to be applied for each metal center, the structure may be regarded as resonance of two extremes: one with a Mo–Ni σ bond and the hydride bonded solely to Ni; the other with a Mo→Ni dative bond and the hydride bound only to Mo. The reaction stoichiometry and the structure of the bimetallic complex may be reasonably assumed as indicated in eq 2. The nickel moiety must have attacked

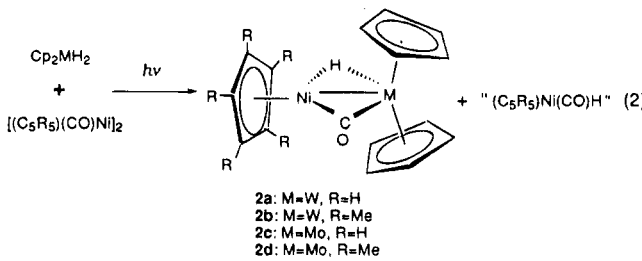

the metallocene dihydride before the latter lost dihydrogen on photolysis. We were unable to detect a (η^5-C_5R_5)Ni(CO)H species, but it is not unexpected since (η^5-C_5R_5)Ni(CO)H must be very unstable and, to our knowledge, no report on its isolation has appeared.

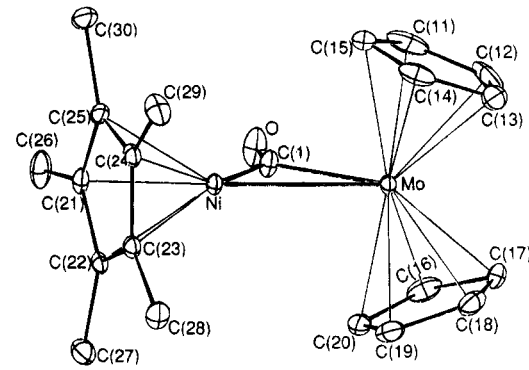

Figure 2. View of Cp_2MoH–$Ni(CO)(C_5Me_5)$ (**2d**) showing the atom-labeling scheme.

Table 3. Selected Bond Distances (Å) and Angles (deg) for 2d

Bond Distances			
Mo–Ni	2.657(1)	Mo–C(1)	2.226(4)
Mo–C(11)	2.291(7)	Mo–C(16)	2.295(6)
Mo–C(12)	2.290(10)	Mo–C(17)	2.263(7)
Mo–C(13)	2.280(7)	Mo–C(18)	2.301(6)
Mo–C(14)	2.296(6)	Mo–C(19)	2.327(6)
Mo–C(15)	2.299(6)	Mo–C(20)	2.306(5)
Ni–C(1)	1.759(5)	Ni–C(21)	2.056(5)
Ni–C(22)	2.132(5)	Ni–C(23)	2.198(5)
Ni–C(24)	2.193(5)	Ni–C(25)	2.109(5)
C(11)–C(12)	1.360(14)	C(16)–C(17)	1.428(10)
C(12)–C(13)	1.357(14)	C(17)–C(18)	1.388(11)
C(13)–C(14)	1.379(13)	C(18)–C(19)	1.331(10)
C(14)–C(15)	1.361(10)	C(19)–C(20)	1.357(9)
C(15)–C(11)	1.389(11)	C(20)–C(16)	1.399(11)
C(21)–C(22)	1.424(7)	C(22)–C(23)	1.407(6)
C(23)–C(24)	1.423(7)	C(24)–C(25)	1.427(6)
C(25)–C(21)	1.424(7)	C(1)–O	1.183(6)

Bond Angles			
Mo–Ni–C(1)	56.2(2)	Ni–C(1)–Mo	82.8(2)
C(1)–Mo–Ni	41.0(1)	Cp–Mo–Cp[a]	139.0(4)
Mo–C(1)–O	135.4(4)	Ni–C(1)–O	141.8(4)
Mo–Ni–C(21)	163.5(1)	Ni–C(21)–C(26)	124.3(4)
Mo–Ni–C(22)	145.3(1)	Ni–C(22)–C(27)	127.0(4)
Mo–Ni–C(23)	129.5(1)	Ni–C(23)–C(38)	128.8(4)
Mo–Ni–C(24)	130.3(1)	Ni–C(24)–C(29)	128.7(4)
Mo–Ni–C(25)	147.4(1)	Ni–C(25)–C(30)	125.8(5)

[a] Angle between the two perpendicular lines from Mo to the Cp rings.

W–Ru and Mo–Ru Complexes. Photolysis of the metallocene dihydride in the presence of the ruthenium dimer $[CpRu(CO)_2]_2$ proceeded smoothly and gave the originally expected hetero*tri*metallic complexes. Thus irradiation and subsequent column chromatography of

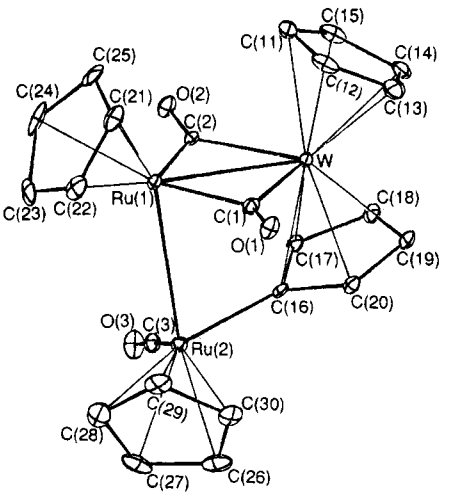

Figure 3. View of $Cp(C_5H_4)W(CO)_2[Cp_2Ru_2(CO)H]$ (**3a**) showing the atom-labeling scheme.

an equimolar mixture of Cp_2MH_2 (M = Mo, W) and $[CpRu(CO)_2]_2$ yielded two complexes, both as air-stable dark-brown crystals. A small amount of $[RuH(CO)Cp]_3$[10] was also obtained as a byproduct. Elemental analysis and spectral data indicated that one of the new complexes had the composition $Cp(C_5H_4)M(CO)_2[Cp_2Ru_2(CO)H]$ (**3a**, M = W, 20%; **3b**, M = Mo, 14% yield) while the other was more symmetric, $(C_5H_4)_2M[CpRu(CO)H]_2$ (**4a**, M = W, 30%; **4b**, M = Mo, 12% yield). The ^1H NMR spectra of complexes **3** exhibit three singlets which indicates that three of the four cyclopentadienyl rings are not metalated, while the fourth Cp ring shows four different multiplets. In addition, a singlet peak assignable to a hydride was observed at −22.06 (**3a**) or −21.82 (**3b**) ppm. Since this peak in the NMR spectra of **3a** has no satellite, it must not be bound to the tungsten but to one of the ruthenium centers. An X-ray analysis of **3a** revealed the structure shown in Figure 3, with bond lengths and angles as tabulated in Table 4. The distance between the two ruthenium atoms is 2.983(2) Å, indicating the presence of a metal−metal single bond. The CO-bridged Ru−Ru bond in the starting dimer $[CpRu(CO)_2]_2$ has a shorter length of 2.735(2) Å.[11] The W−Ru(1) bond with two bridging CO's is also short, 2.784(1) Å, which has a character of dative interaction from W to Ru as is obvious from the electron count at the W center. The third CO is coordinated to Ru(2) as a terminal ligand. Though hydride could not be located from the Fourier map, it must be bonded to Ru(2), as judged by the electron count at the Ru(1) and Ru(2) centers. Inspection of the bond angles at Ru(2) indicates that the hydride occupies the position between Ru(2)−Ru(1) and Ru(2)−C(3) bonds, the angles Ru(1)−Ru(2)−C(16), C(3)−Ru(2)−C(16), and Ru(1)−Ru(2)−C(3) being 77.0, 88.1, and 105.0°, respectively (Table 4). The bond angles at the two Ru centers do not support a structure with a hydride bridge between Ru(1) and Ru(2).

The proton NMR spectra of complexes **4** show two singlet signals of Cp protons, eight multiplets due to two different (μ,σ-η^5-C_5H_4) units, and two nonequivalent hydride peaks. The hydride absorptions in **4a** are observed as two doublets at −24.47 and −24.96 ppm with satellite peaks (J_{HH} = 4.0, $|J_{WH}|$ = 59.4 Hz), and those in **4b**, as two well-defined doublets at δ −22.12 and −22.20 (J_{HH} = 3.6) ppm. The observed H−H coupling and the $^{183}W-^1H$ satellites are indications that the hydrides are interacting with the central metallocene center. The X-ray structure of **4a** has been determined and is shown in Figure 4. Each of the metallocene Cp rings has been metalated by ruthenium, and the two ruthenium moieties differ in the orientation of the Cp and CO ligands. The Ru−Ru distance is 4.697(2) Å; therefore, no direct interaction between them exists. Table 5 contains important bond lengths and angles. The W−Ru(1) bond length of 3.048(1) Å is a little longer than W−Ru(2) of 3.033(1) Å, but the IR carbonyl absorptions in solution appear at the same position (1924 cm^{-1}). These bond lengths are much longer than the W−Ru(1) bond in **3a** (2.784(1) Å) since the bond character is much different, i.e. the W−Ru in **3a** is a pure dative bond with two bridging ligands. Though the positions of hydrides could not be located from the difference-Fourier map, we assume that hydrides bonded to the metallocene center are also interacting with ruthenium atoms since the configuration

Table 4. Selected Bond Distances (Å) and Angles (deg) for 3a

Bond Distances			
W−Ru(1)	2.784(1)	Ru(1)−Ru(2)	2.983(2)
W−C(1)	2.177(9)	W−C(2)	2.192(10)
W−C(16)	2.392(10)	Ru(1)−C(1)	1.978(11)
W−C(17)	2.304(10)	Ru(1)−C(2)	1.950(9)
W−C(18)	2.318(10)	Ru(2)−C(3)	1.832(12)
W−C(19)	2.327(12)	Ru(2)−C(16)	2.051(8)
W−C(20)	2.377(12)		
Ru(1)−C(21)	2.296(12)	Ru(2)−C(26)	2.237(13)
Ru(1)−C(22)	2.281(12)	Ru(2)−C(27)	2.221(11)
Ru(1)−C(23)	2.301(11)	Ru(2)−C(28)	2.287(11)
Ru(1)−C(24)	2.265(13)	Ru(2)−C(29)	2.320(11)
Ru(1)−C(25)	2.275(16)	Ru(2)−C(30)	2.291(12)
C(16)−C(17)	1.457(15)	C(17)−C(18)	1.421(13)
C(18)−C(19)	1.431(17)	C(19)−C(20)	1.442(14)
C(20)−C(16)	1.474(13)	C(1)−O(1)	1.178(13)
C(2)−O(2)	1.191(11)	C(3)−O(3)	1.157(16)

Bond Angles			
W−Ru(1)−Ru(2)	84.52(4)	Cp−W−Cp[a]	134.2(6)
Ru(1)−Ru(2)−C(16)	77.0(3)	Ru(2)−C(16)−W	47.5(4)
W−C(1)−Ru(1)	84.0(4)	W−C(2)−Ru(1)	84.2(4)
W−C(1)−O(1)	138.1(7)	Ru(1)−C(1)−O(1)	137.6(7)
W−C(2)−O(2)	136.3(7)	Ru(1)−C(2)−O(2)	139.1(7)
C(3)−Ru(2)−C(16)	88.1(4)	Ru(1)−Ru(2)−C(3)	105.0(3)
C(1)−Ru(1)−C(2)	102.6(4)	C(1)−Ru(1)−Ru(2)	80.5(3)
C(2)−Ru(1)−Ru(2)	93.4(3)		

[a] Angle between the two perpendicular lines from W to the Cp rings.

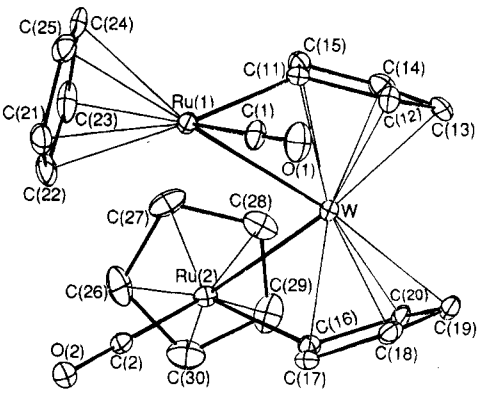

Figure 4. View of $(C_5H_4)_2W[CpRu(CO)H]_2$ (**4a**) showing the atom-labeling scheme.

(10) Forrow, N. J.; Knox, S. A. R.; Morris, M. J. *J. Chem. Soc., Chem. Commun.* **1983**, 234.
(11) Mills, O. S.; Nice, J. P. *J. Organomet. Chem.* **1967**, *9*, 339.

around each ruthenium atom deviates from regular tripod piano stool orientation, as is obvious from the environment of Ru(2) in Figure 4. Two possible bonding descriptions of **4** which are consistent with the 18-electron rule at each metal center are one with two dative bonds from M (M = W or Mo) to Ru and the hydrides bound only to M (form **I**) and the other with two single bonds between M and Ru, the hydrides being bonded only to the Ru centers (form **II**).

The column chromatographic fraction from which **4a** crystallized contained other isomers. The ^{1}H NMR spectrum of the residue showed, except for the peaks due to **4a**, two singlet hydride signals with satellites at −25.12 (isomer **4a′**, $|J_{WH}|$ = 59.4 Hz) and −24.36 ppm (isomer **4a″**, $|J_{WH}|$ = 54.0 Hz) and two singlets due to Cp−Ru at 4.68 (isomer **4a′**) and 4.73 ppm (isomer **4a″**). The (μ,σ-η^5-C_5H_4) signals were too complicated to be analyzed, but from the peak intensities mentioned above the ratio of isomers was **4a/4a′/4a″** ≈ 4/2/1. If we denote the Ru configurations in **4a** as (*R,S*), those in the isomers must be (*R,R*) and (*S,S*) since the hydride signals are observed as singlets. Likewise, isomers of **4b** were found in the ratio **4b/4b′/4b″** ≈ 4/2/1 with singlet peaks at −22.63, 4.63 (**4b′**) and −21.68, 4.72 (**4b″**) ppm.

The reaction is illustrated schematically in eq 3. As a reaction path toward the the formation of **3** and **4**, a

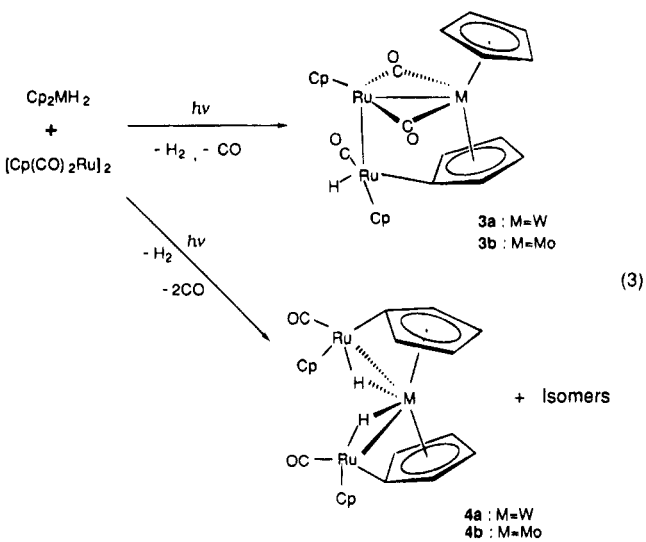

(3)

loss of dihydrogen from the metallocene dihydride in the initial photoreaction is assumed. Attack of the generated metallocene on one of the ruthenium moieties of $[Cp(CO)_2Ru]_2$ and subsequent C−H oxidative addition of the metallocene Cp ring to the other ruthenium, expelling one CO ligand from it, will give **3**. When the metallocene attacks the metal−metal bond and inserts into it, as has been originally expected, one CO ligand is removed from each ruthenium center leading to oxidative addition of the metallocene H_4C_5−H to both of the rutheniums to give **4** (form **II**). Thermal or photochemical conversion of **3** to **4** was not successful.

Experimental Section

Most manipulations were performed in a dry oxygen-free argon atmosphere. Solvents were purified by standard methods and freshly distilled (from Na−benzophenone or CaH_2) under argon before use. Photochemical reactions were performed with a Riko 100-W high-pressure mercury lamp in a Pyrex flask of 150 mL volume. The starting materials and complexes Cp_2MoH_2,[12] Cp_2WH_2,[12] $[CpMo(CO)_3]_2$,[13] $[CpW(CO)_3]_2$,[13] $[CpRu(CO)_2]_2$,[14] $[CpNi(CO)]_2$,[15] and $[Cp^*Ni(CO)]_2$[16] were obtained by published procedures. All other reagents were commercially obtained. ^{1}H- and ^{13}C-NMR spectra were recorded on a JEOL EX-270 spectrometer. The *J*-value signs were not determined. IR spectra were recorded on a Perkin-Elmer FT-1650 spectrometer using THF solutions of samples in a CaF_2 liquid cell. Melting points were measured under argon and were not corrected: all the samples decomposed on melting.

Table 5. Selected Bond Distances (Å) and Angles (deg) for 4a

Bond Distances			
W−Ru(1)	3.047(2)	W−Ru(2)	3.033(1)
W−C(11)	2.191(13)	W−C(16)	2.238(12)
W−C(12)	2.217(13)	W−C(17)	2.271(12)
W−C(13)	2.239(12)	W−C(18)	2.270(12)
W−C(14)	2.291(13)	W−C(19)	2.261(12)
W−C(15)	2.281(12)	W−C(20)	2.256(14)
Ru(1)−C(1)	1.816(12)	Ru(2)−C(2)	1.798(12)
Ru(1)−C(11)	2.032(12)	Ru(2)−C(16)	1.995(11)
C(11)−C(12)	1.435(16)	C(16)−C(17)	1.453(17)
C(12)−C(13)	1.400(21)	C(17)−C(18)	1.425(17)
C(13)−C(14)	1.465(20)	C(18)−C(19)	1.428(19)
C(14)−C(15)	1.358(19)	C(19)−C(20)	1.466(18)
C(15)−C(11)	1.411(18)	C(20)−C(16)	1.424(17)
C(1)−O(1)	1.177(15)	C(2)−O(2)	1.169(15)
Bond Angles			
Ru(1)−W−Ru(2)	101.15(4)	Cp−W−Cp[a]	146.3(6)
W−Ru(1)−C(11)	45.9(4)	W−Ru(2)−C(16)	47.5(4)
W−Ru(1)−C(1)	96.0(2)	W−Ru(2)−C(2)	95.4(4)

[a] Angle between the two perpendicular lines from W to the Cp rings.

Cp(C_5H_4)(CO)W−Mo(CO)$_2$Cp (1a). A mixture of Cp_2WH_2 (123 mg, 0.39 mmol) and $[CpMo(CO)_3]_2$ (188 mg, 0.38 mmol) in DME (120 ml) was irradiated until most of Cp_2WH_2 was consumed (35 h) as monitored by ^{1}H NMR spectra. The initially red solution became dark red, and a small quantity of dark-red material precipitated. The solvent was evaporated under reduced pressure. The residual dark-red solid was chromatographed on alumina (deactivated with 5 wt % H_2O, 2 × 18 cm). Elution with hexane gave a mixture of Cp_2WH_2 and $[CpMo(CO)_3]_2$ as a pink band. Further elution with CH_2Cl_2 gave a dark red fraction which after evaporation to dryness yielded **1a** as dark-red solid (95.2 mg, 0.17 mmol, 43% yield). The analytically pure sample was obtained by recrystallization from THF−hexane as dark-red plates (mp 235−237 °C). ^{1}H NMR (CD_2Cl_2): δ 5.55 (m, μ,σ-η^5-C_5H_4, 1H), 5.32 (m, μ,σ-η^5-C_5H_4, 1H), 5.23 (s, η^5-C_5H_5, 5H), 5.14 (bs, μ,σ-η^5-C_5H_4, 1H), 5.02 (s, η^5-C_5H_5, 5H), 4.04 (m, μ,σ-η^5-C_5H_4, 1H). IR ν(CO): 1961 (s), 1882 (s), 1799 (s) cm^{-1}. Anal. Calcd for $C_{18}H_{14}O_3MoW$: C, 38.74; H, 2.53. Found: C, 39.03; H, 2.50.

Cp(C_5H_4)(CO)Mo−W(CO)$_2$Cp (1b). A procedure similar to that for **1a**, using Cp_2MoH_2 (88 mg, 0.39 mmol) and $[CpW(CO)_3]_2$ (258 mg, 0.39 mmol) and irradiating for 14 h, yielded **1b** as a dark-red powder (90.8 mg, 0.16 mmol, 42% yield, mp 220−222 °C). Crystallization was not successful. ^{1}H NMR (DMSO-d_6): δ 5.59 (m, μ,σ-η^5-C_5H_4, 2H), 5.45 (s, η^5-C_5H_5, 5H), 5.21 (s, η^5-C_5H_5, 5H), 5.04 (m, μ,σ-η^5-C_5H_4, 1H), 3.86 (m, μ,σ-η^5-C_5H_4, 1H). IR ν(CO): 1971 (s), 1880 (s), 1790 (s) cm^{-1}.

(12) (a) Green, M. L. H.; McCleverty, J. A.; Wilkinson, G. *J. Chem. Soc.* **1961**, 4854. (b) Green, M. L. H.; Knowles, P. J. *J. Chem. Soc., Perkin Trans. 1* **1973**, 989.
(13) Birdwhistell, R.; Hackett, P.; Manning, A. R. *J. Organomet. Chem.* **1978**, *157*, 239.
(14) Humphries, A. P.; Knox, S. A. R. *J. Chem. Soc., Dalton Trans.* **1975**, 1710.
(15) King, R. B. In *Organometallic Syntheses*; Academic: New York, 1965; Vol. 1.
(16) Mise, T.; Yamazaki, H. *J. Organomet. Chem.* **1979**, *164*, 391.

$Cp(C_5H_4)(CO)W-W(CO)_2Cp$ (1c). A solution of Cp_2WH_2 (123 mg, 0.39 mmol) and $[CpW(CO)_3]_2$ (258 mg, 0.39 mmol) in DME (120 mL) was irradiated for 35 h. Treatment of the mixture in a similar way to that described for **1a** gave dark-red crystals of **1c** (107.3 mg, 0.17 mmol, 43% yield, mp 212–214 °C). ^1H NMR (DMSO-d_6): δ 5.77 (m, μ,σ-η^5-C_5H_4, 1H), 5.53 (m, μ,σ-η^5-C_5H_4, 1H), 5.40 (s, η^5-C_5H_5, 5H), 5.21 (s, η^5-C_5H_5, 5H), 5.11 (m, μ,σ-η^5-C_5H_4, 1H), 3.66 (m, μ,σ-η^5-C_5H_4, 1H). IR ν(CO): 1962 (s), 1876 (s), 1788 (s) cm^{-1}. Anal. Calcd for $C_{18}H_{14}O_3W_2$: C, 33.77; H, 2.35. Found: C, 33.47; H, 2.18.

$Cp(C_5H_4)(CO)Mo-Mo(CO)_2Cp$ (1d). A solution of Cp_2MoH_2 (88 mg, 0.39 mmol) and $[CpMo(CO)_3]_2$ (188 mg, 0.38 mmol) in DME (120 mL) was irradiated for 12 h. Treatment of the mixture in a similar way to that described for **1a** gave dark-red crystals of the known complex **1d** (104.8 mg, 0.22 mmol, 56% yield).[6,8]

$Cp_2WH-Ni(CO)Cp$ (2a). A solution of Cp_2WH_2 (100 mg, 0.32 mmol) and $[CpNi(CO)]_2$ (96 mg, 0.32 mmol) in DME (120 mL) was irradiated until most of the Cp_2WH_2 was consumed (37 h) as monitored by ^1H NMR spectra. The initially red solution became black, and a small quantity of black material precipitated. The solvent was evaporated under reduced pressure. The residual black solid was chromatographed on alumina (deactivated by 10 wt % H_2O, 2 × 16 cm). Elution with hexane gave a brown band of $[CpNi(CO)]_2$ (38.3 mg, 0.13 mmol, 40%). Further elution with CH_2Cl_2 gave a red band. Evaporation of the solvent from the red eluate to dryness gave **2a** as dark-red solid (82.9 mg, 0.18 mmol, 56% yield). The analytically pure sample was obtained by recrystallization from THF–hexane as dark-red plates (mp 210–212 °C). ^1H NMR (CD_2Cl_2): δ 5.22 (s, η^5-C_5H_5, 5H), 4.72 (s, η^5-C_5H_5, 10H), −5.83 (s, W–H, satellite J_{W-H} = 73.7 Hz, 1H). IR ν(CO): 1732 (s) cm^{-1}. Anal. Calcd for $C_{16}H_{16}ONiW$: C, 41.17; H, 3.45. Found: C, 41.02; H, 3.49.

$Cp_2WH-Ni(CO)(C_5Me_5)$ (2b). A solution of Cp_2WH_2 (123 mg, 0.39 mmol) and $[(C_5Me_5)Ni(CO)]_2$ (172 mg, 0.39 mmol) in DME (120 mL) was irradiated at room temperature for 36 h. The initially red solution became dark red, and a small quantity of black material precipitated. The solvent was evaporated under reduced pressure, and the residual black solid was chromatographed on alumina (deactivated by 10 wt % H_2O, 2 × 18 cm). Elution with hexane gave a red band from which $[(\eta^5$-$C_5Me_5)Ni(CO)]_2$ was recovered (73.6 mg, 0.17 mmol, 43%). Further elution with hexane/CH_2Cl_2 (1/2) gave an orange band. The orange eluate was collected and evaporated to dryness to yield dark-red solid of **2b** (48.2 mg, 0.09 mmol, 23% yield). The analytically pure sample was obtained by recrystallization from THF–hexane as dark-red plates (mp 229–230 °C). ^1H NMR (C_6D_6): δ 4.17 (s, η^5-C_5H_5, 10H), 2.14 (s, C_5Me_5, 15H), −6.47 (s, W–H, satellite J_{W-H} = 76.8 Hz, 1H). IR ν(CO): 1718 (s) cm^{-1}. Anal. Calcd for $C_{21}H_{26}ONiW$: C, 46.97; H, 4.87. Found: C, 46.98; H, 4.87.

$Cp_2MoH-Ni(CO)Cp$ (2c). A mixture of Cp_2MoH_2 (88 mg, 0.39 mmol) and $[CpNi(CO)]_2$ (118 mg, 0.39 mmol) in DME (120 mL) was irradiated for 14 h. The solvent was evaporated under reduced pressure, and the residual black solid was treated as described above. Complex **2c** crystallized from THF–hexane as dark-red plates (51.6 mg, 0.14 mmol, 35% yield, mp 215–216 °C). ^1H NMR (CD_2Cl_2): δ 5.16 (s, η^5-C_5H_5, 5H), 4.75 (s, η^5-C_5H_5, 10H), −6.43 (s, Mo–H, 1H). IR ν(CO): 1755 (s) cm^{-1}. Anal. Calcd for $C_{16}H_{16}OMoNi$: C, 50.17; H, 3.96. Found: C, 50.49; H, 3.96.

$Cp_2MoH-Ni(CO)(C_5Me_5)$ (2d). A solution of Cp_2MoH_2 (88 mg, 0.39 mmol) and $[(\eta^5$-$C_5Me_5)Ni(CO)]_2$ (172 mg, 0.39 mmol) in DME (120 mL) was irradiated for 35 h. The initially red solution became dark red, and a small quantity of black material precipitated. The solvent was evaporated under reduced pressure, and the residual black solid was treated as described above. Recrystallization from THF–hexane gave **2d** as dark-red plates (43.9 mg, 0.10 mmol, 25% yield, mp 235–237 °C). ^1H NMR (C_6D_6): δ 4.21 (s, η^5-C_5H_5, 10H), 2.11 (s, C_5Me_5, 15H), −5.57 (s, Mo–H, 1H). IR ν(CO): 1741 (s) cm^{-1}. Anal. Calcd for $C_{21}H_{26}OMoNi$: C, 56.17; H, 5.84. Found: C, 56.28; H, 5.79.

Preparation of $Cp(C_5H_4)W(CO)_2[Cp_2Ru_2(CO)H]$ (3a) and $(C_5H_4)_2W[CpRu(CO)H]_2$ (4a). A mixture of Cp_2WH_2 (123 mg, 0.39 mmol) and $[CpRu(CO)_2]_2$ (172 mg, 0.39 mmol) in DME (120 mL) was irradiated until most of Cp_2WH_2 was consumed (64 h) as monitored by ^1H NMR spectra. The initially yellow solution became dark red, and a small quantity of orange material precipitated. The solvent was evaporated under reduced pressure, and the residual dark-red solid was chromatographed on alumina (deactivated with 5 wt % H_2O, 2 × 15 cm). Three bands separated. The first blue bland which was eluted with hexane gave, after evaporation of the solvent and recrystallization from toluene, blue crystals (19.4 mg, 0.04 mmol) of the known triruthenium cluster [RuH(CO)-Cp]$_3$, as identified by spectral data and the unit cell dimension from X-ray diffraction.[10] The second brown band was eluted with hexane. Crystallization from toluene gave brown plates of **4a** (87.5 mg, 0.12 mmol, 30% yield, mp 138–140 °C). Elution of the third orange band with CH_2Cl_2/THF (4/1), evaporation of the solvent, and recrystallization from THF–hexane gave red crystals of **3a** (57.0 mg, 0.08 mmol, 20% yield, mp 193–194 °C). **3a:** ^1H NMR (CD_2Cl_2) δ 5.68 (m, μ,σ-η^5-C_5H_4, 1H), 5.32 (m, μ,σ-η^5-C_5H_4, 1H),5.06 (m μ,σ-η^5-C_5H_4, 1H), 5.02 (s, η^5-C_5H_5, 5H), 4.92 (s, η^5-C_5H_5, 5H), 4.81 (s, η^5-C_5H_5, 5H), 4.73 (m, μ,σ-η^5-C_5H_4, 1H), −22.06 (s, Ru–H, 1H); IR ν(CO) 2048 (s), 1995 (s), 1921 (s), 1694 (s) cm^{-1}. Anal. Calcd for $C_{23}H_{20}O_3Ru_2W$: C, 37.82; H, 2.76. Found: C, 37.66; H, 2.96. **4a:** ^1H NMR (C_6D_6) δ 5.47 (m, μ,σ-η^5-C_5H_4, 1H), 5.11 (m, μ,σ-η^5-C_5H_4, 2H), 4.98 (m, μ,σ-η^5-C_5H_4, 1H), 4.95 (s, η^5-C_5H_5, 5H), 4.51 (s, η^5-C_5H_5, 5H), 4.50 (sh, μ,σ-η^5-C_5H_4, 1H), 4.48 (m, μ,σ-η^5-C_5H_4, 1H), 2.95 (m μ,σ-η^5-C_5H_4, 1H), 2.90 (m, μ,σ-η^5-C_5H_4, 1H), −24.47 (d, M–H, J_{H-H} = 4.0, satellite J_{W-H} = 59.4 Hz, 1H), −24.96 (d, M–H, J_{H-H} = 4.0, satellite J_{W-H} = 59.4 Hz, 1H); IR (THF) ν(CO) 1924 (s) cm^{-1}. Anal. Calcd for $C_{22}H_{20}O_2Ru_2W\cdot{}^1/_2C_7H_8$: C, 40.92; H, 3.23. Found: C, 41.14; H, 3.23.

Preparation of $Cp(C_5H_4)Mo(CO)_2[Cp_2Ru_2(CO)H]$ (3b) and $(C_5H_4)_2Mo[CpRu(CO)H]_2$ (4b). A solution of Cp_2MoH_2 (96 mg, 0.42 mmol) and $[CpRu(CO)_2]_2$ (184 mg, 0.42 mmol) in DME (120 mL) was irradiated for 66 h. After the solvent was evaporated under reduced pressure, the residual dark-red solid was treated on column chromatography (Al_2O_3 deactivated with 5 wt % H_2O, 2 × 15 cm). Elution of three bands were performed using the same reaction mixtures as in the case of the W analog described above. Besides the triruthenium cluster [RuH(CO)Cp]$_3$ (37.2 mg, 0.06 mmol), red crystals of **3b** (39.4 mg, 0.06 mmol, 14% yield, mp 190–191 °C) and brown crystals of **4b** (29.9 mg, 0.05 mmol, 12% yield, mp 143–145 °C) were isolated. **3b:** ^1H NMR ($CDCl_3$) δ 5.63 (m, μ,σ-η^5-C_5H_4, 1H), 5.48 (m, μ,σ-η^5-C_5H_4, 1H), 5.14 (m μ,σ-η^5-C_5H_4, 1H), 5.09 (s, η^5-C_{55}, 5H), 4.93 (s, η^5-C_5H_5, 5H), 4.90 (m, μ,σ-η^5-C_5H_4, 1H), 4.71 (s, η^5-C_5H_5, 5H), −21.82 (s, Ru–H, 1H); IR ν(CO) 2048 (s), 1995 (s), 1922 (s), 1717 (s) cm^{-1}. Anal. Calcd for $C_{23}H_{20}O_3MoRu_2$: C, 43.00; H, 3.14. Found: C, 43.01; H, 3.15. **4b:** ^1H NMR (C_6D_6) δ 5.73 (m, μ,σ-η^5-C_5H_4, 1H), 5.30 (m, μ,σ-η^5-C_5H_4, 1H), 4.97 (s, η^5-C_5H_5, 5H), 4.76 (m, μ,σ-η^5-C_5H_4, 1H), 4.71 (m, μ,σ-η^5-C_5H_4, 1H), 4.48 (s, η^5-C_5H_5, 5H), 4.15 (m, μ,σ-η^5-C_5H_4, 2H), 3.33 (m, μ,σ-η^5-C_5H_4, 1H), 3.29 (m, μ,σ-η^5-C_5H_4, 1H), −22.12 (d, M–H, J_{H-H} = 3.6 Hz, 1H), −22.20 (d, M–H, J_{H-H} = 3.6 Hz, 1H); IR ν(CO) 1924 (s) cm^{-1}. Anal. Calcd for $C_{22}H_{20}O_2MoRu_2\cdot{}^1/_2C_7H_8$: C, 46.36; H, 3.69. Found: C, 46.58; H, 3.66.

X-ray Crystallographic Analysis of 1a, 2d, 3a, and 4a. Crystal, data collection, and refinement parameters are summarized in Table 1. Single crystals were grown from THF–hexane (**1a, 2d, 3a**) or from saturated toluene (**4a**). Reflection data were collected at room temperature on an Enraf-Nonius CAD-4 diffractometer using graphite-monochromated Mo Kα radiation and the $2\theta-\omega$ scan technique. The structures were solved from direct and Fourier methods and refined by block-diagonal least squares with anisotropic thermal parameters in the last cycles for all non-hydrogen atoms. Hydrogen atoms

for the cyclopentadienyl rings in **1a** and **4a** were placed in calculated positions, while methyl hydrogens in **2d** were located from a difference Fourier map. These hydrogen atoms were included in subsequent refinements with isotropic thermal parameters. The metal-bound hydrogen atoms could not be located. Only three carbon atoms of crystallized solvent (toluene) in **4a** could be located in a gap of the crystal lattice, suggesting high disorder of the C_7H_8 group, and these were included in subsequent refinements with isotropic thermal parameters. In the refinements unit weight was applied. The function minimized in the least-squares refinement was $\sum w(|F_o| - |F_c|)^2$. The computational program package used in the analysis was the UNICS 3 program system.[17] Neutral atomic scattering factors were taken from ref 18. Important bond lengths and angles are given in Tables 2–5.

Acknowledgment. We are grateful for financial support of this work by a Grant-in-Aid for Scientific Research from the Ministry of Education, Science, and Culture of Japan.

Supporting Information Available: Tables of positional and thermal parameters and bond distances and angles (31 pages). Ordering information is given on any current masthead page.

OM950520G

(17) Sakurai, T.; Kobayashi, K. *Rikagaku Kenkyusho Hokoku* **1979**, *55*, 69.

(18) *International Tables for X-Ray Crystallography*; Kynoch: Birmingham, England, 1974; Vol. IV.

Evidence for the Ligation of Palladium(0) Complexes by Acetate Ions: Consequences on the Mechanism of Their Oxidative Addition with Phenyl Iodide and $PhPd(OAc)(PPh_3)_2$ as Intermediate in the Heck Reaction

Christian Amatore,* Emmanuelle Carré, Anny Jutand,*
Mohamed Amine M'Barki,† and Gilbert Meyer

Ecole Normale Supérieure, Département de Chimie, URA CNRS 1679, 24 Rue Lhomond, 75231 Paris Cédex 5, France

Received June 2, 1995[⊗]

Addition of acetate anions to solutions of $Pd^0(PPh_3)_4$ results in the formation of anionic species in which the acetate ion coordinates the palladium(0) center, $Pd^0(PPh_3)_3(OAc)^-$, which is in equilibrium with the less ligated complex, $Pd^0(PPh_3)_2(OAc)^-$. The latter undergoes oxidative addition with phenyl iodide to afford a mixture of $PhPdI(PPh_3)_2$ and $PhPd(OAc)(PPh_3)_2$. Acetate ions react with $PhPdI(PPh_3)_2$ to afford $PhPd(OAc)(PPh_3)_2$. Mixtures of $Pd(OAc)_2$ and $nPPh_3$ ($n \geq 4$), commonly used as catalysts in Heck reactions, afford a palladium(0) complex that is ligated by one acetate ion, yielding the anionic species $Pd^0(PPh_3)_3(OAc)^-$ and $Pd^0(PPh_3)_2(OAc)^-$. The latter reacts with phenyl iodide. However, this reaction does not afford the expected $PhPdI(PPh_3)_2$ complex but instead affords $PhPd(OAc)(PPh_3)_2$. Reaction of $PhPd(OAc)(PPh_3)_2$ with styrene results in the formation of stilbene, demonstrating that $PhPd(OAc)(PPh_3)_2$ is an intermediate in the Heck reaction.

Introduction

We have reported in previous papers[1] that catalytic systems commonly used in Heck[2] reactions, *i.e.*, $Pd(OAc)_2(PPh_3)_2$ or a mixture of $Pd(OAc)_2$ and $nPPh_3$ ($n \geq 2$), spontaneously and quantitatively generate *in situ* a zero-valent palladium complex that can activate aryl iodides by oxidative addition. Indeed, we demonstrated that triphenylphosphine was able to reduce the bivalent palladium to a zero-valent palladium from the complex $Pd(OAc)_2(PPh_3)_2$ by an intramolecular reaction whereas triphenylphosphine was oxidized to triphenylphosphine oxide[3] according to the following mechanism (eqs 1–3):[1b]

$$Pd(OAc)_2 + 2\,PPh_3 \xrightarrow{\text{fast}} Pd(OAc)_2(PPh_3)_2 \quad (1)$$

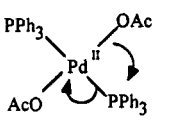

$$\xrightarrow{\text{slow}} \text{"}Pd^0(PPh_3)(OAc)^-\text{"} + AcO\text{-}PPh_3^+ \quad (2)$$

$$AcO\text{-}PPh_3^+ + H_2O \longrightarrow AcOH + O{=}PPh_3 + H^+ \quad (3)$$

In the presence of excess phosphine, a stable palladium(0) was formed, but up to now it was not possible to determine precisely the fate of the acetate anion originating from reaction 2 or to determine whether or not the resulting stable palladium(0) complex was ligated by an acetate ion (eqs 4 and 5):

$$\text{"}Pd^0(PPh_3)(OAc)^-\text{"} + 2PPh_3 \xrightarrow{\text{fast}} Pd^0(PPh_3)_3 + OAc^- \quad (4)$$

$$\text{or } Pd^0(PPh_3)_3(OAc)^- \; ? \quad (5)$$

Chloride (or bromide) anions were able to coordinate low-ligated zero-valent palladium complexes to afford anionic species[4] $[Pd^0(PPh_3)_2X_x]_n^{nx-}$ as well as more saturated complexes such as $Pd^0(PPh_3)_3Cl^-$ when chloride ions were added to $Pd^0(PPh_3)_4$.[4c] Therefore, it was of interest to investigate whether or not acetate anions were able to coordinate palladium(0) complexes, particularly in the case of palladium(0) complexes generated *in situ* from $Pd(OAc)_2$ and triphenylphosphine (reaction 4 or 5). It was also important to investigate the consequences of hypothetical ligation of palladium(0) complexes by acetate ions on the reactivity of the resulting palladium(0) complexes in oxidative additions. We report therefore our investigations concerning the fate and role of the acetate anions that are released during the intramolecular reduction of $Pd(OAc)_2(PPh_3)_2$ by triphenylphosphine. Moreover, palladium(0) complexes such as $Pd^0(PPh_3)_4$ are also efficient catalysts in

* To whom any correspondence should be addressed.
† Present address: Université Ibn Tofail, Faculté des Sciences, BP 133, 14000 Kénitra, Morocco.
⊗ Abstract published in *Advance ACS Abstracts,* October 15, 1995.
(1) (a) Amatore, C.; Jutand, A.; M'Barki, M. A. *Organometallics* **1992,** *11,* 3009. b) Amatore, C.; Carré, E.; Jutand, A.; M'Barki, M. A. *Organometallics* **1995,** *14,* 1818.
(2) For reviews, see: (a) Heck, R. F. *Acc. Chem. Res.* **1979,** *12,* 146. (b) Tsuji, J. *Organic Syntheses via Palladium Compounds*; Springer Verlag: New York, 1980. (c) Kumada, M. *Pure Appl. Chem.* **1980,** *52,* 669. (d) Negishi, E. I. *Acc. Chem. Res.* **1982,** *15,* 340. (e) Heck, R. F. *Org. React.* **1982,** *27,* 345. (f) Heck, R. F. *Palladium Reagents in Organic Syntheses*; Academic Press: New York, 1985. (g) Stille, J. K. *Angew. Chem., Int. Ed. Engl.* **1986,** *25,* 508. (h) De Meijere, A.; Meyer, F. M. *Angew. Chem., Int. Ed. Engl.* **1994,** *33,* 2379. (i) Cabri, W.; Candiani, I. *Acc. Chem. Res.* **1995,** *28,* 2.
(3) (a) Palladium(0) and BINAP oxide are formed from a mixture of $Pd(OAc)_2$ and 2BINAP. See: Ozawa, F.; Kubo, A.; Hayashi, T. *Chem. Lett.* **1992,** 2177. (b) Palladium(0) and tributylphosphine oxide are formed from a mixture of $Pd(OAc)_2$ and $1PBu_3$. See: Mandai, T.; Matsumoto, T.; Tsuji, J. *Tetrahedron Lett.* **1993,** 2513.
(4) (a) Negishi, E.; Takahashi, T.; Akiyoshi, K. *J. Chem. Soc., Chem. Commun.* **1986,** 1338. (b) When X = Cl, $n = 2$ and $x = 2$; $n = 1$ and $x = 1$ or 2. When X = Br. $n = 1$ and $x = 1$ or 2. See: (c) Amatore, C.; Azzabi, M.; Jutand, A. *J. Am. Chem. Soc.* **1991,** *113,* 8375.

0276-7333/95/2314-5605$09.00/0

Table 1. Oxidation Peak Potentials of Palladium(0) Complexes in the Absence and in the Presence of Acetate Ions

entry no.	palladium(0) complexes	E^{p}_{Ox} (V *vs* SCE) in DMF	E^{p}_{Ox} (V *vs* SCE) in THF
1	Pd^0 generated from $Pd(OAc)_2$ + 5PPh_3	+0.02	+0.13, +0.25
2	$Pd^0(PPh_3)_4$	+0.06	+0.26, +0.36
3	$Pd^0(PPh_3)_4$ + 1AcO^- [a]	+0.02	+0.11, +0.21
4	$Pd^0(PPh_3)_4$ + 2AcO^- [a]	+0.01	+0.14
5	$Pd^0(PPh_3)_4$ + 5AcO^- [a]	+0.00	+0.11
6	$Pd^0(PPh_3)_4$ + 10AcO^- [a]	−0.11	nd[b]
7	Pd^0 generated from $Pd(OAc)_2$ + 10PPh_3	+0.02	+0.13, +0.24
8	$Pd^0(PPh_3)_4$ + 5PPh_3	+0.06	+0.26, +0.41
9	$Pd^0(PPh_3)_4$ + 5PPh_3 + 1AcO^- [a]	+0.02	+0.13, +0.23
10	$Pd^0(PPh_3)_4$ + 5PPh_3 + 2AcO^- [a]	+0.01	+0.15
11	$Pd^0(PPh_3)_4$ + 5PPh_3 + 5AcO^- [a]	+0.00	+0.12
12	$Pd^0(PPh_3)_4$ + 5PPh_3 + 10AcO^- [a]	−0.01	+0.12

[a] The acetate ions were introduced as nBu_4NOAc. [b] Not determined.

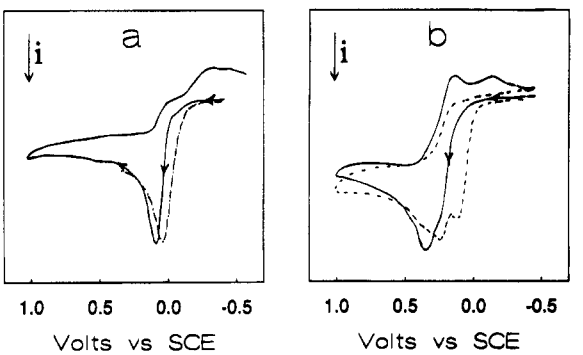

Figure 1. (a) Cyclic voltammetry of $Pd^0(PPh_3)_4$ (2 mM) in DMF (nBu_4NBF_4, 0.3 M) at a stationary gold disk electrode (ø 0.5 mm) with a scan rate of 0.2 V s^{-1}(—). Same experiment in the presence of nBu_4NOAc (1 equiv) (·-·-·). (b) Cyclic voltammetry of $Pd^0(PPh_3)_4$ (2 mM) in THF (nBu_4NBF_4, 0.3 M) (—). Same experiment in the presence of nBu_4NOAc (1 equiv) (- - -).

nucleophilic substitutions on allylic acetates in which acetate ions are continuously released during the reaction.[5] Thus the possible ligation of $Pd^0(PPh_3)_4$ by acetate ions was also investigated.

Results and Discussion

A. Ligation of Palladium(0) Complexes by Acetate Ions. Investigation by Cyclic Voltammetry. As we have already reported,[1] mixtures of $Pd(OAc)_2$ and 5PPh_3 immediately afforded bivalent palladium complex $Pd(OAc)_2(PPh_3)_2$. This complex led spontaneously to a palladium(0) complex, which was detected by its oxidation peak in cyclic voltammetry at E^{p}_{Ox} = +0.02 V *vs* SCE, in DMF. In THF, the oxidation peak of the palladium(0) complex at E^{p}_{Ox} = +0.25 V exhibited a shoulder at +0.13 V (Table 1 and Figure 1). Formally the palladium(0) complex generated *in situ* from the mixture of $Pd(OAc)_2$ and 5PPh_3 should be similar to $Pd^0(PPh_3)_4$ since only one PPh_3 among the five is oxidized to O=PPh_3. As already reported, tetrakis(triphenylphosphine)palladium(0), $Pd^0(PPh_3)_4$, exhibits an oxidation peak at E^{p}_{Ox} = +0.06 V in DMF. This oxidation peak is assigned to the oxidation of the main species in solution, $(DMF)Pd^0(PPh_3)_3$.[6] In THF, the oxidation peak at +0.36 V exhibits a shoulder at +0.26 V. These two oxidation peaks are respectively assigned to the oxidation of $(THF)Pd^0(PPh_3)_3$ and $Pd^0(PPh_3)_3$.[6] Comparison of the oxidation potentials of the palladium(0) complex generated *in situ* from $Pd(OAc)_2$ and 5PPh_3 with those of $Pd^0(PPh_3)_4$ either in THF or in DMF suggests that the complex is not $Pd^0(PPh_3)_4$ (compare entries 1 and 2 in Table 1).

Addition of increasing amounts of acetate ions, introduced as nBu_4NOAc, to $Pd^0(PPh_3)_4$ in DMF results in a shift of the initial oxidation peak to less and less positive potentials (Figure 1a and Table 1). We observed that the shift was the most important in the case of the addition of the first equivalent of AcO^-. The same phenomenon was observed when increasing amounts of acetate ions were added to a solution of $Pd^0(PPh_3)_4$ containing 5 equiv of PPh_3 (Table 1). The new oxidation peak observed in the presence of acetate ions suggests that one acetate ion is able to coordinate the palladium(0) center almost quantitatively to afford an anionic species such as $Pd^0(PPh_3)_3(OAc)^-$ that is more easily oxidized than the initial complex. In THF, after introduction of 1 equiv of acetate ion to a solution of $Pd^0(PPh_3)_4$, a new oxidation peak appeared at a less positive potential, +0.21 V, with a shoulder still present at +0.11 V (Figure 1b and Table 1). In the presence of ≥2 equiv of acetate ions, only one oxidation peak was observed (Table 1). The same phenomenon was observed when increasing amounts of acetate ions were added to a solution of $Pd^0(PPh_3)_4$ containing 5 equiv of PPh_3. The most important shift was always observed in the case of the addition of the first equivalent of AcO^-. Thus it seems that in the presence of 1 equiv of AcO^- two species were formed, $(THF)Pd^0(PPh_3)_3$ and $Pd^0(PPh_3)_3(OAc)^-$, whereas only the $Pd^0(PPh_3)_3(OAc)^-$ complex was produced when >2 equiv of AcO^- was added.

These results suggest that in THF as well as in DMF acetate ions can coordinate $Pd^0(PPh_3)_3$ to afford anionic species that are more easily oxidizable than the initial complex. Comparison of the oxidation potentials of the palladium(0) complex generated *in situ* from $Pd(OAc)_2$ and $nPPh_3$ (n ≥ 5) with those of $Pd^0(PPh_3)_4$ in the presence of one acetate ion, shows a great similitude both in THF and DMF (compare entries 1, 3, 7, and 9 in Table 1). Thus we can tentatively conclude that the palladium(0) complex generated *in situ* from mixtures of $Pd(OAc)_2$ and $nPPh_3$ is also ligated by one acetate ion, $Pd^0(PPh_3)_3(OAc)^-$ (eq 5).

(5) (a) Trost; B. M. *Acc. Chem. Res.* 1980, *13*, 358. (b) Tsuji, J. *Tetrahedron* **1986**, *42*, 4365.

(6) Amatore, C.; Jutand, A.; Khalil, F.; Mottier, L. *Organometallics* **1993**, *12*, 3168.

Table 2. ^{31}P NMR Shifts (in ppm) of $Pd^0(PPh_3)_4$ in the Absence and in the Presence of Acetate Ions in DMF[a]

concn		+ 1AcO$^-$	+ 10AcO$^-$	+ 500AcO$^-$
11.5 mM	12.42	17.69	18.72	21.36
17.0 mM	7.12	12.75	13.12	nd[b]

[a] δ values are relative to H_3PO_4 (external reference). [b] Not determined.

However, these results are deduced from observations taken from cyclic voltammetry. We cannot exclude at this stage the possibility that the shift in the oxidation peak potentials, observable when acetate ions were added to a solution of $Pd^0(PPh_3)_4$, is not due to the formation of a new anionic species, $Pd^0(PPh_3)_3(OAc)^-$, but to a reaction of the acetate ion with the palladium(I) generated by oxidation of $Pd^0(PPh_3)_3$. Indeed, under some specific circumstances[7b] such a chemical reaction could make the $Pd^0(PPh_3)_3$ complex more easily oxidized. Also, the anionic species could exist only within an uphill equilibrium, continuously displaced by the electrode reaction.[7c]

In order to validate our above hypothesis, the effect of acetate ions on solutions of $Pd^0(PPh_3)_4$ was investigated by a technique that allows the observation of the species in solution in their initial state without any chemical or electrochemical transformation, such as ^{31}P NMR spectroscopy.

B. Ligation of Palladium(0) Complexes by Acetate Anions. Investigation by ^{31}P NMR Spectroscopy. The ^{31}P NMR spectrum of a solution of $Pd^0(PPh_3)_4$ in DMF exhibited a broad unique signal characteristic of the species $Pd^0(PPh_3)_3$, $Pd^0(PPh_3)_2$, and PPh_3 involved in a fast equilibrium (the solvent is omitted for simplification).[6,8] As evidenced in Table 2, the chemical shift of the ^{31}P NMR signal strongly depends on the overall concentration of the palladium(0) complex that affects the two equilibria 6 and 7.

$$Pd^0(PPh_3)_4 \rightleftharpoons Pd^0(PPh_3)_3 + PPh_3 \quad (6)$$
$$Pd^0(PPh_3)_3 \rightleftharpoons Pd^0(PPh_3)_2 + PPh_3 \quad (7)$$

When only 1 equiv of AcO$^-$ was added as solid nBu_4NOAc to solutions of $Pd^0(PPh_3)_4$, a new broad signal was observed that was located at lower field, at around 5 ppm from the initial complex (Table 2). Whatever the palladium(0) concentration, addition of >1 equivalent of acetate also resulted in a shift of the signal to lower field, but the shift per equivalent was smaller. These results demonstrate that the acetate ions interfere in equilibria 6 and 7 by coordinating the palladium(0) complexes. The high variation of the chemical shift observed when only 1 equiv of AcO$^-$ was introduced suggests that a new species was formed, such as $Pd^0(PPh_3)_3(OAc)^-$, in the exergonic reaction 8. Since the resulting ^{31}P NMR signal was still broad, it is presumable that this reaction is followed by a fast equilibrium involving the less ligated $Pd^0(PPh_3)_2(OAc)^-$ complex and PPh_3 (reaction 9). Therefore we can assume that

$$Pd^0(PPh_3)_4 + OAc^- \rightleftharpoons Pd^0(PPh_3)_3(OAc)^- + PPh_3 \quad (8)$$
$$Pd^0(PPh_3)_3(OAc)^- \rightleftharpoons Pd^0(PPh_3)_2(OAc)^- + PPh_3 \quad (9)$$

acetate ions can coordinate unsaturated palladium(0) complexes to form anionic species characterized by ^{31}P NMR spectroscopy and cyclic voltammetry. Let us now examine the consequences on the oxidative addition of aryl halides to these new anionic palladium(0) complexes.

C. Characterization of the Arylpalladium Complexes Formed by Oxidative Addition of Iodobenzene with Palladium(0) Complexes Ligated by Acetate Anions. The final product resulting from the oxidative addition of triphenylphosphine ligated palladium(0) complexes with aryl halides is a stable *trans*-σ-arylpalladium complex, $ArPdXL_2$.[9] However, some of us have recently reported that when the oxidative addition was performed with a low-valent palladium(0) complex ligated by chloride, such as $Pd^0(PPh_3)_2Cl^-$, the resulting *trans-s*-arylpalladium complex was slowly formed *via* an anionic pentacoordinated σ-arylpalladium species according to the following mechanism (reactions 10–12)[10]

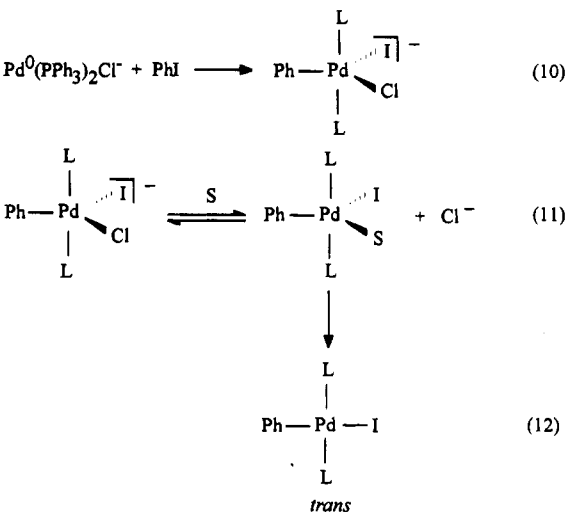

whereas oxidative addition of $Pd^0(PPh_3)_4$ with aryl halides rapidly affords a *trans*-σ-arylpalladium complex from the low-ligated $Pd^0(PPh_3)_2$ complex (eq 13) after deligation of two phosphine ligands through the equilibria 6 and 7.[8]

$$Pd^0(PPh_3)_2 + PhI \rightarrow \underset{trans}{PhPdI(PPh_3)_2} \quad (13)$$

In the latter case, no intermediate has been detected, even in the presence of chloride ions. Also, triphen-

(7) (a) The peak potential of a chemically irreversible voltammogram depends on thermodynamics (*i.e.*, structural effects) as well as on kinetics of electron transfer and homogeneous proceeding of follow-up chemical steps. In the present case, two homogeneous chemical reactions involving acetate ions and $Pd^0(PPh_3)_3$ could be tentatively considered. (b) Follow-up complexation of the Pd^I species formed upon the first electron transfer, by acetate ions, according to a classical "EC" electrochemical sequence.[7d,e] (c) An uphill pre-equilibrium involving a coordination of the Pd^0 center by acetate ions prior to the first electron transfer, according to a classical "CE" electrochemical process. See for example refs 6 and 7d: (d) Bard, A. J.; Faulkner, L. R. *Electrochemical Methods: Fundamentals and Applications*; Wiley: New York, 1980. (e) Howell, J. O.; Goncalves, J. M.; Amatore, C.; Klasinc, L.; Wightman, R. M.; Kochi, J. K. *J. Am. Chem. Soc.* **1984**, *106*, 3968.

(8) (a) Fauvarque, J. F.; Pflüger, F.; Troupel, M. *J. Organomet. Chem.* **1981**, *208*, 419. (b) Amatore, C.; Pflüger, F. *Organometallics* **1990**, *9*, 2276.

(9) (a) Fitton, P.; Johnson, M. P.; Mc Keon, J. E. *J. Chem. Soc., Chem. Commun.* **1968**, 6. (b) Fitton, P.; Rick, E. A. *J. Organomet. Chem.* **1971**, *28*, 287.

(10) (a) Amatore, C.; Jutand, A.; Suarez, A. *J. Am. Chem. Soc.* **1993**, *115*, 9531. (b) Other trigonal bipyramidal structures are obviously possible see reference 32c in ref 10a.

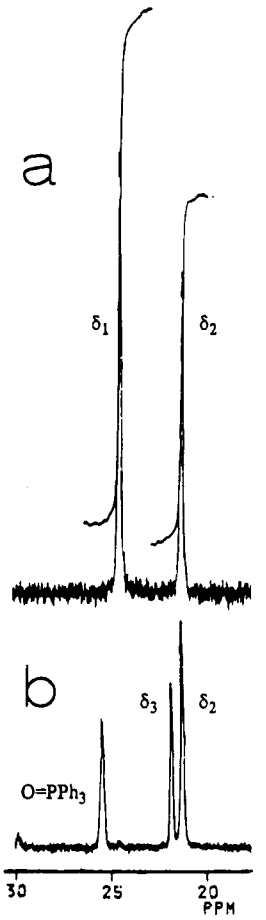

Figure 2. (a) ^{31}P NMR spectrum (162 MHz) of a mixture of *trans*-$PhPdI(PPh_3)_2$ (20.4 mg) and 1.5 equiv of nBu_4NOAc (11 mg) in 3 mL of DMF and 0.2 mL of acetone-d_6, with H_3PO_4 as an external reference. (b) ^{31}P NMR spectrum (162 MHz) of the solution resulting from the oxidative addition of PhI (1 equiv, 7 μL) to the palladium(0) complex generated *in situ* from the mixture $Pd(OAc)_2$ (14.8 mg) and $4PPh_3$ (69 mg) in 3 mL of DMF and 0.2 mL of acetone-d_6, with H_3PO4 as an external reference. The ^{31}P NMR signal at 25.43 ppm is that of the triphenylphosphine oxide that was generated together with the palladium(0) complex.

ylphosphine was found to be an efficient catalyst for the formation of the *trans* complex resulting from the overall reaction 10 + 11 + 12.[10a]

When the oxidative addition with iodobenzene was performed from $Pd^0(PPh_3)_4$ in the presence of acetate ions (1 or 10 equiv), we found that the resulting ^{31}P NMR spectrum exhibited, in addition to the characteristic signals of *trans*-$PhPdI(PPh_3)_2$ at δ_1 24.44 ppm in DMF (23.42 ppm in THF) and of the free phosphine at δ_0 −5.50 ppm in DMF (−5.22 ppm in THF), an additional signal at δ_2 21.25 ppm in DMF (21.15 ppm in THF). This shows that the oxidative addition, when performed in the presence of acetate ions, affords another complex besides the usual *trans* $PhPdI(PPh_3)_2$ complex.[11] In order to identify the complex characterized by the signal at δ_2, we investigated whether acetate ions could react with the *trans* $PhPdI(PPh_3)_2$ complex or not. ^{31}P NMR spectra of solutions of the *trans* $PhPdI(PPh_3)_2$ complex in THF or in DMF, containing acetate ions exhibited, in addition to the signal δ_1 of the *trans* complex, a signal at δ_2 (Figure 2a) identical to that

(11) Another signal was also detected at long times at δ 25.4 ppm in DMF (23.7 ppm in THF) corresponding to triphenylphosphine oxide.

Table 3. Equilibrium Constants *K* Determined at 27 °C for the Reaction $PhPdX(PPh_3)_2 + AcO^- \leftrightharpoons PhPd(OAc)(PPh_3)_2 + X^-$[a,b]

X	*K* DMF	*K* THF
I	0.30 (0.45)	1.30
Br	0.10 (0.20)	0.20 (0.20)
Cl	0.04	nd[c]

[a] $K = [PhPd(OAc)L_2][X^-]/[PhPdXL_2][AcO^-]$. [b] Values in parentheses were determined in the presence of nBu_4NBF_4 (0.3 M). [c] Not determined.

resulting from the oxidative addition described above. The ratio of the two signals was constant as a function of time, but the signal at δ_2 increased at the expense of that of δ_1 when the amount of AcO^- was increased. Introduction of iodide ions resulted in the reverse effect, *viz.* increase of the signal at δ_1 at the expense of that at δ_2. An authentic sample of the *trans*-$PhPd(OAc)(PPh_3)_2$ complex has been synthesized (by reacting *trans*-$PhPdI(PPh_3)_2$ with AgOAc) and characterized by its ^{31}P NMR signal at δ_2.[12] This evidences that acetate ions react with the *trans* $PhPdI(PPh_3)_2$ complex to form a new complex, *trans*-$PhPd(OAc)(PPh_3)_2$,[13] and that this reaction is an equilibrium (eq 14). This reaction is

$$\underset{trans\ \delta_1}{PhPdI(PPh_3)_2} + AcO^- \overset{K}{\rightleftharpoons} \underset{trans\ \delta_2}{PhPd(OAc)(PPh_3)_2} + I^- \quad (14)$$

general whatever the halide of the arylpalladium halide complex, and addition of chloride ions to a solution of the *trans* $PhPd(OAc)(PPh_3)_2$ complex resulted in the formation of some *trans*-$PhPdCl(PPh_3)_2$, which was detected by its ^{31}P NMR signal at 24.40 ppm in DMF. The equilibrium constants *K* (eq 14) have been estimated by integration of the ^{31}P NMR signals at δ_1 and δ_2. From the values of *K*, collected in Table 3, we can conclude that the iodide ion is more easily substituted by the acetate ion than the chloride ion and that the substitution is easier in THF than in DMF.

Performing cyclic voltammetry on solutions of *trans*-$PhPdX(PPh_3)_2$ (X = I, Br) in DMF[14a] showed that these complexes were in equilibrium with the cationic complex $PhPd(PPh_3)_2^+$ (which has been synthesized by reacting *trans*-$PhPdI(PPh_3)_2$ with $AgBF_4$) and the corresponding equilibrium constant K_{Br} (in eq 15) has been determined by chronoamperometry.[15] Thus, the substitution of the halide by the acetate ion probably goes through a cationic complex (S_N1 mechanism), the latter being better solvated by DMF rather than by THF (eqs 15 and 16).[16]

(12) Some triphenylphosphine oxide was detected in the ^{31}P NMR spectrum of solutions containing $PhPd(OAc)(PPh_3)_2$. It seems that in solution $PhPd(OAc)(PPh_3)_2$ can spontaneously and slowly produce triphenylphosphine oxide *via* an intramolecular reduction in a way similar to that we have reported from $Pd(OAc)_2(PPh_3)_2$ (reactions 2 and 3).[1] The formation of triphenylphosphine oxide in high yield has also been observed in the electrochemical reduction of allylic acetates catalyzed by the complex $Pd(OAc)_2$ combined with $6PPh_3$ probably *via* an allyl−$Pd(OAc)(PPh_3)_2$ complex. Torii, S.; Tanaka, H., et al. Private communication, Paris, March 1995.

(13) (a) While this paper was being written, we were informed (N. Miyaura, personal communication to A. Jutand during the 209th American Chemical Society National Meeting in Anaheim, CA, April 2−6, 1995) that (i) $PhPd(OAc)(PPh_3)_2$ has been synthesized simultaneously by N. Miyaura and co-workers and that (ii) Miyaura and co-workers have also observed the formation of $PhPd(OAc)(PPh_3)_2$ from $PhPdI(PPh_3)_2$ in the presence of acetate ions. (b) Preliminary results (in ii above) have already been reported by our group in ref 1a and at the same conference by A. Jutand.

$$PhPdX(PPh_3)_2 \overset{K_X}{\rightleftharpoons} PhPd(PPh_3)_2^+ + X^- \quad (15)$$
with $K_{Br} = [PhPdBrL_2]/[PhPdL_2^+][Br^-] = 3.5 \times 10^3\ M^{-1}$

$$PhPd(PPh_3)_2^+ + AcO^- \overset{K_{OAc}}{\rightleftharpoons} PhPd(OAc)(PPh_3)_2 \quad (16)$$
with $K_{OAc} = [PhPd(OAc)L_2]/[PhPdL_2^+][AcO^-]$

Since $K = [PhPd(OAc)L_2][Br^-]/[PhPdBrL_2][AcO^-] = K_{OAc}/K_{Br}$, the equilibrium constant K_{OAc} of eq 16 can be calculated in DMF, $K_{OAc} = 7 \times 10^2\ M^{-1}$. From the values of K_{OAc} and K (Table 3) we can determine $K_I = 1.5 \times 10^3\ M^{-1}$ and $K_{Cl} = 1.7 \times 10^4\ M^{-1}$. Comparison of the respective values of K_X (X = Cl, Br, and I) and K_{OAc} indicates that, as expected, the affinity of palladium(II) for the anion X′ in $PhPdX'(PPh_3)_2$ complexes follows the order $Cl^- > Br^- > I^- > AcO^-$.

Therefore, the oxidative addition of $Pd^0(PPh_3)_4$ with iodobenzene performed in the presence of acetate ions affords a mixture of two complexes (eq 17).

$$Pd^0(PPh_3)_4 + AcO^- + PhI \rightarrow \rightarrow x PhPdI(PPh_3)_2 + (1-x)PhPd(OAc)(PPh_3)_2 + (1-x)I^- + xAcO^- + 2PPh_3 \qquad 0 < x < 1 \quad (17)$$

But at this stage of the study we could not determine whether the *trans* $PhPd(OAc)(PPh_3)_2$ complex was formed directly from the reaction of $Pd(PPh_3)_2(OAc)^-$ with iodobenzene or resulted from the equilibrium 14.

When the oxidative addition with iodobenzene was performed from the palladium(0) complex that spontaneously generated from the mixtures of $Pd(OAc)_2$ and nPPh$_3$ (n = 4 or 10) in DMF or THF, surprisingly the signal at δ_1 24.44 ppm in DMF (23.42 ppm in THF), characteristic of *trans*-$PhPdI(PPh_3)_2$, was not detected but the signal of the *trans* $PhPd(OAc)(PPh_3)_2$ complex at δ_2 21.25 ppm in DMF (21.15 ppm THF) was present with an additional signal at δ_3 21.81 ppm in DMF (21.41 ppm in THF) (Figure 2b). The signal at δ_3 was found to be identical to that of the cationic complex $PhPd(PPh_3)_2^+BF_4^-$. The complex $PhPdI(PPh_3)_2$ was never observed even at very long times (overnight).[17] Therefore, investigation of the oxidative addition by ^{31}P NMR spectroscopy demonstrates that the complex $PhPd(OAc)(PPh_3)_2$ is the final product of the oxidative addition. Investigation of the oxidative addition by cyclic voltammetry also led to the same conclusion since the cyclic voltammogram of an authentic sample of $PhPd(OAc)(PPh_3)_2$[14b] (Figure 3a) was similar to that of the final complex resulting from the oxidative addition (Figure 3b).

In an earlier paper we reported how to monitor the reactivity of the palladium(0) complex generated *in situ* from mixtures of $Pd(OAc)_2$ and nPPh$_3$ (n = 10) with iodobenzene by recording the variation of its oxidation plateau current as a function of time after addition of PhI.[1b] We observed that, when the electrode was polarized at +0.2 V, the oxidation current of the palladium(0) gradually dropped to zero and stabilized at this value, signifying the end of the oxidative addition. However, when the electrode was polarized at a more positive potential, *i.e.*, at +0.4 V, the current first dropped to zero and then slowly increased so as to reach a plateau (Figure 4a). Cyclic voltammetry of the final solution exhibited the characteristic oxidation peak of iodide ions (see Figure 4b) at $E^p_{Ox} = +0.44$ V in DMF. Thus, when the electode was polarized at a potential where iodide ions are oxidized, the decreasing part of the curve represents the kinetics of the oxidative addition of iodobenzene to the palladium(0) complex whereas the rising part of the curve represents the kinetics of release of iodide ions from an intermediate complex that affords $PhPd(OAc)(PPh_3)_2$ as the final product. Since we know from above that this complex is not $PhPdI(PPh_3)_2$, we are forced to conclude that the kinetic intermediate contains both acetate and iodide ions. These results suggest that the oxidative addition affords $PhPd(OAc)(PPh_3)_2$ *via* a pentacoordinated phenylpalladium complex containing one iodide ion and one acetate ion according to the following mechanism (eq 9 and eqs 18 and 19):

$$Pd^0(PPh_3)_3(OAc)^- \rightleftharpoons Pd^0(PPh_3)_2(OAc)^- + PPh_3 \quad (9)$$

$$Pd^0(PPh_3)_2(OAc)^- + PhI \longrightarrow \begin{matrix} L \\ | \\ Ph-Pd \\ | \\ L \end{matrix} \begin{matrix} \overline{I}^- \\ \diagdown \\ OAc \end{matrix} \quad (18)$$

$$\begin{matrix} L \\ | \\ Ph-Pd \\ | \\ L \end{matrix} \begin{matrix} \overline{I}^- \\ \diagdown \\ OAc \end{matrix} \xrightarrow{k_1} \begin{matrix} L \\ | \\ Ph-Pd-OAc \\ | \\ L \end{matrix} + I^- \quad (19)$$

trans

The formation of rather stable pentacoordinated anionic arylpalladium complexes $ArPdICl_2^-$ has already been reported by our group in the case of the oxidative addition of $Pd^0(PPh_3)_2Cl^-$ with PhI (see eq 10).[10] The value of the rate constant k_1 of the formation of $PhPd(OAc)(PPh_3)_2$ from the pentacoordinated anionic species (eq 19) can be determined from the rising part of the curve in Figure 4a by plotting the variation of $\ln[(i_{lim} - i)/i_{lim}]$ (i, oxidation current of I^- at +0.4 V at t; i_{lim}, limit of i at infinite time) as a function of time (Figure 4c). From the slope of the straight line, one obtains $k_1 = 2.8 \times 10^{-2}\ s^{-1}$. The half-life of this anionic pentacoordinated complex (≈40 s) obtained from a palladium(0) complex generated from $Pd(OAc)_2$ combined with 10PPh$_3$ was very similar to that obtained

(14) (a) In DMF, the cyclic voltammograms of $PhPdX(PPh_3)_2$ complexes (X = I, Br, Cl) exhibited two successive irreversible reduction peaks R_1 and R_2. The ratio of the two reduction peak currents, i_1/i_2, increased when the scan rate decreased, characteristic of two species in equilibrium.[6,7d] The first reduction peak was assigned to the reduction of the cationic complex $PhPd(PPh_3)_2^+$, whereas the second peak was assigned to the neutral complex $PhPdX(PPh_3)_2$. Indeed, the addition of X^- ions to $PhPdX(PPh_3)_2$ resulted in an increase of the second reduction peak at the expense of the first one.[15] (b) In DMF, the cyclic voltammogram of $PhPd(OAc)(PPh_3)_2$ (Figure 3a) exhibited two successive irreversible reduction peaks. The first one, R_1 at −1.84 V, was assigned to the reduction of $PhPd(PPh_3)_2^+$, and the second one, R_2 at −2.08 V, was assigned to the reduction of $PhPd(OAc)(PPh_3)_2$. Addition of AcO^- ions resulted in an increase of the second reduction peak at the expense of the first peak.[15]

(15) Amatore, C.; Carré, E.; Jutand, A. Unpublished results, 1994.

(16) A mechanism similar to S_N2 can probably be excluded since we have shown in a previous work that *trans* $PhPdX(PPh_3)_2$ complexes did not react with halide ions X'^- to form pentacoordinated species such as $PhPdXX'(PPh_3)_2^-$.[10a]

(17) (a) In a previous paper[1a] δ_3 was uncorrectly assigned to $PhPdI(PPh_3)_2$. (b) At long times, a fourth signal was detected at δ_4 23.30 ppm in DMF that could be assigned to $PhPd(OH)(PPh_3)_2$. Indeed we got the same signal by reacting $PhPd(PPh_3)_2^+BF_4^-$ with water or $PhPdI(PPh_3)_2$ with nBu_4NOH. The complex $PhPd(OH)(PPh_3)_2$ was recently reported to be formed from a mixture of $Ph_2Pd_2(\mu OH)_2(PPh_3)_2$ and PPh_3, but due to the equilibrium $Ph_2Pd_2(\mu OH)_2(PPh_3)_2 + 2PPh_3 \leftrightharpoons 2PhPd(OH)(PPh_3)_2$, the signal of $PhPd(OH)(PPh_3)_2$ was not observed. See: (c) Grushin V. V.; Alper, H. *J. Am. Chem. Soc.* **1995**, *117*, 4305.

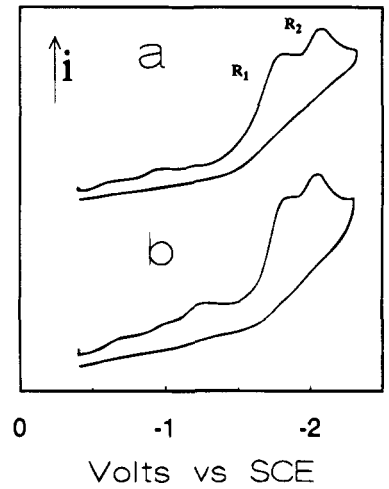

Figure 3. (a) Cyclic voltammetry of an authentic sample of $PhPd(OAc)(PPh_3)_2$ (2 mM) in DMF (nBu_4NBF_4, 0.3 M) at 25 °C, at a stationary gold disk electrode (ø 0.5 mm) with a scan rate of 0.2 V s^{-1}. (b) Cyclic voltammetry of the complex $PhPd(OAc)(PPh_3)_2$ resulting from the oxidative addition of PhI (2 mM) with the palladium(0) complex generated *in situ* from $Pd(OAc)_2$ (2 mM) and PPh_3 (8 mM), in DMF (nBu_4NBF_4, 0.3 M) at 25 °C.

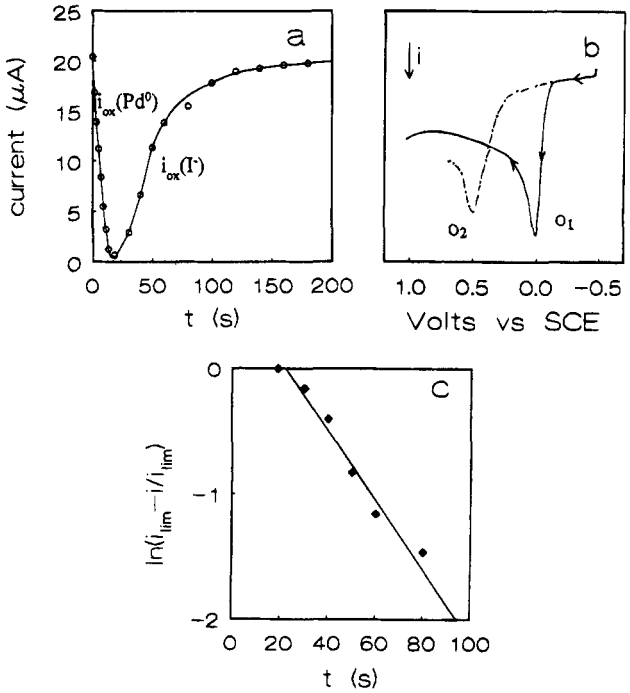

Figure 4. Oxidative addition of phenyl iodide with the palladium(0) complex generated *in situ* from $Pd(OAc)_2$ (2 mM) and PPh_3 (20 mM), in DMF (nBu_4NBF_4, 0.3 M) at 25 °C. (a) Variation of the oxidation plateau current at +0.4 V, at a rotating gold disk electrode (ø 2 mm; $v = 0.02$ Vs^{-1}; $\omega = 105$ rad s^{-1}) in the presence of phenyl iodide (20 mM) as a function of time. (b) Cyclic voltammetry of the palladium(0) complex generated *in situ* from $Pd(OAc)_2$ (2 mM) and PPh_3 (20 mM), in DMF (nBu_4NBF_4, 0.3 M) at 25 °C, performed just before the oxidative addition with PhI (—). Cyclic voltammetry performed after the oxidative addition with PhI (·-·-·). (c) Variation of $\ln[(i_{lim} - i)/i_{lim}]$ as a function of time.

when $Pd(OAc)_2$ was combined with $5PPh_3$. Therefore PPh_3 does not seem to catalyze the formation of the *trans* $PhPd(OAc)(PPh_3)_2$ complex from the anionic pentacoordinated $PhPdI(OAc)(PPh_3)_2^-$, a result that was observed for the formation of the *trans* $PhPdI(PPh_3)_2$ complex from $PhPdICl(PPh_3)_2^-$.[10a]

Although iodide ions were released from reaction 19, they did not react with $PhPd(OAc)(PPh_3)_2$ to produce $PhPdI(PPh_3)_2$ according to the equilibrium 14, since $PhPdI(PPh_3)_2$ was never observed in the ^{31}P NMR spectrum recorded after the oxidative addition. This suggests that the iodide ions, liberated in reaction 19, were not completely free. The formation of the palladium(0) complex from the mixtures of $Pd(OAc)_2$ and $n PPh_3$ is concomitant with the formation of AcOH and H^+ according to reaction 3. Iodide ions might be involved in an equilibrium with the proton ($I^- + H^+ \leftrightarrows$ HI) and therefore might not be able to react significantly with $PhPd(OAc)(PPh_3)_2$. This hypothesis was confirmed by the fact that when no protons were present in the medium, *i.e.*, when the oxidative addition with PhI was performed from a mixture of $Pd^0(PPh_3)_4$ and AcO^-, both $PhPdI(PPh_3)_2$ and $PhPd(OAc)(PPh_3)_2$ were produced.

We can thus assume that the oxidative addition of iodobenzene with the palladium(0) complex formed *in situ* from the mixtures of $Pd(OAc)_2$ and $n PPh_3$, does not afford the *trans* $PhPdI(PPh_3)_2$ complex but rather the *trans* $PhPd(OAc)(PPh_3)_2$ complex. This occurs most presumably *via* pentacoordinated species $PhPdI(OAc)(PPh_3)_2^-$. Conversely, a mixture of *trans*-$PhPdI(PPh_3)_2$ and *trans*-$PhPd(OAc)(PPh_3)_2$ is obtained when the oxidative addition is performed from a mixture of $Pd^0(PPh_3)_4$ and AcO^-.

D. Reactivity of Palladium(0) Complexes Ligated by Acetate Anions in Oxidative Addition with Iodobenzene in DMF at 25 °C. We established above that the products resulting from the oxidative addition strongly depend on the precursor of the palladium(0) complex. We wish now to investigate the reactivity of different palladium(0) complexes in the oxidative addition as a function of the precursor. As mentioned above and in our previous paper,[1b] it is possible to monitor the reactivity of palladium(0) complexes in oxidative addition with phenyl iodide by recording its oxidation plateau current at +0.2 V as a function of time (Figure 5a). A plot of the ratio i_0/i as a function of time, resulted in a straight line ($i_0/i = k_{app}C_0t + 1$, when $[PhI] = [Pd^0] = C_0$), demonstrating that the oxidative addition was first order in palladium(0) and in iodobenzene (Figure 5b). The value of the apparent rate constant k_{app} of the oxidative addition could then be deduced from the slope of the straight line (eq 20).

$$\text{“}Pd^0L_n, AcO^-\text{”} + PhI \xrightarrow{k_{app}} PhPdXL_2 + (n-2)L \quad (20)$$

From the values of k_{app} determined when the oxidative addition of PhI with $Pd^0(PPh_3)_4$ was performed in the absence or in the presence of acetate (Table 4, entries 1–4) we can deduce that the presence of acetate anions does not have a significant influence on the apparent rate constant of the oxidative addition. In the absence of acetate, it is reported that the low-ligated palladium(0) complex $Pd^0(PPh_3)_2$ is more reactive in oxidative addition than the more ligated complex $Pd^0(PPh_3)_3$. Its overall rate depends on its concentration, which is controlled by the value of the equilibrium constant K (eq 7).[8]

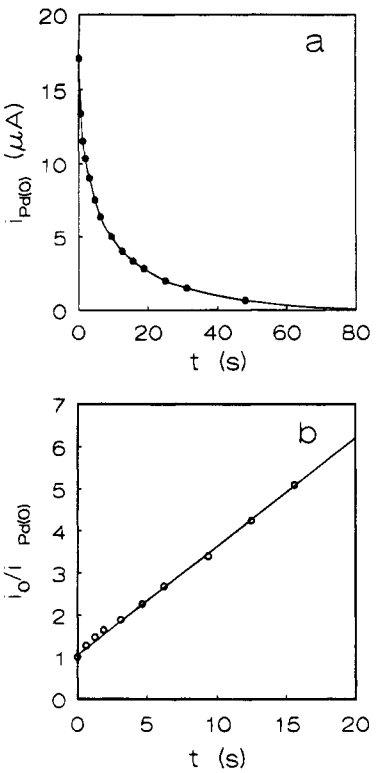

Figure 5. Oxidative addition of phenyl iodide with the palladium(0) complex quantitatively generated *in situ* from $Pd(OAc)_2$ (2 mM) and PPh_3 (6 mM), in DMF (nBu_4NBF_4, 0.3 M) at 25 °C. (a) Variation of the oxidation plateau current $i_{Pd(0)}$ at +0.2 V, at a rotating gold disk electrode (ø = 2 mm; v = 0.02 V s^{-1}; ω = 105 rad s^{-1}) in the presence of phenyl iodide (2 mM) as a function of time. (b) Variation of i_0/i as a function of time.

$$Pd^0(PPh_3)_3 \rightleftharpoons Pd^0(PPh_3)_2 + PPh_3 \qquad K \qquad (7)$$

$$+ PhI \downarrow k$$

$$PhPdI(PPh_3)_2$$

In the presence of an excess of phosphine, the corresponding apparent rate constant of the oxidative addition is given by the relation $k_{app} = kK/[PPh_3]$.[8] In the presence of acetate ions, the corresponding apparent rate constant of the oxidative addition is: $k'_{app} = k'K'/[PPh_3]$ (eq 9).

$$Pd^0(PPh_3)_3(OAc)^- \rightleftharpoons Pd^0(PPh_3)_2(OAc)^- + PPh_3 \qquad K' \qquad (9)$$

$$+ PhI \downarrow k'$$

$$PhPdI(PPh_3)_2 + PhPd(OAc)(PPh_3)_2$$

The complex $Pd^0(PPh_3)_2(OAc)^-$ would be the reactive species rather than $Pd^0(PPh_3)_2$. Indeed, since the rate of the oxidative addition was not sensitive to the acetate concentration, one can exclude the participation of the following equilibrium (eq 21)

$$Pd^0(PPh_3)_2(OAc)^- \rightleftharpoons Pd^0(PPh_3)_2 + AcO^- \qquad (21)$$

which would yield an apparent rate constant $k''_{app} = k''K''/[AcO^-]$.

Surprisingly, the fact that the rate does not depend on the acetate concentration implies that the value of $k'K'$ is very close to that of kK. The ligation of $Pd^0(PPh_3)_2$ by one acetate ion produces a species $Pd^0(PPh_3)_2(OAc)^-$ that ought to be more nucleophilic and more reactive in the oxidative addition with PhI. Thus k' is expected to be higher than k, which implies that $K' < K$.

However, one observes from the values of k_{app} (Table 4, compare entries 2 and 5) that the oxidative addition with phenyl iodide was slightly faster with the palladium(0) generated from the mixture of $Pd(OAc)_2$ and $5PPh_3$ than with $Pd^0(PPh_3)_4$ and $1AcO^-$, although the two systems are formally equivalent, since one triphenylphosphine is oxidized to triphenylphosphine oxide in the first system. In some way, it could seem that internal acetate ions play a more efficient role than external ones. However, it must be noted that the generation of the palladium(0) complex from mixtures of $Pd(OAc)_2$ and $n PPh_3$ is concomitant with the formation of triphenylphosphine oxide and protons (reaction 3). These two species may interfere in the kinetics of the oxidative addition. It has been postulated that phosphine oxide may coordinate palladium complexes,[3b] but we observed that adjunction of 1 equiv of $O{=}PPh_3$ to the mixture of $Pd^0(PPh_3)_4$ and $1AcO^-$ did not change the value of the apparent rate constant of the oxidative addition with PhI. The role of the proton may be the complexation of the reactive anionic species $Pd^0(PPh_3)_2(OAc)^-$. In order to clarify the role of the proton, the oxidative addition was performed with the palladium(0) complex generated from the mixture $Pd(OAc)_2$ and $5PPh_3$ but in the presence of 3 equiv of a base, NEt_3. Under these conditions the value of the apparent rate constant of the oxidative addition was k_{app} = 22 M^{-1} s^{-1}, a value similar to that found for the oxidative addition performed from the mixture of $Pd^0(PPh_3)_4$ and $nAcO^-$ (entries 2–4, Table 4) where, of course, no proton was present. Therefore protons appear to play the same role with $Pd^0(PPh_3)_2(OAc)^-$ as cations do with the anionic species $Pd^0(PPh_3)_2Cl^-$, *i.e.*, coordinating the negatively charged palladium(0) species with the result of enhancing its reactivity.[4c]

In the presence of excess phosphine (more than 5 equiv per palladium(0)) the reactivity of the palladium(0) complex did not depend significantly on its precursor (Table 4, compare entries 7–9). As expected the oxidative addition became slower upon increasing the phosphine concentration. This is rationalized considering that the concentration of the reactive species $Pd^0(PPh_3)_2(OAc)^-$ became smaller because the presence of an excess of phosphine results in the shift of the equilibrium 9 to its left-hand side.

As expected, the most reactive palladium(0) complex was that generated from the mixture of $Pd(OAc)_2$ and $3PPh_3$ (Table 4, entry 6) in which the resulting palladium(0), $Pd^0(PPh_3)_2(OAc)^-$, could not be ligated by more than two phosphines and is thus the only Pd(0) species in solution. Therefore mixing $Pd(OAc)_2$ and $3PPh_3$ allows the direct and quantitative synthesis of $Pd^0(PPh_3)_2(OAc)^-$ ligated by only two phosphines, which undergoes a fast reaction with iodobenzene. In this case, since no extra phosphine is present in solution, we do not measure the value of an apparent rate constant but measure directly the value of the rate constant k' of the intrinsic oxidative addition (eq 22).

$$Pd^0(PPh_3)_2(OAc)^- + PhI \xrightarrow{k_2} PhPd(OAc)(PPh_3)_2 + I^-$$

$$k_2 = 140\ M^{-1}\ s^{-1} \text{ in DMF at } 25\ °C \qquad (22)$$

Table 4. Apparent Rate Constant k_{app} of the Oxidative Addition of Palladium(0) Complexes with PhI as a Function of Their Precursors in DMF at 25 °C

entry no.	precursor of "Pd^0"	main species in solution	k_{app} (M^{-1} s^{-1})
1	$Pd^0(PPh_3)_4$	$Pd^0(PPh_3)_3 + 1PPh_3$	25
2	$Pd^0(PPh_3)_4 + 1AcO^-$	$Pd^0(PPh_3)_3(OAc)^- + 1PPh_3$	21
3	$Pd^0(PPh_3)_4 + 10AcO^-$	$Pd^0(PPh_3)_3(OAc)^- + 1PPh_3 + 9AcO^-$	24
4	$Pd^0(PPh_3)_4 + 100AcO^-$	$Pd^0(PPh_3)_3(OAc)^- + 1PPh_3 + 99AcO^-$	26
5	$Pd(OAc)_2 + 5PPh_3$	$Pd^0(PPh_3)_3(OAc)^- + 1PPh_3 + O{=}PPh_3$	41
6	$Pd(OAc)_2 + 3PPh_3$	$Pd^0(PPh_3)_2(OAc)^- + O{=}PPh_3$	140
7	$Pd^0(PPh_3)_4 + 5PPh_3$	$Pd^0(PPh_3)_3 + 6PPh_3$	9.5
8	$Pd^0(PPh_3)_4 + 5PPh_3 + 1AcO^-$	$Pd^0(PPh_3)_3(OAc)^- + 6PPh_3$	12.5
9	$Pd(OAc)_2 + 10PPh_3$	$Pd^0(PPh_3)_3(OAc)^- + 6PPh_3 + O{=}PPh_3$	12

Scheme 1

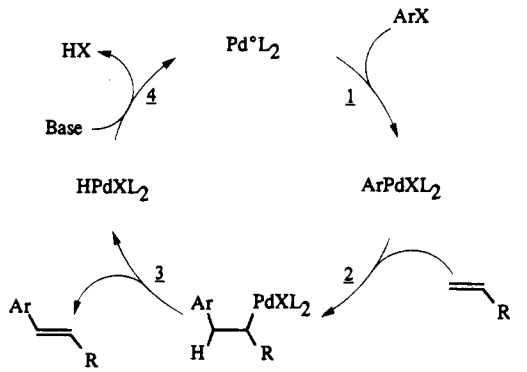

E. $PhPd(OAc)(PPh_3)_2$ as Intermediate in the Heck Reaction. Mixtures of $Pd(OAc)_2$ and $nPPh_3$ ($n \geq 2$) are efficient catalysts for Heck reactions (eq 23).[2]

$$ArX + R{-}CH{=}CH_2 + NR'_3 \xrightarrow{Pd(OAc)_2 + nPPh_3} R{-}CH{=}CH{-}Ar + HNR'_3{}^+X^- \quad (23)$$

The mechanism generally accepted is recalled in Scheme 1.[2h] The rate determining step of the catalytic cycle has never been clearly established. There is general agreement on the fact that the first step of the reaction is oxidative addition of a palladium(0) complex with the aryl halide ArX (step 1) to form an $ArPdXL_2$ complex prone to add on the olefin (step 2). In the present study, we have observed that complexes such as $ArPdX(PPh_3)_2$ (step 1) were not formed during the oxidative addition but that the final product was $ArPd(OAc)(PPh_3)_2$ involved in an equilibrium with the cationic complex $ArPd(PPh_3)_2^+$ (eq 16). It is thus of interest to determine the real intermediate involved in the Heck reaction, *i.e.*, the arylpalladium(II) complex able to react with olefins (step 2). The reaction was followed by cyclic voltammetry with styrene as the olefin. The final expected product, *trans*-stilbene, can be easily detected by its reduction peak at −2.20 V, which is located at a more negative potential than that of $PhPd(OAc)(PPh_3)_2$ (−2.04 V) and at a less negative potential than the reduction potential of styrene (−2.60 V).

From the results collected in Table 5, we observe that under our experimental conditions (DMF, 20 °C) stilbene was formed by reacting styrene with the complex $PhPd(OAc)(PPh_3)_2$ resulting from the oxidative addition of PhI (1 equiv) with the palladium(0) complex generated from the mixture of $Pd(OAc)_2$ and $4PPh_3$. Yields were higher when some triethylamine was present (entries 1−3). The amine is usually described as a reagent able to regenerate the palladium(0) catalyst in step 4 (Scheme 1), *i.e.*, in the step following the formation of the final product. Since we have operated under non catalytic conditions in which the iodobenzene was in stoichiometric proportion relative to the palladium(0) complex, it seems that the amine interferes also in previous steps, unless step 3 is an equilibrium. This latter hypothesis was disproved by the fact that introduction of NEt_3 at the end of the reaction did not improve the yield of stilbene. In a previous study we demonstrated that acetic acid and a proton were formed with the palladium(0) generated from $Pd(OAc)_2$ and $nPPh_3$ (eq 3).[1b] Therefore, in stoichiometric conditions the role of the amine might be the neutralization of the medium. The role of the amine might, however, become more complex under catalytic conditions by regenerating the palladium(0) complex (see step 4).

Table 5. Reaction of Styrene with Isolated $PhPdI(PPh_3)_2$ Complex and with $PhPd(OAc)(PPh_3)_2$ Resulting from the Oxidative Addition of PhI with the Palladium(0) Complex Generated *in Situ* from $Pd(OAc)_2$ and $4PPh_3$ in DMF at 25 °C

entry no.	$PhPdX(PPh_3)_2$	NEt_3 (no. of equiv)	time (h)	stilbene (%)[a]
1	$PhPd(OAc)(PPh_3)_2$[b]	0	20	35
2	$PhPd(OAc)(PPh_3)_2$[b]	1[c]	17	70, 70
3	$PhPd(OAc)(PPh_3)_2$[b]	3[c]	19	75, 66
4	$PhPdI(PPh_3)_2$[d]	0	24	0
5	$PhPdI(PPh_3)_2$[d] + $2AcO^-$	0	22	57
6	$PhPdI(PPh_3)_2$[d] + $2AcO^-$	1	48	72
7	$PhPd(PPh_3)_2{}^+BF_4{}^-$[e]	0	25	27
8	$PhPd(PPh_3)_2{}^+BF_4{}^-$[e]	1	18	22

[a] Yields are relative to the initial $PhPdX(PPh_3)_2$ complexes. [b] Reaction performed on the $PhPd(OAc)(PPh_3)_2$ complex resulting from the oxidative addition of PhI with the palladium(0) complex generated *in situ* from $Pd(OAc)_2$ and $4PPh_3$. Styrene/PhI/$Pd(OAc)_2$ = 100/1/1 with $[Pd(OAc)_2]$ = 2 mM. [c] NEt_3 was introduced at the beginning of the reaction together with the mixture of $Pd(OAc)_2$ and $4PPh_3$. [d] Reaction performed on an authentic sample of $PhPdI(PPh_3)_2$ in the absence or presence of nBu_4NOAc. Styrene/$PhPdI(PPh_3)_2$ = 100/1 with $[PhPdI(PPh_3)_2]$ = 2 mM. [e] Reaction performed on an authentic sample of $PhPd(PPh_3)_2{}^+BF_4{}^-$ with Styrene/$PhPd(PPh_3)_2{}^+BF_4{}^-$ = 100/1 and $[PhPd(PPh_3)_2{}^+BF_4{}^-]$ = 2 mM.

The role of $PhPd(OAc)(PPh_3)_2$ as intermediate in Heck reactions is confirmed by the results of entries 4−6 in Table 5. While $PhPdI(PPh_3)_2$ did not react with styrene under our experimental conditions,[18] the adjunction of acetate ions allowed the reaction to proceed. Since we have demonstrated above that acetate ions were able to substitute the iodide ion from $PhPdI(PPh_3)_2$ to afford $PhPd(OAc)(PPh_3)_2$ (eq 14), this establishes that PhPd-

(18) (a) Some $ArPdX(PPh_3)_2$ complexes can react with styrene but under more drastic conditions than ours, at least at 80 °C. See: (b) Dieck, H. A.; Heck, R. F. *J. Am. Chem. Soc.* **1974**, *96*, 1133. c) Andersson, C. M.; Hallberg, A.; Doyle Daves, G., Jr. *J. Org. Chem.* **1987**, *52*, 3529.

$(OAc)(PPh_3)_2$ is essential and is the species that reacts with the olefin.

The cationic complex $PhPd(PPh_3)_2^+$ formed by dissociation of $PhPd(OAc)(PPh_3)_2$ (eq 16) also reacts with styrene[19] but afforded lower yields and required longer reaction times whatever the triethylamine concentration (Table 5, entries 7 and 8). Since $PhPd(OAc)(PPh_3)_2$ reacts faster than the cationic complex, it cannot react through its cationic complex *via* eq 16. The fact that triethylamine did not affect the yield of the reaction with the cationic complex when no acid was present confirms our above conclusion concerning the role of the amine as a neutralizing reagent.

Therefore we can assume that the first two steps of the catalytic cycle presented in textbooks (Scheme 1) are not operating under the conditions of the Heck reaction, at least when the catalyst is ligated by triphenylphosphine which was the only ligand investigated here.[19,21,22] Indeed, we have demonstrated that $ArPd(OAc)(PPh_3)_2$ complexes are formed by the oxidative addition and give rise to Heck reactions. Further kinetic investigations to clarify this mechanism are presently on the way.

Conclusion

Acetate anions can coordinate palladium(0) centers to form unprecedented anionic species that are in equilibrium, $Pd^0(PPh_3)_3(OAc)^-$ and $Pd^0(PPh_3)_2(OAc)^-$. Such species are formed when acetate ions are added to solutions of $Pd^0(PPh_3)_4$ or when the palladium(0) is generated *in situ* from mixtures of $Pd(OAc)_2$ and $nPPh_3$. It is noteworthy that the latter mixtures are the usual catalyst precursors in the Heck reactions. In both cases the low-ligated complex $Pd^0(PPh_3)_2(OAc)^-$ undergoes an oxidative addition with iodobenzene. In the first case a mixture of $PhPdI(PPh_3)_2$ and $PhPd(OAc)(PPh_3)_2$ is produced, whereas in the second case only $PhPd(OAc)(PPh_3)_2$ is detected. The latter complex reacts with styrene to form stilbene, and this new complex was established as an essential intermediate of the Heck reaction, at least within the first catalytic cycle.

Therefore acetate anions can coordinate palladium(0) complexes as halides have been reported to do.[4] A consequence is that low-ligated palladium(0) complexes such as $Pd^0(PPh_3)_3$ or $Pd^0(PPh_3)_2$ do not exist as soon as halide or acetate anions are present in solution. The result of the ligation of palladium(0) complexes by anions is the formation of new intermediates in the oxidative addition with phenyl iodide, such as $PhPdICl(PPh_3)_2^-$[10] or $PhPdI(OAc)(PPh_3)_2^-$, which is a precursor of new final complexes such as $PhPd(OAc)(PPh_3)_2$.

(19) Cationic arylpalladium complexes have been postulated as intermediates in the Heck reaction.[20] This hypothesis is generally developed in the case of bidentate ligands[2i,21,22] or when the Heck reaction is performed from aryl triflates[2i,22] that afford cationic complexes by reacting with palladium(0) complexes in the absence of any anions.[23]

(20) Karabellas, K.; Westerlund, C.; Hallberg, A. *J. Org. Chem.* **1985**, *50*, 3896. Brown, J. M.; Pérez-Torrente, J. J.; Alcock, N. W.; Clase, H. J. *Organometallics* **1995**, *14*, 207.

(21) (a) Portnoy, M.; BenDavid, Y.; Rousso, I.; Milstein, D. *Organometallics* **1994**, *13*, 3465. (b) Kraatz, H. B.; Milstein, D. *J. Organomet. Chem.* **1995**, *448*, 223.

(22) (a) Osawa, F.; Kubo, A.; Hayashi, T. *J. Am. Chem. Soc.* **1991**, *113*, 1417. (b) Cabri, W.; Candiani, I.; DeBernardinis, S.; Francalanci, F.; Penco, S.; Santi, R. *J. Org. Chem.* **1991**, *56*, 5796. (c) Cabri, W.; Candiani, I.; Bedeshi, A.; Penco, S.; Santi, R. *J. Org. Chem.* **1992**, *57*, 1481. (d) Cabri, W.; Candiani, I.; Bedeshi, A.; Santi, R. *J. Org. Chem.* **1992**, *57*, 3358.

Experimental Section

^{31}P NMR spectra were recorded on a Bruker spectrometer (162 MHz) using H_3PO_4 as an external reference. ^1H NMR spectra were recorded on a Bruker spectrometer (250 MHz). All experiments were performed under argon.

Chemicals. DMF was distilled over calcium hydride, dichloromethane over CaH_2, and petroleum ether over P_2O_5. Iodobenzene was from a commercial source (Janssen) and used after filtration on alumina. Triethylamine was commercial and distilled. $Pd(OAc)_2$, AgOAc, $AgBF_4$, nBu_4NI, styrene, and triphenylphosphine were from commercial sources (Janssen or Aldrich). nBu_4NOAc was synthesized as previously reported.[1a] Authentic samples of $PhPdX(PPh_3)_2$ (X = I,[9] Br,[9] and Cl[24]) were prepared according to described procedures.

Synthesis of $PhPd(OAc)(PPh_3)_2$. The synthesis was carried out using Schlenk techniques under argon. To 0.1 g (0.12 mmol) of $PhPdI(PPh_3)_2$ in 15 mL of CH_2Cl_2 was added 0.04 g (0.24 mmol) of AgOAc. The mixture was stirred at room temperature and in the dark. A grey precipitate was formed. After filtration of the precipitate and evaporation of the filtrate, 0.035 g of a beige precipitate was collected. Yield: 38%. ^{31}P NMR (162 MHz, DMF, acetone-d_6, H_3PO_4) δ, ppm: 21.36. ^1H NMR (250 MHz, $CDCl_3$, TMS) δ, ppm: 2.01 (m, 3H), 6.31 (t, 1H, J = 7.5 Hz), 6.55 (d, 2H, J = 7.5 Hz), 6.63 (t, 2H, J = 7.5 Hz), 7.25 (m, 12H), 7.42 (m, 18H).

Synthesis of $PhPd(PPh_3)_2^+BF_4^-$. The synthesis was carried out using Schlenk techniques under argon. To 0.2 g (0.24 mmol) of $PhPdI(PPh_3)_2$ in 20 mL of CH_2Cl_2 was added 0.07 g (0.36 mmol) of $AgBF_4$. The mixture was stirred for 4 h at room temperature and in the dark. A black precipitate was formed. After filtration of the precipitate and almost complete evaporation of the filtrate, the resulting mixture was poured into a large volume of petroleum ether. A pink-orange precipitate was formed, filtered, dried under vacuum, and stored under argon. A 0.12 g amount of an orange powder was collected. Yield: 62%. ^{31}P NMR (162MHz, DMF, acetone-d_6, H_3PO_4) δ, ppm: 21.70. ^1H NMR (250 MHz, $CDCl_3$, TMS) δ, ppm: 7.38 (m, 2H), 7.49 (dd, 2H, J = 7.5 Hz), 7.53 (t, 1H, J = 7.5 Hz), 7.62 (dd, 6H, J = 7.5 Hz, J = 2 Hz), 7.68 (dd, 6H, J = 7.5 Hz, J = 2 Hz), 7.78 (t, 6H, J = 7.5 Hz), 7.79 (t, 6H, J = 7.5 Hz), 7.91 (td, 6H, J = 7.5 Hz, J = 2 Hz). Anal. Calcd for $C_{42}H_{35}P_2PdBF_4$: C, 63.46; H, 4.44. Found: C, 63.32; H, 4.40.

Electrochemical Setup and Procedure for Cyclic Voltammetry. Cyclic voltammetry was performed with a homemade potentiostat and a wave-form generator, PAR model 175. Cyclic voltammograms were recorded with a Nicolet 3091 digital oscilloscope. Experiments were carried out in a three-electrode cell connected to a Schlenk line. The cell was equipped with a double envelope in order to perform the reactions at constant temperature, 25 °C, using a Lauda M3 thermostat. The counter electrode was a platinum wire of *ca.* 1 cm^2 apparent surface area; the reference was a saturated calomel electrode (Tacussel) separated from the solution by a bridge (3 mL) filled with a 0.3 M nBu_4NBF_4 solution in DMF. A 12-mL volume of DMF containing 0.3 M nBu_4NBF_4 was poured into the cell. A 27.7 mg amount (2×10^{-3} M) of $Pd^0(PPh_3)_4$ was then added. Cyclic voltammetry was performed at a stationary disk electrode (a gold disk made from cross section of wire, 0.5 mm diameter, sealed into glass) at a scan rate of 0.2 V s^{-1}. Suitable amounts of required reagents (*e.g.*, nBu_4NOAc) were then added to the cell, and the cyclic voltammetry was performed again.

In another experiment, a 5.4 mg amount (2×10^{-3} M) of $Pd(OAc)_2$ was added followed by the suitable amount of triphenylphosphine. The formation of the Palladium(0) complex from the mixture $Pd(OAc)_2$ and $nPPh_3$ was monitored by steady state cyclic voltammetry at a rotating disk electrode (a gold disk, 2 mm i.d.) inserted into a Teflon holder (Tacussel EDI 65109) at a scan rate of 0.02 V s^{-1} and an angular velocity of 105 rad s^{-1} (Tacussel controvit). The potential was set on

the plateau of the oxidation wave of the palladium(0) complex, and the oxidation current was monitored as a function of time. When the limit of the oxidation current was reached (100% conversion), the suitable amount of iodobenzene was added to the cell and the oxidation current of the palladium(0) complex was recorded as a function of time to follow the kinetics of oxidative addition with PhI.[1b] Cyclic voltammetry was performed on the resulting solution in reduction and in oxidation in order to characterize the products resulting from the oxidative addition.

Procedure for the Heck Reaction. From $PhPd(OAc)(PPh_3)_2$: A 5.4 mg amount (0.024 mmol) of $Pd(OAc)_2$ was added to the cell followed by a 25 mg amount (0.096 mmol) of triphenylphosphine. The formation of the palladium(0) complex was monitored by steady state cyclic voltammetry at a rotating disk electrode (same conditions as above). When the limit of the oxidation current was reached (100% conversion), 2.7 μL (0.024 mmol) of iodobenzene was added. Cyclic voltammetry was performed on the resulting solution and exhibited the characteristic reduction peaks of $PhPd(OAc)(PPh_3)_2$. A 275 μL amount (2.4 mmol) of styrene was added. The formation of *trans*-stilbene was followed by cyclic voltammetry (reduction peak at -2.20 V) performed as a function of time. The yield in *trans*-stilbene was determined by cyclic voltammetry by comparison of the magnitude of its reduction peak current with that of a known amount of an authentic sample of *trans*-stilbene.

The same reactions were performed in the presence of various amounts of NEt_3 introduced at the beginning of the reaction together with $Pd(OAc)_2$ and $4PPh_3$.

From $PhPdI(PPh_3)_2$: A 20 mg amount (0.024 mmol) of $PhPdI(PPh_3)_2$ was added to the cell followed by 275 μL (2.4 mmol) of styrene, and the reaction was followed by cyclic voltammetry as described above. In another experiment a 14.4 mg amount (0.048 mmol) of nBu_4NOAc was added to the solution followed (or not) by addition of 3.5 μL (0.024 mmol) of NEt_3.

From $PhPd(PPh_3)_2{}^+BF_4{}^-$: A 19 mg amount (0.024 mmol) of $PhPd(PPh_3)_2{}^+BF_4{}^-$ was added to the cell followed by 275 μL (2.4 mmol) of styrene. The reaction was followed by cyclic voltammetry as described above. In another experiment, 3.5 μL (0.024 mmol) of NEt_3 was added to the solution.

Acknowledgment. This work has been supported in part by the Centre National de la Recherche Scientifique (CNRS, URA 1679, "Processus d'Activation Moléculaire") and the Ministère de l'Enseignement Supérieur et de la Recherche (Ecole Normale Supérieure, Département de Chimie).

OM950412U

(23) Jutand, A.; Mosleh, A. *Organometallics* **1995**, *14*, 1810.
(24) Coulson, D. R. *J. Chem. Soc., Chem. Commun.* **1968**, 1530.

Physical Organic Chemistry of Transition Metal Carbene Complexes. 6. Kinetics and Mechanism of the Thermal and Photochemical Hydrolysis of $(CO)_5M{=}C(OMe)CH_2Ph$ (M = Cr, W) in Aqueous Acetonitrile[1]

Claude F. Bernasconi* and Weitao Sun

Department of Chemistry and Biochemistry, University of California, Santa Cruz, California 95064

Received July 14, 1995[⊗]

An extensive kinetic study of the hydrolysis of (benzylmethoxycarbene)pentacarbonylchromium(0), **7-Cr**, and a more limited study of the hydrolysis of its tungsten analog, **7-W**, in 50% acetonitrile–50% water is reported. Both lead to β-methoxystyrene as the main organic product; with **7-W**, phenylacetaldehyde is a significant second product, while with **7-Cr** only traces of phenylacetaldehyde are found. The kinetic results which include the demonstration of general base catalysis and of a kinetic solvent isotope effect are consistent with a mechanism in which **7-M** (M = Cr, W) undergoes a rapid, reversible deprotonation of the α-carbon to form **7-M**$^-$, followed by rate-limiting reaction of **7-M**$^-$ with water, H_3O^+, or buffer acids. This latter step most likely involves protonation of the carbene carbon concerted with cleavage of the C–Cr bond. The hydrolysis of both **7-Cr** and **7-M** is strongly accelerated by light; a limited study of this photochemical pathway at high pH, which also leads to β-methoxystyrene as the principal organic product, suggests a mechanism which most likely involves a ligand exchange between CO and acetonitrile prior to the water-induced rate-limiting product-forming step.

Despite the explosive development of the chemistry of Fischer type transition metal carbene complexes ("Fischer carbenes") over the last 20 years,[2] the hydrolysis of these compounds has, thus far, only received scant attention. In 1993 Aumann et al.[3] reported a product study of the hydrolysis of several Fischer carbenes of the type **1** (R = Ph, CH=CHPh, C_4H_3S, CH=CHC_4H_3S,

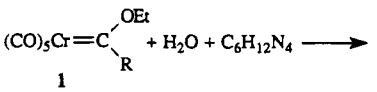

1

$$EtOH + RCH{=}O + (CO)_5CrC_6H_{12}N_4 \quad (1)$$

2

and C≡CPh) in THF containing small quantities of water. In the presence of the tricyclic amine urotropine ($C_6H_{12}N_4$), aldehydes such as **2** are formed in ≥90% yield with all R groups except when R is CH≡CPh; in this latter case the triple bond undergoes nucleophilic attack by the amine. The reaction was assumed to occur via a tetrahedral intermediate, T$^-$, which, after loss of EtO^-, yields **3**, a type of carbene complex known[4] to break down to the corresponding aldehyde **2**.

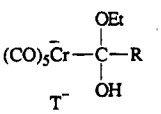

T$^-$

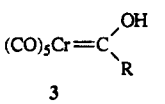

3

The hydrolysis of (methoxymethylcarbene)pentacarbonylchromium(0), **4a**, and (ethoxymethylcarbene)pentacarbonylchromium(0), **4b**, in 50% acetonitrile–50% water yields analogous products as eq 1, i.e., acetaldehyde and methanol in the case of **4a** and acetaldehyde

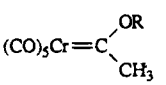

4a (R = CH_3)
4b (R = CH_3CH_2)

and ethanol in the case of **4b**.[1] However, on the basis of a kinetic analysis of these reactions, a mechanism was proposed that is quite different from that suggested by Aumann et al. for eq 1. This mechanism, whose key feature is that it involves the conjugate base of the carbene complex, **4**$^-$, rather than a T$^-$-like adduct as the intermediate, is shown in Scheme 1.[5] This mechanism is apparently more efficient for carbene complexes with acidic α-hydrogen than the alternative pathway via nucleophilic attack by OH^- on the carbene carbon.

The evidence for the mechanism of Scheme 1 can be summarized as follows.[1]

[⊗] Abstract published in *Advance ACS Abstracts,* November 1, 1995.

(1) Part 5: Bernasconi, C. F.; Flores, F. X.; Sun, W. *J. Am. Chem. Soc.* **1995**, *117*, 4875.

(2) For recent reviews see: (a) Dötz, K. H.; Fischer, H.; Hofmann, P.; Kreissl, F. R.; Schubert, U.; Weiss, K. *Transition Metal Carbene Complexes*; Verlag Chemie: Deerfield Beach, FL, 1983. (b) Dötz, K. H. *Angew. Chem., Int. Ed. Engl.* **1984**, *23*, 587. (c) Gallop, M. A.; Roper, W. R. *Adv. Organomet. Chem.* **1986**, *25*, 121. (d) Wulff, W. D. *Adv. Met.-Org. Chem.* **1989**, *1*, 209. (e) Schubert, U., Ed. *Advances in Metal Carbene Chemistry*; Kluwer: Dordrecht, Holland, 1989. (f) Dötz, K. H. *New J. Chem.* **1990**, *14*, 433. (g) Wulff, W. D. In *Comprehensive Organic Synthesis*; Trost, B. M., Fleming, I., Eds.; Pergamon Press: New York, 1990; Vol. 5. (h) Schmidt, M. A.; Miller, J. R.; Hegedus, L. S. *J. Organomet. Chem.* **1991**, *413*, 143. (i) Veillard, A. *Chem. Rev.* **1991**, *91*, 743.

(3) Aumann, R.; Hinterding, P.; Krüger, C.; Goddard, R. *J. Organomet. Chem.* **1993**, *459*, 145.

(4) Fischer, E. O.; Massböl, A. *Chem. Ber.* **1967**, *100*, 2445.

(5) In the presence of buffers, conversion of **4**$^-$ to **5** involves the buffer acid instead of water as the proton donor, while in acidic solution H_3O^+ takes on the role of proton donor.

0276-7333/95/2314-5615$09.00/0

Scheme 1

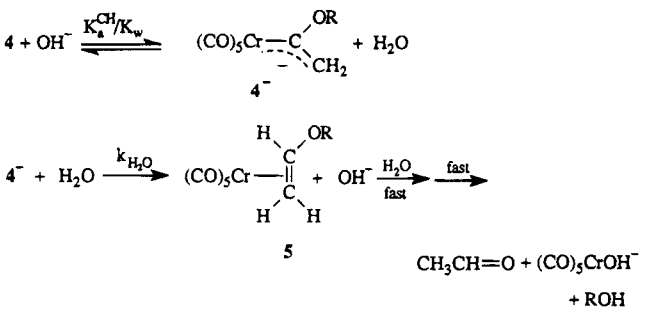

Scheme 2

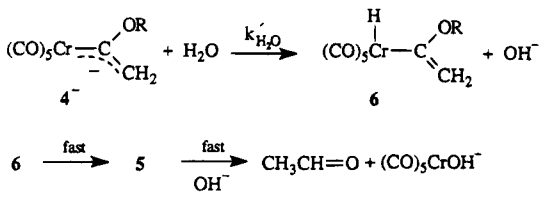

(1) The reversible deprotonation of **4**, whose rate had been measured previously,[6] is much faster than the hydrolysis reaction and hence acts as a rapid preequilibrium in front of the rate-limiting k_{H_2O} step.

(2) The break in the pH–rate profiles (log k_{obsd} vs pH, with k_{obsd} being the observed pseudo-first-order rate constant) occurs at pH $\approx$ 12.35 $\pm$ 0.15 for **4a** and pH $\approx$ 12.80 $\pm$ 0.15 for **4b**, consistent with pK_a^{CH} = 12.50 for **4a** and 12.97 for **4b**.[6]

(3) The rates are substantially reduced when the reactions are conducted in 50% acetonitrile–50% D_2O. At pH $\gg K_a^{CH}$ where $k_{obsd} = k_{H_2O}$, k_{H_2O}/k_{D_2O} ratios in the order of 4 and 7 were determined for **4a**,**b**, respectively. This constitutes a substantial primary kinetic isotope effect and indicates a rate-limiting step that involves a proton transfer.

(4) Even though vinyl ethers are stable in basic solution, it is plausible that complexation of $ROCH{=}CH_2$ with $Cr(CO)_5$ can activate them toward OH^--promoted hydrolysis.[7] Support for this contention comes from control experiments in which acetaldehyde was produced when $EtOCH{=}CH_2$ was added to a basic solution of $(CO)_5Cr(CH_3CN)$ generated by UV irradiation of $Cr(CO)_6$ in acetonitrile.

In Scheme 1 the k_{H_2O} step implies that protonation of the carbene carbon of 4^- is concerted with cleavage of the Cr–C bond. The kinetic data are, however, also consistent with a two-step process in which rate-limiting protonation of 4^- on the metal is followed by a rapid reductive elimination (Scheme 2). This alternative could not be rigorously excluded, but the concerted mechanism was preferred on the grounds that Scheme 2 requires the pK_a of **6** to be unrealistically high.

In this paper we report results of a detailed product and kinetic study of the hydrolysis of (benzylmethoxycarbene)pentacarbonylchromium(0), **7-Cr**, and a more

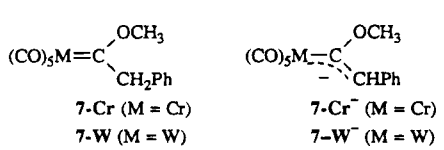

7-Cr (M = Cr) **7-Cr$^-$** (M = Cr)
7-W (M = W) **7-W$^-$** (M = W)

limited study of the hydrolysis of the tungsten analogue, **7-W**. Even though the reactions of **7-Cr** and **7-W** show similar kinetics as the hydrolysis of **4a**,**b**, the major organic product is not the corresponding aldehyde, $PhCH_2CH{=}O$, but β-methoxystyrene. It will be shown that this result does not necessitate the postulation of a different mechanism for the hydrolysis of **7-Cr** and **7-W** but actually adds further support to the mechanism of hydrolysis of **4a**,**b** shown in Scheme 1. We also report that the hydrolysis of **7-Cr** and **7-W** is strongly accelerated by UV light.

Results

General Features. All experiments were conducted in 50% acetonitrile–50% water (v/v). Rates were measured in HCl and KOH solutions as well as in acetate, *N*-morpholine, and triethylamine buffers, spanning a pH range from 2.0 to 14.2. The main hydrolysis products of **7-Cr** are β-methoxystyrene, **8**, and $(CO)_5CrX$; this

$PhCH{=}CHOCH_3$

8

latter is probably present as a mixture where X may be OH^-, the buffer base, CH_3CN and perhaps H_2O, as shown previously.[1] The identity of **8** was confirmed by HPLC and ^1H NMR analysis; both methods showed a $\geq$90% yield of **8** which is formed in an *E*/*Z* ratio of approximately 6. Furthermore, trace amounts of $PhCH_2CH{=}O$ were detected by ^1H NMR which, however, were too small to quantify. On the other hand, the hydrolysis of **7-W** yielded about 25% $PhCH_2CH{=}O$ and $\geq$70% of **8**, the latter in an *E*/*Z* ratio of approximately 5.9.

Kinetic Measurements. 7-Cr. At pH $\ll 10.4 = pK_a$ (**7-Cr**) only one kinetic process could be observed which corresponds to the conversion of **7-Cr** to hydrolysis products. At pH $\geq$ 10.4 the acid–base equilibrium between **7-Cr** and its conjugate base favors **7-Cr$^-$**. Under these conditions two kinetic processes were observed: a rapid reaction that corresponds to the reversible proton transfer, **7-Cr** + OH^- / **7-Cr$^-$** + H_2O, discussed in a previous paper,[6] and conversion of **7-Cr$^-$** to **8** and $(CO)_5CrX$. Figure 1 shows time-resolved spectra illustrating this latter situation. A spectrum of **7-Cr** is also included in Figure 1.

All rates were determined under pseudo-first-order conditions, with the carbene complex as the minor component. The ionic strength was maintained at 0.1 M with KCl. In HCl and in acetate, *N*-methylmorpholine, and triethylamine buffers (pH 2.00–10.60), the rates were measured in a conventional spectrophotometer by monitoring the disappearance of **7-Cr** at 380 nm. In KOH solution (pH $\geq$ 11.5) where **7-Cr** is mainly present as **7-Cr$^-$**, conversion to products was initially monitored at 360 or 320 nm in a stopped-flow spectrophotometer equipped with a high-intensity xenon lamp; in a second series of experiments the reaction was measured at 320 nm in a conventional spectrophotometer equipped with a low-intensity deuterium lamp. Figure 2 shows a plot of log k_{obsd} vs pH, with k_{obsd} being the observed pseudo-first-order rate constant. The k_{obsd} values determined in buffer solutions showed dependence on buffer concentration; the values plotted in Figure 2 represent extrapolations to zero buffer concentration. From the slopes of the buffer plots (k_{obsd} vs [B]) k_B values for general base catalysis were determined as follows: (2.93 $\pm$ 0.45) $\times$ 10^{-3} M^{-1} s^{-1} for

(6) Bernasconi, C. F.; Sun, W. *J. Am. Chem. Soc.* **1993**, *115*, 12526.
(7) Crabtree, R. H. *The Organometallic Chemistry of the Transition Metals*; Wiley-Interscience: New York, 1988; p 91.

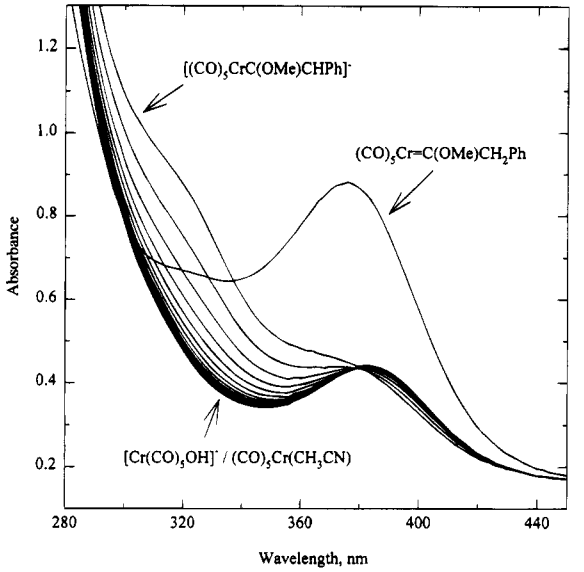

Figure 1. Time-resolved absorption spectra showing the hydrolysis of **7-Cr** in a KOH solution where the proton transfer equilibrium favors **7-Cr**$^-$. The first spectrum was taken 80 s after mixing, which corresponds to 10 half-lives of the proton transfer reaction; subsequent spectra were taken at 50 s intervals. A spectrum of **7-Cr** in neutral solution is also shown.

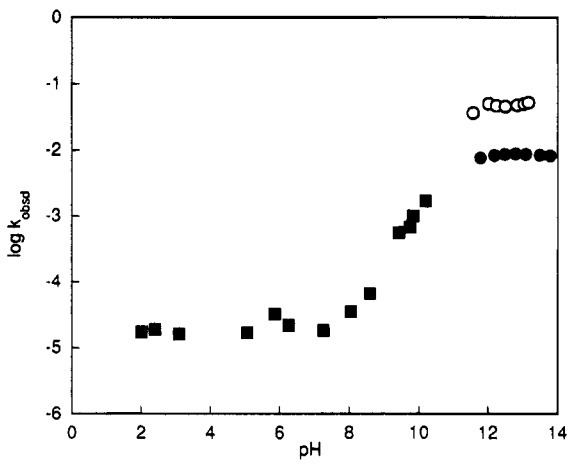

Figure 2. pH–rate profile for the hydrolysis of **7-Cr**: Filled symbols, reaction monitored with low-intensity deuterium lamp; squares, reaction in acetate, N-morpholine, and triethylamine buffers with k_{obsd} being extrapolated to zero buffer concentration; filled circles, reaction in KOH; open circles, reaction in KOH monitored with high-intensity xenon lamp.

acetate ion, $(1.70 \pm 0.38) \times 10^{-3}$ M^{-1} s^{-1} for *N*-methylmorpholine, and $(6.76 \pm 1.65) \times 10^{-2}$ M^{-1} s^{-1} for triethylamine.

As is apparent from Figure 2, k_{obsd} measured in KOH solutions is substantially higher when the reaction is monitored with a high-intensity xenon lamp compared to the situation with a low-intensity deuterium lamp. This indicates that under the former conditions there is a contribution by a photochemical pathway. Figure 3 shows a plot of k_{obsd} at 0.1 M KOH as a function of monochromator slit width of the stopped-flow spectrophotometer with the high-intensity lamp; the reaction was monitored at 320 nm. This plot demonstrates clearly the dependence of the photochemical reaction on light intensity; the fact that a plateau is reached suggests that at high intensity the reaction follows exclusively the photochemical pathway. It should be noted that the photochemical pathway is still substantial at 360 nm, the wavelength used for the experiments shown in Figure 2 (open circles), but becomes insignificant at 380 nm.

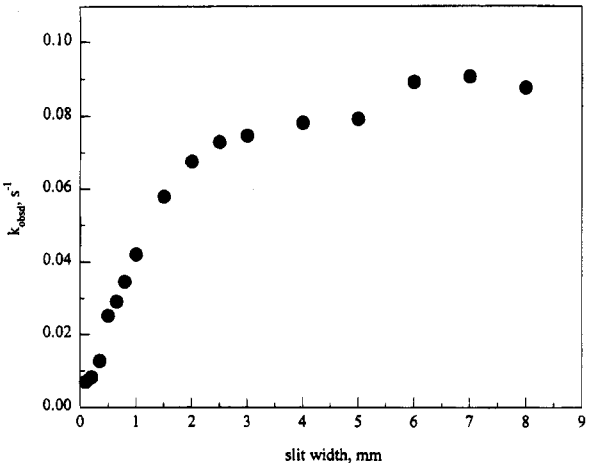

Figure 3. k_{obsd} for the hydrolysis of **7-Cr** in the presence of 0.1 M KOH as function of monochromator slit width. The reaction was monitored at 320 nm in DX.17MV Applied Photophysics stopped-flow apparatus.

Table 1. Kinetic Solvent Isotope Effect in the Hydrolysis of 7-Cr and 7-W

[KOL]^a (M)	$k_{obsd}(H_2O)$ (s^{-1})	$k_{obsd}(D_2O)$ (s^{-1})	$k_{obsd}(H_2O)/k_{obsd}(D_2O)^b$
	7-Cr: Thermal Reaction		
0.008	8.79×10^{-3}	3.17×10^{-3}	2.77
0.02	8.59×10^{-3}	3.14×10^{-3}	2.74
0.04	8.25×10^{-3}	2.92×10^{-3}	2.83
	7-Cr: Photochemical Reaction		
0.0004	3.6×10^{-2}	1.9×10^{-2}	1.89
0.008	5.0×10^{-2}	2.5×10^{-2}	2.00
0.002	4.6×10^{-2}	2.2×10^{-2}	2.09
	7-W: Thermal Reaction		
0.008	7.46×10^{-3}	2.89×10^{-3}	2.58
0.02	7.40×10^{-3}	2.75×10^{-3}	2.69
0.04	6.95×10^{-3}	2.63×10^{-3}	2.64
	7-W: Photochemical Reaction		
0.01	4.78×10^{-2}		
0.02	4.61×10^{-2}		
0.04	4.46×10^{-2}		
0.06	4.44×10^{-2}		

^{a} L = H or D. ^{b} $k_{obsd}(H_2O)/k_{obsd}(D_2O)$ corresponds to $k_2^{H_2O}/k_2^{D_2O}$ (thermal reaction, Scheme 3) and $k_{2'}^{H_2O}/k_{2'}^{D_2O}$ (photochemical reaction, Scheme 4), respectively; see text. The average $k_2^{H_2O}/k_2^{D_2O}$ is 2.78 ± 0.05 for the thermal reaction of **7-Cr**$^-$ and 2.64 ± 0.05 for the thermal reaction of **7-W**$^-$, while the average $k_{2'}^{H_2O}/k_{2'}^{D_2O}$ is 1.99 $\pm$ 0.10 for the photochemical reaction of **7-Cr**$^-$.

HPLC analysis of the products obtained under photochemical conditions revealed β-methoxystyrene to be again the main product; its yield was determined to be at least 87%, with an *E*/*Z* ratio of approximately 4.6. In order to ensure that the analysis was performed on reaction mixtures that were subjected to the same conditions as those in the kinetic experiments, the product study was carried out on the effluent of the stopped-flow apparatus, as described in the Experimental Section.

A few experiments aimed at determining the kinetic solvent isotope effect were conducted in 50% acetonitrile–50% D_2O at high pH. They are summarized in Table 1. The average isotope effect for the thermal reaction is 2.78 $\pm$ 0.05, while for the light enhanced reaction it is 1.99 $\pm$ 0.10.

Scheme 3

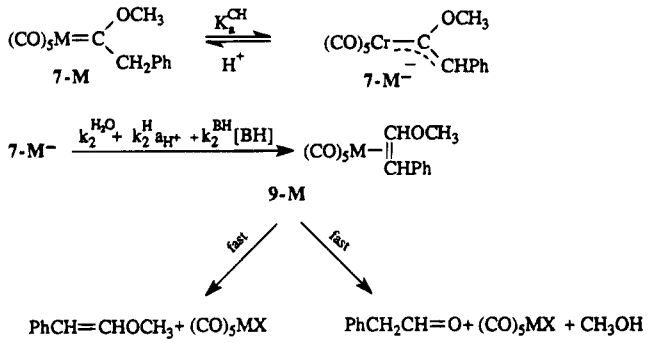

7-W. A limited number of kinetic experiments were performed with the tungsten carbene complex in KOH and KOD solutions. The results are reported in Table 1. In all runs the pH was well above the pK_a of **7-W** (pK_a = 10.18);[8] i.e., the acid–base equilibrium strongly favored **7-W**$^-$. Just as was the case with **7-Cr**$^-$, the reaction is substantially accelerated by light. We also determined the kinetic solvent isotope effect on the thermal reaction which is virtually the same as that for the reaction of **7-Cr**$^-$ (2.65 ± 0.05, Table 1).

Discussion

Thermal Reaction. The formation of β-methoxystyrene in the reaction of **7-M** is reminiscent of the formation of vinyl ethers from various (alkylmethoxycarbene)pentacarbonylchromium(0) complexes in the presence of neat pyridine and *N*-methylmorpholine,[9] or of quinuclidine in hexane,[9] and the formation of 2,3-dihydrofuran in the thermal decomposition of (2-oxacyclopentylidene)pentacarbonylchromium(0) in pyridine.[10] In these systems the absence of water of course precludes hydrolytic conversion of the vinyl ether into the corresponding aldehyde.

The combined results of the present investigation (**7-Cr** and **7-W**) and those of our previous study (**4a,b**) show that vinyl ether and aldehyde formation compete with each other, in some cases overwhelmingly favoring the aldehyde (**4a,b**), in another overwhelmingly favoring the vinyl ether (**7-Cr**), and in a third case leading to a somewhat more equal distribution of products (**7-W**).

The simplest mechanism that is consistent with all experimental observations is shown in Scheme 3 for **7-Cr** and **7-W**. It is basically the same mechanism as in Scheme 1 except that it includes a pathway to the vinyl ether as final product; for alternative views see ref 11.

The fact that in the hydrolysis of **7-Cr** and **7-W** the aldehyde is the minor product, whereas in the hydrolysis of **4a,b** the aldehyde is the major product, may be attributed to a steric effect: β-methoxystyrene being quite bulky apparently forms a less stable and/or shorter-lived complex with M(CO)$_5$ (**9-M**) than $CH_3OCH{=}CH_2$ or $CH_3CH_2OCH{=}CH_2$ (**5** in Scheme 1). In fact, with the chromium derivative, the aldehyde pathway is barely detectable, suggesting that **9-Cr** is even less stable and/or less long-lived than **9-W**. This reduced stability may be a consequence of the smaller size of chromium compared to tungsten, which should lead to more crowding around the metal. In agreement with the extremely low yield of phenylacetaldehyde in the reaction of **7-Cr**, control experiments in which β-methoxystyrene was added to a solution of $(CO)_5Cr(CH_3CN)$ did not yield $PhCH_2CH{=}O$; this contrasts with similar control experiments in our study of the hydrolysis of **4a,b** where ethyl vinyl ether was shown to yield acetaldehyde in the presence of $(CO)_5Cr(CH_3CN)$.[1]

The pseudo-first-order rate constant for Scheme 3 is given by eq 2, which, in the absence of buffer, or after

$$k_{obsd} = \frac{K_a^{CH}}{K_a^{CH} + a_{H^+}}(k_2^{H_2O} + k_2^{H}a_{H^+} + k_2^{BH}[BH]) \quad (2)$$

extrapolation to zero buffer concentration, simplifies to eq 3. At pH ≫ pK_a^{CH}, eq 3 becomes eq 4, which in

$$k_{obsd} = \frac{K_a^{CH}}{K_a^{CH} + a_{H^+}}(k_2^{H_2O} + k_2^{H}a_{H^+}) \quad (3)$$

$$k_{obsd} = k_2^{H_2O} \quad (4)$$

Figure 2 corresponds to the plateau at high pH (filled circles). This is the pH range where the kinetic isotope

(8) Bernasconi, C. F.; Sun, W. Unpublished results.
(9) (a) Fischer, E. O.; Massböl, A. *J. Organomet. Chem.* **1968**, *12*, P15. (b) Fischer, E. O.; Plabst, W. *Chem. Ber.* **1974**, *107*, 3362.
(10) Casey, C. P.; Anderson, R. L. *J. Chem. Soc., Chem. Commun.* **1975**, 895.

(11) A reviewer has suggested that the anionic intermediate involved in the reaction may be **10-M**$^-$ rather than **7-M**$^-$, with **10-M**$^-$ and **7-M**$^-$ being in rapid equilibrium with each other.

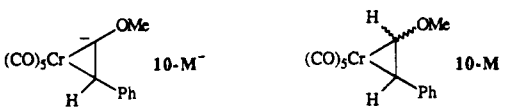

This would imply that the rate-limiting step (k_2) is protonation of **10M**$^-$ to form **10-M**, followed by rapid conversion to **9-M**. This suggestion was based on the reviewer's contention that if **7-Cr**$^-$ were the observed product of deprotonation of **7-Cr**, the UV spectrum should show a red shift relative to **7-Cr** rather than the observed blue shift (Figure 1). Some attractive features of this proposal include "a better electronic rationale for delivery of a proton to the (otherwise) electron deficient carbene carbon" and the fact that **10-M**$^-$ "initiates the structural reorganization necessary for creating the coordinated alkene". In our view there are several problems with the reviewer's proposal. (1) It ignores IR evidence which shows that deprotonation of **4a** in THF leads to **4a**$^-$.[12] (2) It is difficult to understand why **10-M**$^-$, with a negative charge that cannot be delocalized, could be more stable than **7-M**$^-$ with its highly dispersed charge. (3) If cyclopropyl anions can serve as a model for **10-M**$^-$, the basicity of the anionic site of **10-M**$^-$ should be extremely high,[13] even if a substantial stabilization by the $(CO)_5Cr$ moiety is assumed. This means that protonation by all acids used in this study should be close to diffusion controlled and the k_2^{BH} values should show little variation (Brønsted α close to zero).[14] This contrasts with the strong dependence of k_2^{BH} on pK_a^{BH} (Table 2) which is typical for thermodynamically unfavorable reactions that involve a proton transfer. Another reviewer regards protonation of the carbene carbon of **7-M**$^-$ as "unlikely" and suggests slow thermal and/or photochemical disengagement of one CO molecule from **7-M**$^-$ to form **11-M**$^-$.[15]

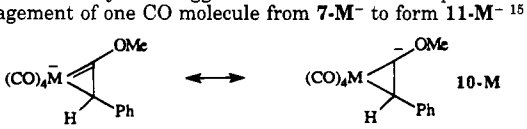

which can be stabilized by charge delocalization and may then be protonated at the carbene carbon. According to this reviewer formation of such a metallacycle could explain why the hydrolysis of **7-M** is accelerated by UV light. The problem with this suggestion is that if formation of **11-M**$^-$ were rate-limiting, the kinetic solvent isotope effect and buffer catalysis would be difficult to explain. If, on the other hand, formation of **11-M**$^-$ represented a fast equilibrium which is followed by rate-limiting protonation, the generation of CO in the course of reaction would lead to strong deviations from first-order kinetics; no such deviations were observed.
(12) Casey, C. P.; Anderson, R. L. *J. Am. Chem. Soc.* **1974**, *96*, 1230.
(13) The pK_a of cyclopropane has been estimated to be 51 ± 5.[14]
(14) Battiste, M. A.; Coxon, J. M. In *The Chemistry of the Cyclopropyl Group*; Rappoport, Z., Ed.; Wiley: New York, 1987; p 255.

Table 2. Rate Constants for the Reactions of 7^-, $4a^-$, and $4b^-$ with Water, Buffer Acids, and H_3O^+ in 50% Acetonitrile–50% Water (v/v) at 25 °C

proton donor (pK_a^{BH})	symbol	**7-Cr**$^-$ (pK_a^{CH} = 10.40)	**7-W**$^-$ (pK_a^{CH} = 10.18)	**4a**$^-$ (pK_a^{CH} = 12.50)	$k_2^{BH}(\mathbf{4a}^-)/k_2^{BH}(\mathbf{7\text{-}Cr}^-)^e$
H_2O (16.63)	$k_2^{H_2O}$, M^{-1} s^{-1}	8.5×10^{-3} [b]	7.3×10^{-3} [c]	0.16[d]	1.88×10^1
Et_3NH^+ (10.45)	k_2^{BH}, M^{-1} s^{-1}	6.0×10^{-2}			
N-MeMorH$^+$ (7.43)	k_2^{BH}, M^{-1} s^{-1}	1.6		$\approx 4.1 \times 10^2$	2.56×10^2
AcOH (5.93)	k_2^{BH}, M^{-1} s^{-1}	8.6×10^1		$\approx 3.2 \times 10^4$	3.72×10^2
H_3O^+ (−1.44)	k_2^{H}, M^{-1} s^{-1}	4.3×10^5		1.9×10^8	4.60×10^2

[a] μ = 0.1 M. [b] $k_2^{H_2O} = 4.4 \times 10^{-2}$ s^{-1} for the photochemical reaction of **7-Cr**$^-$. [c] $k_2^{H_2O} = 4.6 \times 10^{-2}$ s^{-1} for the photochemical reaction of **7-W**$^-$. [d] $k_2^{H_2O} = 0.29$ s^{-1} for **4b** (pK_a^{CH} = 12.97). [e] Here BH stands for either H_2O, H_3O^+, or buffer acid.

effect experiments were conducted, and hence $k_{obsd}(H_2O)/k_{obsd}(D_2O)$ corresponds to $k_2^{H_2O}/k_2^{D_2O}$. The average $k_2^{H_2O}/k_2^{D_2O}$ ratios of 2.78 for **7-Cr** and 2.64 for **7-W** (Table 1) are not as large as in the case of **4a** (3.97)[6] or **4b** (6.96)[6] but still suggest a primary kinetic isotope effect, as expected for a reaction that involves a proton transfer from water to a carbon.

At pH ≪ pK_a^{CH}, eq 3 reduces to eq 5, with $K_a^{CH}k_2^{H_2O}/a_{H^+}$ describing the sloping part of the pH–rate

$$k_{obsd} = K_a^{CH}k_2^{H_2O}/a_{H^+} + K_a^{CH}k_2^{H} \qquad (5)$$

profile and $K_a^{CH}k_2^{H}$ corresponding to the plateau at pH < 8. The break in the pH–rate profile around pH 10.5–10.6 for the reaction of **7-Cr** is consistent with the pK_a^{CH} of 10.4 determined independently.[6]

The slopes of the buffer plots, k_B, which were all determined at pH < (≪) pK_a^{CH}, are given by eq 6, with pK_a^{BH} being the acid dissociation constant of the buffer acid.

$$k_B = K_a^{CH}k_2^{BH}/K_a^{BH} \qquad (6)$$

Table 2 summarizes the, $k_2^{H_2O}$, k_2^{H}, and k_2^{BH} values obtained from the above analysis, along with the corresponding parameters for **4a,b**. The following conclusions may be drawn from Table 2.

(1) As seen from the $k_2^{BH}(\mathbf{4a}^-)/k_2^{BH}(\mathbf{7\text{-}Cr}^-)$ ratios[23] (last column in Table 2), the reaction of **7-Cr**$^-$ is considerably slower than that of **4a**$^-$ or **4b**$^-$. The lower reactivity of **7-Cr**$^-$ can be mainly attributed to the stabilization of the negative charge in **7-Cr**$^-$ by the phenyl group, as reflected in the higher acidity of **7-Cr** (pK_a^{CH} = 10.40) compared to **4a** (pK_a^{CH} = 12.50) and **4b** (pK_a^{CH} = 12.97).

(2) The $k_2^{H}(\mathbf{4a}^-)/k_2^{H}(\mathbf{7\text{-}Cr}^-)$ ratio (460) for the H^+-catalyzed reaction is considerably larger than the $k_2^{H_2O}(\mathbf{4a}^-)/k_2^{H_2O}(\mathbf{7\text{-}Cr}^-)$ ratio (18.8) for the water reaction. This indicates an increasing sensitivity to electronic effects (phenyl vs hydrogen) as the reaction becomes thermodynamically more favorable with a stronger proton donor. The large $k_2^{BH}(\mathbf{4a}^-)/k_2^{BH}(\mathbf{7\text{-}Cr}^-)$ ratios for *N*-methylmorpholinium ion and AcOH also fit into this pattern of increasing selectivity with increasing acidity of the proton donor. This pattern is opposite to expectations based on the Hammond[24] –Leffler[25] postulate or the reactivity–selectivity principle[26] and thus adds to a growing list of examples that do not adhere to this principle.[26b,e,27] A possible factor that may contribute to the relatively low $k_2^{H_2O}(\mathbf{4a}^-)/k_2^{H_2O}(\mathbf{7\text{-}Cr}^-)$ ratio is a transition state stabilization by a field effect between the electron-withdrawing phenyl group and the negative charge on the incipient OH^- in the reaction of **7-Cr**$^-$ with water.[28] This stabilizing effect is absent in reactions of **7-Cr**$^-$ with H_3O^+ or *N*-methylmorpholinium ion, and there might even be a repulsive interaction with the positive charge. In the reaction of **7-Cr**$^-$ with AcOH the negative charge on the incipient acetate ion is more dispersed than on the incipient OH^- in the water reaction and hence the stabilizing field effect is probably negligible.

(3) The number of buffer acids used is too limited to permit the determination of an accurate Brønsted coefficient, especially since not all buffers belong to the same family. Nevertheless, on the basis of the points for the Et_3NH^+ and *N*-methylmorpholinium ions, an approximate α value of ≤0.47 may be estimated for the reaction of **7-Cr**$^-$ with tertiary ammonium ions. The α value is given as an upper limit because the greater bulk of Et_3NH^+ compared to *N*-methylmorpholinium ion may possibly depress k_2^{BH} for Et_3NH^+ due to a steric effect.

Photochemical Reaction. A plausible mechanism

(15) Neutral metallocyclopropenes are known, see, e.g.: (a) Templeton, J. L. *Adv. Organomet. Chem.* **1989**, *29*, 71. (b) Aumann, R.; Heinen, H.; Krüger, C.; Betz, P. *Chem. Ber.* **1990**, *123*, 599.

(16) It is unclear at this point why there are such large differences in $k_2^{H_2O}/k_2^{D_2O}$ for the reactions of 7^-, $4a^-$, and $4b^-$. One factor that may play a role is the possible change in the symmetry of the O---H---C portion of the transition state (Melander–Westheimer model)[17,18] as the basicity of the carbon increases from 7^- to $4a^-$ to $4b^-$.[19] Another is that the degree of coupling to heavy atom motion caused by the cleavage of the C–Cr bond could be different in the three reactions and hence affect the isotope effects differently.[20] In case tunneling[21] is important, different degrees of such tunneling could contribute to the differences in $k_2^{H_2O}/k_2^{D_2O}$. An additional complication is that the contribution to $k_2^{H_2O}/k_2^{D_2O}$ by a *secondary* isotope effect[22] may not be the same for the three reactions.

(17) (a) Melander, L. *Isotope Effects on Reaction Rates*; Ronald Press: New York, 1960; pp 24–32. (b) Westheimer, F. H. *Chem. Rev.* **1961**, *61*, 265. (c) More O'Ferrall, R. A. In *Proton Transfer Reactions*; Caldin, E. F., Gold, V., Eds.; Wiley & Sons: New York, 1975; p 201.

(18) For an example of a concerted E2 elimination which shows this effect, see Smith, P. J.; Amin, M. *Can. J. Chem.* **1989**, *67*, 1457.

(19) It is assumed that the basicity of the carbene carbon follows the basicity of the α-carbon; see Table 2 for the relevant pK_a^{CH} values.

(20) See, e.g.: (a) Saunders, W. H.; Katz, A. M. *J. Am. Chem. Soc.* **1969**, *91*, 4469. (b) Kaldor, S. B.; Saunders, W. H., Jr. *J. Am. Chem. Soc.* **1979**, *101*, 7594.

(21) (a) Bell, R. P. *The Proton in Chemistry*, 2nd ed.; Cornell University Press: Ithaca, NY, 1973; Chapter 12. (b) Saunders, W. H., Jr. *J. Am. Chem. Soc.* **1985**, *107*, 164. (c) Amin, M.; Price, R. C.; Saunders, W. H., Jr. *J. Am. Chem. Soc.* **1990**, *112*, 4467.

(22) (a) Schowen, R. L. *Prog. Phys. Org. Chem.* **1972**, *9*, 275. (b) Schowen, K. J. B. In *Transition States of Biochemical Processes*; Gandour, R. D., Schowen, R. L., Eds.; Plenum: New York, 1978; p 225.

(23) Here BH stands for either H_2O, H_3O^+, or a buffer acid.

(24) Hammond, G. S. *J. Am. Chem. Soc.* **1955**, *77*, 334.

(25) Leffler, J. E.; Grunwald, E. *Rates and Equilibria of Organic Reactions*; Wiley: New York, 1963; p 153.

(26) (a) Pross, A. *Adv. Phys. Org. Chem.* **1977**, *14*, 69. (b) *Isr. J. Chem.* **1985**, *26*, pp 303–428 (Reactivity and Selectivity issue). (c) Jencks, W. P. *Chem. Rev.* **1985**, *85*, 511. (d) Buncel, E.; Wilson, H. *J. Chem. Educ.* **1987**, *64*, 475. (e) Exner, O. *J. Chem. Soc., Perkin Trans. 2* **1993**, 973.

(27) (a) Kemp, D. S.; Casey, M. L. *J. Am. Chem. Soc.* **1973**, *95*, 6670. (b) Johnson, C. D. *Chem. Rev.* **1975**, *75*, 755. (c) Johnson, C. D. *Tetrahedron* **1980**, *36*, 3461. (d) Arnett, E. M.; Reich, R. *J. Am. Chem. Soc.* **1978**, *100*, 2930.

(28) For an example where field effects of the type visualized in this reaction have been shown to be significant in the transition state of a proton transfer, see: Kresge, A. J. *Can. J. Chem.* **1974**, *52*, 1897.

Scheme 4

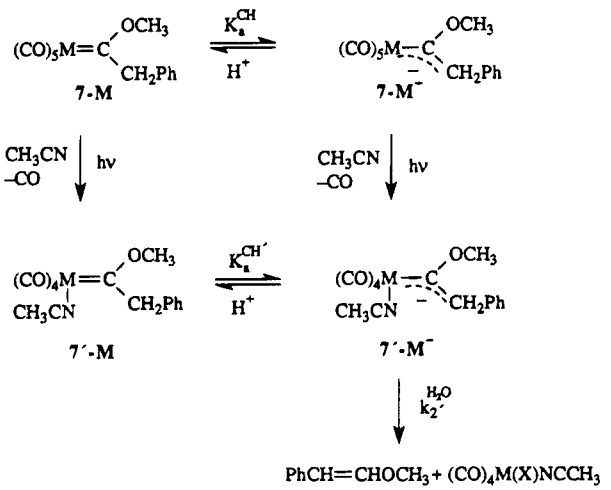

for this reaction is shown in Scheme 4. This mechanism is consistent with the fact that β-methoxystyrene is the main organic product, just as for the thermal reaction, and with the kinetic solvent isotope effect (Table 1) which suggests that the reaction of **7'-M⁻** with water is rate-limiting.[29] The fact that k_{obsd} is pH independent in KOH solution implies that at high pH **7-M** is essentially quantitatively converted to **7'-M⁻** before the onset of the $k_{2'}^{H_2O}$ step. It is also noteworthy that $k_{2'}^{H_2O}$ is about 6- (**7-W⁻**) to 8-fold (**7-Cr⁻**) higher than $k_2^{H_2O}$ (Scheme 3). The increased reactivity of **7'-M⁻** compared to **7-M⁻** is consistent with a higher electron density induced by replacing one of the strongly electron-withdrawing CO ligands by acetonitrile. This is reminiscent of the higher reactivity of **4a⁻** and **4b⁻** compared to **7-M⁻** due to the replacement of the electron-withdrawing phenyl group by hydrogen.

Our results do not allow a distinction between the pathways **7-M** → **7-M⁻** → **7'-M⁻** and **7-M** → **7'-M** → **7'-M⁻**. There exist numerous precedents for the photochemically induced substitution of a CO ligand by acetonitrile in neutral Fischer carbene complexes (such as **7-M**),[30] but we are not aware of any study demonstrating the same process with an anionic complex such as **7-M⁻**. This, of course, does not necessarily exclude the pathway **7-M** → **7-M⁻** → **7'-M⁻**. The fact that the rate of the reversible deprotonation of **7-M** is not affected by light is consistent with the pathway **7-M** → **7-M⁻** → **7'-M⁻**; however, if one assumes that the proton transfer equilibrium is rapidly established compared to the photochemically induced ligand exchange, the pathway **7-M** → **7'-M** → **7'-M⁻** is also consistent with the absence of a photochemically induced acceleration of the proton transfer reaction.

Before we became aware of the photochemical reaction, all stopped-flow experiments had been performed in an instrument equipped with a high-intensity xenon lamp and using a fairly large monochromator slit width of 2 mm (open circles in Figure 2). The pH–rate profile constructed from these data points (**7-Cr**) combined with the data determined at lower pH in a conventional spectrophotometer equipped with a low-intensity deuterium lamp (points below pH 10.7) indicated the presence of a break at pH ~ 11.5, about 1.1 pH units higher than the pK_a^{CH} of **7-Cr**. It is this inconsistency that led us to suspect the presence of a photochemical pathway. No such inconsistency had been observed in the hydrolysis of **4a** or **4b** monitored with the same xenon lamp, and the rates are the same when monitored with a low-intensity deuterium lamp.[1] This indicates that for **4a,b** the photochemical pathway must be negligible under our reaction conditions.

On the other hand, our findings that the photochemical hydrolysis of **7-M** is considerably faster than the thermal reaction, even at relatively low light intensities (Figure 3), leave open the possibility that there may be a small contribution of the photochemical pathway to the rates measured for the thermal reaction.

Conclusions

(1) In contrast to the hydrolysis of **4a,b**, where the initially formed vinyl ethers are further hydrolyzed to the corresponding aldehyde and alcohol, the hydrolysis of **7-Cr** and **7-W** essentially stops at the vinyl ether stage (β-methoxystyrene) although, especially with **7-W**, some further hydrolysis to the phenylacetaldehyde is observed. Another contrast with **4a,b** is that the reactions of **7-M** occur both thermally and photochemically, while for **4a,b** no photochemical pathway was observed.

(2) Despite the different products formed, the hydrolysis mechanisms of **4a,b** and **7-M** are quite similar in that they all involve rapid equilibrium deprotonation of the α-carbon of the carbene complex followed by rate-limiting protonation by water, H_3O^+, or buffer acids. The protonation step probably involves transfer of a proton to the carbene carbon concerted with C–M bond cleavage, although rate-limiting protonation of the metal followed by rapid reductive elimination cannot be excluded, and other possibilities have been suggested.[11] The main difference between **4a** and **4b** compared to **7-M** is that with **4a** and **4b** the vinyl ether /$Cr(CO)_5$ complex (**5**) formed in the rate-limiting step is apparently stable and long-lived enough to make hydrolysis competitive with dissociation, while with **7-M**, and particularly **7-Cr**, the complex **9-M** is too crowded and dissociates too easily for hydrolysis to be very significant.

(3) Field effect interactions between the phenyl group and the charge on the proton donor in the transition state of the reaction of **7-Cr⁻** with acids may be responsible for the nonadherence to the reactivity–selectivity principle of the k_2^{BH}(**4a⁻**)/k_2^{BH}(**7-Cr⁻**) ratios.[23]

(4) The proposed mechanism for the photochemical reaction **7-M⁻** (Scheme 4) is not as firmly established as that for the thermal pathway but is consistent with all experimental facts as well as with literature precedents regarding the ligand exchange between CO and acetonitrile.

Experimental Section

Materials. (Benzylmethoxy)carbenepentacarbonylchromium-(0), **7-Cr**, was prepared as described by Fischer et al.:[31] yield 49%; mp 39–39.5 °C (lit.[31] mp 39 °C); ^{1}H NMR (250 MHz,

(29) The reasons that $k_{2'}^{H_2O}/k_{2'}^{D_2O}$ (1.99) for the photochemical reaction is smaller than $k_2^{H_2O}/k_2^{D_2O}$ (2.78) for the thermal reaction are not known. Comments similar to those made in ref 16 may be relevant here.

(30) (a) Foley, H. C.; Strubinger, L. M.; Targos, T. S.; Geoffroy, G. L. *J. Am. Chem. Soc.* **1983**, *105*, 3064. (b) Bell, S. E. J.; Gordon, K. C.; McGarvey, J. J. *J. Am. Chem. Soc.* **1988**, *110*, 3107. (c) Servaas, P. C.; Stufkens, D. J.; Oskam, A. J. *Organomet. Chem.* **1990**, *390*, 61.

acetone-d_6), δ 4.70 (s, 2H, CH_2), 4.85 (s, 3H, CH_3) and 7.16–7.34 (m, 5H, C_6H_5); UV (50% acetonitrile–50% water) λ_{max} 376, log ϵ = 3.80. Amines were refluxed over NaOH and freshly distilled under argon prior to use. Acetic acid was distilled under argon. KOH and HCl solutions were prepared using "dilut-it" from Baker Analytical. Acetonitrile (Fisher, 99.9%) and D_2O (Aldrich, 99.9 atom % D) were used as received. Water was taken from a Milli-Q water purification system. NaOD in D_2O was prepared by adding carefully cleaned sodium metal to D_2O, and its concentration was determined by titration with a standard HCl solution.

(Benzylmethoxy)carbenepentacarbonyltungsten(0), **7-W**, was prepared by the same procedure as **7-Cr**: yield 65%; mp 49–50 °C; ^{1}H NMR (250 MHz, CD_3CN), δ 4.50 (s, 2H, CH_2), 4.60 (s, 3H, CH_3) and 7.16–7.32 (m, 5H, Ph); ^{13}C NMR (300 MHz, CD_3CN), δ70.51 (CH_2), 72.23 (CH_3), 127.8, 129.5, 130.7 and 136.4 (Ph), 192.6, 198.1, 198.9, 204.8 and 211.7 (CO), 333.1 (C=); EIMS, *m/z* 458 (M^+), 430, 375, 359, 331 (100%), 303, 275, 149 and 91; FTIR, ν 1922 and 2070 cm^{-1} (CO); UV (50% acetonitrile–50% water) λ_{max} 370, log ϵ = 3.87.

Product Studies. A. Thermal Hydrolysis of 7-Cr. A 200 mg (0.61 mmol) amount of **7-Cr** was added to 2 mL of 50% CD_3CN[32] –50% water with 0.5 M KOH. The heterogeneous mixture was stirred at ambient temperature for 2 h. After extraction with 0.5 mL of $CDCl_3$ and drying over Na_2SO_4, the products were analyzed by ^{1}H NMR. All the major peaks were identified as those of β-methoxystyrene. A tiny, yet detectable peak at δ 9.98 ppm was observed. It is attributed to $PhCH_2CHO$.

The hydrolysis products of **7-Cr** were also analyzed by HPLC. A 3.8 mg (0.012 mmol) amount of **7-Cr** was hydrolyzed in 1 mL of 50% acetonitrile–50% water with 0.05 M KOH and 0.05 M KCl at ambient temperature for 4 h. The hydrolysis solution was subjected to analysis on an HP 1090 liquid chromatograph equipped with an HP ODS Hypersil, 5 μm, 200 × 4.6 mm column. A 50% acetonitrile–50% water solution was used as eluent. Detection wavelengths were 240, 260, 280, 320, and 370 nm. A solution containing a known amount of authentic β-methoxystyrene (Aldrich) was analyzed under the same conditions and served as reference. It was found that about 90% of **7-Cr** was converted to β-methoxystyrene. The *E/Z* ratio of β-methoxystyrene was approximately 6 based on the area ratio of the two isomers. No $PhCH_2CHO$ could be detected, presumably due to its low UV extinction coefficient as well as low concentration. The metal fragment was found as $[Cr(CO)_5OH]^-$ and $Cr(CO)_5(CH_3CN)$.[1]

The hydrolysis was also carried out with smaller concentrations of KOH (0.001, 0.1 M), with similar results. In view of the heterogeneous nature of the reaction solutions the absence of an effect of [KOH] on product distribution is difficult to interpret.

B. Thermal Hydrolysis of 7-W. The procedures were the same as for **7-Cr** except that 95.0 mg (0.21 mmol) of **7-W** was used. The ^{1}H NMR analysis showed that besides β-methoxystyrene there is about 25% $PhCH_2CH{=}O$ in the product solution. As in the case of **7-Cr**, different [KOH] had a negligible effect on the product distribution which, due to the heterogeneous nature of the solutions, is again difficult to interpret.

C. Hydrolysis of 7-Cr and 7-W under the Influence of UV Light. A substrate solution was mixed with a KOH solution in an Applied Photophysics DX.17MV stopped-flow apparatus under the following conditions: 50% acetonitrile–50% water (v/v) as solvent, $[\mathbf{7\text{-}M}]_0$, $[\mathbf{7\text{-}Cr}]_0$ = 0.23–0.5 mM, [KOH] = 0.10 M, μ = 0.10 M, 25 °C, 320 nm, and monochromator entrance and exit slit widths of 2 mm. The volume of the stop syringe was set at 20 μL, which corresponds to the volume of the optical cell. This setting ensured that the entire solution flowing through the optical cell would be exposed to the light for the duration of the hydrolysis process. The effluent was collected and analyzed by HPLC (for the conditions, see above). Major peaks in HPLC spectrum were identified as those of β-methoxystyrene. About 90% of **7-M** was converted to β-methoxystyrene; for **7-Cr** the *E/Z* ratio was 4.6, and for **7-W** 3.2.

D. Hydrolysis of β-Methoxystyrene in the Presence of $Cr(CO)_5(CH_3CN)$. $Cr(CO)_3(CH_3CN)$ was generated in situ by irradiating $Cr(CO)_6$ in acetonitrile.[33] The solvent used was distilled over CaH_2 under argon. The aqueous base solution was degassed. The entire procedure was carried out under argon protection. A 0.14 g (0.65 mmol) amount of $Cr(CO)_6$ in 20 mL of acetonitrile was irradiated for 2 h with a UVSL-25 Mineralight lamp (254/366) at ambient temperature; the formation of $Cr(CO)_5(CH_3CN)$ was followed by UV spectroscopy. After the irradiation was discontinued, 0.56 g (4.2 mmol) of β-methoxystyrene was added to the solution and stirred for 0.5 h at ambient temperature. No change was observed. A 5 mL volume of 0.02 M KOH aqueous solution was then added. Some white precipitate formed immediately. The suspension was stirred at ambient temperature for 15 h. A 3 mL volume of $CDCl_3$ was used to extract the organic products. After washing with water and drying over $CaCl_2$, the $CDCl_3$ solution was analyzed by ^{1}H NMR. No product other than β-methoxystyrene was detected. Under the same conditions, the reaction of ethyl vinyl ether with $Cr(CO)_5(CH_3CN)$ leads to acetaldehyde.[1]

Kinetic Runs and Spectra. Reaction solutions were always freshly prepared just prior to measurement by injecting a small amount of stock solution of **7-M** in acetonitrile into the 50% acetonitrile–50% water medium. Most kinetic measurements were carried out in a Perkin-Elmer Lambda 2 UV/vis spectrophotometer. At pH < 10.2, where the reaction corresponds to conversion of **7-M** to products, the kinetics were monitored at 380 nm; in KOH solution, where the reactant is mainly in the form of $\mathbf{7\text{-}M}^-$, the measurements were performed at 320 nm. A number of kinetic runs at pH > 11.5 were also performed in an Applied Photophysics DX.17MV stopped-flow apparatus at 320 and 360 nm and monochromator entrance and exit slit widths of 2 mm. The data relating to the influence of the light intensity on the rate of conversion of **7-M** to products were obtained in a 0.1 M KOH solution by varying the monochromator slit width from 0.1 to 8 mm; again, both the entrance and exit slit had the same setting.

Time resolved spectra (Figure 1) were taken at 25 °C in a Hewlett Packard HP8452A diode array spectrophotometer equipped with a deuterium and a tungsten lamp; $[\mathbf{7\text{-}Cr}]_0$ = 0.18 mM, [KOH] = 0.0008 M, and μ = 0.10 M (KCl). Under these conditions the observed process represents mainly the thermal reaction.

pH and pK_a Measurements. The pH in 50% acetonitrile–50% water was determined according to eq 7[34] with pH_{meas}

$$pH = pH_{meas} + 0.18 \qquad (7)$$

referring to the reading of a pH meter calibrated with standard aqueous buffers. pK_a^{BH} values of acetic acid, *N*-methylmorpholine, and triethylamine were measured as the pH of buffer solutions prepared in a 1:1 ratio of B:BH. Prior to a kinetic run, the buffer solutions of a given B to BH ratio were adjusted for constant pH by adding microliter amounts of HCl or KOH, as needed.

Acknowledgment. This research was supported by Grant CHE-9307659 from the National Science Foundation.

OM950544N

(31) Fischer, E. O.; Kreiter, C. G.; Kollmeier, H. J. *J. Organomet. Chem.* **1971**, *28*, 237.
(32) To reduce the intensity of the signal from acetonitrile in ^{1}H NMR, CD_3CN was used instead of CH_3CN.
(33) Strohmeier, W. Z.; Gerlach, K. *Z. Naturforsch.* **1961**, *15B*, 622.
(34) Allen, A. D.; Tidwell, T. T. *J. Am. Chem. Soc.* **1987**, *109*, 2774.

Metallotrihydridosilanes of Molybdenum and Tungsten: Synthesis, Characterization, and Vibrational Studies of $(C_5R_5)(OC)_2(Me_3P)M-SiH_3$ (M = Mo, W; R = H, Me)[1,2]

Wolfgang Malisch,*[,†] Reiner Lankat,[†] Siegfried Schmitzer,[†] Ralf Pikl,[‡] Uwe Posset,[‡] and Wolfgang Kiefer*[,‡]

Institut für Anorganische Chemie, Universität Würzburg, Am Hubland, D-97074 Würzburg, Germany, and Institut für Physikalische Chemie, Universität Würzburg, Marcusstrasse 9-11, D-97070 Würzburg, Germany

Received May 23, 1995[⊗]

The lithium metalates $Li[M(CO)_2(PMe_3)C_5R_5]$ (**2a–c**), prepared from the corresponding metal hydrides $C_5R_5(OC)_2(Me_3P)M-H$ [R = H, M = Mo (**1a**), W (**1b**); R = Me, M = Mo (**1c**)] with *n*-butyllithium, react with $HSiCl_3$ (**5**) to give $C_5R_5(OC)_2(Me_3P)M-Si(H)Cl_2$ (**6a–c**). Compound **6b** is additionally obtained, starting with the tetramethylphosphonium metalate $[Me_4P][W(CO)_2(PMe_3)C_5H_5]$ (**4**), generated from **1b** with the ylide $Me_3P{=}CH_2$ (**3**). On treatment with $LiAlH_4$, **6a–c** undergo smooth Cl/H exchange at the silicon to afford the metallotrihydridosilanes $C_5R_5(OC)_2(Me_3P)M-SiH_3$ (**7a–c**). The spectroscopic properties of all the compounds have been extensively studied by NMR and IR spectroscopy. In the case of **7a–c**, detailed studies of the Raman spectra have been performed as well as force field calculations for the $M-SiH_3$ units, yielding valuable information with respect to Si–H and M–Si force constants.

Introduction

Metallohydridosilanes bearing a $C_5R_5L_nM$ fragment (n = 2, M = Fe, Ru; n = 3, M = Mo, W; R = H, Me; L = CO, phosphine) offer a variety of interesting reactivities at the functionalized silicon atom due to the activation of the Si–H unit arising from the pronounced electron-donor capacity of the σ-bonded transition metal ligand. In this context, interest is focused on the insertion of oxygen into the Si–H bond offering access to preparatively valuable metallosilanols[3] and on the substitution of hydrogen by transition metal groups leading to silicon-bridged dinuclear complexes.[4] These reactivities should also be valid for SiH_3–metal complexes which offer the possibility to repeat these processes to obtain, e.g., metallosilanetriols[3] or metal clusters with the silicon surrounded by the maximum of four transition metal groups,[5] but evidence has been provided only by an extremely limited number of experiments. In addition, it is of interest to perform these reactions stepwise to produce multifunctionalized metal–silicon species of the type $L_nM-SiH_nX_{3-n}$ (n = 1, 2; X = OH, ML_n). Moreover, SiH_3–metal complexes have gained increasing interest with respect to the generation of thin-film metal silicides by OMCVD.[6]

For the preparation of metallosilanes L_nM-SiH_3 the literature mainly offers the reaction of transition metal anions with halosilanes H_3SiX (X = halogen).[7,8] In practice, this method creates considerable difficulties concerning the preparation and handling of the silicon component. A more efficient and convenient route has recently been established with the hydrogenation of metal-bound chlorosilyl groups by $LiAlH_4$.[9] An essential requirement for this procedure is sufficient metal–silicon bond strength to prevent heterolytic cleavage by the hydride. It is guaranteed by coordination of ligands with a high σ-donor/π-acceptor ratio (e.g., C_5Me_5 and PMe_3) to the transition metal, demonstrated for the first time in connection with the synthesis of $C_5Me_5(OC)_2(Me_3P)W-SiH_3$.[9] As this paper shows, this kind of SiH_3 group formation is also possible for the corresponding molybdenum compound as well as for species bearing an "ordinary" cyclopentadienyl ligand in combination with trimethylphosphine. In addition, the normal coordinate analysis of the $M-SiH_3$ moiety in these novel silyl complexes has been established to conform the assignments and to clarify the bond properties.

† Institut für Anorganische Chemie.
‡ Institut für Physikalische Chemie.
⊗ Abstract published in *Advance ACS Abstracts,* November 1, 1995.
(1) Synthesis and Reactivity of Silicon Transition Metal Complexes, Part 27: Malisch, W.; Möller, S.; Lankat, R.; Reising, J.; Schmitzer, S.; Fey, O. In *Organosilicon Chemistry: From Molecules to Materials*; Auner, N., Weis, J., Eds.; VCH: Weinheim, Germany, *1995*; p 575.
(2) First results concerning this paper were presented at the 10th International Symposium on Organosilicon Chemistry (Poznan, Poland, 1993; Abstracts of Papers, p 80) and at the 10th FECHEM Conference on Organometallic Chemistry (Crete, 1993; Abstract of Papers, p 59).
(3) Malisch, W.; Schmitzer, S.; Kaupp, G.; Hindahl, K.; Käb, H.; Wachtler, U. In *Organosilicon Chemistry*; Auner, N., Weis, J., Eds.; VCH: Weinheim, Germany, 1994; p 185. Malisch, W.; Grün, K.; Gunzelmann, N.; Möller, S.; Lankat, R.; Reising, J.; Neumayer, M.; Fey, O. In *Stereoselective Reactions of Metal-Activated Molecules*: Werner, H., Sundermeyer, J., Eds.; Vieweg: Braunschweig, Germany, 1995; p 183. Adam, W.; Azzena, U.; Prechtl, F.; Hindahl, K.; Malisch, W. *Chem. Ber.* **1992**, *125*, 1409.
(4) Tobita, H.; Kawano, Y.; Shimoi, M.; Ogino, H. *Chem. Lett.* **1987**, 2247. Malisch, W.; Hindahl, K.; Käb, H.; Reising, J.; Adam, W.; Prechtl, F. *Chem. Ber.* **1995**, *128*, 963.
(5) Malisch, W.; Wekel, H.-U.; Grob, I. *Z. Naturforsch.* **1982**, *37b*, 601. Wekel, H.-U.; Malisch, W. *J. Organomet. Chem.* **1984**, *264*, C10. Gusbeth, P.; Vahrenkamp. H. *Chem. Ber.* **1985**, *118*, 1143.
(6) Suhr, H. *Surf. Coat. Technol.* **1991**, *49*, 233. Maury, F. *Adv. Mater.* **1991**, *3*, 542. Kodas, T. T.; Hampden-Smith, M. J. In *The Chemistry of Metal CVD*; VCH: Weinheim, Germany, 1994.
(7) Hagen, A. P.; Higgins, C. R.; Russo, P. J. *Inorg. Chem.* **1971**, *10*, 1657.
(8) Aylett, B. J.; Campbell, J. M. *J. Chem. Soc., Chem. Commun.* **1965**, 217.
(9) Schmitzer, S.; Weis, U.; Käb, H.; Buchner, W.; Malisch, W.; Polzer, T.; Posset, U.; Kiefer, W. *Inorg. Chem.* **1993**, *32*, 303.

0276-7333/95/2314-5622$09.00/0

Scheme 1

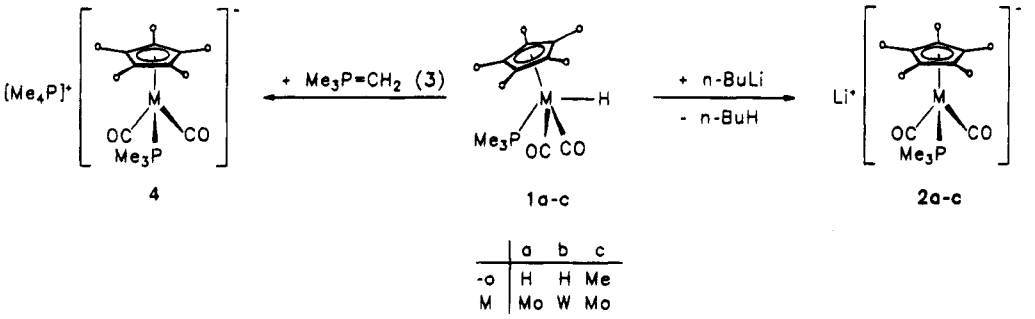

	a	b	c
-o	H	H	Me
M	Mo	W	Mo

Scheme 2

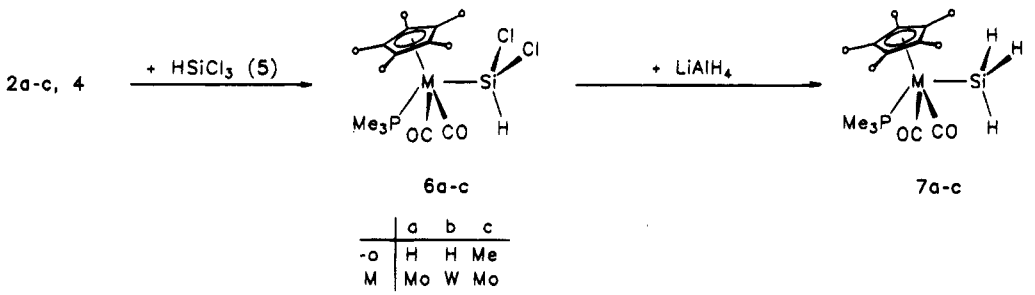

	a	b	c
-o	H	H	Me
M	Mo	W	Mo

Results and Discussion

Synthesis of the Silyl–Metal Complexes 6a–c and 7a–c. For the synthesis of the required carbonyl metalates, CO/Me_3P exchange in the known anions $[C_5R_5(OC)_3M]^-$ (M = Mo, W; R = H, Me) can be envisaged. However, this reaction is inhibited by the strong coordination of the carbon monoxide ligands[10] that is derived from the anionic charge. A successful approach is offered via the metal hydrides **1a–c**, which are easily deprotonated to the corresponding anions by *n*-BuLi. The reaction is conducted in petroleum ether at 0 °C and leads to the formation of a precipitate of the lithium metalates **2a–c** (Scheme 1).

Compounds **2a–c** are highly pyrophoric beige to yellow powders, which could not be characterized analytically. Spectroscopic data are available due to a reasonable solubility in THF. The anionic character of the transition metal fragment is indicated by extremely low values of the $\nu(CO)_{as}$ and the $\nu(CO)_s$ absorptions in the infrared as well as the low $^2J(PCH)$ coupling in the ^1H NMR spectra. According to our experience in metalate chemistry,[11] exchange of Li^+ by an $[R_4P]^+$ group significantly increases the solubility of the metalate, a property which is of importance in context with the generation of donor/solvent-labile main group element–transition metal bonds. Simple access to phosphonium metalates is offered by the interaction of a phosphorous ylide with metal hydrides, a process that in the case of highly nucleophilic metalates can create difficulties due to the abstraction of an organic group from the phosphonium unit.[11] As the synthesis of **4** demonstrates, the metal hydride **1b** is cleanly deprotonated by $Me_3P{=}CH_2$ (**3**) in benzene at ambient temperature (Scheme 1). The phosphonium metalate **4** spontaneously precipitates and can be directly isolated in the pure state by simple filtration.

The reaction of the lithium/tetramethylphosphonium metalates **2a–c** and **4** with $HSiCl_3$ (**5**) in cyclohexane results in the formation of the dichlorosilyl metal complexes **6a–c** in yields of 60%–90%. Due to the good solubility of **4**, the metalation process is complete within less than 1 min compared to 40 h in the case of **2a–c**. Compounds **6a–c** were obtained as pale yellow crystalline powders, showing high thermal stability and resistance toward air.

Metal–silicon bond stabilization by the cyclopentadienyl and the phosphine ligand proves to be high enough to guarantee total Cl/H exchange at the metal-coordinated $SiHCl_2$ group of **6a–c**. Thus, treatment with $LiAlH_4$ in a mixture of toluene/diethyl ether at −78 °C gives access to the metallotrihydrosilanes **7a–c** after an additional period of stirring (4 h) at ambient temperature (Scheme 2).

Compounds **7a–c**, obtained in 74%–80% yield, are yellow solids, which are soluble in aromatic solvents. Increasing stability in solution is found in the order **7a** < **7b** < **7c**, which is in accordance with the increase of the donor character of the metal fragment. Storage of **7a–c** under nitrogen at −20 °C is recommended. Under these conditions **7a–c** show no decomposition even after a period of months. The resistance to light exposure is high and enables laser spectroscopic investigations.

Spectroscopic Characterization of the Silyl Metal Complexes 6a–c and 7a–c. NMR Spectra. The NMR, IR, and Raman spectra of the silyl complexes **6a–c** and **7a–c** [for comparison, the data of the formerly described complex $C_5Me_5(OC)_2(Me_3P)W{-}SiH_3$[9] (**7d**) are included in the following discussion][12] guaran-

(10) Malisch, W. Unpublished results.

(11) Malisch, W. *Angew. Chem.* **1973**, *85*, 228; *Angew. Chem., Int. Ed. Engl.* **1973**, *12*, 235. Angerer, W.; Fiederling, N.; Grötsch, G.; Malisch, W. *Chem. Ber.* **1983**, *116*, 3947.

(12) NMR data of $C_5Me_5(OC)_2(Me_3P)W{-}SiH_3$ (**7d**): ^1H NMR (200 MHz, d_6-benzene): δ 1.24 [d, $^2J(PCH)$ = 9.0 Hz, 9 H, $(H_3C)_3P$], 1.72 [d, $^4J(PWCCH)$ = 0.5 Hz, 15 H, $C_5(CH_3)_5$], 4.26 ppm [d, $^3J(PWSiH)$ = 0.4 Hz, $^1J(SiH)$ = 180.2 Hz, 3 H, SiH_3]. ^{13}C NMR (50 MHz, d_6-benzene): δ 10.66 [s, $C_5(CH_3)_5$], 20.13 [d, $^1J(PC)$ = 33.2 Hz, $(H_3C)_3P$], 100.00 [s, $C_5(CH_3)_5$], 227.34 ppm [d, $^2J(PWC)$ = 18.1 Hz, $^1J(WC)$ = 150.1 Hz, CO]. ^{31}P NMR (36 MHz, d_6-benzene): δ −13.92 ppm [s, $^1J(WP)$ = 278.3 Hz]. ^{29}Si NMR (18 MHz, d_6-benzene): δ −43.18 ppm [d, $^2J(PWSi)$ = 13.2 Hz, $^1J(WSi)$ = 49.8 Hz].

Table 1. Selected Raman Frequencies and IR Absorptions (in Parentheses) in cm^{-1}, and Force Constants *f*(M−Si) and f(Si−H) in N cm^{-1} of 7a−d[a]

$Cp(OC)_2(Me_3P)Mo-SiH_3$ (**7a**)	$Cp(OC)_2(Me_3P)W-SiH_3$ (**7b**)	$C_5Me_5(OC)_2(Me_3P)Mo-SiH_3$ (**7c**)	$C_5Me_5(OC)_2(Me_3P)W-SiH_3$ (**7d**)	assignts
2102 st (2102 w)[b]	2102 m (2080 w, sh)[b]	2089 m, p (2090 w)[c]	2083 st (2075 w)[d]	$\nu_s(SiH_3)$
2082 st (2075 m)[b]	2074 sh (2068 m)[b]	2075 m (2075 w)[c]	2063 sh (2065 m)[d]	$\nu_d(SiH_3)$
1916 m (1910 s)[b]	1909 m (1915 st)[b]	1904 m (1915 st)[c]	1892 m (1903 st)[c,d]	$\nu_s(CO)$
1842 m (1842 vs)[b]	1835 m (1833 vs)[b]	1830 m (1842 vs)[c]	1814 m (1832 vs)[d]	$\nu_{as}(CO)$
1110 vs, p	1109 vs, p	592 st, p	593 st, p	ν_s(ring)
732 w	734/727 w	n.o.	727 m	$\nu_d(PC_3)$
677 st, p	677 st, p	n.o.	675 st, p	$\nu_s(PC_3)$
481 sh	498 w	480 m	503 m	$\nu_{as}(MC)$
463 vs, p	479 vs, p	454 vs	473 vs, p	$\nu_s(MC)$
344 m, p	357 m	n.o.	359 m	ν_s(M−ring)
314 vs, p	315 st, p	335 st, p	326 st, p	ν(M−Si)
1.433	1.640	1.641	1.778	*f*(M−Si)
2.461	2.470	2.448	2.432	*f*(Si−H)

[a] Abbreviations: vs, very strong; st, strong; m, medium; w, weak; sh, shoulder; p, polarized; s, symmetric; as, antisymmetric; d, degenerate; n.o., not observed. [b] Benzene solvent. [c] Pentane solvent. [d] Cyclohexane solvent.

tee unequivocal determination of the stereochemistry at the pseudotetragonal−monopyramidal-coordinated metal center. In all cases the *trans*-position of the Me_3P and the silyl unit is deduced from the appearance of one CO resonance, showing the typical value of 20−30 Hz for the ^2J(PMC) coupling to the *cis*-positioned Me_3P ligand. Moreover, the coupling constant $^1J(^{183}W^{31}P)$ of 244−278 Hz is characteristic for *trans*-configurated tungsten complexes $C_5R_5(OC)_2(Me_3P)WX$ (X as σ-bonded ligand).[13] Consistent with the higher electron-withdrawing character of the dichlorosilyl compared to the trihydridosilyl ligand, the coupling is reduced by ca. 33 Hz on going from **6b** to **7b**, which is indicative of a decrease of the s-electron density in the P−M bond. For the ^{31}P NMR shift of the Me_3P ligand a significant dependence on the metal is observed, with the tungsten species appearing more than 30 ppm upfield from the molybdenum compounds, while the substituents at the silyl ligand show a minor effect (ca. 1−3 ppm).

In connection with the ^{29}Si NMR chemical shifts the following features are notable, which resembles observations made by Berry for the $Cp_2M(H)(SiR_3)$ (M = Mo, W) systems.[14] (1) The metallodichlorosilanes **6a−c** and the tungsten compound described above, $C_5Me_5(OC)_2(Me_3P)W-SiHCl_2$[9] (**7d**), generally show low-field resonances (60.87−83.81 ppm), implying a strong downfield shift by the transition metal fragment [H_2SiCl_2: δ(Si) −11.03 ppm].[15] (2) The metallotrihydridosilanes afford resonances in the negative δ-region [−30.13 (**7c**) to −56.87 ppm (**7b**)], but a significant transition metal effect is still operating (SiH_4: δ −93.10 ppm).[15] It is reduced in comparison to **6a−c**. (3) Changing the metal from molybdenum to tungsten effects an upfield shift of about 14 ppm. Introduction of the C_5Me_5 ligand instead of a Cp group produces an effect of a similar magnitude but in the opposite direction. (4) The coupling constant $^1J(^{183}W^{29}Si)$ in the ^{29}Si NMR spectra is nearly doubled going from the SiH_3 to the $SiHCl_2$ species (**7b,d**, 44.0/49.8 Hz; **6b**, 82 Hz). C_5H_5/C_5Me_5 exchange produces an increase of 6 Hz. Due to the higher electron density caused by electropositive ligands on the metal center or/and on the silicon, the metallotrihydridosilanes **7** exhibit lower ^2J(PMSi) values than the metallochlorosilanes **6** (ΔJ = 2.4−6.2 Hz).

Especially useful for the estimation of the electronic properties of the silicon and its ligand sphere is the ^1J(SiH) coupling constant, which reflects the s-electron density in the Si−H bond.[15] In accordance with Bent's rule[16] the ^1H NMR spectra reveal a significant decrease of ^1J(SiH) when chlorine is substituted by hydrogen [cf.: **6a**, ^1J(SiH) = 244.9 Hz; **7a**, ^1J(SiH) = 183.7 Hz]. The influence of the metal fragment is less significant, resulting in a variation in ^1J(SiH) from 245 to 237 Hz (**6a−c**) and from 183.7 to 180.2 (**7a−d**), respectively, which indicates only a small decrease with respect to metal fragment donor capacity increasing in the series $C_5H_5(OC)_2(Me_3P)Mo$ < $C_5H_5(OC)_2(Me_3P)W$ < $C_5Me_5(OC)_2(Me_3P)Mo$ < $C_5Me_5(OC)_2(Me_3P)W$.

Vibrational Spectra. The vibrational spectra of some silyl tungsten complexes of the type $C_5Me_5(OC)_2(Me_3P)W-SiR_3$ (R = H, Cl, Me) have already been reported.[9] Due to the close similarity to the species presented here, the main features of the vibrational analysis and assignments can be adopted. Therefore, only the most important spectral features are discussed. Spectral data and selected force constants are compiled in Table 1.

Both Raman and IR spectra show the expected two (CO) modes of symmetry species $A_1 + B_2$ (assuming local C_{2v} symmetry for the $M(CO)_2$ oscillators) arising around 1910 (symmetric; IR, s; Raman, m, p) and 1835 cm^{-1} (antisymmetric; IR, vs; Raman, m, dp). The higher electron-releasing character of the C_5Me_5 ligand compared to C_5H_5 finds its expression only in the frequency of the $\nu(CO)A_1$ vibration, which is located 5 cm^{-1} higher for the Cp derivatives (**7a,b**). The $\nu(CO)B_2$ band remains essentially fixed on going from C_5H_5 to C_5Me_5.

SiH_3 stretching gives rise to two bands of symmetry species $A_1 + E$ (assuming local C_{3v} symmetry) in the 2100 cm^{-1} spectral region. Whereas IR absorptions are frequently weak, strong features are observed in the Raman spectra. Both the A_1 and the E modes are usually superimposed and appear as one strong, broad band which could be deconvoluted by curve-fitting procedures and resolved experimentally in the solid state spectra (Figure 1). Polarization data clearly

(13) Keiter, R. L.; Verkade, J. G. *Inorg. Chem.* **1969**, *10*, 2115. Nixon, J. F.; Pidcock, A. *Annu. Rev. NMR Spectrosc.* **1969**, *2*, 345.
(14) Koloski, T. S.; Pestana, D. C.; Carroll, P. J.; Berry, D. H. *Organometallics* **1994**, *13*, 489.
(15) Marsmann, H. ^{29}Si-NMR-Spectroscopic Results. In *NMR Basic Principles and Progress*; Springer: Berlin 1981; Vol. 17, p 65.
(16) Bent, H. A. *Chem. Rev.* **1961**, *61*, 275.

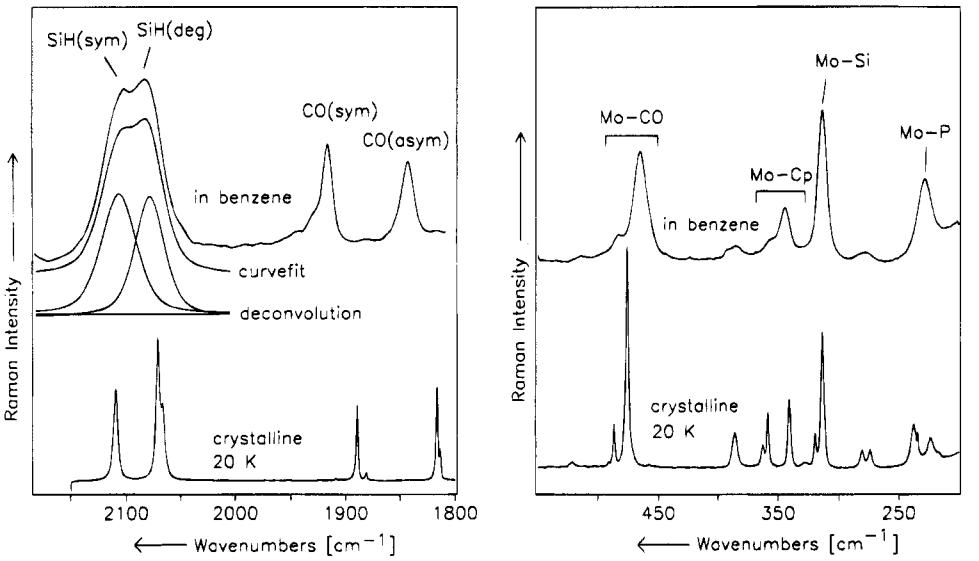

Figure 1. Raman spectra of $Cp(OC)_2(Me_3P)Mo-SiH_3$ (**7a**) in the $\nu(CO)/\nu(SiH)$ and metal–ligand region. Upper trace: in benzene, spectral resolution s = 5 cm^{-1}, temperature T = 300 K. Lower trace: polycrystalline, s = 1 cm^{-1}, T = 20 K.

suggest the higher frequency band to be due to symmetric SiH_3 stretching. From force field calculations[17] the Si–H force constants are determined between 2.432 (**7d**) and 2.470 N cm^{-1} (**7b**) and hence arise within a narrow range. The force constants correlate well with the ^1J(SiH) values of 182.2 (**7b**) and 180.2 Hz (**7d**) found in the ^{1}H NMR spectra, indicating less Si–H bond strength of **7d** (Table 1).

A vibration of great interest in silyl complexes is the metal–silicon stretching mode that gives rise to an intense polarized Raman band in the 300 cm^{-1} region, as previously reported[9,18] (see Figure 1). A special feature of this mode is the insensitivity of its frequency toward exchange of the metal. This is clearly demonstrated by comparing the ν(MSi) frequencies for the homologues **7a** (314 cm^{-1}) and **7b** (315 cm^{-1}) that definitely show no mass effect. On the other hand, on replacing C_5H_5 with C_5Me_5, one observes a shift of about 20 cm^{-1} to higher wavenumbers, reflecting the increased electron density at the metal.

With regard to bond cleavage processes, the strength of the metal–silicon bond is of special interest. The calculation of M–Si force constants *via* a normal coordinate analysis provides a measure for the M–Si bond strengths that can easily be obtained. The results are listed in Table 1. The M–Si force constants increase in the order **7a** < **7b** ≈ **7c** < **7d**. This result is in perfect agreement with the observation that the C_5Me_5 tungsten complex **7d** shows reasonable stability,[9] whereas the C_5H_5 molybdenum derivative **7a** decomposes in solution and under photolysis with M–Si bond cleavage.

Experimental Section

^{1}H, ^{13}C, ^{31}P, and ^{29}Si NMR spectra were obtained on Varian T60, Jeol FX 90 Q, and Bruker AMX 400 spectrometers. $\delta(^{31}P)/\delta(^{29}Si)$ chemical shifts are measured relative to external H_3PO_4(85%)/$Si(CH_3)_4$. $\delta(^1H)/(^{13}C)$ are reported downfield from Me_4Si referenced to the residual proton signal (^{1}H) or natural abundant carbon signal of CD_3CN and C_6D_6. Infrared spectra were recorded on a Perkin-Elmer 283 grating spectrometer. The solutions were measured in NaCl cells with 0.1 mm path length with a resolution of about 2 cm^{-1}. Melting points were measured on a Cu block (closed capillary, not corrected). Mass spectra were recorded at 70 eV on a Varian MAT-SM-CH7 mass spectrometer. Elemental analyses were performed in the microanalytical laboratory of the Institut für Anorganische Chemie der Universität Würzburg. Raman spectra were excited with the 647.1 nm line of a krypton ion laser (Spectra Physics model 2025). Spectra were taken from benzene solutions in NMR tubes filled under a dry argon atmosphere. The scattered light was dispersed by means of a Spex model 1404 double monochromator and detected with a CCD (charge-coupled device) camera system (Photometrics model RDS 2000).[19] The spectra have been evaluated and fitted with standard software. The spectral resolution was 5 cm^{-1}. Plasma lines from the laser tubes were filtered out by means of a modified Anaspec prism filter. The force field calculations were carried out on personal computers and SUN workstations with the program packages QCMP-067 (modified version)[20] and VIA.[21]

Literature procedures were employed to synthesize $Me_3P{=}CH_2$[22] and $C_5R_5(OC)_2(Me_3P)M-H$ (R = H, Me; M = Mo, W).[23] $HSiCl_3$, *n*-BuLi, and $LiAlH_4$ were obtained commercially. All operations were conducted under an atmosphere of purified nitrogen.

1. Lithium [Dicarbonyl(η^5-cyclopentadienyl)(trimethylphosphine)molybdenum(0)] (2a). A solution of 2.56 g (8.70 mmol) of $C_5H_5(OC)_2(Me_3P)Mo-H$ (**1a**) in 40 mL of petroleum ether is cooled to 0 °C. A 4.0 mL (10.0 mmol) amount of a 2.5 M solution of *n*-BuLi in *n*-hexane is added via syringe, causing the immediate precipitation of **2a**, which is filtered off, washed with petroleum ether until the filtrate is colorless, and dried in vacuo. Yield: 2.43 g (93%), beige pyrophoric powder. ^{1}H NMR (400 MHz, d_8-THF): δ 1.32 [d, ^2J(PCH) = 7.2 Hz, 9 H, $(H_3C)_3P$], 4.79 ppm (s, 5 H, C_5H_5). ^{13}C NMR (101 MHz, d_8-THF): δ 26.50 [d, ^1J(PC) = 21.2 Hz, $(H_3C)_3P$], 84.92 (s, C_5H_5), 243.45 ppm [d, ^2J(PMoC) = 14.1 Hz, CO]. ^{31}P NMR (162 MHz, d_8-THF): δ 28.04 ppm. IR (THF): ν(CO) = 1786 (vs), 1646 (vs) cm^{-1}.

(17) Pikl, R.; Posset, U.; Möller, S.; Lankat, R.; Malisch, W.; Kiefer, W. *Vibr. Spectrosc.*, in press.
(18) Van der Berg, G. C.; Oskam, A. J. *J. Organomet. Chem.* **1975**, *91*, 1.
(19) Deckert, V.; Kiefer, W. *Appl. Spectrosc.* **1992**, *46*, 322.
(20) McIntosh, D. F.; Peterson, M. R. *QCPE* **1991**, *342*.
(21) Fleischhauer, H. C. Ph.D. Thesis, University of Düsseldorf, Düsseldorf, Germany, 1991.
(22) Schmidbauer, H.; Tronich, W. *Chem. Ber.* **1968**, *101*, 595.
(23) Alt, H. G.; Englehardt, H. E.; Kläeui, W.; Müller, A. *J. Organomet. Chem.* **1987**, *331*, 317. Bainbridge, A.; Craig, R. J.; Green, M. *J. Chem. Soc. A* **1968**, 2715. Kalck, P.; Pince, R.; Poilblanc, R.; Roussel, J. *J. Organomet. Chem.* **1970**, *24*, 445.

2. Lithium [Dicarbonyl(η^5-cyclopentadienyl)(trimethylphosphine)tungsten(0)] (2b). According to the procedure above for **2a**, **2b** is obtained from 5.26 g (13.8 mmol) of $C_5H_5(OC)_2(Me_3P)W-H$ (**1b**) dissolved in 100 mL of petroleum ether and 6.6 mL (16.5 mmol) of a 2.5 M solution of *n*-BuLi in *n*-hexane. Yield: 5.09 g (95%), beige pyrophoric powder. ^{1}H NMR (400 MHz, d_8-THF): δ 1.48 [d, ^2J(PCH) = 7.8 Hz, 9 H, $(H_3C)_3P$], 4.78 ppm (s, 5 H, C_5H_5). ^{13}C NMR (101 MHz, d_8-THF): δ 27.69 [d, ^1J(PC) = 26.7 Hz, $(H_3C)_3P$], 82.91 (s, C_5H_5), 236.63 ppm [d, ^2J(PWC) = 5.7 Hz, ^1J(WC) = 209.3 Hz, CO]. ^{31}P NMR (162 MHz, d_8-THF): δ −12.92 ppm [s, ^1J(WP) = 462.9 Hz]. IR (THF): ν(CO) = 1782 (vs), 1649 (vs) cm^{-1}.

3. Lithium [Dicarbonyl(η^5-pentamethylcyclopentadienyl)(trimethylphosphine)molybdenum(0)] (2c). According to the procedure above for **2a**, **2c** is obtained from 3.98 g (10.9 mmol) of $C_5Me_5(OC)_2(Me_3P)Mo-H$ (**1c**) dissolved in 100 mL of petroleum ether and 5.2 mL (13.0 mmol) of a 2.5 M solution of *n*-BuLi in *n*-hexane. Yield: 3.85 g (95%), yellow pyrophoric powder. ^{1}H NMR (400 MHz, d_8-THF): δ 1.27 [d, ^2J(PCH) = 6.6 Hz, 9 H, $(H_3C)_3P$], 1.98 ppm [s, 15 H, $C_5(CH_3)_5$]. ^{13}C NMR (101 MHz, d_8-THF): δ 12.80 [s, $C_5(CH_3)_5$], 24.49 [d, ^1J(PC) = 20.0 Hz, $(H_3C)_3P$], 98.42 [s, $C_5(CH_3)_5$], 246.62 ppm [d, ^2J(PMoC) = 12.8 Hz, CO]. ^{31}P NMR (162 MHz, d_8-THF): δ 23.15 ppm. IR (THF): ν(CO) = 1770 (vs), 1638 (vs) cm^{-1}.

4. Tetramethylphosphonium [(Dicarbonyl)(η^5-cyclopentadienyl)(trimethylphosphine)tungsten(0)] (4). To a solution of 578 mg (1.51 mmol) of $Cp(OC)_2(Me_3P)W-H$ (**1b**) in 40 mL of benzene is added 136 mg (1.51 mmol) of $Me_3P{=}CH_2$ (**3**) dissolved in 5 mL of diethyl ether dropwise under vigorous stirring at room temperature within 45 min. The precipitate of **4** that forms is immediately filtered off, washed twice with 20 mL of benzene and 20 mL of pentane, and dried in vacuo. Yield: 663 mg (93%), yellow solid. Mp: 174 °C. ^{1}H NMR (60 MHz, d_3-acetonitrile): δ 1.55 [d, ^2J(PCH) = 7.0 Hz, 9 H, $(H_3C)_3P$], 1.83 [d, ^2J(PCH) = 15.0 Hz, 12 H, $(H_3C)_4P^+$], 4.80 ppm (bs, 5 H, C_5H_5). ^{31}P NMR (162 MHz, d_3-acetonitrile): δ −15.52 [s, ^1J(PW) = 463 Hz, $(H_3C)_3P$], 22.42 ppm [s, $(H_3C)_4P^+$]. IR (acetonitrile): ν(CO) = 1762 (vs), 1681 (vs) cm^{-1}. Anal. Calcd for $C_{14}H_{26}O_2P_2W$ (472.2): C, 35.61; H, 5.55. Found: C, 37.42; H, 5.74.

5. Dicarbonyl(dichlorosilyl)(η^5-cyclopentadienyl)(trimethylphosphine)molybdenum(II) (6a). A suspension of 2.43 g (8.103 mmol) of **2a** in 60 mL of cyclohexane is combined with 3.28 g (24.3 mmol) of $HSiCl_3$ (**5**). Immediately after the addition, the reaction mixture becomes dark brown. After the mixture has been stirred for 40 h, all volatile materials are removed in vacuo, the residue is extracted with 30 mL of toluene, and the extract is filtered over Celite. Solvent is removed in vacuo, and the residue of **6a** is washed at −30 °C with 20 mL of pentane to separate oily side products. Yield: 2.39 g (75%), golden yellow crystals. Mp: 143 °C. ^{1}H NMR (60 MHz, d_6-benzene): δ 1.00 [d, ^2J(PCH) = 10.0 Hz, 9 H, $(H_3C)_3P$], 4.77 [d, ^3J(PMoCH) = 1.0 Hz, 5 H, C_5H_5], 7.57 ppm [d, ^3J(PMoSiH) = 0.3 Hz, ^1J(SiH) = 244.9 Hz, 1 H, $SiHCl_2$]. ^{13}C NMR (101 MHz, d_6-benzene): δ 20.89 [d, ^1J(PC) = 31.8 Hz, $(H_3C)_3P$], 91.65 (s, C_5H_5), 230.31 ppm [d, ^2J(PMoC) = 25.2 Hz, CO]. ^{31}P NMR (162 MHz, d_6-benzene): δ 18.22 ppm. ^{29}Si NMR (79 MHz, d_6-benzene): δ 78.86 ppm [d, ^2J(PMoSi) = 21.9 Hz]. IR (benzene): ν(SiH) = 2134 (w) cm^{-1}; ν(CO) = 1936 (s), 1869 (vs) cm^{-1}. MS (^{28}Si, ^{35}Cl, ^{98}Mo, 70 eV, 30 °C): *m/e* = 394 [2, (M)$^+$], 366 [4, (M − CO)$^+$], 338 [8, (M − 2CO)$^+$], 296 [49, $(C_5H_5(OC)_2(Me_3P)MoH)^+$, $(C_5H_5(OC)(Me_3P)MoSiH)^+$], 274 [60, $(C_5H_5(Me_3P)MoCl)^+$], 266 [60, $(C_5H_5(OC)_2(Me_3P)MoH)^+$, $(C_5H_5(OC)(MeP)MoSiH)^+$], 236 [100, $(C_5H_5(OC)MoSiH_2Me)^+$], 220 [56, $(C_5H_5(OC)_2MoH)^+$, $(C_5H_5(OC)MoSiH)^+$], 207 [59, $(C_5H_5(OC)MoHMe)^+$, $(C_5H_5MoSiHMe)^+$], 198 [82, $(C_5H_5MoCl)^+$], 163 [35, $(C_5H_5Mo)^+$], 118 [8, $(C_5H_5(OC)MoSiH_2Me)^{2+}$], 110 [7, $(C_5H_5(OC)_2MoH)^{2+}$], 81.5 [4, $(C_5H_5Mo)^{2+}$]. Anal. Calcd for $C_{10}H_{15}Cl_2MoO_2PSi$ (393.1): C, 30.55; H, 3.85; Cl, 18.04. Found: C, 30.21; H, 3.81; Cl, 17.83.

6. Dicarbonyl(dichlorosilyl)(η^5-cyclopentadienyl)(trimethylphosphine)tungsten(II) (6b). (a) Metalation of $HSiCl_3$ (5) with $[Me_4P][W(CO)_2(PMe_3)Cp]$ (4). To a suspension of 390 mg (0.83 mmol) of **4** in 25 mL of benzene is added 279 mg (2.06 mmol) of $HSiCl_3$ (**5**) in 5 mL of benzene dropwise under vigorous stirring within 30 s at room temperature. Subsequently $[Me_4P]Cl$ (65 mg, 93%) is separated, and the filtrate is evaporated to dryness. The residue is dissolved in 5 mL of pentane, and **6b** crystallizes on cooling to −78 °C. Yield: 359 mg (90%), yellow crystalline powder. Mp: 137 °C. (b) **Metalation of $HSiCl_3$ (5) with $Li[W(CO)_2(PMe_3)Cp]$ (2b).** According to section 5 above, **6b** is obtained from 563 mg (1.60 mmol) of $Li[W(CO)_2(PMe_3)Cp]$ (**2b**) and 0.30 mL (0.30 mmol) of $HSiCl_3$ (**5**) in 20 mL of cyclohexane. Yield: 515 mg (67%). ^{1}H NMR (60 MHz, d_6-benzene): δ 1.15 [d, ^2J(PCH) = 9.4 Hz, 9 H, $(H_3C)_3P$], 4.82 [d, ^3J(PWCH) = 1.3 Hz, 5 H, C_5H_5], 7.94 ppm [d, ^3J(PWSiH) = 0.3 Hz, ^1J(SiH) = 248.1 Hz, 1 H, $SiHCl_2$]. ^{13}C NMR (101 MHz, d_6-benzene): δ 20.68 [d, ^1J(PC) = 35.5 Hz, $(H_3C)_3P$], 89.94 (s, C_5H_5), 222.30 ppm [d, ^2J(PWC) = 20.1 Hz, ^1J(WC) = 134.4 Hz, CO]. ^{31}P NMR (162 MHz, d_6-benzene): δ −18.30 ppm [^1J(PW) = 244 Hz]. ^{29}Si NMR (79 MHz, d_6-benzene): δ 52.58 ppm [d, ^2J(PWSi) = 21.3 Hz, ^1J(WSi) = 82 Hz]. IR (cyclohexane): ν(SiH) = 2137 (w) cm^{-1}; ν(CO) = 1942 (s), 1863 (m) (*cis*); 1935 (m), 1855 (vs) (*trans*) cm^{-1}. MS (^{28}Si, ^{35}Cl, ^{184}W, 70 eV, 70 °C): *m/e* = 480 [2, (M)$^+$], 452 [3, (M − CO)$^+$], 422 [3, $(C_5H_5(OC)(MeP)WSiCl_2H)^+$], 382 [52, $(C_5H_5(OC)_2(Me_3P)WH)^+$], 352 [59, $(C_5H_5(OC)_2(MeP)WH)^+$], 322 [100, $(C_5H_5(OC)WSiMeH_2)^+$], 306 [50, $(C_5H_5(OC)_2WH)^+$, $(C_5H_5(OC)WSiH)^+$], 292 [31, $(C_5H_5(OC)_2WMe)^+$], 277 [13, $(C_5H_5(OC)WH)^+$, $(C_5H_5WSi)^+$], 160 [12, $(C_5H_5(OC)_2WSiMe)^{2+}$], 153 [13, $(C_5H_5(OC)WSiH)^{2+}$, $(C_5H_5(OC)_2WH)^{2+}$]. Anal. Calcd for $C_{10}H_{15}Cl_2PO_2SiW$ (481.1): C, 24.97; H, 3.14; Cl, 14.74. Found: C, 24.49; H, 3.18; Cl, 14.39.

7. Dicarbonyl(dichlorosilyl)(η^5-pentamethylcyclopentadienyl)(trimethylphosphine)molybdenum(II) (6c). According to the procedure above for **6a**, **6c** is obtained from 1.20 g (3.24 mmol) of $Li[Mo(CO)_2(PMe_3)C_5Me_5]$ (**2c**) and 805 mg (5.94 mmol) of $HSiCl_3$ (**5**) in 50 mL of cyclohexane. Yield: 839 mg (56), beige crystalline powder. Mp: 86 °C. ^{1}H NMR (400 MHz, d_6-benzene): δ 1.05 [d, ^2J(PCH) = 8.9 Hz, 9 H, $(H_3C)_3P$], 1.62 [s, 15 H, $C_5(CH_3)_5$], 7.20 ppm [d, ^3J(PMoSiH) = 2.0 Hz, ^1J(SiH) = 236.9 Hz, 1 H, $SiHCl_2$]. ^{13}C NMR (101 MHz, d_6-benzene): δ 10.87 [s, $C_5(CH_3)_5$], 19.23 [d, ^1J(PC) = 30.7 Hz, $(H_3C)_3P$], 103.15 [s, $C_5(CH_3)_5$], 236.11 ppm [d, ^2J(PMoC) = 29.1 Hz, CO]. ^{31}P NMR (162 MHz, d_6-benzene): δ 19.06 ppm. ^{29}Si NMR (79 MHz, d_6-benzene): δ 83.81 ppm [d, ^2J(PMoSi) = 15.7 Hz]. IR (toluene): ν(SiH) = 2093 (w) cm^{-1}; ν(CO) = 1930 (s), 1855 (vs) cm^{-1}. Anal. Calcd for $C_{15}H_{25}Cl_2MoO_2PSi$ (463.3): C, 38.89; H, 5.44; Found: C, 37.33; H, 6.06.

8. Dicarbonyl(η^5-cyclopentadienyl)(trimethylphosphine)(silyl)molybdenum(II) (7a). To a solution of 354 mg (0.90 mmol) of $Cp(OC)_2(Me_3P)Mo-SiHCl_2$ (**6a**) in 20 mL of diethyl ether/toluene (4:1) is added 105 mg (2.76 mmol) of $LiAlH_4$ at −78 °C. After being stirred for 2 h at this temperature, the mixture is warmed up to room temperature and stirred for another 4 h. Volatile materials are removed in vacuo, and the remaining residue is repeatedly extracted with 20 mL of benzene. After filtration over Celite, the solvent is evaporated and the residual **6a** washed at −78 °C with 20 mL of pentane. Yield: 225 mg (77%), pale yellow solid. Mp: 148 °C. ^{1}H NMR (60 MHz, d_6-benzene): δ 1.07 [d, ^2J(PCH) = 9.0 Hz, 9 H, $(H_3C)_3P$], 4.50 [d, ^3J(PMoSiH) = 0.4 Hz, ^1J(SiH) = 183.7 Hz, 3 H, SiH_3], 4.64 ppm [d, ^3J(PMoCH) = 1.0 Hz, 5 H, C_5H_5]. ^{13}C NMR (101 MHz, d_6-benzene): δ 21.20 [d, ^1J(PC) = 30.4 Hz, $(H_3C)_3P$], 89.47 (s, C_5H_5), 230.42 ppm [d, ^2J(PMoC) = 24.1 Hz, CO]. ^{31}P NMR (162 MHz, d_6-benzene): δ 16.21 ppm. ^{29}Si NMR (79 MHz, d_6-benzene): δ −42.65 ppm [d, ^2J(PMoSi) = 15.9 Hz]. MS (^{28}Si, ^{98}Mo, 70 eV, 35 °C): *m/e* = 326 [21%, (M)$^+$], 311 [12, $(C_5H_5(OC)_2(Me_2P)MoH)^+$, 295 [31, $(C_5H_5(OC)_2(Me_3P)Mo)^+$], 281 [21, $(C_5H_5(OC)_2(Me_2P)MoH)^+$, $(C_5H_5(OC)(Me_2P)MoSiH)^+$], 252 [21, $(C_5H_5(OC)(Me_2P)Mo)^+$, $(C_5H_5(Me_2P)MoSi)^+$], 235 [15, $(C_5H_5(OC)MoMeSiH)^+$], 220 [11, $(C_5H_5(OC)_2MoH)^+$], 191 [18, $(C_5H_5(OC)Mo)^+$, $(C_5H_5MoSi)^+$], 163 [32, $(C_5H_5Mo)^+$], 61 [100, $(Me_2P)^+$]. Anal. Calcd for $C_{10}H_{17}$-

MoO_2PSi (324.3): C, 37.04; H, 5.28; Mo, 29.60. Found: C, 36.29; H, 4.91; Mo, 28.42.

9. Dicarbonyl(η^5-cyclopentadienyl)(trimethylphosphine)(silyl)tungsten(II) (7b). According to the procedure above for **7a**, **7b** is obtained from 478 mg (0.99 mmol) of $Cp(OC)_2(Me_3P)W-SiHCl_2$ (**6b**) and 132 mg (3.48 mmol) of $LiAlH_4$ in 20 mL of diethyl ether/toluene (4:1). Yield: 325 mg (80%), pale yellow solid. Mp: 162 °C. ^{1}H NMR (60 MHz, d_6-benzene): δ 1.05 [d, ^2J(PCH) = 9.4 Hz, 9 H, $(H_3C)_3P$], 4.48 [d, ^3J(PWCH) = 1.1 Hz, 5 H, C_5H_5], 4.52 ppm [s, ^1J(SiH) = 182.8 Hz, 3 H, SiH_3]. ^{13}C NMR (101 MHz, d_6-benzene): δ 21.53 [d, ^1J(PC) = 34.8 Hz, $(H_3C)_3P$], 87.72 (s, C_5H_5), 221.59 ppm [d, ^2J(PWC) = 18.1 Hz, ^1J(WC) = 151.8 Hz, CO]. ^{31}P NMR (162 MHz, d_6-benzene): δ −16.75 ppm [^1J(WP) = 277 Hz]. ^{29}Si NMR (79 MHz, d_6-benzene): δ −56.87 ppm [d, ^2J(PWSi) = 15.1 Hz, ^1J(WSi) = 44.0 Hz]. MS (^{28}Si, ^{184}W, 70 eV, 60 °C): *m/e* = 412 [30, $(M)^+$], 381 [47, $(M - SiH_3)^+$], 351 [60, $(C_5H_5(OC)_2(MeP)W)^+$, $(C_5H_5(OC)(MeP)WSi)^+$], 322 [60, $C_5H_5(OC)WMeSiH_2)^+$], 334 [18, $(C_5H_5(OC)_2WSiH_3)^+$], 320 [60, $(C_5H_5(OC)WSiMe)^+$, $(C_5H_5(OC)_2WMe)^+$], 306 [33, $(C_5H_5(OC)WSiH)^+$, $(C_5H_5(OC)_2WH)^+$], 305 [32, $(C_5H_5(OC)_2W)^+$, $(C_5H_5(OC)WSi)^+$], 292 (17, $(C_5H_5WSiMe)^+$, $(C_5H_5(OC)WMe)^+$], 277 [9, $(C_5H_5WSi)^+$, $(C_5H_5(OC)W)^+$], 191 [3, $(C_5H_5(OC)_2(Me_3P)WH)^{2+}$], 160 [8, $C_5H_5(OC)_2WMe)^{2+}$], 153 [8, $(C_5H_5(OC)_2WH)^{2+}$], 61 [100, $(Me_2P)^+$]. Anal. Calcd for $C_{10}H_{17}O_2PSiW$ (412.2): C, 29.14; H, 4.16; W, 44.61. Found: C, 29.07; H, 4.11; W, 43.82.

10. Dicarbonyl(η^5-pentamethylcyclopentadienyl)(trimethylphosphine)(silyl)molybdenum(II) (7c). According to the procedure above for **7a**, **7c** is obtained from 565 mg (1.22 mmol) of $C_5Me_5(OC)_2(Me_3P)Mo-SiHCl_2$ (**6c**) and 125 mg (3.29 mmol) of $LiAlH_4$ in 50 mL of diethyl ether/toluene (4:1). Yield: 354 mg (74%), yellow solid. Mp: 54 °C. ^{1}H NMR (400 MHz, d_6-benzene): δ 1.12 [d, ^2J(PCH) = 8.6 Hz, 9 H, $(H_3C)_3P$], 1.66 [s, 15 H, $C_5(CH_3)_5$], 4.19 ppm [s, ^1J(SiH) = 180.9 Hz, 3 H, SiH_3]. ^{13}C NMR (101 MHz, d_6-benzene): δ 10.60 [s, $C_5(CH_3)_5$], 19.78 [d, ^1J(PC) = 29.4 Hz, $(H_3C)_3P$], 101.25 [*s*, $C_5(CH_3)_5$], 234.58 ppm [d, ^2J(PMoC) = 26.6 Hz, CO]. ^{31}P NMR (162 MHz, d_6-benzene): δ 22.22 ppm. ^{29}Si NMR (18 MHz, d_6-benzene): δ −30.13 ppm [d, ^2J(PMoSi) = 13.3 Hz]. Anal. Calcd for $C_{15}H_{27}MoO_2PSi$ (394.4): C, 45.68; H, 6.90. Found: C, 45.57; H, 7.27.

Acknowledgment. We gratefully acknowledge financial support from the Deutsche Forschungsgemeinschaft (Sonderforschungsbereich 347, "Selektive Reaktionen Metall-aktivierter Moleküle", Projects B-2 and C-2) as well as from the Fonds der Chemischen Industrie. We also thank R. Schedl, U. Neumann, and C. P. Kneis for the elemental analyses and Dr. W. Buchner and M. L. Schäfer for recording part of the NMR-spectra.

OM950380A

High-Pressure NMR and *ab Initio* Computational Studies on the Insertion Mechanism of Carbon Monoxide into Cationic Monoorganopalladium(II) Complexes Bearing Tridentate Nitrogen Donor Ligands

Bertus A. Markies,[†] Peter Wijkens,[†] Alain Dedieu,*[,§,∥] Jaap Boersma,*[,†] Anthony L. Spek,[‡,⊥] and Gerard van Koten[†]

Debye Institute, Department of Metal-Mediated Synthesis, Utrecht University, Padualaan 8, 3584 CH Utrecht, The Netherlands, Bijvoet Center for Biomolecular Research, Laboratory of Crystal and Structural Chemistry, Utrecht University, Padualaan 8, 3584 CH Utrecht, The Netherlands, and Laboratoire de Chimie Quantique, UPR 139 du CNRS, Université Louis Pasteur, 4 Rue Blaise Pascal, 67070 Strasbourg Cédex, France

Received March 1, 1995[⊗]

A number of methyl and arylpalladium(II) cations bearing tridentate nitrogen-donor ligands has been prepared, and their reactivity in the insertion of carbon monoxide has been studied. The resulting acetyl and aroylpalladium complexes of the ligands *N*-(2-picolyl)-*N*,*N*′,*N*′-trimethylethylenediamine (pico) and *N*,*N*,*N*′,*N*″,*N*″-pentamethyldiethylenetriamine (pmdeta) were isolated and characterized. In the case of the 4-nitrophenylpalladium and 2,4,6-trimethylphenylpalladium pico- and pmdeta complexes, no carbonylation products could be isolated. In these cases, either the equilibrium of the carbonylation reaction did not lie fully to the side of the insertion product even at 10 atm of CO or the insertion product decarbonylated upon attempted isolation. The methylpalladium complex of the 2,6-bis-[(dimethylamino)methyl]pyridine (NN′N) ligand reacted quantitatively with CO in CD_3COCD_3 to give acetic anhydride, palladium metal, and the protonated ligand; a mechanism for the anhydride formation is proposed. With the exception of the 1-naphthoyl derivative, the aroyl complexes of the NN′N ligand could not be isolated due to decarbonylation upon attempted isolation. Most of the unstable insertion products could, however, be characterized by IR and high-pressure NMR. Crystals of the 1-naphthoylpalladium complex with the NN′N ligand were obtained from acetone/pentane under a CO atmosphere. This complex is the first example of an aroylpalladium(II) cation. Two reaction pathways for the carbonyl insertion reaction, *i.e.*, dissociative and associative, have been evaluated using ^{1}H NMR studies and *ab initio* calculations. The insertion reaction at 10 atm of CO pressure in CD_3COCD_3 is complete within 2.5 min for most complexes, with the exception of those bearing strongly electron-withdrawing para substituents (*e.g.*, NO_2) or sterically demanding ortho substituents (*e.g.*, 2,4,6-trimethyl) on the aryl ring. *Ab initio* calculations at the RHF, MP2//SCF, and CAS–SCF/CI levels on the cationic model system $[Pd(CH_3)(NH_3)_3]^+$ + CO and the neutral system $[Pd(CH_3)_2(NH_3)_2]$ + CO show that the carbonylation reaction follows a hybrid pathway, *i.e.*, a concerted replacement of NH_3 by CO followed by migratory insertion of CO into the Pd–C bond instead of a purely dissociative or associative mechanism. For both the neutral and the cationic systems the rate-determining step is the migratory insertion. The insertion process is enhanced by coordination of the dissociated amine and is slightly more favorable in the neutral system. Together with the low-energy replacement of NH_3 by CO, this implies that in both systems the rate of carbonyl insertion should be independent of the applied CO pressure.

Introduction

The insertion of carbon monoxide into metal-to-carbon σ-bonds is one of the most important steps in homogeneous catalysis by transition metal complexes.[1] It is generally accepted, both on experimental[1,2] and theoretical[3] grounds, that CO insertion involves migration of the hydrocarbyl group to the coordinated CO ligand. Very recently, Van Leeuwen *et al.* presented evidence for such migration in the case of square planar palladium and platinum bidentate diphosphine complexes.[4]

Garrou and Heck showed that, in *trans*-$MXR(PR_3)_2$

* To whom general correspondence should be addressed.
† Debye Institute.
‡ Bijvoet Center for Biomolecular Research.
§ Laboratoire de Chimie Quantique.
∥ Address correspondence regarding the calculations to this author.
⊥ Address correspondence regarding the crystallography to this author.
⊗ Abstract published in *Advance ACS Abstracts,* September 15, 1995.

(1) (a) Parshall, G. W.; Ittel, S. D. *Homogeneous Catalysis. The Applications and Chemistry of Catalysis by Soluble Transition Metal Complexes*, 2nd ed.; Wiley: New York, 1992. (b) Collman, J. P.; Hegedus, L. S.; Norton, J. R.; Finke, R. G. *Principles and Applications of Organotransition Metal Chemistry*; Oxford University Press: Oxford, 1987.
(2) Ozawa, F.; Yamamoto, A. *Chem. Lett.* **1981**, 289.

0276-7333/95/2314-5628$09.00/0

complexes (M = Pd or Pt; R = alkyl or aryl; X = I, Br, Cl), insertion proceeds via an initial five-coordinate intermediate $MXR(CO)(PR_3)_2$ and then follows a dissociative or a migratory pathway.[5] In the dissociative pathway, which is slowed down in the presence of excess phosphine, this intermediate loses one phosphine ligand prior to CO insertion, which then proceeds from a four-coordinate complex. In the migratory pathway direct CO insertion occurs.

Little is known about the insertion mechanism when bi-[6] or tridentate donor ligands[6j,7,8] are used. Early studies by Anderson and Lumetta suggested the dissociation of one of the chelate donor atoms when mixed phosphorus/sulfur (P–S) or phosphorus/nitrogen (P–N) ligands were used.[6f] Cavell *et al.* observed similar effects in the carbonylation of palladium(II) complexes $PdMe(XY)(PPh_3)$ in which XY is a β-diketonate or a monothio-β-diketonate ligand.[6n,o] Van Leeuwen and Vrieze *et al.*[6d,g] recently investigated the influence of the bite angle of the ligand for both neutral and cationic complexes of the type PdClMe(P–P) on the insertion rate.

So far, only two reports have appeared on the carbonylation of palladium(II) complexes containing a terdentate ligand, both of which describe complexes of N-donor ligands. Vrieze *et al.* reported the synthesis and subsequent carbonylation of the methylpalladium(II) complexes $[PdMe(terpy)]Cl\cdot 2H_2O$, PdClMe(*i*-Pr-DIP), and [PdMe(*i*-Pr-DIP)]OTf (terpy = 2,2′:6′,2″-terpyridyl; *i*-Pr-DIP = 2,6-bis(*N*-isopropylcarbaldimino)pyridine),[7] and we gave a preliminary account of the synthesis and carbonylation of arylpalladium(II) complexes of the type [PdAr(NN′N)]OTf with Ar = phenyl or 1-naphthyl and NN′N = 2,6-bis[(dimethylamino)-methyl]pyridine.[8] We chose tridentate ligands to diminish the degrees of freedom for rearrangements around the metal center.

In the present paper we present the results of high-pressure NMR measurements and *ab initio* calculations on the carbonyl insertion reaction of palladium complexes containing the NN′N, pmdeta (*N,N,N′,N″,N″*-pentamethyldiethylenetriamine), and pico (*N,N,N′*-trimethyl-*N′*-(2-picolyl)ethylenediamine) ligands.

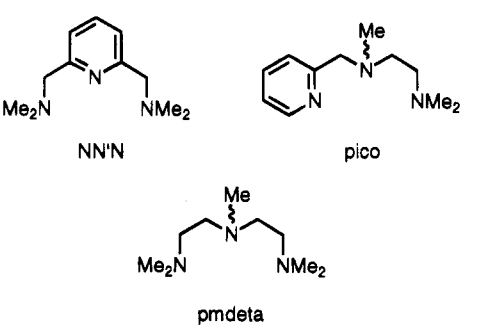

Table 1. Summary and Numbering of the Complexes

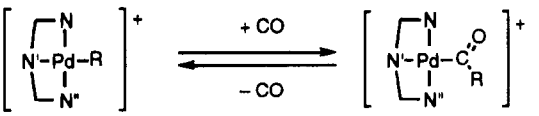

	R–Pd			R–CO–Pd		
R	NN′N	pico	pmdeta	NN′N	pico	pmdeta
Me	**1a**	**2a**	**3a**		**5a**	**6a**
Ph	**1b**	**2b**	**3b**	**4b**	**5b**	**6b**
4-$O_2NC_6H_4$	**1c**	**2c**	**3c**	**4c**	**5c**	**6c**
2-MeC_6H_4	**1d**	**2d**	**3d**	**4d**	**5d**	**6d**
1-naphthyl	**1e**	**2e**	**3e**	**4e**	**5e**	**6e**
mesityl[a]	**1f**	**2f**	**3f**	**4f**	**5f**	**6f**

[a] 2,4,6-Trimethylphen-1-yl.

Results

Insertion and Deinsertion of Carbon Monoxide. The methyl (**1–3a**) and aryl compounds (**1b–f, 2b–e,** and **3b–f**) used in this study were prepared via reported procedures and are listed in Table 1.[9]

Insertion of carbon monoxide (eq 1) was performed

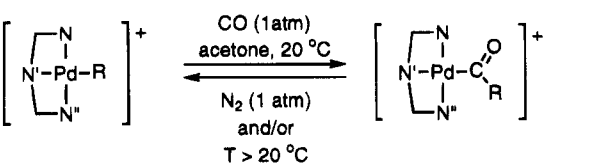

(1)

by bubbling CO at atmospheric pressure through a CD_3-

(3) For semiempirical calculations see: (a) Berke, H.; Hoffmann, R. *J. Am. Chem. Soc.* **1978**, *100*, 7224. (b) Ruiz, M. E.; Flores-Riveros, A.; Novaro, O. *J. Catal.* **1980**, *64*, 1. (c) Calhorda, M. J.; Brown, J. M.; Cooley, N. A. *Organometallics* **1991**, *10*, 1431. For *ab initio* calculations see: (d) Sakaki, S.; Kitaura, K.; Morokuma, K.; Ohkubo, K. *J. Am. Chem. Soc.* **1983**, *105*, 2280. (e) Koga, N.; Morokuma, K. *J. Am. Chem. Soc.* **1986**, *108*, 6136. (f) Ziegler, T.; Versluis, L.; Tschinke, V. *J. Am. Chem. Soc.* **1986**, *108*, 612. (g) Axe, F. U.; Marynick, D. S. *Organometallics* **1987**, *6*, 572. (h) Dedieu, A.; Sakaki, S.; Strich, A.; Siegbahn, P. E. M. *Chem. Phys. Lett.* **1987**, *133*, 317. (i) Shusterman, A. J.; Tamir, I.; Pross, A. *J. Organomet. Chem.* **1988**, *340*, 203. (j) Versluis, L.; Ziegler, T.; Baerends, E. J.; Ravenek, W. *J. Am. Chem. Soc.* **1989**, *111*, 2018. (h) Koga, N.; Morokuma, K. *New J. Chem.* **1991**, *15*, 749. (k) Koga, N.; Morokuma, K. *Chem. Rev.* **1991**, *91*, 823. (l) Tchougreeff, A. L.; Gulevich, Yu. V.; Misurkin, I. A.; Beletskaya, I. P. *J. Organomet. Chem.* **1993**, *455*, 261. (m) Blomberg, M. R. A.; Karlsson, C. A. M.; Siegbahn, P. E. M. *J. Phys. Chem.* **1993**, *97*, 9341.

(4) Van Leeuwen, P. W. N. M.; Roobeek, C. F.; Van der Heijden, H. *J. Am. Chem. Soc.* **1994**, *116*, 12117.

(5) Garrou, P. E.; Heck, R. F. *J. Am. Chem. Soc.* **1976**, *98*, 4115.

(6) For P–P complexes see: (a) Bennett, M. A.; Rokicki, A. *J. Organomet. Chem.* **1983**, *244*, C31. (b) Ozawa, F.; Hayashi, T.; Koide, H.; Yamamoto, A. *J. Chem. Soc., Chem. Commun.* **1991**, 1469. (c) Dekker, G. P. C. M.; Elsevier, C. J.; Vrieze, K.; van Leeuwen, P. W. N. M.; Roobeek, C. F. *J. Organomet. Chem.* **1992**, *430*, 357. (d) Dekker, G. P. C. M.; Elsevier, C. J.; Vrieze, K.; van Leeuwen, P. W. N. M. *Organometallics* **1992**, *11*, 1598. (e) Tóth, I.; Elsevier, C. J. *J. Chem. Soc., Chem. Commun.* **1993**, 529. For P–N complexes see: (f) Anderson, G. K.; Lumetta, G. J. *Organometallics* **1985**, *4*, 1542. (g) Dekker, G. P. C. M.; Buijs, A.; Elsevier, C. J.; Vrieze, K.; van Leeuwen, P. W. N. M.; Smeets, W. J. J.; Spek, A. L.; Wang, Y. F.; Stam, C. H. *Organometallics* **1992**, *11*, 1937. For N–N complexes see: (h) de Graaf, W.; Boersma, J. van Koten, G. *Organometallics* **1990**, *9*, 1479. (i) Markies, B. A.; Rietveld, M. H. P.; Boersma, J.; Spek, A. L.; van Koten, G. *J. Organomet. Chem.* **1992**, *424*, C12. (j) Rülke, R. E. Thesis, University of Amsterdam, Amsterdam, The Netherlands, 1995. (k) Brookhart, M.; Rix, F. C.; DeSimone, J. M. *J. Am. Chem. Soc.* **1992**, *114*, 5894. (l) van Asselt, R.; Gielens, E. E. C. G.; Rülke, R. E.; Elsevier, C. J. *J. Chem. Soc., Chem. Commun.* **1993**, 1203. (m) Markies, B. A.; Verkerk, K. A. N.; Rietveld, M. H. P.; Boersma, J.; Kooijman, H.; Spek, A. L.; van Koten, G. *ibid.* **1993**, 1317. Other ligands or mixed systems: (n) Anderson, G. K.; Lumetta, G. J. *Organometallics* **1985**, *4*, 1542. (o) Cavell, K. J.; Jin, H.; Skelton, B. W.; White, A. H. *J. Chem. Soc., Dalton Trans.* **1992**, 2923. (p) Cavell, K. J.; Jin, H.; Skelton, B. W.; White, A. H. *ibid.* **1993**, 1973. (q) Lindner, E.; Dettinger, J.; Fawzi, R.; Steimann, M. *Chem. Ber.* **1993**, *126*, 1347. (r) Reger, D. L.; Garza, D. G. *Organometallics* **1993**, *12*, 554.

(7) (a) Rülke, R. E.; Han, I. M.; Elsevier, C. J.; Vrieze, K.; van Leeuwen, P. W. N. M.; Roobeek, C. F.; Zoutberg, M. C.; Wang, Y. F.; Stam, C. H. *Inorg. Chim. Acta* **1990**, *169*, 5. (b) Wehman, P.; Rülke, R. E.; Kaasjager, V. E.; Kamer, P. C. J.; Koopman, H.; Spek, A. L.; Elsevier, C. J.; Vrieze, K.; van Leeuwen, P. W. N. M. *J. Chem. Soc., Chem. Commun.* **1995**, 331.

(8) Markies, B. A.; Wijkens, P.; Boersma, J.; Spek, A. L.; van Koten, G. *Recl. Trav. Chim. Pays-Bas* **1991**, *110*, 133.

(9) Markies, B. A.; Wijkens, P.; Kooijman, H.; Veldman, N.; Spek, A. L.; Boersma, J.; van Koten, G. *Organometallics* **1994**, *13*, 3244.

$COCD_3$ solution of the methyl and aryl complexes at room temperature. Decarbonylation of the CO-insertion products was carried out by bubbling nitrogen gas through the solution and/or heating the solution (up to 55 °C, *i.e.*, the boiling point of CD_3COCD_3).

The NN'N-coordinated methyl complex (**1a**) reacted at atmospheric pressure with CO in CD_3COCD_3 to give palladium metal, the quaternary ammonium salt [NN'(NH)]OTf, and acetic anhydride in 84% yield (calculated on **1a**) (eq 2). Acetic anhydride was also obtained when

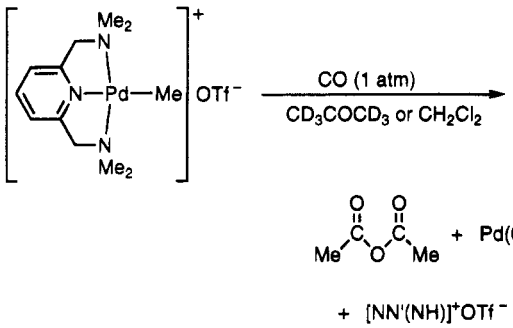

(2)

this reaction was carried out in methylene chloride that had been predried over calcium hydride. Apparently, the acetyl complex is extremely easily hydrolyzed by traces of water. In contrast, the pico- and pmdeta-coordinated methyl complexes (2a and 3a, respectively) gave the corresponding acetyl complexes (**5** and **6a**) as isolable solids, which were readily crystallized from methanol/diethyl ether without apparent methanolysis.

Most of the aryl complexes insert carbon monoxide at 1 atm to give the corresponding aroyl complexes (eq 1). Exceptions are the complexes containing 4-nitrophenyl (**1c**, **2d**, and **3d**) or 2,4,6-trimethylphenyl (mesityl, **1f**, **2e**, and **3e**) groups, which show only partial insertion at 1 atm, and the insertion products could not be isolated in pure form. The insertion equilibrium (eq 1) was shifted to the right by applying higher pressures (10–25 atm of CO) in a high-pressure NMR tube. In this way, ^1H and ^{13}C NMR spectra of the unstable products were obtained *in situ*, except for **4c,f**, which decomposed significantly during the ^{13}C NMR experiments, allowing only ^1H NMR spectra to be obtained. The benzoyl (**5b** and **6b**), and 4-methoxybenzoyl (**5c** and **6c**) complexes were purified by recrystallization from methanol/diethyl ether without apparent methanolysis. The 1-naphthoyl complex **4e** was successfully recrystallized from acetone/pentane under a CO atmosphere, and its solid state structure has been determined.

High-Pressure NMR Studies on the Insertion of Carbon Monoxide. We studied the insertion of carbon monoxide in CD_3COCD_3 solution at 10 atm of CO using a 10 mm high-pressure NMR tube[10] at 295 K. Under these conditions most of the complexes reacted completely to the corresponding acyl complexes within 2.5 min (the minimum time for the first spectrum to be obtained). The 4-nitrophenyl (**1c**, **2d**, and **3d**) and mesityl (**1f** and **2e**) complexes reacted much more slowly, but a reasonable to good conversion (79%–100%) was reached within 60 min. The mesityl complex **3e** did not react at all under these conditions (Table 2).

The methyl complex **1a** reacted within 2.5 min to give the same hydrolysis products as obtained at atmospheric pressure. Attempts to follow the deinsertion of the carbonylation products (obtained at 10 atm of CO) by ^1H NMR, after release of the pressure, failed because this process was very slow. Apparently, for the deinsertion to proceed at a reasonable rate, nitrogen gas needs to be bubbled through the solution. Attempted deinsertion by raising the temperature to 55 °C (the boiling point of CD_3COCD_3) also failed, since decomposition to palladium metal is faster than deinsertion under these conditions.

(10) Roe, D. C. *J. Magn. Reson.* **1985**, *63*, 388.

Table 2. Influence of the Aryl Group on CO Insertion Time

ligand	R	time (min)	conversion (%)[a]
NN'N	4-$O_2NC_6H_4$ (**1c**)	20	89
	mesityl[b] (**1f**)	45	100
pico	4-$O_2NC_6H_4$ (**2d**)	36	100
	mesityl[b] (**2e**)	60	79
pmdta	4-$O_2NC_6H_4$ (**3d**)	60	34
	mesityl[b] (**3e**)	60	0

[a] Conversion at 10 atm of CO and 296 K. [b] 2,4,6-Trimethylphen-1-yl.

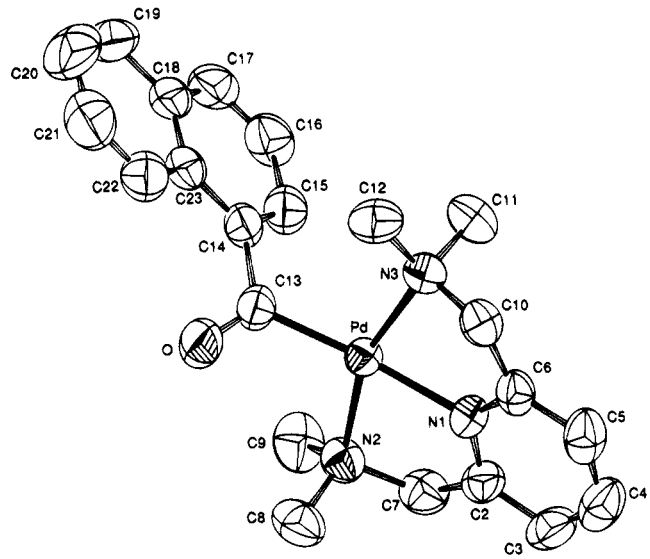

Figure 1. ORTEP representation (50% probability) of the cation $[Pd(COC_{10}H_7)(NN'N)]^+$ (**4e**).

Table 3. Selected Bond Distances (Å) and Angles (deg) of the Cation [Pd(1-naphthoyl)(NN'N)]⁺ (4e)

Pd–N(1)	2.042(4)	Pd–C(13)	1.966(6)
Pd–N(2)	2.120(5)	C(13)–O	1.205(9)
Pd–N(3)	2.118(5)	C(13)–C(14)	1.509(10)
N(1)–Pd–N(2)	80.6(2)	N(3)–Pd–C(13)	100.7(2)
N(1)–Pd–N(3)	79.3(2)	Pd–C(13)–O	119.0(5)
N(1)–Pd–C(13)	172.4(3)	Pd–C(13)–C(14)	120.8(5)
N(2)–Pd–N(3)	159.7(2)	O–C(13)–C(14)	120.3(6)
N(2)–Pd–C(13)	99.6(2)		

Molecular Structure of the Cation [Pd(1-naphthoyl)(NN'N)]⁺ (4e). The molecular structure of this cation is shown in Figure 1 with relevant bond distances and angles presented in Table 3. This structure is the first example of an aroylpalladium(II) cation.

In this square planar palladium(II) complex the 1-naphthoyl group is bonded *via* the carbonyl carbon atom in a position trans to the pyridine nitrogen atom N(1). The nitrogen atoms of the CH_2NMe_2 groups, N(2) and N(3), are bonded mutually trans, forming two fixed PdNCCN(1) five-membered chelate rings. These two chelate rings are puckered with an angle of 15.2(3)° between the mean planes through N1, N2, N3, and C13

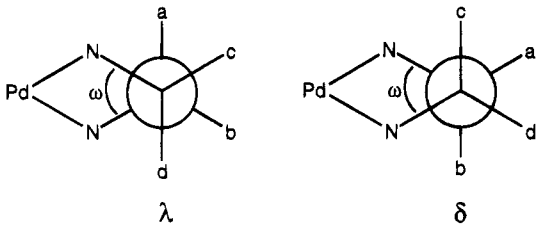

Figure 2. Newman projections of the λ and δ conformations of a five-membered diamine chelate ring.

and the pyridine moiety. The Pd–N(1) bond distance (2.042(4) Å) is short in comparison with the Pd–N(pyridyl) bond distance (2.131(4) Å) trans to the methyl group in [PdMe(2,2′-bipyridyl)(γ-picoline)]BF_4.[11] The short Pd–N(1) bond is accompanied by a small N(2)–Pd–N(3) angle (159.67(19)°). Similar features are present in the related complexes [PdMe(NN′N)]OTf,[9] [PdCl(pico)]Cl,[9] [PdX(2,2′:6,2″-terpyridyl)]Cl·$2H_2O$ (X = Cl[12a] or Me[7]), [Pd(OH)(2,2′:6,2″-terpyridyl)]ClO_4·H_2O,[12b] and [PdCl{2,6-bis(2-imidazolin-2-yl)pyridine}]Cl.[12c] Apparently, the tridentate ligand in these complexes is unable to accommodate a perfect square planar geometry. The Pd–C bond distance in **4e** (1.966(6) Å) is close to other reported Pd–C(acyl) bond distances.[13,14] The carbonyl group of the 1-naphthoyl ligand has a normal Pd–C(13)–O angle (119.0(5)°) and must hence be η^1-bonded to palladium; this angle is much smaller for an η^2-bonded carbonyl group.[15]

Solution Properties of the CO Insertion Products. The ^{1}H NMR resonances of the methylene protons of the pico ligand show well-defined multiplet (td) patterns at *ca.* 3.5 ppm and, in most cases, a poorly resolved ddd pattern at higher field. The patterns for these protons of the pmdeta ligand were much more complex, due to the small differences in chemical shift, but could still be analyzed by computer simulation. These patterns were used to determine the conformations of the NCH_2CH_2N chelate rings of the pico and pmdeta complexes as reported for the chloro, methyl, and aryl complexes of these ligands.[6b,c] The pico and pmdeta complexes all prefer the δ[17] or $\delta\delta$ conformation (Figure 2), respectively.

The $\delta\delta$ conformation of the pmdeta ligand is defined here with respect to the view of the complexes as depicted below.

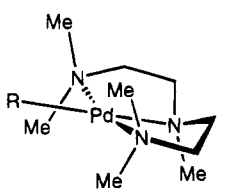

The analysis could not be carried out for [Pd(COMe)(pmdeta)]OTf (**6a**) due to fluxionality of this complex (*vide infra*).

Scheme 1

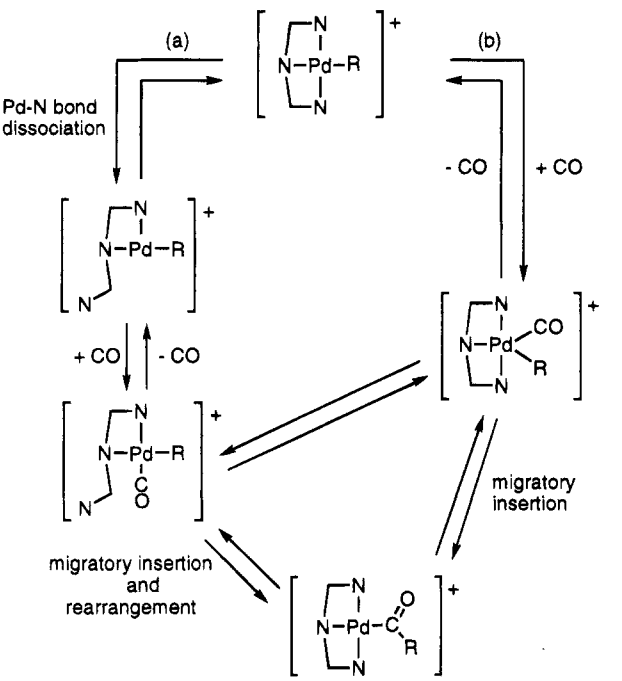

The NMR spectra of the CO insertion products of the NN′N ligand (**4b–f**) showed in all cases well-defined resonances, with singlets for the CH_2 and NMe_2 groups, indicating that rotation around the Pd–C_{CO} and C_{CO}–C_{aryl} bonds is not hindered at ambient temperature (hindered rotation around the Pd–C_{ipso} bond in arylpalladium NN′N complexes was found earlier[9]). The NMR spectra of the acetyl and aroyl pico (**5a–c**) and the aroyl pmdeta complexes (**6b,c**) also did not indicate hindered rotation, except for [Pd(COMe)(pmdeta)]OTf (**6a**). The resonances of the CH_2CH_2 moieties of **6a** are relatively broad at ambient temperature, become sharper on lowering the temperature to ≈271 K, and broaden again upon further lowering of the temperature.

***Ab Initio* Calculations of the Insertion Process.** To get some insight into the mechanism of the CO insertion process, we have carried out *ab initio* calculations on the cationic model system $[Pd(CH_3)(NH_3)_3]^+$ + CO. This model closely resembles the actual complexes and still allows reasonable geometry optimization calculations. Solvent effects were not incorporated at this stage, and thus the calculations should be viewed as providing information on the *intrinsic* ability of such cationic systems to follow a specific pathway. Our working hypothesis for the mechanism of the insertion reaction is outlined in Scheme 1.

(11) Byers, P. K.; Canty, A. J.; Skelton, B. W.; White, A. H. *J. Organomet. Chem.* **1987**, *336*, C55.

(12) (a) Intille, G. M.; Pfluger, C. E.; Baker, W. A., Jr. *J. Cryst. Mol. Struct.* **1973**, *3*, 47. (b) Castan, P.; Dahan, F.; Wimmer, S.; Wimmer, F. L. *J. Chem. Soc., Dalton Trans.* **1990**, 2679. (c) Baker, A. T.; Craig, D. C.; Singh, P. *Aust. J. Chem.* **1991**, *44*, 1659.

(13) (a) Fayos, J.; Dobrzynski, E.; Angelici, R. J.; Clardy, J. *J. Organomet. Chem.* **1973**, *59*, C33. (b) Bardi, R.; Piazessi, A. M.; Cavinato, G.; Cavoli, P.; Toniolo, L. *J. Organomet. Chem.* **1982**, *224*, 407. See also refs 3m and 4l.

(14) The structures of PdCl(COMe)(L_2), with L_2 = 2-(isopropylcarbaldimino)pyridine or 2,2′-bipyridyl, have been solved only recently and have Pd–C(acyl) bond distances of 1.964(5) and 1.94(1) Å, respectively. Rülke, R. E.; Elsevier, C. J.; Vrieze, K. Unpublished results.

(15) For a review on η^2-acyl coordination see: Durfee, L. D.; Rothwell, I. P. *Chem. Rev.* **1988**, *88*, 1059.

(16) (a) Sudmeier, J. L.; Blackmer, G. L. *Inorg. Chem.* **1971**, *10*, 2010. (b) Hawkins, C. J.; Peachey, R. M. *Aust. J. Chem.* **1976**, *29*, 33. (c) Hambley, T. W.; Hawkins, C. J.; Martin, J.; Palmer, J. A.; Snow, M. R. *Aust. J. Chem.* **1981**, *34*, 2505. (c) Hawkins, C. J.; Palmer, J. A. *Coord. Chem. Rev.* **1982**, *44*, 1.

(17) The central NMe group of the pico complexes is chiral, and these complexes are obtained as a 1:1 mixture of enantiomers, with the enantiomer containing the *S* configuration showing the δ conformation. Because the two enantiomers have a reversed preference for the conformation of the NCCN chelate rings, the enantiomer with the *R* configuration for the NMe group will show the λ conformation.

Scheme 2

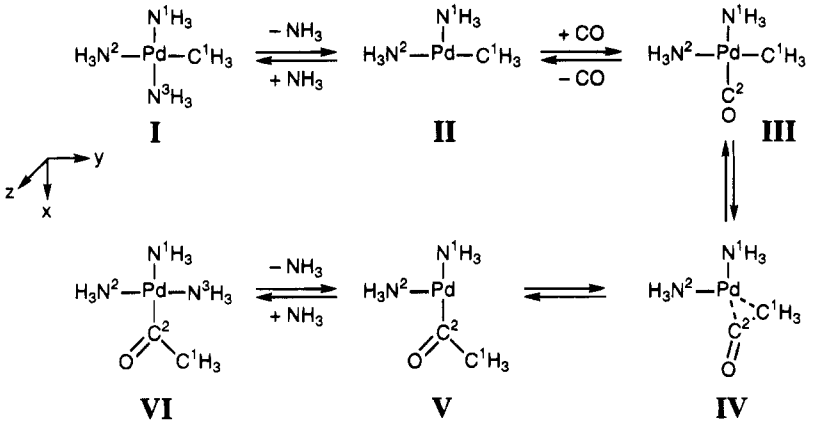

Scheme 3

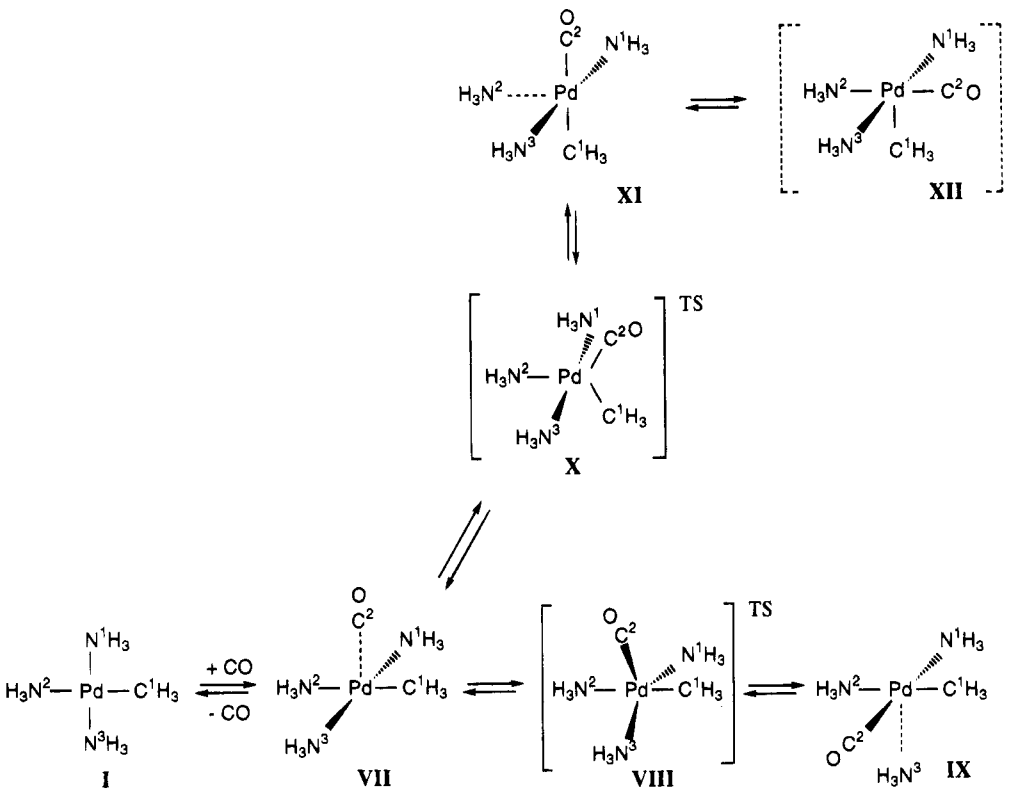

Two main routes could be considered *a priori*: a purely dissociative one, a, in which one amine arm dissociates prior to CO coordination; and a purely associative one, b, in which CO coordinates first and the migratory insertion occurs from a five-coordinate *intermediate*. This d^8 intermediate could have a trigonal bipyramidal structure, as drawn here, but another likely alternative is a square pyramid. We could not exclude, following the work of Garrou and Heck,[3c] a third possibility in which these two routes are linked at a five-coordinate structure $[Pd(NH_3)_3(CH_3)(CO)]^+$. The dissociation of one amine ligand from this structure could then lead to the four-coordinate carbonyl complex of the dissociative route. Note, however, that, at variance with Garrou and Heck, we do not make any assumption in this case as to whether this five-coordinate structure is an intermediate or a transition state.

In order to discriminate between these various possibilities we first optimized the structures **I**–**XI** at the SCF level. Electron-correlation effects were then taken into account by performing MP2 calculations on these SCF-optimized structures (hereafter denoted MP2// SCF). Structures **I**–**VI** are involved in the dissociative route (Scheme 2), **IV** being the transition state for the CO insertion step. Structures **VII**–**XI** (Scheme 3) pertain to the two other routes. It is important to note here that **VIII** and **X** are found to be transition states and not intermediates on the potential-energy hypersurface of the $\{[Pd(CH_3)(NH_3)_3]^+ + CO\}$ composite system. The bond distances and angles are collected in Table 4, and the relative SCF and MP2 energies are given in Table 5.

In addition to and in order to check the validity of the MP2 calculations, CAS–SCF and CAS–SCF/CI calculations were carried out for the NH_3 dissociation step on the structures **I** and **II**···NH_3 (Pd···NH_3 = 100 Å, Table 6) and on the structures **III** and **V** of the CO insertion step (Table 7).

Table 4. Calculated Bond Distances and Angles of Structures I–XIII

	Bond Distances (Å)						
structure	Pd–N^1	Pd–N^2	Pd–N^3	Pd–C^1	Pd–C^2	C^1–C^2	C^2–O
I	2.184	2.275	2.182	2.048			
II	2.247	2.253		1.995			
III	2.182	2.265		2.056	2.106		1.125
IV	2.214	2.248		2.436	1.888	1.897	1.153
V	2.241	2.252			1.962	1.521	1.193
VI	2.235	2.180	2.167		2.054	1.521	1.224
VII	2.183	2.266	2.187	2.047	3.371		1.133
VIII	2.316	2.269	2.539	2.019	2.399		1.129
IX	2.216	2.268	2.841	2.049	2.128		1.126
X	2.175	2.870	2.175	2.044	2.732		1.130
XI	2.198	3.181	2.198	2.032	2.250		1.128
XIII	2.215	2.278	2.782	2.419	1.884	1.929	1.154

	Bond Angles (deg)					
structure	N^1–Pd–N^2	N^1–Pd–C^1	N^1–Pd–N^3	N^2–Pd–C^1	N^2–Pd–N^3	N^3–Pd–C^1
I	92.14	87.83	175.48	178.07	91.80	88.16
II	98.02	89.31		172.64		
III	92.59	87.69		178.37		
IV	95.73	111.67		152.60		
V	99.88					
VI	90.32		90.47		179.12	
VII	91.87	88.13	176.08	179.47	91.83	88.15
VIII	90.81	89.78	125.00	179.41	89.53	90.13
IX	92.29	87.96	93.00	177.51	87.60	94.86
X	92.16	88.57	175.67	131.26	92.17	88.57
XI	93.75	88.74	172.50	109.68	93.75	88.74
XIII	95.32	110.54	92.06	153.19	92.03	93.93

	Bond Angles (deg)					
intermediate	C^1–Pd–C^2	N^1–Pd–C^2	N^2–Pd–C^2	N^3–Pd–C^2	Pd–C^2–O	Pd–C^2–C^1
I						
II						
III	85.62		94.04	173.00	179.97	
IV	50.10	161.77	102.50		157.28	80.11
V		171.34	88.78		127.77	103.25
VI		176.73	92.90	86.32	117.25	123.68
VII	92.01	89.56	87.46	89.30	184.85	
VIII	90.18	144.29	89.34	90.71	179.32	
IX	85.79	169.30	93.59	96.17	178.61	
X	155.22	90.61	73.51	90.62	177.33	
XI	180.74	91.31	69.58	91.31	174.03	
XIII	51.45	161.94	102.40	90.82	159.51	78.73

Table 5. Calculated SCF and MP2 Energies (kcal mol^{-1}) of Structures I–XIII[a]

structure	energy	structure	RHF
I	0	**VII**	−3.1 (−5.6)
II	35.0 (42.2)	**VIII**	6.0 (1.7)
III	14.2 (7.0)	**IX**	4.1 (−4.6)
IV	41.2 (25.8)	**X**	8.1
V	15.8 (12.7)	**XI**	4.8
VI	−16.1 (−16.1)	**XIII**	23.5 (16.3)

[a] All energies are relative to the energy of intermediate I + CO. MP2//SCF values are in parentheses.

Table 6. Comparison of the Energy Differences (kcal mol^{-1}) between Structures I and II (Scheme 2) as a Function of the Calculational Method

method	ΔE	method	ΔE
RHF	35.0	CAS–SCF	30.0
MP2	42.2	SD–CI+Q	31.9

Discussion

Carbonylation of Organopalladium(II) Cations and NMR Studies. The insertion of carbon monoxide into the palladium–carbon bond of the complexes bearing tridentate ligands occurs easily. Most of the insertion products are much more stable toward decarbonylation than the acylpalladium(II) complexes of mono- or bidentate ligands. The reaction is reversible under forcing conditions and can, in most cases, be repeated several times at room temperature without significant loss of the parent complex involved.

Table 7. Dependency of the Relative Energy Values (kcal mol^{-1}) of the Process II → III → IV on the Calculational Method and the Type of Complex

method	reactant	TS	product
RHF	0.0	27.0	1.6
MP2	0.0	18.8	5.7
CAS–SCF	0.0		6.2
SD–CI	0.0		1.2
SD–CI+Q	0.0		−1.4

For most of the complexes carbonylation is complete within 2.5 min at 10 atm of CO in CD_3COCD_3. Only the complexes with a mesityl (**1f** and **2,3e**) or a 4-nitrophenyl group (**1c** and **2,3d**) react slower, and some of these do not even fully carbonylate under these conditions. The carbonylation under high CO pressure is much faster than our earlier reported results at atmospheric pressure, *i.e.*, under the latter conditions the complex [PdPh(NN'N)]OTf (**1b**) reacts about 6 times faster with CO (30 min) than the 1-naphthyl analog **1e** (3 h).[8] These differences were attributed to the larger bulk of the 1-naphthyl group with respect to the phenyl group. The fast insertion under high CO pressure is a

Scheme 4

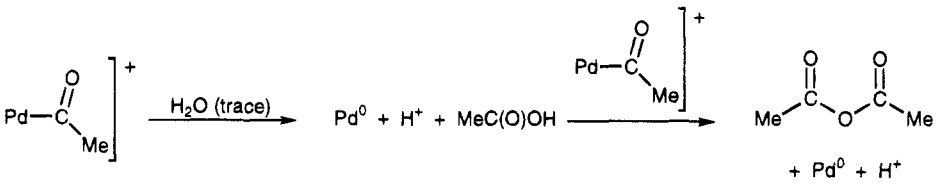

Scheme 5

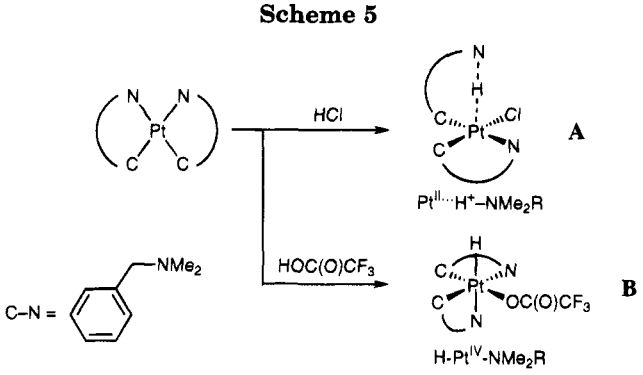

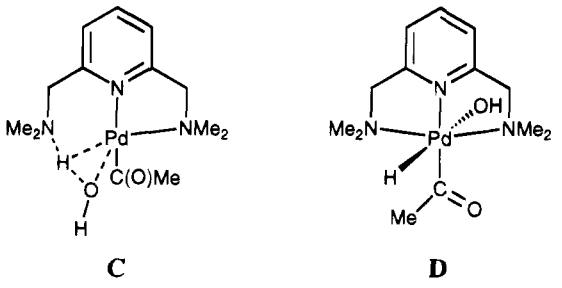

consequence of the higher CO concentration in solution, but the mixing of CO into the solution is a limiting factor. This is supported by an experiment in which [PdPh(NN'N)]OTf (**1b**) was added in one portion as a solid to an acetone solution saturated with CO at 1 atm. This resulted in instantaneous CO insertion. The conversion times given in Table 2 therefore do not have more than a qualitative value.

The stability of the CO inserted products depends on the nature of the tridentate ligand. Whereas all three ligands give aroyl complexes that can be characterized and in most cases isolated as stable solids, only the pmdeta and pico lignds allow isolation of their acetyl complexes. The surprising formation of acetic anhydride upon the CO insertion in [PdMe(NN'N)]OTf (**1a**, eq 2) is probably due to the presence of trace amounts of water in the solvent (CD_3COCD_3 or methylene chloride). A possible reaction path to acetic anhydride is presented in Scheme 4. It is based on the intermediacy of an acetylpalladium species, and it is proposed that the acetic anhydride is formed by attack of acetic acid on this acetyl intermediate.

The conversion of the acyl group into acetic acid can be rationalized on the basis of our earlier observation of tautomeric products **A** and **B** in the protonation of bis-*C,N*-chelated platinum complexes (Scheme 5).[18]

We presume that in the present case the water acts as a nucleophile leading to the tautomeric structures **C** [Pd^{II}(acyl)(water)] and/or **D** [Pd^{IV}(acyl)(hydride)(hydroxyl)].

Although the linear N–H···Pt arrangement in **A** cannot be attained by **C**, the similarity is evident. The formation of **D** requires only a small geometrical change of the N, H, and OH ligands in **C** to give formally a palladium(IV) center, *i.e.*, an oxidative addition of water to palladium(II). The C–OH bond may then be formed by a reductive elimination from **D** or a nucleophilic addition (intramolecularly or by a second water molecule assisted by the Pd–OH bond). To our knowledge, there are very few examples of reactions of palladium complexes with water, probably due to the low polarizability of the Pd–C bond.[19] Because of the higher electrophilicity of palladium(II) cations, reaction with water may be more facile. The difference in this respect between the NN'N complex and the pico/pmdeta complexes is not yet understood.

***Ab Initio* Studies on the Carbonylation Mechanism.** A look at the Table 4 indicates that most of the calculated bond distances and bond angles are within reasonable range of those obtained from X-ray molecular structures for similar systems.[20] Also the geometry of the transition state **IV** is quite close to the one reported by Koga and Morokuma[2e] for the CO insertion into the Pd–CH_3 bond of the neutral [$Pd(PH_3)(H)(CH_3)(CO)$] system despite the use of a different basis set. (In fact, pilot calculations which we carried out on the reaction **III** → **IV** → **V** indicated that the corresponding geometries are not very sensitive to the quality of the basis set.) The most noticeable exceptions are for the apical bonds of the intermediates with five surrounding groups, **VII** (Pd–C^2 = 3.371Å), **IX** (Pd–N^3 = 2.841Å), and **XI** (Pd–N^2 = 3.181Å). Thus these intermediates had rather be viewed as square planar Pd complexes weakly interacting with a fifth moiety. The interaction is particularly weak for **VII**, which is computed at the SCF level to be more stable than **I** + CO by only 3.1 kcal mol^{-1}. The MP2 calculations increase this stabilization to 5.6 kcal mol^{-1} (SCF-optimized geometry), but one should subtract from this value the basis set superposition error which is estimated (at the SCF level using

(18) (a) Wehman-Ooyevaar, I. C. M.; Grove, D. M.; van der Sluis, P.; Spek, A. L.; van Koten, G. *J. Chem. Soc., Chem. Commun.* **1990**, 1367. (b) Wehman-Ooyevaar, I. C. M.; Grove, D. M.; Kooijman, H.; van der Sluis, P.; Spek, A. L.; van Koten, G. *J. Am. Chem. Soc.* **1992**, *114*, 9916. (c) Wehman-Ooyevaar, I. C. M.; Grove, D. M.; de Vaal, P.; Dedieu, A.; van Koten, G. *Inorg. Chem.* **1992**, *31*, 5484. (d) Pregosin, P. S.; Rüegger, H.; Wombacher, F.; van Koten, G.; Grove, D. M.; Wehman-Ooyevaar, I. C. M. *Magn. Reson. Chem.* **1992**, *30*, 548.

(19) See for example: (a) Vicente, J.; Abad, J.-A.; Gil-Rubio, J.; Jones, P. G.; Bembenek, E. *Organometallics* **1993**, *12*, 4151. (b) Canty, A. J.; Honeyman, R. T.; Roberts, A. S.; Traill, P. R.; Colton, R.; Skelton, B. W.; White, A. H. *J. Organomet. Chem.* **1994**, *471*, C8. (c) Valk, J. M.; van Belzen, R.; Kooijman, H.; Spek, A. L.; Boersma, J.; van Koten, G. Manuscript in preparation.

(20) (a) de Graaf, W.; Harder, S.; Boersma, J.; van Koten, G.; Kanters, J. A. *J. Organomet. Chem.* **1988**, *358*, 545. (b) de Graaf, W.; Boersma, J.; Smeets, W. J. J.; Spek, A. L.; van Koten, G. *Organometallics* **1989**, *8*, 2907. (c) Alsters, P. L.; Baesjou, P. J.; Janssen, M. D.; Kooijman, H.; Sicherer-Roetman, A.; Spek, A. L.; van Koten, G. *Organometallics* **1992**, *11*, 4124. (d) Alsters, P. L.; Boersma, J.; Smeets, W. J. J.; Spek, A. L.; van Koten, G. *Organometallics* **1993**, *12*, 1639. (e) Alsters, P. L.; Engel, P. F.; Hogerheide, M. P.; Copijn, M.; Spek, A. L.; van Koten, G. *Organometallics* **1993**, *12*, 1831. (f) Markies, B. A.; Canty, A. J.; de Graaf, W.; Boersma, J.; Janssen, M. D.; Hogerheide, M. P.; Smeets, W. J. J.; Spek, A. L.; van Koten, G. *J. Organomet. Chem.* **1994**, *482*, 191.

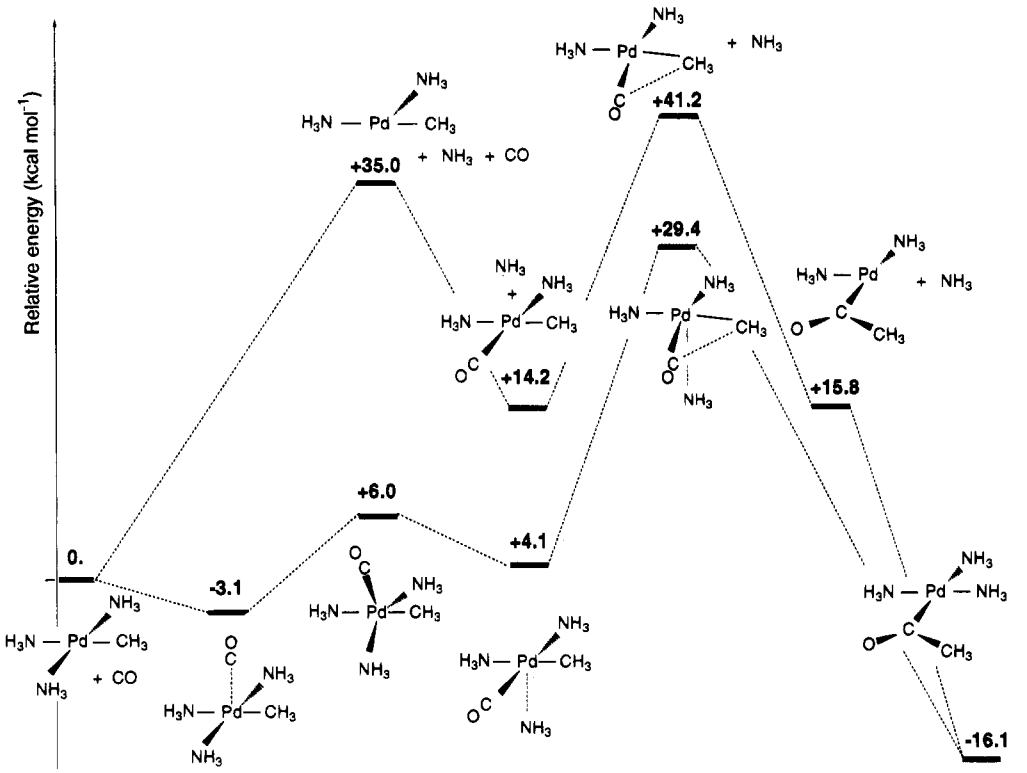

Figure 3. Energy profiles (SCF level) of the cationic system.

the counterpoise method) to be 4.6 kcal mol^{-1}. In **IX**, the stabilization of $[Pd(NH_3)_2(CH_3)(CO)]^+$ by the association with NH_3 is somewhat larger: 10.1 kcal mol^{-1} at the SCF level and 11.6 kcal mol^{-1} at the MP2//SCF level. It should not be offset by the basis set superposition error which we estimate to be less than 6–7 kcal mol^{-1}.[21] In line with these results one gets a shorter apical bond length in **IX**, see Table 4. Like in the naked $Pd(NH_3)$ system recently computed by Blomberg *et al.*,[22] the interaction energy may involve an electron nuclear attraction between the lone pair and the palladium core. It may also be simply the result of some electrostatic attraction between the dipole of the NH_3 molecule and the positive charge of the cationic $[Pd(NH_3)_2(CH_3)(CO)]^+$ entity.

It should be stressed here that the optimization procedures never led to trigonal bipyramidal (TBP) intermediates. Distorted TBP structures, **VIII** and **X**, were instead found and characterized as *transition states* for NH_3 substitution by CO. In these structures the N^1–Pd–N^3 angle is close to 180°, but the angle between the CO incoming group and the NH_3 leaving group is much smaller than 120°. A similar feature has been already recognized by Lin and Hall in square planar Pt(II) and Rh(I) substitution reactions, and they ascribe it to the minimization of the repulsion between the electron concentration on the central atom and the electron concentration on the entering and leaving ligands.[23] In both cases the angle between CO and the spectator equatorial ligand (either NH_3 or CH_3) is quite large (144° in **VIII** and 155° in **X**). This reflects the late nature of these two transition states, *i.e.*, they are product-like, as expected from the endothermicity computed for the NH_3 substitution by CO (*vide infra*). Finally the larger trans influence of CH_3 compared to NH_3 is best seen in the comparison of the lengths of the equatorial Pd–NH_3 bond that is trans either to NH_3 (2.539 Å in **VIII**) or to CH_3 (2.870 Å in **X**).

Thus it seems from these results that, at least in the gas phase, a purely associative pathway (*i.e.*, involving intermediates with five ligands *firmly* attached to the central atom and in which the CO insertion step takes place) can be ruled out for the cationic palladium complexes. Another possible candidate for a five-coordinate intermediate, *i.e.*, **XII**, is not a local minimum since its optimization led directly to **XI**.

We are therefore left with two alternative pathways for the carbonylation process: either a dissociative pathway involving the three coordinate $[Pd(NH_3)_2(CH_3)]^+$ system as a key intermediate or a hybrid pathway where the associative nature of the mechanism is essentially limited to the amine substitution step. The two corresponding energy profiles are shown in Figure 3 (SCF values).

The MP2 calculations lead to overall conclusions that are similar to the ones obtained at the SCF level (*vide infra*), and we will therefore base our discussion mostly on the SCF values.

Dissociative Pathway. The formation of the transition state **IV** (+41.2 kcal mol^{-1}, SCF value) appears to be the rate-determining step and not the dissociation of NH_3 from the initial $[Pd(NH_3)_3(CH_3)]^+$ cation (+35 kcal mol^{-1}, SCF value), whatever the level of calculation is, see the Tables 6 and 7. It should be noted that the MP2 calculations overestimate the binding of NH_3: the NH_3 bond dissociation energy increases from 35 to 42.2 kcal mol^{-1}, whereas CAS–SCF/CI calculations lead to a slight decrease from 35 to 31.9 kcal mol^{-1}. The

(21) A counterpoise calculation carried out for a similar geometry but with the two NH_3 ligands trans to each other and a Pd–N_{axial} bond length of 2.48 Å yielded a basis set superposition error of 6.7 kcal mol^{-1}. The longer Pd–N_{axial} bond in **IX** (2.84 Å) should lead to a smaller error.

(22) Blomberg, M. R. A.; Siegbahn, P. E. M.; Svensson, M. *Inorg. Chem.* **1993**, *32*, 4218.

(23) Lin, Z.; Hall, M. B. *Inorg. Chem.* **1991**, *30*, 646.

thermodynamics of the insertion step is also less favorable at the MP2 level (+5.7 kcal mol^{-1}) than at the CAS–SCF level (−1.4 kcal mol^{-1}). This corresponds to the result that we obtained some years ago for the model reaction $[Pd(H)(CO)]^+ \rightarrow [Pd(CHO)]^+$.[3h] In contrast, the inclusion of correlation leads to a decrease of the energy barrier between **III** and **IV**: the MP2 value is 18.8 kcal mol^{-1}. CAS–SCF/CI calculations are expected to give a value similar to the MP2 value: pilot calculations which were carried out for a structure quite close to the transition state yielded MP2 and CAS–SCF/CI values differing by only 0.5 kcal mol^{-1}.[24] Thus the decrease of the energy barrier obtained at the MP2 level is probably meaningful.

Since **IV** is coordinatively unsaturated, one may wonder whether a η^2 structure might be more stable. We find such a structure, see **V'**, as a local minimum.

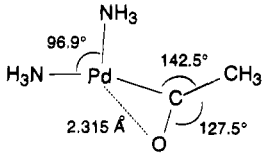

V'

However, the Pd–O bond distance of 2.315 Å points to a rather weak Pd–O interaction. Moreover, **V'** is found to be more stable than **V** by only 2.6 kcal mol^{-1} at the SCF level and *destablized* by 0.4 kcal mol^{-1} at the MP2 level. Thus the recombination of the dissociated amine to yield the final four-coordinate acyl product is energetically favored.

Hybrid Pathway. The high energy required for the dissociation of NH_3 from $[Pd(NH_3)_3(CH_3)]^+$ makes a purely dissociative pathway rather unlikely. In fact the NH_3 substitution by CO turns out to be easier when going through the five-coordinate *transition state* **VIII**. The energy barrier from **I** + CO is computed to be 6.0 kcal mol^{-1} only at the SCF level. MP2 calculations even lower this value to 1.7 kcal/mol. The MP2 value may be too low owing to some overestimation of the metal–carbonyl bond energy.[25,26] In **VIII**, the NH_3 ligand cis to CH_3 is slightly elongated (by 0.36 Å) and the N^1–Pd–N^3 angle amounts to 125°. The tridendate nitrogen donor ligands should be able to achieve this arrangement: we note that in the crystal structures of [Pd(Me)(NN'N)]$^+$,[9] $[Pd(COC_{10}H_7)(NN'N)]^+$, and $[Pd(C_6H_4\text{-}o\text{-}C_7H_{11})(pmdeta)]^+$,[27] the N^1–Pd–N^3 angle is much smaller than 180°, ranging from 159.7 to 165.5°. These systems are therefore deformed in the right direction, and the substitution step should likely proceed through a transition state analogous to **VIII**. Another transition state for the CO/NH_3 substitution might be **X**, but this one is slightly higher in energy than **VIII** (by 2.1 kcal mol^{-1}). Moreover, the nitrogen atom which is pushed away from the metal in this transition state is the one corresponding to the central atom of the tridentate ligands that evidently cannot dissociate in the actual system.

We have already mentioned that before and after the transition state there might be some stabilization of the four-coordinate intermediates by the incoming CO and the leaving NH_3, respectively. However, the stabilization by CO, if any, is very weak (*vide supra*). The stabilization by NH_3 is greater. Interestingly too, the presence of NH_3 in the vicinity of the Pd coordination sphere also stabilizes the transition state of the insertion step through a loose association, see **XIII**.

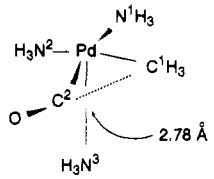

XIII

The barrier for the insertion in the presence of ammonia is computed to be 23.5 kcal mol^{-1} at the SCF level. Electron correlation again lowers this barrier, bringing it down to 16.3 kcal mol^{-1} at the MP2 level. The stabilization of the transition state is slightly greater than the stabilization of the four-coordinate carbonyl complex (at both SCF and MP2//SCF levels). Although this differential effect is quite small, it is corroborated by the change in the Pd–NH_3 distance, 2.78 vs. 2.84 Å. The effect might be greater with a ligand that is more basic than NH_3, such as the tertiary amine end of the pico or pmdeta terdentate ligands, thus providing some sort of nucleophilic catalysis for the insertion. Alternatively acetone, which is a coordinating solvent, might provide the same type of catalysis. The fact that nucleophiles can catalyze the formation of coordinatively unsaturated acyl intermediates has been already recognized experimentally for the CO insertion in some manganese aryl complexes.[28] The strong exothermicity computed for the formation of the four-coordinate acyl product and the presence of the dissociated amine in the vicinity of the coordination sphere might well drive the system directly to this final acyl product, as depicted in Figure 3.[29]

Comparison with the Neutral System. In order to shed some more light on the comparison between the ionic and the neutral system, similar calculations were performed on the neutral {*trans*-$[Pd(NH_3)_2(CH_3)_2]$ + CO} system, obtained by replacing the NH_3 ligand trans to the migrating methyl by a CH_3 group. The corresponding results are summarized in Figure 4 (SCF values only, the MP2//SCF calculations yielding again the same overall conclusions).

As for the cationic system the dissociative pathway is not favored. Instead, the NH_3 substitution by CO takes place associatively and the five-coordinate transition state lies 7 kcal mol^{-1} above the reactants (MP2 calculations lower this value down to 2.9 kcal mol^{-1}). In contrast to the ionic system, the five-coordinate equilibrium structures which have either CO or NH_3

(24) This structure was obtained by using the C_{Me}–C_{CO} distance as a reaction coordinate carrying out a gradient optimization for discrete points of this reaction coordinate and then performing a quadratic interpolation of the energies of the corresponding geometries. The structure obtained through this procedure was found to be quite similar to the transition state structure except for the Pd–C_{Me} bond length, which was too short by 0.15 Å.

(25) Rohlfing, C.; Hay, P. J. *J. Chem. Phys.* **1985**, *83*, 4641.

(26) Ehlers, A. W.; Frenking, G. *J. Am. Chem. Soc.* **1994**, *116*, 1514.

(27) Markies, B. A.; Wijkens, P.; Kooijman, H.; Spek, A. L.; Boersma, J.; van Koten, G. *J. Chem. Soc., Chem. Commun.* **1992**, 1420.

(28) Webb, S. L.; Giandomenico, C. M.; Halpern, J. *J. Am. Chem. Soc.* **1986**, *108*, 345.

(29) In that sense the reaction profile would look like the reaction profile expected for the associative mechanism. The difference here is that at least one ligand (either CO or NH_3) stays quite distant from the metallic center.

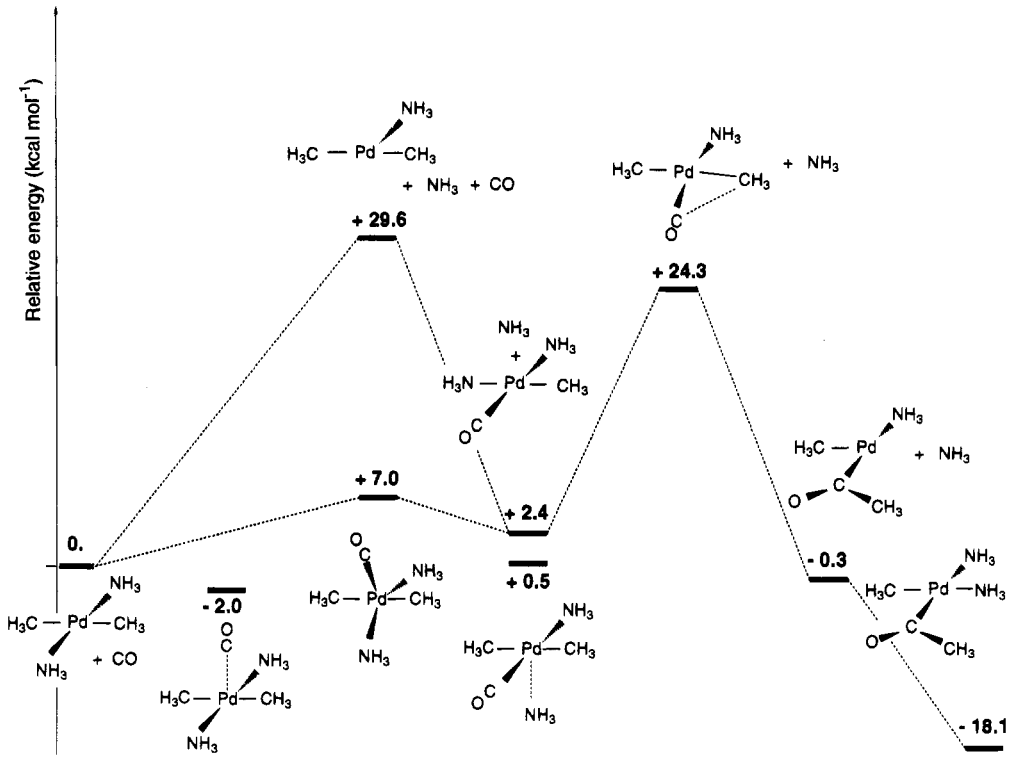

Figure 4. Energy profiles (SCF level) of the neutral system.

loosely bound at the apex of the square pyramid are hardly stabilized with respect to their dissociated counterparts, the interaction energy being only 2 kcal mol^{-1}. The Pd···CO and Pd···NH_3 distances (3.36 and 3.11 Å, respectively) are also much larger than in the ionic case. Thus these structures are most likely artefacts of the basis set superposition error and do not correspond to actual intermediates in the substitution process.

We were also unable to find an equilibrium structure for a transition state which has the NH_3 ligand in the vicinity of the coordination sphere. The optimized transition state corresponds therefore to the reaction taking place in the square planar $[Pd(NH_3)(CH_3)_2(CO)]$ complex. The associated barrier is computed to be 21.9 kcal mol^{-1} at the SCF level and 15.6 kcal mol^{-1} at the MP2//SCF level, *i.e.*, slightly lower at both levels than the barrier in the $[Pd(NH_3)_2(CH_3)(CO)]^+$ ionic system. Moreover, both the insertion step and the overall process are more exothermic in the neutral system. Thus the greater reactivity of the cationic systems which is observed experimentally,[6d,g] does not seem to be an intrinsic property of the cationic character, at least in the gas phase. The lowering of the energy barrier might well result from a difference in the trans influence of the ligand sitting trans to the migrating group: the neutral system mentioned above has a trans CH_3 group instead of the trans NH_3 ligand present in the cationic system. To test this hypothesis we have also determined the energy barrier for the insertion process in the $[Pd(Cl)(NH_3)(CH_3)(CO)]$ system with the chlorine ligand either cis or trans to the CH_3 migrating group. As seen from Table 8 the energy barrier in this neutral system is greater than the barrier in the cationic $[Pd(NH_3)_2(CH_3)(CO)]^+$ system.

Finally one should not overlook differential solvation effects. Solvation effects might be greater for the cationic system than for the neutral one. In particular, a coordinating solvent such as acetone with its oxygen lone pair might catalyze more efficiently the insertion step in the cationic system. Calculations are presently under way to test this hypothesis.

Table 8. Energy Barrier (MP2//SCF Value, in kcal mol^{-1}) for the CO Insertion into the Pd–CH_3 Bond of Various Cationic and Neutral Square Planar Complexes

system	$\Delta E^{\ddagger}_{insertion}$
$H_3N-Pd(NH_3)(CO)-CH_3]^+$	18.8
$H_3C-Pd(NH_3)(CO)-CH_3$	15.4
$Cl-Pd(NH_3)(CO)-CH_3$	21.2
$H_3N-Pd(Cl)(CO)-CH_3$	22.3

Direct Insertion of CO. It has been suggested from calculations carried out on the $PdCH_3$ + CO system that CO might well insert directly into the Pd–C bond without prior coordination to the palladium center.[3m] We do not find any transition state corresponding to this behavior in our calculations. Structure **X**, which has the CO and CH_3 ligands cis to each other, is not a transition state for a direct CO insertion, according to both its geometry (the C^1–Pd–C^2 angle is quite obtuse) and the eigenvector corresponding to the negative eigenvalue of the Hessian matrix, but is instead the transition state between **VII** and **XI**. Moreover, an attempt to locate a transition state corresponding to the

direct insertion resulted in a structure with a coordinated acetyl ligand lying perpendicularly to the $Pd-N_3$ plane. This structure, which lies 6.1 kcal mol^{-1} (SCF value) above **VI**, is therefore the transition state for the rotation of the acetyl ligand. Thus the perpendicular disposition of the aroyl ligand in Figure 1 should be traced to steric rather than to electronic requirements.

Concluding Remarks

We have shown that acetyl and aroyl cations containing the tridentate nitrogen-donor ligands *N*-(2-picolyl)-*N*,*N*′,*N*′-trimethylethylenediamine (pico) and *N*,*N*,*N*′,*N*′′,*N*′′-pentamethyldiethylenetriamine (pmdeta) can be easily isolated, except for the 4-nitrophenyl and mesityl derivatives which decarbonylate upon attempted isolation. The aroyl complexes of the ligand 2,6-bis[(dimethylamino)methyl]pyridine (NN′N) can be observed using high-pressure NMR, but most of them decarbonylate upon attempted isolation except for the 1-naphthoyl derivative of which an X-ray molecular structure was obtained. Moreover, the pico and pmdeta complexes are all stable toward methanol, whereas the NN′N complexes immediately decompose in this solvent. The unexpected formation of acetic anhydride upon carbonylation of [PdMe(NN′N)]OTf with subsequent hydrolysis is a striking example of the ligand-dependent stability of the carbonylation products. Qualitative interpretation of NMR results shows that the carbonylation is influenced by (a) the ligand, (b) the size of the aryl moiety, and (c) the presence of strong electron-withdrawing groups in the aryl group.

The *ab initio* calculations on the system $[Pd(CH_3)(NH_3)_3]^+ + CO$ did provide, however, more insight into the carbonylation mechanism as well as into the differences between neutral and ionic palladium(II) complexes. According to our calculations, a purely dissociative mechanism should not be expected to occur as the Pd−N bond dissociation is found to be a high-energy process. The calculations also show that strong CO coordination to give a five-coordinate complex is not feasible in the chosen model system and that a purely associative CO insertion process is thus unlikely to occur. Nevertheless, a five-coordinate complex occurs as a *transition state* in the concerted ligand exchange of NH_3 for CO, which appeared to be a low-energy process. According to the energy profiles (Figures 3 and 4), this step should always be faster than the CO insertion step. Thus, irrespective of the nature of the palladium species (neutral or cationic), the migratory insertion and not the ligand substitution is the rate-determining step in the carbonylation process. Moreover, because of the low-energy pathway for substitution of a NH_3 for a CO ligand, the overall process should be independent of the CO pressure. This is corroborated by the experimental results. The overall process is highly dependent on the overall difference between these two barriers, the first being more sensitive to steric factors, *i.e.*, to the structure of both the tridentate N-donor ligand and the aryl group. This explains the incoherent results of the carbonylation reaction under different circumstances as well as the lower carbonylation rate found for sterically hindered aryls. Most interestingly, the insertion seems to be assisted by the dissociated amine which is kept in the vicinity of the coordination sphere. The solvent might play a similar role. The relative energetics of the neutral and the cationic system, although similar, seem to depend on the ligand environment, at least for the gas-phase species investigated here. The greater reactivity of the ionic system which is experimentally observed might also be due to a greater solvent assistance. These features are currently being explored. The model system used here, and possible variations of it, can be expected to provide good leads to more insight into the basic steps of insertion-type reactions. The reactivity of these cationic complexes toward other nucleophilic reagents, *i.e.*, alkenes, has also been explored.[27]

Experimental Section

All procedures were carried out in standard Schlenk-type glassware. The alkyl- and arylpalladium complexes were prepared using established methods.[6b] Acetone (p.A.) was obtained from Janssen Chimica, and CD_3COCD_3 was obtained from ISOTEC Inc.; both solvents were used without further purification. ^1H (200 or 300 MHz) and ^{13}C (50 or 75 MHz) NMR spectra were recorded on Bruker AC200 or AC300 spectrometers in air at 1 atm pressure and ambient temperature unless noted otherwise. Chemical shifts (δ) are given in ppm relative to tetramethylsilane, and coupling constants are presented in Hz. Accurate chemical shifts and coupling constants for conformational analyses were obtained using IvorySoft's geNMR simulation program (version 3.4 for MS-DOS). FTIR spectra were obtained on a Mattson Galaxy 5000 spectrometer. GLC analyses were performed on a Philips PU4600 gas chromatograph equipped with a capillary column (DB17, J&W Scientific). The GCMS analyses were performed by the Department of Mass Spectrometry, Utrecht University, The Netherlands. Elemental analyses were performed by Dornis u. Kolbe, Mülheim a. d. Ruhr, Federal Republic of Germany.

Synthesis and Characterization of the Acetyl and Aroyl Complexes. All isolated complexes were prepared using the following typical procedure: Carbon monoxide (1 atm) was bubbled through a solution of 0.10 g (0.2 mmol) [PdPh(pmdeta)]OTf (**3b**) in acetone (5 mL) for 1 min. The vessel was then closed, and the solution was stirred for 1 h. Subsequently, the solution was filtered through filter-aid, and the volatiles evaporated *in vacuo*. The residue was recrystallized from methanol/diethyl ether to give 0.10 g (95%) of yellow crystalline [Pd(COPh)(pmdeta)]OTf (**6b**). Most complexes could also be recrystallized from acetone/pentane. IR spectra of the unstable complexes were obtained by rapid precipitation of the complexes from CD_3COCD_3 solution by addition of a large volume of pentane, except for **4c** which decarbonylated too quickly upon pressure release.

(Benzoyl){2,6-bis[(dimethylamino)methyl]pyridine}palladium Trifluoromethanesulfonate (4b). ^1H NMR (200 MHz, CD_3COCD_3, δ): 2.79 (s, 12, NMe_2); 4.53 (s, 4, CH_2); 7.58 (m, 3, Ph[3,4,5]); 7.64 (d, ^3J = 7.8, 2, Py[3,5]); 8.14 (t, 2 × ^3J = 7.8, 1, Py[4]); 8.42 (m, 2, Ph[2,6]). ^{13}C NMR (50 MHz, CD_3COCD_3, 10 atm of CO, δ): 52.48 (NMe_2); 72.86 (CH_2); 122.11 (Py[3,5]); 129.72, 130.03, 133.00, 136.57 (Ph); 141.78 (Py[4]); 156.30 (Py[2,6]); 237.26 (CO). IR (KBr): 1626 cm^{-1}.

(4-Nitrobenzoyl){2,6-bis[(dimethylamino)methyl]pyridine}palladium Trifluoromethanesulfonate (4c). ^1H NMR (200 MHz, CD_3COCD_3, 25 atm of CO, δ): 2.81 (s, 12, NMe_2); 4.56 (s, 4, CH_2); 7.65 (d, ^3J = 7.8, 2, Py[3,5]); 8.15 (t, 2 × ^3J = 7.8, 1, Py[4]); 8.40 (m, 2, Py[3,5]); 8.67 (m, 2, Py[2,6]).

(2-Methyl-1-benzoyl){2,6-bis[(dimethylamino)methyl]pyridine}palladium Trifluoromethanesulfonate (4d). ^1H NMR (200 MHz, CD_3COCD_3, δ): 2.53 (s, 3, Me-tolyl); 2.72 (s, 12, NMe_2); 4.48 (s, 4, CH_2); 7.25 (m, 1, Ph); 7.45 (m, 2, Ph); 7.61 (d, ^3J = 7.8, 2, Py[3,5]); 8.11 (t, 2 × ^3J = 7.8, 1, Py[4]); 8.91 (m, 1, Ph). ^{13}C NMR (50 MHz, CD_3COCD_3, δ): 20.75 (Me-tolyl); 51.90 (NMe_2); 72.56 (CH_2); 122.08 (Py[3,5]); 123.60,

127.00, 131.57, 131.96, 134.44, 136.15 (Ph); 141.79 (Py[4]); 156.18 (Py[2,6]), 237.24 (CO). IR (KBr): 1630 cm^{-1}.

(1-Naphthoyl){2,6-bis[(dimethylamino)methyl]-pyridine}palladium Trifluoromethanesulfonate (4e). Recrystallization could only be performed from acetone/pentane under a CO atmosphere. Yield: 86%. Mp: 142 °C (decomp). ^1H NMR (200 MHz, CD_3COCD_3, 10 atm of CO, δ): 2.75 (s, 12, NMe_2); 4.52 (s, 4, CH_2); 7.62 (m, 4, naphthyl + Py[3,5]); 7.79 (m, 1, naphthyl); 8.01 (m, 1, naphthyl); 8.14 (m, 2, naphthyl + Py[4]); 8.83 (m, 1, naphthyl); 9.31 (m, 1, naphthyl). ^{13}C NMR (50 MHz, CD_3COCD_3, 10 atm of CO, δ): 52.02 (NMe_2); 72.65 (CH_2); 122.15 (Py[3,5]); 126.10, 126.28, 127.46, 128.35, 129.11, 132.92, 133.40, 134.70, 135.47 (naphthyl); 141.85 (Py[4]); 156.35 (Py[2,6]); CO not observed. IR (KBr): 1610 cm^{-1}. Anal. Calcd for $C_{23}H_{24}N_3F_3O_4PdS$: C, 45.59; H, 4.66; N, 6.93. Found: C, 45.82; H, 4.49; N, 7.10.

(2,4,6-Trimethylbenzoyl){2,6-bis[(dimethylamino)-methyl]pyridine}palladium Trifluoromethanesulfonate (4f). ^1H NMR (200 MHz, CD_3COCD_3, 25 atm of CO, δ): 2.28 (s, 3, Me-mesityl); 2.66 (s, 6, NMe_2); 2.72 (s, 3, Me-mesityl); 2.96 (s, 3, Me-mesityl); 4.42 (s, 4, CH_2); 6.95 (s, 2, mesityl); 7.62 (d, ^3J = 7.8, 2, Py[3,5]); 8.12 (t, 2 × ^3J = 7.8, 1, Py[4])). IR (KBr): 1643 cm^{-1}.

(Acetyl){*N*-(2-picolyl)-*N*,*N*′,*N*′-trimethylethylenediamine}palladium Trifluoromethanesulfonate (5a). Yield: 89%. Mp: 122 °C (decomp). ^1H NMR (300 MHz, CD_3COCD_3, δ): 2.52 (s, 3, NMe); 2.86 (m, ABXY, 1, CH_2CH_2-eq); 2.88 (m, ABXY, 1, CH_2CH_2-eq); 3.08 (s, 6, NMe_2); 3.56 (m, ABXY, 1, CH_2CH_2-ax); 3.70 (m, ABXY, 1, CH_2CH_2-ax); 4.11 (d, AX, ^2J = 15.1, 1, CH_2); 4.80 (d, AX, ^2J = 15.1, 1, CH_2); 7.59 (m, 1, Py); 7.71 (m, 1, Py); 8.15 (m, 2, Py). ^{13}C NMR (50 MHz, CD_3COCD_3, δ): 32.72 (CO*Me*); 42.13 (NMe); 50.24, 52.90 (NMe_2); 56.52, 64.86, 66.99 (CH_2); 125.84, 126.30, 141.20, 152.25, 164.07 (Py); 236.77 (CO). IR (KBr): 1676 cm^{-1}. Anal. Calcd for $C_{14}H_{22}N_3F_3O_4PdS$: C, 34.19; H, 4.51; N, 8.54. Found: C, 34.13; H, 4.58; N, 8.57.

(Benzoyl){*N*-(2-picolyl)-*N*,*N*′,*N*′-trimethylethylenediamine}palladium Trifluoromethanesulfonate (5b). Yield: 70%. Mp: 143–145 °C. ^1H NMR (200 MHz, CD_3COCD_3, δ): 2.63 (s, 3, NMe); 2.73 (s, 3, NMe_2); 2.94 (s, 3, NMe_2); 2.97 (m, ABXY, 1, CH_2CH_2-eq); 2.98 (m, ABXY, 1, CH_2CH_2-eq); 3.72 (m, ABXY, 1, CH_2CH_2-ax); 3.84 (m, ABXY, 1, CH_2CH_2-ax); 4.24 (d, AX, ^2J = 15.3, 1, CH_2); 5.01 (d, AX, ^2J = 15.3, 1, CH_2); 7.39 (m, 1, Py[5]); 7.58 (m, 4, Ph[3,4,5] + Py[6]); 7.74 (d, ^3J = 7.8, 2, Py[3]); 8.09 (td, ^3J = 7.8, ^4J = 1.6, 1, Py-[4]); 8.42 (m, 2, Ph[2,6]). ^{13}C NMR (50 MHz, CD_3COCD_3, δ): 42.38 (NMe); 50.07, 53.39 (NMe_2); 56.71, 64.97, 67.25 (CH_2); 125.82, 126.08 (Py[3,5]); 129.76 (Ph[3,5]); 130.68 (Ph[2,6]); 133.53 (Ph[4]); 136.34 (Ph[1]), 141.24 (Py[4]); 151.71 (Py[2]); 164.64 (Py[6]); 232.30 (CO). IR (KBr): 1638 cm^{-1}. Anal. Calcd for $C_{19}H_{24}N_3F_3O_4PdS$: C, 41.20; H, 4.37; N, 7.59. Found: C, 41.24; H, 4.45; N, 7.62.

(4-Methoxy-1-benzoyl){*N*-(2-picolyl)-*N*,*N*′,*N*′-trimethylethylenediamine}palladium Trifluoromethanesulfonate (5c). Yield: 81%. Mp: 137 °C. ^1H NMR (300 MHz, CD_3COCD_3, δ): 2.63 (s, 3, NMe); 2.72 (s, 3, NMe_2); 2.93 (m, ABXY, 1, CH_2CH_2-eq); 2.94 (s, 3, NMe_2); 2.96 (m, ABXY, 1, CH_2CH_2-eq); 3.70 (m, ABXY, 1, CH_2CH_2-ax); 3.82 (m, ABXY, 1, CH_2CH_2-ax); 3.88 (s, 3, OMe); 4.21 (d, AX, ^2J = 15.2, 1, CH_2); 4.99 (d, AX, ^2J = 15.2, 1, CH_2); 7.03 (m, 2, Ph[3,5]); 7.40 (m, 1, Py[5]); 7.66 (m, 1, Py[6]); 7.73 (m, 1, Py[3]); 8.09 (m, 1, Py[4]); 8.40, (m, 2, Ph[2,6]). ^{13}C NMR (50 MHz, CD_3COCD_3, δ): 42.31 (NMe); 50.05, 53.36 (NMe_2); 56.01 (OMe); 56.67, 64.92, 67.17 (CH_2); 114.85 (Ph[3,5]); 125.78, 126.06 (Py[3,5]); 129.15 (Ph-[1]); 132.92 (Ph[2,6]); 141.15 (Py[4]); 151.69 (Py[2]); 164.13 (Ph-[4]); 164.62 (Py[6]); 229.66 (CO). IR (KBr): 1627 cm^{-1}. Anal. Calcd for $C_{20}H_{23}N_3F_3O_5PdS$: C, 41.35; H, 3.99; N, 7.23. Found: C, 41.22; H, 4.15; N, 7.29.

(4-Nitro-1-benzoyl){*N*-(2-picolyl)-*N*,*N*′,*N*′-trimethylethylenediamine}palladium Trifluoromethanesulfonate (5d). ^1H NMR (200 MHz, CD_3COCD_3, 25 atm CO, δ): 2.67 (s, 3, NMe); 2.75 (s, 3, NMe_2); 2.90 (m, 2, CH_2CH_2-eq); 2.96 (s, 3, NMe_2); 3.82 (m, 2, CH_2CH_2-ax); 4.23 (d, AX, ^2J = 15.2, 1, CH_2); 5.13 (d, AX, ^2J = 15.2, 1, CH_2); 7.39 (m, 1, Py[5]); 7.66 (m, 1, Py[6]); 7.75 (m, 1, Py[3]); 8.10 (m, 1, Py[4]); 8.36 (m, 2, Ph[3,5]); 8.67 (m, 2, Ph[2,6]). ^{13}C NMR (50 MHz, CD_3COCD_3, 25 atm of CO, δ): 42.64 (NMe); 50.46, 53.31 (NMe_2); 56.77, 65.05, 67.51 (CH_2); 124.96 (Ph[3,5]); 125.83, 126.20 (Py[3,5]); 131.59 (Ph[2,6]); 140.27 (Ph[1]); 141.42 (Py[4]); 150.65 (Ph-[4]); 151.88 (Py[2]); 164.84 (Py[6]); 232.85 (CO). IR (KBr): 1633 cm^{-1}.

(Acetyl){*N*,*N*,*N*′,*N*″,*N*″-pentamethyldiethylenetriamine}-palladium Trifluoromethanesulfonate (6a). Yield: 93%. Mp: 135 °C (decomp). ^1H NMR (300 MHz, CD_3COCD_3, 300 K, δ): 2.47 (s, 3, NMe); 2.67 (s, br, 6, NMe_2); 2.76 (s, 3, COMe); 2.87 (s, br, 6, NMe_2); 3.38 (m, ABXY, 2, CH_2CH_2-ax); 3.48 (m, ABXY, 2, CH_2CH_2-ax). ^{13}C NMR (50 MHz, CD_3COCD_3, δ): 30.53 (CO*Me*); 40.64 (NMe); 49.95, 53.73 (NMe_2); 57.03, 66.20 (CH_2); 240.79 (CO). IR (KBr): 1664 cm^{-1}. Anal. Calcd for $C_{12}H_{26}N_3F_3O_4PdS$: C, 30.55; H, 5.55; N, 8.91. Found: C, 30.56; H, 5.62; N, 8.84.

(Benzoyl){*N*,*N*,*N*′,*N*″,*N*″-pentamethyldiethylenetriamine}palladium Trifluoromethanesulfonate (6b). Yield: 95%. Mp: 146 °C. ^1H NRM (300 MHz, CD_3COCD_3, δ): 2.37 (s, 6, NMe_2); 2.74 (m, ABXY, 2, CH_2CH_2-eq); 2.83 (m, ABXY, 2, CH_2CH_2-eq); 2.91 (s, 6, NMe_2); 2.94 (s, 3, NMe); 3.57 (m, ABXY, 2, CH_2CH_2-ax); 3.58 (m, ABXY, 2, CH_2CH_2-ax); 7.58 (m, 3, Ph[3,4,5]); 8.49 (m, 2, Ph[2,6]). ^{13}C NMR (50 MHz, CD_3COCD_3, δ): 40.56 (NMe); 49.96, 54.26 (NMe_2); 57.19, 66.63 (CH_2); 129.75 (Ph[3,5]); 130.60 (Ph[2,6]); 133.21 (Ph[4]); 135.85 (Ph[1]); 236.13 (CO). IR (KBr): 1637 cm^{-1}. Anal. Calcd for $C_{17}H_{28}N_3F_3O_4PdS$: C, 38.24; H, 5.29; N, 7.87. Found: C, 38.21; H, 5.34; N, 7.92.

(4-Methoxybenzoyl){*N*,*N*,*N*′,*N*″,*N*″-pentamethyldiethylenetriamine}palladium Trifluoromethanesulfonate (6c). Yield: 79%. Mp: 144–147 °C (decomp). ^1H NMR (300 MHz, CD_3COCD_3, δ): 2.38 (s, 6, NMe_2); 2.75 (m, ABXY, 2, CH_2-CH_2-eq); 2.83 (m, ABXY, 2, CH_2CH_2-eq); 2.90 (s, 6, NMe_2); 2.92 (s, 3, NMe); 3.56 (m, ABXY, 2, CH_2CH_2-ax); 3.57 (m, ABXY, 2, CH_2CH_2-ax); 3.90 (s, 3, OMe); 7.07 (m, 2, Ph[3,5]); 8.47 (m, 2, Ph[2,6]). ^{13}C NMR (50 MHz, CD_3COCD_3, δ): 40.45 (NMe); 19.90, 54.22 (CH_2); 55.97 (OMe); 57.20, 66.57 (NMe_2); 114.78 (Ph[3,5]); 128.75 (Ph[4]); 132.73 (br, Ph[2,6]); 163.90 (Ph[1]); 233.10 (CO). IR (KBr): 1628 cm^{-1}. Anal. Calcd for $C_{18}H_{30}N_3F_3O_5PdS$: C, 38.34; H, 5.36; N, 7.45. Found: C, 38.29; H, 5.30; N, 7.50.

Reaction of Methyl{2,6-bis[(dimethylamino)methyl]-pyridine}palladium(II) Trifluoromethanesulfonate (1a) with Carbon Monoxide. Carbon monoxide (1 atm) was bubbled through an ice-cold solution of 232 mg of **1a** and 30 μL of 2,2-diphenylpropane (internal standard) in 2 mL CD_3COCD_3 for 1 min, resulting in the immediate precipitation of palladium black. The reaction vessel was then closed, and the solution was stirred for 30 min at 0 °C. The solution was filtered through Celite and subsequently analyzed by GLC, GC–MS, and ^1H NMR spectroscopy. The conversion of **1a** was 100% as shown by ^1H NMR, and GLC analysis (SE-30 column) showed that acetic anhydride was formed in 84% yield (based on **1a**). GC–MS analysis of the NMR solution showed the sole formation of acetic anhydride ($[M + H]^+$ at *m/e* 103) which was confirmed by comparison with reference MS spectra. The ^1H NMR spectrum showed signals that correspond to acetic anhydride (2.20 ppm) and the quaternary ammonium salt [NN′(NH)]OTf (δ(NHMe$_2$) 4.85 ppm), respectively. The assignment of the acetic anhydride resonance was substantiated by addition of a tiny amount of acetic anhydride (15 μL). This resulted in the signal enhancement of the acetic anhydride methyl resonance, and no shifts or additional signals were observed. No resonances corresponding to acetylacetone, acetaldehyde, acetic acid, or diketene were present.

High-Pressure NMR Studies of the Carbon Monoxide Insertion. A solution of 40 mg of the complex in 2 mL of CD_3COCD_3 was transferred to a high-pressure NMR tube. The tube was then pressurized to 10 atm of carbon monoxide, and

Table 9. Coupling Constants[a] and Conformational Data of the NCH_2CH_2N Fragments in 5b–d and 6c,d[b]

R	$^2J_{a,b}$	$^2J_{a,c}$	$^2J_{a,d}$	$^2J_{b,c}$	$^2J_{b,d}$	$^2J_{c,d}$
MeCO **5b**	−13.81 ± 0.18	3.17 ± 0.18	1.45 ± 0.13	13.30 ± 0.13	3.11 ± 0.17	−13.72 ± 0.17
Bz[c] **5c**	−13.90 ● 0.27	3.41 ± 0.27	1.33 ± 0.27	13.29 ± 0.24	3.17 ± 0.35	−14.01 ± 0.32
4-MeOBz[c] **5d**	−13.63 ± 0.72	3.33 ± 0.72	1.35 ± 0.72	13.17 ± 0.72	3.34 ± 0.72	−13.82 ± 0.72
Bz[c] **6c**	−13.42 ± 0.65	3.09 ± 0.66	0.97 ± 0.11	13.87 ± 0.09	3.09 ± 0.63	−13.79 ± 0.64
4-MeOBz[c] **6d**	−13.38 ± 0.86	3.11 ± 0.88	1.13 ± 0.13	13.89 ± 0.14	3.14 ± 0.91	−13.85 ± 0.93

R	X	Y	ω (deg)	n_δ
MeCO **5b**	0.46 ± 0.05	4.20 ± 0.24	56.7 ± 0.7	1.06 ± 0.02
Bz[c] **5c**	0.39 ± 0.08	3.90 ± 0.32	55.4 ± 1.0	1.06 ± 0.03
4-MeOBz[c] **5d**	0.41 ± 0.23	3.95 ± 0.88	55.3 ± 3.0	1.07 ± 0.05
Bz[c] **6c**	0.31 ± 0.08	4.49 ± 0.96	56.8 ± 2.7	1.11 ± 0.06
4-MeOBz[c] **6d**	0.36 ± 0.11	4.47 ± 1.26	56.7 ± 3.6	1.10 ± 0.07

[a] In Hz, values and deviations were determined by spin simulation. [b] The assignments of the protons are shown in Figure 2. [c] Bz = benzoyl.

after 1.5 min inverted 5 times before transferring it to the NMR probe. The data collection for the first spectrum was started 2.5 min after pressurizing the tube. After 30 min the tube was again inverted 5 times. Spectra were obtained at regular intervals until either the conversion stopped above 50% before 30 min had passed or until 60 min had passed.

Conformational Analysis. NMR simulation of the experimental data gave accurate chemcial shifts and coupling constants with their standard deviations, allowing the determination of the conformation (δ or λ) and the NCCN torsion angle (ω) of the five-membered chelate rings using the following equations:[16]

$$n_\lambda = [X\cos^2\omega - \cos^2(120-\omega)]/[\alpha\cos^2(120+\omega) - \cos^2(120-\omega)] \quad (3)$$

$$n_\lambda = [Y\cos^2\omega - \alpha\cos^2(120+\omega)]/[\cos^2(120-\omega) - \alpha\cos^2(120+\omega)] \quad (4)$$

$$n_\lambda + n_\delta = 1 \quad (5)$$

where n_λ (n_δ) = the mole fraction of the λ (δ) conformation (Figure 2), $X = {}^3J_{a,d}/{}^3J_{a,c}$, and $Y = {}^3J_{b,c}/{}^3J_{a,c}$. A value of 1.208 was previously determined for the ratio of the Karplus constants (α).[16b] The standard deviations in the coupling constants (Table 9) were obtained from the NMR simulation, while those of X, Y, n_δ, and ω were obtained from these *via* standard mathematical methods.

Computational Details. The SCF calculations were carried out partly with the ASTERIX system of programs[30] and partly with the GAUSSIAN 92 system of programs[31] using the following basis set for the SCF geometry optimization: (15,9,8) contracted to ⟨6,4,4⟩ for the palladium atom;[32] (9,5) contracted to ⟨3,2⟩ for the first-row atoms;[34] and (4) contracted to ⟨2⟩ for the hydrogen atom.[35] The same basis set was used for the CAS–SCF and SD–CI+Q and the MP2 calculations.

Table 10. Crystal Data and Details of the Structure Determination of 4e

Crystal data	
empirical formula	$C_{23}H_{26}F_3N_3O_4PdS$
fw	603.95
cryst syst	triclinic
space group	$P\bar{1}$ (No. 2)
a, b, c (Å)	8.742(1), 12.303(1), 13.563(1)
α, β, γ (deg)	116.33(1), 89.92(1), 103.47(1)
V_{calcd} (Å^3)	1262.7(2)
Z	2
D_{calcd} (g/cm^3)	1.588
F(000) (electrons)	612
μ(Mo Kα) (cm^{-1})	8.6
cryst size (mm^3)	0.05 × 0.10 × 0.50
Data Collection	
temp (K)	295
radiation, Mo Kα (Zr-filtered) (Å)	0.71073
θ_{min}, θ_{max} (deg)	0.1, 27.5
scan type	$\omega/2\theta$
scan (deg)	0.65 + 0.35 tan θ
ref refln(s)	1,−2,0; 1,0,−3; 0,4,−2
data set	0−11; −15 to 15; −17 to 17
tot., unique data	6775, 5784
no. of obsd data ($I > 2.5\sigma(I)$)	4201
Refinement	
N_{ref}, N_{par}	330, 4201
R, wR, S	0.055, 0.052, 1.40
wting scheme, w^{-1}	$\sigma^2(F)$
max and av shift/error	0.16, 0.01
min and max resd density (e/Å^3)	−0.80, 1.01

For the CAS–SCF calculations[36] on $[Pd(NH_3)_2(CH_3)(CO)]^+$, $[Pd(NH_3)_2(COCH_3)]^+$, and on the system with a geometry close to the transition state connecting them, the active space was made of 10 active orbitals populated by 12 electrons (10a12e CAS–SCF). This active space was set to account for the main bonding interactions and to remain coherent along the reaction path as much as possible. For the $[Pd(NH_3)_2(CH_3)(CO)]^+$ reactant and for the structure close to the transition state of the insertion reaction the active orbitals turned out to be 4σ(CO), 5σ(CO), π_z(CO), π_y(CO), $4d_{xz}$(Pd), $\sigma(CH_3) + 4d_{x^2-y^2}$, $4d_{x^2-y^2} - \sigma(CH_3)$, σ^*(CO), π^*_z(CO), and π^*_y(CO), see Scheme 2 for the choice of axes. For the $[Pd(NH_3)_2(COCH_3)]^+$ product, they turned out to be $\sigma_{C-C}(COCH_3)$, $\sigma_{C-O}(COCH_3)$, π_z(CO), π_y(CO), $4d_{xz}$(Pd), $[\pi^*_y(CO) + \sigma(CH_3)] + 4d_{x^2-y^2}$, $4d_{x^2-y^2} - [\pi^*_y(CO) + \sigma(CH_3)]$, π^*_z(CO), $\sigma^*_{C-O}(COCH_3)$, and $\sigma^*_{C-C}(COCH_3)$ (with some $4p_x$(O) character). For the CAS–SCF calculations on $[Pd(NH_3)_3(CH_3)]^+$ and $[Pd(NH_3)_2(CH_3)\cdots(NH_3)] + (Pd\cdots NH_3 = 100$ Å) the active space was made of eight active orbitals populated by eight electrons (8a8e CAS–SCF). The active orbitals were the three $\sigma(NH_3)$, the $\sigma(CH_3)$ orbitals and their correlated counterparts. The CI calculations were multireference con-

(30) (a) Ernenwein, R.; Rohmer, M.-M.; Bénard, M. *Comput. Phys. Commun.* **1990**, *58*, 305. (b) Rohmer, M.-M.; Demuynck, J.; Bénard, M.; Wiest, R. *Comput. Phys. Commun.* **1990**, *60*, 127. (e) Wiest, R.; Demuynck, J.; Bénard, M.; Rohmer, M.-M.; Ernenwein, R. *Comput. Phys. Commun.* **1991**, *62*, 107.

(31) Frisch, M. J.; Trucks, G. W.; Head-Gordon, M.; Gill, P. M. W.; Wong, M. W.; Foresman, J. B.; Johnson, B. G.; Schlegel, H. B.; Robb, M. A.; Reploge, E. S.; Gomperts, R.; Andres, J. L.; Raghavachari, K.; Binkley, J. S.; Gonzales, C.; Martin, R. L.; Fox, D. J.; Defrees, D. J.; Baker, J.; Stewart, J. J. P.; Pople, J. A. *Gaussian 92*, Revision, E.2.; Gaussian, Inc.: Pittsburgh, PA, 1992.

(32) The original (14,9,8) basis set[33] was modified by the addition of a p function of exponent 0.08386.

(33) Veillard, A. and Dedieu, A. *Theor. Chim. Acta* **1984**, *65*, 215.

(34) Huzinaga, S. *Technical Report*; University of Alberta: Edmonton, Canada, 1971.

(35) Huzinaga, S. *J. Chem. Phys.* **1965**, *42*, 1293.

(36) (a) Roos, B. O.; Taylor, P. R.; Siegbahn, P. E. M. *Chem. Phys.* **1980**, *48*, 157. (b) Siegbahn, P. E. M.; Almlöf, J.; Heiberg, A.; Roos, B. O. *J. Chem. Phys.* **1981**, *74*, 2384. (c) Roos, B. O. *Int. J. Quantum Chem., Symp.* **1980**, *14*, 175.

Table 11. Final Coordinates (Å) and Equivalent Isotropic Thermal Parameters (Å²) of the Non-Hydrogen Atoms for 4e

atom	x	y	z	U_{eq}[a]
Pd	0.86503(5)	0.55189(4)	−0.15802(4)	0.0417(1)
O	0.7659(6)	0.5273(4)	0.0260(3)	0.086(2)
N(1)	0.9582(5)	0.4856(4)	−0.3051(3)	0.0480(17)
N(2)	0.6678(5)	0.4032(4)	−0.2581(4)	0.0545(17)
N(3)	1.0901(5)	0.6823(4)	−0.1139(4)	0.0515(17)
C(2)	0.8610(8)	0.3992(5)	−0.3944(5)	0.056(2)
C(3)	0.9228(9)	0.3437(6)	−0.4942(5)	0.069(3)
C(4)	1.0830(10)	0.3826(7)	−0.4957(6)	0.076(3)
C(5)	1.1814(8)	0.4732(6)	−0.4003(6)	0.067(3)
C(6)	1.1135(7)	0.5237(5)	−0.3035(5)	0.052(2)
C(7)	0.6896(7)	0.3794(6)	−0.3752(5)	0.064(2)
C(8)	0.6710(8)	0.2897(6)	−0.2465(6)	0.076(3)
C(9)	0.5114(7)	0.4309(7)	−0.2347(6)	0.078(3)
C(10)	1.1979(6)	0.6135(5)	−0.1888(5)	0.055(2)
C(11)	1.0730(8)	0.7843(6)	−0.1408(6)	0.072(3)
C(12)	1.1629(8)	0.7389(6)	0.0023(5)	0.068(2)
C(13)	0.7873(7)	0.6006(6)	−0.0122(5)	0.055(2)
C(14)	0.7539(7)	0.7273(5)	0.0510(5)	0.053(2)
C(15)	0.6873(7)	0.7722(6)	−0.0092(5)	0.063(2)
C(16)	0.6342(8)	0.8809(6)	0.0439(6)	0.075(3)
C(17)	0.6496(8)	0.9429(6)	0.1552(7)	0.076(3)
C(18)	0.7217(8)	0.9030(6)	0.2203(6)	0.065(3)
C(19)	0.7405(10)	0.9695(7)	0.3383(7)	0.096(3)
C(20)	0.8142(12)	0.9308(9)	0.3994(7)	0.113(4)
C(21)	0.8756(10)	0.8262(8)	0.3476(7)	0.099(4)
C(22)	0.8580(8)	0.7589(6)	0.2364(6)	0.071(3)
C(23)	0.7782(7)	0.7936(5)	0.1682(5)	0.057(2)
S	0.4087(3)	0.2353(2)	0.3197(2)	0.0879(9)
F(1)	0.3011(7)	0.0035(5)	0.2823(6)	0.157(3)
F(2)	0.1412(8)	0.1061(6)	0.3299(8)	0.231(5)
F(3)	0.2162(14)	0.0479(6)	0.1734(7)	0.265(5)
O(1)	0.3350(8)	0.3149(5)	0.3032(5)	0.123(3)
O(2)	0.4322(16)	0.2667(10)	0.4271(9)	0.327(8)
O(3)	0.5206(11)	0.2037(7)	0.2585(12)	0.306(8)
C(1)	0.2508(16)	0.0961(8)	0.2795(8)	0.122(5)

[a] U_{eq} = 1/3 of the trace of the orthogonalized **U** tensor.

tracted CI calculations[37] using as references the configurations which were found to have an expansion coefficient greater than 0.05 in the CAS−SCF wavefunction. A total of 12 electrons were correlated (the same as in the CAS−SCF wavefunction), and single and double excitations to all virtual valence orbitals were included. The CI results reported here include the Davidson correction[38] to provide an estimate of the inclusion of higher than double excitations.

The geometry optimization was carried out from analytical SCF energy first derivatives. In a few instances some internal coordinates were kept constant, *e.g.*, as to force C_s symmetry in the transition state determination of the insertion step. The final energies (au), with the methods in brackets, calculated for structures **I**−**XIII** were as follows **I**, −5135.1276 (SCF), −5135.7128 (MP2), −5135.2042 (CAS−SCF), −5135.2156 (SD−CI+Q); **II**, −5078.9403 (SCF); **II** + NH_3 (**II**···NH_3 = 100 Å), −5135.078 (SCF), −5135.6455 (MP2), −5135.1564 (CAS−SCF), −5135.1648 (SD−CI+Q); **III**, −5191.5662 (SCF), −5192.2593 (MP2), −5191.7504 (CAS−SCF), −5191.8070 (SD−CI+Q); **IV**, −5191.5230 (SCF), −5192.2294 (MP2); **V**, −5191.5636 (SCF), −5192.2502 (MP2), −5191.7405 (CAS−SCF), −5191.8092 (SD−CI+Q); **VI**, −5247.7460 (SCF), −5248.5399 (MP2); **VII**, −5247.7253 (SCF), −5248.5233; **VIII**, −5247.7107 (SCF), −5248.5116 (MP2); **IX**, −5247.7138 (SCF), −5248.5216 (MP2); **X**, −5247.7074 (SCF); **XI**, −5247.7127 (SCF); **XIII**, −5247.6734 (SCF), −5248.4956 (MP2). The energy of NH_3 is as follows: −56.1316 (SCF), −56.2438 (MP2). The energy of CO is as follows: −112.5927 (SCF), −112.8015 (MP2).

X-ray Structure Determination of [Pd(1-naphthoyl)(NN'N)]OTf (4e). A data set was collected for a needle-shaped crystal mounted on top of a glass fiber on an Enraf-Nonius CAD-4 diffractometer. Unit cell parameters were derived from the SET4 setting angles of 25 reflections in the range $9 < \theta < 16°$. The data were corrected for Lp, a small linear decay of 2.5%, and absorption (DIFABS;[39] correction range 0.78, 1.10). The structure was solved by Patterson techniques (SHELXS86/PATT[40]) and refined on F by full-matrix least-squares techniques (SHELX76[41]). Hydrogen atoms were taken into account at calculated positions (C−H = 0.98 Å) riding on their carrier atoms with two common isotropic thermal parameters. Some residual density in the triflate region (~1 e/Å³) indicates some disorder in that region. Scattering factors were taken from Cromer and Mann,[42] corrected for anomalous dispersion.[43] Geometrical calculations, including the ORTEP illustration, were done with PLATON.[44] Calculations were performed on a MicroVax-II cluster. Numerical details of the structure determination are given in Table 10, and positional data are collected in Table 11.

Acknowledgment. X-ray data were kindly collected by A. J. M. Duisenberg. This work was supported in part (A.L.S.) by the Netherlands Foundation for Chemical Research (SON) with financial support from the Netherlands Organization for Scientific Research (NWO). We are grateful to the European Community Science Plan SCI-0319-C (GDF) and the Utrecht University for providing financial support for a visit by B.A.M. to Strasbourg, France. Kindly acknowledged are also Mr. D. Kruis for his help in some of the preparations and Ms. N. Veldman for her help with the PLATON program. We kindly thank Prof. Dr. A. J. Canty for critical reading of the manuscript.

Supporting Information Available: Further details of the structure determination, including atomic coordinates, bond distances and angles, and thermal parameters (10 pages). Ordering information is given on any current masthead page.

OM950163+

(37) Siegbahn, P. E. M. *Int. J. Quantum Chem.* **1983**, *23*, 1869.
(38) Davidson, E. R. *The World of Quantum Chemistry*; Daudel, R., Pullman, B., Eds.; Reidel: Dordrecht, 1974.
(39) Walker, N.; Stuart, D. *Acta Crystallogr.* **1983**, *A39*, 158.
(40) Sheldrick, G. M. *SHELXS86, Program for Crystal Structure Determination*; University of Göttingen: Göttingen, Germany, 1986.
(41) Sheldrick, G. M. *SHELX76, Program for Crystal Structure Analysis Package*; University of Cambridge: Cambridge, U.K., 1976.
(42) Cromer, D. T.; Mann, J. B. *Acta Crystallogr.* **1968**, *A24*, 321.
(43) Cromer, D. T.; Liberman, D. *J. Chem. Phys.* **1970**, *53*, 1981.
(44) Spek, A. L. *Acta Crystallogr.* **1990**, *A46*, C34.

Synthesis, Characterization, and Reactions of a Mononuclear Tantalum–Benzyne Complex, $Ta(\eta^5\text{-}C_5Me_5)(\eta^4\text{-}C_4H_6)(\eta^2\text{-}C_6H_4)$

Kazushi Mashima,*,† Yoshiyuki Tanaka,‡ and Akira Nakamura*,‡

Department of Chemistry, Faculty of Engineering Science, Osaka University, Toyonaka, Osaka 560, Japan, and Department of Macromolecular Science, Faculty of Science, Osaka University, Toyonaka, Osaka 560, Japan

Received April 18, 1995®

The preparation and crystal structure of the tantalum–benzyne complex $TaCp^*(\eta^4\text{-buta-1,3-diene})(\eta^2\text{-}C_6H_4)$ (**8**) ($Cp^* = \eta^5$-pentamethylcyclopentadienyl) together with its reactions were studied. The benzyne complex **8** was prepared by thermolysis (70 °C, 21 h) of the methyl phenyl complex $Ta(CH_3)(C_6H_5)Cp^*(\eta^4\text{-buta-1,3-diene})$ (**7**), which was synthesized by successive treatment of $TaCl_2Cp^*(\eta^4\text{-buta-1,3-diene})$ (**5**) with 1 equiv of PhMgI and with 1 equiv of MeMgI in THF. The rate of thermolysis of **7** in C_6D_6 measured at the temperature range between 50 and 75 °C gave the thermodynamic data $\Delta G^{\ddagger}(55\ °C) = 27.2 \pm 0.5$ kcal/mol. In the ^{13}C NMR spectrum of **8**, a signal due to the *ipso* carbon atoms of benzyne was observed at 203.0 ppm. The monomeric structures of **7** and **8** were confirmed by single-crystal X-ray analysis. Complex **8** is the first example of the parent benzyne complex bearing a metallocene-like MCp(diene) fragment and thus expected to react with a wide range of organic substrates. Ethylene and 2-butyne inserted into the tantalum benzyne bond of **8** to form the metallacycles $\overline{TaCp^*(C_6H_4CH_2CH_2)}(\eta^4\text{-}C_4H_6)$ (**10**) and $\overline{TaCp^*(C_6H_4CH_2CH_2)}(\eta^4\text{-}C_4H_6)$ (**11**), respectively. Acetonitrile and carbon dioxide inserted also to give $\overline{TaCp^*\{C_6H_4C(Me)=N\}}(\eta^4\text{-}C_4H_6)$ (**12**) and $\overline{TaCp^*\{C_6H_4C(=O)O\}}(\eta^4\text{-}C_4H_6)$ (**13**), respectively. Complex **8** was protonated by methanol and 3,3-dimethyl-1-butyne to form phenyl complexes $Ta(OMe)(Ph)Cp^*(\eta^4\text{-}C_4H_6)$ (**14**) and $Ta(C{\equiv}CCMe_3)(Ph)Cp^*(\eta^4\text{-}C_4H_6)$ (**15**), respectively. The structures of **11**, **12**, **14**, and **15** were elucidated by single-crystal X-ray analysis.

Introduction

The synthesis and reactivity of mononuclear and polynuclear benzyne complexes of transition metals have been the focus of numerous studies.[1] Interest in these complexes stems from the bonding nature and the unique reactivity, depending on the kinds of metals as well as their coordination geometry.[2-23] Since Schrock *et al.* reported the first mononuclear benzyne complex of tantalum, $TaCp^*(\eta^2\text{-}C_6H_4)Me_2$ (**1**) ($Cp^* = \eta^5$-pentamethylcyclopentadienyl), by thermolysis of $TaCp^*Me_3(C_6H_5)$,[17] the organometallic approach to isolating mononuclear benzyne complexes has been actively studied. In the 1970s, thermolysis of diphenyl complexes of group

† Faculty of Engineering Science, Osaka University.

‡ Faculty of Science, Osaka University.

® Abstract published in *Advance ACS Abstracts,* November 1, 1995.

(1) Review: Bennett, M. A.; Schwemlein, H. P. *Angew. Chem., Int. Ed. Engl.* **1989**, *28*, 1296. Buchwald, S. L.; Nielsen, R. B. *Chem. Rev.* **1988**, *88*, 1047.

(2) (a) Kolomnikov, I. S.; Lobeeva, T. S.; Gorbachevskaya, V. V.; Aleksandrov, G. G.; Struckhov, Y. T.; Vol'pin, M. E. *J. Chem. Soc., Chem. Commun.* **1971**, 972. (b) Shur, V. B.; Berkovitch, E. G.; Vasiljeva, L. B.; Kudryavtsev, R. V.; Vol'pin, M. E. *J. Organomet. Chem.* **1974**, *78*, 127. (c) Berkovich, E. G.; Shur, V. B.; Vol'pin, M. E.; Lorenz, B.; Rummel, S.; Wahren, M. *Chem. Ber.* **1980**, *113*, 70. (d) Shur, V. B.; Berkovich, E. G.; Vol'pin, M. E.; Lorenz, B.; Wahren, M. *J. Organomet. Chem.* **1982**, *228*, C36.

(3) (a) Erker, G. *J. Organomet. Chem.* **1977**, *134*, 189. (b) Erker, G. *J. Organomet. Chem.* **1977**, *134*, 189. (c) Erker, G.; Kropp, K. *J. Am. Chem. Soc.* **1979**, *101*, 3659. (d) Erker, G.; Kropp, K. *J. Organomet. Chem.* **1980**, *194*, 45. (e) Erker, G.; Kropp, K. *Organometallics* **1982**, *1*, 1246. (f) Erker, G.; Czisch, P.; Mynott, R.; Tsay, Y.-H.; Krüger, C. *Organometallics* **1985**, *4*, 1310. (g) Erker, G.; Dorf, U.; Mynott, R.; Tsay, Y.-H.; Krüger, C. *Angew. Chem., Int. Ed. Engl.* **1985**, *24*, 584. (h) de Boer, H. J. R.; Akkermann, O. S.; Bickelhaupt, F.; Erker, G.; Czisch, P.; Mynott, R.; Wallis, J. M.; Krüger, C. *Angew. Chem., Int. Ed. Engl.* **1986**, *25*, 639. (i) Erker, G.; Mühlenbernd, T. *J. Organomet. Chem.* **1987**, *319*, 201. (j) Erker, G.; Korek, U.; Rheingold, A. L. *J. Organomet. Chem.* **1993**, *454*, 113.

(4) (a) Buchwald, S. L.; Watson, B. T.; Huffman, J. C. *J. Am. Chem. Soc.* **1986**, *108*, 7411. (b) Buchwald, S. L.; Sayers, A.; Watson, B. T.; Dewan, J. C. *Tetrahedron Lett.* **1987**, *28*, 3245. (c) Buchwald, S. L.; Lucas, E. A.; Davis, W. M. *J. Am. Chem. Soc.* **1989**, *111*, 397. (d) Buchwald, S. L.; Fisher, R. A.; Foxman, B. M. *Angew. Chem., Int. Ed. Engl.* **1990**, *29*, 771. (e) Cuny, G. D.; Gutiérrez, A.; Buchwald, S. L. *Organometallics* **1991**, *10*, 537. (f) Cuny, G. D.; Buchwald, S. L. *Organometallics* **1991**, *10*, 363.

(5) Cámpora, J.; Buchwald, S. L. *Organometallics* **1993**, *12*, 4182.

(6) Rausch, M. D.; Mintz, E. A. *J. Organomet. Chem.* **1980**, *190*, 65.

(7) Legrand, G.; Meunier, P.; Petersen, J. L.; Tavares, P.; Bodiguel, J.; Gautheron, B.; Dousse, G. *Organometallics* **1995**, *14*, 162.

(8) Schock, L. E.; Brock, C. P.; Marks, T. J. *Organometallics* **1987**, *6*, 232.

(9) Miller, F. D.; Sanner, R. D. *Organometallics* **1988**, *7*, 818.

(10) Gautheron, B.; Tainturier, G.; Pouly, S.; Théobald, F.; Vivier, H.; Laarif, A. *Organometallics* **1984**, *3*, 1495.

(11) Kanj, A.; Meunier, P.; Gautheron, B.; Dubac, J.; Daran, J.-C. *J. Organomet. Chem.* **1993**, *454*, 51.

(12) Boekel, C. P.; Teuben, J. H.; Meijer, H. J. L. *J. Organomet. Chem.* **1975**, *102*, 161.

(13) Mattia, J.; Humphrey, M. B.; Rogers, R. D.; Atwood, J. L.; Rausch, M. D. *Inorg. Chem.* **1978**, *17*, 3257.

(14) Fagan, P. J.; Manriquez, J. M.; Maatta, E. A.; Seyam, A. M.; Marks, T. J. *J. Am. Chem. Soc.* **1981**, *103*, 6650.

(15) Cockcroft, J. K.; Gibson, V. C.; Howard, J. A. K.; Poole, A. D.; Siemeling, U.; Wilson, C. *J. Chem. Soc., Chem. Commun.* **1992**, 1668.

(16) Houseknecht, K. L.; Stockman, K. E.; Sabat, M.; Finn, M. G.; Grimes, R. N. *J. Am. Chem. Soc.* **1995**, *117*, 1163.

(17) (a) McLain, S. J.; Schrock, R. R.; Sharp, P. R.; Churchill, M. R.; Youngs, W. J. *J. Am. Chem. Soc.* **1979**, *101*, 263. (b) Churchill, M. R.; Youngs, W. J. *Inorg. Chem.* **1979**, *18*, 1697.

(18) Chamberlain, L. R.; Rothwell, I. P. *J. Am. Chem. Soc.* **1983**, *105*, 1665. Chamberlain, L. R.; Kerschner, J. L.; Rothwell, A. P.; Rothwell, I. P.; Huffman, J. C. *J. Am. Chem. Soc.* **1987**, *109*, 6471.

0276-7333/95/2314-5642$09.00/0

4 metallocene was utilized for generating nascent 16-electron benzyne intermediates "$MCp_2(\eta^2\text{-}C_6H_4)$" (M = group 4 metals; Cp = η^5-cyclopentadienyl). The presence of the benzyne species was revealed by labeling and kinetic studies as well as trapping reactions with various organic substrates such as alkenes, alkynes, carbonyl compounds, nitriles, and so on.[2-4,8b] In 1986, Buchwald *et al.* reported the 18-electron benzyne complex $ZrCp_2(\eta^2\text{-}C_6H_4)(PMe_3)$ (**2**), which was stabilized by the additional donor PMe_3.[4a] Recently two reports appeared on 18-electron benzyne complexes of niobium, $NbCp[NC_6H_3(CHMe_2)_2\text{-}2,6](\eta^2\text{-}C_6H_4)(PMe_3)$ (**3**)[15] and $TaCp(Et_2C_2B_4H_4)(\eta^2\text{-}C_6H_4)(PMe_3)$ (**4**),[16] which have metallocene-like 14-electron fragments stabilized by PMe_3. However, until now the parent benzyne complexes of these group 4 metallocenes or metallocene-like fragments have not yet been isolated.

As a part of our research on tantalum–diene system, we used the 14-electron $TaCp^*(\eta^4\text{-butadiene})$ fragment[24-32] in order to isolate the parent benzyne complex. Herein we report on the isolation and characterization of a tantalum–benzyne complex, $TaCp^*(\eta^4\text{-buta-1,3-diene})(\eta^2\text{-}C_6H_4)$ (**8**), together with the formation of metallacyclic compounds and phenyl derivatives. Some of their structures were determined by X-ray crystallographic studies.

Results and Discussion

Preparation of Benzyne Complex 8. The starting compound, methyl phenyl complex $Ta(CH_3)(C_6H_5)Cp^*(\eta^4\text{-buta-1,3-diene})$ (**7**), was prepared by a two step reaction from $TaCl_2Cp^*(\eta^4\text{-buta-1,3-diene})$ (**5**).[24,27,30] Treatment of **5** with 1 equiv of PhMgI in THF and crystallization of the product from hexane afforded purple crystals of monophenyl complex $TaCl(C_6H_5)Cp^*(\eta^4\text{-buta-1,3-diene})$ (**6**) in 94% yield. Even when an excess amount of Grignard reagent was used, the product is mostly the monophenyl complex, although the dimethyl derivative is easily prepared by treatment of **5** with 2 equiv of MeMgI.[28,30] Such selective formation of a monophenyl complex of thorium Cp^*_2ThPhX has recently been reported.[33]

Reaction of **6** with 1 equiv of MeMgI in THF afforded the methyl phenyl complex **7** in 62% yield after crystallization from hexane. Alternatively, **7** could be synthesized in 74% yield by successive treatment of **5** with 1 equiv of PhMgI and with 1 equiv of MeMgI (eq 1). The

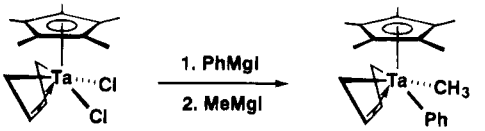

5 7 (1)

^1H NMR spectrum of **7** displayed a singlet at δ −0.12 due to one methyl, three signals at δ 6.51, 6.81, and 6.92 due to three kinds of phenyl protons, and six multiplets due to the butadiene moiety at δ −0.97, −0.74, 0.18, 0.68, 6.51, and 6.69. The dissymmetric structure of **7** was confirmed by single-crystal X-ray analysis (*vide infra*).

During the measurement of the melting point of **7**, we observed the color of the crystals changed from purple to dark red around 114–120 °C before the crystals melted at 130–140 °C. This observation suggested to us that thermolysis of **7** resulted in the formation of another complex before melting. Thermolysis of **7** at 70 °C for 21 h resulted in a loss of methane (by ^1H NMR) and formation of **8** in 69% yield after crystallization from hexane (eq 2). Complex **8** is air and moisture sensitive and gradually decomposed at 70 °C in solution.

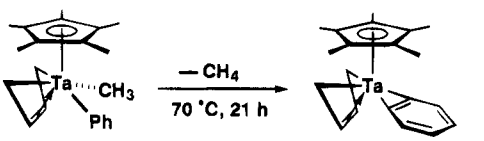

7 8 (2)

The ^1H NMR spectrum of **8** displayed AA'BB'-type signals assignable to protons of benzyne at δ 7.19 and 7.87 together with three signals due to the butadiene moiety, suggesting that **8** has a mirror plane. In the ^{13}C NMR spectrum of **8**, a signal due to the *ipso* carbon atoms of the benzyne was observed at δ 203.0, indicating that the benzyne is donating four electrons to give the metal atom 18 electrons. The chemical shift value for alkynes acting as four π-electron donors has been observed in the region δ ca. 200–240.[1,34,35] The highest δ-value for 2e benzyne so far reported (Table 1) is 174.3 in $ZrCp_2(\eta^2\text{-}C_6H_4)(PMe_3)$.[4a] The higher shielding of δ_c in **8** relative to that (δ 230.5) in **1** could be ascribed to competition for vacant metal orbitals between the π-orbitals of benzyne and those of butadiene; such competition could not occur in **1**.

The rate of formation of **8** from **7** in C_6D_6 was measured at the temperature range 50–75 °C. The reaction was followed by monitoring the disappearance of **7**, giving pseudo-first-order kinetic behavior (Table 2). The Arrhenius plot afforded the thermodynamic

(19) Bartlett, R. A.; Power, P. P.; Shoner, S. C. *J. Am. Chem. Soc.* **1988**, *110*, 1966.
(20) Bunel, G. P. E.; Burger, B. J.; Trimmer, M. S.; Asselt, A. V.; Bercaw, J. E. *J. Mol. Catal.* **1987**, *41*, 21.
(21) (a) Hartwig, J. F.; Andersen, R. A.; Bergman, R. G. *J. Am. Chem. Soc.* **1989**, *111*, 2717. (b) Hartwig, J. F.; Bergman, R. G.; Andersen, R. A. *J. Am. Chem. Soc.* **1991**, *113*, 3404.
(22) Arnold, J.; Wilkinson, G.; Hussain, B.; Hursthouse, M. B. *J. Chem. Soc., Chem. Commun.* **1988**, 704. Arnold, J.; Wilkinson, G.; Hussain, B.; Hursthouse, M. B. *Organometallics* **1989**, *8*, 415.
(23) Bennett, M. A.; Hambley, T. W.; Roberts, N. K.; Robertson, G. B. *Organometallics* **1985**, *4*, 1992.
(24) Yasuda, H.; Tatsumi, K.; Okamoto, T.; Mashima, K.; Lee, K.; Nakamura, A.; Kai, Y.; Kanehisa, N.; Kasai, N. *J. Am. Chem. Soc.* **1985**, *107*, 2410 and references cited therein.
(25) Okamoto, T.; Yasuda, H.; Nakamura, A.; Kai, Y.; Kanehisa, N.; Kasai, N. *Organometallics* **1988**, *7*, 2266.
(26) Okamoto, T.; Yasuda, H.; Nakamura, A.; Kai, Y.; Kanehisa, N.; Kasai, N. *J. Am. Chem. Soc.* **1988**, *110*, 5008.
(27) Mashima, K.; Yamanaka, Y.; Fujikawa, S.; Yasuda, H.; Nakamura, A. *J. Organomet. Chem.* **1992**, *428*, C5.
(28) Mashima, K.; Fujikawa, S.; Nakamura, A. *J. Am. Chem. Soc.* **1993**, *115*, 10990.
(29) Mashima, K.; Fujikawa, S.; Urata, H.; Tanaka, E.; Nakamura, A. *J. Chem. Soc., Chem. Commun.* **1994**, 1623.
(30) Mashima, K.; Fujikawa, S.; Tanaka, Y.; Urata, H.; Oshiki, T.; Tanaka, E.; Nakamura, A. *Organometallics* **1995**, *14*, 2633.
(31) Herberich, G. E.; Englert, U.; Linn, K.; Ross, P.; Runsink, J. *Chem. Ber.* **1991**, *124*, 975.
(32) Herberich, G. E.; Englert, U.; Ross, P. *Chem. Ber.* **1991**, *124*, 2663.
(33) England, A. F.; Burns, C. J.; Buchwald, S. L. *Organometallics* **1994**, *13*, 3491.
(34) Strickler, J. R.; Wexler, P. A.; Wigley, D. E. *Organometallics* **1991**, *10*, 118.
(35) Freundlich, J. S.; Schrock, R. R.; Commins, C. C.; Davis, W. M. *J. Am. Chem. Soc.* **1994**, *116*, 6476.

Table 1. Comparison of NMR Data for Benzyne–Metal Complexes

complex	electron count[a]	δ(ipso-C)	ref
1	4e (16e)	230.5	17
8	4e (18e)	203.0	this work
2	2e (18e)	174.3	4a
		154.1	
3	2e (18e)	162.7	15
		153.7	
4	2e (18e)	168.6	16
		141.8	
Ti(η^2-C_6H_3-3-OMe)(PMe_3)Cp_2	2e (18e)	156.2	5
		149.9	
Ni(η^2-C_6H_4)(DCPE)[b]	2e (16e)	145.2	23
Ru(η^2-C_6H_4)(PMe_3)$_4$	2e (16e)	142.1	21b

[a] Electron count for the benzyne ligand followed by the electron count for complexes in parentheses. [b] DCPE = 1,2-bis(dicyclohexylphosphino)ethane.

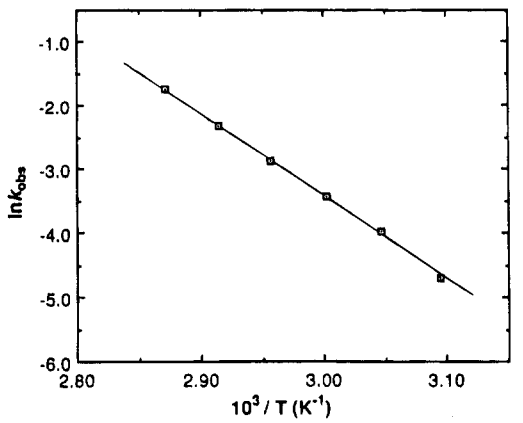

Figure 1. Arhenius plot for the thermolysis of **7** to generate **8**.

Table 2. Observed Rate Constants and Half-Lives at Various Temperatures for Thermolysis of 7 To Give 8

temp, °C	10^5k_{obs}, s^{-1}	$t_{1/2}$, h	temp, °C	10^5k_{obs}, s^{-1}	$t_{1/2}$, h
75	4.86	3.96	60	0.89	21.7
70	2.72	7.07	55	0.52	37.0
65	1.58	12.2	50	0.26	75.1

data $\Delta G^{\ddagger}$(55 °C) = 27.2 ± 0.5 kcal/mol (Figure 1). This value is comparable to those (26.4–27.3 kcal/mol) observed for thermolysis of the diphenyl complexes of titanocene[12] and zirconocene[3b,8] to give benzyne intermediates. The small negative value of $\Delta S^{\ddagger}$ indicates that thermolysis occurred by an intramolecular process through a four-centered intermediate, which is in contrast to the mechanism of late transition metal benzyne complexes, where oxidative addition is followed by reductive elimination.[21b]

In reactions of **8** with *tert*-butyl isocyanide and carbon monoxide, we did not obtain any detectable products. The reaction of **8** with 1 equiv of PMe_3 produced the adduct TaCp*(butadiene)(η^2-C_6H_4)(PMe_3) (**9**) in 61% yield. Complex **9** was thermally unstable and decomposed gradually in solution. The ^{1}H NMR spectrum of **9** showed sharp signals assignable to PMe_3 and Cp* together with six multiplets due to the dissymmetrical butadiene ligand. We observed AA'BB'-type quartet signals due to the benzyne moiety in ^{1}H NMR spectrum. This is in sharp contrast to the ABCD-type (four nonequivalent) protons in the dissymmetric benzyne ligands of **2**–**4**. A plausible explanation of this observation is that complex **9** is in equilibrium with **8** and a small amount of PMe_3 is formed by dissociation. This is supported by the fact that $ZrCp_2(\eta^2$-$C_6H_4)(PMe_3)$ readily dissociates PMe_3.[4a] The ^{31}P NMR spectrum of **9** displayed a singlet at δ −14.5. In the ^{13}C NMR spectrum, we observed two broad resonances at δ 127.9 and 129.2 assignable to four of C_6H_4 carbons, but the signals due to the two *ipso* carbon atoms of the benzyne moiety could not be detected due to its thermal instability as well as the presence of the equilibrium.

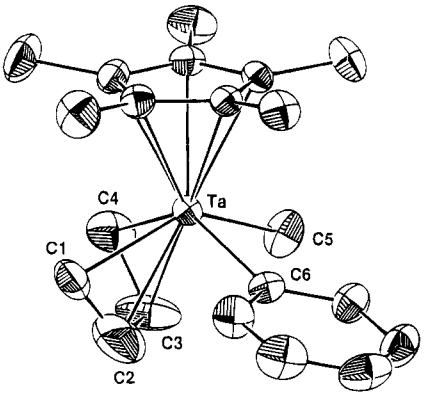

Figure 2. ORTEP drawing of complex **7** with the numbering scheme. Hydrogen atoms are omitted for clarity.

Table 3. Selected Bond Distances (Å) and Angles (deg) for 7

(a) Bond Distances

Ta–C1	2.254(6)	Ta–C6	2.234(5)
Ta–C2	2.32(1)	Ta–CCP[a]	2.114
Ta–C3	2.377(7)	C1–C2	1.50(2)
Ta–C4	2.281(6)	C2–C3	1.53(2)
Ta–C5	2.220(6)	C3–C4	1.43(1)

(b) Bond Angles

C1–Ta–C4	76.0(3)	CCP–Ta–C5	112.1
C1–Ta–C6	89.1(2)	CCP–Ta–C6	110.6
C4–Ta–C5	75.7(3)	θ[b]	89.6
C5–Ta–C6	88.0(2)	φ[c]	61.4
CCP–Ta–C1	111.4	$\varphi 1$[d]	30.4
CCP–Ta–C4	112.4	$\varphi 2$[e]	31.6

[a] CCP: centroid of Cp ring. [b] θ: dihedral angle between the C1–Ta–C4 plane and the C1–C2–C3–C4 plane. [c] φ: dihedral angle between the C1–C2–C3–C4 plane and Cp plane. [d] $\varphi 1$: dihedral angle between the C5–Ta–C6 plane and Cp plane. [e] $\varphi 2$: dihedral angle between the C5–Ta–C6 plane and the C1–C2–C3–C4 plane.

Crystal Structures of 7 and 8. Figure 2 shows the dissymmetric structure of **7**. Selected bond distances and angles are summarized in Table 3. The bond distance [2.220(6) Å] of Ta–C(5) lies in the range observed for Ta–C(sp^3) distances: **1** [2.169(6) and 2.181(6) Å],[17] TaCp*[$(CH_2)_2P(Ph)_2$]Me_2 [2.230(16) and 2.198(17) Å],[36] $TaCp_2$(=CH_2)Me [2.246(12) Å],[37] Ta{N(CH_2-$CH_2NSiMe_3)_3$}Me(OTf) [2.159 Å],[35] and TaCp*(butadiene)Me(OTf) [2.21(1) Å].[30] The bond distance [2.234(5) Å] of Ta–C(6) is longer than the Ta–C(5) bond distance, although C(6) and C(5) are sp^2 and sp^3 carbon atoms, respectively. The diene moiety coordinated to the tantalum center of **7** in *supine* fashion[24] and deviated from the expected planarity, indicating some contribution of the σ,π^3-diene canonical form. The bond distances of C(1)–C(2), C(2)–C(3), and C(3)–C(4) are 1.50(2), 1.53(2), and 1.43(1) Å, respectively, and the bond

(36) Gómez, M.; Jimenez, G.; Royo, P.; Pelinghelli, M. A.; Tiripicchio, A. *J. Organomet. Chem.* **1992**, *439*, 309.
(37) Guggenberger, J. L.; Schrock, R. R. *J. Am. Chem. Soc.* **1975**, *97*, 6578.

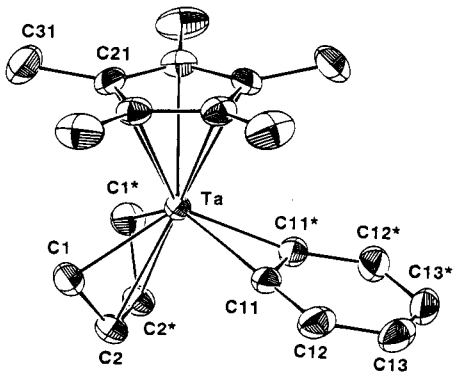

Figure 3. ORTEP drawing of complex **8** with the numbering scheme. Molecule **8** has a mirror plane through the tantalum atom. Hydrogen atoms are omitted for clarity.

Table 4. Selected Bond Distances (Å) and Angles (deg) for 8

	(a) Bond Distances		
Ta–C1	2.219(5)	C2–C2*	1.36(1)
Ta–C2	2.350(4)	C11–C11*	1.370(6)
Ta–C11	2.114(4)	C11–C12	1.387(6)
Ta–CCP[a]	2.112	C12–C13	1.383(8)
C1–C2	1.440(6)	C13–C13*	1.37(1)
	(b) Bond Angles		
C1–Ta–C1*	82.1(3)	C11–C12–C13	117.6(6)
C1–Ta–C11	99.1(2)	C12–C13–C13*	121.2(4)
C11–Ta–C11*	37.8(2)	θ[b]	102.1
CCP–Ta–C1	115.1	φ[c]	68.2
CCP–Ta–C11	113.5	$\varphi 1$[d]	25.4
Ta–C11–C11*	71.7(1)	$\varphi 2$[e]	42.8
C11*–C11–C12	121.2(3)	ϕ[f]	172.1

[a] CCP: centroid of Cp ring. [b] θ: dihedral angle between the C1–Ta–C1* plane and the C1–C2–C2*–C1* plane. [c] φ: dihedral angle between the C1–C2–C2*–C1* plane and Cp plane. [d] $\varphi 1$: dihedral angle between the C11–Ta–C11* plane and Cp plane. [e] $\varphi 2$: dihedral angle between the C11–Ta–C11* plane and the C1–C2–C2*–C1* plane. [f] ϕ: dihedral angle between the C11–Ta–C11* plane and the C11–C12–C13–C13*–C12*–C11* plane.

lengths of Ta–C(1) and Ta–C(2) are shorter than those of Ta–C(4) and Ta–C(3), respectively. The torsion angle of C(1)–C(2)–C(3)–C(4) is −10(1)°.

The monomeric structure of **8** is confirmed by single-crystal X-ray analysis (Figure 3). Selected bond distances and angles are summarized in Table 4. The crystal contained discrete monomers, and the structural features within the $TaCp^*(\eta^4\text{-}C_4H_6)$ fragment are normal. The most interesting feature is the orientation of the benzyne plane parallel to the Cp* plane. This orientation is in sharp contrast to the reported one that is approximately perpendicular (85.3°) to the Cp* plane in **1**.[17] The Ta–C(11) bond distance of 2.114(4) Å in **8** is shorter than that [2.234(5) Å] of the Ta–C(6) in complex **7**. This Ta–C(benzyne) bond distance is longer by ca. 0.04 Å than that of **1**[17] but is shorter than those of the ionic bis(benzyne) complex $[TaPh_4(\eta^2\text{-}C_6H_4)_2\{Li(thf)\}_2]_2[Li_4Cl_2(thf)_{10}]$ [2.214(4)–2.228(6) Å][19] and **4** [average 2.187(3) Å].[16] The C(11)–C(11*) bond distance [1.370(6) Å] of **8** is comparable with that of **1** [1.364(5) Å], **2** [1.364(8) Å], **3** [1.34(1) Å],[15] and **4** [1.344(6) Å].[16] The uncoordinated C–C bond lengths [1.37(1)–1.387(6) Å] of the benzyne ligand of **8** are equivalent within experimental error.

Insertion Reactions. Complex **8** is the first example of a parent benzyne complex bearing a metallocene-like MCp(diene) fragment. Thus, **8** is expected to undergo insertion reaction with a wide range of unsaturated organic compounds since **8** is sterically less hindered than the very unreactive 18-electron Ta–benzyne complex **4**.[16] The results are summarized in Scheme 1.

Scheme 1

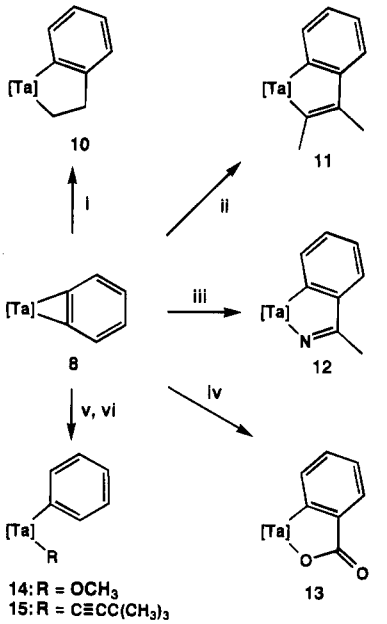

[Ta] = $Ta(\eta^5\text{-}C_5Me_5)(\eta^4\text{-}C_4H_6)$: (i) $CH_2{=}CH_2$ in hexane; (ii) 2-butyne in toluene; (iii) acetonitrile in hexane; (iv) CO_2 in C_6D_6; (v) methanol in hexane; (vi) 3,3-dimethyl-1-butyne in hexane.

Complex **8** reacted with ethylene at atmospheric pressure by insertion into the tantalum–benzyne bond to form dark brown needles of **10** in 47% yield. The metallaindane structure of **10** was confirmed by the ^1H–^1H NOESY and ^1H–^{13}C COSY spectra. Chemical shift values of four methylene protons are δ −0.18, 0.29, 3.57, and 3.90 from ^1H NMR spectroscopy, and the ^{13}C NMR spectrum showed two methylene carbons at δ 55.6 and 43.6.

Complex **8** reacted with an internal alkyne; e.g., 2-butyne gave **11** in 69% yield by heating at 75 °C, while reaction with diphenylacetylene did not proceed due to the steric crowding. Reaction with a terminal alkyne occurred in a different manner, leading ultimately to a σ-alkynyl complex (*vide infra*). The tantalaindene structure of **11** was characterized by conventional spectroscopy and X-ray analysis.

Acetonitrile and carbon dioxide inserted into the tantalum–benzyne bond of **8** gave rise to the products **12** (70% yield) and **13** (50% yield), respectively. Their ^1H and ^{13}C NMR spectra revealed the metallacylic structures. The structure of **12** is closely related to that of similarly formed complexes of ruthenium[21b] and zirconium.[4b] In the infrared spectrum of **13**, a strong absorption at 1670 cm^{-1} corresponded to the carbonyl stretching frequency and was comparable to those (1636 and 1660 cm^{-1}) of analogous complexes of nickel[23] and titanium.[2a]

Crystal Structures of Metallacyclic Compounds 11 and 12. Two crystallographically independent, but otherwise nearly identical, molecules of **11** are present in the asymmetric unit, and each molecule is an enantiomorphic pair. Figure 4 shows an ORTEP drawing of one of two enantiomorphic molecules **11**, and struc-

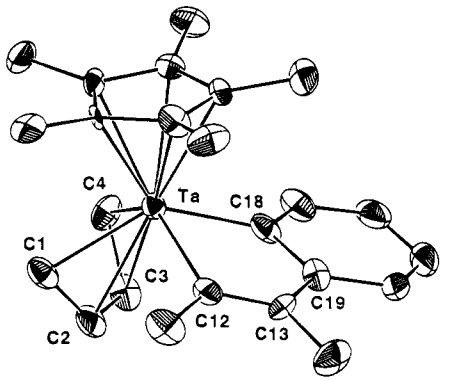

Figure 4. ORTEP drawing of complex **11** with the numbering scheme. One of two crystallographically independent, but part of an enantiomorphic pair, is presented. Hydrogen atoms and the other enantiomer are omitted for clarity.

Table 5. Selected Bond Distances (Å) and Angles (deg) for 11

	(a) Bond Distances		
Ta–C1	2.24(1)	C1–C2	1.43(2)
Ta–C2	2.36(1)	C2–C3	1.41(2)
Ta–C3	2.37(1)	C3–C4	1.45(2)
Ta–C4	2.23(1)	C12–C13	1.35(2)
Ta–C12	2.20(2)	C13–C19	1.49(2)
Ta–C18	2.16(2)	C18–C19	1.40(2)
Ta–CCP[a]	2.078		
	(b) Bond Angles		
C1–Ta–C4	75.3(6)	C12–C13–C19	116(1)
C1–Ta–C12	87.5(5)	C13–C19–C18	113(1)
C4–Ta–C18	87.3(6)	Ta–C18–C19	117(1)
C12–Ta–C18	75.1(6)	θ[b]	94.0
CCP–Ta–C1	113.2	φ[c]	62.7
CCP–Ta–C4	115.4	$\varphi 1$[d]	27.3
CCP–Ta–C12	111.2	$\varphi 2$[e]	35.3
CCP–Ta–C18	111.5	ϕ[f]	172.6
Ta–C12–C13	116(1)		

[a] CCP: centroid of Cp ring. [b] θ: dihedral angle between the C1–Ta–C4 plane and the C1–C2–C3–C4 plane. [c] φ: dihedral angle between the C1–C2–C3–C4 plane and Cp plane. [d] $\varphi 1$: dihedral angle between the C12–Ta–C18 plane and Cp plane. [e] $\varphi 2$: dihedral angle between the C12–Ta–C18 plane and the C1–C2–C3–C4 plane. [f] ϕ: dihedral angle between the Ta–C12–C13–C19–C18 plane and the C14–C19 plane.

tural parameters for one molecule are summarized in Table 5. As the difference between the two molecules is minimal, only one of them will be discussed here. All atoms of the five-membered ring are placed in this plane within a ±0.08 Å deviation. In the tantalacyclopentadiene moiety, the bond length [1.35(2) Å] of C12–C13 is normal for a double bond and the bond distance [1.40(2) Å] of C18–C19 is somewhat longer than the former distance. This tendency has been observed in similar titanocene and zirconocene complexes already reported.[11,13] The bond distances of Ta–C12 [2.20(2) Å] and Ta–C18 [2.16(2) Å] are normal for Ta–C(sp^2) single bond distances. The parameters associated with the Cp*(butadiene)Ta portion of these molecules are not significantly different from those of the other tantalum–butadiene structures.

The molecular structure of **12** is shown in Figure 5, and selected metrical data for **12** are given in Table 6. The monomeric structure of **12** is in sharp contrast to the dimeric pentacoordinated structure of $[Cp_2ZrN{=}C(C_3H_7)C_6H_4]_2$,[4b] which was formed by the insertion reaction of a transient zirconocene–benzyne complex with butyronitrile. The zirconium atom in dimer com-

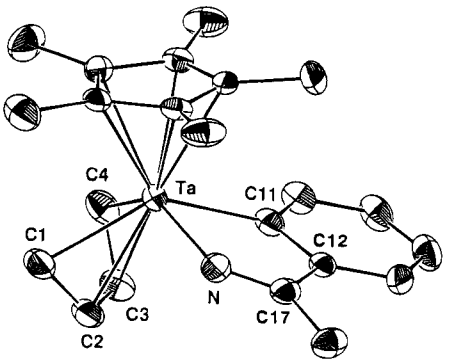

Figure 5. ORTEP drawing of complex **12** with the numbering scheme. Hydrogen atoms are omitted for clarity.

Table 6. Selected Bond Distances (Å) and Angles (deg) for 12

	Bond Distances		
Ta–C1	2.245(6)	C1–C2	1.429(9)
Ta–C2	2.351(6)	C2–C3	1.331(9)
Ta–C3	2.363(6)	C3–C4	1.416(9)
Ta–C4	2.238(6)	C11–C12	1.418(8)
Ta–C11	2.266(6)	C12–C17	1.497(8)
Ta–N	1.999(5)	C17–N	1.259(7)
Ta–CCP[a]	2.122		
	Bond Angles		
C1–Ta–C4	74.5(2)	C11–C12–C17	112.8(5)
C1–Ta–N	94.0(2)	C12–C17–N	114.4(6)
C4–Ta–C11	83.6(2)	Ta–N–C17	126.7(5)
C11–Ta–N	74.0(2)	θ[b]	95.0
CCP–Ta–C1	114.9	φ[c]	63.9
CCP–Ta–C4	113.6	$\varphi 1$[d]	26.2
CCP–Ta–C11	110.9	$\varphi 2$[e]	38.1
CCP–Ta–N	110.3	ϕ[f]	174.1
Ta–C11–C12	111.5(4)		

[a] CCP: centroid of Cp ring. [b] θ: dihedral angle between the C1–Ta–C4 plane and the C1–C2–C3–C4 plane. [c] φ: dihedral angle between the C1–C2–C3–C4 plane and Cp plane. [d] $\varphi 1$: dihedral angle between the C11–Ta–N plane and Cp plane. [e] $\varphi 2$: dihedral angle between the C11–Ta–N plane and the C1–C2–C3–C4 plane. [f] ϕ: dihedral angle between the Ta–C11–C12–C17–N plane and the C11–C16 plane.

plex is coordinated by N and C atoms and the neighboring N atom. The Ta–C11 bond distance of 2.266(6) Å is normal for a Ta–C(sp^2) single bond distance, compared with the Ta–C(sp^2) bond distance [2.234(5) Å] found in **7**. The N–C17 bond distance [1.259(7) Å] is short enough to be regarded as a double bond.

Protonolysis of 8. Complex **8** was protonated by adding methanol and 3,3-dimethyl-1-butyne to form phenyl σ-alkynyl complexes **14** and **15**, respectively. Addition of methanol to a solution of **8** in hexane led to formation of the methoxyphenyl complex **14** in 82% yield. The product was characterized by the ^1H and ^{13}C NMR spectra. Such alcoholysis of benzyne complexes of Zr[4a] and Ru[21] has already been reported.

Figure 6 shows an ORTEP drawing of **14**. Selected bond distances and bond angles are listed in Table 7. The butadiene ligand coordinates to the tantalum atom in *supine* fashion,[24] and the structure within the TaCp*(butadiene) moiety is not exceptional. The Ta–C(6) bond distance [2.247(7) Å] is normal for a single bond and comparable to that of **7**. The Ta–O bond length [1.894(5) Å] is shorter by 0.2–0.3 Å compared to those of TaCp*(butadiene)Me(OTf) [2.097(9) Å][30] and Ta{$N(CH_2CH_2NSiMe_3)_3$}Me(OTf) [2.243 Å],[35] and thereby this bond of **14** has double-bond character. The larger bond angle of Ta–O–C(5) [142.9(6)°] is additional

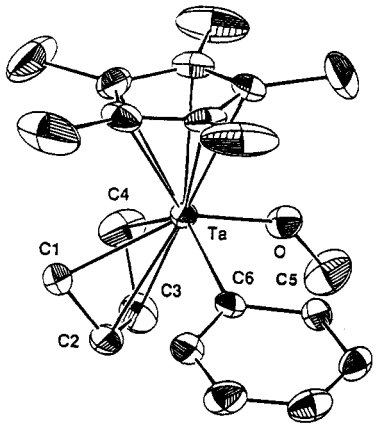

Figure 6. ORTEP drawing of complex **14** with the numbering scheme. Hydrogen atoms are omitted for clarity.

Table 7. Selected Bond Distances (Å) and Angles (deg) for 14

	(a) Bond Distances		
Ta–C1	2.294(7)	Ta–O	1.894(5)
Ta–C2	2.398(7)	Ta–CCP[a]	2.117
Ta–C3	2.385(8)	C1–C2	1.42(1)
Ta–C4	2.259(8)	C2–C3	1.38(1)
Ta–C6	2.247(7)	C3–C4	1.45(1)
	(b) Bond Angles		
C1–Ta–C4	71.6(4)	CCP–Ta–O	118.3
C1–Ta–C6	85.2(3)	Ta–O–C5	142.9(6)
C4–Ta–O	85.5(3)	θ[b]	92.3
C6–Ta–O	90.9(2)	φ[c]	66.0
CCP–Ta–C1	108.1	$\varphi 1$[d]	28.1
CCP–Ta–C4	114.0	$\varphi 2$[e]	38.0
CCP–Ta–C6	110.3		

[a] CCP: centroid of Cp ring. [b] θ: dihedral angle between the C1–Ta–C4 plane and the C1–C2–C3–C4 plane. [c] φ: dihedral angle between the C1–C2–C3–C4 plane and Cp plane. [d] $\varphi 1$: dihedral angle between the C6–Ta–O plane and Cp plane. [e] $\varphi 2$: dihedral angle between the C6–Ta–O plane and the C1–C2–C3–C4 plane.

evidence for the Ta–O double-bond character. These facts indicate that π-donation from the in-plane pπ orbital of the oxygen atom to the laterally directed acceptor dπ-orbital of tantalum is significant. A similar tendency has been observed for alkoxymetallocene complexes of group 4 metals.[38]

Treatment of **8** with 1 equiv of 3,3-dimethyl-1-butyne in hexane resulted in the formation of the σ-alkynyl monophenyl complex **15** as dark-blue crystals in 63% yield. The solid sample of **15** is moderately air and moisture stable, and **15** is thermally stable in solution. Decomposition of **15** was not observed by heating in C_6D_6 at 60 °C after 29 h. The structure of **15** was inferred from NMR spectroscopy to be comprised of one phenyl and one 3,3-dimethyl-1-butynyl group bound to the TaCp*(butadiene) fragment. The ^{13}C NMR spectrum of **15** displayed two singlets assignable to two acetylenic carbons at δ 147.7 and 144.2, whose chemical shift values correspond to those of a metal–acetylide complex such as $TiCp^*_2(C{\equiv}CMe)Et$.[39] In the IR spectrum of **15**, the absorption at 2077 cm^{-1} due to $\nu(C{\equiv}C)$ lies in the expected region.

Figure 7 shows an ORTEP drawing of **15**, and selected bond distances and angles are shown in Table 8.

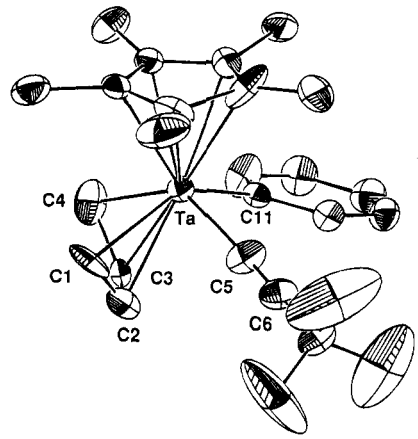

Figure 7. ORTEP drawing of complex **15** with the numbering scheme. Hydrogen atoms are omitted for clarity.

Table 8. Selected Bond Distances (Å) and Angles (deg) for 15

	(a) Bond Distances		
Ta–C1	2.29(2)	Ta–CCP[a]	2.107
Ta–C2	2.38(2)	C1–C2	1.36(3)
Ta–C3	2.35(2)	C2–C3	1.39(3)
Ta–C4	2.25(2)	C3–C4	1.44(3)
Ta–C5	2.20(2)	C5–C6	1.21(3)
Ta–C11	2.22(2)		
	(b) Bond Angles		
C1–Ta–C4	70.3(8)	CCP–Ta–C5	108.7
C1–Ta–C5	80.9(8)	CCP–Ta–C11	111.7
C4–Ta–C11	85.9(7)	θ[b]	91.1
C5–Ta–C11	93.7(7)	φ[c]	64.5
Ta–C5–C6	172(1)	$\varphi 1$[d]	30.4
CCP–Ta–C1	112.0	$\varphi 2$[e]	34.1
CCP–Ta–C4	111.1		

[a] CCP: centroid of Cp ring. [b] θ: dihedral angle between the C1–Ta–C4 plane and the C1–C2–C3–C4 plane. [c] φ: dihedral angle between the C1–C2–C3–C4 plane and Cp plane. [d] $\varphi 1$: dihedral angle between the C5–Ta–C11 plane and Cp plane. [e] $\varphi 2$: dihedral angle between the C5–Ta–C11 plane and the C1–C2–C3–C4 plane.

Figure 8. Schematic drawings for three coordination mode of mononuclear diene complexes: **A**, η^4-diene; **B**, metallacyclo-3-pentene.

Bonding features in the butadiene, phenyl, and Cp* ligands are almost the same as that of **7**. The bond distance [1.21(3) Å] of C(5)–C(6) is normal for a triple bond, *e.g.* $VCp_2(C{\equiv}CCMe_3)$ [1.191(7) Å].[40] The bond angle of Ta–C(5)–C(6) [172(1)°] indicates the acetylide moiety is linearly coordinated to tantalum atom but slight bending in order to minimize the interaction with the phenyl group bound to the Ta atom was discerned.

Structural Features of Butadiene Coordination in the Solution and Solid States. In general, the *s-cis*-1,3-diene coordinated to various transition metals has two possible canonical forms, **A** and **B**, as illustrated schematically in Figure 8.

Structural features of the newly prepared butadiene complexes were able to be evaluated by NMR spectroscopy (Table 9) as well as by X-ray analysis. The values

(38) Mashima, K.; Haraguchi, H.; Ohyoshi, A.; Sakai, N.; Takaya, H. *Organometallics* **1991**, *10*, 2731 and references cited therein.
(39) Cohen, S. A.; Bercaw, J. E. *Organometallics* **1985**, *4*, 1006.
(40) Evans, W. J.; Bloom, I.; Doedens, R. *J. Organomet. Chem.* **1984**, *265*, 249.

Table 9. NMR Data for the Butadiene Moiety Coordinated to Tantalum

complex	chem shift values δ (J_{C-H}, Hz)[a]				
	H1 anti, H4 anti	H1 syn, H4 syn	H2, H3	C1, C4	C2, C3
5	−0.08	0.86	7.09	62.0 (151)	127.0 (169)
6	−0.41, −0.06	0.40, 1.47	6.73, 7.07	58.5 (148), 64.8 (147)	118.9 (170), 121.0 (167)
7	−0.97, −0.74	0.18, 0.68	6.51, 6.69	58.2 (147), 59.7 (147)	114.7 (166), 117.1 (166)
8	−1.29	2.24	5.80	53.4 (146)	108.2 (165)
9a	−0.61, −0.58	0.17, 0.98	4.39, 5.63	39.6 (148), 56.9 (150)	98.6 (167), 99.6 (161)
10	−1.56, −1.45	0.29, 0.85	6.68, 6.24	57.5 (147), 55.0 (149)	112.6 (163), 115.0 (167)
11	−1.25, −1.10	0.69, 0.88	6.56, 6.60	56.6 (148), 58.1 (147)	109.0 (169), 112.2 (168)
12	−0.29, −0.35	1.45, 0.78	6.23, 5.54	53.5 (147), 53.6 (146)	117.6 (170), 111.7 (166)
13	−0.16, −0.81	1.86, 0.97	5.83, 6.32	57.5 (147), 59.1 (145)	116.1 (164), 122.1 (168)
14	−0.38, 0.28	0.54, 1.15	5.81, 6.41	52.3 (151), 59.4 (147)	109.7 (163), 124.2 (167)
15	−0.64, −0.60	0.73, 0.78	6.40, *b*	58.6 (148), 62.7 (140)	113.7 (168), 114.7 (168)

[a] Protons and carbons of butadiene moiety coordinated to tantalum are numbered by 1−4, which is different from the numbering shown in Scheme 2. [b] Not observed due to other peaks.

of the coupling constant J_{C-H} observed in ^{13}C NMR spectroscopy afforded direct information about the σ-character of the Ta−C bond.[24] The values of n for sp^n hybridization estimated for 1,4-carbon atoms and 2,3-carbon atoms in the butadiene moiety on tantalum are found in the ranges 2.4−2.5 and 2.0−2.1, respectively. Thus, the butadiene−tantalum complexes are better represented by **B** rather than **A**. The presence essentially of the latter form **A** has been observed in butadiene complexes of late transition metals where n for sp^n hybridization for 1,4-carbon atoms lies in a range 2.2−2.3.[41] The contribution of the canonical form **B** in the present case is also supported by ^1H NMR spectroscopy. We observed proton signals due to the 2,3-positions of butadiene coordinated to tantalum at rather deshielded values (ca. 5.63−7.09 ppm) except in phosphine adduct **9** (δ 4.39 and 5.63 ppm), as compared with those (4.3−5.27 ppm) of butadiene coordinated to late transition metals. This trend detected by NMR spectroscopy has already been found in various diene complexes of early transition metals and actinide metals.[42,43]

Our X-ray analyses show that all the butadiene complexes of tantalum have *supine* geometry and the diene moiety is better represented by form **B**. We estimated the difference in M−C bond distances (Δd) and C−C bond distances (Δl) by $\Delta d = [d(M-C1) + d(M-C4)]/2 - [d(M-C2) + d(M-C3)]/2$ and $\Delta l = [l(C1-C2) + l(C3-C4)]/2 - l(C2-C3)$, respectively.[24,44] For all known mono(diene) complexes of tantalum, the Δd values and bent angles (θ) lie in the range of −0.2 to −0.1 Å and 91−102°, respectively, though the bent angles (95−125°) reported for some other diene complexes of early transition metals are larger than that of the mono(diene) complexes of tantalum (Table 10).[24,30,42,45-48]

Table 10. Comparison of Structural Features of Butadiene Coordination with Diene Complexes of Actinide and Early Transition Metals

complex	θ, deg	Δd, Å	Δl, Å	ref
Cp^*_2Th(butadiene)	107.4	−0.165	0.02	42
Cp_2Zr(2,3-dimethylbutadiene)	112.0	−0.297	0.053	45
Cp_2Hf(2,3-dimethylbutadiene)	116.5	−0.374	0.094	46
$TiCp^*$(2,3-diphenylbutadiene)Cl	106.8	−0.260	0.097	47
7	89.6	−0.081	−0.065	this work
8	102.1	−0.131	0.080	this work
11	94.0	−0.130	0.030	this work
12	95.0	−0.116	0.092	this work
14	92.3	−0.115	0.055	this work
15	91.1	−0.095	0.010	this work
$TaCp$(butadiene)Cl_2	94.9	−0.160	0.081	24
$TaCp^*$(isoprene)Me(OTf)	93.4	−0.190	0.080	30
$MoCp$(isoprene)$[P(OMe)_3]Cl$	93.2	−0.090	0.033	48

Conclusion

We synthesized the monomeric benzyne complex **8** by thermolysis of methyl phenyl compound **7** through β-hydrogen abstraction and the release of methane. Its structure was characterized on the basis of NMR and X-ray analysis. Complex **8** is highly reactive. Coupling reactions of **8** with unsaturated organic substrates such as ethylene, 2-butyne, carbon dioxide, and acetonitrile give metallacyclic compounds, and protonolysis of **8** smoothly produced monophenyl complexes. Thus, we have demonstrated the fact that structural and chemical properties of MCp^*(buta-1,3-diene) (M = Nb and Ta) fragments are similar to those found for the metallocene fragment of group 4 metals.[15,49] Living polymerization of ethylene by cationic species[28-30] and all-*cis* selective ring opening metathesis polymerization of norbornene by carbene species[50] by using MCp^*(buta-1,3-diene) (M = Nb and Ta) fragments are typical examples to support our concept that the MCp^*(buta-1,3-diene) (M = Nb and

(41) Nakamura, A. *Coord. Chem. Rev.* **1991**, *109*, 207.
(42) Smith, G. M.; Suzuki, H.; Sonnenberger, D. C.; Day, V. C.; Marks, T. J. *Organometallics* **1986**, *5*, 549.
(43) Erker, G.; Mühlenbernd, T.; Benn, R.; Rufiska, A. *Organometallics* **1986**, *5*, 402.
(44) Yasuda, H.; Nakamura, A. *Angew. Chem., Int. Ed. Engl.* **1987**, *26*, 723.
(45) Erker, G.; Engel, K.; Krüger, C.; Chiang, A.-P. *Chem. Ber.* **1982**, *115*, 3311.
(46) Krüger, C.; Müller, G.; Erker, G.; Dorf, U.; Engel, K. *Organometallics* **1985**, *4*, 215.
(47) Yamamoto, H.; Yasuda, H.; Tatsumi, K.; Lee, K.; Nakamura, A.; Chen, J.; Kai, Y.; Kasai, N. *Organometallics* **1989**, *8*, 105.
(48) Kingsbury, K. B.; Carter, J. D.; McElwee-White, L.; Ostrander, R. L.; Rheingold, A. L. *Organometallics* **1994**, *13*, 1635.
(49) Recent examples of group 4 metallocene-like fragments: Gibson, V. C. *J. Chem. Soc., Dalton Trans.* **1994**, 1607. Gibson, V. C. *Angew. Chem., Int. Ed. Engl.* **1994**, *33*, 1565. Siriwardane, U.; Zhang, H.; Hosmane, N. S. *J. Am. Chem. Soc.* **1990**, *112*, 9637. Crowther, D. J.; Baenzinger, N. C.; Jordan, R. F. *J. Am. Chem. Soc.* **1991**, *113*, 1455. Poole, A. D.; Gibson, V. C.; Clegg, W. *J. Chem. Soc., Chem. Commun.* **1992**, 237. Uhrhammer, R.; Crowther, D. J.; Olson, J. D.. Swenson, D. C.; Jordan, R. F. *Organometallics* **1992**, *11*, 3098; Dyer, P. W.; Gibson, V. C.; Howard, J. A. K.; Whittle, B.; Wilson, C. *J. Chem. Soc., Chem. Commun.* **1992**, 1666. Buijink, J.-K.; Teuben, J. H.; Kooijman, H.. Spek, A. L. *Organometallics* **1994**, *13*, 2922; Williams, D. S.; Schofield, M. H.; Anhaus, J. T.; Schrock, R. R. *J. Am. Chem. Soc.* **1990**, *112*, 6728. Williams, D. S.; Schofield, M. H.; Schrock, R. R. *Organometallics* **1993**, *12*, 4560.
(50) Mashima, K.; Tanaka, Y.; Kaidzu, M.; Nakamura, A. Manuscript in preparation.

Ta) fragments are isoelectronic and isolobal to group 4 metallocene fragments.

Experimental Section

General Procedures. All manipulations involving air- and moisture-sensitive organometallic compounds were carried out by use of standard Schlenk techniques under an argon atmosphere. Hexane, THF, toluene, and pentane were dried over sodium benzophenone ketyl. Acetonitrile was dried over P_2O_5. Methanol was dried over magnesium. Benzene-d_6 and THF-d_8 were distilled from Na/K alloy and thoroughly degassed by trap-to-trap distillation before use. 2-Butyne (Aldrich Chemical Co., Inc.) was dried over activated 4-Å molecular sieves, and 3,3-dimethyl-1-butyne (Lancaster Synthesis Inc.) was stirred over CaH_2. A toluene solution of PMe_3 (1.0 M) and diphenylacetylene purchased from Aldrich Chemical Co., Inc., were used as received. Carbon monoxide, carbon dioxide, and ethylene were purchased from Seitetsu Kagaku Co., Aldrich Chemical Co., Inc., and Seitetsu Kagaku Co., respectively, and were used as received. The complex $TaCl_2(\eta^5\text{-}C_5Me_5)(\eta^4\text{-buta-1,3-diene})$ (**5**) was prepared according to the literature.[24,27]

The ^1H (500, 400, and 270 MHz) and ^{13}C (68 MHz) NMR spectra in C_6D_6 or THF-d_8 were measured on a JEOL JNM-GX500, a JEOL JNM-GSX400, or a JEOL JNM-EX270 spectrometer. The $^{31}P\{^1H\}$ NMR spectra were recorded at 109.25 MHz on the JEOL JNM-GSX 270. Infrared spectra were recorded on a Jasco FT/IR-8300 or a Jasco FT/IR-3 spectrometer with the samples as KBr pellets. Elemental analyses were performed at the Elemental Analysis Center, Faculty of Science, Osaka University. The melting points of all complexes were measured in sealed tubes under argon atmosphere and were not corrected.

Preparation of $TaClPh(\eta^5\text{-}C_5Me_5)(\eta^4\text{-buta-1,3-diene})$ (6). To a solution of **5** (0.548 g, 1.24 mmol) in THF (40 mL) cooled at −78 °C was added a solution of PhMgI (1.06 equiv, 1.32 mmol) in ether (0.18 M, 7.30 mL) *via* syringe. The reaction mixture was stirred for 13 h at 25 °C. Precipitated magnesium salts were removed by a centrifuge separation, and then all volatiles were removed under reduced pressure. The residue was extracted with hexane (60 mL). The extract was concentrated and then cooled at −20 °C overnight to afford **6** as dark-purple crystals in 94% yield, mp 191−192 °C. ^1H NMR (C_6D_6): δ −0.41, −0.06, 0.40, 1.47 (4H, m, $=CH_2$), 1.77 (15H, s, C_5Me_5), 6.73, 7.07 (2H, m, $=CH-$), 7.12 (1H, t, ^3J = 6.9 Hz, p-C_6H_5), 7.24 (2H, d, ^3J = 6.9 Hz, o-C_6H_5), 7.27 (2H, t, ^3J = 6.9 Hz, m-C_6H_5). $^{13}C\{^1H\}$ NMR (C_6D_6): δ 11.6 (C_5Me_5), 58.4, 64.5 ($=CH_2$), 118.6, 120.6 ($=CH-$), 122.6 (C_5Me_5), 125.0 (p-C_6H_5), 139.5 (o-C_6H_5), 197.1 (*ipso*-C_6H_5). The m-C_6H_5 resonance in the ^{13}C NMR was not assigned because it was overlapped by C_6D_5H signals. Anal. Calcd for $C_{20}H_{26}ClTa$: C, 49.75; H, 5.43. Found: C, 49.72; H, 5.43.

Preparation of $TaMePh(\eta^5\text{-}C_5Me_5)(\eta^4\text{-buta-1,3-diene})$ (7). To a solution of **5** (0.509 g, 1.15 mmol) in THF (60 mL) cooled at −78 °C was added a solution of PhMgI (1.05 equiv, 1.22 mmol) in ether (0.81 M, 1.50 mL) *via* syringe. The reaction mixture was stirred for 9 h at 20 °C and then added to a solution of MeMgI (1.15 equiv, 1.33 mmol) in ether (1.11 M, 1.20 mL) at −78 °C. The reaction mixture was stirred for 4 h at 20 °C. Precipitated magnesium salts were removed by centrifuge separation, and then all volatiles were removed under reduced pressure. The residue was extracted with hexane (60 mL). The extract was concentrated and then cooled at −20 °C overnight to afford **7** as dark-purple crystals in 74% yield, mp 114−120 °C (dec). Complex **7** was also prepared in 62% yield by the reaction of **6** and MeMgI. ^1H NMR (THF-d_8): δ −0.97, −0.74, 0.18, 0.68 (4H, m, $=CH_2$), −0.12 (3H, s, Ta−CH_3), 1.97 (15H, s, C_5Me_5), 6.51, 6.69 (2H, m, $=CH-$), 6.51 (2H, dd, ^3J = 8.1 Hz, ^4J = 1.3 Hz, o-C_6H_5), 6.81 (1H, tt, ^3J = 7.2 Hz, ^4J = 1.3 Hz, p-C_6H_5), 6.92 (2H, t, ^3J = 7.2 Hz, m-C_6H_5). ^{13}C NMR (THF-d_8): δ 11.7 (q, $^1J_{CH}$ = 127 Hz, C_5Me_5), 47.5 (q, $^1J_{CH}$ = 119 Hz, Ta−CH_3), 58.2 (t, $^1J_{CH}$ = 147 Hz, $=CH_2$), 59.7 (t, $^1J_{CH}$ = 147 Hz, $=CH_2$), 114.7 (d, $^1J_{CH}$ = 166 Hz, $=CH-$), 117.1 (d, $^1J_{CH}$ = 166 Hz, $=CH-$), 121.0 (s, C_5Me_5), 124.6 (d, $^1J_{CH}$ = 157 Hz, p-C_6H_5), 127.9 (d, $^1J_{CH}$ = 155 Hz, m-C_6H_5), 136.3 (d, $^1J_{CH}$ = 154 Hz, o-C_6H_5), 200.1 (s, *ipso*-C_6H_5). Anal. Calcd for $C_{21}H_{29}Ta$: C, 54.55; H, 6.32. Found: C, 54.47; H, 6.35.

Preparation of $Ta(\eta^5\text{-}C_5Me_5)(\eta^4\text{-buta-1,3-diene})(\eta^2\text{-benzyne})$ (8). Hexane (4.0 mL) was added to **7** (0.185 g, 0.40 mmol) placed in a glass reaction vessel. The vessel was sealed and then heated at 70 °C for 21 h. The color of the solution turned gradually to dark-red upon heating. And then the vessel was cooled at −20 °C to afford **8** as dark-red crystals in 69% yield, mp 130−131 °C (dec). ^1H NMR (C_6D_6): δ −1.29 (2H, m, $=CH_2$ anti), 1.74 (15H, s, C_5Me_5), 2.24 (2H, m, $=CH_2$ syn), 5.80 (2H, m, $=CH-$), 7.19, 7.87 (4H, AA′BB′ pattern, C_6H_4). ^{13}C NMR (C_6D_6): δ 11.5 (q, $^1J_{CH}$ = 127 Hz, C_5Me_5), 53.4 (td, $^1J_{CH}$ = 146 Hz, $^2J_{CH}$ = 10 Hz, $=CH_2$), 108.2 (dt, $^1J_{CH}$ = 165 Hz, $^2J_{CH}$ = 5 Hz, $=CH-$), 117.1 (s, C_5Me_5), 128.3 (d, $^1J_{CH}$ = 159 Hz, C_6H_4), 135.4 (d, $^1J_{CH}$ = 158 Hz, C_6H_4), 203.0 (s, Ta−C(benzyne)). Anal. Calcd for $C_{20}H_{25}Ta$: C, 53.82; H, 5.64. Found: C, 53.32; H, 5.62.

Kinetics for Thermolysis of 7 to 8. Complex **7** (0.086 g, 0.186 mmol) was dissolved in C_6D_6 (5.00 mL) at room temperature, and the solution (0.037 M) was divided equally between eight NMR tubes. They were sealed under reduced pressure and kept at −20 °C until they were used. As the sample was thermolyzed in a temperature-controlled (±0.2 °C) oil bath, progress of thermolysis was monitored by ^1H NMR at 30 °C; at this temperature thermolysis of **7** did not proceed. The value $[C]_t$, the concentration of **7** at the reaction time t, was determined by the sum of intensities of areas assignable to four terminal protons ($=CH_2$) of the butadiene ligand in **7**. Treatment of the data is described in the text.

Preparation of $Ta(\eta^5\text{-}C_5Me_5)(\eta^4\text{-buta-1,3-diene})(\eta^2\text{-benzyne})(PMe_3)$ (9). To a solution of **8** (0.135 g, 0.30 mmol) in toluene (3 mL) at 20 °C was added a solution of PMe_3 (1.06 equiv, 0.32 mmol) in toluene (1.0 M, 0.32 mL) *via* syringe. The color of the solution changed immediately from dark-red to reddish-brown. The resulting solution was concentrated to ca. 1 mL and then kept at −20 °C, giving **9** as brown crystals in 61% yield, mp 101−106 °C (dec). Complex **9** is air and moisture sensitive in the solid state and thermally unstable in hydrocarbon solvents. ^1H NMR (270 MHz, THF-d_8, 303 K): δ −0.61, −0.58, 0.17, 0.98 (4H, m, $=CH_2$), 1.57 (15H, s, C_5Me_5), 1.58 (9H, d, $^2J_{HP}$ = 7.6 Hz, PMe_3), 4.39, 5.63 (2H, m, $=CH-$), 6.90 (2H, m, C_6H_4), 7.42 (2H, m, C_6H_4). ^{13}C NMR (68 MHz, THF-d_8, 303 K): δ 11.6 (q, $^1J_{CH}$ = 126 Hz, C_5Me_5), 19.4 (qd, $^1J_{CH}$ = 128 Hz, $^1J_{CP}$ = 25 Hz, PMe_3), 39.6 (t, $^1J_{CH}$ = 148 Hz, $=CH_2$), 56.9 (t, $^1J_{CH}$ = 150 Hz, $=CH_2$), 98.6 (d, $^1J_{CH}$ = 167 Hz, $=CH-$), 99.6 (d, $^1J_{CH}$ = 161 Hz, $=CH-$), 107.5 (s, C_5Me_5), 127.9 (d, $^1J_{CH}$ = 152 Hz, C_6H_4), 129.2 (d (br), $^1J_{CH}$ = 151 Hz, C_6H_4). The resonance for Ta−C(benzyne) was not observed. $^{31}P\{H\}$ NMR (109 MHz, THF-d_8, 303 K): δ −14.5 (PMe_3). Anal. Calcd for $C_{23}H_{34}PTa$: C, 52.88; H, 6.56. Found: C, 52.61; H, 6.53.

Preparation of $\overline{TaCp^*(C_6H_4CH_2CH_2)}(\eta^4\text{-}C_4H_6)$ (10). A solution of **8** (0.091 g, 0.20 mmol) in hexane (7 mL) was cooled at −78 °C and degassed under reduced pressure. After ethylene (1 atm) was introduced to the reaction vessel, the mixture was gradually warmed to room temperature. The color of the solution changed from dark-red to dark-brown. The solution was concentrated to 5 mL and kept at −20 °C to afford **10** as dark-brown crystals in 47% yield, mp 137−139 °C. The 2D ^1H−^1H NOESY spectrum indicated neighboring protons in the molecule. ^1H NMR (THF-d_8): δ −1.56 (1H, m, $H^{11'}$), −1.45 (1H, m, $H^{14'}$), −0.18 (1H, m, ^2J = 13.2 Hz, ^3J = 5.9 Hz, ^3J = 3.0 Hz, $H^{2'}$), 0.29 (1H, m, H^{11}), 0.50 (1H, m, ^2J = 13.2 Hz, ^3J = 9.6 Hz, ^3J = 6.9 Hz, H^2), 0.85 (1H, m, H^{14}), 2.02 (15H, s, C_5Me_5), 3.57 (1H, m, ^2J = 15.8 Hz, ^3J = 6.9 Hz, ^3J = 3.0 Hz, H^3), 3.90 (1H, m, ^2J = 15.8 Hz, ^3J = 9.9 Hz, ^3J = 5.9 Hz, $H^{3'}$),

Table 11. Crystal Data and Data Collection Parameters

complex	**7**	**8**	**12**	**11**	**14**	**15**
formula	$C_{21}H_{29}Ta$	$C_{20}H_{25}Ta$	$C_{22}H_{28}NTa$	$C_{24}H_{31}Ta$	$C_{21}H_{29}OTa$	$C_{27}H_{35}Ta$
fw	462.41	446.37	487.42	500.46	478.41	540.52
cryst system	monoclinic	monoclinic	triclinic	monoclinic	monoclinic	monoclinic
space group	$P2_1/n$	$P2_1/m$	$P\bar{1}$	$P2_1/c$	$P2_1/n$	$P2_1/a$
a, Å	8.529(4)	8.478(1)	8.783(3)	8.452(2)	9.011(5)	12.069(4)
b, Å	16.760(3)	12.955(2)	14.133(4)	28.50(1)	14.256(7)	10.097(3)
c, Å	13.021(4)	8.714(1)	8.388(3)	16.780(5)	15.150(5)	19.035(4)
α, deg			99.28(2)			
β, deg	97.25(3)	115.807(8)	113.01(3)	92.92(2)	95.02(4)	94.94(2)
γ, deg			90.05(3)			
Z	4	2	2	8	4	4
V, Å^3	1846(1)	861.6(2)	943.4(6)	4036(1)	1938(1)	2311(1)
D_{calcd}, g/cm^{-3}	1.663	1.720	1.716	1.647	1.639	1.553
$F(000)$	912	436	480	1984	944	1080
radiation	Mo Kα	Mo Kα	Mo Kα	Mo Kα	Mo Kα	Mo Kα
cryst size, mm	0.8 × 0.3 × 0.3	0.8 × 0.3 × 0.2	0.5 × 0.4 × 0.2	0.6 × 0.3 × 0.2	0.7 × 0.5 × 0.3	0.5 × 0.3 × 0.2
abs coeff, cm^{-1}	58.79	63.61	58.19	54.41	56.05	47.58
scan mode	$\omega-2\theta$	$\omega-2\theta$	$\omega-2\theta$	ω	$\omega-2\theta$	$\omega-2\theta$
temp, °C	23	23	23	23	23	23
scan speed, deg/min	8	8	8	8	8	8
scan width, deg	1.42 + 0.35 tan θ	1.26 + 0.35 tan θ	1.52 + 0.35 tan θ	0.92 + 0.35 tan θ	1.73 + 0.35 tan θ	1.31 + 0.35 tan θ
$2\theta_{max}$, deg	60.2	55.1	60.2	55.3	60.1	60.1
unique data	5608	2089	5546	8180	5908	6280
unique data ($I > 3\sigma(I)$)	4083	1887	4476	5170	3968	3084
no. of variables	200	121	217	452	208	245
R	0.031	0.023	0.048	0.054	0.036	0.072
R_w	0.039	0.028	0.029	0.060	0.043	0.076
GOF	1.61	1.34	2.95	2.35	2.35	2.95
Δ, e Å^{-3}	2.55, −0.76	0.99, −1.31	5.19, −3.14	1.82, −1.31	2.26, −1.31	2.74, −3.38

Scheme 2. Numbering for NMR Data

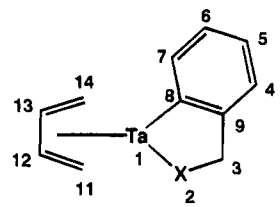

6.24 (1H, m, H^{13}), 6.45 (1H, m, H^7), 6.68 (1H, m, H^{12}), 6.66 (1H, m), 6.69 (1H, m), and 6.71 (1H, m) for H^4 or H^5 or H^6. ^{13}C NMR (THF-d_8): δ 11.9 (q, $^1J_{CH}$ = 127 Hz, C$_5$*Me*$_5$), 43.6 (t, $^1J_{CH}$ = 125 Hz, C^3), 55.0 (t, $^1J_{CH}$ = 149 Hz, C^{14}), 55.6 (t, $^1J_{CH}$ = 117 Hz, C^2), 57.5 (t, $^1J_{CH}$ = 147 Hz, C^{11}), 112.6 (d, $^1J_{CH}$ = 163 Hz, C^{12}), 115.0 (d, $^1J_{CH}$ = 167 Hz, C^{13}), 121.5 (s, *C*$_5$Me$_5$), 136.0 (d, $^1J_{CH}$ = 155 Hz, C^7), 159.0 (s, C^9), 192.7 (s, C^8), 124.0 (d, $^1J_{CH}$ = 150 Hz), 124.5 (d, $^1J_{CH}$ = 154 Hz), and 125.4 (d, $^1J_{CH}$ = 156 Hz) for C^4 or C^5 or C^6. Anal. Calcd for $C_{22}H_{29}Ta$: C, 55.70; H, 6.16. Found: C, 55.43; H, 6.13. See Scheme 2 for numbering of atoms.

Preparation of TaCp*{C$_6$H$_4$C(Me)=C(Me)}(η^4-C$_4$H$_6$) (11). A reaction mixture of **8** (0.098 g, 0.22 mmol) and 2-butyne (1.21 equiv, 0.26 mmol) in toluene (4 mL) was heated at 75 °C for a period of 10 h, giving a reddish-purple solution. All volatiles were removed under reduced pressure, and the resulting residue was recrystallized from THF to afford **11** as dark-reddish-purple crystals in 69% yield, mp 192−193 °C (dec). ^{1}H NMR (THF-d_8): δ −1.25 (1H, m, H$^{11'}$), −1.10 (1H, m, H$^{14'}$), 0.69 (1H, m, H^{11}), 0.88 (1H, m, H^{14}), 1.55 (3H, s, C^2-C*H*$_3$), 1.66 (3H, s, C^3-C*H*$_3$), 2.00 (15H, s, C$_5$*Me*$_5$), 6.44 (1H, d, ^3J = 7.1 Hz, H^7), 6.56 (1H, m, H^{12}), 6.60 (1H, m, H^{13}), 6.63 (1H, td, ^3J = 7.1 Hz, ^4J = 1.4 Hz, H^6), 6.77 (1H, td, ^3J = 7.4 Hz, ^4J = 1.4 Hz, H^5), 6.81 (1H, d, ^3J = 7.6 Hz, H^4). ^{13}C NMR (THF-d_8): δ 11.6 (q, $^1J_{CH}$ = 128 Hz, C$_5$*Me*$_5$), 15.4 (q, $^1J_{CH}$ = 125 Hz, C^3-*C*H$_3$), 22.6 (q, $^1J_{CH}$ = 124 Hz, C^2-*C*H$_3$), 56.6 (t, $^1J_{CH}$ = 148 Hz, C^{11}), 58.1 (t, $^1J_{CH}$ = 147 Hz, C^{14}), 109.0 (d, $^1J_{CH}$ = 169 Hz, C^{12}), 112.2 (d, $^1J_{CH}$ = 168 Hz, C^{13}), 120.6 (dd, $^1J_{CH}$ = 151 Hz, $^2J_{CH}$ = 7 Hz, C^4), 122.2 (s, *C*$_5$Me$_5$), 123.8 (dd, $^1J_{CH}$ = 156 Hz, $^2J_{CH}$ = 6 Hz, C^6), 125.3 (dd, $^1J_{CH}$ = 156 Hz, $^2J_{CH}$ = 7 Hz, C^5), 135.4 (dd, $^1J_{CH}$ = 154 Hz, $^2J_{CH}$ = 6 Hz, C^7), 140.5 (s) and 153.4 (s) for C^3 or C^9, 198.5 (s) and 202.6 (s) for C^2 or C^8. Anal. Calcd for $C_{24}H_{31}Ta$: C, 57.60; H, 6.24. Found: C, 57.32; H, 6.20.

Preparation of TaCp*{C$_6$H$_4$C(Me)=N}(η^4-C$_4$H$_6$) (12). Addition of a solution of CH_3CN (1.11 equiv, 0.31 mmol) in hexane (0.38 M, 0.80 mL) to a solution of **8** (0.123 g, 0.28 mmol) in hexane (7 mL) at 20 °C induced a rapid change in the color of the solution to orange-brown. The resulting solution was kept at −20 °C to afford **12** as reddish-brown crystals in 70% yield, mp 91−93 °C (dec). ^{1}H NMR (THF-d_8): δ −0.35 (1H, m, H$^{14'}$), −0.29 (1H, m, H$^{11'}$), 0.78 (1H, m, H^{14}), 1.45 (1H, m, H^{11}), 1.91 (15H, s, C$_5$*Me*$_5$), 1.95 (3H, m, C*H*$_3$), 5.54 (1H, m, H^{13}), 6.23 (1H, m, H^{12}), 6.92 (1H, td, ^3J = 7.0 Hz, ^4J = 1.5 Hz, H^6), 6.95 (1H, td, ^3J = 7.2 Hz, ^4J = 1.5 Hz, H^5), 6.98 (1H, dd, ^3J = 7.4 Hz, ^4J = 1.5 Hz, H^4), 7.02 (1H, dd, ^3J = 6.9 Hz, ^4J = 1.5 Hz, H^7). ^{13}C NMR (THF-d_8): δ 11.6 (q, $^1J_{CH}$ = 127 Hz, C$_5$*Me*$_5$), 23.8 (q, $^1J_{CH}$ = 126 Hz, *C*H$_3$), 53.5 (t, $^1J_{CH}$ = 147 Hz, C^{11}), 53.6 (t, $^1J_{CH}$ = 146 Hz, C^{14}), 111.7 (d, $^1J_{CH}$ = 166 Hz, C^{13}), 117.6 (d, $^1J_{CH}$ = 170 Hz, C^{12}), 118.1 (s, *C*$_5$Me$_5$), 125.0 (d, $^1J_{CH}$ = 158 Hz, C^5), 125.2 (d, $^1J_{CH}$ = 154 Hz, C^4), 126.8 (d, $^1J_{CH}$ = 156 Hz, C^6), 138.5 (d, $^1J_{CH}$ = 153 Hz, C^7), 164.1 (s, C^9), 171.3(s, C^3), 199.3 (s, C^8). Anal. Calcd for $C_{22}H_{28}NTa$: C, 54.21; H, 5.79; N, 2.87. Found: C, 54.00; H, 5.78; N, 2.86.

Preparation of TaCp*{C$_6$H$_4$C(=O)O}(η^4-C$_4$H$_6$) (13). A solution of **8** (0.116 g, 0.26 mmol) in THF (7 mL) was cooled at −78 °C and then degassed under reduced pressure. After carbon dioxide (1 atm) was introduced to the reaction vessel, the mixture was gradually warmed to room temperature. The color of the solution changed from dark-red to wine-red. The resulting solution was concentrated to ca. 4 mL and then kept at −20 °C, affording **13** as crimson microcrystals in 50% yield, mp 170−175 °C (dec). ^{1}H NMR (THF-d_8): δ −0.81 (1H, m, H$^{14'}$), −0.16 (1H, m, H$^{11'}$), 0.97 (1H, m, H^{14}), 1.86 (1H, m, H^{11}), 2.07 (15H, s, C$_5$*Me*$_5$), 5.83 (1H, m, H^{12}), 6.32 (1H, m, H^{13}), 7.09 (1H, t, ^3J = 7.3 Hz, H^5), 7.10 (1H, d, ^3J = 6.9 Hz, H^7), 7.23 (1H, t, ^3J = 6.9 Hz, H^6), 7.47 (1H, d, ^3J = 6.9 Hz, H^4). ^{13}C NMR (THF-d_8): δ 11.5 (q, $^1J_{CH}$ = 128 Hz, C$_5$*Me*$_5$), 57.5 (t, $^1J_{CH}$ = 147 Hz, C^{11}), 59.1 (t, $^1J_{CH}$ = 145 Hz, C^{14}), 116.1 (d, $^1J_{CH}$ = 164 Hz, C^{12}), 122.1 (d, $^1J_{CH}$ = 168 Hz, C^{13}), 123.0 (s, *C*$_5$Me$_5$), 126.3 (dd, $^1J_{CH}$ = 159 Hz, $^2J_{CH}$ = 7 Hz, C^5), 129.3 (dd, $^1J_{CH}$ = 159 Hz, $^2J_{CH}$ = 7 Hz, C^4), 131.5 (dd, $^1J_{CH}$ = 156 Hz, $^2J_{CH}$ = 6 Hz, C^6), 137.9 (dd, $^1J_{CH}$ = 157 Hz, $^2J_{CH}$ = 8 Hz, C^7), 147.9 (s, C^9), 176.2 (s, C^3), 192.4 (s, C^8). IR (KBr cm^{-1}): 1670 (s, OCO), 1620 (w, OCO). Anal. Calcd for $C_{21}H_{25}O_2Ta$: C, 51.44; H, 5.14. Found: C, 51.46; H, 5.14.

Preparation of Ta(OMe)(C_6H_5)(η^5-C_5Me_5)(η^4-buta-1,3-diene) (14). A solution of methanol (1.07 equiv, 0.21 mmol) in hexane (0.37 M, 0.56 mL) was added to a solution of **8** (0.087 g, 0.19 mmol) in hexane (6 mL). Concentration of the resulting brown-orange solution afforded **14** as orange crystals in 82% yield, mp 143–144 °C. ^{1}H NMR (THF-d_8): δ −0.38, 0.28, 0.54, 1.15 (4H, m, =CH_2), 1.88 (15H, s, C_5Me_5), 4.02 (3H, s, O*Me*), 5.81, 6.41 (2H, m, =C*H*−), 6.87–7.02 (5H, m, C_6H_5). ^{13}C NMR (THF-d_8): δ 11.4 (q, $^1J_{CH}$ = 127 Hz, C_5Me_5), 52.3 (t, $^1J_{CH}$ = 151 Hz, =CH_2), 59.4 (t, $^1J_{CH}$ = 147 Hz, =CH_2), 62.4 (q, $^1J_{CH}$ = 140 Hz, O*Me*), 109.7 (d, $^1J_{CH}$ = 163 Hz, =C*H*−), 119.5 (s, C_5Me_5), 124.2 (d, $^1J_{CH}$ = 167 Hz, =C*H*−), 124.7 (d, $^1J_{CH}$ = 158 Hz, *p*-C_6H_5), 128.4 (d, $^1J_{CH}$ = 155 Hz, *m*-C_6H_5), 139.7 (d, $^1J_{CH}$ = 156 Hz, *o*-C_6H_5), 188.6 (s, *ipso*-C_6H_5). Anal. Calcd for $C_{21}H_{29}OTa$: C, 52.72; H, 6.11. Found: C, 52.55; H, 6.23.

Preparation of Ta(C≡CBu^t)(C_6H_5)(η^5-C_5Me_5)(buta-1,3-diene) (15). To a solution of **8** (0.116 g, 0.26 mmol) in hexane (12 mL) cooled at −78 °C was added a solution of 3,3-dimethyl-1-butyne (1.10 equiv, 0.29 mmol) in hexane (0.11 M, 2.60 mL) *via* syringe. The reaction mixture was stirred for 1 h at room temperature. The resulting dark-blue solution was concentrated to ca. 3 mL. Recrystallization at −20 °C afforded **15** as dark-blue crystals in 63% yield, mp 147–148 °C. ^{1}H NMR (THF-d_8): δ −0.64, −0.60, 0.73, 0.78 (4H, br, =CH_2), 1.21 (9H, s, *tert*-Bu), 2.06 (15H, s, C_5Me_5), 6.40 (1H, m, =C*H*−), 6.80 (1H, m, *p*-C_6H_5), 6.95–7.05 (5H, m, =C*H*−, *o*- and *m*-C_6H_5). ^{13}C NMR (THF-d_8): δ 12.2 (q, $^1J_{CH}$ = 128 Hz, C_5Me_5), 29.9 (s, −*C*Me$_3$), 31.3 (q, $^1J_{CH}$ = 127 Hz, −C*Me*$_3$), 58.6 (t, $^1J_{CH}$ = 148 Hz, =*C*H_2), 62.7 (t, $^1J_{CH}$ = 140 Hz, =*C*H_2), 113.7 (d, $^1J_{CH}$ = 168 Hz, =CH−), 114.7 (d, $^1J_{CH}$ = 168 Hz, =CH−), 122.1 (s, C_5Me_5), 124.4 (d, $^1J_{CH}$ = 159 Hz, *p*-C_6H_5), 127.9 (d, $^1J_{CH}$ = 155 Hz, *m*-C_6H_5), 138.1 (d, $^1J_{CH}$ = 159 Hz, *o*-C_6H_5), 144.2 and 147.7 (s, Ta*C*≡*C*−), 200.9 (s, *ipso*-C_6H_5). IR (KBr cm^{-1}): 2077 (s, C≡C). Anal. Calcd for $C_{26}H_{35}Ta$: C, 59.09; H, 6.67. Found: C, 59.11; H, 6.76.

Crystallographic Data Collections and Structure Determinations of 6, 8, 11, 12, 14, and 15. The crystals of **7**, **8**, **11**, **12**, **14**, and **15** suitable for X-ray diffraction studies were sealed in glass capillaries under argon atmosphere, and then a crystal of each of the complexes was mounted on a Rigaku AFC-5R four-circle diffractometer for data collection using Mo Kα radiation. Relevant crystal and data statistics are summarized in Table 11. The unit cell parameters at 23 °C were determined by a least-squares fit to 2θ values of 20 reflections for all complexes. Three standard reflections were chosen and monitored every 100 reflections. Empirical absorption corrections were carried out based on an azimuthal scan. Every sample showed no significant intensity decay during data collection. The crystal structures of **8**, **14**, and **15** were solved by the heavy-atom method (SAPI 91),[51] while the crystal structures of **7**, **11**, and **12** were solved by direct methods [**7** (MITHRIL),[52] **11** (SIR 88),[53] **12** (SHELX 86)[54]] and then refined by full-matrix least-squares methods. Measured nonequivalent reflections with $I > 3.0\sigma(I)$ were used for the structure determination. In the subsequent refinement, the function $\sum\omega(|F_o| - |F_c|)^2$ was minimized, where $|F_o|$ and $|F_c|$ are the observed and calculated structure factors amplitudes, respectively. The agreement indices are defined as $R = \sum||F_o| - |F_c||/\sum|F_o|$ and $R_w = [\sum\omega(|F_o| - |F_c|)^2/\sum\omega(|F_o|)^2]^{1/2}$, where $\omega^{-1} = \sigma^2(F_o) = \sigma^2(F_o^2)/(4F_o^2)$. The positions of all non-hydrogen atoms for all complexes were found from a difference Fourier electron density map and refined anisotropically. Hydrogen atoms for each complex were placed as follows: For complex **8**, hydrogen atoms of the butadiene and benzyne ligands were found from a difference Fourier map and were refined isotropically, and the other hydrogen atoms were placed at calculated positions (C−H = 0.95 Å) and constrained to ride on their respective carbon atoms. For complexes **7**, **11**, and **15**, all hydrogen atoms were placed at calculated positions (C−H = 0.95 Å) and kept fixed. Hydrogen atoms of the butadiene ligands for **12** and **14** were located from difference Fourier syntheses and were included as fixed contributions after idealization (C−H = 0.95 Å), and the other hydrogen atoms for **12** and **14** were placed at calculated positions (C−H = 0.95 Å) and kept fixed. All calculations were performed using the TEXSAN crystallographic software package, and illustrations were drawn with ORTEP. A molecule of **8** has a mirror plane through the Ta, C(21), and C(31) atoms. In complex **11**, two crystallographically independent but closely analogous molecules (an enantiomorphic pair) are present in the asymmetric unit.

Acknowledgment. A.N. and K.M. are grateful for financial support from the Ministry of Education, Science and Culture of Japan (Grant Nos. 06101004 and 07216249).

Supporting Information Available: Tables of final positional parameters, final thermal parameters, and bond distances and angles and ORTEP diagrams for **7**, **8**, **11**, **12**, **14**, and **15** (73 pages). This material is contained in many libraries on microfiche, immediately follows this article in the microfilm version of the journal, and can be ordered from the ACS; see any current masthead page for ordering information.

OM950272O

(51) Hai-Fu, F. *SAPI91 Structure Analysis Programs with Intelligent Control*; Rigaku Corp.: Tokyo, Japan, 1991.
(52) Gilmore, G. J. *J. Appl. Crystallogr.* **1984**, *17*, 42.
(53) Burla, M. C.; Camalli, M.; Cascarano, G.; Giacovazzo, C.; Polidori, G.; Spagna, R.; Viterbo, D. *J. Appl. Crystallogr.* **1989**, *22*, 389.
(54) Sheldrick, G. M. In *Crystallographic Computing 3*; Scheldrick, G. M., Krüger, C., Goddard, R., Eds.; Oxford University Press: Oxford, U.K., 1985; p 175.

Heterobimetallic Dibridged Complexes $[Cp_2Ta(\mu\text{-}CO)(\mu\text{-}PMe_2)M'(CO)_4]$ (M′ = Cr, W): Synthesis and Reactivity toward Two-Electron Donor Ligands L (L = PR_3, $Me_2P(CH_2)_nPMe_2$, CNR)

Gilles Boni, Philippe Sauvageot, Emmanuel Marpeaux, and Claude Moïse*

Laboratoire de Synthèse et d'Electrosynthèse Organométalliques (Unité de recherche associée au CNRS 1685), Université de Bourgogne, Faculté des Sciences, 6 Boulevard Gabriel, 21000 Dijon, France

Received July 18, 1995[⊗]

The heterobimetallic phosphido-bridged complexes $Cp_2Ta(CO)(\mu\text{-}PMe_2)M'(CO)_5$ (M′ = Cr, Mo, W) (**2a-c**) were prepared by the reaction of the terminal phosphido complex $Cp_2Ta(CO)(PMe_2)$ with $M'(CO)_5(THF)$. Photolytic elimination of one CO from the monobridged complexes produced the dibridged compounds $Cp_2Ta(\mu\text{-}CO)(\mu\text{-}PMe_2)M'(CO)_4$ (M′ = Cr, W) (**3a,b**). Addition reactions between **3a** and **3b** and Lewis bases L (L = phosphines, diphosphines, isonitriles) lead to $Cp_2Ta(CO)(\mu\text{-}PMe_2)M'(CO)_4(L)$ (**4a,b–10a,b**, **11**) with L regiospecifically coordinating to M′. Depending upon the nature of L and M′, the reaction may be stereospecific, since the coordination of L can lead to cis or trans arrangements (with respect to the PMe_2 bridge) on the M′ site. All new bimetallic complexes have been characterized by ^1H and ^{31}P NMR and IR spectroscopy and elemental analyses.

Introduction

Heterobimetallic systems containing both an early and a late transition metal are of great interest for stoichiometric or catalytic reactions.[1] To prevent metal separation during reaction, complexes with phosphorus bridging ligands are a common structural feature and examples of group 4 terminal diphosphido complexes and group 6 monophosphido complexes have been prepared.[2] We have recently developed a new synthetic approach involving group 5 terminal phosphido complexes. These metallaphosphines are synthesized from chlorophosphines and d^2 monohydrido complexes[3,4] or three hydrido complexes[5,6] and are able to bind unsaturated organometallic fragments to give μ-phosphido-bridged complexes.

Scheme 1

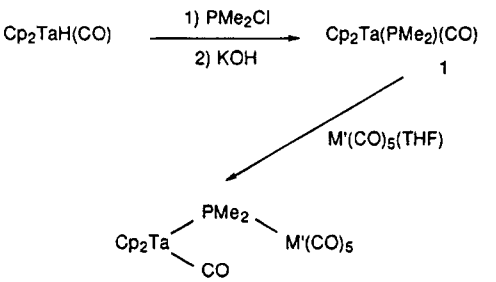

In such a context, we wish to describe the preparation and reactivity of new dinuclear tantalum–chromium or tantalum–tungsten mono- and dibridged systems. Preliminary results concerning this work have been published elsewhere.[7]

Results and Discussion

Synthesis. The (dimethylphosphido)tantalocene complex is obtained by the synthetic route outline in Scheme 1. Treatment of $Cp_2TaH(CO)$ with PMe_2Cl in toluene leads to the phosphine salt $[Cp_2Ta(CO)(PMe_2H)]^+Cl^-$, which is deprotonated in aqueous KOH. The resulting $Cp_2Ta(PMe_2)(CO)$ reacts rapidly at room temperature with $M'(CO)_5(THF)$ in THF solution leading exclusively

[⊗] Abstract published in *Advance ACS Abstracts,* November 1, 1995.

(1) (a) Hostetler, M. J.; Butts, M. D.; Bergman, R. G. *J. Am. Chem. Soc.* **1993**, *115*, 2743. (b) Nielsen-Marsh, S; Crowte, R. J.; Edwards, P. G. *J. Chem. Soc., Chem. Commun.* **1992**, 699. (c) Baker, R. T.; Glassman T. E.; Ovenall, D. W.; Calabrese, J. C. *Isr. J. Chem.* **1991**, *31*, 33. (d) Hostetler, M. J.; Bergman, R. G. *J. Am. Chem. Soc.* **1990**, *112*, 8621. (e) Stephan, D. W. *Coord. Chem. Rev.* **1989**, *95*, 41. (f) Gelmini, L.; Stephan, D. W. *Organometallics* **1988**, *7*, 849. (g) Choukroun, R.; Gervais, D.; Jaud, J.; Kalck, P.; Senocq, R. *Organometallics* **1986**, *5*, 67. (h) Roberts, D. A.; Geoffroy, G. L. *Comprehensive Organometallic Chemistry*; Wilkinson, G., Stone, F. G. A., Abel, E. W., Eds.; Pergamon: Oxford, U.K., **1982**; Vol. 6, 763.

(2) (a) Barré, C.; Boudot, P.; Kubicki, M. M.; Moïse, C. *Inorg. Chem.* **1995**, *34*, 284. (b) Barré, C.; Kubicki, M. M.; Leblanc, J. C.; Moïse, C. *Inorg. Chem.* **1990**, *29*, 5244. (c) Vaughan, G. A.; Hillhouse, G. L.; Rheingold, A. L. *Organometallics* **1989**, *8*, 1760. (d) Kubicki, M. M.; Kergoat, R.; Cariou, M.; Guerchais, J. E.; L'Haridon, P. *J. Organomet. Chem.* **1987**, *322*, 357. (e) Baker, R. T.; Tulip, T. H.; Wreford, S. S. *Inorg. Chem.* **1985**, *24*, 1379. (f) Targos, T. S.; Rosen, R. P.; Whittle, R. R.; Geoffroy, G. L. *Inorg. Chem.* **1985**, *24*, 1375. (g) Wade, S. R.; Wallbridge, M. G. H.; Willey, J. R. *J. Chem. Soc., Dalton Trans.* **1983**, 2555. (h) Baker, R. T.; Whitney, J. F.; Wreford S. S. *Organometallics* **1983**, *2*, 1049.

(3) (a) Lavastre, O.; Bonnet, G.; Leblanc, J. C.; Moïse, C. *Polyhedron* **1995**, *2*, 307. (b) Boni, G.; Kubicki, M. M.; Moïse, C. *Bull. Soc. Chim. Fr.* **1994**, *131*, 895. (c) Challet, S.; Lavastre, O.; Moïse, C.; Leblanc, J. C.; Nuber, B. *New J. Chem.* **1994**, *18*, 1155. (d) Bonnet, G.; Kubicki, M. M.; Moïse, C.; Lazzaroni, R.; Salvadori, P.; Vitulli, G. *Organometallics* **1992**, *11*, 964. (e) Bonnet, G.; Lavastre, O.; Leblanc, J. C.; Moïse, C. *New J. Chem.* **1988**, *12*, 551.

(4) Oudet, P.; Kubicki, M. M.; Moïse, C. *Organometallics* **1994**, *13*, 4278.

(5) (a) Bonnet, G.; Lavastre, O.; Boni, G.; Leblanc, J. C.; Moïse, C. *C. R. Acad. Sci. Paris, Ser. 2*, **1994**, *319*, 1293. (b) Manuscript to be submitted for publication.

(6) (a) Nikonov, G. I.; Kuzmina, L. G.; Mountford, P.; Lemenovskii, D. A. *Organometallics* **1995**, *14*, 3588. (b) Nikonov, G. I.; Lemenovskii, D. A. *Organometallics* **1994**, *13*, 3127.

(7) Boni, G.; Sauvageot, P.; Moïse C. *J. Organomet. Chem.* **1995**, *489*, C32.

0276-7333/95/2314-5652$09.00/0

Scheme 2

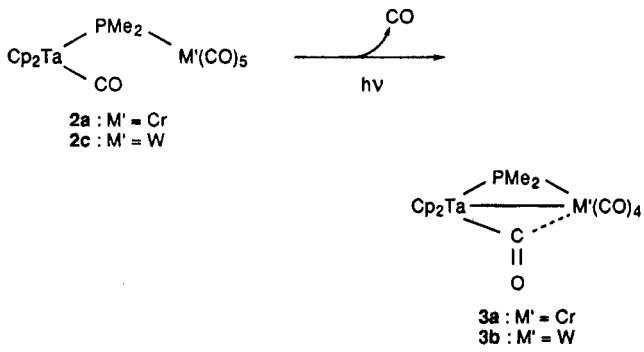

to monobridged phosphido complexes **2a-c** (overall yield 45%). In contrast with previous results observed with niobium–iron derivatives,[4] no trace of dibridged complexes (**3a,b**) is detected: this fact supports an "endo" type situation for the dimethylphosphido ligand which places the $M'(CO)_5$ fragment opposite to the Ta–CO moiety and renders their interactions difficult. However, a photochemical process can be used to convert complexes **2a,c** to μ-CO, μ-P dibridged complexes **3a,b** respectively, with good yields (75%) (Scheme 2). Surprisingly, the expected μ-CO, μ-P tantalum–molybdenum complex was not formed after irradiation of **2b**.

Spectroscopic data for complexes **2a-c** and **3a,b** (Table 1) provide good structural information. In complexes **2**, the ^{31}P NMR spectra reveal expected effects upon coordination of the $M'(CO)_5$ moiety: the resonance of the PMe_2 group is deshielded when M' = Cr whereas it is shifted to higher fields when M' = W. Very characteristic of the dibridged structures **3a,b** are the weak IR absorption at 1725 cm^{-1}, the deshielded ^{13}C resonance for the μ-CO group ($\Delta\delta \approx 55-65$ ppm), and the dramatic downfield shift of the ^{31}P resonance ($\Delta\delta \approx 160-170$ ppm/H_3PO_4) indicating a large decrease in angle with respect to the parent complexes **2a,c**. Cp ring protons of **3a,b** exhibit in the ^1H NMR spectrum a doublet at δ 4.25 ppm (J_{PH} = 1.7 Hz) shifted to higher fields with respect to the corresponding signals of the open compounds **2a,c**. This means that some electron density may be transferred from the $M'(CO)_4$ fragment to the Cp_2Ta moiety via the CO bridging ligand. In the IR, the red shift observed in complexes **3a,b** is in accordance with a high electron density located at the $M'(CO)_4$ fragment. All these data are consistent with a Ta–M' bond.[8]

Two limiting valence bond representations **A** and **B** can account for such a metal–metal bonding (Scheme 3). Electronic structure **A** suggests a donor–acceptor interaction between the filled $1a^1$ orbital of the tantalum atom and a vacant orbital on M', allowing this metal to reach an 18-electron configuration. The semibridging carbonyl permits a transfer of electron density from M' to the tantalocene fragment and helps the metal M' to relieve from its excess of electron density. Representation **B** postulates a normal covalent metal–metal bond together with a symmetrical carbonyl bonding.

X-ray analyses of three related dibridged complexes $Cp_2Ta[\mu\text{-}PPh(i\text{-}Pr)](\mu\text{-}CO)Cr(CO)_4$,[9] $Cp_2Nb(\mu\text{-}PPh_2)(\mu\text{-}CO)Fe(CO)_3$[4] and $Cp_2Nb(\mu\text{-}PPh_2)(\mu\text{-}CO)Cr(CO)_3(PMe_2H)$[10] yielded M–C–O angles (M = Nb, Ta) equal to 144.7, 141.5, and 131.0°, respectively. In accordance with the structural analysis performed by Crabtree,[11] the data of the Nb–Fe and Ta–Cr complexes fall in the range of bent semibridging carbonyl whereas the 131° angle value agrees with a symmetrical bridging. Therefore, no conclusive formulation can be put forward for **3a,b** in the absence of structural data.

Reactivity of Complexes 3a,b with Lewis Bases. As previously reported by Vahrenkamp et al.[12] and others[13] metal–metal bonds can be cleaved by reaction with two-electron donor ligands. We have therefore examined the behavior of the Ta–M' (M' = Cr, **3a**; M' = W, **3b**) toward carbon monoxide, phosphines, diphosphines, and isonitriles (Scheme 4). After bubbling CO through a solution of **3b** in THF, we recovered the expected phosphido-monobridged complex **2c**. The reaction was monitored by IR, and after 20 min, the characteristic semibridging carbonyl band (1725 cm^{-1}) disappears.

The reaction with phosphines and isonitriles proceeds quickly, at room temperature, and the products are easily isolated and characterized (see Experimental Section). With complex **3a**, the addition of L is regiospecific and can lead to cis or trans arrangements at the Cr site. Bonding of phosphines or diphosphines to chromium rather than tantalum is clearly indicated by the absence of a doublet of doublets (or triplet) for the ^1H resonances of cyclopentadienyl ligands in complexes **4a-7a**: the signal appears as a doublet with $J \approx 2$ Hz. With PMe_2Ph, dmpm ($PMe_2(CH_2)PMe_2$), and dmpe ($PMe_2(CH_2)_2PMe_2$) complex **3a** leads to a mixture of cis and trans "open" structures **4a-6a** with a slight excess of the cis (L = PMe_2Ph, **6a**, 64%) or trans (L = dmpm, **4a**, 70%; L = dmpe, **5a**, 77%) isomers. Stereospecific addition in the trans position is observed with bulky PPh_3. These results illustrate the dependence of the coordination site on the bulk of incoming ligands.[14] The isonitriles t-BuNC, 2,6-$Me_2C_6H_3NC$, and PhHMeC*NC give exclusively cis isomers **8a-10a** in accordance with the relatively small steric requirements of this type of ligand. It is worth noting that no cis → trans rearrangement occurs when structures **4a-10a** are heated (80 °C in toluene). IR data establish unambiguously the geometry around chromium atom: a cis arrangement gives rise to four absorption bands whereas only one band would be expected for a trans isomer. The ^1H NMR data provide information on the selectivity of the addition at the Cr site but cannot show whether a cis

(8) (a) Carty, A. J. *Adv. Chem. Ser.* **1982**, *No. 196*, 163. (b) Carty, A. J.; MacLaughlin, S. A.; Taylor, N. J. *J. Organomet. Chem.* **1981**, *204*, C27. (c) Garrou, P. E. *Chem. Rev.* **1981**, *81*, 229. (d) Petersen, J. L.; Stewart, R. P., Jr. *Inorg. Chem.* **1980**, *19*, 186.

(9) Bonnet, G.; Lavastre, O.; Kubicki, M. M.; Leblanc, J. C.; Moïse, C. In *Proceedings from the XVth International Union of Crystallography*; Authier, A., Ed.; Bordeaux, France, 1990; p C227.

(10) Oudet, P.; Moïse, C.; Kubicki, M. M. *Inorg. Chim. Acta*, submitted for publication.

(11) Crabtree, R. H.; Lavin, M. *Inorg. Chem.* **1986**, *25*, 805.

(12) (a) Langenbach, H. J.; Vahrenkamp, H. *Chem. Ber.* **1977**, *110*, 1195. (b) Langenbach, H. J.; Vahrenkamp, H. *Chem. Ber.* **1977**, *110*, 1206.

(13) (a) Shyu, S. G.; Wu, W. J.; Wen, Y. S.; Peng, S. M.; Lee, G. H. *J. Organomet. Chem.* **1995**, *489*, 113. (b) Shyu, S. G.; Hsu, J. Y.; Lin, P. J.; Wu, W. J.; Peng, S. M.; Lee, G. H.; Wen, Y. S. *Organometallics* **1994**, *13*, 1699. (c) Baker, R. T.; Calabrese, J. C.; Krusic, P. J.; Therien M. J.; Trogler W. C. *J. Am. Chem. Soc.* **1988**, *110*, 8392. (d) Mercer, W. C.; Whittle, R. R.; Burkhardt, E. W.; Geoffroy, G. L. *Organometallics* **1985**, *4*, 68. (e) Roberts, D. A.; Steinmetz, G. R.; Breen, M. J.; Shulman, P. M.; Morrison, E. D.; Duttera, M. R.; DeBrosse, C. W.; Whittle, R. R.; Geoffroy, G. L. *Organometallics* **1983**, *2*, 846.

(14) (a) Brown, T. L. *Inorg. Chem.* **1992**, *31*, 1286. (b) Tolman, C. A. *Chem. Rev.* **1977**, *77*, 313.

Table 1. ^1H and ^{31}P NMR and IR (ν(CO)) Data for 1, 2a-c, and 3a,b

complex	^1H (ppm, C_6D_6)[a] Cp	Me	^{31}P (ppm, C_6D_6)	IR (cm^{-1}, THF)
1	4.41 (d) (1.5)	1.48 (d) (4.6)	-96 (s)	1890 vs
2a	4.45 (d) (2.0)	1.55 (d) (5.8)	−80 (s)	2038 m, 1935 vs, 1910 s
2b	4.41 (d) (2.0)	1.54 (d) (5.3)	−100 (s)	2052 m, 1921 vs, 1906 s
2c	4.42 (d) (2.0)	1.68 (d) (5.9)	−122 (s) (J_{PW} = 170)	2051 m, 1974 vs, 1913 s
3a	4.25 (d) (1.7)	1.51 (d) (9.0)	93 (s)	1987 s, 1909 s, 1892 s, 1875 s, 1725 w
3b	4.27 (d) (1.7)	1.52 (d) (8.9)	35 (s) (J_{PW} = 173)	2001 s, 1908 m, 1880 s, 1860 s, 1722 w

[a] J values in Hz in parentheses.

Scheme 3

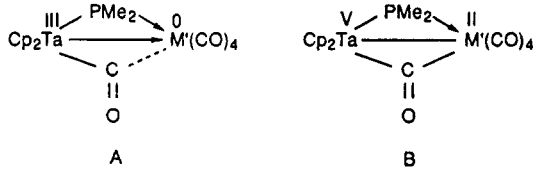

Scheme 4

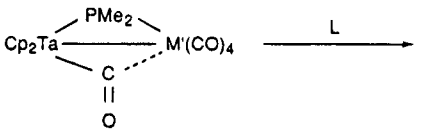

3a : M' = Cr
3b : M' = W

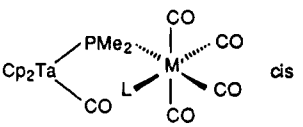

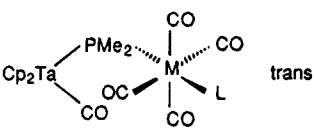

4a,b , L = dmpm ; M' = Cr, W
5a,b , L = dmpe ; M' = Cr, W
6a,b , L = PMe_2Ph ; M' = Cr, W
7a,b , L = PPh_3 ; M' = Cr, W
8a,b , L = ^{t}BuNC ; M' = Cr, W
9a,b , L = 2,6-$Me_2C_6H_3$-NC ; M' = Cr, W
10a,b , L = PhHMeC*NC ; M' = Cr, W
11 , L = P*MePho-An ; M' = W

or a trans arrangement is formed. However, a decisive configurational assignment is available from ^{31}P NMR chemical shifts since a trans configuration involves a systematic deshielding of phosphorus resonances.[15] Noteworthy, cis and trans $^2J_{PP}$ values are very similar[16] and thus do not afford more conclusive structural information. With dmpm or dmpe, the ^{31}P NMR data confirm the presence of a "free" phosphine group since two distinct resonances are observed for the diphosphine ligand: a downfield doublet assigned to the metal-bonded phosphorus atom and a more shielded signal for the terminal phosphorus whose chemical shift is very close to that of the free phosphine.

In contrast, the regiospecific coordination of L ligands on the larger tungsten center gives exclusively the cis isomers **4b-10b** and **11**. However, with very bulky PPh_3, a small amount of the trans isomer (5%) is detected and we have observed, in a THF solution, that a cis → trans isomerization process occurs presumably due to steric factors; after 2 days, an equilibrium is reached with 80% of the trans product. Such a rearrangement, which has some literature precedence, is indicating the thermodynamic nature of the trans isomer.[17]

With the aim of further stereochemical studies, we have introduced a chiral group on the metal fragment (M' = Cr, W; **10a,b**) by using the racemic isonitrile PhHMeC*NC. Surprisingly, in the ^1H NMR, the Cp ligands are equivalent. This lack of Cp resonance differentiation could be explained by distance effects between the metallocene moiety and the asymmetric ligand which place the two cyclopentadienyl rings in almost identical environments. The fact that two distinct resonances ($\Delta\nu \approx 1.7$ Hz) are clearly visible when the chiral phosphine "PAMP" (P*MePh(o-An); o-An = *ortho*-anisyl) is reacted (**11**) supports this explanation. In addition, two doublets are found for the μ-PMe_2 group.

Conclusions

Heterobimetallic phosphido-bridged complexes with or without a metal−metal bond were synthesized from reaction of the terminal phosphido derivative of tantalocene $Cp_2Ta(CO)(PMe_2)$ with unsaturated fragments $M'(CO)_5(THF)$. Addition of CO or Lewis bases to **3a,b** was regiospecific on the metal M' and, depending on the nature of L, was cis or trans to the phosphido bridge. Reactivity studies of dibridged complexes **3a,b** show that the metal−metal bond is a rather weak one. In accordance with our results with the chiral phosphine "PAMP", work to resolve chiral binuclear systems is currently in progress.

Experimental Section

All reactions were carried out under an argon atmosphere with use of standard Schlenk techniques. The solvents and eluents were dried and distilled under argon from sodium and benzophenone immediately before use. Column chromatography was performed under argon and with silica gel (70−230 mesh). $Cp_2Ta(CO)H$, $Cp_2Ta(CO)(PMe_2)$ and $M'(CO)_5(THF)$ were prepared according to literature procedures.[3e,18,19] The synthesis of PhHMeC*NC was adaptated from the literature procedure.[20] The optically active phosphine "PAMP" was

(15) (a) Kubicki, M. M.; Le Gall, J. F.; Kergoat, R.; Gomes De Lima, L. C. *Can. J. Chem.* **1987**, *65*, 1292. (b) Jameson, C. J.; Gutowsky, H. S. *J. Chem. Phys.* **1964**, *40*, 1914.
(16) Nixon, J. F.; Pidcock, A. *Annual Reviews of NMR Spectroscopy* ;Academic Press: London, 1969; Vol. 2, p 346.
(17) (a) Phang, L. T.; Gan, K. S.; Lee, H. K.; Hor, T. S. A. *J. Chem. Soc., Dalton Trans.* **1993**, 2697. (b) Darensbourg, D. J. *Inorg. Chem.* **1979**, *18*, 14.
(18) Foust, D. F.; Rogers, R. D.; Rausch, M. D.; Atwood, J. L. *J. Am. Chem. Soc.* **1982**, *104*, 5646.
(19) Strohmeier, W.; Mueller, F. J. *Chem. Ber.* **1969**, *102*, 3608.

provided by Professor S. Jugé. PMe_2Cl, PMe_2Ph, PPh_3, dmpm, and dmpe (Strem) were used as received.

Elemental analyses (C, H) were performed by the "Service Central d'Analyse du CNRS" (Gif-sur-Yvette, France). Infrared spectra were recorded on a Nicolet 205 IR-FT. Mass spectroscopy was recorded on a Kratos Concept 32 S spectrometer. ^1H, ^{31}P, and ^{13}C NMR spectra were recorded on a Bruker AC 200 spectrometer; chemical shifts are given in ppm relative to Me_4Si (^1H, ^{13}C) or (external) H_3PO_4 (^{31}P).

Synthesis of $Cp_2Ta(\mu\text{-}PMe_2)(CO)M'(CO)_5$ (M' = Cr, Mo, W). General Procedure. To a THF solution (20 mL) of $Cp_2Ta(CO)(PMe_2)$ (0.4 g, 1 mmol) was added an excess (20%) of $M'(CO)_5(THF)$. The mixture was stirred for 20 min at room temperature (the reaction was monitored by IR spectroscopy). The solvent was removed under vacuum, and the crude reaction product was chromatographed on silica gel with toluene as eluant. The brown bimetallic complex was obtained with a 75–80% yield.

$Cp_2Ta(\mu\text{-}PMe_2)(CO)Cr(CO)_5$ (2a). NMR (δ, ppm): $^{13}C\{^1H\}$ ($CDCl_3$) 25.8 (d, J = 10.1 Hz, Me), 90.2 (d, J = 1.2 Hz, Cp), 220.8 (d, J = 10.4 Hz, *cis*-$Cr(CO)_4$), 224.3 (d, J = 8.4 Hz, *trans*-Cr(CO)), 247.2 (d, J = 5.2 Hz, Ta–CO). Anal. Calcd for $C_{18}H_{16}CrO_6PTa$: C, 36.51; H, 2.72. Found: C, 36.56; H, 2.71.

$Cp_2Ta(\mu\text{-}PMe_2)(CO)Mo(CO)_5$ (2b). NMR (δ, ppm): $^{13}C\{^1H\}$ ($CDCl_3$) 26.3 (d, J = 10.1 Hz, Me), 90.3 (s, Cp), 209.2 (d, J = 7.3 Hz, *cis*-$Mo(CO)_4$), 213.4 (d, J = 14.7 Hz, *trans*-Mo(CO)), 250.6 (d, J = 5.5 Hz, Ta–CO). Mass spectrum EI [70 eV, m/z (%)]: 638 (15.8) $[M]^+$; 610 (6.1) $[M - (CO)]^{+\bullet}$, 582 (15.8) $[M - 2(CO)]^{+\bullet}$, 554 (10.8) $[M - 3(CO)]^{+\bullet}$, 526 (10.8) $[M - 4(CO)]^{+\bullet}$, 498 (45.3) $[M - 5(CO)]^{+\bullet}$, 372 (64.7) $[Cp_2Ta(PMe_2)]^{+\bullet}$, 69 (100). Anal. Calcd for $C_{18}H_{16}MoO_6PTa$: C, 33.98; H, 2.54. Found: C, 33.81; H, 2.67.

$Cp_2Ta(\mu\text{-}PMe_2)(CO)W(CO)_5$ (2c). NMR (δ, ppm): $^{13}C\{^1H\}$ ($CDCl_3$) 26.8 (d, J = 12.8 Hz, Me), 90.3 (s, Cp), 201.1 (s, *cis*-$W(CO)_4$), 202.8 (d, J = 12.9 Hz, *trans*-W(CO)), 250.0 (d, J = 4.6 Hz, Ta–CO). Anal. Calcd for $C_{18}H_{16}O_6PTaW$: C, 29.86; H, 2.23. Found: C, 29.83; H, 2.28.

Synthesis of $Cp_2Ta(\mu\text{-}PMe_2)(\mu\text{-}CO)M'(CO)_4$ (M' = Cr, W). General Procedure. A solution of $Cp_2Ta(\mu\text{-}PMe_2)(CO)Cr(CO)_5$ (0.4 g, 0.7 mmol) in THF (60 mL) was irradiated in Pyrex filtering vessels with a high-pressure Hanau TQ 150 mercury lamp for 2 h at room temperature (the reaction was monitored by IR spectroscopy). The solvent was evaporated to dryness under reduced pressure, and the crude reaction product was chromatographed on silica gel with toluene:THF (75:25) as eluant. The red bimetallic complex was obtained with a 70–75% yield.

$Cp_2Ta(\mu\text{-}PMe_2)(\mu\text{-}CO)Cr(CO)_4$ (3a). NMR (δ, ppm): $^{13}C\{^1H\}$ (THF-d_8) 16.2 (d, J = 20.9 Hz, Me), 94.2 (s, Cp), 218.6 (d, J = 8.4 Hz, 2CO), 227.3 (s, 1CO), 229.1 (s, 1CO), 312.5 (s, μ-CO). Mass spectrum EI [70 eV, m/z (%)]: 564 (28.8) $[M]^+$; 536 (17.9) $[M - (CO)]^{+\bullet}$, 480 (40.0) $[M - 3(CO)]^{+\bullet}$, 452 (37.4) $[M - 4(CO)]^{+\bullet}$, 424 (100) $[Cp_2Ta(PMe_2)Cr]^{+\bullet}$, 372 (23.7) $[Cp_2Ta(PMe_2)]^{+\bullet}$, 312 (24.5). Anal. Calcd for $C_{17}H_{16}CrO_5PTa$: C, 36.19; H, 2.86. Found: C, 35.91; H, 2.99.

$Cp_2Ta(\mu\text{-}PMe_2)(\mu\text{-}CO)W(CO)_4$ (3b). NMR (δ, ppm): $^{13}C\{^1H\}$ (THF-d_8) 17.6 (d, J = 19.2 Hz, Me), 93.6 (s, Cp), 199.4 (d, J = 6.3 Hz, 2CO), 201.0 (s, 1CO), 202.7 (s, 1CO), 304.5 (d, J = 25.1 Hz, μ-CO). Mass spectrum EI [70 eV, m/z (%)]: 564 (28.8) $[M]^+$; 536 (17.9) $[M - (CO)]^{+\bullet}$, 480 (40.0) $[M - 3(CO)]^{+\bullet}$, 452 (37.4) $[M - 4(CO)]^{+\bullet}$, 424 (100) $[Cp_2Ta(PMe_2)Cr]^{+\bullet}$, 372 (23.7) $[Cp_2Ta(PMe_2)]^{+\bullet}$. Anal. Calcd for $C_{17}H_{16}O_5PTaW$: C, 29.33; H, 2.32. Found: C, 28.97; H, 2.65.

Synthesis of $Cp_2Ta(\mu\text{-}PMe_2)(CO)M'(CO)_4(L)$ (M' = Cr, W; L = Phosphine, Diphosphine, Isonitrile). General Procedure A. To a THF solution (40 mL) of $Cp_2Ta(\mu\text{-}PMe_2)(CO)M'(CO)_4$ (0.5 mmol) was added 1 equiv of the Lewis base L. The mixture turned green after 15 min of stirring at room temperature. The solvent was removed, and the product was washed with 3 × 20 mL of pentane and dried under vacuum.

General Procedure B. The procedure was the same as above except that the crude product was chromatographed on silica gel with toluene as eluant, yielding a green complex (85–95%).

$Cp_2Ta(\mu\text{-}PMe_2)(CO)Cr(CO)_4$(dmpm) (4a). Procedure A. NMR (δ, ppm): trans isomer (70%) ^1H (C_6D_6) 4.69 (d, J = 1.9 Hz, Cp), 1.88 (d, J = 5.5 Hz, Me), 1.78 (dd, J = 6.1 Hz, J = 3.0 Hz, CH_2), 1.50 (d, J = 7.0 Hz, Me), 0.82 (d, J = 3.7 Hz, Me); ^{31}P (C_6D_6) 37.9 (dd, J = 40 Hz, J = 30 Hz, Cr–PMe_2), −61.0 (d, J = 40 Hz, CH_2-PMe_2), −64.2 (d, J = 30 Hz, μ-PMe_2); cis isomer (30%) ^1H (C_6D_6) 4.67 (d, J = 1.9 Hz, Cp), 1.61 (d, J = 5.1 Hz, Me), 1.39 (d, J = 6.3 Hz, Me), 0.79 (d, J = 3.7 Hz, Me); ^{31}P (C_6D_6) 14.2 (t, J = 33 Hz, Cr–PMe_2), −62.1 (d, J = 33 Hz, CH_2-PMe_2), −76.0 (d, J = 33 Hz, μ-PMe_2). IR (ν(CO), THF): 1979 (m), 1905 (s), 1866 (w), 1847 (vs) cm^{-1}. Mass spectrum EI [70 eV, m/z (%)]: 564 (28.8) $[M]^+$; 536 (17.9) $[M - (CO)]^{+\bullet}$, 480 (40.0) $[M - 3(CO)]^{+\bullet}$, 452 (37.4) $[M - 4(CO)]^{+\bullet}$, 424 (100) $[Cp_2Ta(PMe_2)Cr]^{+\bullet}$, 372 (23.7) $[Cp_2Ta(PMe_2)]^{+\bullet}$. Anal. Calcd for $C_{22}H_{30}CrO_5P_3Ta$: C, 37.73; H, 4.32. Found: C, 37.57; H, 4.29.

$Cp_2Ta(\mu\text{-}PMe_2)(CO)Cr(CO)_4$(dmpe) (5a). Procedure A. NMR (δ, ppm): trans isomer (77%) ^1H (C_6D_6) 4.67 (d, J = 1.9 Hz, Cp), 1.85 (d, J = 5.5 Hz, Me), 1.82–1.55 (m, CH_2), 1.26 (d, J = 7.0 Hz, Me), 0.89 (d, J = 2.8 Hz, Me); ^{31}P (C_6D_6) 34.0 (t, J = 27 Hz, Cr–PMe_2), −49.6 (d, J = 27 Hz, CH_2-PMe_2), −64.5 (d, J = 27 Hz, μ-PMe_2); cis isomer (23%) ^1H (C_6D_6) 4.67 (d, J = 1.8 Hz, Cp), 1.82–1.55 (m, CH_2), 1.57 (d, J = 5.5 Hz, Me), 1.10 (d, J = 6.3 Hz, Me), 0.89 (d, J = 2.8 Hz, Me); ^{31}P (C_6D_6) 13.9 (dd, J = 34 Hz, J = 26 Hz, Cr–PMe_2), −57.6 (d, J = 26 Hz, CH_2-PMe_2), −76.2 (d, J = 34 Hz, μ-PMe_2). IR (ν(CO), THF): 1978 (m), 1905 (s), 1865 (w), 1848 (vs) cm^{-1}. Mass spectrum EI [70 eV, m/z (%)]: 714 (0.7) $[M]^+$; 686 (3.2) $[M - (CO)]^{+\bullet}$, 574 (12.2) $[M - 5(CO)]^{+\bullet}$, 372 (7.2) $[Cp_2TaPMe_2]^{+\bullet}$. Anal. Calcd for $C_{23}H_{32}CrO_5P_3Ta$: C, 38.67; H, 4.52. Found: C, 38.46; H, 4.26.

$Cp_2Ta(\mu\text{-}PMe_2)(CO)Cr(CO)_4(PMe_2Ph)$ (6a). Procedure B. NMR (δ, ppm): cis isomer (64%) ^1H (C_6D_6) 4.58 (d, J = 1.8 Hz, Cp), 1.52 (d, J = 6.5 Hz, Me), 1.27 (d, J = 5.3 Hz, Me), 6.95–7.57 (m, Ph); ^{31}P (C_6D_6) 17.8 (d, J = 34 Hz, Cr–PMe_2-Ph), −75.7 (d, J = 34 Hz, μ-PMe_2); trans isomer (36%) ^1H (C_6D_6) 4.62 (d, J = 1.9 Hz, Cp), 1.84 (d, J = 5.5 Hz, Me), 1.61 (d, J = 7.0 Hz, Me), 6.95–7.57 (m, Ph); ^{31}P (C_6D_6) 38.2 (d, J = 29 Hz, Cr–PMe_2Ph), −61.9 (d, J = 29 Hz, μ-PMe_2). IR (ν(CO), THF): 1980 (m), 1907 (s), 1876 (w), 1867 (s), 1848 (s) cm^{-1}. Mass spectrum EI [70 eV, m/z (%)]: 702 (7.9) $[M]^+$; 620 (27.7), 452 (25.9) $[M - (PMe_2Ph) - 4(CO)]^{+\bullet}$, 424 (87.1) $[M - (PMe_2Ph) - 5(CO)]^{+\bullet}$, 372 (78.1) $[Cp_2TaPMe_2]^{+\bullet}$, 312 (100). Anal. Calcd for $C_{25}H_{27}CrO_5P_2Ta$: C, 42.75; H, 3.87. Found: C, 42.12; H, 3.66.

$Cp_2Ta(\mu\text{-}PMe_2)(CO)Cr(CO)_4(PPh_3)$ (7a). Procedure B. NMR (δ, ppm): trans isomer ^1H (C_6D_6) 4.63 (d, J = 1.9 Hz, Cp), 1.92 (d, J = 5.6 Hz, Me), 7.15–6.99 and 7.87–7.79 (m, Ph); ^{31}P (C_6D_6) 78.6 (d, J = 25 Hz, Cr–PPh_3), −61.4 (d, J = 25 Hz, μ-PMe_2). IR (ν(CO), THF): 1909 (m), 1855 (s) cm^{-1}. Mass spectrum EI [70 eV, m/z (%)]: 686 (4.7) $[M - 5(CO)]^{+\bullet}$, 592 (83.4) $[M - (PPh_3 + CO)]^{+\bullet}$, 564 (14.1) $[M - (PPh_3)]^{+\bullet}$, 536 (28.4) $[M - (PPh_3) - (CO)]^{+\bullet}$, 452 (55.0) $[M - (PPh_3) - 4(CO)]^{+\bullet}$, 424 (93.5) $[M - (PPh_3) - 5(CO)]^{+\bullet}$, 372 (66.2) $[Cp_2TaPMe_2]^{+\bullet}$, 312 (69.8), 262 (100) $[PPh_3]^{+\bullet}$. Anal. Calcd for $C_{35}H_{31}CrO_5P_2Ta$: C, 50.86; H, 3.78. Found: C, 49.38; H, 3.51.

$Cp_2Ta(\mu\text{-}PMe_2)(CO)Cr(CO)_4(^tBuNC)$ (8a). Procedure B. NMR (δ, ppm): cis isomer ^1H (C_6D_6) 4.65 (d, J = 2 Hz, Cp), 1.69 (d, J = 5.4 Hz, Me), 0.93 (s, ^{t}Bu); ^{31}P (C_6D_6) −74.7 (s, μ-PMe_2). IR (ν(CO), THF): 1984 (s), 1907 (s), 1894 (s), 1878 (vs), 1861 (s) cm^{-1}. IR (ν(CN), THF): 2115 (m) cm^{-1}. Mass spectrum EI [70 eV, m/z (%)]: 647 (68.9) $[M]^+$; 563 (18.5) $[M - 3(CO)]^{+\bullet}$, 535 (52.9) $[M - 4(CO)]^{+\bullet}$, 507 (100) $[M - 5(CO)]^{+\bullet}$, 372 (25.5) $[Cp_2TaPMe_2]^{+\bullet}$. Anal. Calcd for $C_{22}H_{25}CrNO_5PTa$: C, 40.82; H, 3.89. Found: C, 40.75; H, 4.17.

(20) Ugi, I.; Meyr, R.; Lipinski, M.; Bodesheim, F.; Rosendahl, F. *Org. Synth.* **1961**, *41*, 13.

$Cp_2Ta(\mu\text{-}PMe_2)(CO)Cr(CO)_4(2,6\text{-}Me_2C_6H_3\text{-}NC)$ (9a). Procedure B. NMR (δ, ppm): cis isomer ^1H (C_6D_6) 4.60 (d, J = 1.7 Hz, Cp), 2.27 (s, Me), 1.69 (d, J = 5.3 Hz, Me), 7.5–6.8 (m, Ph); ^{31}P (C_6D_6) −72.8 (s, μ-PMe_2). IR (ν(CO), THF): 1975 (s), 1905 (s), 1886 (s), 1874 (s), cm^{-1}. IR (ν(CN), THF): 2081 (m) cm^{-1}. Mass spectrum EI [70 eV, m/z (%)]: 695 (95.3) $[M]^+$; 667 (17.6) $[M - (CO)]^{+\bullet}$, 611 (49.6) $[M - 3(CO)]^{+\bullet}$, 583 (57.5) $[M - 4(CO)]^{+\bullet}$, 555 (100) $[M - 5(CO)]^{+\bullet}$. Anal. Calcd for $C_{26}H_{25}CrNO_5PTa$: C, 44.91; H, 3.62. Found: C, 43.97; H, 3.59.

$Cp_2Ta(\mu\text{-}PMe_2)(CO)Cr(CO)_4$(PhHMeC*NC) (10a). Procedure B. NMR (δ, ppm): cis isomer ^1H (C_6D_6) 4.59 (d, J = 1.9 Hz, Cp), 4.11 (dq, J = 6.5 Hz, J = 1.8 Hz, H), 1.64 (d, J = 5.3 Hz,PMe_2), 1.13 (d, J = 6.8 Hz, Me), 7.13–6.92 (m, Ph); ^{31}P (C_6D_6) −72.2 (s, μ-PMe_2). IR (ν(CO), THF): 1984 (s), 1907 (s), 1896 (s), 1880 (vs),1863 (s), cm^{-1}. IR (ν(CN), THF): 2175 (m) cm^{-1}. Mass spectrum EI [70 eV, m/z (%)]: 695 (25.2) $[M]^+$; 611 (7.0) $[M -3 (CO)]^{+\bullet}$, 583 (12.0) $[M -4(CO)]^{+\bullet}$, 555 (36.7) $[M -5(CO)]^{+\bullet}$, 452 (31.2) [M-4(CO)-(CNR)]$^+$, 424 (100) [M-5(CO)-(CNR)]$^+$, 372 (9.0) $[Cp_2TaPMe_2]^{+\bullet}$ Anal. Calcd for $C_{26}H_{25}CrNO_5PTa$: C, 44.91; H, 3.62. Found: C, 45.09; H, 3.44.

$Cp_2Ta(\mu\text{-}PMe_2)(CO)W(CO)_4$(dmpm) (4b). Procedure A. NMR (δ, ppm): cis isomer ^1H (C_6D_6) 4.70 (d, J = 1.9 Hz, Cp), 1.83 (dd, J = 5.3 Hz, J = 2.7 Hz, CH_2), 1.73 (d, J = 5.1 Hz, Me), 1.47 (d, J = 6.4 Hz, Me), 0.80 (d, J = 3.7 Hz, Me); ^{31}P (C_6D_6) 32.2 (dd, J = 42 Hz, J = 28 Hz, $J(P-^{183}W)$ = 210 Hz, W−PMe_2), −61.8 (d, J = 42 Hz, CH_2-PMe_2), −119.9 (d, J = 28 Hz, $J(P-^{183}W)$ = 170 Hz, μ-PMe_2). IR (ν(CO), THF): 1992 (m), 1905 (s), 1880 (s), 1868 (s), 1840 (s) cm^{-1}. Anal. Calcd for $C_{22}H_{30}O_5P_3TaW$: C, 31.75; H, 3.63. Found: C, 31.76; H, 3.66.

$Cp_2Ta(\mu\text{-}PMe_2)(CO)W(CO)_4$(dmpe) (5b). Procedure A. NMR (δ, ppm): cis isomer ^1H (C_6D_6) 4.71 (d, J = 1.9 Hz, Cp), 1.81–1.60 (m, CH_2), 1.69 (d, J = 5.1 Hz, Me), 1.21 (d, J = 6.5 Hz, Me), 0.91 (d, J = 2.8 Hz, Me); ^{31}P (C_6D_6) −29.9 (t, J = 25 Hz, $J(P-^{183}W)$ = 165 Hz, W−PMe_2), −49.4 (d, J = 25 Hz, CH_2-PMe_2), −120.4 (d, J = 25 Hz, $J(P-^{183}W)$ = 169 Hz, μ-PMe_2). IR (ν(CO), THF): 1992 (m), 1906 (s), 1881 (s), 1869 (s), 1840 (s) cm^{-1}. Mass spectrum EI [70 eV, m/z (%)]: 832 (1.4) $[M]^+$; 804 (2.1) $[M - (CO)]^{+\bullet}$, 776 (5.7) $[M - 2(CO)]^{+\bullet}$, 400 (29.1) $[Cp_2TaPMe_2(CO)]^{+\bullet}$, 372 (100) $[Cp_2TaPMe_2]^{+\bullet}$. Anal. Calcd for $C_{23}H_{32}O_5P_3TaW$: C, 32.65; H, 3.81. Found: C, 32.58; H, 3.99.

$Cp_2Ta(\mu\text{-}PMe_2)(CO)W(CO)_4(PMe_2Ph)$ (6b). Procedure B. NMR (δ, ppm): cis isomer ^1H (C_6D_6) 4.65 (d, J = 1.9 Hz, Cp), 1.62 (d, J = 4 Hz, Me), 1.38 (d, J = 6 Hz, Me), 7.42–6.91 (m, Ph); ^{31}P (C_6D_6) −28.8 (d, J = 24 Hz, $J(P-^{183}W)$ = 173 Hz, W−PMe_2Ph), −128.8 (d, J = 24 Hz, $J(P-^{183}W)$ = 173 Hz, μ-PMe_2). IR (ν(CO), THF): 1993 (s), 1907 (s), 1882 (s), 1870 (vs), 1841 (s) cm^{-1}. Anal. Calcd for $C_{25}H_{27}O_5P_2TaW$: C, 35.99; H, 3.26. Found: C, 35.73; H, 3.04.

$Cp_2Ta(\mu\text{-}PMe_2)(CO)W(CO)_4(PPh_3)$ (7b). Procedure B. NMR (δ, ppm): trans isomer (5%) ^1H (C_6D_6) 4.63 (d, J = 2 Hz, Cp), 2.20 (d, J = 6.3 Hz, Me), 7.91–7.70 and 7.14–6.90 (m, Ph); ^{31}P (C_6D_6) −117.83 (d, J = 35 Hz, $J(P-^{183}W)$ = 192 Hz, μ-PMe_2), 29.4 (d, J = 35 Hz, $J(P-^{183}W)$ = 192 Hz, W−PPh_3); cis isomer (95%) ^1H (C_6D_6) 4.61 (d, J = 2 Hz, Cp), 1.45 (d, J = 5.4 Hz, Me), 7.91–7.70 and 6.90–7.14 (m, Ph); ^{31}P (C_6D_6) 19.8 (d, J = 25 Hz, $J(P-^{183}W)$ = 173 Hz, W−PPh_3), −126.0 (d, J = 25 Hz, $J(P-^{183}W)$ = 173 Hz, μ-PMe_2). IR (ν(CO), THF): 1996 (m), 1908 (vs), 1887 (s), 1872 (s), 1859 (s), 1848 (s) cm^{-1}. Anal. Calcd for $C_{35}H_{31}O_5P_2TaW$: C, 43.86; H, 3.26. Found: C, 42.58; H, 3.23.

$Cp_2Ta(\mu\text{-}PMe_2)(CO)W(CO)_4(^tBuNC)$ (8b). Procedure B. NMR (δ, ppm): cis isomer ^1H (C_6D_6) 4.65 (d, J = 1.9 Hz, Cp), 1.83 (d, J = 5 Hz, Me), 0.89 (s, ^{t}Bu); ^{31}P (C_6D_6) −118.3 (s, $J(P-^{183}W)$ = 173 Hz, μ-PMe_2). IR (ν(CO), THF): 1991 (s), 1907 (s), 1894 (s), 1880 (vs), 1859 (s) cm^{-1}. IR (ν(CN), THF): 2123 (m) cm^{-1}. Anal. Calcd for $C_{22}H_{25}NO_5PTaW$: C, 33.91; H, 3.23. Found: C, 33.31; H, 3.15.

$Cp_2Ta(\mu\text{-}PMe_2)(CO)W(CO)_4(2,6\text{-}Me_2C_6H_3\text{-}NC)$ (9b). Procedure B. NMR (δ, ppm): cis isomer ^1H (C_6D_6) 4.60 (d, J = 2 Hz, Cp), 2.20 (s,Me), 1.84 (d, J = 5 Hz, Me), 7.81–6.50 (m, Ph); ^{31}P (C_6D_6) −118.5 (s, $J(P-^{183}W)$ = 173 Hz, μ-PMe_2). IR (ν(CO), THF): 1980 (s), 1905 (s), 1885 (s), 1871 (s), cm^{-1}. IR (ν(CN), THF): 2088 (m) cm^{-1}. Anal. Calcd for $C_{26}H_{25}NO_5$-PTaW: C, 37.75; H, 3.05. Found: C,37.71; H, 3.18.

$Cp_2Ta(\mu\text{-}PMe_2)(CO)W(CO)_4$(PhHMeC*NC) (10b). Procedure B. NMR (δ, ppm): cis isomer ^1H (C_6D_6) 4.60 (d, J = 2.2 Hz, Cp), 4.12 (dq, J = 6.8 Hz, J = 1.8 Hz, H), 1.78 (d, J = 5.6 Hz, PMe_2), 1.09 (d, J = 6.8 Hz, Me), 7.10–6.92 (m, Ph); ^{31}P (C_6D_6) −115.7 (s, $J(P-^{183}W)$ = 173 Hz, μ-PMe_2). IR (ν(CO), THF): 1990 (s), 1906 (s), 1895 (s), 1879 (vs),1862 (s), cm^{-1}. IR (ν(CN), THF): 2123 (m) cm^{-1}. Anal. Calcd for $C_{26}H_{25}NO_5$-PTaW: C, 37.75; H, 3.05. Found: C, 37.67; H, 2.78.

$Cp_2Ta(\mu\text{-}PMe_2)(CO)W(CO)_4$(P*MePh(o-An)) (11). Procedure B. NMR (δ, ppm): cis isomer ^1H (C_6D_6) 4.63 (d, J = 1.7 Hz, Cp), 4.62 (d, J = 1.7 Hz, Cp), 3.25 (s, OMe), 2.08 (d, J = 5.6 Hz, P*Me), 1.45 (d, J = 4.9 Hz, μ-PMe), 1.43 (d, J = 4.9 Hz, μ-PMe), 7.9–6.3 (m, Ph); ^{31}P (C_6D_6) −122.3 (d, J = 27.2 Hz, $J(P-^{183}W)$ = 171.1 Hz, μ-PMe_2), −13.9 (d, J = 27.2 Hz, $J(P-^{183}W)$ = 171.1 Hz, W−P*). IR (ν(CO), THF): 1993 (s), 1904 (s), 1883 (s), 1867 (vs), 1841 (s) cm^{-1}. Anal. Calcd for $C_{31}H_{31}O_6P_2TaW$: C, 40.20; H, 3.37. Found: C, 40.76; H, 3.20. $[\alpha]^{25}_D$ −32.5° (c 6.0, toluene).

Acknowledgment. We thank Professor S. Jugé for the gift of a sample of optically active phosphine "PAMP".

OM9505524

Heterobimetallic Alkyl Polyhydride Complexes of Rhenium and Platinum

Andrei D. Batsanov,† Judith A. K. Howard,† Jason B. Love,‡ and John L. Spencer*,‡

Chemical Sciences Division, Science Research Institute, University of Salford, Salford M5 4WT, U.K., and Department of Chemistry, University of Durham, Durham DH1 3LE, U.K.

Received February 23, 1995⊗

The utilization of the rhenium heptahydride complex [ReH_7(dbpe)] [dbpe = $Bu^t_2P(CH_2)_2PBu^t_2$] in reactions with bis(alkene) complexes of platinum has facilitated the isolation of the heterobimetallic alkyl polyhydride complexes [Re(dbpe)H_6Pt(R′)(PR_3)] [R′ = C_2H_5, PR_3 = PCy_3 (Cy = cyclohexyl); R′ = C_7H_{11} (2-norbornyl), PR_3 = PPh_3, PCy_3, PBu^t_3], which are resistant to the reductive elimination of alkane. The crystal structure of [Re(dbpe)H_6Pt(C_2H_5)(PCy_3)] was elucidated by X-ray crystallography. The molecule was shown to have a short Re–Pt bond [2.643(1) Å]. For the case R′ = 2-norbornyl and PR_3 = PBu^t_3, the β-elimination of norbornene is observed, resulting in the formation of the bimetallic heptahydride complex [Re(dbpe)H_7Pt(PBu^t_3)]. The complex [ReH_7(dbpe)Pt(PCy_3)] may be made by the direct reaction of [$Pt(cod)_2$] with [ReH_7(dbpe)] and PCy_3. All of the bimetallic complexes undergo H/D exchange reactions in C_6D_6 at ambient temperatures, with both metal hydride and methyl protons of the dbpe ligand being active. The reaction between [ReH_7(dbpe)] and [$Pt(nb)_3$] (nb = norbornene) affords a species capable of polymerizing norbornene.

Introduction

Facile, thermally induced, reductive elimination of molecular hydrogen from rhenium heptahydride complexes such as [$ReH_7(PPh_3)_2$] has allowed access to a wealth of organorhenium complex chemistry over the past 20 years.[1a,b] The creation of coordinative unsaturation at the metal center by this method enables two-electron-donor ligands to coordinate,[2] and in the presence of the hydrogen acceptor, 3,3-dimethylbutene, the catalytic dehydrogenation of alkanes can be induced.[3] The observed lability with respect to the loss of dihydrogen has also prompted a reinvestigation of the structures of rhenium heptahydrides, with Crabtree proposing the formulation of some complexes as [Re(η^2-H_2)H_5(PR_3)$_2$], i.e., containing ligated molecular hydrogen.[4] The complex [ReH_7(P{*p*-tolyl}$_3$)$_2$] has been shown by neutron diffraction studies to contain a short H···H distance of 1.357(7) Å, which is between that for a classical dihydride and that for a nonclassical dihydrogen ligand.[5]

An alternative to the thermal activation of rhenium polyhydride complexes is one that utilizes the incorporation of a second, different metal center in order to proffer coordinative unsaturation, a route that has the added promise of metal–metal cooperativity. The synthesis of several mixed-metal polyhydride complexes has been realized,[6] for example, the Re–Ru complex [$ReRuH_5$(CO)(PPh_3)$_4$], which, upon protonation, formed the first Re–Ru dihydrogen complex [Re(PPh_3)$_2$H(μ-H)$_3$(μ-CO)Ru(η^2-H_2)(PPh_3)$_2$]$^+$ [7] and the Ir–Ru complex [$IrRuH_3$(1,5-cod)(PPh_3)$_3$] (cod = cyclooctadiene), which reversibly dehydrogenates at room temperature to yield the cyclometalated complex [Ir(1,5-cod)(μ-H)Ru(H)(PPh_2{C_6H_4})(PPh_3)$_2$].[8]

A reaction of particular interest to us was that leading to the formation of [$ReH_3(C_2H_4)_2(PR_3)_2$] complexes, which, although formed in low yields from the parent heptahydride complex with ethene at high temperature, are best synthesized from [$ReH_7(PR_3)_2$] and ethene in the presence of catalytic amounts of Pt^0 species at ambient temperatures.[9,10] This latter reaction was believed to proceed (Scheme 1) via the formation of a transient Re–Pt bimetallic complex that decomposed by the reductive elimination of ethane and cleavage of the Re–Pt bond, generating the coordinatively unsaturated

† University of Durham.
‡ University of Salford.
⊗ Abstract published in *Advance ACS Abstracts,* October 15, 1995.

(1) (a) Chatt, J.; Coffey, R. S. *J. Chem. Soc. A* **1969**, 1963. (b) Hlatky, G. G.; Crabtree, R. H. *Coord. Chem. Rev.* **1985**, *65*, 1.
(2) Baudry, D.; Ephritikhine, M.; Felkin, H. *J. Organomet. Chem.* **1982**, *224*, 363.
(3) (a) Baudry, D.; Boydell, P.; Ephritikhine, M. *J. Chem. Soc., Dalton Trans.* **1986**, 525. (b) Baudry, D.; Ephritikhine, M.; Felkin, M.; Jeannin, Y.; Robert, F. *J. Organomet. Chem.* **1981**, *220*, C7. (c) Baudry, D.; Ephritikhine, M.; Felkin, H. *J. Chem. Soc., Chem. Commun.* **1982**, 606.
(4) Hamilton, D. G.; Crabtree, R. H. *J. Am. Chem. Soc.* **1988**, *110*, 4126.
(5) Brammer, L.; Howard, J. A. K.; Johnson, O.; Koetzle, T. F.; Spencer, J. L. *J. Chem. Soc., Chem. Commun.* **1991**, 241.
(6) (a) Baudry, D.; Ephritkhine, M. *J. Organomet. Chem.* **1986**, *311*, 189. (b) Bruno, J. W.; Hoffman, J. C.; Green, M. A.; Caulton, K. G. *J. Am. Chem. Soc.* **1984**, *106*, 8310. (c) Skupinski, W. A.; Hoffman, J. C.; Bruno, J. W.; Caulton, K. G. *J. Am. Chem. Soc.* **1984**, *106*, 8128. (d) Carr, S. W.; Fontaine, K. L. R.; Shaw, B. L. *J. Chem. Soc., Dalton Trans.* **1991**, 1025. (e) Connelly, N. G.; Howard, J. A. K.; Spencer, J. L.; Woodley, P. K. *J. Chem. Soc., Dalton Trans.* **1984**, 2003.
(7) Cazanoue, M.; Neibecker, D.; Mathieu, R. *J. Chem. Soc., Chem. Commun.* **1991**, 307.
(8) Poulton, J. T.; Folting, K.; Caulton, K. G. *Organometallics* **1992**, *11*, 1364.
(9) Hazel, N. J.; Howard, J. A. K.; Spencer, J. L. *J. Chem. Soc., Chem. Commun.* **1984**, 1663.
(10) Dix, N.; Spencer, J. L.; Bradley, M. R.; Hazel, N. J.; Howard, J. A. K. Unpublished.

0276-7333/95/2314-5657$09.00/0

Scheme 1

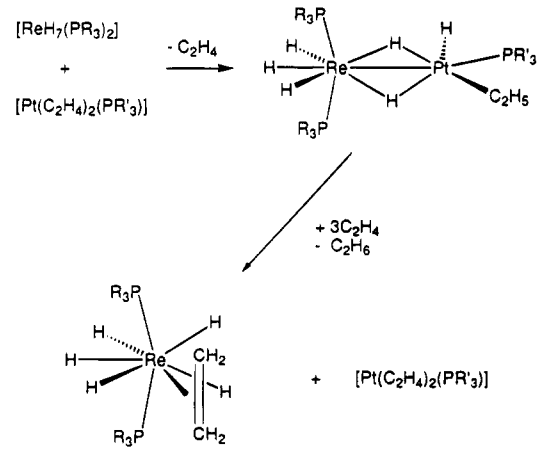

rhenium species $[ReH_5(PR_3)_2]$ to which ethene could coordinate. Further reaction of the pentahydride complex with ethene affords the bis(ethene) complex. Although the bimetallic complex was clearly observed in the ^{31}P NMR spectrum, it proved to be too unstable to isolate despite the use of a range of monodentate phosphine ligands.

A strategy that has been used to confer kinetic stability on metal complexes is to incorporate chelating ancillary ligands. The iridium complex $[IrH_2(Et)(triphos)]$[11] [triphos = $Ph_2PCH_2C\{CH_3\}\{CH_2PPh_2\}_2$] and the rhenium polyhydride $[ReH_6(triphos)]^+$ [12] are stabilized against the reductive elimination of ethane or H_2, respectively, by the incorporation of the tripodal ligand. In other work we have observed the protecting influence of sterically demanding chelating diphosphines on reactive metal centers.[13] We therefore reasoned that the incorporation of a chelating diphosphine at the rhenium center would stabilize the Re–Pt bimetallic complex against the reductive elimination of the alkane by restraining the position of the ligating phosphorus atoms, while at the same time providing steric protection through the bulky substituent groups.

This paper describes the synthesis of the novel rhenium heptahydride complex $[ReH_7(dbpe)]$ and its reactions with Pt^0 complexes, forming heterobimetallic polyhydride and alkyl polyhydride complexes of rhenium and platinum.

Results and Discussion

The preferred route to rhenium heptahydride chemistry is via the complex $[ReOCl_3(PPh_3)_2]$, from which the triphenylphosphine ligands are readily displaced by more basic phosphines such as PPh^iPr_2.[1a,6e] The reaction between equimolar quantities of $[ReOCl_3(PPh_3)_2]$ and the chelating diphosphine 1,2-bis(di-*tert*-butylphosphino)ethane (dbpe) in dichloromethane for 30 min was found to result in the formation of *fac*-$[ReOCl_3(dbpe)]$ (**1**) in high yield (85%), isolated as a pale green solid by precipitation from solution upon the addition of Et_2O (Scheme 2). The IR spectrum of **1** displays a characteristic ν(Re=O) absorption at 985 cm^{-1}.[14] The assignment of the fac isomer follows from the $^{31}P\{^1H\}$ NMR spectrum, which showed that the phosphorus nuclei were equivalent, resonating at δ 20.2 as a singlet. Similar fac geometries have been observed for the complexes $[ReOCl_3(\sqcap\!\!\sqcap PP)]$, where $\sqcap\!\!\sqcap PP$ is a chelating tetraphenyldiphosphine such as 1,1′-bis(diphenylphosphino)ferrocene (dppf).[15] Complex **1** is moisture sensitive, which may be a result of the lability of the chloride ligand trans to the Re=O bond, and thus for storage purposes complex **1** was converted into the ethoxy derivative $[ReOCl_2(OEt)(dbpe)]$ (**2**). The addition of ethanol to a dichloromethane solution of **1** at 20 °C immediately generated the dark blue complex **2** in good yield (80%). In the infrared spectrum, this complex shows characteristic ν(ReO) and ν(ReOEt) absorptions at 963 and 909 cm^{-1} respectively.[14]

Scheme 2

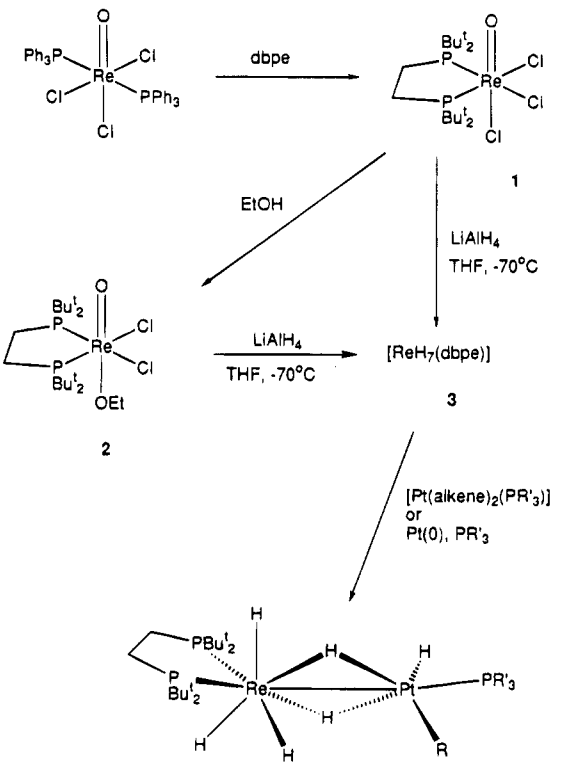

	R	R'
4	Et	Cy
5	C_7H_{11}	Ph
6	C_7H_{11}	Cy
7	C_7H_{11}	Bu^t
8	H	Bu^t
9	H	Cy

The treatment of complexes **1** or **2** with $LiAlH_4$ in THF at −70 °C generated the desired rhenium heptahydride complex $[ReH_7(dbpe)]$ (**3**) as air-stable, white platelets in fair yield (60%). The ^1H NMR spectrum of **3** in C_6D_6 displays a triplet resonance at δ −6.87, integrating as seven protons that can be ascribed to the fluxional hydride ligands. Unfortunately, even with the conformational restraints imposed on this complex by the chelating diphosphine, the hydride ligands were still

(11) Barbaro, P.; Bianchini, C.; Meli, A.; Peruzzini, M.; Vacca, A.; Vizza, F. *Organometallics* **1991**, *10*, 2227.
(12) Luo, X.-L.; Crabtree, R. H. *J. Chem. Soc., Dalton Trans.* **1991**, 587.
(13) (a) Mole, L.; Spencer, J. L.; Carr, N.; Orpen, A. G. *Organometallics* **1991**, *10*, 49. (b) Carr, N.; Dunne, B. J.; Mole, L.; Orpen, A. G.; Spencer, J. L. *J. Chem. Soc., Dalton Trans.* **1991**, 863.
(14) Johnson, N. P.; Lock, C. J.; Wilkinson, G. *J. Chem. Soc.* **1964**, 1054.
(15) Luo, X.-L.; Crabtree, R. H. *J. Am. Chem. Soc.* **1990**, *112*, 4813.

Table 1. Selected Spectroscopic Data[a] for the Complexes [Re(dbpe)H$_6$Pt(R′)(PR$_3$)]

complex	PR$_3$	R′	δ_H	J_{PtH}	$\delta_{C\alpha}$	$J_{PtC\alpha}$	δ_P[b]	J_{PtP}
4[c]	PCy_3	Et	−5.01	250	2.02	570	101.3	
							33.7	3856
5	PPh_3	C_7H_{11}	−5.22	264	35.7	563	101.24	18.3
							27.7	4302
6	PCy_3	C_7H_{11}	−5.21	240	31.2	593	102.3	
							34.9	4082
7	PBu^t_3	C_7H_{11}	−5.40	251	25.2	642	102.6	
							83.7	4096

[a] C_4D_8O, 298 K. Chemical shifts are in ppm, relative to $SiMe_4$. Coupling constants are in Hz. [b] Re*P* then Pt*P*. [c] Solvent: C_6D_6.

observed to be undergoing fast site exchange at 190 K, in contrast to the behavior observed for the complex [ReH$_7$(dppf)].[15] Hydride multiplicity was unambiguously determined by the selective decoupling of the nonhydride protons in the ^{31}P NMR spectrum. The resonance at δ 90.7 then appeared as a binomial octet due to the residual coupling of seven hydrides.

Synthesis of the Complexes [Re(dbpe)H$_6$Pt(R′)(PR$_3$)] [R′ = Et, PR$_3$ = PCy$_3$; R′ = (2-norbornyl), PR$_3$ = PPh$_3$, PCy$_3$, PBu$^t_3$]. Monitoring of the stoichiometric reaction between the polyhydride **3** and the platinum complex [Pt(C$_2$H$_4$)$_2$(PCy$_3$)] (Cy = cyclohexyl, C$_6$H$_{11}$) in toluene at 25 °C by ^{31}P{^{1}H} NMR spectroscopy revealed that the immediate, clean conversion of the precursors into the heterobimetallic complex [Re(dbpe)H$_6$Pt(Et)(PCy$_3$)] (**4**) had occurred, as described in Scheme 2, with the appearance of related resonances at δ 101.3 and 33.7. The latter resonance has associated ^{195}Pt satellites with a large coupling constant $^1J_{PtP}$ (3856 Hz) and so is attributed to the PCy$_3$ ligand.

As no further reaction was observed after a period of 1 day, the original premise that the use of a bulky, chelating diphosphine would stabilize the transient Re–Pt complex is apparently valid. Complex **4** was isolated in excellent yield as a moderately air-stable, yellow powder and recrystallized as orange prisms from hexane at −20 °C. Selected spectroscopic data are detailed in Table 1. Only limited information is available from the ^{1}H NMR spectrum of **4**. The low-frequency pseudoquartet at δ −5.01 confirmed the presence of fluxional hydride ligands, with the coupling to platinum of 250 Hz representing an average for six hydride ligands shared between the two metals. Unfortunately, the hydride site exchange process was still rapid at 183 K.

Three broad resonances at 2.05, 1.70, and 1.20 ppm in the ^{1}H NMR spectrum can be assigned to the tricyclohexylphosphine ligand. The signal due to the Bu^t protons was clearly observed as a sharp doublet, but the resonances due to the ethyl ligand and ethylene bridge of dbpe were obscured by the cyclohexyl signals. However, the presence of the ethyl ligand was confirmed in the ^{13}C{^{1}H} NMR spectrum, in which the platinum-bound methylene group resonates as a doublet at δ 2.02, coupled to both phosphorus and platinum, and the methyl group is seen as a singlet at δ 25.7, the assignment of which was aided by a 135° DEPT ^{13}C NMR spectrum. The chemical shifts and the magnitudes of the coupling constants of the ethyl group resonances are similar to those of other heterobimetallic platinum ethyl complexes, such as [Ir(PEt$_3$)$_3$(H)(μ-H)$_2$Pt(Et)(PEt$_3$)].[16] The hydride multiplicity could not be proven unambiguously by selective ^{1}H decoupling techniques, which is presumably due to the more complex

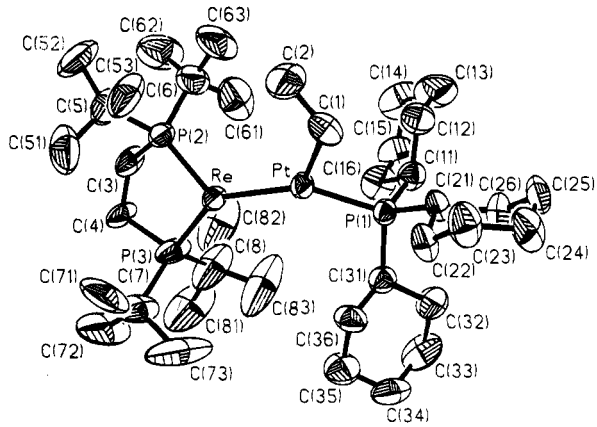

Figure 1. Molecular structure of [Re(dbpe)H$_6$Pt(Et)(PCy$_3$)] (**4**) with thermal ellipsoids at 50% probability.

spin system of complex **4**. Nevertheless, the ratio of integrals of hydridic to aliphatic protons did suggest the presence of six hydride ligands. This is supported by the precedent of the ReH$_6$L$_2$ unit in other heterobimetallic polyhydride complexes, as observed with [Re(PPh$_3$)$_2$H$_6$U(η^5-C$_5$H$_5$)$_3$],[6a] [Re(PPhMe$_2$)$_2$H$_6$Zr(CH$_3$)(η^5-C$_5$H$_5$)$_2$],[6b] and [Re(PPhMe$_2$)$_2$H$_6$AlMe$_2$].[6c] The stereochemical arrangement of the hydride ligands is more ambiguous. An X-ray diffraction study of a crystal of **4** was undertaken with the intention of resolving the remaining structural questions. The molecular structure of **4** is shown in Figure 1, and Tables 2–4 contain the atomic coordinates and bond distances and angles. Both rhenium and platinum atoms have slightly pyramidalized trigonal coordination if only the non-hydrogen atoms are considered. The Re atom deviates by 0.23 Å from the PtP(2)P(3) plane, and the Pt atom deviates by 0.16 Å from the ReP(1)C(1) plane to the same side. However, the two planes are not coplanar, forming a dihedral angle of 36.5°. All cyclohexyl rings adopt chair conformations. The five-membered chelate metallacycle adopts a half-chair conformation, with the C(3) and C(4) atoms tilted out of the ReP(2)P(3) plane by 0.24 and −0.27 Å (in opposite directions).

The Re—Pt bond distance of 2.643(1) Å is the shortest reported to date, as the previously observed values range from 2.788 to 2.906 Å.[17] It is comparable to the length of Re=Re double bonds (which fall mainly in the range 2.35–2.70 Å). In the unique structurally characterized compound with a formal Re=Pd double bond, [RePd(PMe$_3$)$_3${P(C$_6$H$_{11}$)$_2$}$_3$], this bond has a somewhat longer length of 2.758 Å.[18] The X-ray diffraction study of an osmium analogue of **4**, the complex [Os{P(cyclo-C$_5$H$_9$)$_3$}$_2$H$_5$Pt(Et){P(cyclo-C$_5$H$_9$)$_3$}], revealed one platinum- and two osmium-bound terminal hydrides, with the two remaining hydrides occupying bridging positions.[19] A similar stereochemical arrangement can be envisaged for complex **4**, with, in this case, three terminal hydrides at the rhenium center. Although the IR spectrum does suggest the presence of both terminal rhenium and platinum hydrides, no absorptions that could be assigned to bridging hydrides were observed.

(16) Boron, P.; Musco, A.; Venanzi, L. M. *Inorg. Chem.* **1982**, *21*, 4192.
(17) Cambridge Crystallographic Database, Version 4.5, July 1991.
(18) Baker, R. T.; Calabrese, J. C.; Glassman, T. E. *Organometallics* **1988**, *7*, 1889.
(19) Howard, J. A. K.; Weinberg, L. F.; Spencer, J. L. Unpublished.

Table 2. Atomic Coordinates ($\times 10^4$) and Equivalent Isotropic Displacement Coefficients (Å^2 $\times$ 10^3) for 4 (Non-Hydrogen Atoms)

atom	x	y	z	U_{eq}[a]
Pt	8903(1)	8087(1)	1667(1)	45(1)
Re	7874(1)	7138(1)	2272(1)	53(1)
P(1)	10586(2)	8235(2)	1721(1)	44(1)
P(2)	6468(2)	6227(2)	1797(1)	62(1)
P(3)	8012(3)	6407(3)	3249(2)	93(2)
C(1)	8373(10)	8751(7)	808(5)	60(5)
C(2)	7316(12)	8467(11)	408(7)	100(7)
C(3)	6429(10)	5428(8)	2401(6)	75(5)
C(4)	6850(10)	5708(9)	3096(5)	81(6)
C(5)	5092(11)	6679(11)	1533(8)	93(7)
C(6)	6588(14)	5549(11)	1104(7)	96(8)
C(7)	7844(21)	7052(19)	3960(8)	156(14)
C(8)	9210(15)	5694(17)	3534(11)	156(12)
C(11)	11049(10)	7344(7)	1352(6)	59(5)
C(12)	10474(11)	7294(9)	623(7)	77(6)
C(13)	10820(14)	6525(11)	320(9)	112(9)
C(14)	10675(15)	5750(10)	657(9)	120(10)
C(15)	11249(14)	5784(9)	1377(8)	101(8)
C(16)	10916(12)	6529(7)	1691(7)	77(6)
C(21)	10952(9)	9133(6)	1315(5)	51(4)
C(22)	10733(10)	9956(7)	1619(6)	62(5)
C(23)	10782(12)	10668(8)	1165(8)	84(7)
C(24)	11822(13)	10711(8)	1042(8)	91(8)
C(25)	12090(11)	9894(8)	767(7)	79(6)
C(26)	12041(10)	9176(9)	1199(7)	75(6)
C(31)	11399(9)	8192(7)	2585(5)	53(4)
C(32)	12578(10)	8215(10)	2733(7)	84(6)
C(33)	13124(11)	8025(10)	3451(8)	98(7)
C(34)	12763(12)	8544(10)	3914(7)	88(6)
C(35)	11576(11)	8561(10)	3746(6)	83(6)
C(36)	11027(10)	8749(8)	3034(5)	65(5)
C(51)	4811(13)	6873(13)	2154(9)	131(11)
C(52)	4201(12)	6139(14)	1120(8)	147(11)
C(53)	5122(11)	7498(11)	1193(9)	113(8)
C(61)	7713(16)	5184(11)	1263(10)	126(11)
C(62)	5857(17)	4794(12)	969(9)	146(12)
C(63)	6442(16)	6084(12)	484(7)	131(10)
C(71)	6931(25)	7634(19)	3714(11)	196(20)
C(72)	7660(21)	6472(16)	4507(8)	211(16)
C(73)	8918(22)	7521(16)	4277(8)	229(18)
C(81)	9403(17)	5399(16)	4255(9)	208(14)
C(82)	9047(16)	4968(15)	3085(13)	176(16)
C(83)	10195(14)	6188(18)	3509(11)	233(17)

[a] Equivalent isotropic U is defined as one-third of the trace of the orthogonalized $\mathbf{U}_{ij}$ tensor.

Table 3. Selected Bond Lengths (Å) for 4 Excluding Distances to Hydrogen

Pt–Re	2.643(1)	Pt–P(1)	2.215(3)
Pt–C(1)	2.073(11)	Re–P(2)	2.359(3)
Re–P(3)	2.371(4)	P(1)–C(11)	1.841(13)
P(1)–C(21)	1.836(12)	P(1)–C(31)	1.850(10)
P(2)–C(3)	1.847(14)	P(2)–C(5)	1.890(15)
P(2)–C(6)	1.897(17)	P(3)–C(4)	1.863(14)
P(3)–P(7)	1.920(24)	P(3)–C(8)	1.913(23)
C(1)–C(2)	1.48(2)	C(3)–C(4)	1.50(2)

However, bridging hydride vibrations frequently are broad and difficult to observe.[20]

A mechanism proposing the role of the transient Re–Pt bimetallic complex in the formation of the rhenium–ethene complexes [ReH$_5$(C$_2$H$_4$)(PR$_3$)$_2$] and [ReH$_3$(C$_2$H$_4$)$_2$(PR$_3$)$_2$] has been discussed earlier (Scheme 1), and it is likely that complex **4** models this species, although no further reaction by **4** to form rhenium–ethene complexes was observed. It is apparent that the incorporation of the chelating diphosphine, dbpe, in the rhenium moiety imparts stability against the reductive elimination of ethane from complex **4**. This effect might derive from reduced steric interactions in **4**, as although the dbpe ligand is sterically demanding it is less likely to interact repulsively with the platinum-based ligands than would two bulky mononuclear phosphines.[21] This is corroborated by the short Re–Pt bond length of 2.643(1) Å for complex **4**. An interesting feature of the stability of **4** is the presence of hydride and alkyl ligands in close proximity, as the reductive elimination of alkane from *cis*-alkyl hydride complexes is often facile.[22] However, as remarked earlier, the presence of ancillary chelating ligands often confers stability, possibly by imposing stereochemical restrictions or by limiting ligand dissociation.

Table 4. Selected Bond Angles (deg) for 4

Re–Pt–P(1)	134.4(1)	Re–Pt–C(1)	130.9(4)
P(1)–Pt–C(1)	93.3(4)	Pt–Re–P(2)	127.6(1)
Pt–Re–P(3)	144.3(1)	P(2)–Re–P(3)	85.0(1)
Pt–P(1)–C(11)	110.7(4)	Pt–P(1)–C(21)	117.9(4)
C(11)–P(1)–C(21)	104.4(6)	Pt–P(1)–C(31)	108.9(4)
C(11)–P(1)–C(31)	103.5(5)	C(21)–P(1)–C(31)	110.5(5)
Re–P(2)–C(3)	108.7(4)	Re–P(2)–C(5)	117.0(5)
C(3)–P(2)–C(5)	104.8(7)	Re–P(2)–C(6)	117.5(6)
C(3)–P(2)–C(6)	99.9(7)	C(5)–P(2)–C(6)	106.8(7)
Re–P(3)–C(4)	107.9(4)	Re–P(3)–C(7)	115.9(8)
C(4)–P(3)–C(7)	100.7(10)	Re–P(3)–C(8)	115.1(8)
C(4)–P(3)–C(8)	104.6(9)	C(7)–P(3)–C(8)	111.0(10)
Pt–C(1)–C(2)	111.4(9)	P(2)–C(3)–C(4)	114.0(10)
P(3)–C(4)–C(3)	113.7(10)	P(2)–C(5)–C(51)	106.6(10)

A convenient one-pot reaction between the heptahydride **3**, an appropriate phosphine, and [Pt(nb)$_3$] (nb = norbornene) yielded norbornyl polyhydride complexes of the type [Re(dbpe)H$_6$Pt(C$_7$H$_{11}$)(PR$_3$)] [C$_7$H$_{11}$ = 2-norbornyl; PR$_3$ = PPh$_3$ (**5**), PCy$_3$ (**6**)] (Scheme 2) as moderately air-sensitive, yellow microcrystals. Selected spectroscopic data are listed in Table 1.

The order of addition in this synthesis is critical, with the platinum complex added to a solution of the polyhydride and the appropriate phosphine. If no phosphine is present, rapid decomposition to intractable products is observed. Complexes **5** and **6** are spectroscopically similar to the ethyl analogue **4**, with the ^{13}C{^{1}H} NMR spectra providing evidence for a static structure for the norbornyl ligand. Thus, the ^{13}C{135° DEPT} NMR spectrum of **5** revealed the presence of four CH$_2$ and three CH groups for the norbornyl ligand. The arrangement of the hydride ligands in **5** and **6** is expected to be similar to that of the ethyl complex **4** although, as with **4**, little information could be gained from the ^{1}H NMR spectra as the hydride resonances remained fluxional at 183 K.

Synthesis of Re–Pt Heptahydride Complexes [Re(dbpe)H$_7$Pt(PR$_3$)] (PR$_3$ = PBu$^t_3$, PCy$_3$). A significant change in the stability of the norbornyl complex is observed by increasing the steric influence of the platinum-bound phosphine. The reaction between the heptahydride **3** and the platinum complex [Pt(nb)$_2$(PBu$^t_3$)] immediately forms the PBu$^t_3$ analogue of complexes **5** and **6**, [Re(dbpe)H$_6$Pt(C$_7$H$_{11}$)(PBu$^t_3$)] (**7**) (Scheme 2). However, complex **7** undergoes slow decomposition by β-elimination and alkene dissociation,

(20) Cooper, C. B.; Shriver, D. F.; Onaka, S. *Adv. Chem. Ser.* **1978**, *167*, 232.

(21) PReP bond angles in [ReH$_7$(PR$_3$)$_2$] lie in the range 135–145°, compared with 84° in [ReH$_7$(dbpe)]. See, for example, Bau, R. *Adv. Chem. Ser.* **1978**, *167*, 73; Howard, J. A. K.; Mead, K. A.; Spencer, J. L. *Acta Crystallogr.* **1983**, *C39*, 555; ref 5; and Howard, J. A. K.; Spencer, J. L. Unpublished.

(22) See, for example, Abis, L.; Sen, A.; Halpern, J. *J. Am. Chem. Soc.* **1978**, *100*, 2915.

Table 5. Selected Spectroscopic Data[a] for the Complexes [Re(dbpe)H$_7$Pt(PR$_3$)]

complex	PR$_3$	δ_H	J_{PtH}	δ_P[b]	J_{PtP}
8	PBu$^t_3$	−5.72	258	102.3	24
				87.9	3459
9	PCy$_3$	−5.72	250	102.7	29
				44.1	3369

[a] C_4D_8O, 298 K. Chemical shifts are in ppm, relative to $SiMe_4$. Coupling constants are in Hz. [b] Re*P* resonance, upper value.

forming the heptahydrido heterobimetallic complex [Re(dbpe)H$_7$Pt(PBu$^t_3$)] (**8**), although **7** may be stabilized in solution for spectroscopic characterization by the addition of a small excess of norbornene. Selected spectroscopic data are detailed in Table 5.

The β-elimination reaction was monitored over a 3 day period by $^{31}P\{^1H\}$ and ^1H NMR spectroscopy. In the $^{31}P\{^1H\}$ NMR spectrum, the resonances due to the norbornyl complex **7** at δ 102.6 and 83.7 (J_{PtP} = 4076 Hz) slowly diminished, with the concurrent emergence of resonances due to **8** at δ 102.3 and 87.9 (J_{PtP} = 3453 Hz). Some further decomposition products were also observed, notably the parent polyhydride [ReH$_7$(dbpe)]. In the ^1H NMR spectrum, free norbornene is recognized by the alkene protons resonating at $\delta \approx 6$. However, this resonance diminishes over time, implying that the norbornene generated is being consumed in an additional reaction. The isolation of **8** in a pure form was accomplished by passing the crude reaction mixture as a brown hexane solution through a column of neutral alumina and eluting the yellow band with Et$_2$O. The evaporation of the eluent yielded microcrystalline **8** in 35% yield. Attempts to grow crystals that were suitable for X-ray diffraction were unsuccessful. The ^1H NMR spectrum of **8** in C_4D_8O at 298 K displayed a hydride signal at δ −5.72 as a pseudoquartet with ^{195}Pt satellites, a resonance that remained unchanged at 183 K, implying that the hydrides undergo a low-energy intramolecular rearrangement involving both metal centers. The methyl protons are observed as two doublets at δ 1.31 (36 protons, dbpe) and 1.50 (27 protons, PBu$^t_3$). This is different from the spectrum of the asymmetric norbornyl complex **7**, in which two doublets are observed for the methyl protons of the dbpe ligand at δ 1.33 and 1.29. The hydride stoichiometry has not been proven unambiguously, as all selective decoupling experiments were unsuccessful, although the integration ratio between hydridic and aliphatic protons strongly indicates the presence of seven hydride ligands.

Metal alkyl complexes frequently decompose by β-elimination,[23] although this route is rare for alkyl hydride complexes in which the precedent is for the reductive elimination of alkane. The fact that β-elimination is observed implies that the preceding alkyl polyhydride complexes are coordinatively unsaturated (electron counting suggests double unsaturation, with 30 electrons instead of the expected 34) or that coordinative unsaturation is achieved in preliminary equilibrium. Also, it is apparent that this reaction is sterically promoted. The transition state of the β-elimination pathway has recently been modeled on platinum by the agostic alkyl complexes [PtR(P⌐P⌐)]$^+$ (R = ethyl, norbornyl; P⌐P⌐ = bulky chelating diphosphine).[13] These

(23) Wilkinson, G. *Science* **1974**, *185*, 1091.

Scheme 3

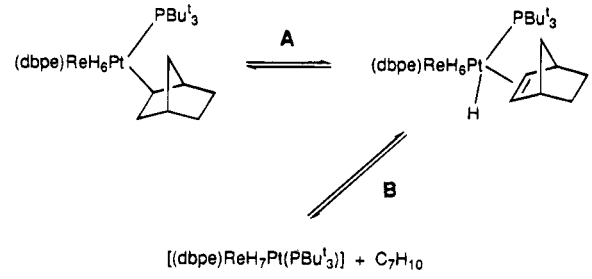

studies showed that whereas increasing the bulk of the phosphine decreased the extent of transfer of the β-hydrogen to the metal in the ground state it nevertheless increased the rate of alkene exchange, suggesting that the rate-determining step in β-elimination in that system was the elimination of alkene. It also appears that for complex **7** the β-elimination reaction is controlled by the elimination of norbornene, which is favored by the increase in the steric influence of the phosphine ligand.

Therefore, while step A (Scheme 3) is expected to be inhibited by an increase in the steric influence of the platinum-bound phosphine, step B is favored due to a relaxation of the crowded ligand environment. The steps described earlier were shown to be partly reversible, as first the formation of **8** is inhibited by the presence of excess norbornene, and second complex **8** slowly reacts with norbornene to generate a small quantity of complex **7** [by $^{31}P\{^1H\}$ NMR spectroscopy]. However, this reaction is complicated by the further reaction of **8** in the presence of norbornene, yielding unidentified products, as noted earlier.

As access to the Re−Pt heptahydride complex **8** via the decomposition of the norbornyl complex **7** was restrictive, more direct routes to **8** were sought. The platinum bis(phosphine) complex [Pt(PBu$^t_3$)$_2$] was shown to be an active catalyst in the formation of [ReH$_3$(C$_2$H$_4$)$_2$(PR$_3$)$_2$] type complexes,[9] presumably through the initial loss of one phosphine ligand, and so was envisaged as a promising precursor for complex **8**. Unfortunately, no reaction was observed between [Pt(PBu$^t_3$)$_2$] and the heptahydride **3**. The one-pot reaction between molar equivalents of the polyhydride **3**, PBu$^t_3$, and [Pt(1,5-cod)$_2$] was attempted on the premise that the cod ligand would not compete with the polyhydride for coordination to platinum. In this case, only the heptahydride **3** and the complex [Pt(PBu$^t_3$)$_2$] were discernible in the $^{31}P\{^1H\}$ NMR spectrum of the reaction mixture. In contrast, this direct route was successful when employing the smaller phosphine PCy$_3$. The slow addition of [Pt(cod)$_2$] to a solution of **3** and PCy$_3$ in toluene resulted in the formation of the yellow complex [Re(dbpe)H$_7$Pt(PCy$_3$)] (**9**) in 55% yield (Scheme 2). Selected spectroscopic data are detailed in Table 5. Again, no definitive determination of the hydride stoichiometry was possible as selective decoupling experiments were unsuccessful, although the integration ratios suggested the presence of seven hydride ligands.

Adducts of rhenium heptahydrides with silver, copper, and mercury have been synthesized previously and have been shown by X-ray crystallography to possess bonding interactions between the metals, as well as bridging hydride interactions.[6e] Complexes **8** and **9** can be viewed as donor−acceptor adducts between the hep-

tahydride and a $Pt(PR_3)$ fragment, with the polyhydride acting as a hydride donor. It is probable that both metal−metal bonding and bridging hydride interactions are present in these complexes. There may also be terminal hydrides attached to platinum, as suggested by analogy with the alkyl polyhydrides **4**−**7**. Limited structural information is available from the spectroscopic data. The averaged J_{PtH} values for the hydride ligands of **8** and **9** suggest a larger platinum-based proportion of hydrides than in the ethyl and norbornyl complexes, as would be the case if one of the hydride ligands occupied the same terminal position as the alkyl ligands in **4**−**7**. Also, in the infrared spectrum, new absorptions are observed at 2174 and 1978 cm^{-1}, which can be tentatively assigned to terminal Pt−H and Re−H absorptions, respectively.

Norbornene Polymerization. Reactions between the heptahydride **3** and $[Pt(nb)_3]$ yielded intractable decomposition products. In an attempt to stabilize the initial products of the reaction, a large excess of norbornene was added, but this led to rapid polymerization, resulting in non-stereospecific ring-opened polynorbornene, containing roughly equal amounts of (**E**) and (**Z**) isomeric forms (by infrared analysis of the film):

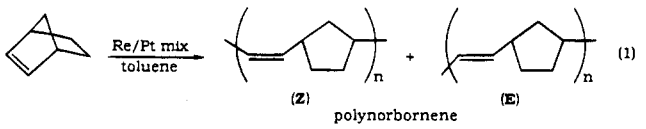

The reaction between the osmium hexahydride complex $[OsH_6(PR_3)_2]$ and $[Pt(nb)_3]$ generates the stable Os−Pt complex $[Os(PR_3)_2H_5Pt(C_7H_{11})(nb)]$,[24] so it is likely that a similar complex is initially formed in this case, i.e., $[Re(dbpe)H_6Pt(C_7H_{11})(nb)]$.

Such a proposal is corroborated spectroscopically. If the reaction between **3** and $[Pt(nb)_3]$ is monitored by $^{31}P\{^1H\}$ NMR spectroscopy, a single resonance of a new complex is observed initially at δ 100.2 and assigned to equivalent ^{31}P nuclei coordinated to the rhenium. Also, the hydride region of the ^1H NMR spectrum displays a triplet resonance at δ −6.15, with associated ^{195}Pt coupling of 369 Hz, implying a bimetallic complex in which the hydride presence at platinum is greatly increased relative to the phosphine derivatives discussed earlier. Polymer chain growth therefore can conceivably occur via the ring-opening metathesis of the norbornene/norbornyl ligands in a manner similar to that proposed by Grubbs et al. for the metathesis polymerization of norbornene by the titanacyclobutane $[Ti(C_6H_{10})(\eta^5\text{-}C_5H_5)_2]$.[25]

Significantly, neither $[Pt(nb)_3]$ nor **3** has been observed to polymerize norbornene under similar conditions. It is often very difficult to identify the true catalytic species, but in this case the evidence suggests that both Pt and Re must be present and that this may represent an example of cooperativity between two metal centers.

H/D Exchange. A reaction that necessitated the change from C_6D_6 to C_4D_8O solvent for ^1H and ^{13}C NMR spectroscopy was the facile exchange (25 °C) between the metal hydrides and deuterium of C_6D_6 for all of the previously isolated heterobimetalic complexes. The ^1H NMR spectrum of the norbornyl complex **5** after a few days at 298 K (or 1 h at 313 K) in C_6D_6 shows significant loss in the intensity of the hydridic resonance and also in that due to the methyl protons of the dbpe ligand, with a concomitant increase in the C_6D_5H resonance. The signals that are attributable to the platinum-bound ligands remain unaffected. The ^2H NMR spectrum of this deuterium-exchanged complex at 298 K in C_4H_8O reveals that deuterium has been incorporated at the metal hydride and phosphine Bu^t sites, with resonances at δ −5.3 (with ^{195}Pt satellites) and 1.1, respectively.

The mononuclear heptahydride complex $[ReH_7(PCy_3)_2]$ has been shown to be thermally activated toward the H/D exchange of the metal hydrides and also the C_2 and C_3 sites of the cyclohexyl groups of the phosphine with deuterium from C_6D_6.[26] The intramolecular oxidative addition of the cyclohexyl C−H bonds to the unsaturated intermediate $[ReH_5(PCy_3)_2]$ (generated by the reversible, thermally promoted elimination of H_2) was postulatd as a mechanism. The heterobimetallic complex **5** is already coordinatively unsaturated, and so unlike $[ReH_7(PCy_3)_2]$ requires no thermal activation. It is thought that the coordination of the deuteriobenzene in an η^2 fashion to a metal center is the primary step in this reaction.[27] Although the intrinsic coordinative unsaturation provided by the platinum moiety suggests that the initial interaction between **5** and the solvent should occur at the platinum center, the isotopic exchange observed for the methyl protons of the dbpe ligand suggests that the rhenium center is, or readily becomes, coordinatively unsaturated. The exchange of the methyl protons of the dbpe ligand with metal deuterides can be rationalized by a reversible intramolecular oxidative addition reaction of this ligand to the rhenium.

The H/D exchange reaction has only been observed with deuteriobenzene. The addition of cyclohexane to a solution of **5** in C_6D_6 and subsequent analysis of the volatile material by ^2H NMR spectroscopy after 2 h at 313 K showed that no deuterium had been incorporated into the cyclohexane. Tetrahydrofuran was also unreactive.

Conclusions

The isolation of heterobimetallic, alkyl polyhydride complexes of rhenium and platinum (**4**−**7**) has been accomplished by the incorporation of the sterically demanding chelating diphosphine, dbpe, in the rhenium polyhydride moiety. Unlike the transient analogues observed during the Pt^0-catalyzed formation of $[ReH_3(C_2H_4)_2(PR_3)_2]$ complexes, these compounds show no propensity to decompose via the reductive elimination of the alkane at ambient temperatures and so can be viewed as rare examples of coordinatively unsaturated, bimetallic, alkyl hydride complexes. In contrast to the 32-electron Re−Zr alkyl polyhydride complex $[Re(PPhMe_2)_2H_6Zr(CH_3)(\eta^5\text{-}C_5H_5)_2]$,[6b] the intrinsic unsaturation of the 30-electron Re−Pt complexes promotes interesting reaction chemistry. In the first instance, it is possible to induce the decomposition of the metal alkyl ligand via β-elimination by increasing the steric requirement of the platinum-bound tertiary phosphine

(24) Hazel, N. J.; Howard, J. A. K.; Spencer, J. L. Unpublished.
(25) Gilliom, L. R.; Grubbs, R. H. *J. Am. Chem. Soc.* **1986**, *108*, 733; Grubbs, R. H.; Tumas, W. *Science* **1989**, *243*, 907 (and references therein).
(26) Caulton, K. G.; DeWit, D. G.; Zeiher, C. M. K. *J. Am. Chem. Soc.* **1984**, *106*, 7006.
(27) Jones, W. D.; Feher, F. J. *J. Am. Chem. Soc.* **1982**, *104*, 4240.

ligand. Furthermore, the inclusion of the platinum moiety promotes the H/D exchange reaction at the rhenium center, a reaction that is not readily accessible in the parent heptahydride complex **3**. Cooperativity between the two metal moieties is also of possible significance in the polymerization of norbornene.

Experimental Section

All experiments were carried out under dry, oxygen-free nitrogen using Schlenk tube techniques. Solvents were dried and distilled under nitrogen immediately prior to use. NMR spectra were recorded on Bruker AC300 and Jeol EX90 spectrometers: ^{1}H spectra at 300 and 90 MHz, ^{13}C spectra at 75 MHz, and ^{31}P spectra at 36.2 MHz. Chemical shifts are quoted relative to $SiMe_4$ (^{1}H, ^{13}C) and $P(OPh)_3$ (external, ^{31}P). Infrared spectra were recorded on a Perkin-Elmer 1710 spectrophotometer. The diphosphine $Bu^t_2P(CH_2)_2PBu^t_2$ (dbpe)[28] and the complexes $[ReOCl_3(PPh_3)_2]$,[29] $[Pt(C_2H_4)_2(PCy_3)]$,[30] $[Pt(nb_3]$[30] and $[Pt(1,5\text{-}C_8H_{12})_2]$[30] were prepared according to literature methods, and $[Pt(nb)_2(PBu^t_3)]$ was made by the addition of a stoichiometric quantity of PBu^t_3 to a suspension of $[Pt(nb)_3]$ in hexane at 5 °C.

Synthesis of [ReOCl$_3$(dbpe)] (1). A solution of dpbe (3.52 g, 11.0 mmol) in dichloromethane (25 mL) was added to a stirred slurry of $[ReOCl_3(PPh_3)_2]$ (9.16 g, 11.0 mmol) in dichloromethane (50 mL), resulting in the dissolution of the solids after 10 min. The dark green solution was reduced in volume in vacuo to approximately 20 mL of solvent, and diethyl ether (100 mL) was added, causing the deposition of [ReOCl$_3$(dbpe)] as pale green microcrystals, which were isolated by decanting the liquors, washing with Et_2O (3 × 25 mL), and drying in vacuo (5.86 g, 85%). ^{1}H NMR (CD_2Cl_2, 298 K): δ 1.57 (d, J_{PH} = 13.4 Hz, CH_3), 1.42 (d, J_{PH} = 13.4 Hz, CH_3), bridge proton resonances were obscured by the methyl proton signals. ^{31}P NMR (CD_2Cl_2): δ 20.2 (s, Re-dbpe). IR (KBr disk): ν_{ReO} 987 (vs) cm^{-1}. Anal. Calcd for $C_{18}H_{40}Cl_3OP_2Re$: C, 34.48; H, 6.43. Found: C, 34.24; H, 6.42.

Synthesis of [ReO(OEt)Cl$_2$(dbpe)] (2). Ethanol (15 mL) was added to a green solution of **1** (1.52 g, 2.42 mmol) in CH_2Cl_2 (15 mL), resulting in the formation of a dark blue solution after 5 min. The partial evaporation of the solvents in vacuo, followed by cooling to −20 °C, resulted in the deposition of blue, microcrystalline [ReO(OEt)Cl$_2$(dbpe)], which was isolated by decanting the liquors, washing with ethanol (5 mL) and Et_2O (2 × 5 mL), and drying in vacuo (1.23 g, 80%). ^{1}H NMR (CD_2Cl_2): δ 3.82 (q, 2 H, J_{HH} = 7.5 Hz, CH_2CH_3), 2.12 (br, m, 4 H, PCH_2CH_2P), 1.43 (d, 18 H, J_{PH} = 13.0 Hz, CH_3), 1.42 (d, 18 H, J_{PH} = 13.2 Hz, CH_3), 0.91 (t, 3 H, J_{HH} = 7.5 Hz, CH_2CH_3). ^{31}P NMR (CD_2Cl_2): δ 46.4 (s, Re-dbpe). IR (KBr disk): ν_{ReO} 963 (vs), ν_{ReOEt} 908 (vs) cm^{-1}. Anal. Calcd for $C_{20}H_{45}Cl_2O_2P_2Re$: C, 37.73; H, 7.12. Found: C, 37.66; H, 6.80.

Synthesis of [ReH$_7$(dbpe)] (3). Solid $LiAlH_4$ (0.922 g, 24.3 mmol) was added in portions via a solids addition funnel to a stirred slurry of **1** (1.903 g, 3.03 mmol) in tetrahydrofuran (50 mL) at −78 °C. When the addition was complete, the mixture was allowed to warm to room temperature and stirred for an additional 1 h. The resultant gray slurry was again cooled to −78 °C, and the excess $LiAlH_4$ was carefully hydrolyzed by the addition of degassed water over 1 h. The yellow mixture was allowed to warm to room temperature and then evaporated to dryness in vacuo. The product was extracted into toluene (3 × 50 mL) and quickly filtered through a glass frit in air, and the filtrate was then evaporated to dryness using a rotary evaporator. Dissolving the dry residue in ethanol (20 mL) and cooling to −20 °C caused the deposition of [ReH$_7$(dbpe)] as white platelets, which were isolated by decanting the liquors, washing with cold hexane (2 × 2 mL), and drying in vacuo (0.916 g, 59%). ^{1}H NMR (C_6D_6): δ 1.31 (d, 4 H, J_{PH} = 9.6 Hz, PCH_2CH_2P), 1.19 (d, 36 H, J_{PH} = 12.4 Hz, CH_3), −6.87 (t, 7 H, J_{PH} = 13.0 Hz, ReH). ^{13}C NMR (C_6D_6): δ 35.1 (m, $PCMe_3$), 30.2 (s, CH_3), 25.4 (t, J_{PC} = 14.5 Hz, $P(CH_2)_2P$). ^{31}P NMR (C_6D_6): δ 90.7 (s, Re-dbpe). IR (KBr disk): ν_{ReH} 1998 (sh), 1975 (br, s), 1958 (sh) cm^{-1}. Anal. Calcd for $C_{18}H_{47}P_2Re$: C, 42.45; H, 9.26. Found: C, 42.43; H, 8.98.

Synthesis of [Re(dbpe)H$_6$Pt(Et)(PCy$_3$)] (4). All manipulations involving the bis(ethene) complex $[Pt(C_2H_4)_2(PCy_3)]$ were carried out under an ethene atmosphere. A solution of $[Pt(C_2H_4)_2(PCy_3)]$ (48 mg, 0.09 mmol) in toluene (5 mL) was added to a solution of **3** (46 mg, 0.09 mmol) in toluene (5 mL); a yellow color was observed immediately upon mixing. The solution was left to stand for 1 h, after which time the solvents were evaporated in vacuo. The yellow residue was dissolved in hexane (5 mL) and loaded on a short, neutral alumina column (5 cm), from which it was eluted with Et_2O. The evaporation of the eluent in vacuo resulted in pure **5** as yellow microcrystals (87 mg, 94%). ^{1}H NMR (C_6D_6, 298 K): δ 1.33 (d, 36 H, J_{PH} = 11.9 Hz, CH_3), −5.01 (q, 6 H, J_{PH} = 13.5 Hz, J_{PtH} = 250 Hz, RePtH), the ethyl and phosphine bridge resonances are obscured by the three broad cyclohexyl resonances at 2.05, 1.70, and 1.20 ppm. ^{13}C NMR (C_6D_6): δ 36.2 (d, J_{PC} = 21.3 Hz, $PCMe_3$), 34.8 (d, J_{PC} = 29.1 Hz, CH), 30.6 (s, CH_3), 30.0 (s, CH_2), 27.9 (d, J_{PC} = 10.5 Hz, CH_2), 26.9 (s, CH_2), 25.7 (s, $PtCH_2CH_3$), 2.02 (d, J_{PC} = 6.4 Hz, J_{PtC} = 570 Hz, $PtCH_2CH_3$), the phosphine bridge carbons were obscured by the resonance at δ 26.9. ^{31}P NMR (C_6D_6): δ 101.3 (d, J_{PP} = 3.7 Hz, Re-dbpe), 33.7 (t, J_{PP} = 3.7 Hz, J_{PtP} = 3856 Hz, Pt-PCy_3). IR (KBr disk): $\nu_{Re/PtH}$ 2082 (m), 2057 (m), 1895 (br), 1830 (br) cm^{-1}. Anal. Calcd for $C_{38}H_{84}P_3PtRe$: C, 44.91; H, 8.43. Found: C, 44.44; H, 8.23.

Synthesis of the Complexes [Re(dbpe)H$_6$Pt(C$_7$H$_{11}$)(PR$_3$)] 5–6. (i) To a stirred solution of the polyhydride **3** (84 mg, 0.164 mmol) and triphenylphosphine (43 mg, 0.164 mmol) in toluene (10 mL) was added solid $[Pt(nb)_3]$ (78 mg, 0.164 mmol), causing an immediate yellow coloration. This solution was left to stand for 10 min, after which time it was evaporated to dryness in vacuo. The yellow residue was then partially dissolved and suspended in hexane (10 mL), loaded on a short (5 cm), neutral alumina column as a slurry, and washed on the column with hexane (3 × 10 mL). The product was then eluted with Et_2O; the eluent yielded [Re(dbpe)H$_6$Pt(C$_7$H$_{11}$)(PPh$_3$)] (**5**) as yellow microcrystals upon the evaporation of the solvent in vacuo (155 mg, 89%). ^{1}H NMR (C_4D_8O, 298 K): δ 7.8 (m, 6 H, *o*-phenyl), 7.31 (m, 9 H, phenyl), 2.31 (m, 1 H, norbornyl), 2.02 (d, 1 H, J_{HH} = 2.7 Hz, norbornyl), 1.80 (s, 1 H, norbornyl), 1.72 (br, m, 1 H, norbornyl), 1.50 (m, 4 H, PCH_2-CH_2P), 1.32 (d, 18 H, J_{PH} = 12.0 Hz, CH_3), 1.31 (d, 18 H, J_{PH} = 12.0 Hz, CH_3), 0.97 (m, 1 H, norbornyl), 0.89 (m, 2 H, norbornyl), 0.76 (m, 1 H, norbornyl), 0.42 (m, 1 H, norbornyl), −5.22 (q, 6 H, J_{PH} = 14.3 Hz, J_{PtH} = 265 Hz, RePtH). ^{13}C NMR (C_4D_8O): δ 135.6 (d, J_{PC} = 11.4 Hz), 130.4 (s), 128.4 (d, J_{PC} = 10.3 Hz, phenyl), 47.8 (s, CH), 47.4 (s, CH_2), 39.6 (s, CH), 37.8 (s, CH_2), 36.9 (dd, J_{PC} = 20.0 and 4.3 Hz, $PC(Me_3)$), 85.7 (d, J_{PC} = 4.9 Hz, J_{PtC} = 563 Hz, PtCH), 31.9 (s, CH_2), 30.9 (s, CH_3), 30.6 (s, CH_2), 27.5 (m, PCH_2CH_2P). ^{31}P NMR (C_4D_8O): δ 101.2 (d, J_{PP} = 4.0 Hz, J_{PtP} = 18.3 Hz, Re-dbpe), 27.7 (t, J_{PP} = 4.0 Hz, J_{PtP} = 4302 Hz, Pt-PPh_3). IR (KBr disk): $\nu_{Re/PtH}$ 2070 (m), 2044 (m), 1959 (br), 1905 (br), 1847 (br), 1737 (w), 1722 (w) cm^{-1}. Anal. Calcd for $C_{43}H_{72}P_3PtRe$: C, 48.57; H, 6.83. Found: C, 48.10; H, 6.75.

(ii) In a manner similar to that used for complex **5**, the polyhydride **3** (101 mg, 0.197 mmol), PCy_3 (55 mg, 0.197 mmol), and $[Pt(nb)_3]$ (95 mg, 0.197 mmol) were reacted in toluene, resulting in the isolation of [Re(dbpe)H$_6$Pt(C$_7$H$_{11}$)(PCy$_3$)] (**6**) as yellow microcrystals (171 mg, 80%). ^{1}H NMR (C_4D_8O, 298 K): δ 1.33 (d, 18 H, J_{PH} = 12.0 Hz, CH_3), 1.31 (d, 18 H, J_{PH} = 12.0 Hz, CH_3), −5.21 (q, 6 H, J_{PH} = 13.4 Hz, J_{PtH} = 240 Hz, Re/PtH), the norbornyl and cyclohexyl resonances

(28) del Paggio, A. A.; Anderson, R. A.; Muettities, E. L. *Organometallics* **1987**, *6*, 1260 (and references therein).
(29) Parshall, G. W. *Inorg. Synth.* **1977**, *17*, 110.
(30) Spencer, J. L. *Inorg. Synth.* **1990**, *28*, 130; Spencer, J. L.; Crascall, L. E. *Inorg. Synth.* **1990**, *28*, 126.

were substantially overlapped. ^{13}C NMR (C_4D_8O): δ 48.0 (s, CH), 47.6 (s, CH_2), 39.4 (s, CH), 37.4 (s, CH_2), 36.9 (dd, J_{PC} = 21.5 and 5.3 Hz, P*C*Me$_3$), 35.6 (d, J_{PC} = 28.8 Hz, CH PCy$_3$), 32.8 (s, CH_2), 32.5 (s, CH_2), 31.2 (d, J_{PC} = 5.4 Hz, J_{PtC} = 593 Hz, Pt*C*H), 30.9 (s, CH_3), 30.6 (s, CH_2 PCy$_3$), 28.6 (d, J_{PC} = 10.8 Hz, CH_2 PCy$_3$), 27.6 (s, CH_2 PCy$_3$), the phosphine bridge resonance was obscured by the signal at δ 27.6. ^{31}P NMR (C_4D_8O): δ 102.2 (d, J_{PP} = 3.7 Hz, Re-dbpe), 34.9 (t, J_{PP} = 3.7 Hz, J_{PtP} = 4082 Hz, PtPCy$_3$). IR (KBr disk): $\nu_{Re/PtH}$ 2072 (m), 2047 (m), 1910 (br), 1867 (br) cm^{-1}. Anal. Calcd for $C_{43}H_{90}P_3$PtRe: C, 47.76; H, 8.39. Found: C, 47.72; H, 8.61.

Synthesis of [Re(dbpe)H$_6$Pt(C$_7$H$_{11}$)(PBu$^t_3$)] (7). A solution of [Pt(nb)$_2$(PBu$^t_3$)] (179 mg, 0.306 mmol) plus several small crystals of norbornene in Et_2O (10 mL) was added to a suspension of the polyhydride **3** (157 mg, 0.306 mmol) in Et_2O (10 mL), resulting in the immediate formation of a red solution. After stirring for 1 min, the ethereal solution was reduced in volume under vacuum to approximately 2 mL and passed through a neutral alumina pad (5 cm), eluting with more Et_2O as required. The red eluent was evaporated to dryness, and the resulting oily solid was redissolved in hexane (5 mL). The slow evaporation of this solution resulted in the deposition of [Re(dbpe)H$_6$Pt(C$_7$H$_{11}$)(PBu$^t_3$)] (**7**) as red microcrystals, which were isolated by decanting the supernatant liquors and drying in vacuo (295 mg, 95%). ^1H NMR (C_4D_8O, with excess norbornene): δ 1.55 (d, 27 H, J_{PH} = 11.5 Hz, CH_3), 1.33 (d, 18 H, J_{PH} = 16.2 Hz, CH_3), 1.29 (d, 18 H, J_{PH} = 16.2 Hz, CH_3), −5.40 (q, 6 H, J_{PH} = 14.2 Hz, J_{PtH} = 251 Hz, Re/Pt-H), other resonances were observed for norbornyl and bridge protons but were substantially overlapped. ^{13}C NMR (C_4D_8O): δ 47.6 (s, CH), 40.2 (s, CH), 39.5 (d, J_{PC} = 15 Hz, P*C*Me$_3$), 38.0 (s, CH_2), 37.1 (m, P*C*Me$_3$), 33.8 (s, CH_3), 31.4 (s, CH_2), 31.1 (s, CH_3), 31.0 (s, CH_3), 30.5 (s, CH_2), 27.7 (dd, J_{PC} = 20.4 and 7.7 Hz, PCH_2-CH_2P), 27.5 (s, CH_2), 25.2 (d, J_{PC} = 4 Hz, J_{PtC} = 642 Hz, Pt*C*H). ^{31}P NMR (C_4D_8O): δ 102.6 (d, J_{PP} < 1 Hz, Re-dbpe), 83.7 (t, J_{PP} < 1 Hz, J_{PtP} = 4076 Hz, PtPBu$^t_3$). Anal. Calcd for $C_{37}H_{84}P_3$PtRe: C, 44.30; H, 8.44. Found: C, 44.49; H, 8.08.

Synthesis of [Re(dbpe)H$_7$Pt(PBu$^t_3$)] (8). Complex **7** (230 mg, 0.229 mmol) was dissolved in toluene (5 mL) and allowed to stand for 3 days, after which time the solvents were evaporated in vacuo. The brown residue was partially dissolved in hexane and loaded onto a 5 cm neutral alumina column as a slurry. The addition of Et_2O eluted [Re(dbpe)H$_7$-Pt(PBu$^t_3$)] (**8**) only as a yellow band, which yielded yellow microcrystals of **8** upon evaporation of the eluent (73 mg, 35%). ^1H NMR (C_4D_8O, 298 K): δ 1.50 (d, 27 H, J_{PH} = 12.4 Hz, CH_3 PBu$^t_3$), 1.31 (d, 36 H, J_{PH} = 11.9 Hz, CH_3 dbpe), −5.72 (q, 7 H, J_{PH} = 13.3 Hz, J_{PtH} = 258 Hz, Re/Pt-H), the phosphine bridge resonances were obscured by the signal at δ 1.50. ^{13}C NMR (C_4D_8O): δ 39.2 (d, J_{PC} = 19.3 Hz, P*C*Me$_3$), 36.5 (d, J_{PC} = 22.2 Hz, P*C*Me$_3$), 32.7 (br, s, CH_3 PBu$^t_3$), 30.9 (s, CH_3 dbpe), 27.4 (m, PCH_2CH_2P). ^{31}P NMR (C_4D_8O): δ 102.3 (d, J_{PP} = 4.0 Hz, J_{PtP} = 24 Hz, Re-dbpe), 87.9 (t, J_{PP} = 4.0 Hz, J_{PtP} = 3453 Hz, PtPBu$^t_3$). IR (KBr disk): $\nu_{Re/Pt-H}$ 2081 (m), 2057 (m), 1975 (ms), 1905 (br), 1876 (br), 1799 (w), 1779 (w) cm^{-1}. Anal. Calcd for $C_{30}H_{74}P_3$PtRe: C, 39.63; H, 8.20. Found: C, 39.32; H, 7.75.

Synthesis of [Re(dbpe)H$_7$Pt(PCy$_3$)] (9). Solid [Pt(1,5-cod)$_2$] (174 mg, 0.423 mmol) was added in portions over 30 min to a quickly stirred solution of the polyhydride **3** (0.216 g, 0.423 mmol) and PCy_3 (119 mg, 0.423 mmol) in toluene (15 mL), allowing the deep red color that was observed immediately upon addition to lighten before the next addition. The resultant yellow solution was stirred for 30 min, after which time it was evaporated to dryness in vacuo. The oily solid was loaded onto a neutral alumina column (10 cm) with hexane, washed on the column with hexane (3 × 10 mL), and eluted with Et_2O. The eluent yielded yellow [Re(dbpe)H$_7$Pt(PCy$_3$)] (**9**), which precipitated from a saturated hexane solution as microcrystals (221 mg, 53%) at −20 °C. ^1H NMR (C_4D_8O): δ 1.31 (d, 36 H, J_{PH} = 11.9 Hz, CH_3), −5.72 (q, 7 H, J_{PH} = 13.2 Hz, J_{PtH} = 250 Hz, RePtH), the cyclohexyl resonances are broad features at δ 2.0, 1.75, and 1.5 and obscure the diphosphine bridge protons. ^{13}C NMR (C_4D_8O): δ 33.5 (d, J_{PC} = 30.7 Hz, CH), 32.8 (d, J_{PC} = 21.9 Hz, P*C*Me$_3$), 27.6 (s, CH_2 PCy$_3$), 27.4 (s, CH_3), 24.7 (d, J_{PC} = 11 Hz, CH_2 PCy$_3$), 23.8 (s, CH_2 PCy$_3$), the diphosphine bridge resonance is obscured by that at δ 24.7. ^{31}P NMR (C_4D_8O): 102.7 (d, J_{PP} = 3.7 Hz, J_{PtP} = 29.4 Hz, Re-dbpe), 44.1 (t, J_{PP} = 3.7 Hz, J_{PtP} = 3369 Hz, Pt PCy$_3$). IR (KBr disk): $\nu_{Re/Pt-H}$) 2174 (ms), 2087, 2062, 1978 (br, w), 1903 (br, m), 1870 (br, m) cm^{-1}. Anal. Calcd for $C_{36}H_{80}P_3$PtRe: C, 43.80; H, 8.17. Found: C, 44.22; H, 8.21.

Norbornene Polymerization: Synthesis of [Re(dbpe)-H$_6$Pt(C$_7$H$_{11}$)(nb)] (10). The addition of [Pt(nb)$_3$] (51 mg, 0.106 mmol) to a solution of the polyhydride **3** (54 mg, 0.106 mmol) plus a 10-fold molar excess of norbornene in toluene (0.7 mL) resulted in an orange solution, of which NMR spectra were recorded immediately. ^1H NMR (toluene): δ (hydride region only) −6.15 (t, J_{PH} = 12.9 Hz, J_{PtH} = 369 Hz, Re/PtH). ^{31}P NMR (toluene): δ 100.2 (s, Re-dbpe).

The preceding solution was transferred to a small Schlenk tube and allowed to stand for 3 h at ambient temperature. The resultant viscous solution was evaporated to dryness in vacuo, and the brown residue was treated with methanol (3 × 10 mL), resulting in a brown, plastic film (88 mg, 88%). IR (plastic film): $\nu_{C=C}$ 965, 736 cm^{-1} (*E*- and *Z*-alkenes).

Reaction between 5 and C$_6$D$_6$. A solution of the norbornyl complex **5** in C_6D_6 was allowed to stand at 313 K for 3 h, during which time the color changed from yellow to brown. After this time, the solvents were evaporated in vacuo and the residue was dissolved in THF, enabling the ^2H NMR spectrum to be recorded. ^2H NMR (THF): δ 1.1 (br, s, Bu$^t_2$-D), −5.3 (br, m, J_{PtD} ~ 261 Hz, Re/Pt-D).

Reaction between 5 and C$_6$D$_6$/C$_6$H$_{12}$. In a manner similar to that used in the preceding paragraph, a solution of complex **5** in a 1:1 C_6D_6/C_6H_{12} solvent mixture was warmed for 3 h at 313 K, after which time the volatile material was distilled trap-to-trap. Analysis of this material by ^2H NMR spectroscopy showed only the presence of C_6D_6.

Crystal Structure Determination of 4. The single-crystal X-ray diffraction experiment was carried out using a Siemens R3m/V four-circle computer-controlled diffractometer (room temperature, graphite-monochromated Mo Kα radiation, γ = 0.710 73). All computations were performed with a MicroVAX II computer using the SHELXTL PLUS set of programs. Crystal data: $C_{38}H_{84}P_3$PtRe: M = 1015.2; monoclinic; a = 13.267(4), b = 16.223(4), c = 21.505(5) Å; β = 107.39(2)°; V = 4417(2) Å^3; space group $P2_1/n$; Z = 4; D_{calcd} = 1.52 g cm^{-3}; μ(Mo Kα) = 60.3 cm^{-1}; F(000) = 2016 (the six metal hydrides were not included in the refinement).

The intensities of 9128 independent reflections with $2\theta \leq 54°$ were measured by the Wyckoff (limited ω) scan technique; 6588 reflections with $I > 2\sigma(I)$ were used in the calculations. A crystal of dimensions 0.37 × 0.43 × 0.62 mm was used for data collection, and a semiempirical absorption correction was applied. The structure was solved by direct methods. The positional and anisotropic thermal displacement parameters of all non-hydrogen atoms were refined by full-matrix least-squares techniques (including all hydrocarbon hydrogen atoms in a riding model). It was impossible to locate the positions of hydride ligands from the difference Fourier map. Neglecting them, the refinement converged at R = 0.060, R_w = 0.062.

Supporting Information Available: Tables of calculated hydrogen atom parameters, non-hydrogen atom anisotropic thermal parameters, and all non-hydrogen bond distances and angles for **4**, together with diagrams of the unit cell and crystal packing (7 pages). This material is contained in many libraries on microfiche, immediately follows this article in the microfilm version of the journal, can be ordered from the ACS, and can be downloaded from the Internet; see any current masthead page for ordering information and Internet access instructions.

OM9501438

$[(\eta\text{-}C_5H_5)M]_4O_6$ (M = Nb, V): Ab Initio Calculations Predict Equivalent Metal Atoms in a Rectangular Conformation

Jose Pedro Sarasa,[†] Josep-M. Poblet,[‡] Marie-Madeleine Rohmer,[§] and Marc Bénard*,[§]

Laboratoire de Chimie Quantique, UPR 139 du CNRS, Université Louis Pasteur, F-67000 Strasbourg, France, Applications Scientifiques du Calcul Intensif (ASCI), UPR 9029 du CNRS, Orsay, France, and Departament de Quimica, Universitat Rovira i Virgili, Pç Imperial Tarraco 1, 43005 Tarragona, Spain

Received July 12, 1995[⊗]

Ab initio SCF calculations have been carried out on the organometallic model clusters $[(\eta\text{-}C_5H_5)M]_4O_6$ (M = Nb, V), for the purpose of comparing the energies of the various conformations proposed for the niobium complex $[(\eta\text{-}C_5Me_5)Nb]_4O_6$. It is shown that a reliable energy comparison requires for this specific problem a fine tuning of the Gaussian basis sets. After the inclusion of diffuse and polarization functions in the basis set describing the metal–oxygen core, it is shown that the most stable conformation for the niobium complex is the quasi-planar form with D_{2h} symmetry, as tentatively proposed by Bottomley on the basis of NMR spectra and magnetic behavior. The observed temperature dependence of the magnetic moment could be explained by the close vicinity of three states with different spin multiplicities. The $[(\eta\text{-}C_5H_5)M]_4O_6$ model also predicts a conformation with D_{2h} symmetry for M = V. This prediction is in contradiction with the reported T_d structure of the $[(\eta\text{-}C_5Me_5)V]_4O_6$ complex, because the model does not account for the important steric strain induced by the coplanar position of the centroids of the C_5Me_5 ligands. A change in the structure of the vanadium complex could therefore be expected from the replacement of C_5Me_5 by less bulky Cp ligands.

Introduction

The synthesis and characterization of clusters with general formula $[L_nM_4](\mu_2\text{-}A_6)$ has been extended in the last decade to non-d^{10} transition metal atoms.[1,2] The $M_4(\mu_2\text{-}A_6)$ core of those clusters has an adamantane-like structure similar to the one represented in Figure 1a. Recently, three clusters have been characterized that provide an alternative to the adamantane-like structure. $[(\eta\text{-}C_5H_5)Ti]_4Se_6$,[3] $(\eta\text{-}C_5Me_5)_6Mo_8O_{16}$,[4] and $(\eta\text{-}C_5Me_5)_4Mo_5O_{11}$[5] display the $M_4(\mu_2\text{-}A)_3(\mu_3\text{-}A)_3$ structure represented in Figure 1c. An analysis of the relationship between the observed conformations of those clusters and their electronic structures has been given by Bottomley, based upon extended Hückel calculations.[6]

The case of $[(\eta\text{-}C_5Me_5)M]_4O_6$ (M = Nb, Ta)[7] for which no X-ray structure could be obtained appears more puzzling. At variance from the other clusters with d^1 metal ions, the magnetic behavior of those molecules is not characteristic of an open-shell ground state. The small temperature-independent magnetic susceptibility observed for $[(\eta\text{-}C_5Me_5)Nb]_4O_6$ rather suggests a diamagnetic ground state interacting with a low-lying multiplet. This magnetic behavior is therefore incompatible with the ground state configuration $1a_1^21e^2$ obtained from extended Hückel calculations on the adamantane structure as on the $M_4(\mu_2\text{-}A)_3(\mu_3\text{-}A)_3$ one.[6,7] In order to solve this contradiction, two other structures with nondegenerate ground states were proposed by Bottomley.[7] The structure of Figure 1d has been observed previously for the complexes $[M_2Cl_2(S(CH_2)_2NMeCH_2)_2]_2$ (M = Zn,[8] Cd[9]), whereas the structure of Figure 1b, a dimer of $Cp_2Nb_2(\mu_2\text{-}O_2)$ units with D_{2h} symmetry connected by two extra bridging oxygens, has apparently no precedent.[7] In spite of that, Bottomley tentatively assigned this latter structure to $[(\eta\text{-}C_5Me_5)Nb]_4O_6$ because of the ^1H and ^{13}C NMR spectra suggesting a unique type of $\eta\text{-}C_5Me_5$ ligand.

The goal of the present work is to carry out ab initio Hartree–Fock calculations on the model system $[(\eta\text{-}C_5H_5)Nb]_4O_6$ in order to characterize the optimal geometry corresponding to each of those conformations, to compare those energies, and to detect the origin of the low-lying paramagnetic states leading to the temperature-independent magnetic susceptibility. Similar calculations will be reported concerning the isoelectronic

[†] Universitat Rovira i Virgili. Permanent address: Departamento de Quimica Fisica y Quimica Orgánica, Universidad de Zaragoza, Ciudad Universitaria s/n, 50009 Zaragoza, Spain.

[‡] Universitat Rovira i Virgili.

[§] Laboratoire de Chimie Quantique and ASCI.

[⊗] Abstract published in *Advance ACS Abstracts,* November 1, 1995.

(1) Babcock, L. M.; Day, V. W.; Klemperer, W. G. *J. Chem. Soc., Chem. Commun.* **1987**, 858.

(2) (a) Bottomley, F.; Magill, C. P.; Zhao, B. *Organometallics* **1990**, *9*, 1700. (b) Bottomley, F.; Magill, C. P.; Zhao, B. *Organometallics* **1991**, *10*, 1946.

(3) Bottomley, F.; Day, R. W. *Organometallics* **1991**, *10*, 2560.

(4) Harper, J. R.; Rheingold, A. L. *J. Am. Chem. Soc.* **1990**, *112*, 4037.

(5) Bottomley, F.; Chen, J.; Preston, K. F.; Thompson, R. C. *J. Am. Chem. Soc.* **1994**, *116*, 7989.

(6) Bottomley, F. *Organometallics* **1993**, *12*, 2652. For a general review on cyclopentadienyl metal oxides, see ref 23.

(7) Bottomley, F.; Boyle, P. D.; Karslioglu, S.; Thompson, R. C. *Organometallics* **1993**, *12*, 4090.

(8) Hu, W. J.; Barton, D.; Lippard, S. J. *J. Am. Chem. Soc.* **1973**, *95*, 1170.

(9) Fawcett, T. G.; Ou, C.-C.; Potenza, J. A.; Schugar, H. J. *J. Am. Chem. Soc.* **1978**, *100*, 2058.

0276-7333/95/2314-5665$09.00/0

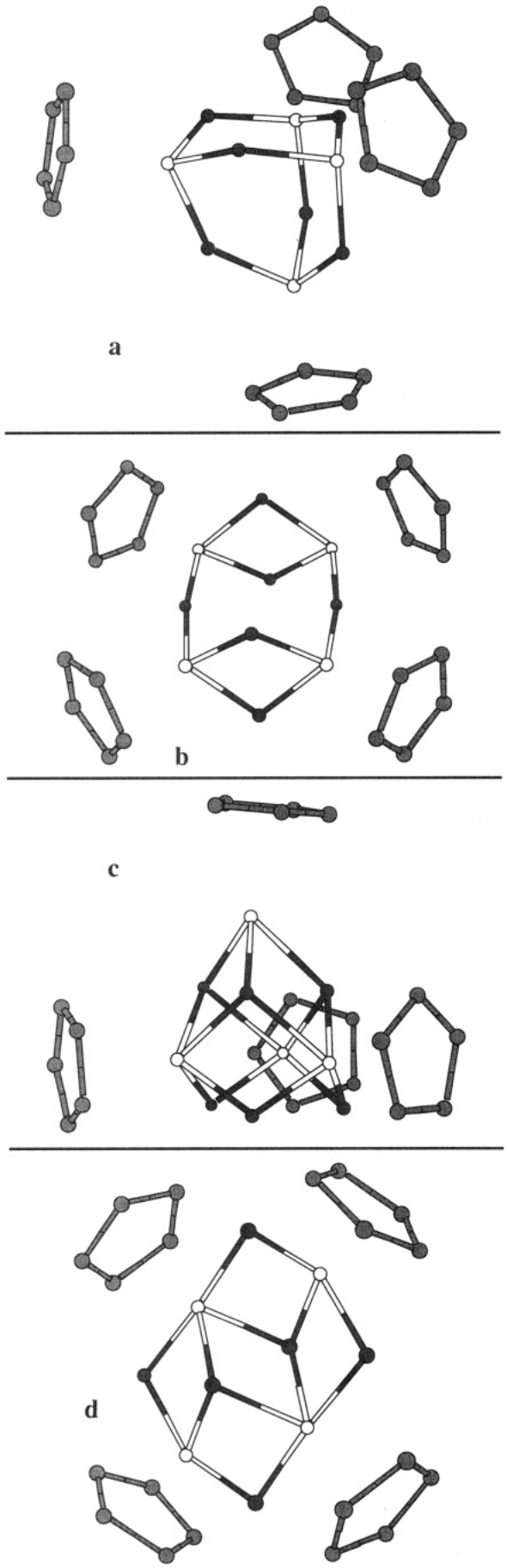

Figure 1. XMOL representation of the four possible conformations considered for $[(\eta\text{-}C_5Me_5)Nb]_4O_6$: (a) adamantanelike form; (b) D_{2h} conformation; (c) pseudo-C_{3v} form with three μ_3-O; (d) pseudo-C_{2h} conformation with two μ_3-O.

complex of vanadium, for which the adamantane-like structure has been confirmed,[2] and the influence of the steric strain induced by the bulky C_5Me_5 ligands will be discussed.

$[(\eta\text{-}C_5H_5)Nb]_4O_6$: Computational Details and Results

The geometry optimizations have been carried out by means of the TURBOMOLE program.[10] The final calculations including polarization functions on the niobium and oxygen atoms were carried out with the ASTERIX program.[11] Triplet and singlet coupling of the four metal electrons, carried out at the optimal geometries, were performed by means of the internally contracted CI program written by Siegbahn and interfaced to ASTERIX.[12]

The energy balance between the two most stable conformations, namely the adamantane-like one (D_{2d} symmetry, conformation **a**) and the one with D_{2h} symmetry (conformation **b**) was found to be extremely sensitive to the quality of the basis set. Four sets of atomic bases were used, corresponding to increasing accuracy in the valence-shell description of the metal−oxygen core or of the carbon atoms (Table 1). Basis set I uses the core potential derived by Hay and Wadt[13] to represent the Ar core of niobium. All-electron, double-ζ basis sets are used for the other atoms. Basis set II (496 contracted Gaussians (CGTOs)) represents the metal atoms with an all-electron basis, minimal for the inner shells but triple-ζ for the valence d shell. The valence shell of the oxygen atoms, formally O^{2-}, is also described with an extended basis set composed of 4 s-type and 4 p-type CGTOs. The carbon and hydrogen atoms of the Cp rings are described with a split-valence basis. Basis set III differs from basis set II by giving more flexibility to the set of Gaussian functions describing the p shell of carbons. Finally, basis set IV (708 CGTOs) adds two polarization functions to each atomic Gaussian set of the metal oxygen core.

Geometry optimizations have been carried out with basis set I assuming the four geometric conformations postulated by Bottomley et al. for $[(\eta\text{-}C_5Me_5)Nb]_4O_6$. In those optimization processes, the four metal electrons were accommodated into separate, singly occupied orbitals, giving rise to quintet states. The optimization process carried out with basis set I yielded the lowest energy for the adamantane-like conformation with D_{2d} symmetry (Table 1). The open-shell quintet electronic configuration is $a_1^1b_2^1e^2$. This state correlates with

(10) (a) TURBOMOLE: a direct SCF program from the Quantum Chemistry Group of the University at Karlsruhe under the directorship of Prof. R. Ahlrichs. (b) Ahlrichs, R.; Bär, M.; Häser, M.; Horn, H.; Kölmel, C. *Chem. Phys. Lett.* **1989**, *162*, 165.

(11) (a) Ernenwein, R.; Rohmer, M.-M.; Bénard, M. *Comput. Phys. Comm.* **1990**, *58*, 305. (b) Rohmer, M.-M.; Demuynck, J.; Bénard, M.; Wiest, R.; Bachmann, C.; Henriet, C.; Ernenwein, R. *Comp. Phys. Comm.* **1990**, *60*, 127. (c) Wiest, R.; Demuynck, J.; Bénard, M.; Rohmer, M.-M.; Ernenwein, R. *Comp. Phys. Commun.* **1991**, *62*, 107. (d) Rohmer, M.-M.; Ernenwein, R.; Ulmschneider, M.; Wiest, R.; Bénard, M. *Int. J. Quantum Chem.* **1991**, *40*, 723.

(12) Siegbahn, P. E. M. *Int. J. Quantum Chem.* **1983**, *23*, 1869. The CI program has been interfaced with ASTERIX by C. Daniel, M.-M. Rohmer, and M. Spéri.

(13) Hay, P. J.; Wadt, W. R. *J. Chem. Phys.* **1985**, *82*, 270, 299.

(14) (a) Huzinaga, S. *Tech. Rep. Univ. Alberta, Dep. Chem., Div. Theor. Chem.* **1971**. (b) Huzinaga, S.; McWilliams, D.; Domsky, B. *J. Chem. Phys.* **1971**, *54*, 2283.

(15) Veillard, A.; Dedieu, A. *Theor. Chim. Acta* **1984**, *65*, 215.

(16) Huzinaga, S. *J. Chem. Phys.* **1965**, *42*, 1293. The contraction into 6s, 4p is carried out according to Dunning's procedure.[17]

(17) Dunning, T. H. *J. Chem. Phys.* **1971**, *55*, 716.

Table 1. $[(C_5H_5)M]_4O_6$: Gaussian Basis Sets[a] Used for the Open-Shell RHF Calculation and Energies (hartrees) Obtained at the Optimal Geometry for the Open-Shell Quintet States Corresponding to the Most Probable Conformations of the Clusters with Relative Energies (kcal·mol^{-1}) in Parentheses

	basis set no.			
	I	II	III	IV
		Basis Sets		
Nb	core potential + (8,6,4) → [3,3,2][13]	(15,10,8) → [6,4,4][15]	same as II	(15,10,8,2)[b] → [6,4,4,2]
V		(13, 7, 5) → [5,3,3][24]		(13,7,5,2)[b] → [5,3,3,2]
O	(8, 4) → [4, 2][14]	(11, 7) → [6, 4][16]	same as II	(11, 7, 2)[b] → [6, 4, 2]
C	(8, 4) → [4, 2][14]	(9, 5) → [3, 2][14]	(9, 5) → [3, 3][14]	same as III
H	(4) → [2][14]	same as I	same as I	same as I
		$[(C_5H_5)Nb]_4O_6$: Energies[c]		
D_{2h} (**b**)	−1440.939 45 (+14.2)	−16202.114 66 (0)	−16202.160 00 (0)	−16202.632 34 (0)
D_{2d} (**a**)	−1440.962 06 (0)	−16202.111 93 (+1.7)	−16202.153 71 (+3.9)	−16202.588 44 (+27.5)
C_s (**c**)	−1440.824 07 (+86.5)			
C_s (**d**)	no local minimum[d]			
		$[(C_5H_5)V]_4O_6$: Energies[c]		
D_{2h} (**b**)		−4982.000 15 (+6.2)		−4982.309 39 (0)
D_{2d} (**a**)		−4982.010 10 (0)		−4982.267 72 (+26.1)

[a] Figures in parentheses represent the number of s-, p-, d-, and f-type primitive Gaussians. The size of the contracted basis set is given within brackets. [b] Exponents of the polarization functions: for niobium and vanadium (f-type), 0.8 and 0.25; for oxygen (d-type), 1.2 and 0.4. [c] The geometries have been fully optimized with basis sets I and II for M = Nb and with basis set II for M = V. Calculations with basis sets III and IV (with basis set IV only for M = V) have been carried out using the geometries optimized with basis set II. [d] The gradient optimization converged toward the geometry obtained for conformation **b**.

an $a_1^1t_2^3$ state in the T_d point group. Then comes the quintet state associated with conformation **b**, 14 kcal·mol^{-1} higher in energy. This conformation belongs to symmetry point group D_{2h} and the electronic configuration is $a_{1g}^1b_{2g}^1b_{1u}^1b_{3u}^1$. Conformation **c** corresponds to the coordination pattern $[(\eta\text{-Cp})Nb]_4(\mu_2\text{-O})_3(\mu_3\text{-O})_3$. The C_{3v} symmetry is lowered to C_s by the top Cp ring (Figure 1). An energy minimum was characterized for this conformation at +86.5 kcal·mol^{-1} with respect to the lowest state. Finally, no minimum could be characterized for conformation **d**, the gradient calculation leading back to the optimal geometry of conformation **b**.

Geometry optimization carried out with basis set II, which includes diffuse orbitals on all atoms of the metal−oxygen core, reverses the energy order of conformations **a** and **b**. The D_{2h} form is now found more stable by 1.7 kcal·mol^{-1}. No further calculation has been carried out on form **c**. The geometries optimized with basis set II have been used for single point calculations carried out with basis sets III and IV. Basis set III increases to 4 kcal·mol^{-1} the energy gap in favor of conformation **b**. Finally, the addition of polarization functions to the atoms of the Nb_4O_6 core leads to an unambiguous assignment of conformation **b** as the most stable one. The energy difference with conformation **a** reaches 27.5 kcal·mol^{-1} at this level of calculation. The most important geometrical parameters of conformations **b** and **a** as optimized with basis set II are displayed in Table 2.

The niobium−oxygen distances optimized for the D_{2d} conformation (1.924 and 1.935 Å) are quite similar to the Nb−O distances reported for $[(\eta\text{-}C_5Me_5)Nb(\mu\text{-Cl})(\mu\text{-O})]_3^+$ (1.937 Å)[18] and for $[(\eta\text{-}C_5Me_5)NbCl_2]_2(\mu\text{-OH})_2(\mu\text{-O})$ (1.942 Å).[7] The Nb−O distances optimized for the D_{2h} structure (1.885 Å for the double Nb−O bridges, 1.961 Å for the single Nb−O bridges) correspond to the same order of magnitude. The distances from the metal to the centroid of the Cp ring are computed to be larger by 0.10−0.15 Å than the currently reported values. This lengthening of the metal−Cp distances optimized at the SCF level of calculation is a well-documented artifact due to the neglect of electron correlation.[19]

Table 2. $[(\eta\text{-}C_5H_5)M]_4O_6$ (M = Nb, V): Selected Interatomic Distances (Å) of Conformations a (D_{2d} Symmetry) and b (D_{2h} Symmetry) from Gradient Optimization of the Quintet Electronic States

	conformation **a** (D_{2d})			conformation **b** (D_{2h})		
	dist			dist		
	M = Nb	M = V	n[a]	M = Nb	M = V	n[a]
M_1-M_3	3.431	3.251	2	3.012	2.711	2
M_1-M_2	3.635	3.234	4	3.758	3.419	2
M_1-O_1	1.924	1.778	4	1.885	1.767	4
M_1-O_3	1.935	1.795	8	1.961	1.803	8
$M_1-\Omega_1$[b]	2.27	2.04	4	2.26	2.06	4
H···H[c]	4.74	3.92		3.40	2.65	

[a] Number of equivalent parameters. [b] Centroid of the C_5H_5 ring. [c] Closest contact between hydrogen atoms belonging to different C_5H_5 rings.

An important information is provided by the Nb−Nb distances. In the conformation with D_{2d} symmetry, those distances are 3.43 and 3.63 Å. It should be noticed first that those distances differ one from another by 0.2 Å, which means that the Nb_4O_6 core significantly departs from its postulated T_d symmetry. This may be interpreted as a trend of the Nb_4O_6 core toward fluxionality due to the lack of direct metal−metal interaction. Metal−metal distances of ~3.5 Å are usually thought to preclude such interactions,[20] an assumption which is substantiated by the orbital energy sequence of the four open-shell metal orbitals. Those orbitals belong to the a_1, b_2, and e representations of the D_{2d} point group. They are made of different combinations of the same d atomic orbitals. Those four-lobe d orbitals are contained in planes approximately parallel to the Cp cycles. This orientation allows for more efficient donation interactions from both the oxygen and the Cp

(18) Bottomley, F.; Karslioglu, S. *Organometallics* **1992**, *11*, 326.

(19) (a) Lüthi, H. P.; Ammeter, J. H.; Almlöf, J.; Faegri, K., Jr. *J. Chem. Phys.* **1982**, *77*, 2002. (b) Almlöf, J.; Faegri, K., Jr.; Schilling, B. E.; Lüthi, H. P. *Chem. Phys. Lett.* **1984**, *106*, 266. (c) Lüthi, H. P.; Siegbahn, P. E. M.; Almlöf, J.; Faegri, K., Jr.; Heiberg, A. *Chem. Phys. Lett.* **1984**, *111*, 1. (d) Lüthi, H. P.; Siegbahn, P. E. M.; Almlöf, J. *J. Phys. Chem.* **1985**, *89*, 2156.

(20) Unusually long metal−metal bonds were however characterized in relation with steric strain in some dinuclear complexes of Zr(III): (a) Rohmer, M.-M.; Bénard, M. *Organometallics* **1991**, *10*, 157. (b) Bénard, M.; Rohmer, M.-M. *J. Am. Chem. Soc.* **1992**, *114*, 4785. (c) DeKock, R. L.; Peterson, M. A.; Reynolds, L. E. L.; Chen, L. H.; Baerends, E. J.; Vernoijs, P. *Organometallics* **1993**, *13*, 2794.

Table 3. $[(\eta\text{-}C_5H_5)Nb]_4O_6$: Computed Energies (hartrees; Shifted by 16 202) of the Lowest Quintet, Triplet, and Singlet States Resulting from the Appropriate Coupling of the Four Metal Electrons in the Adamantane-like (D_{2d}) and in the D_{2h} Conformations with Relative Energies (cm^{-1}) in Parentheses

conformation **a** (D_{2d})		conformation **b** (D_{2h})	
state	energy	state	energy
$^5B_1$	−0.588 444 (0)	^5A_g	−0.632 357 (0)
^3E	−0.587 324 (+246)	$^3B_{1u}$	−0.632 335 (+5)
$^3A_2$	−0.586 222 (+488)	$^3B_{2g}$	−0.631 128 (+270)
$^1A_1$	−0.587 315 (+248)	^1A_g	−0.632 323 (+7)

ligands, but it drastically reduces the possibility for a through-space coupling between the metal electrons. Such a coupling could be effective through the orbital combination with a_1 symmetry, which is in phase and formally bonding with respect to the four metal atoms of the core.[21,22] The three other metal orbitals are nonbonding with respect to the core of metal atoms and correlate with the triply degenerate $1t_2$ orbital reported for the T_d symmetry.[2b,23] The orbital energy obtained for the formally bonding $1a_1$ orbital is −2.34 eV, to be compared with −1.99 eV ($1b_2$) and −2.01 eV (1e) for the set of nonbonding orbitals. The in-phase character of the $1a_1$ orbital does not provide it with much stabilization, indicating that the through-space metal−metal interaction is not far from being negligible.

The geometry optimized for the D_{2h} conformation displays a rectangular arrangement for the metal atoms. The large Nb−Nb distances (3.758 Å) are obtained along the single oxygen bridges, due to a widely open Nb−O−Nb angle (171°). The metal atoms connected by a double bridge are separated by a relatively short distance of 3.012 Å. This distance is compatible with the presence of a metal−metal bond, but it could also be induced by the interactions with the bridging ligands as in the d^0 dimer $[(\eta\text{-}C_5Me_5)NbCl_2]_2(\mu\text{-}OH)_2(\mu\text{-}O)$ for which the Nb−Nb distance is 3.027 Å.[7] Assuming the metal framework to lie in the xy plane (x collinear to the short side of the rectangle), the four open shell metal orbitals are made of approximate $d_{x^2-z^2}$ atomic orbitals. The lobe oriented along the x axis is expected to ensure some through-space coupling between the doubly bridged metal atoms. As a matter of fact, the two combinations that are in phase with respect to the short Nb−Nb distances have energies of −2.75 and −2.59 eV, to be compared with −2.12 and −2.23 eV for the out-of-phase combinations. The energy gap is larger than for the D_{2d} conformation but cannot be interpreted as characteristic of a strong metal−metal interaction. This weak metal−metal bonding that emerges from the analysis of the quintet wave functions obtained for both geometric conformations has direct consequences on the coupling of the four metal electrons. Table 3 reports for each conformation the energy computed using basis set IV for coupled states, respectively ^5A_g, $^3B_{1u}$, $^3B_{2g}$, and ^1A_g for the D_{2h} conformation and $^5B_1$, $^3A_2$, ^3E, and $^1A_1$ for the conformation with D_{2d} symmetry.

Singlet and triplet coupling of the four metal d electrons starting from the SCF orbitals of the quintet state leads for both conformations to intermediate and low-spin states energetically less stable than the quintets (Table 3). For the D_{2d} conformation, this energy difference is 248 cm^{-1} with respect to the $^1A_1$ state and about the same with respect to the lowest triplet (Table 3). For the D_{2h} conformation, the ^5A_g state is computed to be almost degenerate with the two coupled states $^3B_{1u}$ and ^1A_g, with energy differences less than 10 cm^{-1} (Table 3). The triplet state next in energy ($^3B_{2g}$) is higher by ~270 cm^{-1}. A near degeneracy of states with different spin multiplicities could explain the observed magnetic behavior, i.e. the small temperature-independent paramagnetism and the increase of the magnetic moment with temperature. The singlet state would have been expected however to be lowest in energy. In view of the very small energy gaps obtained from the couplings of the four d electrons, a change in the sequence of states is not excluded from further improvement of the basis set quality or from a proper account of electron correlation. Even if a change in the energy sequence of the coupled states was to be obtained for the D_{2h} conformation at a higher level of approximation, the energy gaps are not expected to change much and the three states of lowest energy will remain quasi degenerate.

Vanadium Complex: Results and Discussion

SCF calculations and geometry optimization have been carried out on the isoelectronic complex of vanadium, $[(\eta\text{-}C_5H_5)V]_4O_6$, with basis sets similar to those referred to as II and IV for the calculations on the niobium complex (Table 1). The basis set used for vanadium is taken from the (13s 7p 5d) basis optimized by Hyla-Kryspin et al.,[24] augmented with one p-type function (ζ = 0.15) and contracted to [5, 3, 3]. In the large molecular basis equivalent to IV, polarization functions were added to the vanadium and oxygen atoms with the same exponents as those used for the niobium complex. The results are reported in Table 1.

The effect of polarization functions appears still more dramatic than for niobium, since they induce a reversal of the relative energies obtained for the D_{2h} and D_{2d} conformations. The crucial importance of polarization functions and, more generally, of the valence basis set extension in this specific problem could be explained by the different occupation of space characteristic of the competing conformations. The conformation with D_{2d} symmetry isotropically extends in the three dimensions of space due to the quasi-tetrahedral pattern of the metal atoms and Cp centroids. At variance from that, the D_{2h} conformation is almost planar when the Cp ligands are restricted to their centroids. The doubly bridging oxygens only depart from planarity. In the tetrahedral conformation, the need for angular flexibility is taken care of, at least partly, by the unoccupied basis functions of the surrounding atoms, in a classical "basis set superposition effect" (BSSE). This BSSE is obviously less efficient when the molecular conformation

(21) Such a coupling involving four metal d electrons in a complex with T_d symmetry has been evidenced for metallocarbohedrenes M_8C_{12}. The four d orbitals taking part in this interaction are d_{z^2}-like orbitals defined in a local reference system attached to each metal atom with the z axis pointing toward the center of the tetrahedral molecule. The in-phase combination with a_1 symmetry was in this case strongly stabilized with respect to the nonbonding combination with t_2 symmetry.[22] In the present niobium complex, the singly occupied orbital combinations are made of $d_{x^2-y^2}$-like orbitals (defined in the same local reference system) with lobes directed outside the Nb_4O_6 core.

(22) (a) Rohmer, M.-M.; Bénard, M.; Henriet, C.; Bo, C.; Poblet, J.-M. *J. Chem. Soc., Chem. Commun.* **1993**, 1182. (b) Rohmer, M.-M.; Bénard, M.; Henriet, C.; Poblet, J.-M. *J. Am. Chem. Soc.* **1995**, *117*, 508.

(23) Bottomley, F. *Polyhedron* **1992**, *11*, 1707.

(24) Hyla-Kryspin, I.; Demuynck, J.; Strich, A.; Bénard, M. *J. Chem. Phys.* **1981**, *75*, 3954.

does not equally extend in the three dimensions of space. The extreme case corresponds to diatomic molecules, the energy of which is very slowly convergent with respect to the angular quantum number of the polarization functions.[25] It is therefore not surprising that the extension of the basis set is consistently more favorable to the quasi-planar conformation of the niobium complex and of its vanadium equivalent.

The result found for the vanadium complex raises a problem, however, since the structure of the parent complex $[(\eta\text{-}C_5Me_5)V]_4O_6$ has been characterized and is reported to have T_d symmetry within experimental error.[2] Since the energy difference computed in favor of the quasi-planar, D_{2h} conformation reaches 26 kcal·mol^{-1} with the large basis set (Table 1), the contradiction is expected to lie in the model chosen for the calculations, i.e. the complex with unsubstituted Cp rings $[(\eta\text{-}C_5H_5)V]_4O_6$. It has been proved already that the accumulation of four C_5H_5 ligands around a small organometallic core is susceptible to induce an important distortion of the core because of interligand H···H repulsive contacts.[20] Such repulsions are not expected to develop in either configuration of the $[(\eta\text{-}C_5H_5)M]_4O_6$ complexes (M = Nb or V) since the shortest H···H distance, obtained in the D_{2h} conformation of the vanadium complex, reaches 2.65 Å (Table 2). H···H distances are significantly larger for the D_{2h} conformation of the niobium complex (3.40 Å) and particularly for the D_{2d} conformations of both complexes (3.92 Å for M = V; 4.74 Å for M = Nb). This situation is likely to change when C_5H_5 is replaced by the bulky $C_5(CH_3)_5$, as in the complexes of niobium and vanadium reported experimentally. If a strict rectangular arrangement is maintained for the centroids of the C_5Me_5 rings in the D_{2h} conformation, H···H contacts of ~1.8 Å should develop in the niobium complex. The repulsion generated by such contacts is not anymore negligible.[20] However, the flexibility of the C_5Me_5 ring provides several possibilities to relax this small strain at low cost: rotation of the methyl groups; bending of the C–CH_3 bonds out of the cycle plane; slight deviation of the Cp centroids out of the plane defined by the rectangle of metal atoms. A combination of those slight deformations apparently allows the Nb_4O_6 core to accommodate the bulky C_5Me_5 ligands without departing from its preferred D_{2h} conformation. It should be noted that the adamantane-like conformation can accommodate C_5Me_5 ligands without generating H···H contacts shorter than ~3.2 Å.

Replacing niobium by vanadium yields a contraction of all interatomic distances by ~10% (Table 2). This is sufficient for the steric strain to become dramatic for the planar conformation of $[(\eta\text{-}C_5Me_5)V]_4O_6$ with H···H repulsive contacts of ~1 Å. Even though this conformation is electronically favored as shown in the present work, the centroids of the C_5Me_5 rings cannot remain coplanar. They are expected to undergo a displacement toward a tetrahedral conformation which would most efficiently reduce the steric strain. This displacement would be the driving force leading the vanadium–oxygen core toward the adamantane-like stable conformation.

(25) See for instance: (a) McLean, A. D.; Liu, B. *Chem. Phys. Lett.* **1983**, *101*, 144. (b) Walch, P.; Bauschlicher, C. W., Jr.; Roos, B. O.; Nelin, C. J. *Chem. Phys. Lett.* **1983**, *103*, 175. (c) Bauschlicher, C. W., Jr.; Partridge, H.; Langhoff, S. R.; Taylor, P. R.; Walch, S. P. *J. Chem. Phys.* **1987**, *86*, 7007.

Summary and Conclusion

Ab initio SCF and electron-coupling calculations have been carried out on $[(\eta\text{-}C_5H_5)M]_4O_6$ (M = Nb and V) taken as models for the recently synthesized $[(\eta\text{-}C_5Me_5)M]_4O_6$ complexes. Two main conclusions emerge from this work. The first one is of theoretical interest and concerns the crucial importance of basis set extension and, more specifically, of including polarization functions to decide between the relative stabilities of the two most probable conformations. Those conformations are (i) an adamantane-like structure close to tetrahedral symmetry and (ii) a structure with D_{2h} symmetry characterized by a planar arrangement of the metal atoms and of the Cp centroids. The use of a nonpolarized basis set artificially favors the conformation that extends in the three dimensions of space and can take advantage from the unoccupied basis functions of the surrounding atoms (basis set superposition error). A geometry optimization carried out with a basis set including diffuse functions but devoid of polarization functions gives a slight energetic advantage to the D_{2h} form with Nb and to the D_{2d} form with V. Including polarization functions on all atoms of the metal–oxygen core clearly shows that the D_{2h} conformation is more stable with vanadium as with niobium. The energy difference is comprised between 25 and 30 kcal·mol^{-1} in both cases.

This result is in agreement with the NMR spectra and magnetic behavior reported for the real niobium complex $[(\eta\text{-}C_5Me_5)Nb]_4O_6$. The four d electrons of the niobium cluster undergo a very weak coupling leading to the presence of three states with different spin multiplicities (^1A_g, $^3B_{1u}$, and ^5A_g) within a few cm^{-1}. No such coupling exists for the D_{2d} conformation, and the quintet state $^5B_1$ is found lowest by ~250 cm^{-1} with respect to quasidegenerate singlet and triplet states.

A contradiction appears however between our calculations on the model complex of vanadium and the X-ray characterization of a tetrahedral conformation for the real molecule. The theoretical result is easily reconciled with the observed structure when considering the steric strain induced by the four bulky C_5Me_5 ligands in the D_{2h} form. The present calculations eventually suggest that a vanadium complex incorporating four unsubstituted C_5H_5 cycles, would it be feasible, would probably adopt the conformation with D_{2h} symmetry as the $[(\eta\text{-}C_5Me_5)Nb]_4O_6$ complex.

Acknowledgment. Calculations have been carried out in part on the Cray C98 computer of the Institut de Développement et de Ressources en Informatique Scientifique (IDRIS) and IBM RS6000 workstations purchased with funds provided by the DGICYT of the Government of Spain and by the CIRIT of Generalitat de Catalunya (Grant Nos. PB92-0766-C02-02 and GR9Q93-7003). The cooperation between the Strasbourg and Tarragona groups has been supported by the HCM Contract ERBCHRXCT-930156.

OM950538R

Kinetics and Reaction Mechanisms of Copper(I) Complexes with Aliphatic Free Radicals in Aqueous Solutions. A Pulse-Radiolysis Study

Nadav Navon, Gilad Golub, Haim Cohen, and Dan Meyerstein*

Nuclear Research Centre Negev, R. Bloch Coal Research Center, and Chemistry Department, Ben-Gurion University of the Negev, Beer-Sheva 84105, Israel, and College of Judea and Samaria, Ariel, Israel

Received June 8, 1995[⊗]

The reactions ($Cu^{I}L + {}^{\bullet}R \rightarrow LCu^{II}-R$ and the mechanism of decomposition of the transient complexes $LCu^{II}-R$ were studied using the pulse-radiolysis technique ($L^1 = H_2O$, L^2 = 2,5,8,11-tetramethyl-2,5,8,11-tetraazadodecane; ${}^{\bullet}R = {}^{\bullet}CH_3$, ${}^{\bullet}CH_2COOH$, ${}^{\bullet}CH(CH_3)COOH$, ${}^{\bullet}CH_2CH_2COOH$.) The kinetics of formation of the transient complexes obey pseudo-first-order rate laws. The rate constants measured for these reactions are in the range $(2-4) \times 10^9$ M^{-1} s^{-1} for L^1 and $6 \times 10^6-1 \times 10^8$ M^{-1} s^{-1} for L^2. The mechanisms of decomposition of the transient complexes depend on the nature of R and L as follows: 1. For $R = CH_3$ ethane is the final product. The kinetics of its formation obey second-order rate laws. Free methyl radicals are not intermediates in these processes. 2. For $R = CH_2CH_2COOH$ the transient complexes decompose via an analogous mechanism to that of $R = CH_3$ for L^1 and via homolysis of the copper–carbon σ bond for L^2. 3. For $R = CH_2COOH$ and $CH(CH_3)$-COOH the transient complexes decompose via heterolysis of the copper–carbon σ bonds forming $Cu^{II}L$. The effect of the nature of R and L on the kinetics of these reactions is discussed.

Introduction

Many organic processes of industrial and synthetic interest which are catalyzed by copper complexes involve free radicals as key intermediates.[1,2] These include among others the Meerwein reaction,[3] the addition of polyhalides to alkenes,[4] and the Ullmann reaction.[5] Copper(I) complexes are the active species in these catalytic processes. Furthermore it has been proposed[1,2,4,5] that transient complexes with copper–carbon σ bonds are key intermediates in these catalytic processes. The latter transient complexes are believed to be formed via the reactions of the aliphatic free radicals with the copper complexes present in the system. The interest in the reactivity of Cu(I) complexes toward organic free radicals has also increased due to the role of copper ions in deleterious biological processes initiated by free radicals.[6]

The role of the copper(I) complexes in most systems is dual as follows.

a. Forming the free radicals via halogen abstraction or via the modified Fenton reagent:[7-9]

$$Cu(I) + RX \rightarrow Cu^{II}-X^{+} + {}^{\bullet}R \quad (1)$$

$$Cu(I) + H_2O_2 \rightarrow Cu(II) + OH^{-} + {}^{\bullet}OH \xrightarrow{RH} H_2O + {}^{\bullet}R \quad (2)$$

b. Affecting the nature of the final products due to the formation of transient complexes with copper–carbon σ bonds via

$$Cu(I) + {}^{\bullet}R \rightarrow Cu^{II}-R^{10,11} \quad (3)$$

$$Cu(II) + {}^{\bullet}R \rightarrow Cu^{III}-R^{12} \quad (4)$$

The kinetics of reactions 3 and 4 were studied in aqueous solutions by applying the pulse-radiolysis technique, for several free radicals.[10-12] The results point out that reaction 3 is fast and its rate usually approaches the diffusion-controlled limit, *i.e.* $k_3 > 10^9$ M^{-1} s^{-1}, whereas the rates of reaction 4 are usually considerably slower, *i.e.* $8 \times 10^5 < k_4 < 8 \times 10^8$ M^{-1} s^{-1}.[12] Thus even when the concentration of the Cu(I) complex is considerably lower than that of the Cu(II) complex the free radicals will react mainly via reaction 3.

The mechanisms of decomposition of the transient complexes $Cu^{II}-R$ and $Cu^{III}-R$ clearly determines the composition of the products of these catalytic processes.

* To whom correspondence should be addressed at Ben-Gurion University of the Negev.

⊗ Abstract published in *Advance ACS Abstracts,* November 1, 1995.

(1) Regitz, M., Giese, B., Eds. *Houben-Weyl*; Thieme: Stuttgart, Germany, 1989; Vol. E19a.

(2) (a) Kochi, J. K. *Organometallic Mechanisms and Catalysis*; Academic Press: New York, 1978. (b) Sheldon, R. A.; Kochi, J. K. *Metal Catalyzed Oxidations of Organic Compounds*; Academic Press: New York, 1981.

(3) Rondestvedt, C. S., Jr. *Org. React.* **1976**, *24*, 225.

(4) Bellus, D. *Pure Appl. Chem.* **1985**, *57*, 1827.

(5) (a) Weingarten, H. *J. Org. Chem.* **1964**, *29*, 3624. (b) Schwartz, M. A.; Crowell, J. D.; Musser, J. H. *J. Am. Chem. Soc.* **1972**, *94*, 4363.

(6) Goldstein, S.; Czapski, G. *J. Free Rad. Biol. Med.* **1986**, *2*, 3.

(7) Nonhebel, D. C. Essays on Free Radical Chemistry. *Chem. Soc. Spec. Publ.* **1970**, *24*, 409.

(8) Goldstein, S.; Czapski, G.; Meyerstein, D. J. *Free Rad. Biol. Med.* **1993**, *15*, 435.

(9) Masarwa, M.; Cohen, H.; Meyerstein, D.; Hickman, J.; Bakac, A.; Espenson, J. H. *J. Am. Chem. Soc.* **1988**, *110*, 4293.

(10) Freiberg, M.; Mulac, W. A.; Schmidt, K. H.; Meyerstein, D. *J. Chem. Soc., Faraday Trans. 1* **1980**, *76*, 1838.

(11) Cohen, H.; Meyerstein, D. *Inorg. Chem.* **1986**, *25*, 1506.

(12) (a) Freiberg, M.; Meyerstein, D. *J. Chem. Soc., Faraday Trans. 1* **1980**, *76*, 1825. (b) Masarwa, M.; Cohen, H.; Meyerstein, D. *Inorg. Chem.* **1986**, *25*, 4897.

0276-7333/95/2314-5670$09.00/0

The following mechanisms of decomposition of the transient complexes of the type $Cu^{II}-R$ have been reported.

1. Homolysis of the copper–carbon σ bond.[10,13]

$$Cu^{II}-R \rightleftharpoons Cu(I) + {}^{\bullet}R \quad (5)$$

2. Heterolysis of the copper–carbon σ bond:[11]

$$Cu^{II}-R + H_2O \rightarrow Cu(II) + RH + OH^- \quad (6)$$

3. β-Elimination processes when a good leaving group is bound to the β carbon atom, *e.g.* X = OH, OR, and NR_2:[13c,d]

$$Cu^{II}-CR^1R^2CR^3R^4X \rightarrow Cu(II) + R^1R^2C{=}CR^3R^4 + X^- \quad (7)$$

4. Carbon–carbon bond formation processes, *e.g.*

$$2Cu^{II}-CH_3{}^+{}_{aq} \rightarrow 2Cu^+{}_{aq} + C_2H_6{}^{11} \quad (8)$$

$$(CO)Cu^{II}-CH_3{}^+{}_{aq} \rightarrow Cu^{II}-C(O)CH_3{}^+{}_{aq} \rightarrow Cu^{2+}{}_{aq} + CH_3CHO + OH^-{}^{14} \quad (9)$$

5. Rearrangement of the carbon skeleton of the organic residue:[15]

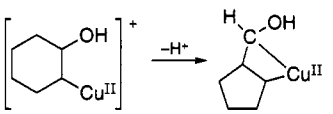

These examples clearly point out the large variety of mechanisms by which the transient complexes with copper–carbon σ bonds might react.

To date, due to the unstable nature of $Cu^+{}_{aq}$, it has been prepared in situ by reduction with $e^-{}_{aq}$, using ionizing radiation, or by the reduction of $Cu^{2+}{}_{aq}$ by $Cr^{2+}{}_{aq}$; in these systems the $Cu^{2+}{}_{aq}$ concentration was high, and thus, the involvement of $Cu^{2+}{}_{aq}$ reactions with the radical, added to the complexity of the reactions studied, and reactions of free radicals, *e.g.* $^{\bullet}CH_2CO_2^-$ for which $k_4 > 5 \times 10^7\ M^{-1}\ s^{-1}$, with Cu(I) could not be studied.

Recently, we have found that solutions containing up to 2×10^{-4} M $Cu^+{}_{aq}$, free of $Cu^{2+}{}_{aq}$, at pH $\leq$ 4.0 can be prepared by adding $[Cu(NH_3)_2]^+{}_{aq}$[16] into acidic solutions. The $Cu^+{}_{aq}$ thus prepared is stable for several hours.

It was therefore decided to measure the mechanisms of reaction of the free radicals $^{\bullet}CH_3$, $^{\bullet}CH_2CO_2H$, $^{\bullet}CH(CH_3)CO_2H$, and $^{\bullet}CH_2CH_2CO_2H$ with $Cu^+{}_{aq}$. Furthermore it was decided to study the mechanisms of reaction of the same free radicals with L^2Cu^+, where L^2 = 2,5,8,-11-tetramethyl-2,5,8,11-tetraazadodecane, with the hope of elucidating the effect of a relatively sterically hindered ligand which induces a hydrophobic nature to the Cu(I) complex[17] on the reaction mechanism. It was recently shown that the latter ligand, which is a pure σ donor, stabilizes Cu(I) in neutral and alkaline aqueous solutions.[17]

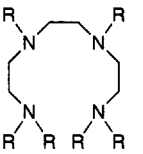

R = H, L
R = CH_3, L^2

Experimental Section

Materials. All solutions were prepared from AR grade chemicals and from distilled water further purified by passing through a Milli Q Millipore setup, final resistivity >10 M Ω/cm. The ligand L^2 was prepared by N-methylation of the unmethylated ligand (L = 1,4,7,10-tetraaza-decane, Aldrich) using formaldehyde and formic acid according to a procedure described in the literature[18] and crystallized as its HCl salt. The degree of N-methylation obtained was verified by C, H, and N analyses and by H-NMR and ^{13}C-NMR measurements. Both analytical techniques indicated that more than 97% of the ligand molecules were hexamethylated.

Cu(I) Preparation. Solutions of L^2Cu^+ were prepared via the comproportionation process:

$$Cu_s + L^2Cu^{2+} + L^2 \rightleftharpoons 2L^2Cu^+ \quad (10)$$

$Cu^+{}_{aq}$ was obtained via comproportionation of $Cu(NH_3)_4{}^{2+}$ in concentrated NH_3 (Linde Inc.), aliquots of which were added to acidic solutions.

The pH was measured with a Corning 220 pH meter and was adjusted by $HClO_4$ and/or NaOH. For the L^2Cu^+ system the pH was adjusted by HCl.

Irradiations. Pulse-radiolysis experiments were carried out using the Varian 7715 linear electron accelerator of the Hebrew University of Jerusalem. The pulse duration was 0.1–1.5 μs with a 200-mA current of 5-MeV electrons. The dose per pulse was 300–3000 rad. Irradiations were carried out in a 4-cm spectrosil optical cell, the analyzing light passing three times through the cell. A 150-W xenon arc produced the analyzing light. The experimental setup was identical with that described earlier in detail.[12a,19]

For dosimetry, a N_2O-saturated solution containing 1×10^{-3} M KSCN was used. The yield of $(SCN)_2{}^{\bullet-}$ was measured by taking $\epsilon_{475} = 7600\ M^{-1}\ cm^{-1}$, and the dose per pulse was calculated assuming $G(SCN)_2{}^{\bullet-} = 6.0$[19] and an optical path of 12.3 cm. The dose per pulse was set so that the initial free radical concentration was 2–20 μM.

The values of the molar extinction coefficients calculated from the dosimetry measurements have an error limit of 15% due to the scatter in the pulse intensity and due to uncertainties in G values. The dose delivered to vials, identical to those irradiated for final product analysis, was measured using the Fricke dosimeter taking $G(Fe(III)) = 15.6$ and $\epsilon_{302} = 2197\ M^{-1}\ cm^{-1}$.[19]

A ^{60}Co source, Noratom, with a dose rate of 1300 rad/min was used for low-dose-rate experiments and product analysis.

Product Analysis. Yield of Cu(I). The stability constant of the formation of the d $\rightarrow$ π complex of $Cu^+{}_{aq}$ with fumaric

(13) (a) Cohen, H.; Meyerstein, D. *Inorg. Chem.* **1987**, *26*, 2342. (b) Meyerstein, M. *Pure Appl. Chem.* **1989**, *61*, 885. (c) Masarwa, M.; Cohen, H.; Saar, J.; Meyerstein, D. *Isr. J. Chem.* **1990**, *61*, 361. (d) Goldstein, S.; Czapski, G.; Cohen, H.; Meyerstein, D. *Inorg. Chem.* **1992**, *31*, 2439.

(14) Szulz, A.; Cohen, H.; Meyerstein, D. To be published.

(15) Masarwa, M.; Cohen, H.; Meyerstein, D. *Inorg. Chem.* **1991**, *30*, 1849.

(16) Parker, A. J. *Search* **1973**, 4.

(17) (a) Golub, G.; Cohen, H.; Meyerstein, D. *J. Chem. Soc., Chem. Commun.* **1992**, 398. (b) Golub, G.; Cohen, H.; Paoletti, P.; Bencini, A.; Bertini, I.; Messori, L.; Meyerstein, D. *J. Am. Chem. Soc.* **1995**, *117*, 8353. (c) Golub, G.; Zilbermann, I.; Cohen, H.; Meyerstein, D. *Supramolecular Chem.*, in press.

(18) Icke, R. N.; Wisegarver, B. B.; Alles, G. A.; Snyder, H. R. *Org. Synth. Synth. Coll.* **1941**, *3*, 723.

(19) Matheson, M. S.; Dorfman, M. L. *Pulse Radiolysis*; MIT Press: Cambridge, MA, 1969.

acid at pH 2.0 is $K = 7500\ M^{-1}$.[20] This complex has an absorption band with $\lambda_{max} = 356$ nm and $\epsilon = 1000 \pm 100\ M^{-1}\ cm^{-1}$ at pH 2.0.[20] The change in the concentration of Cu^{+}_{aq} caused by the reaction was measured by adding fumaric acid at pH 2.0 to the sample so that the final concentration of the fumaric acid was 2.0×10^{-2} M and measuring the absorbance at 356 nm. For the L^2Cu^+ system, the change in the concentration was determined by measuring the absorption due to L^2Cu^{2+}.

UV–vis spectra were recorded using a Hewlett Packard 8452A diode array spectrophotometer.

GC Analysis. The 10 mL samples in glass vials were irradiated by the linac. The gaseous products were analyzed using a Varian Model 3700 gas chromatograph.

Production of Free Radicals. The radiolysis of water in dilute aqueous solutions can be summarized:[19]

$$H_2O \xrightarrow{\gamma, e^-} e^-_{aq}\ (2.65),\ {}^{\bullet}OH\ (2.65),\ H^{\bullet}\ (0.60),\ H_2\ (0.45),\ H_2O_2\ (0.75) \quad (11)$$

(G value, in parentheses, is defined as the number of molecules of each product/100 eV radiation absorbed by the solution.) In concentrated solutions, the yields of the primary free radicals are somewhat higher and those of H_2O_2 and H_2 are somewhat lower.[19]

In neutral N_2O-saturated solutions ($[N_2O] = 0.022$ M) the hydrated electron is converted into the hydroxyl radical via

$$e^-_{aq} + N_2O \xrightarrow{H_2O} N_2 + OH^- + {}^{\bullet}OH \qquad k_{12} = 8.7 \times 10^9\ M^{-1}\ s^{-1}\ [22] \quad (12)$$

In acidic solutions the reaction of e^-_{aq} with H^+, which produces $H^{\bullet}$ atoms, becomes important

$$e^-_{aq} + H^+ \rightarrow H^{\bullet} \qquad k_{14} = 2.2 \times 10^{10}\ M^{-1}\ s^{-1}\ [22] \quad (14)$$

but at pH > 3 the contribution of $H^{\bullet}$ atoms to the total free radical yield is less than 10%. The methyl free radicals were produced via

$$(CH_3)_2SO + {}^{\bullet}OH \rightarrow (CH_3)_2{}^{\bullet}S(O)OH \qquad k_{15} = 6.6 \times 10^9\ M^{-1}\ s^{-1}\ [23] \quad (15)$$

$$(CH_3)_2{}^{\bullet}S(O)OH \rightarrow {}^{\bullet}CH_3 + CH_3S(O)OH \qquad k_{16} = 1.5 \times 10^7\ s^{-1}\ [23] \quad (16)$$

The ${}^{\bullet}CH_2CO_2H/{}^{\bullet}CH_2CO_2^-$, $pK_a = 4.5$,[24] free radicals were prepared via

$$CH_3CO_2H + {}^{\bullet}OH/H \rightarrow {}^{\bullet}CH_2CO_2H + H_2O/H_2 \qquad k_{OH} = (2.3-8.5) \times 10^7\ M^{-1}\ s^{-1}\ [25,26] \quad (17)$$

$$k_H = (1.2-3.5) \times 10^5\ M^{-1}\ s^{-1}\ [27]$$

Table 1. Reactions of Primary Free Radicals with the Solutes Used in this Study

reaction	k ($M^{-1}\ s^{-1}$)	pH
$(CH_3)_2SO + {}^{\bullet}OH \rightarrow (CH_3)_2\dot{S}(O)OH$ followed by	6.6×10^9 [23]	
$(CH_3)_2\dot{S}(O)OH \rightarrow {}^{\bullet}CH_3 + CH_3S(O)OH$	$1.5 \times 10^7\ s^{-1}$ [23]	
$(CH_3)_2SO + {}^{\bullet}H \rightarrow (CH_3)_2S(OH)$	2.7×10^6 [31a]	
$(CH_3)_2SO + e^-_{aq} \rightarrow$ products	1.6×10^6 [31b]	
$e^-_{aq} + Cu^+_{aq} \rightarrow Cu^0$	2.7×10^{10} [32]	5.8
${}^{\bullet}OH + Cu^+_{aq} \rightarrow Cu^{2+}_{aq}$	2.0×10^{10} [32]	
${}^{\bullet}H + Cu^+_{aq} \rightarrow CuH^+_{aq}$ (followed by $Cu{-}H^+_{aq} \rightarrow Cu^{2+}_{aq} + H_2$)	$>5.0 \times 10^9$ [33]	5.6
${}^{\bullet}OH + Cu^{2+}_{aq} \rightarrow CuOH^{2+}$	3.1×10^8 [32]	3–6
${}^{\bullet}H + Cu^{2+}_{aq} \rightarrow Cu^+_{aq} + H^+$	$<10^6$ [12]	
$e^-_{aq} + Cu^{2+}_{aq} \rightarrow Cu^+_{aq}$	3.0×10^{10} [32]	6.8
${}^{\bullet}OH + CH_3CH_2COOH \rightarrow$ products	6.2×10^8 [34]	2
${}^{\bullet}H + CH_3CH_2COOH \rightarrow {}^{\bullet}CH(CH_3)COOH + H_2$	5.9×10^6 [35]	1
$e^-_{aq} + CH_3CH_2COOH \rightarrow CH_3CH_2COO^- + H^{\bullet}$	2.2×10^7 [36]	3–4
${}^{\bullet}OH + CH_3CH_2COO^- \rightarrow$ products	8.2×10^8 [29]	9
${}^{\bullet}H + CH_3CH_2COO^- \rightarrow {}^{\bullet}CH(CH_3)COO^- + H_2$	1.7×10^7 [38]	7
${}^{\bullet}OH + CH_3COOH \rightarrow {}^{\bullet}CH_2COOH + H_2O$	2.3×10^7 [25]	1
${}^{\bullet}H + CH_3COOH \rightarrow {}^{\bullet}CH_2COOH + H_2$	1.2×10^5 [27]	1
$e^-_{aq} + CH_3COOH \rightarrow CH_3COO^- + H^{\bullet}$	1.8×10^8 [37]	5.4
${}^{\bullet}OH + CH_3COO^- \rightarrow {}^{\bullet}CH_2COO^- + H_2O$	8.5×10^7 [26]	10.7
${}^{\bullet}H + CH_3COO^- \rightarrow {}^{\bullet}CH_2COO^- + H_2$	3.5×10^5 [27]	7
$e^-_{aq} + CH_3COO^- \rightarrow$ products	$<1.0 \times 10^6$ [37]	10

The ${}^{\bullet}CH_2CH_2CO_2H$ and ${}^{\bullet}CH(CH_3)CO_2H$ free radicals were prepared via

$$CH_3CH_2CO_2H + {}^{\bullet}OH \xrightarrow{55\%} {}^{\bullet}CH(CH_3)CO_2H + H_2O \xrightarrow{45\%} {}^{\bullet}CH_2CH_2CO_2H + H_2O \quad (18)$$

$$k_{18} = (3.8-8.2) \times 10^8\ M^{-1}\ s^{-1}\ [29]$$

The relative yields given are those for pH 9.0; at pH 3.0 the yield of the α radicals is ~40% and that of the β radicals is ~60%.[24]

Results and Discussion

N_2O-saturated solutions containing $(0.3-1) \times 10^{-4}$ M of Cu^+_{aq}, pH 3.0, or $(1-10) \times 10^{-4}$ M of L^2Cu^+, pH 10.0 (the concentration of L^2 was always twice that of the Cu(I) concentration), and 0.1–0.3 M CH_3CO_2H or $CH_3CH_2CO_2H$ or 0.3 M $(CH_3)_2SO$ were irradiated by a short electron pulse from the linear accelerator. Under these conditions all the primary free radicals are transformed into the desired aliphatic free radicals during the pulse, Table 1.[23,25–29,31–38]

In all the systems studied two consecutive processes are observed after the formation of the aliphatic free radicals, Figure 1. The system containing CH_3CH_2-

(20) Navon, N.; Cohen, H.; Meyerstein, D. To be published. (The stability constant is pH dependent; this is the reason for the difference between K at pH 2.0 and K at pH 3.6 in ref 21.)
(21) Meyerstein, D. *Inorg. Chem.* **1975**, *14*, 1716.
(22) Anbar, M.; Bambenck, M.; Ross, A. B. *Natl. Stand. Ref. Data Ser. (U.S., Natl. Bur. Stand.)* **1973**, NSRDS-NBS 43.
(23) Veitwisch, D.; Janata, E.; Asmus, K. D. *J. Chem. Soc., Perkin Trans.* **1980**, *2*, 146.
(24) Neta, P.; Simic, M.; Hayon, E. *Aust. J. Chem.* **1976**, *29*, 637.
(25) Ebert, M.; Keene, J. P.; Swallow, A. J.; Baxendale, J. H. *Pulse Radiolysis*; Academic Press: New York, 1965; p 131.
(26) Willson, R. L.; Greenstock, C. L.; Adams, G. E.; Wagenman, R.; Dorfman, L. M. *Int. J. Radiat. Phys. Chem.* **1971**, *3*, 211.
(27) (a) Neta, P.; Holdern, G. R.; Schuler, R. H. *J. Phys. Chem.* **1971**, *75*, 449. (b) Appleby, A.; Scholes, G.; Simic, M. *J. Am. Chem. Soc.* **1963**, *85*, 3891.
(28) Zuberbühler, A. D. *Helv. Chim. Acta* **1970**, *53*, 473.
(29) Anbar, M.; Meyerstein, D.; Neta, P. *J. Chem. Soc. B* **1966**, 742.
(30) (a) Espenson, J. H. *Adv. Inorg. Bioinorg. Mech.* **1982**, *1*, 1. (b) Cohen, H.; Meyerstein, D. *Inorg. Chem.* **1974**, *13*, 2432.
(31) (a) Chardhri, S. A.; Goebl, M.; Freyholdt, T.; Asmus, K. D. *J. Am. Chem. Soc.* **1984**, *106*, 5988. (b) Koulkes-Pujo, A. M.; Michael, B. D.; Hart, E. J. *J. Radiat. Phys. Chem.* **1971**, *3*, 333.
(32) Buxton, G. V.; Greenstock, C. L.; Helman, W. P.; Ross, A. B. *J. Phys. Chem. Ref Data* **1988**, *17*, 513.
(33) Mulac, W. A.; Meyerstein, D. *Inorg. Chem.* **1982**, *21*, 1782.
(34) Scholes, G.; Willson, R. L. *Trans. Faraday Soc.* **1967**, *63*, 2983.
(35) Neta, P.; Fessenden, R. W.; Schuler, R. H. *J. Phys. Chem.* **1971**, *75*, 1654.
(36) Micic, O. J.; Markovic, V. *Int. J. Radiat. Phys. Chem.* **1972**, *4*, 43.
(37) Gordon, S.; Hart, E. J.; Matheson, M. S.; Rabani, J.; Thomas, J. K. *Discuss Faraday Soc.* **1963**, *36*, 193.
(38) Neta, P.; Schuler, R. H. *J. Phys. Chem.* **1972**, *76*, 2673.

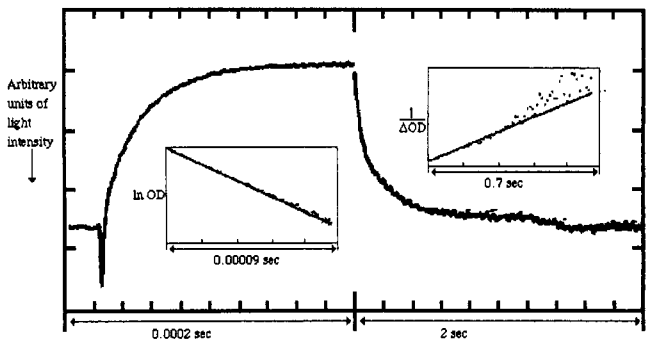

Figure 1. Computer output of light intensity vs time. Solution composition: N_2O-saturated, containing 3×10^{-4} M Cu(I), 6×10^{-4} M L^2, and 0.1 M DMSO at pH 7.0. Insets: Kinetics of formation of the intermediate, a fit to a first-order rate law; kinetics of decomposition of the intermediate, a fit to a second-order rate law.

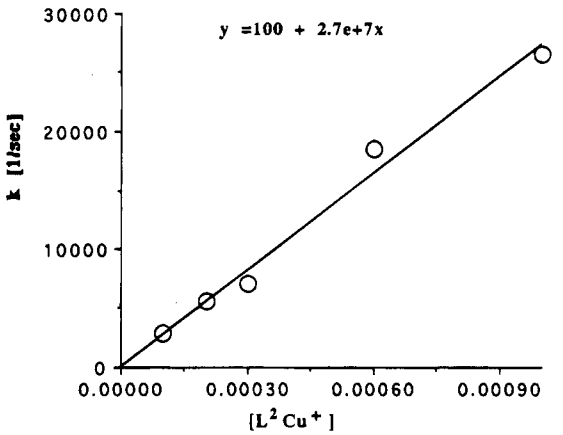

Figure 2. Dependence of the rate of formation of (L^2Cu^{II}–CH_2COO^-) on [L^2Cu^+]. Solution composition: N_2O-saturated, 0.1 M CH_3COO^-, pH 8.0.

CO_2H is an exception to this statement; in this system three consecutive processes are observed.

The first process, the formation of the intermediates, always obeys a first-order rate law; see for example Figure 1. The observed rates are proportional to the concentration of the Cu(I) complexes; see for example Figure 2. The rates are independent of the concentrations of all other components of the solution, pulse intensity, and wavelength of observation. Therefore it is reasonable to propose that the unstable intermediates formed in this process are LCu^{II}–R and that the reactions observed are those depicted in eq 3a, *i.e.*

$$Cu^IL + {}^\bullet R \rightarrow LCu^{II}\text{–}R \qquad (3a)$$

complexes with a copper–carbon σ bond; the results are summed up in Table 2. Indeed the spectra of the intermediates formed, Table 3, are similar to those of other complexes of this type; see below. A typical spectrum is shown in Figure 3. The rates of reaction 3, Table 2, for $Cu^IL = Cu^+_{aq}$ all approach the diffusion-controlled limit in accord with reported data on the reactions of other free radicals with this complex. The rates of reaction 3 for $Cu^IL = L^2Cu^+$ are considerably lower. The order of reactivity is ${}^\bullet CH_3 > {}^\bullet CH_2CO_2^- > {}^\bullet CH_2CH_2CO_2^- > {}^\bullet CH(CH_3)CO_2^-$. The reaction of the latter radical is too slow to be observed; see below. The latter result indicates that the very large effect of this ligand on the rates of reaction stems mainly from the steric hindrance imposed by it.

Table 2. Rates of Reaction of Aliphatic Free Radicals with Cu(I) Complexes

reaction	k_3 (M^{-1} s^{-1})[a]
$Cu^+_{aq} + {}^\bullet CH_3 \rightarrow (Cu^{II}\text{–}CH_3)^+$	3.5×10^9 [d]
$Cu^+_{aq} + {}^\bullet CH_2COOH \rightarrow (Cu^{II}\text{–}CH_2COOH)^+$	2.8×10^9 [d]
$Cu^+_{aq} + {}^\bullet CH(CH_3)COOH/{}^\bullet CH_2CH_2COOH \rightarrow$ $(Cu^{II}\text{–}CH(CH_3)COOH)^+/$ $(Cu^{II}\text{–}CH_2CH_2COOH)^+$ [b]	4.0×10^9 [d]
$L^2Cu^+ + {}^\bullet CH_3 \rightarrow (L^2Cu^{II}\text{–}CH_3)^+$	1.2×10^8 [e,f]
$L^2Cu^+ + {}^\bullet CH_2COO^- \rightarrow (L^2Cu^{II}\text{–}CH_2COO^-)$	2.7×10^7 [e,g]
$L^2Cu^+ + {}^\bullet CH_2CH_2COO^- \rightarrow$ $(L^2Cu^{II}\text{–}CH_2CH_2COO^-)$ [c]	6.3×10^6 [e,g]

[a] All experiments were carried out at room temperature, 22 ± 2 °C. Error limit ±15%. [b] The two reactions are experimentally nonseparable. [c] The reaction of ${}^\bullet CH(CH_3)COOH$ is too slow to be observed; see text. [d] pH 3.0; the results are independent of pH in the range 2–4, $I \leq 0.005$ M. [e] pH 8.0; the results are independent of pH in the range 7–10. [f] $I \leq 0.001$ M. [g] $I = 0.30$ M.

Table 3. Spectra of the Transient Complexes LCu^{II}–R[a]

transient complex	λ_{max} (nm)[b]	ϵ (M^{-1} cm^{-1})[c]
$(Cu^{II}\text{–}CH_3)^+$	375	2700
$(Cu^{II}\text{–}CH_2COOH)^+$	360	1700
$(Cu^{II}\text{–}CH(CH_3)COOH)^+$	410	1750
$(Cu^{II}\text{–}CH_2CH_2COOH)^+$	390	1750
$(L^2Cu^{II}\text{–}CH_3)^+$	380	3000
$(L^2Cu^{II}\text{–}CH_2COO^-)$	405	2700
$(L^2Cu^{II}\text{–}CH_2CH_2COO^-)$	390	2450

[a] Experimental conditions as in Table 1. [b] Error limit ±5 nm. [c] Error limit ±15%.

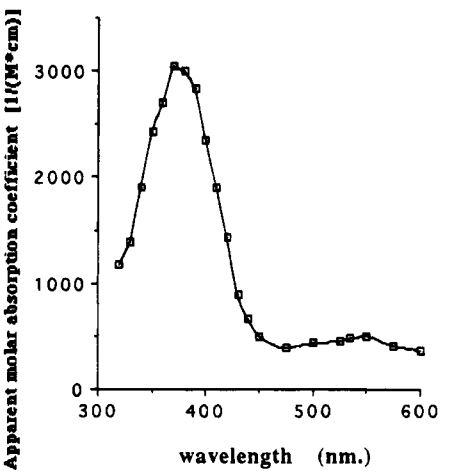

Figure 3. Spectrum of $(L^2Cu^{II}\text{–}CH_3)^+_{aq}$ measured 200 μs after the pulse: N_2O-saturated solution containing 3×10^{-4} M Cu(I), 6×10^{-4} ML^2, and 0.1 M DMSO at pH 7.0.

The mechanism of decomposition of the transient complexes LCu^{II}–R depends on both the nature of R and that of L. In the following paragraphs these mechanisms are discussed separately for each R.

Mechanism of Decomposition of the Complexes LCu^{II}–CH_3^+. The reaction $Cu^+_{aq} + {}^\bullet CH_3$ was studied previously in the presence of excess Cu^{2+}_{aq} as Cu^+_{aq} was prepared via the reduction of Cu^{2+}_{aq} by Cr^{2+}_{aq}.[11] The results obtained under the present experimental conditions, Table 4, are in accord with the previous ones and indicate that above pH 2 the mechanism of decomposition is

$$2Cu^{II}\text{–}CH_3{}^+_{aq} \rightarrow 2Cu^+_{aq} + C_2H_6$$
$$2k_{19} = 3.0 \times 10^8\ M^{-1}\ s^{-1} \qquad (19)$$

The mechanism does not involve homolysis of the

Table 4. Observed Kinetic Parameters

10^3[Cu$^+$] (M)	10^3[L] (M)	solute	[solute] (M)	pH	λ (nm)	k_f[a] (s^{-1})	k_{d1}[b]	k_{d2}[c]	comments
0.2	0.4	DMSO	0.1	10	400	3.0×10^4	128 $M^{-1} s^{-1}$ [d]		
1.0	2.0	DMSO	0.1	10	400	1.17×10^5	158 $M^{-1} s^{-1}$ [d]		
0.3	0.6	DMSO	0.1	7	380	3.1×10^4	124 $M^{-1} s^{-1}$ [d]		
0.3	0.6	DMSO	0.3	7	380	3.6×10^4	131 $M^{-1} s^{-1}$ [d]		
0.3	0.6	DMSO	0.1	7	380	3.6×10^4	130 $M^{-1} s^{-1}$ [d]		0.1 mM Cu^{2+}
0.3	2.6	DMSO	0.1	7	380	3.8×10^4	141 $M^{-1} s^{-1}$ [d]		
0.3	0.6	HAc	0.1	8	450	8.1×10^3	11.1 s^{-1}		
0.3	0.6	HAc	0.3	8	405	7.2×10^3	11.9 s^{-1}		
0.3	0.6	HAc	0.3	8	405	6.7×10^3	12.4 s^{-1}		0.1 mM Cu^{2+}
0.3	2.6	HAc	0.3	8	405	9.5×10^3	16.5 s^{-1}		
0.3	0.6	HAc	0.3	10	405	7.3×10^3	11.6 s^{-1}		
0.6	1.2	HAc	0.3	8	405	1.94×10^4	11.6 s^{-1}		
0.2	0.4	HAc	0.3	8	405	5.5×10^3	11.8 s^{-1}		
0.2	0.4	HPr	0.1	8	420	4.6×10^3	1.0×10^4 $M^{-1} s^{-1}$ [d]		
0.5	1.0	HPr	0.1	8	400	7.1×10^3	3.2×10^3 $M^{-1} s^{-1}$ [d]		
0.8	1.6	HPr	0.1	8	420	8.2×10^3	1.7×10^3 $M^{-1} s^{-1}$ [d]		
		HPr	0.1	8	340		1.3×10^5 $M^{-1} s^{-1}$ [d]		
0.064	H_2O	DMSO	0.3	3	380	2.8×10^5	6.1×10^3 $M^{-1} s^{-1}$ [d]		see ref 11
0.064	CH_3CN	DMSO	0.3	3	380	2.8×10^5	6.6×10^3 $M^{-1} s^{-1}$ [d]		
0.096	H_2O	HAc	0.1	3	400	3.3×10^5	2.6×10^4 s^{-1}		
0.064	H_2O	HAc	0.1	3	400	2.5×10^5	2.4×10^4 s^{-1}		
0.096	H_2O	HAc	0.1	2.5	400	4.3×10^5	6.6×10^4 s^{-1}		
0.096	H_2O	HAc	0.5	3	400	4.8×10^5	6.8×10^4 s^{-1}		
0.096	H_2O	HAc	0.1	3	400		2.3×10^4 s^{-1}		
0.096	H_2O	HPr	0.1	3	400	3.9×10^5	2.5×10^4 s^{-1}	1.6×10^4 $M^{-1} s^{-1}$ [d]	
0.064	H_2O	HPr	0.1	3	400	2.4×10^5	2.0×10^4 s^{-1}	1.6×10^4 $M^{-1} s^{-1}$ [d]	
0.032	H_2O	HPr	0.1	3	400	1.3×10^5		1.7×10^4 $M^{-1} s^{-1}$ [d]	
0.096	H_2O	HPr	0.1	2.5	400	3.9×10^5	8.9×10^4 s^{-1}	1.5×10^4 $M^{-1} s^{-1}$ [d]	

[a] Observed rate of formation of the transient complex. [b] Observed rate of the second process. [c] Observed rate of the third process. [d] $2k/\Delta\epsilon \cdot L$.

copper–carbon σ bond as the rate of reaction is independent of [Cu$^+_{aq}$], Table 4. The rate of reaction 19 is also independent of the presence of excess Cu^{2+}_{aq};[11] however, the observed rate is higher by 1 order of magnitude than that previously reported. The source of this discrepancy is not clear.

The decomposition of the transient complex $L^2Cu^{II}-CH_3^+$ also obeys a second-order rate law. The rate of this process is independent of [L^2Cu^+], Table 4. The results thus indicate that $L^1Cu^{II}-CH_3^+$ and $L^2Cu^{II}-CH_3^+$ decompose via an analogous mechanism. Indeed the product analysis corroborates this conclusion because ethane is the only organic product observed, its yield exceeding 90% of that of the methyl radicals. The observed process is therefore attributed to the reaction

$$2L^2Cu^{II}-CH_3^+{}_{aq} \rightarrow 2L^2Cu^+{}_{aq} + C_2H_6 \qquad 2k_{19} = 8.6 \times 10^6\ M^{-1}\ s^{-1} \quad (19a)$$

In principle reaction 19, taking into account that it does not involve homolysis, may proceed via one of the following routes:

1. Methyl transfer from one of the $LCu^{II}-CH_3^+{}_{aq}$ complexes to the second followed by reductive elimination, *i.e.* via

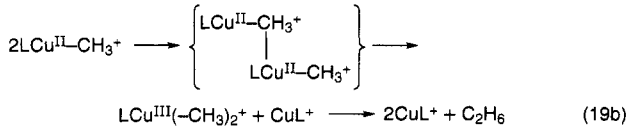

(It should be noted that $LCu^{III}-R$ transient complexes are formed in many reactions of alkyl radicals with Cu(II) complexes.[12])

2. Via a transition state in which the two methyl groups bridge between the two copper ions, *i.e.* via

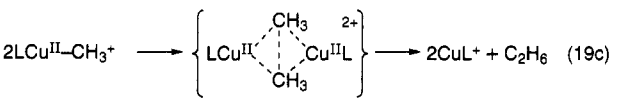

3. Via a transition state in which a carbon–carbon bond is formed directly while each methyl is bound to another copper, *i.e.* via

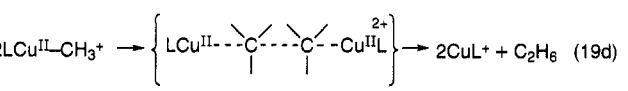

The observation that k_{19a} is only slower by a factor of ~35 than k_{19}, though steric factors slow down k_3 by a similar factor for the same ligands, L, seems to rule out transition states in which one of the methyls is bound coherently to the two copper ions, *i.e.* mechanisms (19b) and (19c). Thus the results indicate that mechanism (19d) describes best the detailed mechanism of the observed process.

It is of interest to note that the addition of 0.1 M CH_3CN to solutions containing Cu$^+_{aq}$ has no effect on the kinetics of decomposition of $LCu^{II}-CH_3^+{}_{aq}$, Table 4. As the Cu(I) under these conditions is present as $Cu(CH_3CN)_2^+{}_{aq}$, $\log \beta_2 = 4.35$,[28] one has to conclude that either $(CH_3CN)_nCu^{II}-CH_3^+{}_{aq}$ decomposes at the same rate of $Cu^{II}-CH_3^+{}_{aq}$ or that the CH_3CN ligands are lost prior to this reaction.

Mechanisms of Decomposition of the Complexes $LCu^{II}-CH_2COOH^+$/($LCu^{II}-CH_2COO^-$). The process of decomposition of the transient complex $Cu^{II}-CH_2COOH^+{}_{aq}$ obeys a first-order rate law. The observed rate constant obeys the equation $k_d = k_0 + k[H^+]$, Figure 4. The reaction is accompanied by a decrease in [Cu$^+_{aq}$]. The yield of this decrease, $G(-Cu^+_{aq})$, equals the yield of $^\bullet CH_2COOH$ free radicals. These results indicate that the observed process is

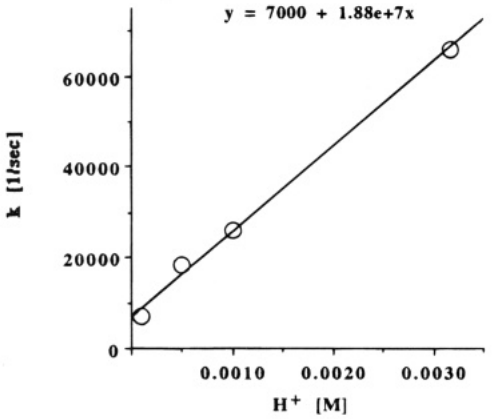

Figure 4. Dependence of the rate of decomposition of $Cu^{II}-CH_2COOH^+_{aq}$ on $[H^+]$. Solution Composition: N_2O-saturated, 1.0×10^{-4} M Cu^+_{aq}, and 0.1 M CH_3COOH.

$$Cu^{II}-CH_2COOH^+_{aq} + H_3O^+/H_2O \rightarrow Cu^{2+}_{aq} + CH_3COOH + H_2O/OH^- \quad k_{20} = (7000 + 1.88 \times 10^7[H^+])\ s^{-1} \quad (20)$$

This rate law is in accord with reports on the heterolysis of various transient complexes with metal–carbon σ bonds[30] and with the observation that $Cu^{II}-CH_3^+{}_{aq}$ decomposes heterolytically at pH < 1.[11] The observation that $Cu^{II}-CH_2COOH^+_{aq}$ decomposes heterolytically under conditions where $Cu^{II}-CH_3^+{}_{aq}$ decomposes via an alternative mechanism is not surprising as the electron-withdrawing substituent, –COOH, increases the polar nature of the metal–carbon σ bond. Analogous observations were reported for the $(H_2O)_5Cr^{III}-R^{2+}$ complexes.[30]

Also the process of decomposition of the transient complex $L^2Cu^{II}-CH_2COO^-{}_{aq}$ obeys a first-order rate law, Table 4. The spectrum of the final product points out that $L^2Cu^{2+}_{aq}$ is one of the final products and that its yield equals the yield of the $^\bullet CH_2COO^-$ free radicals. Thus the results indicate that the observed process is

$$(L^2Cu^{II}-CH_2COO^-)_{aq} + H_2O \rightarrow L^2Cu^{2+}_{aq} + CH_3COO^- + OH^- \quad k_{21} = 11\ s^{-1} \quad (21)$$

The observation that the rate of this reaction is pH independent, in the range 7 < pH < 10 (Table 4), indicates only that the acid-dependent term is smaller than $3 \times 10^7[H^+]\ s^{-1}$. The fact that k_{21} is considerably smaller than the acid-independent component of k_{20} is attributed to the steric hindrance imposed by L^2 which slows down the approach of the water molecule to the copper–carbon bond.

Mechanisms of Decomposition of the Complexes $LCu^{II}-CH_2CH_2COOH^+$/($LCu^{II}-CH_2CH_2COO^-$) and $LCu^{II}-CH(CH_3)COOH^+$/($LCu^{II}-CH(CH_3)COO^-$). In acidic solutions the reaction of $^\bullet OH$ free radicals with propionic acid yields 40% of $^\bullet CH(CH_3)COOH$ and 60% of $^\bullet CH_2CH_2COOH$ free radicals.[24] The reaction of the mixture of these radicals with Cu^+_{aq} cannot be resolved into two processes. The spectrum of the product of these processes, which is expected to be a mixture of $Cu^{II}-CH_2CH_2COOH^+_{aq}$ and $Cu^{II}-CH(CH_3)COOH^+_{aq}$, is shown in Figure 5, the spectrum 22 μs after the pulse.

The mechanism of decomposition of the mixture of these transient complexes consists of two processes

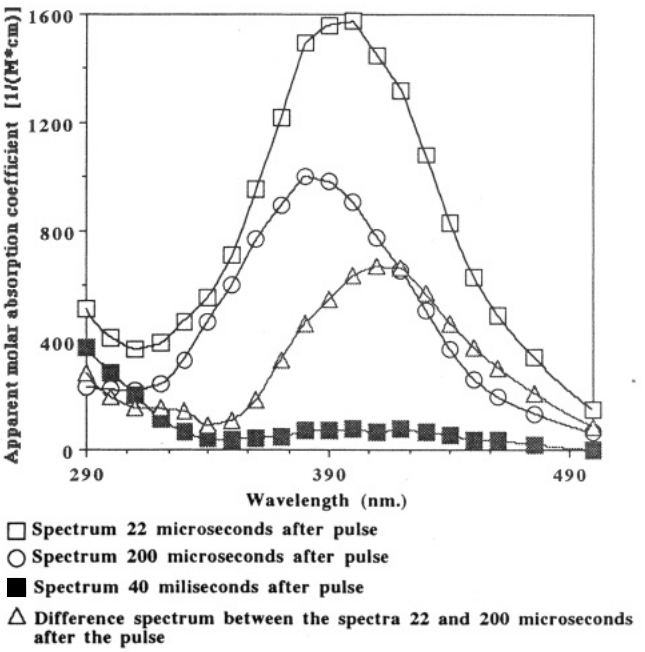

Figure 5. Spectra of the transient complexes formed when a mixture of the free radicals $^\bullet CH_2CH_2CO_2^-$ and $^\bullet CH(CH_3)CO_2^-$ are reacted with Cu^+_{aq}. Solution composition: N_2O-saturated, 1.0×10^{-4} M Cu^+_{aq}, and 0.1 M propionic acid, pH 3.0.

which are well separated in time. The first process obeys a first-order rate law. The rate of the latter reaction increases linearly with $[H_3O^+]$, Table 4, with a rate constant which obeys the relation $k_{ob} = (8300 + 2.5 \times 10^7[H^+])\ s^{-1}$. The spectrum of the transient complex present in the solution after this process is plotted in Figure 5, the spectrum 200 μs after the pulse. The second process obeys a second-order rate law; the rate of this process is independent of $[Cu^+_{aq}]$ and of the concentrations of all the other components of the solution, Table 4. The decrease in $[Cu^+_{aq}]$ points out that $G(-Cu^+_{aq})$ equals ca. half the yield of the aliphatic free radicals. These results indicate that the observed processes are as follows.

1. The first process observed is probably

$$Cu^{II}-CH(CH_3)COOH^+_{aq} + H_3O^+/H_2O \rightarrow Cu^{2+}_{aq} + CH_3CH_2COOH + H_2O/OH^- \quad k_{21} = (8300 + 2.5 \times 10^7[H^+])\ s^{-1} \quad (22)$$

This proposal is based on the following arguments: a. The rate law of this process is very similar to that obtained for the decomposition of $Cu^{II}-CH_2COOH^+_{aq}$. b. $G(-Cu^+_{aq})$ equals the yield of the $^\bullet CH(CH_3)COOH$ free radicals.

2. The second process observed is probably

$$2Cu^{II}-CH_2CH_2COOH^+_{aq} \rightarrow 2Cu^+_{aq} + (HOOCCH_2CH_2-)_2 \quad k_{23} = 1.7 \times 10^8\ M^{-1}\ s^{-1} \quad (23)$$

This proposal is based on the following arguments: a. The rate law of this process is very similar to that obtained for the decomposition of $Cu^{II}-CH_3^+{}_{aq}$. b. If Cu^{2+}_{aq} is indeed the product of the first process, then $G(-Cu^+_{aq}) = 0$ for this process. It should be pointed out that the dimer could not be detected under our

Table 5. Mechanisms and Rates of Decomposition of the Transient Complexes $LCu^{II}-R$[a]

reaction	k_d[b]
$2Cu^{II}-CH_3^+{}_{aq} \rightarrow 2Cu^+{}_{aq} + C_2H_6$	$3.0 \times 10^8\ M^{-1}\ s^{-1}$ [c]
$Cu^{II}-CH_2COOH^+ + H_3O^+/H_2O \rightarrow Cu^{2+}{}_{aq} + CH_3COOH$	$(7000 + 1.90 \times 10^7[H^+])\ s^{-1}$
$Cu^{II}-CH(CH_3)COOH^+ + H_3O^+/H_2O \rightarrow Cu^{2+}{}_{aq} + CH_3CH_2COOH$	$(8300 + 2.5 \times 10^7[H^+])\ s^{-1}$
$2Cu^{II}-CH_2CH_2COOH^+{}_{aq} \rightarrow 2Cu^+{}_{aq} + (HOOCCH_2CH_2^-)_2$	$3.4 \times 10^8\ M^{-1}\ s^{-1}$ [c]
$2L^2Cu^{II}-CH_3^+{}_{aq} \rightarrow L^2Cu^+{}_{aq} + C_2H_6$	$8.6 \times 10^6\ M^{-1}\ s^{-1}$ [c]
$(L^2Cu^{II}-CH_2COO^-)_{aq} + H_2O \rightarrow L^2Cu^{2-}{}_{aq} + CH_3COO^- + OH^-$	$11\ s^{-1}$
$(L^2Cu^{II}-CH_2CH_2COO^-)_{aq} \rightleftharpoons L^2Cu^{2-}{}_{aq} + {}^\bullet CH_2CH_2COO^-$	$1.3 \times 10^{-4}\ M^{-1}$
$2CH_2CH_2COO^- \rightarrow {}^-OOCCH_2CH_2-CH_2CH_2COO^-$	$1.1 \times 10^9\ M^{-1}\ s^{-1}$ [c,d]

[a] Experimental conditions as in Table 1. [b] Error limit ±15%. [c] Value given for $2k$. [d] Measured in this study, the value is an average one for all the possible reactions between the free radicals $^\bullet CH_2CH_2COO^-$ and $^\bullet CH(CH_3)COO^-$, which are not separated in time.

experimental conditions. c. Acrylic acid, an alternative product of reaction 23, if disproportionation and not dimerization occurs, is not formed in this process, G(acrylic acid) < 0.5.

Therefore the spectrum measured 200 μs after a pulse is attributed to $Cu^{II}-CH_2CH_2COOH^+{}_{aq}$ and the difference spectrum between the spectra measured 22 and 200 μs after the pulse, Figure 5, is attributed to $Cu^{II}-CH_2CH_2COOH^+{}_{aq}$.

When N_2O-saturated solutions containing $(1-10) \times 10^{-4}$ M of L^2Cu^+, pH 7–10 (the concentration of L^2 was always twice that of [Cu(I)]) and 0.1–0.3 M $CH_3CH_2CO_2H$ are irradiated, the primary free radicals are transformed into a mixture of 55% $^\bullet CH(CH_3)CO_2^-$ and 45% $^\bullet CH_2CH_2CO_2^-$ free radicals.[24] The reaction of this mixture with L^2Cu^+ was studied. The formation of an unstable intermediate with an absorption band at 390 nm and apparent, assuming that the yield of the intermediate equals the total free radical yield, $\epsilon_{max} = (1100 \pm 150)\ M^{-1}\ cm^{-1}$ is observed. This intermediate decomposes in a process which obeys a second-order rate law, Table 4. L^2Cu^{2+} is not a product of this process.

It is proposed that these results indicate that under our experimental conditions only the $^\bullet CH_2CH_2CO_2^-$ free radical reacts with L^2Cu^+. This proposal is based on the following observations: 1. The kinetics of decomposition indicate that only one transient complex is formed. 2. The apparent molar absorption coefficient of this transient, $\epsilon_{max} = 1100\ M^{-1}\ cm^{-1}$ is considerably smaller than that of the other transients of the type $L^2Cu^{II}-R$, Table 3. 3. L^2Cu^{2+} is not a product of this process suggesting that the transient is not $(L^2Cu^{II}-CH(CH_3)CO_2^-)$. 4. The rates of reaction of free radicals with L^2Cu^+, Table 2, indicate that steric hindrance affects them considerably. The free radical $^\bullet CH(CH_3)CO_2^-$ is considerably more hindered than $^\bullet CH_2CH_2CO_2^-$. Therefore the correct molar absorption coefficient of this transient is $2500 \pm 400\ M^{-1}\ cm^{-1}$, as its yield is only 45% of that of $^\bullet OH$ free radicals.

The rate of decomposition of the transient complex $(L^2Cu^{II}-CH_2CH_2COO^-)$ obeys a second-order rate law. The observed rate decreases with the increase in $[L^2Cu^+]$, $2k = 4.2 \times 10^7$, 7.8×10^7, and $2.7 \times 10^8\ M^{-1}\ s^{-1}$ for $[L^2Cu^+] = 8 \times 10^{-4}$, 5×10^{-4}, and 2×10^{-4} M, respectively. These results suggest that the mechanism of decomposition involves the homolysis of the copper–carbon σ bond:

$$(L^2Cu^{II}-CH_2CH_2COO^-)_{aq} \rightleftharpoons L^2Cu^+{}_{aq} + {}^\bullet CH_2CH_2COO^- \quad (24)$$

This reaction might be followed by one of the following:

$$2{}^\bullet CH_2CH_2COO^- \rightarrow {}^-OOCCH_2CH_2CH_2CH_2COO^- \qquad k_{25} = 1.1 \times 10^9\ M^{-1}\ s^{-1} \quad (25)$$

$$^\bullet CH_2CH_2COO^- + (L^2Cu^{II}-CH_2CH_2COO^-)_{aq} \rightarrow L^2Cu^+{}_{aq} + {}^-OOCCH_2CH_2CH_2CH_2COO^- \quad (26)$$

As the observed rate of decomposition approaches at low $[L^2Cu^+{}_{aq}]$ k_{25}, it was checked whether the data are in accord with the assumption that the observed process involves reactions 24 and 25. Indeed the experimental data are in accord with $K_{24} = 1.3 \times 10^{-4}$ M. As $k_{-24} = 6.3 \times 10^6\ M^{-1}\ s^{-1}$, one calculates $k_{24} = 800\ s^{-1}$.

Concluding Remarks

The results, summed up in Table 5, clearly point out that a variety of mechanisms contribute to the decomposition of transient complexes of the type $LCu^{II}-R$. Thus even if β-elimination is ruled out, by the absence of appropriate leaving groups, one observes the following mechanisms: 1. Heterolysis of the copper–carbon σ bond occurs; this mechanism is prominent mainly when electron-withdrawing groups are bound to the α carbon. This mechanism is acid catalyzed. 2. Homolysis of the copper–carbon σ bond occurs; this mechanism is enhanced if the free radical formed is stabilized by resonance[10,13b] and by steric hindrance imposed by the ligand, L, or by substituents on the aliphatic residue R.[13c] 3. There is a reaction of two transient complexes with each other to form a carbon–carbon bond between the two aliphatic residues.

Finally it is of interest to note that none of the transient complexes decomposes via a mechanism involving a β-hydride shift, though copper is known to oxidize aliphatic free radicals via this mechanism in other solvents.[2]

Acknowledgment. This study was supported in part by The Israel Science Foundation administered by The Israel Academy of Sciences and Humanities and by a grant from the Budgeting and Planing Committee of the Council of Higher Education and the Israel Atomic Energy Commission. D.M. wishes to express his thanks to Mrs. Irene Evens for her ongoing interest and support.

OM950434G

Substituent Effects on Reductive Elimination from Disubstituted Aryl Hydride Complexes: Mechanistic and Thermodynamic Considerations

Anthony D. Selmeczy,[†] William D. Jones,*[,†] Robert Osman,[‡] and Robin N. Perutz*[,‡]

Departments of Chemistry, University of Rochester, Rochester, New York 14627, and University of York, York YO1 5DD, U.K.

Received May 16, 1995[⊗]

The complexes $(C_5Me_5)Rh(PMe_3)(3,5\text{-}C_6H_3R_2)H$ for R = $C(CH_3)_3$, $CH(CH_3)_2$, $Si(CH_3)_3$, CH_3, and CF_3 (**1c–g**) have been prepared both by irradiation of $(C_5Me_5)Rh(PMe_3)(C_2H_4)$ in neat arene and by thermolysis of $(C_5Me_5)Rh(PMe_3)(Ph)H$ (**1a**) in neat arene. Quenching the hydride species with $CHBr_3$ allowed isolation of the corresponding bromide complexes $(C_5Me_5)Rh(PMe_3)(3,5\text{-}C_6H_3R_2)Br$ (**2c–g**). Rates of reductive elimination of arene for the series of disubstituted aryl hydride complexes were measured at various temperatures and activation parameters $\Delta H^{\ddagger}$ and $\Delta S^{\ddagger}$ obtained and compared with those of (C_5Me_5)-$Rh(PMe_3)(Ph)H$ (**1a**) and $(C_5Me_5)Rh(PMe_3)(tolyl)H$ (**1b**). $\Delta H^{\ddagger}$ values range from +35 to +18 kcal/mol, and $\Delta S^{\ddagger}$ values range from +16.4 to −19 cal/mol K. Laser flash photolysis experiments using $(C_5Me_5)Rh(PMe_3)(C_2H_4)$ in neat toluene at various temperatures allowed the determination of activation parameters $\Delta H^{\ddagger}$ and $\Delta S^{\ddagger}$ for intramolecular C–H bond oxidative addition of the η^2-arene complex **3b**. Equilibrium measurements allowed determination of ΔG° values for several of the disubstituted aryl hydride complexes versus the parent phenyl hydride complex. A kinetic isotope effect of $k_H/k_D = 1.0 \pm 0.1$ was measured for the reaction of $(C_5Me_5)Rh(PMe_3)(C_2H_4)$ with a 1:1 mixture of 5-deuterio-1,3-di-*tert*-butylbenzene and 1,3-di-*tert*-butylbenzene. The equilibrium isotope effect for the same reaction $K_{eq} = 2.27(1)$ favors the aryl hydride and free deuterated arene.

Introduction

Two of the most fundamental steps in organometallic reaction mechanisms are oxidative addition and its microscopic reverse, reductive elimination.[1] Most catalytic and stoichiometric processes that utilize transition metals in the functionalization of hydrocarbon substrates invoke oxidative addition and reductive elimination pathways, and the nature of these steps has been probed in detail. Much work has been done on intramolecular and intermolecular C–H bond activation of alkanes and arenes,[2] yet reductive elimination has received somewhat less attention.[3]

It is now well established that oxidative addition products derived from alkanes are inherently less stable than their aryl counterparts despite the fact that the C–H bond is significantly stronger in arenes than in alkanes. The reason for this apparent discrepancy lies in the much greater range of C–M bond strengths versus C–H bond strengths (for the system (C_5Me_5)-$Rh(PMe_3)(R)H$, $D_{Rh-Phenyl} - D_{Rh-Methyl} \approx 13$ kcal/mol and $D_{H-Phenyl} - D_{H-Methyl} \approx 6$ kcal/mol).[4]

Although much work has been done by organic researchers regarding substituent effects on the rates and mechanisms of organic reactions, few studies of this type have been attempted for organometallic systems. Two classic examples of arene substituent effects in organic chemistry are electrophilic aromatic substitution and dissociation constants of benzoic acid derivatives. Strongly electron-donating or -withdrawing substituents dramatically change the rate and stereochemistry of electrophilic attack on benzene derivatives, and K_{eq} values for *para*-substituted benzoic acid derivatives span ~1.5 pK_a units, reflecting a difference of ~2.0 kcal/mol in O–H bond strengths.[5]

The work detailed in this report was undertaken in order to probe (i) electronic effects on the rate of reductive elimination and (ii) η^2-complex stability for a series of disubstituted aryl hydride complexes of the type $(C_5Me_5)Rh(PMe_3)(3,5\text{-}C_6H_3R_2)H$ where R = CF_3, H, CH_3, $Si(CH_3)_3$, $CH(CH_3)_2$, and $C(CH_3)_3$. The *meta*-disubstituted derivatives were chosen rather than *para*-monosubstituted derivatives to avoid the facile equilibration with their *meta*-substituted isomers, which is known to occur in this system.[4] Measurement of rate constants for reductive elimination at various temperatures allowed the determination of activation parameters $\Delta H^{\ddagger}$ and $\Delta S^{\ddagger}$ for the series, and flash photochemi-

[†] University of Rochester.
[‡] University of York.
[⊗] Abstract published in *Advance ACS Abstracts,* October 15, 1995.

(1) (a) Collman, J. P.; Hegedus, L. S. *Principles and Application of Organotransition Metal Chemistry*; University Science: Mill Valley, CA, 1987, and references therein. (b) Parshall, G. W. *Homogeneous Catalysis*; Wiley-Interscience: New York, 1980. (c) Stille, J. K. The Nature and Cleavage of Metal–Carbon Bonds. In The Chemistry of the Metal–Carbon Bond; Hartley, F. R., Patai, S., Eds.; Wiley-Interscience: New York, 1985; Vol. II.

(2) (a) Crabtree, R. H. *Chem. Rev.* **1985**, *85*, 245–269. (b) Ryabov, A. D. *Chem. Rev.* **1990**, *90*, 403–424. (c) Bergman, R. *Science* **1984**, *223*, 902–908. (d) Hill, C. L. *Activation and Functionalization of Alkanes*; Wiley: New York, 1989. (e) Davies, J. A.; Watson, P. L.; Liebman, J. F.; Greenberg, A. *Selective Hydrocarbon Activation*; VCH Publishers, Inc.: New York, 1990. (f) Jones, W. D.; Feher, F. J. *Acc. Chem. Res.* **1989**, *22*, 91–100.

(3) Abis, L.; Sen, A.; Halpern, J. *J. Am. Chem. Soc.* **1978**, *100*, 2915–2916.

(4) Jones, W. D.; Feher, F. J. *J. Am. Chem. Soc.* **1984**, *106*, 1650–1663.

(5) (a) Lowry, T. H.; Richardson, K. S. *Mechanism and Theory in Organic Chemistry*; Harper and Row: New York, 1981.

0276-7333/95/2314-5677$09.00/0

Scheme 1

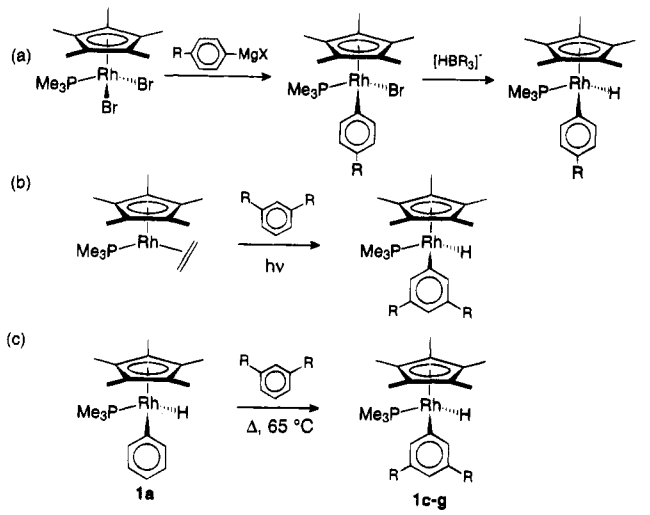

cal experiments were carried out in order to determine activation parameters for the intramolecular oxidative addition of the η^2-arene complex Cp*Rh(PMe$_3$)(η^2-toluene) to form the corresponding aryl hydride. The kinetic isotope effect for C–H vs C–D bond oxidative addition of di-*tert*-butylbenzene to the fragment [Cp*Rh(PMe$_3$)] was measured. On the basis of these data, mechanistic conclusions are drawn regarding reductive elimination from this series of complexes.

Results

Synthesis of Compounds. Several synthetic routes leading to the 3,5-disubstituted aryl hydride complexes were examined. Earlier work with monosubstituted arenes indicated that reaction of (C$_5$Me$_5$)Rh(PMe$_3$)Br$_2$ with aryl Grignard reagents would lead to the aryl bromide complexes, which could then be converted to the desired aryl hydride complexes using LiB(*sec*-butyl)$_3$H (L-selectride).[6] A series of monosubstituted complexes having the general formula (C$_5$Me$_5$)Rh(PMe$_3$)(4-C$_6$H$_4$R)Br, R = CH$_3$, CF$_3$, Si(CH$_3$)$_3$, and C(CH$_3$)$_3$ (Scheme 1a), were easily synthesized from (C$_5$Me$_5$)Rh(PMe$_3$)Br$_2$ and the corresponding aryl Grignard reagent. However, attempts to use similar techniques for the preparation of the 3,5-disubstituted analogs generally met with failure due to difficulties encountered in preparing the Grignard reagent or the aryl bromide precursor. In addition, attempts to generate (C$_5$Me$_5$)Rh(PMe$_3$)[3,5-C$_6$H$_3$(CH$_3$)$_2$]H from the corresponding bromide complex using L-selectride produced a mixture of the desired aryl hydride along with some (C$_5$Me$_5$)Rh(PMe$_3$)H$_2$.

A more successful method for preparing the desired complexes took advantage of the photochemical lability of (C$_5$Me$_5$)Rh(PMe$_3$)(C$_2$H$_4$) to generate the reactive 16-electron intermediate [(C$_5$Me$_5$)Rh(PMe$_3$)] (Scheme 1b). Prolonged photolysis of (C$_5$Me$_5$)Rh(PMe$_3$)(C$_2$H$_4$) in neat 1,3-disubstituted arene (λ > 345 nm) led to loss of ethylene and oxidative addition of the solvent. This procedure was used to prepare the complexes (C$_5$Me$_5$)Rh(PMe$_3$)(3,5-C$_6$H$_3$R$_2$)H for R = CF$_3$ (**1g**), CH$_3$ (**1f**), and C(CH$_3$)$_3$ (**1c**). Although this procedure worked well for dilute samples [<10 mg of (C$_5$Me$_5$)Rh(PMe$_3$)(C$_2$H$_4$)], more concentrated solutions darkened considerably and photolysis became ineffective at long reaction times. Maximum yields of 85% were attained, and significant amounts (>5%) of (C$_5$Me$_5$)Rh(PMe$_3$)$_2$ were also detected after prolonged photolysis.

A third route to the disubstituted aryl hydride complexes proved to be the most efficient (Scheme 1c). Thermolysis of (C$_5$Me$_5$)Rh(PMe$_3$)(Ph)H (**1a**) in neat arene at 67 °C overnight resulted in loss of benzene and generation of the 16e intermediate [(C$_5$Me$_5$)Rh(PMe$_3$)], which then reacted rapidly with the arene solvent. The complexes (C$_5$Me$_5$)Rh(PMe$_3$)(3,5-R$_2$C$_6$H$_3$)H for R = C(CH$_3$)$_3$, CH(CH$_3$)$_2$, Si(CH$_3$)$_3$, CH$_3$, and CF$_3$ (**1c–g**, Scheme 1) were produced cleanly and in high yield by this method. For 1,3-bis(trifluoromethyl)benzene, *m*-xylene, and 1,3-bis(trimethylsilyl)benzene, the reaction went virtually to completion, whereas reaction with 1,3-diisopropylbenzene and 1,3-di-*tert*-butylbenzene only went to partial completion due to equilibration with the free benzene produced. In the latter two cases, the solvent was removed under high vacuum at room temperature and fresh arene was introduced. Repetition of the thermolysis conditions led to >95% yield (^{31}P NMR) of the desired products. In all cases only a single aryl hydride isomer was formed.

Spectroscopic data for the series of 3,5-disubstituted aryl hydride complexes are typical of other aryl hydride complexes of this type. Single resonances are observed by ^{1}H NMR spectroscopy for the *ortho*-hydrogens of the aromatic ring. Equivalent arene substituent resonances are seen in the ^{1}H NMR spectrum, indicating activation solely at the 5-position of the arene ring and free rotation of the Rh–aryl bond. In addition, resonances attributable to bound (C$_5$Me$_5$) and PMe$_3$ ligands are visible, and a hydride resonance is seen in the upfield region with the expected couplings to rhodium and phosphorus. ^{31}P NMR spectroscopy shows a doublet near δ 8–9 ppm with a coupling constant indicative of rhodium in the +3 formal oxidation state ($J_{Rh-P} \approx 150$ Hz).[7]

The materials were further characterized by conversion to the air-stable aryl bromides by reaction with CHBr$_3$ (eq 1). Addition of several drops of CHBr$_3$ to a

$$(C_5Me_5)Rh(PMe_3)(aryl)H \xrightarrow{CHBr_3} (C_5Me_5)Rh(PMe_3)(aryl)Br \quad (1)$$

benzene solution of (C$_5$Me$_5$)Rh(PMe$_3$)(3,5-C$_6$H$_3$R$_2$)H produced an immediate color change to bright orange-red. Chromatography on silica plates with 4% THF/CH$_2$Cl$_2$ led to the isolation of the complexes (C$_5$Me$_5$)Rh(PMe$_3$)(3,5-C$_6$H$_3$R$_2$)Br (**2c–g**) in moderate yields. Spectroscopic data are given in the Experimental Section.

Kinetic Studies. Thermolysis of these aryl hydride complexes in C$_6$D$_6$ led to the reductive elimination of arene and the formation of **1a**-*d*$_6$ (eq 2). The rates of

$$(C_5Me_5)Rh(PMe_3)(aryl)H \xrightarrow{C_6D_6} (C_5Me_5)Rh(PMe_3)(C_6D_5)D \quad (2)$$

these reactions were monitored by ^{1}H NMR spectroscopy at various temperatures. Temperature dependent rates were also obtained for the hydride complex (C$_5$Me$_5$)Rh-

(6) Jones, W. D.; Feher, F. J. *Inorg. Chem.* **1984**, *23*, 2376–2388.

(7) Klingert, B.; Werner, H. *Chem. Ber.* **1983**, *116*, 1450–1462.

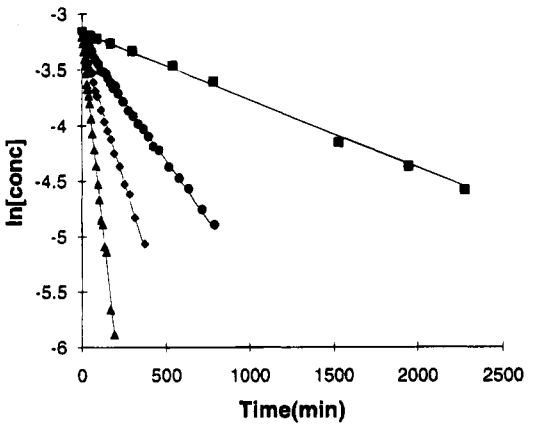

Figure 1. Plot of ln[**1c**] vs time for the elimination of 1,3-$C_6H_4(t\text{-}Bu)_2$ from $(C_5Me_5)Rh(PMe_3)(3,5\text{-}C_6H_3(t\text{-}Bu)_2)H$ in C_6D_6 at 301 (■), 313 (●), 323 (◆), and 333 K (▲).

(PMe_3)(tolyl)H (**1b**), which is known to exist as a rapidly equilibrating 2:1 mixture of *meta*- and *para*-isomers.[8] Rate constants were determined by a single-exponential fit to eq 3, except for **1g**, which exhibited behavior characteristic of an approach to equilibrium and was therefore fitted to the form of eq 4. Fits were optimized

$$[1] = [1]_0\, e^{-k_{obs}t} \tag{3}$$

$$[1] = [1]_\infty + ([1]_0 - [1]_\infty)e^{-k_{obs}t} \tag{4}$$

by varying k_{obs} for **1b**–**g** and also $[Rh(aryl)H]_\infty$ for **1g**. For the reactions of **1b**–**g** first-order behavior was observed (Figure 1) with k_{obs} representing the rate of arene loss; for **1g** the first-order rate constant k_{obs} represents the sum of $k_{forward} + k_{reverse}$. On the basis of the equilibrium constant for this reaction (*vide infra*), the contribution of $k_{reverse}$ to the observed rate constant is 3% or less, which is smaller than the errors (typically 5%–10%) of the measured rate constants. This contribution was therefore disregarded. These results are summarized in Table 1. Details of the kinetic experiments are given in the Experimental Section.

Activation parameters were determined on the basis of the rates listed in Table 1. Eyring plots of $\ln(k_{obs}/T)$ vs $1/T$ over at least a 32 °C temperature range give linear plots with good correlation (Figure 2), yielding enthalpies ($\Delta H^{\ddagger}$) and entropies ($\Delta S^{\ddagger}$) of activation as summarized in Table 2. The limited statistical basis for extracting these values introduces large 95% confidence limits on these values. Also, the values for the rate constants for the reaction of **1g** are somewhat suspect due to a competing H/D exchange reaction (*vide infra*). Calculated $\Delta G^{\ddagger}$ values at 298 K are also reported in Table 2 (there is no statistical basis for including confidence limits on these values).

Equilibrium measurements were also made in order to determine the difference in $\Delta G°$ values for the various disubstituted arene complexes versus the parent phenyl hydride **1a**. For the cases where equilibrium was reached in the preparation of the aryl hydride from reaction of **1a** in neat arene [R = $C(CH_3)_3$, $CH(CH_3)_2$], equilibrium values were obtained based on ^{31}P NMR integrations of reactant and product resonances. K_{eq} values were calculated on the basis of simple bimolecular equilibrium behavior according to eq 5, and $\Delta G°$ was

$$K_{eq} = \frac{[Rh(Ar)H][PhH]}{[Rh(Ph)H][ArH]} \tag{5}$$

obtained from the equation $\Delta G° = -RT\ln(K_{eq})$. Equilibrium values for **1g** were obtained by optimizing the least-squares fit of the kinetic data through variation of the final equilibrium value $[Rh(aryl)H]_\infty$. Equilibrium and $\Delta G°$ values are given in Table 3. Equilibrium concentrations were also measured at various temperatures for the complex **1c**, and a van't Hoff plot of $\ln(K_{eq})$ vs $1/T$ allowed determination of $\Delta H°$ and $\Delta S°$ relative to **1a**. These values are listed as well in Table 3.

Table 1. Kinetic Data for Reductive Elimination of Arene from the Complexes $(C_5Me_5)Rh(PMe_3)(aryl)H$

aryl	T, K	$k \times 10^5$, s^{-1} [a]
C_6H_5, **1a**[b]	299	0.0622 (0.0035)[b]
	325	3.11 (0.13)[b]
	332	11.1 (1.1)[b]
	345	66.1 (9.8)[b]
$C_6H_4(CH_3)$, **1b**	298	0.189 (0.008)
	313	1.72 (0.11)
	323	6.43 (0.12)
	333	23.3 (0.7)
$3,5\text{-}C_6H_3(t\text{-}Bu)_2$, **1c**	301	1.01 (0.02)
	313	3.63 (0.07)
	323	9.00 (0.41)
	333	23.3 (0.5)
$3,5\text{-}C_6H_3(i\text{-}Pr)_2$, **1d**	298	0.698 (0.076)
	313	4.16 (0.11)
	323	13.8 (0.33)
	333	37.5 (1.9)
$3,5\text{-}C_6H_3(SiMe_3)_2$, **1e**	298	0.127 (0.005)
	313	0.845 (0.020)
	323	3.08 (0.16)
	333	8.93 (0.44)
$3,5\text{-}C_6H_3(CH_3)_2$, **1f**	301	1.05 (0.09)
	313	5.06 (0.14)
	324	21.8 (2.3)
	333	51.5 (3.2)
$3,5\text{-}C_6H_3(CF_3)_2$, **1g**	325	0.0108 (0.0004)
	343	0.112 (0.004)
	353	0.751 (0.095)
	363	3.56 (0.12)

[a] 95% confidence limits are shown in parentheses. [b] Data from ref 4.

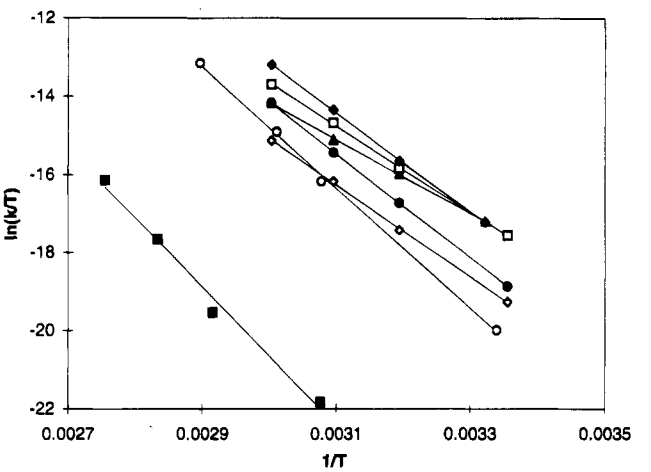

Figure 2. Eyring plots for the determination of $\Delta H^{\ddagger}$ and $\Delta S^{\ddagger}$ for the reductive elimination of arene from $(C_5Me_5)Rh(PMe_3)(aryl)H$ in benzene, where aryl = C_6H_5 (○), $C_6H_4CH_3$ (●), $3,5\text{-}C_6H_3(t\text{-}Bu)_2$ (▲), $3,5\text{-}C_6H_3(i\text{-}Pr)_2$ (□), $3,5\text{-}C_6H_3(SiMe_3)_2$ (◇), $3,5\text{-}C_6H_3(CH_3)_2$ (◆), and $3,5\text{-}C_6H_3(CF_3)_2$ (■).

(8) Jones, W. D.; Feher, F. J. *J. Am. Chem. Soc.* **1982**, *104*, 4240–4242.

Table 2. Activation Parameters for Reductive Elimination of Arene from the Complexes $(C_5Me_5)Rh(PMe_3)(aryl)H$

aryl	$\Delta H^{\ddagger}$, kcal/mol[a]	$\Delta S^{\ddagger}$, cal/mol K[a]	$\Delta G^{\ddagger}_{298}$, kcal/mol	σ_m for aryl substituent
C_6H_5, **1a**	30.6 (2.4)	15.1 (7.4)	26.1	0
$C_6H_4CH_3$, **1b**	26.5 (0.3)	4.1 (1.1)	25.3	−0.07
3,5-$C_6H_3(t\text{-}Bu)_2$, **1c**	18.8 (0.8)	−19.0 (2.5)	24.5	−0.10
3,5-$C_6H_3(i\text{-}Pr)_2$, **1d**	21.9 (0.9)	−8.5 (2.8)	24.4	−0.04
3,5-$C_6H_3(SiMe_3)_2$, **1e**	23.5 (1.1)	−6.7 (3.5)	25.5	−0.04
3,5-$C_6H_3(CH_3)_2$, **1f**	24.1 (4.0)	−1.1 (12.7)	24.4	−0.07
3,5-$C_6H_3(CF_3)_2$, **1g**	35.2 (8.3)	17 (24)	30.0	+0.43

[a] 95% confidence limits for 2 degrees of freedom ($n = 4$) are shown in parentheses.

Table 3. K_{eq} and $\Delta G°$ Values for the Complexes $(C_5Me_5)Rh(PMe_3)(aryl)H$ Equilibrating with C_6H_6

aryl	T, K	K_{eq}	$\Delta G°$, kcal/mol
3,5-$C_6H_3(CF_3)_2$, **1g**	325	40.1	−2.38
$C_6H_4(CH_3)$, **1b**	323	0.37	0.64
3,5-$C_6H_3(CH_3)_2$, **1f**	323	0.083	1.60
3,5-$C_6H_3(i\text{-}Pr)_2$, **1d**	298	0.132	1.20
3,5-$C_6H_3(t\text{-}Bu)_2$, **1c**[a]	298	0.0165	2.43
	311	0.0160	2.56
	324	0.0203	2.51
	338	0.0208	2.60
	347	0.0231	2.60

[a] $\Delta H° = 1.5(0.6)$ kcal/mol; $\Delta S° = -3(2)$ cal/mol K.

Scheme 2

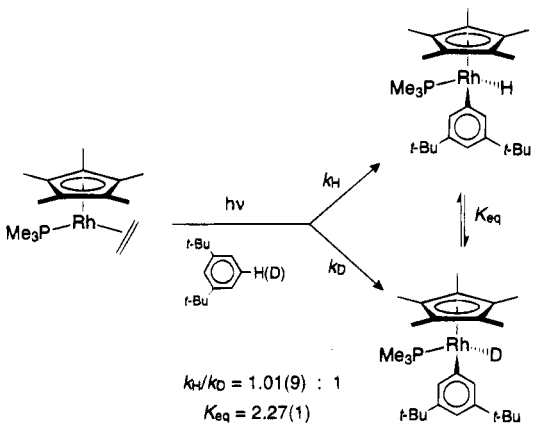

The kinetic isotope effect for C−H bond activation of 1,3-di-*tert*-butylbenzene was measured (Scheme 2). Photolysis of $(C_5Me_5)Rh(PMe_3)(C_2H_4)$ in 1,3-di-*tert*-butylbenzene that was 50% enriched at the 5-position at 10 °C produced both **1c** and **1c**-d_1, yielding a kinetic isotope effect of 1.0 ± 0.1 at early reaction times. An equilibrium isotope effect of 2.27(1) (favoring aryl hydride + free deuterated arene) was observed after the sample had equilibrated at room temperature for 10 days (>10 half-lives).

H/D Exchange in 1g. While the loss of arene from **1g** in C_6D_6 was monitored, a competing H/D exchange reaction was observed which deuterates both the hydride and the methyl groups of the (C_5Me_5) ligand (Scheme 3). Although the concentrations of **1g** and **1a** were monitored by ^1H NMR integration of the corresponding PMe_3 resonances, it became readily apparent that the intensities of the (C_5Me_5) resonances for **1g** and **1a** began to broaden and decrease in intensity relative to the PMe_3 resonances. Inspection of the hydride resonance showed that it also diminished in intensity. A ^2H NMR spectrum taken after 2000 h of thermolysis at 54 °C (<2 half-lives; ~60% arene exchange) confirmed

Scheme 3

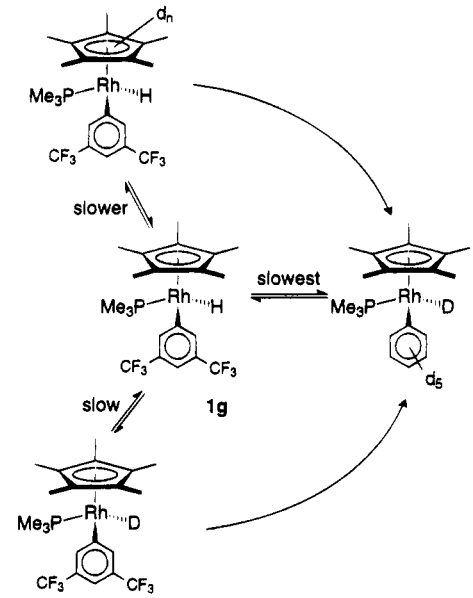

deuterium enrichment of both the (C_5Me_5) ligand and of the hydride. ^{31}P NMR spectra also obtained after 2000 h showed a progressive series of resonances with an upfield shift of 35.5 Hz/D for both **1g**-d_n and for **1a**-d_n (Figure 3). These peaks exhibited the expected large coupling to rhodium, but also a smaller 1:1:1 triplet splitting attributable to a rhodium−deuterium coupling. This monotonic upfield shift is attributed to an isotopic perturbation of resonance due to successive deuterium incorporation into the (C_5Me_5) ligand of the starting material. This effect has also been noted in the ^1H NMR spectra in exchange reactions of fluorinated aryl hydrides.[9] Because the kinetic scheme for this reaction is complicated by this H/D exchange process and its associated isotope effects, suspicion must be raised regarding the validity of the measured rate constants and the activation parameters that are derived from them.

Flash Photolysis Studies. Flash photochemical experiments were carried out in order to examine oxidative addition intermediates with these arenes (Scheme 4). Laser flash photolysis (308 nm, excimer laser) of $(C_5Me_5)Rh(PMe_3)(C_2H_4)$ in neat toluene produced the transient intermediate $[(C_5Me_5)Rh(PMe_3)]$, which reacted rapidly with the solvent to produce the η^2-arene complex **3b** within the lifetime of the flash. Monitoring the lifetime of the intermediate η^2-complex by UV−vis absorption spectroscopy at various temperatures allowed determination of the first-order rate constants and the activation parameters for intramolecular oxidative addition (Table 4). Similar experiments were described in previous work that established the activation parameters for intramolecular oxidative addition of benzene.[10] The activation parameters for intramolecular oxidative addition of toluene were found to be $\Delta H^{\ddagger} = 14.4(2.4)$ kcal/mol and $\Delta S^{\ddagger} = 2.0(0.7)$ cal/mol K. Attempts to perform similar experiments with other disubstituted arenes were unsuccessful due to

(9) Selmeczy, A. D.; Jones, W. D.; Partridge, M. G.; Perutz, R. N. *Organometallics* **1994**, *13*, 385−396.
(10) Belt, S. T.; Dong, L.; Duckett, S. B.; Jones, W. D.; Partridge, M. G.; Perutz, R. N. *J. Chem. Soc., Chem. Commun.* **1991**, 266−269.

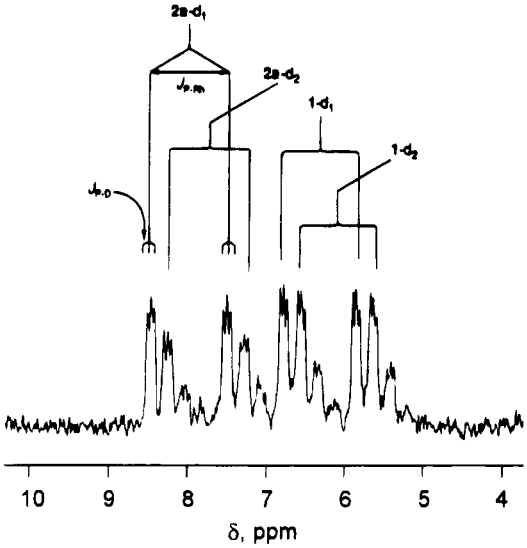

Figure 3. ^{31}P NMR spectrum after heating $(C_5Me_5)Rh(PMe_3)[2,6\text{-}C_6H_3(CF_3)_2]H$ at 54 °C in C_6D_6 for 2000 h.

Scheme 4

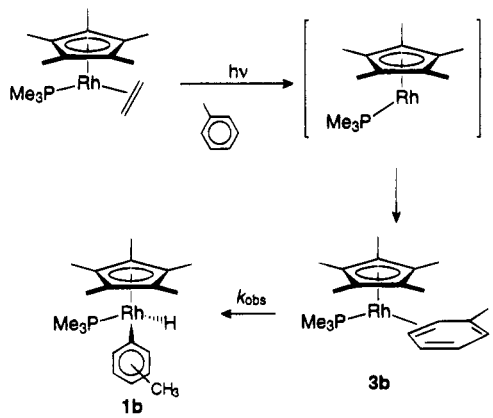

Table 4. Rate Constants for the Conversion of $(C_5Me_5)Rh(PMe_3)(\eta^2\text{-}C_6H_5CH_3)$ to $(C_5Me_5)Rh(PMe_3)(C_6H_4CH_3)H$ from Flash Photochemical Experiments

T, K	k_{obs}, s^{-1} [a]
295	363 (35)
305	780 (50)
310	983 (80)
310	1030 (45)
323	3610 (260)
333	6180 (550)

[a] 95% confidence limits are shown in parentheses.

substantial UV absorption of the arene at the wavelength of the laser pulse (308 nm).

Discussion

The mechanism for reductive elimination of benzene from the metal complex $(C_5Me_5)Rh(PMe_3)(Ph)H$ (**1**) has been well studied. Earlier work from our laboratories has provided support for the intermediacy of a stable η^2-arene complex along the oxidative addition/reductive elimination pathways with benzene.[4,11] The free-energy diagram shown in Scheme 5 has been established by self-exchange of C_6H_6 for C_6D_6 ($\Delta G^{\ddagger}_1$), spin-saturation

Scheme 5

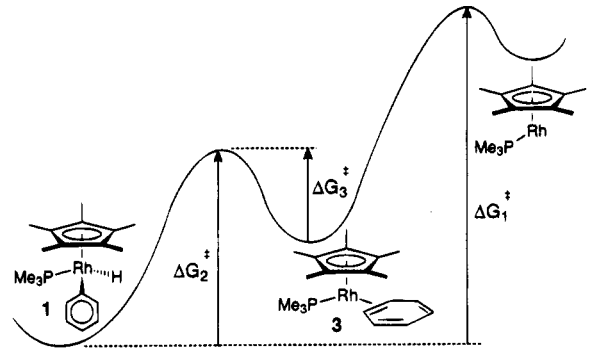

transfer ($\Delta G^{\ddagger}_2$), and flash photolysis experiments ($\Delta G^{\ddagger}_3$). No kinetic isotope effect (KIE) was found for the reaction of the photochemically generated intermediate $[(C_5Me_5)Rh(PMe_3)]$ with a 50/50 mixture of C_6H_6/C_6D_6, but a KIE of 1.40 was observed in the reaction of $[(C_5Me_5)Rh(PMe_3)]$ with 1,3,5-trideuteriobenzene.[12] These results were taken as strong evidence for the existence of an η^2-benzene complex along the reaction coordinate for oxidative addition leading to formation of the phenyl hydride complex **1a**. This η^2-benzene complex was also observed directly in the laser flash experiments of $(C_5Me_5)Rh(PMe_3)(C_2H_4)$.[10] For the reductive elimination of the *m*-xylyl hydride complex **1f**, independent determination of rate constants for loss of *m*-xylene and *m*-xylene-d_1 from the complexes $(C_5Me_5)Rh(PMe_3)[3,5\text{-}C_6H_3(CH_3)_2]H$ and $(C_5Me_5)Rh(PMe_3)[3,5\text{-}C_6H_3(CH_3)_2]D$, respectively, in C_6D_6 showed an inverse kinetic isotope effect $k_H/k_D = 0.51$.[12] The existence of a KIE effect for reductive elimination of Rh(aryl)H vs Rh(aryl)D but not for oxidative addition of aryl–H vs aryl–D is consistent with irreversible formation of an intermediate arene π complex prior to C–H oxidative addition.

The work described in this paper was undertaken in order to examine how electron-donating and electron-withdrawing substituents on the bound arene would affect (i) the rates of reductive elimination of aryl–H and (ii) the stability of the intermediate π-arene complexes. It was anticipated that good σ-donating groups on the aromatic ring would weaken the M–C bond (relative to the parent phenyl hydride **1a**) and would show faster rates of reductive elimination. Conversely, a strong σ-withdrawing aryl substituent should show the opposite behavior through strengthening of the M–C bond, thereby slowing the rate of reductive elimination. A similar trend was anticipated in terms of π-complex stability. Electron withdrawing groups should make the arene a better π-acceptor and stabilize this interaction relative to benzene,[13] while electron-donating substituents make the π-system more electron rich and consequently a poorer π-acceptor than benzene.

The 3,5-disubstituted materials **1c–g** were targeted in order to simplify the experimental rate constant measurements for reductive elimination of aryl–H. Had the monosubstituted series of complexes $(C_5Me_5)Rh(PMe_3)(C_6H_4R)H$ been employed, complications might have arisen due to interconversion of *meta*- and *para*-

(11) Chin, R. M.; Dong, L.; Duckett, S. B.; Partridge, M. G.; Jones, W. D.; Perutz, R. N. *J. Am. Chem. Soc.* **1993**, *115*, 7685–7695.

(12) Jones, W. D.; Feher, F. J. *J. Am. Chem. Soc.* **1986**, *108*, 4814–4819.

(13) (a) Belt, S. T.; Duckett, S. B.; Helliwell, M.; Perutz, R. N. *J. Chem. Soc., Chem. Commun.* **1989**, 928–930. (b) Jones, W. D.; Partridge, M. G.; Perutz, R. N. *J. Chem. Soc., Chem. Commun.* **1991**, 264–266.

isomers. The previously studied tolyl complex **1b** was used since it had been established earlier that equilibration of the *meta*- and *para*-isomers was rapid compared to loss of arene from the intermediate π-complex. Although similar behavior is expected for the monosubstituted series $(C_5Me_5)Rh(PMe_3)(C_6H_4R)H$, this has not yet been confirmed. In addition, two substituent groups should produce a larger inductive effect compared to only one, and the effect on the activation parameters should be more pronounced.

Upon heating the aryl hydride complexes **1b**–**g** in C_6D_6 solvent, first-order loss of arene was observed as **1a**-d_6 formed. The reaction goes to completion with complexes **1b**–**1f**. Only in the case of m-$C_6H_4(CF_3)_2$, a more electron-deficient arene than benzene, did the reaction not go to completion. This observation is somewhat remarkable in that the concentration of liberated m-$C_6H_4(CF_3)_2$ was approximately 1/250th that of the benzene solvent. The large equilibrium constant favoring activation of the fluorinated aromatic accounts for this observation. It is also worth noting that only in the case of **1g** was loss of arene slower than in the parent complex **1a**. All other arenes are lost more rapidly than benzene at a given temperature. The increased lability of **1b**–**f** compared with **1a** can be attributed to a decrease in the ground-state energy of the complexes rather than to a lowering of the transition-state energy for arene dissociation (*vide infra*).

Further insight into the way that substituents affect the rate of arene exchange comes from examination of the temperature dependence of these rates. In the series of reactions studied for this report, a trend emerges from the Eyring data shown in Table 2. The notion that electron-withdrawing substituents would slow reductive elimination rates appears correct, in that the barrier for arene loss ($\Delta G^{\ddagger}$ values) correlates with the electron-withdrawing ability of the substituent. The effect of the electron-donating substituents is similar, as all show a smaller barrier for arene loss than **1a**. Examination of the σ_m values for these substituents accounts roughly for the observed trend and its magnitude.[14] $\Delta H^{\ddagger}$ follows the same trend (**1g** > **1a** > **1b** > **1f** > **1e** > **1d** > **1c**). This trend was not entirely unexpected, since metal–carbon bond strengths are believed to parallel carbon–hydrogen bond strengths.[15] The range of values is quite large ($\Delta\Delta H^{\ddagger} \approx 16$ kcal/mol), however, and is certainly far greater than the range of corresponding C–H bond strengths in the arenes (estimated as 3–4 kcal/mol). Previous work in our laboratory has shown that **1a** is thermodynamically favored over the n-propyl complex $(C_5Me_5)Rh(PMe_3)(CH_2CH_2CH_3)H$ by ~9 kcal/mol, although the C–H bonds in benzene are approximately 8 kcal/mol stronger than the C–H bonds in propane. This thermodynamic preference translates to a Rh–C_6H_5 bond that is ~17 kcal/mol stronger than a Rh–propyl bond in this series of complexes. Since this difference is roughly twice that for the corresponding H–propyl vs H–phenyl bond enthalpies, a large range of metal–arene bond strengths compared with the H–aryl bond strengths is consistent with these earlier studies, but the magnitude of the range is larger than anticipated.

Scheme 6

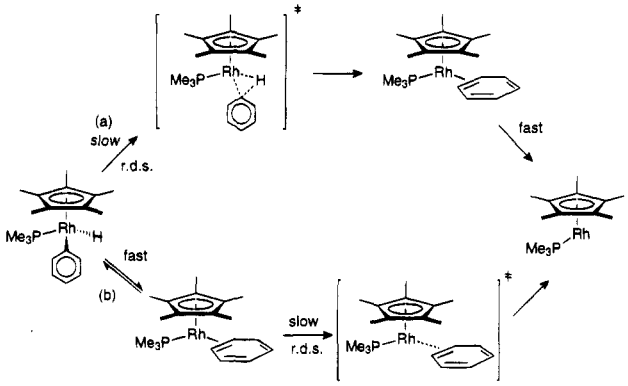

Another intriguing feature of the Eyring data is the change in entropy of activation that occurs when the arene substituent is changed from R = CF_3 to R = $C(CH_3)_3$. These values range from what would be considered a dissociative transition state ($\Delta S^{\ddagger} \approx +16$ cal/mol K) to what would be considered an associative one ($\Delta S^{\ddagger} \approx -19$ cal/mol K). A dissociative transition state is consistent with the initially proposed reaction mechanism of rapid and reversible reductive elimination/oxidative addition processes interconverting the aryl hydride and the η^2-arene complexes, followed by rate-determining loss of π-bound arene. Earlier work with isotopically labeled materials showed that the degenerate isomerization of $(C_5Me_5)Rh(PMe_3)(p\text{-xylyl})H$ at temperatures below which exchange of bound and free arene occurs yields activation parameters $\Delta H^{\ddagger} = +16.3$ kcal/mol and $\Delta S^{\ddagger} = -6.3$ cal/mol K. The slightly negative entropy of activation was interpreted to suggest the ordered transition state for C–H bond formation. The observation of a substantially negative entropy of activation for the complexes where R = $CH(CH_3)_2$ and $C(CH_3)_3$ suggested that a change in the rate-determining step might have occurred. Rate-determining formation of the η^2-arene complex followed by rapid loss of coordinated arene would be consistent with the negative activation entropies for the electron-rich arenes on the basis of the associative three-centered transition state in Scheme 6a. This hypothesis is also supported by the fact that electron-donating substituents on the aromatic ring destabilize the π-complex that is formed, and therefore loss of bound arene might be more favorable.

The notion that C–H bond formation is involved in the rate-determining step led to the prediction of a kinetic isotope effect (KIE) in the *reverse* reaction of the unsaturated intermediate $[(C_5Me_5)Rh(PMe_3)]$ with 5-deuterio-1,3-di-*tert*-butylbenzene (Scheme 2). It had already been shown that irradiation of $(C_5Me_5)Rh(PMe_3)H_2$ in a 50/50 mixture of C_6H_6/C_6D_6 resulted in no measurable KIE ($k_H/k_D = 1.05$), yet the same reaction using 1,3,5-trideuteriobenzene does exhibit a small KIE ($k_H/k_D = 1.40$), since the KIE in the latter reaction reflects the step in which a C–H or C–D bond is broken in the η^2-arene complex. A similar experiment was performed using 1,3-di-*tert*-butylbenzene which had been 50% deuterium-enriched at the 5-position, generating the same unsaturated intermediate via photolysis

(14) Hansch, C.; Leo, A.; Taft, R. W. *Chem. Rev.* **1991**, *91*, 165–195.

(15) Data for substituted arene C–H bond strengths is very limited, but two examples demonstrate the small range of H–Ar enthalpies: for C_6H_6, $D_{C-H} = 110$ kcal/mol, and for C_6F_5H, $D_{C-H} = 114$ kcal/mol. (a) Chamberlain, G. A.; Whittle, E. *Trans. Faraday Soc.* **1971**, *67*, 2077. (b) Choo, K. Y.; Golden, D. M.; Benson, S. W. *Int. J. Chem. Kinet.* **1975**, *7*, 713.

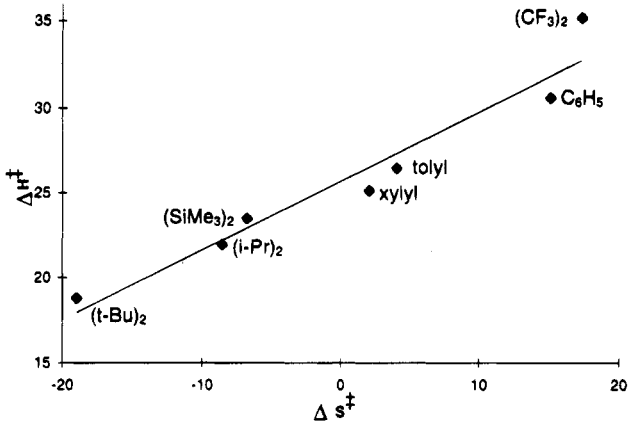

Figure 4. Plot of $\Delta H^{\ddagger}$ vs $\Delta S^{\ddagger}$ for the reductive elimination of arene from $(C_5Me_5)Rh(PMe_3)(aryl)H$ in benzene.

of $(C_5Me_5)Rh(PMe_3)(C_2H_4)$. Again no KIE was measured ($k_H/k_D = 1.0$), leading to the conclusion that arene precoordination is still the rate-determining step in all of these C−H bond activation processes (Scheme 6b). Consequently, the negative entropy of activation for **1c** (and **1d** or **1e**) indicates more order in the transition state for dissociation of η^2-1,3-di-*tert*-butylbenzene from the $(C_5Me_5)Rh(PMe_3)$ fragment. Perhaps lack of rotation about the Rh−(η^2-arene) bond with these more hindered arenes accounts for the negative values. The equilibrium isotope effect between **1c** and **1c**-d_1 of 2.27(1) is similar to that seen earlier in **1a**-d_5.[12]

Flash photochemical experiments were performed in order to determine substituent effects on the rate of intramolecular oxidative addition for the η^2-complex **3b**. Irradiation of a solution of $(C_5Me_5)Rh(PMe_3)(C_2H_4)$ in neat toluene led to formation of the transient species **3b**. The rate of intramolecular oxidative addition leading to complex **1b** was calculated by monitoring the single-exponential decay of the UV−vis absorbance at 370 nm to a steady-state value. Determination of rate constants over a 38 °C temperature range allowed the calculation of activation parameters $\Delta H^{\ddagger}$ and $\Delta S^{\ddagger}$ for **3b**, $\Delta H^{\ddagger} = 14.4(2.4)$ kcal/mol and $\Delta S^{\ddagger} = 2.0(0.7)$ cal/mol K. Comparison of the lifetimes for the η^2-toluene vs the η^2-benzene complexes reveals that the rate of intramolecular oxidative addition is slower for toluene than for benzene. This was surprising, since it was believed that the less stable π-complex with toluene (worse π-acid) should have reacted more quickly than the corresponding benzene species. The $\Delta H^{\ddagger}$ value for the transformation **3b** → **1b** is roughly 3 kcal/mol higher than that for benzene [for **3a** → **1a**, $\Delta H^{\ddagger} = 11.15(0.31)$ kcal/mol], and the $\Delta S^{\ddagger}$ value is near zero [$\Delta S^{\ddagger} = -4.9(1.1)$ cal/mol K for benzene]. These values indicate a slightly greater degree of bond-breaking and less order in the transition state for the toluene complex compared to the benzene complex, but the differences are small.

Several authors have pointed out that entropy−enthalpy compensation effects can occur when studying a homologous series of reactions. The current data for this series of compounds *appears* to follow such a compensation relationship; as $\Delta H^{\ddagger}$ decreases, $\Delta S^{\ddagger}$ also decreases so as to make $\Delta G^{\ddagger}$ change only slightly. Indeed, a plot of $\Delta H^{\ddagger}$ vs $\Delta S^{\ddagger}$ is linear (Figure 4). A systematic relation between the mechanism(s) for arene elimination leads to the principle that there should be a temperature at which all the rates are the same, i.e., an isokinetic temperature. Under such circumstances, the $\ln(k/T)$ vs $1/T$ plots should intersect at a common point. Detailed treatments by Exner,[16] Leffler,[17] and more recently a review by Linert[18] give proper statistical treatments for testing the validity of such a relationship. Examination of the Eyring plots in Figure 2 does not support the presence of an isokinetic relationship, however, *as there is no single point where all lines intersect*, i.e., there is no isokinetic temperature. Peterson has pointed out that a linear $\Delta H^{\ddagger}$ vs $\Delta S^{\ddagger}$ plot does not require an isokinetic relationship,[19] and the data here fall into the same category. Using the statistical methods outlined by Exner and Linert, there is no reason to believe that the current trends in activation parameters are consistent with an isokinetic relationship.

At the same time, the underlying physical reason for the large range of enthalpy and entropy values is not clear. Although earlier results have shown that a significant difference between C−M and C−H bond strengths exists, the magnitude of the effect observed in this study seems remarkable. The result from the KIE study is more consistent with C−H bond cleavage not being involved in the rate-determining step, thus arguing against a change in rate-determining step in the mechanism as the cause for the observed entropy values. We tend to believe that the $\Delta H^{\ddagger}$ and $\Delta S^{\ddagger}$ values reflect the tightness of the bound η^2-arene during dissociation from the metal. The larger amount of bond-breaking required for the electron-deficient arenes would be consistent not only with a complex of lower ground-state energy but also with a transition state with relatively more freedom to rotate about the metal−(η^2-arene) bond, and hence a larger $\Delta S^{\ddagger}$. The magnitude of the changes in $\Delta H^{\ddagger}$ and $\Delta S^{\ddagger}$, however, are still larger than one would have anticipated.

Finally, it is tempting to use the equilibrium and rate data presented here to predict kinetic selectivities for oxidative addition of the 16-electron fragment with mixtures of arenes ($\Delta\Delta G^{\ddagger}_{oa} = \Delta G^{\ddagger}_{1g} - \Delta G^{\ddagger}_{1a} + \Delta G^{\circ}$). Unfortunately, the ΔG° values were not measured at the same temperature, and even so, the range of $\Delta\Delta G^{\ddagger}_{oa}$ values calculated is small (~2 kcal/mol). The uncertainty associated with these values renders their use in the prediction of selectivity as less than reliable.

Conclusions

The free-energy barrier to reductive elimination in a series of disubstituted aryl hydride complexes has been shown to increase as the substituents are more electron withdrawing than H and to decrease when the substituents are more electron donating than H. The range of C−Rh enthalpy of activation values is large (~16 kcal/mol), which translates as a large range in Rh−C bond enthalpy values. This range is certainly much greater than the range of corresponding C−H bond enthalpies (estimated between 3 and 4 kcal/mol). Correlated with the large enthalpy change, a dramatic change in the activation entropies suggests that a looser transition

(16) Exner, O. *Prog. Phys. Org. Chem.* **1973**, *10*, 411−483. Exner, O.; Beranek, V. *Collect. Czech. Chem. Commun.* **1975**, *40*, 781−798.
(17) Leffler, J. E. *J. Org. Chem.* **1955**, *20*, 1202−1231.
(18) Linert, W. *Chem. Soc. Rev.* **1994**, *23*, 429−438.
(19) Peterson, R. C. *J. Org. Chem.* **1964**, *29*, 3133−3135.

state is achieved for electron-poor arenes as compared to the electron-rich arenes.

Experimental Section

General Procedures. All operations and routine manipulations were performed under an atmosphere of nitrogen, either on a high-vacuum line using modified Schlenk techniques or in a Vacuum Atmospheres Dri-Lab. Benzene, THF, and hexanes were distilled from dark purple solutions of benzophenone ketyl and stored in glass ampules fitted with Teflon-sealed vacuum line adapters. Alkane solvents were made olefin-free by stirring over H_2SO_4, washing with aqueous $KMnO_4$ and water and distilling from dark purple solutions of tetraglyme/benzophenone ketyl. *m*-Xylene, 1,3-diisopropylbenzene, and 1,3-bis(trifluoromethyl)benzene were purchased from Aldrich and dried and distilled before use. 1,3-Dichlorobenzene, 1,3,5-tri-*tert*-butylbenzene, (*n*-butyl)$_3$SnD, 4-*tert*-butylphenylmagnesium bromide, and hexamethylphosphoramide (HMPA) were purchased from Aldrich and used as received. $Si(CH_3)_3Cl$ was purchased from Huls (formerly Petrarch) and used as received.

^1H, ^2H, and ^{31}P spectra were recorded on Bruker AMX400 NMR or Bruker WP200 spectrometers. All chemical shifts are reported in ppm (δ) relative to TMS (tetramethylsilane) and referenced to the residual solvent resonances (benzene, δ 7.15; chloroform, δ 7.24; acetone, δ 2.04). Fits for kinetic data, Eyring and van't Hoff plots, and least-squares analysis were performed using Microsoft Excel. All temperatures for variable temperature NMR spectroscopy were calibrated relative to the chemical shift differences in the NMR spectra of known standards (4% methanol in methanol-d_4). The complexes $(C_5Me_5)Rh(PMe_3)(aryl)Br$ and $(C_5Me_5)Rh(PMe_3)(aryl)H$ for aryl = C_6H_5, 4-$(CH_3)C_6H_4$, 4-$(CF_3)C_6H_4$, and 3,5-$(CH_3)_2C_6H_3$ have been described previously.[4,6] 1,3-Bis(trimethylsilyl)benzene was synthesized using a modified procedure from the one described previously.[20] 1-Bromo-3,5-di-*tert*-butylbenzene was prepared as described.[21] $(C_5Me_5)Rh(PMe_3)(C_2H_4)$ was prepared using a modified procedure of Maitlis[22] (for the triphenylphosphine analog) or using the procedure of Werner.[23]

Preparation of 1,3-Bis(trimethylsilyl)benzene. A 30 g (0.204 mol) amount of *m*-dichlorobenzene was dissolved in 50 mL of HMPA and added slowly to a mixture of 100 mL of HMPA/75 mL (0.585 mol) of $Si(CH_3)_3Cl$/12 g (0.494 mol) of Mg turnings in a 500 mL flask equipped with a reflux condenser. The solution was stirred at 120 °C for 7 days under nitrogen. At this point, an additional 30 mL (0.234 mol) of $Si(CH_3)_3Cl$ was added to the mixture via syringe and the reaction continued for 12 h. The solution was cooled and poured onto 300 g of ice. Extraction of the organic layer with 5 × 200 mL of diethyl ether and removal of volatiles gave a mixture of *m*-chlorophenyltrimethylsilane and 1,3-bis(trimethylsilyl)benzene. Distillation under 0.1 Torr vacuum gave 12 g of a fraction with bp 95–97 °C (26% yield). ^1H NMR (C_6D_6): δ 7.875 (s, 1 H); 7.503 (d, J = 7.6, 2 H); 7.276 (t, J = 7.6 Hz, 1 H); 0.245 (s, 18 H).

Preparation of 5-Deuterio-1,3-di-*tert*-butylbenzene. A 6.0 g (31.6 mmol) amount of 5-bromo-1,3-di-*tert*-butylbenzene was dissolved in 10 g (34.2 mmol) of (*n*-butyl)$_3$SnD and heated to 150 °C under a nitrogen atmosphere in a 50 mL flask equipped with a reflux condenser for 6 h. Fractional distillation under 0.1 Torr vacuum gave 4.2 g of a fraction with bp 55 °C. ^1H NMR (acetone-d_6): δ 7.468 (s, 1 H); 7.205 (s, 1 H); 7.198 (s, 1 H); 1.306 (s, 18 H). ^2H NMR (C_6H_6): δ 7.24 (s). GC/MS (70 eV): 191 $(M)^+$, 176 $(M - 15)^+$, 148 $(M - 43)^+$, 116 $(M - 75)^+$, 92 $(M - 99)^+$, 57 $(M - 134)^+$.

Photochemical Preparation of $(C_5Me_5)Rh(PMe_3)(aryl)H$. This method was used for the preparation of aryl hydride complexes where aryl = 1,3-dimethylphenyl, 1,3-bis(trifluoromethyl)phenyl, and 1,3-di-*tert*-butylphenyl. A 25 mg (0.073 mmol) amount of $(C_5Me_5)Rh(PMe_3)(C_2H_4)$ was dissolved in 0.7 mL of the neat arene which had been dried and freeze–pump–thaw degassed three times. The solution was placed in a resealable NMR tube and photolyzed using a λ > 345 nm long-pass filter for 2 days. The solution gradually darkened to a dark red, at which point continued photolysis did not result in further reaction. Typical yields (^{31}P NMR integration) were 80%–85%.

Preparation of $(C_5Me_5)Rh(PMe_3)[4\text{-}(C(CH_3)_3C_6H_4]Br$. A 200 mg (0.421 mmol) amount of $(C_5Me_5)Rh(PMe_3)Br_2$ was dissolved in 25 mL of anhydrous THF. A 0.75 mL amount of 2 M 4-*tert*-butylphenylmagnesium bromide was added under nitrogen. The mixture was stirred for 30 min. The excess Grignard reagent was quenched with 200 μL of saturated aqueous NH_4Br, and the volatiles were removed under vacuum. The red solid was extracted with CH_2Cl_2 and filtered. Chromatography using 4% THF/CH_2Cl_2 on silica gave 120 mg (0.227 mmol, 54%) of $(C_5Me_5)Rh(PMe_3)$(4-*tert*-butylphenyl)Br. ^1H NMR (C_6D_6): δ 8.5 (br s, 2 H), 7.202 (d, J = 7.5 Hz, 2 H), 1.425 (d, J = 1.6 Hz, 15 H), 1.355 (s, 9 H), 1.098 (d, J = 10.3 Hz, 9 H). $^{31}P\{^1H\}$ NMR (C_6D_6): δ 4.565 (d, J = 154 Hz).

Preparation of $(C_5Me_5)Rh(PMe_3)[4\text{-}Si(CH_3)_3C_6H_4]Br$. 4-(Trimethylsilyl)phenylmagnesium bromide (0.25 M) was prepared from 4-bromophenyltrimethylsilane and Mg in refluxing THF at 65 °C. A 150 mg (0.316 mmol) amount of $(C_5Me_5)Rh(PMe_3)Br_2$ was dissolved in anhydrous THF, and 10 mL of the 0.25 M 4-(trimethylsilyl)phenyl Grignard reagent was added under nitrogen. The mixture was stirred for 1 h. Addition of 200 μL of saturated aqueous NH_4Br and removal of volatiles gave a red oil. Extraction with CH_2Cl_2 and chromatography using 4% THF/CH_2Cl_2 on silica gave 80 mg of $(C_5Me_5)Rh(PMe_3)$(4-(trimethylsilyl)phenyl)Br (0.147 mmol, 46%). ^1H NMR (C_6D_6): δ 8.6 (br s, 2 H), 7.321 (d, J = 7.8 Hz, 2 H), 1.358 (d, J = 2 Hz, 15 H), 1.027 (d, J = 9.6 Hz, 9 H), 0.276 (s, 9 H).

Reaction of $(C_5Me_5)Rh(PMe_3)[4\text{-}(CH_3)C_6H_4]Br$ with L-Selectride. A 50 mg (0.103 mmol) amount of $(C_5Me_5)Rh(PMe_3)[4\text{-}(CH_3)C_6H_4]Br$ was dissolved in anhydrous THF, and 1.0 mL of 1 M L-selectride (in THF) was added under nitrogen. The volatiles were removed under vacuum, and the remaining gel was reacted for 2 h. The solid lightened to a straw-yellow color. Flash chromatography on silica using a 3:5 hexanes/THF mixture left a dark oil. ^1H and ^{31}P NMR show formation of $(C_5Me_5)Rh(PMe_3)[4\text{-}(CH_3)C_6H_4]H$ and $(C_5Me_5)Rh(PMe_3)H_2$.

Preparation of $(C_5Me_5)Rh(PMe_3)(aryl)H$. This method was used for the preparation of the 3,5-disubstituted aryl hydride complexes $(C_5Me_5)Rh(PMe_3)(3,5\text{-}C_6H_3R_2)H$ for R = CF_3, CH_3, $Si(CH_3)_3$, $CH(CH_3)_2$, and $C(CH_3)_3$. An 80–100 mg amount of $(C_5Me_5)Rh(PMe_3)(Ph)Br$ was converted to $(C_5Me_5)Rh(PMe_3)(Ph)H$ by a previously published procedure.[4] The yellow solid $(C_5Me_5)Rh(PMe_3)(Ph)H$ was then dissolved in 0.7 mL of the 1,3-disubstituted arene, and the mixture was heated at 67 °C for 10–15 h. The reaction went to >95% completion for the complexes where R = CF_3, CH_3, and $Si(CH_3)_3$. An equilibrium mixture was obtained for the complexes where R = $CH(CH_3)_2$ and $C(CH_3)_3$. Removal of the solvent under high vacuum gave dark oils. In the cases where equilibrium mixtures were obtained, fresh arene was introduced into the isolated oil and the reaction conditions were repeated to obtain >95% yield of the desired product.

Spectroscopic Data for Complexes $(C_5Me_5)Rh(PMe_3)(aryl)H$. $(C_5Me_5)Rh(PMe_3)[3,5\text{-}(CF_3)_2C_6H_3]H$. ^1H NMR (C_6D_6): δ 8.088 (s, 2 H), 7.617 (s, 1 H), 1.601 (d, J = 1 Hz, 15 H), 0.735 (d, J = 10 Hz, 9 H), −13.290 (dd, J = 48, 32 Hz, 1 H). $^{31}P\{^1H\}$ NMR (C_6D_6): δ 7.717 (d, J = 149 Hz). $(C_5Me_5)Rh(PMe_3)[3,5\text{-}(Si(CH_3)_3)_2C_6H_3]H$. ^1H NMR (C_6D_6): δ 7.857 (s,

(20) Bourgeois, P.; Calas, R. *J. Organomet. Chem.* **1975**, *84*, 165–175.
(21) Bartlett, P. D.; Roha, M.; Stiles, R. M. *J. Am. Chem. Soc.* **1954**, *76*, 2349–2353.
(22) Kang, J. W.; Maitlis, P. M. *J. Organomet. Chem.* **1971**, *26*, 393–404.
(23) Werner, H.; Klingert, B. *J. Organomet. Chem.* **1981**, *218*, 395–407.

2 H), 7.548 (s, 1 H), 1.807 (d, J = 3 Hz, 15 H), 0.933 (d, J = 9 Hz, 9 H), 0.394 (s, 18 H), −13.476 (dd, J = 49.1, 32.7 Hz, 1 H). $^{31}P\{^1H\}$ NMR (C_6D_6): δ 7.85 (d, J = 155.2 Hz). $(C_5Me_5)Rh(PMe_3)[3,5\text{-}(CH(CH_3)_2)_2C_6H_3]H$. ^1H NMR (C_6D_6): δ 7.329 (s, 2 H), 6.764 (s, 1 H), 2.876 (sept, J = 7.4 Hz, 2 H), 1.833 (s, 15 Hz), 1.365 (dd, J = 7.4, 3 Hz, 12 H), 0.956 (d, J = 10.4 Hz, 9 H), −13.577 (dd, J = 50.6, 32 Hz, 1 H). $^{31}P\{^1H\}$ NMR (1,3-diisopropylbenzene solvent): δ 7.990 (d, J = 156.6 Hz). $(C_5Me_5)Rh(PMe_3)[3,5\text{-}(C(CH_3)_3)_2C_6H_3]H$. ^1H NMR (C_6D_6): δ 7.498 (s, 2 H), 7.295 (s, 1 H), 1.846 (s, 15 H), 1.461 (s, 18 H), 0.979 (d, J = 9 Hz, 9 H), −13.540 (dd, J = 48.5, 32 Hz, 1 H). $^{31}P\{^1H\}$ NMR (C_6D_6): δ 8.520 (d, J = 157 Hz).

Preparation of $(C_5Me_5)Rh(PMe_3)(aryl)Br$. To a benzene solution of $(C_5Me_5)Rh(PMe_3)(aryl)H$ was added several drops of $CHBr_3$. The solution immediately became red. Chromatography on silica using 4% THF/CH_2Cl_2 allowed isolation of the complexes $(C_5Me_5)Rh(PMe_3)(3,5\text{-}C_6H_3R_2)Br$ for R = CF_3, $Si(CH_3)_3$, $CH(CH_3)_2$, $C(CH_3)_3$.

Spectroscopic Data for Complexes $(C_5Me_5)Rh(PMe_3)(aryl)Br$. $(C_5Me_5)Rh(PMe_3)[3,5\text{-}(CF_3)_2C_6H_3]Br$ ^1H NMR (C_6D_6): δ 9.2 (br s, 1 H), 7.702 (s, 2 H), 1.234 (s, 15 H), 0.905 (d, J = 10.2 Hz, 9 H). $^{31}P\{^1H\}$ NMR (C_6D_6): δ 3.285 (d, J = 147.6 Hz). $(C_5Me_5)Rh(PMe_3)[3,5\text{-}(Si(CH_3)_3)_2C_6H_3]Br$ ^1H NMR (C_6D_6): δ 8.7 (br s, 1 H), 7.650 (s, 2 H), 1.430 (d, J = 2.8 Hz, 15 H), 1.116 (d, J = 9.7 Hz, 9 H), 0.396 (s, 18 H). $^{31}P\{^1H\}$ NMR (C_6D_6): δ 4.494 (d, J = 155.4 Hz). $(C_5Me_5)Rh(PMe_3)[3,5\text{-}(CH(CH_3)_2)_2C_6H_3]Br$ ^1H NMR (C_6D_6): δ 8.28 (br s, 1 H), 6.813 (s, 2 H), 2.89 (br s, 2 H), 1.448 (d, J = 2.7 Hz, 15 H), 1.356 (d, J = 7.6 Hz, 12 H), 1.129 (d, J = 10.4 Hz, 9 H). $^{31}P\{^1H\}$ NMR (C_6D_6): δ 5.43 (d, J = 155.2 Hz). $(C_5Me_5)Rh(PMe_3)[3,5\text{-}(C(CH_3)_3)_2C_6H_3]Br$ ^1H NMR (C_6D_6): δ 8.51 (br s, 1 H), 7.203 (t, J = 1.8 Hz, 1 H), 6.975 (br s, 1 H), 1.45 (br s, 18 H), 1.449 (d, J = 2.8 Hz, 15 H), 1.140 (d, J = 10.3 Hz, 9 H). $^{31}P\{^1H\}$ NMR (C_6D_6): δ 4.28 (d, J = 146 Hz).

Kinetic Studies. In a typical experiment, 80−100 mg of $(C_5Me_5)Rh(PMe_3)(Ph)Br$ was converted to the phenyl hydride $(C_5Me_5)Rh(PMe_3)(Ph)H$ with L-selectride using a published procedure.[4] The $(C_5Me_5)Rh(PMe_3)(Ph)H$ was converted to the 3,5-disubstituted aryl hydride complex as described above. The dark oil was dissolved in C_6D_6 and diluted to 2.8−3.5 mL with C_6D_6 to yield 4 or 5 NMR samples. The solutions were placed in NMR tubes with vacuum adapters, freeze−pump−thaw degassed and flame-sealed under vacuum and stored at −20 °C until ready to use. For reactions with half-lives of 4 h or less, the NMR probe was heated to the desired temperature and spectra were obtained at 10, 5, or 3 min intervals using the Bruker 2D program KINETICS. For slower reactions, the sample was kept in an equilibrated oil-bath for elevated temperatures or a constant temperature room for room temperature and NMR spectra were obtained at appropriate intervals. Kinetics were monitored for a minimum of 3 half-lives, with one exception being the reaction of $(C_5Me_5)Rh(PMe_3)[3,5\text{-}(CF_3)_2C_6H_3]H$ at 54 °C, which has a half-life of 1600 h. In this case the reaction was followed for 2000 h.

Equilibrium Studies. Equilibrium values were obtained with samples used in the synthesis of the $(C_5Me_5)Rh(PMe_3)(3,5\text{-}C_6H_3R_2)H$ complexes. For R = $CH(CH_3)_2$ and $C(CH_3)_3$, equilibrium was attained with the C_6H_6 released from $(C_5Me_5)Rh(PMe_3)(Ph)H$. Measurements were made by $^{31}P\{^1H\}$ NMR spectroscopy using inverse-gated decoupling to insure accuracy of the integration. Equilibrium values for R = CF_3 were obtained using final ratios of aryl hydride to phenyl hydride values from the kinetic experiments in C_6D_6, as equilibrium was achieved with the $1,3\text{-}(CF_3)_2C_6H_4$ released.

Kinetic Isotope Effect of $(C_5Me_5)Rh(PMe_3)(C_2H_4)$ with 1,3-Di-*tert*-butylbenzene/5-Deuterio-1,3-di-*tert*-butylbenzene. A sample of composition 50% 5-deuterio-1,3-di-*tert*-butylbenzene was prepared by dilution of >90% 5-deuterio-1,3-di-*tert*-butylbenzene with proteo 1,3-di-*tert*-butylbenzene. The composition was confirmed by GC−MS analysis of the parent ions at 191 and 190 mass units using low ionization voltage. Integration of the phenyl resonances by ^1H NMR spectroscopy quantitatively confirmed the amount of the deuterium enrichment. A 25 mg (0.053 mmol) amount of $(C_5Me_5)Rh(PMe_3)Br_2$ was converted to $(C_5Me_5)Rh(PMe_3)(C_2H_4)$ and sublimed twice onto a liquid nitrogen cold finger. The $(C_5Me_5)Rh(PMe_3)(C_2H_4)$ was dissolved in 0.5 mL of the deuterium-enriched arene and photolyzed at 10 °C with a high-pressure Hg lamp using a λ > 345 nm long-pass filter. ^{31}P inverse-gated NMR spectra were recorded at 15 min intervals. The relative amounts of aryl hydride and aryl deuteride complexes were determined by integration of the base line-resolved peaks for the two isotopomers.

Flash Photochemical Studies. Flash photolysis experiments were carried out using a flash photochemical apparatus which has been described previously.[10] In a typical experiment, several mg of twice-sublimed $(C_5Me_5)Rh(PMe_3)(C_2H_4)$ was dissolved in high-purity toluene or *m*-xylene which had been distilled and thoroughly dried and degassed. The sample was placed in a flash cell and diluted until the absorbance at 308 nm was between 0.8 and 1.2. The sample was then freeze−pump−thaw degassed three times.

Acknowledgment is made to the U.S. Department of Energy (Grant DE-FG02-86ER13569) for their support of this work and to NATO for a travel grant.

OM950353K

Spectroscopic Characterization and Dynamic Properties of Cationic η^2-Silane and η^2-H_2 Complexes of General Structure $Cp(CO)(L)Fe(HSiR_3)^+$ and $Cp(CO)(L)Fe(H_2)^+$ (L = PEt_3, PPh_3)[1]

Eric Scharrer,[†] Seok Chang, and Maurice Brookhart*

Department of Chemistry, The University of North Carolina, Chapel Hill, North Carolina 27599

Received May 17, 1995[⊗]

The η^2-H_2 complexes $Cp(CO)(PEt_3)Fe(H_2)^+$, **4**, and $Cp(CO)(PPh_3)Fe(H_2)^+$, **9**, were generated by protonation of the neutral monohydride complexes with $H(OEt_2)_2BAr'_4$ (Ar' = 3,5-$(CF_3)_2C_6H_3$) at −78 °C in CD_2Cl_2. The η^2-H_2 bonding mode was verified by observation of J_{HD} = 31.6 Hz for **4** and J_{HD} = 31.7 Hz for **9** in the η^2-HD complexes. The classical trans dihydride $Cp(CO)(PEt_3)Fe(H)_2^+$, **5**, could be detected at low temperature but converts to the more stable η^2-H_2 complex at higher temperatures. The η^2-silane complex $Cp(CO)(PEt_3)Fe(HSiEt_3)^+$, **1**, was prepared by protonation of $Cp(CO)(PEt_3)FeSiEt_3$ with $H(OEt_2)_2BAr'_4$, and the nonclassical structure was verified by observation of a Si–H coupling constant of 62.4 Hz. A more convenient and general method involving displacement of H_2 from $Cp(CO)(PR_3)Fe(H_2)^+$ by free silane was used to prepare a series of η^2-silane complexes including $Cp(CO)(PEt_3)Fe(H_2SiPh_2)^+$, **12**, $Cp(CO)(PEt_3)Fe(H_2SiMePh)^+$, **13**, $Cp(CO)(PEt_3)Fe(H_3SiPh)^+$, **16**, $Cp(CO)(PPh_3)Fe(HSiEt_3)^+$, **11**, and $Cp(CO)(PPh_3)Fe(H_2SiMePh)^+$, **15**. Complex **13** exists as a pair of diastereomers which interconvert above −20 °C ($\Delta G^{\ddagger}$ = 12.6 kcal/mol). A mechanism involving pseudorotation in an Fe(IV) silyl hydride intermediate, $Cp(CO)(PEt_3)Fe(H)(SiMeHPh)^+$, was proposed to account for this dynamic process. Similar dynamic properties were observed for **15** and **16**.

Introduction

The coordination of an Si–H bond to a transition metal center has been extensively studied by a number of research groups.[2–9] In particular, Schubert has prepared a wide variety of manganese silane complexes of the type $Cp'(CO)(L)Mn(HSiX_3)$ and has described the changes in structure and bonding which result from systematic variations in substituents on silicon and the Cp ring as well as variations of the ligand, L.[7] It was found that both steric and electronic factors play a role in determining whether the silane oxidatively adds to the metal center and the extent of Si–H bond breaking in η^2-silane complexes. While there are numerous examples of neutral transition metal silane complexes, cationic complexes of this type are quite rare. During his investigations of silane alcoholysis catalyzed by a cationic Ir complex, Crabtree spectroscopically observed $Ir(Et_3SiH)_2(THF)_2(PPh_3)_2^+SbF_6^-$.[10] Lemke has recently reported observation of $Cp(PMe_3)_2Ru(HSiCl_3)^+BAr'_4$.[11]

During our mechanistic investigations of the insertion reactions of cationic iron carbene complexes into Si–H bonds of organosilanes, a cationic iron silane complex was invoked as an intermediate in an effort to explain certain experimental observations.[12] When the BF_4^- salts of iron carbene complexes of the type $Cp(CO)(PEt_3)Fe{=}CHR^+$ were treated with Et_3SiH, the insertion product was formed together with Et_3SiF. The reaction sequence shown in eq 1 was invoked. The formation of **1** presumably results in an extremely electrophilic silicon center capable of reaction with BF_4^-.

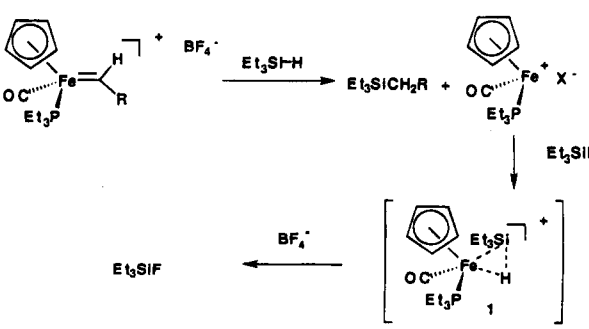

(1)

Evidence supporting this pathway was obtained by carrying out the reaction shown in eq 2. Treatment of

[†] Current address: Department of Chemistry, Franklin and Marshall College, P.O. Box 3003, Lancaster, PA 17604-3003.

[⊗] Abstract published in *Advance ACS Abstracts,* October 1, 1995.

(1) Reported in part at the 205th National Meeting of the American Chemical Society, Denver, CO, March, 1993; INOR 132.

(2) (a) Hart-Davis, A. J.; Graham, W. A. G. *J. Am. Chem. Soc.* **1971**, *94*, 4388. (b) Jetz, W.; Graham, W. A. G. *Inorg. Chem.* **1971**, *10*, 4.

(3) Colomer, E.; Corriu, R. J. P.; Marzin, C.; Vioux, A. *Inorg. Chem.* **1982**, *21*, 368.

(4) Matarasso-Tchiroukhine, E.; Jouen, G. *Can. J. Chem.* **1988**, *66*, 2157.

(5) Luo, X.; Kubas, G. J. *J. Am. Chem. Soc.* **1995**, *117*, 1159.

(6) (a) Lichtenberger, D. L.; Rai-Chaudhuri, A. *J. Am. Chem. Soc.* **1990**, *112*, 2492. (b) Lichtenberger, D. L.; Rai-Chaudhuri, A. *J. Am. Chem. Soc.* **1989**, *111*, 3583.

(7) (a) Schubert, U. *Adv. Organomet. Chem.* **1990**, *30*, 151. (b) Schubert, U.; Scholz, G.; Müller, J.; Ackermann, K.; Wörle, B.; Stansfield, R. F. D. *J. Organomet. Chem.* **1986**, *306*, 303. (c) Kraft, G.; Kalbas, C.; Schubert, U. *J. Organomet. Chem.* **1985**, *289*, 247.

(8) Sun, J.; Lu, R. S.; Bau, R.; Yang, G. K. *Organometallics* **1994**, *13*, 1317.

(9) (a) Luo, X.; Kubas, G. J.; Bryan, J. C.; Burns, C. J.; Unkefer, C. J. *J. Am. Chem. Soc.* **1994**, *116*, 10312. (b) Luo, X.; Kubas, G. J.; Burns, C. J.; Bryan, J. C.; Unkefer, C. J. *J. Am. Chem. Soc.* **1995**, *117*, 1159.

(10) Luo, X.; Crabtree, R. H. *J. Am. Chem. Soc.* **1989**, *111*, 2527.

(11) Lemke, F. R. *J. Am. Chem. Soc.* **1994**, *116*, 11183.

(12) Brookhart, M.; Scharrer, E. *J. Organomet. Chem.* **1995**, *497*, 61.

(13) (a) Brookhart, M.; Grant, B. E.; Volpe, A. F., Jr. *Organometallics* **1992**, *11*, 3920. (b) Taube, R.; Wache, S. *J. Organomet. Chem.* **1992**, *428*, 431.

0276-7333/95/2314-5686$09.00/0

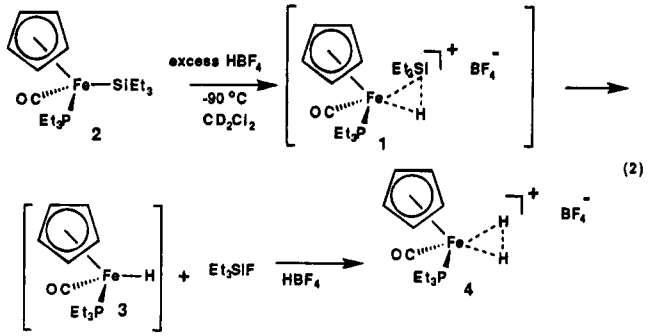

2 with excess HBF_4 resulted in formation of Et_3SiF and a species which was tentatively assigned as the η^2-H_2 complex, **4**. Remarkably, complex **1** apparently reacts with BF_4^- even at −90 °C. By employment of the non-nucleophilic counterion ($(CF_3)_2C_6H_3)_4B^-$ ($BAr'_4{}^-$), the nucleophilic trapping of **1** was avoided and it could be observed spectroscopically at −78 °C as shown in eq 3. Complex **1** is exceedingly sensitive to water and above −40 °C reacts rapidly with trace moisture to yield the η^2-H_2 complex, **4**.

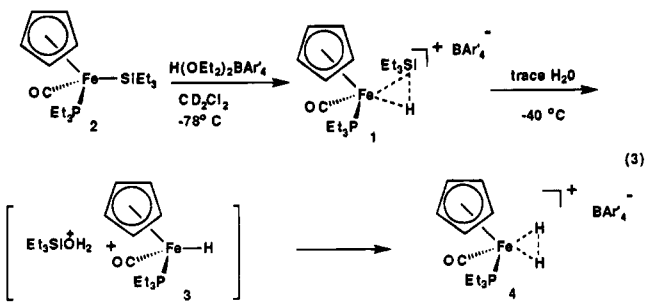

The lack of examples of cationic η^2-silane complexes can be attributed in large measure to their extreme sensitivity to weak nucleophiles, even traditionally non-nucleophilic counterions such as BF_4^-. As demonstrated above, the use of the non-nucleophilic counterion $(CF_3)_2C_6H_3)_4B^-$ now allows access to such species. We report here, the generation, spectroscopic characterization, and dynamic behavior of η^2-silane complexes of the type $Cp(CO)(L)Fe(HSiR_3)^+BAr'_4{}^-$ (L = PEt_3, PPh_3). The dynamic behavior of these species is related to the dynamics of manganese silyl hydride complexes of the type $Cp(P(CH_2)_nP)Mn(H)(SiHPh_2)$ recently reported by Yang.[8] In addition, the corresponding η^2-H_2 complexes, $Cp(CO)(L)Fe(H_2)^+$ (L = PEt_3, PPh_3), are also described.

Results and Discussion

A. Spectroscopic Characterization of Cp(CO)(L)Fe(H$_2$)$^+$BAr'$_4^-$, 4 (L = PEt$_3$) and 9 (L = PPh$_3$), and *trans*-Cp(CO)(PEt$_3$)Fe(H)$_2^+$ BAr'$_4^-$, 5. As noted in the Introduction, $Cp(CO)(L)Fe(H_2)^+$, **4**, was generated by an indirect method through hydrolysis of the cationic silane complex, **1**. Protonation of the neutral iron hydride, **3**, provides a direct route to this species as well as to the partially labeled η^2-HD complex and thus a means to verify the structure and nature of the bonding in **4**.

The neutral iron hydride, **3**, was obtained as an unstable yellow oil by lithium aluminum hydride reduction of the iodide, $Cp(CO)(PEt_3)FeI$. ^1H NMR spectroscopy showed a characteristic doublet at −14.55 ppm for the hydride resonance (J_{PH} = 75 Hz). When this species was protonated using $H(OEt_2)_2BAr'_4$ in CD_2Cl_2 at −78 °C, a broad peak at −11.8 ppm which integrated for 2 protons was observed which corresponds exactly to the final product seen in the silane hydrolysis reactions. This complex is stable to about 10 °C at which point H_2 slowly dissociates from the metal center as is evident from an NMR resonance at 4.6 ppm corresponding to dissolved H_2. The HD complex was prepared by protonation of the neutral iron deuteride, and the value of J_{HD} was determined to be 31.6 Hz which is diagnostic of an η^2-HD bonding interaction and unequivocally establishes the structure of **4** as shown (eq 4).[14]

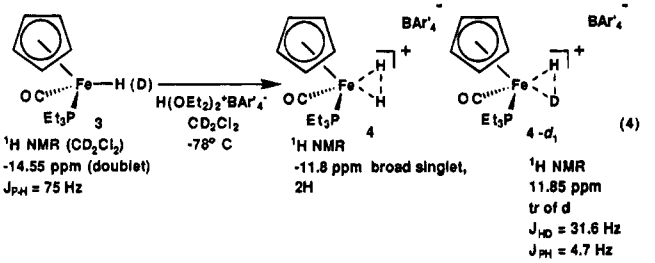

Through a fortuitous observation we have also been able to characterize the classical *trans*-dihydride complex $Cp(CO)(PEt3)Fe(H)_2^+BAr'_4{}^-$, **5**. When the neutral iron silyl complex, $Cp(CO)(PEt_3)FeSiEt_3$, **2**, was protonated with $H(OEt_2)_2^+BAr'_4{}^-$ in CD_2Cl_2 containing significant amounts of water at −78 °C, no η^2-silane complex was observed. We expected to observe only the dihydrogen complex, **4** (−11.8 ppm), and a small amount of this species was present. However, the major resonance in the hydride region was a sharp doublet at −7.9 ppm. The large J_{PH} of 69.7 Hz led us to assign this resonance to the classical dihydride complex, **5**, in which the two hydrogen atoms are trans to each other (eq 5).

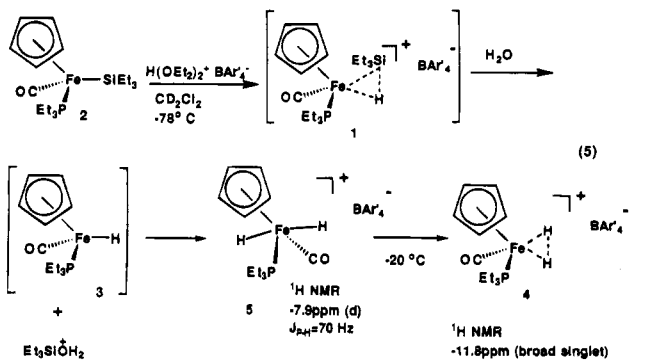

The initially formed silane complex must rapidly react with water to give $Et_3SiOH_2^+$ and the iron hydride complex, **3**. Apparently, under these conditions, subsequent protonation of **3** occurs at the metal to give predominantly the dihydride complex, **5**. Upon warming though, the dihydride complex converts to the η^2-H_2 complex which at −20 °C is the exclusive product. If the sample is recooled to −78 °C, no dihydride complex re-forms which indicates that this is not a reversible process and that the η^2-H_2 complex is the thermodynamically more stable isomer.[15]

These results can be contrasted with those reported

(14) Heinekey, D. M.; Oldham, W. J., Jr. *Chem. Rev.* **1993**, *93*, 913.

by Lapinte.[16] Protonation of Cp*(dppe)FeH at −80 °C initially gave the η^2-H_2 complex, **6**. Upon warming, this species converted to the trans dihydride complex, **7** (eq 6). The Cp*(dppe)Fe metal center in this complex is

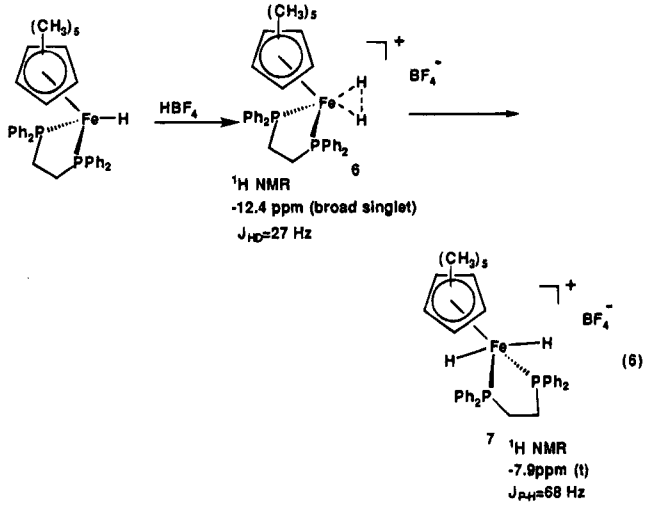

more electron rich than that in the $Cp(CO)(PPh_3)Fe$ fragment. This electronic difference manifests itself in the spectroscopic data. The H−H bond should be stretched to a greater extent in this complex, and indeed J_{HD} is less for **6** than for **4** (27 Hz vs 32 Hz). Additionally, the increased electron density at iron favors oxidative addition as is demonstrated by the irreversible conversion to the dihydride complex, **7**. Lapinte cites the fact that the η^2-H_2 complex is initially formed as evidence that protonation at the M−H bond to give the η^2-H_2 complex, **6**, is kinetically favored over protonation at the iron center to give the dihydride complex. However, in the system studied by us, protonation at the metal must be faster than protonation at the Fe−H bond in order to account for the initially formed dihydride complex, $Cp(CO)(PEt_3)Fe(H)_2$. A possible explanation for the differing results is that steric effects determine the kinetic product of protonation. The bulky bidentate phosphine ligand of Cp*(dppe)FeH can presumably shield the metal center from trans protonation which would give the trans dihydride complex. On the other hand, the metal hydride bond is relatively accessible. By comparison, protonation of **3** at the metal center trans to the hydride ligand is relatively unhindered.[17] This behavior has direct analogy to the studies of Simpson who showed that protonation of $(Ph_2P(CH_2)_3PPh_2)CpRuH$ yields only the cationic *trans*-dihydride while protonation of the more restricted $(Ph_2PCH_2PPh_2)CpRuH$ yields only the η^2-H_2 complex (cis protonation). Protonation of $(Ph_2PCH_2CH_2PPh_2)CpRuH$ yields a mixture of *trans*-dihydride and η^2-H_2 complexes.[18]

The PPh_3-substituted η^2-H_2 complex, **9**, was generated by protonation of the hydride complex, $Cp(CO)(PPh_3)FeH$, **8**, with $H(OEt_2)_2^+BAr'_4^-$ in CD_2Cl_2 at −78 °C as shown in eq 7. The η^2-H_2 signal appears as a broad singlet at

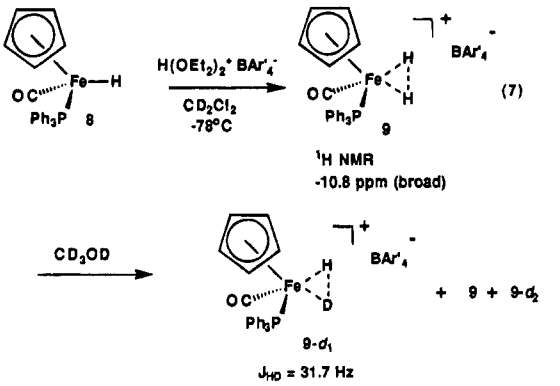

−10.8 ppm. As with complex **4**, the η^2-HD complex was prepared, but in this case, the method of generation relied upon H/D exchange using CD_3OD. Addition of CD_3OD to a −78 °C CD_2Cl_2 solution of **4** resulted in H/D exchange to yield the η^2-HD complex, **9**-d_1, together with presumably the η^2-D_2 complex. Some of the η^2-H_2 complex also was present. The observed J_{HD} of 31.7 Hz clearly establishes an η^2-H_2 structure for complex **9**. Loss of H_2 from both **4** and **9** above 10 °C precluded their isolation.

B. Generation, Spectroscopic Characterization, and Dynamic Behavior of η^2-Silane Complexes of $Cp(CO)(L)Fe^+$ (L = PEt_3, PPh_3). $Cp(CO)(L)Fe(HSiEt_3)^+BAr'_4^-$, 1 (L = PEt_3) and 11 (L = PPh_3). As noted in the Introduction, the cationic silane complex $Cp(CO)(PEt_3)Fe(HSiEt_3)^+BAr'_4^-$, **1**, was observed by low-temperature protonation of the silyl complex $Cp(CO)(PEt_3)FeSiEt_3$ but is hydrolyzed by trace water upon warming to yield the η^2-H_2 complex, **4**, which in turn liberates H_2 above 10 °C. It was anticipated that silane complexes could be generated by displacement of the H_2 ligand from the metal center by excess silane above 10 °C. Indeed, this proved a very convenient method for generating η^2-silane complexes for spectroscopic observation. $Cp(CO)(PEt_3)FeSiEt_3$, **2**, was protonated in CD_2Cl_2 at −78 °C with $H(OEt_2)_2^+BAr'_4^-$, and 5 equivs of Et_3SiH was added. Observation by ^1H NMR spectroscopy at −78 °C showed the silane complex to be present; however, as before, it was converted to **4** upon warming (eq 8).[19] At −20 °C, **4** was the only species present. Upon warming of this solution to room temperature, vigorous outgassing of H_2 was observed. Examination of this solution by ^1H NMR spectroscopy indicated that the η^2-silane complex, **1**, was the only organometallic species present. Clearly, the exchange

(15) There are many examples of an equilibrium between an η^2-H_2 complex and a dihydride complex: (a) Kubas, G. J.; Ryan, R. R.; Wrobleski, D. A. *J. Am. Chem. Soc.* **1986**, *108*, 1339. (b) Kubas, G. J.; Unkefer, C. J.; Swanson, B. I.; Fukushima, E. *J. Am. Chem. Soc.* **1986**, *108*, 7000. (c) Kubas, G. J.; Ryan, R. R.; Unkefer, C. J. *J. Am. Chem. Soc.* **1987**, *109*, 8113. (d) Chinn, M. S.; Heinekey, D. M. *J. Am. Chem. Soc.* **1990**, *112*, 5166. (e) Chinn, M. S.; Heinekey, D. M. *J. Am. Chem. Soc.* **1987**, *109*, 5865. (f) Luo, X. L.; Michos, D.; Crabtree, R. H. *Organometallics* **1992**, *11*, 237.

(16) Hamon, P.; Toupet, L.; Hamon, J.; Lapinte, C. *Organometallics* **1992**, *11*, 1429.

(17) The explanation for the variation in the ratios of **4**:**5** with reaction conditions is not entirely clear but probably rests with the nature of the Bronsted acid responsible for proton transfer. In protonations of hydride **3** with $H(OEt_2)_2^+BAr'_4^-$, proton transfer likely occurs from the Bronsted acid Et_2OH^+ although some H_3O^+ is always present. Hydrolysis of silane complex **1** with water present produces initially $Et_3SiOH_2^+$ which may serve as the acid or proton exchange may generate H_3O^+ as the reactive acid.

(18) Conroy-Lewis, F. M.; Simpson, S. J. *J. Chem. Soc., Chem. Commun.* **1987**, 1675.

(19) Et_3SiOH could not be identified since the ^1H signals of the ethyl group overlap with those of excess Et_3SiH. However, its formation can be inferred due to the conversion of the silane complex to the hydrogen complex. Moreover, we have demonstrated that the the cationic iron η^2-silane complexes are extremely susceptible to nucleophilic attack and react with EtOH to give $EtOSiEt_3$. Silane alcoholysis using these species occurs in a catalytic fashion, and this is the subject of another paper: Chang, S.; Scharrer, E.; Brookhart, M. To be submitted to *J. Mol. Catal.*

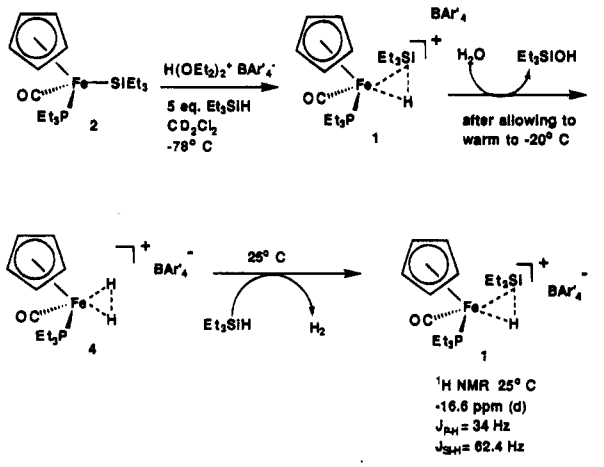

reaction is quantitative since no η^2-H_2 complex remained. Remarkably, **1** was stable even at room temperature as long as excess silane was present.[20] Some of the added free Et_3SiH will also be hydrolyzed via the η^2-complex until all of the water is consumed. This technique provides a method to "dry" the solution to the point where the silane complex is no longer subject to hydrolysis.[21] All attempts to completely eliminate all traces of water from CD_2Cl_2 and $H(OEt_2)_2^+BAr'_4^-$ so that hydrolysis of freshly generated silane complexes would not occur were unsuccessful. Under our normal reaction conditions, it was found that 5–10 equivs of added free silane was sufficient to accomplish water scavenging and allow observation of the silane complex.

The ^{29}Si satellites of the hydride signal were located, and J_{SiH} was determined to be 62.4 Hz. This value clearly indicates that the silane is bound to the iron center in a three-center, two-electron fashion and falls in the upper end of the known range of J_{SiH} values for M–H–Si bonds.[7a] Since these complexes are cationic, back-donation from the iron center into the σ^* orbital of the Si–H bond should be less than in the neutral manganese analogs. Indeed, for the phosphine-substituted manganese silane complexes, $Cp(CO)(PR_3)Mn(HSiR_3)$, J_{SiH} is about 40 Hz which is indicative of greater metal to ligand back-donation. The J_{SiH} values for the iron complexes compare more closely to that observed for $Cp(CO)_2Mn(H_2SiPh_2)$ (J_{SiH} = 63.5 Hz) where there is weaker back-donation from the $Cp'(CO)_2Mn$ fragment to the silane as compared to $Cp'(CO)(PR_3)Mn$.[7a]

An interesting feature of complex **1** is the strong temperature dependence of the chemical shift of the bridging hydride resonance. At −80 °C the signal is observed at −15.2 ppm, but it moves upfield with increasing temperature and at 25 °C appears at −16.6 ppm. One possible explanation for this phenomenon is that the Si–H group is bound to the chiral iron center in two orientations, each of which are significantly populated and rapidly interconvert by rotation about the iron–silane bond and exhibit quite different chemical shifts. A temperature-dependent variation in the population of these rotamers could then account for the observed temperature-dependent chemical shift.

The exchange procedure was also used to generate $Cp(CO)(PPh_3)Fe(HSiEt_3)^+BAr'_4^-$, **11**. As before, the neutral silyl complex, **10**, was protonated at low temperature with $H(OEt_2)_2^+BAr'_4^-$ and 5 equivs of Et_3SiH was added. Initially, only **9** was observed even at −78 °C suggesting that **11** is more rapidly hydrolyzed than **1**. However, upon warming of the sample to 25 °C, loss of H_2 occurs at which point the free Et_3SiH coordinates to the iron center giving the η^2-silane complex, **11** (eq 9). This complex exhibited characteristic NMR behavior

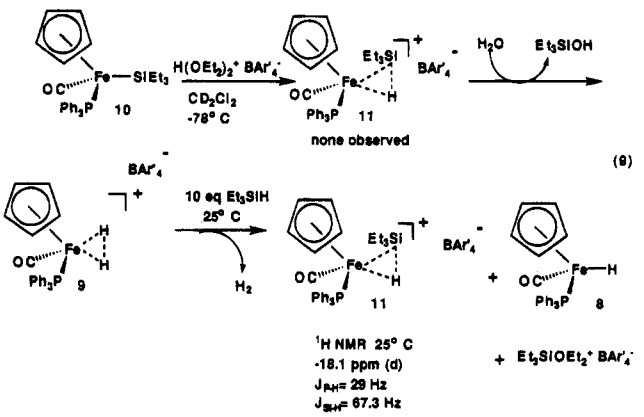

for the bridging hydride (−18.1 ppm, J_{SiH} = 67 Hz, J_{PH} = 29 Hz). Significantly, a small amount of the neutral iron hydride complex was also present along with $Et_3SiOEt_2^+BAr'_4^-$.[22] The latter two species must be formed by reaction of Et_2O with the silane complex. Apparently, in complex **11**, the silicon atom is sufficiently electrophilic to be attacked by Et_2O whereas in complex **1** it is not. The amounts of iron hydride and $Et_3SiOEt_2^+BAr'_4^-$ present are very sensitive to the amount of ether present. When 2 equivs of acid is used to generate the silane complex, more of these species are formed due to the presence of more ether.

$Cp(CO)(PEt_3)FeSiEt_3$, **2**, was protonated with $H(OEt_2)_2^+BAr'_4^-$ in CD_2Cl_2 at room temperature and 5 equiv of diphenylsilane was added (eq 10). ^1H NMR spectroscopy indicated that only the diphenylsilane complex, **12**, was present. One Si–H (H_a) is bound to the metal center and is observed at −12.9 ppm. As with the Et_3SiH complex, the value of J_{SiH} (58 Hz) suggests that the

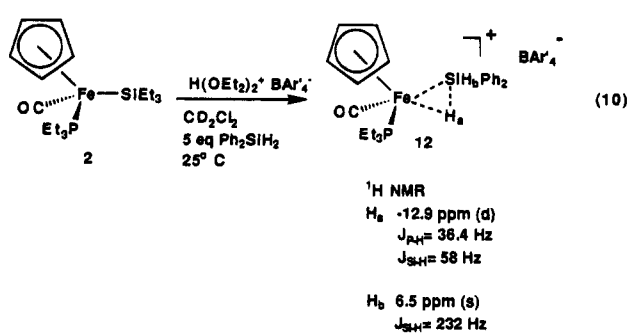

(20) It is interesting to note that the naked silicenium ion, $Et_3Si^+BAr'_4^-$, is not observed upon treatment of Et_3SiH with $Ph_3C^+BAr'_4^-$ in CH_2Cl_2. Instead, flouride is abstracted to give Et_3SiF: Bahr, S.; Boudjouk, P. *J. Am. Chem. Soc.* **1993**, *115*, 4514.

(21) It is likely that Et_3SiOH can also attack the η^2-silane complex and produce $(Et_3Si)_2OH^+$. Thus, 1 equiv of water can result in consumption of 2 equivs of silane.

(22) Confirmation of the formation of this species was obtained by its independent synthesis using the method of Kira: Kira, M.; Hino, T.; Sakurai, H. *J. Am. Chem. Soc.* **1992**, *114*, 6697. The ^1H NMR resonances for the ether protons $(CH_3CH_2)_2OSi(CH_2CH_3)_3^+BAr'_4^-$ were observed at 4.46 ppm (q) and 1.48 ppm (t) and matched those observed upon generation of **11**. The resonances for the triethylsilyl protons were obscured by excess Et_3SiH.

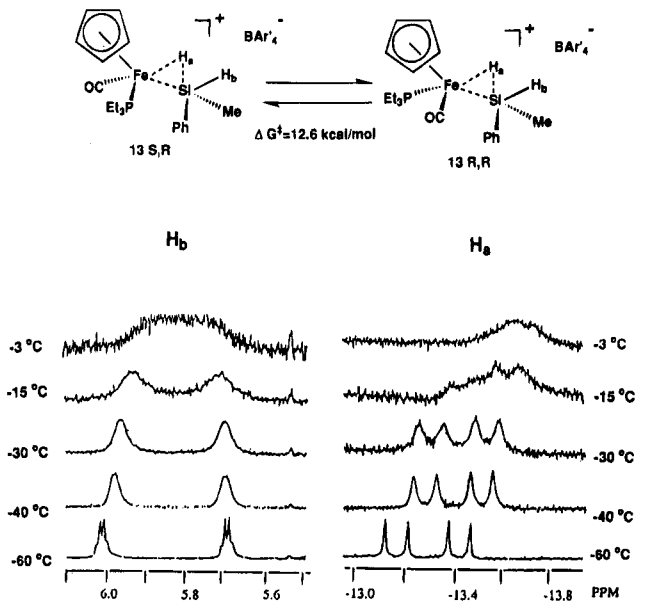

Figure 1. Variable-temperature ^{1}H NMR spectra of the interconversion of **13**-*S,R* and **13**-*R,R* (CD_2Cl_2, 400 MHz).

silane is bound to the metal center in a two-electron, three-center fashion. The terminal Si–H (H_b) does not interact with the metal and is observed at 6.5 ppm with a large value of J_{Si-H} (232 Hz). It is of interest to note that H_a and H_b do not interchange on the NMR time scale. From line width measurements, a maximum possible rate of exhange was estimated to be 5 s^{-1} at room temperature ($\Delta G^{\ddagger} \geq 16.2$ kcal/mol).[23]

The value of J_{SiH} for the terminal SiH bond (H_b) of 232 Hz can be compared with the analogous J_{SiH} value of 205 Hz in the neutral manganese diphenylsilane complex $Cp'(CO)_2Mn(H_2SiPh_2)$.[7a] A possible explanation for the higher value in **12** is that in the cationic iron complex there is a significant positive charge buildup on the silicon atom resulting in a contraction of the Si–H bond and thus increasing the value of J_{SiH}.

Structure and Dynamics of Cp(CO)(L)Fe(H_2SiMePh)$^+$, 13 (L = PEt_3) and 15 (L = PPh_3), and Cp(CO)(PEt_3)Fe(H_3SiPh)$^+$, 16. The iron center in the phosphine-substituted iron silane complexes is chiral. If a prochiral silane were bound to the iron center, then it should be possible to generate diastereomeric silane complexes. With this prospect in mind, the methylphenylsilane complex, **13**, was generated via the exchange method (eq 11). As expected, ^{1}H NMR observation at

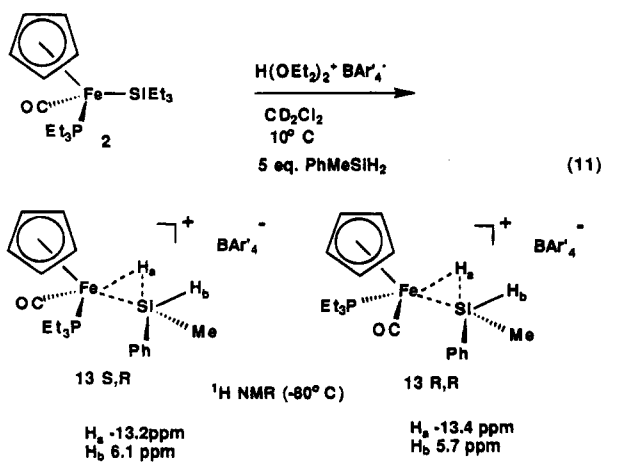

−80 °C showed that two diastereomers were present in ca. a 1:1 ratio. Two doublets were present at −13.2 ppm (J_{PH} = 36 Hz) and −13.4 ppm (J_{PH} = 36 Hz) corresponding to H_a in each diastereomer, and two quartets were observed at 6.1 ppm and 5.7 ppm corresponding to H_b in each diastereomer. Upon warming, the peaks broadened and eventually the two quartets coalesced and the two doublets coalesced, which is indicative of diastereomer interconversion (Figure 1). At 10 °C, a broad doublet was observed at −13.7 ppm along with a broad peak at 5.8 ppm. As with the diphenylsilane complex, the bridging hydride, H_a, did not interchange with the terminal Si–H, H_b. This implies that the diastereomer interconversion is an intramolecular process. If intermolecular exchange were responsible, then H_a and H_b would be expected to exchange with coalescence at a chemical shift between the two individual values (ca. −4 ppm). Using line shape analysis, a $\Delta G^{\ddagger}$ of 12.6 kcal/mol (k = 310 s^{-1} at −3 °C) was calculated for the diastereomer interconversion (eq 12).

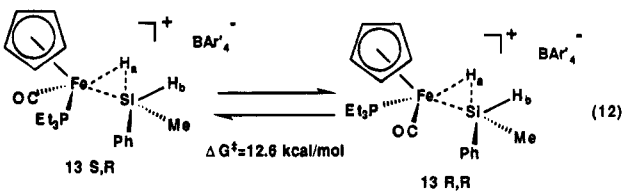

Diastereomer interconversion is not intermolecular and does not involve a rapid migration of iron between H_a and H_b. The process must involve a rapid intramolecular inversion of stereochemistry at either the iron center or the silicon center. The most plausible mechanism involves scrambling of stereochemistry at the iron center via the mechanism shown in Scheme 1. If a complete oxidative addition of the η^2-Si–H bond occurs, then the 7-coordinate iron(IV) intermediate, **14**, would be formed and scrambling of the substituents can occur via a pseudorotation process (**14a** to **14b**).[24] If the phosphine and CO ligands switch positions and the silyl hydride "reductively eliminates" re-forming the η^2-silane complex, then the stereochemistry at iron has been inverted while the stereochemistry at silicon has been maintained. This would interconvert the diastereomers and account for the observed NMR data.

For comparison, the PPh_3-substituted analog, Cp(CO)(PPh_3)Fe(H_2SiMePh)$^+$, **15**, was examined. It was generated by the standard exchange method, but upon NMR observation, this complex showed somewhat different behavior than **13**. Two diastereomers were observed at very low temperature in a 3:1 ratio. At −105 °C, a broad doublet at −13.5 ppm was observed

(23) Thermolysis of certain complexes of the type LnM(alkyl)(H) leads to intramolecular scrambling of the the metal hydride with the α-hydrogens of the alkyl ligands. This scrambling is proposed to occur via a σ-alkane complex which, in contrast to these silane complexes, rapidly interchanges "bridged" and "terminal" hydrogens. For leading references see: (a) Buchanan, J. M.; Stryker, J. M.; Bergman, R. G. *J. Am. Chem. Soc.* **1986**, *108*, 1537. (b) Periana, R. A.; Bergman, R. G. *J. Am. Chem. Soc.* **1986**, *108*, 7332. (c) Periana, R. A.; Bergman, R. G. *J. Am. Chem. Soc.* **1986**, *108*, 7346. (d) Bullock, R. M.; Headford, C. F. L.; Hennessy, K. M.; Kegley, S. E.; Norton, J. R. *J. Am. Chem. Soc.* **1989**, *111*, 3897. (e) Gould, G. L.; Heinekey, D. M. *J. Am. Chem. Soc.* **1989**, *111*, 5502.

(24) Flood, T. C.; Rosenberg, E.; Sarhangi, A. *J. Am. Chem. Soc.* **1977**, *99*, 4334.

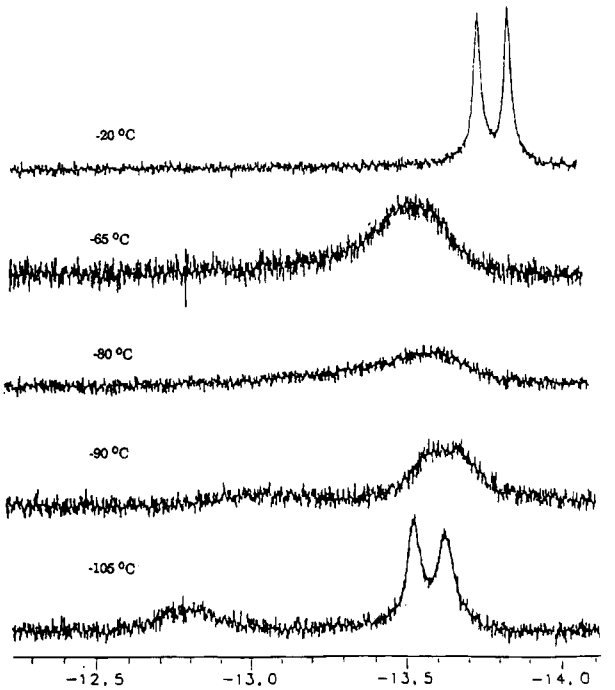

Figure 2. Variable-temperature ^{1}H NMR spectra of the interconversion of **15**-*S*,*R* and **15**-*R*,*R* Cp(CO)(PPh$_3$)Fe(H$_2$-SiMePh)$^+$ (CD_2Cl_2, 400 MHz).

Scheme 1

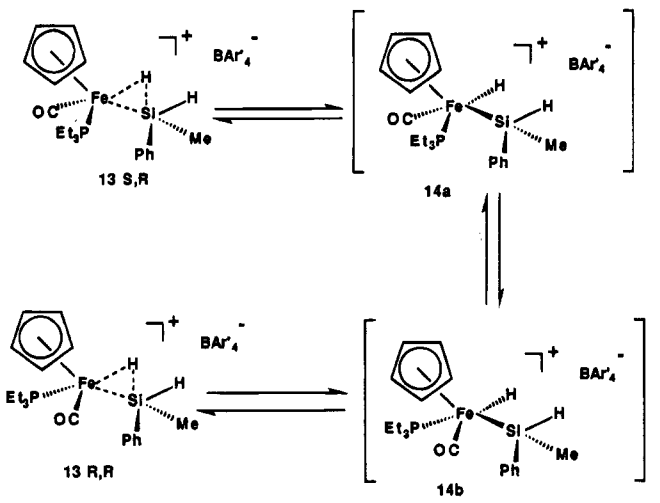

corresponding to the major diastereomer while a smaller, very broad peak was also observed at −12.8 ppm for the minor diastereomer. Upon warming, the peaks broadened further and merged at about −65 °C (Figure 2). Upon further warming, the single broad peak sharpened and was observed as a doublet at −13.7 ppm. Once again, this behavior is indicative of diastereomer interconversion (eq 13) and the mechanism is presumed to be the same as that discussed for complex **13**. There is no obvious reason why diastereomer interconversion is more rapid in **15** than in **13**.

In an attempt to further probe the dynamics of this system, the phenylsilane complex, Cp(CO)(PEt$_3$)Fe(H$_3$-SiPh)$^+$, **16**, was examined. This complex should show two diastereotopic terminal Si−H resonances (H_A and H_B) at low temperatures if the stereochemistry at metal is maintained. Complex **16** was generated by the exchange method described above and characterized by

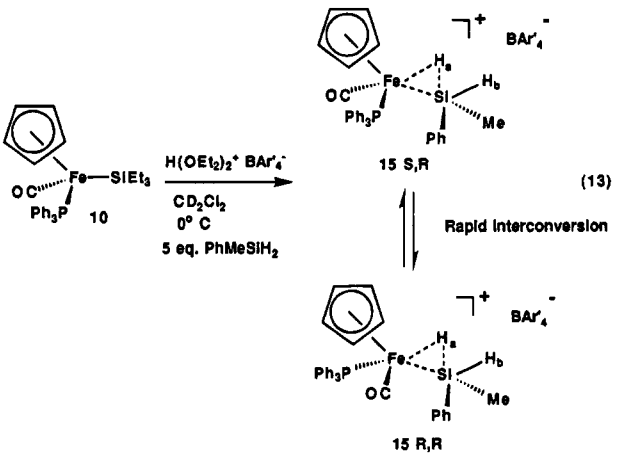

(13)

low-temperature NMR spectroscopy (eq 14). A doublet

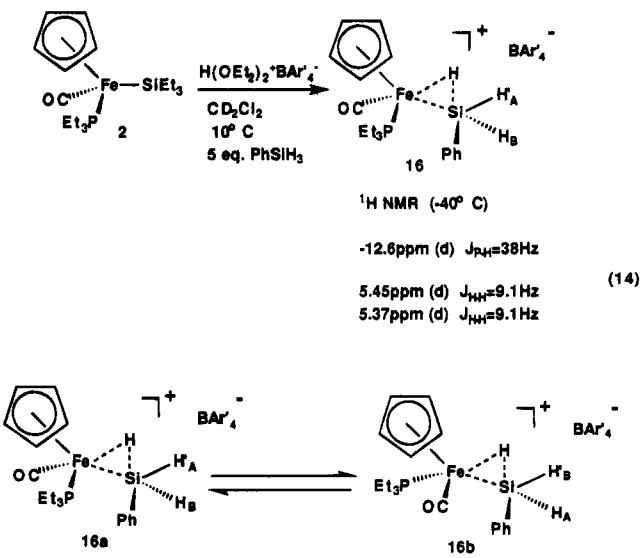

(14)

at −12.6 ppm (J_{PH} = 38 Hz) was observed for the Si−H interacting with the iron center. As expected, H_A and H_B exhibited unique resonances due to the chiral metal center. At −60 °C, two doublets were observed at 5.45 and 5.37 ppm corresponding to these two protons. Upon warming of the sample to 0 °C, the doublets appeared to broaden somewhat, and at 25 °C, very significant broadening had occurred. Although coalescence was not achieved, the extensive line broadening indicates site exchange of H_A and H_B which can occur through inversion of stereochemistry at the iron center via the mechanism proposed in Scheme 1.

The dynamic processes observed here for **13**, **15**, and **16** are similar to the dynamic behavior observed by Yang in related manganese silyl hydride complexes.[8] For example, a dynamic NMR study of Cp(dmpe)Mn-(H)(SiHPh$_2$) showed that the silyl and hydride ligands interchange. A mechanism in which the Si−H interacting with the metal center and the terminal Si−H rapidly interchange was ruled out by an isotopic labeling experiment which also allowed the elimination of a dissociation−reassociation process. The mechanism proposed as most likely to account for the observed results was based on pseudorotation (eq 15) which exchanges the silyl and hydride ligands and is similar to the mechanism proposed for our system in Scheme 1.

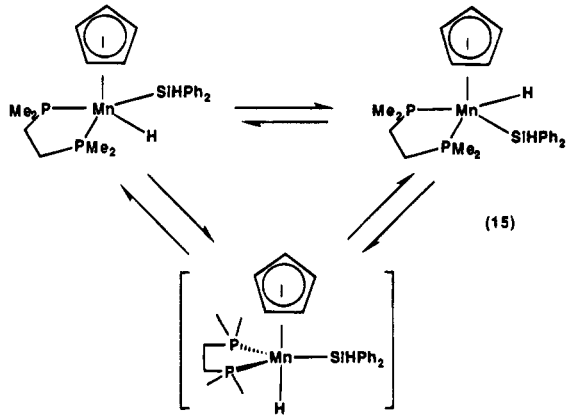

A process involving formation of the η^2-silane complex followed by rotation and readdition to form the silyl hydride complex could not be ruled out by Yang to account for the dynamics in the manganese systems. Such a rotation in the cationic iron species studied here does not result in interchange of diastereomers and thus cannot account for the dynamic behavior of **13** and **15**. Thus, our observations support the operation of the Yang pseudorotation mechanism in both systems.

Summary

A general method has been developed for the generation of cationic iron η^2-silane complexes, $Cp(CO)(L)Fe(HSiR_3)^+$, which are stabilized through the use of the noncoordinating counterion BAr'_4^- ($Ar' = (CF_3)_2C_6H_3$). These species are easily formed by displacement of H_2 from the cationic η^2-H_2 complex by free silane. In both the H_2 and silane complexes, the binding mode of the ligand to the metal has been determined to be nonclassical. Diastereomeric iron silane complexes have been generated which exhibit dynamic behavior that results from interconversion of the diastereomers. An intramolecular mechanism involving scrambling of stereochemistry via a pseudorotation process in an Fe(IV) silyl hydride intermediate was invoked. Support for this mechanism was obtained through observation of interconversion of diastereotopic Si–H resonances in a phenylsilane complex.

Experimental Section

General Methods. Unless otherwise noted, all reactions were carried out under a dry, N_2 atmosphere using Schlenk techniques or a Vacuum Atmospheres drybox. Methylene chloride was distilled from P_2O_5 prior to use. THF, Et_2O, hexanes, and toluene were distilled from sodium–benzophenone ketyl. Solvents used for chromatography were degassed via a N_2 purge for 10 min. Fisher brand alumina (80–200 mesh) was used for chromatography. CD_2Cl_2 was dried on CaH_2 and vacuum transferred to a Kontes flask. C_6D_6 was used as received. Et_3SiH, $MePhSiH_2$, Ph_2SiH_2, and $PhSiH_3$ were purchased from Petrarch or Aldrich and stored over 4 Å molecular sieves. $H(OEt_2)_2^+BAr'_4^-$ [13] was prepared by published methods.

Chemical shifts were referenced to the protonated residue of the deuterated solvents ($CDHCl_2$, δ 5.32 ppm;, C_6HD_5 δ 7.15 ppm). IR spectra were taken in solution using a CaF_2 cell on a Mattson Polaris FT-IR spectrometer. Photolyses were carried out using a reflector flood lamp, GE No. HR100PFL44. Elemental analyses was performed by Oneida Research Services of Whitesboro, NY.

Cp(CO)(PEt$_3$)FeI. A two-necked Schlenk flask was charged with 1.0 g (3.4 mmol) of $Cp(CO)_2FeI$, and this was dissolved in 40 mL of hexanes and 20 mL of toluene. PEt_3 (3 equiv, 10.2 mmol, 1.2 g) was syringed into the reaction vessel, and the Schlenk flask was equipped with a reflux condenser. Photolysis was started while maintaining a constant N_2 purge via a syringe needle. After 20 min, a significant amount of precipitate ($Cp(CO)_2PEt_3Fe^+I^-$) had formed and photolysis was stopped. The green solution exhibited an IR stretching frequency at 1946 cm^{-1} which corresponded to the desired product. This material was transferred via cannula to another flask.

The solid material was redissolved in 40 mL of methylene chloride, and photolysis with an N_2 purge was reinitiated. It was necessary to monitor solvent loss and to add more methylene chloride as needed. After 3 h, the reaction was judged to be complete by IR spectroscopy. Only Cp(CO)(PEt$_3$)FeI was present. All fractions of the product were combined, and solvent was removed in vacuo leaving a green oil. This was then redissolved in diethyl ether and filtered through Celite. Removal of solvent gave 1.3 g (97% yield) of a green powder. Spectroscopic data matched the reported values.[25] ^1H NMR (C_6D_6, 25 °C): δ 4.1 ppm (s, C_5H_5); 1.6–1.4 (broad mult, PCH_2CH_3); 0.8–0.6 (d of t, J_{HH} = 7.5 Hz, PCH_2CH_3). $^{13}C\{^1H\}$ NMR (C_6D_6, 25 °C): δ 221.8 (d, J_{PC} = 32.0 Hz, *C*O); 80.8 ppm (s, C_5H_5); 21.9 (d, J_{PH} = 26 Hz, PCH_2CH_3); 8.5 (s, PCH_2CH_3). ν_{CO} (CH_2Cl_2): 1944 cm^{-1}.

Cp(CO)(PPh$_3$)FeI. A two-necked Schlenk flask was charged with 0.5 g (1.6 mmol) of $Cp(CO)_2FeI$ and 1 equiv (1.6 mmol, 0.42 g) of PPh_3. This was dissolved in 40 mL of methylene chloride, and the Schlenk flask was equipped with a reflux condenser. Photolysis was started while maintaining a constant N_2 purge via a syringe needle. After 0.5 h, the reaction was determined to be complete by IR spectroscopy. The green solution was filtered through an alumina plug, and solvent was removed to give 0.75 g (85% yield) of product as a green powder. Spectroscopic data matched the reported values.[26] ^1H NMR (CD_2Cl_2, 25 °C): δ 7.65–7.5 (mult, 6H, aryl); 7.5–7.35 (m, 9H, aryl); 4.5 ppm (s, C_5H_5). $^{13}C\{^1H\}$ NMR (CD_2Cl_2, 25 °C): δ 221.4 (d, J_{PC} = 32 Hz, *C*O); 136.2 (d, J_{PC} = 44 Hz, C_{ipso}); 133.9 (d, J_{PC} = 10 Hz,); 130.5 (s); 128.5 (d, J_{PC} = 10 Hz); 83.3 (s, C_5H_5). ν_{CO} (CH_2Cl_2: 1952 cm^{-1}.

Cp(CO)(PPh$_3$)FeH. Cp(CO)(PPh_3)FeI (0.33 g, 0.61 mmol) was dissolved to the extent possible in 10 mL of diethyl ether and 20 mL of tetrahydrofuran (it was not completely soluble). The green solution was cooled to −30 °C and 2 equiv (1.2 mmol, 1.2 mL) of lithium aluminum hydride (1.0M in THF) was added. At low temperature, no reaction occurred, but upon being warmed to room temperature, the solution rapidly took on a yellow color. The solution was stirred for 15 more minutes and then recooled to −30 °C. Degassed water was added to quench excess LAH. Diethyl ether (50 mL) was also added. The mixture was shaken in a separatory funnel, and the yellow organic layer was dried on $MgSO_4$. The aqueous layer was washed with two more 40 mL portions of diethyl ether, and these were also dried. The dried ether solution was filtered, and solvent was stripped off giving a yellow oil. This was dissolved in a 2:1 hexanes:Et_2O mixture and loaded onto an alumina column. A yellow band eluted and was collected as a yellow solution. Removal of solvent gave Cp(CO)(PPh_3)FeH as a yellow solid, 0.13 g (52% yield). NMR data matched the reported values.[27] ν_{CO} (Et_2O): 1930 cm^{-1}.

Cp(CO)(PEt$_3$)FeH. Cp(CO)(PEt_3)FeI (0.81 g, 2.1 mmol) was dissolved in 40 mL of diethyl ether and cooled to −40 °C. Lithium aluminum hydride (2 equiv of 1.0 M Et_2O solution, 4.2 mL) was then carefully syringed into the reaction vessel.

(25) Haines, R. J.; Du Preez, A. L.; Marais, T. L. *J. Organomet. Chem.* **1971**, *28*, 405.
(26) Treichel, P. M.; Shubkin, R. L.; Barnett, K. W.; Reichard, D. *Inorg. Chem.* **1966**, *5*, 1177.
(27) Reger, D. L.; Culbertson, E. C. *J. Am. Chem. Soc.* **1976**, *98*, 2789.

Upon warming, the solution slowly changed color from a dark green to a pale yellow. The reaction mixture was then recooled to −20 °C, and degassed water was added to quench any excess LAH. After vigorous stirring, the salts were allowed to settle and the organic layer was transferred into a flask containing $MgSO_4$. The aqueous layer was washed with two more 30 mL portions of diethyl ether, and these were also dried. Upon filtration and solvent removal, 0.33 g (60% yield) of Cp(CO)(PEt$_3$)FeH was obtained as a yellow oil. This material is unstable at room temperature and must be stored in the freezer. ^{1}H NMR (250 MHz, C_6D_6): δ 4.4 ppm (s, C_5H_5); 1.4–1.2, (m, PCH_2CH_3); 1.0–0.8 (m, PCH_2CH_3); −14.1 (d, J_{PH} = 74.8 Hz, Fe-*H*). ^{13}C{^{1}H} NMR (C_6D_6, 25 °C): δ 221.0 ppm (d, J_{PC} = 28 Hz, *C*O); 78.6 (s, C_5H_5); 22.9 (d, J_{PC} = 26 Hz, PCH_2CH_3); 8.2 (s, PCH_2CH_3). ν_{CO} (Et_2O) 1927 cm^{-1}.

Cp(CO)$_2$FeSiEt$_3$. Fp$^-$K$^+$ (1.0 g, 4.6 mmol) was dissolved in 150 mL of THF, and the solution was cooled to −60 °C. Et_3SiCl (1.5 equiv, 1.0 g) was syringed into the reaction mixture, and the solution was allowed to warm. After being stirred overnight, the reaction was judged to be complete by IR spectroscopy. The solution was filtered through Celite to remove salts, and solvent was removed giving a brown oil. This was redissolved in 2-methylbutane and loaded onto an alumina column. A yellow band quickly eluted giving a brown solution. Upon removal of solvent 1.1 g (72% yield) of $FpSiEt_3$ was obtained as a brown oil. Note: This material darkens and converts to unidentifiable products over a relatively short period of time (hours). It is best to use it shortly after preparation. ^{1}H NMR (250 MHz, C_6D_6): δ 4.2 pppm (s, C_5H_5); 1.15–1.05 (t, J_{HH} = 7.3 Hz, CH_3); 0.95–0.85 (q, J_{HH} =7.3 Hz, CH_2). ^{13}C{^{1}H} NMR (250 MHz, C_6D_6): δ 216.3 ppm (s, CO); 83.2 (s, C_5H_5); 12.2 (s, CH_3); 9.4 (s, CH_2). ν_{CO} (THF): 1988, 1932 cm^{-1}.

Cp(CO)(PPh$_3$)FeSiEt$_3$. Cp(CO)$_2$FeSiEt$_3$ (1.0 mmol, 0.3 g) was dissolved in 40 mL of toluene in a Schlenk flask equipped with a reflux condenser. Triphenylphosphine (8 equiv, 8 mmol, 2.1 g) was added, and a nitrogen purge was initiated. The stirring solution was photolyzed with a sun lamp, and progress was monitored by IR spectroscopy.

After 6 h, the reaction was essentially complete. Methyl iodide was added to react with excess phosphine, and after the mixture was stirred for 1 h, significant quantities of the phosphonium salt had precipitated. The solution was filtered to remove salts, and the solvent was pumped off yielding an orange solid. This material was dissolved in 2-methylbutane and loaded onto an alumina column. An orange band stayed near the top of the column as the column was flushed with 2-methylbutane to remove any starting material. The solvent mixture was then changed to 10:1 2-methylbutane:diethyl ether, and the orange band eluted and was collected as a clear orange solution. Solvent was pumped off giving 0.3 g (65% yield) of Cp(CO)(PPh$_3$)FeSiEt$_3$ as an orange solid. ^{1}H NMR (400 MHz, CD_2Cl_2): δ 7.65–7.45 ppm (mult, 6H, aryl); 7.4–7.3 (mult, 9H, aryl); 4.25 (d, J_{PH} = 1.45 Hz, C_5H_5); 0.9 (t, J_{HH} = 7.8 Hz, 9H, $SiCH_2CH_3$); 0.75–0.6 (mult, 3H, $SiCHH'CH_3$); 0.45–0.3 (mult, 3H, $SiCHH'CH_3$). ^{13}C NMR (400 MHz, CD_2Cl_2): δ 221.2 ppm (d, J_{PC} = 29 Hz, CO); 139.4 (d, J_{PC} = 40 Hz, C_{ipso}); 133.8 (d of d, J_{CH} = 160 Hz, J_{PC} = 10 Hz, aryl); 129.5 (d, J_{CH} = 161 Hz, C_{para}); 128.2 (d of d, J_{CH} = 162 Hz, J_{PC} = 9 Hz, aryl); 83.3 (d, J_{CH} = 177 Hz, C_5H_5); 12.2 (t, J_{CH} = 118 Hz, $SiCH_2CH_3$); 10.0 (q, J_{CH} = 123 Hz, $SiCH_2CH_3$). ν_{CO} (Et_2O): 1907 cm^{-1}. Anal. Calcd for $C_{30}H_{35}OPSiFe$: C, 68.44; H, 6.70. Found: C, 68.46; H, 6.63.

Cp(CO)(PEt$_3$)FeSiEt$_3$. Cp(CO)$_2$FeSiEt$_3$ (0.76 g, 2.6 mmol) was dissolved in 40 mL of hexanes in a Schlenk flask equipped with a reflux condenser. Triethylphosphine (8 equiv, 20.8 mmol, 2.4 g) was added to this solution, and a N_2 purge was initiated. The stirring solution was then photolyzed with a sun lamp. After 4 h, the reaction was deemed to be 95% complete by IR spectroscopy, and the photolysis was stopped.

The solution was concentrated and was chromatographed on an alumina column using 2-methylbutane. A yellow band spread quickly across the column, and an initial fraction was collected which contained significant quantities of free triethylphosphine. A second fraction was then collected from the column which upon removal of solvent gave 0.62 g (62% yield) of pure Cp(CO)(PEt$_3$)FeSiEt$_3$ as a yellow solid. ^{1}H NMR (400 MHz, CD_2Cl_2): δ 4.45 ppm (d, J_{PH} = 1.1 Hz, C_5H_5); 1.78–1.64 (m, 3H, $PCH'HCH_3$); 1.58–1.46 (m, 3H, $PCH'HCH_3$); 1.08–0.96 (m, 18H, PCH_2CH_3 and $SiCH_2CH_3$); 0.95–0.84 (m, 3H, $SiCH'HCH_3$); 0.77–0.64 (m, 3H, $SiCH'HCH_3$). ^{13}C{^{1}H} NMR (400 MHz, CD_2Cl_2): δ 221.3 ppm (d, J_{PC} = 29.0 Hz, CO); 80.8 (s, C_5H_5); 22.3 (d, J_{PC} = 25 Hz, PCH_2CH_3); 13.0 (s, $SiCH_2CH_3$); 10.0 (s, $SiCH_2CH_3$); 8.1 (d, J_{PC} = 3 Hz, PCH_2CH_3). ν_{CO} (2-methylbutane): 1909 cm^{-1}. Anal. Calcd for $C_{18}H_{35}OPSiFe$: C, 56.55, H, 9.23. Found: C, 55.76, H, 9.19.

Generation and Spectroscopic Characterization of η^2-H_2 Complexes. Cp(CO)(PEt$_3$)Fe(H$_2$)$^+$BAr′$_4^-$. Cp(CO)(PEt$_3$)FeH (9 mg, 0.05 mmol) was transferred to an NMR tube under a N_2 atmosphere. The tube was cooled to −78 °C, and 0.6 mL of CD_2Cl_2 was added. $H(OEt_2)_2^+BAr'_4^-$ (51 mg, 0.05 mmol) was dissolved in 0.2 mL of CD_2Cl_2, and this was syringed into the NMR tube. The tube was quickly inverted to ensure complete mixing and introduced to the NMR probe which was precooled to −80 °C. The H_2 complex was stable to about 10 °C at which point loss of H_2 gas was observed. ^{1}H NMR (400 MHz, 0 °C, CD_2Cl_2): δ 7.8–7.6 ppm (broad s, aryl, 8H); 7.6–7.5 (broad s, aryl, 4H); 5.0 (s, C_5H_5); 2.0–1.7 (m, PCH_2CH_3); 1.1–1.0 (m, PCH_2CH_3); −11.8 (broad, Fe(H_2)). ^{13}C{^{1}H} NMR (400 MHz, 0 °C, CD_2Cl_2): δ 211 ppm (d, J_{PC} = 26 Hz, CO); 162 (q, J_{BC} = 50 Hz, ipso C); 135 (s, ortho C); 129 (q, J_{CF} = 30 Hz, meta C); 125 (q, J_{CF} = 271 Hz, CF_3); 118 (s, para C); 83.0 (s, C_5H_5); 21.5 (d, J_{PH} = 31 Hz, PCH_2CH_3); 7.9 (d, J_{PH} = 3.0 Hz, PCH_2CH_3).

Cp(CO)(PEt$_3$)Fe(HD)$^+$BAr′$_4^-$. Cp(CO)(PEt$_3$)FeI (0.4 g, 1.6 mmol) was dissolved in 40 mL of Et_2O and cannulated into a −78 °C solution of LAD (0.1 g, 7.3 mmol). The solution was allowed to warm to room temperature. It was then recooled to −30 °C and quenched with water. The organic layer was extracted and dried on $MgSO_4$. It was then filtered, and upon removal of solvent, a yellow oil was obtained. ^{1}H NMR spectroscopy showed the product to contain approximately 20% of the protio compound, **3**.

Complex **3**-d_1 (3.7 mg, 0.02 mmol) was weighed into an NMR tube and cooled to −78 °C. It was then dissolved in 0.5 mL of CD_2Cl_2. $H(OEt_2)_2^+BAr'_4^-$ (0.02 mmol, 20 mg) was dissolved in 0.2 mL of CD_2Cl_2 and transferred to the cold NMR tube. The contents were mixed, and a ^{1}H NMR spectrum was obtained at −78 °C. The HD complex was clearly present along with the H_2 complex. ^{1}H NMR (400 MHz, 0 °C, CD_2Cl_2): δ 7.8–7.6 ppm (broad s, aryl, 8H); 7.6–7.5 (broad s, aryl, 4H); 5.0 (s, C_5H_5); 2.0–1.7 (m, PCH_2CH_3); 1.1–1.0 (m, PCH_2CH_3); −11.85 (t of d, J_{HD} = 31.6 Hz, J_{PH} = 4.7 Hz).

Cp(CO)(PEt$_3$)Fe(H$_2$)$^+$ and Cp(CO)(PEt$_3$)Fe(H)$_2^+$. Cp(CO)(PEt$_3$)FeSiEt$_3$ (14.5 mg, 0.04 mmol) and $H(OEt_2)_2^+BAr'_4^-$ (39 mg, 0.04 mmol) were combined in an NMR tube in the drybox. The NMR tube was cooled to −78 °C under N_2, and 0.8 mL of CD_2Cl_2 was added. The tube was quickly inverted to mix the contents. The NMR tube was introduced into the NMR probe at −80 °C, and presumably due to moisture, the silane complex was not observed. Along with the η^2-H_2 complex, which was the minor compound present, the dihydride complex was also observed as the major product. Upon warming, the dihydride complex converted to the H_2 complex which at −20 °C was the exclusive product. When the sample was recooled, the H_2 complex did not reconvert to the dihydride complex. ^{1}H NMR (400 MHz, −80 °C, CD_2Cl_2): δ 5.1 ppm (s, C_5H_5); 1.8–1.6 (mult, PCH_2CH_3); 1.1–1.0 (mult, PCH_2CH_3); −7.9 (d, J_{PH} = 69.7 Hz, Fe(H)$_2$).

Cp(CO)(PPh$_3$)Fe(H$_2$)$^+$. Cp(PPh$_3$)(CO)FeH (15 mg, 0.037 mmol) and $H(OEt_2)_2^+$ BAr'_4^- (37 mg, 0.037 mmol) were combined in an NMR tube in the drybox. At −78 °C, under N_2, 0.7 mL of CD_2Cl_2 was added. The H_2 complex was observed by low-temperature NMR spectroscopy. Alternatively, protonation of Cp(PPh$_3$)(CO)FeSiEt$_3$ with HBAr′$_4$ in the presence

of Et_3SiH (10 equiv, 37 mmol, 0.04 g) also led to exclusive formation of the H_2 complex via hydrolysis of the initially formed silane complex. ^1H NMR (400 MHz, −80 °C, CD_2Cl_2): δ 7.8−7.1 ppm (mult, aryl); 5.0 (s, C_5H_5); −10.8 (broad, Fe-(H_2)).

Cp(CO)(PPh$_3$)Fe(HD)$^+$. Cp(PPh$_3$)(CO)FeSiEt$_3$ (16 mg, 0.03 mmol) and H(OEt$_2$)$_2^+$BAr′$_4^-$ (31 mg, 0.03 mmol) were combined in an NMR tube in the drybox. After the NMR tube was cooled to −78 °C, 0.7 mL of CD_2Cl_2 was added and the solution was mixed while keeping it cold. Spectroscopic observation at low temperature showed only the η^2-H_2 complex. The tube was removed from the probe and 1 equiv (1.2 mL, 0.03 mmol) of CD_3OD was added. Subsequent NMR observation showed that isotopic scrambling had occurred giving the H_2 and HD complexes. ^1H NMR (400 MHz, 0 °C, CD_2Cl_2): δ 7.8−7.1 ppm (mult, aryl); 5.0 (s, C_5H_5); −10.85 ppm (t of d, J_{HD} = 31.7 Hz, J_{PH} = 4.6 Hz, Fe−H−D).

Generation and Spectroscopic Characterization of η^2-Silane Complexes. Cp(CO)(PEt$_3$)Fe(HSiEt$_3$)$^+$BAr′$_4^-$. In the drybox, an NMR tube was charged with 10.3 mg (0.027 mmol) of Cp(CO)(PEt$_3$)FeSiEt$_3$ and 27.4 mg (0.027 mmol) of H(OEt$_2$)$_2^+$BAr′$_4^-$. The tube was capped with a septum and removed from the drybox. The sample was kept under N_2 via a syringe needle and cooled to −78 °C. CD_2Cl_2 (0.8 mL) was added via syringe. The needle was removed, and the septa was wrapped in parafilm and covered with grease. The tube was quickly inverted to ensure complete mixing and then returned to the cold bath.

The tube was introduced into a cold NMR probe (−80 °C), and the Et_3SiH complex was observed if very little trace water was present. The η^2-H_2 complex was also present along with the dihyride complex as discussed earlier.

After initial observation, the tube was removed from the probe and returned to the cold bath. Under a N_2 atmosphere, 5 equiv of Et_3SiH (0.14 mmol, 0.015 g) was added. The tube was shaken and warmed to room temperature briefly. H_2 was observed to evolve. The tube was then reintroduced to the cooled NMR probe, and now the Et_3SiH complex was the only species present. This complex was relatively stable at room temperature in the presence of excess Et_3SiH. ^1H NMR (400 MHz, 25 °C, CD_2Cl_2): δ 7.8−7.7 ppm (broad s, aryl, 8H); 7.6−7.5 (broad s, 4 H, aryl); 4.9 (s, C_5H_5); 2.0−1.8 (mult, PCH_2-CH_3); 1.2−1.1 (mult, PCH_2CH_3); 1.0−0.9 (mult, partially obscured, $SiCH_2CH_3$); 0.7−0.6 (mult, partially obscured, $SiCH_2$-CH_3); −16.6 (d, J_{PH} = 34 Hz, J_{SiH} = 62.4 Hz, Fe−H−Si). $^{13}C\{^1H\}$ NMR (400 MHz, 25 °C, CD_2Cl_2): δ 213.5 ppm (d, J_{PC} = 27 Hz, CO); 162 (q, J_{BC} = 50 Hz, ipso C); 135 (s, ortho C); 129 (q, J_{CF} = 26 Hz, meta C); 125 (q, J_{CF} = 271 Hz, CF_3); 118 (s, para C); 84.5 (s, C_5H_5); 22.9 (d, J_{PH} = 30 Hz, PCH_2CH_3); 11.2 (s, $SiCH_2CH_3$); 9.0 (s, $SiCH_2CH_3$) 8.2 (s, PCH_2CH_3).

Cp(CO)(PPh$_3$)Fe(HSiEt$_3$)$^+$BAr′$_4^-$. An NMR tube was charged with Cp(CO)(PPh$_3$)FeSiEt$_3$ (0.03 mmol, 14.1 mg) and H(OEt$_2$)$_2^+$BAr′$_4^-$ (0.03 mmol, 27 mg), and this was dissolved with 0.7 mL of CD_2Cl_2 at −78 °C. At −80 °C, ^1H NMR spectroscopy indicated that only the η^2-H_2 complex was present. Et_3SiH (10 equiv, 0.3 mmol, 0.035 g) was added to the NMR tube, and it was allowed to warm. H_2 gas was observed to evolve. NMR spectroscopy showed only the silane complex to be present. This complex is slightly less stable than the PEt$_3$ complex. ^1H NMR (400 MHz, 25°C, CD_2Cl_2): δ 7.9−7.2 ppm (mult, aryl); 4.8 (d, J_{PH} = 1.7 Hz, C_5H_5); 1.2−1.0 (mult, partially obscured, $SiCH_2CH_3$); 0.8−0.6 (mult, partially obscured, $SiCH_2CH_3$); −18.1 (d, J_{PH} = 29 Hz, J_{SiH} = 67.3 Hz, Fe−H−Si).

Cp(CO)(PEt$_3$)Fe(H$_2$SiPh$_2$)$^+$BAr′$_4^-$. An NMR tube was charged with Cp(CO)(PEt$_3$)FeSiEt$_3$ (0.04 mmol, 14.5 mg) and H(OEt$_2$)$_2^+$BAr′$_4^-$ (0.04 mmol, 38 mg). The solids were cooled to −78 °C, and 0.7 mL of CD_2Cl_2 was syringed into the tube. After initial observation at low temperature of the Et_3SiH complex and the H_2 complex, Ph_2SiH_2 (0.2 mmol, 0.035 g) was syringed into the NMR tube and it was allowed to warm to room temperature briefly. H_2 gas was observed to evolve. Low-temperature NMR observation (−20 °C) showed only the Ph_2-SiH_2 complex to be present . ^1H NMR (400 MHz, −20 °C, CD_2Cl_2): δ 7.9−7.2 ppm (mult, aryl); 4.9 (d, J_{PH} = 1.2 Hz, C_5H_5); 6.5 (s, J_{SiH} = 232 Hz, Si−H); 1.7−1.5 (mult, PCH_2CH_3); 1.1−1.0 (mult, PCH_2CH_3); −12.9 (d, J_{PH} = 36.4 Hz, J_{SiH} = 58 Hz, Fe−H−Si).

Cp(CO)(PEt$_3$)Fe(H$_2$SiMePh)$^+$BAr′$_4^-$. An NMR tube was charged with Cp(CO)(PEt$_3$)FeSiEt$_3$ (0.03 mmol, 12.4 mg) and H(OEt$_2$)$_2^+$BAr′$_4^-$ (0.03 mmol, 32.9 mg). The solids were cooled to −78 °C, and 0.7 mL of CD_2Cl_2 was syringed into the tube. $PhMeSiH_2$ (10 equiv, 0.3 mmol, 0.04 g) was syringed into the solution, and the sample was treated in the same manner as the diphenylsilane complex. At temperatures less than −20 °C, two well-resolved diastereomers were observed in a 1:1 ratio which interconverted upon warming. The rate of interconversion was determined to be 310 s^{-1} at −3 °C by line shape analysis at the coalescence point ($k = \pi(\nu_A - \nu_X)/\sqrt{2}$). This corresponds to a $\Delta G^‡$ of 12.6 kcal/mol. ^1H NMR (400 MHz, −40 °C, CD_2Cl_2): δ 7.9−7.1 (mult, aryl); 4.9 (d, J_{PH} = 1.0 Hz, C_5H_5); 4.8 (d, J_{PH} = 1.4 Hz, C_5H_5); 6.0 (q, J_{HH} = 3.6 Hz, Si−H); 5.7 (q, J_{HH} = 3.6 Hz, Si−H); 1.7−1.4 (mult, PCH_2CH_3); 1.1−0.9 (mult, PCH_2CH_3); the $SiCH_3$ resonances are obscured; −13.1 (d, J_{PH} = 36 Hz, Fe−H−Si); −13.4 (d, J_{PH} = 36 Hz, Fe−H−Si).

Cp(CO)(PPh$_3$)Fe(H$_2$SiMePh)$^+$BAr′$_4^-$. An NMR tube was charged with Cp(CO)(PPh$_3$)FeSiEt$_3$ (0.03 mmol, 16 mg) and H(OEt$_2$)$_2^+$BAr′$_4^-$ (0.03 mmol, 31 mg). The solids were cooled to −78 °C, and 0.7 mL of CD_2Cl_2 was syringed into the tube. $PhMeSiH_2$ (3 equiv, 0.09 mmol, 0.01 g) was added, and the sample was treated as discussed above and observed by low-temperature NMR spectroscopy. At −105 °C, two diastereomers were observed in a 3:1 ratio. At higher temperatures these lines broadened and coalesced around −80 °C, and upon further warming the resonance sharpened. ^1H NMR (400 MHz, 0 °C, CD_2Cl_2): δ 7.9−7.1 ppm (mult, aryl); 4.7 (s, C_5H_5); 5.4 (s, Si−H); the $SiCH_3$ resonances are obscured; −14.0 (d, J_{PH} = 40.4 Hz, Fe−H−Si).

Cp(CO)(PEt$_3$)Fe(H$_3$SiPh)$^+$BAr′$_4^-$. An NMR tube was charged with Cp(CO)(PEt$_3$)FeSiEt$_3$ (0.027 mmol, 10.5 mg) and H(OEt$_2$)$_2^+$BAr′$_4^-$ (0.027 mmol, 27.4 mg). The solids were cooled to −78 °C, and 0.7 mL of CD_2Cl_2 was syringed into the tube. $PhSiH_3$ (5 equiv, 0.14 mmol, 0.015 g) was added to the solution. At −60 °C, the two diastereotopic terminal Si−H protons exhibit separate NMR resonances. Upon warming, these resonance broaden substantially and converge. ^1H NMR (400 MHz,-40 °C, CD_2Cl_2): δ 7.9−7.3 ppm (mult, aryl); 5.0 (s, C_5H_5); 5.45 (d, J_{HH} = 9.0 Hz, Si*H*H′); 5.37 (d, J_{HH} = 9.0 Hz, SiH*H*′); 1.8−1.6 (mult, PCH_2CH_3); 1.1−1.0 (mult, PCH_2CH_3); −12.6 (d, J_{PH} = 38 Hz, Fe−H−Si).

Acknowledgment. We thank the National Institutes of Health (Grant No. GM 28938) for support of this work.

OM950354C

Reactions of a Disilene and a Silylene with Cyclopentadiene, Furan, and Thiophene: [2 + 4]-Cycloadditions versus Chalcogen Abstraction[1]

Edwin Kroke, Manfred Weidenbruch,* Wolfgang Saak, and Siegfried Pohl

Fachbereich Chemie der Universität Oldenburg, Carl-von-Ossietzky-Strasse 9-11, D-26111 Oldenburg, Germany

Heinrich Marsmann

Fachbereich Chemie der Universität–Gesamthochschule Paderborn, Warburger Strasse 100, D-33095 Paderborn, Germany

Received June 19, 1995[⊗]

Tetra-*tert*-butyldisilene (**2**) and di-*tert*-butylsilylene (**3**), generated by photolysis of hexa-*tert*-butylcyclotrisilane (**1**), react with the double bonds of cyclopentadiene (**4**) to provide the [2 + 4]- and [1 + 2]-cycloaddition products 2,2,3,3-tetra-*tert*-butyl-2,3-disilabicyclo[2.2.1]-cyclohept-5-ene (**5**) and 6,6-di-*tert*-butyl-6-silabicyclo[3.1.0]hex-2-ene (**6**), which are isolated together with two rearranged ene reaction products of **4** with **2**. Photolysis of **1** in the presence of furan yields *exo*-3,3,6,6,7,7-hexa-*tert*-butyl-3,6,7-trisila-8-oxatricyclo[3.2.1.$0^{2,4}$]-octane (**9**) in addition to 1,1-di-*tert*-butyl-2,2-dimethyl-1-silacyclopropane (**10**) and *trans*-1,1,2,3,3,4-hexa-*tert*-butylcyclotetrasilane. Reaction of **2** and **3** with thiophene gives the sulfur abstraction product 1,1,2,2-tetra-*tert*-butyl-1,2-disilathiirane (**13**) together with 2,2,6,6-tetra-*tert*-butyl-2,6-disilabicyclo[3.1.0]hex-3-ene, 1,1,2,2-tetra-*tert*-butyl-1,2-disilacyclohexa-3,5-diene, and **10**. The structures of **5**, **9**, and **13** were determined by X-ray crystallography.

Introduction

Similar to the C=C double bonds of alkenes, the Si=Si double bonds of disilenes participate in a wide variety of addition and cycloaddition reactions; this behavior has been summarized in several review articles.[2] The differences between the two types of double bonds arise first from the higher lying 3pπ level of the disilenes in comparison to the 2pπ level of the alkenes and second from the appreciably smaller HOMO–LUMO separation in molecules containing the Si=Si structural unit.[2a] The stable or marginally stable disilenes thus behave like highly strained, electron-rich olefins and accordingly should preferentially react with electron-poor reaction partners.[3,4] This hypothesis is supported by their smooth additions to α-diketones, 1,4-diazabutadienes, and α-ketoimines, which can all be considered Diels–Alder reactions with inverse electron demand.[5] On the other hand, [2 + 4]-cycloadditions of the stable tetraaryldisilenes to the double bonds of conjugated 1,3-dienes as well as [2 + 2]-cycloadditions to alkenes are still unknown.[2] Indications that such systems are indeed able to react with disilenes were provided by the recently reported isolation of a [4 + 2]-cycloadduct from the reaction of 3,4,5-trimethoxybenzoyl chloride with tetramesityldisilene in which the oxygen atom and a ring carbon atom reacted with the Si=Si double bond.[6]

Scheme 1 [a]

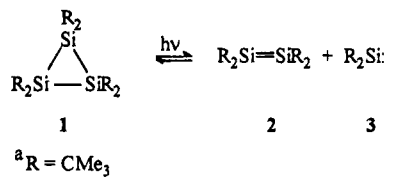

[a] R = CMe_3.

The marginally stable tetraalkyldisilene **2** is somewhat more reactive than the stable tetraaryldisilenes. Previously the only known example of a [2 + 4]-cycloaddition to a diene was the reaction of **2** with 2,3-dimethylbutadiene, from which the corresponding Diels–Alder adduct was isolated in 4% yield together with the ene adduct and an additional compound.[7] Very recently, the [2 + 2]-cycloaddition of a disilene to an alkene was achieved for the first time by the reaction of **2** with *o*-methylstyrene.[8]

Currently, the best approach to **2** is the photolysis of the cyclotrisilane **2**, which gives the desired species together with the silylene **3** (Scheme 1).[10] We now

[⊗] Abstract published in *Advance ACS Abstracts,* October 15, 1995.

(1) Silicon Compounds with Strong Intramolecular Steric Interactions. 58. Part 57: Weidenbruch, M.; Pellmann, A.; Pohl, S.; Saak, W.; Marsmann, H. *Chem. Ber.* **1995**, *128*, 935.

(2) Reviews: (a) West, R. *Angew. Chem.* **1987**, *99*, 1231; *Angew. Chem., Int. Ed. Engl.* **1987**, *26*, 1202; (b) Raabe, G.; Michl, J. In *The Chemistry of Organic Silicon Compounds Part 2*; Patai, S., Rappoport, Z., Eds.; Wiley: Chichester, UK, 1989; p 1015; (c) Tsumuraya, T.; Batcheller, S. A.; Masamune, S. *Angew. Chem.* **1991**, *103*, 916; *Angew. Chem., Int. Ed. Engl.* **1991**, *30*, 902; (d) Weidenbruch, M. *Coord. Chem. Rev.* **1994**, *130*, 275.

(3) Boger, D. L.; Weinreb, S. M. *Hetero Diels-Alder Methodology*; Academic Press: San Diego, 1987.

(4) Schöller, W. W. *J. Chem. Soc., Chem. Commun.* **1985**, 334.

(5) For example: (a) Boudjouk, P.; Han, B.-H.; Anderson, K. R. *J. Am. Chem. Soc.* **1982**, *104*, 4992; (b) Weidenbruch, M.; Schäfer, A.; Thom, K.-L. *Z. Naturforsch.* **1983**, *38B*, 1695; (c) Weidenbruch, M.; Lesch, A.; Peters, K.; von Schnering, H. G. *J. Organomet. Chem.* **1991**, *407*, 31; (d) Weidenbruch, M.; Piel, H.; Lesch, A.; Peters, K.; von Schnering, H. G. *J. Organomet. Chem.* **1993**, *454*, 35.

(6) Fanta, A. D.; Belzner, J.; Powell, J. R.; West, R. *Organometallics* **1993**, *12*, 2177.

(7) Masamune, S.; Murakami, S.; Tobita, H. *Organometallics* **1983**, *2*, 1464.

(8) Weidenbruch, M.; Kroke, E.; Marsmann, H.; Pohl, S.; Saak, W. *J. Chem. Soc., Chem. Commun.* **1994**, 1233.

(9) Jutzi, P. *Chem. Rev.* **1986**, *86*, 983.

(10) Weidenbruch, M. *Chem. Rev.* **1995**, *95*, 1479.

0276-7333/95/2314-5695$09.00/0

Scheme 2 [a]

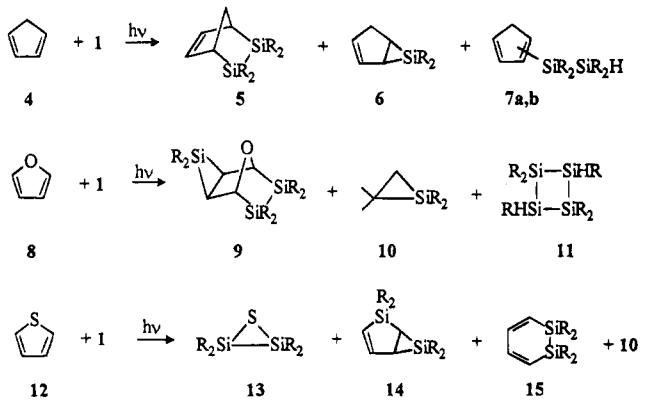

[a] R = CMe_3.

report on the photolysis of **1** in the presence of the five-membered-ring compounds cyclopentadiene, furan, and thiophene. All three reactions give rise to a different spectrum of products.

Results and Discussion

A solution of **1** was irradiated in the presence of an excess of cyclopentadiene **(4)** until the pale yellow color of **1** had disappeared. Subsequent short-path distillation first resulted in the isolation of the bicyclic compound **6** in high yield. This product is formed by the [2 + 1]-cycloaddition of **3** to one of the double bonds in **4**; its constitution was confirmed by a complete NMR analysis as well as mass and IR spectral data. Of particular diagnostic value is the position of the ^{29}Si NMR signal at −55.99 ppm in the region typical for siliranes (Scheme 2).

Whereas the reaction of **3** with **4** gave rise to a major product, the reaction of the disilene **2** with **4** furnished a mixture of products that were difficult to separate. After various methods such as fractional crystallization or HPLC separation had failed, we finally obtained gas chromatographic evidence for the presence of at least three products in an approximate ratio of 2:5:3 in the distillation residue. Three fractions were then separated by preparative GC; of these, only the smallest mass fration (no. 1 ca. 20%) has not yet been identified unequivocally. The main fraction (no. 2, ca. 50%) was shown to be a 1:1 mixture of the positionally isomeric cyclopentadienyldisilanes **7a,b** by complete NMR analysis, including the two-dimensional techniques $^1H,^1H$-COSY, $^1H,^{13}C$-COLOC (correlation spectroscopy for long-range couplings), and $^1H,^{29}Si$-INEPT. Although conclusive evidence for the mechanism of formation of **7a,b** is still lacking, the most plausible explanation involves a primary ene reaction between **2** and **4** and subsequent 1,*n*-sigmatropic hydrogen shifts within the cyclopentadienyl ring, which finally lead to the constitutionally isomeric compounds **7a,b**. Silatropic rearrangements are also possible, but would appear to be improbable on account of the bulkiness of the *tetra-tert*-butyldisilanyl group. The spatial requirements of this group are also held to be responsible for the fact that the disilanyl group undergoes bonding exclusively to the olefinic carbon atoms of the cyclopentadienyl ring.[9]

The last fraction was found to be the [4 + 2]-cycloadduct of **4** to **2**. Since the preparative GC separation furnished only small amounts of **5**, the structural elucidation is based on an X-ray crystallographic analysis of the colorless crystals of **5** (Figure 1, Tables 1 and 2).

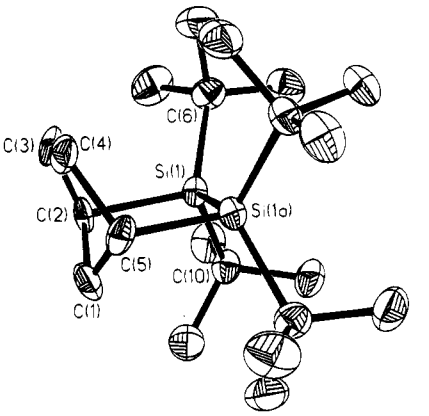

Figure 1. ORTEP drawing and labeling scheme for **5** (hydrogen atoms omitted). Ellipsoids are drawn at 30% probability.

Table 1. Atomic Parameters (×10⁴) and Equivalent Isotropic Displacement Coefficients ($pm^2 \times 10^{-1}$) for 5

	x	*y*	*z*	U_{eq}
Si	695(1)	1935(1)	2363(1)	40(1)
C(1)	48(8)	−802(19)	3174(10)	63(4)
C(2)	607(10)	−554(12)	2483(12)	39(4)
C(3)	226(9)	−1197(15)	1718(11)	66(3)
C(4)	−472(5)	−1168(10)	1852(6)	57(2)
C(5)	−726(12)	−345(25)	2722(14)	47(4)
C(6)	1082(2)	2679(4)	1251(2)	58(1)
C(7)	552(2)	2323(5)	491(2)	80(1)
C(8)	1826(2)	1766(5)	1031(2)	93(1)
C(9)	1213(2)	4557(4)	1244(2)	77(1)
C(10)	1365(1)	2801(3)	3260(2)	53(1)
C(11)	1370(2)	1707(4)	4071(2)	73(1)
C(12)	2206(2)	2882(4)	2986(2)	75(1)
C(13)	1120(2)	4563(3)	3505(2)	68(1)

Table 2. Selected Bond Lengths (pm) and Angles (deg) for 5

Si(1)−Si(1a)	248.49(14)	Si(1)−C(6)	195.5(3)
Si(1)−C(10)	195.9(3)		
C(6)−Si(1)−C(10)	108.05(12)	C(7)−Si(1)−Si(1a)	84.8(5)
C(5)−Si(1)−Si(1a)	92.4(5)	C(2)−C(1)−C(5)	102.7(14)

The most conspicuous feature of this, the first X-ray crystallographic characterization of a Diels−Alder product from a stable or marginally stable disilene, is the Si−Si bond length of 248.5 pm; this is markedly longer than the normal single bond length of 234 pm and also exceeds the bond lengths in other tetra-*tert*-butyldisilanes.[10] However, the Si−Si bond lengths in **1** (251.1 pm)[11] and in hexa-*tert*-butyldisilane (269.7 pm)[12] are appreciably longer; the latter being the longest Si−Si bond length measured to date in a discrete molecule.

The reaction of furan **(8)** with **2** generated by photolysis of **1** is also presumably initiated by a [4 + 2]-cycloaddition. In contrast to the corresponding reaction of **2** with **4**, however, the newly formed double bond in the present case is so activated that an additional [2 + 1]-addition of **3** follows to furnish the tricyclic compound **9** as the final product (Scheme 2). The ^{29}Si

(11) Schäfer, A.; Weidenbruch, M.; Peters, K.; von Schnering, H. G. *Angew. Chem.* **1984**, *96*, 311; *Angew. Chem., Int. Ed. Engl.* **1984**, *23*, 302.

(12) Wiberg, N.; Schuster, H.; Simon, A.; Peters, K. *Angew. Chem.* **1986**, *98*, 100; *Angew. Chem., Int. Ed. Engl.* **1986**, *25*, 79.

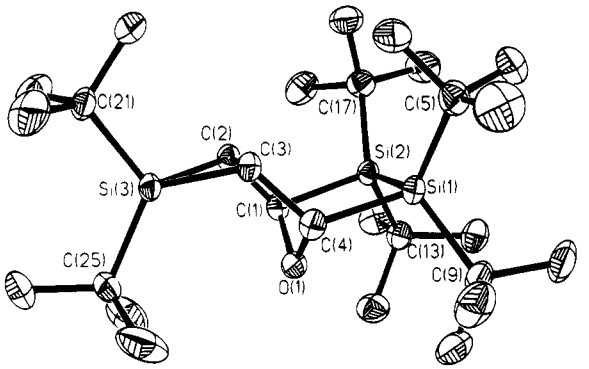

Figure 2. ORTEP drawing and labeling scheme for **9** (hydrogen atoms omitted). Ellipsoids are drawn at 30% probability.

Table 3. Atomic Parameters ($\times 10^4$) and Equivalent Isotropic Displacement Coefficients ($pm^2 \times 10^{-1}$) for 9

	x	y	z	U_{eq}
Si(1)	−2306(1)	652(1)	696(1)	39(1)
Si(2)	−3149(1)	2239(1)	1286(1)	36(1)
Si(3)	429(1)	2899(1)	1614(1)	38(1)
O(1)	−1437(1)	1179(2)	1765(1)	42(1)
C(1)	−1836(2)	2422(3)	1726(1)	39(1)
C(2)	−990(2)	3111(3)	1429(1)	39(1)
C(3)	−433(2)	2110(3)	1050(1)	41(1)
C(4)	−1037(2)	968(3)	1169(1)	41(1)
C(5)	−2289(3)	941(3)	−162(1)	57(1)
C(6)	−3436(3)	1192(4)	−378(2)	85(1)
C(7)	−1893(4)	−95(5)	−537(2)	112(1)
C(8)	−1621(3)	2028(4)	−318(2)	76(1)
C(9)	−2569(3)	−1078(3)	832(2)	54(1)
C(10)	−1632(3)	−1831(3)	642(2)	85(1)
C(11)	−3560(3)	−1528(4)	494(2)	85(1)
C(12)	−2687(3)	−1367(4)	1491(2)	78(1)
C(13)	−4152(2)	1693(3)	1857(1)	50(1)
C(14)	−5000(3)	923(4)	1535(2)	71(1)
C(15)	−4707(3)	2718(4)	2193(2)	71(1)
C(16)	−3606(3)	940(4)	2360(2)	66(1)
C(17)	−3630(2)	3766(3)	930(2)	51(1)
C(18)	−4774(3)	3699(4)	709(2)	79(1)
C(19)	−3497(3)	4768(3)	1413(2)	73(1)
C(20)	−3017(3)	4230(4)	406(2)	67(1)
C(21)	1229(2)	4143(3)	1251(1)	48(1)
C(22)	745(3)	4489(4)	641(2)	79(1)
C(23)	2352(3)	3743(5)	1150(2)	92(2)
C(24)	1253(4)	5275(4)	1640(2)	83(1)
C(25)	963(2)	2165(3)	2341(1)	50(1)
C(26)	156(4)	2304(5)	2823(2)	98(2)
C(27)	1946(4)	2756(5)	2600(2)	123(2)
C(28)	1111(5)	827(4)	2249(2)	113(2)

Table 4. Selected Bond Lengths (pm) and Angles (deg) for 9

Si(1)−Si(2)	246.97(11)	Si(1)−C(9)	196.2(3)
Si(2)−C(13)	195.1(3)	Si(1)−C(4)	193.8(3)
Si(2)−C(1)	192.7(3)	Si(3)−C(2)	186.5(3)
Si(3)−C(3)	186.1(3)	C(2)−C(3)	158.2(4)
C(2)−Si(3)−C(3)	50.25(12)	C(2)−C(3)−Si(3)	65.01(14)
C(3)−C(2)−Si(3)	64.74(14)	C(1)−O−C(4)	103.3(2)

NMR spectrum of **9** shows two signals of differing intensities at 14.65 and −46.67 ppm; the upfield signal again being in the region typical for siliranes. The structure of this double cycloaddition product has been confirmed by an X-ray crystallographic analysis of the colorless crystals of **9** (Figure 2, Tables 3 and 4).

Similar to **5**, the Si−Si bond is markedly stretched (247.0 pm), as are the Si−C bonds, in comparison to normal single bond lengths. On the other hand, the acute C−Si−C angle in the silirane part of **9** corresponds well with the angles observed at the silicon atoms in other siliranes substituted by both sterically unpretentious[13] and sterically demanding groups.[14]

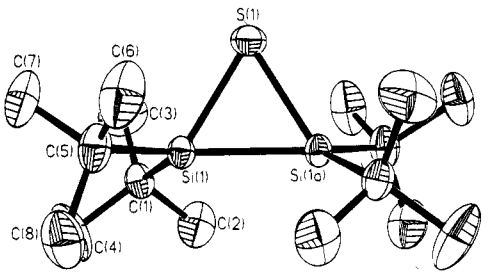

Figure 3. ORTEP drawing and labeling scheme for **13** (hydrogen atoms omitted). Ellipsoids are drawn at 30% probability.

Table 5. Atomic Parameters ($\times 10^4$) and Equivalent Isotropic Displacement Coefficients for 13

	x	y	z	U_{eq}
S	5000	633(1)	2500	64(1)
Si	5052(1)	−2324(1)	3090(1)	44(1)
C(1)	4095(1)	−3108(4)	3376(1)	54(1)
C(2)	3525(2)	−4447(5)	2797(2)	93(1)
C(3)	3641(2)	−1124(6)	3498(2)	103(1)
C(4)	4289(2)	−4558(7)	4017(2)	119(2)
C(5)	6053(1)	−2218(5)	3871(1)	68(1)
C(6)	6749(2)	−1001(7)	3692(2)	106(1)
C(7)	5863(2)	−916(6)	4460(1)	97(1)
C(8)	6355(2)	−4465(6)	4137(2)	101(1)

The low yield of **9** indicates that the [4 + 2]-cycloaddition of **2** to **8** proceeds only very slowly. This assumption is in harmony with the concomitant formation of the cyclotetrasilane **11**, which is often observed when suitable reaction partners are available for **3** but not for **2**.[10] Compound **11** was first detected in the ultrasound-induced dehalogenation of di-*tert*-butyldichlorosilane.[15] The formation of the silirane **10** also supports the impeded reaction between **2** and **8** since irradiation of **1** in the presence of less reactive trapping agents does lead to partial elimination of isobutene,[16] which would then experience a [2 + 1]-cycloaddition of **3** to its double bond to furnish the isolated product **10**. The constitution of this silirane has again been confirmed by a complete NMR analysis.

In comparison to the photolysis of **1** in the presence of **4** or **8**, the corresponding reaction with thiophene (**12**) follows a completely different course. Here, the disilene **2** abstracts the sulfur atom from **12** to furnish the 1,2-disilathiirane **13** as the major product (Scheme 2). Since the structure of only one tetraaryl-substituted disilathiirane had been reported previously,[17] we have also characterized **13** by X-ray crystallography (Figure 3, Tables 5 and 6).

The Si−Si bond in **13** is extraordinarily short (230.5 pm) and remains under those of the corresponding

(13) For example: Delker, G. L.; Wang, Y.; Stucky, G. D.; Lambert, R. L.; Haas, C. K.; Seyferth, D. *J. Am. Chem. Soc.* **1976**, *98*, 1779.
(14) For example: (a) Ando, W.; Fujita, M.; Yoshida, H.; Sekiguchi, A. *J. Am. Chem. Soc.* **1988**, *110*, 3310; (b) Pae, D. H.; Xiao, M.; Chiang, M. Y.; Gaspar, P. P. *J. Am. Chem. Soc.* **1991**, *113*, 1281.
(15) Boudjouk, P.; Samaraweera, K.; Sooriyakumaran, R.; Chrisciel, K.; Anderson, K. R. *Angew. Chem.* **1988**, *100*, 1406; *Angew. Chem., Int. Ed. Engl.* **1988**, *27*, 1355.
(16) Weidenbruch, M.; Brand-Roth, B.; Pohl, S.; Saak, W. *J. Organomet. Chem.* **1989**, *379*, 217.
(17) West, R.; DeYoung, D. J.; Haller, K. J. *J. Am. Chem. Soc.* **1985**, *107*, 4942.

Table 6. Selected Bond Lengths (pm) and Angles (deg) for 13

Si(1)–Si(1a)	230.49(11)	Si(1)–S	217.13(9)
Si(1)–C(1)	194.1(2)	Si(1)–C(5)	194.4(2)
Si(1)–S–Si(1a)	64.11(4)	C(1)–Si(1)–C(5)	112.84(10)
C(1)–Si(1)–Si(1a)	118.71(8)	C(5)–Si(1)–Si(1a)	127.12(8)

compounds **5** and **9** by about 17 pm. Although the bond length in tetramesityldisilathiirane is even shorter (228.9 pm),[17] it must be remembered that the lengths of the Si–Si bonds in tetra-*tert*-butyldisilanes are, on average, 10 pm greater than those in tetramesityldisilanes; hence, the compression of this bond in **13** is even more pronounced than that in the tetramesityl derivative. Compound **13** thus can be considered to provide further support for the assumption that the disiliranes occupy a position in the continuum between the classical three-membered ring structure and that of a π-complex of the respective disilene with the heteroatom.[2] A further indication of the predominance of the π-complex form is given by the almost planar orientation about each silicon atom of the quaternary carbon atoms and the respective other silicon atoms (angular sum = 358.7°).

The first 1,2-disilathiiranes were obtained by the addition of sulfur to tetramesityl- and 1,2-di-*tert*-butyldimesityldisilenes.[17] It was recently demonstrated that the reaction of cyclohexene sulfide with tetramesityldisilene also gave rise to the disilathiirane.[18] Although this reaction does have a formal similarity to the sulfur abstraction reaction described in the present work, the differences are, in fact, considerable: in the case of cyclohexene sulfide, a thermally stable olefin is formed, whereas in the present case cyclobutadiene—which is not known in the free form—would be the corresponding product. As illustrated by the isolation of the bicyclic compound **14** and the 1,2-disilacyclohexadiene **15**, sulfur abstraction from **12** is only possible when the simultaneous insertion of the silylene **3** or the disilene **2** into the hole resulting from the sulfur elimination occurs. It is interesting to note, however, that not the silole expected from silylene insertion but rather the bicyclic product **14** is isolated; compound **14** presumably arises from an additional [2 + 1]-cycloaddition of a further silylene molecule to the double bond of the silole.[19] The constitutions of both products **14** and **15** were elucidated by comprehensive spectroscopic analyses. Thus, the ^{29}Si NMR spectrum of **15** reveals only one signal at 22.44 ppm, whereas that of **14** contains a singlet for the silicon atom in the five-membered ring (34.38 ppm), as well as a singlet for the silicon atom in the three-membered ring (−36.32 ppm).

The results of the present work are worthy of note in that the replacement of the CH_2 group in **4** by an oxygen or a sulfur atom gives rise to widely different product patterns. It thus will be of interest to subject other five-membered heterocyclic compounds of this type to photolysis in the presence of **1**.

Experimental Section

General Procedures. All reactions were carried out in oven-dried glassware under an atmosphere of dry argon. Photolyses were carried out at −25 °C by using a high-pressure mercury immersion lamp (Heraeus TQ 150).

The ^{1}H and ^{13}C NMR spectra were obtained on a Bruker AM 300 spectrometer using C_6D_6 as solvent. The ^{29}Si and two-dimensional NMR spectra were recorded on a Bruker AMX 300 spectrometer. IR spectra were taken on a Bio-Rad FTS-7 spectrometer. Mass spectra were recorded on a Varian-MAT 212 or Finnigan-MAT 95 instrument. Elemental analyses were performed by Analytische Laboratorien (D-51647 Gummersbach, Germany).

The cyclotrisilane **1** was prepared according to the literature procedure.[11]

Photolysis of 1 in the Presence of Cyclopentadiene (4). A solution of **1** (0.505 g, 1.18 mmol) and **4** (0.802 g, 12.1 mmol) in *n*-hexane (100 mL) was irradiated for 2 h. After this time, the reaction was shown to be complete by the disappearance of the pale yellow color of **1**. The solvent was removed by vacuum destillation and the residue was transfered to a molecular still. Distillation at 60–70 °C/1 mbar yielded 0.206 g (84%) of **6**.

The distillation residue (0.6 g) was redissolved in *n*-hexane (15 mL) and filtered through a 2 cm layer of silica gel. According to GC analysis, the residue contained three fractions in a ratio of 20:50:30%. A part of the residue was separated by preparative GC. While the minor fraction 1 (20%) could not be identified unambiguously, the main fraction 2 (50%) was shown to consist of a 1:1 mixture of the cyclopentadienyldisilanes **7a,b**. Fraction 3 (30%) was identified as the [4 + 2]-cycloadduct **5**.

2,2,3,3-Tetra-*tert*-butyl-2,3-disilabicyclo[2.2.1]hept-5-ene (5): colorless crystals; mp 200–204 °C; ^{1}H NMR δ 1.18 (s, 18H), 1.25 (s, 18H), 2.05–2.14, 2.20–2.28 (m, 4H, 2 × C*H*, CH_2), 5.91 (s, 2H, *H*C=C); ^{13}C NMR δ 22.77 (C_q), 31.45 (CH_2), 32.77 (C_p), 33.20 (C_p), 42.33 (*C*H), 133.16 (*C*=C) (C_p and C_q refer to primary and quaternary carbon atoms); mass spectrum (CI, isobutane) *m*/*z* 350 (M^+, 17); HRMS calcd for $C_{21}H_{42}Si_2$ 350.2825, found 350.2826.

6,6-Di-*tert*-butyl-6-silabicyclo[3.1.0]hex-2-ene (6): colorless liquid; ^{1}H NMR δ 0.99 (s, 9H), 1.12 (s, 9H), 1.58 (pseudo-t of d, 1H, ^3J = 19 Hz, ^3J = 2 Hz, CH_2CH), 2.15 (m, 1H), 2.77 (m, 1H), 3.07 (m, 1H), 5.38 (m, 1H), 6.88 (m, 1H); ^{13}C NMR δ 17.32 (*C*H), 18.99 (C_q), 22.25 (C_q), 29.88 (C_p), 30.03 (*C*H), 31.48 (C_p), 35.39 (CH_2), 127.67 (*C*=C), 131.59 (C=*C*); ^{29}Si NMR δ −55.99; IR (KBr) ν 1653, 1597 (C=C) cm^{-1}; mass spectrum (EI, 70 eV) *m*/*z* 208 (M^+, 12), 151 (M^+ − *t*Bu, 88); HRMS calcd for $C_{13}H_{24}Si$ 208.1647, found 208.1632.

1,1,2,2-Tetra-*tert*-butyl-1-(cyclopenta-1,3-dienyl)disilane and 1,1,2,2-tetra-*tert*-butyl-1-(cyclopenta-2,4-dienyl-)disilane (7a,b): colorless oil; ^{1}H NMR (C_6D_6, 500 MHz) δ 1.17 (s, 9H), 1.211 (s, 9H), 1.214 (s, 9H), 1.26 (s, 9H), 2.75 (pseudo-q, 2H, ^3J = ^4J = 1.5 Hz, CH_2), 3.12 (2H, AB system, CH_2), 4.03 (s, 1H, Si*H*), 4.10 (s, 1H, Si*H*), 6.32 (dq, 1H, ^3J = 5.1 Hz, ^4J = 1.5 Hz, C*H*=C), 6.54 (2H, AB system, C*H*=C), 6.77 (pseudo-quint, 1H, ^3J = ^4J = 1.5 Hz, C*H*=C), 6.92 (dq, 1H, ^3J = 5.1 Hz, ^4J = 1.5 Hz, C*H*=C), 7.07 (quint, 1H, ^3J = ^4J = 1.5 Hz, C*H*=C); ^{13}C NMR δ 21.71 (C_q), 21.80 (C_q), 22.14 (C_q), 31.45 (C_p), 32.68 (C_p), 32.74 (C_p), 43.40 (CH_2), 48.88 (CH_2), 131.34 (=*C*H), 132.99 (=*C*H), 137.35 (=*C*H), 138.94 (=*C*H), 144.02 (C_q), 144.09 (C_q), 144.17 (=*C*H), 144.95 (=*C*H); ^{29}Si NMR δ −0.50 (s, *Si*H), −1.03 (s), −1.22 (s, *Si*H), −2.01 (s); IR (KBr) ν 2070 (m, SiH), 1765, 1719 (C=C) cm^{-1}; mass spectrum (CI, isobutane) *m*/*z* 351 (MH^+, 100); HRMS calcd for $C_{21}H_{42}Si_2$ 350.2825, found 350.2732.

Photolysis of 1 in the Presence of Furan (8). A solution of **1** (0.608 g, 1.42 mmol) and **8** (0.832 g, 13.7 mmol) in *n*-hexane (80 mL) was irradiated at −25 °C for 4 h. After this time, the pale yellow color of **1** had disappeared. The solvent was removed by evaporation and the residue was transferred to a molecular still. Distillation at 36 °C/1.5 mbar yielded 0.082 g (29%) of **10** as a colorless liquid. At 50–70 °C/0.01 mbar, 0.070 g of a second colorless fraction was obtained. It consisted of several compounds that could not be identified.

(18) Mangette, J. E.; Powell, D. R.; West, R. *J. Chem. Soc., Chem. Commun.* **1993**, 1384.

(19) One referee pointed out that compound **13** may also arise from a [2 + 4]-cycloaddition of **2** to **12** followed by sulfur abstraction and that compound **14** is formed by photochemically induced rearrangement[21] of **15**. In fact, these possibilities cannot be excluded.

Table 7. Crystallographic Data

	5	9	13
empirical formula	$C_{21}H_{42}Si_2$	$C_{28}H_{58}OSi_3$	$C_{16}H_{36}SSi_2$
fw	350.73	495.01	316.69
a (pm)	1762.4(4)	1284.1(1)	1703.2(3)
b (pm)	809.2(2)	1102.4(1)	622.3(1)
c (pm)	1555.3(2)	2243.2(1)	1992.8(4)
β (deg)		92.43(1)	107.03(3)
V (pm^3)	2281(9) × 10^6	3127.6(4) × 10^6	2019.6(6) × 10^6
Z	4	4	4
D(calcd) (g cm^{-3})	1.050	1.036	1.042
cryst syst	orthorhombic	monoclinic	monoclinic
space group	*Pbcn*	$P2_1/n$	$C2/c$
cryst size (mm)	0.46 × 0.38 × 0.30	0.61 × 0.45 × 0.45	1.15 × 0.49 × 0.49
data collection mode	$\omega-2\theta$ scan	ω scan	$\omega-2\theta$ scan
$2\theta_{max}$ (deg)	50	50	50
no. of rfls measd	1956	5843	1848
no. of unique rfls	1956	5575	1784
no. of rfls [$I > 2\sigma(I)$]	1287	3749	1437
GOF (F^2)	1.003	1.039	1.034
R, R_{w2} [$I > 2\sigma(I)$]	0.048, 0.107	0.056, 0.128	0.043, 0.107
residual electron density	267	354	311
e nm^{-3}	−169	−201	−156

The solid distillation residue was dissolved in *n*-hexane, filtered, and concentrated to 5 mL. Cooling at −25 °C for 1 week afforded 0.068 g (10%) of colorless crystals of **9**. Crystallization of the residue (from the mother liquor after the separation of **9**) from a minimum amount of *n*-hexane at −50 °C provided 0.064 g (20%) of colorless crystals of **11**.

***exo*-3,3,6,6,7,7-Hexa-*tert*-butyl-3,6,7-trisila-8-oxatricyclo-[3.2.1.0^{2,4}]octane (9):** mp 202−206 °C (dec); ^{1}H NMR δ 1.09 (s, 9H), 1.33 (s, 18H), 1.34 (s, 27H), 1.83 (s, 2H), 4.64 (s, 2H); ^{13}C NMR δ 19.23, 21.71, 22.24, 22.68, 23.01, 30.32, 31.04, 32.58, 33.25, 73.65; ^{29}Si NMR δ −46.75, 14.65; mass spectrum (CI, isobutane) m/z 496 (MH^+, 7), 438 ($M^+ - t$Bu, 16), 353 (100). Anal. Calcd for $C_{28}H_{58}OSi_3$: C, 67.94; H, 11.81. Found: C, 67.71; H, 11.74.

1,1-Di-*tert*-butyl-2,2-dimethyl-1-silacyclopropane (10): ^{1}H NMR δ 0.54 (s, 2H, CH_2), 1.08 (s, impurity, <5%), 1.13 (s, 18H), 1.43 (s, 6H); ^{13}C NMR δ 14.89 (CH_2), 17.49 (C_q), 20.10 (C_q, *t*Bu), 28.81 (CH_3), 31.61 (C_p, *t*Bu); ^{29}Si NMR δ −40.54; mass spectrum (EI, 70 eV) m/z 198 (M^+, 6), 141 ($M^+ - t$Bu, 24); HRMS calcd for $C_{13}H_{24}Si$ 198.1804, found 198.1801.

***trans*-1,1,2,3,3,4-Hexa-*tert*-butylcyclotetrasilane (11):** [15] mp 325−328 °C (dec); ^{1}H NMR δ 1.26 (s, 18H), 1.32 (s, 36H), 4.20 (s, 2H, Si*H*); ^{13}C NMR δ 21.23, 23.49, 32.24, 32.89; IR (KBr) ν 2066 (SiH) cm^{-1}; mass spectrum (CI, isobutane) m/z 456 (M^+, 60), 399 ($M^+ - t$Bu, 100). Anal. Calcd for $C_{24}H_{56}Si_4$: C, 63.07; H, 12.35. Found: C, 62.83; H, 12.17.

Photolysis of 1 in the Presence of Thiophene (12). A solution of **1** (0.572 g, 1.34 mmol) and **12** (0.899 g, 10.7 mmol) in *n*-hexane (80 mL) was irradiated until the pale yellow color of **1** had disappeared (200 min). Evaporation of the reaction mixture under vacuum to 10 mL and cooling to −50 °C yielded 0.206 g (49%) of colorless crystals of **13**. The mother liquor was transferred to a molecular still and distilled under reduced pressure. At 35 °C/1.5 mbar, 0.088 g of a colorless liquid was collected and shown by NMR spectroscopy to consist of an approximately 1:1 mixture of **10** (0.042 g, 16%) and **15** (0.046 g, 10%). Continued distillation at approximately 50 °C/0.01 mbar provided 0.076 g (8%) of colorless **14**.

1,1,2,2-Tetra-*tert*-butyl-1,2-disilathiirane (13): mp 120−124 °C (dec); ^{1}H NMR δ 1.25 (s); ^{13}C NMR δ 23.53 (C_q), 31.79 (C_p); ^{29}Si NMR δ −4.59 (s); mass spectrum (field desorption) m/z 317 (M^+, 100). Anal. Calcd for $C_{16}H_{36}SSi_2$: C, 60.68; H, 11.46; S, 10.13. Found: C, 60.53; H, 11.32; S, 10.03.

2,2,6,6-Tetra-*tert*-butyl-2,6-disilabicyclo[3.1.0]hex-3-ene (14): purity 85%; ^{1}H NMR δ 0.25 (d, 1H, ^3J = 8.8 Hz), 1.05 (s, 9H), 1.12 (s, 9H), 1.15 (s, 9H), 1.24 (s, 9H), 2.15 (dt, 1H, ^3J = 8.8 Hz, $^3J = {}^4J$ = 2.1 Hz), 5.74 (dd, 1H, ^3J = 10 Hz, ^3J = 2.1 Hz), 6.94 (dd, 1H, ^3J = 10 Hz, ^4J = 2.1 Hz); ^{13}C NMR δ 0.66 (Si*C*Si), 19.12 (C_q), 20.18 (C_q), 22.08 (C_q), 22.52 (C_q), 28.02 (C_p), 30.46 (C_p), 31.01 (C_p), 31.45 (C_p), 32.54, 123.47 (=*C*), 153.14 (=*C*); ^{29}Si NMR δ −36.32 (s), 34.38 (s); mass spectrum (CI, isobutane) m/z 337 (MH^+, 100); HRMS calcd for $C_{20}H_{40}Si_2$ 336.2669, found 336.2672.

1,1,2,2-Tetra-*tert*-butyl-1,2-disilacyclohexa-3,5-diene (15). Since this compound was obtained as a 1:1 mixture with **10** (vide supra), the corresponding signals are also present in the spectra. These peaks are omitted from the following list: ^{1}H NMR δ 1.08 (s, 36H), 6.01 (d, broad, 2H, AA′MM′ spin system, ^3J = 12 Hz), 6.90 (d, broad, 2H, ^3J = 12 Hz); ^{13}C NMR δ 18.91 (C_q), 29.08 (C_p), 129.85 (=*C*), 147.43 (=*C*); ^{29}Si NMR δ 22.44 (s); mass spectrum (CI, isobutane) m/z 195 ($M^+ - Si t Bu_2$, 100); HRMS calcd for $C_{20}H_{40}Si_2$ 336.2669, found 336.2671.

Crystallographic Analyses. Crystal data and numerical data of the structure determinations are given in Table 7. The colorless crystals of **5** were grown by slow evaporation of an *n*-hexane solution at 0 °C. The crystals of **9** and **13** were obtained by cooling *n*-hexane solutions to −25 **(9)** or −50 °C **(13)**. In each case, the crystal was mounted in a thin-walled glass capillary. Data collection was performed at room temperature on a Siemens Stoe AED 2 spectrometer using graphite-monochromated Mo Kα radiation.

The structures were solved by direct phase determination using the Siemens SHELXTL PLUS and SHELX 93 program systems[20] and refined by full-matrix least-squares techniques. Hydrogen atoms were placed in calculated positions, and all other atoms were refined anisotropically.

The cyclopentene ring of **5** is disordered around the 2-fold axis, resulting in a C(3)−C(4) bond length between those of double and triple bonds. It was refined in two positions, each with an occupancy factor of 0.5.

Acknowledgment. Financial support of our work from the Volkswagen-Stiftung, the Deutsche Forschungsgemeinschaft, and the Fonds der Chemischen Industrie is gratefully acknowledged.

Supporting Information Available: Tables of crystal data, atomic coordinates for H atoms, bond lengths, bond angles, and anisotropic displacement coefficients for **5**, **9**, and **13** (19 pages). Ordering information is given on any current masthead page.

OM950473S

(20) *SHELXTL PLUS*, Siemens Analytical X-RAY Instruments, 1989. Sheldrick, G. M. *SHELXL-93*, Program for the Refinements of Structures, Universität Göttingen, 1993.

(21) Nakadaira, Y.; Kanouchi, S.; Sakurai, H. *J. Am. Chem. Soc.* **1974**, *96*, 5623.

Digermylplatinum(II) Organometallic Rings $L_2PtGe(Me_2)EGeMe_2$ [E = N-, O, S, $(\eta$-$C_5H_4)_2Fe$]

J. Barrau,* G. Rima, V. Cassano, and J. Satgé

Laboratoire de chimie des Organominéraux, URA 477 du CNRS, Université Paul Sabatier, 118 route de Narbonne, 31062 Toulouse Cedex, France

Received February 21, 1995[⊗]

The synthesis, reactivity, and characterization of the digermylplatinum(II) linear complexes $(ClMe_2Ge)_2Pt(PPh_3)_2$ (**1**) and $(ClMe_2Ge)_2Pt$(diphos) (**2**) and cyclic complexes (diphos)$PtGe(Me_2)EGeMe_2$ [E = S (**3**), -NPh (**4**), $(\eta^5$-$C_5H_4)Fe(\eta^5$-$C_5H_4)$ (**5**), O (**6**)] are reported. The chemistry of **2**–**6** is illustrated through their reactions with phenylacetylene and N-methyltriazolinedione. Complexes **3** and **6** give double germylation of these unsaturated systems, while **2**, by reaction with triazolinedione, gives the monogermylated complex $Me_2(Cl)GePt(Cl)$diphos and the dimer of the germylated heterocycle $Me_2GeNC(O)N(Me)C(O)N$.

Introduction

There recently has been a great interest in the use of transition-metal complexes to catalyze the formation and cleavage of metal 14–metal 14 bonds.[1] In continuation of our studies on cyclic silyl- or germyliron, -ruthenium, -dicobalt, and -platinum complexes,[2,3] we have explored the potential of new three-, four-, and five-membered cyclic germanium–transition-metal compounds in the context of (i) new germanium–transition-metal chemistry and (ii) stabilization of strained cyclic, transient divalent, or unsaturated germanium–transition-metal compounds. In this area the chemistry of silyl–transition-metal complexes[4–10] is more advanced than that of germyl–transition-metal complexes.

We report here the details of the synthesis and characterization of new digermylplatinum(II) four-membered cyclic compounds of type $L_2PtGe(Me_2)EGeMe_2$ [E = N-, O, S, $(\eta^5$-$C_5H_4)Fe(\eta^5$-$C_5H_4)$].

Results and Discussion

For these syntheses, treatment of bis(chlorogermyl) derivatives with alkali-metal reagents, the classic route to germanium-containing heterocycles with Ge–E–Ge linkages, was applied to a *cis*-bis(chlorogermyl)platinum complex (eq 1).

$$\begin{aligned} &cis\text{-}ClMe_2GePt(L_2)GeMe_2Cl \quad + \\ &M_2E = Na_2S,\ PhNLi_2,\ (\eta\text{-}C_5H_4Li)_2Fe \end{aligned}$$

$$M_2E \xrightarrow{-2MCl} L_2PtGe(Me_2)EGeMe_2 \quad (1)$$

1. *cis*-Bis(chlorogermyl)platinum Complexes. When 1,2-dichlorotetramethyldigermane in benzene was treated with the platinum complex $Pt(C_2H_4)(PPh_3)_2$, a selective oxidative addition of the germanium–germanium bond gave a mixture of *cis*- and *trans*-bis(chlorogermyl)platinum complexes, **1** (eq 2). When the solution

$$Pt(C_2H_4)(PPh_3)_2 + ClMe_2GeGeMe_2Cl \xrightarrow[-C_2H_4]{C_6H_6} \underset{\mathbf{1}}{trans,cis\text{-}(ClMe_2Ge)_2Pt(PPh_3)_2} \quad (2)$$

was 0.05 M in platinum, the *trans/cis* ratio was 95/5. When the solution was more concentrated [0.2 M in Pt], the ratio was 80/20.

From dilute solution *cis* complex **1** was isolated by crystallization as yellow crystals. When these were dissolved in CD_2Cl_2, rapid isomerization occurred to give, at room temperature, a 90/10 *cis/trans* mixture after 30 min and a 70/30 equilibrium mixture after 3 h; this ratio did not change after several hours.

Treatment of the *cis* and *trans* complexes with 1,2-bis(diphenylphosphino)ethane (diphos) produced the *cis* complex **2** (eq 3). The latter was characterized by mass

trans, cis-$(ClMe_2Ge)_2Pt(PPh_3)_2$ + $Ph_2PCH_2CH_2PPh_2$

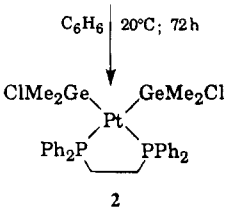

(3)

2

spectroscopy and NMR analyses.

[⊗] Abstract published in *Advance ACS Abstracts,* September 15, 1995.

(1) (a) Yamashita, H.; Tanaka, M.; Goto, M. *Organometallics* **1992,** *11,* 3227. (b) Pannell, K. H.; Cervantes, J.; Parkanyi, L.; Cervantes Lee, F. *Organometallics* **1990,** *9,* 859. (c) Pannell, K. H.; Brun, M. C.; Sharma, H.; Jones, K.; Sharma, S. *Organometallics* **1994,** *13(4),* 1075. (d) Finckh, W.; Tang, B. Z.; Lough, A.; Manners, I. *Organometallics* **1992,** *11,* 2904. (e) Ishikawa, M.; Naka, A.; Okazaki, S.; Sakamoto, H. *Organometallics* **1993,** *12,* 87 and references therein.

(2) Barrau, J. *Heteroat. Chem.* **1991,** *2(6),* 601.

(3) Barrau, J.; Rima, G.; Cassano, V.; Satgé, J. *Inorg. Chim. Acta* **1992,** *198–200,* 461.

(4) Belluco, V.; Croatto, V.; Uguagliati, P.; Pietropaolo, R. *Inorg. Chem.* **1967,** *6,* 718.

(5) Zybill, C.; West, R. *J. Chem. Soc., Chem. Comm.* **1986,** 8571.

(6) Campion, B. K.; Heyn, R. H.; Tilley, T. D. *J. Am. Chem. Soc.* **1988,** *110,* 7558.

(7) Pham, E. K.; West, R. *J. Am. Chem. Soc.* **1989,** *111,* 7667.

(8) Koloski, T. S.; Carroll, P. J.; Berry, D. H. *J. Am. Chem. Soc.* **1990,** *112,* 6405.

(9) Pham, E. K.; West, R. *Organometallics* **1990,** *9,* 1517.

(10) Berry, D. H.; Chey, J.; Zipin, H. S.; Carroll, P. J. *J. Am. Chem. Soc.* **1990,** *112,* 452; *Tetrahedron* **1991,** *10,* 1189.

0276-7333/95/2314-5700$09.00/0

Scheme 1

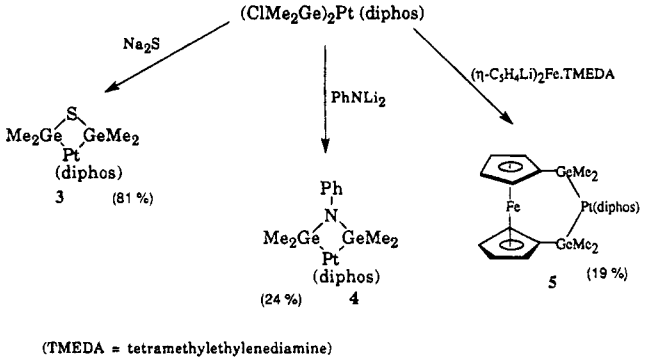

(TMEDA = tetramethylethylenediamine)

These bis(chlorogermyl)platinum complexes are stable at room temperature but decompose when heated. A study of the thermal decomposition of a mixture of *cis,trans*-(chlorogermyl)platinum complexes **1** showed that at 120 °C a complex mixture of chlorogermanium derivatives and metallic platinum is produced (eq 4).

$$cis,trans\text{-}(ClMe_2Ge)_2Pt(PPh_3)_2 \xrightarrow[-\,[Pt]]{120^\circ C;\ C_6H_6} \begin{array}{l} Me_2ClGeGeClMe_2\ (12\%) + Me_3GeGeMe_2Cl\ (5\%) \\ + Me_2ClGePh\ (60\%) + Me_2GeCl_2\ (14\%) \\ + (Me_2GeO)_3\ (\text{traces}) \end{array} \quad (4)$$

No trace of the monogermylated platinum complex $ClMe_2GePt(PPh_3)_2Cl$ or the dimethylgermylene-derived products was observed. Thus, this decomposition is different from that observed by Tanaka[11] for the analogous complex $(ClMe_2Ge)_2Pt(PEt_3)_2$. The difference must be due to the difference in the phosphino ligands, triethylphosphine in Tanaka's case and triphenylphosphine in ours. It is also noteworthy that the Ge–Cl bond of Me_2GeCl_2 oxidatively adds to the Pt(0) complex $Pt(PEt_3)_3$[11] but not to $Pt(PPh_3)_2(C_2H_4)$.

2. (diphos)PtGe(Me$_2$)EGeMe$_2$. The action of a dichlorodigermanium compound with a dialkali derivative, the classic route to germyl sulfides, amines, and ferrocenophanes, was used in further conversions of *cis*-bis(chlorodimethylgermyl)platinum complex **2**.

These cyclization reactions were carried out at room temperature, except for the case where E = NPh, and the expected complexes were isolated in variable yield depending on the nature of the dialkali derivative (Scheme 1).

Reactions of **3**–**5** with diverse reagents have been studied (Scheme 2). Bromine and iodomethane, as expected, cleave the platinum–germanium bond to give platinum complexes and the corresponding bis(bromodimethylgermyl) and bis(trimethylgermyl) sulfides (in the case of E = S). These cleavages probably proceed *via* octahedral platinum(IV) intermediates.[12]

Hydrolysis of the Ge–N bond of **4** afforded the four-membered digermoxane **6**.

Scheme 2

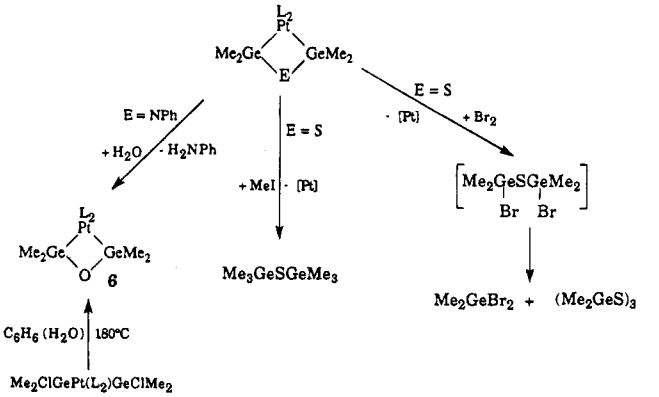

Scheme 3

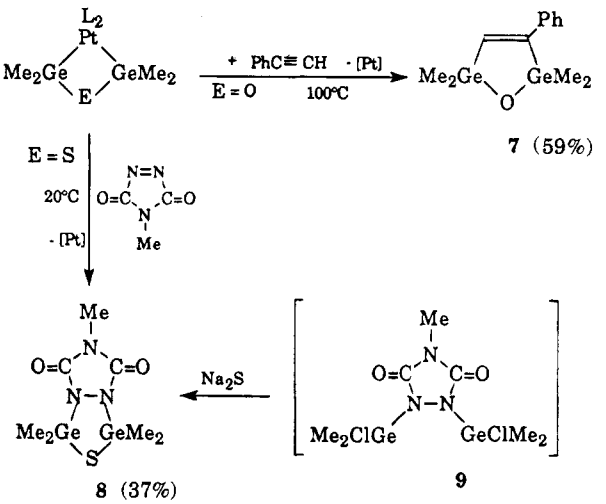

Upon treatment of L$_2$PtGe(Me$_2$)EGeMe$_2$ with triazolinedione and phenylacetylene, double germylation of the unsaturated systems occurred (Scheme 3). For example, the four-membered oxide **6** and sulfide **3** reacted instantaneously at room temperature with *N*-methyltriazolinedione but only at 100 °C with phenylacetylene, producing, in each case, new digermanium heterocycles. These are *formally* adducts of the oxa- or thiadigermirane with phenylacetylene or with *N*-methyltriazolinedione. They were characterized by NMR, mass spectroscopy, and elemental analysis.

To confirm the structure of the thiadiazadigermolane **8**, an alternate synthesis, the direct cyclization of the bis(chlorodimethylgermyl)triazolidine **9** with sodium sulfide was sought. Thus, in order to obtain **9**, the reaction of bis(chlorodimethylgermyl)platinum(II)–diphos with 4-methyl-1,2,4-triazolinedione was carried out. The double germylation of this unsaturated system was not the main path observed for this reaction, the expected dihalodigermanium **9** being obtained in solution, in only low yield, as an unisolated intermediate only. Trapping with Na_2S resulted in formation of **8** in approximately 10% yield.

In effect, somewhat unexpected is the reaction of bis(chlorodimethylgermyl)platinum–diphos) with triazolinedione to form dichlorodimethylgermanium, the tetraazadigerminane **12**, and, an interesting feature, the monogermylated platinum complex **10**.

The formation of dichlorodimethylgermanium and of platinum complex **10** suggests that the reaction pro-

(11) Yamashita, H.; Kobayashi, T.; Tanaka, M.; Samuels, J. A.; Streib, W. E. *Organometallics* **1992**, *11*, 2330.

(12) Hartley, F. R. In *Comprehensive Organometallic Chemistry*; Wilkinson, G., Stone, F. G. A., Abel, E. W., Eds.; Pergamon Press: Oxford, 1982; Vol. 6, Chapter 39, p 471, and references therein.

Scheme 4

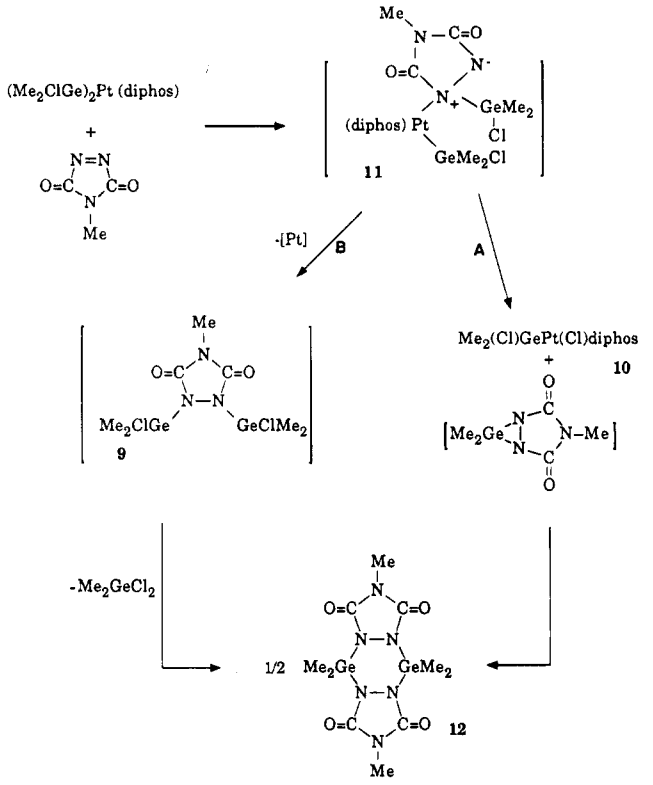

ceeds in a stepwise fashion probably involving a zwitterionic intermediate **11**. The formation of the monogermylated platinum complex **10** is most likely explained by rearrangement of **11** with a shift of chlorine to platinum (path A). The formation of the dichlorodimethylgermane indicates the existence of path B involving extrusion of platinum from **11**, leading to the expected bis(chlorodimethylgermyl)triazolidine which decomposes slowly at room temperature to give dichlorodimethylgermanium and **12** (Scheme 4).

We now are investigating the chemistry of these four-membered heterocycles with various other unsaturated compounds. With judiciously selected ligands, these digermylplatinum(II) organometallic rings should have potential, especially as precursors of species containing germanium in low-coordination states.

Experimental Section

General Procedures. All reactions and manipulations were carried out under an argon or nitrogen atmosphere with the use of Schlenk techniques. The solvents were dried and deoxygenated by standard methods. The ^1H NMR spectra were recorded on an AC Bruker spectrometer operating at 80 MHz; the ^{31}P spectra were measured on a Bruker AC-200 (spectrometer frequency 81.015 Hz). The ^1H chemical shifts are given in ppm (δ) relative to Me_4Si. ^{31}P spectra are externally referenced to 85% H_3PO_4. Gas-phase chromatography was effected on an HP 5890 series II apparatus (capillary column, HP1 methylsilicone gum, 10 m × 0.53 mm × 2.65 μm film thickness) using nitrogen as carrier gas. Infrared spectra were obtained of samples in KBr pellets and were recorded on a Perkin-Elmer 1600 series FTIR instrument. Mass spectra were recorded on a Nermag R10-10H or a Hewlett Packard 5989 instrument operating in the electron impact mode at 70 eV, and samples were contained in glass capillaries under argon or in the chemical ionization mode (CH_4). In all cases, the complex envelope of peaks obtained for polygermanes agreed with the isotopic distribution characteristic of germanium.[13] Melting points were measured on an Electrothermal digital melting point apparatus in sealed glass capillaries. Elemental analyses were performed by the Microanalytic Laboratory of CNRS or ENSCT, Toulouse, France.

$(ClMe_2Ge)_2Pt(PPh_3)_2$, 1. A solution of $Pt(C_2H_4)(PPh_3)_2$ (0.40 g, 0.535 mmol) in C_6H_6 (1.5 mL) was added to a solution of *sym*-dichlorotetramethyldigermane (0.148 g, 0.535 mmol) in C_6H_6 (1 mL). The resulting yellow suspension was stirred for 1 h at room temperature. The resulting mixture was filtered, and the yellow filtrate was washed with C_6H_6 (5 mL). Filtration gave 0.48 g (91%) of **1**; mp 195–200 °C. NMR analyses showed that the *cis/trans* ratio is 20/80. In a second identical experiment, starting from 1.27 g (1.70 mmol) of $Pt(C_2H_4)(PPh_3)_2$ in 10 mL of C_6H_6 and 0.47 g (1.70 mmol) of *sym*-dichlorotetramethyldigermane, the NMR analyses of the resulting solution showed the formation of a mixture of *cis*- and *trans*-**1** with the ratio 5/95. From this mixture, *cis*-**1** crystallized after 12 h as pale yellow crystals. Dissolution of these crystals in CH_2Cl_2 gave a mixture of *cis*- and *trans*-**1** in *cis/trans* ratio 90/10 after 30 min.

trans-**1**: ^1H NMR (C_6H_6) δ 0.98 [s, with two satellites $J(^1H-C-Ge-^{195}Pt)$ = 8.2 Hz, 12H], 6.90 (m, 18H), 7.56 (m, 12H); $^{31}P\{^1H\}$ NMR (C_6H_6) δ 25.17 [s, with two satellites $J(^{195}Pt-^{31}P)$ = 2327 Hz]; IR (KBr) ν(Pt–P) 422, ν(Ge–C) 573, ϱ(Me) 835; MS *m/z* 818 (M^+ – MeCl).

cis-**1**: ^1H NMR (CD_2Cl_2) δ 0.32 [d, $J(^1H-C-Ge-Pt-^{31}P)$ = 1.7 Hz with two satellites (d) $J(^1H-C-Ge-^{195}Pt)$ = 10.1 Hz, 12H]; $^{31}P\{^1H\}$ NMR (CD_2Cl_2) δ 21.31 [s, with two satellites $J(^{195}Pt-^{31}P)$ = 2210 Hz]; IR (KBr) ν(Pt–P) 450, ν(Ge–C) 573, ϱ(Me) 835. Anal. Calcd for $C_{40}H_{42}Cl_2Ge_2P_2Pt$ (mixture of *cis/trans*, 20/80): C, 48.23; H, 4.22. Found: C, 48.40; H, 4.20.

$(ClMe_2Ge)_2Pt(diphos)$, 2. A solution of **1** (1.00 g, 1.00 mmol) and 1,2-bis(diphenylphosphino)ethane (0.40 g, 1.00 mmol) in C_6H_6 (10 mL) was stirred for 3 days at room temperature. The precipitate was filtered and washed twice with C_6H_6 (5 mL). Drying in *vacuo* gave **2** as yellow crystals (0.61 g; 70%). ^1H NMR (CD_2Cl_2) δ 0.57 [d, $J(^1H-C-Ge-Pt-^{31}P)$ = 1.3 Hz, with two satellites (d) $J(^1H-C-Ge-^{195}Pt)$ = 12.0 Hz, 12H], 2.05 [d, $J(^1H-C-^{195}P)$ = 19.9 Hz, with two satellites (dd) $J(^1H-C-P-^{195}Pt)$ = 18.5 Hz, 4H], 7.53 (m, 12H), 7.75 (m, 8H); $^{31}P\{^1H\}$ NMR (CD_2Cl_2) δ 55.36 [s, with two satellites $J(^{195}Pt-^{31}P)$ = 2025 Hz]; IR (KBr) ν(Ge–Pt) 392, ν(Pt–P) 441, ν(Ge–C) 529, ϱ(Me) 830. MS *m/z* 833 (M^+ – Cl). Anal. Calcd for $C_{30}H_{36}Ge_2Cl_2P_2Pt$: C, 41.39; H, 4.14. Found: C, 41.68; H, 4.08.

Thermolysis of 1. A benzene solution (1 mL) of **1** (0.05 g, 0.05 mmol) was heated at 120 °C for 4 h in a degassed sealed tube. Analyses by ^1H NMR spectroscopy, GC (including coinjection with authentic samples), and GCMS showed $Me_2GePhCl$ [^1H NMR (C_6D_6) δ 0.37 (s, 6 H)]; *m/z* 216 (M^+)], Me_2GeCl_2 [^1H NMR (C_6D_6) δ 0.59(s); *m/z* 174 (M^+)], $Me_2(Cl)GeGe(Cl)Me_2$ [^1H NMR (C_6D_6) 0.62(s); *m/z* 276 (M^+)],[14] $Me_3GeGe(Cl)Me_2$ [^1H NMR (C_6D_6) 0.27(s, 9 H), 0.59 (s, 6 H); *m/z* 256 (M^+)][14] to be present in this solution in relative amounts of 60%, 14%, 12%, and 5%, respectively.

$Me_2GeSGe(Me_2)Pt(diphos)$, 3. To a solution of 0.20 g (0.23 mmol) of **2** in 10 mL of CH_2Cl_2 was added 0.60 g (7.6 mmol) of Na_2S. The resulting mixture was sonicated for 12 h. After the remaining Na_2S and resulting NaCl were filtered, CH_2Cl_2 was evaporated. A 5 mL amount of C_6H_6 was added to the residue. Pure **3** was obtained by filtration as a white solid (0.16 g, 81%), mp 243–245 °C (decomp). ^1H NMR (CD_2Cl_2): δ 0.29 [d, $J(^1H-C-Ge-Pt-^{31}P)$ = 1.7 Hz, with two satellites (d) $J(^1H-C-Ge-^{195}Pt)$ = 14.2 Hz, 12H], 2.18 [d, $J(^1H-C-^{31}P)$ = 18.1 Hz, with two satellites (dd) $J(^1H-C-P-^{195}Pt)$ = 15.2 Hz, 4H], 7.47 (m, 12H), 7.73 (m, 8H); $^{31}P\{^1H\}$ NMR (CD_2Cl_2) δ 55.22 [s, with two satellites $J(^{195}Pt-^{31}P)$ =

(13) Carrick, A.; Glockling, F. *J. Chem. Soc. A* **1966**, 623.
(14) Barrau, J.; Rima, G.; El-Amine, M.; Satgé, J. *Synth. React. Inorg. Met.–Org. Chem.* **1988**, *18*, 21.

1868 Hz]. MS *m/z* 832 (M^+). Anal. Calcd for $C_{30}H_{36}Ge_2P_2PtS$: C, 43.33; H, 4.33; S, 3.85. Found: C, 43.16; H, 4.29; S, 3.73.

$Me_2GeN(Ph)Ge(Me_2)Pt$ (diphos), 4. To a solution of 0.110 g (0.118 mmol) of **2** in 5 mL of C_6H_6 was added dropwise a solution of 0.118 mmol of $PhNLi_2$ [prepared from 0.011 g (0.118 mmol) of aniline and 0.15 mL of a solution 1.6 M of butyllithium; addition at −78 °C and heating to reflux for 36 h] in 2 mL of xylene at room temperature. The mixture was heated at reflux for 12 h. After filtration the solvent was removed under vacuum, yielding 0.025 g (24%) of **4** as an orange powder, mp 116−118 °C (decomp). ^1H NMR (CD_2Cl_2) δ 0.30 [d, $J(^1H-C-Ge-Pt-^{31}P)$ = 1.5 Hz, with two satellites (d) $J(^1H-C-Ge-^{195}Pt)$ = 12.6 Hz, 12H], 2.25 [d, $J(^1H-C-^{31}P)$ = 17.7 Hz, with two satellites (dd) $J(^1H-C-P-^{195}Pt)$ = 14.4 Hz, 4H], 7.48 (m, 12H), 7.53 (m, 8H); $^{31}P\{^1H\}$ NMR (CD_2Cl_2) δ 58.10 [s, with two satellites $J(^{195}Pt-^{31}P)$ = 1863 Hz]. MS *m/z* 875 (M^+ − Me). Anal. Calcd for $C_{36}H_{41}Ge_2NP_2Pt$: C, 48.58; H, 4.64; N, 1.57. Found: C, 48.77; H, 1.65; N, 1.38.

$Me_2Ge[(\eta^5\text{-}C_5H_4)Fe(\eta^5\text{-}C_5H_4)]Ge(Me_2)Pt$(diphos), 5. To a suspension of 1,1′-ferrocenylenedilithium·TMEDA[15] (0.06 g, 0.19 mmol) in pentane (5 mL) at −78 °C was added a cooled (−78 °C) solution of **2** (0.17 g, 0.19 mmol) in diethyl ether (3 mL). The reaction mixture was warmed slowly to room temperature and then was stirred overnight. The reaction mixture was filtered, and the solvent was removed. Residual TMEDA was removed under vacuum (25 °C, 0.002 mmHg). The red orange residue was identified as **5** (0.035 g, 19%), mp 166−168 °C (decomp). ^1H NMR (C_6D_6) δ 0.29 [d, $J(^1H-C-Ge-Pt-^{31}P)$ = 1.4 Hz, with two satellites (d) $J(^1H-C-Ge-^{195}Pt)$ = 11.4 Hz, 12H], 2.31 [d, $J(^1H-C-^{31}P)$ = 17.6 Hz, with two satellites (dd) $J(^1H-C-P-^{195}Pt)$ = 14.2 Hz, 4H], 4.14 (m, 4H), 4.24 (m, 4H), 7.45 (m, 12H), 7.62 (m, 8H). Anal. Calcd for $C_{40}H_{44}FeGe_2P_2Pt$: C, 48.88; H, 4.51. Found: C, 49.10; H, 4.39.

$Me_2GeOGe(Me_2)Pt$(diphos), 6. Compound **2** (0.10 g, 0.11 mmol), 1 mL of benzene, and 0.1 mL of water were placed in a sealed tube and heated at 180 °C for 12 h. ^1H NMR, GC, and MS analysis of the reaction mixture showed the presence of **6** and $(Me_2GeO)_3$ in 58% and 37% yield, respectively. ^1H NMR (C_6D_6) δ 1.14 [d, $J(^1H-C-Ge-Pt-^{31}P)$ = 1.3 Hz, with two satellites (d) $J(^1H-C-Ge-^{195}Pt)$ = 7.2 Hz, 12H], 1.93 [d, $J(^1H-C-^{31}P)$ = 20.1 Hz, with two satellites (dd) $J(^1H-C-P-^{195}Pt)$ = 15.1 Hz, 4H], 7.06 (m, 12H), 7.74 (m, 8H); $^{31}P\{^1H\}$ NMR (C_6D_6) δ 46.62 [s, with two satellites $J(^{195}Pt-^{31}P)$ = 1760 Hz]. MS *m/z* 814 (M^+).

Compound **4** (0.012 g, 0.013 mmol) was dissolved in CD_2Cl_2 (0.5 mL) in an NMR tube. The opened NMR tube stood at ambient temperature for a few hours. ^1H NMR, GC, and MS analysis of the reaction mixture after 2 h showed the presence of **6** and $(Me_2GeO)_3$ in 69% and 31% yield, respectively.

Any attempt to obtain pure **6** by addition of pentane was unsuccessful.

Reaction of 3 with Br_2 and MeI. Equimolar amounts of **3** and Br_2 or MeI reacted in the presence of benzene at 20 °C to give the results recorded in Scheme 2. In all cases, after elimination of inorganic platinum products by filtration, the remaining mixtures were analyzed by GC, ^1H NMR, and GCMS.

The known compounds Me_2GeBr_2, $(Me_2GeS)_3$, and $(Me_3Ge)_2S$ were detected in 80% (both Me_2GeBr_2 and $(Me_2GeS)_3$) or 85% yield, respectively (comparisons with authentic samples).

Reaction of 6 with Phenylacetylene. A 0.10 g amount of a mixture of **6** (68%) and $(Me_2GeO)_3$ (27%) and 0.12 g (1 mmol) of phenylacetylene in 1 mL of benzene were heated in a sealed glass tube at 100 °C for 3 h. Analysis by ^1H NMR and GCMS of the resulting mixture showed that the oxide $Me_2GeCH{=}C(Ph)Ge(Me_2)O$, **7**, had been formed in 59% yield (comparison with authentic sample obtained by hydrolysis of $ClMe_2GeC(Ph){=}CHGeMe_2Cl$).[16] ^1H NMR (C_6D_6) δ 0.87 (s, 6H), 1.10 (s, 6H), 6.87 (s, 1H), 7.04−7.35 (m, 5H). MS *m/z* 324 (M^+).

Reaction of 3 with 4-Methyl-1,2,4-triazolinedione. To a solution of **3** (0.10 g, 0.12 mmol) in CH_2Cl_2 (1 mL) was added dropwise 0.014 g (0.12 mmol) of 4-methyl-1,2,4-triazolinedione. After decolorization of the reaction mixture, the platinum products were filtered and the filtrate was evaporated to dryness. The solid residue was treated with 0.2 mL of benzene. Filtration and removal of the solvent under vacuum yielded 0.015 g of $Me_2GeNC(O)N(Me)C(O)NGe(Me_2)S$, **8** (37%) as a yellow powder, mp 154−156 °C. ^1H NMR (C_6D_6) δ 0.54 (s, 12H), 2.90 (s, 3H). MS *m/z* 351 (M^+). Anal. Calcd for $C_7H_{15}Ge_2N_3O_2$: C, 26.41; H, 4.75. Found: C, 26.53; H, 4.57.

Reaction of 2 with 4-Methyl-1,2,4-triazolinedione. A solution of 4-methyl-1,2,4-triazolinedione (0.013 g, 0.115 mmol) in C_6H_6 (1 mL) was added to a solution of **2** (0.10 g, 0.115 mmol). After decolorization of the reaction mixture, the mixture was analyzed by ^1H NMR spectroscopy. Appearance of new signals in the range of $\delta(Me_2Ge)$ at δ 0.26 (d), 0.84 (s), 1.01 (s), and 1.12 (s) were observed, establishing that **10**, **12**, and Me_2GeCl_2 had been formed (comparisons with authentic samples); the signal at δ 1.01 could be consistent with the proposed intermediate structure **9**. After 2 h at room temperature, the resulting mixture was filtered; the white residue was washed with C_6H_6 (1 mL); filtration gave 0.06 g (68%) of **10**. Removal of solvent from the filtrate under vacuum yielded compound **12** as an analytically pure white powder.

Data for **10**: mp 309−312 °C; ^1H NMR (CD_2Cl_2) δ 0.26 [d, $J(^1H-C-Ge-Pt-^{31}P)$ = 0.8 Hz with two satellites (d) $J(^1H-C-Ge-^{195}Pt)$ = 12.6 Hz, 6H], 2.26 [d, $J(^1H-C-^{31}P)$ = 18.9 Hz, with two satellites (dd) $J(^1H-C-P-^{195}Pt)$ = 17.1 Hz, 4H], 7.47 (m, 12H), 7.71 (m, 8H); $^{31}P\{^1H\}$ NMR (CD_2Cl_2) δ 53.10 [s, with two satellites $J(^{195}Pt-^{31}P)$ = 1990 Hz]; MS *m/z* 731 (M^+ − Cl). Anal. Calcd for $C_{28}H_{30}Cl_2GeP_2Pt$: C, 43.82; H, 3.91; Cl, 9.26. Found: C, 43.74; H, 3.86; Cl, 9.20.

For **12**: mp 167−169 °C; ^1H NMR (CD_2Cl_2) δ 0.84 (s, 12H), 2.72 (s, 6H); IR (C_6D_6) ν(CO) 1710, 1670. MS *m/z* 432 (M^+). Anal. Calcd for $C_{10}H_{18}N_6O_4Ge_2$: C, 27.82; H, 4.17; N, 19.48. Found: C, 26.92; H, 4.21; N, 19.27.

Immediately after a mixture of 4-methyl-1,2,4-triazolinedione (0.013 g, 0.115 mmol) and **2** (0.10 g, 0.115 mmol) in CH_2Cl_2 (1 mL) was decolorized, 0.10 g (1.28 mmol) of Na_2S was added. The resulting mixture was sonicated for 1 h. After the remaining Na_2S and resulting NaCl were filtered, and ^1H NMR and MS showed formation of **8** (~10%), $(Me_2GeS)_3$ (15%), and unidentified products (yields estimated by ^1H NMR).

OM950149X

(15) Rausch, M. I.; Cappanelli, D. J. *J. Organomet. Chem.* **1967**, *10*, 127.

(16) Hayashi, T.; Yamashita, H.; Sakakura, T.; Uchimaru, Y.; Tanaka, M. *Chem. Lett.* **1991**, 245.

Notes

Facile Retro-[1,4]-Brook Rearrangement of a [(2-Siloxycyclopentyl)methyl]lithium Species

Xing-Long Jiang and William F. Bailey*

Department of Chemistry, University of Connecticut, Storrs, Connecticut 06269

Received August 9, 1995®

*Summary: The [1,4]-O → C migration of the TBDMS group in the [(2-(tert-butyldimethylsiloxy)cyclopentyl)-methyl]lithium system (**1** and **2**) has been found to be confined to the cis-isomer (**1**).*

The relatively facile [1,2]-migration of a silyl substituent from carbon to oxygen, first recognized by Brook in the late 1950's,[1] is the prototype of a class of [1,*n*]-C → O silyl migrations that are commonly termed Brook rearrangements.[2] More recently, examples of the reverse of this process, involving transfer of a silyl substituent from oxygen to a formally anionic carbon (retro-Brook rearrangement), have been documented.[3] In light of the current interest in [1,4]- and [1,5]-O → C silyl migrations,[4] we were prompted to communicate the results of a study of [(2-(*tert*-butyldimethylsiloxy)cyclopentyl)methyl]lithiums (**1** and **2**) demonstrating that the retro-[1,4]-Brook rearrangement in this system is confined exclusively to the *cis*-isomer (**1**).

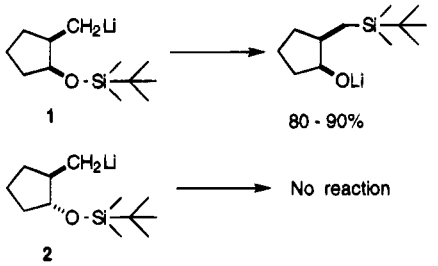

1 2

In the course of a continuing investigation of the cyclization of 5-hexenyllithiums bearing various heteroatomic substituents,[5] we had occasion to explore the ring-closure of [4-(*tert*-butyldimethylsiloxy)-5-hexenyl]-lithium (**3**) generated, as shown below, from iodide **4** by low-temperature lithium–iodine exchange with *t*-BuLi.[6]

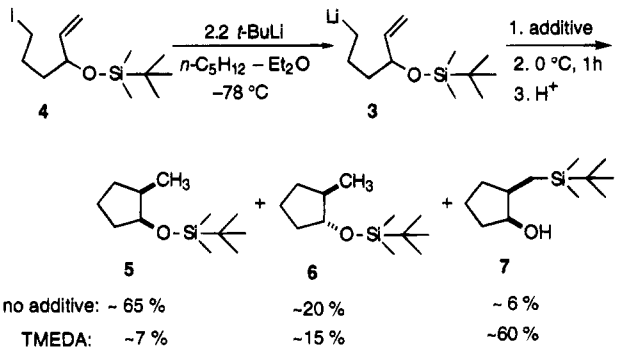

Quenching reaction mixtures that had been warmed and held at 0 °C for 1 h delivered not only the expected *cis*-(**5**) and *trans*-2-methyl-1-(*tert*-butyldimethylsiloxy)cyclopentane (**6**) products[7] but also a small quantity of *cis*-2-[(*tert*-butyldimethylsilyl)methyl]cyclopentanol (**7**). Moreover, alcohol **7** becomes the major product of the isomerization when the cyclization of **3** is conducted at higher temperatures or, as illustrated below, in the presence of *N,N,N′,N′*-tetramethylethylenediamine (TMEDA). In no instance was the *trans*-isomer of **7** detected in any of the reaction mixtures nor was there any evidence of [1,5]-O → C TBDMS migration in **3**.

Alcohol **7** is undoubtedly formed via retro-[1,4]-Brook rearrangement following cyclization of **3**. We were intrigued by the fact that TBDMS migration was apparently limited to the *cis*-isomer of the cyclic organolithium (**1**). In order to confirm this observation, the behavior of authentic samples of *cis*- (**1**) and *trans*-[(2-(*tert*-butyldimethylsiloxy)cyclopentyl)methyl]lithium (**2**) was investigated.

To this end, [4-(*tert*-butyldimethylsiloxy)-5-hexenyl)-lithium (**3**) was isomerized for 1 h at 0 °C in a solution

® Abstract published in *Advance ACS Abstracts,* November 1, 1995.

(1) Brook, A. G. *J. Am. Chem. Soc.* **1958**, *80*, 1886.

(2) (a) Brook, A. G. *Acc. Chem. Res.* **1974**, *7*, 77. (b) Brook, A. G.; Bassindale, A. R. In *Rearrangements in Ground and Excited States*; De Mayo, P., Ed.; Academic Press: New York, 1980; Vol. 2, p 149. (c) Colvin, E. W. In *Silicon in Organic Synthesis*; Butterworths: London, 1981; p 30.

(3) (a) West, R.; Lowe, R.; Stewart, H. F.; Wright, A. *J. Am. Chem. Soc.* **1971**, *93*, 282. (b) Wright, A.; West, R. *J. Am. Chem. Soc.* **1974**, *96*, 3214. (c) Evans, D. A.; Takacs, J. M.; Hurst, K. M. *J. Am. Chem. Soc.* **1979**, *101*, 371. (d) Eisch, J. J.; Tsai, M. R. *J. Organomet. Chem.* **1982**, *225*, 5 and references therein. (e) Linderman, R. J.; Ghannam, A. *J. Am. Chem. Soc.* **1990**, *112*, 2392.

(4) (a) For a concise summary of the literature relating to [1,4]- and [1,5]-Brook and retro-Brook rearrangements, see: Lautens, M.; Delanghe, P. H. M.; Goh, J. B.; Zhang, C. H. *J. Org. Chem.* **1995**, *60*, 4213. (b) Bures, E. J.; Keay, B. A. *Tetrahedron Lett.* **1987**, *28*, 5965. (c) Spinazzé, P. G.; Keay, B. A. *Tetrahedron Lett.* **1989**, *30*, 1765 and references therein. (d) Kim, K. D.; Magriotis, P. A. *Tetrahedron Lett.* **1990**, *31*, 6137. (e) Hoffmann, R. W.; Bewersdorf, M. *Tetrahedron Lett.* **1990**, *31*, 67. (f) Hoffmann, R.; Brückner, R. *Chem. Ber.* **1992**, *125*, 2731. (g) Clayden, J.; Julia, M. *Synlett* **1995**, 103.

(5) The results of study of the cyclization of (4-methoxy-5-hexenyl)-lithium have been published: Bailey, W. F.; Jiang, X-L. *J. Org. Chem.* **1994**, *59*, 6528.

(6) Bailey, W. F.; Punzalan, E. R. *J. Org. Chem.* **1990**, *55*, 5404.

(7) Cyclization of **3** under a variety of experimental conditions has been found to give *cis*-rich mixtures of **5** and **6**. It is of some interest to note that the stereochemistry of the cyclization of the related ether, (4-methoxy-5-hexenyl)lithium, is strongly dependent on the solvent system in which the isomerization is conducted.[5] The diastereoselectivity of the ring-closure of **3** and related substrates will be presented in the full account of an ongoing investigation of the cyclization of a range of 5-hexenyllithiums bearing heteroatomic substituents capable of coordination with lithium.

0276-7333/95/2314-5704$09.00/0

Scheme 1

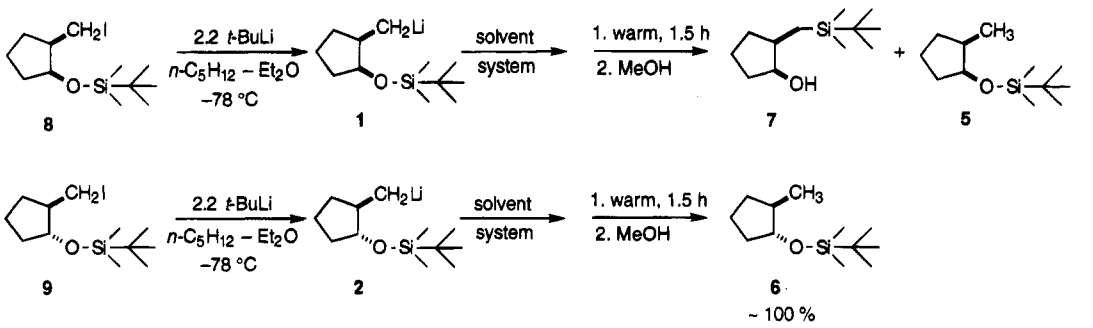

Table 1. Retro-[1,4]-Brook Rearrangement (Scheme 1) of *cis*-[(2-(*tert*-Butyldimethylsiloxy)-cyclopentyl)methyl]lithium (1)[a]

entry no.	solvent syst	temp, °C	products, % yield[b] 7	5
1	n-C_5H_{12}–Et_2O (3:2 by vol)	+20	83	17
2	TMEDA	0	88	12
3		+22	83	17
4	HMPA	0	80	20

[a] *cis*-[(2-(*tert*-Butyldimethylsiloxy)cyclopentyl)methyl]lithium (1) was generated at −78 °C by addition of 2.2 equiv of *t*-BuLi to a solution of iodide **8** in *n*-pentane–diethyl ether (3:2 by vol). Where indicated, 2.2 molar equiv of dry TMEDA or HMPA was added at −78 °C after completion of the exchange reaction. The cooling bath was then removed, and the mixture stood at the specified temperature for 1.5 h before the addition of an excess of oxygen-free methanol. [b] Yields were determined by capillary GC using *n*-heptane as an internal standard.

of *n*-pentane–diethyl ether and the resulting cyclic organolithium products (**1** and **2**) were trapped with iodine to deliver a mixture of the corresponding iodides (**8** and **9**) along with a small amount of **7**. Careful

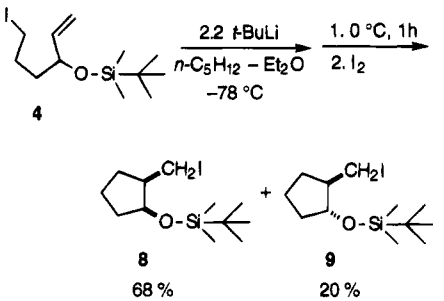

chromatography of the product mixture on silica gel provided pure samples of **8** and **9** in isolated yields of 68% and 20%, respectively. Treatment of either **8** or **9** with *t*-BuLi at −78 °C returned isomerically pure organolithium (**1** or **2**) in virtually quantitative yield as demonstrated by the fact that quench of each reaction mixture with MeOH at −78 °C delivered the corresponding *cis*- (**5**) or *trans*-2-methyl-1-(*tert*-butyldimethylsiloxy)cyclopentane (**6**) in 97%–99% yield.

With a method in hand for the generation of isomerically pure samples of **1** and **2**, the tendency of each isomer to undergo retro-[1,4]-Brook rearrangement was explored (Scheme 1). As demonstrated by the results summarized in Table 1, [1,4]-migration of the TBDMS moiety in **1** is a facile, high-yield process at room temperature in *n*-pentane–diethyl ether solvent or at 0 °C in the presence of TMEDA or HMPA: pure **7** was isolated in 85% yield when the rearrangement of **1** was conducted at 0 °C in a solvent mixture containing 2.2 equiv of TMEDA (Table 1, entry 2). In striking contrast to the behavior of **1**, the *trans*-isomer, **2**, proved to be totally resistant to retro-[1,4]-Brook rearrangement. Indeed, a series of experiments in which solutions of **2** stood at room temperature in the presence of TMEDA (or other Lewis bases) for periods of 1–2 h provided no evidence of rearrangement: quenching such mixtures delivered pure *trans*-2-methyl-1-(*tert*-butyldimethylsiloxy)cyclopentane (**6**) in essentially quantitative yield (Scheme 1).

The complete absence of any product derived from [1,4]-O → C migration of the silyl substituent in **2** implies that *intermolecular* rearrangement is not occurring in this system.[8] This conclusion was confirmed by the result of the following experiment: a 2:1 mixture of iodides **8** and **9** in *n*-pentane–diethyl ether (3:2 by vol) was treated with *t*-BuLi at −78 °C, and the resulting mixture of **1** and **2** was warmed and stood at +20 °C for 1 h prior to quench. As expected (Table 1, entry 1, and Scheme 1), all of the *trans*-isomer (**2**) was recovered as **6** while 85% of the *cis*-isomer (**1**) was converted to **7**.

Given the intramolecular nature of the retro-[1,4]-Brook rearrangement in the [(2-(*tert*-butyldimethylsiloxy)cyclopentyl)methyl]lithium system, it is perhaps not surprising, albeit in retrospect, that migration is confined to the *cis*-isomer (**1**).[9] The [1,4]-O → C migration of the TBDMS group in **1** may proceed, either in a concerted fashion or via the intermediacy of a pentavalent silicon intermediate,[4] with little distortion of the carbon skeleton. Such intramolecular migration would be energetically costly in the *trans*-isomer (**2**) since it would involve severe steric strain in the transition state for the process.

The generation of a lithium alkoxide following retro-[1,4]-Brook rearrangement of **1** presumably provides the thermodynamic driving force for the reaction.[2-4] Literature precedent suggests that replacement of lithium by sodium should reverse the direction of the migration.[2-4] Indeed, as illustrated below, treatment of *cis*-2-[(*tert*-butyldimethylsilyl)methyl]cyclopentanol (**7**) with 5 equiv of NaH in DMF at room temperature led to virtually complete conversion of the alcohol to **5**.

(8) Intermolecular [1,4]- and [1,5]-O → C silyl migrations are documented; see, for example: Smichen, G.; Pfletschinger, J. *Angew. Chem, Int. Ed. Engl.* **1976**, *15*, 428.

(9) It is of some interest to note that intramolecular retro-[1,4]-Brook rearrangement is a facile process for the *trans*-isomer of the related [(2-siloxycyclohexyl)methyl]lithium system. See: Rücker, C. *Tetrahedron Lett.* **1984**, *25*, 4349.

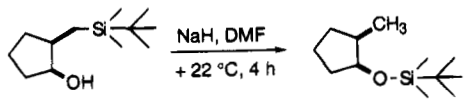

7 5

94 %

Experimental Section

General Procedures. General spectroscopic and chromatographic procedures, methods used for the purification of reagents and solvents, and precautions regarding the manipulation of organolithiums have been previously described.[10]

Literature procedures, incorporating some minor modifications, were followed for the preparation of 6-chloro-1-hexen-3-ol,[11] *trans*-2-methylcyclopentanol,[5] *cis*-2-methylcyclopentanol,[5] and 1-hexen-3-ol.[5]

3-[(*tert*-Butyldimethyl)siloxy]-6-iodo-1-hexene (4). A solution of 7.50 g (55.8 mmol) of 6-chloro-1-hexen-3-ol,[11] 9.48 g (139 mmol) of imidazole, and 10.1 g (66.9 mmol) of *tert*-butyldimethylsilyl chloride in 18 mL of dry DMF was heated at 35 °C for 24 h and then diluted with 40 mL of diethyl ether. The resulting mixture was poured into 20 mL of water, the organic layer was separated, and the aqueous phase was extracted with several portions of diethyl ether. The combined organic extracts were washed sequentially with 30 mL of saturated aqueous ammonium chloride solution, 30 mL of water, and 30 mL of brine, dried ($MgSO_4$), and concentrated at reduced pressure. The residue was purified by flash chromatography on silica gel (petroleum ether; $R_f = 0.67$) to give 11.2 g (81%) of the TBDMS ether, which was used without further purification for the preparation of the iodide: ^{1}H NMR δ 0.027 (s, 3 H), 0.048 (s, 3 H), 0.89 (s, 9 H), 1.26–1.80 (m, 4 H), 3.53 (t, J = 6.68 Hz, 2 H), 4.13–4.15 (m, 1 H), 5.04 (apparent d of t, J_{cis} = 10.5 Hz, J_{gem} = 1.48 Hz, ^4J = 1.46 Hz, 1 H), 5.15 (apparent d of t, J_{trans} = 17.1 Hz, ^4J = 1.55 Hz, J_{gem} = 1.48 Hz, 1 H), 5.78 (ddd, J_{trans} = 17.1 Hz, J_{cis} = 10.5 Hz, ^3J = 5.91 Hz, 1 H); ^{13}C NMR δ −4.86, −4.37, 22.63, 25.87, 28.33, 35.20, 45.24, 73.08, 114.07, 141.31.

A solution of 7.00 g (46.6 mmol) of sodium iodide and 5.30 g (21.3 mmol) of the chloride in 70 mL of dry acetone was heated at gentle reflux for 24 h. The reaction mixture was cooled and filtered, and the precipitate was washed with acetone. The combined filtrate and washings were concentrated, and the residue was taken up in 50 mL of diethyl ether. The ethereal solution was washed with 30 mL of 5% aqueous sodium thiosulfate and 30 mL of brine, dried ($MgSO_4$), and concentrated under reduced pressure. The residue was purified by flash chromatography on silica gel (petroleum ether) to give 6.31 g (87%) of the title iodide which was pure by GC analysis: (petroleum ether; $R_f = 0.70$) ^{1}H NMR δ 0.014 (s, 3 H), 0.037 (s, 3 H), 0.884 (s, 9 H), 1.48–1.93 (m, 4 H), 3.18 (t, J = 5.53 Hz, 2 H), 4.11–4.13 (m, 1 H), 5.03 (apparent d of t, J_{cis} = 10.3 Hz, J_{gem} = 1.48 Hz, ^4J = 1.34 Hz, 1 H), 5.14 (apparent d of t, J_{trans} = 17.1 Hz, ^4J = 1.52 Hz, J_{gem} = 1.48 Hz, 1 H), 5.77 (ddd, J_{trans} = 17.1 Hz, J_{cis} = 10.3 Hz, ^3J = 6.00 Hz, 1 H); ^{13}C NMR δ −4.85, −4.39, 7.11, 25.86, 29.17, 32.46, 38.65, 72.72, 114.06, 141.16; HRMS calcd for $C_8H_{16}ISiO$ ($M^+ - C_4H_9$) m/z 283.0015, found m/z 283.0012.

***cis*-2-Methyl-1-(*tert*-butyldimethylsiloxy)cyclopentane (5).** A solution of 1.00 g (10 mmol) of *cis*-2-methylcyclopentanol,[5] 1.81 g (12.0 mmol) of *tert*-butyldimethylsilyl chloride, and 1.70 g (25.0 mmol) of imidazole in 2.5 mL of dry DMF was heated at 35 °C for 24 h. The cooled reaction mixture was diluted with 25 mL of water and 30 mL of diethyl ether, the layers were separated, and the aqueous layer was extracted with two 20 mL portions of diethyl ether. The combined extract and washings were washed successively with 20 mL of aqueous ammonium chloride, 20 mL of water, and 20 mL of brine, dried ($MgSO_4$), and concentrated under reduced pressure. The residue was purified by preparative GC on a 10-ft, 10% FFAP on Chromosorb W NAW (80/100 mesh) column at 150 °C to afford 1.95 g (91%) of the title compound: ^{1}H NMR δ 0.023 (s, 6 H), 0.88 (s, 9 H), 0.93 (d, J = 6.63 Hz, 3 H),1.55–1.75 (m, 7 H), 3.99–4.01 (m, 1 H); ^{13}C NMR δ −4.89, −4.59, 14.34, 18.40, 21.96, 25.91, 30.85, 35.11, 39.99, 76.33. Anal. Calcd for $C_{12}H_{26}OSi$: C, 67.22; H, 12.22. Found: C, 67.46; H, 12.43.

***trans*-2-Methyl-1-(*tert*-butyldimethylsiloxy)cyclopentane (6).** A solution of 0.500 g (10.0 mmol) of *trans*-2-methylcyclopentanol,[5] 0.910 g (6.00 mmol) of *tert*-butyldimethylsilyl chloride, and 0.850 g (12.5 mmol) of imidazole in 1.5 mL of dry DMF was heated at 35 °C for 24 h. The cooled reaction mixture was worked up as described above for the *cis*-isomer, and the residue was purified by preparative GC on a 10-ft, 10% FFAP on Chromosorb W NAW (80/100 mesh) column at 150 °C to afford 0.950 g (89%) of the title compound: ^{1}H NMR δ 0.029 (s, 3 H), 0.039 (s, 3 H), 0.89 (s, 9 H), 0.93 (d, J = 6.63 Hz, 3 H), 1.48–1.84 (m, 7 H), 3.58–3.61 (m, 1 H); ^{13}C NMR δ −4.68, −4.49, 18.08, 18.14, 21.23, 25.93, 31.17, 34.36, 42.51, 80.89. Anal. Calcd for $C_{12}H_{26}OSi$: C, 67.22; H, 12.22. Found: C, 66.79; H, 12.32.

***cis*- (8) and *trans*-2-(Iodomethyl)-1-(*tert*-butyldimethylsiloxy)cyclopentane (9).** A 100 mL flame-dried flask was charged with a solution of 1.85 g (5.45 mmol) of 3-(*tert*-butyldimethyl)siloxy-6-iodo-1-hexene (**4**) in 32.7 mL of dry pentane and 21.8 mL of dry diethyl ether. The solution was cooled to −78 °C, and 6.32 mL of a 1.89 M solution of *t*-BuLi (11.9 mmol) in pentane was added dropwise by syringe. The resulting mixture was stirred at −78 °C for 5 min, the cooling bath was then removed, and the solution was warmed and stood at 0 °C for 1 h to effect cyclization to a mixture of **1** and **2**. In another flask, a solution of 2.79 g (10.9 mmol) of iodine in 35 mL of dry diethyl ether was cooled to −78 °C under an atmosphere of argon. The solution of **1** and **2** was then added dropwise to the iodine solution via a Teflon cannula. The resulting mixture was stirred at −78 °C for 0.5 h and was then warmed to room temperature and poured into 20 mL of 5% aqueous sodium thiosulfate. The organic phase was separated, washed with brine, dried over $MgSO_4$, and concentrated under reduced pressure. Flash chromatography of the residue over silica gel using hexanes as eluent served to separate the thermally and light-sensitive isomeric products. The major product (1.25 g, 68%), which eluted first (R_f = 0.57), was identified as *cis*-2-(iodomethyl)-1-(*tert*-butyldimethylsiloxy)-cyclopentane (**8**) on the basis of the following spectroscopic data: ^{1}H NMR δ 0.06 (s, 3 H), 0.10 (s, 3 H), 0.88 (s, 9 H), 1.39–1.45 (m, 1 H), 1.67–1.87 (m, 5 H), 2.09–2.24 (m, 1 H), 3.15 (A portion of ABX, J_{AB} = 9.19 Hz, J_{AX} = 6.56 Hz, 1 H), 3.28 (B portion of ABX, J_{AB} = 9.19 Hz, J_{BX} = 8.75 Hz, 1 H), 4.17–4.18 (m, 1 H); ^{13}C NMR δ −4.62, −4.33, 7.43, 18.03, 22.31, 25.86, 29.67, 34.99, 49.92, 74.86. HRMS calcd for $C_8H_{16}ISiO$ ($M^+ - C_4H_9$) m/z 283.0015, found m/z 283.0009. The minor product (0.377 g, 20%; R_f = 0.29) was identified as *trans*-2-(iodomethyl)-1-(*tert*-butyldimethylsiloxy)cyclopentane (**9**) on the basis of the following spectroscopic data: ^{1}H NMR δ 0.04 (s, 3 H), 0.07 (s, 3 H), 0.88 (s, 9 H), 1.23–1.29 (m, 1 H), 1.51–1.62 (m, 1 H), 1.68–1.91 (m, 5 H), 3.16 (A portion of ABX, J_{AB} = 9.65 Hz, J_{AX} = 6.80 Hz, 1 H), 3.33 (B portion of ABX, J_{AB} = 9.65 Hz, J_{BX} = 4.38 Hz, 1 H), 3.74–3.77 (m, 1 H); ^{13}C NMR δ −4.57, −4.36, 12.17, 17.97, 21.71, 25.85, 30.05, 34.71, 49.62, 78.30. HRMS calcd for $C_8H_{16}ISiO$ ($M^+ - C_4H_9$) m/z 283.0015, found m/z 283.0019.

Retro-[1,4]-Brook Rearrangement: Preparation of *cis*-2-[(*tert*-butyldimethylsilyl)methyl]cyclopentanol (7). An approximately 0.1 M solution of *cis*-2-(iodomethyl)-1-(*tert*-butyldimethylsiloxy)cyclopentane (**8**) in *n*-pentane–diethyl ether (3:2 by vol) containing an accurately weighed quantity of *n*-heptane as internal standard was cooled to −78 °C, and

(10) Bailey, W. F.; Khanolkar, A. D.; Gavaskar, K.; Ovaska, T. V.; Rossi, K.; Thiel, Y.; Wiberg, K. B. *J. Am. Chem. Soc.* **1991**, *113*, 5720.
(11) Meyer, C.; Marek, I.; Courtemanche, G.; Normant, J.-F. *Tetrahedron* **1994**, *50*, 1665.

2.2 molar equiv of *t*-BuLi in pentane was added dropwise via syringe over a 5 min period. The resulting mixture was stirred at −78 °C for 5 min before treatment in one of the following ways. (A) The cooling bath was removed, and the solution was warmed and stood at +20 °C for 1.5 h before the addition of 1.0 mL of dry, deoxygenated MeOH. (B) The organolithium solution was maintained at −78 °C, and 2.2−2.5 equiv of dry TMEDA or HMPA was added by syringe. The resulting mixture was stirred for an additional 5 min at −78 °C and then was warmed and stood at the appropriate temperature (Table 1, entries 2−4) for 1.5 h prior to the addition of 1.0 mL of dry, deoxygenated MeOH. Reaction mixtures were washed with water, dried ($MgSO_4$), and concentrated under reduced pressure. GC analysis on a 19-m × 0.25-mm methylphenyl silicone capillary column using temperature programming (50 °C for 5 min, 20 °C/min to 250 °C) revealed that the product mixtures consisted of **5** and **7** in the ratios given in Table 1. The minor product, which had the shorter retention time, was identified as *cis*-2-methyl-1-(*tert*-butyldimethylsiloxy)cyclopentane (**5**) by comparison with an authentic sample. The major product, isolated in 85% yield from the reaction conducted in *n*-pentane−diethyl ether by chromatography on silica gel (50% diethyl ether−hexanes; R_f = 0.80), was identified as the title alcohol on the basis of the following spectroscopic data: IR (neat) 3374 (br), 2930, 1464, 1250, and 828 cm^{-1}; ^1H NMR δ −0.039 (s, 3 H), −0.034 (s, 3 H), 0.53−0.59 (m, 2 H), 0.69−0.76 (m, 1 H), 0.86 (s, 9 H), 1.30 (br s, 1 H), 1.64−1.80 (m, 6 H), 3.96−3.98 (m, 1 H); ^{13}C NMR δ −5.76, −5.02, 11.49, 16.64, 22.24, 26.58, 31.28, 34.13, 41.92, 76.52. Anal. Calcd for $C_{12}H_{26}SiO$: C, 67.22; H, 12.22. Found: C, 67.16; H, 12.40.

Repetition of these experiments using *trans*-2-(iodomethyl)-1-(*tert*-butyldimethylsiloxy)cyclopentane (**9**) gave no evidence of rearrangement: in each instance, pure *trans*-2-methyl-1-(*tert*-butyldimethylsiloxy)cyclopentane (**6**) was produced in *ca.* 100% yield.

[1,4]-Brook Rearrangement of *cis*-2-[(*tert*-butyldimethylsilyl)methyl]cyclopentanol (7): Preparation of *cis*-2-Methyl-1-(*tert*-butyldimethylsiloxy)cyclopentane (5). A suspension of 0.380 g (15.8 mmol) of oil-free sodium hydride in 5.0 mL of dry DMF was stirred under a blanket of argon, and 0.678 g (3.17 mmol) of *cis*-2-[(*tert*-butyldimethylsilyl)-methyl]cyclopentanol (**7**) was added to the suspension. The resulting mixture was stirred at room temperature for 4 h, and then diluted with 5.0 mL of diethyl ether, washed with water, and dried over $MgSO_4$. Analysis of the crude product by GC on a 19-m × 0.25-mm methylphenyl silicone capillary column using temperature programming (50 °C for 5 min, 20 °C/min to 250 °C) and by GC−MS on a 25-m × 0.20-mm HP-5 methylphenyl (20%) silicone capillary column using temperature programming (50 °C for 5 min, 20 °C/min to 250 °C) revealed that reaction mixture consisted of 94% *cis*-2-methyl-1-(*tert*-butyldimethylsiloxy)cyclopentane (**5**) and 6% of the starting alcohol (**7**). The identity of the products was confirmed by comparison of GC retention times and mass spectra to those of authentic samples.

Acknowledgment. This work was supported by the Connecticut Department of Economic Development.

OM950631F

Synthesis and Characterization of the First Ruthenium–Lead Clusters, $[Ru_3(\mu\text{-}PbR_2)(\mu\text{-}CO)_2(CO)_9]$ and $[Ru_3(\mu\text{-}PbR_2)_2(\mu\text{-}CO)(CO)_9]$. Single-Crystal X-ray Structure of $[Ru_3(\mu\text{-}PbR_2)_2(\mu\text{-}CO)(CO)_9]$

Nicolas C. Burton,[†] Christine J. Cardin,[†] David J. Cardin,*[,†] Brendan Twamley,[†,‡] and Yan Zubavichus[†,§]

Chemistry Department, University of Reading, Whiteknights, Reading, Berkshire RG6 6AD, U.K., and Chemistry Department, Trinity College, University of Dublin, Dublin 2, Ireland

Received June 14, 1995[⊗]

Summary: Reaction of PbR_2 [R = $CH(SiMe_3)_2$] with $[Ru_3(CO)_{12}]$ at 60 °C afforded the first ruthenium–lead clusters $[Ru_3(\mu\text{-}PbR_2)(\mu\text{-}CO)_2(CO)_9]$ (1) and $[Ru_3(\mu\text{-}PbR_2)_2(\mu\text{-}CO)(CO)_9]$ (2). After separation the compounds were characterized by ^1H and ^{13}C NMR and IR spectroscopies, FAB-MS, and, for 2, by a single-crystal X-ray study. The structure gives the first reported Ru–Pb bond lengths and shows the cluster to have a planar pentametallic array with two PbR_2 and one CO bridging the three sides of an Ru_3 triangle. A greatly improved yield for the preparation of PbR_2 is also reported. Compound 2 crystallizes in the triclinic space group $P\bar{1}$ with unit cell dimensions $a = 12.279(6)$ Å, $b = 15.406(6)$ Å, $c = 20.775(5)$ Å, $\alpha = 99.54(6)°$, $\beta = 107.47(6)°$, $\gamma = 109.59(6)°$, $U = 3373.1(10)$ Å^3, and $Z = 2$. A total of 10 179 unique observations gave a merging R of 0.038 and a conventional R of 0.0756.

Introduction

We report the synthesis of the first ruthenium–lead clusters and the first structural data for lead–transition metal clusters, apart from two reports on Pb–Fe compounds.[1,2] We also report a higher-yield synthesis for our starting material, the lead(II) compound $[Pb\{CH(SiMe_3)_2\}_2]$, previously reported to be obtained in very low yield.[3]

There is extensive literature on heterometallic clusters incorporating main-group metals,[4] but very little relates to clusters having lead atoms in the framework. The published work is restricted to lead–iron systems, which were prepared from lead(IV) species using hydride or halide elimination reactions.[5] We have reported on a number of transition metal clusters in which tin has been introduced using a variety of tin(II) reagents.[6] In these reactions, the nucleophilicity of the tin(II) species is exploited to displace either a carbonyl group (for the lighter metals) or a more labile group, such as acetonitrile (for heavy elements, e.g., osmium). This approach has led to a range of cluster nuclearities from M_3Sn through M_3Sn_3 (M = Fe, Ru, or Os) to Ir_4Sn_5.[6c] To date, no analogous reactions with clusters have been reported for the lead(II) species, though $[Pb\{CH(SiMe_3)_2\}_2]$ (PbR_2) has been shown in a single instance to ligate to a metal center in the species $[(OC)_5MoPb\{CH(SiMe_3)_2\}_2]$, obtained in 4% yield from the parent carbonyl and PbR_2 under ultraviolet irradiation.[7] The other reported chemistry for the lead species relates principally to oxidative additions or, for the case of the isoelectronic amide, to insertion into the Pt–Cl bonds of $[\{PtCl_2(PEt_3)\}_2]$ to give $[\{Pt(ClPb(N(SiMe_3)_2)_2)Cl(PEt_3)\}_2]$.[7]

We now report that the plumbylene reacts thermally with ruthenium carbonyl to afford two clusters and discuss the structure of one of them.

Results and Discussion

The published synthesis of PbR_2 quotes a yield of *ca.* 3%.[3,8] We find that following sublimation of the lead(II) chloride starting material, the procedure reported gives essentially quantitative yields. The compound was obtained as an extremely air–sensitive purple solid after recrystallization from hexane at low temperature.

Where the analogous stannylene, SnR_2 reacts rapidly with $[Ru_3(CO)_{12}]$ in hexane at room temperature, the lead reagent is a less effective nucleophile, failing to react under these conditions. On heating in hexanes (60 °C, 1.5 h) two products were obtained and separated by fractional crystallization from hexanes. Chromatography (silica column/hexanes) is not the preferred

[†] University of Reading.
[‡] University of Dublin.
[§] Present address: Higher Chemical College, Russian Academy of Sciences, Miusskaya Sq. 9, Moscow, Russia.
[⊗] Abstract published in *Advance ACS Abstracts,* October 15, 1995.

(1) Lagrone, C. B.; Whitmire, K. H.; Churchill, M. R.; Fettinger, J. C. *Inorg. Chem.* **1986,** *25,* 2080.
(2) Whitmire, K. H.; Lagrone, C. B.; Churchill, M. R.; Fettinger, J. C.; Robinson, B. H. *Inorg. Chem.* **1987,** *26,* 3491.
(3) Davidson, P. J.; Harris, D. H.; Lappert, M. F. *J. Chem. Soc., Dalton Trans.* **1976,** 2268.
(4) For a leading review see: Whitmire, K. H. *J. Coord. Chem.* **1987,** *17,* 95.
(5) (a) Cotton, J. D.; Knox, S. A. R.; Paul, I.; Stone, F. G. A. *J. Chem. Soc. A* **1967,** 264. (b) Dalton, J.; Paul, I.; Stone, F. G. A. *J. Chem. Soc. A* **1968,** 1215. (c) Marks, T. J.; Newmann, A. R. *J. Am. Chem. Soc.* **1973,** *95,* 769.
(6) See for example: (a) Cardin, C. J.; Cardin, D. J.; Convery, M. A.; Devereux, M. M. *J. Chem. Soc., Chem. Commun.* **1991,** 687. (b) Cardin, C. J.; Cardin, D. J.; Lawless, G. A.; Power, M. B.; Hursthouse, M. B. *J. Organomet. Chem.* **1987,** *325,* 203 and references therein. (c) Cardin, C. J.; Cardin, D. J.; Power, M. B. *J. Organomet. Chem.* **1993,** *462,* C27.
(7) Cotton, J. D.; Davidson, P. J.; Lappert, M. F. *J. Chem. Soc., Dalton Trans.* **1976,** 2275.
(8) Davidson, P. J.; Lappert, M. F. *J. Chem. Soc., Chem. Commun.* **1973,** 317.

0276-7333/95/2314-5708$09.00/0

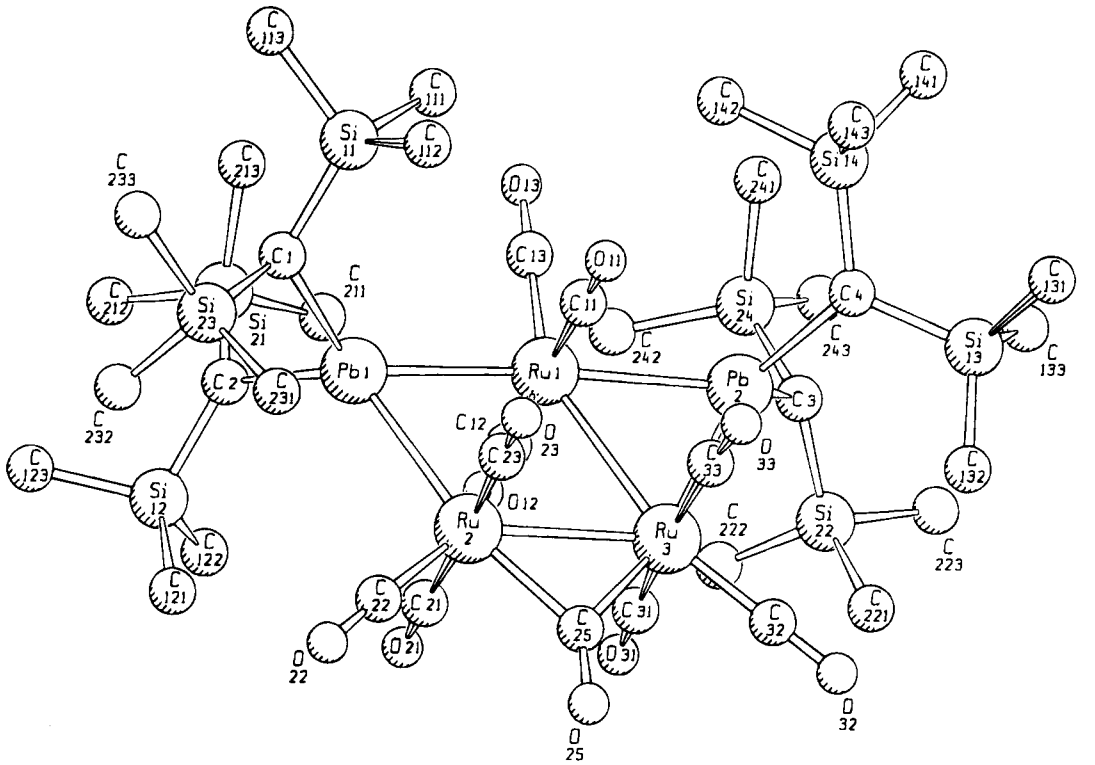

Figure 1. Structure diagram of a single molecule of **2** with the atoms numbered as in Table 1. Hydrogen atoms are omitted for clarity.

method of purification since **1** survives only in low yield and **2** decomposes on the column. Both compounds are

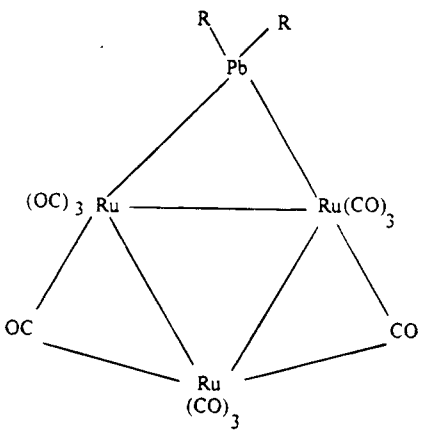

1

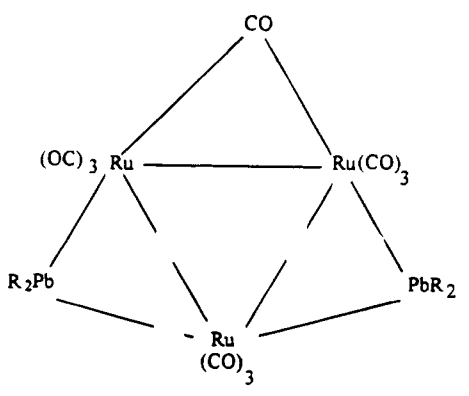

2

sensitive to air and light in solution, though they are moderately air-stable in the solid state.

The IR spectrum of **2** shows terminal CO stretches together with a characteristic single bridging carbonyl band at 1846 cm^{-1}. Since in related reactions of the analogous stannylene, SnR_2,[6b] the tin group almost invariably bridges two transition metal centers, maintaining the 48-electron count for the metal triangle, this strongly suggests the presence of two bridging PbR_2 groups. In contrast, two bridging carbonyl bands are observed in the IR spectrum of **1** at 1877 and 1833 cm^{-1}, implying the addition of a single PbR_2 group. ^1H and ^{13}C NMR spectroscopy indicate the presence of the ligand $CH(SiMe_3)_2$ in both **1** and **2**. Both ^1H and ^{13}C spectra showed inequivalence of the methyl groups, as observed previously in the tin analogue.[6b] The compounds do not survive electron impact mass spectrometry and react with most common matrices employed in the FAB technique. Using *meta*-nitrobenzyl alcohol and FAB, the highest ions were detected at m/z 927, equal to the mass of the fragment $[Ru_3(CO)_9PbR]^+$ (corresponding to the loss of an R group and two CO groups) for compound **1** and, at m/z 1476, equal to the mass of the fragment $[Ru_3(CO)_{10}Pb_2R_3]^+$ (corresponding to loss of a single R group) for compound **2**.

A single-crystal structure determination was carried out for compound **2**, confirming the formulation suggested by the spectroscopic data above. The molecule consists of a pentanuclear metal array, with two sides of an Ru_3 triangle bridged by PbR_2 groups, see Figure 1.

The substituents on the lead atoms are oriented essentially perpendicular to the metal plane with slight deviations [1.74° at Pb1 and 4.47° at Pb2], similar to the geometries found for tin groups bridging ruthenium, osmium, iron, or iridium frameworks.[6] The lead atoms thus have a highly distorted tetrahedral environment with Ru–Pb–Ru angles of 64.12(4) and 64.55(4)° and C–Pb–C angles of 96.7(10) and 102.2(10)° for Pb1 and

Table 1. Selected Bond Lengths (Å) and Angles (deg)

Pb1–Ru1	2.777(2)	Pb1–C1	2.31(2)
Pb1–Ru2	2.790(2)	Pb1–C2	2.27(2)
Pb2–Ru1	2.765(2)	Pb2–C3	2.31(2)
Pb2–Ru3	2.787(2)	Pb2–C4	2.30(2)
Ru1–Ru2	2.955(2)	Ru2–C25	2.06(2)
Ru2–Ru3	2.852(2)	Ru3–C25	2.08(2)
Ru3–Ru1	2.965(2)	C25–O25	1.17(2)
C1–Pb1–C2	96.7(10)	C25–Ru2–Ru3	46.7(5)
Ru1–Pb1–Ru2	64.12(4)	Ru2–C25–Ru3	87.0(7)
Pb1–Ru1–Ru2	58.15(4)	C25–Ru3–Ru2	46.3(5)
Ru1–Ru2–Pb1	57.72(4)	Ru1–Pb2–Ru3	64.55(4)
Ru2–Ru1–Ru3	57.60(5)	Pb2–Ru1–Ru3	58.08(4)
Ru1–Ru2–Ru3	61.37(4)	Pb2–Ru3–Ru1	57.38(4)
Ru1–Ru3–Ru2	61.02(4)	C3–Pb2–C4	102.2(10)

Pb2, respectively. As with the tin analogue, the metal-bridged Ru–Ru vectors are significantly longer than those of the parent carbonyl. The distances in (a) $[Ru_3(CO)_{12}]$, (b) $[Ru_3(\mu\text{-}SnR_2)_2(\mu\text{-}CO)(CO)_9]$, and (c) $[Ru_3(\mu\text{-}PbR_2)_2(\mu\text{-}CO)(CO)_9]$ are (a) 2.854(4), (b) 2.950(2) and 2.963(2), and (c) 2.955(2) and 2.965(2) Å; thus the lengthening produced by both SnR_2 and PbR_2 is remarkably similar. The Ru–Pb distances, the first such to be reported, are given in the table of selected bond lengths and angles (Table 1). These bridges are significantly asymmetrical, the longer Pb–Ru separations in each case being adjacent to the bridging carbonyl. The probable interpretation of this is that the Pb–Ru vector is pseudo *trans* to the (in-plane) bridging carbonyl, which exerts a comparably larger *trans* influence. It is noteworthy that the SnR_2 bridges of the tin analogue (b above) are not significantly asymmetrical, possibly reflecting a greater *trans* influence for the Sn ligand. We have already noted above that the tin reagent is appreciably more reactive in displacing CO from the parent carbonyl.

Experimental Section

The syntheses and subsequent manipulations of the compounds described here were conducted under inert atmosphere conditions using standard Schlenk, vacuum line, and glovebox techniques. Solvents were dried and distilled prior to use. NMR spectra were recorded on a Bruker AM250 instrument, and IR data were obtained using a Perkin-Elmer 1720-X FT instrument.

$[Pb\{CH(SiMe_3)_2\}_2]$.[8] Bis(trimethylsilyl)lithium (20 mL, 6.6 mmol, 0.33 M in Et_2O) was added over 1 h to a suspension of freshly sublimed anhydrous $PbCl_2$ (0.92 g, 3.3 mmol) in diethyl ether (50 mL) at −10 °C, and during the addition the slurry became yellow and quickly darkened to a deep purple. The mixture was stirred for 0.5 h at 0 °C and then for 1 h at room temperature, after which time solvent was removed under vacuum. The remaining purple solid was redissolved in hexane (50 mL), and the solution was filtered. The solution was concentrated and cooled, (−25 °C), and the product was collected (1.65 g, 95%).

$[Ru_3(\mu\text{-}PbR_2)(\mu\text{-}CO)_2(CO)_9]$ (1) and $[Ru_3(\mu\text{-}PbR_2)_2(\mu\text{-}CO)(CO)_9]$ (2). A purple solution of PbR_2 (1.65 g, 3.1 mmol) in hexane (30 mL) was added to a suspension of $[Ru_3(CO)_{12}]$ (0.33 g, 0.53 mmol) in hexane (50 mL), and the mixture was heated at 60 °C for 1.5 h. The reaction was monitored by TLC until completion. After concentration of the solvent and filtration to remove unreacted $[Ru_3(CO)_{12}]$, **2** (0.18 g, 21%) was obtained by crystallization at −25 °C in hexane. Mp 135 °C (decomp). IR (CsI), ν(CO) (cm^{-1}): 2090 s, 2059 s, 2038 s, 2022 s, 2009 s, 1981 s br, 1846 s br. FT-Raman (cm^{-1}): 2954, 2901, 2089, 2051, 2037, 2028, 2005, 1983, 1973, 1841, 460, 448, 149. ^1H NMR (400 MHz, C_6D_6): δ 0.37, 0.39, 0.41, 0.43 (s, 72H), 1.59 (br, 4H). ^{13}C NMR (10 MHz, $CDCl_3$): δ 5.98, 6.07, 6.42, 131.64, 199.64, 204.29. FAB MS: m/z 1476 ($M^+ - 156$). Subsequent recrystallization from the mother liquor gave **1** (0.06 g, 11%). Mp 137 °C (decomp). IR (CsI), ν(CO) (cm^{-1}): 2113 s, 2051 s, 2031 s, 1996 s, 1877 s br, 1831 s br. ^1H NMR (250 MHz, $CDCl_3$): δ 0.29 (s, 36H) 1.19 (s, 2H). ^{13}C NMR (100 MHz, $CDCl_3$): δ 4.8, 128.22, 205.2. FAB MS: m/z 927 ($M^+ - 213$). The light- and air-sensitivity preclude obtaining accurate elemental analytical data for these compounds.

Crystal Data: $C_{38}H_{76}O_{10}Pb_2Ru_3Si_8$. M = 1635.30. Triclinic, space group $P\bar{1}$. a = 12.279(6) Å, b = 15.406(6) Å, c = 20.775(5) Å, α = 99.54(6)°, β = 107.47(6)°, γ = 109.59(6)°, U = 3373.1(10) Å^3, Z = 2, D_c = 1.610 g/cm^{-3}, μ(Mo Kα) = 5.81 mm^{-1}, F(000) = 1584, λ = 0.710 73 Å.

A crystal of approximate dimensions 0.1 × 0.2 × 0.2 mm^3 was mounted on a glass fiber, and intensity data in the range $2.77 \geq \theta \geq 25.02°$ were measured using a MAR Imageplate Scanner. Ninety-five frames were measured with a 2° rotation and an exposure time of 2 min per frame. Data were processed with the XDS package[9] to give a total of 10 179 unique observations with a merging R of 0.038. The structure was solved by Patterson synthesis using SHELX 86 and refined with SHELXL. The final conventional R factor is 0.0756 based on 7 150 observations for which $|F| > 4(\sigma F)$ and 549 parameters, but the structure was refined using all 10 179 observations. SHELX 86 and SHELXL were used by kind permission of Professor G. M. Sheldrick (University of Göttingen, Göttingen, Germany).

Acknowledgment. We thank the EPSRC and the SERC for support, the Research Endowment fund (University of Reading) and the Krieble fund (Trinity College Dublin) for maintenance grants, Dr. P. Turner (Bruker, U.K.) for running the FT Raman spectra, Sun Microsystems, and Caversham Rotary Club (to Y.Z.).

Supporting Information Available: Tables of crystal data, positional and thermal parameters, and distances and angles (16 pages). Ordering information is given on any current masthead page.

OM9504563

(9) Kabsch, W. *J. Appl. Crystallogr.* **1993**, *26*, 795.